

# PRESTRESSED CONCRETE

A FUNDAMENTAL APPROACH

FIFTH EDITION  
UPDATE

ACI, AASHTO, IBC 2009 Codes Version

EDWARD G. NAWY

83.9

139

2010

avis

- $a$  = depth of equivalent rectangular stress block.
- $A_{cp}$  = area enclosed by outside perimeter of concrete cross section.
- $A_g$  = gross area of section, in.<sup>2</sup>
- $A_h$  = area of shear reinforcement parallel to flexural tension reinforcement, in.<sup>2</sup>
- $A_j$  = Effective cross-sectional area within a joint, in.<sup>2</sup> in a plane parallel to plane of reinforcement generating shear in the joint. The joint depth shall be the overall depth of the column. Where a beam frames into a support of larger width, the effective width of the joint shall not exceed the smaller of:
- beam width plus the joint depth
  - twice the smaller perpendicular distance from the longitudinal axis of the beam to the column side.
- $A_l$  = total area of longitudinal reinforcement to resist torsion, in.<sup>2</sup>
- $A_n$  = area of reinforcement in bracket or corbel resisting tensile force  $N_{uc}$ , in.<sup>2</sup>
- $A_o$  = gross area enclosed by shear flow path, in.<sup>2</sup>
- $A_{oh}$  = area enclosed by centerline of the outermost closed transverse torsional reinforcement, in.<sup>2</sup>
- $A_{ps}$  = area of prestressed reinforcement in tension zone, in.<sup>2</sup>
- $A_s$  = area of nonprestressed tension reinforcement, in.<sup>2</sup>
- $A'_s$  = area of compression reinforcement, in.<sup>2</sup>
- $A_{sh}$  = total cross-sectional area of transverse reinforcement (including cross-ties) within spacing  $s$  and perpendicular to dimension  $h_o$ .
- $A_t$  = area of one leg of a closed stirrup resisting torsion within a distance  $s$ , in.<sup>2</sup>
- $A_{tr}$  = total cross-sectional area of transverse reinforcement (stirrup or tie) within a spacing  $s$  and perpendicular to plane of bars being spliced or developed, in.<sup>2</sup>
- $A_v$  = area of shear reinforcement within a distance  $s$ , or area of shear reinforcement perpendicular to flexural tension reinforcement within a distance  $s$  for deep flexural members, in.<sup>2</sup>
- $A_{vf}$  = area of shear-friction reinforcement, in.<sup>2</sup>
- $A_{vh}$  = area of shear reinforcement parallel to flexural tension reinforcement within a distance  $s_2$ , in.<sup>2</sup>
- $b$  = width of compression face of member, in.
- $b_o$  = perimeter of critical section for slabs and footings, in.
- $b_t$  = width of that part of cross section containing the closed stirrups resisting torsion.
- $b_v$  = width of cross section at contact surface being investigated for horizontal shear.
- $b_w$  = web width, or diameter of circular section, in.
- $c$  = distance from extreme compression fiber to neutral axis, in.
- $c_1$  = size of rectangular or equivalent rectangular column, capital, or bracket measured in the direction of the span for which moments are being determined, in.
- $c_2$  = size of rectangular or equivalent rectangular column, capital, or bracket measured transverse to the direction of the span for which moments are being determined, in.
- $d$  = distance from extreme compression fiber to centroid of tension reinforcement, in.
- $d'$  = distance from extreme compression fiber to centroid of compression reinforcement, in.
- $d_b$  = nominal diameter of bar, wire, or prestressing strand, in.
- $d_c$  = thickness of concrete cover measured from extreme tension fiber to center of bar or wire located closest thereto, in.
- $d_p$  = distance from extreme compression fiber to centroid of prestressed reinforcement.
- $e$  = eccentricity of load parallel to axis of member measured from centroid of cross section.
- $E_c$  = modulus of elasticity of concrete, psi.
- $E_s$  = modulus of elasticity of bar reinforcement, psi.
- $E_{ps}$  = modulus of elasticity of prestressing reinforcement.
- $f'_c$  = specified 28-day compressive strength of concrete, psi.
- $f_{cr}$  = average strength to be used as basis for selecting concrete proportions, psi.
- $f'_{cr}$  = required average compressive strength of concrete used as the basis for selection of concrete proportions, psi.
- $\sqrt{f'_c}$  = square root of specified compressive strength of concrete, psi.
- $f'_{ci}$  = compressive strength of concrete at time of initial prestress, psi.
- $\sqrt{f'_{ci}}$  = square root of compressive strength of concrete at time of initial prestress, psi.
- $f_{ct}$  = average splitting tensile strength of lightweight aggregate concrete, psi.

- $f_d$  = stress due to unfactored dead load, at extreme fiber of section where tensile stress is caused by externally applied loads, psi.
- $f_{pc}$  = compressive stress in concrete due to effective prestress forces only (after allowance for all prestress losses) at extreme fiber of section where tensile stress is caused by externally applied loads, psi.
- $f_{ps}$  = stress in prestressed reinforcement at nominal strength.
- $f_{pu}$  = specified tensile strength of prestressing tendons, psi.
- $f_{py}$  = specified yield strength of prestressing tendons, psi.
- $f_r$  = modulus of rupture of concrete, psi.
- $f'_t$  = tensile strength of concrete, psi.
- $f_y$  = specified yield strength of nonprestressed reinforcement, psi.
- $f_{yt}$  = specified yield strength of transverse, reinforcement, psi.
- $h$  = overall thickness of member, in.
- $I$  = moment of inertia of section resisting externally applied factored loads, in.<sup>4</sup>
- $I_b$  = moment of inertia about centroidal axis of gross section of beam, in.<sup>4</sup>
- $I_{cr}$  = moment of inertia of cracked section transformed to concrete, in.<sup>4</sup>
- $I_e$  = effective moment of inertia for computation of deflection, in.<sup>4</sup>
- $I_g$  = moment of inertia of gross concrete section about centroidal axis, neglecting reinforcement, in.<sup>4</sup>
- $k$  = effective length factor for compression members.
- $K_b$  = flexural stiffness of beam; moment per unit rotation.
- $K_c$  = flexural stiffness of column; moment per unit rotation.
- $K_{ec}$  = flexural stiffness of equivalent column; moment per unit rotation.
- $K_s$  = flexural stiffness of slab; moment per unit rotation.
- $K_t$  = torsional stiffness of torsional member; moment per unit rotation.
- $l_{dh}$  = development length of standard hook in tension, measured from critical section to outside end of hook (straight embedment length between critical section and start of hook [point of tangency] plus radius of bend and one bar diameter), in.
- =  $l_{hb}$  × applicable modification factors.
- $M_a$  = maximum moment in member at stage deflection is computed.
- $M_c$  = factored moment to be used for design of compression member.
- $M_d$  = moment due to dead load.
- $M_{cr}$  = cracking moment.
- $M_n$  = nominal moment strength.
- $M_m$  = maximum factored moment at section due to externally applied loads.
- $M_u$  = factored moment at section.
- $n$  = modular ratio of elasticity.  
=  $E_s/E_c$  or  $E_{ps}/E_c$ .
- $N_u$  = factored axial load normal to cross section occurring simultaneously with  $V_u$ ; to be taken as positive for compression, negative for tension, and to include effects of tension due to creep and shrinkage.
- $N_{uc}$  = factored tensile force applied at top of bracket or corbel acting simultaneously with  $V_u$ , to be taken as positive for tension.
- $P_b$  = nominal axial load strength at balanced strain conditions.
- $P_c$  = critical buckling load.
- $P_n$  = nominal axial load strength at given eccentricity.
- $p_{cp}$  = outside perimeter of the concrete cross-section  $A_{cp}$ , in.
- $p_h$  = perimeter of centerline of outermost closed transverse torsional reinforcement, in.
- $r$  = radius of gyration of cross section of a compression member.
- $s$  = spacing of shear or torsion reinforcement in direct parallel to longitudinal reinforcement, in.
- $t$  = thickness of a wall of a hollow section, in.
- $T_u$  = factored torsional moment at section.
- $V_e$  = nominal shear strength provided by concrete.
- $V_{ci}$  = nominal shear strength provided by concrete when diagonal cracking results from combined shear and moment.
- $V_{cw}$  = nominal shear strength provided by concrete when diagonal cracking results from excessive principal tensile stress in web.
- $V_d$  = shear force at section due to unfactored dead load.
- $V_p$  = vertical component of effective prestress force at section.
- $V_s$  = nominal shear strength provided by shear reinforcement.
- $V_u$  = factored shear force at section.

# PRESTRESSED CONCRETE

*A Fundamental Approach*

*Fifth Edition Update*

*ACI, AASHTO, IBC 2009 Codes Version*

**Edward G. Nawy**

*Distinguished Professor Emeritus*

*Department of Civil and Environmental Engineering*

*Rutgers, The State University of New Jersey*

**Prentice Hall**

Upper Saddle River, Boston, Columbus, San Francisco, New York  
London, London, Toronto, Sydney, Singapore, Tokyo, Montreal,  
Delhi, Mexico, New Delhi, Hyderabad, Mumbai, Paris, Amsterdam, Cape Town



# PRESTRESSED CONCRETE

*A Fundamental Approach*

*Fifth Edition Update  
ACI, AASHTO, IBC 2009 Codes Version*

**Edward G. Nawy**

*Distinguished Professor Emeritus  
Department of Civil and Environmental Engineering  
Rutgers, The State University of New Jersey*

**Prentice Hall**

Upper Saddle River Boston Columbus San Francisco New York  
Indianapolis London Toronto Sydney Singapore Tokyo Montreal  
Dubai Madrid Hong Kong Mexico City Munich Paris Amsterdam Cape Town

Vice President and Editorial Director, ECS: *Marcia J. Horton*  
Senior Editor: *Holly Stark*  
Associate Editor: *Dee Bernhard*  
Editorial Assistant: *William Opaluch*  
Director of Team-Based Project Management: *Vince O'Brien*  
Senior Managing Editor: *Scott Disanno*  
Production Editor: *Jane Bonnell/Patty Donovan*  
Senior Operations Supervisor: *Alan Fischer*  
Operations Specialist: *Lisa McDowell*  
Senior Marketing Manager: *Tim Galligan*  
Marketing Assistant: *Mack Patterson*  
Art Director, Cover: *Jayne Conte*  
Cover Designer: *Bruce Kenselaar*  
Art Editor: *Greg Dulles*  
Media Editor: *Daniel Sandin*  
Media Project Manager: *Danielle Leone*  
Composition: *Laserwords Maine*

*About the Cover:* The new I-35W bridge, Minneapolis, Minnesota. Designed for the Minnesota Department of Transportation by FIGG, this new bridge incorporates aesthetics selected by the community using a theme of “Arches–Water–Reflection” to complement the site across the Mississippi River. Curved, 70' tall concrete piers meet the sweeping parabolic arch of the 504' precast, prestressed concrete main span over the river to create a modern bridge. The new 10-lane interstate bridge was constructed by Flatiron-Manson, JV and opened to traffic on September 18, 2008. The bridge was designed and built in 11 months. The bridge incorporates the first use of LED highway lighting, the first major use in the United States of nanotechnology cement that cleans the air (gateway sculptures) and “smart bridge” technology with 323 sensors embedded throughout the concrete to provide valuable data for the future. The photograph of the new I-35W bridge is courtesy of FIGG.

**Copyright 2010, 2006, 2003, 2000, 1996, 1989 by Pearson Education, Inc., Upper Saddle River, New Jersey 07458.** All rights reserved. Manufactured in the United States of America. This publication is protected by Copyright and permissions should be obtained from the publisher prior to any prohibited reproduction, storage in a retrieval system, or transmission in any form or by any means, electronic, mechanical, photocopying, recording, or likewise. To obtain permission(s) to use materials from this work, please submit a written request to Pearson Higher Education, Permissions Department, 1 Lake Street, Upper Saddle River, NJ 07458.

The author and publisher of this book have used their best efforts in preparing this book. These efforts include the development, research, and testing of the theories and programs to determine their effectiveness. The author and publisher make no warranty of any kind, expressed or implied, with regard to these programs or the documentation contained in this book. The author and publisher shall not be liable in any event for incidental or consequential damages in connection with, or arising out of, the furnishing, performance, or the use of these programs.

#### **Library of Congress Cataloging-in-Publication Data**

Nawy, Edward G.

Prestressed concrete : a fundamental approach / Edward G. Nawy.—5th ed.  
p. cm.

ISBN 0-13-608150-9

1. Prestressed concrete. I. Title.

TA683.9.N39 2009

624.1'83412--dc22

2009024405

**Prentice Hall**  
is an imprint of

**PEARSON**

[www.pearsonhighered.com](http://www.pearsonhighered.com)

10 9 8 7 6 5 4 3 2 1

ISBN-13: 978-0-13-608150-0  
ISBN-10: 0-13-608150-9

To  
Rachel E. Nawy

*For her high-limit state of stress endurance over the years,  
which made the writing of this book in its several editions a reality.*





# CONTENTS

## PREFACE **xix**

# 1

## BASIC CONCEPTS **1**

- 1.1 Introduction 1
  - 1.1.1 Comparison with Reinforced Concrete 2
  - 1.1.2 Economics of Prestressed Concrete 4
- 1.2 Historical Development of Prestressing 5
- 1.3 Basic Concepts of Prestressing 7
  - 1.3.1 Introduction 7
  - 1.3.2 Basic Concept Method 10
  - 1.3.3 C-Line Method 12
  - 1.3.4 Load-Balancing Method 15
- 1.4 Computation of Fiber Stresses in a Prestressed Beam by the Basic Method 19
- 1.5 C-Line Computation of Fiber Stresses 21
- 1.6 Load-Balancing Computation of Fiber Stresses 22
- 1.7 SI Working Stress Concepts 23
- Selected References 28
- Problems 28

# 2

## MATERIALS AND SYSTEMS FOR PRESTRESSING **31**

- 2.1 Concrete 31
  - 2.1.1 Introduction 31
  - 2.1.2 Parameters Affecting the Quality of Concrete 31
  - 2.1.3 Properties of Hardened Concrete 32
- 2.2 Stress–Strain Curve of Concrete 36
- 2.3 Modulus of Elasticity and Change in Compressive Strength with Time 36
  - 2.3.1 High-Strength Concrete 38
  - 2.3.2 Initial Compressive Strength and Modulus 39
- 2.4 Creep 43
  - 2.4.1 Effects of Creep 45
  - 2.4.2 Rheological Models 45
- 2.5 Shrinkage 48
- 2.6 Nonprestressing Reinforcement 50
- 2.7 Prestressing Reinforcement 53
  - 2.7.1 Types of Reinforcement 53
  - 2.7.2 Stress-Relieved and Low-Relaxation Wires and Strands 54
  - 2.7.3 High-Tensile-Strength Prestressing Bars 55
  - 2.7.4 Steel Relaxation 56
  - 2.7.5 Corrosion and Deterioration of Strands 58

2.8	ACI Maximum Permissible Stresses in Concrete and Reinforcement	59
2.8.1	Concrete Stresses in Flexure	59
2.8.2	Prestressing Steel Stresses	59
2.9	AASHTO Maximum Permissible Stresses in Concrete and Reinforcement	60
2.9.1	Concrete Stresses before Creep and Shrinkage Losses	60
2.9.2	Concrete Stresses at Service Load after Losses	60
2.9.3	Prestressing Steel Stresses	60
2.9.4	Relative Humidity Values	60
2.10	Prestressing Systems and Anchorages	61
2.10.1	Pretensioning	61
2.10.2	Post-Tensioning	62
2.10.3	Jacking Systems	63
2.10.4	Grouting of Post-Tensioned Tendons	64
2.11	Circular Prestressing	70
2.12	Ten Principles	70
	Selected References	70

### 3

## PARTIAL LOSS OF PRESTRESS 73

3.1	Introduction	73
3.2	Elastic Shortening of Concrete ( $ES$ )	75
3.2.1	Pretensioned Elements	75
3.2.2	Post-Tensioned Elements	78
3.3	Steel Stress Relaxation ( $R$ )	78
3.3.1	Relaxation Loss Computation	80
3.3.2	ACI-ASCE Method of Accounting for Relaxation Loss	80
3.4	Creep Loss ( $CR$ )	80
3.4.1	Computation of Creep Loss	82
3.5	Shrinkage Loss ( $SH$ )	83
3.5.1	Computation of Shrinkage Loss	84
3.6	Losses Due to Friction ( $F$ )	85
3.6.1	Curvature Effect	85
3.6.2	Wobble Effect	86
3.6.3	Computation of Friction Loss	87
3.7	Anchorage-Seating Losses ( $A$ )	88
3.7.1	Computation of Anchorage-Seating Loss	89
3.8	Change of Prestress Due to Bending of a Member ( $\Delta f_{pB}$ )	90
3.9	Step-by-Step Computation of All Time-Dependent Losses in a Pretensioned Beam	90
3.10	Step-by-Step Computation of All Time-Dependent Losses in a Post-Tensioned Beam	96
3.11	Lump-Sum Computation of Time-Dependent Losses in Prestress	99
3.12	SI Prestress Loss Expressions	100
13.12.1	SI Prestress Loss Example	101
	Selected References	104
	Problems	105

### 4

## FLEXURAL DESIGN OF PRESTRESSED CONCRETE ELEMENTS 106

4.1	Introduction	106
4.2	Selection of Geometrical Properties of Section Components	108
4.2.1	General Guidelines	108
4.2.2	Minimum Section Modulus	108

- 4.3 Service-Load Design Examples 115
    - 4.3.1 Variable Tendon Eccentricity 115
    - 4.3.2 Variable Tendon Eccentricity with No Height Limitation 122
    - 4.3.3 Constant Tendon Eccentricity 126
  - 4.4 Proper Selection of Beam Sections and Properties 128
    - 4.4.1 General Guidelines 128
    - 4.4.2 Gross Area, the Transformed Section, and the Presence of Ducts 130
    - 4.4.3 Envelopes for Tendon Placement 130
    - 4.4.4 Advantages of Curved or Harped Tendons 131
    - 4.4.5 Limiting-Eccentricity Envelopes 132
    - 4.4.6 Prestressing Tendon Envelopes 136
    - 4.4.7 Reduction of Prestress Force Near Supports 138
  - 4.5 End Blocks at Support Anchorage Zones 139
    - 4.5.1 Stress Distribution 139
    - 4.5.2 Development and Transfer Length in Pretensioned Members and Design of Their Anchorage Reinforcement 141
    - 4.5.3 Post-Tensioned Anchorage Zones: Linear Elastic and Strut-and-Tie Theories 144
    - 4.5.4 Design of End Anchorage Reinforcement for Post-Tensioned Beams 153
  - 4.6 Flexural Design of Composite Beams 158
    - 4.6.1 Unshored Slab Case 159
    - 4.6.2 Fully Shored Slab Case 161
    - 4.6.3 Effective Flange Width 161
  - 4.7 Summary of Step-by-Step Trial-and-Adjustment Procedure for the Service-Load Design of Prestressed Members 162
  - 4.8 Design of Composite Post-Tensioned Prestressed Simply Supported Section 165
  - 4.9 Ultimate-Strength Flexural Design 178
    - 4.9.1 Cracking-Load Moment 178
    - 4.9.2 Partial Prestressing 179
    - 4.9.3 Cracking Moment Evaluation 180
  - 4.10 Load and Strength Factors 181
    - 4.10.1 Reliability and Structural Safety of Concrete Components 181
  - 4.11 ACI Load Factors and Safety Margins 184
    - 4.11.1 General Principles 184
    - 4.11.2 ACI Load Factors Equations 185
    - 4.11.3 Design Strength vs. Nominal Strength: Strength-Reduction Factor  $\phi$  187
  - 4.12 Limit State in Flexure at Ultimate Load in Bonded Members: Decompression to Ultimate Load 188
    - 4.12.1 Introduction 188
    - 4.12.2 The Equivalent Rectangular Block and Nominal Moment Strength 189
    - 4.12.3 Strain Limits Method for Analysis and Design 191
    - 4.12.4 Negative Moment Redistribution in Continuous Beams 193
    - 4.12.5 Nominal Moment Strength of Rectangular Sections 194
  - 4.13 Preliminary Ultimate-Load Design 202
  - 4.14 Summary Step-by-Step Procedure for Limit-State-at-Failure Design of the Prestressed Members 204
  - 4.15 Ultimate-Strength Design of Prestressed Simply Supported Beam by Strain Compatibility 209
  - 4.16 Strength Design of Bonded Prestressed Beam Using Approximate Procedures 212
  - 4.17 SI Flexural Design Expression 216
    - 4.17.1 SI Flexural Design of Prestressed Beams 218
- Selected References 220
- Problems 221

## 5

## SHEAR AND TORSIONAL STRENGTH DESIGN 223

- 5.1 Introduction 223
- 5.2 Behavior of Homogeneous Beams in Shear 224
- 5.3 Behavior of Concrete Beams as Nonhomogeneous Sections 227
- 5.4 Concrete Beams without Diagonal Tension Reinforcement 228
  - 5.4.1 Modes of Failure of Beams without Diagonal Tension Reinforcement 229
  - 5.4.2 Flexural Failure [ $F$ ] 229
  - 5.4.3 Diagonal Tension Failure [Flexure Shear,  $FS$ ] 229
  - 5.4.4 Shear Compression Failure [Web Shear,  $WS$ ] 231
- 5.5 Shear and Principal Stresses in Prestressed Beams 232
  - 5.5.1 Flexure-Shear Strength [ $V_{ci}$ ] 233
  - 5.5.2 Web-Shear Strength [ $V_{cw}$ ] 236
  - 5.5.3 Controlling Values of  $V_{ci}$  and  $V_{cw}$  for the Determination of Web Concrete Strength  $V_c$  237
- 5.6 Web-Shear Reinforcement 238
  - 5.6.1 Web Steel Planar Truss Analogy 238
  - 5.6.2 Web Steel Resistance 238
  - 5.6.3 Limitation on Size and Spacing of Stirrups 241
- 5.7 Horizontal Shear Strength in Composite Construction 242
  - 5.7.1 Service-Load Level 242
  - 5.7.2 Ultimate-Load Level 243
  - 5.7.3 Design of Composite-Action Dowel Reinforcement 245
- 5.8 Web Reinforcement Design Procedure for Shear 246
- 5.9 Principal Tensile Stresses in Flanged Sections and Design of Dowel-Action Vertical Steel in Composite Sections 249
- 5.10 Dowel Steel Design for Composite Action 250
- 5.11 Dowel Reinforcement Design for Composite Action in an Inverted T-Beam 251
- 5.12 Shear Strength and Web-Shear Steel Design in a Prestressed Beam 253
- 5.13 Web-Shear Steel Design by Detailed Procedures 256
- 5.14 Design of Web Reinforcement for a PCI Double T-Beam 259
- 5.15 Brackets and Corbels 263
  - 5.15.1 Shear Friction Hypothesis for Shear Transfer in Corbels 264
  - 5.15.2 Horizontal External Force Effect 266
  - 5.15.3 Sequence of Corbel Design Steps 269
  - 5.15.4 Design of a Bracket or Corbel 270
  - 5.15.5 SI Expressions for Shear in Prestressed Concrete Beams 272
  - 5.15.6 SI Shear Design of Prestressed Beams 274
- 5.16 Torsional Behavior and Strength 278
  - 5.16.1 Introduction 278
  - 5.16.2 Pure Torsion in Plain Concrete Elements 279
- 5.17 Torsion in Reinforced and Prestressed Concrete Elements 284
  - 5.17.1 Skew-Bending Theory 285
  - 5.17.2 Space Truss Analogy Theory 287
  - 5.17.3 Compression Field Theory 289
  - 5.17.4 Plasticity Equilibrium Truss Theory 293
  - 5.17.5 Design of Prestressed Concrete Beams Subjected to Combined Torsion, Shear, and Bending in Accordance with the ACI 318-08 Code 298
  - 5.17.6 SI-Metric Expressions for Torsion Equations 303
- 5.18 Design Procedure for Combined Torsion and Shear 304
- 5.19 Design of Web Reinforcement for Combined Torsion and Shear in Prestressed Beams 308

- 5.20 Strut-and-Tie Model Analysis and Design of Concrete Elements 317
  - 5.20.1 Introduction 317
  - 5.20.2 Strut-and-Tie Mechanism 318
  - 5.20.3 ACI Design Requirements 321
  - 5.20.4 Example 5.10: Design of Deep Beam by Strut-and-Tie Method 324
  - 5.20.5 Example 5.11: Design of Corbel by the Strut-and-Tie Method 328
- 5.21 SI Combined Torsion and Shear Design of Prestressed Beam 332
  - Selected References 335
  - Problems 337

## 6

### INDETERMINATE PRESTRESSED CONCRETE STRUCTURES 340

- 6.1 Introduction 340
- 6.2 Disadvantages of Continuity in Prestressing 341
- 6.3 Tendon Layout for Continuous Beams 341
- 6.4 Elastic Analysis for Prestress Continuity 344
  - 6.4.1 Introduction 344
  - 6.4.2 Support Displacement Method 344
  - 6.4.3 Equivalent Load Method 347
- 6.5 Examples Involving Continuity 347
  - 6.5.1 Effect of Continuity on Transformation of C-Line for Draped Tendons 347
  - 6.5.2 Effect of Continuity on Transformation of C-Line for Harped Tendons 352
- 6.6 Linear Transformation and Concordance of Tendons 354
  - 6.6.1 Verification of Tendon Linear Transformation Theorem 355
  - 6.6.2 Concordance Hypotheses 358
- 6.7 Ultimate Strength and Limit State at Failure of Continuous Beams 358
  - 6.7.1 General Considerations 358
  - 6.7.2 Moment Redistribution 361
- 6.8 Tendon Profile Envelope and Modifications 362
- 6.9 Tendon and C-Line Location in Continuous Beams 362
- 6.10 Tendon Transformation to Utilize Advantages of Continuity 373
- 6.11 Design for Continuity Using Nonprestressed Steel at Support 378
- 6.12 Indeterminate Frames and Portals 379
  - 6.12.1 General Properties 379
  - 6.12.2 Forces and Moments in Portal Frames 382
  - 6.12.3 Application to Prestressed Concrete Frames 386
  - 6.12.4 Design of Prestressed Concrete Bonded Frame 389
- 6.13 Limit Design (Analysis) of Indeterminate Beams and Frames 401
  - 6.13.1 Method of Imposed Rotations 402
  - 6.13.2 Determination of Plastic Hinge Rotations in Continuous Beams 405
  - 6.13.3 Rotational Capacity of Plastic Hinges 408
  - 6.13.4 Calculation of Available Rotational Capacity 411
  - 6.13.5 Check for Plastic Rotation Serviceability 412
  - 6.13.6 Transverse Confining Reinforcement for Seismic Design 413
  - 6.13.7 Selection of Confining Reinforcement 414
  - Selected References 415
  - Problems 417

## 7

### CAMBER, DEFLECTION, AND CRACK CONTROL 418

- 7.1 Introduction 418
- 7.2 Basic Assumptions in Deflection Calculations 419

7.3	Short-Term (Instantaneous) Deflection of Uncracked and Cracked Members	420
7.3.1	Load-Deflection Relationship	420
7.3.2	Uncracked Sections	423
7.3.3	Cracked Sections	427
7.4	Short-Term Deflection at Service Load	433
7.4.1	Example 7.3 Non-Composite Uncracked Double T-Beam Deflection	433
7.5	Short-Term Deflection of Cracked Prestressed Beams	439
7.5.1	Short-Term Deflection of the Beam in Example 7.3 if Cracked	439
7.6	Construction of Moment-Curvature Diagram	440
7.7	Long-Term Effects on Deflection and Camber	446
7.7.1	PCI Multipliers Method	446
7.7.2	Incremental Time-Steps Method	448
7.7.3	Approximate Time-Steps Method	450
7.7.4	Computer Methods for Deflection Evaluation	452
7.7.5	Deflection of Composite Beams	452
7.8	Permissible Limits of Calculated Deflection	453
7.9	Long-Term Camber and Deflection Calculation by the PCI Multipliers Method	454
7.10	Long-Term Camber and Deflection Calculation by the Incremental Time-Steps Method	458
7.11	Long-Term Camber and Deflection Calculation by the Approximate Time-Steps Method	469
7.12	Long-Term Deflection of Composite Double-T Cracked Beam	472
7.13	Cracking Behavior and Crack Control in Prestressed Beams	479
7.13.1	Introduction	479
7.13.2	Mathematical Model Formulation for Serviceability Evaluation	479
7.13.3	Expressions for Pretensioned Beams	480
7.13.4	Expressions for Post-Tensioned Beams	481
7.13.5	ACI New Code Provisions	483
7.13.6	Long-Term Effects on Crack-Width Development	484
7.13.7	Tolerable Crack Widths	485
7.14	Crack Width and Spacing Evaluation in Pretensioned T-Beam Without Mild Steel	485
7.15	Crack Width and Spacing Evaluation in Pretensioned T-Beam Containing Nonprestressed Steel	486
7.16	Crack Width and Spacing Evaluation in Pretensioned I-Beam Containing Nonprestressed Mild Steel	487
7.17	Crack Width and Spacing Evaluation for Post-Tensioned T-Beam Containing Nonprestressed Steel	488
7.18	Crack Control by ACI Code Provisions	490
7.19	SI Deflection and Cracking Expressions	490
7.20	SI Deflection Control	491
7.21	SI Crack Control	496
	Selected References	496
	Problems	497

## 8

## PRESTRESSED COMPRESSION AND TENSION MEMBERS 500

8.1	Introduction	500
8.2	Prestressed Compression Members: Load–Moment Interaction in Columns and Piles	501
8.3	Strength Reduction Factor $\phi$	507
8.4	Operational Procedure for the Design of Nonslender Prestressed Compression Members	508

- 8.5 Construction of Nominal Load-Moment ( $P_n-M_n$ ) and Design ( $P_u-M_u$ ) Interaction Diagrams 509
- 8.6 Limit State at Buckling Failure of Slender (Long) Prestressed Columns 515
  - 8.6.1 Buckling Considerations 519
- 8.7 Moment Magnification Method: First-Order Analysis 520
  - 8.7.1 Moment Magnification in Non-Sway Frames 521
  - 8.7.2 Moment Magnification in Sway Frames 522
- 8.8 Second-Order Frames Analysis and the  $P - \Delta$  Effects 523
- 8.9 Operational Procedure and Flowchart for the Design of Slender Columns 525
- 8.10 Design of Slender (Long) Prestressed Column 525
- 8.11 Compression Members in Biaxial Bending 531
  - 8.11.1 Exact Method of Analysis 531
  - 8.11.2 Load Contour Method of Analysis 532
  - 8.11.3 Step-by-Step Operational Procedure for the Design of Biaxially Loaded Columns 535
- 8.12 Practical Design Considerations 537
  - 8.12.1 Longitudinal or Main Reinforcement 537
  - 8.12.2 Lateral Reinforcement for Columns 537
- 8.13 Reciprocal Load Method for Biaxial Bending 540
- 8.14 Modified Load Contour Method for Biaxial Bending 542
  - 8.14.1 Design of Biaxially Loaded Prestressed Concrete Column by the Modified Load Contour Method 542
- 8.15 Prestressed Tension Members 544
  - 8.15.1 Service-Load Stresses 544
  - 8.15.2 Deformation Behavior 546
  - 8.15.3 Decompression and Cracking 547
  - 8.15.4 Limit State at Failure and Safety Factors 547
- 8.16 Suggested Step-by-Step Procedure for the Design of Tension Members 548
- 8.17 Design of Linear Tension Members 548
  - Selected References 551
  - Problems 552

## 9

## TWO-WAY PRESTRESSED CONCRETE FLOOR SYSTEMS 554

- 9.1 Introduction: Review of Methods 554
  - 9.1.1 The Semielastic ACI Code Approach 557
  - 9.1.2 The Yield-Line Theory 557
  - 9.1.3 The Limit Theory of Plates 557
  - 9.1.4 The Strip Method 557
  - 9.1.5 Summary 558
- 9.2 Flexural Behavior of Two-Way Slabs and Plates 558
  - 9.2.1 Two-Way Action 558
  - 9.2.2 Relative Stiffness Effects 558
- 9.3 The Equivalent Frame Method 559
  - 9.3.1 Introduction 559
  - 9.3.2 Limitations of the Direct Design Method 560
  - 9.3.3 Determination of the Statical Moment  $M_0$  561
  - 9.3.4 Equivalent Frame Analysis 563
  - 9.3.5 Pattern Loading of Spans 566
- 9.4 Two-Directional Load Balancing 567
- 9.5 Flexural Strength of Prestressed Plates 569
  - 9.5.1 Design Moments  $M_u$  569



- 9.6 Banding of Prestressing Tendons and Limiting Concrete Stresses 572
  - 9.6.1 Distribution of Prestressing Tendons 572
  - 9.6.2 Limiting Concrete Tensile Stresses at Service Load 573
- 9.7 Load-Balancing Design of a Single-Panel Two-Way Floor Slab 577
- 9.8 One-Way Slab Systems 582
- 9.9 Shear-Moment Transfer to Columns Supporting Flat Plates 583
  - 9.9.1 Shear Strength 583
  - 9.9.2 Shear-Moment Transfer 583
  - 9.9.3 Deflection Requirements for Minimum Thickness: An Indirect Approach 586
- 9.10 Step-by-Step Trial-and-Adjustment Procedure for the Design of a Two-Way Prestressed Slab and Plate System 587
- 9.11 Design of Prestressed Post-Tensioned Flat-Plate Floor System 592
- 9.12 Direct Method of Deflection Evaluation 610
  - 9.12.1 The Equivalent Frame Approach 610
  - 9.12.2 Column and Middle Strip Deflections 611
- 9.13 Deflection Evaluation of Two-Way Prestressed Concrete Floor Slabs 613
- 9.14 Yield-Line Theory for Two-Way-Action Plates 616
  - 9.14.1 Fundamental Concepts of Hinge-Field Failure Mechanisms in Flexure 617
  - 9.14.2 Failure Mechanisms and Moment Capacities of Slabs of Various Shapes Subjected to Distributed or Concentrated Loads 622
- 9.15 Yield-Line Moment Strength of a Two-Way Prestressed Concrete Plate 628
  - Selected References 629
  - Problems 630

# 10

## CONNECTIONS FOR PRESTRESSED CONCRETE ELEMENTS 632

- 10.1 Introduction 632
- 10.2 Tolerances 633
- 10.3 Composite Members 633
- 10.4 Reinforced Concrete Bearing in Composite Members 634
  - 10.4.1 Reinforced Bearing Design 638
- 10.5 Dapped-End Beam Connections 640
  - 10.5.1 Determination of Reinforcement to Resist Failure 641
  - 10.5.2 Dapped-End Beam Connection Design 644
- 10.6 Reinforced Concrete Brackets and Corbels 647
- 10.7 Concrete Beam Ledges 647
  - 10.7.1 Design of Ledge Beam Connection 649
- 10.8 Selected Connection Details 651
  - Selected References 659
  - Problems 659

# 11

## PRESTRESSED CONCRETE CIRCULAR STORAGE TANKS AND STEEL ROOFS 660

- 11.1 Introduction 660
- 11.2 Design Principles and Procedures 661
  - 11.2.1 Internal Loads 661
  - 11.2.2 Restraining Moment  $M_0$  and Radial Shear Force  $Q_0$  at Freely Sliding Wall Base Due to Liquid Pressure 664
  - 11.2.3 General Equations of Forces and Displacements 669
  - 11.2.4 Ring Shear  $Q_0$  and Moment  $M_0$  Gas Containment 673

- 11.3 Moment  $M_0$  and Ring Force  $Q_0$  in Liquid Retaining Tank 674
- 11.4 Ring Force  $Q_y$  at Intermediate Heights of Wall 676
- 11.5 Cylindrical Shell Membrane Coefficients 677
- 11.6 Prestressing Effects on Wall Stresses for Fully Hinged, Partially Sliding and Hinged, Fully Fixed, and Partially Fixed Bases 679
  - 11.6.1 Freely Sliding Wall Base 694
  - 11.6.2 Hinged Wall Base 694
  - 11.6.3 Partially Sliding and Hinged Wall Base 695
  - 11.6.4 Fully Fixed Wall Base 695
  - 11.6.5 Partially Fixed Wall Base 699
- 11.7 Recommended Practice for Situ-Cast and Precast Prestressed Concrete Circular Storage Tanks 704
  - 11.7.1 Stresses 704
  - 11.7.2 Required Strength Load Factors 705
  - 11.7.3 Minimum Wall-Design Requirements 706
- 11.8 Crack Control in Walls of Circular Prestressed Concrete Tanks 708
- 11.9 Tank Roof Design 708
  - 11.9.1 Membrane Theory of Spherical Domes 709
- 11.10 Prestressed Concrete Tanks with Circumferential Tendons 715
- 11.11 Seismic Design of Liquid Containment Tank Structures 715
- 11.12 Step-by-Step Procedure for the Design of Circular Prestressed Concrete Tanks and Dome Roofs 720
- 11.13 Design of Circular Prestressed Concrete Water-Retaining Tank and Its Domed Roof 727
  - Selected References 740
  - Problems 741

# 12

## LRFD AND STANDARD AASHTO DESIGN OF CONCRETE BRIDGES 742

- 12.1 Introduction: Safety and Reliability 742
- 12.2 AASHTO Standard (LFD) and LRFD Truck Load Specifications 744
  - 12.2.1 Loads 745
  - 12.2.2 Wheel Load Distribution on Bridge Decks: Standard AASHTO Specifications (LFD) 748
  - 12.2.3 Bending Moments in Bridge Deck Slabs: Standard AASHTO Specifications (LFD) 750
  - 12.2.4 Wind Loads 751
  - 12.2.5 Seismic Forces 751
  - 12.2.6 AASHTO LFD Load Combinations 751
  - 12.2.7 LRFD Load Combinations 753
- 12.3 Flexural Design Considerations 758
  - 12.3.1 Strain  $\epsilon$  and Factor  $\phi$  Variations: The Strain Limits Approach 758
  - 12.3.2 Factored Flexural Resistance 760
  - 12.3.3 Flexural Design Parameters 760
  - 12.3.4 Reinforcement Limits 761
- 12.4 Shear Design Considerations 762
  - 12.4.1 The Modified Compression Field Theory 762
  - 12.4.2 Design Expressions 763
- 12.5 Horizontal Interface Shear 768
  - 12.5.1 Maximum Spacing of Dowel Reinforcement 770
- 12.6 Combined Shear and Torsion 770

- 12.7 AASHTO-LRFD Flexural-Strength Design Specifications vs. ACI Code Provisions 773
- 12.8 Step-by-Step Design Procedure (LRFD) 775
- 12.9 LRFD Design of Bulb-Tee Bridge Deck 780
- 12.10 LRFD Shear and Deflection Design 793
- 12.11 Standard AASHTO Flexural Design of Prestressed Bridge Deck Beams (LFD) 801
- 12.12 Standard AASHTO Shear-Reinforcement Design of Bridge Deck Beams 809
- 12.13 Shear and Torsion Reinforcement Design of a Box-Girder Bridge 813
- 12.14 LRFD Major Design Expressions in SI Format 819
  - Selected References 820
  - Problems for Solution 821

# 13

## SEISMIC DESIGN OF PRESTRESSED CONCRETE STRUCTURES 824

- 13.1 Introduction: Mechanism of Earthquakes 824
  - 13.1.1 Earthquake Ground Motion Characteristics 826
  - 13.1.2 Fundamental Period of Vibration 827
  - 13.1.3 Design Philosophy 828
- 13.2 Spectral Response Method 829
  - 13.2.1 Spectral Response Acceleration Maps 829
  - 13.2.2 Seismic Design Parameters 829
  - 13.2.3 Earthquake Design Load Classifications and Seismic Categories 833
  - 13.2.4 Redundancy 835
  - 13.2.5 General Procedure Response Spectrum 835
- 13.3 Equivalent Lateral Force Method 837
  - 13.3.1 Horizontal Base Shear 837
  - 13.3.2 Vertical Distribution of Forces 840
  - 13.3.3 Horizontal Distribution of Story Shear  $V_x$  841
  - 13.3.4 Rigid and Flexible Diaphragms 841
  - 13.3.5 Torsion 841
  - 13.3.6 Story Drift and the P-Delta Effect 841
  - 13.3.7 Overturning 843
  - 13.3.8 Simplified Analysis Procedure for Seismic Design of Buildings 843
  - 13.3.9 Other Aspects in Seismic Design 844
- 13.4 Seismic Shear Forces in Beams and Columns of a Frame:
  - Strong Column–Weak Beam Concept 845
    - 13.4.1 Probable Shears and Moments 845
    - 13.4.2 Strong Column Weak Beam Concept 847
- 13.5 ACI Confining Reinforcements for Structural Concrete Members 849
  - 13.5.1 Longitudinal Reinforcement in Compression Members 849
  - 13.5.2 Transverse Confining Reinforcement 851
  - 13.5.3 Horizontal Shear at the Joint of Beam–Column Connections 852
  - 13.5.4 Development of Reinforcement 854
  - 13.5.5 Allowable Shear Stresses in Structural Walls, Diaphragms, and Coupling Beams 854
- 13.6 Seismic Design Concepts in High-Rise Buildings and Other Structures 858
  - 13.6.1 General Concepts 858
  - 13.6.2 Ductility of Elements and Plastic Hinging 858
  - 13.6.3 Ductility Demand Due to Drift Effect 859
- 13.7 Structural Systems in Seismic Zones 860
  - 13.7.1 Structural Ductile Frames 860
  - 13.7.2 Dywidag Ductile Beam–Column Connection: DDC Assembly 864

13.7.3	Structural Walls in High-Seismicity Zones (Shear Walls)	867
13.7.4	Unbonded Precast Post-Tensioned Walls	869
13.8	Dual Systems	872
13.9	Design Procedure for Earthquake-Resistant Structures	872
13.10	SI Seismic Design Expressions	876
13.11	Seismic Base Shear and Lateral Forces and Moments by the IBC Approach	879
13.12	Seismic Shear Wall Design and Detailing	882
13.13	Example 13.3 Structural Precast Wall Base Connection Design	888
13.14	Design of Precast Prestressed Ductile Frame Connection in a High-Rise Building in High-Seismicity Zone Using Dywidag Ductile Connection Assembly (DDC)	890
13.15	Design of Precast Prestressed Ductile Frame Connection in a High-Rise Building in High-Seismicity Zone Using a Hybrid Connector System	895
	Selected References	900
	Problems for Solution	902

## **APPENDIX A UNIT CONVERSIONS, DESIGN INFORMATION, PROPERTIES OF REINFORCEMENT 905**

## **APPENDIX B SELECTED TYPICAL STANDARD PRECAST DOUBLE TEES, INVERTED TEES, HOLLOW CORE SECTIONS, AND AASHTO BRIDGE SECTIONS 929**

## **INDEX 943**



# PREFACE

Prestressed concrete is a widely used material in construction. Hence, graduates of every civil engineering program must have, as a minimum requirement, a basic understanding of the fundamentals of linear and circular prestressed concrete. The high technology advancements in the science of materials have made it possible to construct and assemble large-span systems such as cable-stayed bridges, segmental bridges, nuclear reactor vessels, and offshore oil drilling platforms—work impossible to undertake in the past.

Reinforced concrete's tensile strength is limited, while its compressive strength is extensive. Consequently, prestressing becomes essential in many applications in order to fully utilize that compressive strength and, through proper design, to eliminate or control cracking and deflection. Additionally, design of the members of a total structure is achieved only by trial and adjustment: assuming a section and then analyzing it. Hence, design and analysis are combined in this work in order to make it simpler for the student first introduced to the subject of prestressed concrete design.

This completely updated fifth edition of the book revises the previous text so as to conform to the new ACI 318-08 Code and the International Building Code, IBC 2006–2009, for seismic design, stressing the strain limits approach, sometimes termed as the “unified method” in the code.

The text is the outgrowth of the author's lecture notes developed in teaching the subject at Rutgers University over the past 45 years and the experience accumulated over the years in teaching and research in the areas of reinforced and prestressed concrete inclusive of the Ph.D. level, and the consulting engineering and forensic work that the author has been engaged in over the years. The material is presented in such a manner that the student can become familiarized with the properties of plain concrete, both normal and high strength, and its components prior to embarking on the study of structural behavior. The book is uniquely different from other textbooks on the subject in that the major topics of material behavior, prestress loss, flexure, shear, and torsion are self-contained and can be covered in one semester at the senior level and the graduate level. The in-depth discussions of these topics permit the advanced undergraduate and graduate student, as well as the design engineer, to develop with minimum effort a profound understanding of fundamentals of prestressed concrete structural behavior and performance.

The concise discussion presented in Chapters 1 through 3 on basic principles, the historical development of prestressed concrete, the properties of constituent materials, the long-term basic behavior of such materials, and the evaluation of prestress losses should give an adequate introduction to the subject of prestressed concrete. They should also aid in developing fundamental knowledge regarding the reliability of performance of prestressed structures, a concept to which every engineering student should be exposed today.

Chapters 4 and 5 on flexure, shear, and torsion, with the step-by-step logic of trial and adjustment as well as the flowcharts shown, give the student and the engineer a basic understanding of both the service load and the limit state of load at failure, using the new

ACI 318-08 Code requirements for ultimate load design, thereby producing a good feel for the reserve strength and safety factors inherent in the design expressions. Chapter 4 in this edition contains the latest design procedure with numerical examples for the design of end anchorages of post-tensioned members as required by the latest ACI and AASHTO codes.

An extensive Chapter 5 presents, with design examples, the provisions on torsion combined with shear and bending, which include a unified approach to the topic of torsion in reinforced and prestressed concrete members. SI Units examples are included in the text in addition to having equivalent SI conversions for the major steps of examples throughout the book. Additionally, a detailed theoretical discussion is presented on the mechanisms of shear and torsion, the various approaches to the torsional problem and the plastic concepts of the shear equilibrium and torsional equilibrium theories and their interaction. A totally new section is added on the strut-and-tie modeling of forces in deep beams and corbels, with detailed design examples as required by the latest ACI Code provisions.

Furthermore, inclusion in this edition of design examples in SI Units and a listing of the relevant equations in SI format extends the scope of the text to cover wider applications by the profession. In this manner, the student as well as the practicing engineer can avail themselves with the tools for using either the lb-in. (PI) system or the international (SI) system.

Chapter 6 on indeterminate prestressed concrete structures covers in detail continuous prestressed beams as well as portal frames, consistent with the increased use of continuous members in bridge structures. Numerous detailed examples illustrate the use of the basic concepts method, the C-line method, and the balancing method presented in Chapter 1. Chapter 7 discusses in detail the design for camber, deflection, and crack control, considering both short- and long-term effects using three different approaches: the PCI multipliers method, the detailed incremental time steps method, and the approximate time steps method. A state-of-the-art discussion is presented, based on the author's work, of the evaluation and control of flexural cracking in partially prestressed beams. Several design examples are included in the discussion. Chapter 8 covers the proportioning of prestressed compression and tension members, including the buckling behavior and design of prestressed columns and piles and the P- $\Delta$  effect in the design of slender columns.

Chapter 9 presents a thorough analysis of the service load behavior and yield-line behavior of two-way action prestressed slabs and plates. The service load behavior utilizes, with extensive examples, the equivalent frame method of flexural design (analysis) and deflection evaluation. A detailed discussion is presented on the shear-moment transfer at column support section in two-way action prestressed concrete plates, and on deflection of two-way plates. Extensive coverage is presented of the yield-line failure mechanisms of all the usual combinations of loads on floor slabs and boundary conditions, including the design expressions for these various conditions. Chapter 10 on connections for prestressed concrete elements covers the design of connections for dapped-end beams, ledge beams, and bearing, in addition to the design of the beams and corbels presented in Chapter 5 on shear and torsion. It is revised to accommodate the new load and strength reduction factors required in the ACI 318-08 Code.

This book is also unique in that Chapter 11 gives a detailed account of the analysis and design of prestressed concrete tanks and their shell roofs. Presented are the basics of the membrane and bending theories of cylindrical shells for use in the design of prestressed concrete tanks for the various wall boundary conditions of fixed, semi-fixed, hinged, and sliding wall bases, as well as the incorporation of vertical prestressing, using wrapped wires as well as tendons. Chapter 11 also discusses the theory of axisymmetrical shells and domes that are used in the design of domed roofs for circular tanks.

The extensive Chapter 12, added to the previous edition, has been updated to accommodate the latest LRFD and Standard AASHTO 2009 specifications for the design of prestressed bridge deck girders for flexure, shear, torsion, and serviceability, including the design of anchorage blocks. Several extensive examples are given using bulb-tees and box girder sections. It also includes the AASHTO requirements for truck and lane loadings and load combinations as stipulated both by the LRFD and the Standard specifications.

Chapter 13, dealing with the seismic design of prestressed precast structures in high seismicity zones, has been updated based on the new ACI 318-08 and the significantly modified International Building Code, IBC 2009, on seismic design of reinforced and prestressed concrete structures. It contains several design examples and a detailed discussion of ductile moment-resistant connections in high-rise buildings and parking garages in high seismicity zones. A unique approach for the design of such ductile connections in precast beam-column joints in high-rise building structures was extended and updated to conform to the new load and strength reduction factors. It also contains examples of the design of shear walls and hybrid connections—all based on the state of the art in this field.

Selected photographs involving various areas of the structural behavior of concrete elements at failure are included in all the chapters. They are taken from research work conducted and published by the author with many of his MS and PhD students at Rutgers University over the past four decades. Additionally, photographs of some major prestressed concrete landmark structures are included throughout the book to illustrate the versatility of design in pretensioned and post-tensioned prestressed concrete. Appendices have also been included, with monograms and tables on standard properties, sections and charts of flexural and shear evaluation of sections, as well as representative tables for selecting sections such as PCI double-tees, PCI/AASHTO bulb-tees, box girder and AASHTO standard sections for bridge decks. Conversion to SI metric units is included in the examples throughout most chapters of the book.

In summary, the topics of this updated fifth edition of the book have been presented in as concise a manner as possible without sacrificing the need for instructional details. The major portions of the text can be used without difficulty and equally in an advanced senior level and at the graduate level for any student who has had a prior course in reinforced concrete. The contents should also serve as a valuable guideline for the practicing engineer who has to keep abreast of the state-of-the-art in prestressed concrete and the latest provisions of the ACI 318-08 Building Code and PCI Standards, AASHTO 2009 Standards, and the International Building Code (IBC 2009), as well as the designer who seeks a concise treatment of the fundamentals of linear and circular prestressing.

## ACKNOWLEDGMENTS

Grateful acknowledgment is due to the American Concrete Institute, the Prestressed Concrete Institute and the Post-Tensioning Institute for their gracious support in permitting generous quotations from the ACI 318 and other relevant Codes and Reports and the numerous illustrations and tables from so many PCI and PTI publications. Special mention has to be made of the author's original mentor, the late Professor A. L. L. Baker of London University's Imperial College of Science, Technology and Medicine, who inspired him with the affection that he has developed for systems constructed of reinforced and prestressed concrete. Grateful acknowledgment is also made to the author's many students, both undergraduate and graduate, who have had much to do with generating the writing of this book and to the many who assisted in his research activities over the past 50 years. Thanks are also due to the many professors who have been continuously



using this textbook since 1988 in major universities in the United States and their valuable comments, and to the engineers worldwide who have adopted this book as a standard reference on the up-to-date analysis and design of prestressed concrete structures.

Acknowledgment is also made to the many experts who reviewed the manuscript of the first edition including Professors Carl E. Ekberg of Iowa State University; Thomas T. C. Hsu of the University of Houston; Daniel P. Jenny, formerly of the PCI; and Clifford L. Freyrmuth, formerly of the PTI. Thanks are also due to Robert M. Nawy, BA, BS, MBA, Rutgers Engineering class of 1983, who assisted in the work on the first edition, and to Engineer Gregg Romano, MS Rutgers 1999, for his contribution to the last edition's Chapter 12 on LRFD design of bridge decks. For the third edition of this book, particular thanks are due to Professor Thomas Hsu for again reviewing the revised portions on torsional theory and examples and the shear LRFD section; Professor Alex Aswad of Pennsylvania State University at Harrisburg for his valuable input on precast shear walls in seismic regions; George Nasser, formerly Editor-in-Chief, and Paul Johal, Research Director, both of the Precast/Prestressed Concrete Institute, for their support; Mr. Khalid Shawwaf, Vice President-Engineering, Dywidag Systems International, for his cooperation and advice; and Dr. Robert E. Englekirk, President, Englekirk Consulting Engineers, and Visiting Professor at the Universities of California, Los Angeles, and San Diego, for his extensive input, discussions and advice on the subject of ductile moment-resisting frame connections in high seismicity zones. Thanks also go to Ms. Linda Figg, President and CEO, FIGG Bridge Engineers, for her input into this and previous editions of this book.

Grateful acknowledgment is also made to the Prentice Hall officers and staff: Marcia Horton, Vice President and Editorial Director, and Vincent O'Brien, Director of Team-Based Project Management, who both have given me continuous encouragement and support over the years; Holly Stark, Senior Engineering Editor, for her cooperation in processing this updated version; Scott Disanno, Senior Managing Editor, for his continuous guidance in the successful and prompt production of the book; Jane Bonnell, Production Liaison, for her coordinating efforts; Bruce Kenselaar, of the Prentice Hall Art Department, for his admirable artwork on the book cover for this and prior editions of the textbook; and Patty Donovan, Senior Project Coordinator, Laserwords Maine, for commendable efforts over the years in bringing to fruition the several editions of this book. Last but not least, the author is grateful to Mayrai Gindy, Nakin Suksawang, and James Giancastro, all PhD, Rutgers, for their assistance in the fifth edition, and to Joseph Davis, PhD, Rutgers, for his past help and diligent computational and processing work in the new sections of this edition.

*EDWARD G. NAWY  
Rutgers University  
The State University of New Jersey  
Piscataway, New Jersey*

# **PRESTRESSED CONCRETE**





# 1

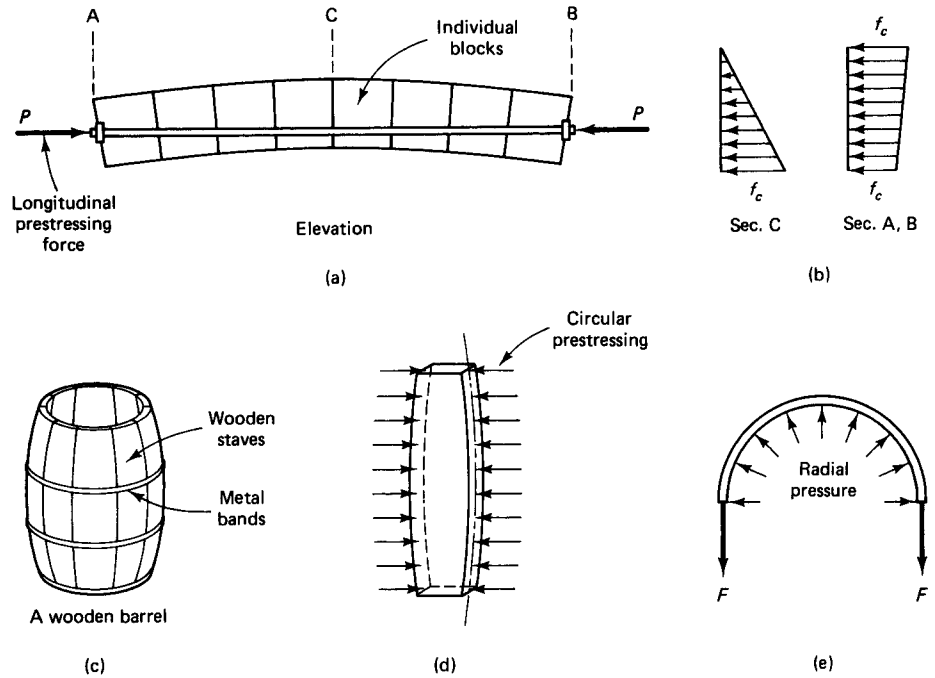
## BASIC CONCEPTS

### 1.1 INTRODUCTION

Concrete is strong in compression, but weak in tension: its tensile strength varies from 8 to 14 percent of its compressive strength. Due to such a low tensile capacity, flexural cracks develop at early stages of loading. In order to reduce or prevent such cracks from developing, a concentric or eccentric force is imposed in the longitudinal direction of the structural element. This force prevents the cracks from developing by eliminating or considerably reducing the tensile stresses at the critical midspan and support sections at service load, thereby raising the bending, shear, and torsional capacities of the sections. The sections are then able to behave elastically, and almost the full capacity of the concrete in compression can be efficiently utilized across the entire depth of the concrete sections when all loads act on the structure.

Such an imposed longitudinal force is called a *prestressing force*, i.e., a compressive force that prestresses the sections along the span of the structural element prior to the application of the transverse gravity dead and live loads or transient horizontal live loads. The type of prestressing force involved, together with its magnitude, are determined mainly on the basis of the type of system to be constructed and the span length and slenderness desired. Since the prestressing force is applied longitudinally along or parallel to

The Diamond Baseball Stadium, Richmond, Virginia. Situ cast and precast post-tensioned prestressed structure. (Courtesy, Prestressed Concrete Institute.)



**Figure 1.1** Prestressing principle in linear and circular prestressing. (a) Linear prestressing of a series of blocks to form a beam. (b) Compressive stress on midspan section C and end section A or B. (c) Circular prestressing of a wooden barrel by tensioning the metal bands. (d) Circular hoop prestress on one wooden stave. (e) Tensile force  $F$  on half of metal band due to internal pressure, to be balanced by circular hoop prestress.

the axis of the member, the prestressing principle involved is commonly known as *linear* prestressing.

*Circular* prestressing, used in liquid containment tanks, pipes, and pressure reactor vessels, essentially follows the same basic principles as does linear prestressing. The circumferential hoop, or “hugging” stress on the cylindrical or spherical structure, neutralizes the tensile stresses at the outer fibers of the curvilinear surface caused by the internal contained pressure.

Figure 1.1 illustrates, in a basic fashion, the prestressing action in both types of structural systems and the resulting stress response. In (a), the individual concrete blocks act together as a beam due to the large compressive prestressing force  $P$ . Although it might appear that the blocks will slip and vertically simulate shear slip failure, in fact they will not because of the longitudinal force  $P$ . Similarly, the wooden staves in (c) might appear to be capable of separating as a result of the high internal radial pressure exerted on them. But again, because of the compressive prestress imposed by the metal bands as a form of circular prestressing, they will remain in place.

### 1.1.1 Comparison with Reinforced Concrete

From the preceding discussion, it is plain that permanent stresses in the prestressed structural member are created before the full dead and live loads are applied, in order to eliminate or considerably reduce the net tensile stresses caused by these loads. With reinforced concrete, it is assumed that the tensile strength of the concrete is negligible



**Photo 1.1** Bay Area Rapid Transit (BART), San Francisco and Oakland, California. Guideways consist of prestressed precast simple-span box girders 70 ft long and 11 ft wide. (Courtesy, Bay Area Rapid Transit District, Oakland, California.)

and disregarded. This is because the tensile forces resulting from the bending moments are resisted by the bond created in the reinforcement process. Cracking and deflection are therefore essentially irrecoverable in reinforced concrete once the member has reached its limit state at service load.

The reinforcement in the reinforced concrete member does not exert any force of its own on the member, contrary to the action of prestressing steel. The steel required to produce the prestressing force in the prestressed member actively preloads the member, permitting a relatively high controlled recovery of cracking and deflection. Once the flex-



**Photo 1.2** Chaco-Corrientes Bridge, Argentina. The longest precast prestressed concrete cable-stayed box girder bridge in South America. (Courtesy, Ammann & Whitney.)



**Photo 1.3** Park Towers, Tulsa, Oklahoma. (Courtesy, Prestressed Concrete Institute.)

ural tensile strength of the concrete is exceeded, the prestressed member starts to act like a reinforced concrete element.

By controlling the amount of prestress, a structural system can be made either flexible or rigid without influencing its strength. In reinforced concrete, such a flexibility in behavior is considerably more difficult to achieve if considerations of economy are to be observed in the design. Flexible structures such as fender piles in wharves have to be highly energy absorbent, and prestressed concrete can provide the required resiliency. Structures designed to withstand heavy vibrations, such as machine foundations, can easily be made rigid through the contribution of the prestressing force to the reduction of their otherwise flexible deformation behavior.

### 1.1.2 Economics of Prestressed Concrete

Prestressed members are shallower in depth than their reinforced concrete counterparts for the same span and loading conditions. In general, the depth of a prestressed concrete member is usually about 65 to 80 percent of the depth of the equivalent reinforced concrete member. Hence, the prestressed member requires less concrete, and about 20 to 35 percent of the amount of reinforcement. Unfortunately, this saving in material weight is balanced by the higher cost of the higher quality materials needed in prestressing. Also, regardless of the system used, prestressing operations themselves result in an added cost: Formwork is more complex, since the geometry of prestressed sections is usually composed of flanged sections with thin webs.

In spite of these additional costs, if a large enough number of precast units are manufactured, the difference between at least the initial costs of prestressed and reinforced concrete systems is usually not very large. And the indirect long-term savings are quite substantial, because less maintenance is needed, a longer working life is possible due to

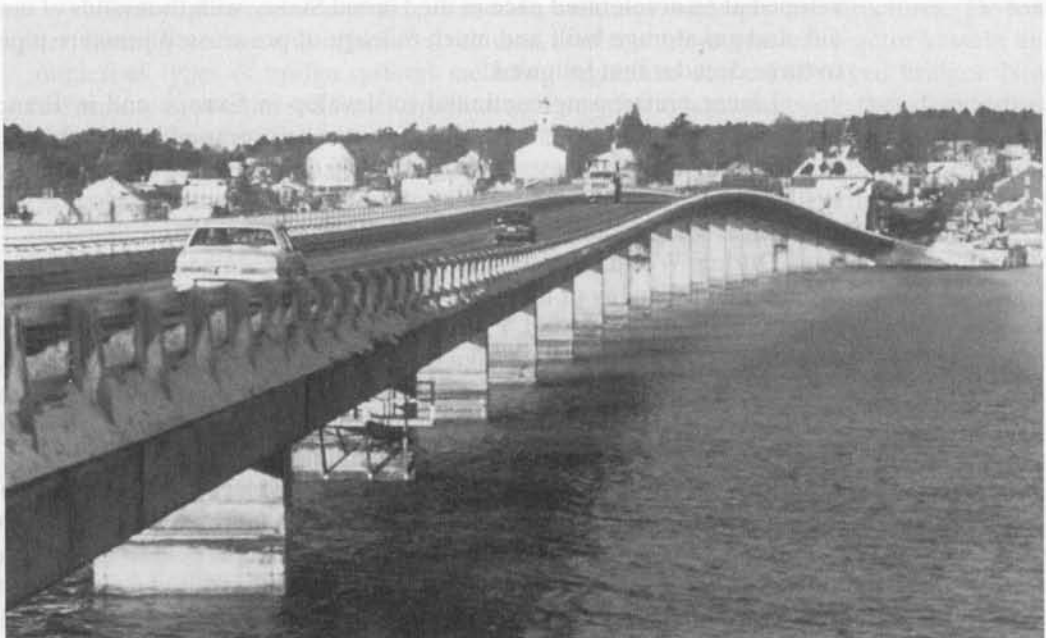
better quality control of the concrete, and lighter foundations are achieved due to the smaller cumulative weight of the superstructure.

Once the beam span of reinforced concrete exceeds 70 to 90 feet, the dead weight of the beam becomes excessive, resulting in heavier members and, consequently, greater long-term deflection and cracking. Thus, for larger spans, prestressed concrete becomes mandatory since arches are expensive to construct and do not perform as well due to the severe long-term shrinkage and creep they undergo. Very large spans such as segmental bridges or cable-stayed bridges can *only* be constructed through the use of prestressing.

## 1.2 HISTORICAL DEVELOPMENT OF PRESTRESSING

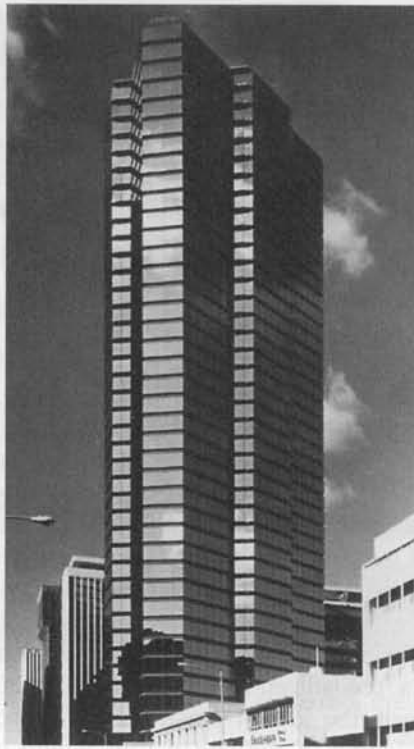
Prestressed concrete is not a new concept, dating back to 1872, when P. H. Jackson, an engineer from California, patented a prestressing system that used a tie rod to construct beams or arches from individual blocks. [See Figure 1.1(a).] In 1888, C. W. Doehring of Germany obtained a patent for prestressing slabs with metal wires. But these early attempts at prestressing were not really successful because of the loss of the prestress with time. J. Lund of Norway and G. R. Steiner of the United States tried early in the twentieth century to solve this problem, but to no avail.

After a long lapse of time during which little progress was made because of the unavailability of high-strength steel to overcome prestress losses, R. E. Dill of Alexandria, Nebraska, recognized the effect of the shrinkage and creep (transverse material flow) of concrete on the loss of prestress. He subsequently developed the idea that successive post-tensioning of *unbonded* rods would compensate for the time-dependent loss of stress in the rods due to the decrease in the length of the member because of creep and shrinkage. In the early 1920s, W. H. Hewett of Minneapolis developed the principles of circular prestressing. He hoop-stressed horizontal reinforcement around walls of concrete tanks through the use of turnbuckles to prevent cracking due to internal liquid pres-



**Photo 1.4** Wiscasset Bridge, Maine. (Courtesy, Post-Tensioning Institute.)





**Photo 1.5** Executive Center, Honolulu, Hawaii. (Courtesy, Post-Tensioning Institute.)

sure, thereby achieving watertightness. Thereafter, prestressing of tanks and pipes developed at an accelerated pace in the United States, with thousands of tanks of water, liquid, and gas storage built and much mileage of prestressed pressure pipe laid in the two to three decades that followed.

Linear prestressing continued to develop in Europe and in France, in particular through the ingenuity of Eugene Freyssinet, who proposed in 1926 through 1928 methods to overcome prestress losses through the use of high-strength and high-ductility steels. In 1940, he introduced the now well-known and well-accepted Freyssinet system comprising the conical wedge anchor for 12-wire tendons.

During World War II and thereafter, it became necessary to reconstruct in a prompt manner many of the main bridges that were destroyed by war activities. G. Magnel of Ghent, Belgium, and Y. Guyon of Paris extensively developed and used the concept of prestressing for the design and construction of numerous bridges in western and central Europe. The Magnel system also used wedges to anchor the prestressing wires. They differed from the original Freyssinet wedges in that they were flat in shape, accommodating the prestressing of two wires at a time.

P. W. Abeles of England introduced and developed the concept of partial prestressing between the 1930s and 1960s. F. Leonhardt of Germany, V. Mikhailov of Russia, and T. Y. Lin of the United States also contributed a great deal to the art and science of the design of prestressed concrete. Lin's load-balancing method deserves particular mention in this regard, as it considerably simplified the design process, particularly in continuous structures. These twentieth-century developments have led to the extensive use of prestressing throughout the world, and in the United States in particular.



**Photo 1.6** Stratford "B" Condeep offshore oil drilling platform, Norway. (Courtesy, the late Ben C. Gerwick.)

Today, prestressed concrete is used in buildings, underground structures, TV towers, floating storage and offshore structures, power stations, nuclear reactor vessels, and numerous types of bridge systems including segmental and cable-stayed bridges. Note the variety of prestressed structures in the photos throughout the book; they demonstrate the versatility of the prestressing concept and its all-encompassing applications. The success in the development and construction of all these landmark structures has been due in no small measure to the advances in the technology of materials, particularly prestressing steel, and the accumulated knowledge in estimating the short- and long-term losses in the prestressing forces.

### 1.3 BASIC CONCEPTS OF PRESTRESSING

#### 1.3.1 Introduction

The prestressing force  $P$  that satisfies the particular conditions of geometry and loading of a given element (see Figure 1.2) is determined from the principles of mechanics and of stress-strain relationships. Sometimes simplification is necessary, as when a prestressed beam is assumed to be homogeneous and elastic.

Consider, then, a simply supported rectangular beam subjected to a *concentric* prestressing force  $P$  as shown in Figure 1.2(a). The compressive stress on the beam cross section is uniform and has an intensity



**Photo 1.7** Sunshine Skyway Bridge, Tampa Bay, Florida. Designed by Figg and Muller Engineers, Inc., the bridge has a 1,200-ft cable-stayed main span with a single pylon, 175-ft vertical clearance, and total length of 21,878 ft. It has twin 40-ft roadways and has 135-ft spans in precast segmental sections and high approaches to elevation + 130 ft. (Courtesy, Figg and Muller Engineers, Inc., now FIGG Engineers)

$$f = -\frac{P}{A_c} \quad (1.1)$$

where  $A_c = bh$  is the cross-sectional area of a beam section of width  $b$  and total depth  $h$ . A *minus* sign is used for compression and a *plus* sign for tension throughout the text. Also, bending moments are drawn on the tensile side of the member.

If external transverse loads are applied to the beam, causing a maximum moment  $M$  at midspan, the resulting stress becomes

$$f^t = -\frac{P}{A} - \frac{Mc}{I_g} \quad (1.2a)$$

and

$$f_b = -\frac{P}{A} + \frac{Mc}{I_g} \quad (1.2b)$$

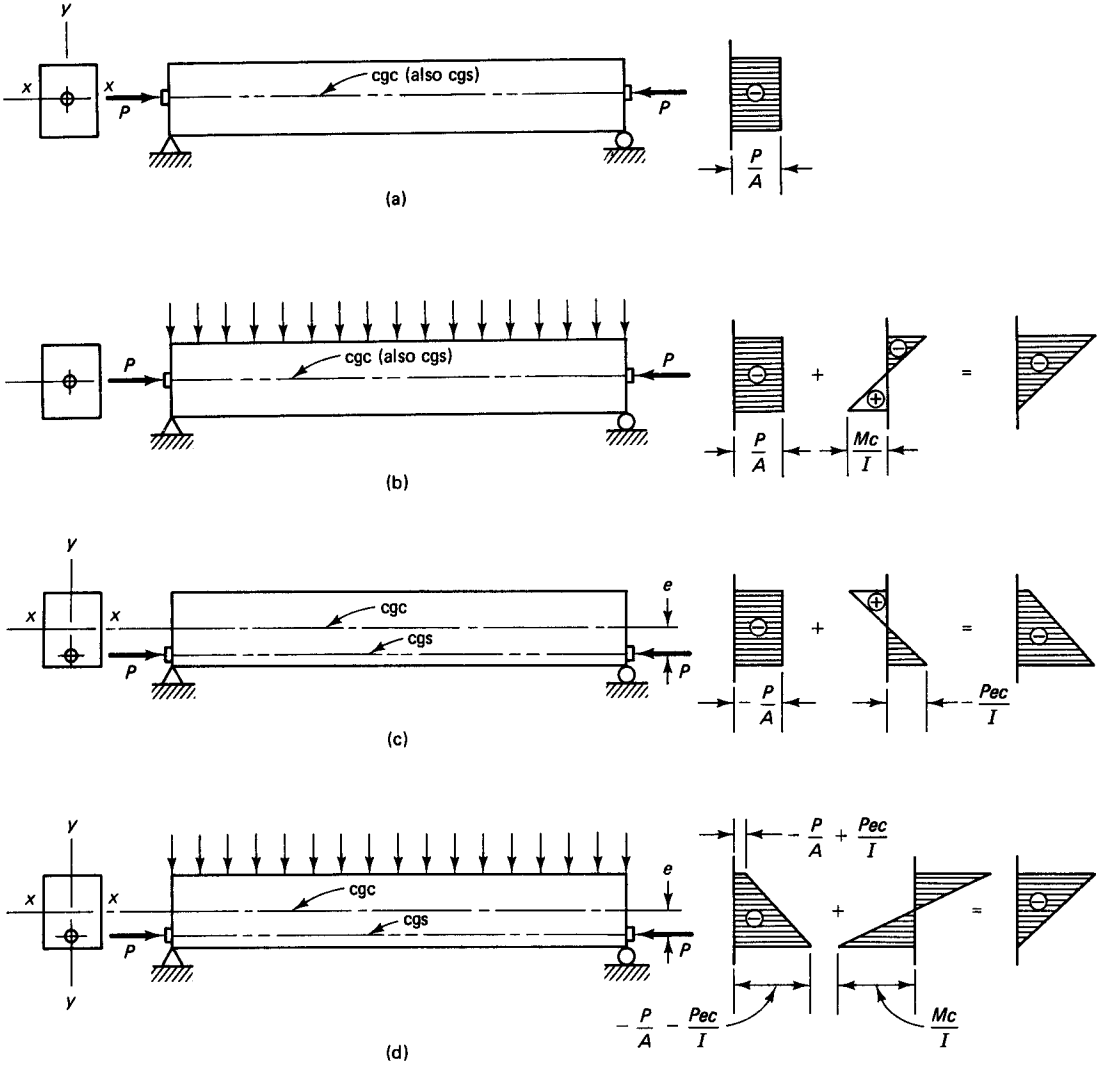
where  $f^t$  = stress at the top fibers

$f_b$  = stress at the bottom fibers

$c = \frac{1}{2}h$  for the rectangular section

$I_g$  = gross moment of inertia of the section ( $bh^3/12$  in this case)

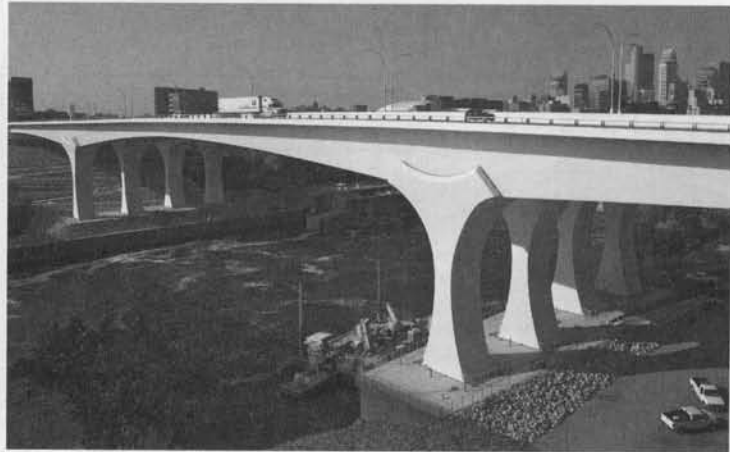
Equation 1.2b indicates that the presence of prestressing-compressive stress  $-P/A$  is reducing the tensile flexural stress  $Mc/I$  to the extent intended in the design, either elimi-



**Figure 1.2** Concrete fiber stress distribution in a rectangular beam with straight tendon. (a) Concentric tendon, prestress only. (b) Concentric tendon, self-weight added. (c) Eccentric tendon, prestress only. (d) Eccentric tendon, self-weight added.

nating tension totally (even inducing compression), or permitting a level of tensile stress within allowable code limits. The section is then considered uncracked and behaves elastically: the concrete’s inability to withstand tensile stresses is effectively compensated for by the compressive force of the prestressing tendon.

The compressive stresses in Equation 1.2a at the top fibers of the beam due to prestressing are compounded by the application of the loading stress  $- Mc/I$ , as seen in Figure 1.2(b). Hence, the compressive stress capacity of the beam to take a substantial external load is reduced by the *concentric* prestressing force. In order to avoid this limitation, the prestressing tendon is placed *eccentrically* below the neutral axis at midspan, to induce tensile stresses at the top fibers due to prestressing. [See Figure 1.2(c), (d).] If the tendon is placed at eccentricity  $e$  from the center of gravity of the concrete, termed the *cgc line*, it creates a moment  $Pe$ , and the ensuing stresses at midspan become



**Photo 1.8** The new I-35W bridge, Minneapolis, Minnesota. Designed by FIGG, the 10-lane interstate bridge has a 504' precast, prestressed concrete span over the Mississippi River, with 75' vertical clearance. The span's 120 precast concrete segments, each 45' wide, up to 25' deep and weighing 200 tons, achieved an average concrete strength of 7600 psi. These segments for the main span were assembled in one directional cantilever from the main piers in just 47 days. The bridge has 50,000 cubic yards of concrete and nearly 3 million pounds of post-tensioning steel that runs the length of the twin 1,214' bridges. This new interstate bridge was designed and built in 11 months, opening on September 18, 2008. (Courtesy of FIGG, the bridge designer)

$$f^t = -\frac{P}{A_c} + \frac{Pec}{I_g} - \frac{Mc}{I_g} \quad (1.3a)$$

$$f_b = -\frac{P}{A_c} - \frac{Pec}{I_g} + \frac{Mc}{I_g} \quad (1.3b)$$

Since the support section of a simply supported beam carries no moment from the external transverse load, high tensile fiber stresses at the top fibers are caused by the eccentric prestressing force. To limit such stresses, the eccentricity of the prestressing tendon profile, the *cgs line*, is made less at the support section than at the midspan section, or eliminated altogether, or else a negative eccentricity above the *cgs line* is used.

### 1.3.2 Basic Concept Method

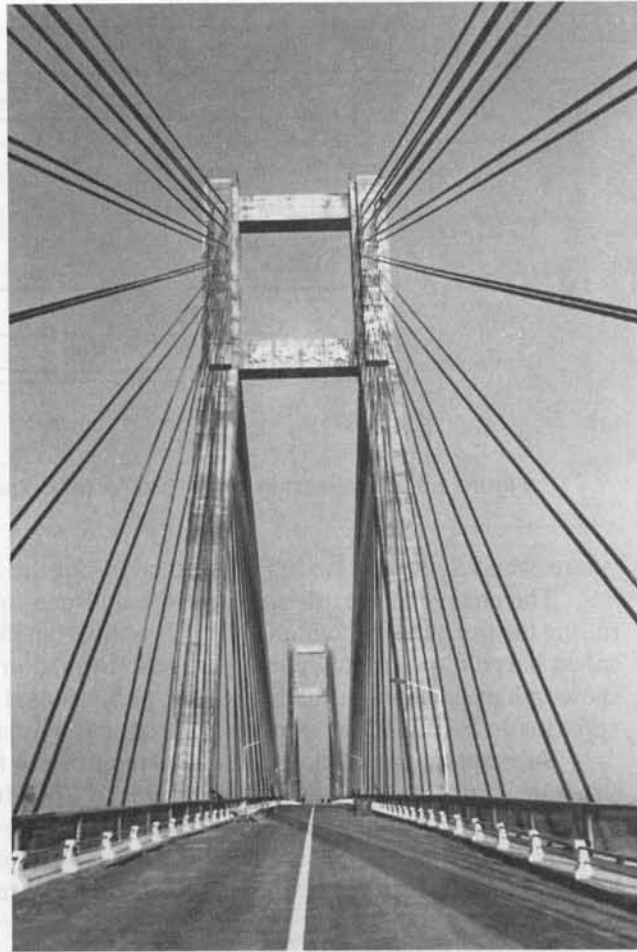
In the basic concept method of designing prestressed concrete elements, the concrete fiber stresses are *directly* computed from the external forces applied to the concrete by longitudinal prestressing and the external transverse load. Equations 1.3a and b can be modified and simplified for use in calculating stresses at the initial prestressing stage and at service load levels. If  $P_i$  is the initial prestressing force before stress losses, and  $P_e$  is the effective prestressing force after losses, then

$$\gamma = \frac{P_e}{P_i} \quad (1.3c)$$

can be defined as the residual prestress factor. Substituting  $r^2$  for  $I_g/A_c$  in Equations 1.3, where  $r$  is the radius of gyration of the gross section, the expressions for stress can be rewritten as follows:

#### (a) Prestressing Force Only

$$f^t = -\frac{P_i}{A_c} \left( 1 - \frac{ec_t}{r^2} \right) \quad (1.4a)$$



**Photo 1.9** Tianjin Yong-He cable-stayed prestressed concrete bridge, Tianjin, China, the largest span bridge in Asia, with a total length of 1,673 ft and a suspended length of 1,535 ft, was completed in 1988. (Credits Owner: Tianjin Municipal Engineering Bureau. General contractor: Major Bridge Engineering Bureau of Ministry of Railways of China. Engineer for project design and construction control guidance: Tianjin Municipal Engineering Survey and Design Institute, Chief Bridge Engineer, Bang-yan Yu.)

$$f_b = -\frac{P_i}{A_c} \left( 1 + \frac{ec_b}{r^2} \right) \quad (1.4b)$$

where  $c_t$  and  $c_b$  are the distances from the center of gravity of the section (the cg line) to the extreme top and bottom fibers, respectively.

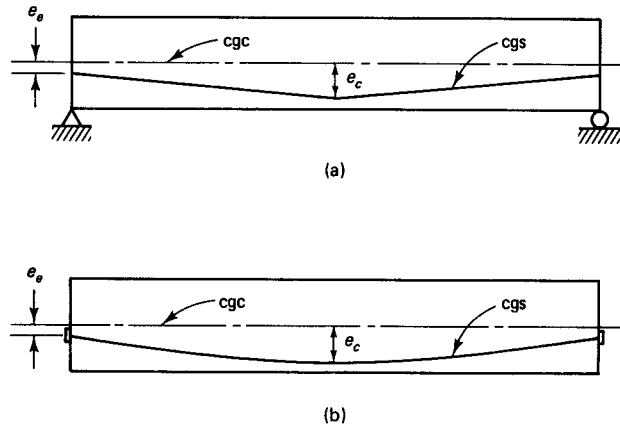
(b) *Prestressing Plus Self-weight*

If the beam self-weight causes a moment  $M_D$  at the section under consideration, Equations 1.4a and b, respectively, become

$$f_t = -\frac{P_i}{A_c} \left( 1 - \frac{ec_t}{r^2} \right) - \frac{M_D}{S_t} \quad (1.5a)$$

and

$$f_b = -\frac{P_i}{A_c} \left( 1 + \frac{ec_b}{r^2} \right) + \frac{M_D}{S_b} \quad (1.5b)$$



**Figure 1.3** Prestressing tendon profile. (a) Harped tendon. (b) Draped tendon.

where  $S^t$  and  $S_b$  are the moduli of the sections for the top and bottom fibers, respectively.

The change in eccentricity from the midspan to the support section is obtained by raising the prestressing tendon either abruptly from the midspan to the support, a process called harping, or gradually in a parabolic form, a process called draping. Figure 1.3(a) shows a harped profile usually used for pretensioned beams and for concentrated transverse loads. Figure 1.3(b) shows a draped tendon usually used in post-tensioning.

Subsequent to erection and installation of the floor or deck, live loads act on the structure, causing a superimposed moment  $M_s$ . The full intensity of such loads normally occurs after the building is completed and some time-dependent losses in prestress have already taken place. Hence, the prestressing force used in the stress equations would have to be the effective prestressing force  $P_e$ . If the total moment due to gravity loads is  $M_T$ , then

$$M_T = M_D + M_{SD} + M_L \quad (1.6)$$

where  $M_D$  = moment due to self-weight

$M_{SD}$  = moment due to superimposed dead load, such as flooring

$M_L$  = moment due to live load, including impact and seismic loads if any

Equations 1.5 then become

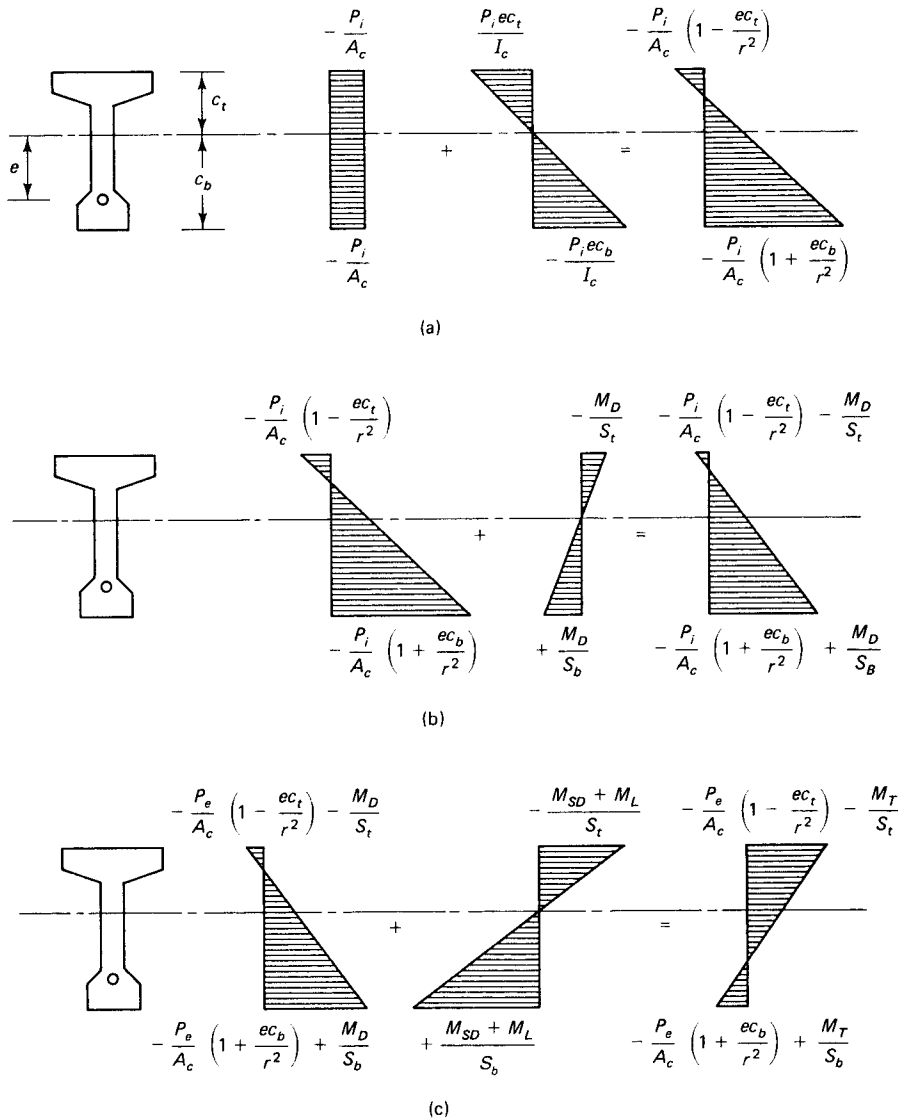
$$f^t = -\frac{P_e}{A_c} \left( 1 - \frac{ec_t}{r^2} \right) - \frac{M_T}{S^t} \quad (1.7a)$$

$$f_b = -\frac{P_e}{A_c} \left( 1 + \frac{ec_b}{r^2} \right) + \frac{M_T}{S_b} \quad (1.7b)$$

Some typical elastic concrete stress distributions at the critical section of a prestressed flanged section are shown in Figure 1.4. The tensile stress in the concrete in part (c) permitted at the extreme fibers of the section cannot exceed the maximum permissible in the code, e.g.,  $f_t = 6\sqrt{f'_c}$  at midspan in the ACI code. If it is exceeded, bonded non-prestressed reinforcement proportioned to resist the total tensile force has to be provided to control cracking at service loads.

### 1.3.3 C-Line Method

In this line-of-pressure or thrust concept, the beam is analyzed as if it were a plain concrete elastic beam using the basic principles of statics. The prestressing force is considered an ex-



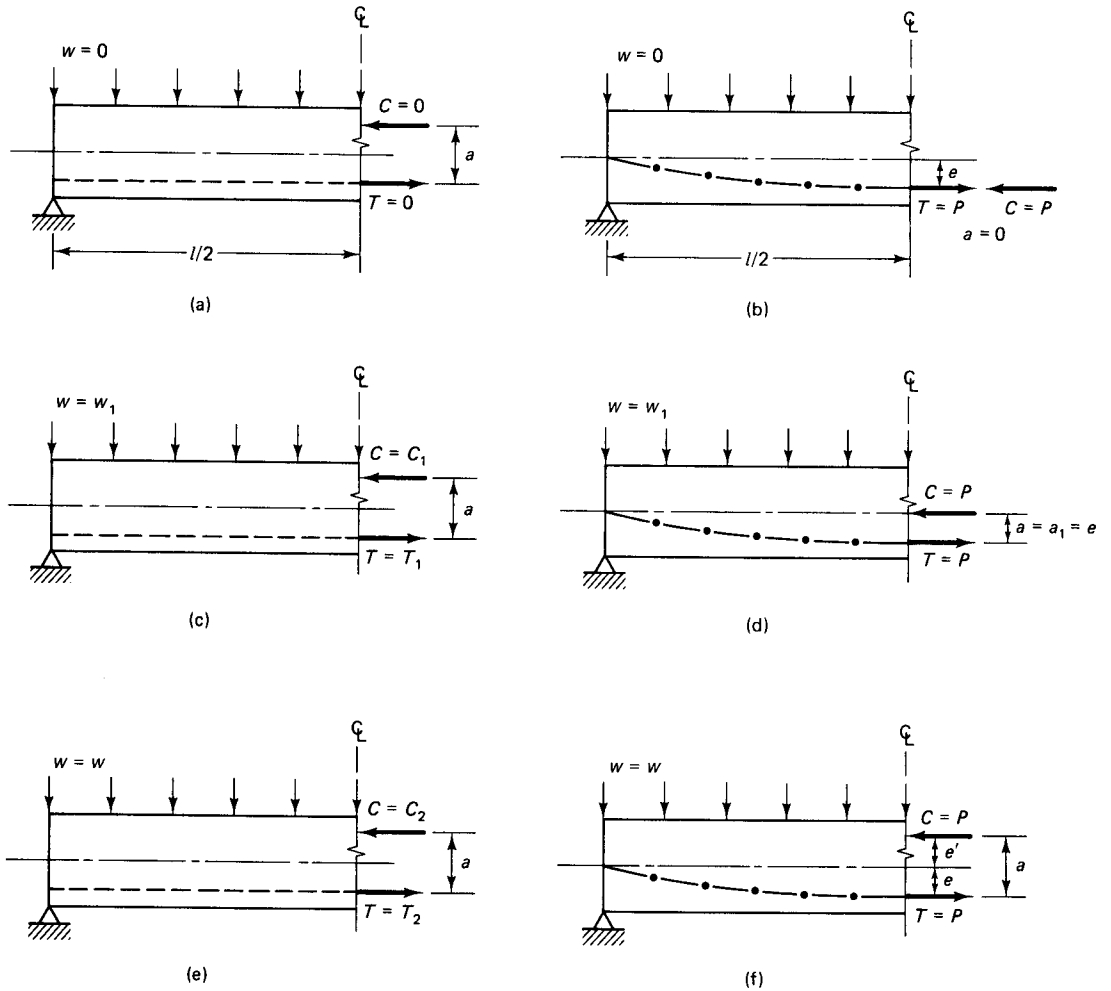
**Figure 1.4** Elastic fiber stresses due to the various loads in a prestressed beam. (a) Initial prestress before losses. (b) Addition of self-weight. (c) Service load at effective prestress.

ternal compressive force, with a constant tensile force  $T$  in the tendon throughout the span. In this manner, the effects of external gravity loads are disregarded. Equilibrium equations  $\Sigma H = 0$  and  $\Sigma M = 0$  are applied to maintain equilibrium in the section.

Figure 1.5 shows the relative line of action of the compressive force  $C$  and the tensile force  $T$  in a reinforced concrete beam as compared to that in a prestressed concrete beam. It is plain that in a reinforced concrete beam,  $T$  can have a finite value only when transverse and other external loads act. The moment arm  $a$  remains basically constant throughout the elastic loading history of the reinforced concrete beam while it changes from a value  $a = 0$  at prestressing to a maximum at full superimposed load.

Taking a free-body diagram of a segment of a beam as in Figure 1.6, it is evident that the C-line, or center-of-pressure line, is at a varying distance  $a$  from the T-line. The moment is given by





**Figure 1.5** Comparative free-body diagrams of a reinforced concrete (R.C.) beam and a prestressed concrete (P.C.) beam. (a) R.C. beam with no load. (b) P.C. beam with no load. (c) R.C. beam with load  $w_1$ . (d) P.C. beam with load  $w_1$ . (e) R.C. beam with typical load  $w$ . (f) P.C. beam with typical load  $w$ .

$$M = Ca = Ta \tag{1.8}$$

and the eccentricity  $e$  is known or predetermined, so that in Figure 1.6,

$$e' = a - e \tag{1.9a}$$

Since  $C = T$ ,  $a = M/T$ , giving

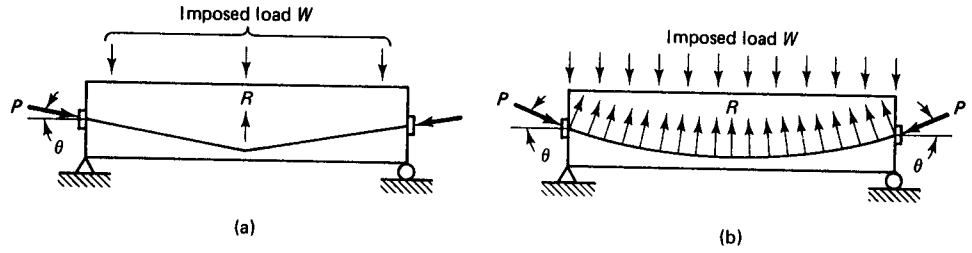
$$e' = \frac{M}{T} - e \tag{1.9b}$$

From the figure,

$$f' = -\frac{C}{A_c} - \frac{Ce'c_t}{I_c} \tag{1.10a}$$

$$f_b = -\frac{C}{A_c} + \frac{Ce'c_b}{I_c} \tag{1.10b}$$





**Figure 1.7** Load-balancing forces. (a) Harped tendon. (b) Draped tendon.

Figure 1.7 demonstrates the balancing forces for both harped- and draped-tendon prestressed beams. The load balancing reaction  $R$  is equal to the vertical component of the prestressing force  $P$ . The horizontal component of  $P$ , as an approximation in long-span beams, is taken to be equal to the full force  $P$  in computing the concrete fiber stresses at *midspan* of the simply supported beam. At other sections, the actual horizontal component of  $P$  is used.

**1.3.4.1 Load-Balancing Distributed Loads and Parabolic Tendon Profile.** Consider a parabolic tendon as shown in Figure 1.8. Let the parabolic function

$$Ax^2 + Bx + C = y \tag{1.13}$$

represent the tendon drape; the force  $T$  denotes the pull to which the tendon is subjected. Then for  $x = 0$ , we have

$$\begin{aligned} y = 0 & \quad C = 0 \\ \frac{dy}{dx} = 0 & \quad B = 0 \end{aligned}$$

and for  $x = l/2$ ,

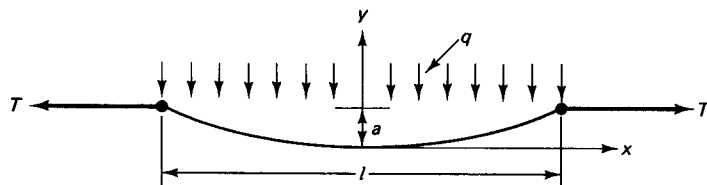
$$y = a \quad A = \frac{4a}{l^2}$$

But from calculus, the load intensity is

$$q = T \frac{\partial^2 y}{\partial x^2} \tag{1.14}$$

Finding  $\partial^2 y / \partial x^2$  in Equation 1.13 and substituting into Equation 1.14 yields

$$q = T \frac{4a}{l^2} \times 2 = \frac{8Ta}{l^2} \tag{1.15a}$$



**Figure 1.8** Sketched tendon subjected to transverse load intensity  $q$ .

or

$$T = \frac{ql^2}{8a} \tag{1.15b}$$

$$Ta = \frac{ql^2}{8} \tag{1.15c}$$

Hence, if the tendon has a parabolic profile in the prestressed beam and the prestressing force is denoted by  $P$ , the balanced-load intensity, from Equation 1.15a, is

$$w_b = \frac{8Pa}{l^2} \tag{1.16}$$

Figure 1.9 gives a free-body diagram of the forces acting on a prestressed beam with a parabolic tendon profile. Clearly, the two sets of equal and opposite transverse loads  $w_b$  cancel each other, and no bending stress is produced. This is reasonable to expect in the load-balancing method, since it is always the case that  $T = C$ , and  $C$  has to cancel  $T$  to satisfy the equilibrium requirement that  $\Sigma H = 0$ . As there is no bending, the beam remains straight, without having a convex shape, or camber, at the top face.

The concrete fiber stress across the depth of the section at midspan becomes

$$f_b^t = -\frac{P'}{A} = -\frac{C}{A} \tag{1.17}$$

This stress, which is constant, is due to the force  $P' = P \cos \theta$ . Figure 1.10 shows the superposition of stresses to yield the net stress. Note that the prestressing force in the load-balancing method has to act at the center of gravity (cgc) of the support section in simply supported beams and at the cgc of the free end in the case of a cantilever beam. This condition is necessary in order to prevent any eccentric unbalanced moments.

When the imposed load exceeds the balancing load  $w_b$  such that an additional *unbalanced* load  $w_{ub}$  is applied, a moment  $M_{ub} = w_{ub}l^2/8$  results at midspan. The corresponding fiber stresses at midspan become

$$f_b^t = -\frac{P'}{A_c} \mp \frac{M_{ub}c}{I_c} \tag{1.18}$$

Equation 1.18 can be rewritten as the two equations

$$f_b^t = -\frac{P'}{A_c} - \frac{M_{ub}}{S^t} \tag{1.19a}$$

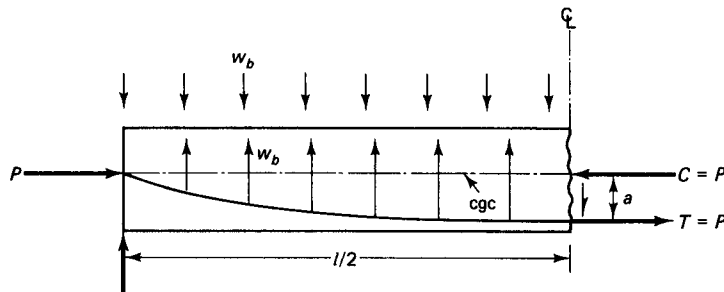
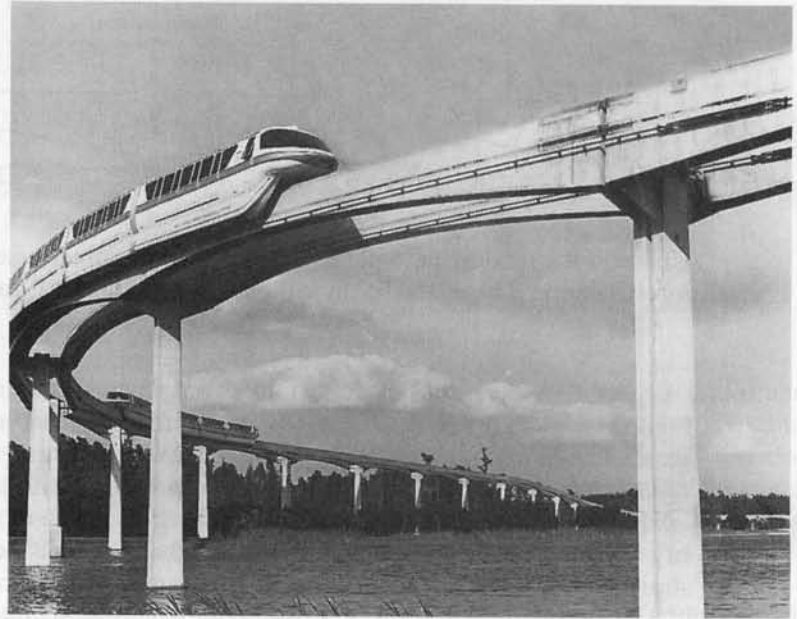


Figure 1.9 Load-balancing force on free-body diagram.

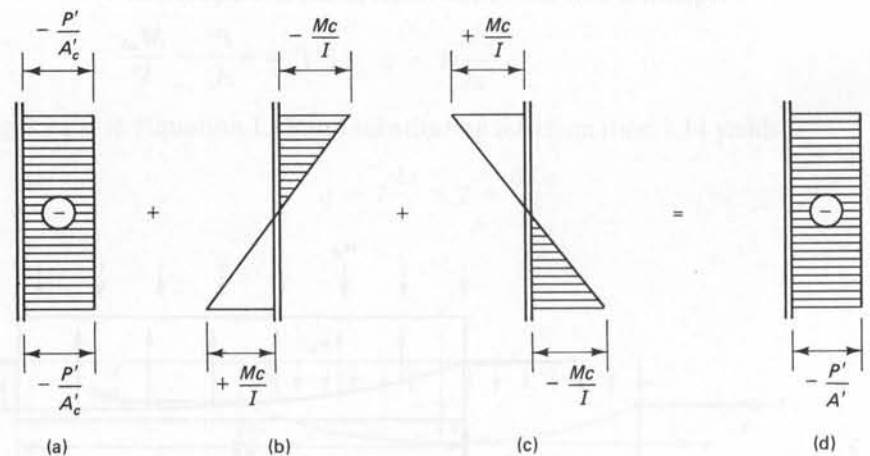


**Photo 1.11** Walt Disney World Monorail, Orlando, Florida. A series of hollow precast prestressed concrete 100-foot box girders individually post-tensioned to provide six-span continuous structure. Designed by ABAM Engineers, Tacoma, Washington. (Courtesy, Walt Disney World Corporation.)

and

$$f_b = -\frac{P'}{A_c} + \frac{M_{ub}}{S_b} \quad (1.19b)$$

Equations 1.19 will yield the same values of fiber stresses as Equations 1.7 and 1.12. Keep in mind that  $P'$  is taken to be equal to  $P$  at the midspan section because the prestressing force is horizontal at this section, i.e.,  $\theta = 0$ .



**Figure 1.10** Load-balancing stresses. (a) Prestress stresses. (b) Imposed-load stresses. (c) Balanced-load stresses. (d) Net stress.

## 1.4 COMPUTATION OF FIBER STRESSES IN A PRESTRESSED BEAM BY THE BASIC METHOD

**Example 1.1**

A pretensioned simply supported 10LDT24 double T-beam without topping has a span of 64 ft (19.51 m) and the geometry shown in Figure 1.11. It is subjected to a uniform superimposed gravity dead-load intensity  $W_{SD}$  and live-load intensity  $W_L$  summing to 420 plf (6.13 kN/m). The initial prestress before losses is  $f_{pi} \cong 0.70 f_{pu} = 189,000$  psi (1,303 MPa), and the effective prestress after losses is  $f_{pe} = 150,000$  psi (1,034 MPa). Compute the extreme fiber stresses at the midspan due to

- (a) the initial full prestress and no external gravity load
- (b) the final service load conditions when prestress losses have taken place.

Allowable stress data are as follows:

$$f'_c = 6,000 \text{ psi, lightweight (41.4 MPa)}$$

$$f_{pu} = 270,000 \text{ psi, stress relieved (1.862 MPa)} = \text{specified tensile strength of the tendons}$$

$$f_{py} = 220,000 \text{ psi (1.517 MPa)} = \text{specified yield strength of the tendons}$$

$$f_{pe} = 150,000 \text{ psi (1,034 MPa)}$$

$$f_t = 12 \sqrt{f'_c} = 930 \text{ psi (6.4 MPa)} = \text{maximum allowable tensile stress in concrete}$$

$$f'_{ci} = 4,800 \text{ psi (33.1 MPa)} = \text{concrete compressive strength at time of initial prestress}$$

$$f_{ci} = 0.6 f'_{ci} = 2,880 \text{ psi (19.9 MPa)} = \text{maximum allowable stress in concrete at initial prestress}$$

$$f_c = 0.45 f'_c = \text{maximum allowable compressive stress in concrete at service}$$

Assume that ten  $\frac{1}{2}$ -in.-dia. Seven-wire-strand (ten 12.7-mm-dia strand) tendons with a 108-D1 strand pattern are used to prestress the beam.

$$A_c = 449 \text{ in.}^2 (2,915 \text{ cm}^2)$$

$$I_c = 22,469 \text{ in.}^4 (935,347 \text{ cm}^4)$$

$$r^2 = I_c/A_c = 50.04 \text{ in.}^2$$

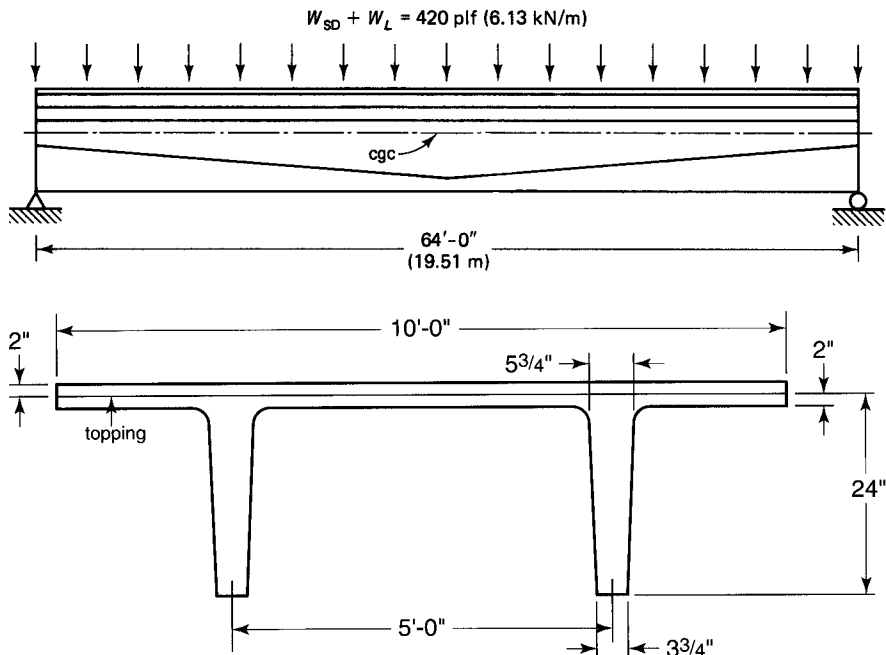
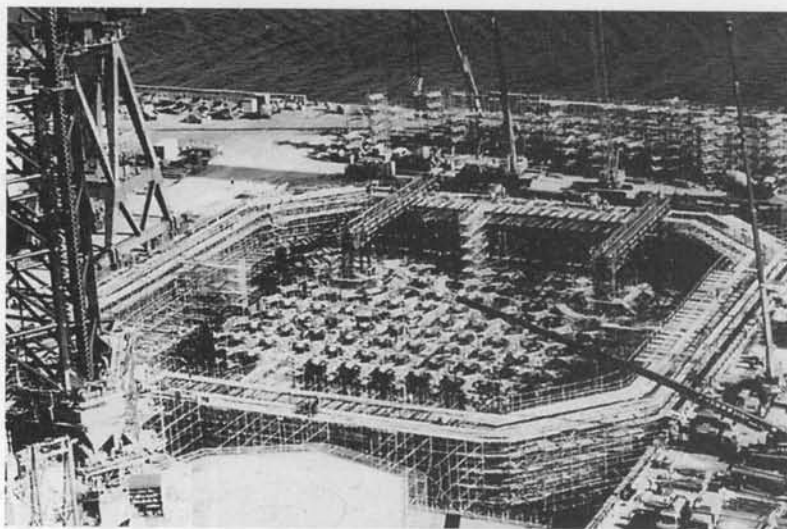


Figure 1.11 Example 1.1



**Photo 1.12** Prestressed lightweight concrete mid-body for Arctic offshore drilling platform. Global Marine Development. (Courtesy, the late Ben C. Gerwick.)

$$c_b = 17.77 \text{ in. (452 mm)}$$

$$c_t = 6.23 \text{ in. (158 mm)}$$

$$e_c = 14.77 \text{ in. (375 mm)}$$

$$e_e = 7.77 \text{ in. (197 mm)}$$

$$S_b = 1,264 \text{ in.}^3 \text{ (20,714 cm}^3\text{)}$$

$$S^t = 3,607 \text{ in.}^3 \text{ (59,108 cm}^3\text{)}$$

$$W_D = 359 \text{ plf (4.45 kN/m)}$$

**Solution:**

**(i) Initial Conditions at Prestressing**

$$A_{ps} = 10 \times 0.153 = 1.53 \text{ in.}^2$$

$$P_i = A_{ps} f_{pi} = 1.53 \times 189,000 = 289,170 \text{ lb (1,287 kN)}$$

$$P_e = 1.53 \times 150,000 = 229,500 \text{ lb (1,020 kN)}$$

The midspan self-weight dead-load moment is

$$M_D = \frac{wl^2}{8} = \frac{359(64)^2}{8} \times 12 = 2,205,696 \text{ in.-lb. (249 kN-m)}$$

From Equations 1.5 and 1.7,

$$\begin{aligned} f^t &= -\frac{P_i}{A_c} \left(1 - \frac{ec_t}{r^2}\right) - \frac{M_D}{S^t} \\ &= -\frac{289,170}{449} \left(1 - \frac{14.77 \times 6.23}{50.04}\right) - \frac{2,205,696}{3,607} \\ &= +540.3 - 611.5 \cong -70 \text{ psi (C)} \end{aligned}$$

$$\begin{aligned} f_b &= -\frac{P_i}{A_c} \left(1 + \frac{ec_b}{r^2}\right) + \frac{M_D}{S_b} \\ &= -\frac{289,170}{449} \left(1 + \frac{14.77 \times 17.77}{50.04}\right) + \frac{2,205,696}{1,264} \end{aligned}$$

$$= -4,022.1 + 1,745.0 \cong -2,277 \text{ psi (C)}$$

$$\leq f_{ci} = -2,880 \text{ psi allowed, O.K.}$$

(ii) **Final Condition at Service Load** Midspan moment due to superimposed dead and live load is

$$M_{SD} + M_L = \frac{420 (64)^2}{8} \times 12 = 2,580,480 \text{ in.-lb}$$

$$\text{Total Moment } M_T = 2,205,696 + 2,580,480$$

$$= 4,786,176 \text{ in.-lb. (541 kN-m)}$$

$$f^t = -\frac{P_e}{A_c} \left( 1 - \frac{ec_t}{r^2} \right) - \frac{M_T}{S^t}$$

$$= -\frac{229,500}{449} \left( 1 - \frac{14.77 \times 6.23}{50.04} \right) - \frac{4,786,176}{3,607}$$

$$= +429 - 1,327 \cong -898 \text{ psi (C) (7 MPa)}$$

$$< f_c = 0.45 \times 6,000 = 2,700 \text{ psi, O.K.}$$

$$f_b = -\frac{P_e}{A_c} \left( 1 + \frac{ec_b}{r^2} \right) + \frac{M_T}{S_b}$$

$$= -\frac{229,500}{449} \left( 1 + \frac{14.77 \times 17.77}{50.04} \right) + \frac{4,786,176}{1,264}$$

$$= -3,192 + 3,786 \cong +594 \text{ psi (T) (5.2 MPa)}$$

$$< f_t = 12\sqrt{f_c} = 930 \text{ psi, O.K.}$$

## 1.5 C-LINE COMPUTATION OF FIBER STRESSES

### Example 1.2

Solve example 1.1 for the final service-load condition by the line-of-thrust, C-line method.

#### Solution:

$$P_e = 229,500 \text{ lb}$$

$$M_T = 4,786,176 \text{ in.-lb}$$

$$a = \frac{M_T}{P_e} = \frac{4,786,176}{229,500} = 20.85 \text{ in.}$$

$$e' = a - e = 20.85 - 14.77 = 6.08 \text{ in.}$$

From Equations 1.12,

$$f^t = -\frac{P_e}{A_c} \left( 1 + \frac{e'c_t}{r^2} \right)$$

$$= -\frac{229,500}{449} \left( 1 + \frac{6.08 \times 6.23}{50.04} \right) \cong -898 \text{ psi (C)}$$

$$f_b = -\frac{P_e}{A_c} \left( 1 - \frac{e'c_b}{r^2} \right)$$

$$= -\frac{229,500}{449} \left( 1 - \frac{6.08 \times 17.77}{50.04} \right) \cong +594 \text{ psi (T)}$$

Notice how the C-line method is shorter than the basic method used in Example 1.1.





**Photo 1.13** Dauphin Island Bridge, Mobile County, Alabama. (Courtesy, Post-Tensioning Institute.)

## 1.6 LOAD-BALANCING COMPUTATION OF FIBER STRESSES

### Example 1.3

Solve Example 1.1 for the final service load condition after losses using the load-balancing method.

### Solution:

$$P' = P_e = 229,500 \text{ lb at midspan}$$

$$\text{At midspan, } a = e_c = 14.77'' = 1.231 \text{ ft}$$

For the balancing load, we have

$$\begin{aligned} W_b &= 8 \frac{Pa}{l^2} = \frac{8 \times 229,500 \times 1.231}{(64)^2} \\ &= 552 \text{ plf (8.1 kN/m)} \end{aligned}$$

Thus, if the total gravity load would have been 552 plf, only the axial load  $P' / A$  would act if the beam had a parabolically draped tendon with no eccentricity at the supports. This is because the gravity load is balanced by the tendon at the midspan. Hence,

$$\begin{aligned} \text{Total load to which the beam is subjected} &= W_D + W_{SD} + W_L \\ &= 359 + 420 = 779 \text{ plf} \end{aligned}$$

$$\text{Unbalanced load } W_{ub} = 779 - 552 = 227 \text{ plf}$$

$$\begin{aligned} \text{Unbalanced moment } M_{ub} &= \frac{W_{ub}(l)^2}{8} = \frac{227(64)^2}{8} \times 12 \\ &= 1,394,688 \text{ in.-lb} \end{aligned}$$

From Equations 1.19,

$$f^t = -\frac{P'}{A_c} - \frac{M_{ub}}{S'} = -\frac{229,500}{449} - \frac{1,394,688}{3,607}$$



**Photo 1.14** Heidrun Offshore Oil Drilling Platform in the North Sea weighing 2.9 million Kg. It measures 110 m on each side; has four slip-form constructed hulls and module-support 50-ft. span beams (Courtesy, C. E. Morrison, CONOCO Inc., Houston, Texas.)

$$= -511 - 387 \cong -898 \text{ psi (C)}$$

$$f_b = -\frac{P'}{A_c} + \frac{M_{ub}}{S_b} = -\frac{229,500}{449} + \frac{1,394,688}{1,264}$$

$$= -511 + 1,104 \cong 594 \text{ psi (T)}$$

$$\leq f_t = 930 \text{ psi allowed, O.K.}$$

## 1.7 SI WORKING LOAD STRESS CONCEPTS

### Example 1.4

Solve Example 1.1 using SI units

#### Given

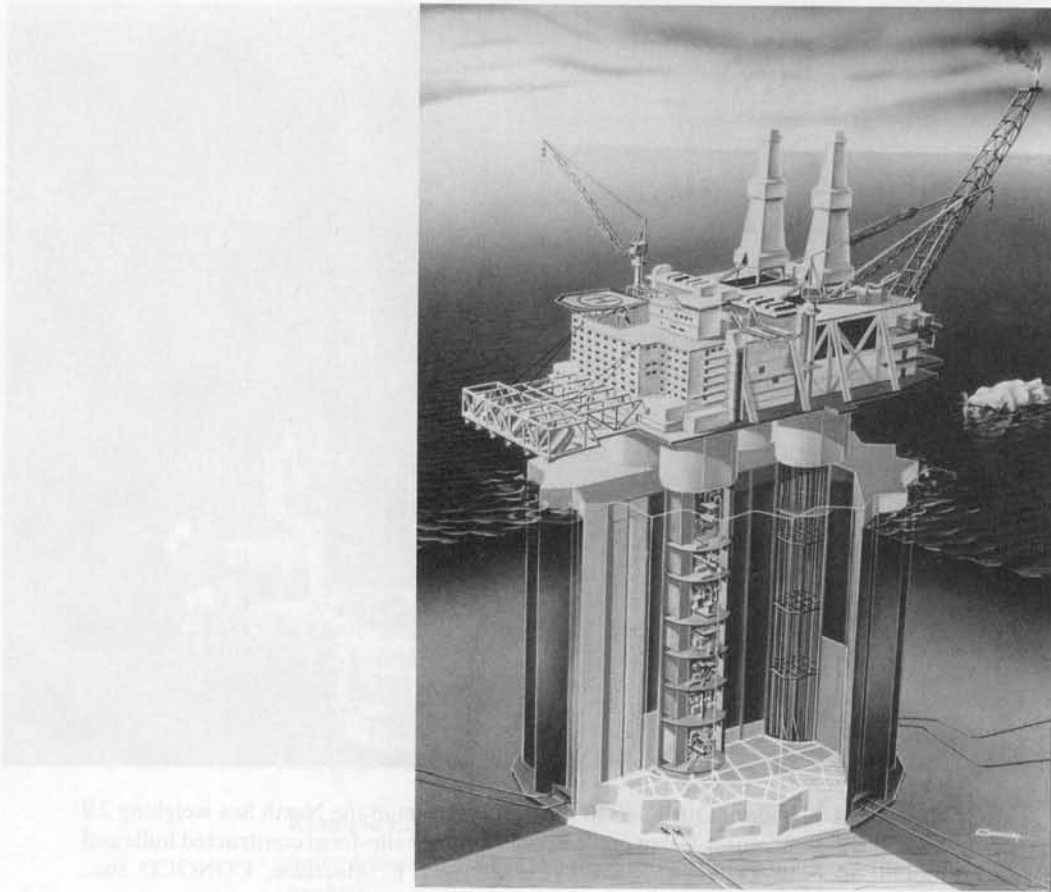
#### Stress Data

$$f'_c = 41.4 \text{ MPa}$$

$$f_{pu} = 1,860 \text{ MPa}$$

$$f_{pt} = 0.70 f_{pu} = 0.70 \times 1860 = 1300 \text{ MPa}$$

$$f_{py} = 1,520 \text{ MPa}$$



**Photo 1.15** Hibernia Platform, Grand Banks, Newfoundland, 1997: 80 m water depth, 165,000 m<sup>3</sup>, 70 MPa strength concrete and 8,000 tons of prestressing tendons; first platform designed for iceberg impacts (Courtesy, Dr. George C. Hoff, Mobile Research and Development Corp.)

$$f_{pe} = 1,034 \text{ MPa}$$

$$f_t = \sqrt{f'_c} \text{ is deflection check O.K.} = 6.4 \text{ MPa, use}$$

$$f_t = \frac{1}{2} \sqrt{f'_c} \text{ if no check made on deflection}$$

$$f'_{ci} \cong 0.8 f'_c = 33.1 \text{ MPa}$$

$$f_{ci} = 0.6 f'_{ci} = 19.9 \text{ MPa}$$

$$f_c = 0.45 f'_c = 18.6 \text{ MPa}$$

$$A_{ps} = 10 \text{ tendons } 17.7 \text{ mm diameter} = 10 \times 99 \text{ mm}^2 = 990 \text{ mm}^2$$

### Section Geometry

Try 108-D1 Strand Pattern

$$A_c = 2897 \text{ cm}^2$$

$$I_c = 935,346 \text{ cm}^4$$

$$r^2 = I_c / A_c = 323 \text{ cm}^2$$



**Photo 1.16** Pier 37 Rebuild, Seattle Washington: a 1200-ft-long by 40-ft wide pier consisting of 20-ft-long prestressed concrete deck panel supported by situ-cast concrete pile caps and prestressed concrete piles (Designed by BERGER/ABAM Engineers, Federal Way, Washington, courtesy Robert Mast, Chairman)

$$c_b = 45.1 \text{ cm} \quad c_t = 15.8 \text{ cm}$$

$$e_c = 37.5 \text{ cm} \quad e_e = 19.74 \text{ cm}$$

$$S^t = 59,108 \text{ cm}^3$$

$$S_b = 20,713 \text{ cm}^3$$

$$W_D = 5.24 \text{ kN/m}$$

$$W_{SD} + W_L = 6.13 \text{ kN/m}$$

$$l = 19.51 \text{ m}$$

**Solution:**

**1. Initial conditions at prestressing**

$$A_{ps} = 990 \text{ mm}^2$$

$$P_i = A_{ps} f_{pi} = 990 \times 1,303 = 1,290 \text{ kN}$$

$$P_e = A_{ps} f_{pe} = 990 \times 1,034 = 1,024 \text{ kN}$$

Midspan self-weight dead-load moment

$$M_D = \frac{wl^2}{8} = \frac{5.24 (19.51)^2}{8} = 249 \text{ kN-m}$$

From Equation 1.1a,

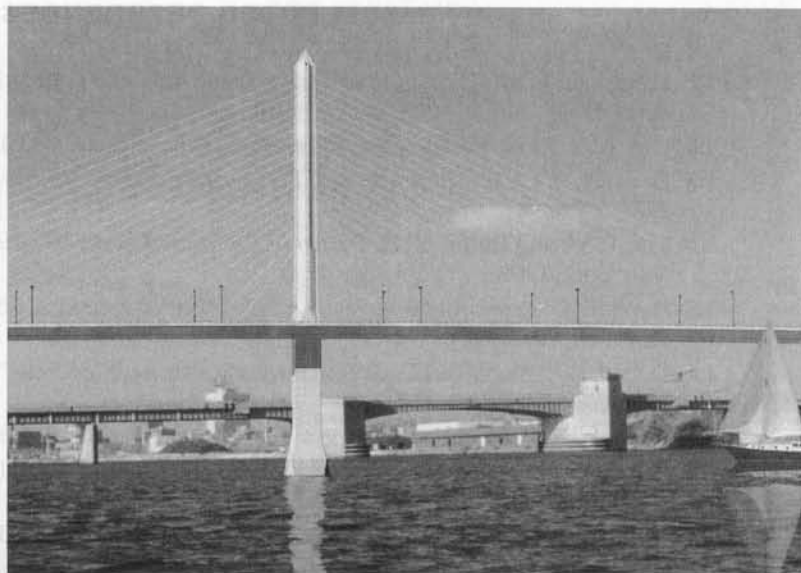
$$\begin{aligned} f_t &= -\frac{P_i}{A_c} \left( 1 - \frac{ec'}{r^2} \right) - \frac{M_d}{S_t} \\ &= -\frac{1290}{2897} \left( 1 - \frac{37.5 \times 15.8}{323} \right) - \frac{249 \times 10^2 \text{ kN-cm}}{59,108 \text{ cm}^2} \\ &= +0.37 - 0.42 \text{ kN/cm}^2 = -0.5 \times 10^6 \text{ N/m}^2 \\ &= 0.5 \text{ MPa (C)} < f_{ti} \text{ in tension} < f_{ci}, \text{ O.K.} \end{aligned}$$

From Equation 1.1b,

$$\begin{aligned} f_b &= -\frac{P_i}{A_c} \left( 1 + \frac{ec_b}{r^2} \right) + \frac{M_D}{S_b} \\ &= -\frac{1290}{2897} \left( 1 + \frac{37.5 \times 45.1}{323} \right) + \frac{249 \times 10^2 \text{ kN-cm}}{20,713 \text{ cm}^2} \end{aligned}$$



**Photo 1.17** Paramount Apartments, San Francisco, CA: the first hybrid precast prestressed concrete moment-resistant 39 floor high-rise frame building in high seismicity zone, 2002. (Courtesy Charles Pankow Ltd., Design/Build contractors. Structural Engineers: Robert Englekirk Inc.; Design Architects: Elkus/Manfredi; Executive Architect: Kwan Henmi, Inc.; Owner: The Related Companies)



**Photo 1.18** Rendering of the New Maumee River Bridge, Toledo. The design includes a unique single pylon clad with glass emitting LED arrays at night, single plane of stays, and a main span of 612 feet in both directions. Courtesy of the designer, FIGG Engineers of Tallahassee, Florida.

$$\begin{aligned}
 &= -2.33 + 1.23 \text{ kN/cm}^2 = -11.0 \times 10^6 \text{ N/m}^2 \\
 &= 11.0 \text{ MPa (C)} < \text{allowable } f_{ci} = 19.9 \text{ MPa, O.K.}
 \end{aligned}$$

## 2. Final condition at service load

$$\begin{aligned}
 W_{SD+L} &= 6.13 \text{ kN/m} \\
 M_{SD+L} &= \frac{6.13(19.51)^2}{8} = 292 \text{ kN-m}
 \end{aligned}$$

Total Moment  $M_T = 343 + 292 = 635 \text{ kN-m}$ . From Eq. 1.7a,

$$\begin{aligned}
 f^t &= -\frac{P_e}{A_c} \left( 1 - \frac{ec^t}{r^2} \right) - \frac{M_T}{S^t} \\
 &= -\frac{1024}{2897} \left( 1 - \frac{37.5 \times 15.8}{323} \right) - \frac{541 \times 10^2 \text{ kN-cm}}{59,108 \text{ cm}^3} \\
 &= +0.29 - 0.92 \text{ kN/cm}^2 = -6.3 \times 10^6 \text{ N/m}^2 \\
 &= -6.3 \text{ MPa (C)} < \text{allow } f_c = 18.6 \text{ MPa, O.K.}
 \end{aligned}$$

From Equation 1.7b,

$$\begin{aligned}
 f_b &= -\frac{P_e}{A_c} \left( 1 + \frac{ec_b}{r^2} \right) + \frac{M_T}{S_b} \\
 &= -\frac{1024}{2897} \left( 1 + \frac{37.5 \times 45.1}{323} \right) + \frac{541 \times 10^2 \text{ kN-cm}}{20,713 \text{ cm}^3} \\
 &= (-2.20 + 2.16) \times 10^7 \text{ N/m}^2 = +4.1 \times 10^6 \text{ N/m}^2 \\
 &= 4.1 \text{ MPa (T)} < \text{allow. } f_t = \sqrt{f_c'} = 6.4 \text{ MPa, O.K.}
 \end{aligned}$$

## SELECTED REFERENCES

- 1.1 Freyssinet, E. *The Birth of Prestressing*. London: Public Translation, Cement and Concrete Association, 1954.
- 1.2 Guyon, Y. *Limit State Design of Prestressed Concrete*, vol. 1. Halsted-Wiley, New York, 1972.
- 1.3 Gerwick, B. C., Jr. *Construction of Prestressed Concrete Structures*. Wiley-Interscience, New York, 1993, 591 p.
- 1.4 Lin, T. Y., and Burns, N. H. *Design of Prestressed Concrete Structures*. 3d ed. John Wiley & Sons, New York, 1981.
- 1.5 Nawy, E. G. *Reinforced Concrete—A Fundamental Approach*. 6th ed., Prentice-Hall, Upper Saddle River, NJ: 2009, 936 p.
- 1.6 Dobell, C. "Patents and Code Relating to Prestressed Concrete." *Journal of the American Concrete Institute* 46, 1950, 713–724.
- 1.7 Naaman, A. E. *Prestressed Concrete Analysis and Design*. McGraw Hill, New York, 1982.
- 1.8 Dill, R. E. "Some Experience with Prestressed Steel in Small Concrete Units." *Journal of the American Concrete Institute* 38, 1942, 165–168.
- 1.9 Institution of Structural Engineers. "First Report on Prestressed Concrete." *Journal of the Institution of Structural Engineers*, September 1951.
- 1.10 Magnel, G. *Prestressed Concrete*. London: Cement and Concrete Association, 1948.
- 1.11 Abeles, P. W., and Bardhan-Roy, B. K. *Prestressed Concrete Designer's Handbook*. 3d ed. Viewpoint Publications, London, 1981.
- 1.12 Nawy, E. G., *Fundamentals of High Performance Concrete*, 2nd ed. John Wiley & Sons, New York, 2001, pp. 460.
- 1.13 Nawy, E. G., editor-in-chief, *Concrete Construction Engineering Handbook*, 2nd ed., CRC Press, Boca Raton, FL, 2008, 1560 p.

## PROBLEMS

- 1.1 An AASHTO prestressed simply supported I-beam has a span of 34 ft (10.4 m) and is 36 in. (91.4 cm) deep. Its cross section is shown in Figure P1.1. It is subjected to a live-load intensity  $W_L = 3,600$  plf (52.6 kN/m). Determine the required  $\frac{1}{2}$ -in.-dia stress-relieved seven-wire strands to resist the applied gravity load and the self-weight of the beam, assuming that the tendon eccentricity at midspan is  $e_c = 13.12$  in. (333 mm). Maximum permissible stresses are as follows:

$$f'_c = 6,000 \text{ psi (41.4 MPa)}$$

$$f_c = 0.45f'_c$$

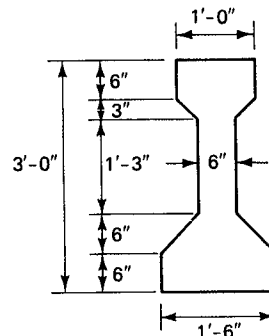


Figure P1.1

$$= 2,700 \text{ psi (19.7 MPa)}$$

$$f_t = 12\sqrt{f'_c} = 930 \text{ psi (6.4 MPa)}$$

$$f_{pu} = 270,000 \text{ psi (1,862 MPa)}$$

$$f_{pi} = 189,000 \text{ psi (1,303 MPa)}$$

$$f_{pe} = 145,000 \text{ psi (1,000 MPa)}$$

The section properties, are:

$$A_c = 369 \text{ in}^2$$

$$I_g = 50,979 \text{ in}^4$$

$$r^2 = I_c/A_c = 138 \text{ in}^2$$

$$c_b = 15.83 \text{ in.}$$

$$S_b = 3,220 \text{ in}^3$$

$$S^t = 2,527 \text{ in}^3$$

$$W_D = 384 \text{ plf}$$

$$W_L = 3,600 \text{ plf}$$

Solve the problem by each of the following methods:

(a) Basic concept

(b) C-line

(c) Load balancing

1.2 Solve problem 1.1 for a 45 ft (13.7 m) span and a superimposed live load  $W_L = 2,000$  plf (29.2 kN/m).

1.3 A simply supported pretensioned pretopped double T-beam for a floor has a span of 70 ft (21.3 m) and the geometrical dimensions shown in Figure P1.3. It is subjected to a gravity live-load intensity  $W_L = 480$  plf (7 kN/m), and the prestressing tendon has an eccentricity at midspan of  $e_c = 19.96$  in. (494 mm). Compute the concrete extreme fiber stresses in this beam at transfer and at service load, and verify whether they are within the permissible limits. Assume that all permissible stresses and materials used are the same as in example 1.1. The section properties are:

#### Section Properties

$$A_c = 1185 \text{ in.}^2$$

$$I_g = 109,621 \text{ in.}^4$$

$$c_b = 25.65 \text{ in.}$$

$$c_t = 8.35 \text{ in.}$$

$$S_b = 4274 \text{ in.}^3$$

$$S^t = 13,128 \text{ in.}^3$$

$$W_D = 1234 \text{ plf}$$

$$82 \text{ psf}$$

$$V/S = 2.45 \text{ in.}$$

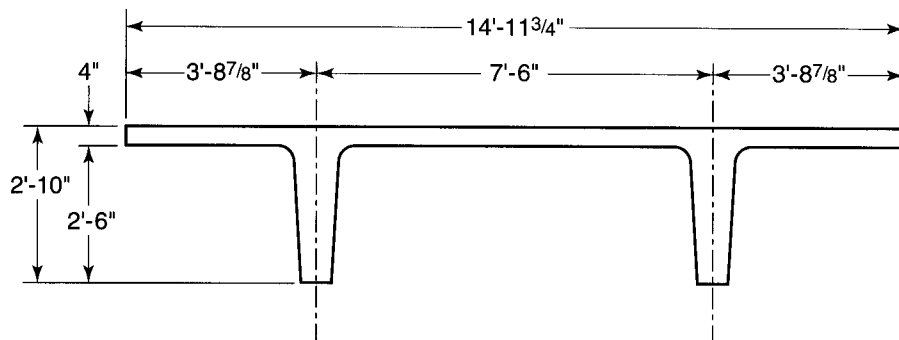


Figure P1.3



Design the prestressing steel needed using  $\frac{1}{2}$ -in.-dia stress-relieved seven-wire strands. Use the three methods of analysis discussed in this chapter in your solution.

- 1.4** A T-shaped simply supported beam has the cross section shown in Figure P1.4. It has a span of 36 ft (11 m), is loaded with a gravity live-load unit intensity  $W_L = 2,500$  plf (36.5 kN/), and is prestressed with twelve  $\frac{1}{2}$ -in.-dia (twelve 12.7-mm-dia) seven-wire stress-relieved strands. Compute the concrete fiber stresses at service load by each of the following methods:

- (a) Basic concept  
 (b) C-line  
 (c) Load balancing

Assume that the tendon eccentricity at midspan is  $e_c = 9.6$  in. (244 mm). Then given that

$$f'_c = 5,000 \text{ psi (34.5 MPa)}$$

$$f_t = 12\sqrt{f'_c} = 849 \text{ psi (5.9 MPa)}$$

$$f_{pe} = 165,000 \text{ psi (1,138 MPa)}$$

the section properties are as follows:

$$A_c = 504 \text{ in}^2$$

$$I_c = 37,059 \text{ in}^4$$

$$r^2 = I_c/A_c = 73.5 \text{ in}^2$$

$$c_b = 12.43 \text{ in.}$$

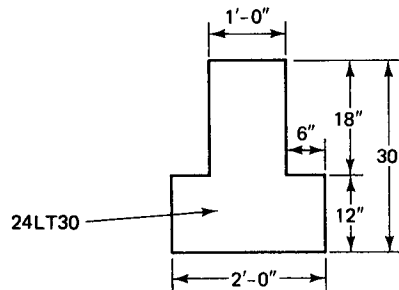
$$S_b = 2,981 \text{ in}^3$$

$$S' = 2,109 \text{ in}^3$$

$$W_D = 525 \text{ plf}$$

$$e_c = 9.6 \text{ in.}$$

$$A_{ps} = \text{twelve } \frac{1}{2}\text{-in.-dia, seven-wire stress-relieved strands}$$



**Figure P1.4**

- 1.5** Solve problem 1.4 if  $f'_c = 7,000$  psi (48.3 MPa) and  $f_{pe} = 160,000$  psi (1,103 MPa).



# 2

## MATERIALS AND SYSTEMS FOR PRESTRESSING

### 2.1 CONCRETE

#### 2.1.1 Introduction

Concrete, particularly high-strength concrete, is a major constituent of all prestressed concrete elements. Hence, its strength and long-term endurance have to be achieved through proper quality control and quality assurance at the production stage. Numerous texts are available on concrete production, quality control, and code requirements. The following discussion is intended to highlight the topics directly related to concrete in prestressed elements and systems; it is assumed that the reader is already familiar with the fundamentals of concrete and reinforced concrete.

#### 2.1.2 Parameters Affecting the Quality of Concrete

Strength and endurance are two major qualities that are particularly important in prestressed concrete structures. Long-term detrimental effects can rapidly reduce the prestressing forces and could result in unexpected failure. Hence, measures have to be taken to ensure strict quality control and quality assurance at the various stages of production

Pasco-Kennewick Intercity Bridge. Segmentally assembled prestressed concrete cable-stayed bridge, spans 407–981–407 ft. (*Courtesy, Arvid Grant and Associates, Inc.*)

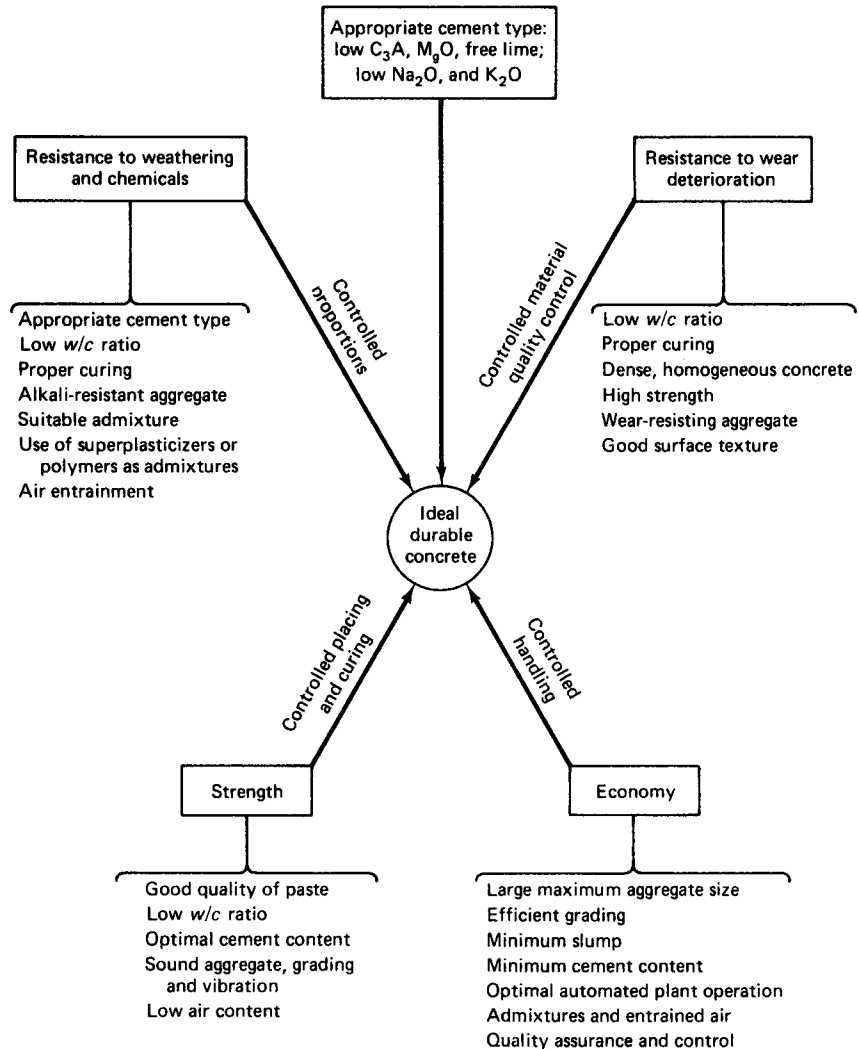


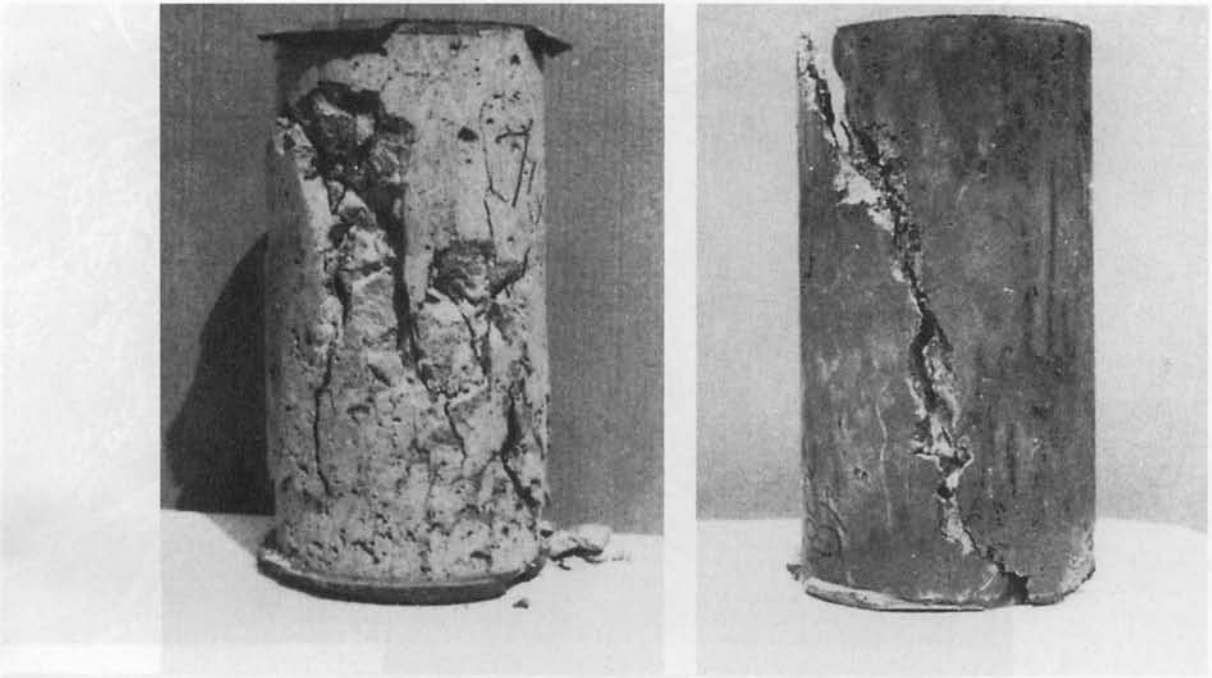
Figure 2.1 Principal properties of good concrete.

and construction as well as maintenance. Figure 2.1 shows the various factors that result in good-quality concrete.

### 2.1.3 Properties of Hardened Concrete

The mechanical properties of hardened concrete can be classified into two categories: short-term or instantaneous properties, and long-term properties. The short-term properties are strength in compression, tension, and shear; and stiffness, as measured by the modulus of elasticity. The long-term properties can be classified in terms of creep and shrinkage. The following subsections present some details on these properties.

**2.1.3.1 Compressive Strength.** Depending on the type of mix, the properties of aggregate, and the time and quality of the curing, compressive strengths of concrete can be obtained up to 20,000 psi or more. Commercial production of concrete with ordinary ag-



**Photo 2.1** Concrete cylinders tested to failure in compression. Specimen A, low-epoxy-cement content; specimen B, high-epoxy-cement content. (Tests by Nawy, Sun, and Sauer.)

gregate is usually in the range 4,000 to 12,000 psi, with the most common concrete strengths being in the 6,000 psi level.

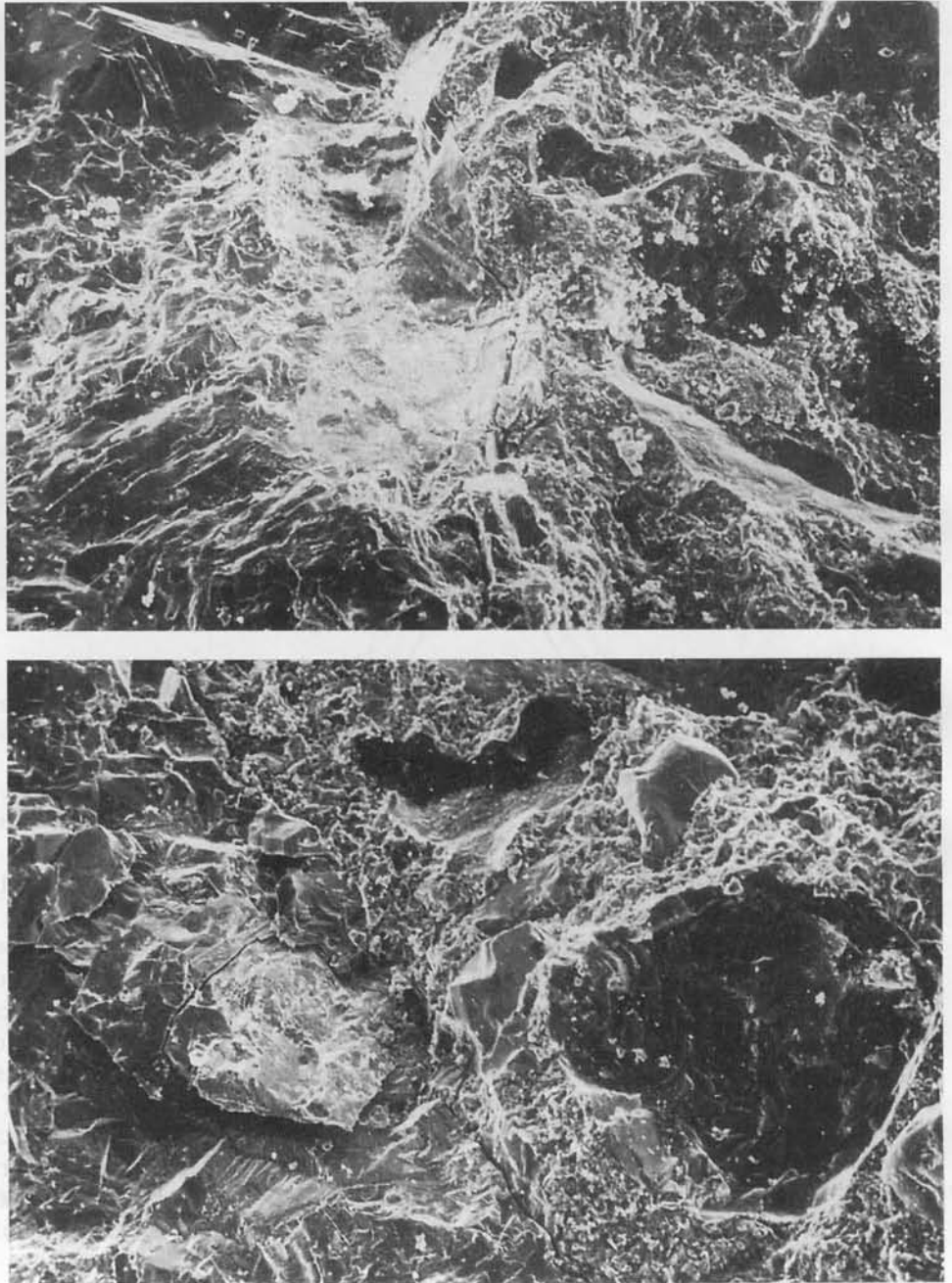
The compressive strength  $f'_c$  is based on standard 6 in. by 12 in. cylinders cured under standard laboratory conditions and tested at a specified rate of loading at 28 days of age. The standard specifications used in the United States are usually taken from ASTM C-39. The strength of concrete in the actual structure may not be the same as that of the cylinder because of the difference in compaction and curing conditions.

For a strength test, the ACI code specifies using the average of two cylinders from the same sample tested at the same age, which is usually 28 days. As for the frequency of testing, the code specifies that the strength of an individual class of concrete can be considered satisfactory if (1) the average of all sets of three consecutive strength tests equals or exceeds the required  $f'_c$ , and (2) no individual strength test (average of two cylinders) falls below the required  $f'_c$  by more than 500 psi. The average concrete strength for which a concrete mixture must be designed should exceed  $f'_c$  by an amount that depends on the uniformity of plant production.

Note that the design  $f'_c$  should not be the average cylinder strength, but rather the minimum conceivable cylinder strength.

**2.1.3.2 Tensile Strength.** The tensile strength of concrete is relatively low. A good approximation for the tensile strength  $f_{ct}$  is  $0.10f'_c < f_{ct} < 0.20f'_c$ . It is more difficult to measure tensile strength than compressive strength because of the gripping problems with testing machines. A number of methods are available for tension testing, the most commonly used method being the cylinder splitting, or Brazilian, test.

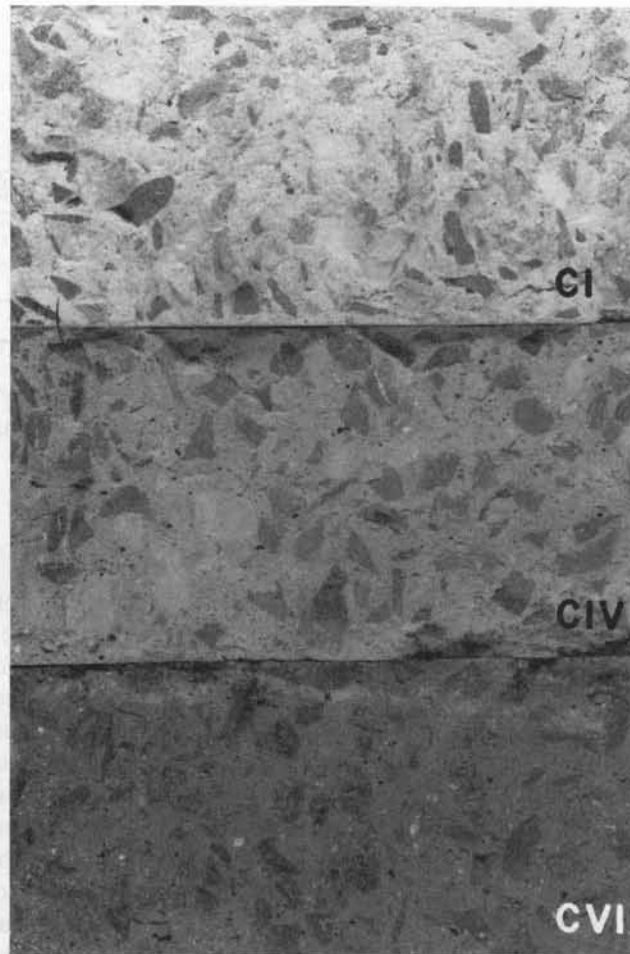
For members subjected to bending, the value of the modulus of rupture  $f_r$ , rather than the tensile splitting strength  $f'_t$  is used in design. The modulus of rupture is measured by testing to failure plain concrete beams 6 in. square in cross section, having a



**Photo 2.2** Electron microscope photographs of concrete from specimens A and B in the preceding photograph. (Tests by Nawy et al.)

span of 18 in., and loaded at their third points (ASTM C-78). The modulus of rupture has a higher value than the tensile splitting strength. The ACI specifies a value of  $7.5 \sqrt{f'_c}$  for the modulus of rupture of normal-weight concrete.

In most cases, lightweight concrete has a lower tensile strength than does normal-weight concrete. The following are the code stipulations for lightweight concrete:



**Photo 2.3** Fracture surfaces in tensile splitting tests of concretes with different  $w/c$  contents. Specimens CI and CIV have higher  $w/c$  content, hence more bond failures than specimen CVI. (Tests by Nawy et al.)

1. If the splitting tensile strength  $f_{ct}$  is specified,

$$f_r = 1.09 f_{ct} \leq 7.5 \sqrt{f'_c} \quad (2.1)$$

2. If  $f_{ct}$  is not specified, use a factor of 0.75 for all-lightweight concrete and 0.85 for sand-lightweight concrete. Linear interpolation may be used for mixtures of natural sand and lightweight fine aggregate.

**2.1.3.3 Shear Strength.** Shear strength is more difficult to determine experimentally than the tests discussed previously because of the difficulty in isolating shear from other stresses. This is one of the reasons for the large variation in shear-strength values reported in the literature, varying from 20 percent of the compressive strength in normal loading to a considerably higher percentage of up to 85 percent of the compressive strength in cases where direct shear exists in combination with compression. Control of a structural design by shear strength is significant only in rare cases, since shear stresses must ordinarily be limited to continually lower values in order to protect the concrete from failure in diagonal tension.

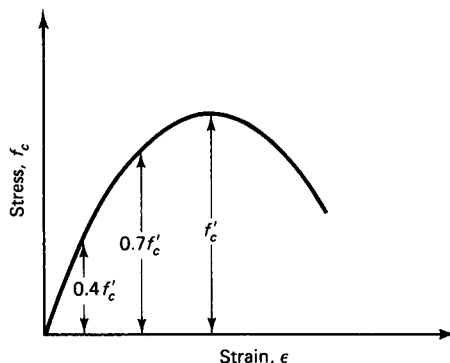


Figure 2.2 Typical stress-strain curve of concrete.

## 2.2 STRESS-STRAIN CURVE OF CONCRETE

Knowledge of the stress-strain relationship of concrete is essential for developing all the analysis and design terms and procedures in concrete structures. Figure 2.2 shows a typical stress-strain curve obtained from tests using cylindrical concrete specimens loaded in uniaxial compression over several minutes. The first portion of the curve, to about 40 percent of the ultimate strength  $f'_c$ , can essentially be considered linear for all practical purposes. After approximately 70 percent of the failure stress, the material loses a large portion of its stiffness, thereby increasing the curvilinearity of the diagram. At ultimate load, cracks parallel to the direction of loading become distinctly visible, and most concrete cylinders (except those with very low strengths) suddenly fail shortly thereafter. Figure 2.3 shows the stress-strain curves of concrete of various strengths reported by the Portland Cement Association. It can be observed that (1) the lower the strength of concrete, the higher the failure strain; (2) the length of the initial relatively linear portion increases with the increase in the compressive strength of concrete; and (3) there is an apparent reduction in ductility with increased strength.

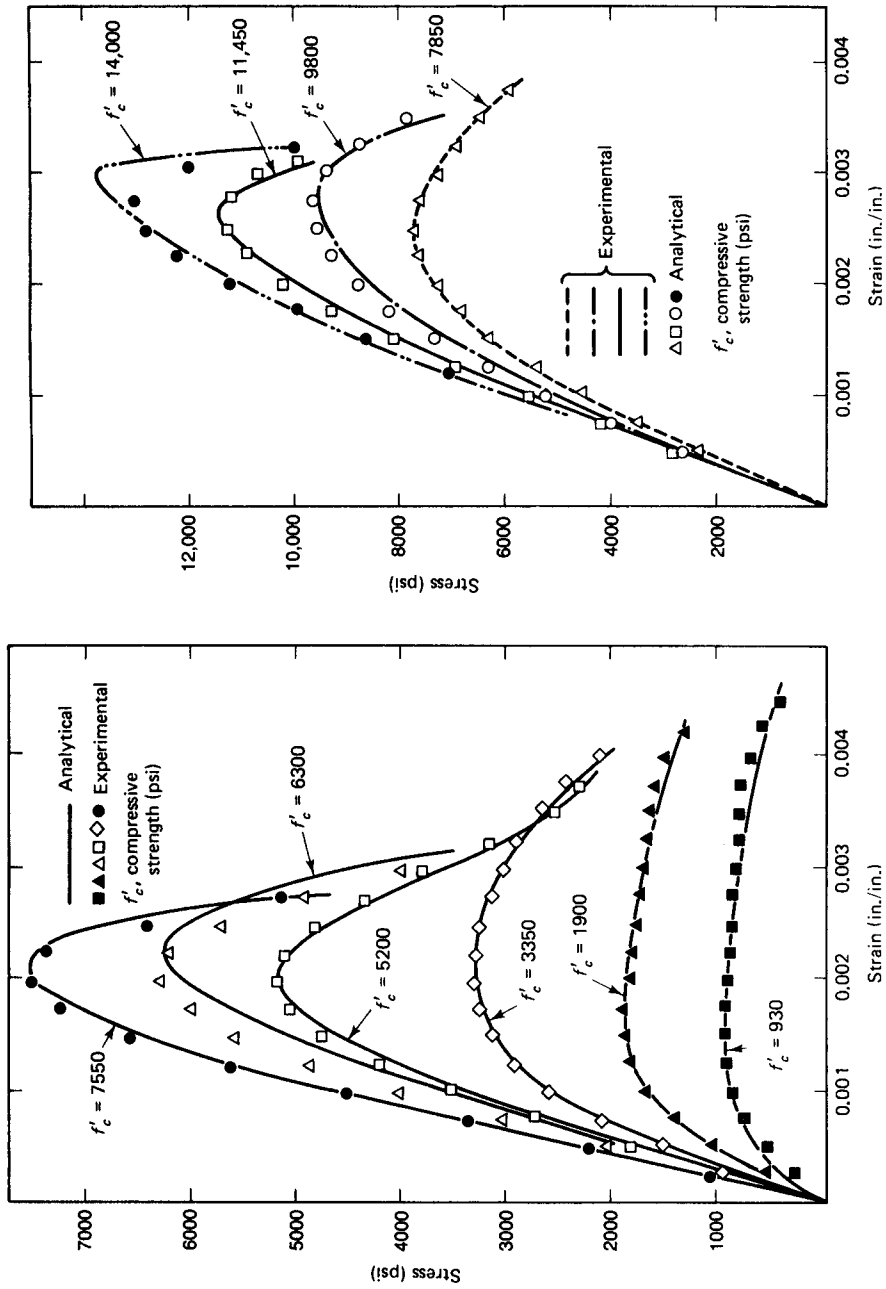
## 2.3 MODULUS OF ELASTICITY AND CHANGE IN COMPRESSIVE STRENGTH WITH TIME

Since the stress-strain curve shown in Figure 2.4 is curvilinear at a very early stage of its loading history, Young's modulus of elasticity can be applied only to the tangent of the curve at the origin. The initial slope of the tangent to the curve is defined as the initial tangent modulus, and it is also possible to construct a tangent modulus at any point of the curve. The slope of the straight line that connects the origin to a given stress (about  $0.4 f'_c$ ) determines the secant modulus of elasticity of concrete. This value, termed in design calculation the *modulus of elasticity*, satisfies the practical assumption that strains occurring during loading can be considered basically elastic (completely recoverable on unloading), and that any subsequent strain due to the load is regarded as creep.

The ACI building code gives the following expressions for calculating the secant modulus of elasticity of concrete,  $E_c$ .

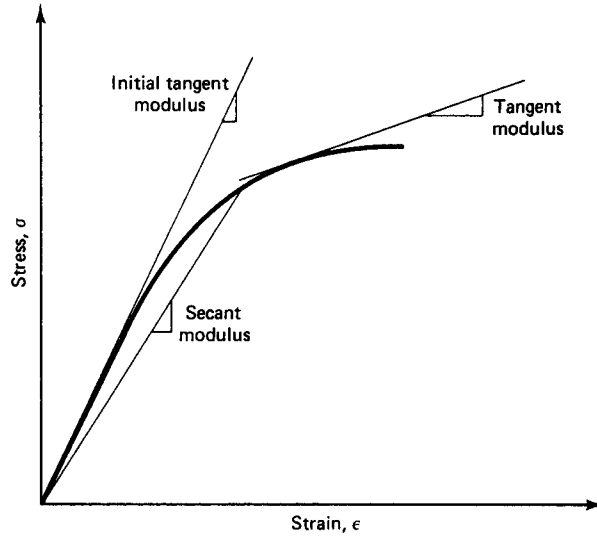
$$E_c = 33w_c^{1.5}\sqrt{f'_c} \quad \text{for } 90 < w_c < 155 \text{ lb/ft}^3 \quad (2.2a)$$

where  $w_c$  is the density of concrete in pounds per cubic foot ( $1 \text{ lb/ft}^3 = 16.02 \text{ kg/m}^3$ ) and  $f'_c$  is the compressive cylinder strength in psi. For normal-weight concrete,



**Figure 2.3** Stress-strain curves for various concrete strengths.





**Figure 2.4** Tangent and secant moduli of concrete.

$$E_c = 57,000\sqrt{f'_c} \text{ psi } (4,700\sqrt{f'_c} \text{ MPa})$$

or

$$E_c = 0.043w^{1.5}\sqrt{f'_c} \text{ MPa} \quad (2.2.b)$$

### 2.3.1 High-Strength Concrete

High-strength concrete is termed as such by the ACI 318 Code when the cylinder compressive strength exceeds 6,000 psi (41.4 MPa). For concrete having compressive strengths 6,000 to 12,000 psi (42–84 MPa), the expressions for the modulus of concrete (Refs. 2.11, 2.35, 2.38)

$$E_c (\text{psi}) = [40,000\sqrt{f'_c} + 10^6] \left(\frac{w_c}{145}\right)^{1.5} \quad (2.3a)$$

where  $f'_c = \text{psi}$  and  $w_c = \text{lb/ft}^3$

or

$$E_c (\text{MPa}) = [3.32\sqrt{f'_c} + 6,895] \left(\frac{w_c}{2320}\right)^{1.5} \quad (2.3b)$$

where  $f'_c = \text{MPa}$  and  $w_c = \text{Kg/m}^3$ .

Today, concrete strength up to 20,000 psi (138 MPa) is easily achieved using a maximum stone aggregate size of  $\frac{3}{8}$  in. (9.5 mm) and pozzolamic cementitious partial replacements for the cement such as silica fume. Such strengths can be obtained in the field under strict quality control and quality assurance conditions. For strengths in the range of 20,000 to 30,000 (138–206 MPa), other constituents such as steel or carbon fibers have to be added to the mixture. In all these cases, mixture design has to be made by several field trial batches (five or more), modifying the mixture components for the workability needed in concrete placement. Steel cylinder molds size 4 in. (diameter)  $\times$  8 in. length have to be used, applying the appropriate dimensional correction. It is also necessary to

grind the cylinder ends, then cap them with high strength capping compound for load testing, or to apply the load directly to the ground ends of the cylinder or through a removable steel cap with a hard neoprene pad bearing directly on the ground specimen ends. Preparation of the cylinders should resemble as closely as possible the field conditions of concrete placement. Mock-up placement of the high-strength concrete is advisable in order to evaluate the construction procedures and performance of the concrete in field conditions and to identify potential problems with batching, placement, and testing of the concrete at early ages. Corrective measures should be taken immediately.

A good example of the use of high-strength concrete in the range 20,000 psi (138 MPa) at 56 days and a concrete modulus  $E_c = 7.8 \times 10^6$  psi ( $53.8 \times 103$  MPa) is the Two Union Square Building, Seattle, Washington (Ref. 2.11, 2.38). Actual typical mixture obtained is listed in Table 2.1, with the design mixture values in parentheses.

A slump of 8 in. with  $w/c \approx 0.22$  resulted from the mix proportions indicated. A typical compressive vs. age plot for the indicated mixture based on 4 in.  $\times$  8 in. cylinder tests is shown in Figure 2.5.

Recent work at Rutgers (Refs. 2.36, 2.37) on high-strength composite construction has resulted in considerable enhancement of the ductility of high-strength reinforced concrete beams. Prestressed concrete prisms of high-strength concrete were used in lieu of the normal mild steel bar reinforcement. The mixture proportions in  $\text{lb}/\text{yd}^3$  were as shown in Table 2.2. The mixture was designed for a seven-day compressive strength of 12,000 psi (84 MPa). The ratio of the cementations/fine/coarse aggregate was 1:1.22:2.06 and the slump varied between 4 to 6 in. (100–150 mm). The prestressing strands were stress-relieved 270K (1900 MPa) 7 wire  $\frac{3}{8}$  in. (9.5 mm) diameter strands. Figure 2.6 shows the cross section of the composite beams. Concrete achieved in some of the mixtures a 7 day strength of 13,250 psi (91.4 MPa). The tested specimens were instrumented with a fiber-optic system developed by the author using Bragg Grating sensors both internally and externally.

### 2.3.2 Initial Compressive Strength and Modulus

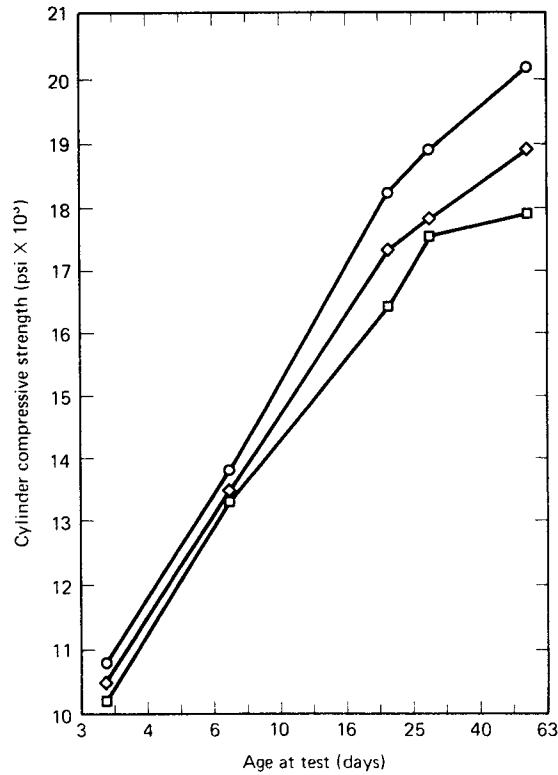
Since prestressing is performed in most cases prior to concrete's achieving its 28 days' strength, it is important to determine the concrete compressive strength  $f'_{ci}$  at the prestressing stage as well as the concrete modulus  $E_c$  at the various stages in the loading history of the element. The general expression for the compressive strength as a function of time (Ref. 2.18) is

$$f'_{ci} = \frac{t}{\alpha + \beta t} f'_c \quad (2.4a)$$

**Table 2.1** Mixture Proportions for  $f'_c > 18,000$  PSI

Coarse aggregate ( $\frac{3}{8}$ in.) (lb)	Fine aggregate (paving sand) (lb)	Cement (lb)	Water (lb)	Silica fume (gal)	Superplasticizer	
					W. R. Grace Dartard 40 (oz/100 lb cement)	Mighty 150 (oz/100 lb cement)
1872	1165	957	217	13	2.1	9.8
1894	1165	956	217	13	2.1	16.4
(1805)	(1100)	(950)	(w/c = 0.22)	(70 lb) <sup>a</sup>	(6.0)	(Up to 24)

<sup>a</sup>Weight of solid silica fume only. Water contained as part of the emulsion must be subtracted from the total water allowed.



**Figure 2.5** Compressive strength versus age of high-strength concrete.

where  $f'_c$  = 28 days' compressive strength

$t$  = time in days

$\alpha$  = factor depending on type of cement and curing conditions

= 4.00 for moist-cured type-I cement and 2.30 for moist-cured type-III cement

= 1.00 for steam-cured type-I cement and 0.70 for steam-cured type-III cement

$\beta$  = factor depending on the same parameters for  $\alpha$  giving corresponding values of 0.85, 0.92, 0.95, and 0.98, respectively

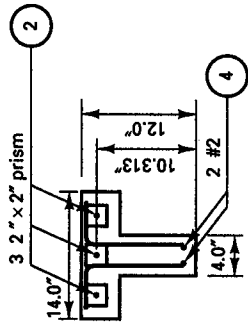
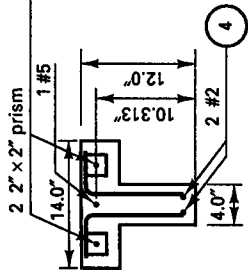
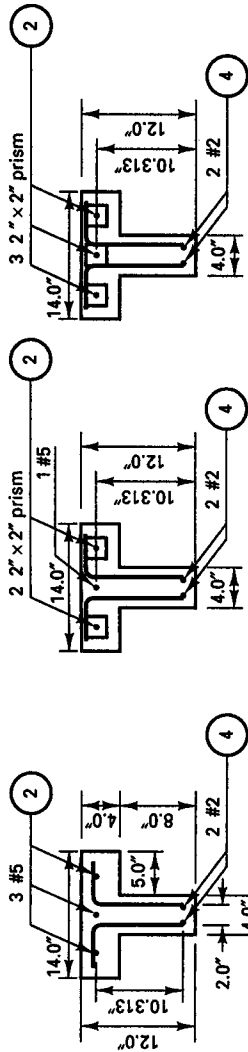
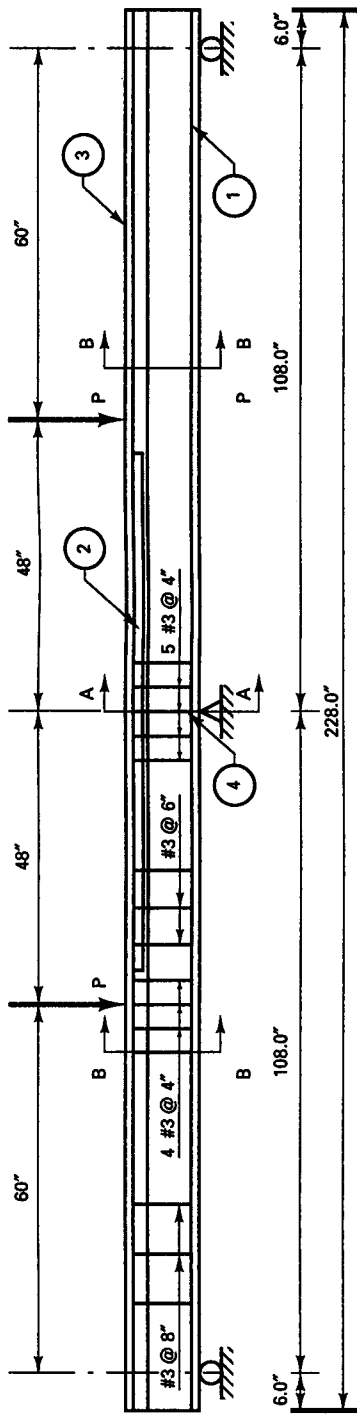
Hence, for a typical moist-cured type-I cement concrete,

$$f'_{ci} = \frac{t}{4.00 + 0.85t} f'_c \quad (2.4b)$$

**Table 2.2** Mixture Proportions in lb/yd<sup>3</sup> For Composite Beams  $f'_c > 13,000$  PSI

Coarse aggregate $\frac{3}{8}$ in.	Fine aggregate (natural sand)	Portland cement type III	Water	Powder silica fume force— 10,000	Liquid super plasticizer (Grace)
(1)	(2)	(3)	(4)	(5)	(6)
1851	1100	720	288	180	54

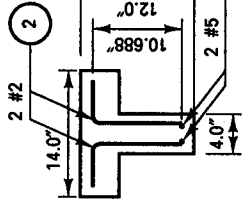
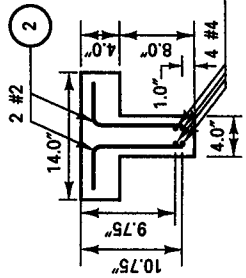
1 lb/yd<sup>3</sup> = 0.59 Kg/m<sup>3</sup>



A-A (C-2)

A-A (C-3, C-4)

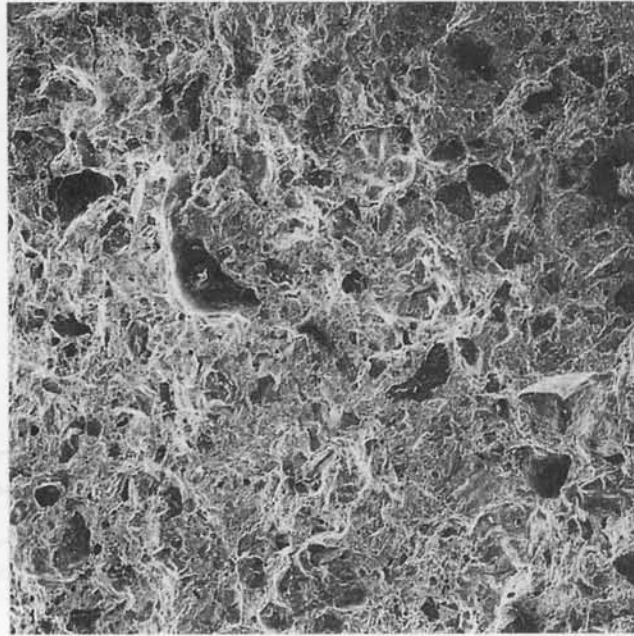
A-A (C-1)



B-B (C-1, C-2, C-3)

B-B (C-4)

**Figure 2.6** High-strength flanged sections reinforced with prestressed concrete prisms instrumented with fiber-optic sensors (Ref. 2.37).



**Photo 2.4** Scanning electron microscope photograph of concrete fracture surface. (Tests by Nawy, Sun, and Sauer.)

The effective modulus of concrete,  $E'_c$ , is

$$E'_c = \frac{\text{stress}}{\text{elastic strain} + \text{creep strain}} \quad (2.5)$$

and the ultimate effective modulus is given by

$$E_{cn} = \frac{E_c}{1 + \gamma_t} \quad (2.6a)$$

where  $\gamma_t$  is the creep ratio defined as

$$\gamma_t = \frac{\text{ultimate creep strain}}{\text{elastic strain}}$$

The creep ratio  $\gamma_t$  has upper and lower limits as follows for prestressed quality concrete:

$$\text{Upper: } \gamma_t = 1.75 + 2.25 \left( \frac{100 - H}{65} \right) \quad (2.6b)$$

$$\text{Lower: } \gamma_t = 0.75 + 0.75 \left( \frac{100 - H}{50} \right) \quad (2.6c)$$

where  $H$  is the mean humidity in percent.

It has to be pointed out that these expressions are valid only in general terms, since the value of the modulus of elasticity is affected by factors other than loads, such as moisture in the concrete specimen, the water/cement ratio, the age of the concrete, and temperature. Therefore, for special structures such as arches, tunnels, and tanks, the modulus of elasticity needs to be determined from test results.

Limited work exists on the determination of the modulus of elasticity in tension because the low-tensile strength of concrete is normally disregarded in calculations. It is, however, valid to assume within those limitations that the value of the modulus in tension is equal to that in compression.

## 2.4 CREEP

*Creep*, or lateral material flow, is the increase in strain with time due to a sustained load. The initial deformation due to load is the *elastic strain*, while the additional strain due to the same sustained load is the *creep strain*. This practical assumption is quite acceptable, since the initial recorded deformation includes few time-dependent effects.

Figure 2.7 illustrates the increase in creep strain with time, and as in the case of shrinkage, it can be seen that creep rate decreases with time. Creep cannot be observed directly and can be determined only by deducting elastic strain and shrinkage strain from the total deformation. Although shrinkage and creep are not independent phenomena, it can be assumed that superposition of strains is valid; hence,

$$\text{Total strain } (\epsilon_t) = \text{elastic strain } (\epsilon_e) + \text{creep } (\epsilon_c) + \text{shrinkage } (\epsilon_{sh})$$

An example of the relative numerical values of strain due to the foregoing three factors for a normal concrete specimen subjected to 900 psi in compression is as follows:

$$\begin{aligned} \text{Immediate elastic strain, } \epsilon_e &= 250 \times 10^{-6} \text{ in./in.} \\ \text{Shrinkage strain after 1 year, } \epsilon_{sh} &= 500 \times 10^{-6} \text{ in./in.} \\ \text{Creep strain after 1 year, } \epsilon_c &= 750 \times 10^{-6} \text{ in./in.} \\ \epsilon_t &= \frac{1,500 \times 10^{-6}}{\text{in./in.}} \end{aligned}$$

These relative values illustrate that stress-strain relationships for short-term loading lose their significance and long-term loadings become dominant in their effect on the behavior of a structure.

Figure 2.8 qualitatively shows, in a three-dimensional model, the three types of strain discussed that result from sustained compressive stress and shrinkage. Since creep is time dependent, this model has to be such that its orthogonal axes are deformation, stress, and time.

Numerous tests have indicated that creep deformation is proportional to applied stress, but the proportionality is valid only for low-stress levels. The upper limit of the relationship cannot be determined accurately, but can vary between 0.2 and 0.5 of the ulti-

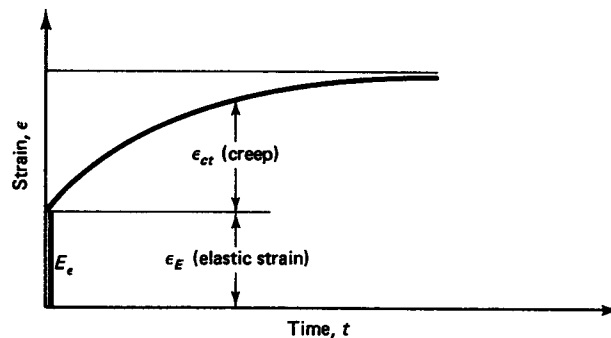
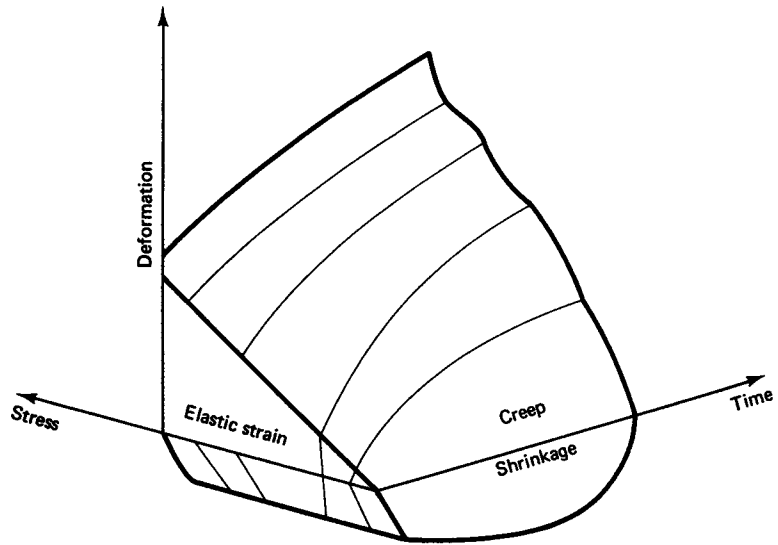


Figure 2.7 Strain-time curve.

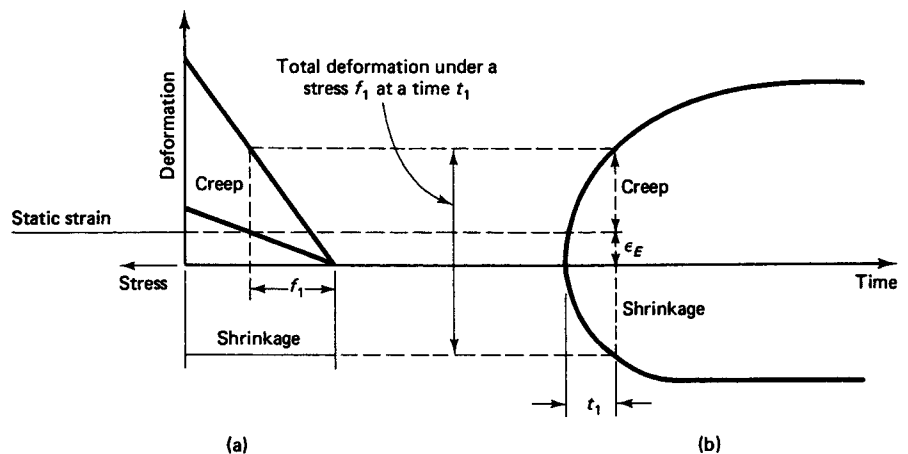


**Figure 2.8** Three-dimensional model of time-dependent structural behavior.

mate strength  $f'_c$ . This range in the limit of the proportionality is due to the large extent of microcracks at about 40 percent of the ultimate load.

Figure 2.9a shows a section of the three-dimensional model in Figure 2.8 parallel to the plane containing the stress and deformation axes at time  $t_1$ . It indicates that both elastic and creep strains are linearly proportional to the applied stress. In a similar manner, Figure 2.9b illustrates a section parallel to the plane containing the time and strain axes at a stress  $f_1$ ; hence, it shows the familiar relationships of creep with time and shrinkage with time.

As in the case of shrinkage, creep is not completely reversible. If a specimen is unloaded after a period under a sustained load, an immediate elastic recovery is obtained which is less than the strain precipitated on loading. The instantaneous recovery is followed by a gradual decrease in strain, called *creep recovery*. The extent of the recovery



**Figure 2.9** (a) Section parallel to the stress-deformation plane. (b) Section parallel to the deformation-time plane.

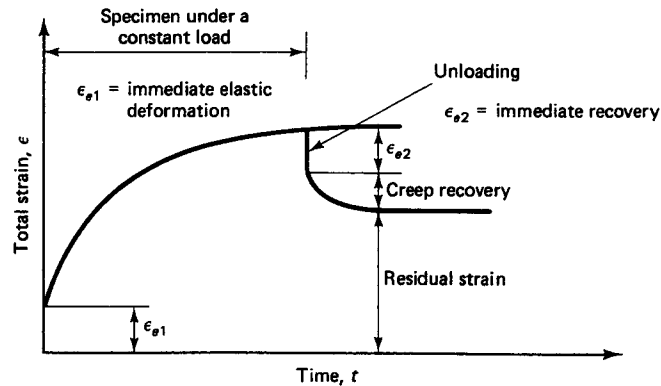


Figure 2.10 Creep recovery versus time.

depends on the age of the concrete when loaded, with older concretes presenting higher creep recoveries, while residual strains or deformations become frozen in the structural element (see Figure 2.10).

Creep is closely related to shrinkage, and as a general rule, a concrete that resists shrinkage also presents a low creep tendency, as both phenomena are related to the hydrated cement paste. Hence, creep is influenced by the composition of the concrete, the environmental conditions, and the size of the specimen, but principally creep depends on loading as a function of time.

The composition of a concrete specimen can be essentially defined by the water/cement ratio and water/cementitious ratio when admixtures are used, aggregate and cement types, and aggregate and cement contents. Therefore, like shrinkage, an increase in the water/cement ratio and in the cement content increases creep. Also, as in shrinkage, the aggregate induces a restraining effect such that an increase in aggregate content reduces creep.

### 2.4.1 Effects of Creep

As in shrinkage, creep increases the deflection of beams and slabs and causes loss of prestress. In addition, the initial eccentricity of a reinforced concrete column increases with time due to creep, resulting in the transfer of the compressive load from the concrete to the steel in the section.

Once the steel yields, additional load has to be carried by the concrete. Consequently, the resisting capacity of the column is reduced and the curvature of the column increases further, resulting in overstress in the concrete, leading to failure.

### 2.4.2 Rheological Models

Rheological models are mechanical devices that portray the general deformation behavior and flow of materials under stress. A model is basically composed of elastic springs and ideal dashpots denoting stress, elastic strain, delayed elastic strain, irrecoverable strain, and time. The springs represent the proportionality between stress and strain, and the dashpots represent the proportionality of stress to the rate of strain. A spring and a dashpot in parallel form a Kelvin unit, and in series they form a Maxwell unit.

Two rheological models will be discussed: the Burgers model and the Ross model. The Burgers model in Figure 2.11 is shown since it can approximately simulate the stress-strain-time behavior of concrete at the limit of proportionality with some limitations. This model simulates the instantaneous recoverable strain,  $\alpha$ ; the delayed recoverable



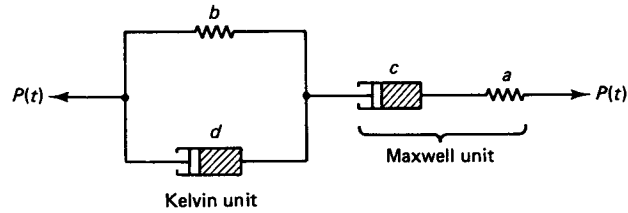


Figure 2.11 Burgers model.

elastic strain in the spring,  $b$ ; and the irrecoverable time-dependent strains in the dashpots,  $c$  and  $d$ . The weakness in the model is that it continues to deform at a uniform rate as long as the load is sustained by the Maxwell dashpot—a behavior not similar to concrete, where creep reaches a limiting value with time, as shown in Figure 2.7.

A modification in the form of the Ross rheological model in Figure 2.12 can eliminate this deficiency.  $A$  in this model represents the Hookian direct proportionality of stress-to-strain element,  $D$  is the dashpot, and  $B$  and  $C$  are the elastic springs that can transmit the applied load  $P(t)$  to the enclosing cylinder walls by direct friction. Since each coil has a defined frictional resistance, only those coils whose resistance equals the applied load  $P(t)$  are displaced; the others remain unstressed, symbolizing the irrecoverable deformation in concrete. As the load continues to increase, it overcomes the spring resistance of unit  $B$ , pulling out the spring from the dashpot and signifying failure in a concrete element. More rigorous models, such as Roll's, have been used to assist in predicting the creep strains. Mathematical expressions for such predictions can be very rigorous. One convenient expression due to Ross defines the creep  $C$  under load after a time interval  $t$  as

$$C = \frac{t}{a + bt} \tag{2.7}$$

where  $a$  and  $b$  are constants determinable from tests.

Work by Branson (Refs. 2.18 and 2.19) has simplified creep evaluation. The additional strain  $\epsilon_{cu}$  due to creep can be defined as

$$\epsilon_{cu} = \rho_u f_{ci} \tag{2.8}$$

where  $\rho_u$  = unit creep coefficient, generally called *specific creep*

$f_{ci}$  = stress intensity in the structural member corresponding to unit strain  $\epsilon_{ci}$

The ultimate creep coefficient,  $C_u$ , is given by

$$C_u = \rho_u E_c \tag{2.9}$$

or average  $C_u \approx 2.35$ .

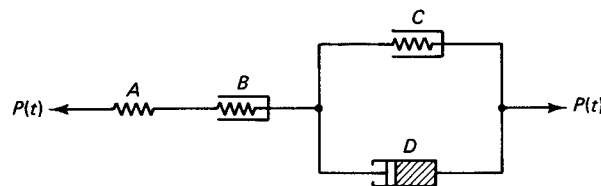


Figure 2.12 Ross model.

Branson's model, verified by extensive tests, relates the creep coefficient  $C_t$  at any time to the ultimate creep coefficient (for standard conditions) as

$$C_t = \frac{t^{0.6}}{10 + t^{0.6}} C_u \quad (2.10)$$

or, alternatively,

$$\rho_t = \frac{t^{0.6}}{10 + t^{0.6}} \quad (2.11)$$

where  $t$  is the time in days and  $\rho_t$  is the time multiplier. Standard conditions as defined by Branson pertain to concretes of slump 4 in. (10 cm) or less and a relative humidity of 40 percent.

When conditions are not standard, creep correction factors have to be applied to Equations 2.10 or 2.11 as follows:

- (a) For moist-cured concrete loaded at an age of 7 days or more,

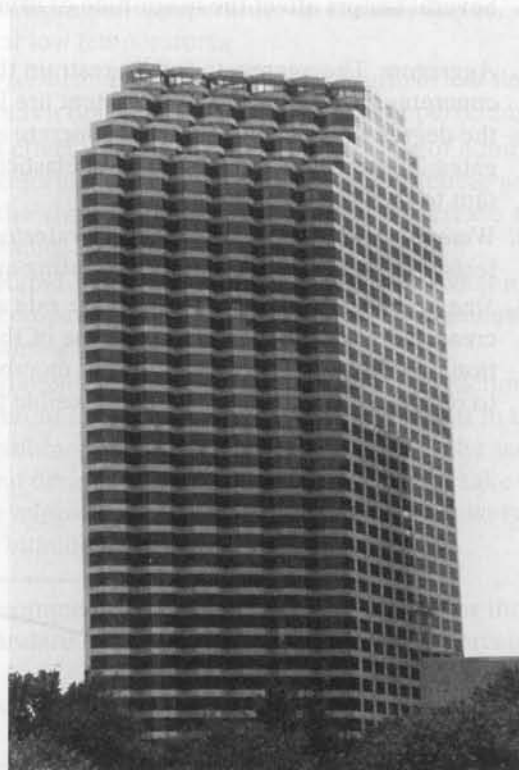
$$k_a = 1.25t^{-0.118} \quad (2.12)$$

- (b) For steam-cured concrete loaded at an age of 1 to 3 days or more,

$$k_a = 1.13t^{-0.095} \quad (2.13)$$

For greater than 40 percent relative humidity, a further multiplier correction factor of

$$k_{c_1} = 1.27 - 0.0067H \quad (2.14)$$



**Photo 2.5** Energy Center, New Orleans, Louisiana. (Courtesy, Post-Tensioning Institute.)

has to be applied in addition to those of Equations 2.12 and 2.13, where  $H$  = relative humidity value in percent.

## 2.5 SHRINKAGE

Basically, there are two types of shrinkage: plastic shrinkage and drying shrinkage. *Plastic shrinkage* occurs during the first few hours after placing fresh concrete in the forms. Exposed surfaces such as floor slabs are more easily affected by exposure to dry air because of their large contact surface. In such cases, moisture evaporates faster from the concrete surface than it is replaced by the bleed water from the lower layers of the concrete elements. *Drying shrinkage*, on the other hand, occurs after the concrete has already attained its final set and a good portion of the chemical hydration process in the cement gel has been accomplished.

Drying shrinkage is the decrease in the volume of a concrete element when it loses moisture by evaporation. The opposite phenomenon, that is, volume increase through water absorption, is termed *swelling*. In other words, shrinkage and swelling represent water movement out of or into the gel structure of a concrete specimen due to the difference in humidity or saturation levels between the specimen and the surroundings irrespective of the external load.

Shrinkage is not a completely reversible process. If a concrete unit is saturated with water after having fully shrunk, it will not expand to its original volume. Figure 2.13 relates the increase in shrinkage strain  $\epsilon_{sh}$  with time. The rate decreases with time since older concretes are more resistant to stress and consequently undergo less shrinkage, such that the shrinkage strain becomes almost asymptotic with time.

Several factors affect the magnitude of drying shrinkage:

1. *Aggregate.* The aggregate acts to restrain the shrinkage of the cement paste; hence, concretes with high aggregate content are less vulnerable to shrinkage. In addition, the degree of restraint of a given concrete is determined by the properties of aggregates: Those with a high modulus of elasticity or with rough surfaces are more resistant to the shrinkage process.
2. *Water/cement ratio.* The higher the water/cement ratio, the higher the shrinkage effects. Figure 2.14 is a typical plot relating aggregate content to water/cement ratio.
3. *Size of the concrete element.* Both the rate and the total magnitude of shrinkage decrease with an increase in the volume of the concrete element. However, the duration of shrinkage is longer for larger members since more time is needed for drying to reach the internal regions. It is possible that 1 year may be needed for the drying

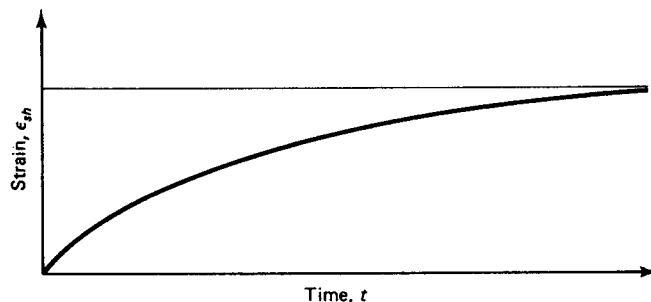
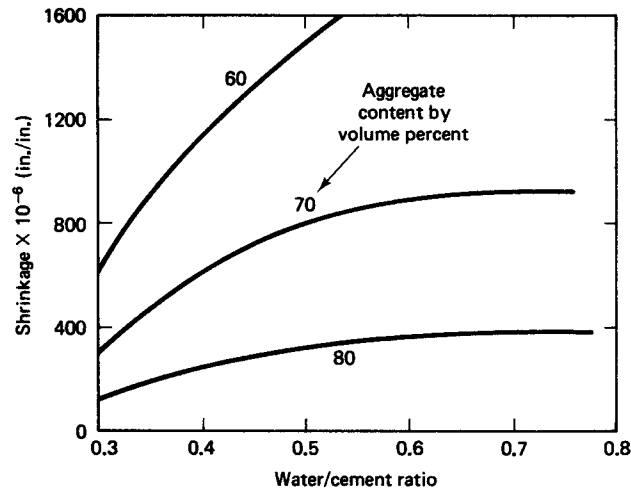


Figure 2.13 Shrinkage-time curve.



**Figure 2.14** w/c ratio and aggregate content effect on shrinkage.

process to begin at a depth of 10 in. from the exposed surface, and 10 years to begin at 24 in. below the external surface.

4. *Medium ambient conditions.* The relative humidity of the medium greatly affects the magnitude of shrinkage; the rate of shrinkage is lower at high states of relative humidity. The environment temperature is another factor, in that shrinkage becomes stabilized at low temperatures.
5. *Amount of reinforcement.* Reinforced concrete shrinks less than plain concrete; the relative difference is a function of the reinforcement percentage.
6. *Admixtures.* This effect varies depending on the type of admixture. An accelerator such as calcium chloride, used to accelerate the hardening and setting of the concrete, increases the shrinkage. Pozzolans can also increase the drying shrinkage, whereas air-entraining agents have little effect.
7. *Type of cement.* Rapid-hardening cement shrinks somewhat more than other types, while shrinkage-compensating cement minimizes or eliminates shrinkage cracking if used with restraining reinforcement.
8. *Carbonation.* Carbonation shrinkage is caused by the reaction between the carbon dioxide (CO<sub>2</sub>) present in the atmosphere and that present in the cement paste. The amount of the combined shrinkage varies according to the sequence of occurrence of carbonation and drying processes. If both phenomena take place simultaneously, less shrinkage develops. The process of carbonation, however, is dramatically reduced at relative humidities below 50 percent.

Branson (Ref. 2.18) recommends the following relationships for the shrinkage strain as a function of time for standard conditions of humidity ( $H \cong 40$  percent):

- (a) For moist-cured concrete any time  $t$  after 7 days,

$$\epsilon_{SH,t} = \frac{t}{35 + t} (\epsilon_{SH,u}) \quad (2.15)$$

where  $\epsilon_{SH,u} = 800 \times 10^{-6}$  in./in. if local data are not available.

(b) For steam-cured concrete after the age of 1 to 3 days,

$$\epsilon_{SH,t} = \frac{t}{55 + t} \epsilon_{SH,u} \quad (2.16)$$

For other than standard humidity, a correction factor has to be applied to Equations 2.15 and 2.16 as follows:

(a) For  $40 < H \leq 80$  percent,

$$k_{SH} = 1.40 - 0.010H \quad (2.17a)$$

(b) For  $80 < H \leq 100$  percent,

$$k_{SH} = 3.00 - 0.030H \quad (2.17b)$$

## 2.6 NONPRESTRESSING REINFORCEMENT

Steel reinforcement for concrete consists of bars, wires, and welded wire fabric, all of which are manufactured in accordance with ASTM standards. The most important properties of reinforcing steel are:

1. Young's modulus,  $E_s$
2. Yield strength,  $f_y$
3. Ultimate strength,  $f_u$
4. Steel grade designation
5. Size or diameter of the bar or wire

To increase the bond between concrete and steel, projections called *deformations* are rolled onto the bar surface as shown in Figure 2.15, in accordance with ASTM specifications. The deformations shown must satisfy ASTM Specification A616-76 for the bars to be accepted as deformed. Deformed wire has indentations pressed into the wire or bar to serve as deformations. Except for wire used in spiral reinforcement in columns, only deformed bars, deformed wires, or wire fabric made from smooth or deformed wire may be used in reinforced concrete under approved practice.

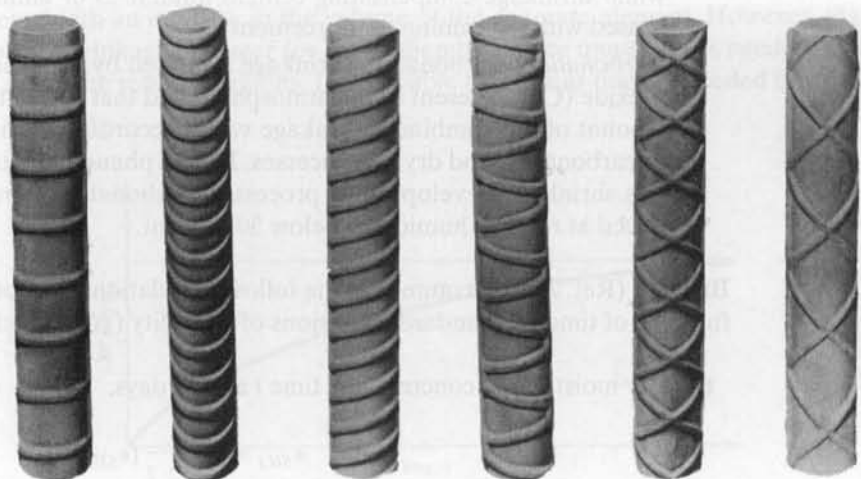
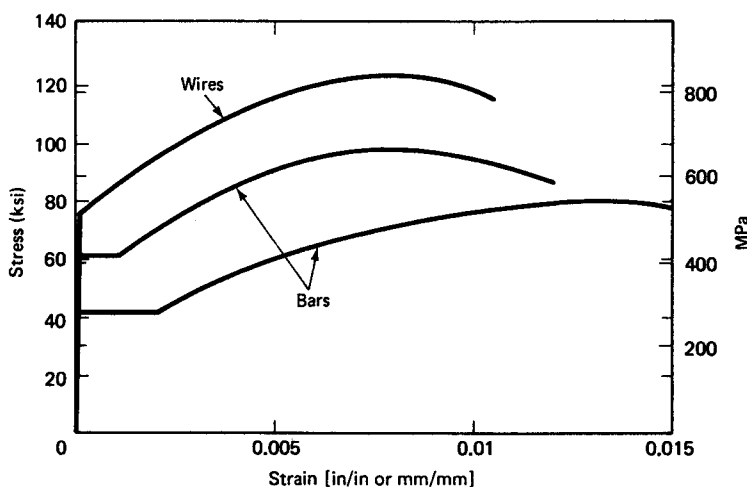


Figure 2.15 Various forms of ASTM-approved deformed bars.



**Figure 2.16** Typical stress-strain diagrams for various nonprestressing steels.

Figure 2.16 shows typical stress-strain curves for grades 40, 60, and 75 steels. These have corresponding yield strengths of 40,000, 60,000, and 75,000 psi (276, 345, and 517 N/mm<sup>2</sup>, respectively) and generally have well-defined yield points. For steels that lack a well-defined yield point, the yield-strength value is taken as the strength corresponding to a unit strain of 0.005 for grades 40 and 60 steels, and 0.0035 for grade 80 steel. The ultimate tensile strengths corresponding to the 40, 60, and 80 grade steels are 70,000, 90,000, and 100,000 psi (483, 621, and 690 N/mm<sup>2</sup>), respectively, and some steel types are given in Table 2.3. The percent elongation at fracture, which varies with the grade, bar diameter, and manufacturing source, ranges from 4.5 to 12 percent over an 8-in. (203.2-mm) gage length.

Welded wire fabric is increasingly used for slabs because of the ease of placing the fabric sheets, the control over reinforcement spacing, and the better bond. The fabric reinforcement is made of smooth or deformed wires which run in perpendicular directions

**Table 2.3** Reinforcement Grades and Strengths

1982 Standard type	Minimum yield point or yield strength, $f_y$ (psi)	Ultimate strength, $f_u$ (psi)
Billet steel (A615)		
Grade 40	40,000	70,000
Grade 60	60,000	90,000
Axle steel (A617)		
Grade 40	40,000	70,000
Grade 60	60,000	90,000
Low-alloy steel (A706): Grade 60	60,000	80,000
Deformed wire		
Reinforced	75,000	85,000
Fabric	70,000	80,000
Smooth wire		
Reinforced	70,000	80,000
Fabric	65,000, 56,000	75,000, 70,000

**Table 2.4 Standard Wire Reinforcement**

W&D size		U.S. customary				Area (in. <sup>2</sup> /ft of width for various spacings)					
		Nominal diameter (in.)	Nominal area (in. <sup>2</sup> )	Nominal weight (lb/ft)	Center-to-center spacing (in.)						
Smooth	Deformed				2	3	4	6	8	10	12
W31	D31	0.628	0.310	1.054	1.86	1.24	0.93	0.62	0.465	0.372	0.31
W30	D30	0.618	0.300	1.020	1.80	1.20	0.90	0.60	0.45	0.366	0.30
W28	D28	0.597	0.280	0.952	1.68	1.12	0.84	0.56	0.42	0.336	0.28
W26	D26	0.575	0.260	0.934	1.56	1.04	0.78	0.52	0.39	0.312	0.26
W24	D24	0.553	0.240	0.816	1.44	0.96	0.72	0.48	0.36	0.288	0.24
W22	D22	0.529	0.220	0.748	1.32	0.88	0.66	0.44	0.33	0.264	0.22
W20	D20	0.504	0.200	0.680	1.20	0.80	0.60	0.40	0.30	0.24	0.20
W18	D18	0.478	0.180	0.612	1.08	0.72	0.54	0.36	0.27	0.216	0.18
W16	D16	0.451	0.160	0.544	0.96	0.64	0.48	0.32	0.24	0.192	0.16
W14	D14	0.422	0.140	0.476	0.84	0.56	0.42	0.28	0.21	0.168	0.14
W12	D12	0.390	0.120	0.408	0.72	0.48	0.36	0.24	0.18	0.144	0.12
W11	D11	0.374	0.110	0.374	0.66	0.44	0.33	0.22	0.165	0.132	0.11
W10.5		0.366	0.105	0.357	0.63	0.42	0.315	0.21	0.157	0.126	0.105
W10	D10	0.356	0.100	0.340	0.60	0.40	0.30	0.20	0.15	0.12	0.10
W9.5		0.348	0.095	0.323	0.57	0.38	0.285	0.19	0.142	0.114	0.095
W9	D9	0.338	0.090	0.306	0.54	0.36	0.27	0.18	0.135	0.108	0.09
W8.5		0.329	0.085	0.289	0.51	0.34	0.255	0.17	0.127	0.102	0.085
W8	D8	0.319	0.080	0.272	0.48	0.32	0.24	0.16	0.12	0.096	0.08
W7.5		0.309	0.075	0.255	0.45	0.30	0.225	0.15	0.112	0.09	0.075
W7	D7	0.298	0.070	0.238	0.42	0.28	0.21	0.14	0.105	0.084	0.07
W6.5		0.288	0.065	0.221	0.39	0.26	0.195	0.13	0.097	0.078	0.065
W6	D6	0.276	0.060	0.204	0.36	0.24	0.18	0.12	0.09	0.072	0.06
W5.5		0.264	0.055	0.187	0.33	0.22	0.165	0.11	0.082	0.066	0.055
W5	D5	0.252	0.050	0.170	0.30	0.20	0.15	0.10	0.075	0.06	0.05
W4.5		0.240	0.045	0.153	0.27	0.18	0.135	0.09	0.067	0.054	0.045
W4	D4	0.225	0.040	0.136	0.24	0.16	0.12	0.08	0.06	0.048	0.04
W3.5		0.211	0.035	0.119	0.21	0.14	0.105	0.07	0.052	0.042	0.035
W3		0.195	0.030	0.102	0.18	0.12	0.09	0.06	0.045	0.036	0.03
W2.9		0.192	0.029	0.098	0.17	0.116	0.087	0.058	0.043	0.035	0.029
W2.5		0.178	0.025	0.085	0.15	0.10	0.075	0.05	0.037	0.03	0.025
W2		0.159	0.020	0.068	0.12	0.08	0.06	0.04	0.03	0.024	0.02
W1.4		0.135	0.014	0.049	0.084	0.056	0.042	0.028	0.021	0.017	0.014

**Table 2.5** Weight, Area, and Perimeter of Individual Bars

Bar designation number	Weight per foot (lb)	Standard nominal dimensions		
		Diameter, $d_b$ [in. (mm)]	Cross-sectional area, $A_b$ (in. <sup>2</sup> )	Perimeter (in.)
3	0.376	0.375 (10)	0.11	1.178
4	0.668	0.500 (13)	0.20	1.571
5	1.043	0.625 (16)	0.31	1.963
6	1.502	0.750 (19)	0.44	2.356
7	2.044	0.875 (22)	0.60	2.749
8	2.670	1.000 (25)	0.79	3.142
9	3.400	1.128 (29)	1.00	3.544
10	4.303	1.270 (32)	1.27	3.990
11	5.313	1.410 (36)	1.56	4.430
14	7.65	1.693 (43)	2.25	5.32
18	13.60	2.257 (57)	4.00	7.09

and are welded together at intersections. Table 2.4 presents geometrical properties for some standard wire reinforcement.

For most mild steels, the behavior is assumed to be elastoplastic and Young's modulus is taken as  $29 \times 10^6$  psi ( $200 \times 10^6$  MPa). Table 2.3 presents the reinforcement-grade strengths, and Table 2.5 presents geometrical properties of the various sizes of bars.

## 2.7 PRESTRESSING REINFORCEMENT

### 2.7.1 Types of Reinforcement

Because of the high creep and shrinkage losses in concrete, effective prestressing can be achieved by using very high-strength steels in the range of 270,000 psi or more (1,862 MPa or higher). Such high-stressed steels are able to counterbalance these losses in the



**Photo 2.6** Prestressed concrete Valdez floating dock. Designed by ABAM Engineers, built in two pieces in Tacoma, Washington, then towed to Alaska by deployment. (Courtesy, ABAM Engineers, Tacoma, Washington.)



surrounding concrete and have adequate leftover stress levels to sustain the required prestressing force. The magnitude of normal prestress losses can be expected to be in the range of 35,000 to 60,000 psi (241 to 414 MPa). The initial prestress would thus have to be very high, on the order of 180,000 to 220,000 psi (1,241 to 1,517 MPa). From the aforementioned magnitude of prestress losses, it can be inferred that normal steels with yield strengths  $f_y = 60,000$  psi (414 MPa) would have little prestressing stress left after losses, obviating the need for using very high-strength steels for prestressing concrete members.

Prestressing reinforcement can be in the form of single wires, strands composed of several wires twisted to form a single element, and high-strength bars. Three types commonly used in the United States are:

- Uncoated stress-relieved or low-relaxation wires.
- Uncoated stress-relieved strands and low-relaxation strands.
- Uncoated high-strength steel bars.

Wires or strands that are not stress-relieved, such as the straightened wires or oil-tempered wires often used in other countries, exhibit higher relaxation losses than stress-relieved wires or strands. Consequently, it is important to account for the appropriate magnitude of losses once a determination is made on the type of prestressing steel required.

## 2.7.2 Stress-Relieved and Low-Relaxation Wires and Strands

Stress-relieved wires are cold-drawn single wires conforming to ASTM standard A421; stress-relieved strands conform to ASTM standard A 416. The strands are made from seven wires by twisting six of them on a pitch of 12- to 16-wire diameter around a slightly larger, straight control wire. Stress-relieving is done after the wires are woven into the strand. The geometrical properties of the wires and strands as required by ASTM are given in Tables 2.6 and 2.7, respectively.

To maximize the steel area of the 7-wire strand for any nominal diameter, the standard wire can be drawn through a die to form a *compacted* strand as shown in Figure 2.17(b); this is opposed to the standard 7 wire strand in Figure 2.17(a). ASTM standard A 779 requires the minimum strengths and geometrical properties given in Table 2.8.

Figure 2.18(a) shows a typical stress-strain diagram for wire and strand prestressing steels, while Figure 2.18(b) shows values relative to those of mild steel.

**Table 2.6** Wire for Prestressed Concrete

Nominal diameter (in.)	Min. tensile strength (psi)		Min. stress at 1% extension (psi)	
	Type BA	Type WA	Type BA	Type WA
0.192		250,000		212,500
0.196	240,000	250,000	204,000	212,500
0.250	240,000	240,000	204,000	204,000
0.276	235,000	235,000	199,750	199,750

Source: Post-Tensioning Institute

**Table 2.7** Seven-Wire Standard Strand for Prestressed Concrete

Nominal diameter of strand (in.)	Breaking strength of strand (min. lb)	Nominal steel area of strand (sq in.)	Nominal weight of strands (lb per 1000 ft)*	Minimum load at 1% extension (lb)
GRADE 250				
$\frac{1}{4}$ (0.250)	9,000	0.036	122	7,650
$\frac{5}{16}$ (0.313)	14,500	0.058	197	12,300
$\frac{3}{8}$ (0.375)	20,000	0.080	272	17,000
$\frac{7}{16}$ (0.438)	27,000	0.108	367	23,000
$\frac{1}{2}$ (0.500)	36,000	0.144	490	30,600
$\frac{3}{5}$ (0.600)	54,000	0.216	737	45,900
GRADE 270				
$\frac{3}{8}$ (0.375)	23,000	0.085	290	19,550
$\frac{7}{16}$ (0.438)	31,000	0.115	390	26,350
$\frac{1}{2}$ (0.500)	41,300	0.153	520	35,100
$\frac{3}{5}$ (0.600)	58,600	0.217	740	49,800

\*100,000 psi = 689.5 MPa

0.1 in. = 2.54 mm; 1 in.<sup>2</sup> = 645 mm<sup>2</sup>

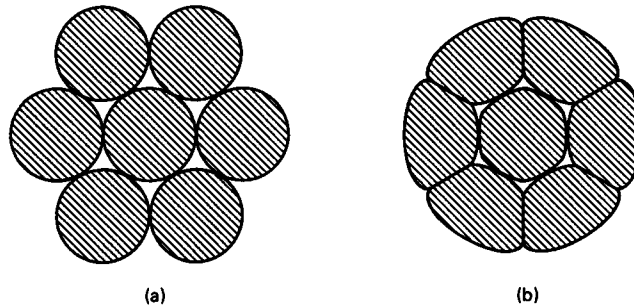
weight: mult. by 1.49 to obtain weight in kg per 1,000 m.

1,000 lb = 4,448 Newton

Source: Post-Tensioning Institute

### 2.7.3 High-Tensile-Strength Prestressing Bars

High-tensile-strength alloy steel bars for prestressing are either smooth or deformed, and are available in nominal diameters from  $\frac{3}{4}$  in. (19 mm) to  $1\frac{3}{8}$  in. (35 mm). They must conform to ASTM standard A 722. Cold drawn in order to raise their yield strength, these bars are stress relieved as well to increase their ductility. Stress relieving is achieved by heating the bar to an appropriate temperature, generally below 500°C. Though essentially the same stress-relieving process is employed for bars as for strands, the tensile strength of prestressing bars has to be a minimum of 150,000 psi (1,034 MPa), with a minimum yield strength of 85 percent of the ultimate strength for smooth bars and 80 percent for deformed bars.



**Figure 2.17** Standard and compacted 7-wire prestressing strands. (a) Standard strand section. (b) Compacted strand section.

**Table 2.8** Seven-Wire Compacted Strand for Prestressed Concrete [ASTM A779]

Nominal diameter (in.)	Nominal Breaking strength of strand (min. lb)*	Nominal steel area (in. <sup>2</sup> )	Nominal weight of strand (per 1,000 ft-lb)
$\frac{1}{2}$	47,000	0.174	600
0.6	67,440	0.256	873
0.7	85,430	0.346	1176

\*1000 lb = 4,448 Newton

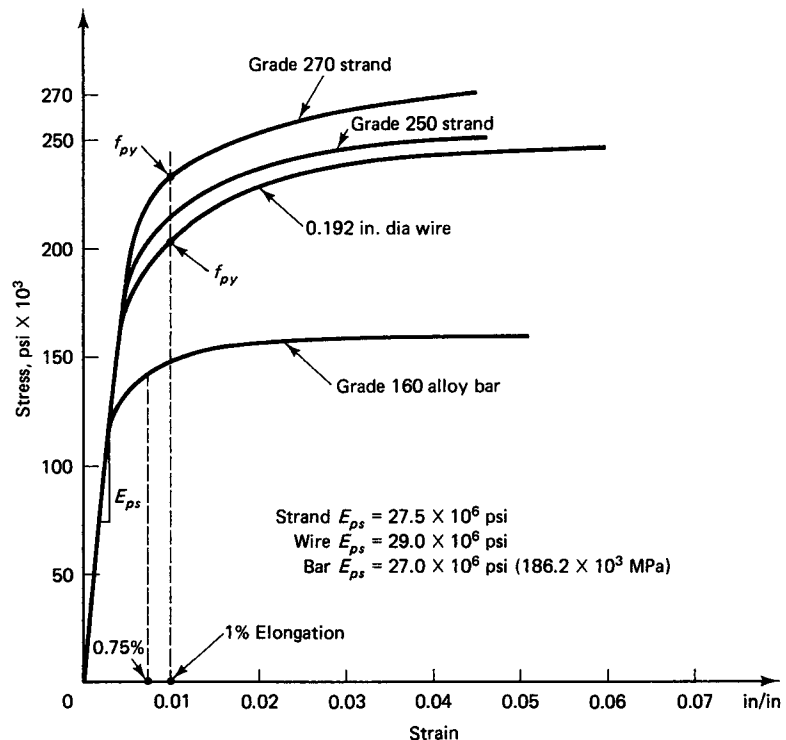
Grade 270;  $f_{pu} = 270,000$  psi ult. strength (1,862 MPa)

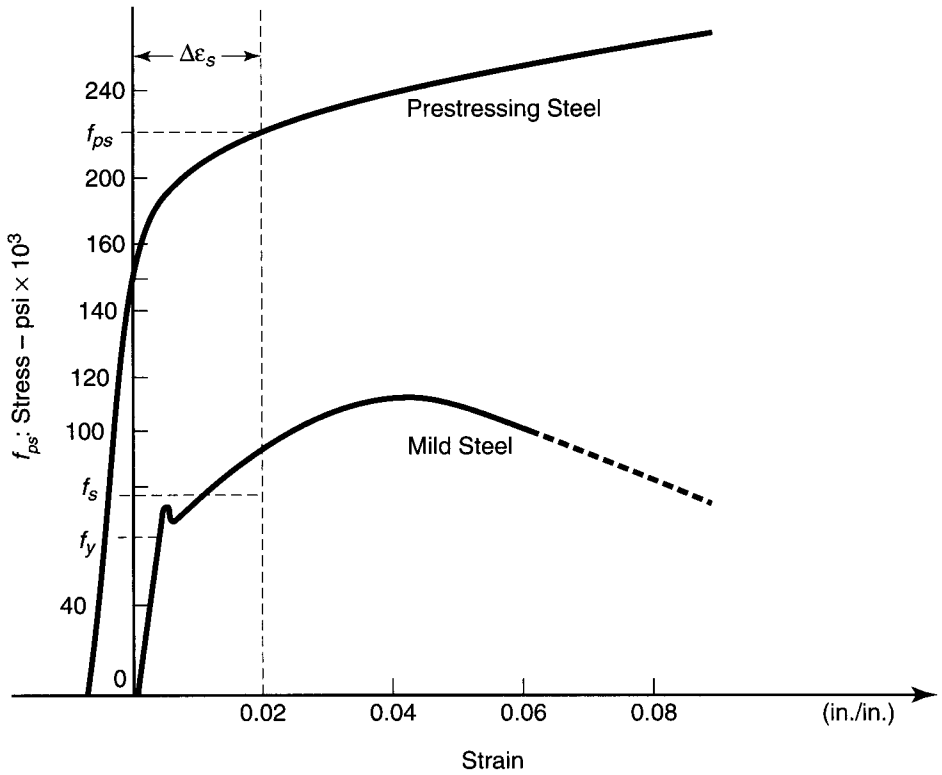
1 in. = 25.4 mm; 1 in.<sup>2</sup> = 645 mm<sup>2</sup>

Table 2.9 lists the geometrical properties of the prestressing bar as required by ASTM standard A 722, and Figure 2.18 shows a typical stress-strain diagram for such bars.

### 2.7.4 Steel Relaxation

Stress relaxation in prestressing steel is the loss of prestress when the wires or strands are subjected to essentially constant strain. It is identical to creep in concrete, except that creep is a *change* in strain whereas steel relaxation is a *loss in steel stress*. Where  $t =$  time,

**Figure 2.18a** Stress-strain diagram for prestressing steel.



**Figure 2.18(b)** Stress-Strain Diagram for Prestressing Steel Strands in Comparison with Mild Steel Bar Reinforcement.

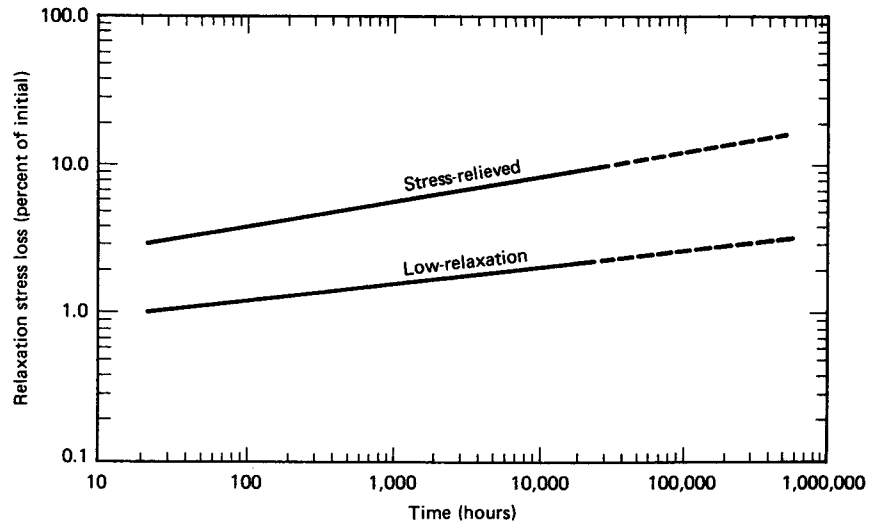
in hours, after prestressing, the loss of stress due to relaxation in stress-relieved wires and strands can be evaluated from the expression

$$\Delta f_R = f_{pi} \frac{\log t}{10} \left( \frac{f_{pi}}{f_{py}} - 0.55 \right) \tag{2.18}$$

**Table 2.9** Steel Bars for Prestressed Concrete

Bar type*	Nominal diameter (in.)	Nominal steel area (in. <sup>2</sup> )
Smooth Alloy	0.750	0.442
Steel Grade	0.875	0.601
145 or 160	1.000	0.785
(ASTM A722)	1.125	0.994
	1.250	1.227
	1.375	1.485
Deformed	0.625	0.280
Bars	1.000	0.852
	1.250	1.295

\*Grade 145:  $f_{pu} = 145,000$  psi (1,000 MPa)  
 Grade 160:  $f_{pu} = 160,000$  psi (1,103 MPa)  
 1 in. = 25.4 mm; 1 in.<sup>2</sup> = 645 mm<sup>2</sup>



**Figure 2.19** Relaxation loss vs. time for stress-relieved low-relaxation prestressing steels at 70 percent of the ultimate. (Courtesy, Post-Tensioning Institute.)

provided that  $f_p/f_{py} \geq 0.55$  and  $f_{py} \cong 0.85 f_{pu}$  for stress-relieved strands and 0.90 for low-relaxation strands. Also,  $f_{pi} = 0.82 f_{py}$  immediately after transfer but  $f_{pi} \leq 0.74 f_{pu}$  for pre-tensioned, and  $0.70 f_{pu}$  for post-tensioned, concrete. In general,  $f_{pi} \cong 0.70 f_{pu}$ .

It is possible to decrease stress relaxation loss by subjecting strands that are initially stressed to 70 percent of their ultimate strength  $f_{pu}$  to temperatures of 20°C to 100°C for an extended time in order to produce a permanent elongation—a process called *stabilization*. The prestressing steel thus produced is termed *low-relaxation steel* and has a relaxation stress loss that is 25 percent of that of normal stress-relieved steel.

The expression for stress relaxation in low-relaxation prestressing steels is

$$\Delta f_R = f_{pi} \frac{\log t}{45} \left( \frac{f_{pi}}{f_{py}} - 0.55 \right) \quad (2.19)$$

Figure 2.19 shows the relative relaxation loss for stress-relieved and low-relaxation steels for 7-wire strands held at constant length at 29.5°C.

### 2.7.5 Corrosion and Deterioration of Strands

Protection against corrosion of prestressing steel is more critical than in the case of non-prestressed steel. Such precaution is necessary since the strength of the prestressed concrete element is a function of the prestressing force, which in turn is a function of the prestressing tendon area. Reduction of the prestressing steel area due to corrosion can drastically reduce the nominal moment strength of the prestressed section, which can lead to premature failure of the structural system. In pretensioned members, protection against corrosion is provided by the concrete surrounding the tendon, provided that adequate concrete cover is available. In post-tensioned members, protection can be obtained by full grouting of the ducts after prestressing is completed or by greasing.

Another form of wire or strand deterioration is *stress corrosion*, which is characterized by the formation of microscopic cracks in the steel which lead to brittleness and fail-

ure. This type of reduction in strength can occur only under very high stress and, though infrequent, is difficult to prevent.

## 2.8 ACI MAXIMUM PERMISSIBLE STRESSES IN CONCRETE AND REINFORCEMENT

Following are definitions of some important mathematical terms used in this section:

- $f_{py}$  = specified yield strength of prestressing tendons, in psi
- $f_y$  = specified yield strength of nonprestressed reinforcement, in psi
- $f_{pu}$  = specified tensile strength of prestressing tendons, in psi
- $f'_c$  = specified compressive strength of concrete, in psi
- $f'_{ci}$  = compressive strength of concrete at time of initial prestress

### 2.8.1 Concrete Stresses in Flexure

Stresses in concrete immediately after prestress transfer (before time-dependent prestress losses) shall not exceed the following:

- (a) Extreme fiber stress in compression . . . . .  $0.60 f'_{ci}$
- (b) Extreme fiber stress in tension except as permitted in (c) . . . . .  $3\sqrt{f'_{ci}}$
- (c) Extreme fiber stress in tension at ends of simply supported members . . . . .  $6\sqrt{f'_{ci}}$

Where computed tensile stresses exceed these values, bonded auxiliary reinforcement (nonprestressed or prestressed) shall be provided in the tensile zone to resist the total tensile force in concrete computed under the assumption of an uncracked section.

Stresses in concrete at service loads (after allowance for all prestress losses) shall not exceed the following:

- (a) Extreme fiber stress in compression due to prestress plus sustained load, where sustained dead load and live load are a large part of the total service load . . . . .  $0.45 f'_c$
- (b) Extreme fiber stress in compression due to prestress plus total load, if the live load is transient . . . . .  $0.60 f'_c$
- (c) Extreme fiber stress in tension in precompressed tensile zone. . . . .  $6\sqrt{f'_c}$
- (d) Extreme fiber stress in tension in precompressed tensile zone of members (except two-way slab systems), where analysis based on transformed cracked sections and on bilinear moment-deflection relationships shows that immediate and long-time deflections comply with the ACI definition requirements and minimum concrete cover requirements . . . . .  $12\sqrt{f'_c}$

### 2.8.2 Prestressing Steel Stresses

Tensile stress in prestressing tendons shall not exceed the following:

- (a) Due to tendon jacking force . . . . .  $0.94 f_{py}$   
but not greater than the lesser of  $0.80 f_{pu}$  and the maximum value recommended by the manufacturer of prestressing tendons or anchorages.
- (b) Immediately after prestress transfer. . . . .  $0.82 f_{py}$   
but not greater than  $0.74 f_{pu}$ .
- (c) Post-tensioning tendons, at anchorages and couplers, immediately after tendon anchorage . . . . .  $0.70 f_{pu}$

**2.9 AASHTO MAXIMUM PERMISSIBLE STRESSES IN CONCRETE AND REINFORCEMENT**

**2.9.1 Concrete Stresses before Creep and Shrinkage Losses**

Compression	
Pretensioned members . . . . .	$0.60 f'_{ci}$
Post-tensioned members . . . . .	$0.55 f'_{ci}$
Tension	
Precompressed tensile zone . . . . .	No temporary allowable stresses are specified.
Other Areas	
In tension areas with no bonded reinforcement. . . . .	200 psi or $3\sqrt{f'_{ci}}$
Where the calculated tensile stress exceeds this value, bonded reinforcement shall be provided to resist the total tension force in the concrete computed on the assumption of an uncracked section. The maximum tensile stress shall not exceed . . . . .	
	$7.5\sqrt{f'_{ci}}$

**2.9.2 Concrete Stresses at Service Load after Losses**

Compression . . . . .	$0.40 f'_c$
Tension in the precompressed tensile zone	
(a) For members with bonded reinforcement . . . . .	$6\sqrt{f'_c}$
For severe corrosive exposure conditions, such as coastal areas . . . . .	$3\sqrt{f'_c}$
(b) For members without bonded reinforcement . . . . .	0

Tension in other areas is limited by the allowable temporary stresses specified in Section 2.8.1.

**2.9.2.1 Cracking Stresses.** Modulus of rupture from tests or if not available.

For normal-weight concrete . . . . .	$7.5\sqrt{f'_c}$
For sand-lightweight concrete . . . . .	$6.3\sqrt{f'_c}$
For all other lightweight concrete . . . . .	$5.5\sqrt{f'_c}$

**2.9.2.2 Anchorage-Bearing Stresses**

Post-tensioned anchorage at service load . . . . . 3,000 psi  
(but not to exceed  $0.9 f'_{ci}$ )

**2.9.3 Prestressing Steel Stresses**

- (a) Due to tendon jacking for . . . . .  $0.94 f_{py} \leq 0.80 f_{pu}$
- (b) Immediately after prestress transfer . . . . .  $0.82 f_{py} \leq 0.74 f_{pu}$
- (c) Post-tensioning tendons at anchorage, immediately after tendon anchorage . . . . .  $0.70 f_{pu}$   
 $f_{py} \approx 0.85 f_{pu}$  (for low-relaxation,  $f_{py} = 0.90 f_{pu}$ )

Hence for 270 K tendons used in the book,  $f_{pi}$  at transfer =  $0.70 \times 270,000 = 189,000$  psi (1300 MPa) is applied for uniformity.

**2.9.4 Relative Humidity Values**

Figure 2.20 gives the mean annual relative humidity values for all regions in the United States in percent, to be used for evaluating shrinkage losses in concrete.

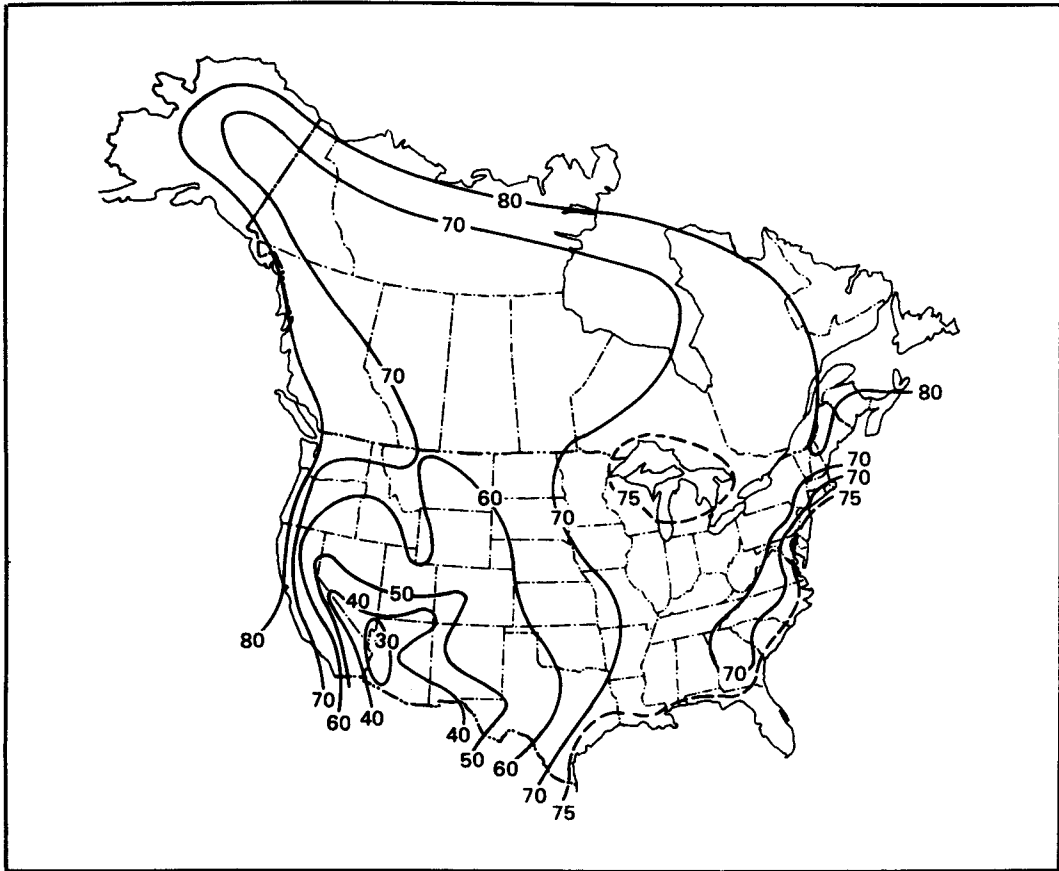


Figure 2.20 Mean annual relative humidity. (Courtesy, Prestressed Concrete Institute.)

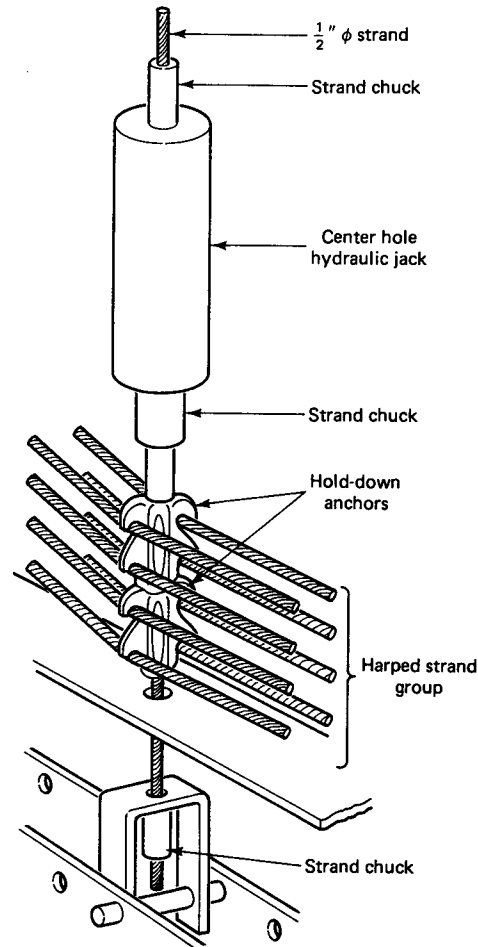
## 2.10 PRESTRESSING SYSTEMS AND ANCHORAGES

### 2.10.1 Pretensioning

Prestressing steel is pretensioned against independent anchorages *prior to* the placement of concrete around it. Such anchorages are supported by large and stable bulkheads to support the exceedingly high concentrated forces applied to the individual tendons. The term “pretensioning” means pretensioning of the prestressing steel, not the beam it serves. Consequently, a *pretensioned beam* is a prestressed beam in which the prestressing tendon is tensioned prior to casting the section, while a *post-tensioned beam* is one in which the prestressing tendon is tensioned after the beam has been cast and has achieved the major portion of its concrete strength. Pretensioning is normally performed at pre-casting plants, where a precasting stressing bed of a long reinforced concrete slab is cast on the ground with vertical anchor bulkheads or walls at its ends. The steel strands are stretched and anchored to the vertical walls, which are designed to resist the large eccentric prestressing forces. Prestressing can be accomplished by prestressing *individual* strands, or *all* the strands at one jacking operation.

For harped tendon profiles, the prestressing bed is provided with hold-down devices as shown in Figure 2.21. Since the bed can be several hundred feet long, several pre-cast prestressed elements can be produced in one operation, and the exposed prestressing strands between them can be cut after the concrete hardens. Pretensioning





**Figure 2.21** Hold-down anchor for harping pretensioning tendons. (Courtesy, Post-Tensioning Institute.)

several elements in a prestressing bed is represented schematically in Figure 2.22, while harping of tendons in a prestressing bed system is shown in Figure 2.23.

In pretensioning, strands and single wires are anchored by several patented systems. One of these, a chuck system by Supreme Products, is used for anchoring tendons in post-tensioning. The gripping mechanism of this system is illustrated in Figure 2.24(c). Other anchorage systems and ductile connections are shown in Figure 2.24(d), (e), and (f). A prestressing bed for moderately sized pretensioned beams up to 24 ft (7.32 m) long was developed and used by the author in Ref. 2.31 for his continuing work on the behavior of pretensioned and post-tensioned structural systems. Supreme Products anchorage chucks have been used together with the Freyssinet jack, where applicable. Figures 2.25 and 2.26 give details of the prestressing bed system also used for post-tensioning developed by Nawy and Potyondy at Rutgers University, while Figure 2.27 shows the dimensional details of the system.

### 2.10.2 Post-Tensioning

In post-tensioning, the strands, wires, or bars are tensioned after hardening of the concrete. The strands are placed in the longitudinal ducts within the precast concrete ele-

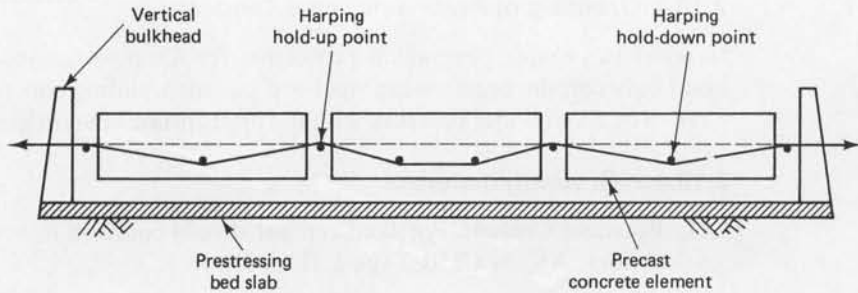


Figure 2.22 Schematic of prestressing bed.

ment. The prestressing force is transferred through end anchorages such as the Supreme Products chucks shown in Figure 2.24. The tendons of strands should *not* be bonded or grouted prior to full prestressing.

### 2.10.3 Jacking Systems

One of the fundamental components of a prestressing operation is the jacking system applied, i.e., the manner in which the prestressing force is transferred to the steel tendons. Such a force is applied through the use of hydraulic jacks of capacity 10 to 20 tons and a stroke from 6 to 48 in., depending on whether prestressing or post-tensioning is used and whether individual tendons are being prestressed or all the tendons are being stressed simultaneously. In the latter case, large-capacity jacks are needed, with a stroke of at least 30 in. (762 mm). Of course, the cost will be higher than sequential tensioning. Figure 2.28 shows a 500-ton multistrand jack for simultaneous jacking through a center hole.



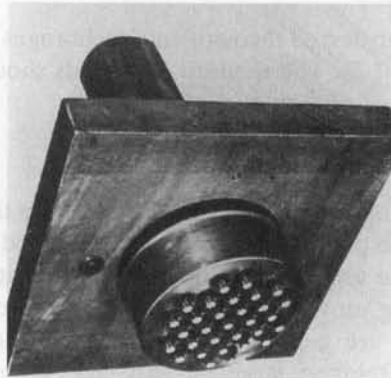
Figure 2.23 Harping of tendons in a prestressing bed system.

### 2.10.4 Grouting of Post-Tensioned Tendons

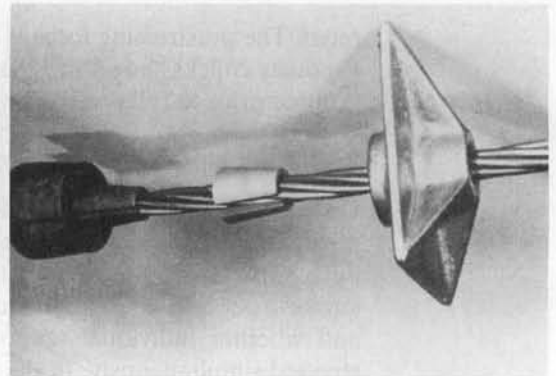
In order to provide permanent protection for the post-tensioned steel and to develop a bond between the prestressing steel and the surrounding concrete, the prestressing ducts have to be filled under pressure with the appropriate cement grout in an injection process.

#### 2.10.4.1 Grouting materials

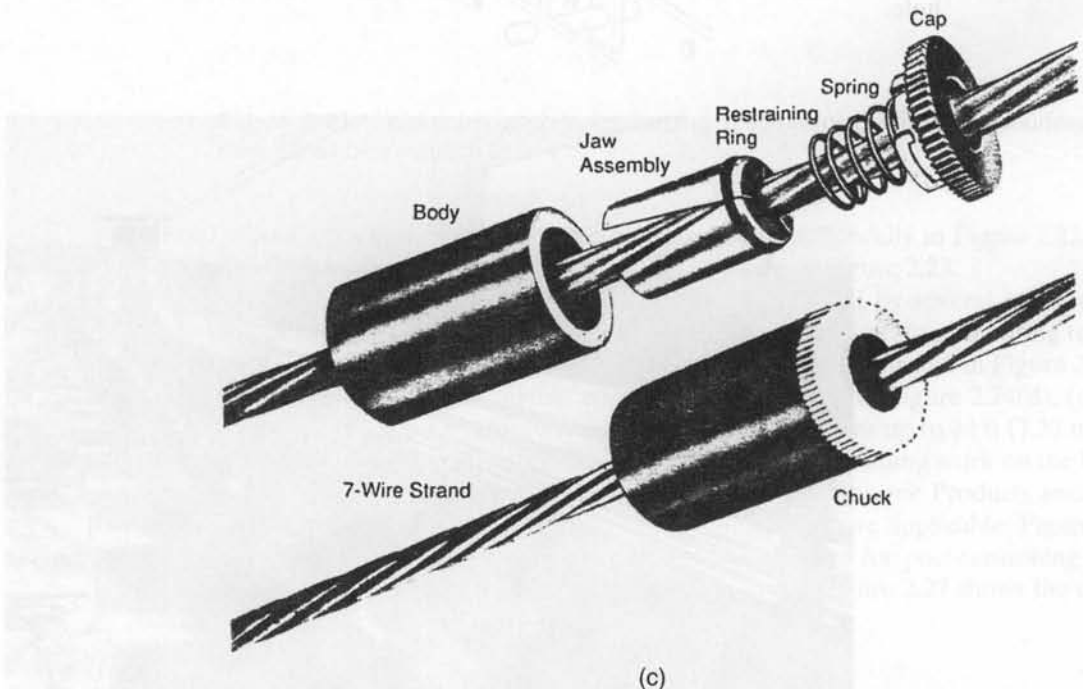
- 1. Portland Cement.** Portland cement should conform to one of the following specifications: ASTM C150, Type I, II, or III.



(a) Strand anchor.



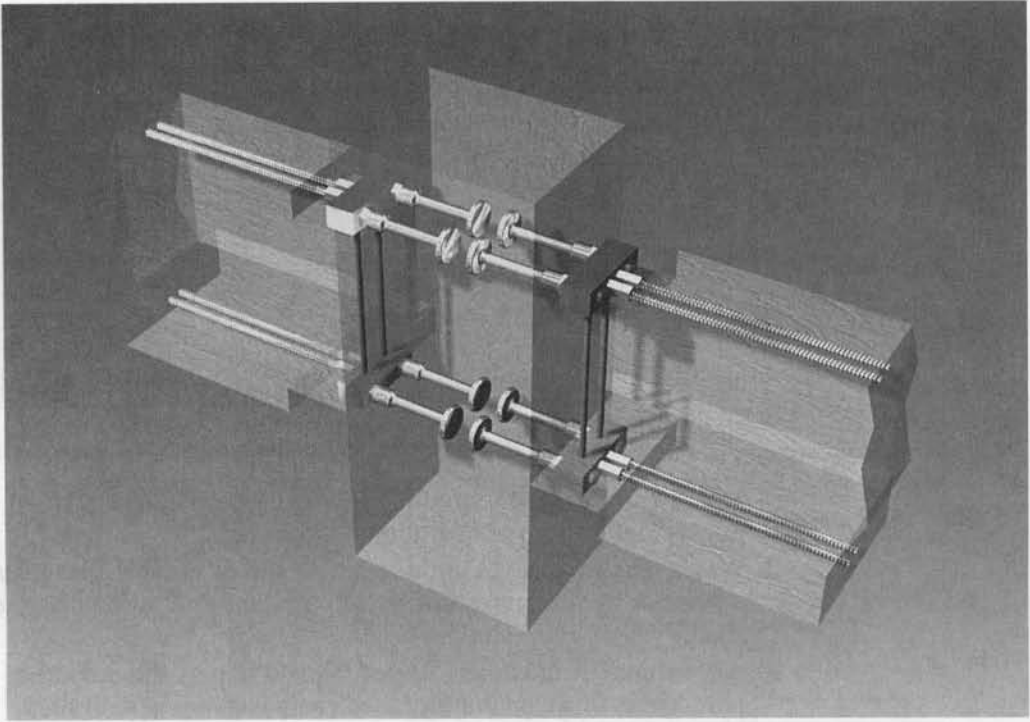
(b) Monostrand anchor.



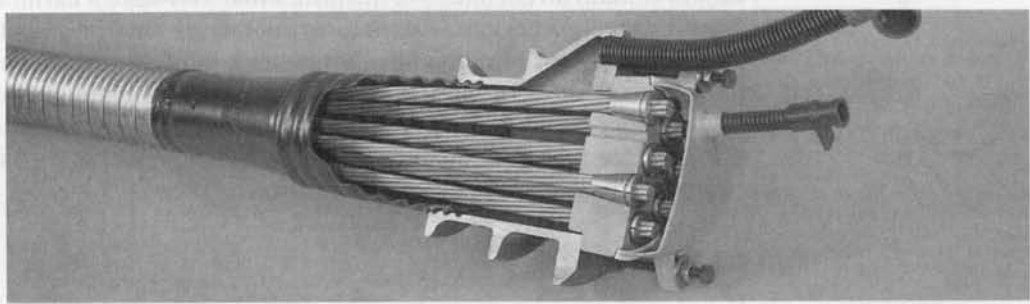
(c)

**Figure 2.24** (a) Stress Strand Anchor, (b) Monostrand anchor, (c) Supreme Products anchorage chuck. (Courtesy, Post-Tensioning Institute.)

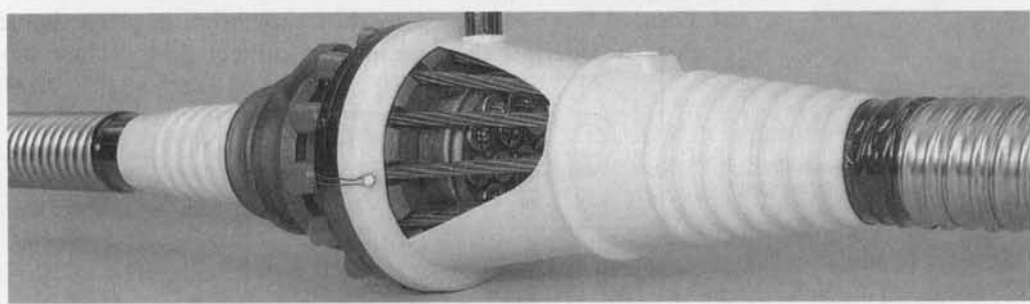
(d)



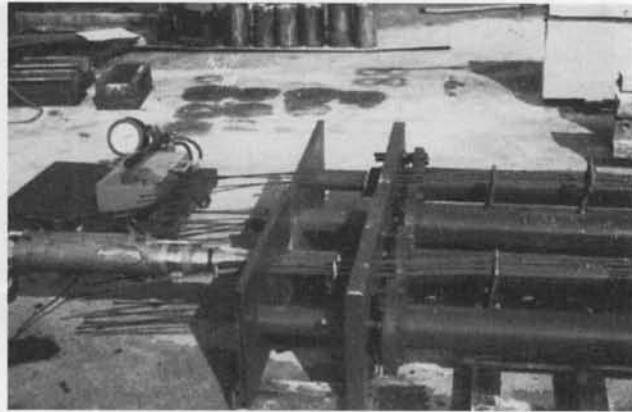
(e)



(f)



**Figure 2.24** (continued) Multiple anchorages, couplers and ductile connectors (Courtesy Dywidag Systems International): (d) Multiple anchorage, (e) Coupler, (f) Dywidag ductile connectors (DDC) for ductile precast beam-column connections in seismic zones. See also details in Figures 13.9 and 13.10.



**Figure 2.25** Prestress tensioning arrangement (Nawy et al.).

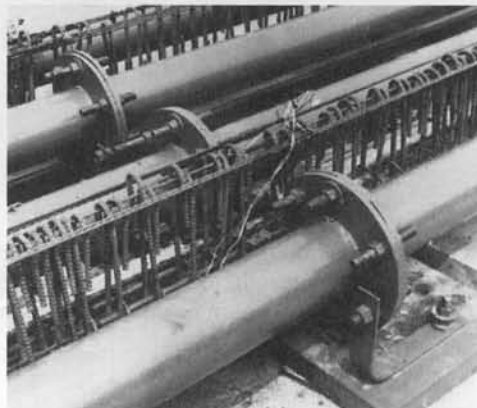
Cement used for grouting should be fresh and should not contain any lumps or other indications of hydration or “pack set.”

2. **Water.** The water used in the grout should be potable, clean, and free of injurious quantities of substances known to be harmful to portland cement or prestressing steel.
3. **Admixtures.** Admixtures, if used, should impart the properties of low water content, good flow, minimum bleed, and expansion if desired. Their formulation should contain no chemicals in quantities that may have a harmful effect on the prestressing steel or cement. Admixtures containing chlorides (as Cl in excess of 0.5 percent by weight of admixture, assuming 1 lb of admixture per sack of cement), fluorides, sulphites, or nitrates should not be used. Aluminum powder of the proper fineness and quantity, or any other approved gas-evolving material which is well dispersed through the other admixture, may be used to obtain 5 to 10 percent unrestrained expansion of the grout (see Refs. 2.11, 2.38).

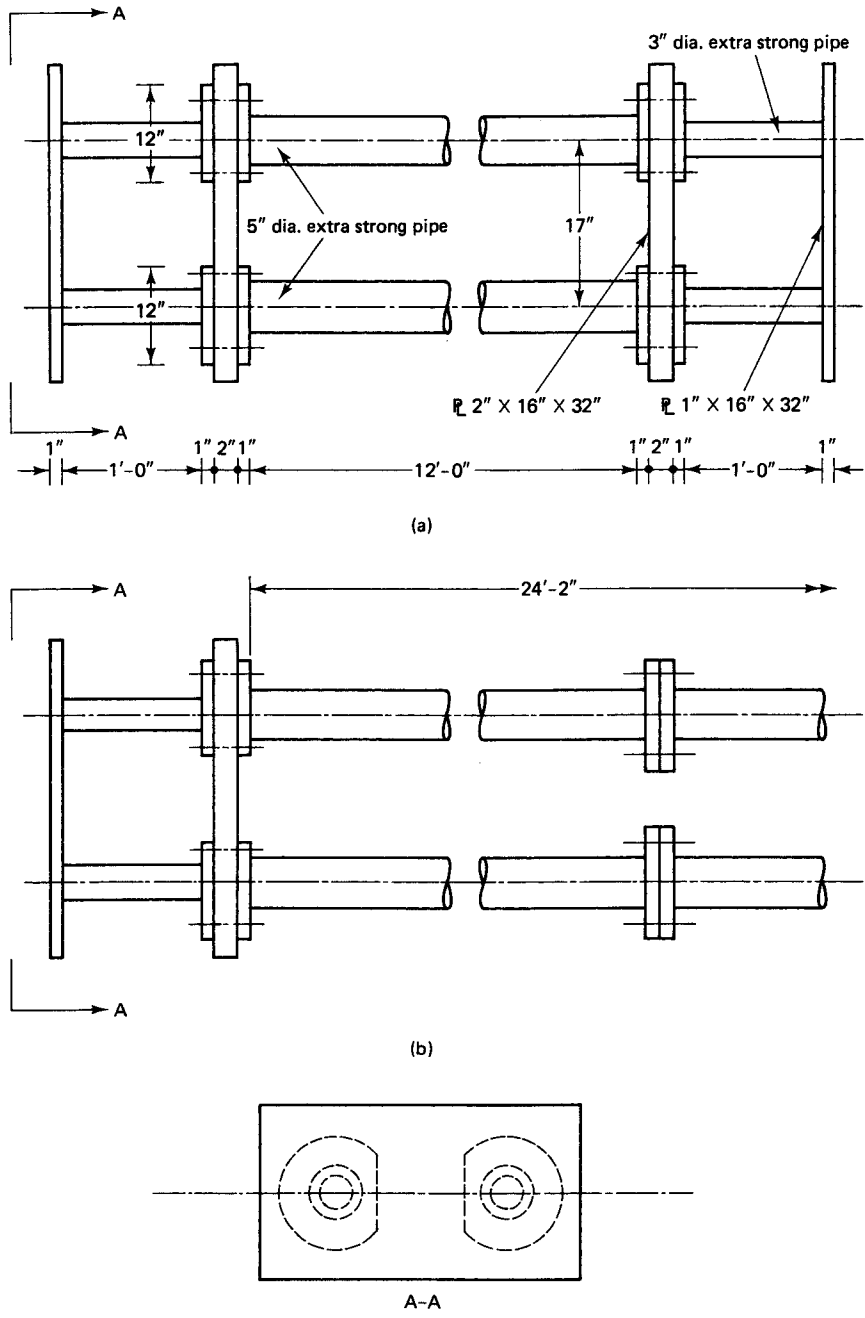
#### 2.10.4.2 Ducts

##### 1. Forming.

- (a) **Formed Ducts.** Ducts formed by sheath left in place should be of a type that does not permit the entrance of cement paste. They should transfer bond



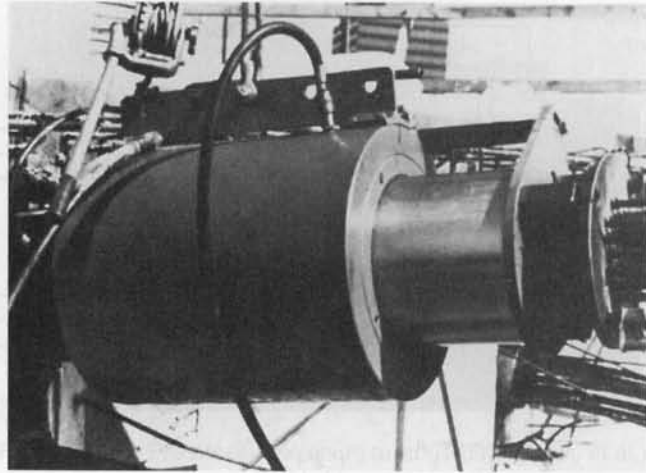
**Figure 2.26** Intermediate connections between frames of the prestressing system for continuous beams (Nawy et al.).



**Figure 2.27** Dimensioning details of the pretensioning or post-tensioning laboratory system used for research at Rutgers (Nawy et al.).

stresses as required and should retain their shape under the weight of the concrete. Metallic sheaths should be of a ferrous metal, and they may be galvanized.

**(b) Cored Ducts.** Cored ducts should be formed with no constrictions which would tend to block the passage of grout. All coring material should be removed.



**Figure 2.28** Stresstek Multistrand 500-ton jack. (Courtesy, Post-Tensioning Institute.)

2. **Grout Openings or Vents.** All ducts should have grout openings at both ends. For draped cables, all high points should have a grout vent except where the cable curvature is small, such as in continuous slabs. Grout vents or drain holes should be provided at low points if the tendon is to be placed, stressed, and grouted in a freezing climate. All grout openings or vents should include provisions for preventing grout leakage.
3. **Duct Size.** For tendons made up of a plurality of wires, bars, or strands, the duct area should be at least twice the net area of the prestressing steel. For tendons made up of a single wire, bar, or strand, the duct diameter should be at least  $\frac{1}{4}$  in. larger than the nominal diameter of the wire, bar, or strand.
4. **Placement of Ducts.** After the placement of ducts, reinforcement, and forming are complete, an inspection should be made to locate possible duct damage. Ducts should be securely fastened at close enough intervals to avoid displacement during concreting. All holes or openings in the duct must be repaired prior to placement of concrete. Grout openings and vents must be securely anchored to the duct and to



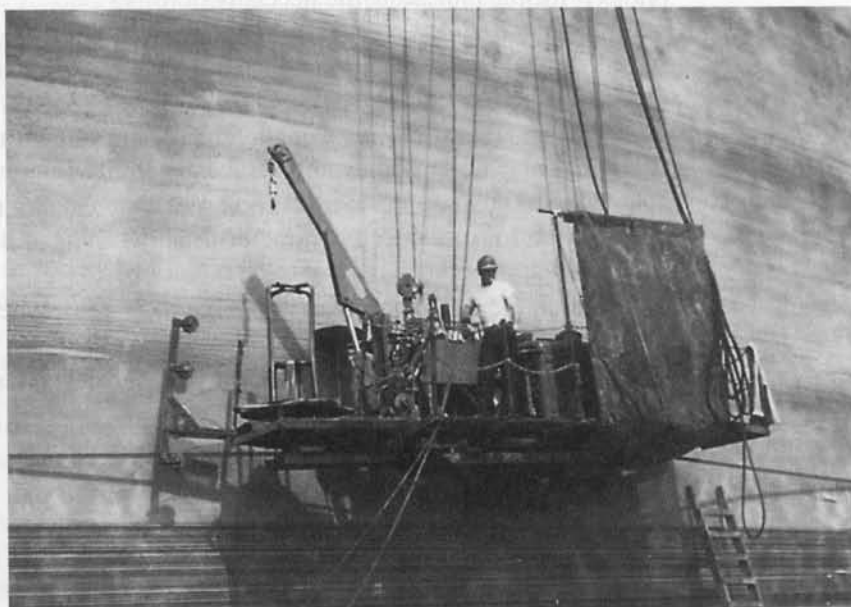
**Photo 2.7** Prestress conduit for a bridge deck.

either the forms or the reinforcing steel, to prevent displacement during concrete-placing operations.

### 2.10.4.3 Grouting Process

1. Ducts with concrete walls (cored ducts) should be flushed to ensure that the concrete is thoroughly wetted.
2. All grout and high-point vent openings should be open when grouting starts. Grout should be allowed to flow from the first vent after the inlet pipe until any residual flushing water or entrapped air has been removed, at which time the vent should be capped or otherwise closed. Remaining vents should be closed in sequence in the same manner. The pumping pressure at the tendon inlet should not exceed 250 psig.
3. Grout should be pumped through the duct and continuously wasted at the outlet pipe until no visible slugs of water or air are ejected. The efflux time of the ejected grout should not be less than the injected grout. To ensure that the tendon remains filled with grout, the outlet and/or inlet should be closed. Plugs, caps, or valves thus required should not be removed or opened until the grout has set.
4. When one-way flow of grout cannot be maintained, the grout should be immediately flushed out of the duct with water.
5. In temperatures below 32°F, ducts should be kept free of water to avoid damage due to freezing.
6. The temperature of the concrete should be 35°F or higher from the time of grouting until job-cured 2-in. cubes of grout reach a minimum compressive strength of 800 psi.
7. Grout should not be above 90°F during mixing or pumping. If necessary, the mixing water should be cooled.

Additional details and specifications on grouting are given by the Post-Tensioning Institute in Ref. 2.29.



**Figure 2.29** Prestressing of preload circular tank. (Courtesy, N.A. Legates, Preload Technology, Inc., New York.)



## 2.11 CIRCULAR PRESTRESSING

Circular prestressing involves the development of hoop or hugging compressive stresses on circular or cylindrical containment vessels, including prestressed water tanks and pipes. It is usually accomplished by a wire-wound technique, in which the concrete pipe or tank is wrapped with continuous high-tensile wire tensioned to prescribed design levels. Such tension results in uniform radial compression that prestresses the concrete cylinder or core and prevents tensile stresses from developing in the concrete wall section under internal fluid pressure. Figure 2.29 shows a preload circular tank being prestressed by the wire-wrapping process along its height.

## 2.12 TEN PRINCIPLES

The following ten principles are taken from Abeles (Ref. 2.32) and applicable not only to prestressing concrete but to any endeavor that the engineer is called upon to undertake:

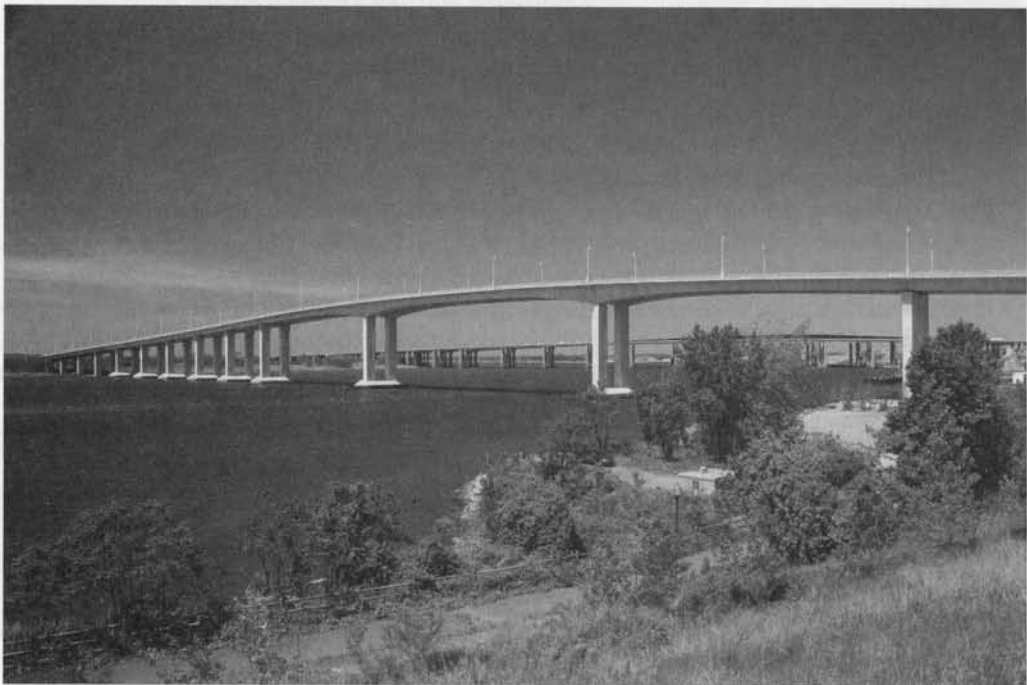
1. You cannot have everything. (Each solution has advantages and disadvantages that have to be tallied and traded off against each other.)
2. You cannot have something for nothing. (One has to pay in one way or another for something which is offered as a “free gift” into the bargain, notwithstanding a solution’s being optimal for the problem.)
3. It is never too late (e.g., to alter a design, to strengthen a structure before it collapses, or to adjust or even change principles previously employed in the light of increased knowledge and experience).
4. There is no progress without considered risk. (While it is important to ensure sufficient safety, overconservatism can never lead to an understanding of novel structures.)
5. The proof of the pudding is in the eating. (This is in direct connection with the previous principle indicating the necessity of tests.)
6. Simplicity is always an advantage, but beware of oversimplification. (The latter may lead to theoretical calculations which are not always correct in practice, or to a failure to cover all conditions.)
7. Do not generalize, but rather qualify the specific circumstances. (Serious misunderstandings may be caused by unreserved generalizations.)
8. The important question is how good, not how cheap an item is. (A cheap price given by an inexperienced contractor usually results in bad work; similarly, cheap, unproved appliances may have to be replaced.)
9. We live and learn. (It is always possible to increase one’s knowledge and experience.)
10. There is nothing completely new. (Nothing is achieved instantaneously, but only by step-by-step development.)

## SELECTED REFERENCES

- 2.1 American Society for Testing and Materials. *Annual book of ASTM Standards: Part 14, Concrete and Mineral Aggregates*. Philadelphia: ASTM, 1994.
- 2.2 Popovices, S. *Concrete-Making Materials*. New York: McGraw-Hill, 1979, 1997.
- 2.3 ACI Committee 221. “Selection and Use of Aggregate for Concrete.” *Journal of the American Concrete Institute*, Farmington Hills, MI, 1992.

- 2.4 American Concrete Institute, *ACI Manual of Concrete Practice*, 2008. *Materials*. American Concrete Institute, Farmington Hills, MI, 2009.
- 2.5 Portland Cement Association. *Design and Control of Concrete Mixtures*, 13th ed. PCA, Skokie, Ill., 1994.
- 2.6 ACI Committee 212. "Admixtures for Concrete," in *ACI Manual of Concrete Practice 1983*. ACI, Farmington Hills, MI, 1995, ACI 212.1 R-81.
- 2.7 Nawy, E. G., Ukadike, M. M., and Sauer, J. A. "High Strength Field Modified Concretes," *Journal of the Structural Division, ASCE*, 103, No. ST12, December 1977, 2307–2322.
- 2.8 American Concrete Institute. *Super-plasticizers in Concrete*, ACI Special Publication SP-62. ACI, Farmington Hills, MI, 1979.
- 2.9 ACI Committee 211. "Standard Practice for Selecting Proportions for Normal, Heavyweight, and Mass Concrete," ACI 211.1–92. American Concrete Institute, Farmington Hills, MI, 1992.
- 2.10 ACI Committee 211. "Standard Practice for Selecting Proportions for Structural Lightweight Concrete," ACI 211.1–92. American Concrete Institute, Farmington Hills, MI.
- 2.11 Nawy, E. G. *Reinforced Concrete—A Fundamental Approach*. Prentice-Hall, Inc., Upper Saddle River, NJ, 6th ed., 2009, 936 p.
- 2.12 ACI Committee 318. "Building Code Requirements for Structural Concrete (ACI 318–08) and Commentary (318 R–08) American Concrete Institute, Farmington Hills, MI, 2005, pp. 442.
- 2.13 American Society for Testing and Materials. *Significance of Tests and Properties of Concrete and Concrete Making Materials*, Special Technical Publication 169B. ASTM, Philadelphia, 1978.
- 2.14 Ross, A. D. "The Elasticity, Creep and Shrinkage of Concrete," in *Proceedings of the Conference on Non-metallic Brittle Materials*. Interscience Publishers, London, 1958.
- 2.15 Neville, A. M. *Properties of Concrete*, 4th ed. Pitman Books, London, 1996.
- 2.16 Freudenthal, A. M., and Roll, F. "Creep and Creep Recovery of Concrete under High Compressive Stress," *Journal of the American Concrete Institute*, Proc. 54, Farmington Hills, MI, June 1958, 1111–1142.
- 2.17 Ross, A. D., "Creep Concrete Data," *Proceedings, Institution of Structural Engineers*, London, 1937, 314–326.
- 2.18 Branson, D. E. *Deformation of Concrete Structures*. New York, McGraw-Hill, 1977.
- 2.19 Branson, D. E. "Compression Steel Effects on Long Term Deflections," *Journal of the American Concrete Institute*, Proc. 68, Farmington Hills, MI, August 1971, 555–559.
- 2.20 Mindess, S., and Young, J. F. *Concrete*. Upper Saddle River, N.J., Prentice-Hall, Inc., 1981.
- 2.21 Nawy, E. G., and Balaguru, P. N. "High Strength Concrete," Chapter 5 in *Handbook of Structural Concrete*. London: Pitman Books, McGraw-Hill, New York, 1983, pp. 5–1 to 5–33.
- 2.22 Mehta, P. Kumar. *Concrete-Structure, Properties, and Materials*, 2nd ed. Prentice Hall, Upper Saddle River, N.J., 1993.
- 2.23 American Society for Testing and Materials. "Standard Specification for Deformed and Plain Billet-Steel Bars for Concrete Reinforcement, A6 15–79." ASTM, Philadelphia, 1980, 588–599.
- 2.24 American Society for Testing and Materials. "Standard Specification for Rail-Steel Deformed and Plain Bars for Concrete Reinforcement, A6 16–79." ASTM, Philadelphia, 1980, 600–605.
- 2.25 American Society for Testing and Materials. "Standard Specification for Axle Steel Deformed and Plain Bars for Concrete Reinforcement, A6 17–79." ASTM, Philadelphia, 1980, 607–611.
- 2.26 American Society for Testing and Materials. "Standard Specification for Cold-Drawn Steel Wire for Concrete Reinforcement, A8 2-79." ASTM, Philadelphia, 1980, 154–157.
- 2.27 American Society for Testing and Materials. "Standard Specification for Low-Alloy Steel Deformed Bars for Concrete Reinforcement, A706–79." ASTM, Philadelphia, 1980, 755–760.
- 2.28 ACI-ASCE Committee 423, "Recommendation for Concrete Members Prestressed with Unbonded Tendons" (ACI 423.3R-83). *Concrete International 5* (1983): 61–76.
- 2.29 Post-Tensioning Institute. "Guide Specifications for Post-Tensioning Materials." In *Post-Tensioning Manual*, 5th ed. Post-Tensioning Institute, Phoenix, Ariz., 2000.
- 2.30 AASHTO. *Standard Specifications for Highway Bridges*, 17th ed. American Association of State Highway and Transportation Officials, Washington, D.C., 2002.

- 2.31 Nawy, E. G., and Potyondy, J. G. "Moment Rotation, Cracking, and Deflection of Spirally Bound Pretensioned Prestressed Concrete Beams." *Engineering Research Bulletin No. 51*. New Brunswick, N.J.: Bureau of Engineering Research, Rutgers University, 1970, pp. 1–97.
- 2.32 Abeles, P. W., and Bardhan-Roy, B. K. *Prestressed Concrete Designer's Handbook*. 3d ed. London: Viewpoint Publications, 1981.
- 2.33 Nawy, E. G. *Simplified Reinforced Concrete*. Prentice Hall, Upper Saddle River, N.J., 1986.
- 2.34 Nawy, E. G., "Concrete." In *Corrosion and Chemical Resistant Masonry Materials Handbook*. Park Ridge, N.J.: Noyes, 1986, pp. 57–73.
- 2.35 ACI Committee 435. "Control of Deflection in Concrete Structures," ACI Committee Report, E. G. Nawy, Chairman, American Concrete Institute, Farmington Hills, MI, 1995, 77 p.
- 2.36 Chen, B., and Nawy, E. G. "Structural Behavior Evaluation of High Strength Concrete Reinforced with Prestressed Prisms Using Fiber Optic Sensors." *Proceedings, ACI Structural Journal*, American Concrete Institute, Farmington Hills, MI, Dec. 1994, pp. 708–718.
- 2.37 Chen, B., Maher, M. H., and Nawy, E. G. "Fiber Optic Bragg Grating Sensor for Non-Destructive Evaluation of Composite Beams." *Proceedings, ASCE Journal of the Structural Division*. American Society of Civil Engineers, New York, Dec. 1994, pp. 3456–3470.
- 2.38 Nawy, E. G. *Fundamentals of High Performance Concrete*, 2nd ed. John Wiley & Sons, New York, 2001, pp. 460.
- 2.39 Nawy, E. G., Editor-in-Chief, *Concrete Construction Engineering Handbook*. Boca Raton, FL: CRC Press, 1998, 1250 p.



**Photo 2.8** Route 35, Victory Bridge over the Raritan River, connecting Perth Amboy and Sayerville, New Jersey. A variable depth precast segmental concrete bridge with spans of 330'–440'–330' built in balanced cantilever, the main 440 ft. span being the longest precast cantilever segmental construction in the United States. (Courtesy of FIGG, the bridge designer)



# 3

## PARTIAL LOSS OF PRESTRESS

### 3.1 INTRODUCTION

It is a well-established fact that the initial prestressing force applied to the concrete element undergoes a progressive process of reduction over a period of approximately five years. Consequently, it is important to determine the level of the prestressing force at each loading stage, from the stage of transfer of the prestressing force to the concrete, to the various stages of prestressing available at service load, up to the ultimate. Essentially, the reduction in the prestressing force can be grouped into two categories:

- Immediate elastic loss during the fabrication or construction process, including elastic shortening of the concrete, anchorage losses, and frictional losses.
- Time-dependent losses such as creep, shrinkage, and those due to temperature effects and steel relaxation, all of which are determinable at the service-load limit state of stress in the prestressed concrete element.

An exact determination of the magnitude of these losses—particularly the time-dependent ones—is not feasible, since they depend on a multiplicity of interrelated factors. Empirical methods of estimating losses differ with the different codes of practice or

Executive Center, Honolulu, Hawaii. (Courtesy, Post-Tensioning Institute.)

**Table 3.1** AASHTO Lump-Sum Losses

Type of prestressing steel	Total loss	
	$f'_c = 4,000$ psi (27.6 N/mm <sup>2</sup> )	$f'_c = 5,000$ psi (34.5 N/mm <sup>2</sup> )
Pretensioning strand		45,000 psi (310 N/mm <sup>2</sup> )
Post-tensioning <sup>a</sup> wire or strand	32,000 psi (221 N/mm <sup>2</sup> )	33,000 psi (228 N/mm <sup>2</sup> )
Bars	22,000 psi (152 N/mm <sup>2</sup> )	23,000 psi (159 N/mm <sup>2</sup> )

<sup>a</sup>Losses due to friction are excluded. Such losses should be computed according to Section 6.5 of the AASHTO specifications.

recommendations, such as those of the Prestressed Concrete Institute, the ACI-ASCE joint committee approach, the AASHTO lump-sum approach, the Comité Eurointernationale du Béton (CEB), and the FIP (Federation Internationale de la Précontrainte). The degree of rigor of these methods depends on the approach chosen and the accepted practice of record.

A very high degree of refinement of loss estimation is neither desirable nor warranted, because of the multiplicity of factors affecting the estimate. Consequently, lump-sum estimates of losses are more realistic, particularly in routine designs and under average conditions. Such lump-sum losses can be summarized in Table 3.1 of AASHTO and Table 3.2 of PTI. They include elastic shortening, relaxation in the prestressing steel, creep, and shrinkage, and they are applicable only to routine, standard conditions of loading; normal concrete, quality control, construction procedures, and environmental conditions; and the importance and magnitude of the system. Detailed analysis has to be performed if these standard conditions are not fulfilled.

A summary of the sources of the separate prestressing losses and the stages of their occurrence is given in Table 3.3, in which the subscript  $i$  denotes “initial” and the subscript  $j$  denotes the loading stage after jacking. From this table, the total loss in prestress can be calculated for pretensioned and post-tensioned members as follows:

**(i) Pretensioned Members**

$$\Delta f_{pT} = \Delta f_{pES} + \Delta f_{pR} + \Delta f_{pCR} + \Delta f_{pSH} \quad (3.1a)$$

**Table 3.2** Approximate Prestress Loss Values for Post-Tensioning

Post-tensioning tendon material	Prestress loss, psi	
	Slabs	Beams and joists
Stress-relieved 270-K strand and stress-relieved 240-K wire	30,000 (207 N/mm <sup>2</sup> )	35,000 (241 N/mm <sup>2</sup> )
Bar	20,000 (138 N/mm <sup>2</sup> )	25,000 (172 N/mm <sup>2</sup> )
Low-relaxation 270-K strand	15,000 (103 N/mm <sup>2</sup> )	20,000 (138 N/mm <sup>2</sup> )

Note: This table of approximate prestress losses was developed to provide a common post-tensioning industry basis for determining tendon requirements on projects in which the magnitude of prestress losses is not specified by the designer. These loss values are based on use of normal-weight concrete and on average values of concrete strength, prestress level, and exposure conditions. Actual values of losses may vary significantly above or below the table values where the concrete is stressed at low strengths, where the concrete is highly prestressed, or in very dry or very wet exposure conditions. The table values do not include losses due to friction.

Source: Post-Tensioning Institute.

**Table 3.3** Types of Prestress Loss

Type of prestress loss	Stage of occurrence		Tendon stress loss	
	Pretensioned members	Post-tensioned members	During time interval ( $t_p$ , $t_j$ )	Total or during life
Elastic shortening of concrete (ES)	At transfer	At sequential jacking	...	$\Delta f_{pES}$
Relaxation of tendons (R)	Before and after transfer	After transfer	$\Delta f_{pR}(t_i, t_j)$	$\Delta f_{pR}$
Creep of concrete (CR)	After transfer	After transfer	$\Delta f_{pC}(t_i, t_j)$	$\Delta f_{pCR}$
Shrinkage of concrete (SH)	After transfer	After transfer	$\Delta f_{pS}(t_i, t_j)$	$\Delta f_{pSH}$
Friction (F)	...	At jacking	...	$\Delta f_{pF}$
Anchorage seating loss (A)	...	At transfer	...	$\Delta f_{pA}$
Total	Life	Life	$\Delta f_{pT}(t_p, t_j)$	$\Delta f_{pT}$

where  $\Delta f_{pR} = \Delta f_{pR}(t_0, t_{tr}) + \Delta f_{pR}(t_{tr}, t_s)$   
 $t_0$  = time at jacking  
 $t_{tr}$  = time at transfer  
 $t_s$  = time at stabilized loss

Hence, computations for steel relaxation loss have to be performed for the time interval  $t_1$  through  $t_2$  of the respective loading stages.

As an example, the transfer stage, say, at 18 h would result in  $t_{tr} = t_2 = 18$  h and  $t_0 = t_1 = 0$ . If the next loading stage is between transfer and 5 years (17,520 h), when losses are considered stabilized, then  $t_2 = t_s = 17,520$  h and  $t_1 = 18$  h. Then, if  $f_{pi}$  is the initial prestressing stress that the concrete element is subjected to and  $f_{pJ}$  is the jacking stress in the tendon, then

$$f_{pi} = f_{pJ} - \Delta f_{pR}(t_0, t_{tr}) - \Delta f_{pES} \quad (3.1b)$$

### (ii) Post-tensioned Members

$$\Delta f_{pT} = \Delta f_{pA} + \Delta f_{pF} + \Delta f_{pES} + \Delta f_{pR} + \Delta f_{pCR} + \Delta f_{pSH} \quad (3.1c)$$

where  $\Delta f_{pES}$  is applicable only when tendons are jacked sequentially, and not simultaneously.

In the post-tensioned case, computation of relaxation loss starts between the transfer time  $t_1 = t_{tr}$  and the end of the time interval  $t_2$  under consideration. Hence

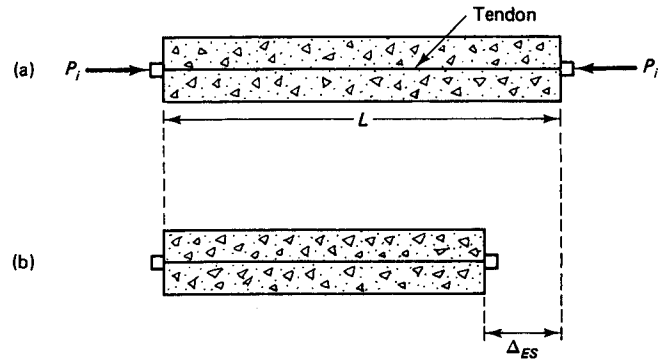
$$f_{pi} = f_{pJ} - \Delta f_{pA} - \Delta f_{pF} \quad (3.1d)$$

## 3.2 ELASTIC SHORTENING OF CONCRETE (ES)

Concrete shortens when a prestressing force is applied. As the tendons that are bonded to the adjacent concrete simultaneously shorten, they lose part of the prestressing force that they carry.

### 3.2.1 Pretensioned Elements

For pretensioned (precast) elements, the compressive force imposed on the beam by the tendon results in the longitudinal shortening of the beam, as shown in Figure 3.1. The unit shortening in concrete is  $\epsilon_{ES} = \Delta_{ES}/L$ , so



**Figure 3.1** Elastic shortening. (a) Unstressed beam. (b) Longitudinally shortened beam.

$$\epsilon_{ES} = \frac{f_c}{E_c} = \frac{P_i}{A_c E_c} \quad (3.2a)$$

Since the prestressing tendon suffers the same magnitude of shortening,

$$\Delta f_{pES} = E_s \epsilon_{ES} = \frac{E_s P_i}{A_c E_c} = \frac{n P_i}{A_c} = n f_{cs} \quad (3.2b)$$

The stress in the concrete at the centroid of the steel due to the initial prestressing is

$$f_{cs} = -\frac{P_i}{A_c} \quad (3.3)$$

If the tendon in Figure 3.1 has an eccentricity  $e$  at the beam midspan and the self-weight moment  $M_D$  is taken into account, the stress the concrete undergoes at the midspan section at the level of the prestressing steel becomes

$$f_{cs} = -\frac{P_i}{A_c} \left( 1 + \frac{e^2}{r^2} \right) + \frac{M_D e}{I_c} \quad (3.4)$$

where  $P_i$  has a lower value after transfer of prestress. The *small* reduction in the value of  $P_j$  to  $P_i$  occurs because the force in the prestressing steel immediately after transfer is less than the initial jacking prestress force  $P_j$ . However, since it is difficult to accurately determine the reduced value of  $P_i$ , and since observations indicate that the reduction is only a few percentage points, it is possible to use the initial value of  $P_i$  before transfer in Equations 3.2 through 3.4, or reduce it by about 10 percent for refinement if desired.

### 3.2.1.1 Elastic shortening loss in pretensioned beams

#### Example 3.1

A pretensioned prestressed beam has a span of 50 ft (15.2 m), as shown in Figure 3.2. For this beam,

$$f'_c = 6,000 \text{ psi (41.4 MPa)}$$

$$f_{pu} = 270,000 \text{ psi (1,862 MPa)}$$

$$f'_{ci} = 4,500 \text{ psi (31 MPa)}$$

$$A_{ps} = 10 - \frac{1}{2}\text{-in dia. seven-wire-strand tendon}$$

$$= 10 \times 0.153 = 1.53 \text{ in.}^2$$

$$E_{ps} = 27 \times 10^6 \text{ psi (1,862 MPa)}$$

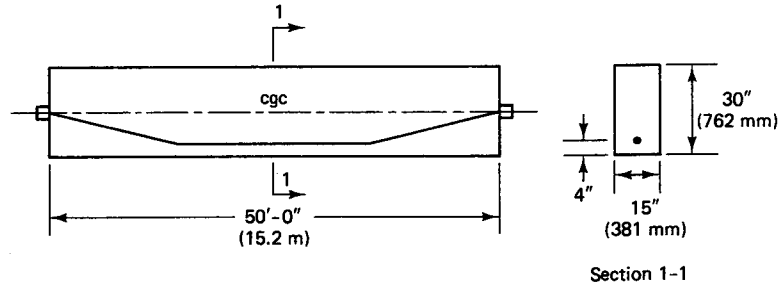


Figure 3.2 Beam in Example 3.1.

Calculate the concrete fiber stresses at transfer at the centroid of the tendon for the midspan section of the beam, and the magnitude of loss in prestress due to the effect of elastic shortening of the concrete. Assume that prior to transfer, the jacking force on the tendon was 75%  $f_{pu}$ .

**Solution:**

$$A_c = 15 \times 30 = 450 \text{ in.}^2$$

$$I_c = \frac{15(30)^3}{12} = 33,750 \text{ in.}^4$$

$$r^2 = \frac{I_c}{A_c} = 75 \text{ in.}^2$$

$$A_{ps} = 10 \times 0.153 = 1.53 \text{ in.}^2$$

$$e_c = \frac{30}{2} - 4 = 11 \text{ in.}$$

$$P_i = 0.75f_{pu}A_{ps} = 0.75 \times 270,000 \times 1.53 = 309,825 \text{ lb}$$

$$M_D = \frac{wl^2}{8} = \frac{15 \times 30}{144} \times 150 \frac{(50)^2}{8} \times 12 = 1,757,813 \text{ in.-lb}$$

From Equation 3.4, the concrete fiber stress at the steel centroid of the beam at the moment of transfer, assuming that  $P_i \cong P_j$ , is

$$\begin{aligned} f_{cs} &= -\frac{P_i}{A_c} \left( 1 + \frac{e^2}{r^2} \right) + \frac{M_D e}{I_c} \\ &= -\frac{309,825}{450} \left( 1 + \frac{11^2}{75} \right) + \frac{1,757,813 \times 11}{33,750} \\ &= -1,799.3 + 572.9 = -1,226.4 \text{ psi (8.50 MPa)} \end{aligned}$$

We also have

$$\text{Initial } E_{ci} = 57,000 \sqrt{f'_{ci}} = 57,000 \sqrt{4,500} = 3.824 \times 10^6 \text{ psi}$$

$$\text{Initial modular ratio } n = \frac{E_s}{E_{ci}} = \frac{27 \times 10^6}{3.824 \times 10^6} = 7.06$$

$$28 \text{ days' strength } E_c = 57,000 \sqrt{6,000} = 4.415 \times 10^6 \text{ psi}$$

$$28 \text{ days' modular ratio } n = \frac{27 \times 10^6}{4.415 \times 10^6} = 6.12$$

From Equation 3.2b, the loss of prestress due to elastic shortening is

$$\Delta f_{pES} = n f_{cs} = 7.06 \times 1,226.4 = 8,659.2 \text{ psi (59.7 MPa)}$$



### 3.2.2 Post-Tensioned Elements

In post-tensioned beams, the elastic shortening loss varies from zero if all tendons are jacked simultaneously to half the value calculated in the pretensioned case if several sequential jacking steps are used, such as jacking two tendons at a time. If  $n$  is the number of tendons or pairs of tendons sequentially tensioned, then

$$\Delta f_{pES} = \frac{1}{n} \sum_{j=1}^n (\Delta f_{pES})_j \quad (3.5)$$

where  $j$  denotes the number of jacking operations. Note that the tendon that was tensioned last does not suffer any losses due to elastic shortening, while the tendon that was tensioned first suffers the maximum amount of loss.

#### 3.2.2.1 Elastic shortening loss in post-tensioned beam

##### Example 3.2

Solve Example 3.1 if the beam is post-tensioned and the prestressing operation is such that

- (a) Two tendons are jacked at a time.
- (b) One tendon is jacked at a time.
- (c) All tendons are simultaneously tensioned.

##### Solution:

- (a) From Example 3.1,  $\Delta f_{pE} = 8,659.2$  psi. Clearly, the last tendon suffers no loss of prestress due to elastic shortening. So only the first four pairs have losses, with the first pair suffering the maximum loss of 8,659.2 psi. From Equation 3.5, the loss due to elastic shortening in the post-tensioned beam is

$$\begin{aligned} \Delta f_{pES} &= \frac{4/4 + 3/4 + 2/4 + 1/4}{5} (8,659.2) \\ &= \frac{10}{20} \times (8,659.2) = 4,330 \text{ psi (29.9 MPa)} \end{aligned}$$

- (b) 
$$\begin{aligned} \Delta f_{pES} &= \frac{9/9 + 8/9 + \dots + 1/9}{10} (8,659.2) \\ &= \frac{45}{90} \times (8,659.2) = 4,330 \text{ psi (29.9 MPa)} \end{aligned}$$

In both cases the loss in prestressing in the post-tensioned beam is half that of the pretensioned beam.

- (c)  $\Delta f_{pES} = 0$

### 3.3 STEEL STRESS RELAXATION ( $R$ )

Stress-relieved tendons suffer loss in the prestressing force due to constant elongation with time, as discussed in Chapter 2. The magnitude of the decrease in the prestress depends not only on the duration of the sustained prestressing force, but also on the ratio

$f_{pi}/f_{py}$  of the initial prestress to the yield strength of the reinforcement. Such a loss in stress is termed *stress relaxation*. The ACI 318-05 Code limits the tensile stress in the prestressing tendons to the following:

- (a) For stresses due to the tendon jacking force,  $f_{pj} = 0.94 f_{py}$ , but not greater than the lesser of  $0.80 f_{pu}$  and the maximum value recommended by the manufacturer of the tendons and anchorages.
- (b) Immediately after prestress transfer,  $f_{pi} = 0.82 f_{py}$  but not greater than  $0.74 f_{pu}$ .
- (c) In post-tensioned tendons, at the anchorages and couplers immediately after force transfer  $= 0.70 f_{pu}$ .

The range of values of  $f_{py}$  is given by the following:

Prestressing bars:  $f_{py} = 0.80 f_{pu}$

Stress-relieved tendons:  $f_{py} = 0.85 f_{pu}$

Low-relaxation tendons:  $f_{py} = 0.90 f_{pu}$

If  $f_{pR}$  is the remaining prestressing stress in the steel after relaxation, the following expression defines  $f_{pR}$  for stress relieved steel:

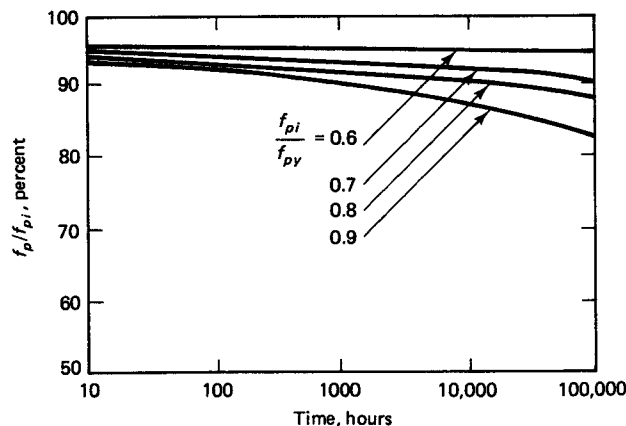
$$\frac{f_{pR}}{f_{pi}} = 1 - \left( \frac{\log t_2 - \log t_1}{10} \right) \left( \frac{f_{pi}}{f_{py}} - 0.55 \right) \quad (3.6)$$

In this expression,  $\log t$  in hours is to the base 10,  $f_{pi}/f_{py}$  exceeds 0.55, and  $t = t_2 - t_1$ . Also, for low-relaxation steel, the denominator of the log term in the equation is divided by 45 instead of 10. A plot of Equation 3.6 is given in Figure 3.3.

An approximation of the term  $(\log t_2 - \log t_1)$  can be made in Equation 3.6 so that  $\log t = \log(t_2 - t_1)$  without significant loss in accuracy. In that case, the stress-relaxation loss becomes

$$\Delta f_{pR} = f_{pi}' \frac{\log t}{10} \left( \frac{f_{pi}'}{f_{py}} - 0.55 \right) \quad (3.7)$$

where  $f_{pi}'$  is the initial stress in steel to which the concrete element is subjected.



**Figure 3.3** Stress-relaxation relationship in stress-relieved strands. (Courtesy, Post-Tensioning Institute.)

If a step-by-step loss analysis is necessary, the loss increment at any particular stage can be defined as

$$\Delta f_{pR} = f'_{pi} \left( \frac{\log t_2 - \log t_1}{10} \right) \left( \frac{f'_{pi}}{f_{py}} - 0.55 \right) \quad (3.8)$$

where  $t_1$  is the time at the beginning of the interval and  $t_2$  is the time at the end of the interval from jacking to the time when the loss is being considered.

For low relaxation steel, the divider is 45 instead of 10 in Equation 3.8, as shown in Equation 2.19.

### 3.3.1 Relaxation Loss Computation

#### Example 3.3

Find the relaxation loss in prestress at the end of 5 years in Example 3.1, assuming that relaxation loss from jacking to transfer, from elastic shortening, and from long-term loss due to creep and shrinkage over this period is 20 percent of the initial prestress. Assume also that the yield strength  $f_{py} = 230,000$  psi (1,571 MPa).

**Solution:** From Equation 3.1b for this stage

$$\begin{aligned} f_{pi} &= f_{pj} - \Delta f_{pR}(t_0, t_r) \\ &= 0.75 \times 270,000 = 202,500 \text{ psi (1,396 MPa)} \end{aligned}$$

The reduced stress for calculating relaxation loss is

$$f'_{pi} = (1 - 0.20) \times 202,500 = 162,000 \text{ psi (1,170 MPa)}$$

The duration of the stress-relaxation process is

$$5 \times 365 \times 24 \cong 44,000 \text{ hours}$$

From Equation 3.7,

$$\begin{aligned} \Delta f_{pR} &= f'_{pi} \frac{\log t}{10} \left( \frac{f'_{pi}}{f_{py}} - 0.55 \right) \\ &= 162,000 \frac{\log 44,000}{10} \left( \frac{162,000}{230,000} - 0.55 \right) \\ &= 162,000 \times 0.4643 \times 0.1543 = 11,606 \text{ psi (80.0 MPa)} \end{aligned}$$

### 3.3.2 ACI-ASCE Method of Accounting for Relaxation Loss

The ACI-ASCE method uses the separate contributions of elastic shortening, creep, and shrinkage in the evaluation of the steel stress-relaxation loss by means of the equation

$$\Delta f_{pR} = [K_{re} - J\Delta(f_{pES} + f_{pCR} + f_{pSH})] \times C$$

The values of  $K_{re}$ ,  $J$ , and  $C$  are given in Tables 3.4 and 3.5.

## 3.4 CREEP LOSS (CR)

Experimental work over the past half century indicates that flow in materials occurs with time when load or stress exists. This lateral flow or deformation due to the longitudinal stress is termed *creep*. A more detailed discussion is given in Ref. 3.9. It must be emphasized that creep stresses and stress losses result *only* from *sustained* loads during the loading history of the structural element.

**Table 3.4** Values of  $C$ 

$f_{pi}/f_{pu}$	Stress-relieved strand or wire	Stress-relieved bar or low-relaxation strand or wire
0.80		1.28
0.79		1.22
0.78		1.16
0.77		1.11
0.76		1.05
0.75	1.45	1.00
0.74	1.36	0.95
0.73	1.27	0.90
0.72	1.18	0.85
0.71	1.09	0.80
0.70	1.00	0.75
0.69	0.94	0.70
0.68	0.89	0.66
0.67	0.83	0.61
0.66	0.78	0.57
0.65	0.73	0.53
0.64	0.68	0.49
0.63	0.63	0.45
0.62	0.58	0.41
0.61	0.53	0.37
0.60	0.49	0.33

Source: Post-Tensioning Institute.

The deformation or strain resulting from this time-dependent behavior is a function of the magnitude of the applied load, its duration, the properties of the concrete including its mixture proportions, curing conditions, the age of the element at first loading, and environmental conditions. Since the stress-strain relationship due to creep is essentially linear, it is feasible to relate the creep strain  $\epsilon_{CR}$  to the elastic strain  $\epsilon_{EL}$  such that a creep coefficient  $C_u$  can be defined as

**Table 3.5** Values of  $K_{RE}$  and  $J$ 

Type of tendon <sup>a</sup>	$K_{RE}$	$J$
270 Grade stress-relieved strand or wire	20,000	0.15
250 Grade stress-relieved strand or wire	18,500	0.14
240 or 235 Grade stress-relieved wire	17,600	0.13
270 Grade low-relaxation strand	5,000	0.040
250 Grade low-relaxation wire	4,630	0.037
240 or 235 Grade low-relaxation wire	4,400	0.035
145 or 160 Grade stress-relieved bar	6,000	0.05

<sup>a</sup>In accordance with ASTM A416-74, ASTM A421-76, or ASTM A722-75.

Source: Prestressed Concrete Institute.

$$C_u = \frac{\epsilon_{CR}}{\epsilon_{EL}} \quad (3.9a)$$

Then the creep coefficient at any time  $t$  in days can be defined as

$$C_t = \frac{t^{0.60}}{10 + t^{0.60}} C_u \quad (3.9b)$$

As discussed in Chapter 2, the value of  $C_u$  ranges between 2 and 4, with an average of 2.35 for ultimate creep. The loss in prestressed members due to creep can be defined for bonded members as

$$\Delta f_{pCR} = C_t \frac{E_{ps}}{E_c} f_{cs} \quad (3.10)$$

where  $f_{cs}$  is the stress in the concrete at the level of the centroid of the prestressing tendon. In general, this loss is a function of the stress in the concrete at the section being analyzed. In post-tensioned, nonbonded members, the loss can be considered essentially uniform along the whole span. Hence, an average value of the concrete stress  $f_{cs}$  between the anchorage points can be used for calculating the creep in post-tensioned members.

The ACI-ASCE Committee expression for evaluating creep loss has essentially the same format as Equation 3.10, viz.,

$$\Delta f_{pCR} = K_{CR} \frac{E_{ps}}{E_c} (\bar{f}_{cs} - \bar{f}_{csd}) \quad (3.11a)$$

or

$$\Delta f_{pCR} = n K_{CR} (\bar{f}_{cs} - \bar{f}_{csd}) \quad (3.11b)$$

where  $K_{CR} = 2.0$  for pretensioned members

$= 1.60$  for post-tensioned members (both for normal concrete)

$\bar{f}_{cs}$  = stress in concrete at level of steel cgs immediately after transfer

$\bar{f}_{csd}$  = stress in concrete at level of steel cgs due to all superimposed dead loads applied after prestressing is accomplished

$n$  = modular ratio

Note that  $K_{CR}$  should be reduced by 20 percent for lightweight concrete.

### 3.4.1 Computation of Creep Loss

#### Example 3.4

Compute the loss in prestress due to creep in Example 3.1 given that the total superimposed load, excluding the beam's own weight after transfer, is 375 plf (5.5 kN/m).

**Solution:** At full concrete strength,

$$E_c = 57,000 \sqrt{6,000} = 4.415 \times 10^6 \text{ psi } (30.4 \times 10^3 \text{ MPa})$$

$$n = \frac{E_s}{E_c} = \frac{27.0 \times 10^6}{4.415 \times 10^6} = 6.12$$

$$M_{SD} = \frac{375(50)^2}{8} \times 12 = 1,406,250 \text{ in.-lb } (158.9 \text{ kN-m})$$

$$\bar{f}_{csd} = \frac{M_{SD}e}{I_c} = \frac{1,406,250 \times 11}{33,750} = 458.3 \text{ psi (3.2 MPa)}$$

From Example 3.1,

$$\bar{f}_{cs} = 1,226.4 \text{ psi (8.5 MPa)}$$

Also, for normal concrete use,  $K_{CR} = 2.0$  (pretensioned beam); so from Equation 3.11a,

$$\begin{aligned} \Delta f_{pCR} &= nK_{CR}(\bar{f}_{cs} - \bar{f}_{csd}) \\ &= 6.12 \times 2.0(1,226.4 - 458.3) \\ &= 9,401.5 \text{ psi (64.8 MPa)} \end{aligned}$$

### 3.5 SHRINKAGE LOSS ( $SH$ )

As with concrete creep, the magnitude of the shrinkage of concrete is affected by several factors. They include mixture proportions, type of aggregate, type of cement, curing time, time between the end of external curing and the application of prestressing, size of the member, and the environmental conditions. Size and shape of the member also affect shrinkage. Approximately 80 percent of shrinkage takes place in the first year of life of the structure. The average value of ultimate shrinkage strain in both moist-cured and steam-cured concrete is given as  $780 \times 10^{-6}$  in./in. in ACI 209 R-92 Report. This average value is affected by the length of initial moist curing, ambient relative humidity, volume-surface ratio, temperature, and concrete composition. To take such effects into account, the average value of shrinkage strain should be multiplied by a correction factor  $\gamma_{SH}$  as follows

$$\epsilon_{SH} = 780 \times 10^{-6} \gamma_{SH} \quad (3.12)$$

Components of  $\gamma_{SH}$  are factors for various environmental conditions and tabulated in Ref. 3.12, Sec. 2.

The Prestressed Concrete Institute stipulates for standard conditions an average value for nominal ultimate shrinkage strain  $(\epsilon_{SH})_u = 820 \times 10^{-6}$  in./in. (mm/mm), (Ref. 3.4). If  $\epsilon_{SH}$  is the shrinkage strain after adjusting for relative humidity at volume-to-surface ratio  $V/S$ , the loss in prestressing in pretensioned member is

$$\Delta f_{pSH} = \epsilon_{SH} \times E_{ps} \quad (3.13)$$

For post-tensioned members, the loss in prestressing due to shrinkage is somewhat less since some shrinkage has already taken place before post-tensioning. If the relative humidity is taken as a percent value and the  $V/S$  ratio effect is considered, the PCI general expression for loss in prestressing due to shrinkage becomes

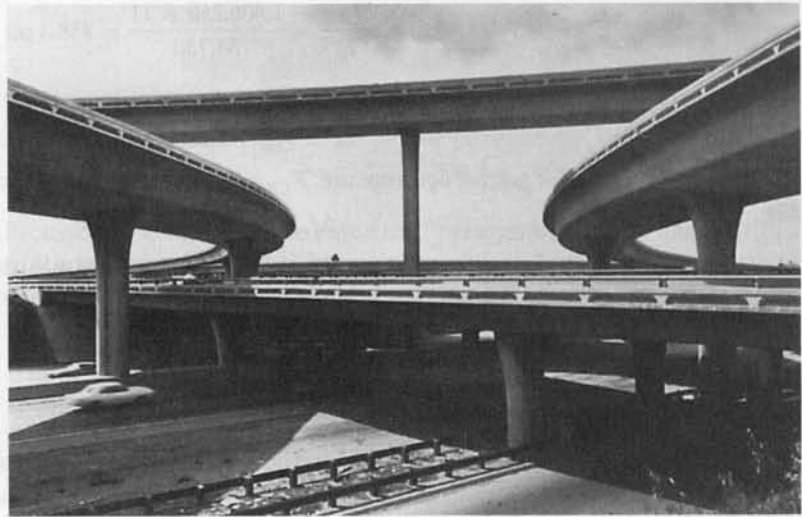
$$\Delta f_{pSH} = 8.2 \times 10^{-6} K_{SH} E_{ps} \left(1 - 0.06 \frac{V}{S}\right) (100 - RH) \quad (3.14)$$

where RH = relative humidity

**Table 3.6** Values of  $K_{SH}$  for Post-Tensioned Members

Time from end of moist curing to application of prestress, days								
	1	3	5	7	10	20	30	60
$K_{sh}$	0.92	0.85	0.80	0.77	0.73	0.64	0.58	0.45

Source: Prestressed Concrete Institute.



**Photo 3.1** 101/280/680 interchange connectors, South San Jose, California.

where  $K_{SH} = 1.0$  for pretensioned members. Table 3.6 gives the values of  $K_{SH}$  for post-tensioned members.

Adjustment of shrinkage losses for standard conditions as a function of time  $t$  in days after 7 days for moist curing and 3 days for steam curing can be obtained from the following expressions

(a) Moist curing, after 7 days

$$(\epsilon_{SH})_t = \frac{t}{35 + t} (\epsilon_{SH})_u \quad (3.15a)$$

where  $(\epsilon_{SH})_u$  is the ultimate shrinkage strain,  $t$  = time in days after shrinkage is considered.

(b) Steam curing, after 1 to 3 days

$$(\epsilon_{SH})_t = \frac{t}{55 + t} (\epsilon_{SH})_u \quad (3.15b)$$

It should be noted that separating creep from shrinkage calculations as presented in this chapter is an accepted engineering practice. Also, significant variations occur in the creep and shrinkage values due to variations in the properties of the constituent materials from the various sources, even if the products are plant-produced such as pretensioned beams. Hence it is recommended that information from actual tests be obtained especially on manufactured products, large span-to-depth ratio cases and/or if loading is unusually heavy.

### 3.5.1 Computation of Shrinkage Loss

#### Example 3.5

Compute the loss in prestress due to shrinkage in Examples 3.1 and 3.2 at 7 days after moist curing using both the ultimate  $K_{SH}$  method of Equation 3.14 and the time-dependent method of Equation 3.15. Assume that the relative humidity  $RH$  is 70 percent and the volume-to-surface ratio is 2.0.

**Solution A** **$K_{SH}$  method**(a) Pretensioned beam,  $K_{SH} = 1.0$ :

From Equation 3.14,

$$\begin{aligned}\Delta f_{pSH} &= 8.2 \times 10^{-6} \times 1.0 \times 27 \times 10^6 (1 - 0.06 \times 2.0)(100 - 70) \\ &= 5,845.0 \text{ psi (40.3 MPa)}\end{aligned}$$

(b) Post-tensioned beam, from Table 3.6,  $K_{SH} = 0.77$ :

$$\Delta f_{pSH} = 0.77 \times 5,845 = 4,500.7 \text{ psi (31.0 MPa)}$$

**Solution B****Time-dependent method**

From Equation 3.15a,

$$\begin{aligned}\epsilon_{SH,t} &= \frac{t}{35 + t} \epsilon_{SH,u} = \frac{7}{35 + 7} \times 780 \times 10^{-6} = 130 \times 10^{-6} \text{ in/in} \\ \Delta f_{pSH} &= \epsilon_{SH,t} E_s = 130 \times 10^{-6} \times 27 \times 10^6 = 3,510 \text{ psi (24.0 MPa)}\end{aligned}$$

**3.6 LOSSES DUE TO FRICTION ( $F$ )**

Loss of prestressing occurs in post-tensioning members due to friction between the tendons and the surrounding concrete ducts. The magnitude of this loss is a function of the tendon form or alignment, called the *curvature effect*, and the local deviations in the alignment, called the *wobble effect*. The values of the loss coefficients are often refined while preparations are made for shop drawings by varying the types of tendons and the duct alignment. Whereas the curvature effect is predetermined, the wobble effect is the result of accidental or unavoidable misalignment, since ducts or sheaths cannot be perfectly placed.

It should be noted that the maximum frictional stress loss would be at the far end of the beam if jacking is from one end. Hence frictional loss varies linearly along the beam span and can be interpolated for a particular location if such refinement in the computations is warranted.

**3.6.1 Curvature Effect**

As the tendon is pulled with a force  $F_1$  at the jacking end, it will encounter friction with the surrounding duct or sheath such that the stress in the tendon will vary from the jacking plane to a distance  $L$  along the span as shown in Figure 3.4. If an infinitesimal length of the tendon is isolated in a free-body diagram as shown in Figure 3.5, then, assuming that  $\mu$  denotes the coefficient of friction between the tendon and the duct due to the curvature effect, we have

$$dF_1 = -\mu F_1 d\alpha$$

or

$$\frac{dF_1}{F_1} = -\mu d\alpha \quad (3.16a)$$

Integrating both sides of this equation yields

$$\log_e F_1 = -\mu\alpha \quad (3.16b)$$



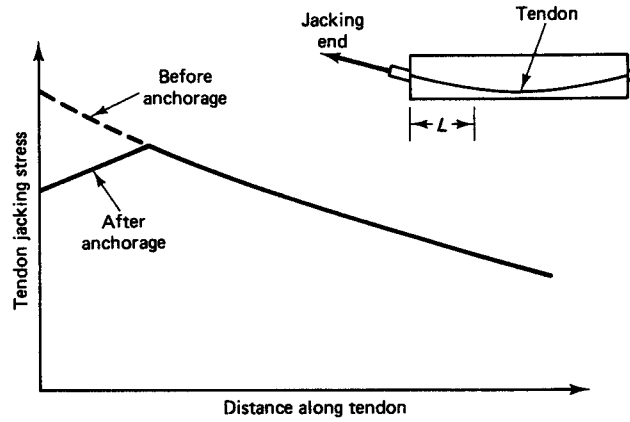


Figure 3.4 Frictional force stress distribution in tendon.

If  $\alpha = L/R$ , then

$$F_2 = F_1 e^{-\mu\alpha} = F_1 e^{-\mu(L/R)} \tag{3.17}$$

### 3.6.2 Wobble Effect

Suppose that  $K$  is the coefficient of friction between the tendon and the surrounding concrete due to wobble effect or length effect. Friction loss is caused by imperfection in alignment along the length of the tendon, regardless of whether it has a straight or draped alignment. Then by the same principles described in developing Equation 3.16,

$$\log_e F_1 = -KL \tag{3.18}$$

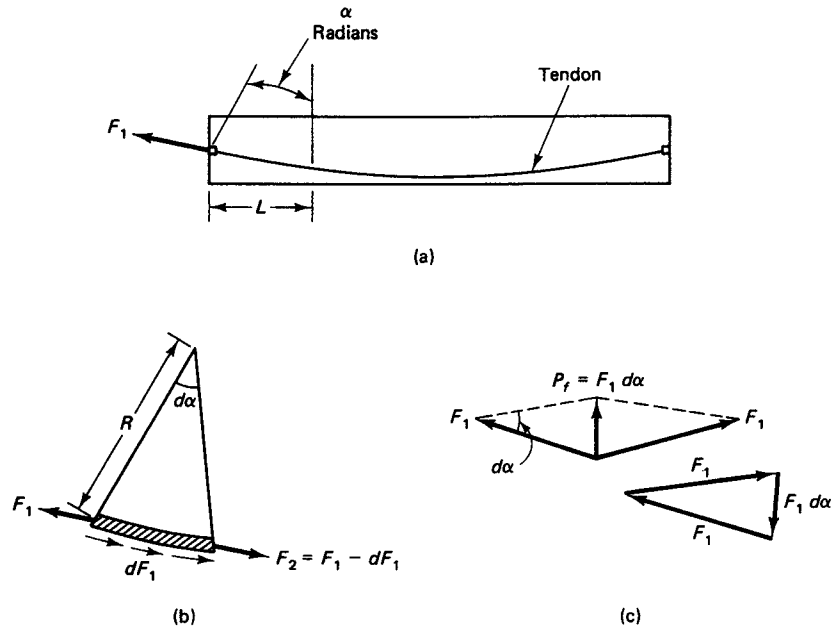


Figure 3.5 Curvature friction loss. (a) Tendon alignment. (b) Forces on infinitesimal length where  $F_1$  is at the jacking end. (c) Polygon of forces assuming  $F_1 = F_2$  over the infinitesimal length in (b).

or

$$F_2 = F_1 e^{-KL} \quad (3.19)$$

Superimposing the wobble effect on the curvature effect gives

$$F_2 = F_1 e^{-\mu\alpha - KL}$$

or, in terms of stresses,

$$f_2 = f_1 e^{-\mu\alpha - KL} \quad (3.20)$$

The frictional loss of stress  $\Delta f_{pF}$  is then given by

$$\Delta f_{pF} = f_1 - f_2 = f_1(1 - e^{-\mu\alpha - KL}) \quad (3.21)$$

Assuming that the prestress force between the start of the curved portion and its end is small ( $\cong 15$  percent), it is sufficiently accurate to use the initial tension for the entire curve in Equation 3.21. Equation 3.21 can thus be simplified to yield

$$\Delta f_{pF} = -f_1(\mu\alpha + KL) \quad (3.22)$$

where  $L$  is in feet.

Since the ratio of the depth of beam to its span is small, it is sufficiently accurate to use the projected length of the tendon for calculating  $\alpha$ . Assuming the curvature of the tendon to be based on that of a circular arc, the central angle  $\alpha$  along the curved segment in Figure 3.6 is twice the slope at either end of the segment. Hence,

$$\tan \frac{\alpha}{2} = \frac{m}{x/2} = \frac{2m}{x}$$

If

$$y \cong \frac{1}{2}m \quad \text{and} \quad \alpha/2 = 4y/x$$

then

$$\alpha = 8y/x \text{ radian} \quad (3.23)$$

Table 3.7 gives the design values of the curvature friction coefficient  $\mu$  and the wobble or length friction coefficient  $K$  adopted from the ACI 318 Commentary.

### 3.6.3 Computation of Friction Loss

#### Example 3.6

Assume that the alignment characteristics of the tendons in the post-tensioned beam of Example 3.2 are as shown in Figure 3.7. If the tendon is made of 7-wire uncoated strands in flexible metal sheathing, compute the frictional loss of stress in the prestressing wires due to the curvature and wobble effects.

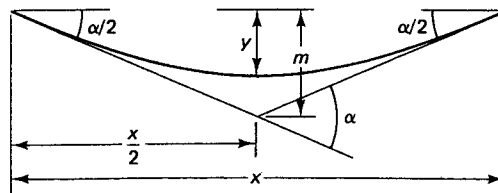


Figure 3.6 Approximate evaluation of the tendon's central angle.

**Table 3.7** Wobble and Curvature Friction Coefficients

Type of tendon	Wobble coefficient, $K$ per foot	Curvature coefficient, $\mu$
Tendons in flexible metal sheathing		
Wire tendons	0.0010–0.0015	0.15–0.25
7-wire strand	0.0005–0.0020	0.15–0.25
High-strength bars	0.0001–0.0006	0.08–0.30
Tendons in rigid metal duct		
7-wire strand	0.0002	0.15–0.25
Mastic-coated tendons		
Wire tendons and 7-wire strand	0.0010–0.0020	0.05–0.15
Pregreased tendons		
Wire tendons and 7-wire strand	0.0003–0.0020	0.05–0.15

Source: Prestressed Concrete Institute.

**Solution:**

$$P_i = 309,825 \text{ lb}$$

$$f_{pi} = \frac{309,825}{1.53} = 202,500 \text{ psi}$$

From Equation 3.23,

$$\alpha = \frac{8y}{x} = \frac{8 \times 11}{50 \times 12} = 0.1467 \text{ radian}$$

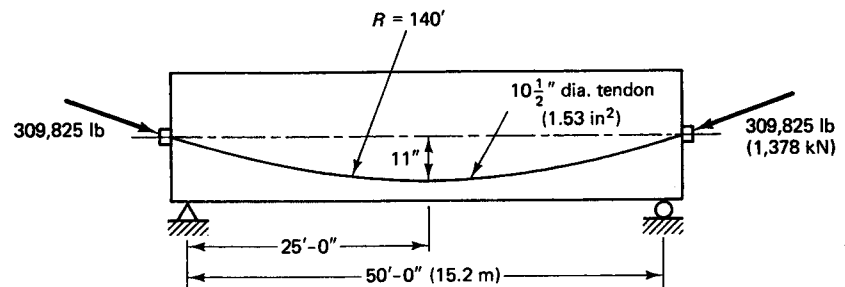
From Table 3.7, use  $K = 0.0020$  and  $\mu = 0.20$ . From Equation 3.22, the prestress loss due to friction is

$$\begin{aligned} \Delta f_{pF} &= f_{pi}(\mu\alpha + KL) \\ &= 202,500(0.20 \times 0.1467 + 0.0020 \times 50) \\ &= 202,500 \times 0.1293 = 26,191 \text{ psi (180.6 MPa)} \end{aligned}$$

This loss due to friction is 12.93 percent of the initial prestress.

**3.7 ANCHORAGE-SEATING LOSSES (A)**

Anchorage-seating losses occur in post-tensioned members due to the seating of wedges in the anchors when the jacking force is transferred to the anchorage. They can also occur in the prestressing casting beds of pretensioned members due to the adjustment

**Figure 3.7** Prestressing tendon alignment.

expected when the prestressing force is transferred to these beds. A remedy for this loss can be easily effected during the stressing operations by overstressing. Generally, the magnitude of anchorage-seating loss ranges between  $\frac{1}{4}$  in. and  $\frac{3}{8}$  in. (6.35 mm and 9.53 mm) for the two-piece wedges. The magnitude of the overstressing that is necessary depends on the anchorage system used since each system has its particular adjustment needs, and the manufacturer is expected to supply the data on the slip expected due to anchorage adjustment. If  $\Delta_A$  is the magnitude of the slip,  $L$  is the tendon length, and  $E_{ps}$  is the modulus of the prestressing wires, then the prestress loss due to anchorage slip becomes

$$\Delta f_{pA} = \frac{\Delta_A}{L} E_{ps} \quad (3.24)$$

### 3.7.1 Computation of Anchorage-Seating Loss

#### Example 3.7

Compute the anchorage-seating loss in the post-tensioned beam of Example 3.2 if the estimated slip is  $\frac{1}{4}$  in. (6.35 mm).

#### Solution:

$$E_{ps} = 27 \times 10^6 \text{ psi}$$

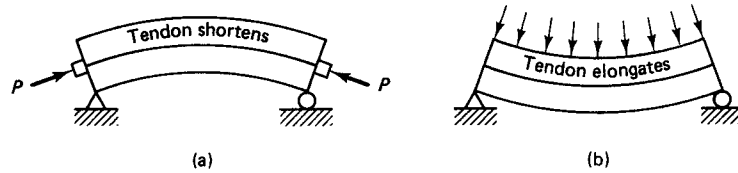
$$\Delta_A = 0.25 \text{ in.}$$

$$\Delta f_{pA} = \frac{\Delta_A}{L} E_{ps} = \frac{0.25}{50 \times 12} \times 27 \times 10^6 = 11,250 \text{ psi (77.6 MPa)}$$

Note that the percentage of loss due to anchorage slip becomes very high in short-beam elements and thus becomes of major significance in short-span beams. In such cases, it becomes difficult to post-tension such beams with high accuracy.



**Photo 3.2** Terracentre, Denver, Colorado. (Courtesy, Post-Tensioning Institute.)



**Figure 3.8** Change in beam longitudinal shape. (a) Due to prestressing. (b) Due to external load.

### 3.8 CHANGE OF PRESTRESS DUE TO BENDING OF A MEMBER ( $\Delta f_{pB}$ )

As the beam bends due to prestress or external load, it becomes convex or concave depending on the nature of the load, as shown in Figure 3.8. If the unit compressive strain in the concrete along the level of the tendon is  $\epsilon_c$ , then the corresponding change in prestress in the steel is

$$\Delta f_{pB} = \epsilon_c E_{ps}$$

where  $E_{ps}$  is the modulus of the steel. Note that any loss due to bending need not be taken into consideration if the prestressing stress level is measured after the beam has already bent, as is usually the case.

Figure 3.9 presents a flowchart for step-by-step evaluation of time-dependent prestress losses without deflection.

### 3.9 STEP-BY-STEP COMPUTATION OF ALL TIME-DEPENDENT LOSSES IN A PRETENSIONED BEAM

#### Example 3.8

A simply supported pretensioned 70-ft-span lightweight steam-cured double T-beam as shown in Figure 3.10 is prestressed by twelve  $\frac{1}{2}$ -in. diameter (twelve 12.7 mm dia) 270-K grade stress-relieved strands. The strands are harped, and the eccentricity at midspan is 18.73 in. (476 mm) and at the end 12.98 in. (330 mm). Compute the prestress loss at the critical section in the beam due to dead load and superimposed dead load. Assume the critical section to be at 0.40 L of the span considering that it can sometimes govern in cases of moving loads and also in continuous spans.

- (a) stage I at transfer
- (b) stage II after concrete topping is placed
- (c) two years after concrete topping is placed

Suppose the topping is 2 in. (51 mm) normal-weight concrete cast at 30 days. Suppose also that prestress transfer occurred 18 h after tensioning the strands. Given

$$f'_c = 5,000 \text{ psi, lightweight (34.5 MPa)}$$

$$f'_{ci} = 3,500 \text{ psi (24.1 MPa)}$$

and the following noncomposite section properties.

$$A_c = 615 \text{ in.}^2 (3,968 \text{ cm}^2)$$

$$I_c = 59,720 \text{ in.}^4 (2.49 \times 10^6 \text{ cm}^4)$$

$$c_b = 21.98 \text{ in. (55.8 cm)}$$

$$c^t = 10.02 \text{ in. (25.5 cm)}$$

$$S_b = 2,717 \text{ in.}^3 (44,520 \text{ cm}^3)$$

$$S^t = 5,960 \text{ in.}^3 (97,670 \text{ cm}^3)$$

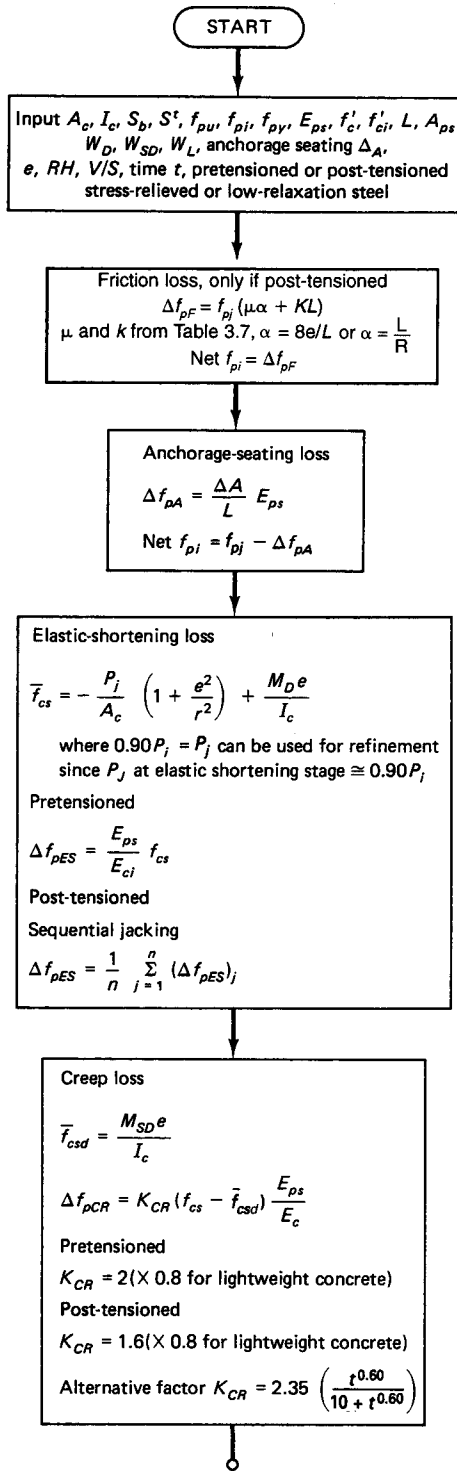


Figure 3.9 Flowchart for step-by-step evaluation of prestress losses.

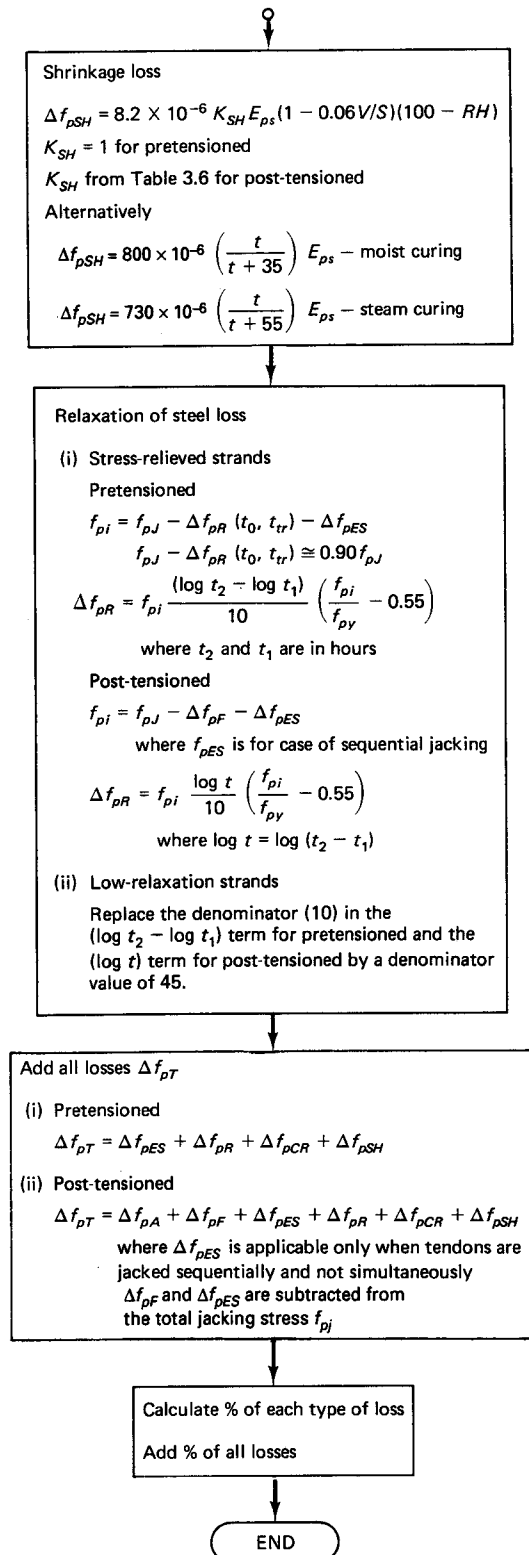
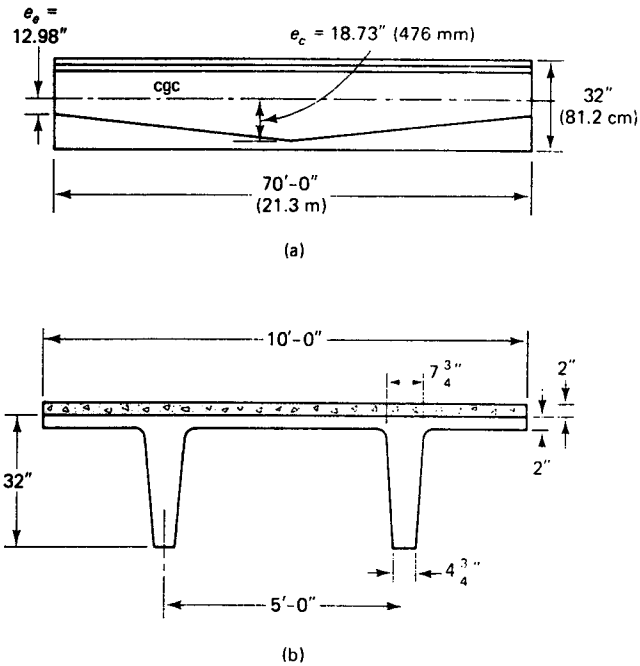


Figure 3.9 Continued



**Figure 3.10** Double-T pretensioned beam. (a) Elevation. (b) Pretensioned section.

$$W_D \text{ (no topping)} = 491 \text{ plf (7.2 kN/m)}$$

$$W_{SD} \text{ (2-in. topping)} = 250 \text{ plf (3.65 kN/m)}$$

$$W_L = 40 \text{ psf (1,915 Pa)—Transient}$$

$$f_{pu} = 270,000 \text{ psi (1,862 MPa)}$$

$$f_{py} = 0.85f_{pu} \approx 230,000 \text{ psi (1,589 MPa)}$$

$$f_{pi} = 0.70f_{pu} = 0.82f_{py} = 0.82 \times 0.85f_{pu} \approx 0.70f_{pu} \\ = 189,000 \text{ psi (1,303 MPa)}$$

$$E_{ps} = 28 \times 10^6 \text{ psi (193.1} \times 10^3 \text{ MPa)}$$

Assume that post-tensioning is applied in 18 hours after concrete curing.

**Solution:**

$$f'_{ci} = 3,500 \text{ psi}$$

$$E_{ci} = 115^{1.5}(33\sqrt{3,500}) = 2.41 \times 10^6 \text{ psi}$$

$$E_c = 115^{1.5}(33\sqrt{5,000}) = 2.88 \times 10^6 \text{ psi}$$

**Stage 1: Stress Transfer**

- (a) *Elastic shortening.* Given critical section distance from support =  $0.40 \times 70 = 28$  ft,  $e$  at critical section =  $12.98 + 0.8(18.73 - 12.98) = 17.58$  in. Dead-load moment  $M_D$  at 0.40 of the span is



$$M_D = W_D \frac{x}{2} (L - x) = 491 \left( \frac{28}{2} \right) (70 - 28)$$

$$= 288,708 \text{ ft-lb} = 3,464,496 \text{ in.-lb} \quad (391 \text{ kN-m})$$

$$f_{pi} = 0.70f_{pu} = 0.70 \times 270,000 = 189,000 \text{ psi}$$

Assume elastic-shortening loss and steel-relaxation loss  $\cong 18,000$  psi; then net-steel stress  $f_{pi} = 189,000 - 18,000 = 171,000$  psi, and

$$P_i = A_p f_{pi} = 12 \times 0.153 \times 171,000 = 313,956 \text{ lb}$$

$$r^2 = \frac{I_c}{A_c} = \frac{59,720}{615} = 97.11 \text{ in}^2$$

$$\bar{f}_{cs} = -\frac{P_i}{A_c} \left( 1 + \frac{e^2}{r^2} \right) + \frac{M_D e}{I_c}$$

$$= -\frac{313,956}{615} \left( 1 + \frac{(17.58)^2}{97.11} \right) + \frac{3,464,496 \times 17.58}{59,720}$$

$$= -2,135.2 + 1,019.9 = -1,115.3 \text{ psi} \quad (7.7 \text{ MPa})$$

$$n = \frac{E_{ps}}{E_{ci}} = \frac{28 \times 10^6}{2.41 \times 10^6} = 11.62$$

$$\Delta f_{pES} = n \bar{f}_{CS} = 11.62 \times 1,115.3 = 12,958 \text{ psi} \quad (85.4 \text{ MPa})$$

If  $f_{pi} = 189,000$  psi is used, then the net  $f_{pi} = 189,000 - 12,958 = 176,042$  psi, and we have

$$\bar{f}_{cs} = -2,135.20 \times \frac{176,042}{171,000} + 1,019.90 = -1178.3 \text{ psi}$$

$$\Delta f_{pES} = n \bar{f}_{CS} = 11.62 \times 1178.3 = 13,690 \text{ psi} \quad (94 \text{ MPa})$$

vs. 12,985 psi in the refined solution, a small difference of ~6 percent. Thus, an assumption of 10-percent loss at the beginning in estimating  $P_i \cong 0.9P_j$  would have been adequate.

**(b) Steel-Stress Relaxation.** Calculate the steel relaxation at transfer.

$$f_{py} = 230,000 \text{ psi}$$

$$f_{pi} = 189,000 \text{ psi} \quad (\text{or net } f_{pi} = 171,000 \text{ psi could be used})$$

$$t = 18 \text{ hours}$$

$$\Delta f_{pR} = f_{pi} \left( \frac{\log t_2 - \log t_1}{10} \right) \left( \frac{f_{pi}}{f_{py}} - 0.55 \right)$$

$$= 189,000 \left( \frac{\log 18}{10} \right) \left( \frac{189,000}{230,000} - 0.55 \right)$$

$$= 6,446.9 \text{ psi} \cong 6,447 \text{ psi}$$

$$\Delta f_{pES} + \Delta f_{pR} = 12,958 + 6,447 = 19,405 \cong 18,000 \text{ psi, assumed OK.}$$

**(c) Creep Loss**

$$\Delta f_{pCR} = 0$$

**(d) Shrinkage Loss**

$$\Delta f_{pSH} = 0$$

The stage-I total losses are

$$\Delta f_{pT} = \Delta f_{pES} + \Delta f_{pR} + \Delta f_{pCR} + \Delta f_{pSH}$$

$$= 12,958 + 6,447 + 0 + 0 = 19,405 \text{ psi} \quad (134 \text{ MPa})$$

The strand stress  $f_{pi}$  at the end of stage I = 189,000 – 19,405 = 169,595 psi (1,169 MPa), giving  $P_i = 311,376$  psi.

### Stage II: Transfer to Placement of Topping after 30 Days

#### (a) Creep Loss

$$E_c = 2.88 \times 10^6 \text{ psi}$$

$$E_{ps} = 28 \times 10^6 \text{ psi}$$

$$n = \frac{E_{ps}}{E_c} = \frac{28 \times 10^6}{2.88 \times 10^6} = 9.72$$

$$\bar{f}_{cs} = 1,115.3 \text{ psi}$$

Intensity of 2-in. normal-weight concrete topping:

$$W_{SD} = \frac{2}{12} \times 10 \times 150 = 250 \text{ plf}$$

The moment due to the 2-in. topping is

$$M_{SD} = W_{SD} \left( \frac{x}{2} \right) (L - x) = 250 \left( \frac{28}{2} \right) (70 - 28) \times 12 = 1,764,000 \text{ in.-lb (199 kN-m)}$$

$$\bar{f}_{csd} = \frac{M_{SD}e}{I_c} = \frac{1,764,000 \times 17.58}{59,720} = 519.3 \text{ psi}$$

Although 30 days' duration is short for long-term effects, sufficient approximation can be justified in stage II using the creep factor  $K_{CR}$  of Equation 3.11 to account for stage III as well (see stage-III creep calculations).

For lightweight concrete, use  $K_{CR} = 2.0 \times 80\% = 1.6$ . Then, from Equation 3.10, the prestress loss due to long-term creep is

$$\Delta f_{pCR} = nK_{CR}(\bar{f}_{cs} - \bar{f}_{csd}) = 9.72 \times 1.6(1,115.3 - 519.3) = 9,269 \text{ psi (63.3 MPa)}$$

#### (b) Shrinkage Loss. Assume relative humidity $RH = 70\%$ . Then, from Equation 3.14, the prestress loss due to long-term shrinkage is

$$\Delta f_{pSH} = 8.2 \times 10^{-6} K_{SH} E_{ps} \left( 1 - 0.06 \frac{V}{S} \right) (100 - RH)$$

$$\frac{V}{S} = \frac{615}{364} = 1.69 \text{ from geometry}$$

$K_{SH} = 1.0$  for pretensioned members; hence,

$$\begin{aligned} \Delta f_{pSH} &= 8.2 \times 10^{-6} \times 1.0 \times 28 \times 10^6 (1 - 0.06 \times 1.69)(100 - 70) \\ &= 6,190 \text{ psi (42.7 MPa)} \end{aligned}$$

#### (c) Steel Relaxation Loss at 30 Days

$$t_1 = 18 \text{ hours}$$

$$t_2 = 30 \text{ days} = 30 \times 24 = 720 \text{ hours}$$

$$f_{ps} = 169,595 \text{ psi from stage I}$$

$$\Delta f_{pR} = 169,595 \left( \frac{\log 720 - \log 18}{10} \right) \left( \frac{169,595}{230,000} - 0.55 \right) = 5,091 \text{ psi (35.1 MPa)}$$

Stage-II total loss is

$$\Delta f_{pT} = \Delta f_{pCR} + \Delta f_{pSH} + \Delta f_{pR} = 9,269 + 6,190 + 5,091 = 20,550 \text{ psi (142 MPa)}$$

The increase in stress in the strands due to the addition of topping is

$$f_{SD} = n\bar{f}_{csd} = 9.72 \times 519.3 = 5,048 \text{ psi (34.8 MPa)}$$

Hence, the strand stress at the end of stage II is

$$f_{pe} = f_{ps} - \Delta f_{pT} + f_{SD} = 169,595 - 20,550 + 5,048 = 154,093 \text{ psi (1,062 MPa)}$$

### Stage III: At End of Two Years

The values for long-term creep and long-term shrinkage evaluated for stage II are assumed not to have increased significantly, since the long-term values of  $K_{CR}$  for creep and  $K_{SH}$  for shrinkage were used in stage-II computations. Accordingly,

$$f_{pe} = 154,093 \text{ psi (1,066 MPa)}$$

$$t_1 = 30 \text{ days} = 720 \text{ hours}$$

$$t_2 = 2 \text{ years} \times 365 \times 24 = 17,520 \text{ hours}$$

The steel relaxation stress loss is

$$\Delta f_{pR} = 154,093 \left( \frac{\log 17,520 - \log 720}{10} \right) \left( \frac{154,093}{230,000} - 0.55 \right) = 2,563 \text{ psi (17.7 MPa)}$$

So the strand stress  $f_{pe}$  at the end of stage III  $\cong 154,093 - 2,563 = 151,530 \text{ psi (1,033 MPa)}$ .

### Summary of Stresses

Stress level at various stages	Steel stress, psi	Percent
After tensioning ( $0.70 f_{pu}$ )	189,000	100.0
Elastic shortening loss	-12,958	-6.9
Creep loss	-9,269	-4.9
Shrinkage loss	-6,190	-3.3
Relaxation loss (6,447 + 5,091 + 2,563)	-14,101	-7.5
Increase due to topping	5,048	2.7
Final net stress $f_{pe}$	151,530 psi (1,045 MPa)	80.1

Percentages of total losses =  $100 - 80.1 = 19.9\%$ , say, 20% for this pretensioned beam.

## 3.10 STEP-BY-STEP COMPUTATION OF ALL TIME-DEPENDENT LOSSES IN A POST-TENSIONED BEAM

### Example 3.9

Solve Example 3.8 assuming that the beam is post-tensioned. Assume also that the anchorage seating loss is  $\frac{1}{4}$  in. and that all strands are simultaneously tensioned in a flexible duct. Also assume that the total jacking force prior to the friction and anchorage seating losses resulted in  $f_{pi} = 189,000 \text{ psi}$  ( $f_{pj} = f_{pi}$  of Equation 3.1d in this case).

#### Solution:

##### (a) Anchorage seating loss

$$\Delta_A = \frac{1''}{4} = 0.25'' \quad L = 70 \text{ ft}$$

From Equation 3.24, the anchorage slip stress loss is

$$\Delta f_{pA} = \frac{\Delta_A}{L} E_{ps} = \frac{0.25}{70 \times 12} \times 28 \times 10^6 \cong 8333 \text{ psi (40.2 MPa)}$$

- (b) *Elastic shortening.* Since all jacks are simultaneously post-tensioned, the elastic shortening will precipitate during jacking. As a result, no elastic shortening stress loss takes place in the tendons. Hence,  $\Delta f_{pES} = 0$ .
- (c) *Frictional loss.* Assume that the parabolic tendon approximates the shape of an arc of a circle. Then, from Equation 3.23,

$$\alpha = \frac{8y}{x} = \frac{8(18.73 - 12.98)}{70 \times 12} = 0.0548 \text{ radian}$$

From Table 3.7, use  $K = 0.001$  and  $\mu = 0.25$ . Then, from Example 3.8,

$$f_{pi} = 189,000 \text{ psi (1,303 MPa)}$$

From Equation 3.22, the stress loss in prestress due to friction is

$$\begin{aligned} \Delta f_{pF} &= f_{pi}(\mu\alpha + KL) \\ &= 189,000(0.25 \times 0.0548 + 0.001 \times 70) \\ &= 15,819 \text{ psi (109 MPa)} \end{aligned}$$

The stress remaining in the prestressing steel after all initial instantaneous losses is

$$f_{pi} = 189,000 - 8,333 - 0 - 15,819 = 164,848 \text{ psi (1,136 MPa)}$$

Hence, the net prestressing force is

$$P_i = 164,848 \times 12 \times 0.153 = 296,726 \text{ lb}$$

compared to  $P_i = 311,376 \text{ lb}$  in the pretensioned case of Example 3.8.



**Photo 3.3** Linn Cove Viaduct, Grandfather Mountain, North Carolina. A 90° cantilever and a 10 percent superelevation in one direction to a full 10 percent in the opposite direction within 180 ft. Designed by Figg and Muller Engineers, Inc., Tallahassee, Florida. (Courtesy, Figg and Muller Engineers, Inc., now FIGG Engineers)

**Stage I: Stress at Transfer****(a) Anchorage Seating Loss**

$$\begin{aligned}\text{Loss} &= 8,333 \text{ psi} \\ \text{Net stress} &= 164,848 \text{ psi}\end{aligned}$$

**(b) Relaxation Loss**

$$\begin{aligned}\Delta f_{pR} &= 164,848 \left( \frac{\log 18}{10} \right) \left( \frac{164,848}{230,000} - 0.55 \right) \\ &\cong 3,450 \text{ psi (23.8 MPa)}\end{aligned}$$

**(c) Creep Loss**

$$\Delta f_{pCR} = 0$$

**(d) Shrinkage Loss**

$$\Delta f_{pSH} = 0$$

So the tendon stress  $f_{pi}$  at the end of stage I is

$$164,848 - 3,450 = 161,398 \text{ psi (1,113 MPa)}$$

**Stage II: Transfer to Placement of Topping after 30 Days****(a) Creep Loss**

$$\begin{aligned}P_i &= 161,398 \times 12 \times 0.153 = 296,327 \text{ lb} \\ \bar{f}_{cs} &= -\frac{P_i}{A_c} \left( 1 + \frac{e^2}{r^2} \right) + \frac{M_D e}{I_c} \\ &= -\frac{296,327}{615} \left( 1 + \frac{(17.58)^2}{97.11} \right) + \frac{3,464,496 \times 17.58}{59,720} \\ &= -2,016.20 + 1,020.00 = -996.2 \text{ psi (6.94 MPa)}\end{aligned}$$

Hence, the creep loss:

For lightweight concrete,  $K_{CR}$  is reduced by 20%, hence =  $1.6 \times 0.80 = 1.28$ .

$$\begin{aligned}\Delta f_{pCR} &= nK_{CR}(\bar{f}_{cs} - \bar{f}_{csd}) \\ &= 9.72 \times 1.28(996.2 - 519.3) \cong 5,933 \text{ psi (41 MPa)}\end{aligned}$$

**(b) Shrinkage Loss.** From Example 3.8, for  $K_{SH} = 0.58$  at 30 days, Table 3.6,

$$\Delta f_{pSH} = 6,190 \times 0.58 = 3,590 \text{ psi (24.8 MPa)}$$

Here, the assumption is made that the major shrinkage occurred in 30 days.

**(c) Steel Relaxation Loss at 30 Days**

$$f_{ps} = 161,398 \text{ psi}$$

The relaxation loss in stress becomes

$$\begin{aligned}\Delta f_{pR} &= 161,398 \left( \frac{\log 720 - \log 18}{10} \right) \left( \frac{161,398}{230,000} - 0.55 \right) \\ &\cong 3,923 \text{ psi (27.0 MPa)}\end{aligned}$$

**Stage II: Total Losses**

$$\begin{aligned}\Delta f_{pT} &= \Delta f_{pCR} + \Delta f_{pSH} + \Delta f_{pR} \\ &= 5,933 + 3,590 + 3,923 = 13,446 \text{ psi (93 MPa)}\end{aligned}$$

From Example 3.8, the increase in stress in the strands due to the addition of topping, is  $f_{SD} = 5,048$  psi (34.8 MPa); hence, the strand stress at the end of stage II is

$$f_{pe} = f_{ps} - \Delta f_{pT} + \Delta f_{SD} = 161,398 - 13,446 + 5,048 = 153,000 \text{ psi (1,055 MPa)}$$

**Stage III: At End of 2 Years**

$$f_{pe} = 153,000 \text{ psi}$$

$$t_1 = 720 \text{ hours}$$

$$t_2 = 17,520 \text{ hours}$$

The steel relaxation stress loss is

$$\begin{aligned} \Delta f_{pR} &= 153,000 \left( \frac{\log 17,520 - \log 720}{10} \right) \left( \frac{153,000}{230,000} - 0.55 \right) \\ &\cong 2,444 \text{ psi (16.9 MPa)} \end{aligned}$$

Using the same assumptions for stage III creep and shrinkage as in Example 3.8, the strand stress  $f_{pe}$  at the end of stage III is approximately

$$153,000 - 2,444 = 150,556 \text{ psi (1,038 MPa)}$$

**Summary of Stresses**

Stress level at various stages	Steel stress psi	Percent
After tensioning ( $0.70f_{pu}$ )	189,000	100.0
Elastic shortening loss	0	0.0
Anchorage loss*	-8,333	-4.4
Frictional loss*	-15,819	-8.4
Creep loss	-5,933	-3.1
Shrinkage loss	-3,590	-1.9
Relaxation loss (3,450 + 3,923 + 2,444)	-9,817	-5.2
Increase due to topping	+5,048	+2.7
Final net stress $f_{pe}$	150,556	79.7
Percentage of total losses = $100 - 79.7 = 20.3\%$ beam.		

\*Frictional and anchorage seating losses are included in this table since the total jacking stress is given as 189,000 psi; otherwise the tendons would have to be jacked an additional stress of such a magnitude as to neutralize the frictional and anchorage seating losses.

### 3.11 LUMP-SUM COMPUTATION OF TIME-DEPENDENT LOSSES IN PRESTRESS

**Example 3.10**

Solve Examples 3.8 and 3.9 by the approximate lump-sum method, and compare the results.

*Solution for Example 3.8.* From Table 3.1, the total loss  $\Delta f_{pT} = 45,000$  psi (228 MPa). So the net final strand stress by this method is

$$f_{pe} = 189,000 - 45,000 = 144,000 \text{ psi (993 MPa)}$$

$$\text{Step-by-step } f_{pe} \text{ value} = 151,530$$

$$\text{Percent difference} = \frac{151,530 - 144,000}{151,530} = 5.0\%$$

*Solution for Example 3.9.* From Table 3.2, the total loss  $\Delta_{pT} = 35,000$  psi (241 MPa). So the net final strand stress by the lump-sum method is

$$f_{pe} = 189,000 - 35,000 = 154,000 \text{ psi (1,062 MPa)}$$

$$\text{Step-by-step } f_{pe} \text{ value} = 150,556$$

$$\text{Percent difference} = \frac{154,000 - 149,232}{154,000} = 2.3\%$$

In both cases, the difference between the step-by-step “exact” method and the approximate lump-sum method is quite small, indicating that in normal, standard cases both methods are equally reliable.

### 3.12 SI PRESTRESS LOSS EXPRESSIONS

$$\Delta f_{pR} = f_{pi} \left( \frac{\log t_2 - \log t_1}{10} \right) \left( \frac{f'_{pi}}{f_{py}} - 0.55 \right) \quad (3.8)$$

for stress-relieved tendons where  $t$  is in hours. The denominator 10 becomes 45 for low-relaxation tendons.

$$\Delta f_{pCR} = n K_{CR} (\bar{f}_{cs} - \bar{f}_{csd}) \quad (3.11b)$$

where for normal concrete

$$\begin{aligned} K_{CR} &= 2.0 \text{ for pretensioned} \\ &= 1.6 \text{ for post-tensioned} \end{aligned}$$

reduced by 20% for lightweight concrete.

$$n = \text{modular ratio} = \frac{E_{ps}}{E_c}$$

$$\Delta f_{pSH} = 8.2 \times 10^{-6} K_{SH} E_{ps} \left( 1 - 0.06 \frac{V}{S} \right) (100 - RH) \quad (3.14)$$

$$\begin{aligned} K_{SH} &= 1.0, \text{ pretensioned} \\ &= \text{range of } 0.92 \text{ (1 day) to } 0.45 \text{ (60 days)} \end{aligned}$$

Equation 3.15a, moist curing for 7 days

$$\epsilon_{SH,t} = \left[ \frac{t}{t + 35} \right] \epsilon_{SH,u}$$

where  $\epsilon_{SH,t} = 800 \times 10^{-6}$  mm/mm

Equation 3.15b, steam curing 1 to 3 days max

$$\epsilon_{SH,t} = \left[ \frac{t}{t + 55} \right] \epsilon_{SH,u}$$

where  $\epsilon_{SH,t} = 730 \times 10^{-6}$  mm/mm

$$\Delta f_{pF} = -f_1 (\mu \alpha + 3.28KL) \quad (3.22)$$

where  $L$ , meter.

$$\Delta f_{pA} = \left( \frac{\Delta_A}{L} \right) E_{ps} \quad (3.24)$$

$$E_c = w^{1.5} 0.043 \sqrt{f'_c} \quad w \text{ (lightweight)} \approx 1830 \text{ Kg/m}^3.$$

$$E_{ci} = w^{1.5} 0.043 \sqrt{f'_{ci}}$$

$$\text{MPa} = 10^6 \text{ N/m}^2 = \text{N/mm}^2$$

$$(\text{psi}) 0.006895 = \text{MPa}$$

$$(\text{lb/ft}) 14.593 = \text{N/m}$$

$$(\text{in.-lb}) = 0.113 = \text{N-m}$$

### 3.12.1 SI Prestress Loss Example

#### Example 3.11

Solve Example 3.9 using SI units for losses in prestress, considering self-weight and superimposed dead load only.

#### Data

$$f'_c = 34.5 \text{ MPa}$$

$$f'_{ci} = 24.1 \text{ MPa}$$

$$A_c = 3,968 \text{ cm}^2$$

$$S' = 97,670 \text{ cm}^3$$

$$I_c = 2.49 \times 10^6 \text{ cm}^4$$

$$S_b = 44,520 \text{ cm}^3$$

$$r^2 = I_c/A_c = 626$$

$$c_b = 55.8 \text{ cm}$$

$$c' = 25.5 \text{ cm}$$

$$e_c = 47.6 \text{ cm}$$

$$e_e = 33.0 \text{ cm}$$

$$f_{pu} = 1,860 \text{ MPa}$$

$$f_{py} = 0.85f_{pu} = 1,580 \text{ MPa}$$

$$f_{pi} = 0.82f_{py} = (0.82 \times 0.85)f_{pu} = 0.7f_{pu} = 1,300 \text{ MPa}$$

$$E_{ps} = 193,000 \text{ MPa}$$

$$\text{Span } l = 21.3 \text{ m}$$

$$A_{ps} = \text{twelve tendons, 12.7-mm diameter (99 mm}^2\text{)}$$

$$= 12 \times 99 = 1,188 \text{ mm}^2$$

$$M_D = 391 \text{ kN-m} \quad M_{SD} = 199 \text{ kN-m}$$

$$\Delta_A = 0.64 \text{ cm}$$

$$V/S = 1.69$$

$$RH = 70\%$$

#### Solution:

##### (a) Anchorage seating loss

$$\Delta A = 0.64 \text{ cm} \quad l = 21.3 \text{ m}$$

$$\Delta f_{pA} = \frac{\Delta A}{l} (E_{ps}) = \frac{0.64}{21.3 \times 100} \times 193,000 = 58.0 \text{ MPa}$$

##### (b) Elastic Shortening

Since all jacks are simultaneously tensioned, the elastic shortening will simultaneously precipitate during jacking. As a result, no elastic shortening loss takes place in the tendons.



Hence

$$\Delta f_{pES} = 0.$$

(c) *Frictional Loss*

Assume that the parabolic tendon approximates the shape of an arc of a circle. Then, from Equation 3.23,

$$\begin{aligned}\alpha &= \frac{8y}{x} = \frac{8(e_c - e_e)}{l} = \frac{8(47.6 - 33.0)}{21.3 \times 100} \\ &= 0.055 \text{ radians}\end{aligned}$$

From Table 3.7,  $K = 0.001$ ,  $\mu = 0.25$ ,  $f_{pi} = 1,300$  MPa

From Equation 3.22,

$$\begin{aligned}\Delta f_{pF} &= f_{pi}(\mu\alpha + 3.28KL) \\ &= 1,300(0.25 \times 0.055 + 0.001 \times 3.28 \times 21.3) \\ &= 109 \text{ MPa}\end{aligned}$$

The stress remaining in the prestressing steel after all instantaneous stresses

$$f_{pi} = 1,300 - (58 + 0 + 109) = 1,133 \text{ MPa}$$

Hence, the net prestressing force is

$$P_i = f_{pi}A_{ps} = 1,133 \times 1,188 = 1.35 \times 10^6 \text{ N}$$

**Stage I: Stress at Transfer**

(a) *Anchorage Seating Loss*  $\Delta f_{fA} = 58$  MPa

(b) *Relaxation Loss*

From Equation 3.8,

$$\begin{aligned}\Delta f_{pR} &= f_{pi} \left( \frac{\log t_2 - \log t_1}{10} \right) \left( \frac{f'_{pi}}{f_{py}} - 0.55 \right) \\ &= 1,133 \left( \frac{\log 18 - \log 0}{10} \right) \left( \frac{1,133}{1,580} - 0.55 \right) \\ &= 24.4 \text{ MPa}\end{aligned}$$

(c) *Creep Loss*  $\Delta f_{cR} = 0$

(d) *Shrinkage Loss*  $\Delta f_{SH} = 0$

Tendon stress at the end of stage I

$$f_{ps} = 1,133 - 24.4 \cong 1,108 \text{ MPa}$$

**Stage II: Transfer to Placement of Topping After 30 Days**

(a) *Creep Loss*

$$P_i = 1,108 \times 1,188 = 1.32 \times 10^6 \text{ N}$$

$$\bar{f}_{cs} = -\frac{P_i}{A_c} \left( 1 + \frac{e^2}{r^2} \right) + \frac{M_D e_b}{I_c} \text{ at tendons centroid}$$

$e$  at 0.4 of span = 17.58 in. = 44.7 cm

$$\begin{aligned}\bar{f}_{cs} &= -\frac{1.32 \times 10^6}{3,968 \times 10^2} \left[ 1 + \frac{(44.6)^2}{626} \right] + \frac{3.91 \times 10^7 \text{ N-cm} \times 44.6 \text{ N/mm}^2}{2.49 \times 10^6} \times \frac{1}{100} \\ &= -13.90 + 7.00 \text{ N/mm}^2 = 6.90 \text{ MPa at cgs}\end{aligned}$$

$w$  (lightweight) = 1,800 Kg/m<sup>3</sup>

$$\begin{aligned}
 E_c (\text{lightweight}) &= w^{1.5} 0.043 \sqrt{34.5} \\
 &= 1,830^{1.5} \times 0.043 \sqrt{34.5} = 19,770 \text{ MPa} \\
 n &= \frac{E_{ps}}{E_c} = \frac{193,000}{19,770} = 9.76
 \end{aligned}$$

$\bar{f}_{csd}$  = stress in concrete at cgs due to all superimposed dead loads after prestressing is accomplished.

$$\begin{aligned}
 \bar{f}_{csd} &= \frac{M_{SDe}}{I_c} = \frac{1.99 \times 10^7 \text{ N-cm} \times 44.7}{2.49 \times 10^6} \times \frac{1}{100} \text{ N/mm}^2 \\
 &= 3.57 \text{ MPa}
 \end{aligned}$$

$K_{CR} = 1.6$  for post-tensioned beam

From Equation 3.11b,

$$\begin{aligned}
 \Delta f_{pCR} &= nK_{CR}(\bar{f}_{cs} - \bar{f}_{csd}) \\
 &= 9.76 \times 1.6(6.90 - 3.57) = 52.0 \text{ MPa}
 \end{aligned}$$

**(b) Shrinkage Loss at 30 Days**

From Equation 3.14,

$$\Delta f_{pSH} = 8.2 \times 10^{-6} K_{SH} E_{ps} \left( 1 - 0.06 \frac{V}{S} \right) (100 - RH)$$

$K_{SH}$  at 30 days = 0.58 (Table 3.6)

$$\begin{aligned}
 \Delta f_{pSH} &= 8.2 \times 10^{-6} \times 0.58 \times 193,000 (1 - 0.06 \times 1.69) (100 - 70) \\
 &= 24.7 \text{ MPa}
 \end{aligned}$$

**(c) Relaxation Loss at 30 Days (720 Hrs)**

$$f_{ps} = 1,108 \text{ MPa}$$

$$\begin{aligned}
 \Delta f_{pR} &= 1,108 \left( \frac{\log 720 - \log 18}{10} \right) \left( \frac{1,108}{1,580} - 0.55 \right) \\
 &= 110.8(2.85 - 1.25)0.151 = 26.8 \text{ MPa}
 \end{aligned}$$

**Stage II: Total Losses**

$$\begin{aligned}
 \Delta f_{pT} &= \Delta f_{pCR} + \Delta f_{pSH} + \Delta f_{pR} \\
 &= 52.0 + 24.7 + 26.8 = 104 \text{ MPa}
 \end{aligned}$$

Increase of tensile stress at bottom cgs fibers due to addition of topping is from before,

$$\begin{aligned}
 \Delta f_{SD} &= n f_{CSD} = 9.76 \times 3.57 = 34.8 \text{ MPa} \\
 f_{pe} &= f_{ps} - \Delta f_{pT} + \Delta f_{SD} \\
 &= 1,108 - 103.5 + 34.5 = 1,039 \text{ MPa}
 \end{aligned}$$

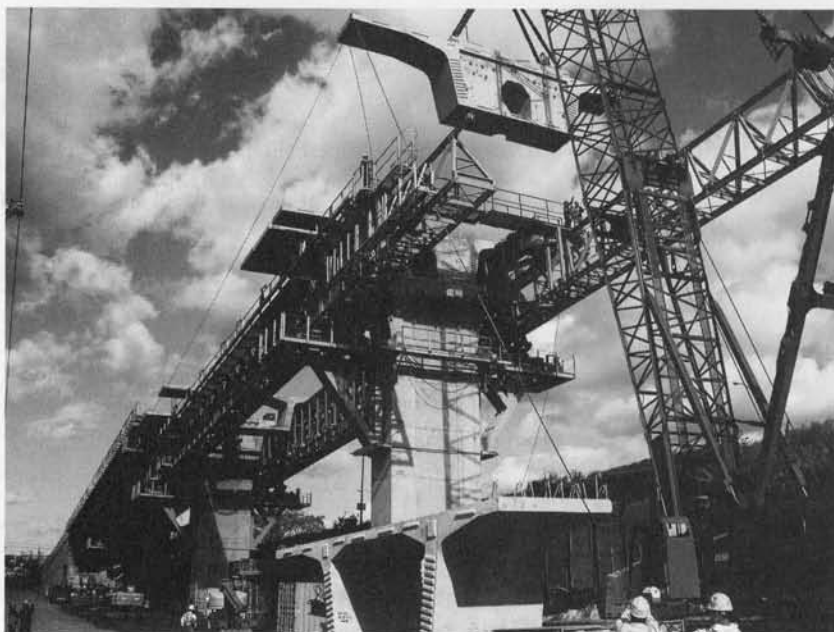
**Stage III: At End of Two Years**

$$f_{pe} = 1,039 \text{ MPa}$$

$$t_1 = 720 \text{ hrs.} \quad t_2 = 17,520 \text{ hrs.}$$

$$\begin{aligned}
 \Delta f_{pR} &= 1,039 \left( \frac{\log 17,520 - \log 720}{10} \right) \left( \frac{1,039}{1,580} - 0.55 \right) \\
 &= 103.9(4.244 - 2.857)0.108 = 15.6 \text{ MPa}
 \end{aligned}$$

On the assumption that  $\Delta f_{pCR}$  and  $\Delta f_{pSH}$  were stable in this case, the stress in the tendons at end of stage III can approximately be  $f_{ps} = 1,039 - 15.6 \cong 1,020 \text{ MPa}$ .



**Photo 3.4** Route 35, Victory Bridge over the Raritan River, connecting Perth Amboy and Sayerville, New Jersey. A variable depth precast segmental concrete bridge with spans of 330'–440'–330' built in balanced cantilever. The first of the twin 3,970' bridges was completed in just 15 months. The speeding of construction was accomplished by erecting the approach spans with span-to-span construction while simultaneously erecting the main 440 ft. span using balanced cantilever construction. At this time, this main span is the longest precast cantilever segmental construction in the United States. The photo shows the span-by-span erection scheme of the approach spans. (Courtesy of FIGG, the bridge designer)

## SELECTED REFERENCES

- 3.1 PCI Committee on Prestress Loss. "Recommendations for Estimating Prestress Loss." *Journal of the Prestressed Concrete Institute* 20 (1975): 43–75.
- 3.2 ACI-ASCE Joint Committee 423. "Tentative Recommendations for Prestressed Concrete." *Journal of the American Concrete Institute* 54 (1957): 548–578.
- 3.3 AASHTO Subcommittee on Bridges and Structures. *Interim Specifications Bridges*. American Association of State Highway and Transportation Officials, Washington, D.C., 1975.
- 3.4 Prestressed Concrete Institute. *PCI Design Handbook*. 5th Ed. PCI, Chicago: 1999.
- 3.5 Post-Tensioning Institute. *Post-Tensioning Manual*. 5th ed. Post-Tensioning Institute, Phoenix, AZ, 2000.
- 3.6 Lin, T. Y. "Cable Friction in Post-Tensioning." *Journal of Structural Division*. ASCE, New York, November 1956, pp. 1107–1 to 1107–13.
- 3.7 Tadros, M. K., Ghali, A., and Dilger, W. H. "Time Dependent Loss and Deflection in Prestressed Concrete Members." *Journal of the Prestressed Concrete Institute* 20, 1975, 86–98.
- 3.8 Branson, D. E. "The Deformation of Noncomposite and Composite Prestressed Concrete Members." In *Deflection of Structures*. American Concrete Institute, Farmington Hills, 1974, pp. 83–128.
- 3.9 Nawy, E. G. *Reinforced Concrete—A Fundamental Approach*. 6th ed. Prentice-Hall, Upper Saddle River, NJ: 2009, 936 pp.
- 3.10 Cohn, M. Z. *Partial Prestressing, From Theory to Practice*. NATO-ASI Applied Science Series, vols 1 and 2. Dordrecht, The Netherlands: Martinus Nijhoff, in Cooperation with NATO Scientific Affairs Division, 1986.
- 3.11 ACI Committee 318, *Building Code Requirements for Structural Concrete (ACI 318-08) and Commentary (ACI 318 R-08)*, American Concrete Institute, Farmington Hills, MI, 2008, pp. 446.
- 3.12 ACI Committee 435, "Control of Deflection in Concrete Structures," ACI Committee Report R435-95, E. G. Nawy, Chairman, American Concrete Institute, Farmington Hills, MI, 1995, pp. 77.

- 3.13 Nawy, E. G., "Concrete—The Sustainable Infrastructure Material for the 21 st. Century," Keynote Address Paper, No. E-C103, Transportation Research Board, National Research Council, Washington, D.C., September 2006, pp. 1–23.
- 3.14 Nawy, E. G., "Concrete—The Sustainable Infrastructure Material for the 21 st. Century," Keynote Address Paper, Proceedings, The First International Conference on Recent Advances in Concrete Technology, Crystal City, Washington, D.C., September 19, 2007, pp. 1–24.

### PROBLEMS

- 3.1 A simply supported pretensioned beam has a span of 75 ft (22.9 m) and the cross section shown in Figure P3.1. It is subjected to a uniform gravitational live-load intensity  $W_L = 1,200$  plf (17.5 kN/m) in addition to its self-weight and is prestressed with 20 stress-relieved  $\frac{1}{2}$ -in. dia (12.7 mm dia) 7-wire strands. Compute the total prestress losses by the step-by-step method, and compare them with the values obtained by the lump-sum method. Take the following values as given:

$$f'_c = 6,000 \text{ psi (41.4 MPa), normal-weight concrete}$$

$$f'_{ci} = 4,500 \text{ psi (31 MPa)}$$

$$f_{pu} = 270,000 \text{ psi (1,862 MPa)}$$

$$f_{pi} = 0.70f_{pu}$$

$$\text{Relaxation time } t = 5 \text{ years}$$

$$e_c = 19 \text{ in. (483 mm)}$$

$$\text{Relative humidity } RH = 75\%$$

$$V/S = 3.0 \text{ in. (7.62 cm)}$$

Assume  $SD$  load = 30%  $LL$ .

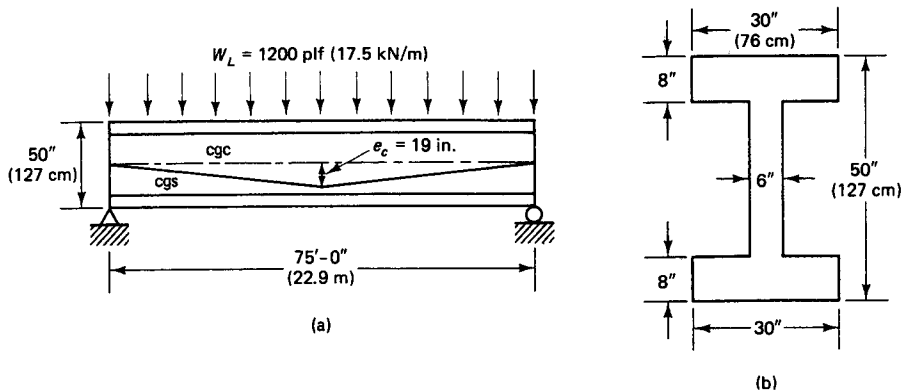


Figure P3.1 (a) Elevation. (b) Section.

- 3.2 Compute, by the detailed step-by-step method, the total losses in prestress of the 10-ft (3.28-m)-wide flange double T-beam in Example 1.1 which has a span of 64 ft (19.5 m) for a steel relaxation period of 7 years. Use  $RH = 70\%$  and  $V/S = 3.5$  in. (8.9 cm), and solve for both pretensioned and post-tensioned prestressing conditions. Assume  $SD$  load = 30%  $LL$ . In the post-tensioned case, assume that the total jacking stress prior to the friction and anchorage seating losses is 189,000 psi.
- 3.3 Compute, by the detailed step-by-step method, the total losses of prestress in the AASHTO 36-in. (91.4 cm)-deep beam used in Problem 1.1 and which has a span of 34 ft (10.4 m) for both the pretensioned and the post-tensioned case. Use all the data of Problem 1.1 in your solution, and assume that the relative humidity  $RH = 70\%$  and the volume-to-surface ratio  $V/S = 3.2$ . Determine the steel relaxation losses at the end of the first year after erection and at the end of 4 years.
- 3.4 Compute, by the detailed step-by-step method, the total prestress losses of the simply supported double T-beam of Example 3.9 if it was post-tensioned using flexible ducts for the tendon. Assume that the tendon profile is essentially parabolic. Assume also that all strands are tensioned simultaneously and that the anchorage slip  $\Delta_A = \frac{3}{8}$  in. (9.5 mm). All the data are identical to those of Example 3.8; the critical section is determined to be at a distance 0.4 times the span from the face of the support.

# 4



## FLEXURAL DESIGN OF PRESTRESSED CONCRETE ELEMENTS

### 4.1 INTRODUCTION

Flexural stresses are the result of external, or imposed, bending moments. In most cases, they control the selection of the geometrical dimensions of the prestressed concrete section regardless of whether it is pretensioned or post-tensioned. The design process starts with the choice of a preliminary geometry, and by trial and adjustment it converges to a final section with geometrical details of the concrete cross section and the sizes and alignments of the prestressing strands. The section satisfies the flexural (bending) requirements of concrete stress and steel stress limitations. Thereafter, other factors such as shear and torsion capacity, deflection, and cracking are analyzed and satisfied.

While the input data for the analysis of sections differ from the data needed for design, every design is essentially an analysis. One assumes the geometrical properties of the section to be prestressed and then proceeds to determine whether the section can safely carry the prestressing forces and the required external loads. Hence, a good understanding of the fundamental principles of analysis and the alternatives presented thereby significantly simplifies the task of designing the section. As seen from the discussion in Chapter 1, the basic mechanics of materials, principles of equilibrium of internal couples, and elastic principles of superposition have to be adhered to in all stages of loading.

Maryland Concert Center parking garage, Baltimore. (*Courtesy, Prestressed Concrete Institute.*)

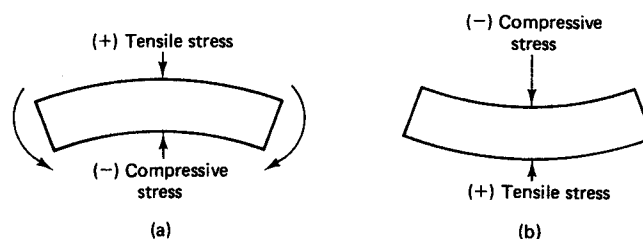
It suffices in the flexural design of reinforced concrete members to apply only the limit states of stress at failure for the choice of the section, provided that other requirements such as serviceability, shear capacity, and bond are met. In the design of prestressed members, however, additional checks are needed at the load transfer and limit state at service load, as well as the limit state at failure, with the failure load indicating the reserve strength for overload conditions. All these checks are necessary to ensure that at service load cracking is negligible and the long-term effects on deflection or camber are well controlled.

In view of the preceding, this chapter covers the major aspects of both the service-load flexural design and the ultimate-load flexural design check. The principles and methods presented in Chapter 1 for service load computations are extended into step-by-step procedures for the design of prestressed concrete linear elements, taking into consideration the impact of the magnitude of prestress losses discussed in Chapter 3. Note that a logical sequence in the design process entails *first* the service-load design of the section required in flexure, and then the analysis of the available moment strength  $M_n$  of the section for the limit state at failure. Throughout the book, a negative sign (–) is used to denote compressive stress and a positive sign (+) is used to denote tensile stress in the concrete section. A convex or hogging shape indicates negative bending moment; a concave or sagging shape denotes positive bending moment, as shown in Figure 4.1.

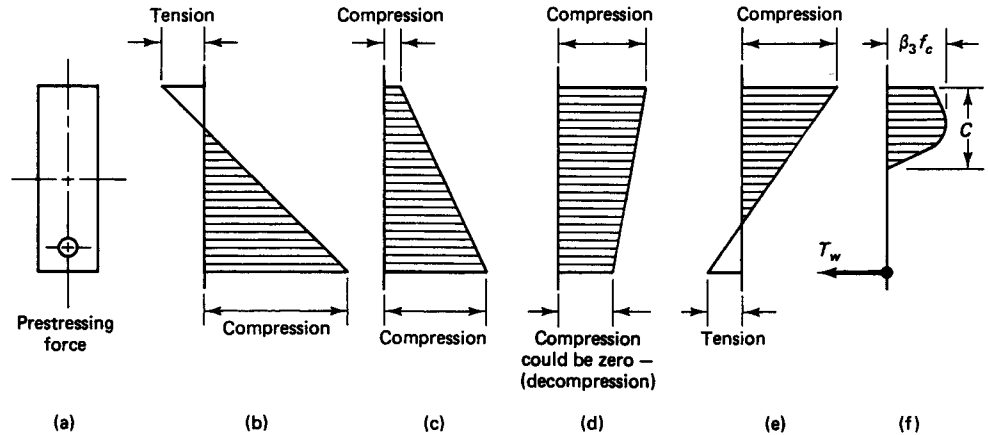
Unlike the case of reinforced concrete members, the external dead load and partial live load are applied to the prestressed concrete member at varying concrete strengths at various loading stages. These loading stages can be summarized as follows:

- Initial prestress force  $P_i$  is applied; then, at transfer, the force is transmitted from the prestressing strands to the concrete.
- The full self-weight  $W_D$  acts on the member together with the initial prestressing force, provided that the member is simply supported, i.e., there is no intermediate support.
- The full superimposed dead load  $W_{SD}$  including topping for composite action, is applied to the member.
- Most short-term losses in the prestressing force occur, leading to a reduced prestressing force  $P_{eo}$ .
- The member is subjected to the full service load, with long-term losses due to creep, shrinkage, and strand relaxation taking place and leading to a net prestressing force  $P_e$ .
- Overloading of the member occurs under certain conditions up to the limit state at failure.

A typical loading history and corresponding stress distribution across the depth of the critical section are shown in Figure 4.2, while a schematic plot of load versus defor-



**Figure 4.1** Sign convention for flexure stress and bending moment. (a) Negative bending moment. (b) Positive bending moment.



**Figure 4.2** Flexural stress distribution throughout loading history. (a) Beam section. (b) Initial prestressing stage. (c) Self-weight and effective prestress. (d) Full dead load plus effective prestress. (e) Full service load plus effective prestress. (f) Limit state of stress at ultimate load for underreinforced beam.

mation (camber or deflection) is shown in Figure 4.3 for the various loading stages from the self-weight effect up to rupture.

## 4.2 SELECTION OF GEOMETRICAL PROPERTIES OF SECTION COMPONENTS

### 4.2.1 General Guidelines

Under service-load conditions, the beam is assumed to be homogeneous and elastic. Since it is also assumed (because expected) that the prestress compressive force transmitted to the concrete closes the crack that might develop at the tensile fibers of the beam, beam sections are considered uncracked. Stress analysis of prestressed beams under these conditions is no different from stress analysis of a steel beam, or, more accurately, a beam column. The axial force due to prestressing is always present regardless of whether bending moments do or do not exist due to other external or self-loads.

As seen from Chapter 1, it is advantageous to have the alignment of the prestressing tendon eccentric at the critical sections, such as the midspan section in a simple beam and the support section in a continuous beam. As compared to a rectangular solid section, a nonsymmetrical flanged section has the advantage of efficiently using the concrete material and of concentrating the concrete in the compressive zone of the section where it is most needed.

Equations 4.1, 4.2, and 4.3 to be subsequently presented are stress equations that are convenient in the analysis of stresses in the section once the section is chosen. For design, it is necessary to transpose the three equations into geometrical equations so that the student and the designer can readily choose the concrete section. A logical transposition is to define the minimum section modulus that can withstand all the loads after losses.

### 4.2.2 Minimum Section Modulus

To design or choose the section, a determination of the required minimum section modulus,  $S_b$  and  $S'$ , has to be made first. If

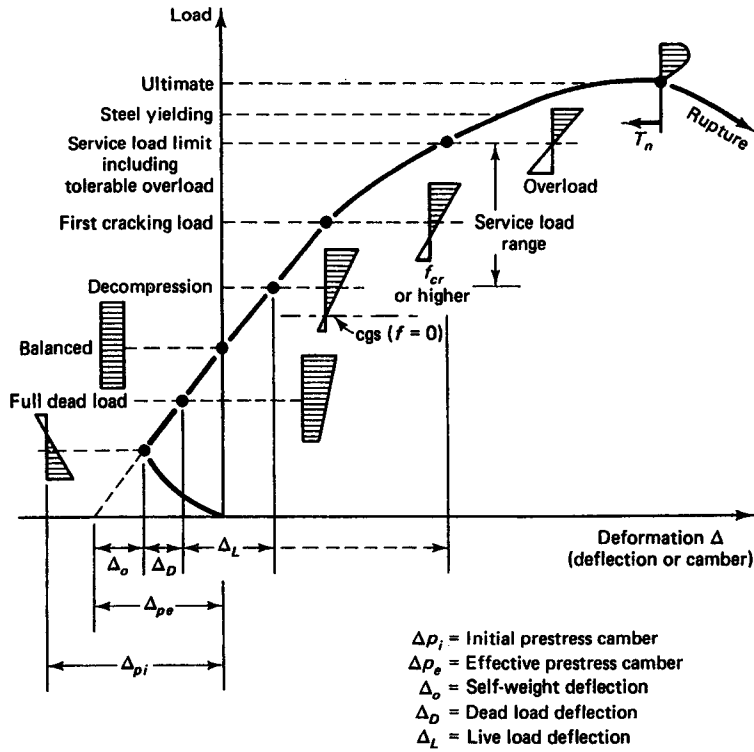


Figure 4.3 Load-deformation curve of typical prestressed beam.

- $f_{ci}$  = maximum allowable compressive stress in concrete immediately after transfer and prior to losses  
 $= 0.60 f'_{ci}$
- $f_{ti}$  = maximum allowable tensile stress in concrete immediately after transfer and prior to losses  
 $= 3\sqrt{f'_{ci}}$  (the value can be increased to  $6\sqrt{f'_{ci}}$  at the supports for simply supported members)
- $f_c$  = maximum allowable compressive stress in concrete after losses at service-load level  
 $= 0.45 f'_c$  or  $0.60 f'_c$  when allowed by the code
- $f_t$  = maximum allowable tensile stress in concrete after losses at service load level  
 $= 6\sqrt{f'_c}$  (the value can be increased in one-way systems to  $12\sqrt{f'_c}$  if long-term deflection requirements are met)

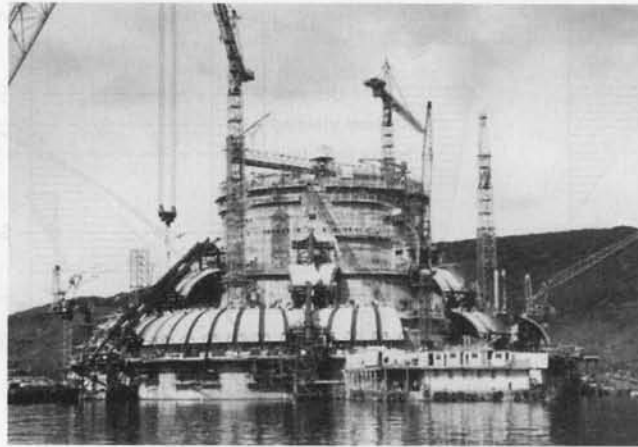
then the *actual* extreme fiber stresses in the concrete cannot exceed the values listed.

Using the uncracked unsymmetrical section, a summary of the equations of stress from Section 1.3 for the various loading stages is as follows.

**Stress at Transfer**

$$f^t = -\frac{P_i}{A_c} \left( 1 - \frac{ec_t}{r^2} \right) - \frac{M_D}{S^t} \leq f_{ti} \tag{4.1a}$$





**Photo 4.1** Ninian Central oil drilling platform, Cheiron, England, and C. G. Doris, Scotland. (Courtesy, Ben C. Gerwick.)

$$f_b = -\frac{P_i}{A_c} \left( 1 + \frac{ec_b}{r^2} \right) + \frac{M_D}{S_b} \leq f_{ci} \quad (4.1b)$$

where  $P_i$  is the initial prestressing force. While a more accurate value to use would be the horizontal component of  $P_i$ , it is reasonable for all practical purposes to disregard such refinement.

#### Effective Stresses after Losses

$$f^t = -\frac{P_e}{A_c} \left( 1 - \frac{ec_t}{r^2} \right) - \frac{M_D}{S^t} \leq f_t \quad (4.2a)$$

$$f_b = -\frac{P_e}{A_c} \left( 1 + \frac{ec_b}{r^2} \right) + \frac{M_D}{S_b} \leq f_c \quad (4.2b)$$

#### Service-load Final Stresses

$$f^t = -\frac{P_e}{A_c} \left( 1 - \frac{ec_t}{r^2} \right) - \frac{M_T}{S^t} \leq f_t \quad (4.3a)$$

$$f_b = -\frac{P_e}{A_c} \left( 1 + \frac{ec_b}{r^2} \right) + \frac{M_T}{S_b} \leq f_c \quad (4.3b)$$

where  $M_T = M_D + M_{SD} + M_L$

$P_i$  = initial prestress

$P_e$  = effective prestress after losses

$t$  denotes the top, and  $b$  denotes the bottom fibers

$e$  = eccentricity of tendons from the concrete section center of gravity,  $ecg$

$r^2$  = square of radius of gyration

$S^t/S_b$  = top/bottom section modulus value of concrete section

The *decompression stage* denotes the increase in steel strain due to the increase in load from the stage when the effective prestress  $P_e$  acts *alone* to the stage when the addi-

tional load causes the compressive stress in the concrete at the cgs level to reduce to zero (see Figure 4.3). At this stage, the *change* in concrete stress due to decompression is

$$f_{\text{decomp}} = \frac{P_e}{A_c} \left( 1 + \frac{e^2}{r^2} \right) \quad (4.3c)$$

This relationship is based on the assumption that the strain between the concrete and the prestressing steel bonded to the surrounding concrete is such that the gain in the steel stress is the same as the decrease in the concrete stress.

**4.2.2.1 Beams With Variable Tendon Eccentricity.** Beams are prestressed with either draped or harped tendons. The maximum eccentricity is usually at the midspan controlling section for the simply supported case. Assuming that the effective prestressing force is

$$P_e = \gamma P_i$$

where  $\gamma$  is the residual prestress ratio, the loss of prestress is

$$P_i - P_e = (1 - \gamma)P_i \quad (a)$$

If the actual concrete extreme fiber stress is equivalent to the maximum allowable stress, the change in this stress after losses, from Equations 4.1a and b, is given by

$$\Delta f'_t = (1 - \gamma) \left( f_{ti} + \frac{M_D}{S'_t} \right) \quad (b)$$

$$\Delta f_b = (1 - \gamma) \left( -f_{ci} + \frac{M_D}{S_b} \right) \quad (c)$$

From Figure 4.4(a), as the superimposed dead-load moment  $M_{SD}$  and live-load moment  $M_L$  act on the beam, the net stress at top fibers is

$$f'_n = f_{ti} - \Delta f'_t - f_c$$

or

$$f'_n = \gamma f_{ti} - (1 - \gamma) \frac{M_D}{S'_t} - f_c \quad (d)$$

The net stress at the bottom fibers is

$$f_{bn} = f_t - f_{ci} - \Delta f_b$$

or

$$f_{bn} = f_t - \gamma f_{ci} - (1 - \gamma) \frac{M_D}{S_b} \quad (e)$$

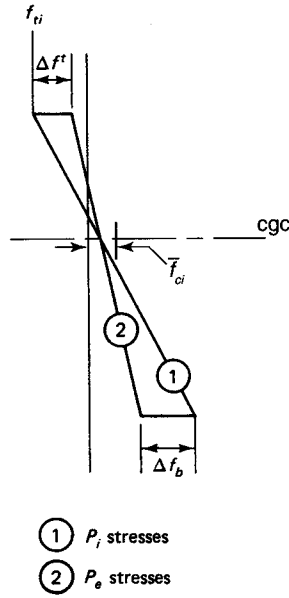
From Equations (d) and (e), the chosen section should have section moduli values

$$S'_t \geq \frac{(1 - \gamma)M_D + M_{SD} + M_L}{\gamma f_{ti} - f_c} \quad (4.4a)$$

and

$$S_b \geq \frac{(1 - \gamma)M_D + M_{SD} + M_L}{f_t - \gamma f_{ci}} \quad (4.4b)$$





**Figure 4.4(b)** Maximum fiber stresses at support section of beams with straight tendons (stress distribution at midspan section similar to that of Figure 4.4a).

**4.2.2.2 Beams with Constant Tendon Eccentricity.** Beams with constant tendon eccentricity are beams with straight tendons, as is normally the case in precast moderate-span simply supported beams. Because the tendon has a large eccentricity at the support, creating large tensile stresses at the top fibers without any reduction due to superimposed  $M_D + M_{SD} + M_L$ , in such beams smaller eccentricity of the tendon at midspan has to be used as compared to a similar beam with a draped tendon. In other words, the controlling section is the support section, for which the stress distribution at the support is shown in Figure 4.4(b). Hence,

$$\Delta f_t' = (1 - \gamma)(f_{ti}) \tag{a'}$$

and

$$\Delta f_b = (1 - \gamma)(-f_{ci}) \tag{b'}$$

The net stress at the service-load condition after losses at the top fibers is

$$f_n^t = f_{ti} - \Delta f_t' - f_c$$

or

$$f_n^t = \gamma f_{ti} - f_{cs} \tag{c'}$$

where  $f_{cs}$  is the actual service-load stress in concrete. The net stress at service load after losses at the bottom fibers is

$$f_{bn} = f_{ti} - f_{ci} - \Delta f_b$$

or

$$f_{bn} = f_{ti} - \gamma f_{ci} \tag{d'}$$

From Equations (c) and (d), the chosen section should have section moduli values

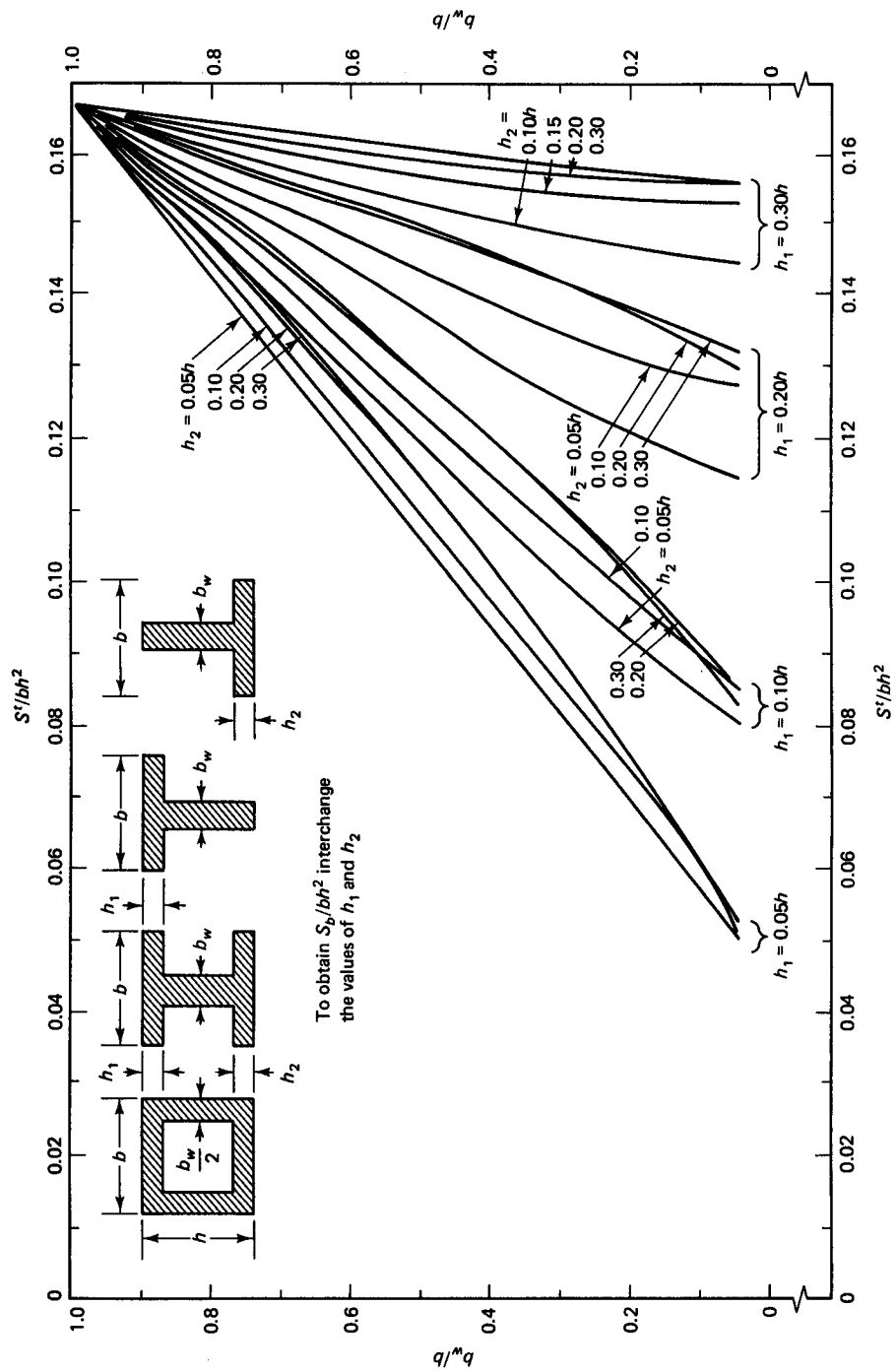


Figure 4.5 Section moduli of flanged and boxed sections (adapted from Ref. 4.16).

$$S' \geq \frac{M_D + M_{SD} + M_L}{\gamma f_{ii} - f_c} \quad (4.5a)$$

and

$$S_b \geq \frac{M_D + M_{SD} + M_L}{f_t - \gamma f_{ci}} \quad (4.5b)$$

The required eccentricity value at the critical section, such as the support for an ideal beam section having properties close to those required by Equations 4.5a and b, is

$$e_e = (f_{ii} - \bar{f}_{ci}) \frac{S'}{P_i} \quad (4.5c)$$

A graphical representation of section moduli of nominal sections is shown in Figure 4.5. It may be used as a speedy tool for the choice of initial trial sections in the design process.

Table 4.1 gives the section moduli of standard PCI rectangular sections. Tables 4.2 and 4.3 give the geometrical outer dimensions of standard PCI T-sections and AASHTO I-sections, respectively, as well as the top-section moduli of those sections needed in the preliminary choice of the section in the service-load analysis. Table 4.4(a) gives dimensional details of the *actual* “as-built” geometry of the standard PCI and AASHTO sections, and Table 4.4(b) gives girder properties of optimized sections used in different states. Properties of bulb sections are given in Appendix C. Additional details are presented in Refs. 4.9 and 4.12.

## 4.3 SERVICE-LOAD DESIGN EXAMPLES

### 4.3.1 Variable Tendon Eccentricity

#### Example 4.1

Design a simply supported pretensioned double-T-beam for a parking garage with harped tendon and with a span of 60 ft (18.3 m) using the ACI 318 Building Code allowable stresses. The beam has to carry a superimposed sustained service live load of 1,100 plf (16.1 kN/m) and superimposed dead load of 100 plf (1.5 kN/m), and has no concrete topping. Assume the beam is made of normal-weight concrete with  $f'_c = 5,000$  psi (34.5 MPa) and that the concrete strength  $f'_{ci}$  at transfer is 75 percent of the cylinder strength. Assume also that the time-dependent losses of the initial prestress are 18 percent of the initial prestress, and that  $f_{pu} = 270,000$  psi (1,862 MPa) for stress-relieved tendons,  $f_t = 12\sqrt{f'_c}$ .

**Table 4.1** Section Properties and Moduli of Standard PCI Rectangular Sections

Designation	12RB16	12RB20	12RB24	12RB28	12RB32	12RB36	16RB32	16RB36	16RB40
Section modulus $S$ , (in. <sup>3</sup> )	512	800	1,152	1,568	2,048	2,592	2,731	3,456	4,267
Width, $b$ (in.)	12	12	12	12	12	12	16	16	16
Depth, $h$ (in.)	16	20	24	28	32	36	32	36	40

**Table 4.2** Geometrical Outer Dimensions and Section Moduli of Standard PCI Double T-Sections

Designation	Top-/bottom-section modulus, in. <sup>3</sup>	Flange width $b_f$ , in.	Flange depth $t_f$ , in.	Total depth $h$ , in.	Web width $2 b_w$ in.
8DT12	1,001/315	96	2	12	9.5
8DT14	1,307/429	96	2	14	9.5
8DT16	1,630/556	96	2	16	9.5
8DT20	2,320/860	96	2	20	9.5
8DT24	3,063/1,224	96	2	24	9.5
8DT32	5,140/2,615	96	2	32	9.5
10DT32	5,960/2,717	120	2	32	12.5
*12DT34	10,458/3,340	144	4	34	12.5
*15DT34	13,128/4,274	180	4	34	12.5

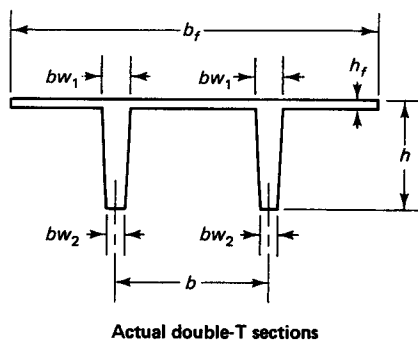
\*Pretopped

**Table 4.3** Geometrical Outer Dimensions and Section Moduli of Standard AASHTO Bridge Sections

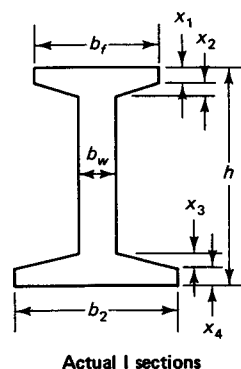
Designation	AASHTO sections					
	Type 1	Type 2	Type 3	Type 4	Type 5	Type 6
Area $A_c$ in. <sup>2</sup>	276	369	560	789	1,013	1,085
Moment of inertia, $I_{g(x-x)}$ in. <sup>4</sup>	22,750	50,979	125,390	260,741	521,180	733,320
$I_{g(y-y)}$ , in. <sup>4</sup>	3,352	5,333	12,217	24,347	61,235	61,619
Top-/bottom-section modulus, in. <sup>3</sup>	1,476	2,527	5,070	8,908	16,790	20,587
	1,807	3,320	6,186	10,544	16,307	20,157
Top flange width, $b_f$ (in.)	12	12	16	20	42	42
Top flange average thickness, $t_f$ (in.)	6	8	9	11	7	7
Bottom flange width, $b_2$ (in.)	16	18	22	26	28	28
Bottom flange average thickness, $t_2$ (in.)	7	9	11	12	13	13
Total depth, $h$ (in.)	28	36	45	54	63	72
Web width, $b_w$ (in.)	6	6	7	8	8	8
$c_t/c_b$ (in.)	15.41	20.17	24.73	29.27	31.04	35.62
	12.59	15.83	20.27	24.73	31.96	36.38
$r^2$ , in. <sup>2</sup>	82	132	224	330	514	676
Self-weight $w_D$ lb/ft	287	384	583	822	1055	1130

**Table 4.4(a)** Geometrical Details of As-Built PCI and AASHTO Sections

Designation	$b_f$ (in.)	$h_f$ (in.)	$b_{w1}$ (in.)	$b_{w2}$ (in.)	$h$ (in.)	$b$ (in.)
8DT12	96	2	5.75	3.75	12	48
8DT14	96	2	5.75	3.75	14	48
8DT16	96	2	5.75	3.75	16	48
8DT18	96	2	5.75	3.75	18	48
8DT20	96	2	5.75	3.75	20	48
8DT24	96	2	5.75	3.75	24	48
8DT32	96	2	7.75	4.75	32	48
10DT32	120	2	7.75	4.75	32	60
12DT34	144	4	7.75	4.75	34	60
15DT34	180	4	7.75	4.75	34	90



Designation	$b_f$ (in.)	$x_1$ (in.)	$x_2$ (in.)	$b_2$ (in.)	$x_3$ (in.)	$x_4$ (in.)	$b_w$ (in.)	$h$ (in.)
AASHTO 1	12	4	3	16	5	5	6	28
AASHTO 2	12	6	3	18	6	6	6	36
AASHTO 3	16	7	4.5	22	7.5	7	7	45
AASHTO 4	20	8	6	26	9	8	8	54
AASHTO 5	42	5	7	28	10	8	8	63
AASHTO 6	42	5	7	28	10	8	8	72

**Solution:**

$$\gamma = 100 - 18 = 82\%$$

$$f'_{ci} = 0.75 \times 5,000 = -3,750 \text{ psi (25.9 MPa)}$$

Use  $f_t = 12\sqrt{5,000} = 849 \text{ psi (5.9 MPa)}$  as the maximum stress in tension, and assume a self-weight of approximately 1,000 plf (14.6 kN/m). Then the self-weight moment is given by

$$M_D = \frac{wl^2}{8} = \frac{1,000(60)^2}{8} \times 12 = 5,400,000 \text{ in.-lb (610 kN-m)}$$

and the superimposed load moment is

$$M_{SD} + M_L = \frac{(1,100 + 100)(60)^2}{8} \times 12 = 6,480,000 \text{ in.-lb (732 kN-m)}$$

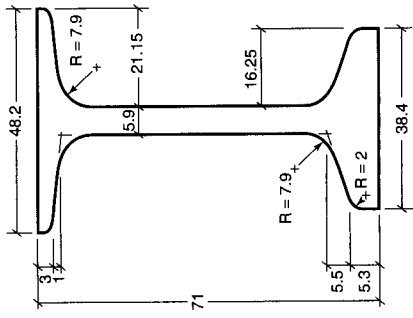
Since the tendon is harped, the critical section is close to the midspan, where dead-load and superimposed dead-load moments reach their maximum. The critical section is in many cases taken at  $0.40L$  from the support, where  $L$  is the beam span. The value  $0.40L$  is used to indicate that under moving load, the critical section can be at  $0.40L$  and not necessarily at midspan. From Equations 4.4a and b,



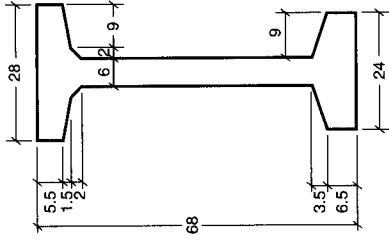
Table 4.4(b) Girder Properties of Optimized Sections

Agency	Girder Type	Depth (in.)	Web Width (in.)	area (in. <sup>2</sup> )	Inertia (in. <sup>4</sup> )	$y_t$ (in.)	$y_b$ (in.)	$S_t$ (in. <sup>3</sup> )	$S_b$ (in. <sup>3</sup> )	$\rho$	$\alpha$
CTL	BT-48	48	6	557	177,736	23.53	24.47	7,553	7,264	0.554	0.940
	BT-60	60	6	629	308,722	29.59	30.41	10,432	10,154	0.545	0.931
	BT-72	72	6	701	484,993	35.64	36.36	13,606	13,340	0.534	0.914
PCI	BT-54	54	6	659	268,077	26.37	27.63	10,166	9,702	0.558	0.943
	BT-63	63	6	713	392,638	30.82	32.12	12,715	12,224	0.556	0.942
	BT-72	72	6	767	545,894	35.40	36.60	15,421	14,915	0.549	0.934
AASHTO	Type VI	72	8	1,085	733,320	35.62	36.38	20,587	20,157	0.522	0.893
	Mod. Type VI	72	6	941	671,088	35.56	36.44	18,871	18,417	0.550	0.941
Washington	80/6	50	6	513	159,191	27.24	22.76	5,844	6,994	0.501	0.943
	100/6	58	6	591	256,560	30.01	27.99	8,549	9,166	0.517	0.925
	120/6	73.5	6	688	475,502	37.68	35.82	12,619	13,275	0.512	0.908
	14/6	73.5	6	736	534,037	35.30	38.20	15,122	13,985	0.538	0.894
Colorado	G54/6	54	6	631	242,592	27.33	26.67	8,877	9,095	0.527	0.924
	G68/6	68	6	701	426,575	33.99	34.01	12,548	12,544	0.526	0.911
Nebraska	1600	63	5.9	852	494,829	32.64	30.36	15,159	16,300	0.586	1.051
	1800	70.9	5.9	898	659,505	36.72	34.18	17,959	19,297	0.585	1.049
	2000	78.7	5.9	944	849,565	40.74	37.96	20,854	22,380	0.582	1.042
	2400	94.5	5.9	1,038	1,323,985	48.84	45.66	27,106	28,999	0.572	1.023
Florida	BT-54	54	6.5	785	311,765	28.11	25.89	11,091	12,042	0.546	0.983
	BT-63	63	6.5	843	458,521	32.88	30.12	13,945	15,223	0.549	0.992
	BT-72	72	6.5	901	638,672	37.64	34.36	16,968	18,588	0.548	0.991
Texas	U54A	54	10.2	1,022	379,857	30.12	23.90	12,612	15,895	0.516	0.996
	U54B	54	10.2	1,118	403,878	31.54	22.48	12,807	17,966	0.509	1.029

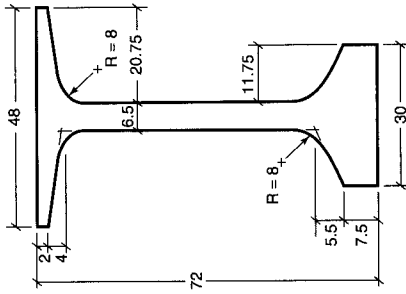
1 in. = 25.4 mm; 1 in.<sup>2</sup> = 645 mm<sup>2</sup>; 1 in.<sup>3</sup> = 16,390 mm<sup>3</sup>; 1 in.<sup>4</sup> = 416,000 mm<sup>4</sup>



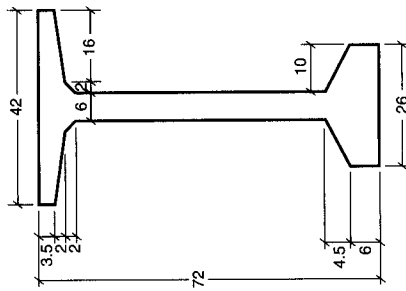
NU 1800



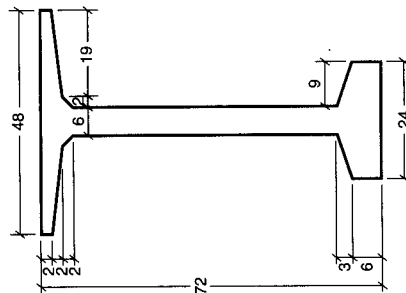
CO G68/6



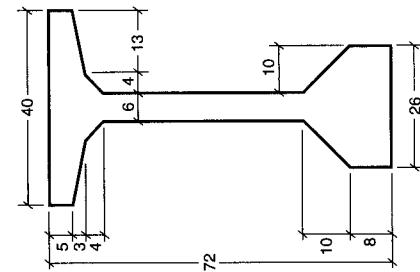
FL BT-72



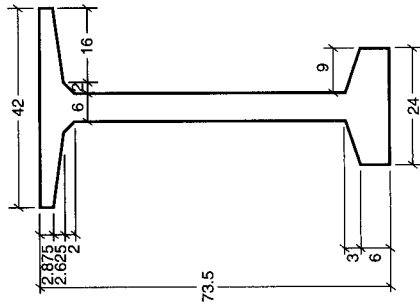
BT-72



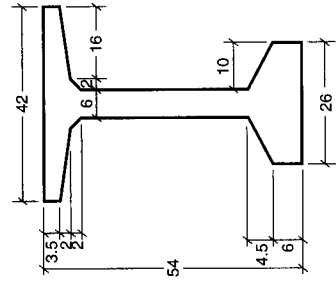
CTL BT-72



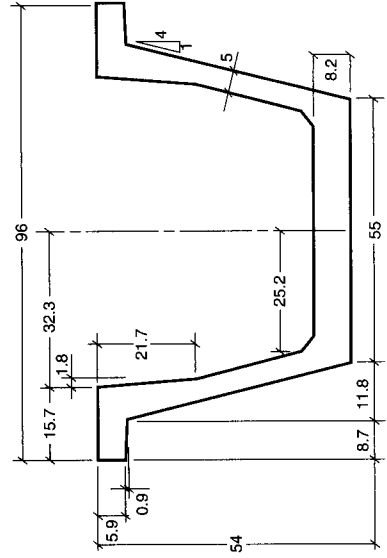
Type VI



WA 14/6



BT-54



U54B

Figure 4.6 Cross Sections of Optimized Bridge Girder Sections [See Table 4.4(b)]

$$\begin{aligned}
 S^t &\geq \frac{(1 - \gamma)M_D + M_{SD} + M_L}{\gamma f_{ti} - f_c} \\
 &\geq \frac{(1 - 0.82)5,400,000 + 6,480,000}{0.82 \times 184 - (-2,250)} = 3,104 \text{ in}^3 (50,860 \text{ cm}^3) \\
 S_b &\geq \frac{(1 - \gamma)M_D + M_{SD} + M_L}{f_t - \gamma f_{ci}} \\
 &\geq \frac{(1 - 0.82)5,400,000 + 6,480,000}{849 - 0.82(-2,250)} = 2,766 \text{ in}^3 (45,330 \text{ cm}^3)
 \end{aligned}$$

From the PCI design handbook, select a nontopped normal weight concrete double-T 12 DT 34 168-D1, since it has the bottom-section modulus value  $S_b$  closest to the required value.

The section properties of the concrete are as follows:

$$\begin{aligned}
 A_c &= 978 \text{ in.}^2 & c_t &= 8.23 \text{ in.} \\
 I_c &= 86,072 \text{ in.}^4 & c_b &= 25.77 \text{ in.} \\
 r^2 &= \frac{I_c}{A_c} = 88.0 \text{ in.}^2 & e_c &= 22.02 \text{ in.} \\
 S^t &= 10,458 \text{ in.}^3 & e_e &= 12.77 \text{ in.} \\
 S_b &= 3,340 \text{ in.}^3 & W_D &= 1,019 \text{ plf} \\
 & & \frac{V}{S} &= 2.39 \text{ in.}
 \end{aligned}$$

**Design of Strands and Check of Stresses.** The assumed self-weight is close to the actual self-weight of Fig. 4-7. Hence, use

$$\begin{aligned}
 M_D &= \frac{1,019}{1,000} \times 5,400,000 = 5,502,600 \text{ in.-lb} \\
 f_{pi} &= 0.70 \times 270,000 = 189,000 \text{ psi} \\
 f_{pe} &= 0.82f_{pi} = 0.82 \times 189,000 = 154,980 \text{ psi}
 \end{aligned}$$

(a) *Analysis of Stresses at Transfer.* From Equation 4.1a,

$$f^t = -\frac{P_i}{A_c} \left( 1 - \frac{ec_t}{r^2} \right) - \frac{M_D}{S^t} \leq f_{ti} = 184 \text{ psi}$$

Then

$$184 = -\frac{P_i}{978} \left( 1 - \frac{22.02 \times 8.23}{88.0} \right) - \frac{5,502,600}{10,458}$$

$$P_i = (184 + 526.16) \frac{978}{1.06} = 655,223 \text{ lb.}$$

$$\text{Required number of tendons} = \frac{655,223}{189,000 \times 0.153} = 22.66 \frac{1}{2}\text{-in. dia. tendons.}$$

Try sixteen  $\frac{1}{2}$ -in. dia. strands for the standard section:

$$A_{ps} = 16 \times 0.153 = 2.448 \text{ in}^2 (15.3 \text{ cm}^2)$$

$$P_i = 2.448 \times 189,000 = 462,672 \text{ lb (2,058 kN)}$$

$$P_e = 2.448 \times 154,980 = 379,391 \text{ lb (1,688 kN)}$$

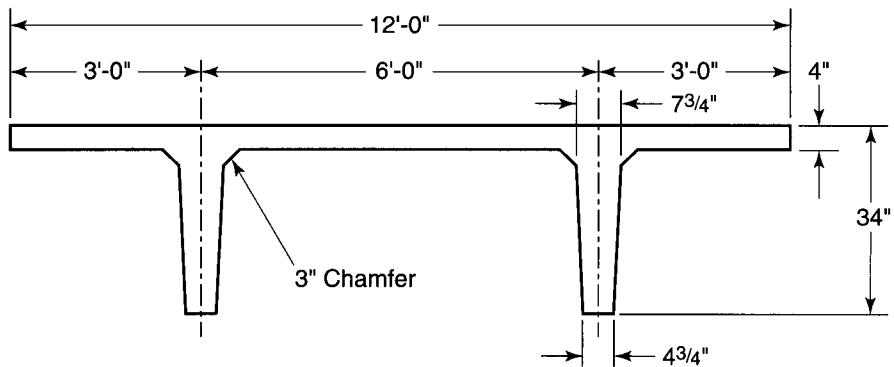


Figure 4.7 Double-T Section (12 DT34)

(b) Analysis of Stresses at Service Load at Midspan

$$P_e = 379,391 \text{ lb}$$

$$M_{SD} = \frac{100(60)^2 12}{8} = 540,000 \text{ in.-lb (61 kN-m)}$$

$$M_L = \frac{1,100(60)^2 12}{8} = 5,940,000 \text{ in.-lb (788 kN-m)}$$

$$\begin{aligned} \text{Total moment } M_T &= M_D + M_{SD} + M_L = 5,502,600 + 6,480,000 \\ &= 11,982,600 \text{ in.-lb (1,354 kN-m)} \end{aligned}$$

From Equation 4.3a,

$$\begin{aligned} f'_t &= -\frac{P_e}{A_c} \left( 1 - \frac{ec'_t}{r^2} \right) - \frac{M_T}{S'_t} \\ &= -\frac{379,391}{978} \left( 1 - \frac{22.02 \times 8.23}{88.0} \right) - \frac{11,982,600}{10,458} \\ &= +411 - 1146 = -735 \text{ psi} < f_c = -2,250 \text{ psi, O.K.} \end{aligned}$$

From Equation 4.3b,

$$\begin{aligned} f_b &= -\frac{P_e}{A_c} \left( 1 + \frac{ec_b}{r^2} \right) + \frac{M_T}{S_b} \\ &= -\frac{379,391}{978} \left( 1 + \frac{22.02 \times 25.77}{88.0} \right) + \frac{11,982,600}{3,340} \\ &= -2,889 + 3,587 = +698 \text{ psi (T)} < f_t = +849 \text{ psi, O.K.} \end{aligned}$$

(c) Analysis of Stresses at Support Section

$$e_e = 12.77 \text{ in. (324 mm)}$$

$$f_{ii} = 6\sqrt{f'_{ci}} = 6\sqrt{3,750} \cong 367 \text{ psi}$$

$$f_t = 12\sqrt{f'_c} = 12\sqrt{5,000} = 849 \text{ psi}$$

## (i) At Transfer

$$f'_t = -\frac{462,672}{978} \left( 1 - \frac{12.77 \times 8.23}{88.0} \right) - 0 = +92 \text{ psi (T)}$$

$$f_b = -\frac{462,672}{978} \left( 1 + \frac{12.77 \times 25.77}{88.0} \right) + 0 = -2,240 \text{ psi (C)}$$

$$< f_{ci} = -2,250 \text{ psi, O.K.}$$

If  $f_b > f_{ci}$ , the support eccentricity has to be changed.

## (ii) At Service Load

$$f'_t = -\frac{379,391}{978} \left( 1 - \frac{12.77 \times 8.23}{88.0} \right) - 0 = +75 \text{ psi (T)} < f_t = 849 \text{ psi, O.K.}$$

$$f_b = -\frac{379,391}{978} \left( 1 + \frac{12.77 \times 25.77}{88.0} \right) + 0 = -1,840 \text{ psi (C)}$$

$$< f_c = -2,250 \text{ psi, O.K.}$$

Adopt the section for service-load conditions using sixteen  $\frac{1}{2}$ -in. (1.7 mm) strands with midspan eccentricity  $e_c = 22.02$  in. (560 mm) and end eccentricity  $e_e = 12.77$  in. (324 mm).

## 4.3.2 Variable Tendon Eccentricity with No Height Limitation

## Example 4.2

Design an I-section for a beam having a 65-ft (19.8 m) span to satisfy the following section modulus values: Use the same allowable stresses and superimposed loads as in Example 4.1.

$$\text{Required } S'_t = 3,570 \text{ in}^3 (58,535 \text{ cm}^3)$$

$$\text{Required } S_b = 3,780 \text{ in}^3 (61,940 \text{ cm}^3)$$

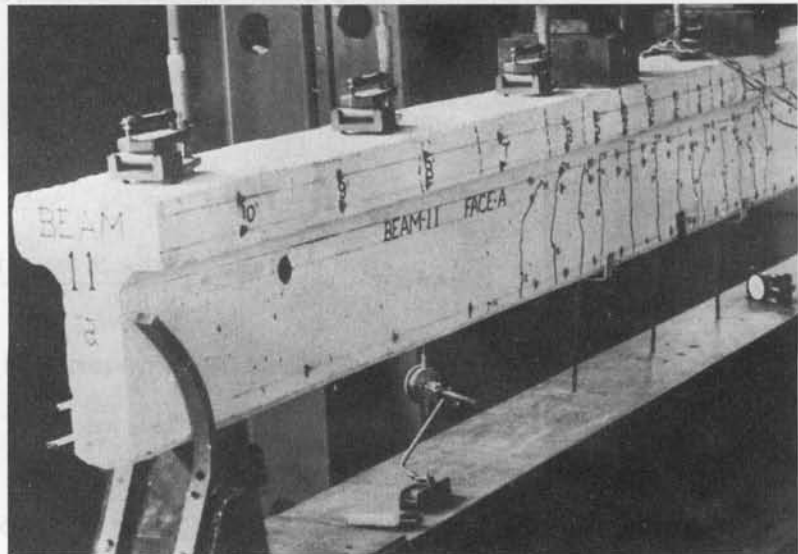


Photo 4.2 Crack development in prestressed T-beam (Nawy et al.).

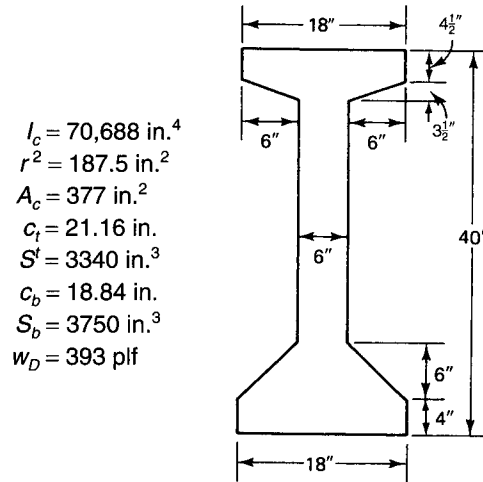


Figure 4.8 I-beam section in Example 4.2.

### Solution

Since the section moduli at the top and bottom fibers are almost equal, a symmetrical section is adequate. Next, analyze the section in Figure 4.8 chosen by trial and adjustment.

**Analysis of Stresses at Transfer.** From Equation 4.4d,

$$\begin{aligned}\bar{f}_{ci} &= f_{ii} - \frac{c_t}{h}(f_{ii} - f_{ci}) \\ &= +184 - \frac{21.16}{40}(+184 + 2,250) \cong -1,104 \text{ psi (C) (7.6 MPa)}\end{aligned}$$

$$P_i = A_c \bar{f}_{ci} = 377 \times 1,104 = 416,208 \text{ lb (1,851 kN)}$$

$$M_D = \frac{393(65)^2}{8} \times 12 = 2,490,638 \text{ in.-lb (281 kN-m)}$$

From Equation 4.4c, the eccentricity required at the section of maximum moment at midspan is

$$\begin{aligned}e_c &= (f_{ii} - \bar{f}_{ci}) \frac{S^t}{P_i} + \frac{M_D}{P_i} \\ &= (184 + 1,104) \frac{3,340}{416,208} + \frac{2,490,638}{416,208} \\ &= 10.34 + 5.98 = 16.32 \text{ in. (415 mm)}\end{aligned}$$

Since  $c_b = 18.84$  in., and assuming a cover of 3.75 in., try  $e_c = 18.84 - 3.75 \cong 15.0$  in. (381 mm).

$$\text{Required area of strands } A_p = \frac{P_i}{f_{pi}} = \frac{416,208}{189,000} = 2.2 \text{ in}^2 (14.2 \text{ cm}^2)$$

$$\text{Number of strands} = \frac{2.2}{0.153} = 14.38$$

Try thirteen  $\frac{1}{2}$ -in. strands,  $A_p = 1.99 \text{ in}^2 (12.8 \text{ cm}^2)$ , and an actual  $P_i = 189,000 \times 1.99 = 376,110 \text{ lb (1,673 kN)}$ , and check the concrete extreme fiber stresses. From Equation 4.1a

$$f^t = -\frac{P_i}{A_c} \left( 1 - \frac{ec_t}{r^2} \right) - \frac{M_D}{S^t}$$

$$= -\frac{376,110}{377} \left( 1 - \frac{15.0 \times 21.16}{187.5} \right) - \frac{2,490,638}{3,340}$$

$$= +691.2 - 745.7 = -55 \text{ psi (C), no tension at transfer, O.K.}$$

From Equation 4.1b

$$f_b = -\frac{P_i}{A_c} \left( 1 + \frac{ec_b}{r^2} \right) + \frac{M_D}{S_b}$$

$$= -\frac{376,110}{377} \left( 1 + \frac{15 \times 18.84}{187.5} \right) + \frac{2,490,638}{3,750}$$

$$= -2,501.3 + 664.2 = -1,837 \text{ psi (C)} < f_{ci} = 2,250 \text{ psi, O.K.}$$

**Analysis of Stresses at Service Load.** From Equation 4.3a

$$f^t = -\frac{P_e}{A_c} \left( 1 - \frac{ec_t}{r^2} \right) - \frac{M_T}{S^t}$$

$$P_e = 13 \times 0.153 \times 154,980 = 308,255 \text{ lb (1,371 kN)}$$

$$M_{SD} + M_L = \frac{(100 + 1100)(65)^2}{8} \times 12 = 7,605,000 \text{ m} \cdot \text{lb}$$

$$\text{Total moment } M_T = M_D + M_{SD} + M_L = 2,490,638 + 7,605,000$$

$$= 10,095,638 \text{ in.} \cdot \text{lb (1,141 kN} \cdot \text{m)}$$

$$f^t = -\frac{308,225}{377} \left( 1 - \frac{15.0 \times 21.16}{187.5} \right) - \frac{10,095,638}{3,340}$$

$$= +566.5 - 3,022.6 = -2,456 \text{ psi (C)} > f_c = -2,250 \text{ psi}$$

Hence, either enlarge the depth of the section or use higher strength concrete. Using  $f'_c = 6,000$  psi,

$$f_c = 0.45 \times 6,000 = -2,700 \text{ psi, O.K.}$$

$$f_b = -\frac{P_e}{A_c} \left( 1 + \frac{ec_b}{r^2} \right) + \frac{M_T}{S_b} = -\frac{308,255}{377} \left( 1 + \frac{15.0 \times 18.84}{187.5} \right) + \frac{10,095,638}{3,750}$$

$$= -2,050 + 2,692.2 = 642 \text{ psi (T), O.K.}$$

#### Check Support Section Stresses

$$\text{Allowable } f'_{ci} = 0.75 \times 6,000 = 4,500 \text{ psi}$$

$$f_{ci} = 0.60 \times 4,500 = 2,700 \text{ psi}$$

$$f_{ii} = 3\sqrt{f'_{ci}} = 201 \text{ psi for midspan}$$

$$f_{it} = 6\sqrt{f'_{ci}} = 402 \text{ psi for support}$$

$$f_c = 0.45f'_c = 2,700 \text{ psi}$$

$$f_{i1} = 6\sqrt{f'_c} = 465 \text{ psi}$$

$$f_{i2} = 12\sqrt{f'_c} = 930 \text{ psi}$$

(a) *At Transfer.* Support section compressive fiber stress.

$$f_b = -\frac{P_i}{A_c} \left( 1 + \frac{ec_b}{r^2} \right) + 0$$

$$P_i = 376,110 \text{ lb}$$

or

$$-2,700 = -\frac{376,110}{377} \left( 1 + \frac{e \times 18.84}{187.5} \right)$$

so that

$$e_e = 16.98 \text{ in.}$$

To ensure a tensile stress at the top fibers within the allowable limits, try  $e_e = 12.49$  in.:

$$f^t = -\frac{376,110}{377} \left( 1 - \frac{12.49 \times 21.16}{187.5} \right) - 0$$

$$= 409 \text{ psi (T)} > f_{ti} = 402 \text{ psi}$$

$$f_b = -2250 \text{ psi}$$

Thus, use mild steel at the top fibers at the support section to take all tensile stresses in the concrete, or use a higher strength concrete for the section, or reduce the eccentricity.

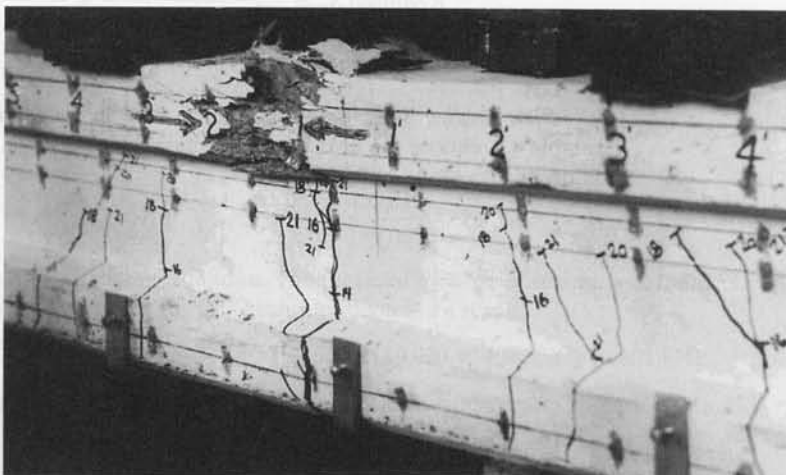
**(b) At Service Load**

$$f^t = -\frac{308,255}{377} \left( 1 - \frac{12.49 \times 21.16}{187.5} \right) - 0 = 335 \text{ psi (T)} < 930 \text{ psi, O.K.}$$

$$f_b = -\frac{308,255}{377} \left( 1 + \frac{12.49 \times 18.84}{187.5} \right) + 0 = -1,844 \text{ psi (C)} < -2,700 \text{ psi, O.K.}$$

Hence, adopt the 40-in. (102-cm)-deep I-section prestressed beam of  $f'_c$  equal to 6,000 psi (41.4 MPa) normal-weight concrete with thirteen  $\frac{1}{2}$ -in. tendons having midspan eccentricity  $e_c = 15.0$  in. (381 mm) and end section eccentricity  $e_e = 12.5$  in. (318 mm).

An alternative to this solution is to continue using  $f'_c = 5,000$  psi, but change the number of strands and eccentricities.



**Photo 4.3** Prestressed beam at failure. Note crushing of concrete on top fibers (Nawy, Potyondy, et al.).



### 4.3.3 Constant Tendon Eccentricity

#### Example 4.3

Solve Example 4.2 assuming that the prestressing tendon has constant eccentricity. Use  $f'_c = 5,000$  psi (34.5 MPa) normal-weight concrete, permitting a maximum concrete tensile stress  $f_t = 12\sqrt{f'_c} = 849$  psi.

**Solution:** Since the tendon has constant eccentricity, the dead-load and superimposed dead- and live-load moments at the support section of the simply supported beam are zero. Hence, the support section controls the design. The required section modulus at the support, from Equation 4.5a, is

$$S^t \geq \frac{M_D + M_{SD} + M_L}{\gamma f_{ti} - f_c}$$

$$S_b \geq \frac{M_D + M_{SD} + M_L}{f_t - \gamma f_{ci}}$$

Assume  $W_D = 425$  plf. Then

$$M_D = \frac{425 \times (65)^2}{8} \times 12 = 2,693,438 \text{ in.-lb (304 kN-m)}$$

$$M_{SD} + M_L = 7,605,000 \text{ in.-lb (859 kN-m)}$$

Thus, the total moment  $M_T = 10,298,438$  in.-lb (1,164 kN-m), and we also have

$$\text{Allowable } f_{ci} = -2,250 \text{ psi}$$

$$f'_{ci} = -3,750 \text{ psi}$$

$$f_{ti} = 6\sqrt{f'_{ci}} \text{ for support section} = 367 \text{ psi}$$

$$f_c = -2,250 \text{ psi (15.5 MPa)}$$

$$f_t = +849 \text{ psi}$$

$$\gamma = 0.82$$

$$\text{Required } S^t = \frac{10,298,438}{0.82 \times 184 + 2,250} = 4,289 \text{ in}^3 (72,210 \text{ cm}^3)$$

$$\text{Required } S_b = \frac{M_D + M_{SD} + M_L}{f_t - \gamma f_{ci}} = \frac{10,298,438}{849 + 0.82 \times 2,250}$$

$$= 3,823 \text{ in}^3 (62,713 \text{ cm}^3)$$

**First Trial.** Since the required  $S^t = 4,289 \text{ in}^3$ , which is greater than the available  $S^t$  in Example 4.2, choose the next larger I-section with  $h = 44$  in. as shown in Figure 4.9. The section properties are:

$$I_c = 92,700 \text{ in}^4$$

$$r^2 = 228.9 \text{ in}^2$$

$$A_c = 405 \text{ in}^2$$

$$c_t = 23.03 \text{ in.}$$

$$S^t = 4,030 \text{ in}^3$$

$$c_b = 20.97 \text{ in}$$

$$S_b = 4,420 \text{ in}^3$$

$$W_D = 422 \text{ plf}$$

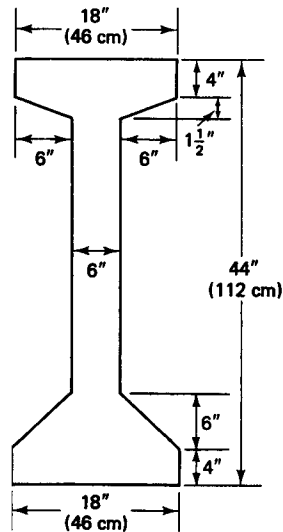


Figure 4.9 I-beam section in Example 4.3.

From Equation 4.5c, the required eccentricity at the critical section at the support is

$$e_e = (f_u - \bar{f}_{ci}) \frac{S^t}{P_i}$$

where

$$\begin{aligned} \bar{f}_{ci} &= f_u - \frac{c_t}{h} (f_u - f_{ci}) \\ &= 367 - \frac{23.03}{44} (367 + 2,250) = -1,002 \text{ psi (6.9 MPa)} \end{aligned}$$

and

$$P_i = A_c \bar{f}_{ci} = 405 \times 1,002 = 405,810 \text{ lb (1,805 kN)}$$

Hence,

$$e = (367 + 1,002) \frac{4,030}{405,810} = 13.60 \text{ in. (346 mm)}$$

The required prestressed steel area is

$$A_p = \frac{P_i}{f_{pi}} = \frac{405,810}{189,000} = 2.15 \text{ in}^2 (14.4 \text{ cm}^2)$$

So we try  $\frac{1}{2}$  in. strands tendon. The required number of strands is  $2.15/0.153 = 14.05$ . Accordingly, use fourteen  $\frac{1}{2}$  in. (12.7 mm) tendons. As a result,

$$P_i = 14 \times 0.153 \times 189,000 = 404,838 \text{ lb (1,801 kN)}$$

(a) *Analysis of Stresses at Transfer at End Section.* From Equation 4.1a,

$$\begin{aligned} f^t &= -\frac{P_i}{A_c} \left( 1 - \frac{ec_t}{r^2} \right) - \frac{M_D}{S^t} = -\frac{404,838}{405} \left( 1 - \frac{13.60 \times 23.03}{228.9} \right) - 0 \\ &= +368.2 \text{ psi (T)} \cong f_u = 367, \text{ O.K.} \end{aligned}$$

From Equation 4.1b,

$$f_b = -\frac{P_i}{A_c} \left( 1 + \frac{ec_b}{r^2} \right) + \frac{M_D}{S_b} = -\frac{404,838}{405} \left( 1 + \frac{13.6 \times 20.97}{228.9} \right) + 0$$

$$= -2,245 \text{ psi (C)} \cong f_{ci} = -2,250, \text{ O.K.}$$

**(b) Analysis of Final Service-Load Stresses at Support**

$$P_e = 14 \times 0.153 \times 154,980 = 331,967 \text{ lb (1,477 kN)}$$

$$\text{Total moment } M_T = M_D + M_{SD} + M_L = 0$$

From Equation 4.3a,

$$f^t = -\frac{P_e}{A_c} \left( 1 - \frac{ec_i}{r^2} \right) - \frac{M_T}{S^t}$$

$$= -\frac{331,967}{405} \left( 1 - \frac{13.60 \times 23.03}{228.9} \right) - 0 = 302 \text{ psi (T)} < f_t = 849 \text{ psi, O.K.}$$

This is also applicable to midspan since eccentricity  $e$  is constant. From Equation 4.3b

$$f_b = -\frac{P_e}{A_c} \left( 1 + \frac{ec_b}{r^2} \right) + \frac{M_T}{S_b}$$

$$= -\frac{331,967}{405} \left( 1 + \frac{13.60 \times 20.97}{228.9} \right) + 0$$

$$= -1,841 \text{ psi (12.2 MPa) (C)} < f_c = -2,250 \text{ psi, O.K.}$$

**(c) Analysis of Final Service-Load Stresses at Midspan.** From before, the total moment  $M_T = M_D + M_{SD} + M_L = 10,298,438 \text{ in.-lb}$ . Revised  $w_D = 422 \text{ plf} = \text{assumed } w_D = 425 \text{ plf}$ ; hence,  $M_T \approx 10,298,438 \text{ in.-lb}$  is sufficiently accurate. So the extreme concrete fiber stress due to  $M_T$  is

$$f_1^t = \frac{M_T}{S^t} = -\frac{10,298,438}{4,030} = -2,555 \text{ psi (C) (17.6 MPa)}$$

$$f_{1b} = \frac{M_T}{S_b} = \frac{10,298,438}{4,420} = +2,330 \text{ psi (T) (16.1 MPa)}$$

Hence, the final midspan fiber stresses are

$$f^t = +302 - 2,555 = -2,253 \text{ psi (C)} \cong f_c = -2,250 \text{ psi, accept}$$

$$f_b = -1,841 + 2,330 = +489 \text{ psi (T)} < f_t = 849 \text{ psi, O.K.}$$

Consequently, accept the trial section with a constant eccentricity  $e = 13.60 \text{ in. (345 mm)}$  for the fourteen  $\frac{1}{2}$ " (12.7 mm dia.) tendons.

## 4.4 PROPER SELECTION OF BEAM SECTIONS AND PROPERTIES

### 4.4.1 General Guidelines

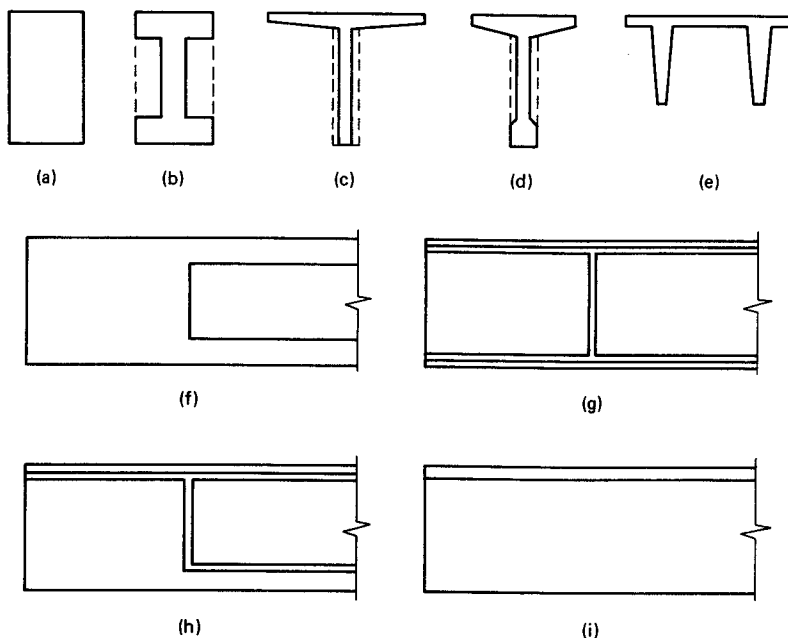
Unlike steel-rolled sections, prestressed sections are not yet fully standardized. In most cases, the design engineer has to select the type of section to be used in the particular project. In the majority of simply supported beam designs, the distance between the cgc and cgs lines, viz., the eccentricity  $e$ , is proportional to the required prestressing force.

Since the midspan moment usually controls the design, the larger the eccentricity at midspan the smaller is the needed prestressing force, and consequently the more economical is the design. For a large eccentricity, a large concrete area at the top fibers is needed. Hence, a T-section or a wide-flange I-section becomes suitable. The end section is usually solid in order to avoid large eccentricities at planes of zero moment, and also in order to increase the shear capacity of the support section, and prevent anchorage zone failures.

Another popular section in wide use is the double-T-section. This section adds the advantages of the single-T-section to its own ease of handling and erection inherent in its stability. Figure 4.10 shows typical sections in general usage. Other sections such as hollow-core slabs and nonsymmetrical sections are also commonly used. Note that flanged sections can replace rectangular solid sections of the same depth without any loss of flexural strength. Rectangular sections, however, are used as short-span supporting girders or ledger beams.

I-sections are used as typical floor beams with composite slab topping action in long-span parking structures. T-sections with heavy bottom flanges, such as that in Figure 4.10(d), are generally used in bridge structures. Double-T-sections are widely used in floor systems in buildings and also in parking structures, particularly because of the composite action advantage of the top wide flange, which is 10 to 15 feet wide in many cases.

Hollow-core cast and extruded sections are shallow one-way beam strips that serve as easily erectable floor slabs. Large, hollow box girders are used as bridge girders for very large spans in what are known as *segmental bridge deck systems*. These segmental girders have large torsional resistance, and their flexural strength-to-weight ratio is relatively higher than in other types of prestressing systems.



**Figure 4.10** Typical prestressed concrete sections. (a) Rectangular beam section. (b) I-beam section. (c) T-beam section. (d) T-section with heavy bottom flange. (e) Double-T-section. (f) End part of beam in (b). (g) End part of beam in (c). (h) End part of beam in (d). (i) End part of beam in (e).

#### 4.4.2 Gross Area, the Transformed Section, and the Presence of Ducts

In general, the gross cross-sectional area of the concrete section is adequate for use in the service-load design of prestressed sections. While some designers prefer refining their designs through the use of the transformed section in their solutions, the accuracy gained in accounting for the contribution of the area of the reinforcement to the stiffness of the concrete section is normally not warranted. In post-tensioned beams, where ducts are grouted, the gross cross section is still adequate for all practical design considerations. It is only in cases of large-span bridge and industrial prestressed beams, where the area of the prestressing reinforcement is large, that the transformed section or the net concrete area excluding the duct openings has to be used.

#### 4.4.3 Envelopes for Tendon Placement

The tensile stress in the extreme concrete fiber under service-load conditions cannot exceed the maximum allowable by codes such as the ACI, PCI, AASHTO, or CEB-FIP. It is therefore important to establish the limiting zone in the concrete section, i.e., an envelope within which the prestressing force can be applied without causing tension in the extreme concrete fibers. From Equation 4.1a, we have

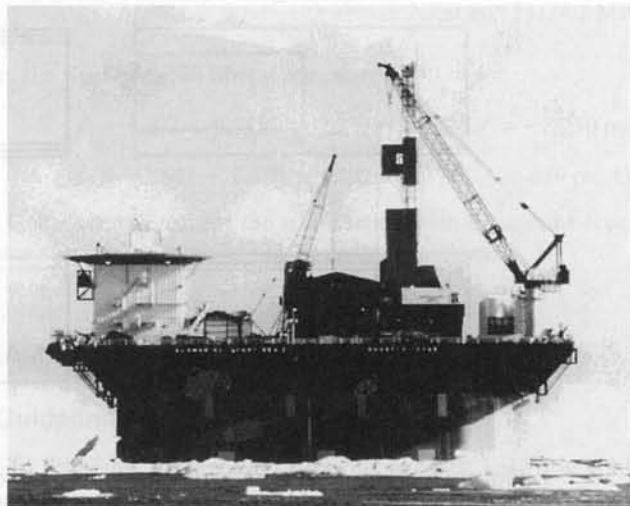
$$f_t = 0 = -\frac{P_i}{A_c} \left( 1 - \frac{ec_t}{r^2} \right)$$

for the prestressing force part only, giving  $e = r^2/c_t$ . Hence, the *lower kern point*

$$k_b = \frac{r^2}{c_t} \quad (4.6a)$$

Similarly, from Equation 4.1b, if  $f_b = 0$ ,  $-e = r^2/c_b$ , where the negative sign represents measurements upwards from the neutral axis, since positive eccentricity is positive downwards. Hence, the *upper kern point*

$$k_t = \frac{r^2}{c_b} \quad (4.6b)$$



**Photo 4.4** Super CIDS offshore platform under tow to Arctic, Global Marine Development. (Courtesy, the late Ben C. Gerwick.)

From the determination of the upper and lower kern points, it is clear that

- (a) If the prestressing force acts below the lower kern point, tensile stresses result at the extreme upper concrete fibers of the section.
- (b) If the prestressing force acts above the upper kern point, tensile stresses result at the extreme lower concrete fibers of the section.

In a similar manner, kern points can be established for the right and left of the vertical line of symmetry of a section so that a central kern or core area for load application can be established, as Figure 4.11 shows for a rectangular section.

#### 4.4.4 Advantages of Curved or Harped Tendons

Although straight tendons are widely used in precast beams of moderate span, the use of curved tendons is more common in in-situ-cast post-tensioned elements. Nonstraight tendons are of two types:

- (a) Draped: gradually curved alignment such as parabolic forms, used in beams subjected primarily to uniformly distributed external loading.
- (b) Harped: inclined tendons with a discontinuity in alignment at planes of concentrated load applications, used in beams subjected primarily to concentrated transverse loading.

Figures 4.12, 4.13, and 4.14 describe the alignment bending moment and stress distribution for beams that are prestressed with straight, draped, and harped tendons, respectively. These diagrams are intended to illustrate the economic advantages of the draped and harped tendons over the straight tendons. In Figure 4.12, at section 1-1, undesirable tensile stress in the concrete is shown at the top fibers. Section 1-1 in Figures 4.13 and 4.14 shows the uniform compression if the tendon acts at the cgc of the section at the support. Another advantage of draped and harped tendons is that they allow the prestressed beams to carry heavy loads because of the balancing effect of the vertical component of the prestressing nonstraight tendon. In other words, the required prestressing forces  $P_p$  for the parabolic tendon in Figure 4.13 and  $P_h$  for the harped tendon in Figure 4.14 are smaller at the midspan than the force required in the straight tendon of Figure 4.12. Hence, for the same stress level, a smaller number of strands are needed in the case of draped or harped tendons, and sometimes smaller concrete sections can be used with the resulting efficiency in the design. (Compare Examples 4.2 and 4.3 again.)

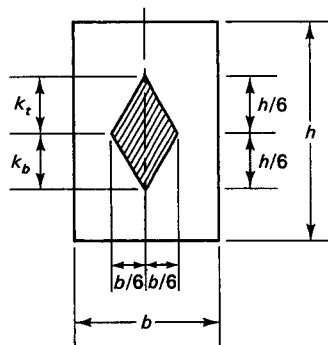
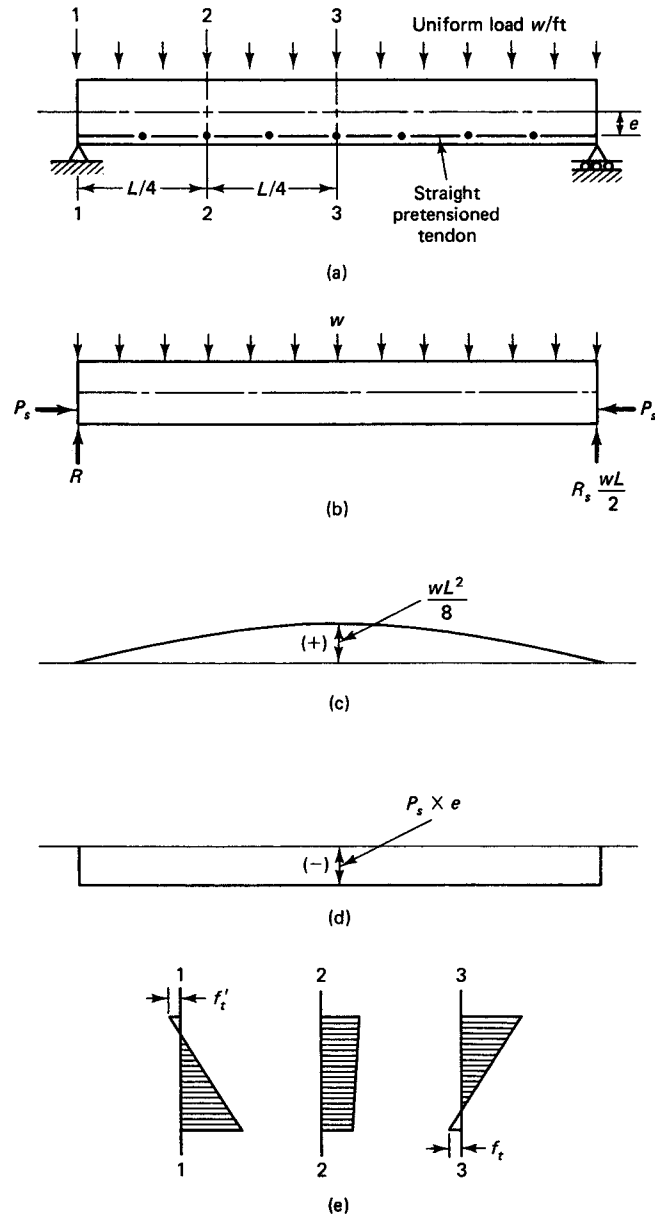


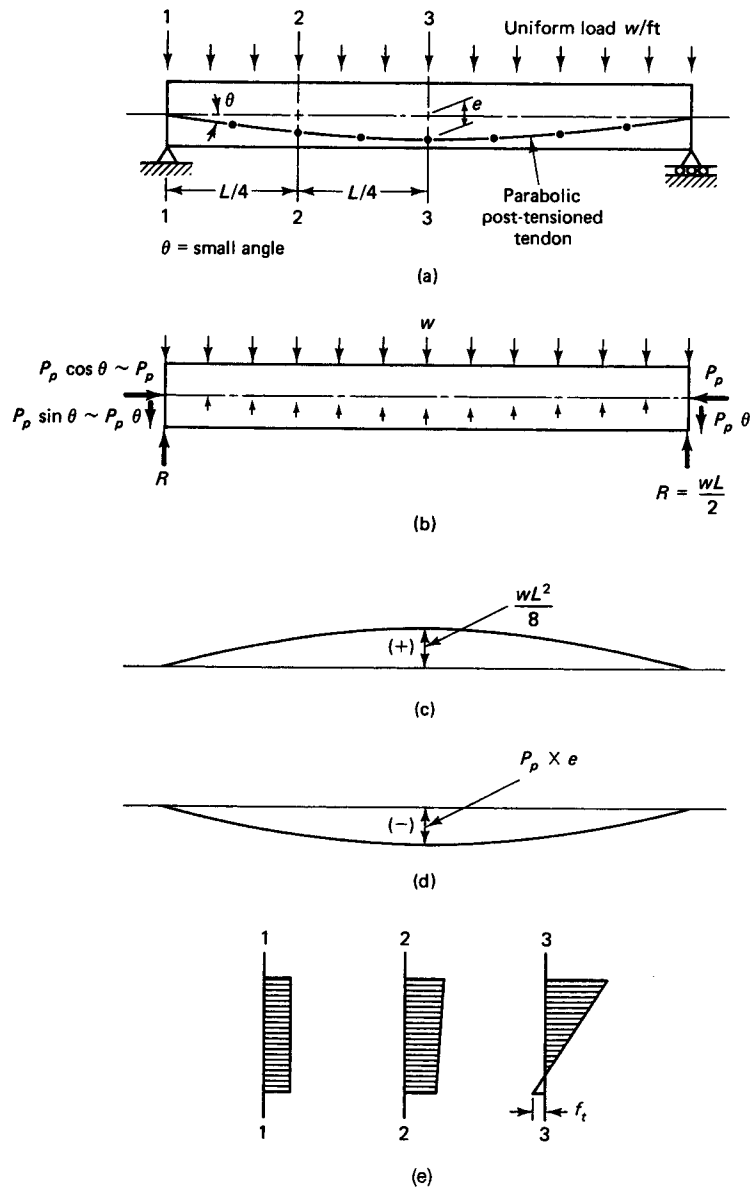
Figure 4.11 Central kern area for a rectangular section.



**Figure 4.12** Beam with straight tendon. (a) Beam elevation. (b) Free-body diagram. (c) External load balancing moment diagram. (d) Prestressing force bending moment diagram. (e) Typical stress distribution in sections 1, 2, and 3 (Equation 4.3).

#### 4.4.5 Limiting-Eccentricity Envelopes

It is desirable that the designed eccentricities of the tendon along the span be such that limited or no tension develops at the extreme fibers of the beam controlling sections. If it is desired to have no tension along the span of the beam in Figure 4.15 with the draped tendon, the controlling eccentricities have to be determined at the sections that follow along the span. If  $M_D$  is the self-weight dead-load moment and  $M_T$  is the total moment



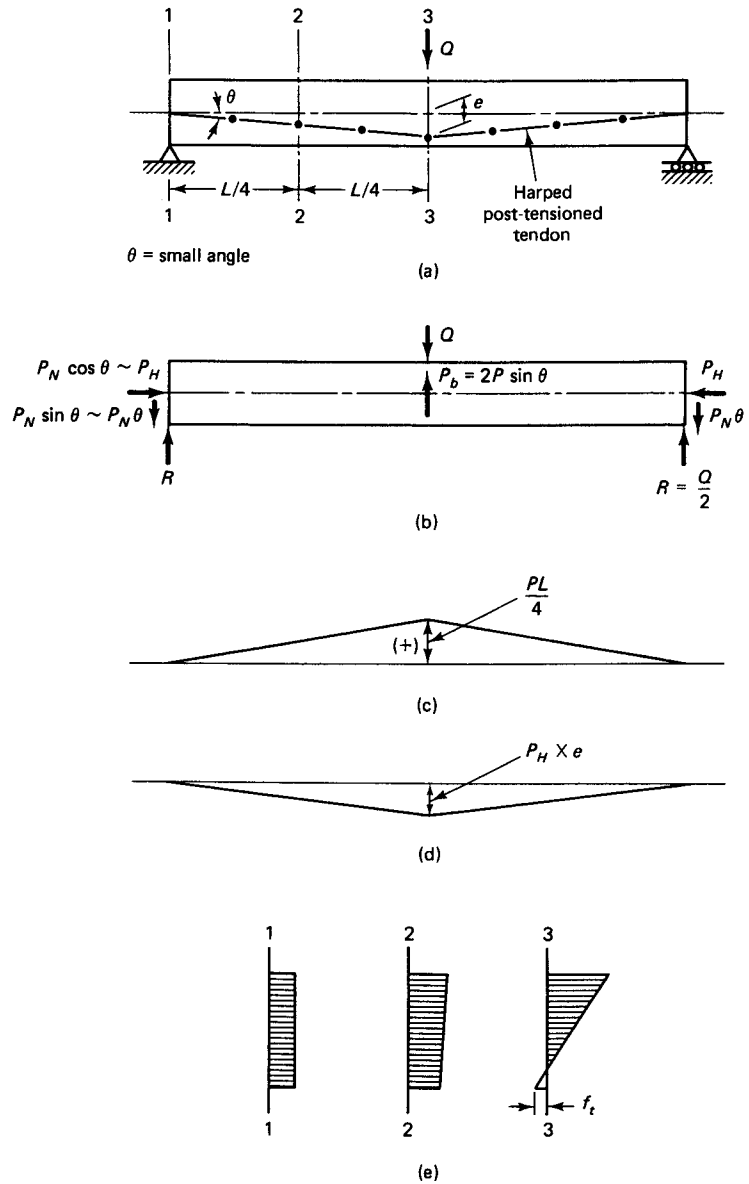
**Figure 4.13** Beam with parabolic draped tendon. (a) Beam elevation. (b) Free-body diagram. (c) External load bending moment diagram. (d) Prestressing force bending moment diagram. (e) Typical stress distribution on sections 1, 2, and 3 (Equation 4.3).

due to all transverse loads, then the arms of the couple composed of the center-of-pressure line (C-line) and the center of the prestressing tendon line (cgs line) due to  $M_D$  and  $M_T$  are  $a_{\min}$  and  $a_{\max}$ , respectively, as shown in Figure 4.15.

**Lower cgs Envelope.** The minimum arm of the tendon couple is

$$a_{\min} = \frac{M_D}{P_i} \quad (4.7a)$$





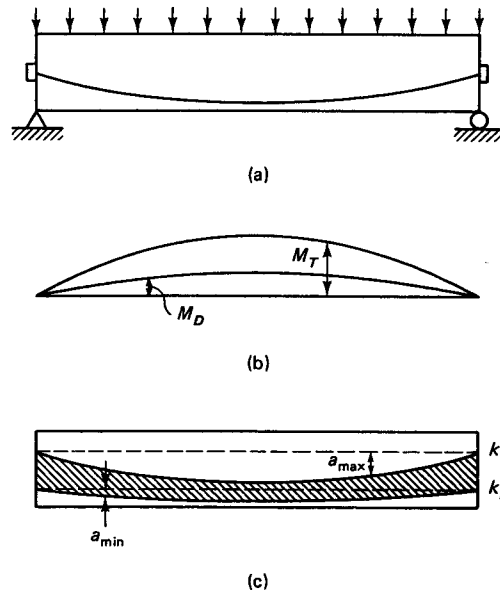
**Figure 4.14** Beam with harped tendon. (a) Beam elevation. (b) Free-body diagram. (c) External load bending moment diagram. (d) Prestressing force bending moment diagram. (e) Typical stress distribution in sections 1, 2, and 3 (Equation 4.3).

This defines the maximum distance below the *bottom* kern where the cgs line is to be located so that the C-line does not fall *below* the *bottom* kern line, thereby preventing tensile stresses at the *top* extreme fibers. Hence, the limiting bottom eccentricity is

$$e_b = (a_{\min} + k_b) \tag{4.7b}$$

**Upper cgs Envelope.** The maximum arm of the tendon couple is

$$a_{\max} = \frac{M_T}{P_e} \tag{4.7c}$$



**Figure 4.15** Cgs envelope determination. (a) One tendon location in beam. (b) Bending moment diagram. (c) Limiting cgs envelope.

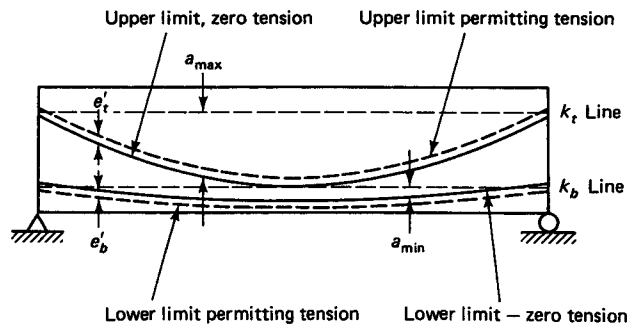
This defines the minimum distance below the *top* kern where the cgs line is to be located so that the C-line does not fall *above* the *top* kern, thereby preventing tensile stresses at the *bottom* extreme fibers. Hence, the limiting top eccentricity is

$$e_t = (a_{max} - k_t) \tag{4.7d}$$

Limited tensile stress is allowed in some codes both at transfer and at service-load levels. In such cases, it is possible to allow the cgs line to fall slightly outside the two limiting cgs envelopes described in Equations 4.7a and c.

If an additional eccentricity  $e'_b$ ,  $e'_t$  is superimposed on the cgs-line envelope that results in limited tensile stress at both the top and bottom extreme concrete fibers, the additional top stress  $f^{(t)}$  and bottom stress  $f_{(b)}$  would be

$$f^{(t)} = \frac{P_i e'_b c_t}{I_c} \tag{4.8a}$$



**Figure 4.16** Envelope permitting tension in concrete extreme fibers.

and

$$f_{t(b)} = \frac{P_e e'_t c_b}{I_c} \quad (4.8b)$$

where  $t$  and  $b$  denote the top and bottom fibers, respectively. From Equation 4.6, the additional eccentricities to be added to Equations 4.7b and d would be

$$e'_b = \frac{f^{(t)} A_c k_b}{P_i} \quad (4.9a)$$

and

$$e'_t = \frac{f_{(b)} A_c k_t}{P_e} \quad (4.9b)$$

The envelope allowing limited tension is shown in Figure 4.16. It should be noted that the upper envelope is outside the section, but the stresses are within the allowable limits, indicating a non-economical section. A change in eccentricity or prestressing force improves the design.

#### 4.4.6 Prestressing Tendon Envelopes

##### Example 4.4

Suppose that the beam in example 4.2 is a post-tensioned bonded beam and that the prestressing tendon is draped in a parabolic shape. Determine the limiting envelope for tendon location such that the limiting concrete fiber stresses are at no time exceeded. Consider the midspan, quarter-span, and beam ends as the controlling sections. Assume that the magnitude of prestress losses is the same as in Example 4.2 but that  $P_i = 549,423$  lb,  $P_e = 450,526$  lb,  $f'_c = 6000$  psi,  $e_c = 13$  in. and  $e_e = 6$  in.

**Solution:** The design moments of the I-beam in Example 4.2 can be summarized together with the section properties needed here:

$$P_i = 549,423 \text{ lb (2,431 kN)}$$

$$P_e = 450,526 \text{ lb (2,004 kN)}$$

$$M_D = 2,490,638 \text{ in.-lb (281 kN-m)}$$

$$M_{SD} + M_L = 7,605,000 \text{ in.-lb (859 kN-m)}$$

$$M_T = M_D + M_{SD} + M_L = 10,095,638 \text{ in.-lb (1,141 kN-m)}$$

$$A_c = 377 \text{ in}^2 (2,536 \text{ cm}^2)$$

$$f'_c = 6,000 \text{ psi}$$

$$r^2 = 187.5 \text{ in}^2 (1,210 \text{ cm}^2)$$

$$c_t = 21.16 \text{ in. (537 mm)}$$

$$c_b = 18.84 \text{ in. (479 mm)}$$

Since bending moments in this example are due to a uniformly distributed load, the shape of the bending moment diagram is parabolic, with the moment value being zero at the simply supported ends. Hence, quarter-span moments are

$$M_D = 0.75 \times 2,490,638 = 1,867,979 \text{ in.-lb (211 kN-m)}$$

$$M_T = 0.75 \times 10,095,638 = 7,571,729 \text{ in.-lb (856 kN-m)}$$

From Equations 4.6a and b, the kern point limits are

$$k_t = \frac{r^2}{c_b} = \frac{187.5}{18.84} = 9.95 \text{ in. (253 mm)}$$

$$k_b = \frac{r^2}{c_t} = \frac{187.5}{21.16} = 8.86 \text{ in. (225 mm)}$$

### **Lower Envelope**

From Equation 4.7a, the maximum distance that the cgs line is to be placed below the *bottom* kern to prevent tensile stress at the top fibers is determined as follows:

#### **(i) Midspan**

$$a_{\min} = \frac{M_D}{P_i} = \frac{2,490,638}{549,423} = 4.53 \text{ in. (115 mm)}$$

giving

$$e_1 = k_b + a_{\min} = 8.86 + 4.53 = 13.39 \text{ in. (340 mm)} \text{ vs } e_c = 15 \text{ in. used in Ex. 4.2 allowing tension at top at transfer}$$

#### **(ii) Quarter span**

$$a_{\min} = \frac{1,867,979}{549,423} = 3.40 \text{ in. (86 mm)}$$

giving

$$e_2 = 8.86 + 3.40 = 12.26 \text{ in. (311 mm)}$$

#### **(iii) Support**

$$a_{\min} = 0$$

giving

$$e_3 = 8.86 + 0 = 8.86 \text{ in. (225 mm)}$$

### **Upper Envelope**

From Equation 4.7b, the maximum distance that the cgs line is to be placed below the *top* kern to prevent tensile stress at the bottom extreme fibers is determined as follows:

#### **(i) Midspan**

$$a_{\max} = \frac{M_T}{P_e} = \frac{10,095,638}{450,526} = 22.41 \text{ in. (569 mm)}$$

$$e_1 = a_{\max} - k_t = 22.41 - 9.95 = 12.46 \text{ in. (316 mm)}$$

Clear minimum cover = 3.0 in.

Note that  $e_1$  cannot exceed  $c_b$ , otherwise tendon is outside the section.

#### **(ii) Quarter span**

$$a_{\max} = \frac{7,571,729}{450,526} = 16.80 \text{ in. (427 mm)}$$

$$e_2 = 16.80 - 9.95 = 6.85 \text{ in. (174 mm)}$$

#### **(iii) Support**

$$a_{\max} = 0$$

$$e_3 = 0 - 9.95 = -9.95 \text{ in. (-253 mm)} \quad (9.95 \text{ in. above cgc line})$$

Now, assume for practical purposes that the maximum fiber tensile stresses under working-load conditions for the purpose of constructing the cgs envelopes does not exceed  $f_t = 6\sqrt{f'_c} = 465$  psi for both top and bottom fibers both at midspan and the support, since  $f'_c = 6,000$  psi from Example 4.2. From Equation 4.9a, this additional eccentricity to add to the *lower* cgs envelope in order to allow limited tension at the *top* fibers is

$$e'_b = \frac{f^{(t)} A_c k_b}{P_i} = \frac{465 \times 377 \times 8.86}{549,423} = 2.83 \text{ in. (72 mm)}$$

Similarly, from Equation 4.9b, the additional eccentricity to add to the *upper* cgs envelope in order to allow limited tension at the *bottom* fibers is

$$e'_t = \frac{f^{(b)} A_c k_t}{P_e} = \frac{465 \times 377 \times 9.95}{450,526} = 3.87 \text{ in. (98 mm)}$$

We thus have the following summary of cgs envelope eccentricities:

	Zero tension, in.	Increment	Allowable tension, in.
Midspan			
Lower envelope	13.39	+2.83	16.22
Upper envelope	12.46	-3.87	8.59
Quarter span			
Lower envelope	12.26	+2.83	15.09
Upper envelope	6.86	-3.87	2.99
Support			
Lower envelope	8.86	+2.83	11.69
Upper envelope	-9.95	-3.87	-13.82
Actual midspan eccentricity $e_c = 13$ in. < 16.22 in.			
Hence, tendon is inside envelope at midspan.			
Actual support eccentricity $e_e = 6$ in. < 11.69 in.			
Hence, tendon is also inside envelope at support.			

Figure 4.17 illustrates the band of the cgs envelopes for both zero and limited tension in the concrete.

#### 4.4.7 Reduction of Prestress Force Near Supports

As seen from Example 4.3 and Sections 4.4.3 and 4.4.5, straight tendons in pretensioned members can cause high-tensile stresses in the concrete extreme fibers at the support sections because of the absence of bending moment stresses due to self-weight and superimposed loads and the dominance of the moment due to the prestressing force alone. Two common and practical methods of reducing the stresses at the support section due to the prestressing force are:

1. Changing the eccentricity of some of the cables by raising them towards the support zone, as shown in Figure 4.18(a). This reduces the moment values.
2. Sheathing some of the cables by plastic tubing towards the support zone, as shown in Figure 4.18(b). This eliminates the prestress transfer of part of the cables at some distance from the support section of the simply supported prestressed beam.

Note that raised cables are also used in long-span post-tensioned prestressed beams, theoretically discontinuing part of the tendons where they are no longer needed



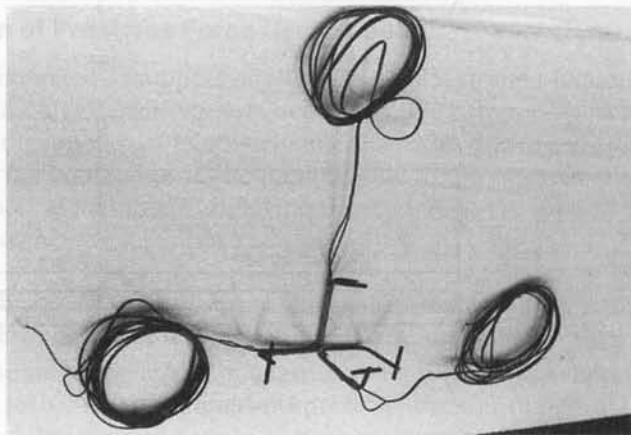
post-tensioned beams, due to the large tendon prestressing forces. In the *pretensioned beams* the concentrated load transfer of the prestressing force to the surrounding concrete gradually occurs over a length  $l_t$  from the face of the support section until it becomes essentially uniform.

In *post-tensioned beams*, this manner of gradual load distribution and transfer is not possible since the force acts directly on the face of the end of the beam through bearing plates and anchors. Also, some or all of the tendons in the post-tensioned beams are raised or draped towards the top fibers through the web part of the concrete section.

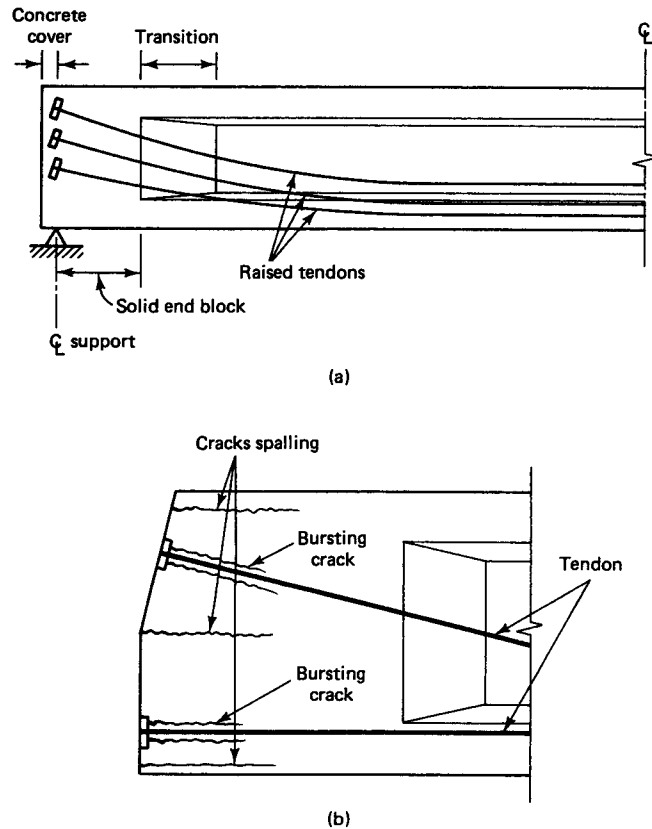
As the nongradual transition of the longitudinal compressive stress from concentrated to linearly distributed produces high transverse *tensile* stresses in the vertical (transverse) direction, longitudinal bursting cracks develop at the anchorage zone. When the stresses exceed the modulus of rupture of the concrete, the end block has to split (crack) longitudinally unless appropriate vertical reinforcement is provided. The location of the concrete-bursting stresses and the resulting bursting cracks as well as the surface-spalling cracks would thus have to depend on the location and distribution of the horizontal concentrated forces applied by the prestressing tendons to the end bearing plates.

It is sometimes necessary to increase the area of the section towards the support by a gradual transmission of the web to a width at the support equal to the flange width, in order to accommodate the raised tendons [see Figure 4.19(a)]. Such an increase in the cross-sectional area does not contribute, however, to preventing bursting or spalling cracks, and has no effect on reducing the transverse tension in the concrete. In fact, both test results and the theoretical analysis of this three-dimensional stress problem demonstrate that the tensile stresses could increase.

Consequently, it is essential to provide the necessary anchorage reinforcement in the load transfer zone in the form of *closed* ties, stirrups, or anchorage devices enclosing all the main prestressing and mild nonprestressed longitudinal reinforcement. However, it is at the same time advisable to insert reinforcing vertical mats and confining hoops close to the end face behind the bearing places in the case of post-tensioned beams. If the design has to follow AASHTO requirements for bridges, properly reinforced end blocks are required. Typical stress contours of equal vertical stress based on three-dimensional



**Photo 4.5** Three-dimensional instrumentation for end-block stress determination (Nawy et al.).



**Figure 4.19** End anchorage zones for bonded tendons. (a) Transition to solid section at support. (b) End-zone bursting and spalling cracks.

analysis and test results from Refs. 4.5, 4.7, 4.28. An idealization of the tensile and compressive stress paths is shown in Figure 4.20.

#### 4.5.2 Development and Transfer Length in Prestensioned Members and Design of Their Anchorage Reinforcement

As the jacking force is released in prestensioned members, the prestressing force is dynamically transferred through the bond interface to the surrounding concrete. The interlock or adhesion between the prestressing tendon circumference and the concrete over a finite length of the tendon gradually transfers the concentrated prestressing force to the entire concrete section at planes away from the end block and towards the midspan. The length of embedment determines the magnitude of prestress that can be developed along the span: the larger the embedment length, the higher is the prestress developed.

As an example for  $\frac{1}{2}$ -in. 7-wire strand, an embedment of 40 in. (102 cm) develops a stress of 180,000 psi (1,241 MPa), whereas an embedment of 70 in. (178 cm) develops a stress of 206,000 psi (1,420 MPa). From Figure 4.21, it is plain that the embedment length  $l_d$  that gives the full development of stress is a combination of the transfer length  $l_t$  and the flexural bond length  $l_f$ . These are given respectively by

$$l_t = \frac{1}{1000} \left( \frac{f_{pe}}{3} \right) d_b \quad (4.10a)$$



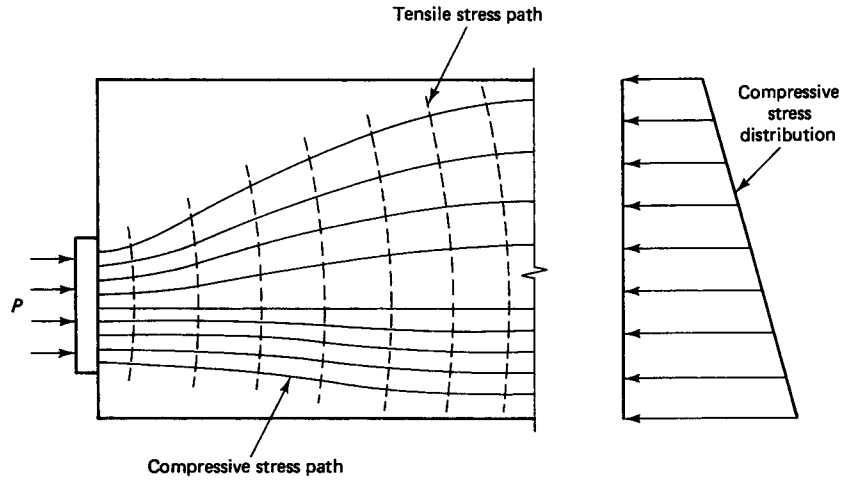


Figure 4.20 Idealized tensile and compressive stress paths at end blocks.

or

$$l_t = \frac{f_{pe}}{3000} d_b \tag{4.10b}$$

and

$$l_f = \frac{1}{1000} (f_{ps} - f_{pe}) d_b \tag{4.10c}$$

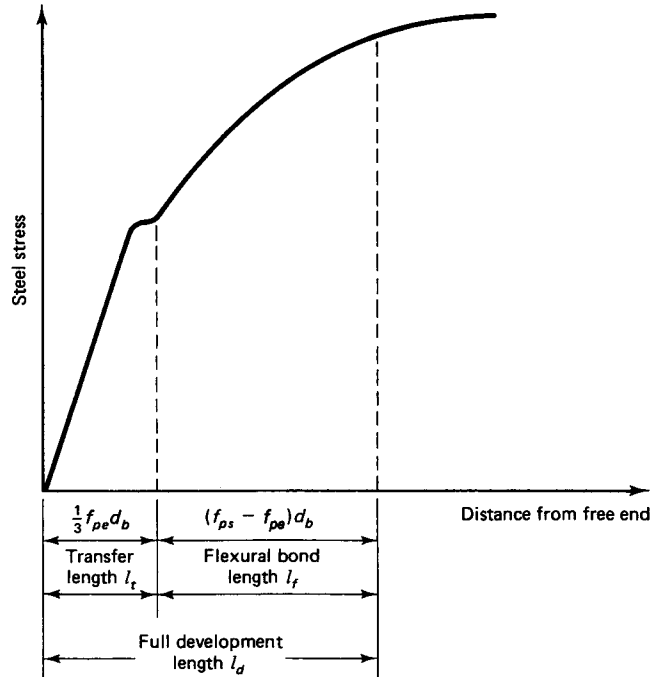


Figure 4.21 Development length for prestressing strand.

where  $f_{ps}$  = stress in prestressed reinforcement at nominal strength (psi)  
 $f_{pe}$  = effective prestress after losses (psi)  
 $d_b$  = nominal diameter of prestressing tendon (in.).

Combining Equations 4.10b and 4.10c gives

$$\text{Min } l_d = \frac{1}{1,000} \left( f_{ps} - \frac{2}{3} f_{pe} \right) d_b \quad (4.10d)$$

Equation 4.10d gives the minimum required development length for prestressing strands. If part of the tendon is sheathed towards the beam end to reduce the concentration of bond stresses near the end, the stress transfer in that zone is eliminated and an increased adjusted development length  $l_d$  is needed.

**4.5.2.1 Design of Transfer Zone Reinforcement in Pretensioned Beams.** Based on laboratory tests, empirical expressions developed by Mattock et al. give the total stirrup force  $F$  as

$$F = 0.0106 \frac{P_i h}{l_t} \quad (4.11)$$

where  $h$  is the pretensioned beam depth and  $l_t$  is the transfer length. If the average stress in a stirrup is taken as *half* the maximum permissible steel  $f_s$ , then  $F = \frac{1}{2} A_t f_s$ . Substituting this for  $F$  in Equation 4.11 gives

$$A_t = 0.021 \frac{P_i h}{f_s l_t} \quad (4.12)$$

where  $A_t$  is the total area of the stirrups and  $f_s \leq 20,000$  psi (138 MPa) for crack-control purposes.

#### 4.5.2.2 Reinforcement Selection in Pretensioned Beams

##### Example 4.5

Design the anchorage reinforcement needed to prevent bursting or spalling cracks from developing in the beam of Example 4.2, pretensioned.

##### Solution:

$$P_i = 376,110 \text{ lb (1,673 kN)}$$

From Equation 4.12,

$$A_t = 0.021 \frac{P_i h}{f_s l_t}$$

From Equation 4.10b, the transfer length is  $l_t = (f_{pe}/3,000)d_b$ . So since  $f_{pe} = 154,980$  psi and  $d_b = \frac{1}{2}$  in., we have

$$l_t = \frac{154,980}{3,000} \times 0.5 = 25.83 \text{ in. (66 cm)}$$

Now,

$$A_t = 0.021 \frac{P_i h}{f_s l_t}$$

So since  $f_s \leq 20,000$  psi, we get

$$A_t = 0.021 \frac{376,110 \times 40}{20,000 \times 25.83}$$

$$= 0.61 \text{ in.}^2 (3.9 \text{ cm}^2)$$

Trying #3 closed ties,

$$2 \times 0.11 = 0.22 \text{ in.}^2 (9.5 \text{ mm dia) ties}$$

$$\text{Min no. of stirrups} = \frac{0.61}{0.22} = 2.78$$

Use three #3 ties to provide the envelope for all the main longitudinal reinforcement.

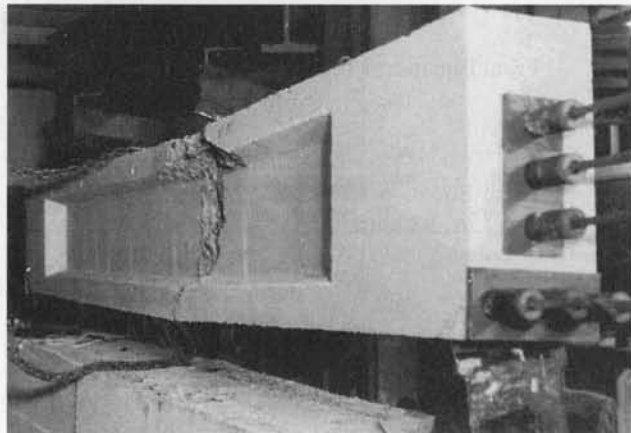
Wrap the tendons with helical steel wire through the development length,  $l_d$ , in order to effect good transfer.

### 4.5.3 Post-Tensioned Anchorage Zones: Linear Elastic and Strut-and-Tie Theories

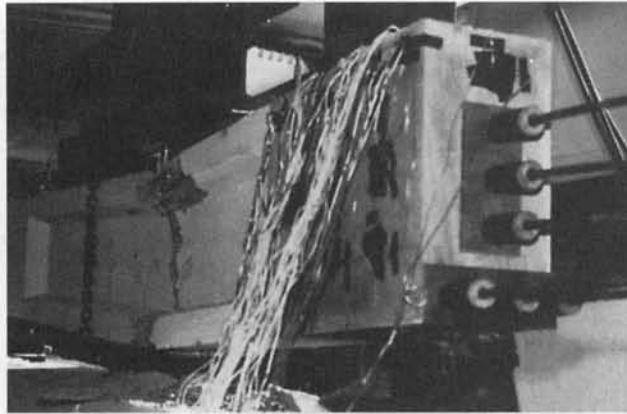
The anchorage zone can be defined as the volume of concrete through which the concentrated prestressing force at the anchorage device spreads transversely to a linear distribution across the entire cross-section depth along the span (Ref. 4.5, 4.7, 4.12, 4.30). The length of this zone follows St. Venant's principle, namely, that the stress becomes uniform at an approximate distance ahead of the anchorage device equal to the depth,  $h$ , of the section. The entire prism which would have a transfer length,  $h$ , is the total anchorage zone.

This zone is thus composed of two parts:

1. *General Zone:* The general extent of the zone is identical to the total anchorage zone. Its length extent along the span is therefore equal to the section depth,  $h$ , in standard cases.
2. *Local Zone:* This zone is the insert prism of concrete surrounding and immediately ahead of the anchorage device and the confining reinforcement it contains. See the shaded area in Figure 4.22(c) and its magnification in Fig. 4.22(a). Also shown are the distribution of tensile and compressive stresses in the local zone and their stress



**Photo 4.6** End block of post-tensioned I-beam at ultimate load (Nawy et al.).



**Photo 4.7** Anchorage block instrumentation (Nawy et al.).

contours obtained from the finite element analysis of the Rutgers tests (Ref. 4.7). The length of the local zone has to be considered as the larger of either its maximum width or the length of the anchorage device confining reinforcement.

The confining reinforcement throughout the entire anchorage zone has to be so chosen as to prevent bursting and splitting which are the result of the high concentrated compressive forces transmitted through the anchorage devices. In addition, checks have to be made of the bearing stresses on the concrete in the local zone due to these high compressive forces to ensure that the allowable compressive bearing capacity of the concrete is never exceeded.

#### 4.5.3.1 Design Methods for the General Zone

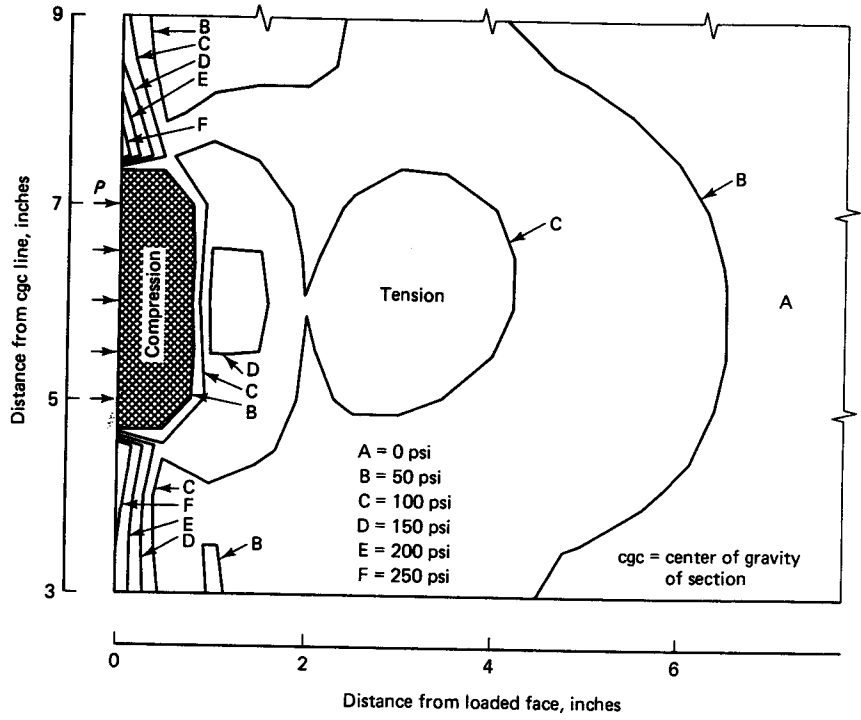
Essentially, three methods are applicable to the design of the anchorage zone.

1. *Linear Elastic Stress Analysis Approach Including Use of Finite Elements:* This involves computing the detailed state of stresses as linearly elastic. The application of the finite element method is somewhat limited by the difficulty of developing adequate models that can correctly model the cracking in the concrete (Ref. 4.30). Nevertheless, appropriate assumptions can always be made to get reasonable results.
2. *Equilibrium-Based Plasticity Approach such as the Strut-and-Tie Models:* The strut-and-tie method provides for idealizing the path of the prestressing forces as a truss structure with its forces following the usual equilibrium principles. The ultimate load predicted by this method is controlled by failure of any one of the component struts or ties. The method usually gives conservative results for this application.
3. *Approximate Methods:* These apply to rectangular cross sections without discontinuities.

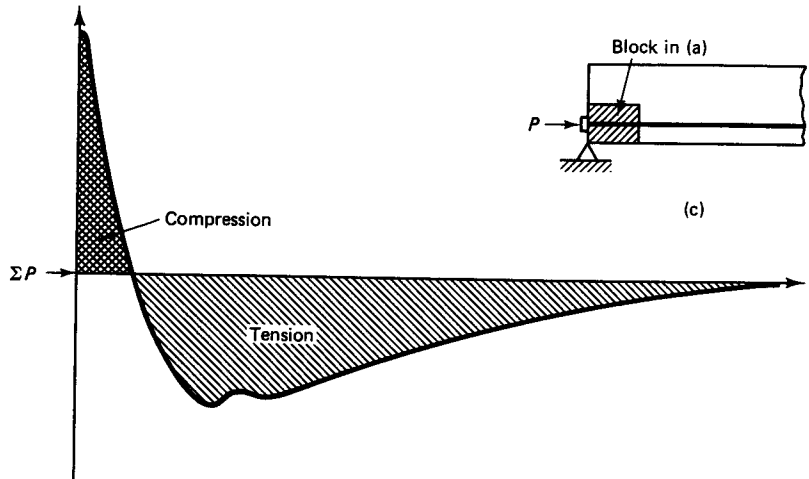
#### 4.5.3.2 Linear Elastic Analysis Method for Confining Reinforcement Determination

The anchorage zone is subjected to three levels of stress as seen in Figure 4.22(a) and the stress contour zones:

- (a) High bearing stresses ahead of the anchorage devices. Proper confinement of the concrete is necessary in order to prevent the compressive failure of the compressive segment shown in the darkly shaded area of Figures 4.22(a) and 4.22(b).



(a)

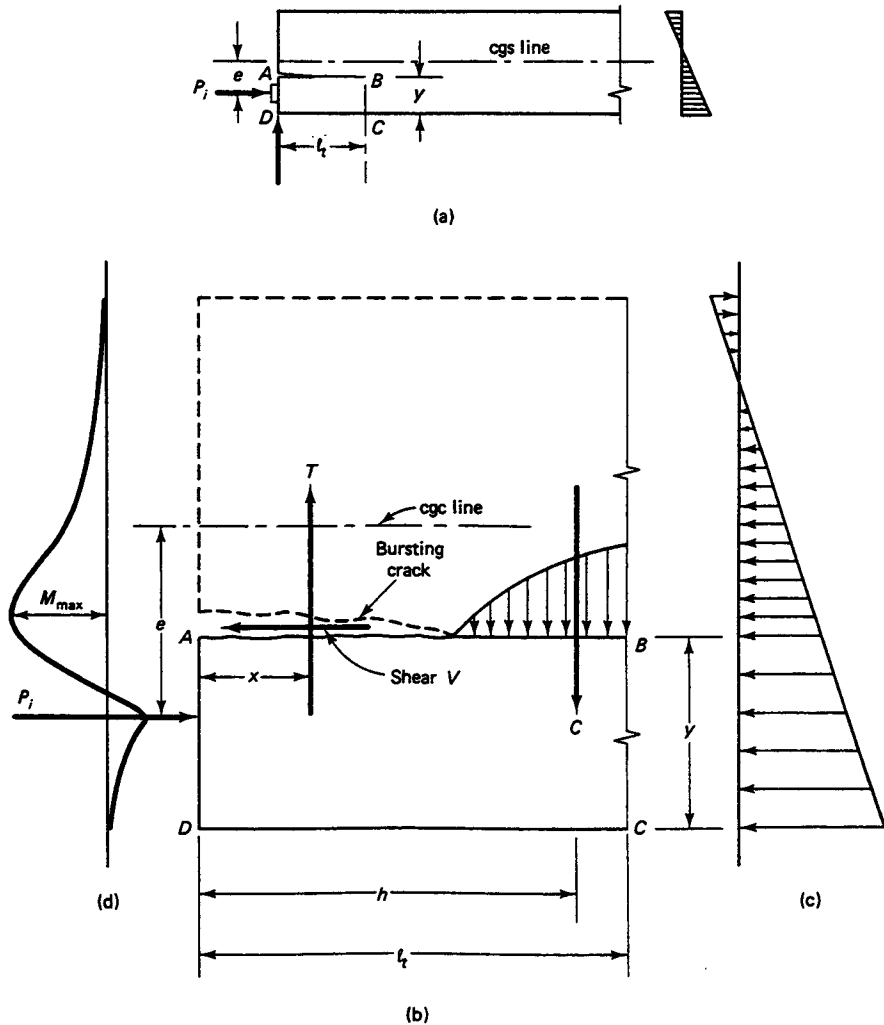


(b)

**Figure 4.22** Principal tensile stress contours of equal vertical stress at anchorage zone (eccentricity  $e_e = 6$  in.). (a) Contours of stress. (b) Stress distribution at 4.5 in. above base. (c) Segment of beam elevation. (Nawy et al., Refs. 4.7, 4.28)

- (b) Extensive tensile-bursting stresses in the tension contour areas, normal to the tendon axis as shown in Figures 4.22(a) and (b) and in Figure 4.23(b).
- (c) High compression in the stress field—areas marked D and E in Figure 4.22(a).

The following discussion illustrates that a linear elastic stress analysis can predict the cracking locations and give a reasonably reliable approximate estimate of the flow of



**Figure 4.23** Post-tensioned beam end-block forces. (a) Beam elevation, showing transfer length  $l_t$ . (b) Free-body diagram ABCD. (c) Fiber stress distribution across beam block depth. (d) Moment values on crack surface AB for all possible locations  $y$  across beam block depth.

stresses after cracking. The area of the tensile reinforcement is computed to carry the total tensile force obtained through integrating the tensile stresses in the concrete. In compressive stress regions, if the compressive force is very high, the provision of additional compressive reinforcement would become necessary.

On a parallel approach, a linearly elastic finite element analysis as shown in Figure 4.22 results in more accurate determination of the state of stresses in the anchorage zone. However, the process of computation is time-consuming and costly. The results can be limited because of the difficulty of developing adequate models that can correctly model the cracking in the concrete. A nonlinear finite element analysis to predict the post-cracking response could resolve this discrepancy. Yet, the design engineer expects less rigor and faster answers in the routine day-to-day office applications.

Figure 4.23 schematically illustrates the linearly elastic end block forces. It shows the end-block forces and the fiber stresses due to the prestressing force  $P_i$ , as well as the bending moment value for each possible crack height  $y$  above the beam bottom  $CD$ . The

maximum moment value  $M_{max}$  determines the potential position of the horizontal bursting crack. This moment is resisted by the couple provided by the tensile force  $T$  of the vertical anchorage zone reinforcement and the compressive force  $C$  provided by the end-block concrete, while the horizontal shear force  $V$  at the crack split surface is resisted by the aggregate interlock forces. From practical observations, the vertical anchorage zone stirrups that provide the force  $T$  should be distributed over a zone width  $h/2$  from the end-face of the beam such that  $x$  in Figure 4.23 can vary between  $h/3$  and  $h/5$ .

From equilibrium of moments,

$$T = \frac{M_{max}}{h - x} \quad (4.13)$$

and the total required area of vertical steel reinforcement becomes

$$A_t = \frac{T}{f_s} \quad (4.14)$$

where the steel stress  $f_s$  used in the calculation should not exceed 20,000 psi (138.5 MPa) for crack-width control purposes.

In summary and in lieu of a linear elastic finite element analysis, the procedure outlined can reasonably though less precisely give a detailed anchorage design as given in Example 4.6 part (a).

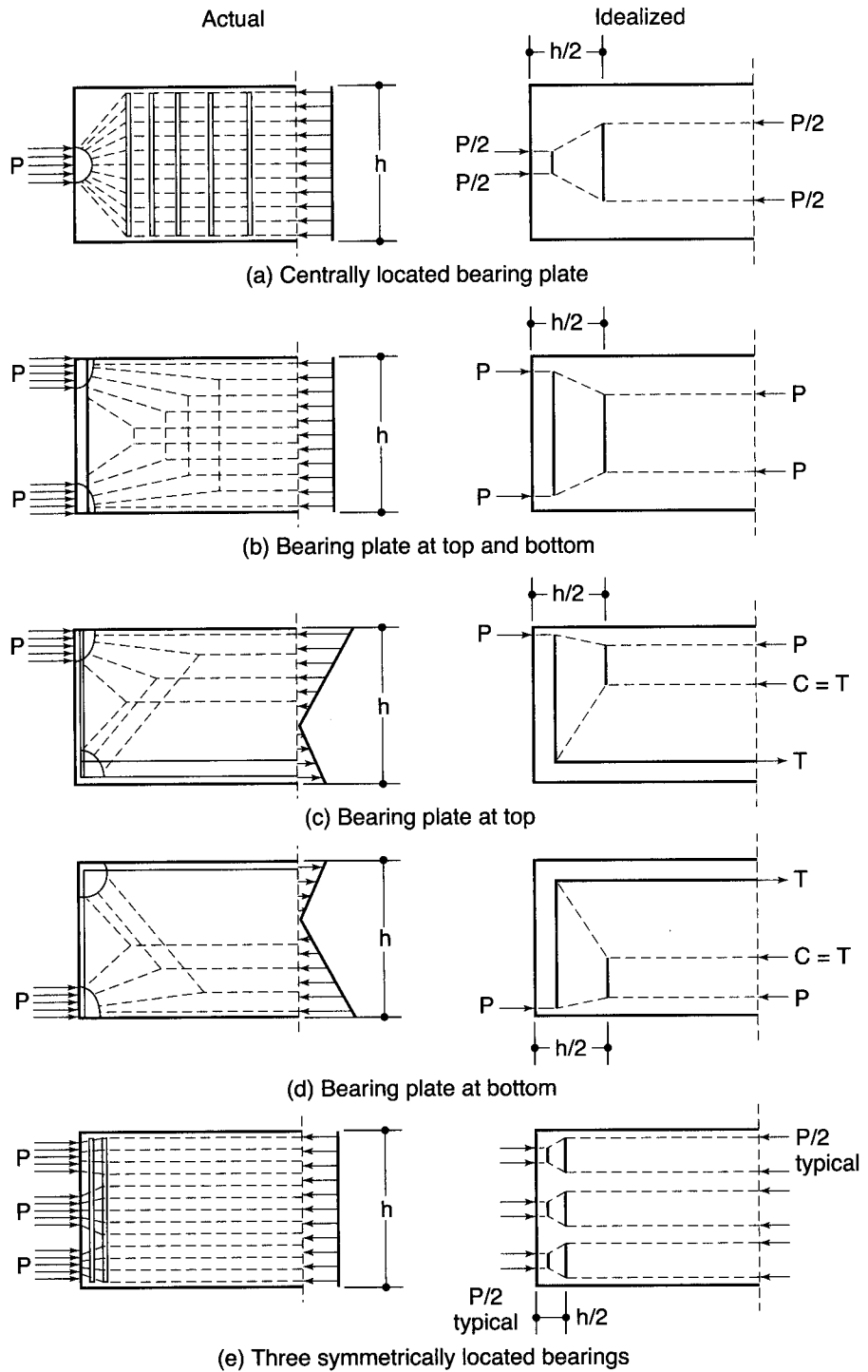
#### 4.5.3.3 Strut-and-Tie Method for Confining End-Block Reinforcement

The strut-and-tie concept is based on a plasticity approach approximating the flow of forces in the anchorage zone by a series of straight compression struts and straight tension ties connected at discrete points that are called nodes to form truss units. The compressive forces are carried by the plastic compression struts and the tensile forces are carried either by non-prestressed reinforcement such as mild steel bars as confining ties or by prestressing steel reinforcement. The yield strength of the anchorage confining reinforcement is used to determine the total area of reinforcement needed in the anchorage block. Figure 4.24 (adapted from Ref. 4.17) illustrates the flow of the concentric and eccentric prestressing forces  $P$  ahead of the point of application of these forces through the anchorage device towards the end of general zone where the stresses become uniform by St. Venant's principle.

A detailed discussion is presented in the author's Ref. 4.2 of the principles governing the strut-and-tie modeling procedures, the B and D regions, evaluation of the compression strut nominal strength, and the range of applicability of this fully plastic approach.

After significant cracking is developed, compressive stress trajectories in the concrete tend to congregate into straight lines that can be idealized as straight compressive struts in uniaxial compression. These struts would become part of truss units where the principal tensile stresses are idealized as tension ties in the truss unit with the nodal locations determined by the direction of the idealized compression struts. Figure 4.25(a) shows the development of a strut and Figure 4.25(b) sketches the resulting strut-and-tie trusses for multiple anchorage in a flanged T-section (Ref. 4.29). Figure 4.26 summarizes the concept of the idealized struts and ties in the anchorage zone. Figure 4.27 sketches standard strut-and-tie idealized trusses for concentric and eccentric cases both for solid and flanged sections as given in ACI 318 Code.

The tension tie in the ensuing truss analogy can be reasonably assumed to be at a distance  $h/2$  from the anchorage device. This assumption is essentially consistent with the approximated location of the tensile force  $T$  in Figure 4.23 of the elastic stress-analysis approach. It is clear from all these diagrams that the designer has to make an engineering judgment on the number of paths of struts, resulting ties, and ensuing nodes, particularly



**Figure 4.24** Schematic of Compression Strut-and-Tie Force Paths (Adapted from Ref. 4.17).



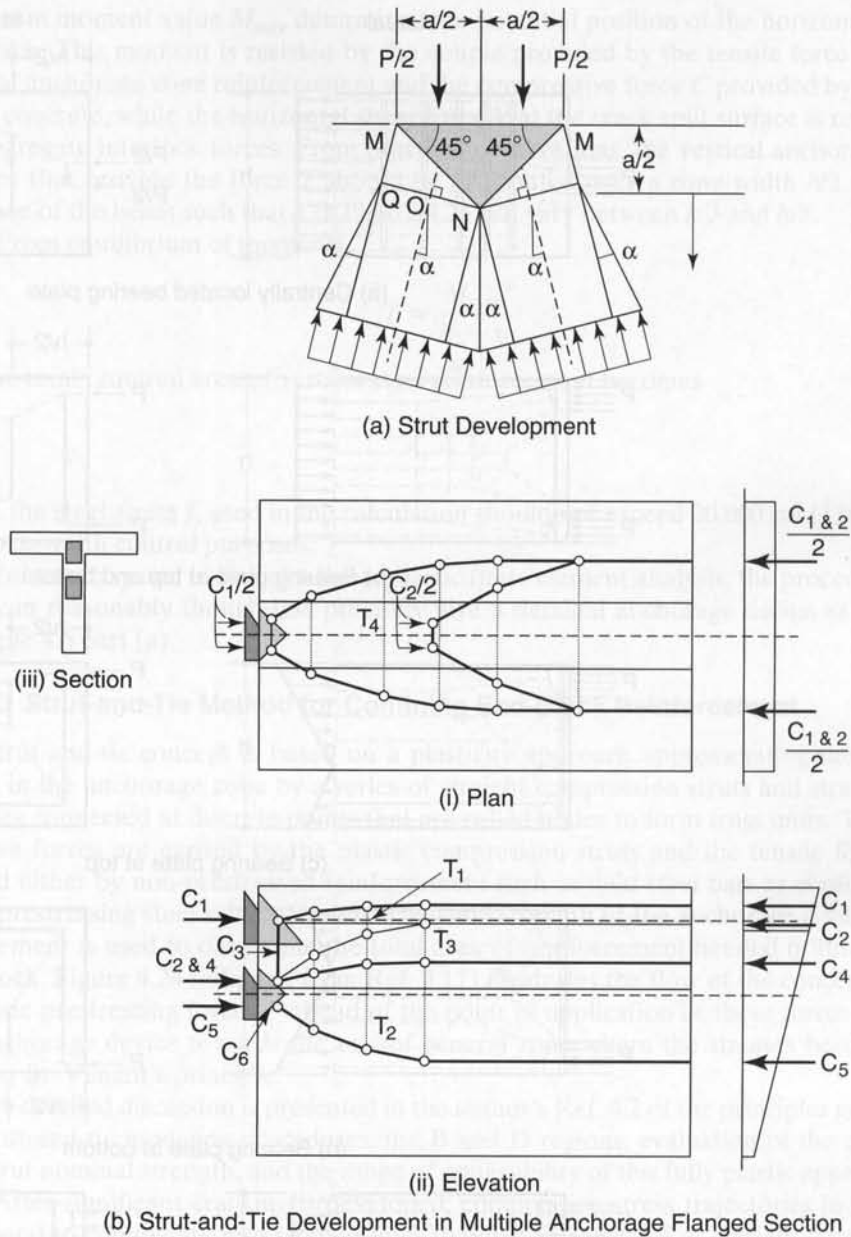


Figure 4.25 Strut-and-Tie Development.

in the usual case of multiple anchorage devices. Part (b) of Example 4.6 illustrates the assumed idealized paths for the anchorage zone in the I-beam under consideration.

Anchorage devices are treated as closely spaced if their center-to-center spacing does not exceed 1.5 times the width of the anchorage device

#### 4.5.3.4 Approximate Method for Confinement of End Block Reinforcement

Simplified equations can be used to compute the magnitude of the bursting force,  $T_{\text{burst}}$  and its centroid distance,  $d_{\text{burst}}$ , from the major bearing surface of the anchorage (Ref. 4.30). The member has to have a rectangular cross-section with no discontinuities

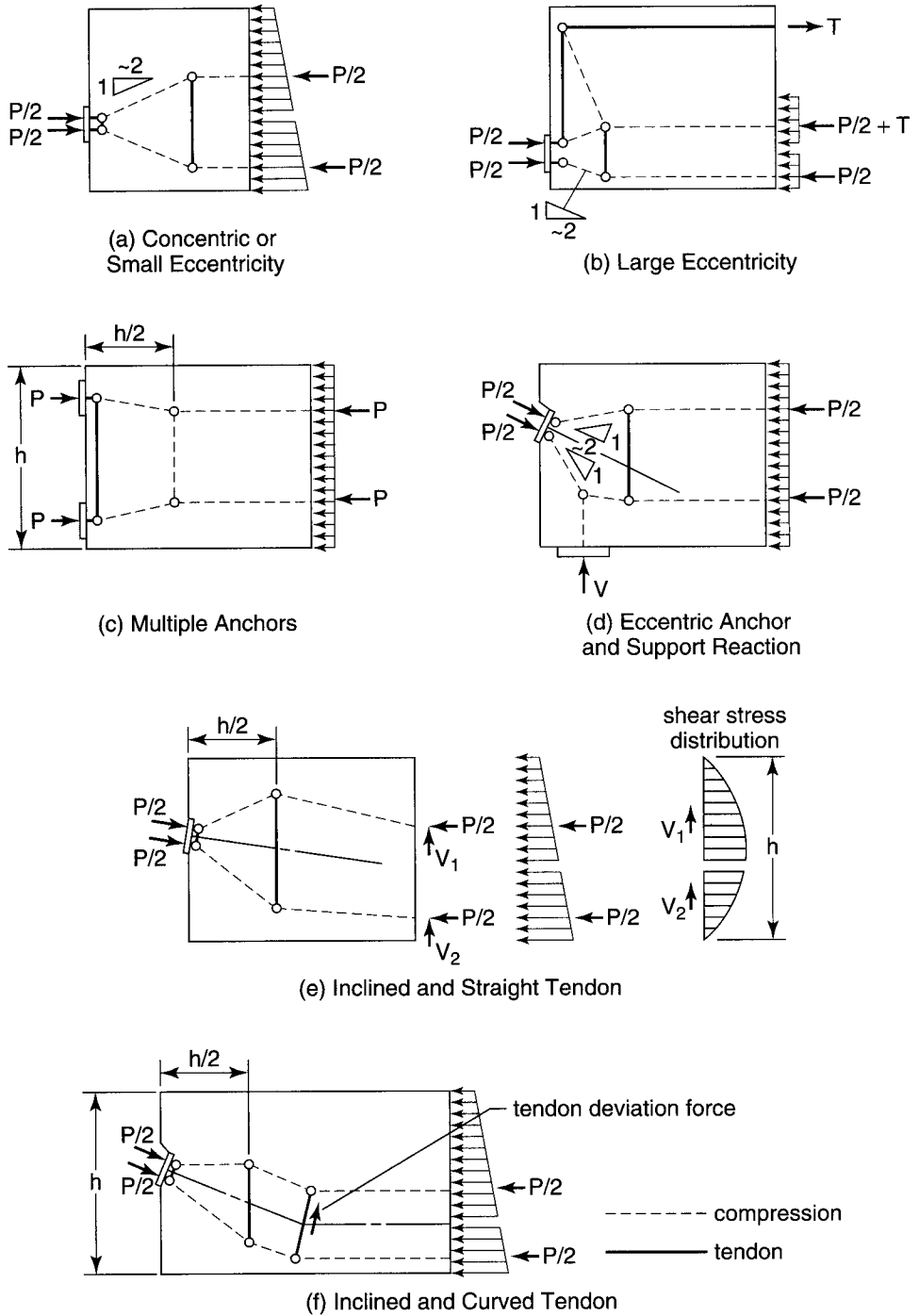
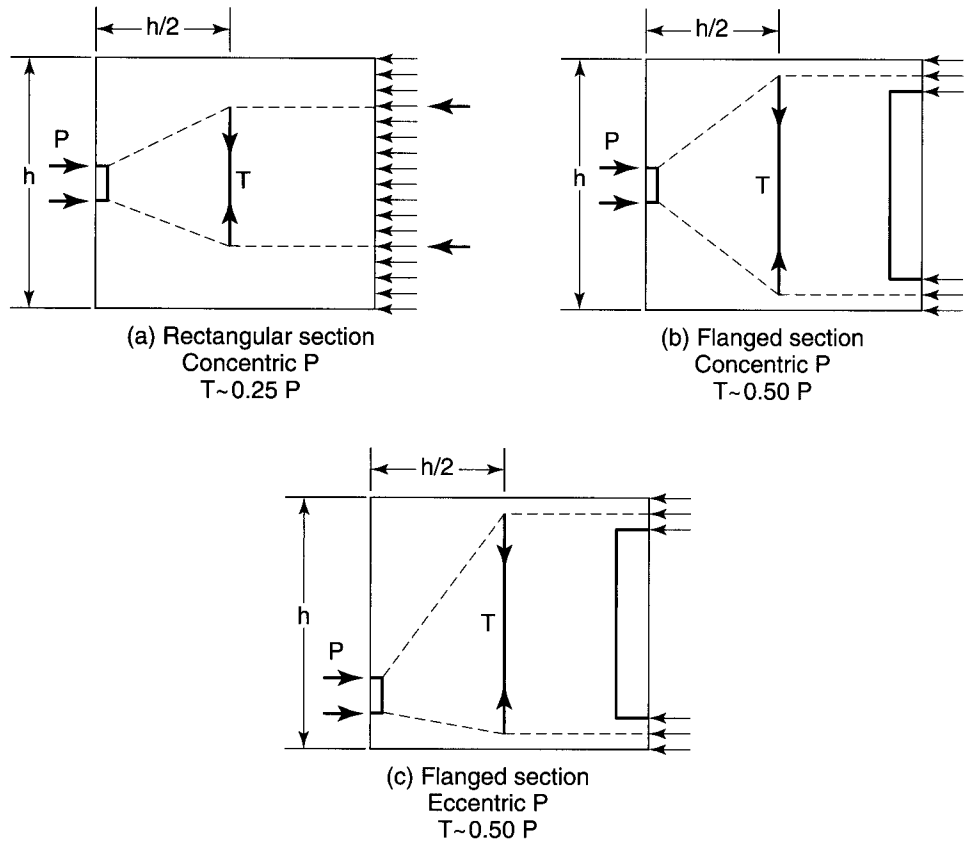


Figure 4.26 Typical Strut-and-Tie Models For End-Block Anchorage Zones.



**Figure 4.27** Strut-and-Tie Idealized Trusses in Standard Concentric and Eccentric Cases, ACI 318.

along the span. The beam cross section would usually be the depth,  $h$ , of the section times the width  $b$ . The bursting force,  $T_{burst}$ , and its distance,  $d_{burst}$ , can be computed from the following expression:

$$T_{burst} = 0.25 \Sigma P_{su} \left( 1 - \frac{a}{h} \right) \quad (4.15a)$$

$$d_{burst} = 0.5(h - 2e) \quad (4.15b)$$

where

$\Sigma P_{su}$  = the sum of the total factored prestress loads for the stressing arrangement considered, lb

$a$  = plate width of anchorage device or single group of closely spaced devices in the direction considered, in.

$e$  = eccentricity (always taken positive) of the anchorage device or group closely spaced devices with respect to the centroid of the cross-section, in.

$h$  = depth of the cross-section in the direction considered, in.

The ACI 318 Code requires that the design of confining reinforcement in the end anchorage block of post-tensioned members be based on the *factored* prestressing force  $P_{su}$  for both the general and local zones described at the outset of Sec. 4.4.3. A load factor of 1.2 is to be applied to an end anchorage stress level  $f_{pi} = 0.80 f_{pu}$  for low-relaxation strands at the *short time* interval of jacking, which can reduce to an average value of  $0.70 f_{pu}$  for the total group of strands at the completion of the jacking process. For stress-

relieved strands, a lower  $f_{pi} = 0.70 f_{pu}$  is advised. The maximum force  $P_{su}$  stipulated in the ACI 318 Code for designing the confining reinforcement at the end-block zone is as follows for the more widely used low-relaxation strands:

$$P_{su} = (1.2) A_{ps} (0.8 f_{pu}) \quad (4.15c)$$

The AASHTO Standard, for the case where  $P_{su}$  acts at an inclined angle  $\alpha$  in the direction of the beam span, adds the term  $[0.5 \Sigma (P_{us} \sin \alpha)]$  to Equation (4.15a) and  $5e(\sin \alpha)$  to Equation (4.15b). For horizontal  $P_{su}$   $\sin \alpha = 0$ .

#### 4.5.3.5 Allowable Bearing Stresses

The maximum allowable bearing stress at the anchorage device seating should not exceed the smaller of the two values obtained from Equations 4.16(a) and 4.16(b) as follows:

$$f_b \leq 0.7 f'_{ci} \sqrt{A/A_g} \quad 4.16 (a)$$

$$f_b \leq 2.25 f'_{ci} \quad 4.16 (b)$$

where  $f_b$  = maximum factored tendon load,  $P_u$ , divided by the effective bearing area  $A_b$

$f'_{ci}$  = concrete compressive strength at stressing

$A$  = maximum area of portion of the supporting surface that is geometrically similar to the loaded area and concentric with it, contained wholly within the section, with the upper base being the loaded surface area of the concrete and sloping sideway with a slope of 1 vertical to 2 horizontal.

$A_g$  = gross area of the bearing plate

Equations 4.16(a) and 4.16(b) are valid only if general zone reinforcement is provided and if the extent of concrete along the tendon axis ahead of the anchorage device is at least twice the length of the local zone.

#### 4.5.4 Design of End Anchorage Reinforcement for Post-tensioned Beams

##### Example 4.6

Design an end anchorage reinforcement for the post-tensioned beam in Example 4.2, giving the size, type, and distribution of reinforcement. Use  $f'_c = 5,000$  psi (34.5 MPa) normal-weight concrete.  $f_{pu} = 270,000$  psi low-relaxation steel.

Assume that the beam ends are rectangular blocks extending 40 in. (104 cm.) into the span beyond the anchorage devices then transitionally reduce to the 6-in. thick web. Solve the problem using (a) the linear elastic stress analysis method, (b) the plastic strut-and-tie method. Sketch the truss model you determine.

##### (a) Solution by the Linear Elastic Stress Method:

1. Establish the configuration of the strands to give eccentricity  $e_e = 12.49$  in. (317 mm)

From Example 4.2,

$c_b = 18.84$  in., hence distance from the beam bottom fibers =  $c_b - e_e = 6.35$  in. (161 mm)

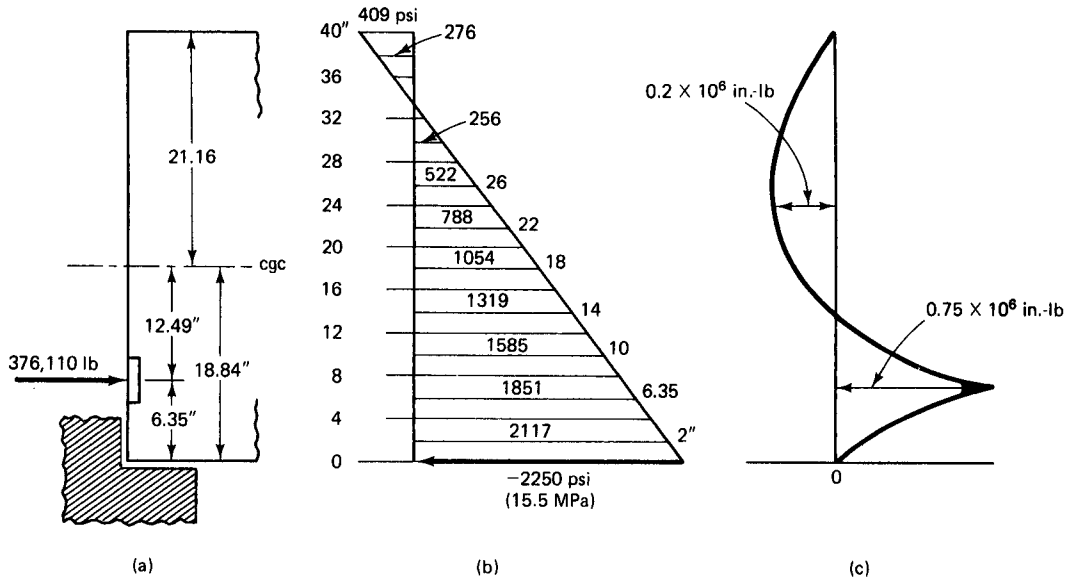
For a centroidal distance of the  $13 - \frac{1}{2}$  in. size tendons = 6.35 in. from the beam bottom fibers, try the following row arrangement:

1st row : 5 strands at 2.5 in.

2nd row : 5 strands at 7.0 in.

3rd row : 3 strands at 11.5 in.

$$\text{distance of the centroid of tendons} = \frac{5 \times 2.5 + 5 \times 7.0 + 3 \times 11.5}{13} \cong 6.35 \text{ in., O.K.}$$



**Figure 4.28** Anchorage zone stresses and moments in Example 4.6. (a) Post-tensioned end-block zone. (b) Transfer concrete stress distribution across depth. (c) Net anchorage zone moments on potential horizontal cracking planes along the beam depth.

## 2. Elastic analysis of forces

Divide the beam depth into 4-in. increments of height as shown in Figure 4.28, and assume that the concrete stress at the center of each increment is uniform across the depth of the increment. Then calculate the incremental moments due to these internal stresses and due to the external prestressing force  $P_i$  about each horizontal plane in order to determine the *net* moment on the section. The net maximum moment will determine the position of the potential horizontal bursting crack and the reinforcement that has to be provided to prevent the crack from developing. Using a plus (+) sign for clockwise moment, the initial prestressing force before losses, from Example 4.2, is  $P_i = 376,110$  lb (1,673 kN). From Figure 4.28, the concrete internal moment at the plane 4 in. from the bottom fibers is

$$\begin{aligned} M_{c4} &= 2,117 \times 4 \times 18 \times (2 \text{ in.}) = 304,848 \text{ in.-lb} \\ &= 0.3 \times 10^6 \text{ in.-lb (34.4 kN-m)} \end{aligned}$$

and that at the plane 8 in. from the bottom fibers is

$$\begin{aligned} M_{c8} &= 2,117 \times 4 \times 18 \times (6 \text{ in.}) + 1,851 \times 4 \times \frac{18 + 10}{2} \times (2 \text{ in.}) \\ &= 1,121,856 \text{ in.-lb} = 1.12 \times 10^6 \text{ in.-lb (127 kN-m)} \end{aligned}$$

The prestressing force moment at the plane 8 in. from the bottom fibers is

$$\begin{aligned} M_{c8} &= 376,110 \times (8 - 6.35) = -620,582 \text{ in.-lb} \\ &= -0.62 \times 10^6 \text{ in.-lb (70.1 kN-m)} \end{aligned}$$

The net moment is then  $1.12 \times 10^6 - 0.62 \times 10^6 = 0.50 \times 10^6$  in.-lb (56.6 kN-m).

In a similar manner, we can find the net moment for all the other incremental planes at 4-in. increments to get the values tabulated in Table 4.5. From the table, the maximum net moments are  $+M_{\max} = 0.75 \times 10^6$  in.-lb (84.6 kN-m) at the horizontal plane 6.35 in. above the beam bottom fibers (bursting potential crack effect) and  $-M_{\max} = -0.20 \times 10^6$  in.-lb at the horizontal plane 24 in. (61 cm) above the beam bottom fibers (spalling potential crack effect).

**Table 4.5** Anchorage Zone Moments for Example 4.6

Moment plane dist. $d$ from bottom in.	Section width in.	Stress at plane $(d - 2.0)^*$ psi	Concrete resistance force at $(d - 2.0)^*$ lb	Moment $M_p$ for a $P_i$ about horiz. plane in col. (1) in.-lb $\times 10^6$	Moment $M_c$ of concrete in col. (4) about horiz. plane in col. (1) in.-lb $\times 10^6$	Net moment $(M_c - M_p)$ col. (6) - col. (5) in.-lb $\times 10^6$
(1)	(2)	(3)	(4)	(5)	(6)	(7)
0	18	-2,250	162,000	0	0	0
4	18	-2,117	152,424	0	+0.30	+0.30
6.35	13.3	-1,851	103,656	0	+0.75	+0.75
8	10	-1,585	63,400	-0.62	+1.12	+0.50
12	6	-1,319	31,656	-2.13	+2.25	+0.12
16	6	-1,054	25,296	-3.63	+3.54	-0.09
20	6	-788	18,912	-5.13	+4.94	-0.19
24	6	-522	12,528	-6.64	+6.44	-0.20
28	6	-256	6,144	-8.14	+7.99	-0.15
32	6	-0	-0	-9.65	+9.61	-0.04
36	18	+276	-19,872	-11.15	+11.13	-0.02
40	18	+409	-29,448	-12.66	+12.65	-0

\* $d$  = distance from plane about which moment is taken less half the depth of one slice (in this example slice depth = 4 in.).

### 3. Design of anchorage reinforcement

From Equation 4.13, assuming that the center of the tensile vertical force  $T$  is at a distance  $x \approx 15$  in., we obtain

$$T = \frac{M_{\max}}{h - x} = \frac{+0.75 \times 10^6}{40 - 15} = 30,000 \text{ lb (133 kN)}$$

Allowing a maximum steel stress,  $f_s = 20,000$  psi, (the Code allows  $0.60 f_y = 36,000$  psi)

The bursting zone reinforcement is

$$A_t = \frac{T_b}{f_s} = \frac{30,000}{20,000} = 1.50 \text{ in.}^2 (968 \text{ mm}^2)$$

So

$$\text{Try No. 3 closed ties } (A_s = 2 \times 0.11 = 0.22 \text{ in.}^2)$$

$$\text{Required no. of stirrups} = \frac{1.50}{0.22} = 6.82$$

Use seven No. 3 ties in addition to what is required for shear.

The spalling zone force

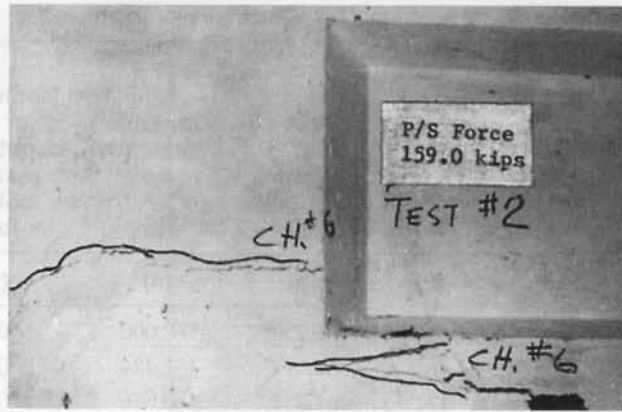
$$T_s = \frac{-0.2 \times 10^6}{40 - 15} = 8,000 \text{ lb}$$

So

$$A_s = \frac{T_s}{f_s} = \frac{8,000}{20,000} = 0.40 \text{ in.}^2 (250 \text{ mm}^2)$$

Hence, we have

$$\text{Req no. of No. 3 stirrups} = \frac{0.40}{0.22} = 1.82$$



**Photo 4.8** Typical bursting crack of the anchorage zone (Nawy et al.).

So use two No. 3 additional stirrups. Then

$$\text{Total number of stirrups} = 6.82 + 1.82 + 4 \approx 12.64$$

Use 13 No. 3 closed ties. Extend the stirrups into the compression zone in Figure 4.23.

Space the No. 3 closed ties at 3 in. center to center with the first stirrup starting 3 in. from the beam end. Also, provide four No. 3 bars 10 in. long at 3 in. center to center each way 2 in. from the end face at the anchor location, since cracking can occur vertically and horizontally. Add spiral reinforcement under the anchors if the manufacturer specifies that such a reinforcement is useful.

Next, check the bearing plate stresses.

**(b) Solution by the Plastic Strut-and-Tie Method:**

1. Establish the configuration of the strands to give eccentricity  $e_e = 12.49$  in. (317 mm)

From Example 4.2,

$$c_b = 18.84 \text{ in.}, \text{ hence distance from the beam fibers} = c_b - e_e = 6.35 \text{ in. (161 mm)}$$

For a centroidal distance of the 13- $\frac{1}{2}$ -in.-size strands = 6.35 in. from the beam bottom fibers, try the following row arrangement of tendons with the indicated distances from the bottom fibers:

- 1st row : 5 tendons at 2.5 in.
- 2nd row : 5 tendons at 7.0 in.
- 3rd row : 3 tendons at 11.5 in.

$$\text{distance of the centroid of tendons} = \frac{5 \times 2.5 + 5 \times 7.0 + 3 \times 11.5}{13} \approx 6.35 \text{ in., O.K.}$$

2. Factored forces in tendon rows and bearing capacity of the concrete

From Equation (4.15c) for low-relaxation strands,  $f_{pi} = 0.80 f_{pu}$ .

The factored jacking force at the short jacking time interval is:

$$P_{su} = 1.2 A_{ps} (0.80 f_{pu}) = 0.96 f_{pu} A_{ps} = 0.96 \times 270,000 A_{ps} = 259,200 A_{ps} \text{ psi.}$$

If stress-relieved strands are used, it would have been advisable to use  $f_{pi} = 0.70 f_{pu}$ .

$$\text{1st row force } P_{u1} = 5 \times 0.153 \times 259,200 = 198,286 \text{ lb. (882 kN)}$$

$$\text{2nd row force } P_{u2} = 5 \times 0.153 \times 259,200 = 198,286 \text{ lb. (882 kN)}$$

$$\text{3rd row force } P_{u3} = 3 \times 0.153 \times 259,200 = 118,973 \text{ lb. (529 kN)}$$

$$\text{Total ultimate compressive force} = 198,286 + 198,286 + 118,973 = 515,545 \text{ lb. (2290 kN)}$$

Total area of rigid bearing plates supporting the Supreme 13-chucks anchorage

$$\text{devices} = 14 \times 11 + 6 \times 4 = 178 \text{ in.}^2 (113 \text{ cm}^2)$$

$$\text{Actual bearing stress } f_b = \frac{515,545}{178} = 2896 \text{ psi (19.9 MPa)}$$

From Equations 4.16(a) and (b), the maximum allowable bearing pressure on the concrete is the lesser of

$$f_b \leq 0.7 f'_{ci} \sqrt{A/A_g}$$

$$f_b \leq 2.25 f'_{ci}$$

$$\begin{aligned} \text{Assume that the initial concrete strength at stressing is } f'_{ci} &= 0.75 f'_c \\ &= 0.75 \times 5,000 = 3750 \text{ psi} \end{aligned}$$

Concentric area,  $A$ , of concrete with the bearing plates  $\cong (14+4)(11+4) + (6+4)(4+4) = 350 \text{ in.}^2$ , as defined for the concrete pyramid base in Section 4.5.3.5.

$$\text{Allowable bearing stress, } f_b = 0.7 \times 3750 \sqrt{\frac{350}{178}} = 3,681 \text{ psi. } > 2,896 \text{ psi, O.K.}$$

The bearing stress from Eq. 4.14 (b) does not control.

As defined in Section 4.5.3.5, it should be noted that the area  $A_g$  of the rigid steel plate or plates, and the corresponding concrete pyramid base area  $A$  within the end block assumed to receive the bearing stress, are purely determined by engineering judgement. The areas are based on the geometry of the web and bottom flange of the section, the rectangular dimension of the beam end, and the arrangement and spacing of the strand anchorages in contact with the supporting steel end bearing plates.

### 3. Draw the strut-and-tie model

Total length of distance  $a$ , as in Figure 4.25 between forces  $P_{u1} - P_{u3} = 11.5 - 2.5 = 9.0 \text{ in.}$

Hence depth  $a/2$  ahead of the anchorages  $= 9.0/2 = 4.5 \text{ in.}$

Construct the strut-and-tie model assuming it to be as shown in Figure 4.29.

The geometrical dimensions for finding the horizontal force components from the ties 1-2 and 3-2 have cotangent values of 26.5/15.5 and 13.0/15.5 respectively. From statics, truss analysis in Figure 4.29 gives the member forces as follows:

$$\text{tension tie 1-2} = 118,973 \times \frac{26.5}{15.5} = 203,405 \text{ lb (904 kN)}$$

$$\text{tension tie 3-2} = 198,286 \times \frac{13}{15.5} = 166,304 \text{ lb (699 kN)}$$

Use the larger of the two values for choice of the closed tension tie stirrups.

Try No. 3 closed ties, giving a tensile strength per tie  $= \phi f_y A_v$

$$= 0.90 \times 60,000 \times 2(0.11) = 11,880 \text{ lb}$$

$$\text{required number of stirrup ties} = \frac{203,405}{11,880} = 17.1$$

For the tension tie a-b-c in Figure 4.29, use the force  $P_u = 166,304 \text{ lb}$  to concentrate additional No. 4 vertical ties ahead of the anchorage devices. Start the first tie at a distance of  $1\frac{1}{2} \text{ in.}$  from the end rigid steel plate transferring the load from the anchorage devices to the concrete.

$$\text{Number of ties} = \frac{166,304}{0.90 \times 60,000(2 \times 0.20)} = 7.7$$

Use eight No. 4 closed ties @  $1\frac{1}{4} \text{ in.}$  (12.7 mm @ 32 mm) center to center with the first tie to start at  $1\frac{1}{2} \text{ in.}$  ahead of the anchorage devices.

Only thirteen ties in lieu of the 15.0 calculated are needed since part of the zone is covered by the No. 4 ties. Use 13 No. 3 closed ties @  $2\frac{1}{2} \text{ in.}$  (9.5 mm @ 57 mm) center to center



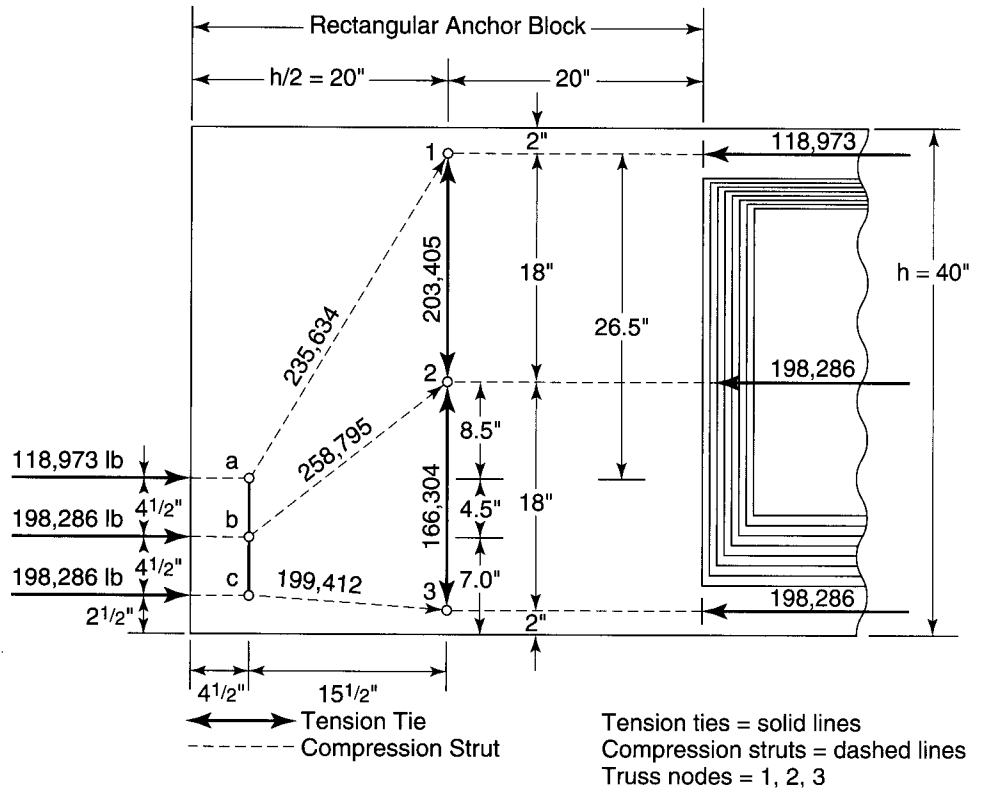


Figure 4.29 Struts-and-Ties in Example 4.6

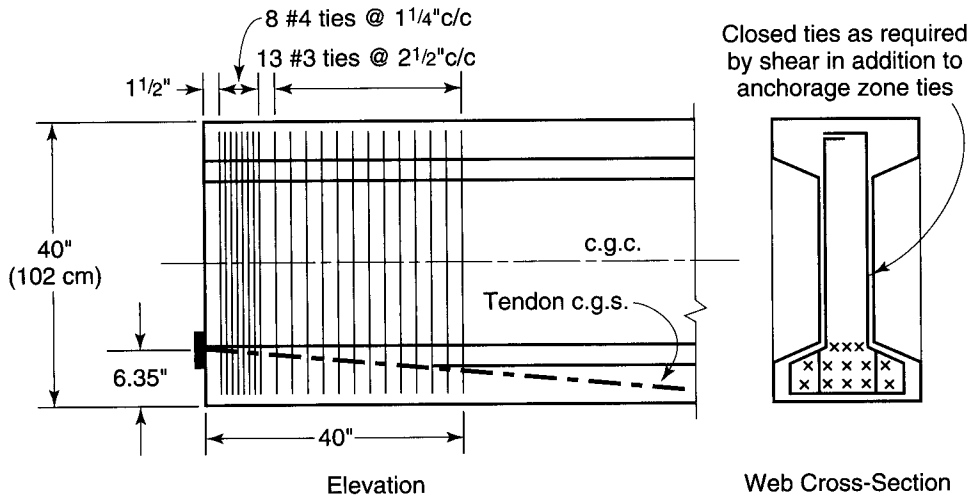
beyond the last No. 4 tie so that a total distance of 40 in. (104 cm) width of the rectangular anchor block is confined by the reinforcement closed ties.

Note that this solution requires a larger number of confining ties than the semi-elastic solution in part (a). Adopt this design of the anchorage zone. Figure 4.30 shows a schematic of the anchorage zone confining reinforcement details resulting from the strut-and-tie analysis.

It should also be noted that the idealized paths of the compression struts for cases where there are several layers of prestressing strands should be such that at each layer level a stress path is assumed in the design. This can be seen in Example 4.7 and Figure 4.39(b). If layers are combined, a more conservative solution with more confining reinforcement area results, which is not necessarily justified.

#### 4.6 FLEXURAL DESIGN OF COMPOSITE BEAMS

Composite sections are normally precast, prestressed supporting elements over which sit situ-cast top slabs that act integrally with them. Composites have the advantage of the precast part becoming in many cases the falsework for supporting the situ-cast top slab and topping in bridges and industrial buildings, as shown in Figure 4.31. Sometimes the precast, prestressed element is shored during the placement and curing of the situ-cast top slab. In such a case, the slab weight acts only on the composite section, which has a substantially larger section modulus than the precast section. Hence, the concrete stress calculations have to take this situation into account in the design. The concrete stress distribution due to composite action can be seen in Figure 4.32, in part (e) of which the load taken by the cured composite section is the sum of  $W_{SD} + W_L$ .



**Figure 4.30** End anchorage reinforcement in Example 4.6. (a) Anchorage zone, (b) Beam cross section.

**4.6.1 Unshored Slab Case**

From Equations 4.2a and b, the extreme concrete fiber stress equations before casting the top slab are

$$f^t = -\frac{P_e}{A_c} \left( 1 - \frac{ec_t}{r^2} \right) - \frac{M_D + M_{SD}}{S^t} \tag{4.17}$$

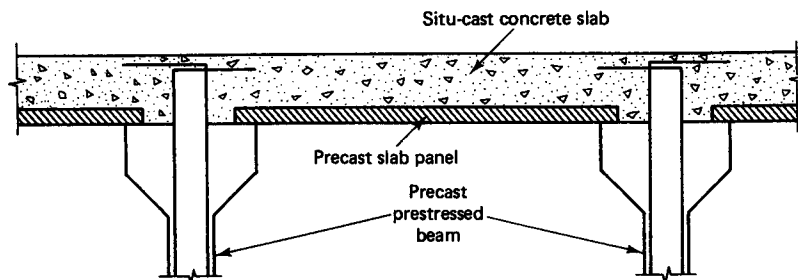
and

$$f_b = -\frac{P_e}{A_c} \left( 1 + \frac{ec_b}{r^2} \right) + \frac{M_D + M_{SD}}{S_b} \tag{4.18}$$

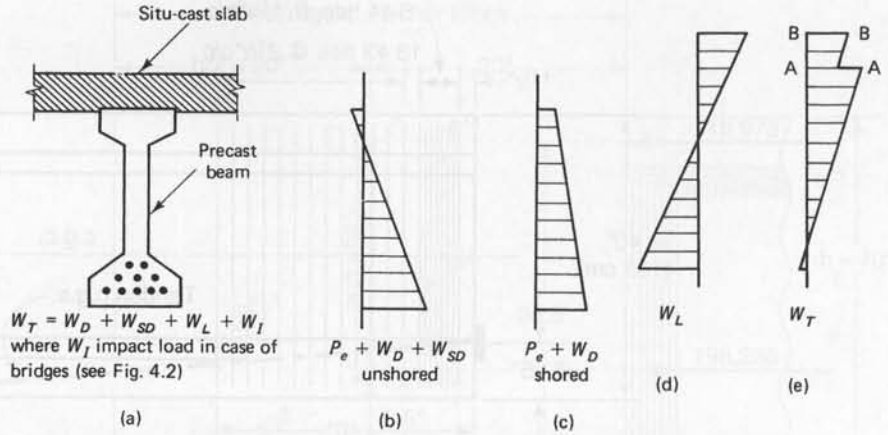
where  $S^t$  and  $S_b$  are the section moduli of the precast section only, and  $M_{SD}$  is any additional superimposed moment such as the wet slab concrete.

After the situ-cast slab hardens and composite action takes place, new higher moduli  $S'_c$  and  $S'_{cb}$  are available, with the cgc line moving upwards towards the top fibers. The concrete fiber stress counterparts to Equations 4.18a and b for the extreme top and bottom fibers of the *precast* part of the composite section (level AA in Figure 4.32(e) are

$$f^t = -\frac{P_e}{A_c} \left( 1 - \frac{ec_t}{r^2} \right) - \frac{M_D + M_{SD}}{S^t} - \frac{M_{CSD} + M_L}{S'_c} \tag{4.19a}$$



**Figure 4.31** Composite prestressed concrete construction.



**Figure 4.32** Flexural stress distribution in composite beams. (a) Composite beam. (b) Concrete stress distribution. (c) Concrete stress distribution with precast beam shored. (d) Live-load stress for shored case, or live load plus superimposed dead load for unshored case. (e) Final service-load stress due to all loads.

and

$$f_b = -\frac{P_e}{A_c} \left( 1 + \frac{ec_b}{r^2} \right) + \frac{M_D + M_{SD}}{S_b} + \frac{M_{CSD} + M_L}{S_{cb}} \quad (4.19b)$$

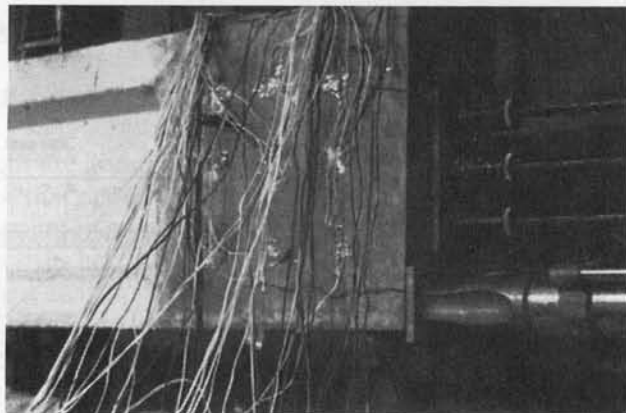
where  $M_{CSD}$  is the additional composite superimposed dead load after erection, i.e., at service, and  $S_c^t$  and  $S_{cb}$  are the section moduli of the composite section at the level of the top and bottom fibers, respectively, of the precast section.

The fiber stresses at the level of the top and bottom fibers of the situ-cast slab (levels *BB* and *AA* of Figure 4.32(e)) are

$$f_{ts} = -\frac{M_{CSD} + M_L}{S_{cs}^t} \quad (4.20a)$$

and

$$f_{bs} = -\frac{M_{CSD} + M_L}{S_{bcs}} \quad (4.20b)$$



**Photo 4.9** Jacking tendons of post-tensioned beam (Nawy et al.).

where  $M_{CSD} + M_L$  are the incremental moments added after composite action has developed, and  $S_{cb}^t$  and  $S_{bc}^b$  are the section moduli of the composite section for the top and bottom fibers  $AA$  and  $BB$ , respectively, of the slab in Figure 4.32(e).

#### 4.6.2 Fully Shored Slab Case

In cases where the situ-cast slab is fully shored until composite action develops, the concrete fiber stresses before shoring and top slab casting become, from Equations 4.18 and 4.19,

$$f^t = -\frac{P_e}{A_c} \left( 1 - \frac{ec_t}{r^2} \right) - \frac{M_D}{S^t} \quad (4.21a)$$

and

$$f_b = -\frac{P_e}{A_c} \left( 1 + \frac{ec_b}{r^2} \right) + \frac{M_D}{S_b} \quad (4.21b)$$

After the top slab is situ cast and full composite action is developed when the concrete hardens, Equations 4.19a and b become, for the beam shored after erection,

$$f^t = -\frac{P_e}{A_c} \left( 1 - \frac{ec_t}{r^2} \right) - \frac{M_D}{S^t} - \frac{M_{SD} + M_{CSD} + M_L}{S_c^t} \quad (4.22a)$$

and

$$f_b = -\frac{P_e}{A_c} \left( 1 + \frac{ec_b}{r^2} \right) + \frac{M_D}{S_b} + \frac{M_{SD} + M_{CSD} + M_L}{S_{cb}^b} \quad (4.22b)$$

Note that adequate check has to be made for the horizontal interface shear stresses between the situ-cast and the precast beams, as will be discussed in Chapter 5.

#### 4.6.3 Effective Flange Width

In order to determine the theoretical composite action that resists the flexural stresses, a determination has to be made of the slab width that can effectively contribute to the stiffness increase resulting from composite action.

Figure 4.33 and Table 4.6 give the ACI and AASHTO requirements for determining the effective top flange width of the composite section. If the topping concrete is of different strength than that of the precast section, the width  $b$  has to be modified to account for the difference in the moduli of the two concretes in order to ensure that the strains in both materials at the interface are compatible. The modified width of the composite topping for calculating the composite  $I_{cc}$  is

$$b_m = \frac{E_{ct}}{E_c} (b) = n_c b \quad (4.23)$$

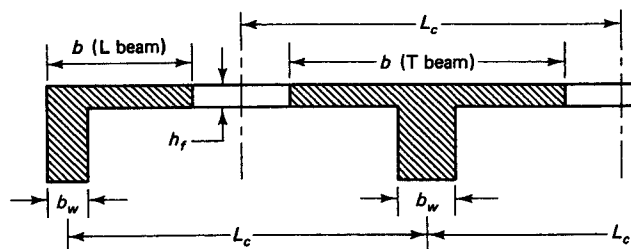


Figure 4.33 Effective flange width of composite section.

**Table 4.6** Values of Effective Flange Width

<b>Width <math>b</math> as the least of the tabulated values (Modify to <math>b_M = n_c b</math>, where <math>n_c = E_{ct}/E_c</math> when flange concrete is of different strength from that of the precast web)</b>		
	<b>End beam</b>	<b>Intermediate beam</b>
ACI	$b_w + 6h_f$	$b_w + 16h_f$
	$b_w + \frac{1}{2}L_c$	$b_w + L_c$
	$b_w + \frac{L}{12}$	$\frac{L}{4}$
AASHTO	$b_w + 6h_f$	$b_w + 12h_f$
	$b_w + \frac{1}{2}L_c$	$b_w + L_c$
	$b_w + \frac{L}{12}$	$\frac{L}{4}$

$L$  = span of end or intermediate beam

where  $E_{ct}$  = modulus of the topping concrete  
 $E_c$  = modulus of the precast concrete

Once the modified width  $b_m$  is defined, the entire composite section is considered to be of the higher strength concrete.

#### 4.7 SUMMARY OF STEP-BY-STEP TRIAL-AND-ADJUSTMENT PROCEDURE FOR THE SERVICE-LOAD DESIGN OF PRESTRESSED MEMBERS

1. Given the superimposed dead-load intensity  $W_{SD}$ , the live-load intensity  $W_L$ , the span and the height limitation, the material strengths  $f_{pu}$ ,  $f'_c$ , the type of concrete, and whether the prestress type is pretensioning or post-tensioning,
2. Assume the intensity of self-weight  $W_D$ , and calculate moments  $M_D$ ,  $M_{SD}$ , and  $M_L$ .
3. Calculate  $f_{pi}$ ,  $f'_{ci}$ ,  $f_{ti}$ ,  $f_t$  and  $f_c$ , where  $f_{pi} = 0.70 f_{pu}$ ,  $f_{ci} = 0.60 f'_{ci}$ , and  $f_{ti} = 3\sqrt{f'_{ci}}$ , for the midspan section,  $f_c = 0.45 f'_c$  or  $0.60 f'_c$  as allowed and  $f_t = 6\sqrt{f'_c}$  to  $12\sqrt{f'_c}$ .
4. Calculate the prestress losses  $\Delta f_{pT} = \Delta f_{pES} + \Delta f_{pR} + \Delta f_{pSH} + \Delta f_{pCR} + \Delta f_{pE} + \Delta f_{pA} + \Delta f_{pB}$  for the type of prestressing used. Determine net stresses  $f_{pe} = f_{pi} - \Delta f_{pT}$ .
5. Find the minimum required section modulus of the minimum efficient section for evaluating the concrete fiber stresses at the top and bottom fibers.
  - (a) For harped or draped tendons, use the midspan controlling section:

$$S^t \geq \frac{(1 - \gamma)M_D + M_{SD} + M_L}{\gamma f_{ti} - f_c}$$

$$S_b \geq \frac{(1 - \gamma)M_D + M_{SD} + M_L}{f_t - \gamma f_{ci}}$$

where

$$\gamma = \frac{P_e}{P_i}$$

- (b) For straight tendons, use the end-support controlling section:

$$S^t \geq \frac{M_D + M_{SD} + M_L}{\gamma f_u - f_c}$$

$$S_b \geq \frac{M_D + M_{SD} + M_L}{f_t - \gamma f_{ci}}$$

6. Select a trial section with section modulus properties close to those required in step 5 to be checked later for composite section fiber stress requirements.
7. For (a) the controlling section in the span (usually the midspan or at 0.4 of span), (b) the controlling section at the support, and (c) any other section along the span if both straight and draped tendons are used, analyze the concrete fiber stresses expected at stress transfer immediately before such transfer:

$$f^t = -\frac{P_i}{A_c} \left( 1 - \frac{ec_t}{r^2} \right) - \frac{M_D}{S^t}$$

$$f_b = -\frac{P_i}{A_c} \left( 1 + \frac{ec_b}{r^2} \right) + \frac{M_D}{S_b}$$

If the stresses exceed the allowable values, enlarge the section, or change the eccentricity  $e_c$  or  $e_e$ , or both.

8. Analyze the concrete fiber stresses for the service-load conditions, as in step 7:

$$f^t = -\frac{P_e}{A_c} \left( 1 - \frac{ec_t}{r^2} \right) - \frac{M_T}{S^t}$$

$$f_b = -\frac{P_e}{A_c} \left( 1 + \frac{ec_b}{r^2} \right) + \frac{M_T}{S_b}$$

where  $M_T = M_D + M_{SD} + M_L$ . If the stresses exceed the allowable values, enlarge the section or change the eccentricity  $e_c$  or  $e_e$ , or both.

9. For cases where many strands have to be used, establish the envelopes of limiting eccentricities for zero tension  $e_b = (k_b + a_{\min})$  and  $e_t = (a_{\max} - k_t)$ , where  $a_{\min} = M_D/P_i$  and  $a_{\max} = M_T/P_e$ . If the tension in the concrete is used in the design, add

$$e'_b = \frac{f^{(t)} A_c k_b}{P_i}$$

and

$$e'_t = \frac{f_{(b)} A_c k_t}{P_e}$$

to the bottom and top envelopes, respectively, where  $f^{(t)}$  and  $f_{(b)}$  are the extreme fiber stresses calculated to be in the concrete.

10. Investigate the end-block anchorage zone stresses, and design the necessary reinforcement to prevent bursting or spalling cracks. Determine the minimum development length

$$l_d = \frac{1}{1,000} \left( f_{ps} - \frac{2}{3} f_{pe} \right) d_b$$

of which the transfer length  $l_t = \frac{f_{pe}}{3,000} d_b$ , where  $f_{pe}$  is in psi units.

**Post-tensioned Anchorage**

Design the anchorage block reinforcement. Use the strut-and-tie plastic truss units to compute the ultimate tension force in the tie for confining reinforcement selection.

**Pretensional Prestress Transfer Zone**

$$A_t = 0.021 \frac{P_t h}{f_s l_t}$$

11. Determine the composite action stresses, and revise the section if these stresses exceed the maximum allowable concrete fiber stresses both in the precast section and the situ-cast top slab. Use the modified effective width  $b_m = (E_{ct}/E_c)b$  for the top composite flange when calculating the section modulus of the composite section.

(a) **Unshored Slab Case.** Before the top slab is situ cast:

$$f^t = -\frac{P_e}{A_c} \left( 1 - \frac{ec_t}{r^2} \right) - \frac{M_D + M_{SD}}{S^t}$$

$$f_b = -\frac{P_e}{A_c} \left( 1 + \frac{ec_b}{r^2} \right) + \frac{M_D + M_{SD}}{S_b}$$

After the top slab is cast and cured to develop full composite action, the stresses at top and bottom fibers of the *precast* part of the composite section will be

$$f^t = -\frac{P_e}{A_c} \left( 1 - \frac{ec_t}{r^2} \right) - \frac{M_D + M_{SD}}{S^t} - \frac{M_{CSD} + M_L}{S_c^t}$$

$$f_b = -\frac{P_e}{A_c} \left( 1 + \frac{ec_b}{r^2} \right) + \frac{M_D + M_{SD}}{S_b} + \frac{M_{CSD} + M_L}{S_{cb}}$$

where  $S_c^t$  and  $S_{cb}$  are the section moduli of the composite section at the level of the top and bottom fibers of the precast section. Also,  $M_L$  includes  $M_I$  if impact stresses exist.

The fibers stresses at the level of the top and bottom fibers of the situ-cast hardened slab are

$$f^{ts} = -\frac{M_{CSD} + M_L}{S_{cs}^t}$$

$$f_{bs} = -\frac{M_{CSD} + M_L}{S_{csb}}$$

where  $S_{cs}^t$  and  $S_{csb}$  are the section moduli of the composite section at the level of the top and bottom of the situ-cast slab.

(b) **Fully Shored Slab Case.** Before shoring, and before the topping is situ-cast,

$$f^t = -\frac{P_e}{A_c} \left( 1 - \frac{ec_t}{r^2} \right) - \frac{M_D}{S^t}$$

$$f_b = -\frac{P_e}{A_c} \left( 1 + \frac{ec_b}{r^2} \right) + \frac{M_D}{S_b}$$

After the situ-cast slab is cured and *full composite action develops*,

$$f_t = -\frac{P_e}{A_c} \left( 1 - \frac{ec_t}{r^2} \right) - \frac{M_D}{S^t} - \frac{M_{SD} + M_{CSD} + M_L}{S_c^t}$$

$$f_b = -\frac{P_e}{A_c} \left( 1 + \frac{ec_b}{r^2} \right) + \frac{M_D}{S_c} + \frac{M_{SD} + M_{CSD} + M_L}{S_{cb}}$$

The effective width of the top flange of the composite section is determined in accordance with the applicable ACI or AASHTO specifications.

$M_D$  = moment due to self-weight of the precast element,  $M_{SD}$  = moment due to situ-cast slab and any other construction load, and  $M_{CSD}$  = moment due to additional composite superimposed load.

12. Proceed to determine the strength of the section for the limit state at failure and for shear and torsional strength.

Figure 4.34 shows a flowchart for the service-load flexural design of prestressed beams.

## 4.8 DESIGN OF COMPOSITE POST-TENSIONED PRESTRESSED SIMPLY SUPPORTED SECTION

### Example 4.7

A two-lane simply supported bridge has a 64 ft (19.5 m) span, center to center, of bearings. The width of the bridge is such that the exterior beams are 28 ft (8.54 m) center to center. The spacing of the interior beams is at 7 ft center to center. Design the supporting interior post-tensioned beams, with deck slab *unshored* during construction, to carry

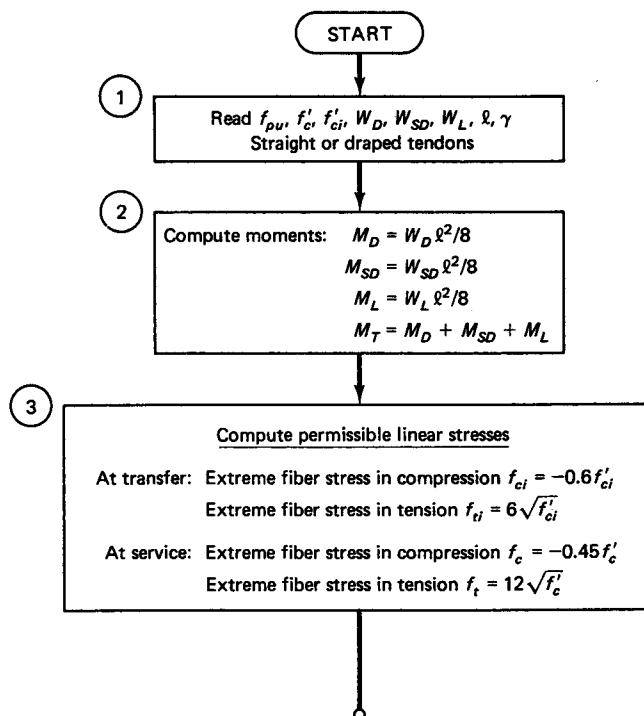


Figure 4.34 Flowchart for service-load flexural design of prestressed beams.



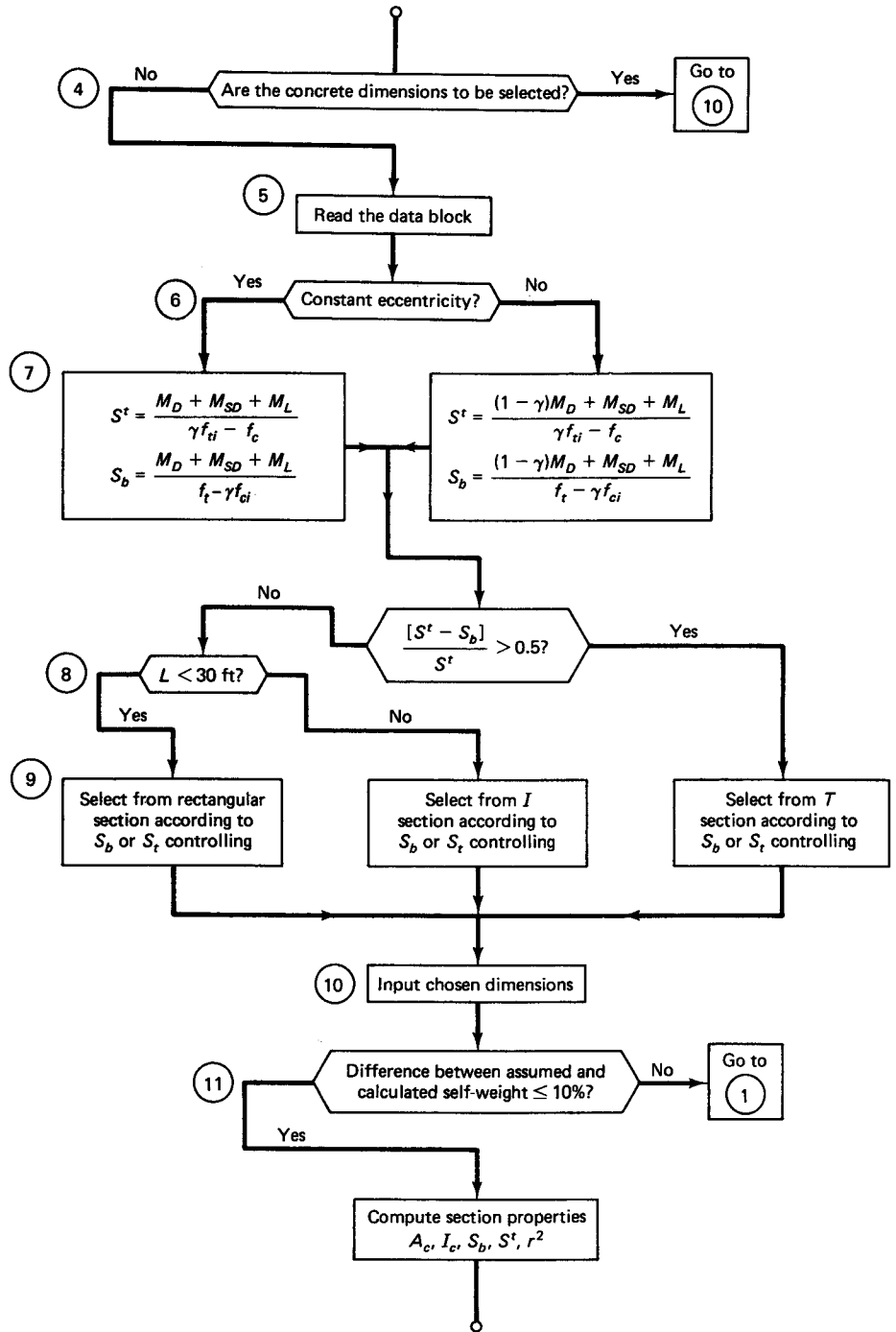


Figure 4.34 (continued)

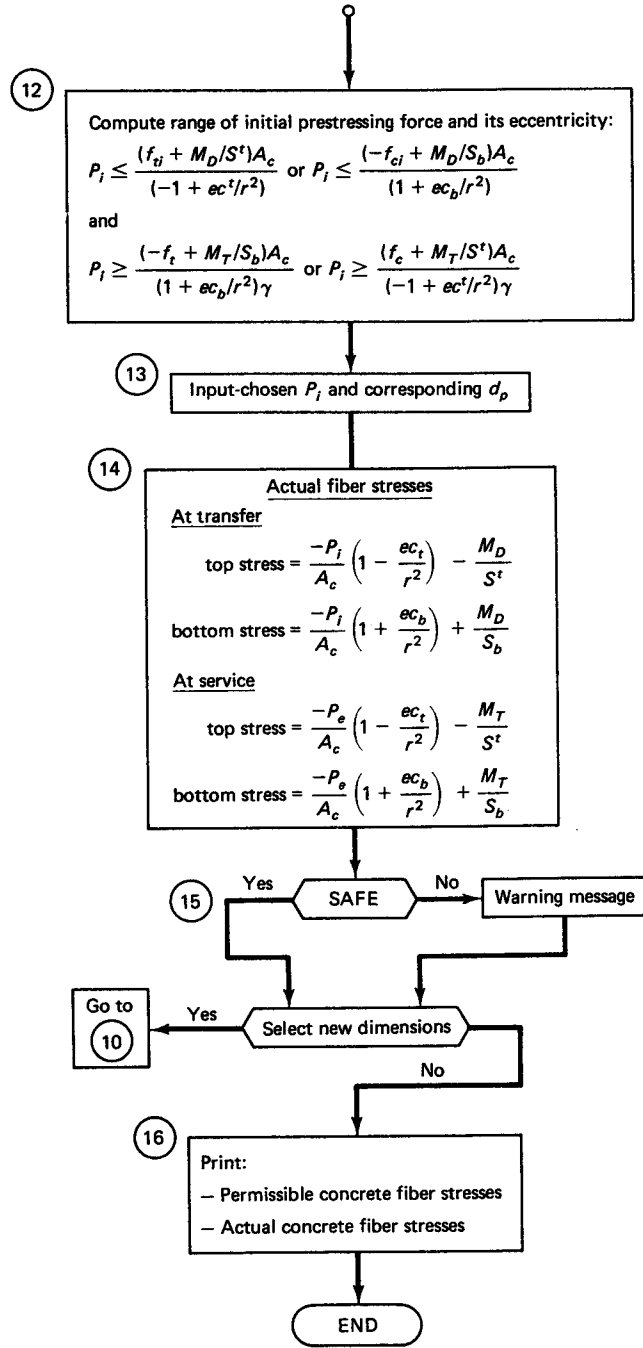


Figure 4.34 (continued)



**Photo 4.10** Photo layout of bridge deck prestressing tendon.

AASHTO HS20-44 loading; establish the tendon eccentricities and tendon envelopes; and design the anchorage block and reinforcement, given the following information:

#### Concrete

Precast beam  $f'_c = 5,000$  psi normal-weight concrete

$5\frac{3}{4}$  in. deck  $f'_c = 3,000$  psi normal-weight concrete

$$f'_{ci} = 4,000 \text{ psi (27.6 MPa)}$$

$$f_{ci} = 0.55f'_{ci} = -2,200 \text{ psi (15.2 MPa)}$$

$$f_c = 0.40f'_c = -2,000 \text{ psi (13.8 MPa)}$$

$$f_{ii} = 212 \text{ psi} = 3\sqrt{f'_c}$$

$$f_t = 6\sqrt{f'_c} = 424 \text{ psi}$$

#### Prestressing Steel

$$f_{pu} = 270,000 \text{ psi (1,862 MPa)}$$

$$f_{py} = 0.90f_{pu} = 243,000 \text{ psi (1,675 MPa)}$$

$$f_{pi} = 0.70f_{pu} = 189,000 \text{ psi (1,303 MPa)}$$

$$f_{pe} \text{ after losses} = 0.80f_{pi} = 151,200 \text{ psi (1,043 MPa)}$$

Locate and draw the distribution of tendons in both the midspan and end sections. Use a live-load moment value including impact due to AASHTO HS20-44 loading for one interior beam of the 64 ft span bridge = 9,300,000 in.-lb (1,051 kN-m).

#### Solution:

**Bending Moments and New Allowable Stresses (Steps 1–4).** Since the beam spacing and span length are known, the moments due to situ-cast slab and diaphragms can be initially determined. The clear distance between the webs of the beams is 7 ft, 0 in. – 6 in. = 6 ft, 6 in. Assume a deck slab  $5\frac{3}{4}$  in. (14.6 cm) thick made of  $1\frac{3}{4}$  in. precast panels and 4 in. situ-cast topping and a diaphragm 8 in. (20 cm) thick at midspan and 45 in. (122 cm) deep, cast integrally with the deck slab. We have:

$$\text{Diaphragm weight} = \frac{8}{12} \times \frac{45}{12} \times 6.5 \times 150 = 2,440 \text{ lb (11.3 kN)}$$

$$1\frac{3}{4} \text{ in. precast formwork panel weight} = \frac{1.75}{12} \times 7 \times 150 = 153 \text{ plf (2.2 kN/m)}$$

$$4 \text{ in. situ-cast topping weight} = \frac{4}{12} \times 7 \times 150 = 350 \text{ plf (5.1 kN/m)}$$

$$M_{SD1} = \frac{153(64)^2}{8} \times 12 = 940,032 \text{ in.-lb}$$

$$M_{CSD} = \text{composite superimposed dead load} = 0$$

$$\begin{aligned} M_{SD2} &= \frac{PL}{4} + \frac{W_{SD}L^2}{8} \\ &= \frac{2,440(64 \times 12)}{4} + \frac{350(64)^2(12)}{8} \\ &= 468,480 + 2,150,400 = 2,618,880 \text{ in.-lb} \end{aligned}$$

$$\text{Total } M_{SD} = 940,032 + 2,618,880 = 3,558,912 \text{ in.-lb (403 kN-m)}$$

$$M_{CSD} = 0 \text{ in this case}$$

#### Minimum Section Moduli and Choice of Trial Section (Steps 5–6)

$$\gamma = \frac{151,200}{189,000} = 0.80$$

$$S' \geq \frac{(1 - \gamma)M_D + M_{SD} + M_L}{\gamma f_{ti} - f_c}$$

$$S_b \geq \frac{(1 - \gamma)M_D + M_{SD} + M_L}{f_t - \gamma f_{ci}}$$

Assume that the self-weight of the precast beam element is approximately 583 plf (8.5 kN/m). Then

$$M_D = \frac{583(64)^2 \times 12}{8} = 3,581,952 \text{ in.-lb (405 kN-m)}$$

$$\text{Min } S' = \frac{(1 - 0.80)3,581,952 + 3,558,912 + 9,300,000}{0.80(212) - (-2,000)} = 6,257 \text{ in.}^3 (102,535 \text{ cm}^3)$$

$$\text{Min } S_b = \frac{(1 - 0.80)3,581,952 + 3,558,912 + 9,300,000}{424 - 0.80(-2,200)} = 6,215 \text{ in.}^3 (101,846 \text{ cm}^3)$$

The expected actual section modulus for the top fibers is usually considerably larger than the section modulus for the bottom fibers of the composite section. So choose the precast element based on  $S_b = 6,215 \text{ in.}^3$ .

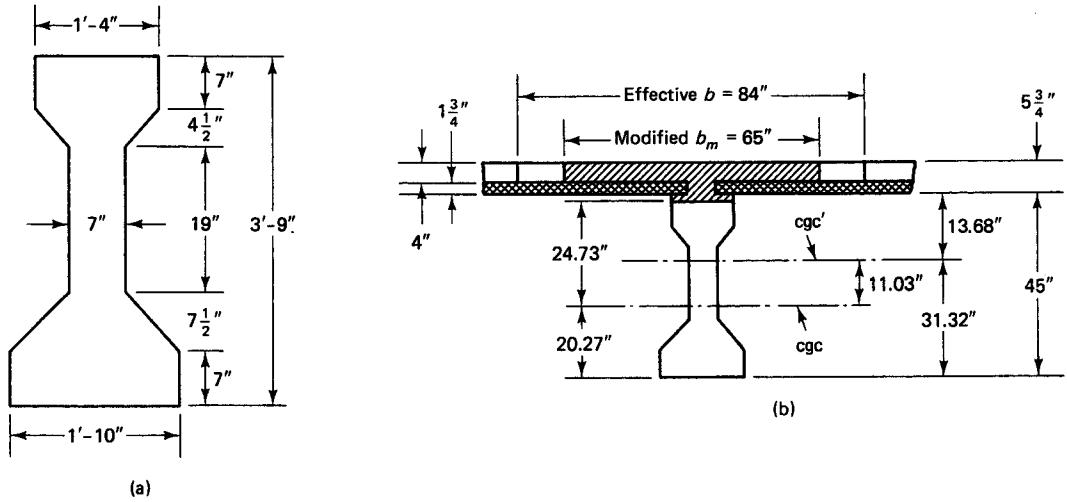
AASHTO type III is chosen as the closest trial section for  $S_b = 6,215 \text{ in.}^3$  since AASHTO type IV has a much larger section modulus. We have as in Figure 4.35.

$$S' = 5,070 \text{ in.}^3 (83,082 \text{ cm}^3)$$

$$S_b = 6,186 \text{ in.}^3 (101,370 \text{ cm}^3)$$

$$I_c = 125,390 \text{ in.}^4 (5.2 \times 10^6 \text{ cm}^4)$$

$$A_c = 560 \text{ in.}^2 (3,613 \text{ cm}^2)$$



**Figure 4.35** Example 4.7. (a) Section (AASHTO-III). (b) Composite section properties.

$$r^2 = 223.9 \text{ in.}^2 (1,445 \text{ cm}^2)$$

$$c_t = 24.73 \text{ in. (62.8 cm)}$$

$$c_b = 20.27 \text{ in. (51.5 cm)}$$

$$W_D = 583 \text{ plf (8.2 kN/m)}$$

Try  $A_{ps}$  = twenty-two  $\frac{1}{2}$ -in. dia (12.7 mm) 7-wire stress-relieved strands.

#### Stresses at Transfer

$$M_T = 3,581,952 + 3,589,632 + 9,300,000 = 16,471,584 \text{ in.-lb (1,861 kN-m)}$$

$$A_{ps} = 22 \times 0.153 = 3.366 \text{ in.}^2 = (21.7 \text{ cm}^2)$$

$$P_i = A_{ps} f_{pi} = 3.366 \times 0.70 \times 270,000 = 636,174 \text{ lb (2,830 kN)}$$

$$P_e = 0.80 P_i = 0.80 \times 636,174 = 508,940 \text{ lb (2,264 kN)}$$

$$k_t = \frac{r^2}{c_b} = \frac{223.91}{20.27} = 11.05 \text{ in. (28.1 cm)}$$

$$k_b = \frac{r^2}{c_t} = \frac{223.91}{24.73} = 9.05 \text{ in. (23.0 cm)}$$

$$a_{\min} = \frac{M_D}{P_i} = \frac{3,581,952}{636,174} = 5.63 \text{ in.}$$

$$a_{\max} = \frac{M_T}{P_e} = \frac{16,471,584}{508,940} = 32.36 \text{ in. (Upper envelope, outside section, hence section can be improved)}$$

$$e_b = a_{\min} + k_b = 5.63 + 9.05 = 14.68 \text{ in.}$$

$$e_t = a_{\max} - k_t = 32.36 - 11.05 = 21.31 \text{ in.}$$

$e'_b = f' A_c K_b / P_i = 212 \times 560 \times 9.05 / 636,174 = 1.69 \text{ in.}$ , giving a maximum  $e_c$  with tension =  $14.69 + 1.69 = 16.37 \text{ in.}$

Using 4 in. cover gives  $e_c = c_b - 4.0 = 20.27 - 4.0 = 16.27 < 16.37 \text{ in.}$ , hence O.K. as the tendon is within the band.

$$\text{Try } e_c = 16.27 \text{ in. (413 mm)} \quad e_e = 10 \text{ in. (254 mm)}$$

**(a) Midspan Section**

$$\begin{aligned}
 f^t &= -\frac{P_i}{A_c} \left( 1 - \frac{e_c c_t}{r^2} \right) - \frac{M_D}{S^t} \\
 &= -\frac{636,174}{560} \left( 1 - \frac{16.27 \times 24.73}{223.91} \right) - \frac{3,581,952}{5,070} \\
 &= 905.4 - 706.5 = 198.9 \text{ psi (T)} < 212 \text{ psi, O.K.} \\
 f_b &= -\frac{P_i}{A_c} \left( 1 + \frac{e_c c_b}{r^2} \right) + \frac{M_D}{S_b} \\
 &= -\frac{636,174}{560} \left( 1 + \frac{16.27 \times 20.27}{223.91} \right) + \frac{3,581,952}{6,186} \\
 &= -2,809.3 + 579.0 = -2,230.3 \text{ (C)} (15.4 \text{ MPa}) \cong f_{ci} = -2,200 \text{ psi, O.K.}
 \end{aligned}$$

**(b) Support Section**

$$\begin{aligned}
 f^t &= -\frac{P_i}{A_c} \left( 1 - \frac{e_c c_t}{r^2} \right) = -\frac{636,174}{560} \left( 1 - \frac{10 \times 24.73}{223.91} \right) \\
 &= +118.7 \text{ psi (T)} < 212 \text{ psi, O.K.} \\
 f_b &= -\frac{P_i}{A_c} \left( 1 + \frac{e_c c_b}{r^2} \right) = -\frac{636,174}{560} \left( 1 + \frac{10 \times 20.27}{223.9} \right) \\
 &= -2,164.4 \text{ psi (C)} < -2,200 \text{ psi, O.K.}
 \end{aligned}$$

**Composite Section Properties**

$$\frac{E_c(\text{topping})}{E_c(\text{precast})} = \frac{57,000 \sqrt{3,000}}{57,000 \sqrt{5,000}} = 0.77$$

$$\text{Effective flange width} = 7 \text{ ft} = 84 \text{ in. (213 cm)}$$

$$\text{Modified effective flange width} = 0.77 \times 84 = 65 \text{ in. (165 cm)}$$

$$c_b = \frac{(5.75 \times 65)(47.875) + (560 \times 20.27)}{(5.75)(65) + 560} = 31.32 \text{ in.}$$

$$I'_c = 125,390 + 560(31.32 - 20.27)^2 + \frac{65(5.75)^3}{12} + 65 \times 5.75(16.56)^2$$

$$= 297,044 \text{ in.}^4$$

$$r^2 = 318.12 \text{ in.}^2$$

$$S_{cb} = 9,490 \text{ in.}^3$$

$$S'_c = 21,714 \text{ in.}^3 \text{ at top of precast section}$$

$$\text{Precast } c^t = 45 - 31.32 = 13.68 \text{ in.}$$

$$S'_c = \frac{297,044}{13.68} = 21,714 \text{ in.}^3$$

$$\text{slab top } c^t = 13.68 + 5.75 = 19.43 \text{ in.}$$

$$S'_{cs} = \frac{297,044}{19.43} = 15,288 \text{ in.}^3 \text{ at top of slab}$$

$$S_{bcs} = \frac{297,044}{(19.43 - 4)} = 19,251 \text{ in.}^3 \text{ at bottom of slab}$$

**Stresses After 1½ In. Precast Panel Is Erected As Formwork,  $M_D + M_{SD}$  (Step 11a) Before Diaphragm and Slab Are Cast,**

(a) Midspan Section

$$f^t = -\frac{P_e}{A_c} \left( 1 - \frac{e_c c_t}{r^2} \right) - \frac{M_D + M_{SD}}{S^t}$$

$$M_D + M_{SD} = 3,581,952 + 940,032 = 4,521,984 \text{ in.-lb}$$

$$f^t = -\frac{508,904}{560} \left( 1 - \frac{16.27 \times 24.73}{223.9} \right) - \frac{4,521,984}{5,070}$$

$$= +724.3 - 891.9 = -167.6 \text{ psi (C), no tension, O.K.}$$

$$f_b = -\frac{P_e}{A_c} \left( 1 + \frac{e_c c_b}{r^2} \right) + \frac{M_D + M_{SD}}{S_b}$$

$$= -\frac{508,940}{560} \left( 1 + \frac{16.27 \times 20.27}{223.9} \right) + \frac{4,521,984}{6,186}$$

$$= -2,247.4 + 731.0 = -1,516.4 \text{ psi (C) } < 2,000 \text{ psi, O.K.}$$

(b) Support Section

$$f^t = -\frac{508,940}{560} \left( 1 - \frac{10 \times 24.73}{223.9} \right) = 94.9 \text{ psi (T) } < f_t = 424 \text{ psi, O.K.}$$

$$f_b = -\frac{508,940}{560} \left( 1 + \frac{10 \times 20.27}{223.9} \right) = -1,731.6 \text{ psi (11.9 MPa) (C)}$$

$$< -2,000 \text{ psi, O.K.}$$

**Stresses Immediately After Casting Concrete Slab Topping: Midspan Section (Slab Concrete Not Hardened)**

$$f^t = -\frac{P_e}{A_c} \left( 1 - \frac{e_c c_t}{r^2} \right) - \frac{M_D + M_{SD}}{S^t}$$

$$M_D + M_{SD} = 4,521,984 + 2,649,600 = 7,171,584 \text{ in.-lb}$$

$$f^t = \frac{508,940}{560} \left( 1 - \frac{16.27 \times 24.73}{223.9} \right) - \frac{7,171,584}{5,070}$$

$$= 724.3 - 1,414.5 = -690.2 \text{ psi (C) } < -2,000 \text{ psi, O.K.}$$

$$f_b = -\frac{P_e}{A_c} \left( 1 + \frac{e_c c_b}{r^2} \right) + \frac{M_D + M_{SD}}{S_b}$$

$$= -\frac{508,940}{560} \left( 1 + \frac{16.27 \times 20.27}{223.9} \right) + \frac{7,171,584}{6,186}$$

$$= -2,247.4 + 1,159.3 = -1,088.1 \text{ psi (C)}$$

$$< -2,000 \text{ psi (7.5 MPa } < 13.8 \text{ MPa), O.K.}$$

**Stresses at Service Load (Step 11) Add the Effect of  $M_{SD2}$  Due to Unshored Slab**

(a) Midspan Section

$$f^t = -\frac{P_e}{A_c} \left( 1 - \frac{e_c c_t}{r^2} \right) - \frac{M_D + M_{SD}}{S^t} - \frac{M_{CSD} + M_L}{S_c^t}$$

$$M_D + M_{SD} = 7,171,584 \text{ in.-lb}$$

$$M_{CSD} + M_L = 0 + 9,300,000 = 9,300,000$$

From the previous stage,  $f^t = -690.2$  psi (C),  $f_b = -1088.1$  psi (C). Stress at top fibers of precast section in composite action is

$$f_c^t = -690.2 - \frac{9,300,000}{21,714} = -690.2 - 428.3 = -1,118.5 \text{ psi (C)} < -2000 \text{ psi, O.K.}$$

$$f_{bc} = -1088.1 + \frac{9,300,000}{9,492} = -1088.1 + 979.8 = -108.3 \text{ psi (C)}$$

Modular ratio  $n = 0.77$  from before. Stress at top fibers of slab after concrete hardened is

$$f_{cs}^t = -\frac{9,300,000}{15,288} \times 0.77 = -468 \text{ psi (C)}$$

stress at bottom fibers of the slab is

$$f_{bcs} = -\frac{9,300,000}{19,251} \times 0.77 = -372 \text{ psi (C)}$$

- (b) *Support Section.* Same kind of calculations as in previous step. Result is  $f^t = +94.9$  psi (T) and  $f_b = -1,731.6$  psi (C).

#### **Tendon Envelope**

- (a) *Midspan Section*

$$a_{\max} = 32.36 \text{ in.}$$

$$a_{\min} = 5.63 \text{ in.}$$

- (b) *Quarter Section*

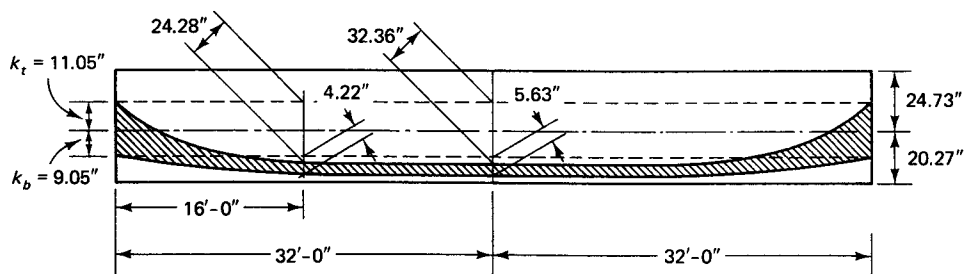
$$M_D = 2,686,464$$

$$a_{\min} = \frac{M_D}{P_i} = 4.22 \text{ in.}$$

$$M_T = 12,355,248$$

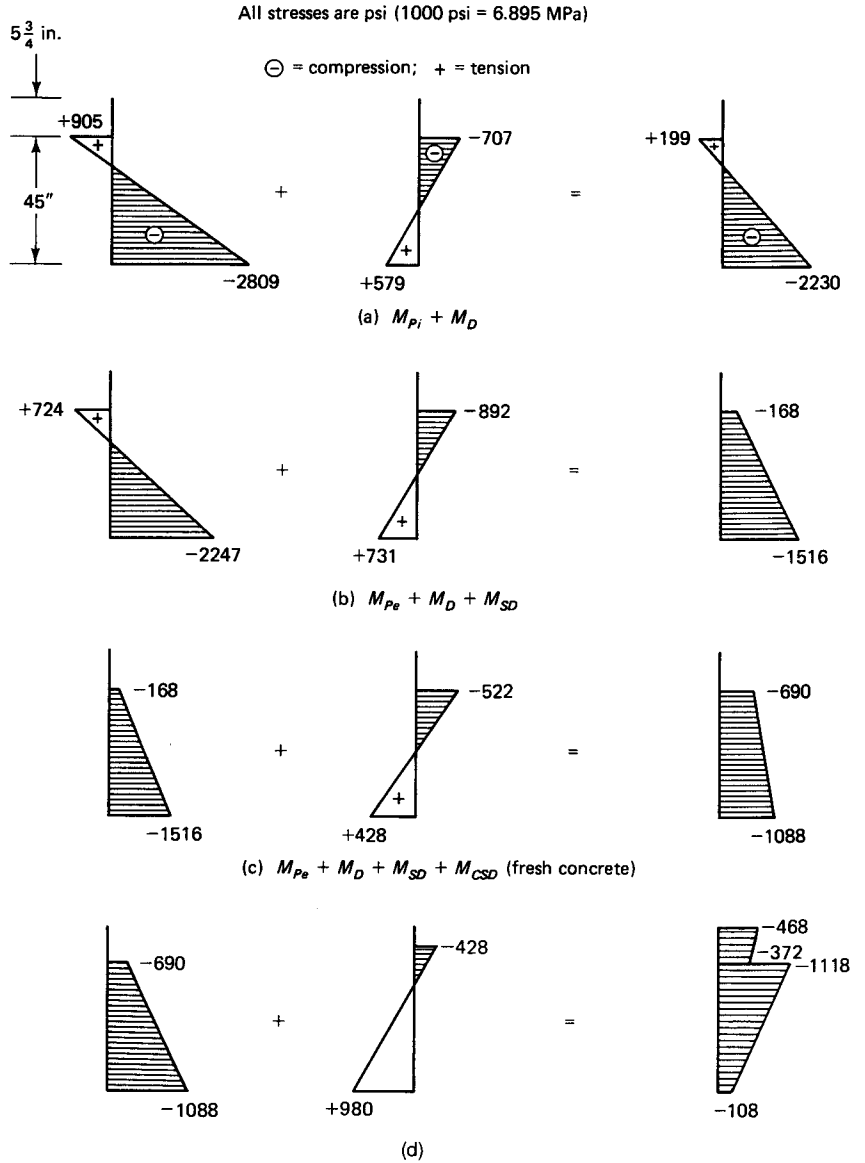
$$a_{\max} = \frac{M_T}{P_e} = 24.28 \text{ in.}$$

See Figure 4.36 for the tendon envelope and Figure 4.37 for the stress distribution. Figure 4.38 gives the anchorage zone stresses and the net moments along the depth of the beam.



**Figure 4.36** Prestressing tendon envelope.





**Figure 4.37** Midspan concrete fiber stresses in Example 4.7. (a) Transfer. (b) Erection. (c) Topping cast. (d) Service-load stage.

**Design of End-Block Anchorage**

(a) *Solution by Linear Elastic Method:*

$$P_i = 636,174 \text{ lb}$$

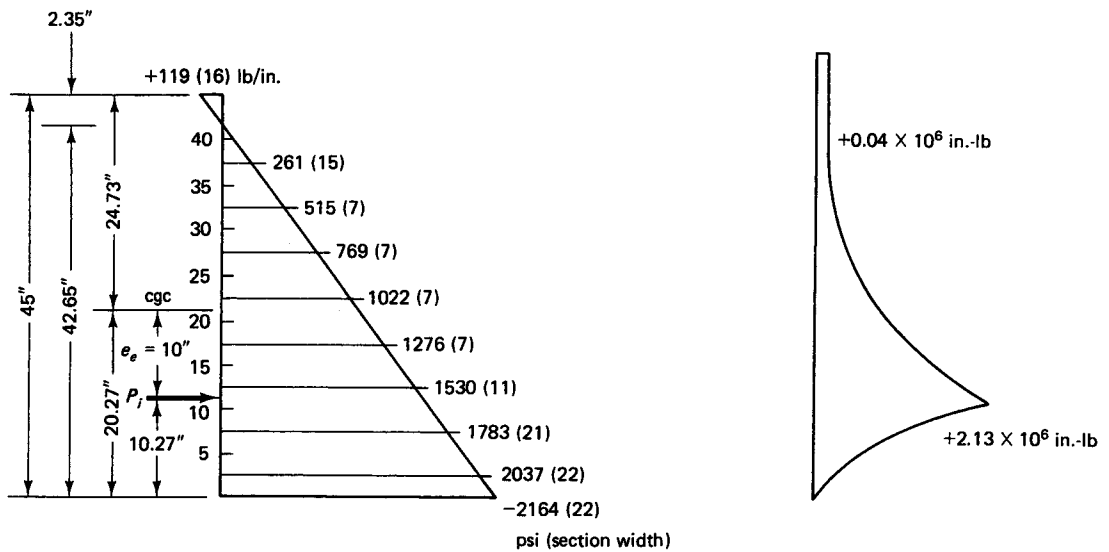
$$e_e = 10 \text{ in.}$$

$$f^t = +119 \text{ psi (T)}$$

$$f_b = -2,164 \text{ psi (C)}$$

(i) *Bursting Crack Reinforcement*

$$h = 45 \text{ in.}$$



**Figure 4.38** Anchorage zone elastic stresses and net moments in Example 4.7. (a) Anchorage zone stresses. Bracketed values are section widths (in.) along which anchorage stresses are acting. (b) Net bursting or splitting moments ( $M_p - M_o$ ) at 5-in. depth intervals.

Use

$$x = h/3 = 15 \text{ in.}$$

$$T_b = \frac{M_{\max}}{h - x} = \frac{2.15 \times 10^6}{45 - 15} = 71,670 \text{ lb (316 kN)}$$

$$A_s = \frac{T_b}{f_s} = \frac{71,670}{20,000} = 3.58 \text{ in}^2 (23.1 \text{ cm}^2)$$

(ii) *Spalling Crack Reinforcement*

$$T_{sp} = \frac{M_{\min}}{h - x} = \frac{+0.04 \times 10^6}{45 - 15} = 1,330$$

$$A_s = \frac{T_{sp}}{20,000} = \frac{1,330}{20,000} = 0.07 \text{ in}^2$$

$$\text{Total reinforcement} = 3.58 + 0.07 = 3.65 \text{ in}^2 (23.5 \text{ cm}^2)$$

Try #4 vertical reinforcement (12.7 mm dia.):

$$\text{Number required} = \frac{3.65}{0.20 \times 2} = 9.13$$

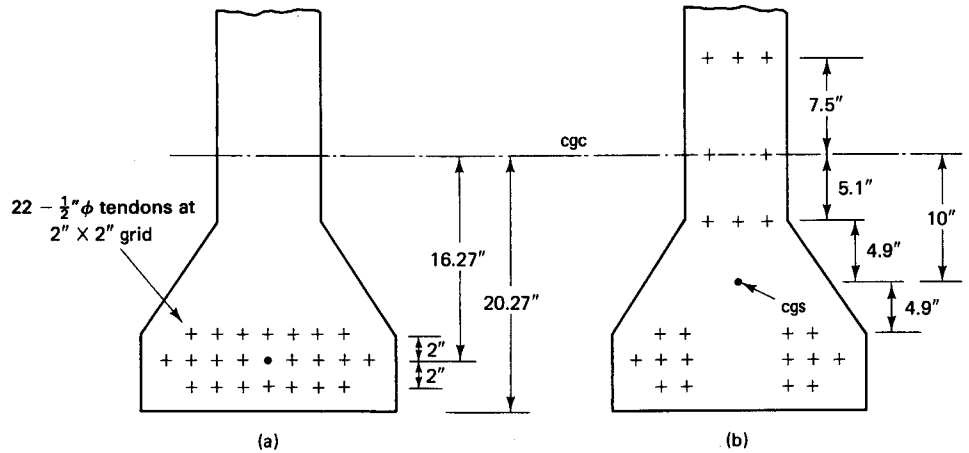
**Arrangement of Strands.** Use a 2 in.  $\times$  2 in. (25 mm  $\times$  25 mm) grid for arranging the distribution of strands. Eccentricities are:

$$e_c = 16.27 \text{ in. (41.3 cm)}$$

$$e_e = 10.0 \text{ in. (25.4 cm)}$$

The arrangement of the strands to develop the required tendon eccentricities are shown in Fig. 4.39(a).

The anchorage zone moments at the various planes at 5-in. intervals along the height of the section are given in Table 4.7.



**Figure 4.39(a)** Strand arrangement in Example 4.7. (a) Midspan ( $e_c = 16.27$  in.). (b) End section ( $e_e = 10.0$  in.).

**(b) Solution by the Plastic Strut-and-Tie Method:**

(1) compute distance of the centroid of strands:

$$= \frac{4(2) + 6(4) + 4(6) + 3(15.8) + 2(20.27) + 3(27.77)}{22} = 10.33 \text{ in.}$$

which is close to  $e_c = 10$  in. used in the design.

(2) determine concrete bearing capacity at the anchorage devices plane:

From Equation (4.15c),  $P_{su} = 1.2 A_{ps} (0.80 f_{pu}) = 1.2 A_{ps} (0.80 \times 270,000) = 259,200 A_{ps}$  lb

row forces:  $P_{u1}, P_{u3} = 4(0.153)(259,200) = 158,630$  lb

$P_{u2} = 6(0.153)(259,200) = 237,936$  lb

**Table 4.7** Anchorage Zone Moments for Example 4.7

Moment plane dist. $d$ from bottom (in.)	Section width (in.)	Stress at plane ( $d - 2.5$ ) (psi)	Concrete resist. force at ( $d - 2.5$ ) (lb)	Moment $M_p$ of force $P_i$ about horiz. plane in col. (1) (in.-lb $\times 10^6$ )	Moment $M_c$ of concrete in col. (4) about horiz. plane in col. (1) (in.-lb $\times 10^6$ )	Net moment ( $M_c - M_p$ ) col. (6) - col. (5) (in.-lb $\times 10^6$ )
(1)	(2)	(3)	(4)	(5)	(6)	(7)
0	22	-2,164	0	0	0	0
5	22	-2,037	237,040	0	+0.56	+0.56
10.27	15	-1,783	133,725	0	+2.15	+2.15
15	7	-1,530	53,550	-3.01	+4.42	+1.41
20	7	-1,276	44,660	-6.19	+7.00	+0.81
25	7	-1,022	35,770	-9.37	+9.80	+0.43
30	7	-769	26,915	-12.55	+12.76	+0.19
35	12	-515	25,750	-15.73	+15.80	+0.07
40	16	-216	20,880	-18.91	+18.95	+0.04
45	16	+119	+9,520	-22.09	+22.15	+0.06

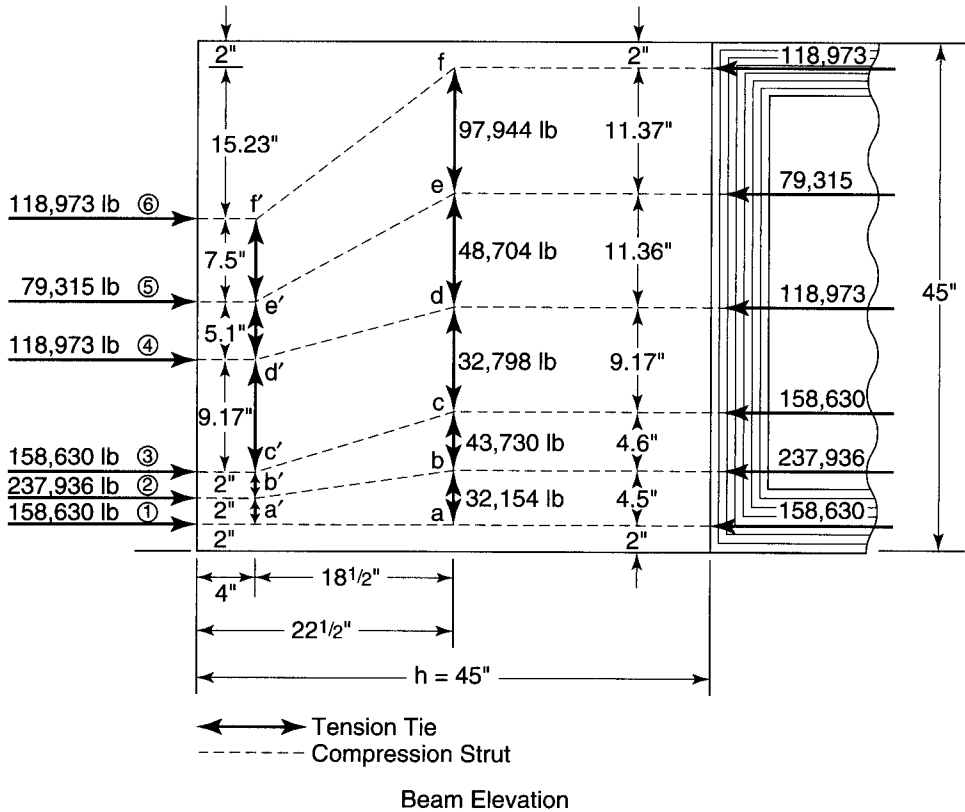


Figure 4.39(b) Strut-and-Tie Forces in Example 4.7.

$$P_{u4}, P_{u6} = 3(0.153)(259,200) = 118,973 \text{ lb}$$

$$P_{u5} = 2(0.153)(259,200) = 79,315 \text{ lb}$$

Total ultimate compressive force =  $2(158,630 + 237,936 + 2(118,973) + 79,315) = 872,457 \text{ lb}$

Total area of rigid bearing plates supporting the anchorage chucks:

$$A_b = 20 \times 12 + 7 \times 16 = 352 \text{ in.}^2$$

$$f_b = \frac{872,457}{352} = 2480 \text{ psi}$$

From Equations 4.16(a) and (b), the maximum allowable bearing pressure on the concrete is

$$f_b \leq 0.7 f'_{ci} \sqrt{A/A_g}$$

$$f_b \leq 2.25 f'_{ci}$$

Assume that the initial concrete strength at stressing is  $f'_{ci} = 0.75 f'_c$

$$= 0.75 \times 5,000 = 3750 \text{ psi}$$

Concentric area,  $A$ , of concrete with the bearing plates  $\cong (20 + 4)(12 + 4) + (7 + 4)(16 + 4) = 604 \text{ in.}^2$ , as defined for the concrete pyramid base in Section 4.5.3.5. Note that the bearings are acting against the rectangular end block section.

$$\text{Allowable bearing stress } f_b = 0.7 \times 3750 \sqrt{\frac{604}{352}} = 3439 \text{ psi.} > 2480 \text{ psi, O.K.}$$

The bearing stress from Eq. 4.14 (b) does not control.

- (3) Draw the strut-and-tie model and select the anchorage reinforcement choose distance  $a$ , as in Figure 4.39(b) between two forces  $P_{u5} - P_{u6} = 7.5$  in.

$$\text{hence, depth } a/2 \text{ ahead of the anchorages} = \frac{7.5}{2} = 3.75 \text{ in., say 4 in.}$$

Construct the strut-and-tie model assuming it to be as shown in Figure 4.39 (b). The tension tie forces range between 32,154 and 97,944 lb. As an example,  $P_{ff}' = 118,973$  (15.23/18.50) = 97,944 lb. Choosing the larger value of 97,944 lb and using No. 3 closed U-stirrups confining reinforcement within the anchorage zone area:

$$\begin{aligned} \text{tensile strength per tie} &= \phi f_y A_v \\ &= 0.90 \times 60,000 \times 2(0.11) = 11,880 \text{ lb} \end{aligned}$$

$$\text{required number of stirrup ties} = \frac{97,944}{11,880} = 8.3, \text{ use nine No. 3 closed U-stirrups}$$

Trying No. 4 closed U-Stirrups in the compression zone adjacent to the anchorage devices plane, the applicable force can also be assumed in this case to be approximately 97,944 lb.

$$\text{Tensile strength of one No. 4 confining tie} = 0.90 \times 60,000 \times 2(0.20) = 21,600 \text{ lb.}$$

$$\text{number of ties} = \frac{97,944}{21,600} = 4.5, \text{ used five No. 4 closed U-stirrups.}$$

Comparing solutions (a) and (b), adopt the following confining reinforcement in the anchorage zone over a distance  $h = 45$  in. from the beam end:

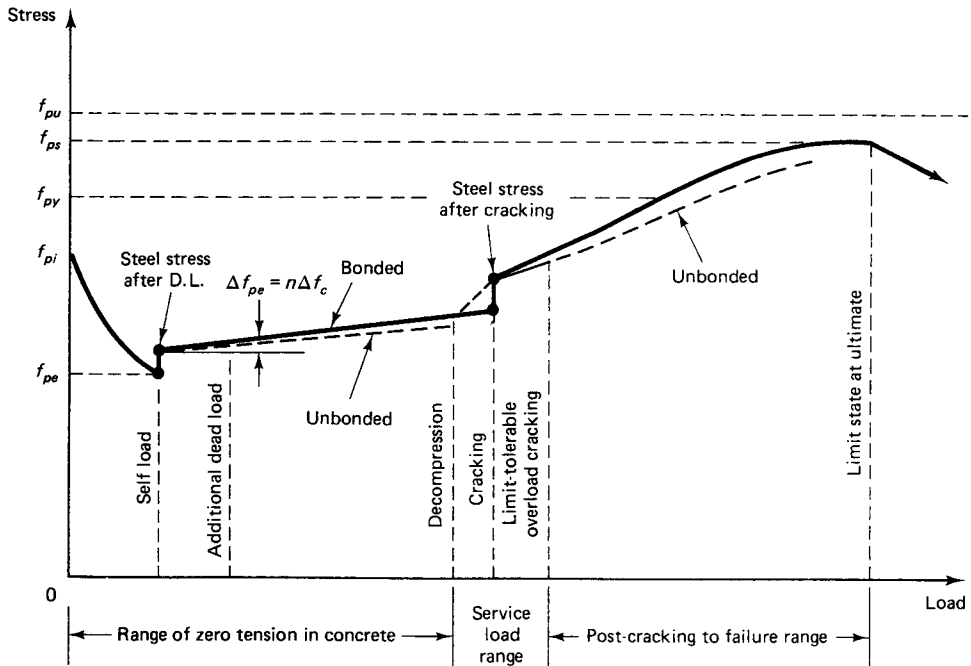
Use five No. 4 closed U-stirrups starting at  $1\frac{1}{2}$  in. from the anchorage devices plane and spaced at  $1\frac{1}{2}$  in. on centers, then continue with the nine stirrups at 5 in. on centers over a distance of 40 in. It should be noted that if a smaller number of path lines are assumed in the idealization of the compression strut paths, the tension tie forces would have been larger resulting in more confining reinforcement.

## 4.9 ULTIMATE-STRENGTH FLEXURAL DESIGN

### 4.9.1 Cracking-Load Moment

As mentioned in Chapter 1, one of the fundamental differences between prestressed and reinforced concrete is the continuous shift in the prestressed beams of the compressive C-line away from the tensile cgs line as the load increases. In other words, the moment arm of the internal couple continues to increase with the load without any appreciable change in the stress  $f_{pe}$  in the prestressing steel. As the flexural moment continues to increase when the full superimposed dead load and live load act, a loading stage is reached where the concrete compressive stress at the bottom-fibers reinforcement level of a simply supported beam becomes zero. This stage of stress is called the limit state of *decompression*: Any additional external load or overload results in cracking at the bottom face, where the modulus of rupture of concrete  $f_r$  is reached due to the cracking moment  $M_{cr}$  caused by the first cracking load. At this stage, a sudden increase in the steel stress takes place and the tension is dynamically transferred from the concrete to the steel.

Figure 4.40 relates load to steel stress at the various loading stages. It shows not only the load-deformation curve, including its abrupt change of slope at the first cracking load, but also the dynamic dislocation in the load-stress diagram at the first cracking load after decompression in a bonded prestressed beam. Beyond that dislocation point the beam can no longer be considered to behave elastically, and the rise in the compressive



**Figure 4.40** Prestressing steel stress at various load levels.

C-line stabilizes and stops so that the section starts to behave like a reinforced concrete section with *constant* moment resistance arm.

It is important to evaluate the first cracking load, since the section stiffness is reduced and hence an increase in deflection has to be considered. Also, the crack width has to be controlled in order to prevent reinforcement corrosion or leakage in liquid containers.

The concrete fiber stress at the tension face is

$$f_b = -\frac{P_e}{A_c} \left( 1 + \frac{ec_b}{r^2} \right) + \frac{M_{cr}}{S_b} = f_r \quad (4.24)$$

where the modulus of rupture  $f_r = 7.5\sqrt{f'_c}$  and the cracking moment  $M_{cr}$  is the moment due to all loads at that load level ( $M_D + M_{SD} + M_L$ ). From Eq. 4.24,

$$M_{cr} = f_r S_b + P_e \left( e + \frac{r^2}{c_b} \right) \quad (4.25)$$

Note that the term  $r^2/c_b$  is the upper kern value  $k_i$  so that  $P_e r^2/c_b$  denotes the elastic moment required to raise the C-line from the prestressing steel level to the upper kern point giving zero tension at the bottom fibers. Consequently, the term  $f_r S_b$  is that additional moment required to cause the development of the first crack at the extreme tension fibers due to overload, such as at the bottom fibers at midspan of a simply supported beam.

### 4.9.2 Partial Prestressing

“Partial prestressing” is a controversial term, since it is *not* intended to denote that a beam is prestressed partially, as might seem to be the case. Rather, partial prestressing describes prestressed beams wherein limited cracking is permitted through the use of additional mild nonprestressed reinforcement to control the extent and width of the cracks

and to assume part of the ultimate flexural moment strength. Two major advantages of partial prestressing are the efficient use of all constituent materials and the control of excessive camber due to the long-term creep of concrete under compression.

Reinforced concrete beams always have to be designed as underreinforced to ensure ductile failure by yielding of the reinforcement. Prestressed beams can be either *underreinforced* using a relatively small percentage of mild nonprestressed steel, leading to rupture of the tensile steel at failure, or essentially *overreinforced*, using a large percentage of steel, resulting in crushing of the concrete at the compression top fibers in a somewhat less ductile failure.

Another type of, say, premature failure occurs at the first cracking load level, where  $M_{cr}$  approximates the nominal moment strength  $M_n$  of the section. This type of failure can occur in members that are prestressed and reinforced with very small amounts of steel, or in members that are concentrically prestressed with small amounts of steel, or in hollow members.

It is generally advisable to evaluate the magnitude of the cracking moment  $M_{cr}$  in order to determine the reserve strength and overload limits that the designed section has.

### 4.9.3 Cracking Moment Evaluation

#### Example 4.8

Calculate the cracking moment  $M_{cr}$  in the I-beam of Example 4.2, and evaluate the magnitude of the overload moment that the beam can tolerate at the modulus of rupture of concrete. Also, determine what safety factor the beam has against cracking due to overload. Given is  $f_r = 7.5\sqrt{f'_c} = 7.5\sqrt{5,000} = 530$  psi (3.7 MPa).

**Solution:** From Example 4.2,

$$P_e = 308,225 \text{ lb (1,371 kN)}$$

$$r^2/c_b = 187.5/18.84 = 9.95 \text{ in. (25.3 cm)}$$

$$S_b = 3,750 \text{ in.}^3 \text{ (61,451 cm}^3\text{)}$$

$$e_c = 14 \text{ in. (35.6 cm) in this example.}$$

$$M_D + M_{SD} = 2,490,638 \text{ in.-lb (281 kN-m)}$$

$$\text{where } M_{SD} = 0$$

$$M_L = 7,605,000 \text{ in.-lb (859 kN-m)}$$

From Equation 4.25,

$$\begin{aligned} M_{cr} &= f_r S_b + P_e \left( e + \frac{r^2}{c_b} \right) \\ &= 530 \times 3750 + 308,255(14 + 9.95) \\ &= 9,370,207 \text{ in.-lb (1,509 kN-m)} \end{aligned}$$

$$\begin{aligned} M_T &= M_D + M_{SD} + M_L = 2,490,638 + 7,605,000 \\ &= 10,095,638 \text{ in.-lb (1,141 kN-m)} \end{aligned}$$

$$\begin{aligned} \text{Overload moment} &= M_T - M_{cr} = 10,095,638 - 9,370,207 \\ &= 725,431 \text{ in.-lb (83 kN-m)} \end{aligned}$$

Since  $M_T > M_{cr}$ , the beam had tensile cracks at service load, as the design in Example 4.2 pre-supposed. The safety factor against cracking is given by

$$\frac{M_{cr}}{M_T} = \frac{9,370,207}{10,095,638} = 0.93$$

If the service load  $M_T$  is less than  $M_{cr}$ , the safety factor against cracking will be greater than 1, as in nonpartially prestressed members.

Note that where nonprestressed reinforcement is used to develop a partially prestressed section, the total factored moment  $\phi M_n \geq 1.2M_{cr}$ , as required by the ACI code.

## 4.10 LOAD AND STRENGTH FACTORS

### 4.10.1 Reliability and Structural Safety of Concrete Components

Three developments in recent decades have majorly influenced present and future design procedures: the vast increase in the experimental and analytical evaluation of concrete elements, the probabilistic approach to the interpretation of behavior, and the digital computational tools available for rapid analysis of safety and reliability of systems. Until recently, most safety factors in design have had an empirical background based on local experience over an extended period of time. As additional experience is accumulated and more knowledge is gained from failures as well as familiarity with the properties of concrete, factors of safety are adjusted and in most cases lowered by the codifying bodies.

In 1956, Baker (Ref. 4.24) proposed a simplified method of safety factor determination, as shown in Table 4.8, based on probabilistic evaluation. This method expects the design engineer to make critical choices regarding the magnitudes of safety margins in a design. The method takes into consideration that different weights should be assigned to the various factors affecting a design. The weighted failure effects  $W_i$  for the various factors of workmanship, loading conditions, results of failure, and resistance capacity are tabulated in the table.

The safety factor against failure is

$$\text{S.F.} = 1.0 + \frac{\sum W_i}{10} \quad (4.26)$$

where the maximum total weighted value of all parameters affecting performance equals 10.0. In other words, for the worst combination of conditions affecting structural performance, the safety factor S.F. = 2.0.

**Table 4.8** Baker's Weighted Safety Factor

Weighted Failure Effect	Maximum $W_i$
1. Results of failure: 1.0 to 4.0	
Serious, either human or economic	4.0
Less serious, only the exposure of nondamageable material	1.0
2. Workmanship: 0.5 to 2.0	
Cast in place	2.0
Precast "factory manufactured"	0.5
3. Load conditions: 1.0 to 2.0	2.0
(high for simple spans and overload possibilities; low for load combinations such as live loads and wind)	
4. Importance of member in structure	0.5
(beams may use lower value than columns)	
5. Warning of failure	1.0
6. Depreciation of strength	0.5
	Total = $\sum W_i = 10.0$

$$\text{S.F.} = 1.0 + \frac{\sum W_i}{10}$$



This method assumes adequate prior performance data similar to a design in progress. Such data in many instances are not readily available for determining safe weighted values  $W_i$  in Eq. 4.26. Additionally, if the weighted factors are numerous, a probabilistic determination of them is more difficult to codify. Hence, an undue value-judgment burden is probably placed on the design engineer if the full economic benefit of the approach is to be achieved.

Another method with a smaller number of probabilistic parameters deals primarily with loads and resistances. Its approaches for steel and concrete structures are generally similar: both the load-and-resistance-factor-design method (LRFD) and first-order second-moment method (FOSM) propose general reliability procedures for evaluating probability-based factored load design criteria (see Refs. 4.25 and 4.26). They are intended for use in proportioning structural members on the basis of load types such that the resisting strength levels are *greater* than the factored load or moment distributions. As these approaches are basically load oriented, they reduce the number of individual variables that have to be considered, such as those listed in Table 4.8.

Assume that  $\phi_i$  represents the resistance factors of a concrete element and that  $\gamma_i$  represents the load factors for the various types of load. If  $R_n$  is the nominal resistance of the concrete element and  $W_i$  represents the load effect for various types of superimposed load,

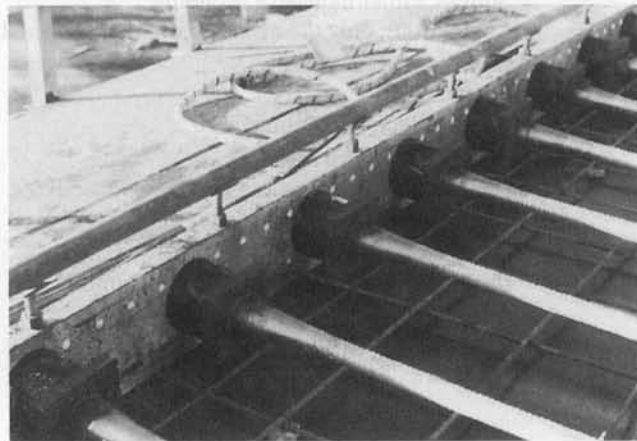
$$\phi_i R_n \geq \gamma_i W_i \quad (4.27)$$

where  $i$  represents the load in question, such as dead, live, wind, earthquake, or time-dependent effects.

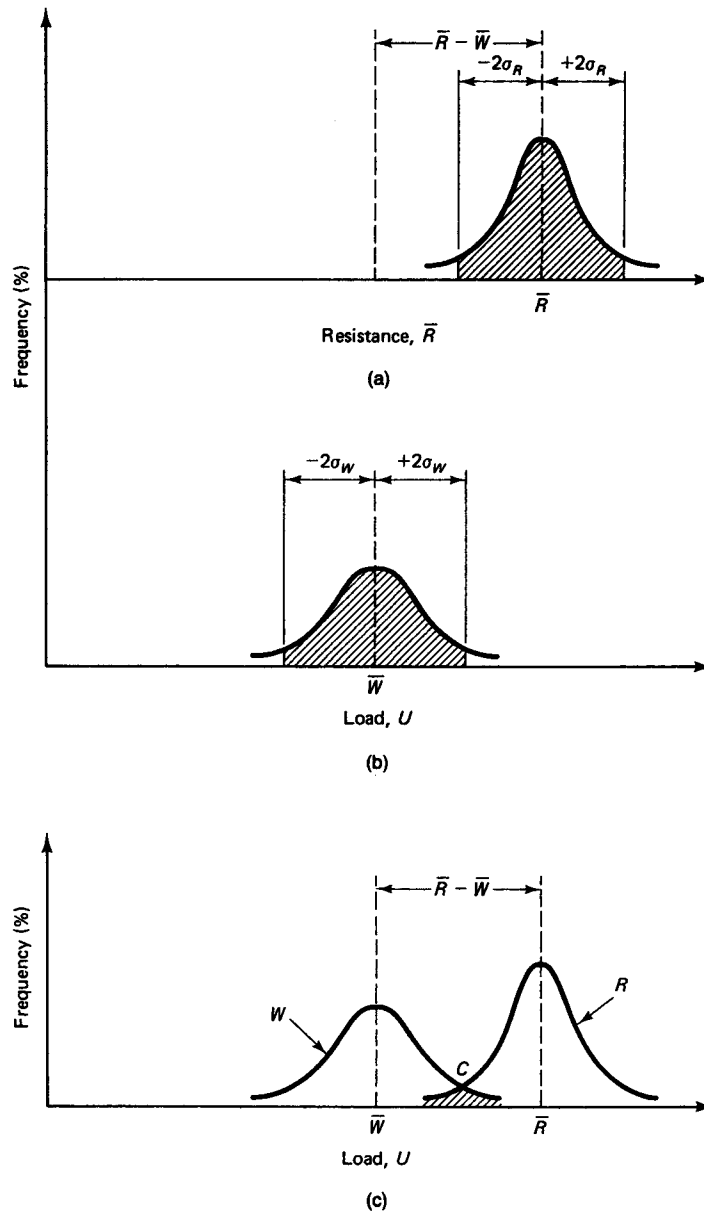
Figures 4.41(a) and (b) show a plot of the separate frequency distributions of the actual load  $W$  and the resistance  $R$  with means values  $\bar{R}$  and  $\bar{W}$ . Figure 4.41(c) gives the two distributions superimposed and intersecting at point  $C$ .

It is recognized that safety and reliable integrity of the structure can be expected to exist if the load effect  $W$  falls at a point to the left of intersection  $C$  on the  $W$  curve, and to the right of intersection  $C$  on the resistance curve  $R$ . Failure, on the other hand, would be expected to occur if the load effect or the resistance fall within the shaded area in Fig. 4.41(c). If  $\beta$  is a safety index, then

$$\beta = \frac{\bar{R} - \bar{W}}{\sqrt{\sigma_R^2 + \sigma_W^2}} \quad (4.28)$$



**Photo 4.11** Post-tensioning bridge deck conduits.

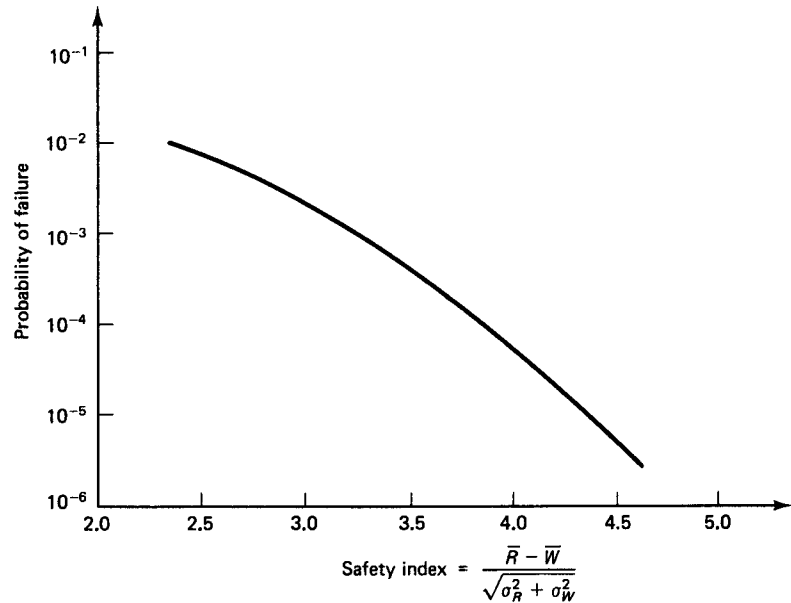


**Figure 4.41** Frequency distribution of loads vs. resistance.

where  $\sigma_R$  and  $\sigma_W$  are the standard deviations of the resistance and the load, respectively.

A plot of the safety index  $\beta$  for a hypothetical structural system against the probability of failure of the system is shown in Fig. 4.42. One can observe that such a probability is reduced as the difference between the mean resistance  $\bar{R}$  and load effect  $\bar{W}$  is increased, or the variability of resistance as measured by their standard deviations  $\sigma_R$  and  $\sigma_W$  is decreased, thereby reducing the shaded area under intersection  $C$  in Fig. 4.41(c).

The extent of increasing the difference  $(\bar{R} - \bar{W})$  or decreasing the degree of scatter of  $\sigma_R$  or  $\sigma_W$  is naturally dictated by economic considerations. It is economically unreasonable to design a structure for zero failure, particularly since types of risk other than load are an accepted matter, such as the risks of severe earthquake, hurricane, volcanic erup-



**Figure 4.42** Probability of failure vs. safety index.

tion, and fire. Safety factors and corresponding load factors would thus have to disregard those types or levels of load, stress, and overstress whose probability of occurrence is very low. In spite of this, it is still possible to achieve reliable safety conditions by choosing such a safety index value  $\beta$  through a proper choice of  $R_n$  and  $W_i$  using the appropriate resistance factors  $\phi_i$  and load factors  $\gamma_i$  in Equation 4.27. A safety index  $\beta$  having the value 1.75 to 3.2 for concrete structures is suggested where the lower value accounts for load contributions from wind and earthquake.

If the factored external load is expressed as  $U_i$ , then  $\Sigma \gamma_i W = U_i$  for the different loading combinations.

In cases where other load combinations, such as snow or lateral pressure are not present, a typical  $U_i$  value recommended in the ASCE-7 Standard (Ref. 4.14) and IBC 2000 (Ref. 4.17) for maximum  $U_i$  to be used in Equation 4.2, that is,  $\phi_i R_n \geq \gamma_i W_i \geq U_{i \max}$ , as follows:

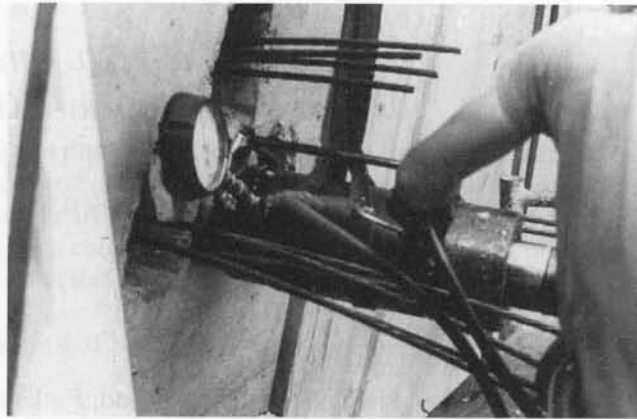
$$U = \phi_i R_n = \text{Maximum} [1.2D + 1.6L] \quad (4.29)$$

As more substantive records of performance are compiled, the details of the foregoing approach to reliability, safety, and reserve strength evaluation of structural components will be more universally accepted and extended beyond the treatment of the component elements to the treatment of the total structural system, such as described in Table 4.8.

## 4.11 ACI LOAD FACTORS AND SAFETY MARGINS

### 4.11.1 General Principles

The general concepts of safety and reliability of performance presented in the preceding section are inherent in a more simplified but less accurate fashion in the ACI code. The load factors  $\gamma$  and the strength reduction factors  $\phi$  give an overall safety factor based on load types such that



**Photo 4.12** Tendon stressing with Freyssinet jack.

$$S.F. = \frac{\gamma_1 D + \gamma_2 L}{D + L} \times \frac{1}{\phi} \quad (4.30)$$

where  $\phi$  is the strength reduction factor and  $\gamma_1$  and  $\gamma_2$  are the respective load factors for the dead load  $D$  and the live load  $L$ . Basically, a single common factor is used for dead load and another for live load. Variation in resistance capacity is accounted for in  $\phi$ . Hence, the method is a simplified empirical approach to safety and the reliability of structural performance that is not economically efficient for every case and not fully adequate in other instances, such as combinations of dead and wind loads.

The ACI factors are termed *load factors*, as they restrict the estimation of reserve strength to the loads only as compared to the other parameters listed in Table 4.8. The estimated service or working loads are magnified by the coefficients, such as a coefficient of 1.2 for dead loads and 1.6 for live load, with the basic combination of vertical gravity loads is dead load plus live load. The *dead load*, which constitutes the weight of the structure and other relatively permanent features, can be estimated more accurately than the live load. The *live load* is estimated using the weight of nonpermanent loads, such as people and furniture. The transient nature of live loads makes them difficult to estimate more accurately. Therefore, a higher load factor is normally used for live loads than for dead loads.

The philosophy used for combining the various load components for earthquake loading is essentially the same as that used for wind loading.

#### 4.11.2 ACI Load Factors Equations

The ACI 318 Building Code for concrete structures is an international code. As such, it has to conform to the International Building Code, IBC, and be consistent with the ASCE-7 Standard on Minimum Design Loads for Buildings and Other Structures (Ref. 4.25). These two standards contain the same probabilistic values for the expected safety resistance factors  $\phi_i R_n$  where  $\phi$  is a strength reduction factor, depending on the type of stress being considered in the design, namely, flexure or shear or compression, etc.

Thus, the current ACI design loads  $U$  (factored loads) have to be at least equal to the values obtained from Equations 4.31(a) through 4.31(g). The effect of one or more loads not acting simultaneously has to be investigated. Structures are seldom subjected to dead and live load alone. The following equations present combinations of loads for situations in which wind, earthquake, or lateral pressures due to earthfill or fluids should be considered:

$$U = 1.4(D + F) \quad (4.31a)$$

$$U = 1.2(D + F + T) + 1.6(L + H) + 0.5(L_r \text{ or } S \text{ or } R) \quad (4.31b)$$

$$U = 1.2D + 1.6(L_r \text{ or } S \text{ or } R) + (1.0L \text{ or } 0.8W) \quad (4.31c)$$

$$U = 1.2D + 1.6W + 0.5L + 1.0(L_r \text{ or } S \text{ or } R) \quad (4.31d)$$

$$U = 1.2D + 1.0E + 1.0L + 0.2S \quad (4.31e)$$

$$U = 0.9D + 1.6W + 1.6H \quad (4.31f)$$

$$U = 0.9D + 1.0E + 1.6H \quad (4.31g)$$

where

$D$  = dead load;  $E$  = earthquake load;  $F$  = lateral fluid pressure load & maximum height;

$H$  = load due to the weight and lateral pressure of soil and water in soil;

$L$  = live load;  $L_r$  = roof load;  $R$  = rain load;  $S$  = snow load;

$T$  = self-straining force such as creep, shrinkage and temperature effects;

$W$  = wind load.

It should be noted that the philosophy used for combining the various load components for earthquake loading is essentially similar to that used for wind loading.

#### Exceptions to the values in these expressions

- (a) The load factor on  $L$  in Eq. 4.31(c) to 4.31(e) is allowed to be reduced to 0.5 except for garages, areas occupied as places of public assembly, and all areas where the live load  $L$  is greater than 100 lb/ft<sup>2</sup>.
- (b) Where wind load  $W$  has not been reduced by a directionality factor, the code permits to use  $1.3W$  in place of  $1.6W$  in Eq. 4.31(d) and 4.31(f).
- (c) Where earthquake load  $E$  is based on service-level seismic forces,  $1.4E$  shall be used in place of  $1.0E$  in Eq. 4.31(e) and 4.31(g).
- (d) The load factor on  $H$  is to be set equal to zero in Eq. 4.31(f) and Eq. 4.31(g) if the structural action due to  $H$  counteracts that due to  $W$  or  $E$ . Where lateral earth pressure provides resistance to structural actions from other forces, it should not be included in  $H$  but shall be included in the design resistance.

Due regard has to be given to sign in determining  $U$  for combinations of loadings, as one type of loading may produce effects of opposite sense to that produced by another type. The load combinations with  $0.9D$  are specifically included for the case where a higher dead load reduces the effects of other loads. Consideration also has to be given to various combinations of loading to determine the most critical design condition, particularly when strength is dependent on more than one load effect, such as strength for combined flexure and axial load or shear strength in members with axial load. In cases where special circumstances require greater reliance on the strength of particular members than encountered in usual practice, the ACI Code allows some reduction in the stipulated strength reduction factors  $\phi$ , or an increase in the stipulated load factors  $U$ .

#### 4.11.2.1 Reduction in Live Loads

For large areas, it is reasonable to assume that the *full* intensity of live load does *not* cover the entire floor area. Hence, members having an influence area of 400 ft<sup>2</sup> (37.2 m<sup>2</sup>) or more can be designed for a reduced live load from the following equation:

$$L = L_0 \left( 0.25 + \frac{15}{\sqrt{A_I}} \right) \quad (4.32a)$$

where

$L$  = Reduced design live load per square foot of area supported by the member,  
 $L_0$  = Unreduced design live load per square foot of area,  
 $A_I$  = Influence area: For other than cantilevered construction,  $A_I$  is the tributary area for a column;  $A_I$  is tributary area for beams, or equal area for a two-way slab (Ref. 4.25).

In SI units, Equation 4.31 becomes

$$L = L_0 \left( 0.25 + \frac{4.57}{\sqrt{A_I}} \right) \quad (4.32b)$$

where  $L$ ,  $L_0$ , and  $A_I$  are in square meters of area.

The reduced design live load cannot be less than 50 percent of the unit live load  $L_0$  for members supporting one floor or less than 40 percent of the unit live load  $L_0$  for members supporting two or more floors. For live loads of 100 lb/ft<sup>2</sup> (4.79 kN/m<sup>2</sup>) or less, no reduction can be made for areas used as places of public assembly, except that in the case of garages for passenger cars a reduction of up to 20 percent can be made. Live loads in all other cases not stipulated by the code cannot be reduced except as accepted by the jurisdictional authority.

### 4.11.3 Design Strength vs. Nominal Strength: Strength-Reduction Factor $\phi$

The strength of a particular structural unit calculated using the current established procedures is termed *nominal strength*. For example, in the case of a beam, the resisting moment capacity of the section calculated using the equations of equilibrium and the properties of concrete and steel is called the *nominal strength moment*  $M_n$  of the section. This nominal strength is reduced using a strength reduction factor  $\phi$  to account for inaccuracies in construction, such as in the dimensions or position of reinforcement or variations in properties. The reduced strength of the member is defined as the design strength of the member.

For a beam, the design moment strength  $\phi M_n$  should be at least equal to, or better, slightly greater than, the external factored moment  $M_u$  for the worst condition of factored load  $U$ . The factor  $\phi$  varies for the different types of behavior and for the different types of structural elements. For beams in flexure, for instance,  $\phi$  is 0.9.

For tied columns that carry dominant compressive loads, the factor  $\phi$  equals 0.65. The smaller strength-reduction factor used for columns is due to the structural importance of the columns in supporting the total structure compared to other members, and to guard against progressive collapse and brittle failure with no advance warning of collapse. Beams, on the other hand, are designed to undergo excessive deflections before failure. Hence, the inherent capability of the beam for advanced warning of failure permits the use of a higher strength reduction factor or resistance factor.

Table 4.9 summarizes the resistance factors  $\phi$  for various structural elements as given in the ACI code. A comparison of these values to those given in Ref. 4.24 indicates that the  $\phi$  values in this table, as well as the load factors of Equation 4.31, are in some cases more conservative than they should be. In cases of earthquakes, wind, and shear forces, the probability of load magnitude and reliability of performance are subject to higher randomness, and hence a higher coefficient of variation than the other types of loading.

**Table 4.9** Resistance or Strength Reduction Factor  $\phi$ 

Structural Element	Factor $\phi$
Beam or slab: bending or flexure	0.9
Columns with ties	0.65
Columns with spirals	0.75
Columns carrying very small axial loads (refer to Chapter 9 for more details)	0.65–0.9, or 0.75–0.9
Beam: shear and torsion	0.75

## AASHTO STRENGTH-REDUCTION FACTORS

**Flexure:** For factory-produced precast prestressed concrete members,  $\phi = 1.0$   
For post-tensioned cast-in-place concrete members,  $\phi = 0.95$

**Shear and Torsion:** Reduction factor for prestressed members,  $\phi = 0.90$   
See LRFD and Standard AASHTO other factors in Chapter 12.

## 4.12 LIMIT STATE IN FLEXURE AT ULTIMATE LOAD IN BONDED MEMBERS: DECOMPRESSION TO ULTIMATE LOAD

### 4.12.1 Introduction

As discussed in Section 4.9.1, the prestressed concrete beam starts to behave like a reinforced concrete beam when the value of the flexural moment is well beyond the cracking moment  $M_{cr}$  and the total service load moment  $M_T$ . The ultimate theory in flexure and the principles and concepts underlying it are thus equally applicable to prestressed concrete. A detailed fundamental treatment of this subject is given in chapter 5 of Ref. 4.2. The same fundamental format of equations will be given here, modified to reflect the characteristics of the different reinforcing materials and the geometry peculiar to prestressed concrete.

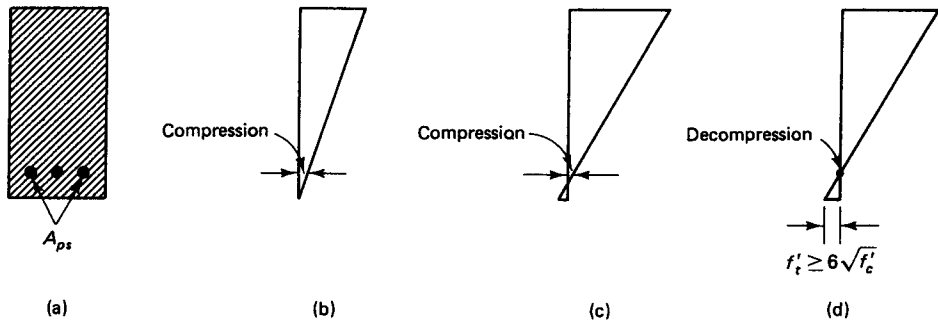
Cracking develops when the tensile stress in the concrete at the extreme fibers of the critical section exceeds the maximum stress level  $f_r \cong 7.5\sqrt{f'_c}$ . Prior to attaining this level, the overload causes the compressive stress in the concrete *at the level of the prestressing steel* to continually decrease until it becomes zero at a load level termed the *decompression load*. The stress level in the tendons is correspondingly termed the *decompression stress* (see Figures 4.3 and 4.43).

Some investigators define the decompression load as the load at which the first crack appears at the extreme fibers of the critical section, such as the bottom midspan fibers of a simply supported beam. A minor difference results in the analysis using this definition of the decompression load.

To follow the loading step-by-step states, suppose that the effective prestress  $f_{pe}$  at service load due to all loads results in a strain  $\epsilon_1$  such that

$$\epsilon_1 = \epsilon_{pe} = \frac{f_{pe}}{E_{ps}} \quad (4.33a)$$

At decompression, i.e., when the compressive stress in the surrounding concrete at the level of the prestressing tendon is neutralized by the tensile stress due to overload, a decompression strain  $\epsilon_{decomp} = \epsilon_2$  results such that



**Figure 4.43** Strain in the concrete up to the decompression stage at the tension reinforcement level. (a) Cross section. (b) Entire section in compression. (c) Tension at the lower fibers below the modulus-of-rupture level. (d) Decompression stage with zero stress in the concrete at the level of the prestressing reinforcement.

$$\epsilon_2 = \epsilon_{\text{decomp}} = \frac{P_e}{A_c E_c} \left( 1 + \frac{e^2}{r^2} \right) \quad (4.33b)$$

Figures 4.43 and 4.44 illustrate the stress distribution at and after the decompression stage where the behavior of the prestressed beam starts to resemble that of a reinforced concrete beam.

As the load approaches the limit state at ultimate, the additional strain  $\epsilon_3$  in the steel reinforcement follows the linear triangular distribution shown in Fig. 4.44(b), where the maximum compressive strain at the extreme compression fibers is  $\epsilon_c = 0.003$  in./in. In such a case, the steel strain increment due to overload above the decompression load is

$$\epsilon_3 = \epsilon_c \left( \frac{d - c}{c} \right) \quad (4.33c)$$

where  $c$  is the depth of the neutral axis. Consequently, the total strain in the prestressing steel at this stage becomes

$$\epsilon_s = \epsilon_1 + \epsilon_2 + \epsilon_3 \quad (4.33d)$$

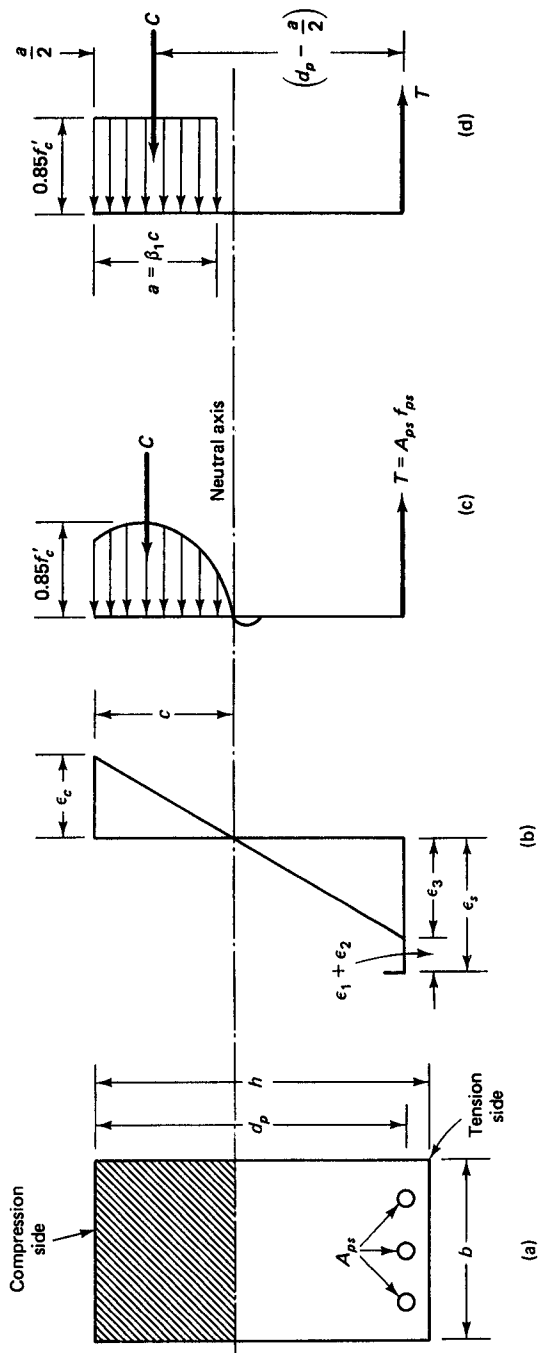
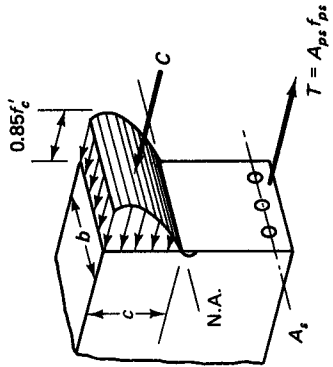
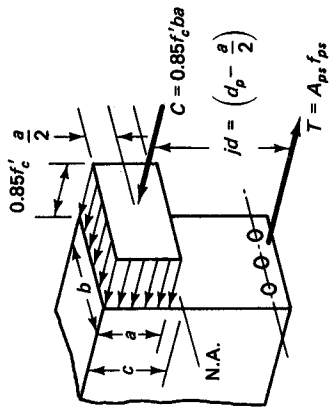
The corresponding stress  $f_{ps}$  at nominal strength can be easily obtained from the stress-strain diagram of the steel supplied by the producer.

### 4.12.2 The Equivalent Rectangular Block and Nominal Moment Strength

It is important to be able to evaluate the reserve strength in the prestressed beam up to failure, as discussed in Chapter 1. Hence, the total design would have to incorporate the moment strength of the prestressed section in addition to the service-load level checks described in detail in Sections 4.1 through 4.7. The following assumptions are made in defining the behavior of the section at ultimate load:

1. The strain distribution is assumed to be linear. This assumption is based on Bernoulli's hypothesis that plane sections remain plane before bending and perpendicular to the neutral axis after bending.
2. The strain in the steel and the surrounding concrete is the same prior to cracking of the concrete or yielding of the steel as after such cracking or yielding.
3. Concrete is weak in tension. It cracks at an early stage of loading at about 10 percent of its compressive strength limit. Consequently, concrete in the tension zone of





**Figure 4.44** Stress and strain distribution across beam depth. (a) Beam cross section. (b) Strains. (c) Actual stress block. (d) Assumed equivalent stress block.

the section is neglected in the flexural analysis and design computations, and the tension reinforcement is assumed to take the total tensile force.

To satisfy the equilibrium of the horizontal forces, the compressive force  $C$  in the concrete and the tensile force  $T$  in the steel should balance each other—that is,

$$C = T \quad (4.34)$$

The terms in Figure 4.44 are defined as follows:

$b$  = width of the beam at the compression side

$d$  = depth of the beam measured from the extreme compression fiber to the centroid of steel area

$h$  = total depth of the beam

### 4.12.3 Strain Limits Method for Analysis and Design

#### 4.12.3.1 General Principles

In this approach, sometimes referred to as the “unified method,” being equally applicable to flexural analysis of prestressed concrete elements, the nominal flexural strength of a concrete member is reached when the net compressive strain in the extreme compression fibers reaches the ACI code-assumed limit 0.003 in./in. It also stipulates that when the net tensile strain in the extreme tension steel,  $\epsilon_p$ , is sufficiently large, as discussed in the previous section, at a value equal to or greater than 0.005 in./in., the behavior is fully ductile. The concrete beam section is characterized as *tension-controlled*, with ample warning of failure as denoted by excessive cracking and deflection.

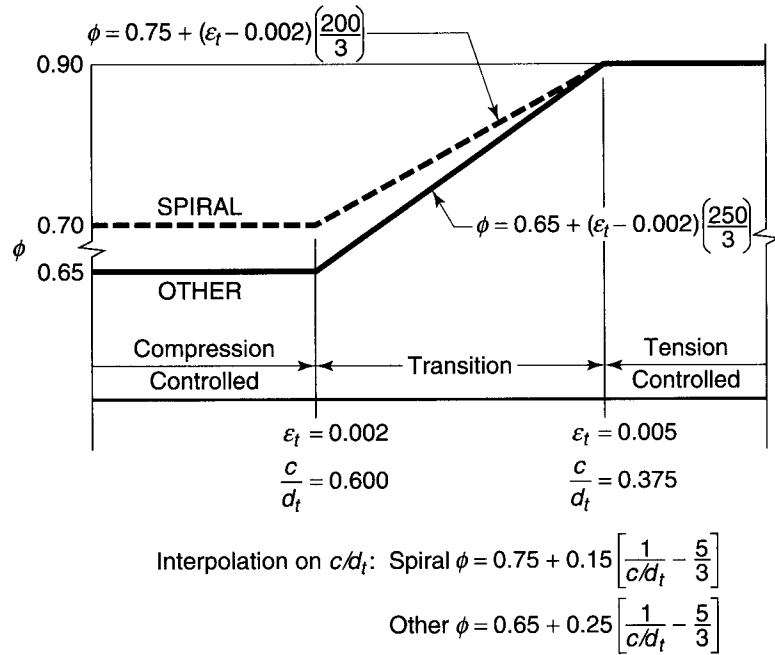
If the net tensile strain in the extreme tension fibers,  $\epsilon_p$ , is small, such as in compression members, being equal to or less than a *compression-controlled* strain limit, a brittle mode of failure is expected, with little warning of such an impending failure. Flexural members are usually tension-controlled. Compression members are usually compression-controlled. However, some sections, such as those subjected to small axial loads, but large bending moments, the net tensile strain,  $\epsilon_p$ , in the extreme tensile fibers, will have an intermediate or transitional value between the two strain limit states, namely, between the compression-controlled strain limit  $\epsilon_t = f_y/E_s = 60,000/29 \times 10^6 = 0.002$  in./in., and the tension-controlled strain limit  $\epsilon_t = 0.005$  in./in. Figure 4.45 delineates these three zones as well as the variation in the strength reduction factors applicable to the total range of behavior.

For the tension-controlled state, the strain limit  $\epsilon_t = 0.005$  corresponds to reinforcement ratio  $\rho/\rho_b = 0.63$ , where  $\rho_b$  is the balanced reinforcement ratio for the balanced strain  $\epsilon_t = 0.002$  in the extreme tensile reinforcement. The net tensile strain  $\epsilon_t = 0.005$  for a tension-controlled state is a single value that applies to all types of reinforcement regardless whether mild steel or prestressing steel. High reinforcement ratios that produce a net tensile strain less than 0.005 result in a  $\phi$ -factor value lower than 0.90, resulting in less economical sections. Therefore, it is more efficient to add compression reinforcement if necessary or deepen the section in order to make the strain in the extreme tension reinforcement,  $\epsilon_p \geq 0.005$ .

**Variation of  $\phi$  as a Function of Strain.** Variation of the  $\phi$  value for the range of strain between  $\epsilon_t = 0.002$  and  $\epsilon_t = 0.005$  can be linearly interpolated to give the following expressions,

Tied Sections:

$$0.65 \leq \left[ \phi = 0.65 + (\epsilon_t - 0.002) \left( \frac{250}{3} \right) \right] \leq 0.90 \quad (4.35a)$$



**Figure 4.45** Strain limit zones and variation of strength reduction factor  $\phi$  with the net Tensile Strain  $\epsilon_t$

Spirally-reinforced sections:

$$0.75 \leq \left[ \phi = 0.75 + (\epsilon_t - 0.002) \left( \frac{200}{3} \right) \right] \leq 0.90 \tag{4.35b}$$

**Variation of  $\phi$  as a Function of Neutral Axis depth Ratio  $c/d_t$ .** Equations 4.35(a) and 4.35(b) can be expressed in terms of the ratio of the neutral axis depth  $c$  to the effective depth  $d_t$  of the layer of reinforcement closest to the tensile face of the section as follows,

Tied sections:

$$0.65 \leq \left( \phi = 0.65 + 0.25 \left[ \frac{1}{c/d_t} - \frac{5}{3} \right] \right) \leq 0.90 \tag{4.36a}$$

Spirally-reinforced sections:

$$0.75 \leq \left( \phi = 0.75 + 0.15 \left[ \frac{1}{c/d_t} - \frac{5}{3} \right] \right) \leq 0.90 \tag{4.36b}$$

For balanced strain, where the reinforcement at the tension side yields at the same time as the concrete crushes at the compression face ( $f_s = f_y$ ), the neutral axis depth ratio for a limit strain  $\epsilon_t = 0.002$  in./in. can be defined as

$$\frac{c_b}{d_t} = \left( \frac{87,000}{87,000 + f_y} \right) \tag{4.37}$$

In summary, when the net tensile strain in the extreme tension reinforcement is sufficiently large (equal or greater than 0.005), the section is defined as tension-controlled, where ample warning of failure with extensive deflection occurs.

#### 4.12.4 Negative Moment Redistribution in Continuous Beams

The Code permits decreasing the negative elastic moment at the supports for continuous members by not more than  $[1000 \epsilon_t]$  percent, with a maximum of 20 percent. The reason is that for ductile members, plastic hinge regions develop at points of maximum moment and cause a shift in the elastic moment diagram. In many cases, the result is a reduction of the negative moment and a corresponding increase in the positive moment. The redistribution of the negative moment as permitted by the code can only be used when  $\epsilon_t$  is equal or greater than about 0.0075 in./in. at the section at which the moment is reduced. Redistribution is inapplicable in the case of slab systems proportioned by the direct design method (DDM).

Figure 4.46 shows the permissible moment redistribution for minimum rotational capacity. A minimum strain of 0.0075 at the tensile face is comparable to the case where the reinforcement ratio for the combined prestressed and mild steel reinforcement has a reinforcement index of  $\omega$  not exceeding  $0.24\beta_1$  as an upper limit for ductile design. A maximum strain 0.005 for the tension-controlled state is comparable to a reinforcement index  $\omega_p = 0.32 \beta_1$  or  $\omega_T = 0.36 \beta_1$  as described in the Code commentary.

The ACI 318 Code stipulates a maximum strength reduction factor  $\phi = 0.90$  for tension-controlled bending, to be used in computing the design strength of flexural members. This corresponds to neutral axis depth ratio  $c/d_t = 0.375$  for a strain  $\epsilon_t = 0.005$ , with a lower  $c/d_t$  ratio recommended. For a useful redistribution of moment in continuous members, this neutral axis depth ratio should be considerably lower, so that the net tensile strain is within the range of  $\epsilon_t = 0.0075$ , giving a 7.5% redistribution, and 0.020, giving 20% redistribution, as shown in Figure 4.46. The tensile strain at the extreme tensile reinforcement has the value

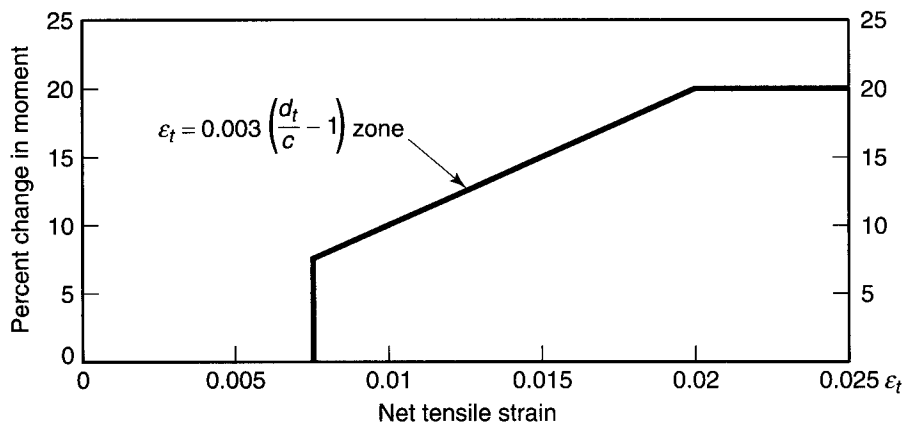
$$\epsilon_t = 0.003 \left( \frac{d_t}{c} - 1 \right) \quad (4.38a)$$

As an example, if  $d_t = 20$  in. and neutral axis depth  $c = 5.1$  in.,

$\epsilon_t = 0.003 \left( \frac{d_t}{c} - 1 \right) = 0.003 \left( \frac{20}{5.1} - 1 \right) = 0.0088$  in./in.  $> 0.0075$  in./in. minimum value for inelastic redistribution to be applied.

In this case, the maximum allowable moment redistribution =  $1000 \epsilon_t = 8.8\%$

This gives a net reduction in the negative moment value =  $(100 - 8.8) = 91.2\%$ .



**Figure 4.46** Allowable redistribution percentage for maximum rotational capacity

A 20 % maximum redistribution is approximately  $= 0.24\beta_1$ , as in previous codes. This limit can be represented by a reinforcement index relationship for bonded prestressed concrete members as follows:

$$\omega_p + \frac{d}{d_p} (\omega - \omega') \leq 0.24\beta_1 \quad (4.38b)$$

Although the code allows a maximum redistribution of 20% or  $1000 \epsilon_t$ , it is more reasonable to limit the redistribution percentage to about 10- 15 percent. Summarizing, the ACI 318-05 code stipulates that a redistribution (reduction) of the moments at supports of continuous flexural members **not to exceed 1000  $\epsilon_t$**  percent, with a maximum of 20 percent, as seen in Figure 4.46, while increasing the positive midspan moment accordingly. But inelastic moment redistribution should only be made when  $\epsilon_t$  is equal or greater than 0.0075 at the section for which moment is reduced. An adjustment in one span should also be applied to all the other spans in flexure, shear and bar cutoffs.

It should be noted that the total amount of prestressed and non-prestressed reinforcement should be adequate to develop a factored load of at least 1.2 times the cracking load computed on the basis of the modulus of rupture  $f_r$ . This provision in ACI 318 Code is permitted to be waived for (a) Two-way, unbonded post-tensioned slabs; and (b) Flexural members with shear and flexural strength at least twice the load level causing the first cracking moment  $M_{cr}$ .

#### 4.12.5 Nominal Moment Strength of Rectangular Sections

The actual distribution of the compressive stress in a section at failure has the form of a rising parabola, as shown in Figure 4.44(c). It is time-consuming to evaluate the volume of the compressive stress block if it has a parabolic shape. An equivalent rectangular stress block due to Whitney can be used with ease and without loss of accuracy to calculate the compressive force and hence the flexural moment strength of the section. This equivalent stress block has a depth  $a$  and an average compressive strength  $0.85f'_c$ . As seen from Figure 4.44(d), the value of  $a = \beta_1 c$  is determined by using a coefficient  $\beta_1$  such that the area of the equivalent rectangular block is approximately the same as that of the parabolic compressive block, resulting in a compressive force  $C$  of essentially the same value in both cases.

The value  $0.85f'_c$  for the average stress of the equivalent compressive block is based on the core test results of concrete in the structure at a minimum age of 28 days. Based on exhaustive experimental tests, a maximum allowable strain of 0.003 in./in. was adopted by the ACI as a safe limiting value. Even though several forms of stress blocks, including the trapezoidal, have been proposed to date, the simplified equivalent rectangular block is accepted as the standard in the analysis and design of reinforced concrete. The behavior of the steel is assumed to be elastoplastic.

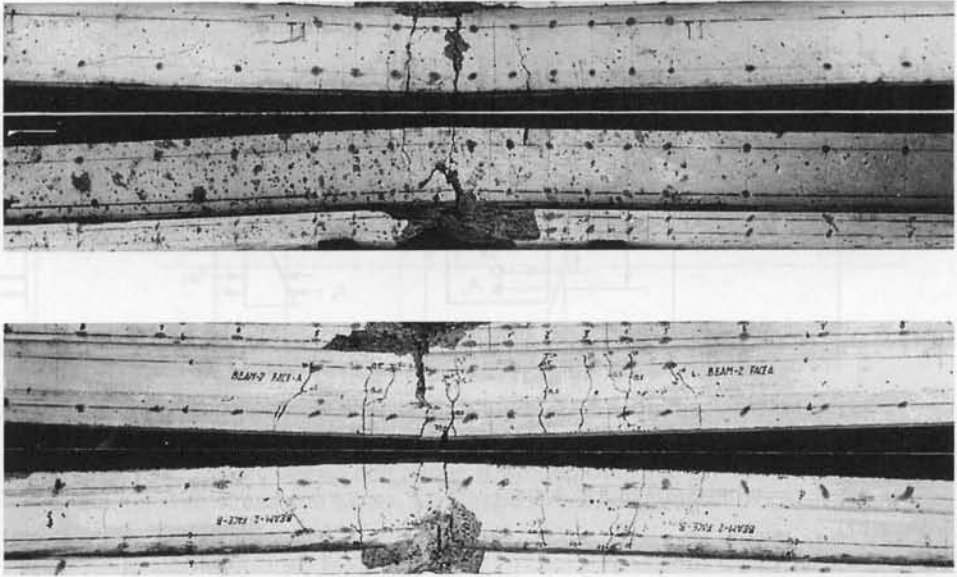
Using all the preceding assumptions, the stress distribution diagram shown in Figure 4.44(c) can be redrawn as shown in Figure 4.44(d). One can easily deduce that the compression force  $C$  can be written  $0.85f'_c ba$ —that is, the *volume* of the compressive block at or near the ultimate when the tension steel has yielded ( $\epsilon_s > \epsilon_y$ ). The tensile force  $T$  can be written as  $A_{ps}f_{ps}$ ; thus, the equilibrium Equation 4.34, equating  $C$  and  $T$ , can be rewritten as

$$A_{ps}f_{ps} = 0.85f'_c ba \quad (4.39)$$

A little algebra yields

$$a = \beta_1 c = \frac{A_{ps} f_{ps}}{0.85f'_c b} \quad (4.40)$$

The nominal moment strength is obtained by multiplying  $C$  or  $T$  by the moment arm  $(d_p - a/2)$ , yielding



**Photo 4.13** Flexural cracks at failure of prestressed T-beams (Nawy, Potyondy).

$$M_n = A_{ps} f_{ps} \left( d_p - \frac{a}{2} \right) \quad (4.41a)$$

where  $d_p$  is the distance from the compression fibers to the center of the prestressed reinforcement. The steel percentage  $\rho_p = A_{ps}/bd_p$  gives nominal strength of the prestressing steel only as follows

$$M_n = \rho_p f_{ps} b d_p^2 \left( 1 - 0.59 \rho_p \frac{f_{ps}}{f'_c} \right) \quad (4.41b)$$

If  $\omega_p$  is the reinforcement index  $= \rho_p (f_{ps}/f'_c)$ , Equation 4.41b becomes

$$M_n = \rho_p f_{ps} b d_p^2 (1 - 0.59 \omega_p) \quad (4.41c)$$

The contribution of the mild steel tension reinforcement should be similarly treated, so that the depth  $a$  of the compressive block is

$$a = \frac{A_{ps} f_{ps} + A_s f_y}{0.85 f'_c b} \quad (4.42a)$$

If  $c = a/\beta_1$ , the strain at the level of the mild steel is (Fig. 4.44)

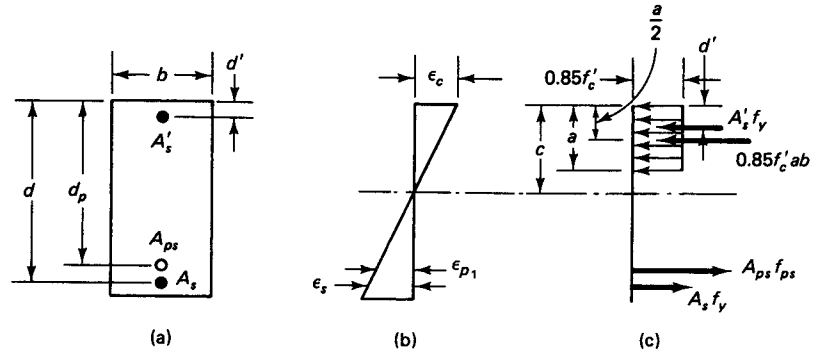
$$\epsilon_3 = \epsilon_c \left( \frac{d - c}{c} \right) \quad (4.42b)$$

Equation 4.41(b), for rectangular sections but with mild tension steel and no compression steel accounted for, becomes

$$M_n = \rho_p f_{ps} b d_p^2 \left( 1 - 0.59 \rho_p \frac{f_{ps}}{f'_c} \right) + \rho f_y b d^2 \left( 1 - 0.59 \frac{f_y}{f'_c} \right) \quad (4.43a)$$

or can be rewritten as either

$$M_n = A_{ps} f_{ps} \left\{ 1 - 0.59 \left( \omega_p + \frac{d}{d_p} \omega \right) \right\} + A_s f_y \left\{ 1 - 0.59 \left( \frac{d_p}{d} \omega_p + \omega \right) \right\} \quad (4.43b)$$



**Figure 4.47** Strain, stress, and forces across beam depth of rectangular section. (a) Beam section. (b) Strain. (c) Stresses and forces.

where  $\omega = \rho(f_y/f'_c)$ , or

$$M_n = A_{ps} f_{ps} \left( d_p - \frac{a}{2} \right) + A_s f_y \left( d - \frac{a}{2} \right) \quad (4.43c)$$

The contribution from compression reinforcement can be taken into account provided it has been found to have yielded,

$$a = \frac{A_{ps} f_{ps} + A_s f_y - A'_s f_y}{0.85 f'_c b} \quad (4.44)$$

where  $b$  is the section width of the compression face of the beam.

Taking moments about the center of gravity of the compressive block in Figure 4.47, the nominal moment strength in Equation 4.43b becomes

$$M_n = A_{ps} f_{ps} \left( d_p - \frac{a}{2} \right) + A_s f_y \left( d - \frac{a}{2} \right) + A'_s f_y \left( \frac{a}{2} - d' \right) \quad (4.45)$$

**4.12.5.1 Nominal Moment Strength of Flanged Sections.** When the compression flange thickness  $h_f$  is less than the neutral axis depth  $c$  and equivalent rectangular block depth  $a$ , the section can be treated as a flanged section as in Figure 4.48. From the figure,

$$T_p + T_s = T_{pw} + T_{pf} \quad (4.46)$$

where  $T_p$  = total prestressing force =  $A_{ps} f_{ps}$

$T_s$  = ultimate force in the nonprestressed steel =  $A_s f_y$

$T_{pw}$  = part of the total force in the tension reinforcement required to develop the web =  $A_{pw} f_{ps}$

$A_{pw}$  = total reinforcement area corresponding to the force  $T_{pw}$

$T_{pf}$  = part of the total force in the tension reinforcement required to develop the flange =  $C_f = 0.85 f'_c (b - b_w) h_f$

$C_w = 0.85 f'_c b_w a$

Substituting in Equation 4.46, we obtain

$$T_{pw} = A_{ps} f_{ps} + A_s f_y - 0.85 f'_c (b - b_w) h_f \quad (4.47)$$

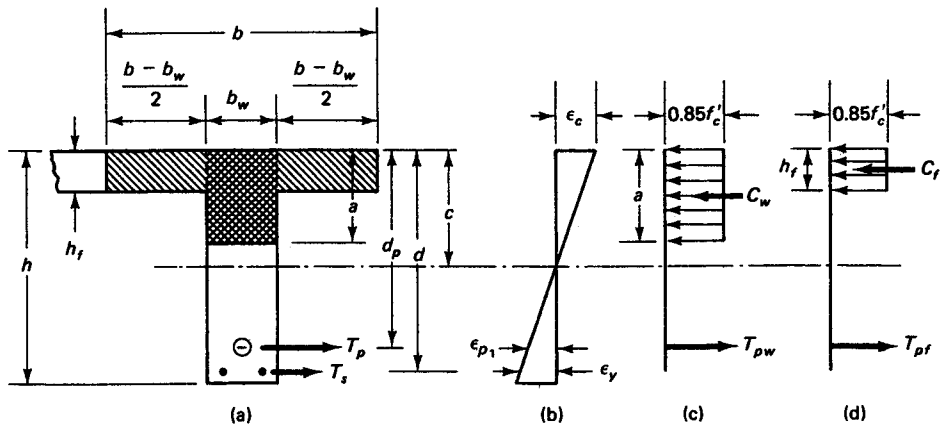
Summing up all forces in Figures 4.48(c) and (d), we have

$$T_{pw} + T_{pf} = C_w + C_f$$

giving

$$a = \frac{A_{pw} f_{ps}}{0.85 f'_c b_w} \quad (4.48a)$$

or



**Figure 4.48** Strain, stress, and forces in flanged sections. (a) Beam section. (b) Strain. (c) Web stress and forces. (d) Flange stress and force.

$$a = \frac{A_{ps} f_{ps} + A_s f_y - 0.85f'_c (b - b_w) h_f}{0.85f'_c b_w} \quad (4.48b)$$

Eq. 4.45 for a beam with compression reinforcement can be rewritten to give the nominal moment strength for a flanged section where the neutral axis falls outside the flange and  $a > h_f$  as follows, taking moments about the center of the prestressing steel:

$$M_n = A_{pw} f_{ps} \left( d_p - \frac{a}{2} \right) + A_s f_y (d - d_p) + 0.85f'_c (b - b_w) h_f \left( d_p - \frac{h_f}{2} \right) \quad (4.49a)$$

The design moment in all cases would be

$$M_u = \phi M_n \quad (4.49b)$$

where  $\phi = 0.90$  for flexure.

In order to determine whether the neutral axis falls outside the flange, requiring a flanged section analysis, one has to determine, as discussed in Ref. 4.2, where the total compressive force  $C_n$  is larger or smaller than the total tensile force  $T_n$ . If  $T_p + T_s$  in Figure 4.48 is larger than  $C_f$ , the neutral axis falls outside the flange and the section has to be treated as a flanged section. Otherwise, it should be treated as a rectangular section of the width  $b$  of the compression flange.

Another method of determining whether the section can be considered flanged is to calculate the value of the equivalent rectangular block depth  $a$  from Eq. 4.48b, thereby determining the neutral axis depth  $c = a/\beta_1$ .

**4.12.5.2 Determination of Prestressing Steel Nominal Failure Stress  $f_{ps}$ .** The value of the stress  $f_{ps}$  of the prestressing steel at failure is not readily available. However, it can be determined by *strain compatibility* through the various loading stages up to the limit state at failure. Such a procedure is required if

$$f_{pe} = \frac{P_e}{A_{ps}} < 0.50f_{pu} \quad (4.50a)$$

Approximate determination is allowed by the ACI 318 building code provided that

$$f_{pe} = \frac{P_e}{A_{ps}} \geq 0.50f_{pu} \quad (4.50b)$$

with separate equations for  $f_{ps}$  given for bonded and nonbonded members.



**Bonded Tendons.** The empirical expression for bonded members is

$$f_{ps} = f_{pu} \left( 1 - \frac{\gamma_p}{\beta_1} \left[ \rho_p \frac{f_{pu}}{f'_c} + \frac{d}{d_p} (\omega - \omega') \right] \right) \quad (4.51)$$

where the reinforcement index for the compression nonprestressed reinforcement is  $\omega' = \rho'(f_y/f'_c)$ . If the compression reinforcement is taken into account when calculating  $f_{ps}$  by Eq. 4.51, the term  $[\rho_p(f_{pu}/f'_c) + (d/d_p)(\omega - \omega')]$  should not be less than 0.17 and  $d'$  should not be greater than  $0.15d_p$ . Also,

$$\begin{aligned} \gamma_p &= 0.55 \text{ for } f_{py}/f_{pu} \text{ not less than } 0.80 \\ &= 0.40 \text{ for } f_{py}/f_{pu} \text{ not less than } 0.85 \\ &= 0.28 \text{ for } f_{py}/f_{pu} \text{ not less than } 0.90 \end{aligned}$$

The value of the factor  $\gamma_p$  is based on the criterion that  $f_{py} = 0.80 f_{pu}$  for high-strength prestressing bars, 0.85 for stress-relieved strands, and 0.90 for low-relaxation strands.

**Unbonded Tendons.** For a span-to-depth ratio of 35 or less,

$$f_{ps} = f_{pe} + 10,000 + \frac{f'_c}{100\rho_p} \quad (4.52a)$$

where  $f_{ps}$  shall not be greater than  $f_{py}$  or  $(f_{pe} + 60,000)$ .

For a span-to-depth ratio greater than 35,

$$f_{ps} = f_{pe} + 10,000 + \frac{f'_c}{300\rho_p} \quad (4.52b)$$

where  $f_{ps}$  shall not be greater than  $f_{py}$  or  $(f_{pe} + 30,000)$ . Figure 4.49, from Ref. 4.9, shows seating losses for typical unbonded tendons.

Note that the AASHTO expressions for the ultimate design strength,  $f_{ps}$ , differ from Equations 4.51 and 4.52, as shown in Section 12.3.3.

**4.12.5.3 Limiting Values of the Reinforcement Index.** The reinforcement index  $\omega_p$ , a measure of the percentage of reinforcement in the section, is given by

$$\omega_p = \frac{A_{ps}f_{ps}}{bd_p f'_c} = \rho_p \frac{f_{ps}}{f'_c} \quad (4.53)$$

**Minimum Reinforcement.** If the percentage of reinforcement is too small, the concrete section will be too weak to resist the tensile stress level after cracking and the section will behave almost as a plain section, with premature abrupt failure through rupture of the reinforcement. Hence, a minimum percentage  $\rho_{\min}$  with a minimum  $\omega_{p \min}$  has to be observed in the design in order to prevent such a failure. The total amount of prestressed and nonprestressed reinforcement required by the ACI should not be less than that required to develop a factored moment  $M_u = \phi M_n$  such that

$$M_u \geq 1.2M_{cr} \quad (4.54a)$$

where  $M_{cr}$  is based on a modulus of rupture  $f_r = 7.5\sqrt{f'_c}$ . An exception can be made where the flexural member has shear and flexural strengths at least twice those of the factored loads in Equations 4.31. Also, the minimum area of bonded nonprestressed reinforcement in beams in accordance with the ACI code has to be computed as

$$\text{Min } A_s = 0.004A_t \quad (4.54b)$$

where  $A_t$  is that part of the cross section between the flexural tension face and the center of gravity cgc of the gross section (in.<sup>2</sup>). This reinforcement has to be uniformly distributed over the precompressed tensile zone as close as possible to the extreme tension fibers.

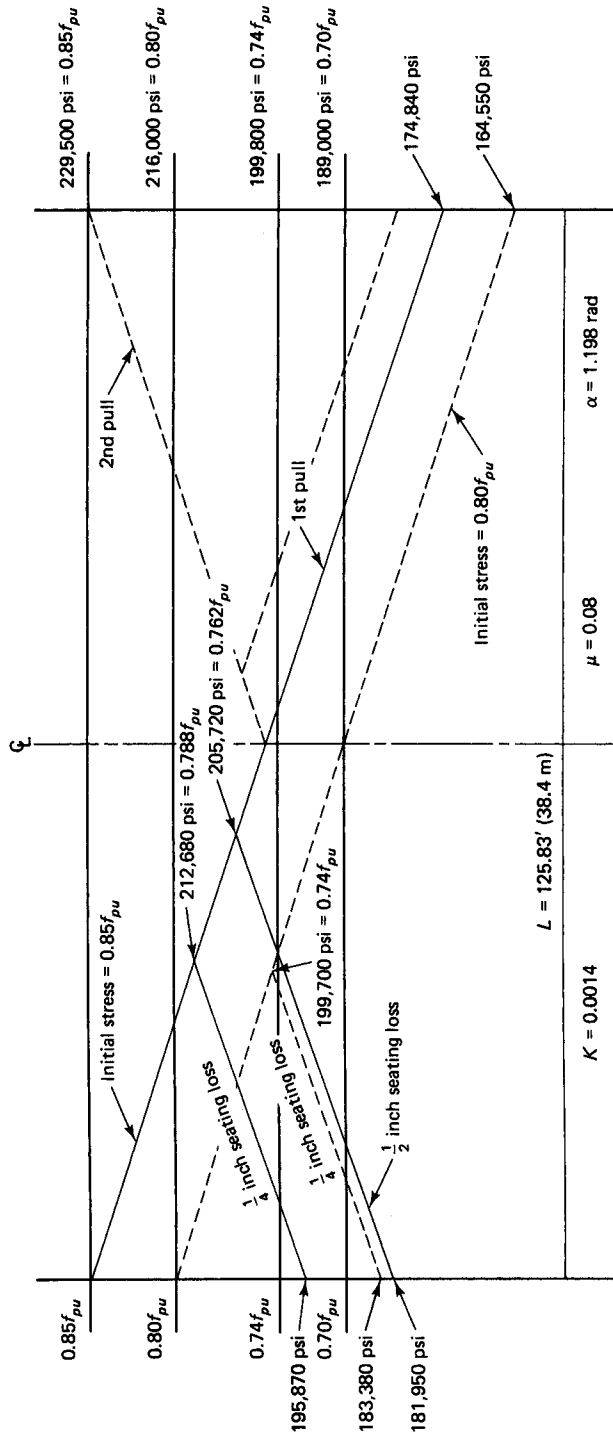


Figure 4.49 Stress diagram for unbonded tendons with various values of initial stress and seating loss (100,000 psi = 689.5 MPa).

In two-way flat plates, where the tension stress in the concrete at service load exceeds  $2\sqrt{f'_c}$ , bonded nonprestressed steel is required such that

$$A_s = \frac{N_c}{0.5f_y} \quad (4.55a)$$

where  $f_y \leq 60,000$  psi

$N_c$  = tensile force in the concrete due to unfactored dead plus live loads ( $D + L$ ).

In the negative-moment areas of slabs at column support, the minimum area of nonprestressed steel in each direction should be

$$A_s = 0.00075hl \quad (4.55b)$$

where  $h$  = total slab thickness

$l$  = span length in the direction parallel to that of the reinforcement being determined.

The reinforcement  $A_s$  has to be distributed with a slab width between lines that are  $1.5h$  outside the faces of the column support, with at least four bars or wires to be provided in each direction and a spacing not to exceed 12 in.

**Maximum Reinforcement.** If the percentage of reinforcement is too large, the concrete section behaves as if it were overreinforced. As a result, a nonductile failure would occur by initial crushing of the concrete at the compression fibers since the reinforcement at the tension side cannot yield first. Reinforced concrete beams always have to be designed as underreinforced with a minimum strain  $\epsilon_t = 0.005$ , as discussed in Sections 4.12.3 and 4.12.4.

In prestressed beams, however, it is not always possible to impose an underreinforced condition. The prestressing forces  $P_i$  and  $P_e$  at transfer and service load also control the value of the area of the tensile reinforcement needed, including the area of the nonprestressed reinforcement. Additionally, the yield strength, and in turn the yield strain value of the prestressing steel is not well defined. Consequently, the prestressed beam designed to satisfy all the service-load requirements could behave as either underreinforced or overreinforced at the limit state of ultimate-load design, particularly if it is a partially prestressed beam.

In order to ensure ductility of behavior, the percentage of reinforcement should be such that the reinforcement index,  $\omega_p$ , does not exceed  $0.36\beta_1$  noting that  $0.32\beta_1$  is comparable to 0.005 in./in., as discussed in Section 4.12.4. The ACI Code, in an indirect measure to limit the reinforcement percentage, requires determining the tension zone in Fig. 4.45 that applies to the analyzed beam section in order to choose the applicable  $\phi$  factor for the design moment  $M_u$ . This is established by finding the ratio  $c/d_t$  at the ultimate limit state, hence the controlling  $\phi$  value for  $M_u = \phi M_n$ , where  $c$  is the depth of the the neutral axis =  $a/\beta_1$ , and  $a$  is the depth of the equivalent rectangular block. Also,  $M_u/M_{cr}$  has to be  $\geq 1.2$  in order to prevent abrupt flexure failure immediately after cracking.

$$\beta_1 = 0.85 - \frac{0.05(f'_c - 4,000)}{1,000} \geq 0.65 \quad (4.56)$$

for a rectangular section with prestressing steel only,

$$\omega_p = \rho_p \frac{f_{ps}}{f'_c} \leq 0.32\beta_1 \quad (4.57a)$$

for rectangular sections with tensile and compressive mild steel,

$$\left[ \omega_p + \frac{d}{d_p} (\omega - \omega') \right] \leq 0.36\beta_1 \quad (4.57b)$$

where

$$\omega = \frac{A_s f_y}{b d f'_c}$$

and

$$\omega' = \frac{A'_s f_y}{b d f'_c}$$

finally, for flanged sections,

$$\left[ \omega_{pw} + \frac{d}{d_p} (\omega_w - \omega'_w) \right] \leq 0.36\beta_1 \quad (4.57c)$$

where  $\omega_{pw}$ ,  $\omega_w$ , and  $\omega'_w$  are computed in the same manner as in Equation 4.57a, b, except that the web width  $b_w$  is used in the denominators of these equations. Note that the terms  $\omega_{ps}$ ,  $(\omega_p + (d/d_p)(\omega - \omega'))$ , and  $(\omega_{pw} + (d/d_p)(\omega_w - \omega'_w))$  are each equal to  $0.85a/d_p$ , where  $a$  is the depth of the equivalent rectangular concrete compressive block as follows:

(a) In rectangular sections and in flanged sections in which  $a \leq h_f$ ,

$$\begin{aligned} \left[ \omega_p + \frac{d}{d_p} (\omega - \omega') \right] &= \left[ \frac{A_{ps} f_{ps}}{b d_p f'_c} + \frac{d}{d_p} \left( \frac{A_s f_y}{b d f'_c} - \frac{A'_s f_y}{b d f'_c} \right) \right] \\ &= \frac{A_{ps} f_{ps} + A_s f_y - A'_s f_y}{b d_p f'_c} = \frac{0.85 f'_c a b}{b d_p f'_c} = \frac{0.85 a}{d_p} \end{aligned}$$

(b) In flanged sections in which  $a > h_f$ , let  $C_F$  be the resultant concrete compression force in outstanding flanges. Then,

$$\begin{aligned} \left[ \omega_{pw} + \frac{d}{d_p} (\omega_w - \omega'_w) \right] &= \left[ \frac{(A_{ps} f_{ps} - C_F)}{b_w d_p f'_c} + \frac{d}{d_p} \left( \frac{A_s f_y}{b_w d f'_c} - \frac{A'_s f_y}{b_w d f'_c} \right) \right] \\ &= \frac{A_{ps} f_{ps} + A_s f_y - A'_s f_y - C_F}{b_w d_p f'_c} \quad (4.57d) \\ &= \frac{\text{compression force in web}}{b_w d_p f'_c} \\ &= \frac{0.85 f'_c b_w a}{b_w d_p f'_c} = \frac{0.85 a}{d_p} \end{aligned}$$

An exception can be made in Equations 4.57a, b, and c, provided that the design moment strength does not exceed the moment strength based on the compression portion of the moment couple. In other words, unless a strain compatibility analysis is performed, the overreinforced prestressed beam moment strength should be determined from the empirical expression

$$M_n = 0.25 f'_c b d^2 \quad (4.58a)$$

for rectangular sections, and

$$M_n = 0.25 f'_c b_w d^2 + 0.85 f'_c (b - b_w) h_f (d - 0.5 h_f) \quad (4.58b)$$

for flanged sections. These equations can be modified as follows:

(a) For the overreinforced rectangular section,

$$M_n = f'_c b d_p^2 (0.36\beta_1 - 0.08\beta_1^2) \quad (4.59a)$$

(b) For the overreinforced flanged section,

$$M_n = f'_c b_w d_p^2 (0.36\beta_1 - 0.08\beta_1^2) + 0.85f'_c (b - b_w) h_f (d_p - 0.5h_f) \quad (4.59b)$$

In summary, the maximum reinforcement index  $\omega$  to be allowed should not exceed  $0.85 a/d_p$  (or  $0.85 a/d_f$ ) in order to ensure ductile behavior through limiting the reinforcement percentage. However, the ACI 318 Code as previously discussed, indirectly stipulates limiting the reinforcement percentage by setting a  $\phi$  value in the tensile zones of Fig. 4.45 from the  $c/d_f$  ratio corresponding to low tensile strain at the limit state at failure.

**4.12.5.4 Limit State in Flexure at Ultimate Load in Nonbonded Tendons.** The discussion presented in Sections 4.12.1 and 4.12.2 defines the design and analysis process for pretensioned beams, where the concrete is cast around the prestressed tendons, thereby achieving full bond, as well as for post-tensioned beams, where the tendons are fully grouted under pressure after the tendons are prestressed.

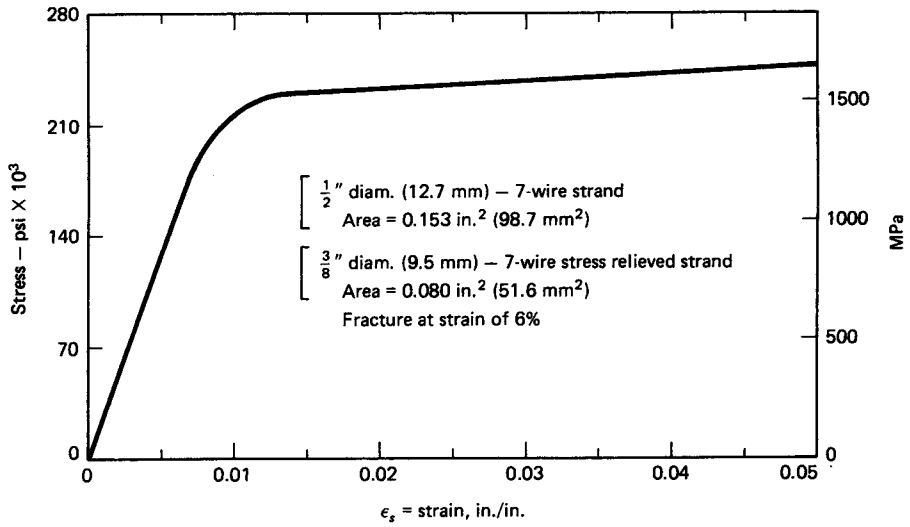
Post-tensioned tendons that are not grouted or that are asphalt coated (many in the United States) are nonbonded tendons. Consequently, as the superimposed load acts on the beam, slip results between the tendons and the surrounding concrete, permitting a uniform deformation along the entire length of the prestressing tendon. As cracks develop at the critical high-moment zones, the increase in the steel tensile stress is not concentrated at the cracks, but is uniformly distributed along the freely sliding tendon. As a result, the net increase in strain and stress is less in the nonbonded case than in the case of bonded tendons as the load continues to increase to the ultimate. Hence a lesser number of cracks, but of larger width, develops in nonbonded prestressing (Ref 4.4). The final stress in the prestressed tendons at ultimate load would be only slightly higher than the effective prestress  $f_{pe}$ .

In order to ensure a structure with good serviceability performance, a reasonable percentage of nonprestressed steel has to be used, within the limitations mentioned in Section 4.12.5.3. The nonprestressed reinforcement controls the flexural crack development and width, and contributes to substantially increasing the moment strength capacity  $M_n$  of the section. It undergoes a strain larger than its yield strain, since its deformation at the postelastic range has to be compatible with the deformation of the adjacent prestressing strands. Hence, the stress level in the nonprestressed steel will always be higher than its yield strength at ultimate load. Figure 4.50 shows a typical stress-strain diagram for a 270-K 7-wire  $\frac{1}{2}$ -in. prestressing strand, while Fig. 4.51 schematically illustrates the relative stresses of the prestressed and the nonprestressed steel and seating losses.

From this discussion, it can be concluded that the expressions presented for the  $M_n$  calculations of the nominal moment strength for bonded beams can be equally used for nonbonded elements. Note that while it is always advisable to grout the post-tensioned tendons, it is sometimes not easy to do so, as, for example, in two-way slab systems or shallow-box elements, where the concrete thickness is small. Also, consideration has to be given to the cost of pressure grouting in cases where there is a congestion of tendons.

## 4.13 PRELIMINARY ULTIMATE-LOAD DESIGN

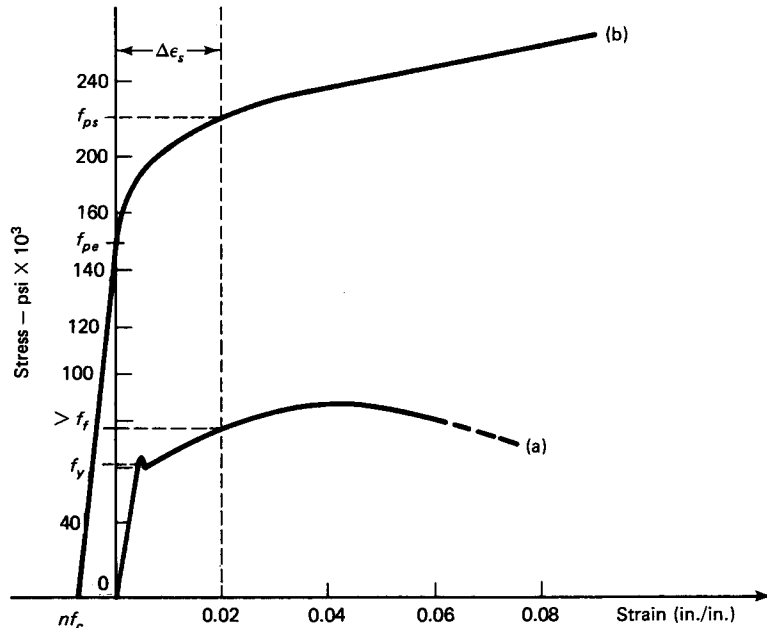
If the preliminary design starts at the ultimate-load level, the required design moment  $M_u = \phi M_n$  has to be at least equal to the factored moment  $M_u$ . The first trial depth has to be based on a reasonable span-to-depth ratio, with the top flange width determined by whether the beam is for residential floors or parking garages, where a double-T-section or a hollow-box shallow section is preferable, or whether the beam is intended to support



**Figure 4.50** Typical stress-strain relationship of 7-wire 270-K prestressing strand.

a bridge deck with spacing decided by load and the number of lanes, where an I-section might be preferable.

As a rule of thumb, the average depth of a prestressed beam is about 75 percent of the depth of a comparably loaded reinforced concrete beam. Another guideline for an initial trial is to use 0.6 in. of depth per foot of span. Once a first-trial depth is chosen, a determination is made of the other geometrical properties of the section.



**Figure 4.51** Stress-strain diagrams for reinforcement. (a) Nonprestressed steel. (b) Prestressed steel (100,000 psi = 689.5 MPa).

Assume that the center of gravity of the prestressing steel is approximately  $0.85/h$  from the middepth of the flange. Then the lever arm of the moment couple  $jd \cong 0.80h$ . Assume also that the nominal strength of the prestressed steel is  $f_{ps} \cong 0.90 f_{pu}$ . Then the area  $A_{ps}$  of the prestressing tendons is

$$A_{ps} = \frac{M_u/\phi}{0.9f_{pu}(0.80h)} \quad (4.60a)$$

or

$$A_{ps} = \frac{M_n}{0.72f_{pu}h} \quad (4.60b)$$

If the compressive block depth  $a$  equals the flange thickness  $h_f$ , the volume of the compressive block of Figure 4.44(d) in terms of the area  $ba = A'_c$  is

$$C = 0.85f'_c A'_c$$

$$T = 0.9f_{pu}A_{ps} = \frac{M_n}{0.8h}$$

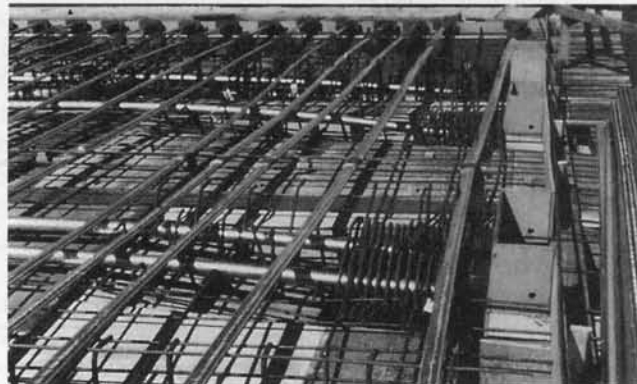
From the equilibrium of forces,  $C = T$ . Hence, the area of the compression flange is

$$A'_c = \frac{M_n}{0.85f'_c(0.8h)} = \frac{M_n}{0.68f'_c h} \quad (4.61)$$

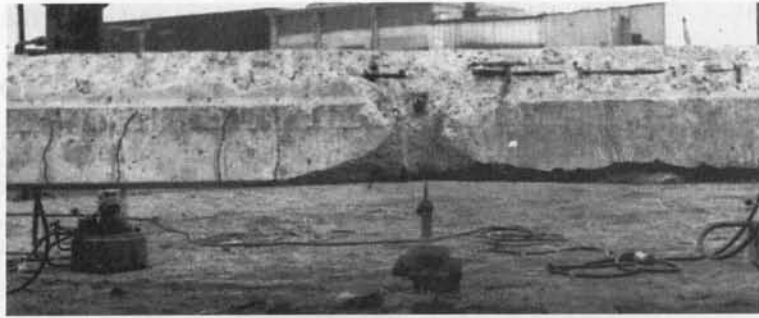
Once the width of the flange is chosen for the first trial and the beam depth is known, the web thickness can be chosen based on the shear requirements to be discussed in Chapter 5. Thereafter, by trial and adjustment, one can select the ideal section for the particular design requirement conditions and proceed to analyze the stresses for the service-load conditions.

#### 4.14 SUMMARY STEP-BY-STEP PROCEDURE FOR LIMIT-STATE-AT-FAILURE DESIGN OF THE PRESTRESSED MEMBERS

1. Determine whether or not partial prestressing is to be chosen, using an effective percentage of nonprestressed steel. Choose a trial depth  $h$  based on either 0.6 in. per ft of span or 75 percent of the depth needed for reinforced concrete sections after calculating the required nominal strength  $M_n = M_u/\phi$ .



**Photo 4.14** Bridge deck prestressing reinforcement set up prior to concreting.



**Photo 4.15** Full-scale bridge test (Nawy, Goodkind).

2. Select a trial flange thickness such that the total concrete area of the flange  $A'_c \cong M_n/0.68f'_c h$ , based on choosing a flange width dictated by planning requirements and spacing of beams. Choose a preliminary area of prestressing steel  $A_{ps} = M_n/0.72f_{pu} h$ .
3. Use a reasonable value for the steel stress  $f_{ps}$  at failure for a first trial. If  $f_{pe} < 0.5f_{pu}$ , strain compatibility analysis would thereafter be needed. Determine whether the tendons are bonded or nonbonded. Use the value of the effective prestress  $f_{pe}$  from the service-load analysis if that design was already made. If  $f_{pe} > 0.5f_{pu}$ , use the approximate values from the following applicable cases by ACI procedures:

(a) *Bonded tendons*

$$f_{ps} = f_{pu} \left( 1 - \frac{\gamma_p}{\beta_1} \left\{ \rho_p \frac{f_{pu}}{f'_c} + \frac{d}{d_p} (\omega - \omega') \right\} \right)$$

(b) *Nonbonded tendons, span/depth ratio  $\leq 35$*

$$f_{ps} = f_{pe} + 10,000 + \frac{f'_c}{100\rho_p}$$

(c) *Nonbonded tendons, span/depth ratio  $> 35$*

$$f_{ps} = f_{pe} + 10,000 + \frac{f'_c}{300\rho_p}$$

Note that AASHTO stipulates different expressions for  $f_{ps}$  as shown in Section 12.3.3.

4. Determine whether the trial section chosen should be considered rectangular or flanged by determining the position of the neutral axis,  $c = a/\beta_1$ . If rectangular,

$$a = \frac{A_{ps} f_{ps} + A_s f_y - A'_s f_y}{0.85f'_c b}$$

If flanged,

$$a = \frac{A_{pw} f_{ps}}{0.85f'_c b_w}$$

where  $A_{pw} f_{ps} = A_{ps} f_{ps} + A_s f_y - 0.85f'_c (b - b_w) h_f$

5. If  $h_f$  is larger than  $c$  and  $a$ , analyze the element as a rectangular section singly or doubly reinforced.



6. Find the reinforcement indices  $\omega_p$ ,  $\omega$ , and  $\omega'$  for the case  $a < h_f$  (neutral axis within the flange; hence, use for a rectangular section).
- (a) Rectangular sections with prestressing steel only:

$$\omega_T = \omega_p = \rho_p \frac{f_{ps}}{f'_c} = \frac{A_{ps} f_{ps}}{b d_p f'_c}$$

- (b) Rectangular sections with compression steel in addition to nonprestressed tension steel:

$$\omega_T = \omega_p + \frac{d}{d_p} (\omega - \omega')$$

If the total index in (a) or (b) is less than or equal to  $0.36\beta_1$ , then the moment strength is

$$M_n = A_{ps} f_{ps} \left( d_p - \frac{a}{2} \right) + A_s f_y \left( d - \frac{a}{2} \right) + A'_s f_y \left( \frac{a}{2} - d' \right)$$

7. Find the reinforcement indices  $\omega_{pw}$ ,  $\omega_w$  and  $\omega'_w$  for the case  $a > h_f$  (neutral axis outside the flange), with the total index

$$\omega_T = \omega_{pw} + \frac{d}{d_p} (\omega_w - \omega'_w)$$

The indices are calculated on the basis of the web width  $b_w$ . If the total index  $\omega_T < 0.36\beta_1$ , then

$$M_n = A_{pw} f_{ps} \left( d_p - \frac{a}{2} \right) + A_s f_y (d - d_p) + 0.85 f'_c (b - b_w) h_f \left( d_p - \frac{h_f}{2} \right)$$

where

$$a = \frac{A_{pw} f_{ps}}{0.85 f'_c b_w}$$

and

$$A_{pw} f_{ps} = A_{ps} f_{ps} + A_s f_y - 0.85 f'_c (b - b_w) h_f$$

If the total index  $\omega_T > 0.36\beta_1$ , the section is overreinforced and the nominal strength is

$$M_n = f'_c b_w d_p^2 (0.36\beta_1 - 0.08\beta_1^2) + 0.85 f'_c (b - b_w) h_f (d_p - 0.5h_f)$$

8. Check for the minimum required reinforcement  $A_s > 0.004A$ . Also, check whether  $M_u \geq 1.2M_{cr}$  to ensure the use of adequate nonprestressed tension steel, particularly in nonbonded tendons.
9. Select the size and spacing of the nonprestressed tension reinforcement, and compression reinforcement where applicable.
10. Verify that the design moment  $M_u = \phi M_n$  is equal to or larger than the factored moment  $M_u$ . If not, adjust the design.

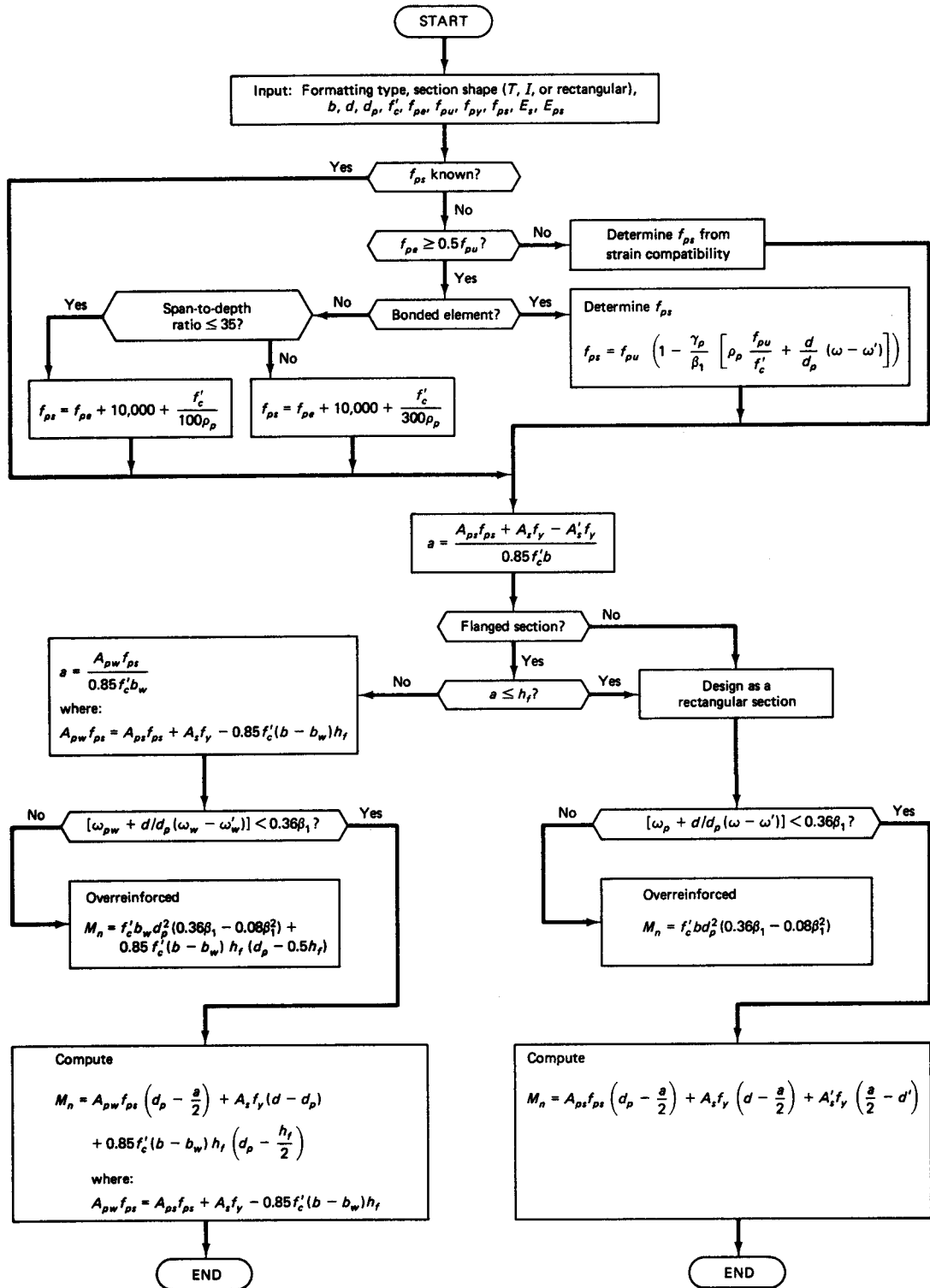
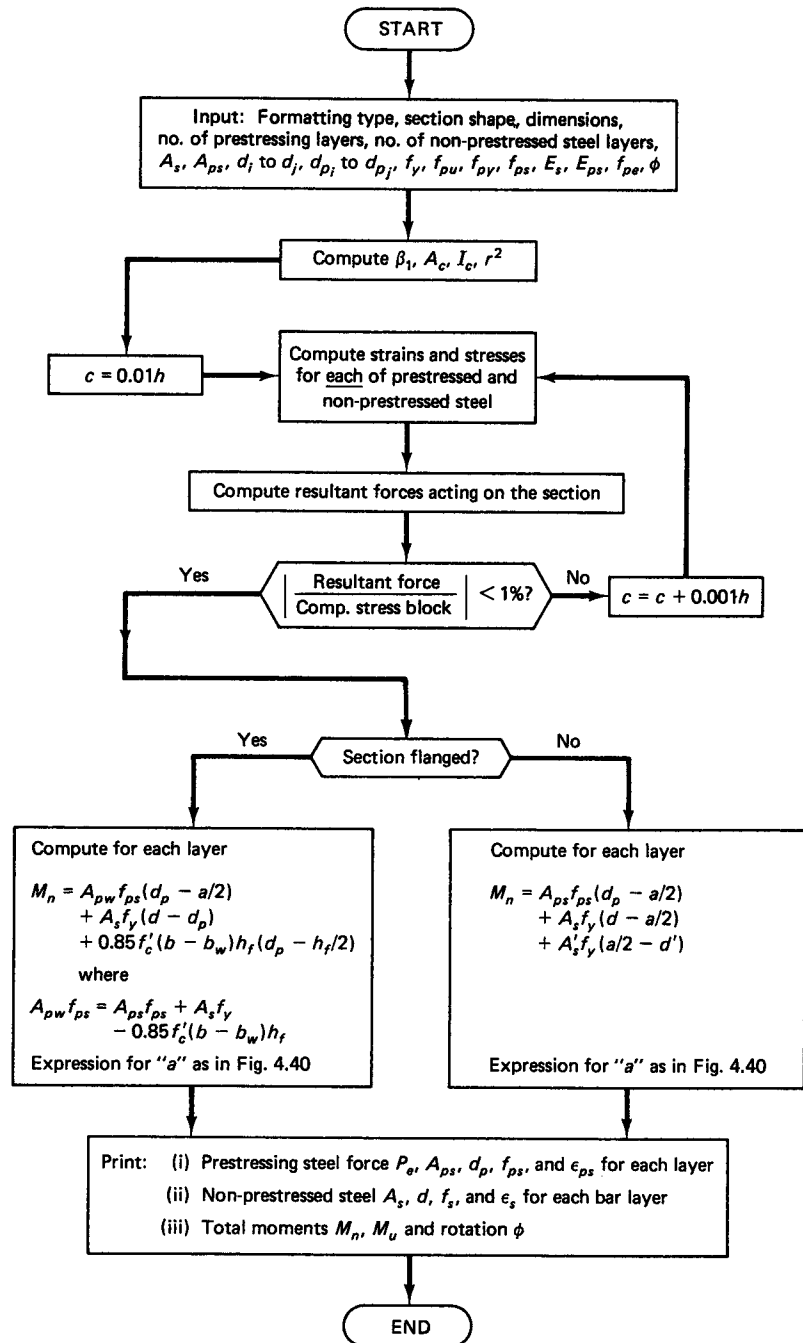


Figure 4.52 Flowchart for flexural analysis of rectangular and flanged prestressed sections based on cgs profile depth.



**Figure 4.53** Flowchart for flexural analysis of rectangular and flanged prestressed sections using compatibility analysis for individual layers of strands and bars.

A flowchart for programming the step-by-step trial-and-adjustment procedure in analyzing the nominal flexural strength of rectangular and flanged prestressed sections taking  $d_p$  as the single-layer cgs depth of tendon is shown in Fig. 4.52. Similarly, a flowchart for programming the nominal flexural strength of prestressed beams using strain-compatibility analysis of *multilayered* strand depths  $d_{p1}$  to  $d_{pn}$  is given in Fig. 4.53. Both charts are applicable to fully prestressed beams that use no mild steel and that allow no tension in the concrete, as well as to “partially prestressed” beams where limited tensile stress is permitted in the concrete through the use of nonprestressed reinforcement. A computer program based on the flowcharts in the two figures can be equally used for a single effective depth  $d_p$  of the cgs tendon profile.

#### 4.15 ULTIMATE-STRENGTH DESIGN OF PRESTRESSED SIMPLY SUPPORTED BEAM BY STRAIN COMPATIBILITY

##### Example 4.9

Design the bonded beam in Example 4.2 by the ultimate-load theory using nonprestressed reinforcement to *partially* carry part of the factored loads. Use strain compatibility to evaluate  $f_{ps}$ , given the *modified* section in Fig. 4.54 with a *composite* 3 in. top slab and

$$f_{pu} = 270,000 \text{ psi (1,862 MPa)}$$

$$f_{py} = 0.85f_{pu} \text{ for stress-relieved strands}$$

$$f_y = 60,000 \text{ psi (414 MPa)}$$

$$f'_c = 5,000 \text{ psi normal-weight concrete (34.5 MPa)}$$

Use 7-wire  $\frac{1}{2}$ -in. dia tendons. The nonprestressed partial mild steel is to be placed with a  $\frac{1}{2}$ -in. clear cover, and no compression steel is to be accounted for. No wind or earthquake is taken into consideration.

**Solution:** From Example 4.2,

$$\text{Service } W_L = 1,100 \text{ plf (16.1 kN/m)}$$

$$\text{Service } W_{SD} = 100 \text{ plf (1.46 kN/m)}$$

$$\text{Assumed } W_D = 393 \text{ plf (5.74 kN/m)}$$

$$\text{Beam span} = 65 \text{ ft (19.8 m)}$$

##### 1. Factored moment (step 1)

$$\begin{aligned} W_u &= 1.2(W_D + W_{SD}) + 1.6W_L \\ &= 1.2(100 + 393) + 1.6(1,100) = 2352 \text{ plf (34.4 kN/m)} \end{aligned}$$

The factored moment is given by

$$M_u = \frac{w_u l^2}{8} = \frac{2352(65)^2 12}{8} = 14,905,800 \text{ in.-lb (1684 kN-m)}$$

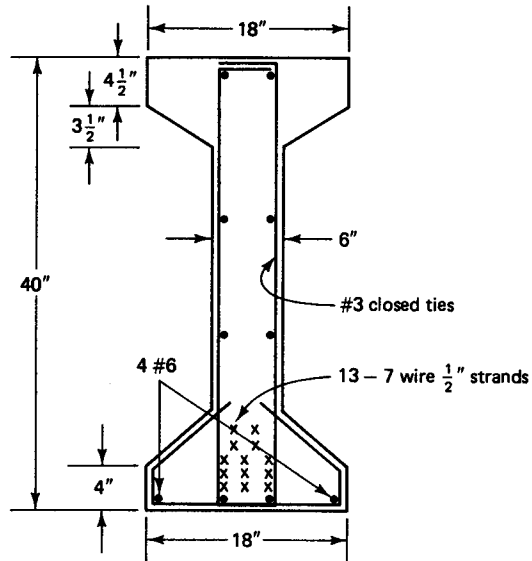
and the required nominal moment strength is

$$M_n = \frac{M_u}{\phi} = \frac{14,905,800}{0.9} = 16,562,000 \text{ in.-lb (1871 kN-m)}$$

##### 2. Choice of preliminary section (step 2)

Assuming a depth of 0.6 in./ft of span, we can have a trial section depth  $h = 0.6 \times 65 \cong 40$  in. (102 cm). Then assume a mild partial steel 4 #6 =  $4 \times 0.44 = 1.76 \text{ in.}^2$  (11.4 cm<sup>2</sup>). From Equation 4.61,

$$A'_c = \frac{M_n}{0.68f'_c h} = \frac{16,562,000}{0.68 \times 5,000 \times 40} = 121.8 \text{ in.}^2 (786 \text{ cm}^2)$$



**Figure 4.54** Midspan section of the beam in Example 4.9.

Assume a flange width of 18 in. Then the average flange thickness =  $121.8/18 \cong 7.0$  in. (178 mm). So suppose the web  $b_w = 6$  in. (152 mm), to be subsequently verified for shear requirements. Then from Equation 4.60b,

$$A_{ps} = \frac{M_n}{0.72f_{pu}h} = \frac{16,562,000}{0.72 \times 270,000 \times 40} = 2.13 \text{ in.}^2 (13.3 \text{ cm}^2)$$

and the number of  $\frac{1}{2}$ -in. stress-relieved wire strands =  $2.13/0.153 = 13.9$ . So try thirteen  $\frac{1}{2}$ -in. tendons.

$$A_{ps} = 13 \times 0.153 = 1.99 \text{ in.}^2 (12.8 \text{ cm}^2)$$

**3. Calculate the stress  $f_{ps}$  in the prestressing tendon at nominal strength using the strain-compatibility approach (step 3)**

The geometrical properties of the trial section are very close to the assumed dimensions for the depth  $h$  and the top flange width  $b$ . Hence, use the following data for the purpose of the example:

$$A_c = 377 \text{ in.}^2$$

$$c_t = 21.16 \text{ in.}$$

$$d_p = 15 + c_t = 15 + 21.16 = 36.16 \text{ in.}$$

$$r^2 = 187.5 \text{ in.}^2$$

$$e = 15 \text{ in. at midspan}$$

$$e^2 = 225 \text{ in.}^2$$

$$e^2/r^2 = 225/187.5 = 1.20$$

$$E_c = 57,000\sqrt{5,000} = 4.03 \times 10^6 \text{ psi } (27.8 \times 10^3 \text{ MPa})$$

$$E_{ps} = 28 \times 10^6 \text{ psi } (193 \times 10^3 \text{ MPa})$$

The maximum allowable compressive strain  $\epsilon_c$  at failure = 0.003 in./in. Assume that the effective prestress at service load is  $f_{pe} \cong 155,000$  psi (1,069 MPa).

$$(a) \quad \epsilon_1 = \epsilon_{pe} = \frac{f_{pe}}{E_{ps}} = \frac{155,000}{28 \times 10^6} = 0.0055 \text{ in./in.}$$

$$P_e = 13 \times 0.153 \times 155,000 = 308,295 \text{ lb}$$

The increase in prestressing steel strain as the concrete is decompressed by the increased external load (see Figure 4.3 and Equation 4.3c) is given as

$$\begin{aligned}\epsilon_2 &= \epsilon_{\text{decomp}} = \frac{P_e}{A_c E_c} \left(1 + \frac{e^2}{r^2}\right) \\ &= \frac{308,295}{377 \times 4.03 \times 10^6} (1 + 1.20) = 0.0004 \text{ in./in.}\end{aligned}$$

- (b) Assume that the stress  $f_{ps} \cong 205,000$  psi as a first trial. Suppose the neutral axis inside the flange is verified on the basis of  $h_f = 3 + 4\frac{1}{2} + 3\frac{1}{2}/2 = 9.25$  in due to the 3 in. topping. Then, from Equation 4.42a

$$\begin{aligned}a &= \frac{A_{ps} f_{ps} + A_s f_y}{0.85 f'_c b} = \frac{1.99 \times 205,000 + 1.76 \times 60,000}{0.85 \times 5,000 \times 18} \\ &= 6.71 \text{ in. (17 cm)} < h_f = 8.00 \text{ in.}\end{aligned}$$

Hence, the equivalent compressive block is inside the flange and the section has to be treated as rectangular.

Accordingly, for 5,000 psi concrete,

$$\beta_1 = 0.85 - 0.05 = 0.8$$

$$c = \frac{a}{\beta_1} = \frac{6.71}{0.80} = 8.39 \text{ in. (22.7 cm)}$$

$$d = 40 - (1.5 + \frac{1}{2} \text{ in. for stirrups} + \frac{5}{16} \text{ in. for bar}) \cong 37.6 \text{ in.}$$

The increment of strain due to overload to the ultimate, from Equation 4.37(c) is

$$\epsilon_3 = \epsilon_c \left(\frac{d-c}{c}\right) = 0.003 \left(\frac{37.6 - 8.39}{8.39}\right) = 0.0104 \text{ in./in.} \gg 0.005 \text{ in./in. O.K.}$$

and the total strain is

$$\begin{aligned}\epsilon_{ps} &= \epsilon_1 + \epsilon_2 + \epsilon_3 \\ &= 0.0055 + 0.0004 + 0.0104 = 0.0163 \text{ in./in.}\end{aligned}$$

From the stress-strain diagram in Figure 4.50 the  $f_{ps}$  corresponding to  $\epsilon_{ps} = 0.0163$  is 230,000 psi.

*Second trial for  $f_{ps}$  value*

Assume

$$f_{ps} = 229,000 \text{ psi}$$

$$a = \frac{1.99 \times 229,000 + 1.76 \times 60,000}{0.85 \times 5,000 \times 18} = 7.34 \text{ in., consider section as a rectangular beam.}$$

$$c = \frac{7.34}{0.80} = 9.17 \text{ in.}$$

$$\epsilon_3 = 0.003 \left(\frac{37.6 - 9.17}{9.17}\right) = 0.0093$$

Then the total strain is  $\epsilon_{ps} = 0.0055 + 0.0004 + 0.0093 = 0.0152$  in./in. From Figure 4.50,  $f_{ps} = 229,000$  psi (1,579 MPa); use

$$A_s = 4 \#6 = 1.76 \text{ in.}^2$$

#### 4. Available moment strength (steps 6 through 10)

From Equation 4.43c, if the neutral axis were to fall within the flange,

$$\begin{aligned}
 M_n &= 1.99 \times 229,000 \left( 36.16 - \frac{7.34}{2} \right) + 1.76 \times 60,000 \left( 37.6 - \frac{7.34}{2} \right) \\
 &= 14,806,017 + 3,583,008 = 18,389,025 \text{ in.-lb (2,078 kN-m)} \\
 &> \text{required } M_n = 16,562,000 \text{ in.-lb, O.K.}
 \end{aligned}$$

A reduction in the area of the mild steel can be made to make the section relatively more efficient since its available moment strength is about 11% larger than the required moment.

### 5. Check for minimum and maximum reinforcement (steps 6 and 9)

(a)  $\text{Min } A_s = 0.004A$

where  $A$  is the area of the part of the section between the tension face and the cgc. From the cross section of Figure 4.8,

$$A = 377 - 18 \left( 4.125 + \frac{1.375}{2} \right) - 6(21.16 - 5.5) \cong 201 \text{ in.}^2$$

$\text{Min } A_s = 0.004 \times 201 = 0.80 \text{ in.}^2 < 1.76 \text{ used, O.K. for non-prestressed reinforcement.}$

As checked in the following Example 4.10,  $M_u = 0.90 \times 18,389 \text{ in.-lb} > 1.2 M_{cr}$ ; hence, the requirement of minimum reinforcement is satisfied for the combined mild and prestressing steel.

(b) The maximum steel index, from Equation 4.57b, is

$$\omega_p + \frac{d}{d_p} (\omega - \omega') \leq 0.36\beta_1 < 0.29 \text{ for } \beta_1 = 0.80$$

and the actual total reinforcement index is

$$\begin{aligned}
 \omega_T &= \frac{1.99 \times 229,000}{18 \times 36.16 \times 5,000} + \frac{37.6}{36.16} \left( \frac{1.76 \times 60,000}{18 \times 37.6 \times 5,000} \right) \\
 &= 0.14 + 0.03 = 0.17 < 0.29, \text{ O.K.}
 \end{aligned}$$

Alternatively, the ACI Code limit strain provisions as given in Fig. 4.45 do not prescribe a maximum percentage of reinforcement. They require that a check be made of the strain  $\epsilon_t$ , at the level of the extreme tensile reinforcement to determine whether the beam is in the tensile, the transition, or the compression zone, for verifying the appropriate  $\phi$  value. In this case, for  $c = 9.17$  and  $d_t = 37.6$  in., and from similar triangles in the strain distribution across the beam depth,

$$\epsilon_t = 0.003 \times (37.6 - 9.17)/9.17 = 0.0093 > 0.005.$$

Hence the beam is in the tensile zone, with  $\phi = 0.90$  as used in the solution and the design is O.K.

### 6. Choice of section for ultimate load (step 11)

From steps 1–5 of the design, the section in Example 4.2 with the modifications shown in Fig. 4.54 has the nominal moment strength  $M_n$  that can carry the factored load, provided that four #6 nonprestressed bars are used at the tension side as a partially prestressed section.

So one can adopt the section for flexure, as it also satisfies the service-load flexural stress requirements both at midspan and at the support. Note that the section could only develop the required nominal strength  $M_n = 16,562,000 \text{ in.-lb}$  by the addition of the nonprestressed bars at the tension face to resist part of the total *required* moment strength. Note also that this section is adequate with a concrete  $f'_c = 5,000 \text{ psi}$ , while the section in Example 4.2 has to have  $f'_c = 6,000 \text{ psi}$  strength in order not to exceed the allowable service-load concrete stresses. Hence, ultimate-load computations are necessary in prestressed concrete design to ensure that the constructed elements can carry all the factored load and are thus an integral part of the total design.

## 4.16 STRENGTH DESIGN OF BONDED PRESTRESSED BEAM USING APPROXIMATE PROCEDURES

### Example 4.10

Design the beam in Example 4.9 as a partially prestressed beam using the ACI approximate procedures if permissible. Use the exact standard section used in Example 4.2 with (a)

bonded prestressing steel, and (b) nonbonded prestressing steel. Neglect the contribution of the compressive nonprestressed steel.

**Solution:**

**1. Section properties (steps 1 and 2)**

The width of the top flange in Example 4.2 is  $b = 18$  in., and its average thickness from Figure 4.8 is

$$h_f = 4\frac{1}{2} + \frac{3\frac{1}{2}}{2} = 6.25 \text{ in}$$

Try four #6 (four 12.7 mm dia) nonprestressed tension steel bars in this cycle in addition to the prestressing reinforcement.

**2. Stress  $f_{ps}$  in prestressing steel at nominal strength (step 3)**

From Example 4.9,

$$f_{pe} \cong 155,000 \text{ psi}$$

$$0.5f_{pu} = 0.50 \times 270,000 = 135,000 \text{ psi}$$

$$f_{pe} > 0.5f_{pu}$$

Hence, one can use the ACI approximate procedure for determining  $f_{ps}$ .

**(A) BONDED CASE**

If the position of the neutral axis is not known, analyze as a rectangular section as follows: From Equation 4.51,

$$f_{ps} = f_{pu} \left( 1 - \frac{\gamma_p}{\beta_1} \left[ \rho_p \frac{f_{pu}}{f'_c} + \frac{d}{d_p} (\omega - \omega') \right] \right)$$

$$\frac{f_{py}}{f_{pu}} = \frac{229,500}{270,000} = 0.85, \text{ use } \gamma_p = 0.40$$

$$A_{ps} = 13 \times 0.153 = 1.99 \text{ in}^2$$

$$A_s = 4 \times 0.44 = 1.76 \text{ in}^2$$

$$\rho_p = \frac{A_{ps}}{bd_p} = \frac{1.99}{18 \times 36.16} = 0.0031$$

$$\omega = \frac{A_s}{bd} \times \frac{f_y}{f'_c} = \frac{1.76}{18 \times 37.6} \times \frac{60,000}{5,000} = 0.0312$$

For  $\omega' = 0$ ,

$$f_{ps} = 270,000 \left( 1 - \frac{0.40}{0.80} \left[ 0.0031 \times \frac{270,000}{5,000} + \frac{37.6}{36.16} (0.0312) \right] \right)$$

$$= 270,000 \times 0.897 = 242,190 \text{ psi (1,670 MPa)}$$

$$a = \frac{1.99 \times 242,190 + 1.76 \times 60,000}{0.85 \times 5,000 \times 18} = 7.68 \text{ in} > h_f = 6.25 \text{ in}$$

Hence, the neutral axis is outside the flange, and analysis has to be based on a T-section. Using in such a case the web width  $b_w$ ,

$$\rho_p = \frac{A_{ps}}{b_w d_p} = \frac{1.99}{6 \times 36.16} = 0.0092$$

$$\omega_w = \frac{A_s}{b_w d} \times \frac{f_y}{f'_c} = \frac{1.76}{6 \times 37.6} \times \frac{60,000}{5,000} = 0.0936$$

$$f_{ps} = 270,000 \left( 1 - \frac{0.40}{0.80} \left[ 0.0092 \times \frac{270,000}{5,000} + \frac{37.6}{36.16} (0.0936 - 0) \right] \right)$$



$$\begin{aligned}
 &= 189,793 \text{ psi (1,309 MPa)} \\
 A_{pw} f_{ps} &= A_{ps} f_{ps} + A_s f_y - 0.85 f'_c (b - b_w) h_f \\
 &= 1.99 \times 189,793 + 1.76 \times 60,000 - 0.85 \times 5,000 (18 - 6) \\
 &\quad \times 6.25 \\
 &= 377,688 + 105,600 - 318,750 = 164,538 \text{ lb} \\
 a &= \frac{164,538}{0.85 \times 5,000 \times 6} = 6.45 \text{ in. (16.4 cm)}
 \end{aligned}$$

### 3. Available nominal moment strength (steps 4–8)

$$\begin{aligned}
 M_n &= A_{pw} f_{ps} \left( d_p - \frac{a}{2} \right) + A_s f_y (d - d_p) + 0.85 f'_c (b - b_w) h_f \left( d_p - \frac{h_f}{2} \right) \\
 &= 164,538 \left( 36.16 - \frac{6.45}{2} \right) + 1.76 (60,000) (37.6 - 36.16) \\
 &\quad + 0.85 (5,000) (18 - 6) \times 6.25 \left( 36.16 - \frac{6.25}{2} \right) = 16,071,226 \text{ in.-lb}
 \end{aligned}$$

(1,816 kN-m) < required  $M_n = 16,562,000 \text{ in.-lb}$  (1871 kN-m), hence the section is inadequate.

Proceed to another trial and adjustment cycle using more nonprestressed reinforcement. Try four #8 bars (four 25 mm dia),  $A_s = 3.16 \text{ in.}^2$  (25 cm<sup>2</sup>). We have

$$\omega_w = \frac{3.16}{6 \times 37.6} \times \frac{60,000}{5,000} = 0.17$$

giving  $f_{ps} = 179,068 \text{ psi}$  and  $A_{pw} f_{ps} = 227,195 \text{ lb}$  (1010 kN). So

$$a = \frac{227,195}{0.85 \times 5,000 \times 6} = 8.9 \text{ in. (22.6 cm)}$$

$$\begin{aligned}
 M_n &= 227,195 \left( 36.16 - \frac{8.9}{2} \right) + 3.16 (60,000) (37.6 - 36.16) \\
 &\quad + 0.85 (5,000) (18 - 6) \times 6.25 \left( 36.16 - \frac{6.25}{2} \right) \\
 &= 18,007,283 \text{ in.-lb (2035 kN-m)} > \text{Required } M_n = 16,562,000 \text{ in.-lb, O.K.}
 \end{aligned}$$

Hence, use four #8 nonprestressed bars at the bottom fibers, and adopt the design for the bonded case.

### (B) NONBONDED CASE

$$\text{Span-to-Depth ratio} = \frac{65 \times 12}{40} = 19.5 < 35$$

Hence, from Equation 4.52a,

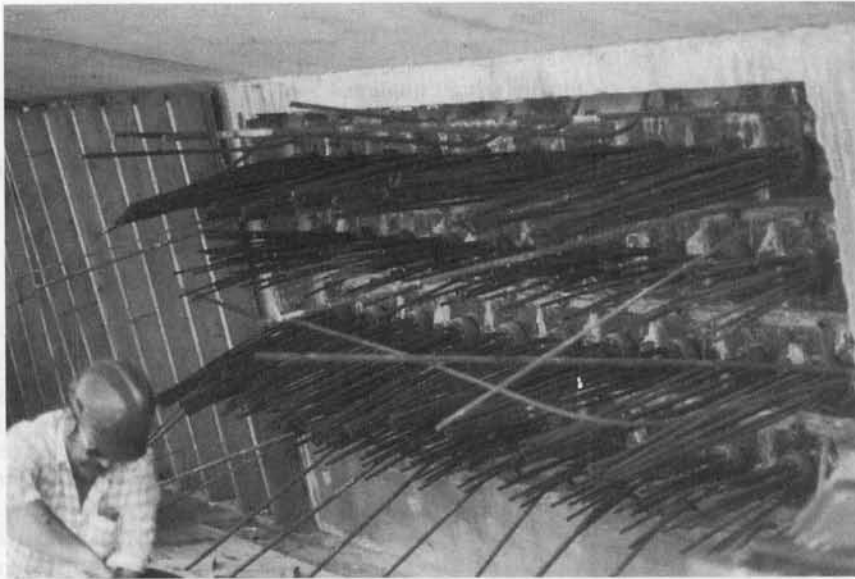
$$\begin{aligned}
 f_{ps} &= f_{pe} + 10,000 + \frac{f'_c}{100\rho_p} = 155,000 + 10,000 + \frac{5,000}{100 \times 1.99 / (6 \times 36.16)} \\
 &= 170,451 \text{ psi (1,175 MPa)}
 \end{aligned}$$

Notice that  $b_w = 6 \text{ in.}$  is used here for  $\rho_p$ , since it is now known that the section behaves like a T-beam, as the neutral axis is below the flange. Thus,

$$f_{ps} = 170,451 \text{ psi (1,175 MPa)}$$

### 1. Selection of nonprestressed steel

Try four #8 nonprestressed tension reinforcements to resist part of the factored moment:



**Photo 4.16** Diaphragm anchorage.

$$A_s = 4 \times 0.79 = 3.16 \text{ in}^2 (19.8 \text{ cm}^2)$$

$$\begin{aligned} A_{pw} f_{ps} &= 1.99 \times 170,451 + 3.16 \times 60,000 - 0.85 \times 5,000(18 - 6)6.25 \\ &= 210,047 \text{ lb} \end{aligned}$$

$$a = \frac{A_{pw} f_{ps}}{0.85 f'_c b_w} = \frac{210,047}{0.85 \times 5,000 \times 6} = 8.24 \text{ in. (20.9 cm)}$$

## 2. Available moment strength (steps 4-8)

From Equation 4.48,

$$\begin{aligned} \text{Available } M_n &= 210,047 \left( 36.16 - \frac{8.24}{2} \right) + 3.16 \times 60,000(37.6 - 36.16) \\ &\quad + 0.85 \times 5,000(18 - 6) \times 6.25 \times \left( 36.16 - \frac{6.25}{2} \right) \\ &= 17,537,057 \text{ in.-lb (1981 kN-m)} \\ &> \text{Req. } M_n = 16,562,000 \text{ in.-lb, O.K.} \end{aligned}$$

## (C) CHECK FOR REINFORCEMENT LIMITS

### 1. Minimum reinforcement

From Equation 4.25, the cracking moment,  $M_{cr}$  is given by

$$M_{cr} = f_r S_b + P_e \left( e + \frac{r^2}{c_b} \right)$$

From Example 4.2,  $f_r = 7.5\sqrt{5,000} = 530.3 \text{ psi (3.7 MPa)}$ . So since  $S_b = 3,750 \text{ in.}^3$ ,  $e = 15 \text{ in.}$ ,  $r^2/c_b = 187.5/18.84 = 9.95 \text{ in.}$ , and  $P_e = 308,255 \text{ lb (1,371 kN)}$ , we get

$$\begin{aligned} M_{cr} &= 530.3 \times 3,750 + 308,295(15 + 9.95) \\ &= 9,680,585 \text{ in.-lb (1,090 kN-m)} \end{aligned}$$

$$1.2M_{cr} = 1.2 \times 9,680,585 = 11,616,702 \text{ in.-lb (1,313 kN-m)}$$

$$\begin{aligned} M_u &= \phi M_n = 0.90 \times 18,026,667 \\ &= 16,224,000 \text{ in.-lb (1,833 kN-m)} \end{aligned}$$

Finally, from Equation 4.54a,

$$M_u > 1.2M_{cr}$$

Hence, the requirement for minimum reinforcement is satisfied for both the non-bonded and the bonded case.

## 2. Maximum reinforcement index

$$\text{Max. allow. } \omega_p = 0.36\beta_1 = 0.36 \times 0.80 = 0.288$$

( $\epsilon_t = 0.005$  in./in. minimum strain is comparable to  $0.32\beta_1$ )

$$\text{From Eq. 4.57d, maximum total } \omega = 0.85a/d_p = \frac{0.85 \times 8.9}{36.16} = 0.209 < 0.288, \text{ O.K.}$$

Alternatively, the ACI Code limit strain provisions as given in Fig. 4.45 do not prescribe a maximum percentage of reinforcement. They require that a check be made of the strain  $\epsilon_t$ , at the level of the extreme tensile reinforcement to determine whether the beam is in the tensile, the transition, or the compression zone, for verifying the appropriate  $\phi$  value. In this case, for  $c = a/\beta_1 = 8.9/0.80 = 11.1$  and  $d_t = 37.6$  in., and from similar triangles in the strain distribution across the beam depth,

$$\epsilon_t = 0.003 \times (37.6 - 11.1) / 11.6 = 0.0072 > 0.005.$$

Hence the beam is in the tensile zone, with  $\phi = 0.90$  as used in the solution and the design is O.K.

Accordingly, adopt the design that uses the concrete section in Example 4.2 and include four #8 nonprestressed steel bars at the tension side. Note that the moment strength capacity of the non-bonded section for the same area of nonprestressed steel is less than the moment strength capacity of the bonded section, which is expected.

If  $f'_c = 6,000$  psi would have been used in the strength design in this example, as it was in the service-load design of this section in Example 4.2, less mild steel reinforcement would have been needed.

## 4.17 SI FLEXURAL DESIGN EXPRESSION

$$f'_{ci} = 0.8f'_c$$

$$f_{ci} = 0.60f'_{ci}$$

$$f_{ii} = \frac{1}{4}\sqrt{f'_c} \text{ (midspan)}$$

$$= \frac{1}{2}\sqrt{f'_{ci}} \text{ (support)}$$

$$f_c = 0.45f'_c \text{ due to prestress + sustained load}$$

$$f_c = 0.6f'_c \text{ due to prestress + total load if it includes transient load}$$

*Stress at transfer*

$$f^t = -\frac{P_i}{A_c} \left( 1 - \frac{ec_t}{r^2} \right) - \frac{M_d}{S^t} \leq f_{ii} \quad (4.1a)$$

$$f_b = -\frac{P_i}{A_c} \left( 1 + \frac{ec_b}{r^2} \right) + \frac{M_D}{S_b} \leq f_{ci} \quad (4.16)$$

*Effective stress after losses*

$$f^t = -\frac{P_e}{A_c} \left( 1 - \frac{ec_t}{r^2} \right) - \frac{M_D}{S^t} \leq f_i \quad (4.2a)$$

$$f_b = -\frac{P_e}{A_c} \left( 1 + \frac{ec_b}{r^2} \right) + \frac{M_D}{S_b} \leq f_c \quad (4.2b)$$

*Service load final stress*

$$f^t = -\frac{P_e}{A_c} \left( 1 - \frac{ec_t}{r^2} \right) - \frac{M_T}{S^t} \leq f_c \quad (4.3a)$$

$$f_b = -\frac{P_e}{A_c} \left( 1 + \frac{ec_b}{r^2} \right) + \frac{M_T}{S_b} \leq f_t \quad (4.3b)$$

$$f_{\text{decomp}} = \frac{P_e}{A_c} \left( 1 + \frac{e^2}{r^2} \right) \quad (4.3c)$$

$$S^t \geq \frac{(1 - \gamma)M_D + M_{SD} + M_L}{\gamma f_{ti} - f_c} \quad (4.4a)$$

$$S_b \geq \frac{(1 - \gamma)M_D + M_{SD} + M_L}{f_t - \gamma f_{ci}} \quad (4.4b)$$

$$e_e = (f_{ti} - \bar{f}_{ci}) \frac{S^t}{P_i} \quad (4.5c)$$

$$k_b = \frac{r^2}{c_t}, \quad k_t = \frac{r^2}{c_b} \quad (4.6)$$

$$b_m = \frac{E_{ct}}{E_c} (b) = n_c b \quad (4.23)$$

*Unshored case*

$$f^t = -\frac{P_e}{A_c} \left( 1 - \frac{ec_t}{r^2} \right) - \frac{M_D + M_{SD}}{S_t} - \frac{M_{CSD} + M_L}{S'_c} \quad (4.19a)$$

$$f_b = -\frac{P_e}{A_c} \left( 1 + \frac{ec_b}{r^2} \right) + \frac{M_D + M_{SD}}{S_b} + \frac{M_{CSD} + M_L}{S_{cb}} \quad (4.19b)$$

*Shored case*

$$f^t = -\frac{P_e}{A_c} \left( 1 - \frac{ec_t}{r^2} \right) - \frac{M_D}{S^t} - \frac{M_{SD} + M_{CSD} + M_L}{S'_c} \quad (4.22a)$$

$$f_b = -\frac{P_e}{A_c} \left( 1 + \frac{ec_b}{r^2} \right) + \frac{M_d}{S_b} + \frac{M_{SD} + M_{CSD} + M_L}{S_{cb}} \quad (4.22b)$$

Equation 4.51 for bonded tendons

$$f_{ps} = f_{pu} \left( 1 - \frac{\gamma_p}{\beta_1} \left[ \rho_p \frac{f_{pu}}{f'_c} + \frac{d}{d_p} (\omega - \omega') \right] \right) \text{MPa}$$

where  $\gamma_p = 0.55$  for  $f_{py}/f_{pu} \geq 0.80$   
 $= 0.40$  for  $f_{py}/f_{pu} \geq 0.85$   
 $= 0.28$  for  $f_{py}/f_{pu} \geq 0.90$

Equation 4.52 for nonbonded tendons

$$f_{ps} = f_{pe} + 70 + \frac{f'_c}{100\rho_p} \text{ MPa for } \frac{\text{span}}{\text{depth}} \leq 35$$

$$f_{ps} = f_{pe} + 70 + \frac{f'_c}{300\rho_p} \text{ MPa for } \frac{\text{span}}{\text{depth}} > 35$$

$$\text{MPa} = \text{N/mm}^2 = 106 \text{ N/m}^2$$

$$(1b) 4.448 = \text{N}$$

$$(\text{psi}) 0.006895 = \text{MPa}$$

$$(\text{lb/ft}) 14.593 = \text{N/m}$$

$$(\text{in.-lb}) 0.113 = \text{N-m}$$

$$1 \text{ Kg force} = 9.806 \text{ N}$$

### 4.17.1 SI Flexural Design of Prestressed Beams

#### Example 4.11

Solve Example 4.10 using SI units. Tendons are bonded.

Data:

$$A_c = 5045 \text{ cm}^2$$

$$b = 45.7 \text{ cm}$$

$$b_w = 15.2 \text{ cm}$$

$$I_c = 7.04 \times 10^6 \text{ cm}^4$$

$$r^2 = 1,394 \text{ cm}^2$$

$$c_b = 89.4 \text{ cm}$$

$$c' = 32.5 \text{ cm}$$

$$e_e = 84.2 \text{ cm}$$

$$e_c = 60.4 \text{ cm}$$

$$S_b = 78,707 \text{ cm}^3$$

$$S_t = 216,210 \text{ cm}^3$$

$$w_D = 11.9 \times 10^3 \text{ kN/m}$$

$$w_{SD} = 1,459 \text{ N/m}$$

$$w_L = 16.1 \text{ kN/m}$$

$$l = 19.8 \text{ m}$$

$$f'_c = 34.5 \text{ MPa}$$

$$f_{pi} = 1,300 \text{ MPa}$$

$$f_{pu} = 1,860 \text{ MPa}$$

$$f_{py} = 1,580 \text{ MPa}$$

$$\text{Prestress loss } \gamma = 18\% \quad f_y = 414 \text{ MPa}$$

$$A_{ps} = 13 \text{ tendons, diameter } 12.7 \text{ mm } (A_{ps} = 99 \text{ mm}^2)$$

$$= 13 \times 99 = 1,287 \text{ mm}^2$$

$$\text{Required } M_n = 16.5 \times 10^6 \text{ in.-lb} = 1871 \text{ kN-m}$$

#### Solution:

##### 1. Section properties (Steps 1 and 2)

$$\text{Flange width } b = 18 \text{ in.} = 45.7 \text{ cm}$$

$$\text{Average thickness } h_f = 4.5 + \frac{1}{2}(3.5) \cong 6.25 \text{ in.} = 15.7 \text{ cm}$$

Try 4 No. 20 M mild steel bars for partial prestressing (diameter = 19.5 mm,  $A_s = 300 \text{ mm}^2$ ).

$$A_s = 4 \times 300 = 1,200 \text{ mm}^2$$

##### 2. Stress $f_{ps}$ in prestressing steel at nominal strength and neutral axis position (Step 3)

$$f_{pe} = \gamma f_{pi} = 0.82 \times 1,300 \cong 1,066 \text{ MPa}$$

##### Verify Neutral Axis Position

If outside flange, its depth has to be greater than  $a = A_{pw} f_{ps} / 0.85 f'_c b_w$

$0.5 f_{pu} = 0.50 \times 1,860 = 930 \text{ MPa} < 1,066$ , hence, one can use ACI approximate procedure for determining  $f_{ps}$ . From equation 4.51,

$$f_{ps} = f_{pu} \left( 1 - \frac{\gamma_p}{\beta_1} \left[ \rho_p \frac{f_{pu}}{f'_c} + \frac{d}{d_p} (\omega - \omega') \right] \right)$$

$$d_p = 36.16 \text{ in.} = 91.8 \text{ cm}, d = 37.6 \text{ in.} = 95.5 \text{ cm}$$

$$\frac{f_{py}}{f_{pu}} = \frac{1,580}{1,860} = 0.85, \text{ use } \gamma_p = 0.40$$

$$\rho_p = \frac{A_{ps}}{bd_p} = \frac{1,287}{457 \times 918} = 0.00306$$

$$\rho = \frac{A_s}{bd} = \frac{1,200}{457 \times 955} = 0.00275$$

$$\omega_p = \frac{A_{ps}}{bd_p} \times \frac{f_{ps}}{f'_c} = 0.00306 \times \frac{1,674}{34.5} = 0.14$$

$$\omega = \frac{A_s}{bd} \times \frac{f_y}{f'_c} = 0.00275 \times \frac{414}{34.5} = 0.033$$

$$\omega' = 0$$

$$\text{For } f'_c = 34.5 \text{ MPa}, \beta_1 = 0.80$$

$$f_{ps} = 1,860 \left( 1 - \frac{0.40}{0.80} \left[ 0.00306 \times \frac{1,860}{34.5} + \frac{955}{918} \times 0.033 \right] \right)$$

$$= 1,860(1 - 0.1) = 1,674 \text{ MPa}$$

From Equation 4.47a,

$$a = \frac{A_{pw}f_{ps}}{0.85f'_c b_w}$$

$$\text{where } A_{pw}f_{ps} = A_{ps}f_{ps} + A_s f_y - 0.85f'_c(b - b_w)h_f$$

$$A_{pw}f_{ps} = 1,287 \times 1,674 + 1,200 \times 414$$

$$- 0.85 \times 34.5 \times (45.7 - 15.2)15.7 \times 10^2$$

$$= 10^6(2.15 + 0.5 - 1.14) \text{ N} = 1,240 \text{ kN}$$

$$a = \frac{1,240 \times 10}{0.85 \times 34.7 \times 15.2} = 24.7 \text{ cm} > h_f = 15.7 \text{ cm}$$

Hence neutral axis is outside the flange and analysis has to be based on a T-section.

### 3. Available nominal moment strength (Step 4-8)

$$\omega_T = \omega_p + \omega = 0.14 + 0.033 = 0.173 < 0.36\beta_1, \text{ hence, O.K.}$$

hence, maximum reinforcement index  $\omega$  is satisfied.

Alternatively, the ACI Code,  $c/d_t = a/\beta_1 d_t = 15.7/(0.80 \times 91.8) = < 0.375$ .

Hence, the beam is in the tensile zone of Fig. 4.45 and did not exceed the maximum permissible reinforcement, allowing  $\phi = 0.90$  for determining the design moment  $M_u$  as assumed, and thus OK for the chosen reinforcement.

$$M_n = A_{pw}f_{ps} \left( d - \frac{a}{2} \right) + A_s f_y (d - d_p) + 0.85f'_c(b - b_w)h_f \left( d_p - \frac{h_f}{2} \right)$$

$$\text{Available } M_n = 1.24 \times 10^6 \left( 91.8 + \frac{27.7}{2} \right) + 1,200 \times 414(95.5 - 91.8)$$

$$+ 0.85 \times 34.5(45.7 - 15.2)15.7 \left( 91.8 - \frac{15.2}{2} \right) \times 10^2$$

$$= 10^6(96.6 + 1.83 + 118.2) \text{ N-cm} = 2,166 \text{ kN-m}$$

$$> \text{Required } M_n = 1871 \text{ kN-m}$$

hence, section is O.K.

## SELECTED REFERENCES

- 4.1 ACI Committee 318. *Building Code Requirements for Structural Concrete (ACI 318-08)* and Commentary, ACI 318R-08. American Concrete Institute, Farmington Hills, MI, 2008, pp. 465
- 4.2 Nawy, E. G., *Reinforced Concrete—A Fundamental Approach*, 6th Ed., Prentice Hall, Upper Saddle River, NJ: 2009, pp. 936.
- 4.3 Nawy, E. G., and Chiang, J. Y., “Serviceability Behavior of Post-Tensioned Beams.” *Journal of the Prestressed Concrete Institute* 25, Chicago Jan.–Feb. 1980: 74–85.
- 4.4 Nawy, E. G., and Potyondy, G. J., “Moment Rotation, Cracking, and Deflection of Spirally Bound Pretensioned Prestressed Concrete Beams.” *Engineering Research Bulletin No. 51*. New Brunswick, N.J.: Bureau of Engineering Research, Rutgers University, 1970, pp. 1–97.
- 4.5 Post-Tensioning Institute, *Post-Tensioning Manual*, 6th Ed., Phoenix, AZ, 2006.
- 4.6 Nawy, E. G., and Goodkind, H. “Longitudinal Crack in Prestressed Box Beam.” *Journal of the Prestressed Concrete Institute* Chicago, (1969): 38–42.
- 4.7 Yong, Y. K., Gadebeku, C. and Nawy, E. G., “Anchorage Zone Stresses of Post-tensioned Prestressed Beams Subjected to Shear Forces,” *ASCE Structural Division Journal*, Vol. 113, No. 8, August 1987, pp. 1789–1805.
- 4.8 Nawy, E. G., and Huang, P. T. “Crack and Deflection Control of Pretensioned Prestressed Beams.” *Journal of the Prestressed Concrete Institute* 22 (1977): 30–47.
- 4.9 Prestressed Concrete Institute. *PCI Design Handbook, Precast and Prestressed Concrete*. 5th ed. Prestressed Concrete Institute, Chicago, 1999.
- 4.10 Gerwick B. C., *Construction of Prestressed Concrete Structures*. 3rd Ed., CRC Press, Boca Raton, FL, 2008.
- 4.11 Nawy, E. G. “Flexural Cracking Behavior of Pretensioned and Post-Tensioned Beams—The State of the Art.” *Journal of the American Concrete Institute*, December 1985, pp. 890–900.
- 4.12 American Association of State Highway and Transportation Officials. *AASHTO Standard Specifications for Highway Bridges*. Washington, D.C.: AASHTO, 18th Ed., Supplements, 2006–2009.
- 4.13 Nilson, A. H. “Flexural Design Equations for Prestressed Concrete Members.” *Journal of the Prestressed Concrete Institute* 14 (1969): 62–71.
- 4.14 Lin, T. Y., and Burns, N. H. *Design of Prestressed Concrete Structures*. John Wiley & Sons, New York, 1981.
- 4.15 Naaman, A. E. *Prestressed Concrete Analysis and Design*. McGraw Hill, New York, 1982.
- 4.16 Federal Highway Administration, “Optimized Sections for High Strength Concrete Bridge Girders,” FHWA Publication No. RD-95-180, Washington, D.C., August 1997, pp. 156.
- 4.17 Collins, M. P. and Mitchell, D., *Prestressed Concrete Structures*, Prentice Hall, Upper Saddle River, NJ, 1991, 1–766 p.
- 4.18 Abeles, P.W., and Bardhan-Roy, B. K. *Prestressed Concrete Designer’s Handbook*. 3d ed. Viewpoint Publications, London, 1981.
- 4.19 Guyon, Y. *Limit State Design of Prestressed Concrete; Vol. 1, Design of Section*. John Wiley & Sons, New York, 1972.
- 4.20 Marshall, W. T., and Mattock, A. H. “Control of Horizontal Cracking in the Ends of Pretensioned Prestressed Concrete Girders.” *Journal of the Prestressed Concrete Institute* 7 (1962): 56–74.
- 4.21 Ezeldin, A., and Balaguru, P. N. “Analysis of Partially Prestressed Beams for Strength and Serviceability Using Microcomputers.” Paper presented at the First Canadian Conference on Computer Applications in Civil Engineering, MacMaster University, Hamilton, Ontario, Canada, May 1986.
- 4.22 Gergely, P., and Sozen, M. A., “Design of Anchorage Zone Reinforcement in Prestressed Concrete Beams.” *Journal of the Prestressed Concrete Institute* 12 (1967): 63–75.
- 4.23 Baker, A. L. L. *The Ultimate Load Theory Applied to the Design of Reinforcement and Prestressed Concrete Frames*. London: Concrete Publications, 1956.
- 4.24 Ellingwood, B., McGregor, J. G., Galambos, T. V., and Cornell, C. A. “Probability Based Load Criteria: Load Factors and Load Combinations.” *Journal of the Structural Division, ASCE* 108 (1982): 978–997.
- 4.25 American National Standards Institute. *Minimum Design Loads for Buildings and Other Structures*, ANSI–ASCE 7-95, 1995, pp. 214.

- 4.26 Stone, W. C., and Breen, J. E. "Design of Post-Tensioned Girder Anchorage Zones." *Journal of the Prestressed Concrete Institute* 29 (1984): 64–109.
- 4.27 Nawy, E. G., Yong, Y. K., and Gadebeku, B. K. "Anchorage Zone Stresses of Post-Tensioned Prestressed Beams." *Proceedings of the International Conference on Structural Mechanics of Reinforced and Prestressed Concrete*, Sept. 1996, Chinese Academy of Sciences, Nanjing Institute of Technology, 1986.
- 4.28 ACI Committee 435, "Control of Deflection in Concrete Structures," ACI Committee Report, E. G. Nawy, Chairman, American Concrete Institute, Farmington Hills, 1995, pp. 77.
- 4.29 Breen J. E., Burdet, O., Roberts, C., Sanders, D., and Wollman, G. "Anchorage Zone Reinforcement for Post-tensioned Concrete Girders," NCHRP Report 356, Transportation Research Board, Washington, D.C., 1994, 204 p.
- 4.30 Nawy E. G., "Cracking of Concrete—ACI and CEB Approaches," *Proceedings, International Conference on Advances in Concrete Technology*, 2nd Edition, V. M. Malhotra, ed., CANMET/ACI, Farmington Hills, MI, 1992, pp 203–242.
- 4.31 Nawy, E. G., *Fundamentals of High Performance Concrete*, 2nd ed. John Wiley and Sons, New York, 2001, 460 pp.
- 4.32 Nawy, E. G., editor-in-chief, *Concrete Construction Engineering Handbook* 2nd ed., CRC Press, Boca Raton, FL, 2008, pp. 1560.

## PROBLEMS

- 4.1 Design, for service-load and ultimate-load conditions, a pretensioned symmetrical I-section beam to carry a sustained superimposed dead load of 750 plf (10.95 kN/m) and a sustained service live load of 1,500 plf (21.90 kN/m) on a 50 ft (15.2 m) simply supported span. Assume that the sectional properties are  $b = 0.5h$ ,  $h_f = 0.2h$ , and  $b_w = 0.40b$ , using the following data:

$$f_{pu} = 270,000 \text{ psi (1,862 MPa)}$$

$$E_{ps} = 28.5 \times 10^6 \text{ psi (196} \times 10^3 \text{ MPa)}$$

$$f'_c = 5,000 \text{ psi (34.5 MPa) normal-weight concrete}$$

$$f'_{ci} = 3,500 \text{ psi (24.1 MPa)}$$

$$f_t = 12\sqrt{f'_c} \text{ assuming deflection is not critical}$$

Sketch the design details, including the anchorage zone reinforcement and arrangement of strands for (a) straight-tendon case, and (b) a harped tendon at the third span points with end eccentricity zero. Assume total prestress losses of 22 percent.

- 4.2 Solve Problem 4.1 if the beam is post-tensioned bonded and the tendon is draped. Use strain compatibility to determine the value of the tendon stress  $f_{ps}$  at nominal strength. Design the anchorage zone reinforcement by the strut-and-tie method.
- 4.3 A double-T pretensioned roof beam is shown in Figure P4.3. It has a simple span of 74 ft (22.6 m) and carries superimposed service live and dead loads of 60 psf (2,873 Pa;  $W_{SD}$  part of load = 25 psf). It also carries a 2-in. (5.1 cm) concrete topping. Design the prestressing reinforcement and the appropriate eccentricities using 270-grade prestressing strands ( $f_{pu} = 1,862 \text{ MPa}$ ) with a total prestress loss of 20 percent. Use the appropriate percentage of nonprestressed mild steel for partial prestressing behavior at the limit state at failure. Assume the strands to be harped at midspan, and sketch the reinforcing details including the anchorage zone strands. Also, draw the distribution of stresses for the various loading stages in your solution. The following data are given:

$$f_{pu} = 270,000 \text{ psi, stress-relieved strands (1,862 MPa)}$$

$$E_{ps} = 28 \times 10^6 \text{ psi (193} \times 10^3 \text{ MPa)}$$

$$f'_c = 5,000 \text{ psi (34.5 MPa) normal-weight concrete}$$

$$f'_c \text{ for topping} = 3,000 \text{ psi (20.7 MPa) normal-weight concrete}$$

$$f'_{ci} = 4,000 \text{ psi}$$

$$V/S = 1.79 \text{ in.}$$



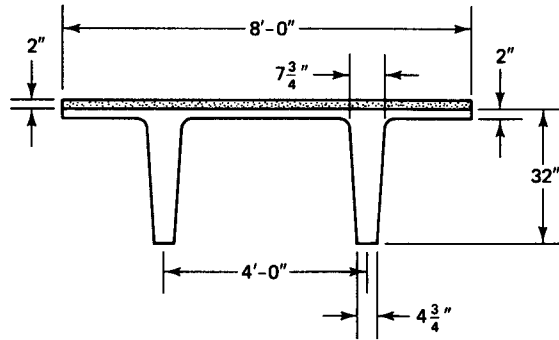


Figure P4.3 Double-T cross section.

$$e_c = 17.71 \text{ in.}$$

	Untopped	Topped
$A_c$	567 in. <sup>2</sup> (3,658 cm <sup>2</sup> )	—
$I_c$	55,464 in. <sup>4</sup>	71,886 in. <sup>4</sup>
$c_b$	21.21 in.	23.66 in.
$c_t$	10.79 in.	10.34 in.
$S_b$	2,615 in. <sup>3</sup>	3,038 in. <sup>3</sup>
$S^t$	5,140 in. <sup>3</sup>	6,952 in. <sup>3</sup>
$W_D$	591 plf	791 plf

- 4.4 A bridge girder has a simple span of 55 ft (16.8 m). It is subjected to a total superimposed service load of 4,600 plf (67.2 kN/m). Design the section as a post-tensioned bonded beam using an AASHTO standard section with parabolically draped tendons. Assume a 7 in. situ-cast slab over the precast section and the following data:

Beams spaced at 7' -6" c. to c.

$$f_{pu} = 270,000 \text{ psi stress relieved (1,862 MPa)}$$

$$E_{ps} = 28 \times 10^6 \text{ psi (193} \times 10^3 \text{ MPa)}$$

$$f'_c = 5,000 \text{ psi (34.5 MPa) normal-weight concrete}$$

$$\text{slab } f'_c = 3,000 \text{ psi (20.7 MPa) normal-weight concrete}$$

$$f'_{ci} = 4,000 \text{ psi (27.6 MPa)}$$

Design the bridge section as unshored for service-load and ultimate-load conditions, and detail all the reinforcement including the anchorage zone steel and the nonprestressed tensile steel. Assume the section to be constant throughout the span, and, for the limit state at failure analysis, find the stress  $f_{ps}$  at nominal strength by (a) the ACI approximate procedure, and (b) strain compatibility. Assume a total prestress loss of 20 percent. Design the anchorage zone reinforcement by the strut-and-tie method and compare the results with those obtained using the linear elastic analysis approach.

- 4.5 Solve problem 4.4 if the draped tendons are nonbonded, and compare the two solutions. Use the tie-and-strut method to design the anchorage zone reinforcement. Assume the tendons are harped at midspan.



# 5

## SHEAR AND TORSIONAL STRENGTH DESIGN

### 5.1 INTRODUCTION

This chapter presents procedures for the design of prestressed concrete sections to resist shear and torsional forces resulting from externally applied loads. Since the strength of concrete in tension is considerably lower than its strength in compression, design for shear and torsion becomes of major importance in all types of concrete structures.

The behavior of prestressed concrete beams at failure in shear or combined shear and torsion is distinctly different from their behavior in flexure: They fail abruptly without sufficient advance warning, and the diagonal cracks that develop are considerably wider than the flexural cracks. Both shear and torsional forces result in shear stress. Such a stress can result in principal tensile stresses at the critical section which can exceed the tensile strength of the concrete.

Photos in this chapter show typical beam shear failure and torsion failure. Notice the curvilinear plane of twist depicting torsional failure caused by the imposed torsional moments. As will be discussed in subsequent sections, the shearing stresses in regular beams are caused, not by direct shear or pure torsion, but by a combination of external

Empire State Performing Arts Center, Albany, New York, Ammann & Whitney design, prestressed concrete shell ring. (*Courtesy, New York Office of General Services.*)

loads and moments. This leads to *diagonal tension*, or flexural shear stresses, in the member. Only in special applications in certain structural systems are direct shear or pure torsion applied. Examples of such cases are corbels or brackets involving direct shear, or a cantilever balcony involving essentially a direct twist on the supporting beam.

## 5.2 BEHAVIOR OF HOMOGENEOUS BEAMS IN SHEAR

Consider the two infinitesimal elements,  $A_1$  and  $A_2$  of a rectangular beam in Figure 5.1(a) made of homogeneous, isotropic, and linearly elastic material. Figure 5.1(b) shows the bending stress and shear stress distributions across the depth of the section. The tensile normal stress  $f_t$  and the shear stress  $v$  are the values in element  $A_1$  across plane  $a_1$ – $a_1$  at a distance  $y$  from the neutral axis. From the principles of classical mechanics, the normal stress  $f$  and the shear stress  $v$  for element  $A_1$  can be written as

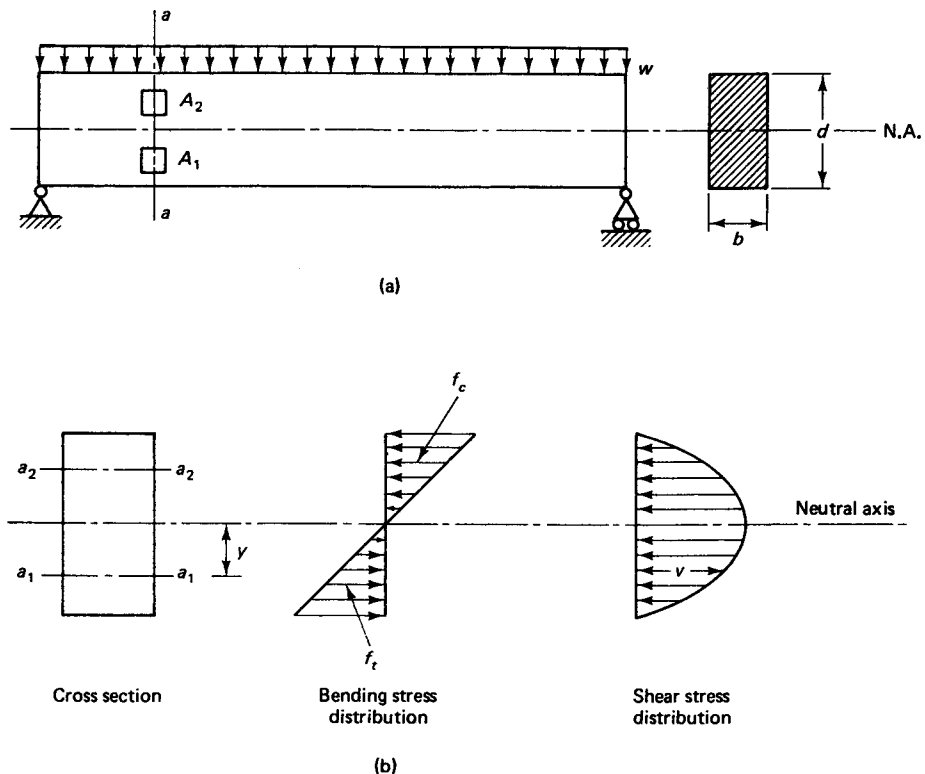
$$f = \frac{My}{I} \quad (5.1)$$

and

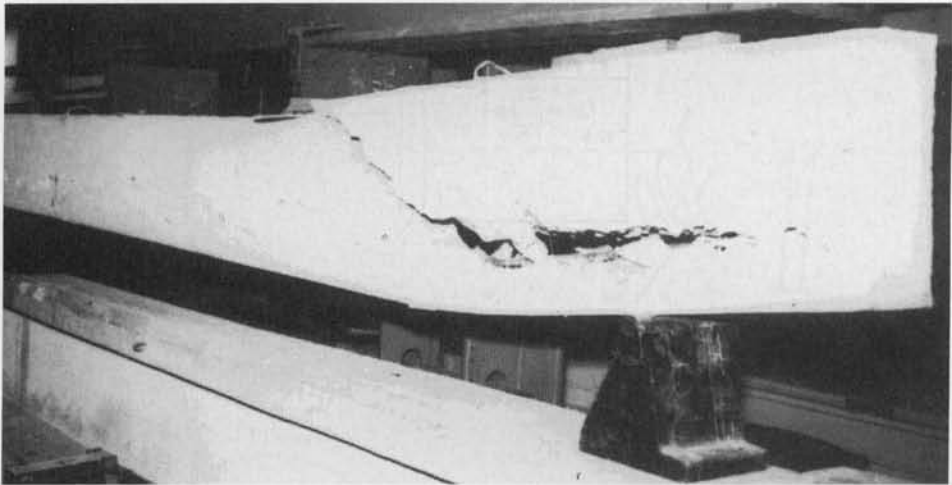
$$v = \frac{VA\bar{y}}{Ib} = \frac{VQ}{Ib} \quad (5.2)$$

where  $M$  and  $V$  = bending moment and shear force at section  $a_1$ – $a_1$

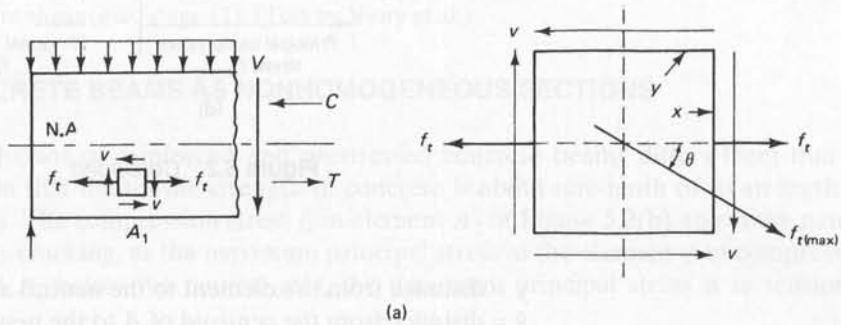
$A$  = cross-sectional area of the section at the plane passing through the centroid of element  $A_1$



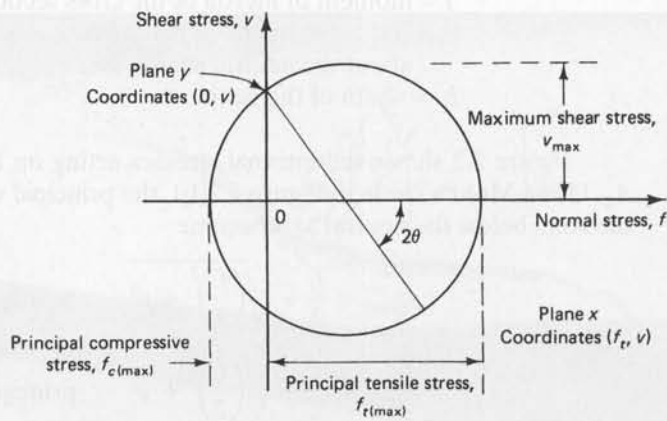
**Figure 5.1** Stress distribution for a typical homogeneous rectangular beam.



**Photo 5.1** Typical diagonal tension (flexure shear) failure at rupture load level. (Test by Nawy et al.)



(a)



(b)

**Figure 5.2** Stress state in elements  $A_1$  and  $A_2$ . (a) Stress state in element  $A_1$ . (b) Mohr's circle representation, element  $A_1$ . (c) Stress state in element  $A_2$ . (d) Mohr's circle representation, element  $A_2$ .

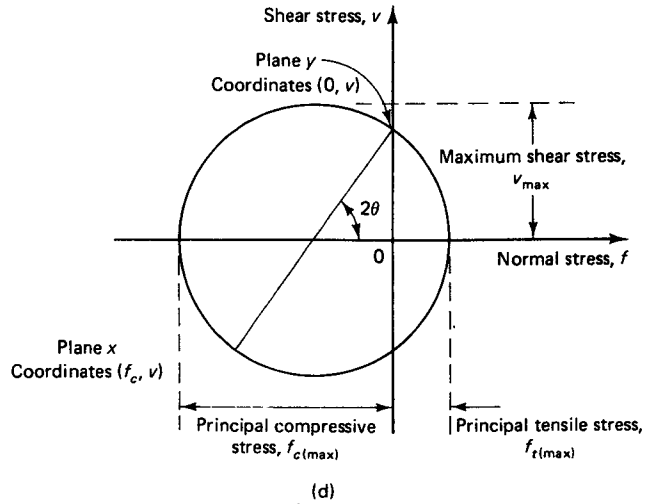
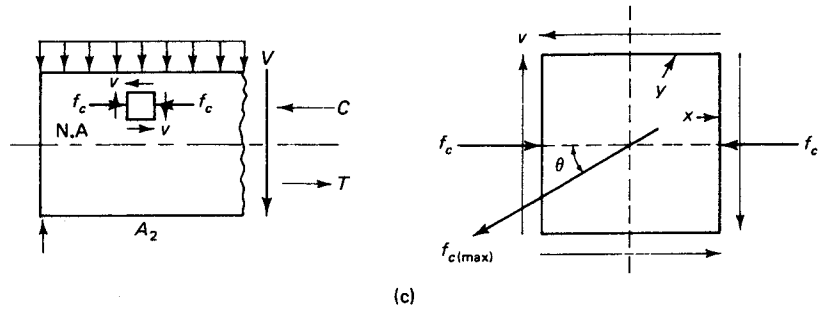


Figure 5.2 Continued

- $y$  = distance from the element to the neutral axis
- $\bar{y}$  = distance from the centroid of  $A$  to the neutral axis
- $I$  = moment of inertia of the cross section
- $Q$  = statical moment of the cross-sectional area above or below that level about the neutral axis
- $b$  = width of the beam

Figure 5.2 shows the internal stresses acting on the infinitesimal elements  $A_1$  and  $A_2$ . Using Mohr's circle in Figure 5.2(b), the principal stresses for element  $A_1$  in the tensile zone below the neutral axis become

$$f_{t(max)} = \frac{f_t}{2} + \sqrt{\left(\frac{f_t}{2}\right)^2 + v^2} \quad \text{principal tension} \quad (5.3a)$$

$$f_{c(max)} = \frac{f_t}{2} - \sqrt{\left(\frac{f_t}{2}\right)^2 + v^2} \quad \text{principal compression} \quad (5.3b)$$

and

$$\tan 2\theta_{max} = \frac{v}{f_t/2} \quad (5.3c)$$



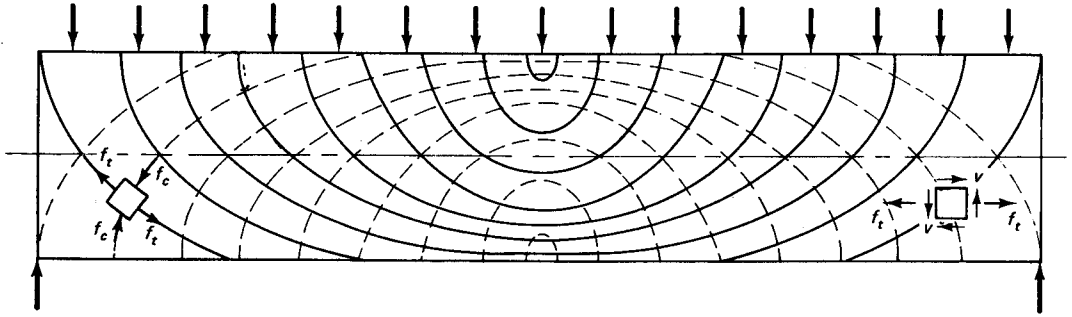
**Photo 5.2** Simply supported beam prior to developing diagonal tension crack in flexure shear (load stage 11). (Test by Nawy et al.)

### 5.3 BEHAVIOR OF CONCRETE BEAMS AS NONHOMOGENEOUS SECTIONS

The behavior of reinforced and prestressed concrete beams differs from that of steel beams in that the tensile strength of concrete is about one-tenth of its strength in compression. The compression stress  $f_c$  in element  $A_2$  of Figure 5.2(b) above the neutral axis prevents cracking, as the maximum principal stress in the element is in compression. For element  $A_1$  below the neutral axis, the maximum principal stress is in tension; hence



**Photo 5.3** Principal diagonal tension crack at failure of beam in the preceding photograph (load stage 12).



**Figure 5.3** Trajectories of principal stresses in a homogeneous isotropic beam. Solid lines are tensile trajectories, dashed lines are compressive trajectories.

cracking ensues. As one moves toward the support, the bending moment and hence  $f_t$  decreases, accompanied by a corresponding increase in the shear stress. The principal stress  $f_{t(\max)}$  in tension acts at an approximately  $45^\circ$  plane to the normal at sections close to the support, as seen in Figure 5.3. Because of the low tensile strength of concrete, diagonal cracking develops along planes perpendicular to the planes of principal tensile stress—hence the term *diagonal tension cracks*. To prevent such cracks from openings, special diagonal tension reinforcement has to be provided.

If  $f_t$  close to the support of Figure 5.3, is assumed equal to zero, the element becomes nearly in a state of pure shear, and the principal tensile stress, using Equation 5.3b, would be equal to the shear stress  $v$  on a  $45^\circ$  plane. It is this diagonal tension stress that causes the inclined cracks.

Definitive understanding of the correct shear mechanism in reinforced concrete is still incomplete. However, the approach of ACI-ASCE Joint Committee 426 gives a systematic empirical correlation of the basic concepts developed from extensive test results.

## 5.4 CONCRETE BEAMS WITHOUT DIAGONAL TENSION REINFORCEMENT

In regions of large bending moments, cracks develop almost perpendicular to the axis of the beam. These cracks are called *flexural cracks*. In regions of high shear due to the diagonal tension, the inclined cracks develop as an extension of the flexural crack and are termed *flexure shear cracks*. Figure 5.4 portrays the types of cracks expected in a reinforced concrete beam with or without adequate diagonal tension reinforcement.

In prestressed beams, the section is mostly in compression at service load. From Figures 5.2(c) and (d), the principal stresses for element  $A_2$  would be

$$f_{t(\max)} = -\frac{f_c}{2} + \sqrt{(f_c/2)^2 + v^2} \quad \text{principal tension} \quad (5.4a)$$

$$f_{c(\max)} = -\frac{f_c}{2} - \sqrt{(f_c/2)^2 + v^2} \quad \text{principal compression} \quad (5.4b)$$

and

$$\tan 2\theta_{\max} = \frac{v}{f_c/2} \quad (5.4c)$$

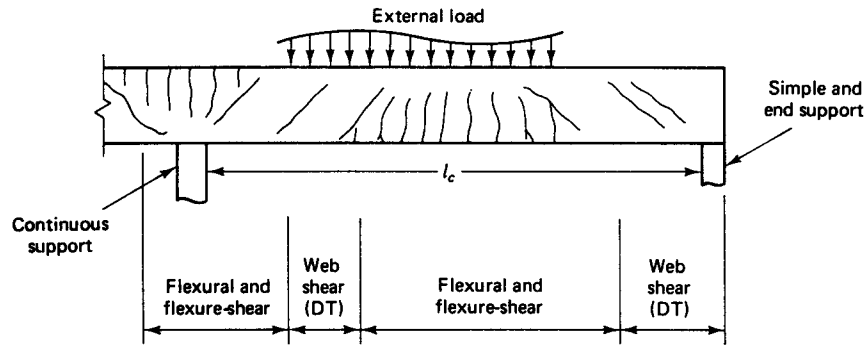


Figure 5.4 Crack categories.

### 5.4.1 Modes of Failure of Beams Without Diagonal Tension Reinforcement

The slenderness of the beam, that is, its shear span-to-depth ratio, determines the failure mode of the beam. Figure 5.5 demonstrates schematically the failure patterns for the different slenderness ratio limits. The shear span  $a$  for concentrated load is the distance between the point of application of the load and the face of support. For distributed loads, the shear span  $l_c$  is the clear beam span. Fundamentally, three modes of failure or their combinations occur: flexural failure, diagonal tension failure, and shear compression failure (web shear). The more slender the beam, the stronger the tendency toward flexural behavior, as seen from the following discussion.

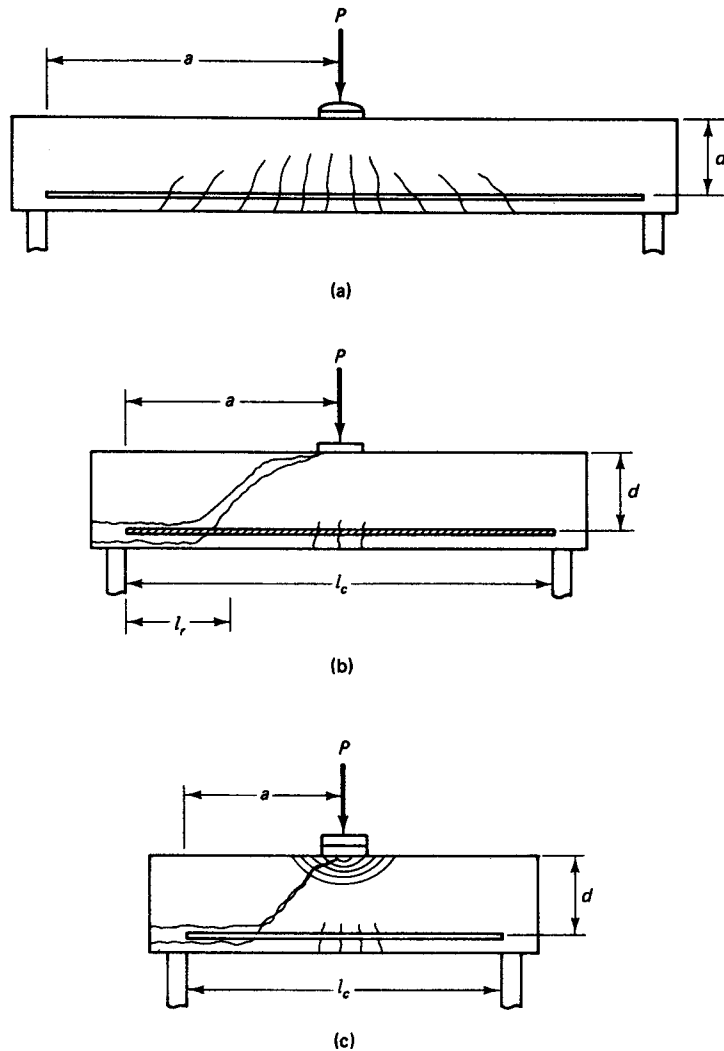
### 5.4.2 Flexural Failure [ $F$ ]

In the region of flexural failure, cracks are mainly vertical in the middle third of the beam span and perpendicular to the lines of principal stress. These cracks result from a very small shear stress  $v$  and a dominant flexural stress  $f$  which results in an almost horizontal principal stress  $f_{t(\max)}$ . In such a failure mode, a few very fine vertical cracks start to develop in the midspan area at about 50 percent of the failure load in flexure. As the external load increases, additional cracks develop in the central region of the span and the initial cracks widen and extend deeper toward the neutral axis and beyond, with a marked increase in the deflection of the beam. If the beam is underreinforced, failure occurs in a ductile manner by initial yielding of the main longitudinal flexural reinforcement. This type of behavior gives ample warning of the imminence of collapse of the beam. The shear span-to-depth ratio for this behavior exceeds a value of 5.5 in the case of concentrated loading, and in excess of 16 for distributed loading.

### 5.4.3 Diagonal Tension Failure [Flexure Shear, $FS$ ]

Diagonal tension failure precipitates if the strength of the beam in diagonal tension is lower than its strength in flexure. The shear span-to-depth ratio is of *intermediate* magnitude, varying between 2.5 and 5.5 for the case of concentrated loading. Such beams can be considered of intermediate slenderness. Cracking starts with the development of a few fine vertical flexural cracks at midspan, followed by the destruction of the bond between the reinforcing steel and the surrounding concrete at the support. Thereafter, without ample warning of impending failure, two or three diagonal cracks develop at about  $1\frac{1}{2}d$  to  $2d$  distance from the face of the support in the case of reinforced concrete beams, and usually at about a quarter of the span in the case of prestressed concrete beams. As they stabilize, one of the diagonal cracks widens into a principal diagonal tension crack and extends to the top compression fibers of the beam, as seen in Figure 5.5(b) and 5.5(c).

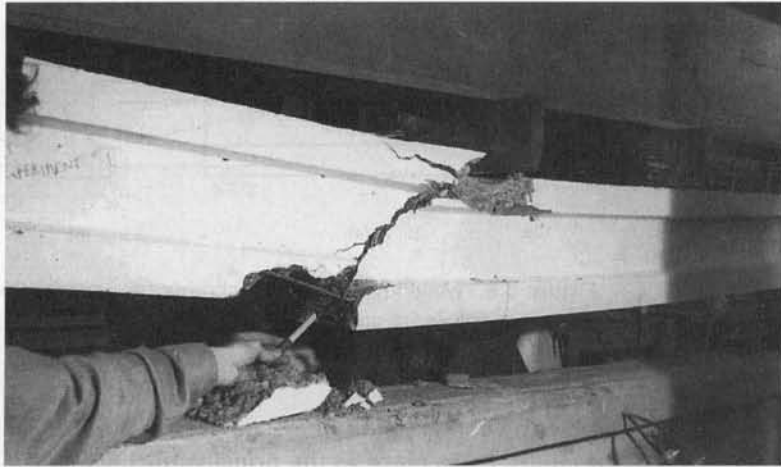




**Figure 5.5** Failure patterns as a function of beam slenderness. (a) Flexural failure. (b) Diagonal tension failure (flexure shear). (c) Shear compression failure (web shear).

Notice that the flexural cracks do not propagate to the neutral axis in this essentially brittle failure mode, which has relatively small deflection at failure.

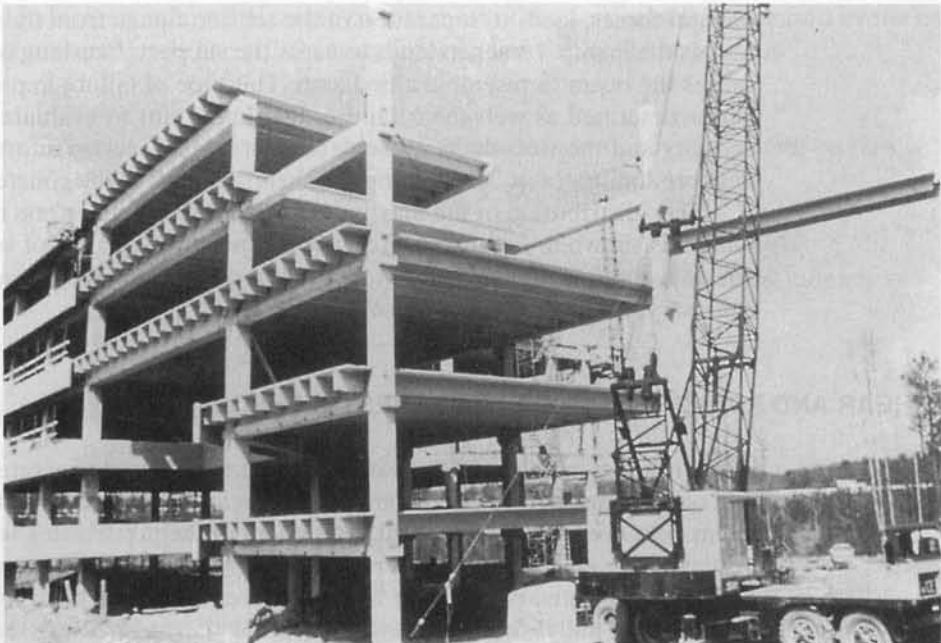
Although the maximum external shear is at the support, the critical location of the maximum principal stress in tension is not. It is considerably reduced at that section because of the high compression force of the prestressing tendon, in addition to the vertical compression force of the beam reaction at the supports. This is the reason why the stabilized diagonal crack is located further into the span, depending on the magnitude of the prestressing force and the variation in its eccentricity, with an average value of about one-quarter of the span in flanged prestressed beams. In sum, the diagonal tension failure is the result of the combination of the flexural and shear stresses, taking into account the balancing contribution of the vertical component of the prestressing force, and noted by a combination of flexural and diagonal cracks. It is best termed *flexure shear* in the case of prestressed beams, and is more common to account for than *web shear*, discussed next.



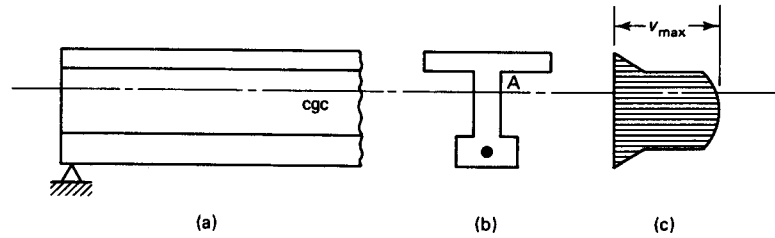
**Photo 5.4** Shear failure in prestressed I-beam (Nawy et al.).

#### 5.4.4 Shear Compression Failure [Web Shear, *WS*]

Beams that are most subject to shear compression failure have a small span-to-depth ratio of magnitude 2.5 for the case of concentrated loading and less than 5.0 for distributed loading. As in the diagonal tension case, a few fine flexural cracks start to develop at midspan and stop propagating as destruction of the bond occurs between the longitudinal bars and the surrounding concrete at the support region. Thereafter, an inclined crack steeper than in the diagonal tension case suddenly develops and proceeds to propagate toward the neutral axis. The rate of its progress is reduced with the crushing of the con-



**Photo 5.5** Installation of precast prestressed double-T floor beams in a multifloor office structure.



**Figure 5.6** Maximum horizontal shear stress distribution across depth. (a) Beam elevation. (b) Beam cross section. (c) Shear stress.

crete in the top compression fibers and a redistribution of stresses within the top region. Sudden failure takes place as the principal inclined crack dynamically joins the crushed concrete zone, as illustrated in Figure 5.5(c). This type of failure can be considered relatively less brittle than the diagonal tension failure due to the stress redistribution. Yet it is, in fact, a brittle type of failure with limited warning, and such a design should be avoided completely.

A concrete beam or element is not homogeneous, and the strength of the concrete throughout the span is subject to a normally distributed variation. Hence, one cannot expect that a stabilized failure diagonal crack occurs at both ends of the beam. Also, because of these properties, overlapping combinations of flexure–diagonal tension failure and diagonal tension–shear compression failure can occur at overlapping shear span-to-depth ratios. If the appropriate amount of shear reinforcement is provided, brittle failure of horizontal members can be eliminated with little additional cost.

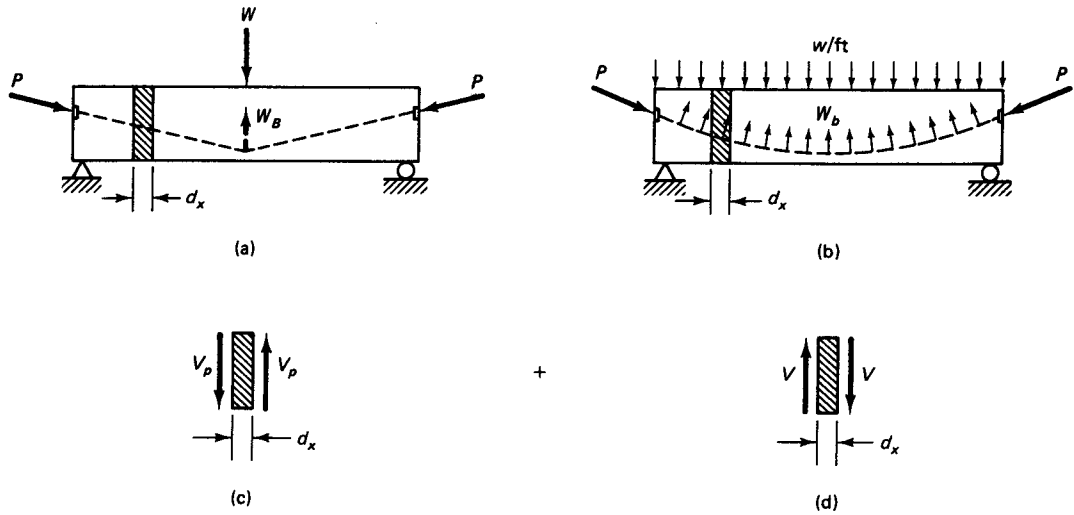
It should be emphasized that most failures tend to occur by diagonal tension, which is a combination of flexure and shear effects. The shear-compression type of failure, with the resulting crushing of the top compressive area of the concrete and failure to resist the flexural forces, leads to separation of the tension flange from the web in the flanged section as the inclined crack extends towards the support. Crushing of the web of the section causes the beam to resemble a tied arch. This type of failure in prestressed beams can be better described as web-shear failure. It is important to evaluate *both* the flexure-shear capacity and the web-shear capacity of each critical section in order to determine which type predominates in determining the shear strength of the concrete section.

The distribution of the maximum horizontal shearing stress in an uncracked flanged section is shown in Figure 5.6. Because of the abrupt change of section width at the corner A, a check of the capacity of the section at critical locations along the span becomes necessary, particularly for web-shear failure.

## 5.5 SHEAR AND PRINCIPAL STRESSES IN PRESTRESSED BEAMS

As mentioned in Section 5.4, flexure shear in prestressed concrete beams includes the effect of the externally applied compressive prestressing force that the reinforced concrete beam does *not* have. The vertical component of the prestressing tendon force reduces the vertical shear caused by the external transverse load, and the *net* transverse load to which a beam is subjected is markedly less in prestressed than in reinforced concrete beams.

Additionally, the compressive force of the prestressing tendon, even in cases of straight tendons, considerably reduces the effect of the tensile flexural stresses, so that the extent and magnitude of flexural cracking in prestressed members are reduced. As a



**Figure 5.7** Balancing load to counteract vertical shear. (a) Beam with harped tendon. (b) Beam with draped tendon. (c) Internal shear vector  $V_p$  due to prestressing force  $P$  on infinitesimal element  $dx$ . (d) Internal shear vector  $V$  due to external load  $W$  on infinitesimal element  $dx$ .

result, the shear forces and the resulting principal stresses in a prestressed beam are considerably lower than those same forces and stresses in reinforced concrete beams, all else being equal. Consequently, the *basic* equations developed for prestressed concrete in shear are identical to those developed for reinforced concrete and described in detail in Refs. 5.3 and 5.4. Figure 5.7 illustrates the contributions of the vertical component of the tendon force in counterbalancing part or most of the vertical shear  $V$  caused by the external transverse load. The net shearing force  $V_c$  carried by the concrete is

$$V_c = V - V_p \quad (5.5)$$

From Equation 5.2, the net unit shearing stress  $v$  at any depth of the cross section is

$$v_c = \frac{V_c Q}{Ib} \quad (5.6)$$

The compressive fiber-stress distribution  $f_c$  due to the external bending moment is

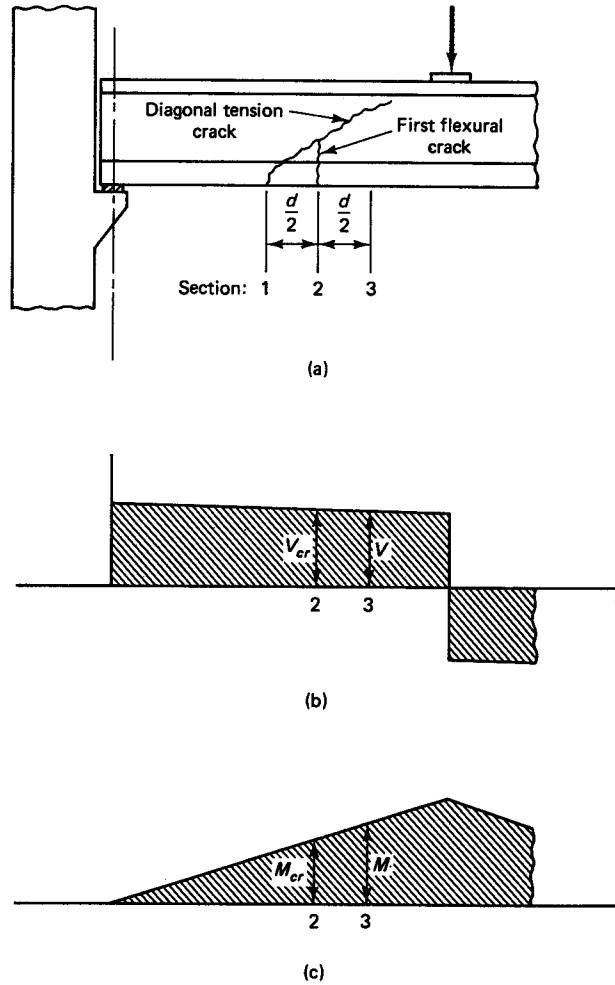
$$f_c = -\frac{P_e}{A_c} \pm \frac{P_e ec}{I_c} \mp \frac{M_T c}{I_c} \quad (5.7)$$

and the principal tensile stress, from Equation 5.4a, is

$$f'_t = \sqrt{(f_c/2)^2 + v_c^2} - \frac{f_c}{2} \quad (5.8)$$

### 5.5.1 Flexure-Shear Strength [ $V_c$ ]

To design for shear, it is necessary to determine whether flexure shear or web shear controls the choice of concrete shear strength  $V_c$ . The inclined stabilized crack at a distance  $d/2$  from a flexural crack that develops at the first cracking load in flexure shear is shown in Figure 5.8. If the effective depth is  $d_p$ , the depth from the compression fibers to the



**Figure 5.8** Flexure-shear crack development. (a) Crack pattern and types. (b) Shear diagram due to external load with frictional shear force  $V_{cr}$  ordinate at section 2. (c) Moment diagram with first cracking moment  $M_{cr}$  ordinate at section 2.

centroid of the longitudinal prestressed reinforcement, the change in moment between sections 2 and 3 is

$$M - M_{cr} \cong \frac{Vd_p}{2} \quad (5.9a)$$

or

$$V = \frac{M_{cr}}{M/V - d_p/2} \quad (5.9b)$$

where  $V$  is the shear at the section under consideration. Extensive experimental tests indicate that an additional vertical shear force of magnitude  $0.6b_w d_p \sqrt{f'_c}$  is needed to fully develop the inclined crack in Figure 5.8 (Ref. 5.5). Hence, the total vertical shear acting at plane 2 of Figure 5.8 is

$$V_{ci} = \frac{M_{cr}}{M/V - d_p/2} + 0.6b_w d_p \sqrt{f'_c} + V_d \quad (5.10)$$

where  $V_d$  is the vertical shear due to self-weight. The vertical component  $V_p$  of the prestressing force is disregarded in Equation 5.10, since it is small along the span sections where the prestressing tendon is not too steep.

The value of  $V$  in Equation 5.10 is the factored shear force  $V_i$  at the section under consideration due to externally applied loads occurring simultaneously with the maximum moment  $M_{\max}$  occurring at that section, i.e.,

$$\begin{aligned} V_{ci} &= 0.6\lambda \sqrt{f'_c} b_w d_p + V_d + \frac{V_i}{M_{\max}} (M_{cr}) \geq 1.7\lambda \sqrt{f'_c} b_w d_p \\ &\leq 5.0\lambda \sqrt{f'_c} b_w d_p \end{aligned} \quad (5.11)$$

where  $\lambda = 1.0$  for normal-weight concrete  
 $= 0.85$  for sand-lightweight concrete  
 $= 0.75$  for all-lightweight concrete

$V_d$  = shear force at section due to unfactored dead load

$V_{ci}$  = nominal shear strength provided by the concrete when diagonal tension cracking results from combined vertical shear and moment

$V_i$  = factored shear force at section due to externally applied load occurring simultaneously with  $M_{\max}$ .

For lightweight concrete,  $\lambda = f_{cr}/6.7 \sqrt{f'_c}$  if the value of the tensile splitting strength  $f_{cr}$  is known. Note that the value  $\sqrt{f'_c}$  should not exceed 100.

The equation for  $M_{cr}$ , the moment causing flexural cracking due to external load, is given by

$$M_{cr} = \frac{I_c}{y_t} (6\sqrt{f'_c} + f_{ce} - f_d) \quad (5.12)$$

In the ACI code,  $f_{ce}$  is termed as  $f_{pe}$

where  $f_{ce}$  = concrete compressive stress due to effective prestress after losses at *extreme* fibers of section where tensile stress is caused by external load, psi. At the centroid,  $f_{ce} = \bar{f}_c$

$f_d$  = stress due to unfactored dead load at extreme fiber of section resulting from self-weight only where tensile stress is caused by externally applied load, psi

$y_t$  = distance from centroidal axis to extreme fibers in tension.

and  $M_{cr}$  = that portion of the applied *live load* moment that causes cracking. For simplicity,  $S_b$  may be substituted for  $I_c/y_t$ .

A plot of Equation 5.10 is given in Figure 5.9 with experimental data from Ref. 5.6. Compare this plot with an analogous one in Figure 6.6 of Ref. 5.3 for reinforced concrete where an asymptotic horizontal value of shear is achieved along the span.

Note that in shear design of composite sections, the same design stipulations used for precast sections apply. This is because design for shear is based on the limit state at failure due to factored loads. Although the entire composite section resists the factored shear as a monolithic section, calculation of the shear strength  $V_c$  should be based on the properties of the *precast* section since most of the shear strength is provided by the web of the precast section. Consequently,  $f_{ce}$  and  $f_d$  in Equation 5.12 are calculated using the precast section geometry.

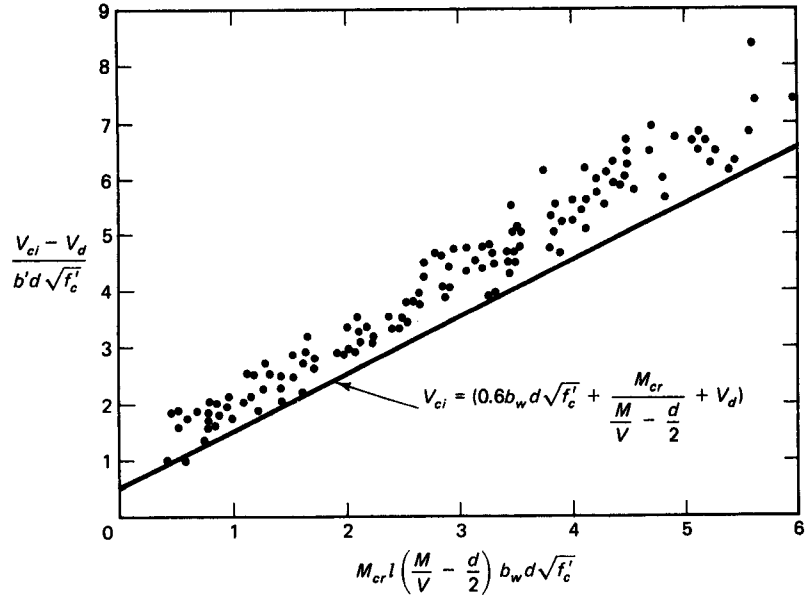


Figure 5.9 Moment-shear relationship in flexure-shear cracking.

**5.5.2 Web-Shear Strength [ $V_{cw}$ ]**

The web-shear crack in the prestressed beam is caused by an indeterminate stress that can best be evaluated by calculating the principal tensile stress at the critical plane from Equation 5.8. The shear stress  $v_c$  can be defined as the web shear stress  $v_{cw}$  and is maximum near the centroid *cgc* of the section where the actual diagonal crack develops, as extensive tests to failure have indicated. If  $v_{cw}$  is substituted for  $v_c$  and  $\bar{f}_c$ , which denotes the concrete stress  $f_c$  due to effective prestress *at the cgc level*, is substituted for  $f_c$  in the equation, the expression equating the principal tensile stress in the concrete to the direct tensile strength becomes

$$f'_t = \sqrt{(f_c/2) + v_{cw}^2} - \frac{\bar{f}_c}{2} \tag{5.13}$$

where  $v_{cw} = V_{cw}/(b_w d_p)$  is the shear stress in the concrete due to all loads causing a nominal strength vertical shear force  $V_{cw}$  in the web. Solving for  $v_{cw}$  in Equation 5.13 gives

$$v_{cw} = f'_t \sqrt{1 + \bar{f}_c/f'_t} \tag{5.14a}$$

Using  $f'_t = 3.5 \sqrt{f'_c}$  as a reasonable value of the tensile stress on the basis of extensive tests, Equation 5.14(a) becomes

$$v_{cw} = 3.5\sqrt{f'_c} (\sqrt{1 + \bar{f}_c/3.5 \sqrt{f'_c}}) \tag{5.14b}$$

which can be further simplified to

$$v_{cw} = 3.5 \sqrt{f'_c} + 0.3 \bar{f}_c \tag{5.14c}$$

In the ACI code,  $\bar{f}_c$  is termed  $f_{pc}$ . The notation used herein is intended to emphasize that this is the stress in the concrete, and not the prestressing steel. The nominal shear strength  $V_{cw}$  provided by the concrete when diagonal cracking results from *excessive principal tensile stress* in the web becomes

$$V_{cw} = (3.5\lambda \sqrt{f'_c} + 0.3\bar{f}_c)b_w d_p + V_p \quad (5.15)$$

where  $V_p$  = the vertical component of the effective prestress at the particular section contributing to added nominal strength

$\lambda = 1.0$  for normal-weight concrete, and less for lightweight concrete

$d_p$  = distance from the extreme compression fiber to the centroid of prestressed steel, or  $0.8h$ , whichever is greater.

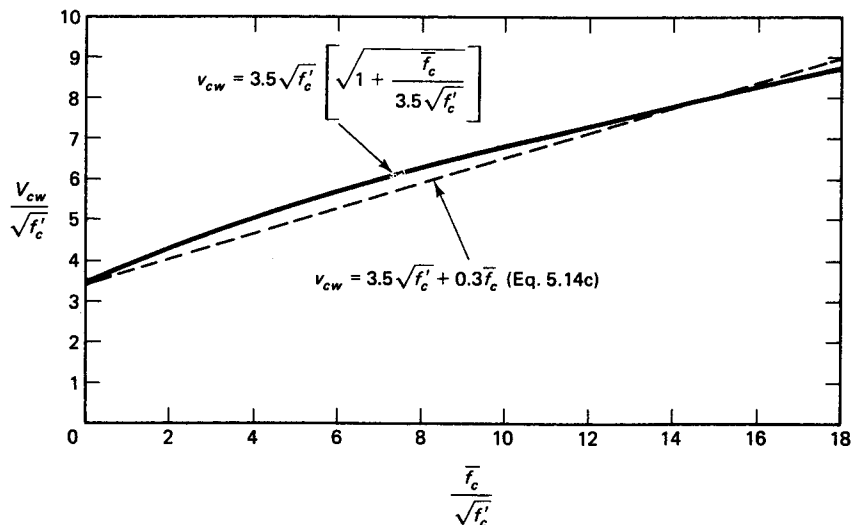
The ACI code stipulates the value of  $\bar{f}_c$  to be the resultant concrete compressive stress at either the centroid of the section or the junction of the web and the flange when the centroid lies within the flange. In case of composite sections,  $\bar{f}_c$  is calculated on the basis of stresses caused by prestress and moments resisted by the precast member acting *alone*. A plot relating the nominal web shear stress  $v_{cw}$  to the centroidal compressive stress in the concrete is given in Figure 5.10. Note the similarity between the plots of Equations 5.14b and c, showing that the approximation used in the latter linearized equation is justified. The code also allows using a value of 1.0 instead of 0.3 in the second term inside the bracket in Equation 5.15.

### 5.5.3 Controlling Values of $V_{ci}$ and $V_{cw}$ for the Determination of Web Concrete Strength $V_c$

The ACI code has the following additional stipulations for calculating  $V_{ci}$  and  $V_{cw}$  in order to choose the required value of  $V_c$  in the design:

- (a) In pretensioned members where the section at a distance  $h/2$  from the face of the support is closer to the end of the member than the transfer length of the prestressing tendon, a reduced prestressed value has to be considered when computing  $V_{cw}$ . This value of  $V_{cw}$  has to be taken as the maximum limit of  $V_c$  in the expression

$$V_{cw} = \left( 0.6\lambda \sqrt{f'_c} + 700 \frac{V_u d_p}{M_u} \right) b_w d_p \geq 2\lambda \sqrt{f'_c} b_w d_p \leq 5\lambda \sqrt{f'_c} b_w d_p \quad (5.16)$$



**Figure 5.10** Centroidal compressive stress vs. nominal shear stress in web-shear cracking.



the value  $V_u d_p / M_u$  cannot exceed 1.0.

- (b) In pretensioned members where bonding of some tendons does not extend to the end of the member, a reduced prestress has to be considered when computing  $V_c$  in accordance with Equation 5.16 or with the *lesser* of the two values of  $V_c$  obtained from Equations 5.11 and 5.15. Also, the value of  $V_{cw}$  calculated using the reduced prestress must consequently be taken to be the maximum limit of Equation 5.16.
- (c) Equation 5.16 can be used in determining  $V_c$  for members where the effective prestress force is not less than 40 percent of the tensile strength of the flexural reinforcement, *unless* a more detailed analysis is performed using Equations 5.11 for  $V_{ci}$  and 5.15 for  $V_{cw}$  and choosing the lesser of these two as the limiting  $V_c$  value to be used as the capacity of the web in designing the web reinforcement.
- (d) The first plane for the total required nominal shear strength  $V_n = V_u / \phi$  to be used for web steel calculation is also at a distance  $h/2$  from the face of the support.

## 5.6 WEB-SHEAR REINFORCEMENT

### 5.6.1 Web Steel Planar Truss Analogy

In order to prevent diagonal cracks from developing in prestressed members, *whether due to flexure-shear or web-shear action*, steel reinforcement has to be provided, ideally in the form of the solid lines depicting tensile stress trajectories in Figure 5.3. However, practical considerations preclude such a solution, and other forms of reinforcement are improvised to neutralize the tensile stresses at the critical shear failure planes. The mode of failure in shear reduces the beam to a simulated arched section in compression at the top and tied at the bottom by the longitudinal beam tension bars, as seen in Figure 5.11(a). If one isolates the main concrete compression element shown in Figure 5.11(b), it can be considered as the compression member of a triangular truss, as shown in Figure 5.11(c), with the polygon of forces  $C_c$ ,  $T_b$ , and  $T_s$  representing the forces acting on the truss members—hence the expression *truss analogy*. Force  $C_c$  is the compression in the simulated concrete strut, force  $T_b$  is the tensile force increment of the main longitudinal tension bar, and  $T_s$  is the force in the bent bar. Figure 5.12(a) shows the analogy truss for the case of using vertical stirrups instead of inclined bars, with the forces polygon having a vertical tensile force  $T_s$  instead of the inclined one in Figure 5.11(c).

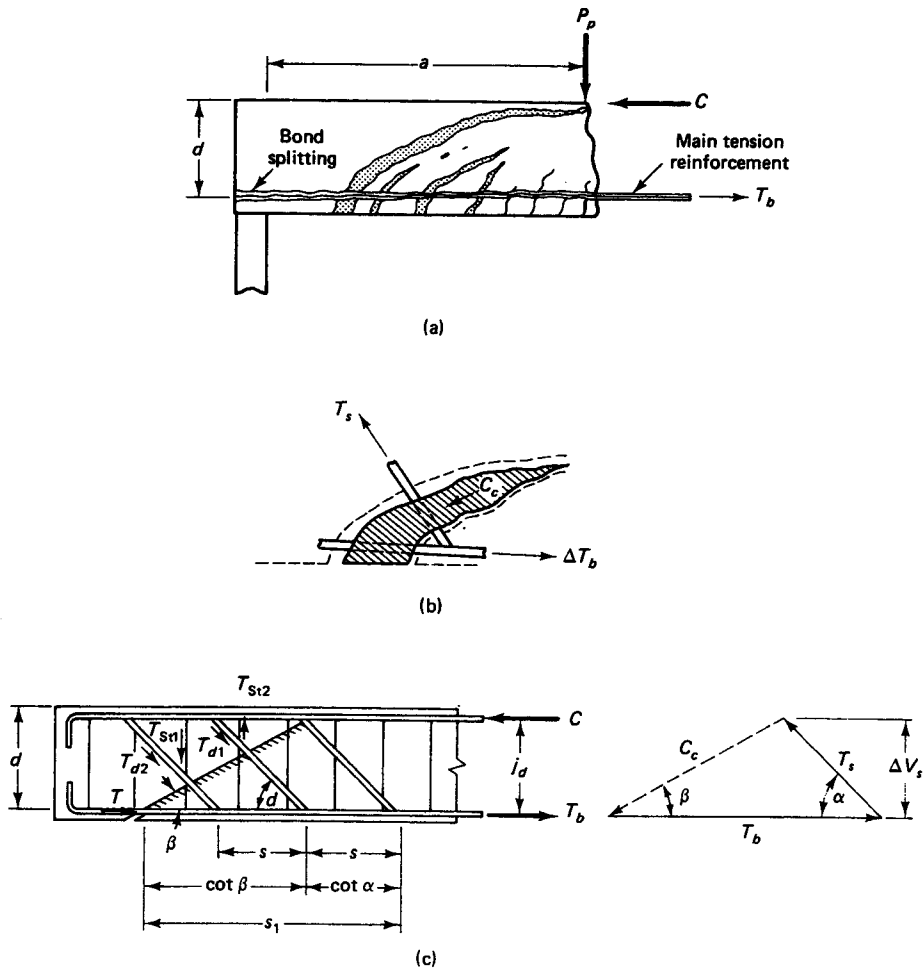
As can be seen from the previous discussion, the shear reinforcement basically performs four main functions:

1. It carries a portion of the external factored shear force  $V_u$ .
2. It restricts the growth of the diagonal cracks.
3. It holds the longitudinal main reinforcing bars in place so that they can provide the dowel capacity needed to carry the flexural load.
4. It provides some confinement to the concrete in the compression zone if the stirrups are in the form of closed ties.

### 5.6.2 Web Steel Resistance

If  $V_c$ , the nominal shear resistance of the plain web concrete, is less than the nominal total vertical shearing force  $V_u / \phi = V_n$ , web reinforcement has to be provided to carry the difference in the two values; hence,

$$V_s = V_n - V_c \quad (5.17)$$



**Figure 5.11** Diagonal tension failure mechanism. (a) Failure pattern. (b) Concrete simulated strut. (c) Planar truss analogy.

Here,  $V_c$  is the lesser of  $V_{ci}$  and  $V_{cw}$ .  $V_c$  can be calculated from Equation 5.11 or 5.15, and  $V_s$  can be determined from equilibrium analysis of the bar forces in the analogous triangular truss cell. From Figure 5.11(c),

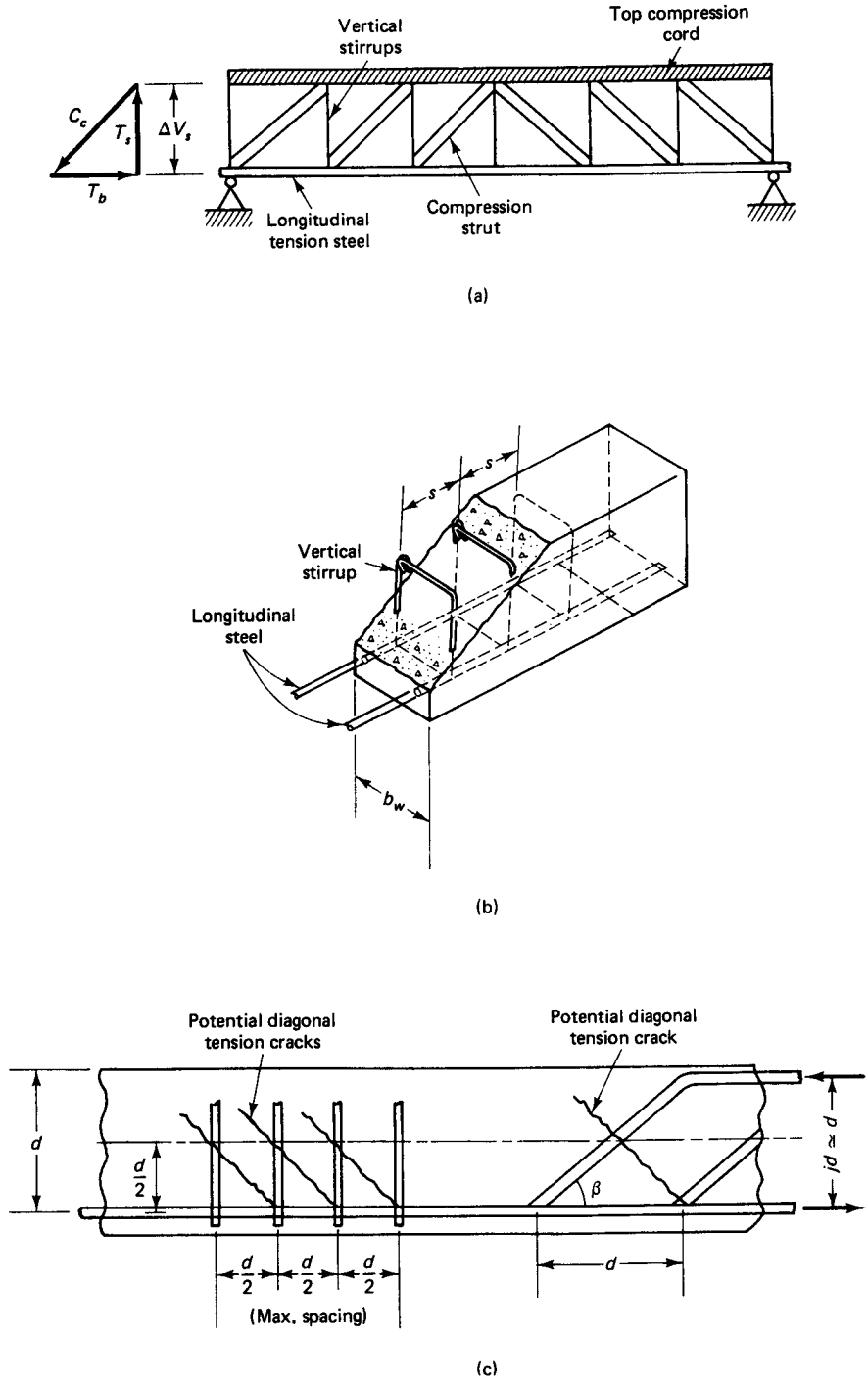
$$V_s = T_s \sin \alpha = C_c \sin \beta \tag{5.18a}$$

where  $T_s$  is the force resultant of all web stirrups across the diagonal crack plane and  $n$  is the number of spacings  $s$ . If  $s_1 = ns$  in the bottom tension chord of the analogous truss cell, then

$$s_1 = jd(\cot \alpha + \cot \beta) \tag{5.18b}$$

Assuming that moment arm  $jd \approx d$ , the stirrup force per unit length from Equations 5.18a and b, where  $s_1 = ns$ , becomes

$$\frac{T_s}{s_1} = \frac{T_s}{ns} = \frac{V_s}{\sin \alpha} \frac{1}{d(\cot \beta + \cot \alpha)} \tag{5.18c}$$



**Figure 5.12** Web steel arrangement. (a) Truss analogy for vertical stirrups. (b) Three-dimensional view of vertical stirrups. (c) Spacing of web steel.

If there are  $n$  inclined stirrups within the length  $s_1$  of the analogous truss chord, and if  $A_v$  is the area of one inclined stirrup, then

$$T_s = nA_v f_{yt} \quad (5.19a)$$

Hence,

$$nA_v = \frac{V_s ns}{d \sin \alpha (\cot \beta + \cot \alpha) f_{yt}} \quad (5.19b)$$

But it can be assumed that in the case of diagonal tension failure the compression diagonal makes an angle  $\beta = 45^\circ$  with the horizontal; so Equation 5.19b becomes

$$V_s = \frac{A_v f_{yt} d}{s} [\sin \alpha (1 + \cot \alpha)]$$

or

$$V_s = \frac{A_v f_{yt} d}{s} (\sin \alpha + \cos \alpha) \quad (5.20a)$$

or, solving for  $s$  and using the fact that  $V_s = V_n - V_c$ ,

$$s = \frac{A_v f_{yt} d}{V_n - V_c} (\sin \alpha + \cos \alpha) \quad (5.20b)$$

If the inclined web steel consists of a single bar or a single group of bars all bent at the same distance from the face of the support, then

$$V_s = A_v f_{yt} \sin \alpha \leq 3.0 \sqrt{f'_c} b_w d$$

If vertical stirrups are used, angle  $\alpha$  becomes  $90^\circ$ , giving

$$V_s = \frac{A_v f_{yt} d_p}{s} \quad (5.21a)$$

or

$$s = \frac{A_v f_{yt} d}{(V_u/\phi) - V_c} = \frac{A_v \phi f_{yt} d_p}{V_u - \phi V_c} \quad (5.21b)$$

In Equations 5.21a and b,  $d_p$  is the distance from the extreme compression fibers to the centroid of the prestressing reinforcement, and  $d$  is the corresponding distance to the centroid of the nonprestressed reinforcement. The value of  $d_p$  need not be less than  $0.80h$ .

### 5.6.3 Limitation on Size and Spacing of Stirrups

Equations 5.20 and 5.21 give an inverse relationship between the spacing of the stirrups and the shear force or shear stress they resist, with the spacing  $s$  decreasing with the increase in  $(V_n - V_c)$ . In order for every *potential* diagonal crack to be resisted by a vertical stirrup, as shown in Figure 5.11(c), maximum spacing limitations are to be applied for the vertical stirrups as follows:

- (a)  $s_{\max} \leq \frac{3}{4}h \leq 24$  in., where  $h$  is the total depth of the section.
- (b) If  $V_s > 4\lambda \sqrt{f'_c} b_w d_p$ , the maximum spacing in (a) shall be reduced by half.
- (c) If  $V_s > 8\lambda \sqrt{f'_c} b_w d_p$ , enlarge the section.

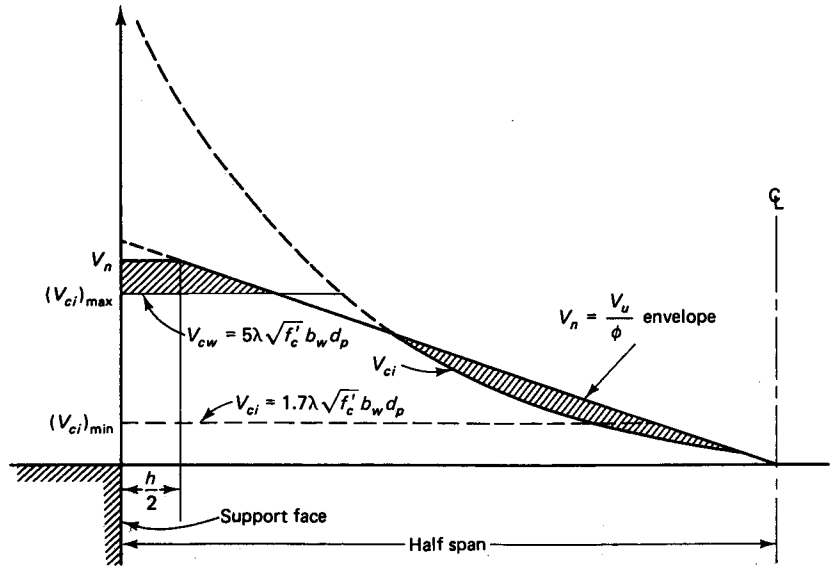


Figure 5.13 Web steel envelope for uniformly loaded prestressed beam.

- (d) If  $V_u = \phi V_n > \frac{1}{2} \phi V_c$ , a minimum area of shear reinforcement has to be provided. This area may be computed by the equation

$$A_v = 0.75 \sqrt{f'_c} \frac{b_w s}{f_{yt}} \text{ or } A_v = \frac{50 b_w s}{f_{yt}} \text{ whichever larger} \quad (5.22a)$$

If the effective prestress force  $P_e$  is equal to or greater than 40 percent of the tensile strength of the flexural reinforcement, the equation

$$A_v = \frac{A_{ps} f_{pu} s}{80 f_y d_p} \sqrt{\frac{d_p}{b_w}} \quad (5.22b)$$

which gives a lesser required minimum  $A_v$ , may be used instead.

- (e) The web reinforcement must develop the full required development length in order to be effective. This means that the stirrups or mesh should extend to the compression and tension surfaces of the section, less the clear concrete cover requirement and a 90° or 135° hook used at the compression side.

A typical qualitative diagram showing the zone along the span of a uniformly loaded prestressed beam for which web reinforcement has to be provided is given in Figure 5.13. The shaded area is the envelope of excess shear  $V_s$  requiring web steel.

## 5.7 HORIZONTAL SHEAR STRENGTH IN COMPOSITE CONSTRUCTION

Full transfer of horizontal shear forces has to be assumed at the contact surfaces of the interconnected elements.

### 5.7.1 Service-Load Level

The maximum horizontal shear stress  $\nu_h$  can be evaluated from the basic principles of mechanics and the equation

$$v_h = \frac{VQ}{I_c b_v} \quad (5.23)$$

where  $V$  = unfactored design vertical shear acting on the composite section  
 $Q$  = moment of area about cgc of the segment above or below cgc  
 $I_c$  = moment of inertia of entire composite section  
 $b_v$  = contact width of precast section web, or width of section at which horizontal shear is being calculated.

Equation 5.23 can be simplified to

$$v_h = \frac{V}{b_v d_{pc}} \quad (5.24)$$

where  $d_{pc}$  is the effective depth from the extreme compression fibers of the composite section to the centroid cgs of the prestressing reinforcement.

### 5.7.2 Ultimate-Load Level

**Direct Method.** In the limit state at failure, Equation 5.24 can be modified such that the factored load  $V_u$  can be substituted for  $V$  to give

$$v_{uh} = \frac{V_u}{b_v d_{pc}} \quad (5.25a)$$

or, in terms of the nominal vertical shear strength  $V_n$

$$v_{nh} = \frac{V_u/\phi}{b_v d_{pc}} = \frac{V_n}{b_v d_{pc}} \quad (5.25b)$$

where  $\phi = 0.75$ . If  $V_{nh}$  is the nominal horizontal shear strength, then  $V_u \leq V_{nh}$  and the total nominal shear strength is

$$V_{nh} = v_{nh} b_v d_{pc} \quad (5.25c)$$

The ACI code limits  $v_{nh}$  to 80 psi if no dowels or vertical ties are provided and the contact surface is roughened, or if minimum vertical ties are provided but there is no roughening of the surface of contact.  $v_{nh}$  can go up to 500 psi; otherwise the friction theory, with the following assumptions, has to be used:

- (a) When no vertical ties are provided, but the contact surface of the precast element is intentionally roughened, use

$$V_{nh} \leq 80A_c \leq 80b_v d_{pc} \quad (5.26a)$$

where  $A_c$  is the area of concrete resisting shear  $= b_v d_{pc}$ .

- (b) When minimum vertical ties are provided, where  $A_v = 50(b_w s)/f_y$ , but the contact surface of precast elements is *not* roughened, use

$$V_{nh} \leq 80b_v d_{pc}$$

- (c) If the contact surface of the precast element is roughened to a full amplitude of  $\frac{1}{4}$  in., and minimum vertical steel in (b) is provided, use

$$V_{nh} \leq 500 b_v d_{pc} \quad (5.26b)$$

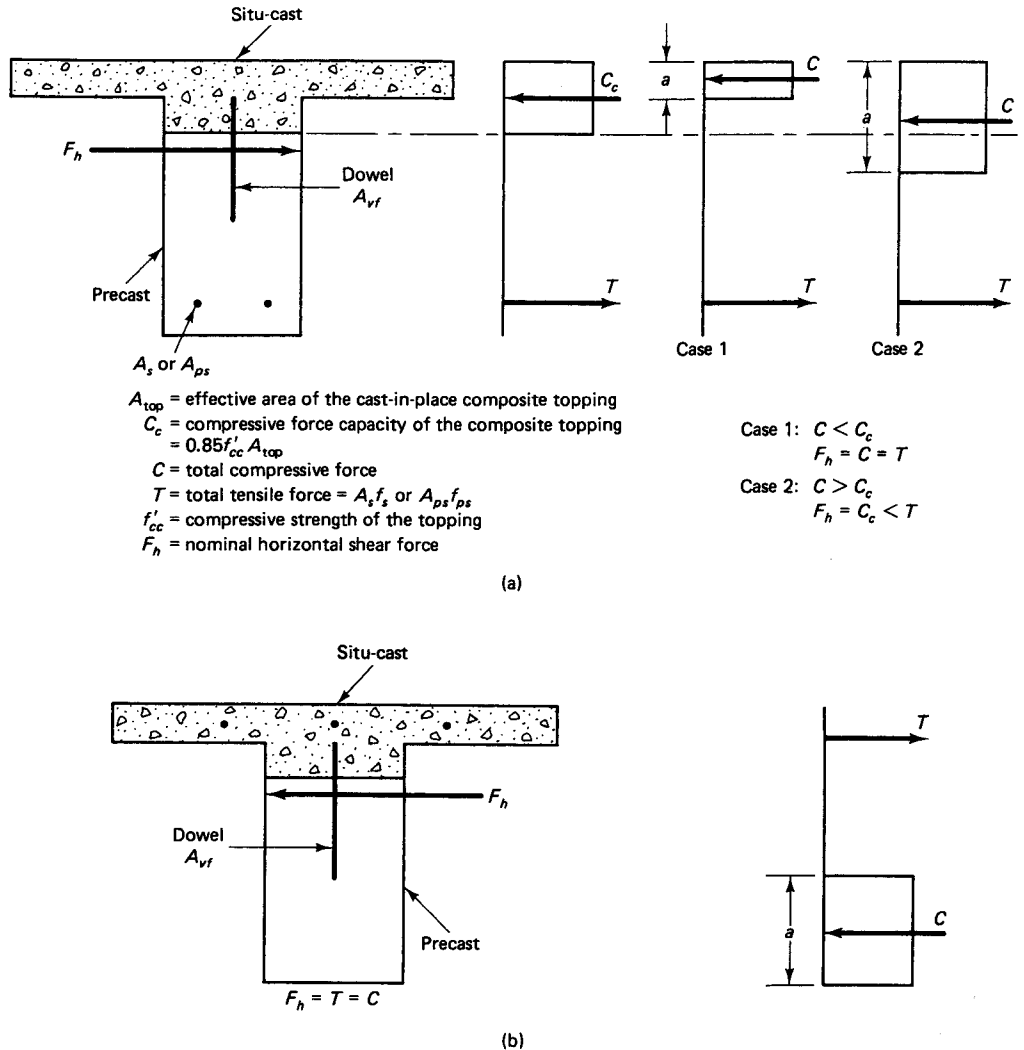
- (d) If the factored shear  $V_u > \phi(500 b_v d_{pc})$ , the shear friction theory can be used to design the dowel reinforcement. In this case, all horizontal shear has to be taken by ties in the perpendicular plane such that

$$V_{nh} = \mu A_{vf} f_{yt} \tag{5.27}$$

where  $A_{vf}$  = area of shear-friction reinforcement, in.<sup>2</sup>  
 $f_y$  = design yield strength, not to exceed 60,000 psi  
 $\mu$  = coefficient of friction  
 =  $1.0\lambda$  for concrete placed against intentionally roughened concrete surface  
 =  $0.60\lambda$  for concrete placed against unroughened concrete surface  
 $\lambda$  = factor for type of concrete.

In all cases, the nominal shear strength  $V_n \leq 0.20f'_c A_{cc} \leq 800 A_{cc}$ , where  $A_{cc}$  is the concrete contact area resisting shear transfer. Note that in most cases, the shear stress  $v_{nh}$  resulting from the factored shear force does not exceed 500 psi. Hence, the shear friction theory is not normally necessary in designing the dowel reinforcement for composite action.

The maximum allowable spacing of the dowels or ties for horizontal shear is the smaller of four times the least dimension of the supported section and 24 inches.



**Figure 5.14** Composite action forces ( $F_h$  acts longitudinally along the beam span). (a) Positive-moment section. (b) Negative-moment section.

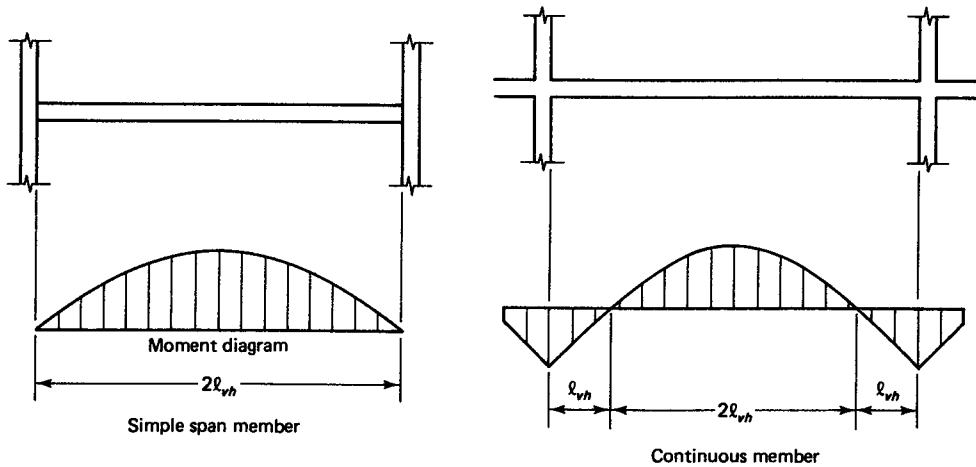


Figure 5.15 Horizontal shear length in composite action.

**Basic Method.** The ACI code allows an alternative method wherein horizontal shear is investigated by computing the actual change in compressive or tensile force in any plane and transferring that force as *horizontal* shear to the supporting elements. The area-of-contact surface  $A_{cc}$  is substituted for  $b_v d_{pc}$  in Equations 5.25b and c to give

$$V_{nh} = v_{nh} A_{cc} \quad (5.28)$$

where  $V_{nh} \geq F_h$ , the horizontal shear force, and is at least equal to the compressive force  $C$  or tensile force  $T$  in Figure 5.14. (See Equation 5.30 for the value of  $F_h$ .)

The value of the contact area  $A_{cc}$  can be defined as

$$A_{cc} = b_v l_{vh} \quad (5.29)$$

where  $l_{vh}$  is the horizontal shear length defined in Figures 5.15(a) and (b) for simple span and continuous span members, respectively.

### 5.7.3 Design of Composite-Action Dowel Reinforcement

Ties for horizontal shear may consist of single bars or wires, multiple leg stirrups, or vertical legs of welded wire fabric. The spacing cannot exceed four times the least dimension of the support element or 24 in., whichever is less. If  $\mu$  is the coefficient of friction, then the nominal horizontal shear force  $F_h$  in Figure 5.14 can be defined as

$$F_h = \mu A_{vf} f_{yt} \leq V_{nh} \quad (5.30)$$

The ACI values of  $\mu$  are based on a limit shear-friction strength of 800 psi, a quite conservative value as demonstrated by extensive testing (Ref. 5.7). The Prestressed Concrete Institute (Ref. 5.8) recommends, for concrete placed against an intentionally roughened concrete surface, a maximum  $\mu_e = 2.9$  instead of  $\mu = 1.0\lambda$ , and a maximum design shear force

$$V_u \leq 0.25\lambda^2 f'_c A_c \leq 1,000\lambda^2 A_{cc} \quad (5.31a)$$

with a required area of shear-friction steel of

$$A_{vf} = \frac{V_{uh}}{\phi f_{yt} \mu_e} \quad (5.31b)$$



or

$$A_{vf} = \frac{V_{nh}}{\mu_e f_y} = \frac{F_h}{\mu_e f_{yt}} \quad (5.31c)$$

Using the PCI less conservative values, Equation 5.31c becomes

$$F_h \leq \mu_e A_{vf} f_{yt} \leq V_{nh} \quad (5.32)$$

with

$$\mu_e = \frac{1,000\lambda^2 b_v I_{vh}}{F_h} \leq 2.9$$

where  $b_v I_{vh} = A_{cc}$ . The minimum reinforcement is

$$A_{vf} = \frac{50b_v s}{f_{yt}} = \frac{50b_v I_{vh}}{f_{yt}} \quad (5.33)$$

## 5.8 WEB REINFORCEMENT DESIGN PROCEDURE FOR SHEAR

The following is a summary of a recommended sequence of design steps:

1. Determine the required nominal shear strength value  $V_n = V_u/\phi$  at a distance  $h/2$  from the face of the support,  $\phi = 0.75$ .
2. Calculate the nominal shear strength  $V_c$  that the web has by one of the following two methods.
  - (a) *ACI conservative method if  $f_{pe} > 0.40 f_{pu}$*

$$V_c = \left( 0.60\lambda\sqrt{f'_c} + \frac{700V_u d_p}{M_u} \right) b_w d_p$$

where  $2\lambda\sqrt{f'_c} b_w d_p \leq V_c \leq 5\lambda\sqrt{f'_c} b_w d_p$  and where  $V_u d_p/M_u \leq 1.0$  and  $V_u$  is calculated at the same section for which  $M_u$  is calculated.

If the average tensile splitting strength  $f_{ct}$  is specified for lightweight concrete, then  $\lambda = f_{ct}/6.7\sqrt{f'_c}$  with  $\sqrt{f'_c}$  not to exceed a value of 100.

- (b) *Detailed analysis where  $V_c$  is the lesser of  $V_{ci}$  and  $V_{cw}$*

$$V_{ci} = 0.60\lambda\sqrt{f'_c} b_w d_p + V_d + \frac{V_i}{M_{\max}} (M_{cr}) \geq 1.7\lambda\sqrt{f'_c} b_w d_p \leq 5.0\lambda\sqrt{f'_c} b_w d_p$$

$$V_{cw} = (3.5\lambda\sqrt{f'_c} + 0.3\bar{f}_c) b_w d_p + V_p$$

using  $d_p$  or  $0.8h$ , whichever is larger, and

where  $M_{cr} = (I_c/y_t) (6\lambda\sqrt{f'_c} + f_{ce} - f_d)$

or  $M_{cr} = S_b (6\lambda\sqrt{f'_c} + f_{ce} - f_d)$

$V_i$  = factored shear force at section due to externally applied loads occurring simultaneously with  $M_{\max}$

$f_{ce}$  = compressive stress in concrete after occurrence of all losses at *extreme fibers* of section where external load causes tension.  $f_{ce}$  becomes  $f'_c$  for the stress at the centroid of the section.

3. If  $V_u/\phi \leq \frac{1}{2}V_c$ , no web steel is needed. If  $V_u/\phi > \frac{1}{2}V_c < V_c$ , provide minimum reinforcement. If  $V_u/\phi > V_c$  and  $V_s = V_u/\phi - V_c \leq 8\lambda\sqrt{f'_c}b_wd_p$ , design the web steel. If  $V_s = V_u/\phi - V_c > 8\lambda\sqrt{f'_c}b_wd_p$ , or if  $V_u > \phi(V_c + 8\lambda\sqrt{f'_c}b_wd_p)$ , enlarge the section.
4. Calculate the required minimum web reinforcement. The spacing is  $s \leq 0.75h$  or 24 in., whichever is smaller.

$$\text{Min. } A_v = 0.75\sqrt{f'_c} \frac{b_w s}{f_{yt}} \quad \text{or} \quad A_v = \frac{50b_w s}{f_{yt}} \quad \text{whichever is larger.}$$

If  $f_{pe} \geq 0.40f_{pu}$ , a less conservative Min  $A_v$  is the smaller of

$$A_v = \frac{A_{ps}f_{pu}s}{80f_y d_p} \sqrt{\frac{d_p}{b_w}}$$

where  $d_p \geq 0.80h$ , and

$$A_v = 50b_w s / f_{yt} \quad \text{or} \quad A_v = 0.75\sqrt{f'_c} \frac{b_w s}{f_{yt}}$$

5. Calculate the required web reinforcement size and spacing. If  $V_s = (V_u/\phi - V_c) \leq 4\lambda\sqrt{f'_c}b_wd_p$ , then the stirrup spacing  $s$  is as required by the design expressions in step 6, to follow. If  $V_s = (V_u/\phi - V_c) > 4\lambda\sqrt{f'_c}b_wd_p$ , then the stirrup spacing  $s$  is half the spacing required by the design expressions in step 6.
- 6.

$$s = \frac{A_v f_y d_p}{(V_u/\phi) - V_c} = \frac{A_v \phi f_y d_p}{V_u - \phi V_c} \leq 0.75h \leq 24 \text{ in. } \geq \text{minimum } s \text{ from step 4}$$

7. Draw the shear envelope over the beam span, and mark the band requiring web steel.
8. Sketch the size and distribution of web stirrups along the span using #3- or #4-size stirrups as preferable, but no larger size than #6 stirrups.
9. Design the vertical dowel reinforcement in cases of composite sections.
  - (a)  $V_{nh} \leq 80b_v d_{pc}$  for both roughened contact and no vertical ties or dowels, and nonroughened but with minimum vertical ties, use

$$A_v = \frac{50b_w s}{f_{yt}} = \frac{50b_v l_{vh}}{f_{yt}}$$

- (b)  $V_{nh} \leq 500b_v d_{pc}$  for a roughened contact surface with full amplitude  $\frac{1}{4}$  in.

- (c) For cases where  $V_{nh} > 500b_v d_{pc}$ , design vertical ties for  $V_{nh} = A_{vf} f_y \mu$ ,

where  $A_{vf}$  = area of frictional steel dowels

$\mu$  = coefficient of friction =  $1.0\lambda$  for intentionally roughened surface, where  $\lambda = 1.0$  for normal-weight concrete. In all cases,  $V_n \leq V_{nh} \leq 0.2f'_c A_{cc} \leq 800 A_{cc}$ , where  $A_{cc} = b_v l_{vh}$ .

An alternative method of determining the dowel reinforcement area  $A_{vf}$  is by computing the horizontal force  $F_h$  at the concrete contact surface such that

$$F_h \leq \mu_e A_{vf} f_y \leq V_{nh}$$

where

$$\mu_e = \frac{1,000\lambda^2 b_v l_{vh}}{F_h} \leq 2.9$$

Figure 5.16 outlines the foregoing steps in flowchart form.

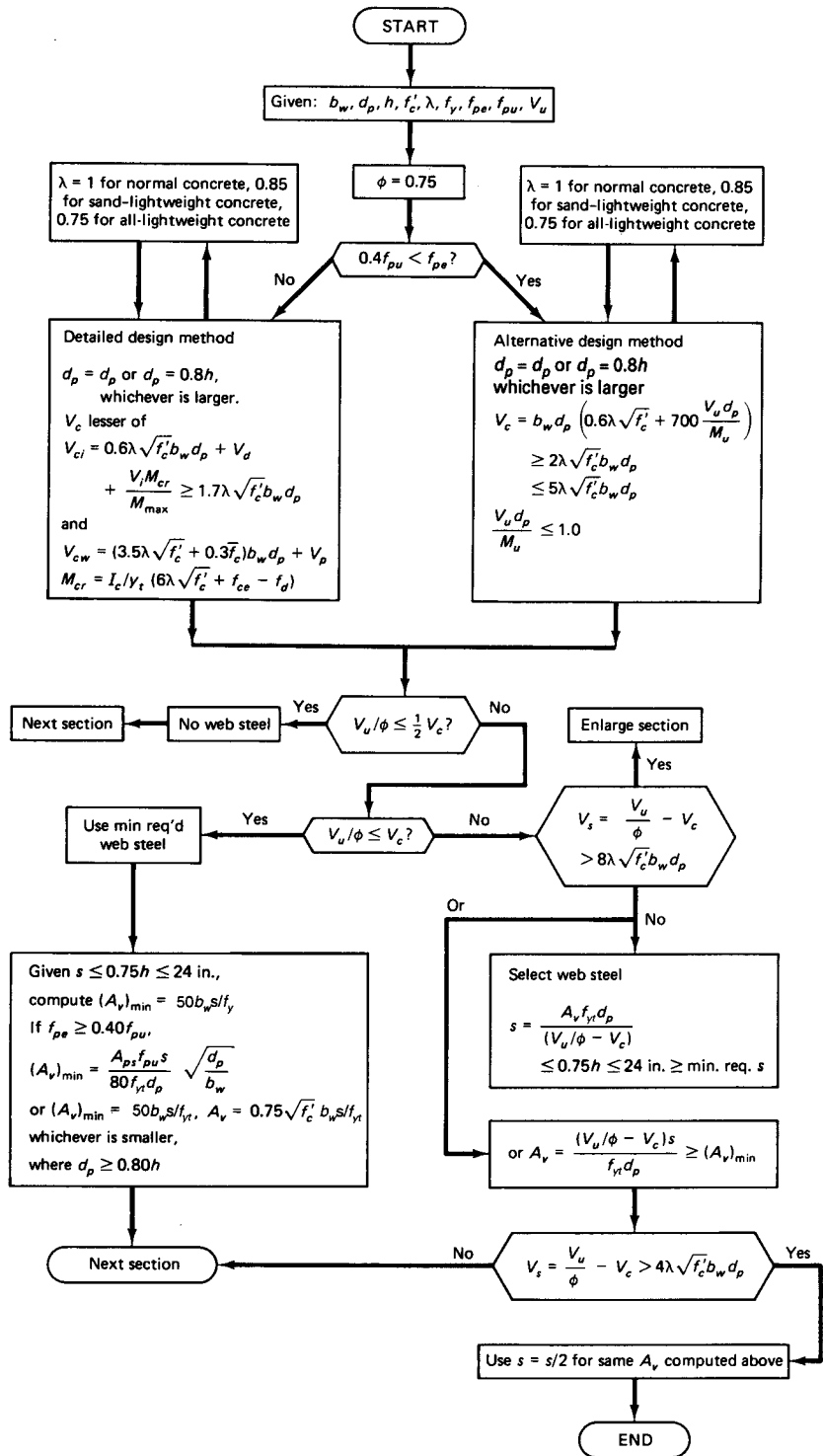


Figure 5.16 Flowchart for shear-web reinforcement.

## 5.9 PRINCIPAL TENSILE STRESSES IN FLANGED SECTIONS AND DESIGN OF DOWEL-ACTION VERTICAL STEEL IN COMPOSITE SECTIONS

### Example 5.1

A prestressed concrete T-beam section has the distribution of compressive service load shown in Figure 5.17. The unfactored design external vertical shear  $V = 120,000$  lb (554 kN), and the factored vertical shear  $V_u = 190,000$  lb (845 kN).

- Compute the principal tensile stress at the centroidal cgc axis and at the reentrant corner A of the web-flange junction, and calculate the maximum horizontal shearing stresses at service load for these locations.
- Compute the required nominal horizontal shear strength at the interaction surface A-A between the precast web and the situ-cast flange, and design the necessary vertical ties or dowels to prevent fracture slip at A-A, thereby ensuring complete composite action. Use the ACI direct method, and assume that the contact surface is intentionally roughened. Given data are as follows:

$$f'_c \text{ for web} = 6,000 \text{ psi normal-weight concrete}$$

$$f'_c \text{ for flange} = 3,000 \text{ psi normal-weight concrete}$$

$$f_{yr} = f_y = 60,000 \text{ psi}$$

$$\text{Effective width of flange } b_m = 60 \text{ in. (152.4 cm)}$$

where  $b_m$  is the modified width to account for the difference in moduli of the concrete of the precast and topping parts.

### Solution:

**Service-Load Horizontal Shear Stresses.** The maximum horizontal shear stress is

$$v_h = \frac{VQ}{Ib_v}$$

Now,

$$Q_A = 60 \times 12(19.32 - 6) = 9,590 \text{ in.}^3 (157,172 \text{ cm}^3)$$

$$Q_{cgc} = 60 \times 12(19.32 - 6) + \frac{12 \times (7.32)^2}{2} = 9,912 \text{ in.}^3 (162,429 \text{ cm}^3)$$

So the horizontal shear stresses at service load are

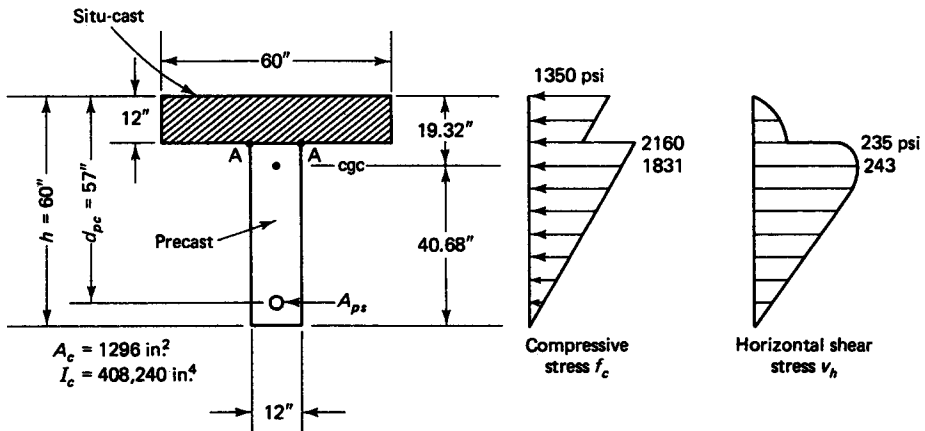


Figure 5.17 Beam cross section in Example 5.1.

$$v_h \text{ at A} = \frac{120,000 \times 9590}{408,240 \times 12} = 235 \text{ psi (1.6 MPa)}$$

and

$$v_h \text{ at cgc} = \frac{120,000 \times 9,912}{408,240 \times 12} = 243 \text{ psi (1.7 MPa)}$$

From Equation 5.13, the corresponding principal tensile stresses are, at A,

$$\begin{aligned} f'_t &= \sqrt{\left(\frac{f_{cA}}{2}\right)^2 + v_h^2} - \frac{f_{cA}}{2} \\ &= \sqrt{\left(\frac{2,160}{2}\right)^2 + (235)^2} - \frac{2,160}{2} = 25 \text{ psi (111 Pa)} \end{aligned}$$

and at cgc,

$$f'_t = \sqrt{\left(\frac{1,831}{2}\right)^2 + (243)^2} - \frac{1,831}{2} = 32 \text{ psi (221 Pa)}$$

Thus, the principal tensile stresses are low and should not cause any cracking at service load.

The horizontal shear stress  $v_h = 235$  psi at contact surface A–A has to be checked to verify whether it is within acceptable limits. In accordance with AASHTO, the maximum allowed is 160 psi < 235 psi, and hence special provision for added vertical ties or dowels has to be made if AASHTO requirements are applicable.

#### **Dowel Reinforcement Design**

$$V_u = 190,000 \text{ lb}$$

$$\text{Req. } V_{nh} = \frac{V_u}{\phi} = \frac{190,000}{0.75} = 253,333 \text{ lb (1126 kN)}$$

$$b_v = 12 \text{ in. (30.5 cm)} \quad d_{pc} = 57 \text{ in. (145 cm)}$$

From Equation 5.26b,

$$\text{Available } V_{nh} = 500b_v d_{pc} = 500 \times 12 \times 57 = 342,000 \text{ lb (1520 kN)} > 253,333 \text{ lb}$$

Hence, specify roughening the contact surface of the precast web fully to  $\frac{1}{4}$  in. amplitude.

From Equation 5.22 (a),  $0.75\sqrt{f'_c} = 0.75\sqrt{6000} = 58 > 50$ , use 58 in the expression.

$$\text{min unit } \frac{A_v}{l_{vh}} = \frac{58b_v}{f_{yt}} = \frac{58 \times 12}{60,000} = 0.0116 \text{ in.}^2/\text{in. along span}$$

So using #3 vertical stirrups,  $A_v = 2 \times 0.11 = 0.22 \text{ in.}^2$ , and  $s = 0.22/0.0116 = 18.9 \text{ in. (48 cm)}$  center to center < 24 in., O.K. Vertical-web steel reinforcement for shear in the web would most probably require smaller spacing. Hence, extend all web stirrups into the situ-cast top slab.

## **5.10 DOWEL STEEL DESIGN FOR COMPOSITE ACTION**

### **Example 5.2**

Using (a) the ACI friction coefficient and (b) the PCI friction coefficient, design the dowel reinforcement of Example 5.1 for full composite action by the alternative method, assuming a simply supported beam of effective 65 ft (19.8 m) span.

**Solution:** From Figures 5.14 and 5.17,

$$A_{\text{top}} = 60 \times 12 = 720 \text{ in}^2 (4,645 \text{ cm}^2)$$

$$C_c = 0.85f'_{cc}A_{\text{top}} = 0.85 \times 3,000 \times 720 = 1,836,000 \text{ lb (8,167 kN)}$$

Assume  $A_{ps}f_{ps} > C_c$ , since the prestressing force is not given. Then

$$F_h = 1,836,000 \text{ lb}$$

$$l_{vh} = \frac{65 \times 12}{2} = 390 \text{ in.}$$

$$b_v = 12 \text{ in.}$$

$$80b_v l_{vh} = 80 \times 12 \times 390 = 374,400 \text{ lb (1,665 kN)} < 1,836,000 \text{ lb}$$

Hence, vertical ties are needed.

For roughened surface to full  $\frac{1}{4}$  in. amplitude and minimum reinforcement,

$$V_{nh} = 500 b_v d = 500 \times 12 \times 57 = 342,000$$

$$\text{Req. } \frac{V_u}{\phi} = \frac{190,000}{0.75} = 253,333 \text{ lb} < V_{nh} = 342,000 < \text{available } F_h = 1,836,000 \text{ lb}$$

Use  $F_h = 253,333 \text{ lb}$  for determining the required composite action reinforcement.

**Using ACI  $\mu$  Value.** From Equation 5.27 and  $\mu = 1.0$ , with  $l_{vh} = 390 \text{ in.}$ ,

$$\text{Total } A_{vf} = \frac{253,333}{1.0 \times 60,000} = 4.2 \text{ in}^2 (26.3 \text{ cm}^2)$$

$$\text{Min } A_{vf} = \frac{50b_v l_{vh}}{f_{yt}} = \frac{50 \times 12 \times 390}{60,000} = 3.90 \text{ in}^2 (25.1 \text{ cm}^2)$$

From Example 5.1,  $\text{min } A_{vf} = 0.01 \text{ in.}^2/\text{in.} = 0.12 \text{ in.}^2/12 \text{ in.}$ , controls. So, trying #3 stirrups, we obtain  $A_v = 2 \times 0.11 = 0.22 \text{ in.}^2$ , and

$$s = \frac{l_{vh} A_v}{A_{vf}} = \frac{390 \times 0.22}{4.2} = 20.42 \text{ in. center-to-center} < 24 \text{ in.} < \text{max. allow. } 4 \times 12 = 48 \text{ in.}$$

So use #3 U ties at 20 in. center to center.

**Using PCI  $\mu_e$  Value**

$$\lambda = 1.0$$

$$\mu_e = \frac{1,000\lambda^2 b_v l_{vh}}{F_h} \leq 2.9$$

$$= \frac{1,000 \times 1 \times 12 \times 390}{1,836,000} = 2.55 < 2.9$$

So use  $\mu_e = 2.55$ ; then, from Equation 5.32,

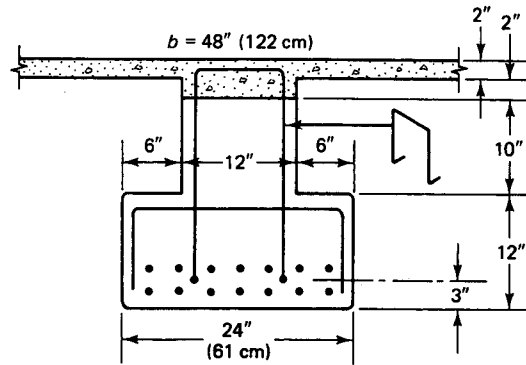
$$\text{Req. } A_{vf} = \frac{253,333}{2.55 \times 60,000} = 1.66 \text{ in.}^2 < \text{min. } A_{vf} = 3.90 \text{ in.}^2, \text{ controls}$$

So use #3 U ties at 20 in. center-to-center (9.5 mm dia at 55 cm).

## 5.11 DOWEL REINFORCEMENT DESIGN FOR COMPOSITE ACTION IN AN INVERTED T-BEAM

### Example 5.3

A simply supported inverted T-beam has an effective 24 ft (7.23 m) span length. The beam, shown in cross section in Figure 5.18, has a 2 in. (5.1 cm) situ-cast topping on a nonroughened surface. Design the required dowel action stirrups to develop full composite behavior, assuming that the factored shear  $V_u$  to which the beam is subjected at the critical section is 160,000 lb (712 kN). Given data are as follows:



**Figure 5.18** Beam cross section in Example 5.3.

$f'_c$  (precast) = 6,000 psi (41.4 MPa), normal-weight concrete

$f'_{cc}$  (topping) = 3,000 psi (20.7 MPa), normal-weight concrete

Prestressing steel:

Twelve  $\frac{1}{2}$  in. dia 270 k strands

$f_{pu} = 270,000$  psi (1,862 MPa)

$f_{ps} = 242,000$  psi (1,669 MPa)

Tie steel  $f_{yt} = 60,000$  psi (414 MPa)

Use both the ACI direct method and the alternative method with effective  $\mu_e$  to carry out your design.

**Solution:**

$$d_p = 2 + 2 + 10 + 12 - 3 = 23 \text{ in.}$$

$$A_{ps} = 12 \times 0.153 = 1.836 \text{ in.}^2$$

$$T_n = A_{ps}f_{ps} = 1.836 \times 242,000 = 444,312 \text{ lb (1,976 kN)}$$

$$b_v = 12 \text{ in.}$$

$$l_{vh} = \frac{24 \times 12}{2} = 144 \text{ in.}$$

$$A_{\text{top}} = 2 \times 48 + 2 \times 12 = 120 \text{ in.}^2$$

$$C_c = 0.85f'_{cc}A_{\text{top}} = 0.85 \times 3,000 \times 120 = 306,000 \text{ lb (1,361 kN)}$$

$$< T_n = 444,312 \text{ lb}$$

Accordingly, use  $F_n = 306,000$  lb (1,361 kN). Then, for a nonroughened surface,

$$\text{Available } V_{nh} = 80b_vl_{vh} = 80 \times 12 \times 144 = 138,240 \text{ lb (615 kN)}$$

$$< C_c = 306,000 \text{ lb}$$

Hence, ties are required for developing full composite action using  $\lambda = 1.0$ .

**ACI Direct Method**

$$\text{Req. } V_{nh} = \frac{V_u}{\phi} = \frac{160,000}{0.75} = 213,333 \text{ lb (949 kN)}$$

Use  $\mu = 1.0$ . Then, from Equation 5.26a, with dowel reinforcement, we have

$$\text{Available } V_{nh} = 80b_v d_{pc} = 80 \times 12 \times 23 = 22,000 \text{ lb} \ll \text{required } V_{nh}$$

From Equation 5.27, for an unroughened surface  $\mu = 0.6\lambda = 0.60$ . Then

$$\text{Req. total } A_{vf} = \frac{V_n}{\mu f_{yt}} = \frac{213,333}{0.60 \times 60,000} = 5.93 \text{ in}^2$$

From Eq. 5.22 (a),  $0.75\sqrt{f'_c} = 0.75\sqrt{6000} = 58 > 50$ , hence use 58 in the expression.

$$\text{Req. min } A_{vf} = \frac{58b_v l_{vh}}{f_{yt}} = \frac{58 \times 12 \times 144}{60,000} = 1.67 \text{ in}^2 < 5.93 \text{ in}^2$$

So use  $A_{vf} = 5.93 \text{ in}^2$  (37.0 cm<sup>2</sup>), and try #3 inverted U ties. Then  $A_{vf} = 2 \times 0.11 = 0.22 \text{ in}^2$  (1.4 cm<sup>2</sup>) and the spacing is

$$s = \frac{l_{vh} A_v}{A_{vf}} = \frac{144 \times 0.22}{5.93} = 5.34 \text{ in. (15.4 cm)}$$

The maximum allowable spacing is  $s = 4(2 + 2) = 16 \text{ in.}$ , or  $0.75h = 0.75 \times 26 = 19.5 \text{ in.} < 24 \text{ in.}$  Thus, use #3 inverted U ties 5 in. (13 cm) center-to-center over the entire simply supported span.

#### *Alternative Method Using $\mu_e$*

$$F_h = 306,000 \text{ lb}$$

$$\mu_e = \frac{1,000\lambda^2 b_v l_{vh}}{F_h} = \frac{1,000 \times 1.0 \times 12 \times 144}{306,000} = 5.65 > 2.9$$

So use  $\mu_e = 2.9$ ; then, from Equation 5.31c, we get

$$\text{Req. } A_{vf} = \frac{F_h}{\mu_e f_{yt}} = \frac{306,000}{2.9 \times 60,000} = 1.76 \text{ in}^2$$

$$\text{Req. min. } A_{vf} \text{ from (a)} = 1.67 \text{ in}^2 < 1.76 \text{ in}^2$$

So use  $A_{vf} = 1.76 \text{ in}^2$ . Then the spacing is four times the least dimension:

$$s = \frac{l_{vh} A_v}{A_{vf}} = \frac{144 \times 0.22}{1.76} = 18 \text{ in. center-to-center}$$

and the maximum allowable spacing is four times the least dimension:

$$s = 4(2 + 2) = 16 \text{ in.} < 24 \text{ in.}$$

Hence, use #3 inverted U ties at 16 in. center to center over the entire simply supported span.

## 5.12 SHEAR STRENGTH AND WEB-SHEAR STEEL DESIGN IN A PRESTRESSED BEAM

### **Example 5.4**

Design the bonded beam of Example 4.2 to be safe against shear failure, and proportion the required web reinforcement.

**Solution:**

#### *Data and Nominal Shear Strength Determination*

$$f_{pu} = 270,000 \text{ psi (1,862 MPa)}$$

$$f_y = f_{yt} = 60,000 \text{ psi (414 MPa)}$$

$$f_{pe} = 155,000 \text{ psi (1,069 MPa)}$$

$$f'_c = 5,000 \text{ psi normal-weight concrete}$$

$$A_{ps} = 13 \text{ 7-wire } \frac{1}{2}\text{-in. tendons} = 1.99 \text{ in}^2 \text{ (12.8 cm}^2\text{)}$$



$$A_s = 4 \text{ #6 bars} = 1.76 \text{ in}^2 (11.4 \text{ cm}^2)$$

$$\text{Span} = 65 \text{ ft (19.8 m)}$$

$$\text{Service } W_L = 1,100 \text{ plf (16.1 kN/m)}$$

$$\text{Service } W_{SD} = 100 \text{ plf (1.46 kN/m)}$$

$$\text{Service } W_D = 393 \text{ plf (5.7 kN/m)}$$

$$h = 40 \text{ in. (101.6 cm)}$$

$$d_p = 36.16 \text{ in. (91.8 cm)}$$

$$d = 37.6 \text{ in. (95.5 cm)}$$

$$b_w = 6 \text{ in. (15 cm)}$$

$$e_c = 15 \text{ in. (38 cm)}$$

$$e_e = 12.5 \text{ in. (32 cm)}$$

$$I_c = 70,700 \text{ in.}^4 (18.09 \times 10^6 \text{ cm}^4)$$

$$A_c = 377 \text{ in.}^2 (2,432 \text{ cm}^2)$$

$$r^2 = 187.5 \text{ in.}^2 (1,210 \text{ cm}^2)$$

$$c_b = 18.84 \text{ in. (48 cm)}$$

$$c_t = 21.16 \text{ in. (54 cm)}$$

$$P_e = 308,255 \text{ lb (1,371 kN)}$$

$$\text{Factored load } W_u = 1.2D + 1.6L$$

$$= 1.2(100 + 393) + 1.6 \times 1,100 = 2352 \text{ plf}$$

$$\text{Factored shear force at face of support} = V_u = W_u L/2$$

$$= (2352 \times 65)/2 = 76,440 \text{ lb}$$

$$\text{Req. } V_n = V_u/\phi = 76,440/0.75 = 101,920 \text{ lb at support}$$

### ***Plane at $\frac{1}{2}d_p$ from Face of Support***

The ACI 318 Code allows in the case of prestressed concrete members to consider the critical section for shear and torsion to be taken at a distance of  $h/2$  from the face of the support while in reinforced concrete members it mandates a distance of  $d/2$ . For uniformity in the treatment of both materials,  $d_p/2$  is chosen in the solutions, which is slightly more conservative.

#### **1. Nominal shear strength $V_c$ of web (steps 2, 3)**

$$\frac{1}{2} d_p = \frac{36.16}{2 \times 12} \cong 1.5 \text{ ft}$$

$$V_n = 101,920 \times \frac{[(65/2) - 1.5]}{65/2} = 97,216 \text{ lb}$$

$$V_u \text{ at } \frac{1}{2} d_p = 0.75 \times 97,216 = 72,912 \text{ lb (} V_u \text{ at } \frac{1}{2} h = 72,206 \text{ lb)}$$

$$f_{pe} = 155,000 \text{ psi}$$

$$0.40f_{pu} = 0.40 \times 270,000 = 108,000 \text{ psi (745 MPa)}$$

$$< f_{pe} = 155,000 \text{ psi (1,069 MPa)}$$

#### ***Use ACI alternate method***

Since  $d_p > 0.8h$ , use  $d_p = 36.16 \text{ in.}$ , assuming that part of the prestressing strands continue straight to the support. From Equation 5.16,

$$V_c = \left( 0.60\lambda \sqrt{f'_c} + 700 \frac{V_u d_p}{M_u} \right) b_w d_p \geq 2\lambda \sqrt{f'_c} b_w d_p \leq 5\lambda \sqrt{f'_c} b_w d_p$$

$\lambda = 1.0$  for normal-weight concrete

$$\begin{aligned} M_u \text{ at } d/2 \text{ from face} &= \text{reaction} \times 1.5 - \frac{W_u(1.5)^2}{2} \\ &= 76,440 \times 1.5 - \frac{2352(1.5)^2}{2} = 112,014 \text{ ft}\cdot\text{lb} = 1,344,168 \text{ in}\cdot\text{lb} \\ \frac{V_u d_p}{M_u} &= \frac{72,912 \times 36.16}{1,344,168} = 1.96 > 1.0 \end{aligned}$$

So use  $V_u d_p / M_u = 1.0$ . Then

$$\text{Min. } V_c = 2\lambda\sqrt{f'_c}b_w d_p = 2 \times 1.0\sqrt{5,000} \times 6 \times 36.16 = 30,683 \text{ lb}$$

$$\text{Max. } V_c = 5\lambda\sqrt{f'_c}b_w d_p = 76,707 \text{ lb}$$

$$\begin{aligned} V_c &= (0.60 \times 1.0\sqrt{5,000} + 700 \times 1.0)6 \times 36.16 \\ &= 161,077 \text{ lb} > \max V_c = 76,707 \text{ lb} \end{aligned}$$

Then  $V_c = 76,707 \text{ lb}$  and controls (341 kN). Also,  $V_u/\phi > \frac{1}{2}V_c$ ; hence, web steel is needed. Accordingly,

$$V_s = \frac{V_u}{\phi} - V_c = 97,216 - 76,707 = 20,509 \text{ lb}$$

$$\begin{aligned} 8\lambda\sqrt{f'_c}b_w d_p &= 8 \times 1.0\sqrt{5,000} \times 6 \times 36.16 = 122,713 \text{ lb (546 kN)} \\ &> V_s = 20,509 \text{ lb} \end{aligned}$$

So the section depth is adequate.

### 2. Minimum web steel (step 4)

From Equation 5.22b,

$$\begin{aligned} \text{Min. } \frac{A_v}{s} &= \frac{A_{ps}f_{pu}}{80f_{yt}d_p}\sqrt{\frac{d_p}{b_w}} \\ &= \frac{1.99 \times 270,000}{80 \times 60,000 \times 36.16}\sqrt{\frac{36.16}{6}} = 0.0076 \text{ in.}^2/\text{in.} \end{aligned}$$

### 3. Required web steel (steps 5, 6)

From Equation 5.21b,

$$s = \frac{A_v f_{yt} d_p}{V_u/\phi - V_c} \leq 0.75h \leq 24 \text{ in.}$$

or

$$\frac{A_v}{s} = \frac{V_s}{f_{yt}d_p} = \frac{20,509}{60,000 \times 36.16} = 0.0095 \text{ in.}^2/\text{in.}$$

(prestressing force is  $> 0.4 \times$  tensile strength)

Then the minimum required web-shear steel  $A_v/s = 0.0095 \text{ in.}^2/\text{in.}$  So trying #3 U stirrups,  $A_v = 2 \times 0.11 = 0.22 \text{ in.}^2$ , and we get  $0.0095 = 0.22/s$ , so that the maximum spacing is

$$s = \frac{0.22}{0.0095} = 23.2 \text{ in. (59 cm)}$$

and

$$4\lambda\sqrt{f'_c}b_w d_p = 4 \times 1.0\sqrt{5,000} \times 6 \times 36.16 = 61,366 \text{ lb} > V_s$$

Hence, we do not need to use  $\frac{1}{2}s$ . Now,

$$0.75h = 0.75 \times 40.0 = 30.0 \text{ in.}$$

Thus, use #3 U web-shear reinforcement at 22 in. center to center (9.5 mm dia at 56 cm center to center).

**Plane at Which No Web Steel Is Needed.** Assume such a plane is at distance  $x$  from support. By similar triangles,

$$\frac{1}{2}V_c = \frac{76,707}{2} = 101,920 \times \frac{65/2 - x}{65/2}$$

or

$$\frac{65}{2} - x = \frac{76,707}{101,920} \times \frac{65}{4}$$

giving

$$x = 20.3 \text{ ft (6.11 m)} \approx 244 \text{ in.}$$

Therefore, adopt the design in question, using #3 U at 22 in. center-to-center over a stretch length of approximately 244 in., with the first stirrup to start at 18 in. from the face of support. Extend the stirrups to the midspan if composite action doweling is needed.

### 5.13 WEB-SHEAR STEEL DESIGN BY DETAILED PROCEDURES

#### Example 5.5

Solve Example 5.4 by detailed procedures, determining the value of  $V_c$  as the smaller of the flexure shear  $V_{ci}$  and the web shear  $V_{cw}$ . Assume that the tendons are harped at midspan and not draped. Also assume  $f'_c = 6000$  psi.

**Solution:** The profile of the prestressing strands is shown in Figure 5.19.

**Plane at  $d/2$  from Face of Support.** From Example 5.4,  $V_n = 97,216$  lb.

#### 1. Flexure-shear cracking, $V_{ci}$ (step 2)

From Equation 5.11,

$$V_{ci} = 0.60\lambda\sqrt{f'_c}b_wd_p + V_d + \frac{V_i}{M_{\max}}(M_{cr}) \geq 1.7\lambda\sqrt{f'_c}b_wd_p$$

From Equation 5.12, the cracking moment is

$$M_{cr} = \frac{I_c}{y_t} (6\lambda\sqrt{f'_c} + f_{ce} - f_d)$$

where  $I_c/y_t = S_b$  since  $y_t$  is the distance from the centroid to the extreme tension fibers. Now,

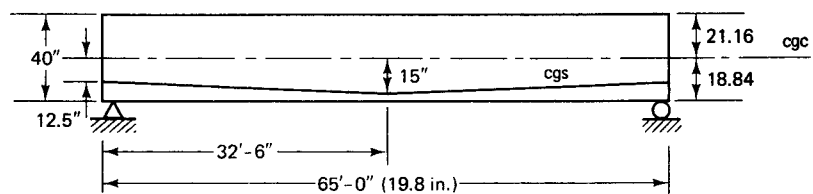


Figure 5.19 Tendon profile in Example 5.5.

$$I_c = 70,700 \text{ in.}^4$$

$$c_b = 18.84 \text{ in.}$$

$$P_e = 308,255 \text{ lb}$$

$$S_b = 3,753 \text{ in.}^3$$

$$r^2 = 187.5 \text{ in.}^2$$

So from Equation 4.3b, the concrete stress at the extreme bottom fibers *due to pre-stress only* is

$$f_{ce} = -\frac{P_e}{A_c} \left( 1 + \frac{ec_b}{r^2} \right)$$

and the tendon eccentricity at  $d_p/2 \cong 1.5$  ft from the face of the support is

$$e = 12.5 + (15 - 12.5) \frac{1.5}{65/2} = 12.62 \text{ in.}$$

Thus,

$$f_{ce} = -\frac{308,255}{377} \left( 1 + \frac{12.62 \times 18.84}{187.5} \right) \cong -1,855 \text{ psi (12.8 MPa)}$$

From Example 4.2, the unfactored dead load due to self-weight  $W_D = 393$  plf (5.7 kN/m) is

$$M_{d/2} = \frac{W_D x(l-x)}{2} = \frac{393 \times 1.5(65 - 1.5) \times 12}{2} = 224,600 \text{ in.-lb (25.4 kN-m)}$$

and the stress due to the unfactored dead load at the extreme concrete fibers where tension is created by the external load is

$$f_d = \frac{M_{d/2} c_b}{I_c} = \frac{224,600 \times 18.84}{70,700} = 60 \text{ psi}$$

Also,

$$\begin{aligned} M_{cr} &= 3,753(6 \times 1.0 \times \sqrt{6,000} + 1,855 - 60) \\ &= 8,480,872 \text{ in.-lb (958 kN-m)} \end{aligned}$$

$$V_d = W_D \left( \frac{l}{2} - x \right) = 393 \left( \frac{65}{2} - 1.5 \right) = 12,183 \text{ lb (54.2 kN)}$$

$$W_{SD} = 100 \text{ plf}$$

$$W_L = 1,100 \text{ plf}$$

$$W_U = 1.2 \times 100 + 1.6 \times 1100 = 1880 \text{ plf}$$

The factored shear force at the section due to externally applied loads occurring simultaneously with  $M_{\max}$  is

$$V_i = W_U \left( \frac{l}{2} - x \right) = 1880 \left( \frac{65}{2} - 1.5 \right) = 58,280 \text{ lb (259 kN)}$$

and

$$\begin{aligned} M_{\max} &= \frac{W_U x(l-x)}{2} = \frac{1880 \times 1.5(65 - 1.5)}{2} \times 12 \\ &= 1,074,420 \text{ in.-lb (122 kN-m)} \end{aligned}$$

Hence,

$$\begin{aligned}
 V_{ci} &= 0.6 \times 1.0\sqrt{6,000} \times 6 \times 36.16 + 12,183 + \frac{58,280}{1,074,420}(8,480,872) \\
 &= 482,296 \text{ lb (54.5 kN-m)} \\
 1.7\lambda\sqrt{f'_c}b_wd_p &= 1.7 \times 1.0\sqrt{6,000} \times 6 \times 36.16 = 28,569 \text{ lb (127 kN)} \\
 &< V_{ci} = 482,296 \text{ lb}
 \end{aligned}$$

Hence,  $V_{ci} = 482,296 \text{ lb (214.5 kN)}$ .

**2. Web-shear cracking,  $V_{cw}$  (step 2)**

From Equation 5.15,

$$\begin{aligned}
 V_{cw} &= (3.5\sqrt{f'_c} + 0.3\bar{f}_c)b_wd_p + V_p \\
 \bar{f}_c &= \text{compressive stress in concrete at the cgc} \\
 &= \frac{P_e}{A_c} = \frac{308,255}{377} \cong 818 \text{ psi (5.6 MPa)}
 \end{aligned}$$

$$\begin{aligned}
 V_p &= \text{vertical component of effective prestress at section} \\
 &= P_e \tan \theta \text{ (more accurately, } P_e \sin \theta)
 \end{aligned}$$

where  $\theta$  is the angle between the inclined tendon and the horizontal. So

$$V_p = 308,255 \frac{(15 - 12.5)}{65/2 \times 12} = 1,976 \text{ lb (8.8 kN)}$$

Hence,  $V_{cw} = (3.5\sqrt{6,000} + 0.3 \times 818) \times 6 \times 36.16 + 1,976 = 114,038 \text{ lb (507 kN)}$ . In this case, web-shear cracking controls (i.e.,  $V_c = V_{cw} = 114,038 \text{ lb (507 kN)}$ ) is used for the design of web reinforcement). Compare this value with  $V_c = 76,707 \text{ lb (341 kN)}$  obtained in Example 5.4 by the more conservative alternative method.

Now, from Example 5.4,

$$V_s = \frac{V_u}{\phi = 0.75} - V_c = (97,216 - 114,038) \text{ lb, namely } V_c > V_u$$

So no web steel is needed unless  $V_u/\phi > \frac{1}{2}V_c$ . Accordingly, we evaluate the latter:

$$\frac{1}{2}V_c = \frac{114,038}{2} = 57,019 \text{ lb (254 kN)} < 97,216 \text{ lb (432 kN)}$$

Since  $V_u/\phi > \frac{1}{2}V_c$  but  $< V_c$ , use minimum web steel in this case.

**3. Minimum web steel (step 4)**

From Example 5.4,

$$\text{Req. } \frac{A_v}{s} = 0.0077 \text{ in.}^2/\text{in.}$$

So, trying #3 U stirrups, we get  $A_v = 2 \times 0.11 = 0.22 \text{ in.}^2$ , and it follows that

$$s = \frac{A_v}{\text{Req. } A_v/s} = \frac{0.22}{0.0077} = 28.94 \text{ in. (73 cm)}$$

We then check for the minimum  $A_v$ , as the lesser of the two values given by

$$A_v = 0.75\sqrt{f'_c} \left( \frac{b_w s}{f_{yt}} \right), A_v = 50b_w s / f_{yt} \text{ whichever is larger,}$$

and

$$A_v = \frac{A_{ps} f_{pu} s}{80 f_{yt} d_p} \sqrt{\frac{d_p}{b_w}}$$

So the maximum allowable spacing  $\leq 0.75h \leq 24 \text{ in.}$  Then use #3 U stirrups at 22 in. center-to-center over a stretch length of 84 in. from the face of the support, as in Example 5.4.

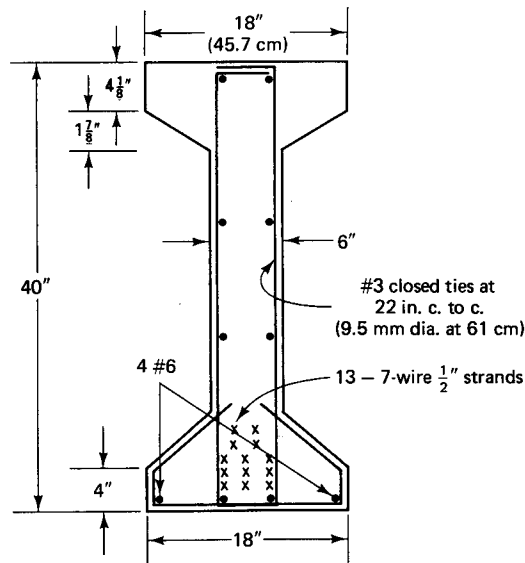


Figure 5.20 Web reinforcement details in Example 5.5.

Details of the section reinforcement (step 8) are shown in Figure 5.20.

## 5.14 DESIGN OF WEB REINFORCEMENT FOR A PCI DOUBLE T-BEAM

### Example 5.6

A simply supported PCI 12 DT 34 pretopped double-T-beam has a span of 70 ft (21.3 m). It is subjected to a superimposed service dead load of 200 plf (2.9 kN/m), including a 2-in. additional topping placed sometime after service, and a service live load  $W_L = 720$  plf. Design the web reinforcement needed to prevent shear cracking at the quarter-span section 17 ft 6 in. (5.3 m) from the support, calculating the nominal web-shear strength  $V_c$  by the detailed design method. Also, design any dowel reinforcement if necessary, assuming that the top surface of the precast T-beam is intentionally unroughened. The section properties are shown in Figure 5.21 and are as follows:

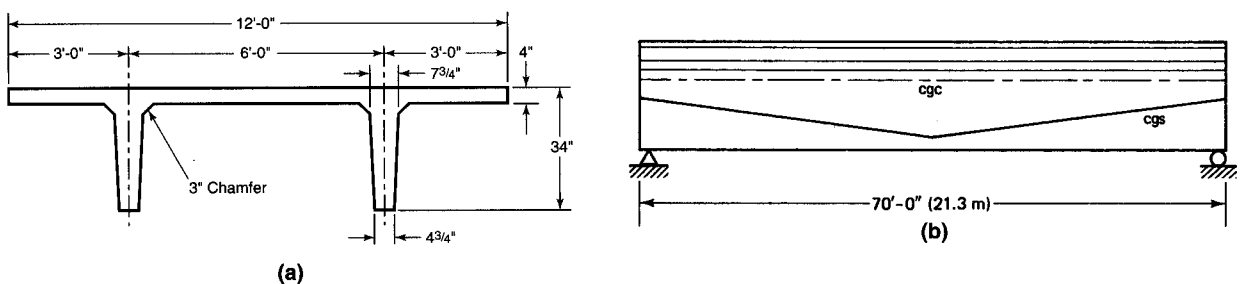


Figure 5.21 Beam geometry in Example 5.5. (a) Section. (b) Elevation.

Section property	Pretopped
$A_c$	978 in. <sup>2</sup>
$I_c$	86,072 in. <sup>4</sup>
$r^2$	88.0 in. <sup>2</sup>
$c_b$	25.77 in.
$c_t$	8.23 in.
$S_b$	3,340 in. <sup>4</sup>
$S^t$	10,458 in. <sup>3</sup>
$W_D$	1,019 plf
$2b_w$	12.50 in.

Other data are:

$f'_c$  (precast) = 5,000 psi (34.5 MPa), normal-weight concrete

$f'_{cc}$  (topping) = 3,000 psi (20.7 MPa), normal-weight concrete, for future topping if used

$f'_{ci}$  = 4,000 psi (27.6 MPa)

$f_{pu}$  = 270,000 psi (1,862 MPa), low-relaxation steel

$f_{ps}$  = 240,000 psi (1,655 MPa)

$f_{pe}$  = 148,000 psi (1,020 MPa)

$e_e$  = 11.38 in. (28.3 cm)

$e_c$  = 21.77 in. (57.2 cm)

$A_{ps}$  = 18  $\frac{1}{2}$ -in. (12.7 mm) dia strands

$f_{yt}$  for stirrups = 60,000 psi (414 MPa)

Use the same value for the effective depth  $d_p$  for the midspan as well as other sections. Note that  $b_w$  for both webs = 2 (4.75 + 7.75)/2 = 12.50 in. (32 cm).

**Solution:**

$$W_u = 1.2(200 + 1,019) + 1.6 \times 720 \cong 2615 \text{ plf (58kN/m)}$$

$$V_u \text{ at face of support} = \frac{2615 \times 70}{2} = 91,525 \text{ lb}$$

$$\begin{aligned} V_n \text{ at 17 ft 6 in. from the face of the support} &= \frac{1}{0.75} \left( 91,525 \times \frac{(35 - 17.5)}{35} \right) \\ &= 61,017 \text{ lb (271 kN)} \end{aligned}$$

1. Flexure-shear cracking,  $V_{ci}$  (step 2)

$$d_p = 34 - 25.77 + 21.77 = 30.0 \text{ in. (76 cm)}$$

$$P_e = 18 \times 0.153 \times 148,000 = 407,592 \text{ lb (18,176 kN)}$$

$$e \text{ at 17 ft, 6 in. from support} = 11.38 + (21.77 - 11.38) \frac{17.5}{35} = 16.58 \text{ in.}$$

Use the precast section properties for computing  $f_{ce}$  and  $f_d$  as discussed in Section 5.5:

$$\begin{aligned} f_{ce} &= -\frac{P_e}{A_c} \left( 1 + \frac{ec_b}{r^2} \right) = -\frac{407,592}{978} \left( 1 + \frac{16.58 \times 25.77}{88.0} \right) \\ &= -2,440 \text{ psi (16.8 MPa)} \end{aligned}$$

Use allowable extreme compressive stresses as follows:

- (a) prestress + sustained load:  $f_c = 0.45f'_c$   
 (b) prestress + total load (allowing 33% increase due to transient load:  $f_c = 0.60f'_c$ )  
 Note that although  $f_{ce} = 0.45f'_c$ , this should not affect the shear strength since  $f_{ce}$  is due to prestress only, and the inclusion of self-weight reduces it to less than  $0.45f'_c$ .  
 We thus have

Self-Weight  $W_D = 1,019$  plf

$$M_{17.5} = \frac{W_D x(l-x)}{2} = \frac{1,019 \times 17.5(70 - 17.5)}{2} \times 12$$

$$= 5,617,238 \text{ in.-lb (634 kN-m)}$$

$$f_d = \frac{M_{c_b}}{I_c} = \frac{5,617,238 \times 25.77}{86,072} = 1,682 \text{ psi (11.6 MPa)}$$

$$M_{cr} = S_b(6.0\lambda\sqrt{f'_c} + f_{ce} - f_d)$$

$$= 3,340(6.0 \times 1.0\sqrt{5,000} + 2,440 - 1,682)$$

$$= 3,948,762 \text{ in.-lb (445 kN-m)}$$

It should be noted that the factor 6.0 in the cracking moment expression is low, since the modulus of rupture is taken 7.5. If 7.5 is used in the expression the cracking moment value would have become 4,303,022 in.-lb, thereby reducing the number of stirrups needed in this design.

Unfactored shear due to self-weight dead load is:

$$V_d = W_D \left( \frac{l}{2} - x \right) = 1,019 \left( \frac{70}{2} - 17.5 \right) = 17,833 \text{ lb}$$

$$W_{SD} = 200 \text{ plf}$$

$$W_L = 720 \text{ plf}$$

Factored external load intensity is:

$$W_U = 1.2 \times 200 + 1.6 \times 720 = 1392 \text{ plf (20.4 kN/m)}$$

$$V_i = W_U \left( \frac{l}{2} - x \right) = 1392 \left( \frac{70}{2} - 17.5 \right) = 24,360 \text{ lb (108 kN)}$$

$$M_{\max} = W_U x \left( \frac{l-x}{2} \right) = \frac{1392 \times 17.5(70 - 17.5)}{2} \times 12$$

$$= 7,673,400 \text{ in.-lb (867 kN-m)}$$

$$V_{ci} = 0.6\lambda\sqrt{f'_c}b_w d_p + V_d + \frac{V_i}{M_{\max}} \times (M_{cr}) \geq 1.7\lambda\sqrt{f'_c}b_w d_p$$

$$= 0.6 \times 1.0 \times \sqrt{5,000} \times 12.5 \times 30.0 + 17,833$$

$$+ \frac{24,360}{7,673,400} (3,948,762)$$

$$= 46,279 \text{ lb (201 kN)}$$

$$1.7\lambda\sqrt{f'_c}b_w d_p = 1.7 \times 1.0\sqrt{5,000} \times 12.5 \times 30.0 = 45,078 \text{ lb} < 46,279 \text{ lb}$$

Hence,  $V_{ci} = 46,279$  controls.

## 2. Web-shear cracking, $V_{cw}$ (step 2)

$$\bar{f}_c = \frac{P_e}{A_c} = \frac{407,592}{978} = 417 \text{ psi (2.9 MPa)}$$



For the vertical component of the prestress force,

$$V_p = P_e \tan \theta = 407,592 \frac{(21.77 - 11.38)}{70/2 \times 12} = 10,083 \text{ lb (44.0 kN)}$$

$$\begin{aligned} V_{cw} &= (3.5\lambda \sqrt{f'_c} + 0.3\bar{f}_c) b_w d_p + V_p \\ &= (3.5 \sqrt{5,000} + 0.3 \times 417) \times 12.5 \times 30.0 + 10,083 \\ &= 149,803 \text{ lb vs. } V_{ci} = 46,279 \text{ lb} \end{aligned}$$

Now,  $V_c$  is the smaller of  $V_{ci}$  and  $V_{cw}$ ; hence,

$$V_c = V_{ci} = 46,279 \text{ lb}$$

### 3. Design of web reinforcement (steps 3–8)

From above,

$$V_c = 46,279 \text{ lb}$$

So

$$\frac{1}{2}V_c = 23,140 \text{ lb}$$

Now,  $V_u / \phi$  at a section 17.5 ft from support = 61,017 lb  $> V_c > \frac{1}{2}V_c$ ; hence design of stirrups is necessary. If  $V_u / \phi < V_c > \frac{1}{2}V_c$ , only minimum-web steel is needed.

$$\begin{aligned} \text{Req. } \frac{A_v}{s} &= \frac{V_n - V_c}{f_{yt} d_p} = \frac{(V_u / \phi) - V_c}{f_{yt} d_p} = \frac{61,017 - 46,279}{60,000 \times 30.0} \\ &= 0.0082 \text{ in.}^2/\text{in. spacing} \end{aligned}$$

Using  $d \cong d_p = 30.0$  in. and  $b_w = 12.5$  in.:

$$\begin{aligned} \text{Min.} \left( \frac{A_v}{s} \right) &= \frac{A_{ps}}{80} \frac{f_{pu}}{f_{yt} d_p} \sqrt{\frac{d_p}{b_w}} = \frac{18 \times 0.153}{80} \times \frac{270,000}{60,000 \times 30.0} \sqrt{\frac{30.0}{12.5}} = 0.0080 \\ &0.75 \sqrt{f'_c} = 0.75 \sqrt{5000} = 53 \\ \text{or Min.} \left( \frac{A_v}{s} \right) &= \frac{53 b_w}{f_{yt}} = \frac{53 \times 12.5}{60,000} = 0.011 \text{ in.}^2/\text{in.} \end{aligned}$$

The *lesser* of the two minimum value applies, consequently, min.  $A_v = 0.0080 \text{ in.}^2/\text{in.}$  applies as the lesser of the two values.

$$\text{Hence controlling } \frac{A_v}{s} = 0.0080 \text{ in.}^2/\text{in.} = 0.10 \text{ in.}^2/\text{ft for both webs or}$$

$$0.05 \text{ in.}^2/\text{ft per web}$$

Try one row of D5 deformed welded wire fabric at 10 in. center-to-center weld spacing.

The maximum allowable spacing is, then  $0.75h \leq 24$  in. So we have

$$0.75h = 0.75 \times 34 = 25.5 \text{ in.}$$

Accordingly, adopt one row D5 WWF web reinforcement in one layer at 10 in. center-to-center weld spacing per web at the quarter-span section.

Note, in comparing the solution for  $V_{ci}$  and  $V_{cw}$  in Example 5.6, that  $V_{ci}$  has its highest value close to the support and *rapidly* decreases toward the midspan, while  $V_{cw}$  has a lesser variation in its value, as can be seen from Figure 5.13. It is important to calculate the flexure shear  $V_{ci}$  and web shear  $V_{cw}$  at several sections along the span in order to determine the most efficient distribution of the web steel. A computer program facilitates finding these values at constant intervals of, say,  $\frac{1}{10}$ th of the span, and a plot can

be made similar to the one in Figure 5.13 showing the variation of the shear strengths of the web along the span.

4. *Design of dowel steel for full composite section of the additional 2-in. topping (step 9), if such topping is added later to the pretopped section.*

*Section at  $\frac{1}{2} d_p$  from face of support*

$$\text{Used } d_p = 30.0 + 2.0 = 32 \text{ in.}$$

$$V_u \text{ at support} = 91,525 \text{ (408 kN)}$$

$$\frac{1}{2} d_p = \frac{32.0}{2 \times 12} = 1.33 \text{ ft (40 cm)} \quad h/2 = 17 \text{ in.} = 1.33 \text{ ft}$$

$$V_u = 91,525 \times \left( \frac{35 - 1.33}{35} \right) = 88,047 \text{ lb (393 kN)}$$

$$\text{Req } V_{nh} = \frac{V_u}{\phi} = \frac{88,047}{0.75} = 117,396 \text{ (522 kN)}$$

$$b_v = 12 \text{ ft.} \quad \text{topping } h = 2 \text{ in.}$$

From Figure 5.14

$$C_c = 0.85 f'_c A_{top} = 0.85 \times 3000 \times 12 \times 12 \times 2 = 734,400 \text{ lb (3,267 kN)}$$

$$T_s = A_{ps} f_{ps} = 18 \times 0.153 \times 240,000 = 660,960 \text{ (2,940 kN)}$$

$$< C_c = 734,400 \text{ lb}$$

Hence,

$$F_h = 660,960 \text{ lb (2,178 kN)}$$

$$l_{vh} = \frac{70 \times 12}{2} = 420 \text{ in. (1,067 cm)}$$

$$b_v = 144 \text{ in. (366 cm)}$$

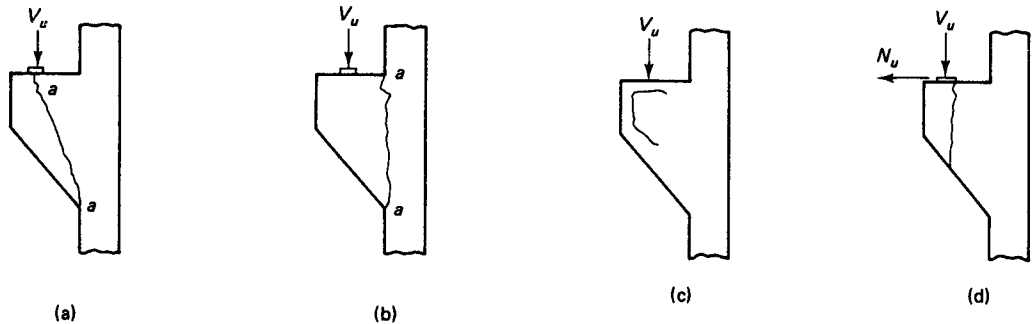
$$80 b_v l_{vh} = 80 \times 144 \times 420 = 4,838,400 \text{ lb (21,520 kN)} \gg 660,960 \text{ lb}$$

No dowel reinforcement is needed to extend to future additional 2-in. topping for full composite action to be developed. The section is adopted when it satisfies the flexural, deflection, and cracking requirements.

## 5.15 BRACKETS AND CORBELS

Brackets and corbels are short-haunched cantilevers that project from the inner face of columns or concrete walls to support heavy concentrated loads or beam reactions. They are very important structural elements for supporting precast beams, gantry girders, and any other forms of precast structural systems. Precast and prestressed concrete is becoming increasingly dominant, and larger spans are being built, resulting in heavier shear loads at supports. Hence, the design of brackets and corbels has become increasingly important. The safety of the total structure could depend on the sound design and construction of the supporting element, in this case the corbel, necessitating a detailed discussion of this subject.

In brackets and corbels, the ratio of the shear arm or span to the corbel depth is often less than 1.0. Such a small ratio changes the state of stress of a member into a two-dimensional one. Shear deformations would hence affect the nonlinear stress behavior of the bracket or corbel in the elastic state and beyond, and the shear strength becomes a major factor. Corbels also differ from deep beams in the existence of potentially large horizontal forces transmitted from the supported beam to the corbel or bracket. These



**Figure 5.22** Failure patterns. (a) Diagonal shear. (b) Shear friction. (c) Anchorage splitting. (d) Vertical splitting.

horizontal forces result from long-term shrinkage and creep deformation of the supported beam, which in many cases is anchored to the bracket.

The cracks are usually mostly vertical or steeply inclined pure shear cracks. They often start from the point of application of the concentrated load and propagate toward the bottom reentrant corner junction of the bracket to the column face, as in Figure 5.22(a). Or they start at the upper reentrant corner of the bracket or corbel and proceed almost vertically through the corbel toward its lower fibers, as shown in Figure 5.22(b). Other failure patterns in such elements are shown in Figure 5.22(c) and (d). They can also develop through a combination of the ones illustrated. Bearing failure can also occur by crushing of the concrete under the concentrated load-bearing plate, if the bearing area is not adequately proportioned.

As will be noticed in the subsequent discussion, detailing of the corbel or bracket reinforcement is of major importance. Failure of the element can be attributed in many cases to incorrect detailing that does not realize full anchorage development of the reinforcing bars.

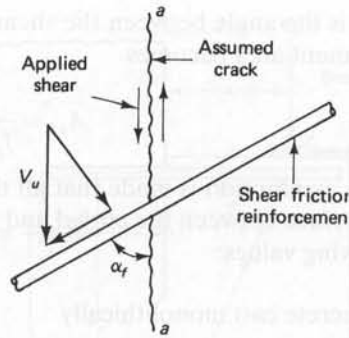
Two approaches can be used for the analysis and design of corbels as deep concrete members: the shear friction hypothesis, and the strut-and-tie modeling of forces hypothesis. In the following section, criteria are presented for computing the forces ensuing from the shear friction approach with the resulting design expressions and the applicable design example of a typical corbel. Section 5.21 presents the strut-and-tie model development for the analysis of deep beams and corbels, with the applicable design examples.

### 5.15.1 Shear Friction Hypothesis for Shear Transfer in Corbels

Corbels cast at different times than the main supporting columns can have a potential shear crack at the interface between the two concretes through which shear transfer has to develop. The smaller the ratio  $a/d$ , the larger the tendency for pure shear to occur through essentially vertical planes. This behavior is accentuated in the case of corbels with a potential interface crack between two dissimilar concretes.

The shear friction approach in this case is recommended by the ACI, as shown in Figure 5.22(b). An assumption is made of an already cracked vertical plane ( $a-a$  in Figure 5.23) along which the corbel is considered to slide as it reaches its limit state of failure. A coefficient of friction  $\mu$  is used to transform the horizontal resisting forces of the well-anchored closed ties into a vertical nominal resisting force larger than the external factored shear load. Hence, the nominal vertical resisting shear force

$$V_n = A_{vf} f_y \mu \quad (5.34a)$$



**Figure 5.23** Shear-friction reinforcement at crack.

to give

$$A_{vf} = \frac{V_n}{f_y \mu} \quad (5.34b)$$

where  $A_{vf}$  is the total area of the horizontal anchored closed shear ties.

The external factored vertical shear has to be  $V_u \leq \phi V_n$ , where for normal concrete,

$$V_n \leq 0.2f'_c b_w d \quad (5.35a)$$

or

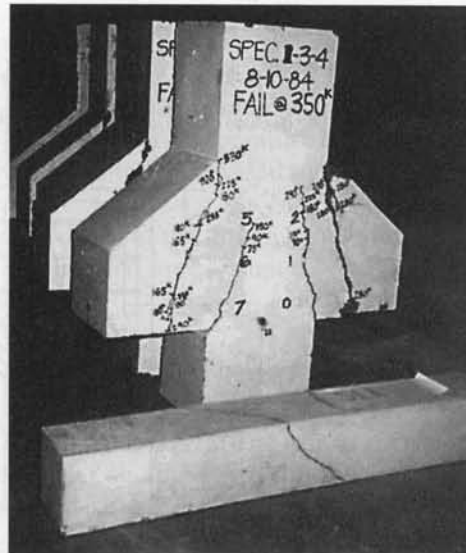
$$V_n \leq 800b_w d \quad (5.35b)$$

whichever is smaller. The required effective depth  $d$  of the corbel can be determined from Equation 5.35a, or b, whichever gives a larger value.

For all-lightweight or sand-lightweight concretes, the shear strength  $V_n$  should not be taken greater than  $(0.2 - 0.07a_v/d)f'_c b_w d$ , or  $(800 - 280a/d)b_w d$  in pounds.

If the shear friction reinforcement is inclined to the shear plane such that the shear force produces some tension in the shear friction steel,

$$V_n = A_{vf} f_y (\mu \sin \alpha + \cos \alpha) \quad (5.35c)$$



**Photo 5.6** High-strength concrete corbel at failure (Nawy et al.).

where  $\alpha_f$  is the angle between the shear friction reinforcement and the shear plane. The reinforcement area becomes

$$A_{vf} = \frac{V_n}{f_y(\mu \sin \alpha + \cos \alpha)} \quad (5.35d)$$

The assumption is made that all the shear resistance is due to the resistance at the crack interface between the corbel and the column. The ACI coefficient of friction  $\mu$  has the following values:

Concrete cast monolithically	1.4 $\lambda$
Concrete placed against hardened roughened concrete	1.0 $\lambda$
Concrete placed against unroughened hardened concrete	0.6 $\lambda$
Concrete anchored to structural steel	0.7 $\lambda$

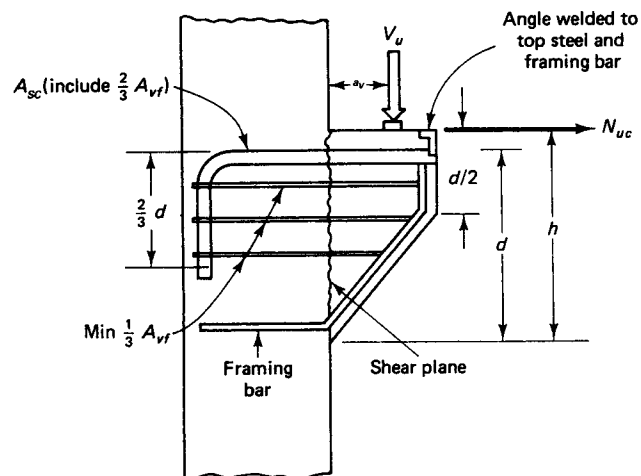
$\lambda = 1.0$  for normal-weight concrete, 0.85 for sand-lightweight concrete, and 0.75 for all-lightweight concrete. The PCI values are less conservative than the ACI values based on comprehensive tests.

If considerably higher strength concretes, such as polymer-modified concretes, are used in the corbels to interface with the normal concrete of the supporting columns, higher values of  $\mu$  could logically be used for such cases as those listed above. Work in the field (Ref. 5.7) substantiates the use of higher values.

Part of the horizontal steel  $A_{vf}$  is incorporated in the top tension tie, and the remainder of  $A_{vf}$  is distributed along the depth of the corbel as in Figure 5.24. Evaluation of the top horizontal primary reinforcement layer  $A_s$  will be discussed in the next section.

### 5.15.2 Horizontal External Force Effect

When the corbel or bracket is cast monolithically with the supporting column or wall and is subjected to a large horizontal tensile force  $N_{uc}$  produced by the beam supported by the corbel, a modified approach is used, often termed the *strut theory approach*. In all cases, the horizontal factored force  $N_{uc}$  cannot exceed the vertical factored shear  $V_u$ . As shown in Figure 5.25, reinforcing steel  $A_n$  has to be provided to resist the force  $N_{uc}$ .



**Figure 5.24** Reinforcement schematic for corbel design by the shear friction hypothesis.

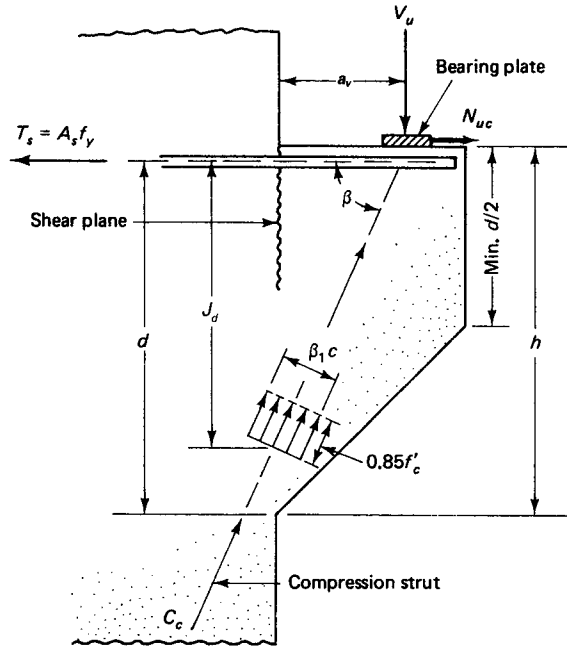


Figure 5.25 Compression strut in corbel.

where

$$A_n = \frac{N_{uc}}{\phi f_y} \quad (5.36)$$

and

$$A_f = \frac{V_u a_v + N_{uc}(h - d)}{\phi f_{yt} j d} \quad (5.37)$$

Reinforcement  $A_n$  to resist tensile force  $N_{ue}$  should be determined from  $N_{ue} \geq \phi A_n f_y$ . Tensile force  $N_{ue}$  should not be taken less than  $0.2 V_u$  unless special provisions are made to avoid tensile forces. Tensile force  $N_{ue}$  should be regarded as a live load even when tension results from creep, shrinkage, or temperature changes.

Reinforcement  $A_f$  also has to be provided to resist the bending moments caused by  $V_u$  and  $N_{uc}$ .

The value of  $N_{uc}$  considered in the design should not be less than  $0.20 V_u$ . The flexural steel area  $A_f$  can be obtained approximately by the usual expression for the limit state at failure of beams, that is,

$$A_f = \frac{M_u}{\phi f_{yt} j d} \quad (5.38)$$

where  $M_u = V_u a_v + N_{uc}(h - d)$  and  $\phi = 0.75$ . The axis of such an assumed section lies along a compression strut inclined at an angle  $\beta$  to the tension tie  $A_s$ , as shown in the figure. The volume of the compressive block is

$$C_c = 0.85 f'_c \beta_1 c b = \frac{T_s}{\cos \beta} = \frac{A_s f_{yt}}{\cos \beta} = \frac{V_u}{\sin \beta} \quad (5.39a)$$

for which the depth  $\beta_1 c$  of the block is obtained perpendicular to the direction of the compressive strut, i.e.,

$$\beta_1 c = \frac{A_s f_y}{0.85 f'_c b \cos \beta} \tag{5.39b}$$

The effective depth  $d$  minus  $\beta_1 c/2 \cos \beta$  in the vertical direction gives the lever arm  $jd$  between the force  $T_s$  and the horizontal component of  $C_c$  in Figure 5.25. Therefore,

$$jd = d - \frac{\beta_1 c}{2 \cos \beta} \tag{5.39c}$$

If the right-hand side is substituted for  $jd$  in Equation 5.38, then

$$A_f = \frac{M_u}{\phi f_y (d - \beta_1 c/2 \cos \beta)} \tag{5.40}$$

To eliminate several trials and adjustments, the lever arm  $jd$  from Equation (5.39c) can be approximated for all practical purposes in most cases as

$$jd \cong 0.85d \tag{5.41a}$$

so that

$$A_f = \frac{M_u}{0.85 \phi f_y d} \tag{5.41b}$$

The area  $A_{sc}$  of the primary tension reinforcement (tension tie) can now be calculated and placed as shown in Figure 5.26:

$$A_{sc} \geq \frac{2}{3} A_{vf} + A_n \tag{5.42}$$

or

$$A_{sc} \geq A_f + A_n \tag{5.43}$$

whichever is larger. Then

$$\rho = \frac{A_{sc}}{bd} \geq 0.04 \frac{f'_c}{f_y}$$

where  $A_n$  = reinforcement area resisting tension.

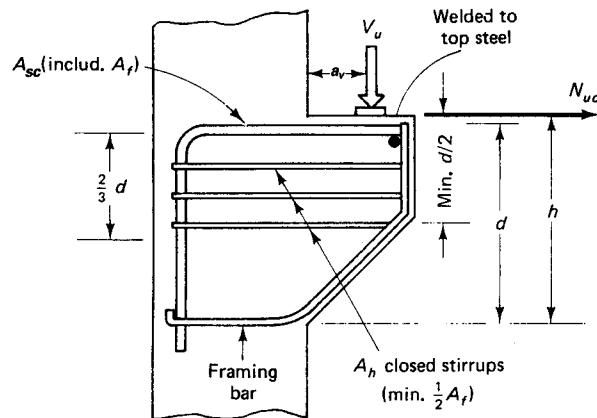


Figure 5.26 Reinforcement schematic for corbel design by strut theory.

If  $A_h$  is assumed to be the total area of the closed stirrups or ties parallel to  $A_{sc}$ , then

$$A_h \geq 0.5(A_{sc} - A_n) \quad (5.44)$$

The bearing area under the external load  $V_u$  on the bracket should not project beyond the straight portion of the primary tension bars,  $A_{sc}$ , nor should it project beyond the interior face of the transverse welded anchor bar shown in Figure 5.26.

### 5.15.3 Sequence of Corbel Design Steps

As discussed in the preceding section, a horizontal factored force  $N_{uc}$ , a vertical factored force  $V_u$ , and a bending moment [ $V_u a + N_{uc}(h - d)$ ] basically act on the corbel. To prevent failure, the corbel has to be designed to resist these three parameters simultaneously by one of the following two methods, depending on the type of corbel construction sequence, that is, whether the corbel is cast monolithically with the column or not:

- (a) For a monolithically cast corbel with the supporting column, by evaluating the steel area  $A_h$  of the closed stirrups which are placed below the primary steel ties  $A_{sc}$ . Part of  $A_h$  is due to the steel area  $A_n$  from Equation 5.36 resisting the horizontal force  $N_{uc}$ .
- (b) By calculating the steel area  $A_{vf}$  by the shear friction hypothesis if the corbel and the column are *not* cast simultaneously, using part of  $A_{vf}$  along the depth of the corbel stem and incorporating the balance in the area  $A_s$  of the primary top steel reinforcing layer.

The primary tension steel area  $A_{sc}$  is the major component of both methods. Calculations of  $A_s$  depend on whether Equation 5.42 or 5.43 governs. If Equation 5.42 controls,  $A_{sc} = \frac{2}{3} A_{vf} + A_n$  is used and the remaining  $\frac{1}{3} A_{vf}$  is distributed over a depth  $\frac{2}{3} d$  adjacent to  $A_{sc}$ . If Equation 5.43 controls,  $A_{sc} = A_f + A_n$ , with the addition of  $\frac{1}{2} A_f$  provided as closed stirrups parallel to  $A_{sc}$  and distributed within  $\frac{2}{3} d$  vertical distance adjacent to  $A_{sc}$ .

In both cases, the primary tension reinforcement plus the closed stirrups automatically yield the total amount of reinforcement needed for either type of corbel. Since the mechanism of failure is highly indeterminate and randomness can be expected in the propagation action of the shear crack, it is sometimes advisable to choose the larger calculated value of the primary top steel area  $A_{sc}$  in the corbel regardless of whether the corbel element is cast simultaneously with the supporting column.

As seen from the foregoing discussions, the horizontal closed stirrups are also a major element in reinforcing the corbel. Occasionally, additional inclined closed stirrups are also used.

The following sequence of steps is proposed for the design of the corbel:

1. Calculate the factored vertical force  $V_u$  and the nominal resisting force  $V_n$  of the section such that  $V_n \geq V_u/\phi$ , where  $\phi = 0.75$  for all calculations.  $V_u/\phi$  should be  $\leq 0.20f'_c b_w d$ , or  $\leq 800b_w d$  for normal-weight concrete. If not, the concrete section at the support should be enlarged.
2. Calculate  $A_{vf} = V_n/f_y \mu$  for resisting the shear friction force, and use in the subsequent calculation of the primary tension top steel  $A_s$ .
3. Calculate the flexural steel area  $A_f$  and the direct tension steel area  $A_n$ , where

$$A_f = \frac{v_u a_v + N_{uc}(h - d)}{\phi f_y J d}$$

and

$$A_n = \frac{N_{uc}}{\phi f_y}$$

where  $\phi = 0.75$



4. Calculate the primary steel area from (a)  $A_{sc} = \frac{2}{3} A_{vf} + A_n$  and (b)  $A_{sc} = A_f + A_n$ , whichever is larger. If case (a) controls, the remaining  $\frac{1}{3} A_{vf}$  has to be provided as closed stirrups parallel to  $A_{sc}$  and distributed with a  $\frac{2}{3} d$  distance adjacent to  $A_{sc}$ , as in Figure 5.24.

If case (b) controls, use in addition  $\frac{1}{2} A_f$  as closed stirrups distributed within a distance  $\frac{2}{3} d$  adjacent to  $A_{sc}$ , as in Figure 5.26. Then

$$A_h \geq 0.5(A_{sc} - A_n)$$

and

$$\rho = \frac{A_{sc}}{bd} \geq 0.04 \frac{f'_c}{f_y}$$

or

$$\text{Min. } A_{sc} = 0.04 \frac{f'_c}{f_y} bd$$

5. Select the size and spacing of the corbel reinforcement with special attention to the detailing arrangements, as many corbel failures are due to incorrect detailing.

Figure 5.27 shows a flowchart for proportioning corbels.

#### 5.15.4 Design of a Bracket or Corbel

##### Example 5.7

Design a corbel to support a factored vertical load  $V_u = 80,000$  lb (160 kN) acting at a distance  $a = 5$  in. (127 mm) from the face of the column. The corbel has a width  $b = 10$  in. (254 mm), a total thickness  $h = 18$  in. (457 mm), and an effective depth  $d = 14$  in. (356 mm). The following data are given:

$$f'_c = 5,000 \text{ psi (34.5 MPa), normal-weight concrete}$$

$$f_y = 60,000 \text{ psi (414 MPa)}$$

Assume the corbel to be either cast after the supporting column was constructed, or cast simultaneously with the column. Neglect the weight of the corbel. Supporting column size is 12 in.  $\times$  12 in.

##### Solution:

##### Step 1

$$V_n \geq \frac{V_u}{\phi} = \frac{80,000}{0.75} = 106,667 \text{ lb}$$

$$0.2f'_c b_w d = 0.2 \times 5,000 \times 10 \times 14 = 140,000 \text{ lb} > V_n$$

$$800b_w d = 800 \times 10 \times 14 = 112,000 \text{ lb} > V_n, \text{ O.K.}$$

##### Step 2

- (a) Monolithic construction, normal-weight concrete  $\mu = 1.4\lambda$ :

$$A_{vf} = \frac{V_u}{\phi f_y \mu} = \frac{106,667}{60,000 \times 1.4} = 1.270 \text{ in.}^2 (819 \text{ mm}^2)$$

- (b) Nonmonolithic construction,  $\mu = 1.0\lambda$ :

$$A_{vf} = \frac{106,667}{60,000 \times 1.0} = 1.777 \text{ in.}^2 (1110 \text{ mm}^2)$$

Choose the larger  $A_{vf} = 1.777 \text{ in.}^2$  as controlling.

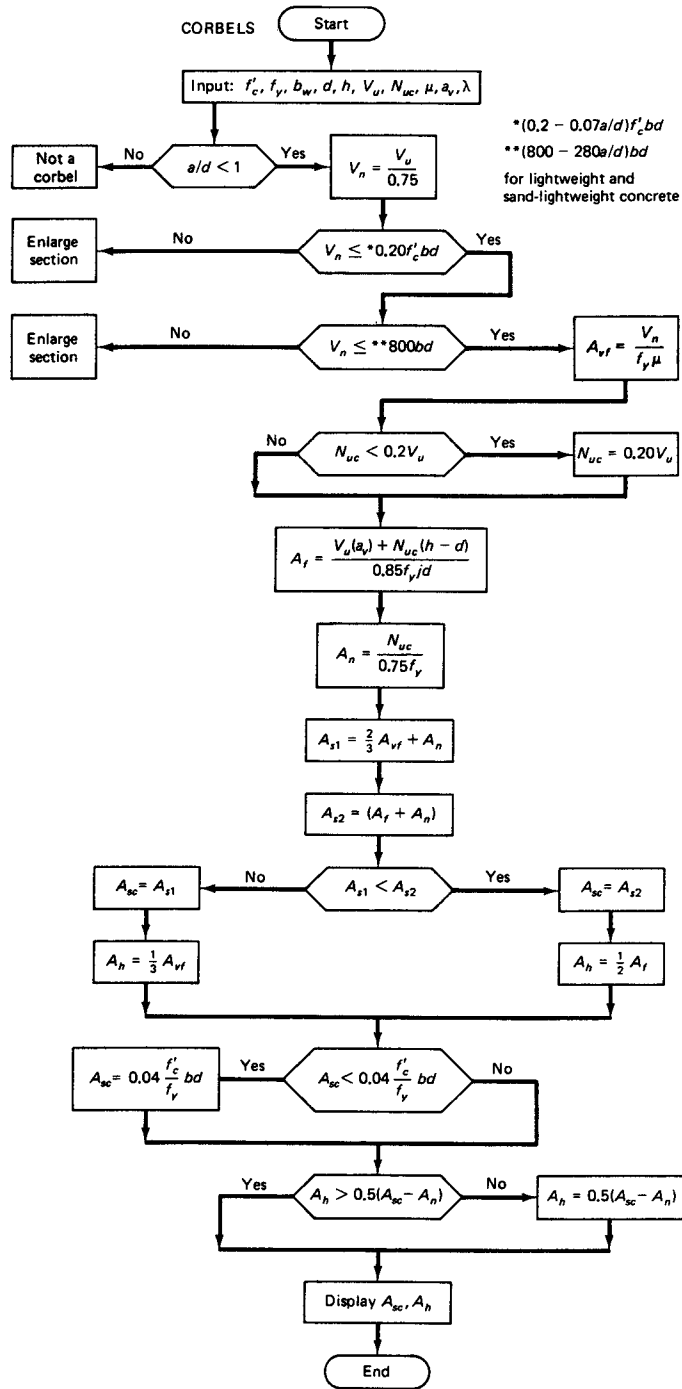


Figure 5.27 Flowchart for proportioning corbels.

**Step 3.** Since no value of the horizontal external force  $N_{uc}$  transmitted from the superimposed beam is given, use

$$\text{Min } N_{uc} = 0.20V_u = 0.2 \times 80,000 = 16,000 \text{ lb}$$

$$A_f = \frac{M_u}{\phi f_y j d} = \frac{V_u a_v + N_{uc}(h - d)}{\phi f_y j d} \quad (\text{where } jd \cong 0.85d)$$

$$= \frac{80,000 \times 5 + 16,000(18 - 14)}{0.90 \times 60,000(0.85 \times 14)} = 0.727 \text{ in}^2 \text{ (524 mm}^2\text{)}$$

$$A_n = \frac{N_{uc}}{\phi f_y} = \frac{16,000}{0.75 \times 60,000} = 0.356 \text{ in}^2 \text{ (280 mm}^2\text{)}$$

**Step 4.** Check the controlling area of primary steel  $A_{sc}$ :

$$(a) A_{sc} = \left(\frac{2}{3} A_{vf} + A_n\right) = \frac{2}{3} \times 1.777 + 0.356 = 1.541 \text{ in.}^2$$

$$(b) A_{sc} = A_f + A_n = 0.727 + 0.356 = 1.083 \text{ in.}^2$$

$$\text{Min } A_{sc} = 0.04 \frac{f'_c}{f_y} b d = 0.04 \times \frac{5,000}{60,000} \times 10 \times 14 = 0.47 \text{ in.}^2$$

$$< 1.541 \text{ in.}^2, \text{ O.K.}$$

Provide  $A_{sc} = 1.541 \text{ in.}^2$  (994 mm<sup>2</sup>).

Horizontal closed stirrups:

Since case (a) controls,

$$\frac{1}{3} A_{vf} = \frac{1}{3} \times 1.777 = 0.592 \text{ in.}^2$$

$$A_h = 0.5(A_{sc} - A_n) = 0.5(1.541 - 0.356) = 0.593 \text{ in.}^2$$

Use the larger of the two values  $\frac{1}{3} A_{vf}$  and  $A_h$ .

**Step 5.** Select bar sizes:

(a) Required  $A_{sc} = 1.541 \text{ in.}^2$ ; use three No. 7 bars =  $1.80 \text{ in.}^2$  (three bars of diameter 22 mm gives  $1,161 \text{ mm}^2$ )  $A_{sc}$ .

(b) Required  $A_h = 0.593 \text{ in.}^2$ ; use three No. 3 closed stirrups =  $2 \times 3 \times 0.11 = 0.66 \text{ in.}^2$  spread over  $\frac{2}{3} d = 9.33 \text{ in.}$  vertical distance. Hence, use three No.-3 closed stirrups at 3 in. center to center. Also use three framing size No.-3 bars and one welded No.-7 anchor to bar.

Details of the bracket reinforcement are shown in Figure 5.28. The bearing area under the load has to be checked, and the bearing pad designed such that the bearing stress at the factored load  $V_u$  should not exceed  $\phi(0.85f'_c A_1)$ , where  $A_1$  is the pad area. We have

Bearing strength reduction factor  $\phi = 0.70$ .

$$V_u = 80,000 \text{ lb} = 0.70(0.85 \times 5,000) A_1$$

$$A_1 = \frac{80,000}{0.70 \times 0.85 \times 5000} = 26.9 \text{ in}^2 \text{ (16,813 mm}^2\text{)}$$

Use a plate  $5\frac{1}{2} \text{ in.} \times 5\frac{1}{2} \text{ in.}$  Its thickness has to be designed based on the manner in which  $V_u$  is applied as an undeformable plate.

### 5.15.5 SI Expressions for Shear in Prestressed Concrete Beams

$$V_{ci} = \left[ \frac{\lambda \sqrt{f'_c}}{20} b_w d + V_d + V_i \left( \frac{M_{cr}}{M_{\max}} \right) \right] \geq \left( \frac{\sqrt{f'_c}}{7} \right) b_w d \quad (5.11)$$

$$M_{cr} = S_b(0.5\lambda \sqrt{f'_c} + f_{ce} - f_d) \quad (5.12)$$

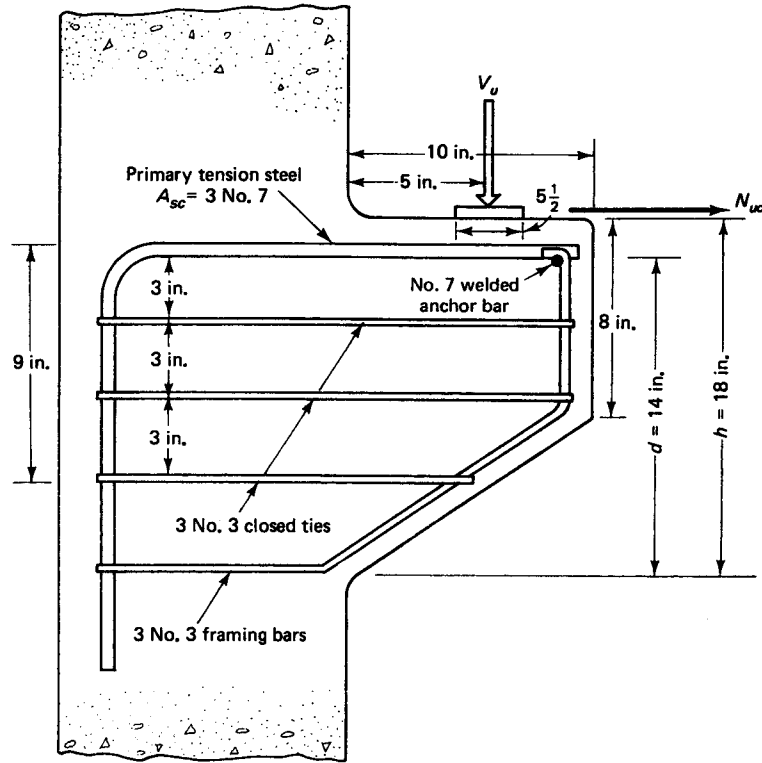


Figure 5.28 Corbel reinforcement details (Example 5.7).

$$V_{cw} = 0.3(\lambda\sqrt{f'_c} + 0.3\bar{f}_c)b_w d + V_p \quad (5.15)$$

(See Sec. 5.5.1 for explanation on  $f'_c$  vs.  $f_{ce}$  of the ACI code).  $M_{cr}$  for shear = moment causing flexural cracking at section due to externally applied load.

$$\begin{aligned} V_c &= \left( \frac{\lambda\sqrt{f'_c}}{20} + 5\frac{V_u d}{M_u} \right) b_w d; & \frac{V_u d}{M_u} &\leq 1.0 \\ &\geq \left[ \lambda \frac{\sqrt{f'_c}}{5} \right] b_w d \\ &\leq [0.4\lambda\sqrt{f'_c} b_w d] \\ s &= \frac{A_v f_{yt} d}{(V_u/\phi) - V_c} = \frac{A_v f_{yt} d}{V_s} \end{aligned} \quad (5.21b)$$

$$\text{Max } s = \frac{3}{4}h \leq 600 \text{ mm}$$

$$\text{when } V_s > (\lambda\sqrt{f'_c}/3)b_w d, \text{ max } s \leq 3/16h \leq 300 \text{ mm}$$

$$V_s > (2\lambda\sqrt{f'_c}/3)b_w d, \text{ enlarge section.}$$

Min.  $A_v$ : the smaller of

$$A_v \geq \frac{0.35b_w s}{f_{yt}} \quad \text{or} \quad \frac{A_p s f_{pu} s}{80f_{yt} d} \sqrt{\frac{d}{b_w}}$$

where  $b_w$ ,  $s$  and  $d$  are in millimeters and  $f_{yt}$  is in MPa.

Max. allowable shear friction force without dowels,  $F_h = 0.55b_v l_{vh}$

$$1 \text{ lb} \times 4.448 = \text{N}$$

$$\text{psi} \times 0.006895 = \text{MPa}$$

$$(\text{in.}\cdot\text{lb}) \times 0.1130 = \text{N}\cdot\text{m}$$

$$1 \text{ Pa} = \text{N}/\text{m}^2$$

$$1 \text{ MPa} = \text{N} \times 10^6/\text{m}^2$$

$$(\text{lb}/\text{ft}) \times 14.593 = \text{N}/\text{m}$$

### 5.15.6 SI Shear Design of Prestressed Beams

#### Example 5.8

Solve Example 5.6 using the SI units system. The sectional geometric properties of the beam are as follows:

Section property	Pretopped
$A_c$	6,310 cm <sup>2</sup>
$I_c$	$3.58 \times 10^6$ cm <sup>4</sup>
$r^2$	568 cm <sup>2</sup>
$c_b$	65.5 cm
$c_t$	20.9 cm.
$S_b$	54,733 cm <sup>3</sup>
$S^t$	171,376 cm <sup>3</sup>
$W_D$	14,870 N/m
$W_D + W_{SD}$	17,789 N/m
$W_L$	10,507 N/m
$2b_w$	32 cm

Other data are:

$f'_c$  (precast) = 34.5 MPa, normal-weight concrete, section pretopped

$f'_{cc}$  (topping) = 20.7 MPa, normal-weight concrete, at a later stage if used

$f'_{ci}$  = 27.6 MPa

$f_{pu}$  = 1,862 MPa, low-relaxation steel

$f_{ps}$  = 1,655 MPa

$f_{pe}$  = 1,020 MPa

$e_e$  = 28.3 cm

$e_c$  = 57.2 cm

$A_{ps}$  = 18 – 12.7 mm diameter tendons = 99 mm<sup>2</sup>

$f_{yt}$  for stirrups = 414 MPa

Use the same value for the effective depth  $d_p$  for the midspan as well as other sections. Note that  $b_w$  for both webs = 32 cm.

#### Solution:

$$W_u = 1.2 \times 17,789 + 1.6 \times 10,507 \cong 38.2 \text{ kN/m}$$

$$V_u \text{ at face of support} = \frac{38.2 \times 21.3}{2} = 407 \text{ kN}$$

$$\frac{1}{4} \text{ of the span} = 21.3/4 = 5.33 \text{ m.}$$

$$\begin{aligned} V_n \text{ at 5.33m. from the face of the support} &= \frac{1}{0.75} \left( 407 \times \frac{(10.67 - 5.33)}{10.67} \right) \\ &= 272 \text{ kN} \end{aligned}$$

(1) Flexure-shear cracking,  $V_{ci}$  (step 2)

$$d_p = 76.2 \text{ cm}$$

$$P_e = 18 \times 99 \times 1,020 \text{ MPa} = 18,176 \text{ kN}$$

$$e \text{ at 5.33 m from support} = 42.1 \text{ cm}$$

Use the precast section properties for computing  $f_{ce}$  and  $f_d$  as discussed in Section 5.5:

$$\begin{aligned} f_{ce} &= -\frac{P_e}{A_c} \left( 1 + \frac{ec_b}{r^2} \right) = -\frac{18,176}{6,310} \left( 1 + \frac{42.1 \times 65.46}{568} \right) \\ &= 16.8 \text{ MPa} \end{aligned}$$

Use allowable extreme compressive stresses as follows:

(a) prestress + sustained load:  $f_c = 0.45 f'_c$

(b) prestress + total load (allowing 33% increase due to transient load:  $f_c = 0.60 f'_c$ )

Note that although  $f_{ce} = 0.45 f'_c$ , this should not affect the shear strength since  $f_{ce}$  is due to prestress only, and the inclusion of self-weight reduces it to less than  $0.45 f'_c$ .

We thus have:

$$\text{Self-weight } W_D = 14,870 \text{ N/m}$$

$$\begin{aligned} M_{5.33} &= \frac{W_D x(l-x)}{2} = \frac{14,870 \times 5.33(21.3 - 5.33)}{2} \\ &= 634 \text{ kN-m} \end{aligned}$$

$$f_d = \frac{M c_b}{I_c} = \frac{6,340,000 \times 65.46}{3.58 \times 10^6} = 11.6 \text{ MPa}$$

$$\begin{aligned} M_{cr} &= S_b(0.50\lambda\sqrt{f'_c} + f_{ce} - f_d) \\ &= 54,733(0.50 \times 1.0\sqrt{34.5} + 16.8 - 11.6) \\ &= 445 \text{ kN-m} \end{aligned}$$

Unfactored shear due to self-weight is

$$V_d = W_D \left( \frac{l}{2} - x \right) = 14,870 \left( \frac{21.3}{2} - 5.33 \right) = 79.1 \text{ kN}$$

$$W_{SD} = 2,919 \text{ N/m}$$

$$W_L = 10,507 \text{ N/m}$$

Factored external load intensity is

$$W_U = 1.2 \times 2,919 + 1.6 \times 10,507 = 20.3 \text{ kN/m}$$

$$V_i = W_U \left( \frac{l}{2} - x \right) = 20.3 \left( \frac{20.3}{2} - 5.33 \right) = 108 \text{ kN}$$

$$\begin{aligned} M_{\max} &= W_U x \left( \frac{l-x}{2} \right) = \frac{20.3 \times 5.33(21.3 - 5.33)}{2} \\ &= 864 \text{ kN-m} \end{aligned}$$

$$V_{ci} = 0.6\lambda\sqrt{f'_c} b_w d_p + V_d + \frac{V_i}{M_{\max}} (M_{cr}) \geq 0.33\lambda\sqrt{f'_c} b_w d_p$$

$$\begin{aligned}
 &= 0.6 \times 1.0 \times \sqrt{34.5} \times 3.18 \times 7.62 + 79.1 \\
 &+ \frac{108}{864}(445) \\
 &= 220 \text{ kN}
 \end{aligned}$$

$$0.33\lambda\sqrt{f'_c}b_wd_p = 0.33 \times 1.0\sqrt{34.5} \times 31.8 \times 76.2 = 202 \text{ kN} < 220 \text{ kN}$$

Hence,  $V_{ci} = 220 \text{ kN}$  controls.

**(2) Web-shear cracking,  $V_{cw}$  (step 2)**

$$\bar{f}_c = \frac{P_e}{A_c} = \frac{18,176}{6,310} = 2.9 \text{ MPa}$$

For the vertical component of the prestress force,

$$V_p = P_e \tan\theta = 18,176 \frac{(55.3 - 28.9)}{21.3/2} = 44.0 \text{ kN}$$

$$\begin{aligned}
 V_{cw} &= [0.3(\lambda\sqrt{f'_c} + \bar{f}_c)]b_wd_p + V_p \\
 &= [0.3(1.0\sqrt{34.5} + 2.9)] \times 318 \times 762 + 44 \\
 &= 681 \text{ kN vs. } V_{ci} = 211 \text{ kN}
 \end{aligned}$$

Now,  $V_c$  is the smaller of  $V_{ci}$  and  $V_{cw}$ ; hence,

$$V_c = V_{ci} = 211 \text{ kN}$$

**(3) Design of web reinforcement (steps 3–8)**

From above,

$$V_c = 211 \text{ kN,}$$

So

$$\frac{1}{2}V_c = 106 \text{ kN}$$

Now,  $V_u / \phi$  at a section 5.33 m. from support = 272 >  $V_c > \frac{1}{2}V_c$ ; hence design of stirrups is necessary. If  $V_u / \phi < V_c > \frac{1}{2}V_c$ , only minimum-web steel is need.

$$\begin{aligned}
 \text{Req. } \frac{A_v}{s} &= \frac{V_n - V_c}{f_{yt}d_p} = \frac{(V_u/\phi) - V_c}{f_{yt}d_p} = \frac{(272 - 211)}{414 \times 762} \\
 &= 0.19 \text{ mm}^2/\text{mm spacing}
 \end{aligned}$$

Using  $d \cong d_p = 762 \text{ mm}$  and  $b_w = 318 \text{ mm}$ :

$$\text{Min.} \left( \frac{A_v}{s} \right) = \frac{A_{ps} f_{pu}}{80 f_{yt} d_p} \sqrt{\frac{d_p}{b_w}} = \frac{18 \times 99}{80} \times \frac{1,860}{414 \times 762} \sqrt{\frac{762}{318}} = 0.20 \text{ mm}^2/\text{mm}$$

Or

$$\text{Min.} \left( \frac{A_v}{s} \right) = \frac{b_w}{3 f_{yt}} = \frac{318}{3 \times 414} = 0.25 \text{ mm}^2/\text{mm}$$

The lesser of the two minimum value applies; consequently, min.  $A_v = 0.20 \text{ mm}^2/\text{mm}$  applies as the lesser of the two values.

Controlling web steel is hence

$$\frac{A_v}{s} = 0.21 \text{ mm}^2/\text{mm for both webs or}$$

0.105 mm<sup>2</sup> / mm per web.

Try one row of D5 deformed welded wire fabric at 254 mm center-to-center weld spacing.

The maximum allowable spacing is, then  $0.75h$  where  $h = 864$  mm but not to exceed 610 mm. So we have

$$0.75 \times 864 = 648$$

Accordingly, adopt using one row D5 WWF in one layer at 254 mm center-to-center of welds per web at the quarter-span section.

Note, in comparing the solution for  $V_{ci}$  and  $V_{cw}$  that  $V_{ci}$  has its highest value close to the support and *rapidly* decreases toward the midspan, while  $V_{cw}$  has a lesser variation in its value, as can be seen from Figure 5.13. It is important to calculate the flexure shear  $V_{ci}$  and web shear  $V_{cw}$  at several sections along the span in order to determine the most efficient distribution of the web steel. A computer program facilitates finding these values at constant intervals of, say, 1/10th of the span, and a plot can be made similar to the one in Figure 5.13 showing the variation of the shear strengths of the web along the span.

- (4) *Design of dowel steel for full composite section of the additional 2-in. topping (step 9), if such topping is added later to the pretopped section.*

Section at  $\frac{1}{2}d_p$  from face of support

$$\text{Use } d_p = 76.2 + 5.1 = 81.3 \text{ cm}$$

$$V_u \text{ at support} = 407 \text{ kN}$$

$$\frac{1}{2}d_p = \frac{81.3}{2} = 41 \text{ cm} \quad h/2 = 0.4 \text{ m}$$

$$V_u = 407 \times \left( \frac{10.7 - 0.4}{10.7} \right) = 392 \text{ kN}$$

$$\text{Req } V_{nh} = \frac{V_u}{\phi} = \frac{392}{0.75} = 523 \text{ kN}$$

$$b_v = 366 \text{ cm} \quad \text{topping } h = 5.08 \text{ cm}$$

From Figure 5.14

$$C_c = 0.85f'_{cc}A_{top} = 0.85 \times 20.7 \times 366 \times 5.08 \times 10^{-3} = 3,267 \text{ kN}$$

$$T_s = A_{ps}f_{ps} = 18 \times 99 \times 1655 \times 10^{-3} = 2,940 \text{ kN}$$

$$< C_c = 3,267 \text{ kN}$$

Then

$$F_h = 2,940 \text{ kN}$$

$$l_{vh} = \frac{21.3}{2} = 10.67 \text{ m} = 1,067 \text{ cm}$$

$$b_v = 366 \text{ cm}$$

$$0.55b_v l_{vh} = 0.55 \times 366 \times 1067 = 21,520 \text{ kN} \gg 2940 \text{ kN}$$

No dowel reinforcement is needed to extend to the additional 5 cm topping for full composite action to be developed. The section is adopted when it satisfies the flexural, deflection, and cracking requirements.



## 5.16 TORSIONAL BEHAVIOR AND STRENGTH

### 5.16.1 Introduction

Torsion occurs in monolithic concrete construction primarily where the load acts at a distance from the longitudinal axis of the structural member. An end beam in a floor panel, a spandrel beam receiving load from one side, a canopy or a bus-stand roof projecting from a monolithic beam on columns, and peripheral beams surrounding a floor opening are all examples of structural elements subjected to twisting moments. These moments occasionally cause excessive shearing stresses. As a result, severe cracking can develop well beyond the allowable serviceability limits unless special torsional reinforcement is provided. Photos in this section illustrate the extent of cracking at failure of a beam in torsion. They show the curvilinear plane of twist caused by the imposed torsional moments. In actual spandrel beams of a structural system, the extent of damage due to torsion is usually not as severe. This is due to the redistribution of stresses in the structure. However, loss of integrity due to torsional distress should always be avoided by proper design of the necessary torsional reinforcement.

An introduction to the subject of torsional stress distribution has to start with the basic elastic behavior of simple sections, such as circular or rectangular sections. Most concrete beams subjected to twist are components of rectangles, for example, flanged sections such as T-beams and L-beams. Although circular sections are rarely a consideration in normal concrete construction, a brief discussion of torsion in circular sections serves as a good introduction to the torsional behavior of other types of sections.

Shear stress is equal to shear strain times the shear modulus at the elastic level in circular sections. As in the case of flexure, the stress is proportional to its distance from the neutral axis (i.e., the axis through the center of the circular section) and is maximum at the extreme fibers. If  $r$  is the radius of the element,  $J = \pi r^4/2$ , its polar moment of inertia, and  $v_{te}$  the elastic shearing stress due to an elastic twisting moment  $T_e$ , then

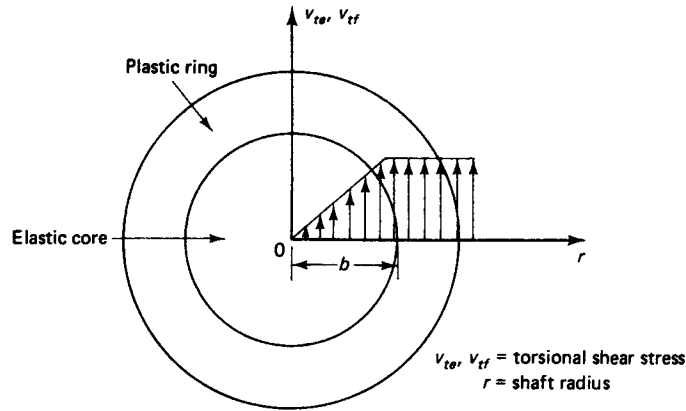
$$v_{te} = \frac{T_e r}{J} \quad (a)$$

When deformation takes place in the circular shaft, the axis of the circular cylinder is assumed to remain straight. All radii in a cross section also remain straight (i.e., there is no warping) and rotate through the same angle about the axis. As the circular element starts to behave plastically, the stress in the plastic outer ring becomes constant while the stress in the inner core remains elastic, as shown in Figure 5.29. As the whole cross section becomes plastic,  $b = 0$  and the shear stress

$$v_{tf} = \frac{3}{4} \frac{T_p r}{J} \quad (b)$$

where  $v_{tf}$  is the nonlinear shear stress due to an ultimate twisting moment  $T_p$ . (The subscript  $f$  denotes failure.)

In rectangular sections, the torsional problem is considerably more complicated. The originally plane cross sections undergo warping due to the applied torsional moment. This moment produces axial as well as circumferential shear stresses with zero values at the corners of the section and the centroid of the rectangle, and maximum values on the periphery at the middle of the sides, as shown in Figure 5.30. The maximum torsional shearing stress would occur at midpoints  $A$  and  $B$  of the larger dimension of the cross section. These complications plus the fact that the reinforced and prestressed concrete sections are neither homogeneous nor isotropic make it difficult to develop exact



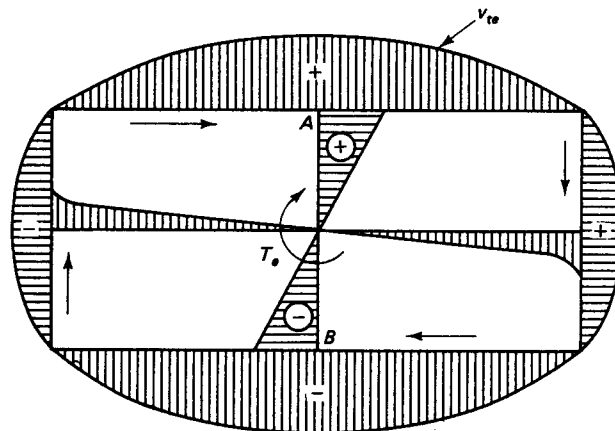
**Figure 5.29** Torsional stress distribution through circular section.

mathematical formulations based on physical models such as Equations (a) and (b) for circular sections.

For over seventy years, the torsional analysis of concrete members has been based on either (1) the classical theory of elasticity developed through mathematical formulations coupled with membrane analogy verifications (St.-Venant's), or (2) the theory of plasticity represented by the sand-heap analogy (Nadai's). Both theories were applied essentially to the state of pure torsion. But it was found experimentally that the elastic theory is not entirely satisfactory for the accurate prediction of the state of stress in concrete in pure torsion. The behavior of concrete was found to be better represented by the plastic approach. Consequently almost all developments in torsion as applied to prestressed concrete and to reinforced concrete have been in the latter direction.

### 5.16.2 Pure Torsion in Plain Concrete Elements

**5.16.2.1 Torsion in elastic materials.** In 1853, St.-Venant presented his solution to the elastic torsional problem with warping due to pure torsion which develops in noncircular sections. In 1903, Prandtl demonstrated the physical significance of the mathematical formulations by his membrane analogy model. The model establishes particular



**Figure 5.30** Pure torsional stress distribution in a rectangular section.

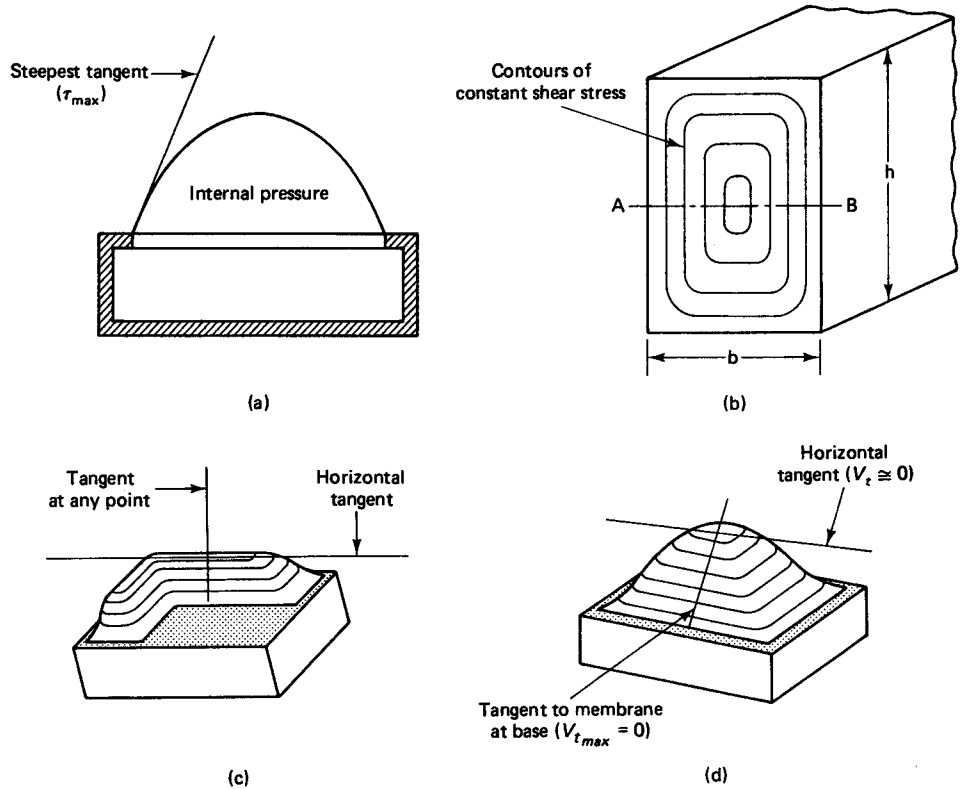
relationships between the deflected surface of the loaded membrane and the distribution of torsional stresses in a bar subjected to twisting moments. Figure 5.31 shows the membrane analogy behavior for rectangular as well as L-shaped forms.

For small deformations, it can be proved that the differential equation of the deflected membrane surface has the same form as the equation that determines the stress distribution over the cross section of the bar subjected to twisting moments. Similarly, it can be demonstrated that (1) the tangent to a contour line at any point of a deflected membrane gives the direction of the shearing stress at the corresponding cross section of the actual membrane subjected to twist; (2) the maximum slope of the membrane at any point is proportional to the magnitude of shear stress  $\tau$  at the corresponding point in the actual member; and (3) the twisting moment to which the actual member is subjected is proportional to *twice* the volume under the deflected membrane.

It can be seen from Figure 5.30 and 5.31(b) that the torsional shearing stress is inversely proportional to the distance between the contour lines. The closer the lines, the higher the stress, leading to the previously stated conclusion that the maximum torsional shearing stress occurs at the middle of the longer side of the rectangle. From the membrane analogy, this maximum stress has to be proportional to the steepest slope of the tangents at points *A* and *B*.

If  $\delta$  is the maximum displacement of the membrane from the tangent at point *A*, then from basic principles of mechanics and St.-Venant's theory,

$$\delta = b^2 G\theta \tag{5.45a}$$



**Figure 5.31** Membrane analogy in elastic pure torsion. (a) Membrane under pressure. (b) Contours in a real beam or in a membrane. (c) L-section. (d) Rectangular section.

where  $G$  is the shear modulus and  $\theta$  is the angle of twist. But  $v_{t(\max)}$  is proportional to the slope of the tangent; hence,

$$v_{t(\max)} = k_1 b G \theta \quad (5.45b)$$

where  $k_1$  is a constant. The corresponding torsional moment  $T_e$  is proportional to *twice* the volume under the membrane, or

$$T_e \propto 2\left(\frac{2}{3}\delta b h\right) = k_2 \delta b h$$

where, again,  $k_2$  is a constant. Or yet again,

$$T_e = k_3 b^3 h G \theta \quad (5.45c)$$

with  $k_3$  constant. From Equations 5.45a and b,

$$v_{t(\max)} = \frac{T_e b}{k b^3 h} \approx \frac{T_e b}{J_1} \quad (5.45d)$$

The denominator  $k b^3 h$  in 5.45d represents the polar moment of inertia  $J_1$  of the section. Comparing this equation to Equation (a) for the circular section shows the similarity of the two expressions, except that the factor  $k$  in the equation for the rectangular section takes into account the shear strains due to warping. Equation 5.45d can be further simplified to give

$$v_{t(\max)} = \frac{T_e}{k b^2 h} \quad (5.46)$$

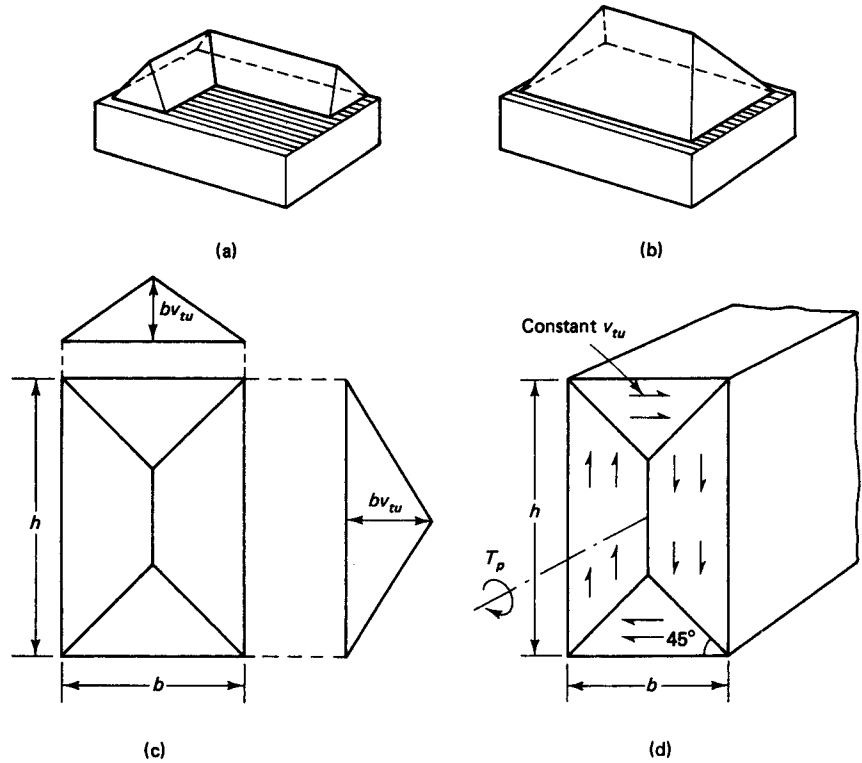
It can also be written to give the stress at planes inside the section, such as an inner concentric rectangle of dimensions  $x$  and  $y$ , where  $x$  is the shorter side, so that

$$v_{t(\max)} = \frac{T_e}{k x^2 y} \quad (5.47)$$

It is important to note in using the membrane analogy approach that the torsional shear stress changes from one point to another along the same axis as  $AB$  in Figure 5.31, because of the changing slope of the analogous membrane, rendering the torsional shear stress calculations lengthy.

**5.16.2.2 Torsion in plastic materials.** As indicated earlier, the plastic sand-heap analogy provides a better representation of the behavior of brittle elements such as concrete beams subjected to pure torsion than does the elastic analogy. The torsional moment is also proportional to *twice* the volume under the heap, and the maximum torsional shearing stress is proportional to the slope of the sand heap. Figure 5.32 is a two- and three-dimensional illustration of the sand heap. The torsional moment  $T_p$  in part (d) of the figure is proportional to twice the volume of the rectangular heap shown in parts (b) and (c). It can also be recognized that the slope of the sand-heap sides as a measure of the torsional shearing stress is *constant* in the sand-heap analogy approach, whereas it is continuously variable in the membrane analogy approach. This characteristic of the sand heap considerably simplifies the solutions.

**5.16.2.3 Sand-heap analogy applied to L-beams.** Most concrete elements subjected to torsion are flanged sections, most commonly L-beams comprising the external wall beams of a structural floor. The L-beam in Figure 5.33 is chosen in applying the plas-



**Figure 5.32** Sand-heap analogy in plastic pure torsion. (a) Sand-heap L-section. (b) Sand-heap rectangular section. (c) Plan of rectangular section. (d) Torsional shear stress.

tic sand-heap approach to evaluate its torsional moment capacity and shear stress to which it is subjected.

The sand heap is broken into three volumes:

$$V_1 = \text{pyramid representing a square cross-sectional shape} = y_1 b_w^2 / 3$$

$$V_2 = \text{tent portion of the web, representing a rectangular cross-sectional shape} = y_1 b_w (h - b_w) / 2$$

$$V_3 = \text{tent representing the flange of the beam, transferring part } PDI \text{ to } NQM = y_2 h_f (b - b_w) / 2$$

The torsional moment is proportional to twice the volume of the sand heaps; hence,

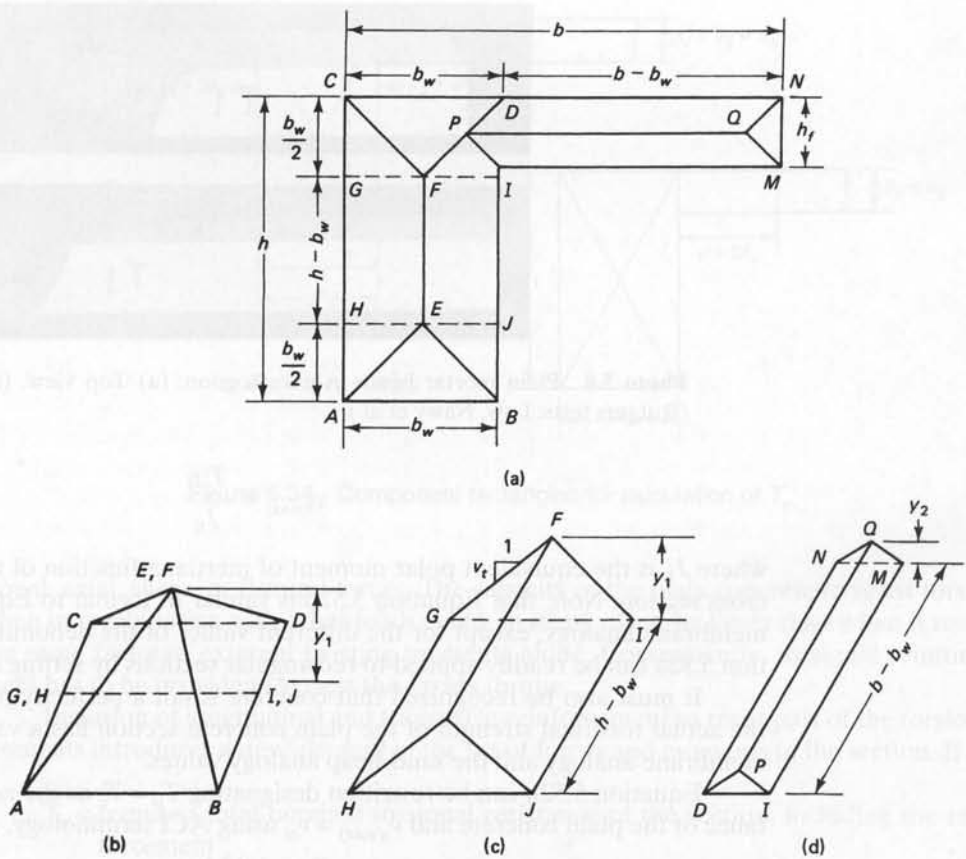
$$T_p \cong \left[ \frac{y_1 b_w^2}{3} + \frac{y_1 b_w (h - b_w)}{2} + \frac{y_2 h_f (b - b_w)}{2} \right] 2 \tag{5.48}$$

Also, the torsional shear stress is proportional to the slope of the sand heaps; hence,

$$y_1 = \frac{v_t b_w}{2} \tag{5.49}$$

$$y_2 = \frac{v_t h_f}{2} \tag{5.50}$$

Substituting  $y_1$  and  $y_2$  from Equations 5.49 and 5.50 into Equation 5.48 give us



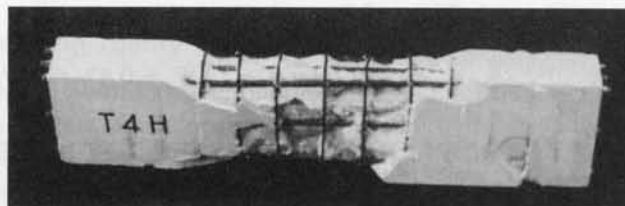
**Figure 5.33** Sand-heap analogy of flanged section. (a) Sand heap on L-shaped cross section. (b) Composite pyramid from web ( $V_1$ ). (c) Tent segment from web ( $V_2$ ). (d) Transformed tent of beam flange ( $V_3$ ).

$$v_{t(max)} = \frac{T_p}{(b_w^2/6)(3h - b_w) + (h_f^2/2)(b - b_w)} \quad (5.51)$$

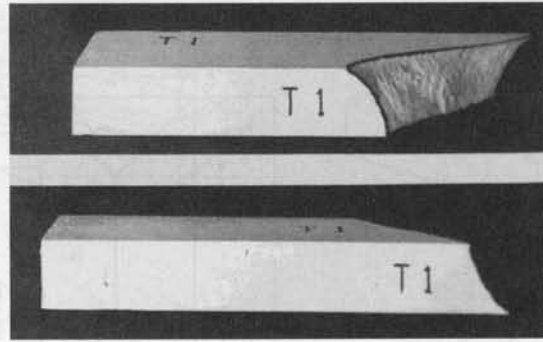
If both the numerator and denominator of Equation 5.51 are divided by  $(b_w h)^2$  and the terms rearranged, we have

$$v_{t(max)} = \frac{T_p h / (b_w h)^2}{[\frac{1}{6}(3 - b_w/h)] + \frac{1}{2}(h_f/b_w)2(b/h - b_w/h)} \quad (5.52a)$$

If one assumes that  $C_t$  is the denominator in this equation and that  $J_E = C_t / (b_w h)^2$ , the equation becomes



**Photo 5.7** Reinforced plaster beam at failure in pure torsion. (Rutgers tests: Law, Nawy, et al.)



**Photo 5.8** Plain mortar beam in pure torsion. (a) Top view. (b) Bottom view. (Rutgers tests: Law, Nawy et al.)

$$v_{t(\max)} = \frac{T_p h}{J_E} \quad (5.52b)$$

where  $J_E$  is the equivalent polar moment of inertia, a function of the shape of the beam cross section. Note that Equation 5.52b is similar in format to Equation 5.45d from the membrane analogy, except for the different values of the denominators  $J$  and  $J_E$ . Equation 5.52a can be readily applied to rectangular sections by setting  $h_f = 0$ .

It must also be recognized that concrete is not a perfectly plastic material; hence, the actual torsional strength of the plain concrete section has a value lying between the membrane analogy and the sand-heap analogy values.

Equation 5.52b can be rewritten designating  $T_p = T_c$  as the nominal torsional resistance of the plain concrete and  $v_{t(\max)} = v_{tc}$  using ACI terminology, so that

$$T_c = k_2 b^2 h v_{tc} \quad (5.53a)$$

or

$$T_c = k_2 x^2 y v_{tc} \quad (5.53b)$$

where  $x$  is the smaller dimension of the rectangular section.

Extensive work on reinforced concrete beams by Hsu and confirmed by others has established that  $k_2$  can be taken as  $\frac{1}{3}$ . This value originated from research in the skew-bending theory of plain concrete. It was also established that  $6\sqrt{f'_c}$  can be considered as a limiting value of the pure torsional strength of a member without torsional reinforcement. Using a reduction factor of 2.5 for the first cracking torsional load  $v_{tc} = 2.4\sqrt{f'_c}$ , and using  $k_2 = \frac{1}{3}$  in Equation 5.53, results in

$$T_c = 0.8\sqrt{f'_c} x^2 y \quad (5.54a)$$

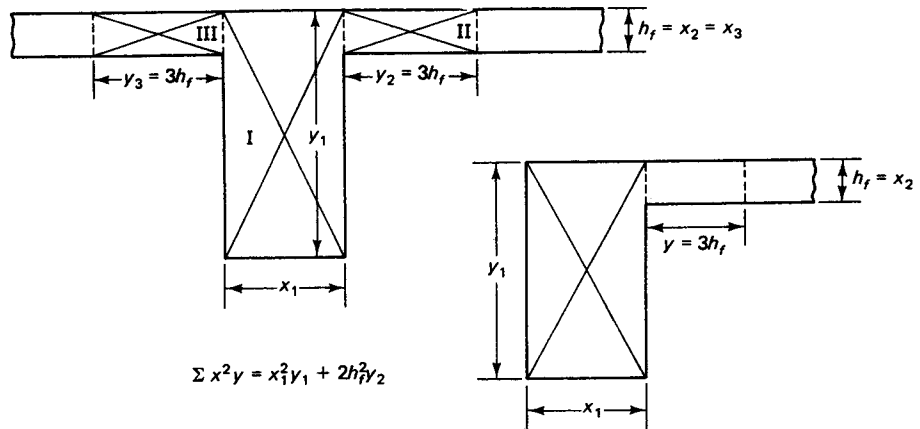
where  $x$  is the shorter side of the rectangular section. The high reduction factor of 2.5 is used to offset any effect of bending moments that might be present.

If the cross section is a T- or L-section, the area can be broken into component rectangles as in Figure 5.34, such that

$$T_c = 0.8\sqrt{f'_c} \sum x^2 y \quad (5.54b)$$

## 5.17 TORSION IN REINFORCED AND PRESTRESSED CONCRETE ELEMENTS

Torsion rarely occurs in concrete structures without being accompanied by bending and shear. The foregoing should give a sufficient background on the contribution of the plain concrete in the section toward resisting *part* of the combined stresses resulting from tor-



**Figure 5.34** Component rectangles for calculation of  $T_c$ .

sional, axial, shear, or flexural forces. The capacity of the plain concrete to resist torsion when in combination with other loads could, in many cases, be lower than when it resists the same factored external twisting moments alone. Consequently, torsional reinforcement has to be provided to resist the excess torque.

Inclusion of longitudinal and transverse reinforcement to resist part of the torsional moments introduces a new element in the set of forces and moments in the section. If

$T_n$  = required total nominal torsional resistance of the section, including the reinforcement

$T_c$  = nominal torsional resistance of the plain concrete

and

$T_s$  = torsional resistance of the reinforcement

then

$$T_n = T_c + T_s \quad (5.55)$$

Several theories have been proposed over the past half century. A general discussion presented here concentrates on (a) the skew bending theory, (b) the space truss analogy theory, (c) the compression field theory, and (d) the plasticity equilibrium truss theory. Except for the skew bending theory, the other models consider the shear flow in hollow box sections as the principal element in evaluating the torsional capacity of solid and hollow sections.

### 5.17.1 Skew-Bending Theory

Skew-bending theory considers in detail the internal deformational behavior of the series of transverse warped surfaces along the beam. Initially proposed by Lessig, it had subsequent contributions from Collins, Hsu, Zia, Gesund, Mattock, and Elfgren among the several researchers in this field. Hsu made a major contribution experimentally to the development of the skew-bending theory as it presently stands. In his book (Ref. 5.9), Hsu details the development of the theory of torsion as applied to concrete structures and how the skew-bending theory formed the basis of the initial ACI code provisions on tor-



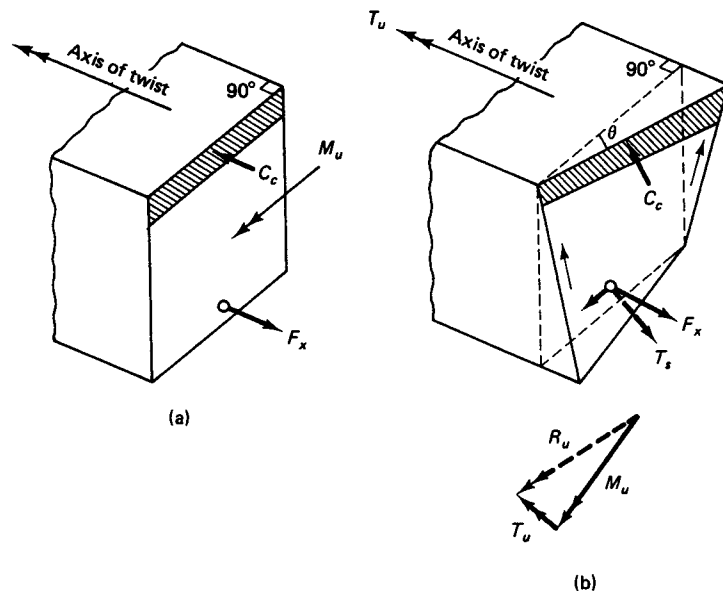
sion. The complexity of the torsional problem permits here only the brief discussion that follows.

The failure surface of the normal beam cross section subjected to bending moment  $M_u$  remains plane after bending, as shown in Figure 5.35(a). If a twisting moment  $T_u$  is also applied exceeding the capacity of the section, cracks develop on three sides of the beam cross section, and compressive stresses appear on portions of the fourth side along the beam. As torsional loading proceeds to the limit state at failure, a skewed failure surface results due to the combined torsional moment  $T_u$  and bending moment  $M_u$ . The neutral axis of the skewed surface and the shaded area in Figure 5.35(b) denoting the compression zone would no longer be straight, but subtend a varying angle  $\theta$  with the original plane cross sections.

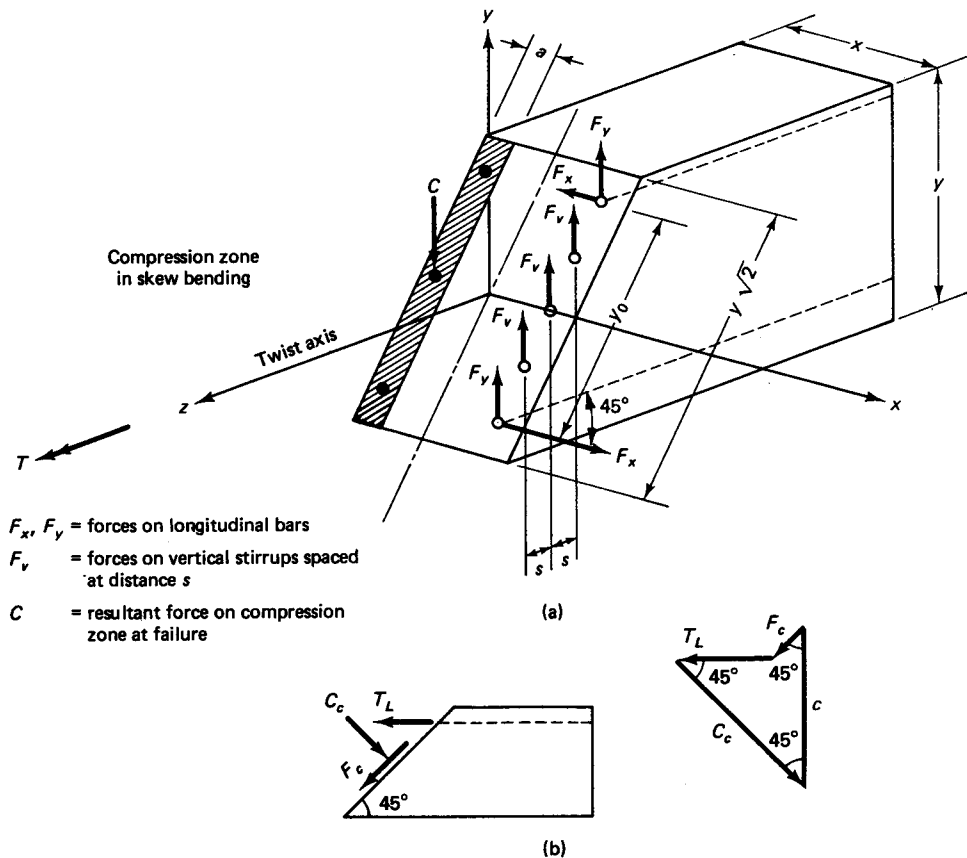
Prior to cracking, neither the longitudinal bars nor the closed stirrups have any appreciable contribution to the torsional stiffness of the section. At the postcracking stage of loading, the stiffness of the section is reduced, but its torsional resistance is considerably increased, depending on the amount and distribution of *both* the longitudinal bars and the transverse *closed* ties. It has to be emphasized that little additional torsional strength can be achieved beyond the capacity of the plain concrete in the beam unless both longitudinal torsion bars and transverse ties are used.

The skew-bending theory idealizes the compression zone by considering it to be of uniform depth. It assumes the cracks on the remaining three faces of the cross section to be uniformly spread, with the steel ties (stirrups) at those faces carrying the tensile forces at the cracks and the longitudinal bars resisting shear through dowel action with the concrete. Figure 5.36(a) shows the forces acting on the skewly bent plane. The polygon in Figure 5.36(b) gives the shear resistance  $F_c$  of the concrete, the force  $T_t$  of the active longitudinal steel bars in the compression zone, and the normal compressive block force  $C_c$ .

The torsional moment  $T_c$  of the resisting shearing force  $F_c$  generated by the shaded compressive block area in Figure 5.36(a) is thus



**Figure 5.35** Skew bending due to torsion. (a) Bending before twist. (b) Bending and torsion.



**Figure 5.36** Forces on the skew-bent planes. (a) All forces acting on skew plane at failure. (b) Vector forces on compression zone.

$$T_c = \frac{F_c}{\cos 45^\circ} \times \text{its arm about forces } F_v \text{ in the figure}$$

OR

$$T_c = \sqrt{2}F_c(0.8x) \quad (5.56a)$$

where  $x$  is the shorter side of the beam. Extensive tests (Refs. 5.9 and 5.10) to evaluate  $F_c$  in terms of the internal stress in concrete  $k_1\sqrt{f'_c}$  and the geometrical torsional constants of the section  $k_2x^2y$  led to the expression

$$T_c = \frac{2.4}{\sqrt{x}} x^2y\sqrt{f'_c} \quad (5.56b)$$

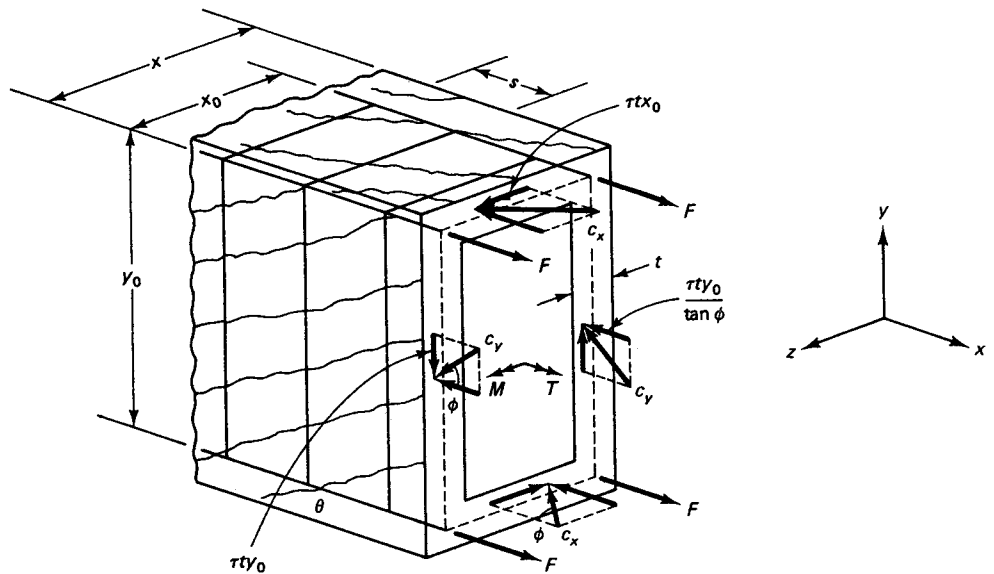
### 5.17.2 Space Truss Analogy Theory

Space truss analogy theory was originally developed by Rausch and later extended by Lampert and Collins, with additional work by Hsu, Thurliman, Elfgren, and others. Further refinement was introduced by Rabbat and Collins (Ref. 5.13) on the variable angle space truss and Collins and Mitchell (Ref. 5.11).

Hsu (Refs. 5.17 and 5.18) proposed combining the equilibrium, compatibility and the softened constitutive laws of concrete in a unified theory that can predict with reasonable accuracy the shear and torsional behavior of beams (the softened truss model). The shear flow concept was utilized in deriving the relevant expressions for shear equilibrium. The space truss analogy is an extension of the model used in the design of the shear-resisting stirrups, in which the diagonal tension cracks, once they start to develop, are resisted by the stirrups. Because of the nonplanar shape of the cross sections due to the twisting moment, a space truss composed of the stirrups is used as the diagonal tension members, and the idealized concrete strips at a variable angle  $\theta$  between the cracks are used as the compression members (struts), as shown in Figure 5.37.

It is assumed in this theory that the concrete beam behaves in torsion similarly to a thin-walled box with a constant shear flow in the wall cross section, producing a constant torsional moment. The use of hollow-walled sections rather than solid sections proved to give essentially the same ultimate torsional moment, provided that the walls were not too thin. Such a conclusion is borne out of tests which have shown that the torsional strength of the solid sections is composed of the resistance of the closed stirrup cage, consisting of the longitudinal bars and transverse stirrups, and the idealized concrete inclined compression struts in the plane of the cage wall. The compression struts are the inclined concrete strips between the cracks in Figure 5.37.

The CEB-FIP code is based on the space truss model. In this code, the effective wall thickness of the hollow beam is taken as  $\frac{1}{8}D_0$ , where  $D_0$  is the diameter of the circle inscribed in the rectangle connecting the corner longitudinal bars, namely,  $D_0 = x_0$  in Figure 5.37. In summary, the absence of the core does not affect the strength of such members in torsion—hence, the acceptability of the space truss analogy approach based on hollow sections.



- $F$  = tensile force in each longitudinal bar
- $c_x$  = inclined compressive force on horizontal side
- $c_y$  = inclined compressive force on vertical side
- $\tau t$  = shear flow force per unit length of wall

Figure 5.37 Forces on hollow-box concrete surface by truss analogy.

### 5.17.3 Compression Field Theory

The compression field theory can be considered a special case of the general truss model theory. Elfgren proposed the compression fields to describe components of the plasticity truss model currently used in the European Code, and Collins and Mitchell modified the approach, proposing the terms to be subsequently discussed. The angle of inclination  $\theta$  in Fig. 5.37 of the diagonal cracks or the compression struts between the diagonal cracks is not idealized to  $45^\circ$ , but rather uses limits based on the areas of the longitudinal tension steel and the transverse torsional web steel (inclined or vertical closed stirrups or ties). Figure 5.38 points up the fact that the torsional force is resisted by the tangential components of the diagonal compression struts, which produce a shear flow  $q$  around the perimeter (Ref. 5.11).

Assuming that concrete carries no tension after cracking, and that torsional shear is carried by the field of diagonal compression struts, the angle of inclination  $\theta$  of these struts can be defined as

$$\tan^2 \theta = \frac{\epsilon_l + \epsilon_d}{\epsilon_t + \epsilon_d} \quad (5.57)$$

where  $\epsilon_l$  = longitudinal tensile strain in the main bars  $A$

$\epsilon_t$  = transverse tensile strain in bars  $B$

$\epsilon_d$  = diagonal compression strain

The area  $A_o$  in the figure enclosed by the shear flow  $q$  can be obtained as

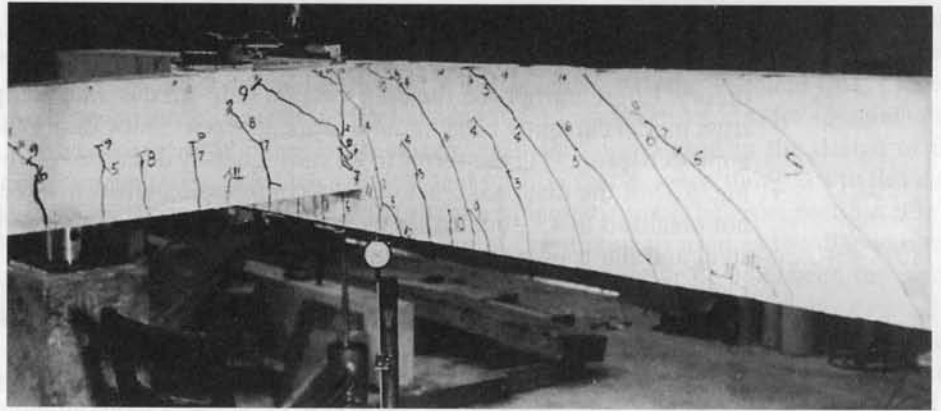
$$A_o = A_{oh} - \frac{a_0}{2} p_h \quad (5.58)$$

where  $A_{oh}$  = area enclosed by the centerline of the hoop

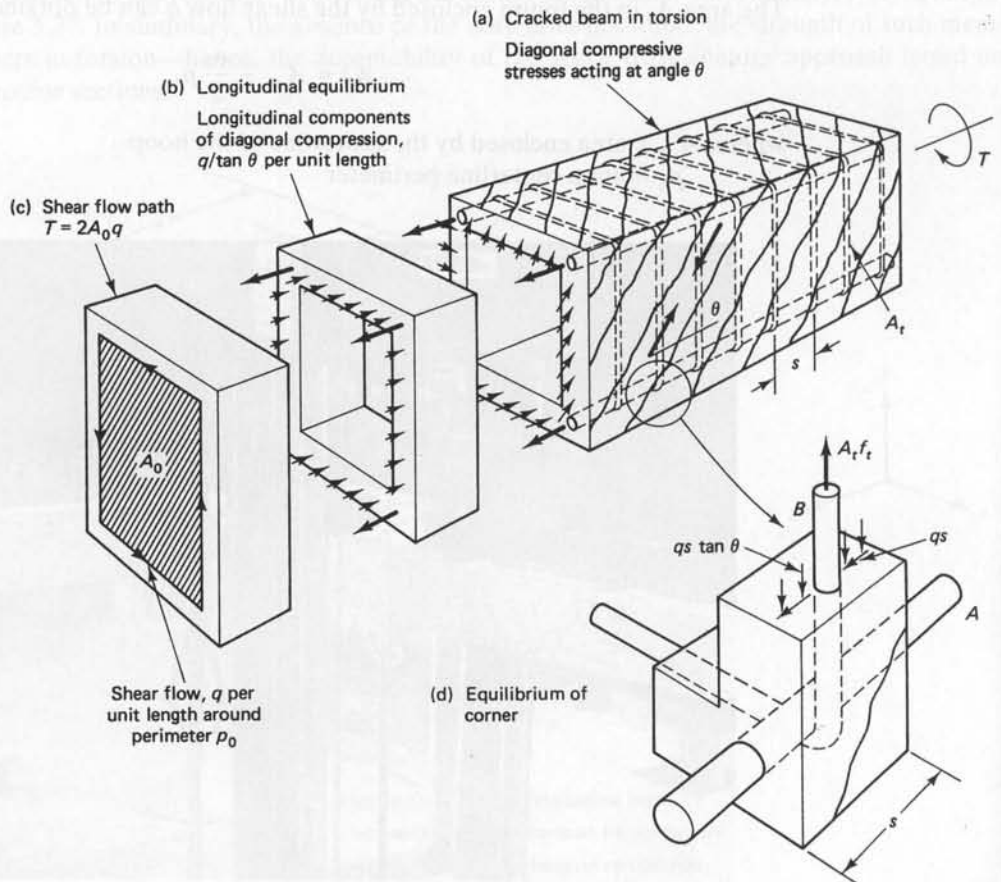
$p_h$  = hoop centerline perimeter



**Photo 5.9** Reinforced concrete beams in torsion, testing setup. (Courtesy, Thomas T. C. Hsu.)



**Photo 5.10** Closeup of torsional cracking of beams in the preceding photograph. (Courtesy, Thomas T. C. Hsu.)



**Figure 5.38** Compression field truss model by Collins and Mitchell (Ref. 5.11).

$a_o$  = compression block depth (identical to the depth  $a$  of the equivalent rectangular block in flexure)

The equivalent wall thickness  $t_d$  in the analysis of the twisted beam is shown in Figure 5.39, and the depth  $a_o$  of the compressive block is defined in Equation 5.61.

The diagonal torsional cracks, as well as the exposed transverse ties after spalling of the concrete cover at torsion failure, are demonstrated in Figure 5.40.

The transverse and longitudinal strains in the steel at the nominal torsional moment  $T_n$  can be respectively defined as

$$\epsilon_t = \left( \frac{0.85\beta_1 f'_c A_o}{\tau_n A_{oh} \tan \theta} - 1 \right) 0.003 \quad (5.59a)$$

$$\epsilon_l = \left( \frac{0.85\beta_1 f'_c A_o}{\tau_n A_{oh}} \tan \theta - 1 \right) 0.003 \quad (5.59b)$$

where the nominal torsional shear stress is

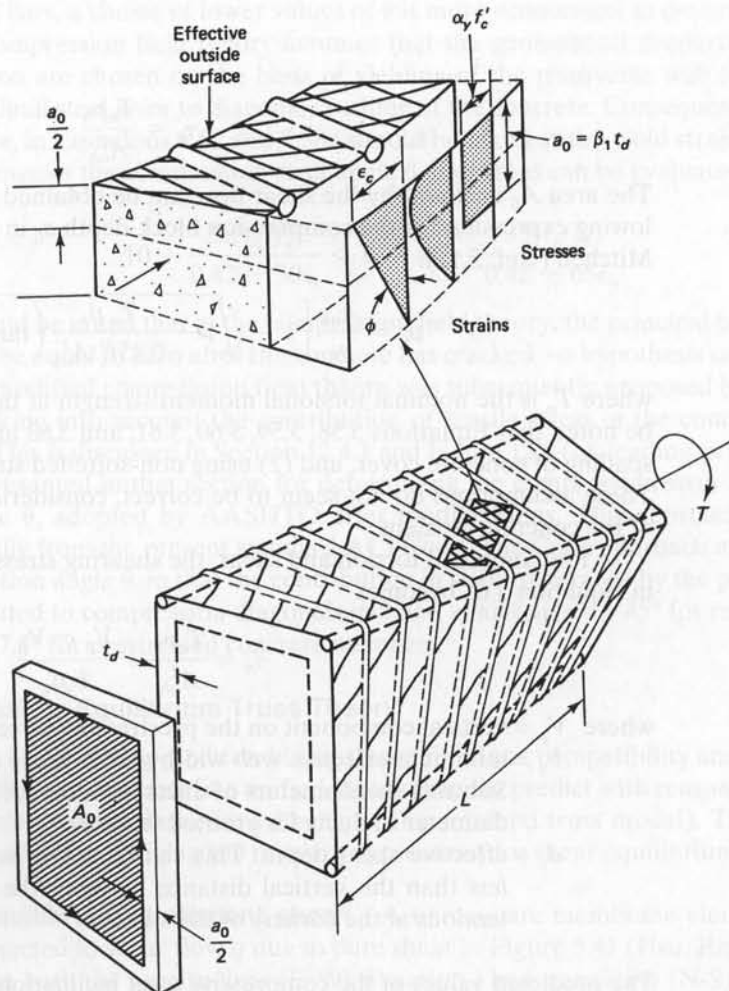
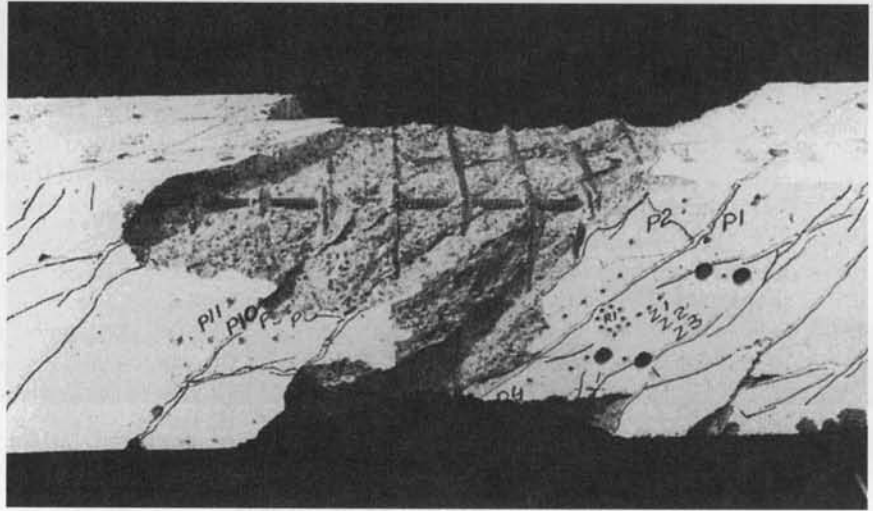


Figure 5.39 Effective thickness  $t_d$  and compression block depth  $a_o$ .



**Figure 5.40** Torsional failure of web-reinforced beam after spalling of cover (Collins and Mitchell, Ref. 5.11).

$$\tau_n = \frac{T_n p_h}{A_{oh}^2} \quad (5.60)$$

The area  $A_0$  enclosed by the shear flow can be obtained from Equation 5.60 and the following expression for the compression block depth  $a_0$  in torsion according to Collins and Mitchell (Ref. 5.11):

$$a_0 = \frac{A_{oh}}{p_h} \left[ 1 - \sqrt{1 - \frac{T_n p_h}{0.85 f'_c A_{oh}^2} \left( \tan \theta + \frac{1}{\tan \theta} \right)} \right] \quad (5.61)$$

where  $T_n$  is the nominal torsional moment strength at the limit state at failure. It should be noted that Equations 5.58, 5.59, 5.60, 5.61, and 5.63 are based on the assumptions: (1) spalling of concrete cover, and (2) using non-softened stress-strain curve of the concrete. These assumptions do not seem to be correct, considering the actual torsional behavior of the concrete element.

For combined torsion and shear, the shearing stress at nominal strengths  $T_n$  and  $V_n$  in Equation 5.61 becomes

$$\tau_n = \frac{T_n p_h}{A_{oh}^2} + \frac{V_n - V_p}{b_v d_v} \quad (5.62)$$

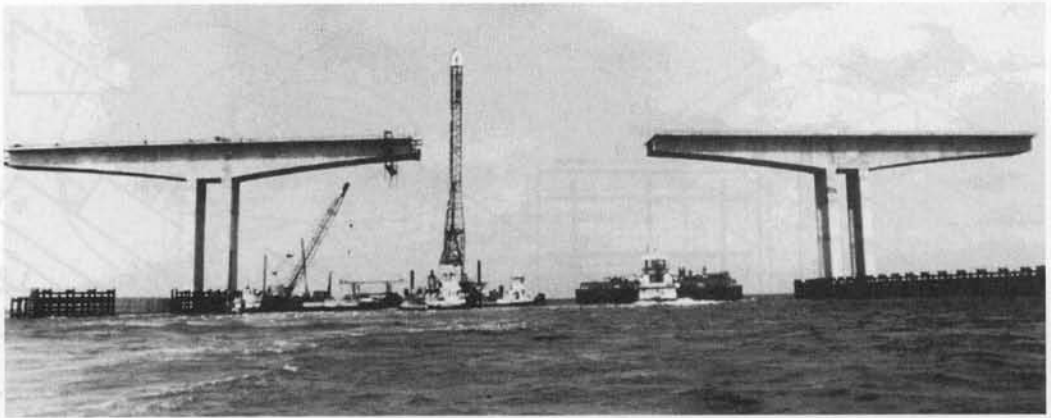
where  $V_p$  = vertical component on the prestressing force.

$b_v$  = minimum effective web width within shear depth  $d_v$  after spalling of cover.

Subtract the diameters of ducts from the web width if ungrouted, or half the diameter of ducts for grouted tendons.

$d_v$  = effective shear depth. This can be taken as the flexural lever arm, but *not less* than the vertical distance between the centers of bars or prestressing tendons at the corners of the stirrups.

The predicted values of the compressive strut inclination  $\theta$  in Figure 5.38 range between  $24^\circ$  for pure torsion and  $90^\circ$  for pure flexure. Hence, the lower the value of  $\theta$  selected for a given torque, the less is the transverse hoop steel needed and the more is the required



**Photo 5.11** Dauphin Island Bridge, Alabama, assembly of segmental bridge units. (Courtesy, Prestressed Concrete Institute.)

area of longitudinal steel. Since transverse closed stirrups or ties are more expensive than longitudinal bars, a choice of lower values of  $\theta$  is more economical in design.

The compression field theory assumes that the geometrical properties of the designed section are chosen on the basis of yielding of the transverse web reinforcement and longitudinal steel *prior* to diagonal crushing of the concrete. Consequently, the transverse strain  $\epsilon_t$  in Equations 5.57 and 5.58a should be taken as the yield strain  $\epsilon_{ty}$ .

The range of the compression strut angle  $\theta$  in degrees can be evaluated from

$$10 + \frac{35(\tau_n/f'_c)}{0.42 - 50\epsilon_t} < \theta < 80 - \frac{35(\tau_n/f'_c)}{0.42 - 65\epsilon_{ty}} \quad (5.63)$$

It should be noted that in the compression field theory, the principal tensile stress is assumed to be equal to zero after the concrete has cracked—a hypothesis subject to justification. A modified compression field theory was subsequently proposed by Collins and Mitchell, taking into account the contribution of tensile stress in the concrete between the cracks. This is discussed in Section 12.4.1 and Figure 12.8 (c), leading to the design expressions presented in that section for determining the compression strut *variable* inclination angle  $\theta$ , adopted by AASHTO after modifications. This approach also differs fundamentally from the present standard ACI Code. The Code approach assumes a *constant* inclination angle  $\theta$ , in that the contribution in shear resistance by the plain concrete,  $V_o$  is attributed to compression diagonals inclined at an angle  $\theta = 45^\circ$  for reinforced concrete, and  $37.5^\circ$  for prestressed concrete members.

#### 5.17.4 Plasticity Equilibrium Truss Theory

Hsu (Ref. 5.17, 5.18) proposed combining the equilibrium, compatibility and the softened constitutive laws of concrete in a unified theory that can predict with reasonable accuracy the shear and torsional behavior of beams (The softened truss model). The shear flow concept is utilized in deriving the relevant expressions for shear equilibrium.

**5.17.4.1 Equilibrium in element shear.** A unit square membrane element of thickness  $t$  is subjected to shear flow  $q$  due to pure shear in Figure 5.41 (Hsu, Ref. 5.18). Reinforcement in both the longitudinal (E-W) direction  $l$  and transverse (N-S) direction  $t$  is subjected to a unit stress  $f_l/s_l$  and  $f_v/s$  respectively such that the shear flow  $q$  can be defined by the equilibrium equations



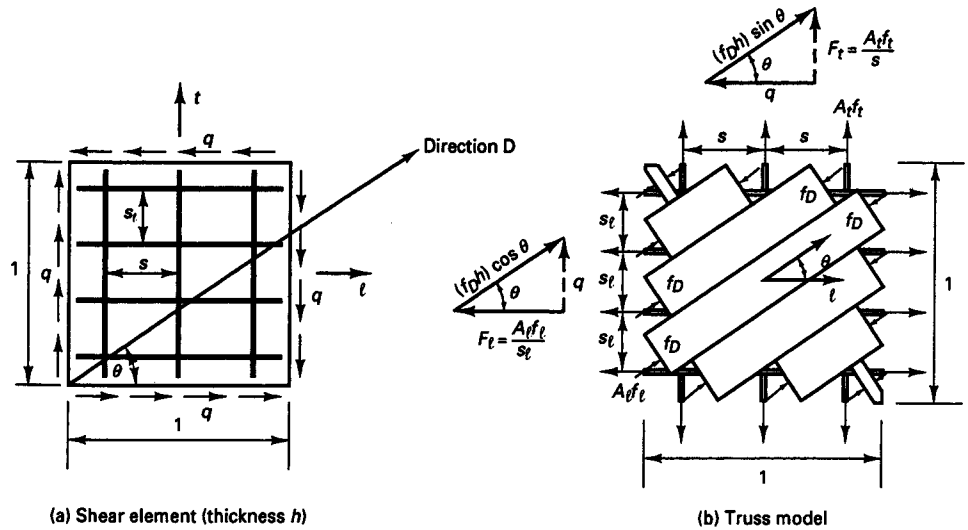


Figure 5.41 Equilibrium forces in element shear (Ref. 5.18).

$$q = (F_l) \tan \theta \tag{5.64a}$$

where unit  $F_l = A_l f_l / s_l$  and

$$q = (F_t) \cot \theta \tag{5.64b}$$

where unit  $F_t = A_t f_t / s$

$A_l$  and  $A_t$  are the cross-sectional areas of the reinforcement, and  $s_l$  and  $s$  are the spacings in the  $l$  and  $t$  directions, respectively.

From the geometry of the triangles in Figure 5.41 the shear flow can also be defined as

$$q = (f_D t) \sin \theta \cos \theta \tag{5.65}$$

If the reinforcement in both directions is assumed to have yielded, Equations 5.64a, b and 5.65 give

$$\tan \theta = \sqrt{\frac{F_{ty}}{F_{ly}}} \tag{5.66a}$$

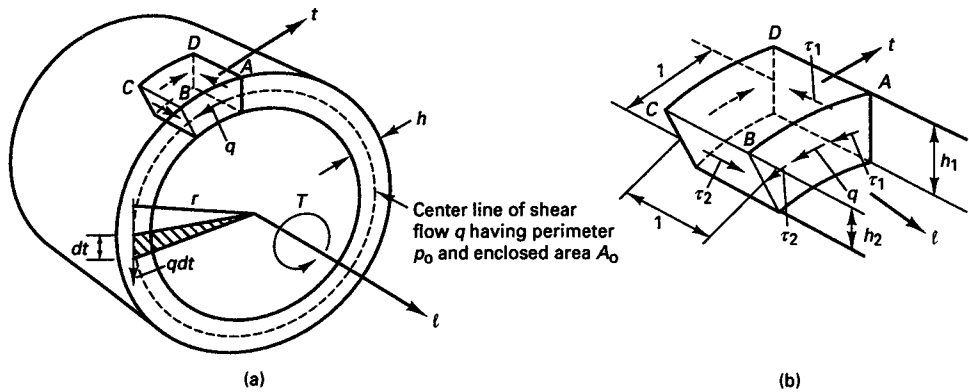
and

$$q_y = \sqrt{F_{ly} F_{ty}} \tag{5.66b}$$

where the subscript  $y$  denotes the yielding of the reinforcement.

**5.17.4.2 Equilibrium in element torsion.** The case of a hollow tube of any shape and variable thickness is considered (Figure 5.42). It is subjected to pure torsion. St.-Venant’s theory stipulates that the cross-sectional shape remains unchanged in elastic small deformations and the warping deformation perpendicular to the cross-section would be the same along the member’s axis. Hence, it can be assumed that only shear stresses develop in the tube wall in the form of shear flow  $q$  in Figure 5.42a and that the in-plane normal stresses in the wall vanish. If an infinitesimal wall element ABCD is isolated as in Figure 5.42b, the shear flow in the  $l$  direction has to be equal to the shear flow in the  $t$  direction or

$$\tau_l t_1 = \tau_t t_2 \tag{5.67}$$



**Figure 5.42** Hollow tube equilibrium torsion forces. (a) Section of tube subjected to torsion  $T$ . (b) Unit shear element from tube wall of varying thickness  $h$ . Note:  $l$  and  $t$  denote the longitudinal and transverse directions.

On this basis, the shear flow  $q$  is considered constant throughout the cross-section (Ref. 5.18). The torsional force over an infinitesimal distance  $dt$  along the shear flow path is  $qdt$  so that the torsional resistance to the external torsional moment  $T$  in Figure 5.42a becomes

$$T = q \oint r dt \quad (5.68)$$

It can be seen from Figure 5.42a that  $r dt$  in the integral is equal to *twice* the area of the shaded triangle formed by  $r$  and  $dt$ . A summation of the total area around the cross section gives

$$\oint r dt = 2A_0 \quad (5.69)$$

where  $A_0$  = cross-sectional area bounded by the shear flow center line. Substituting  $2A_0$  into Equation 5.68 gives

$$q = \frac{T}{2A_0} \quad (5.70)$$

By neglecting warping, the shear element subjected to pure torsion in the tube wall of Figure 5.42a becomes identical to the membrane shear element in Figure 5.41a. Hence, substituting for the shear flow  $q$  from Equation 5.70 into Equations 5.64a, b, and 5.65, the following three equations of equilibrium for torsion result in

$$T = \frac{\bar{F}_l}{p_0} (2A_0) \tan \theta \quad (5.71a)$$

where  $\bar{F}_l = F_l p_0$  and  $p_0$  = perimeter of the shear flow path.  $\bar{F}_l$  is the *total* longitudinal force due to torsion.

$$T = F_l (2A_0) \cot \theta \quad (5.71b)$$

$$T = (f_D t) (2A_0) \sin \theta \cos \theta \quad (5.71c)$$

Equation 5.71b can be written at yield as

$$T_n = \frac{2A_0 A_t f_{yv}}{s} \cot \theta \quad (5.72)$$

where  $T_n$  is the maximum torsional moment strength.

The required torsional reinforcement in the transverse and longitudinal directions become

$$A_t = \frac{T_n s}{2A_0 f_{yv} \cot \theta} \tag{5.73}$$

$$A_{l_i} = \frac{A_t}{s} \left( \frac{f_{yv}}{f_{yl}} \right) (s_l \cot^2 \theta) \tag{5.74a}$$

where  $A_{l_i}$  is the area of one longitudinal bar. If  $s_l$  as the longitudinal reinforcement spacing represents the perimeter  $p_h$  of the center-line of the outermost closed transverse torsional reinforcement, then

$$A_{l_i} = \frac{A_t}{s} p_h \left( \frac{f_{yv}}{f_{yl}} \right) \cot^2 \theta \tag{5.74b}$$

where  $A_t$  = total area of all longitudinal torsional steel in the section.

**5.17.4.3 Shear-torsion-bending interaction.** Consider the rectangular box in Figures 5.37 and 5.43. The shear flow  $q$  will not be the same on the four walls of the box when subjected to combined shear and torsion as shown in Figure 5.43. Failure can precipitate in two distinct modes:

- (a) yielding of the longitudinal bottom tension steel and the transverse stirrups,
- (b) yielding of the longitudinal top compression steel and the transverse stirrups,

**(a) Bottom Tension Steel Yielding**

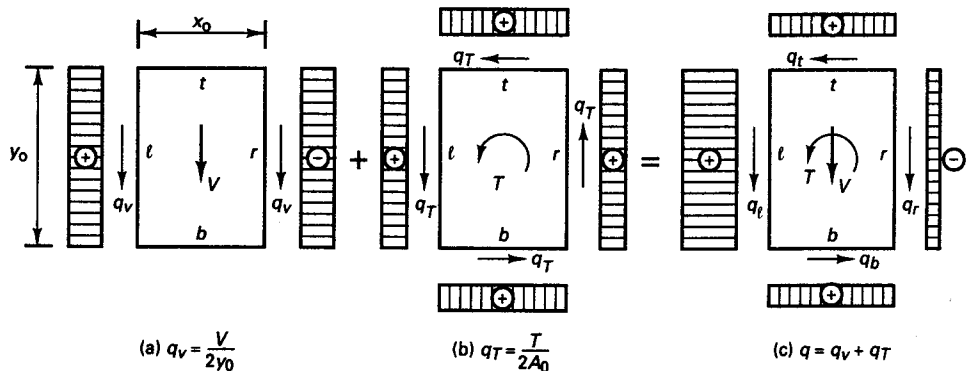
If the failure mode is caused by yielding of the longitudinal bottom stringer (tensile steel) and the transverse stirrups due to combined shear and torsion, the following expression can be derived from equilibrium (Ref. 5.18)

$$\frac{M}{F_B y_0} + \left( \frac{V}{2y_0} \right)^2 \frac{y_0}{F_B} \frac{s}{A_t f_v} + \left( \frac{T}{2A_0} \right)^2 \frac{(y_0 + x_0)}{F_B} \frac{s}{A_t f_v} = 1 \tag{5.75}$$

if  $M_0$ ,  $V_0$ , and  $T_0$  are the moments and forces acting *alone*, they can be defined as follows

$$M_0 = F_B y_0 \tag{5.76a}$$

$$V_0 = 2y_0 \sqrt{\left( \frac{F_T}{y_0} \right) \frac{A_t f_v}{s}} \text{ for a two-web box} \tag{5.76b}$$



**Figure 5.43** Hollow section shear flow  $q$  due to combined shear and torsion.



**Photo 5.12** The Woodley Park Zoo station, Washington, D.C. (Courtesy, H. Wilden & Assoc.).

$$T_0 = 2A_0 \sqrt{\left(\frac{2F_T}{p_0}\right) \frac{A_t f_v}{s}} \quad (5.76c)$$

where  $p_0 = 2(y_0 + x_0)$

$$R = \frac{F_T}{F_B} \quad (5.76d)$$

A nondimensional interaction surface relationship can be obtained by introducing Equation 5.76 into Equation 5.75 such that

$$\left(\frac{M}{M_0}\right) + \left(\frac{V}{V_0}\right)^2 R + \left(\frac{T}{T_0}\right)^2 R = 1 \quad (5.77a)$$

#### (b) Top Compression Steel Yielding

If the failure mode is caused by yielding of the longitudinal top chord (compression steel) and the transverse stirrups, Equation 5.77a becomes

$$-\left(\frac{M}{M_0}\right) \frac{1}{R} + \left(\frac{V}{V_0}\right)^2 + \left(\frac{T}{T_0}\right)^2 = 1 \quad (5.77b)$$

From both Equations 5.77a and 5.77b the interaction of  $V$  and  $T$  is *circular* for a constant bending moment  $M$  for both failure surfaces. The intersection of the two failure surfaces for these two failure modes forms a peak interaction curve between  $V$  and  $T$  that Equations 5.77a and b give

$$\left(\frac{V}{V_0}\right)^2 + \left(\frac{T}{T_0}\right)^2 = \frac{1+R}{2R} \quad (5.78a)$$

Equation 5.78 for  $R = 0.25, 0.5,$  and  $1.0$  on the peak planes gives the circular plots shown in Figure 5.44.

A third mode of failure is caused by yielding in the top bar, in the bottom bar, and in the transverse reinforcement, all on the side where shear flows due to shear and tor-

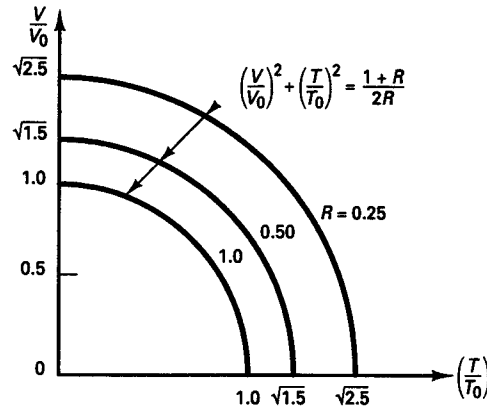


Figure 5.44 Shear-torsion interaction diagram.

sion are additive i.e. left wall (Ref. 5.15). A modified form of Equation 5.78 results as follows

$$\left(\frac{V}{V_0}\right)^2 + \left(\frac{T}{T_0}\right)^2 + \sqrt{2}\left(\frac{VT}{V_0T_0}\right) = \frac{1+R}{2R} \quad (5.78b)$$

The factored torsional moment strength,  $\phi T_n$ , must equal or exceed the external torsion,  $T_u$ , due to the factored loads. In the calculation of  $T_n$  (ACI 318–99, Ref. 5.1), all the torque is assumed to be resisted by the closed stirrups and longitudinal steel with the torsional moment  $T_c$  resisted by the concrete compression struts assumed as zero. At the same time, the shear resisted by concrete,  $V_c$  is assumed to be unchanged by the presence of torsion. This simplification eliminates the need for the rigor of the lengthy interaction expressions for  $V$ ,  $T$ , and  $M$  used in the previous codes. In summary, the web reinforcement for shear is determined by the value of  $V_s = V_n - V_c$  while the web reinforcement for torsion by the  $T_n$  value alone, where  $T_n = T_u/\phi$  with  $\phi = 0.85$ .

### 5.17.5 Design of Prestressed Concrete Beams Subjected to Combined Torsion, Shear, and Bending in Accordance with the ACI 318–08 Code

Adjusting in the equilibrium truss model of Section 5.17.4, the following are the ACI 318 Code provisions for designing the longitudinal and transverse reinforcement in prestressed elements.

**5.17.5.1 Compatibility torsion.** In statically indeterminate systems, stiffness assumptions, compatibility of strains at the joints and redistribution of stresses may affect the stress resultants, leading to a reduction of the resulting torsional shearing stresses. A reduction is permitted in the value of the factored moment used in the design of the member if part of this moment can be redistributed to the intersecting members. The ACI Code permits a maximum factored torsional moment at the critical section  $h/2$  from the face of the supports for prestressed concrete members as follows:

where  $A_{cp}$  = area enclosed by outside perimeter of concrete cross section =  $x_0y_0$   
 $p_{cp}$  = outside perimeter of concrete cross section  $A_{cp}$ , in. =  $2(x_0 + y_0)$

$$T_u = \phi 4 \sqrt{f'_c} \left( \frac{A_{cp}^2}{p_{cp}} \right) \sqrt{1 + \frac{f_c}{4\sqrt{f'_c}}} \quad (5.79)$$

where  $\bar{f}_c$  = average compressive stress in the concrete at the centroidal axis due to effective prestress only after allowing for all losses.  $\bar{f}_c$  is denoted in the ACI Code as  $f_{pc}$ .

Neglect of the full effect of the total value of external torsional moment in this case does **not**, in effect, lead to failure of the structure but may result in excessive cracking if  $\phi 4\sqrt{f'_c}(A_{cp}^2/p_{cp})$  is considerably smaller in value than the actual factored torque.

If the actual factored torque is less than that given in Equation 5.79, the beam has to be designed for the lesser torsional value. Torsional moments are neglected however if for prestressed concrete

$$T_u < \phi \sqrt{f'_c} \left( \frac{A_{cp}^2}{p_{cp}} \right) \sqrt{1 + \frac{\bar{f}_c}{4\sqrt{f'_c}}} \quad (5.80)$$

**5.17.5.2 Torsional moment strength.** The size of the cross section is chosen on the basis of reducing unsightly cracking and preventing the crushing of the surface concrete caused by the inclined compressive stresses due to shear and torsion defined by the left hand side of the expressions in Equation 5.81. The geometrical dimensions for torsional moment strength in both reinforced and prestressed members are limited by the following expressions.

**(a) Solid Sections**

$$\sqrt{\left( \frac{V_u}{b_w d} \right)^2 + \left( \frac{T_u p_h}{1.7 A_{oh}^2} \right)} \leq \phi \left( \frac{V_c}{b_w d} + 8\sqrt{f'_c} \right) \quad (5.81)$$

**(b) Hollow Sections**

$$\left( \frac{V_u}{b_w d} \right) + \left( \frac{T_u p_h}{1.7 A_{oh}^2} \right) \leq \phi \left( \frac{V_c}{b_w d} + 8\sqrt{f'_c} \right) \quad (5.82)$$

where  $A_{oh}$  = area enclosed by the centerline of the outermost closed transverse torsional reinforcement, sq. in.

$p_h$  = perimeter of centerline of outermost closed transverse torsional reinforcement, in.

The area  $A_{oh}$  for different sections are given in Figure 5.45. Figures 5.46 and 5.47 give guidance to the determination of the area  $A_{oh}$  and the shear flow area  $A_0 \cong 0.85A_{oh}$  in Equation 5.84(a).

The sum of the stresses at the left hand side of Equation 5.82 should not exceed the stresses causing shear cracking plus  $8\sqrt{f'_c}$ . This is similar to the limiting strength  $V_s \leq 8\sqrt{f'_c}$  for shear without torsion.

**5.17.5.3 Hollow sections wall thickness.** The shear stresses due to shear and to torsion both develop in the walls of the hollow section as seen in Figure 5.48a. Note that in a solid section the shear stresses due to torsion still concentrate in the outer zones of the section as in Figure 5.48b and as discussed in Section 5.17.3.1.

If the wall thickness in the hollow section varies around its perimeter, the section geometry has to be evaluated at such a location where the left-hand side of Equation 5.82 has a maximum value. Also, if the wall thickness  $t < A_{oh}/p_h$  the left-hand side of Equation 5.82 should be taken as

$$\left( \frac{V_u}{b_w d} \right) + \left( \frac{T_u}{1.7 A_{oh} t} \right)$$

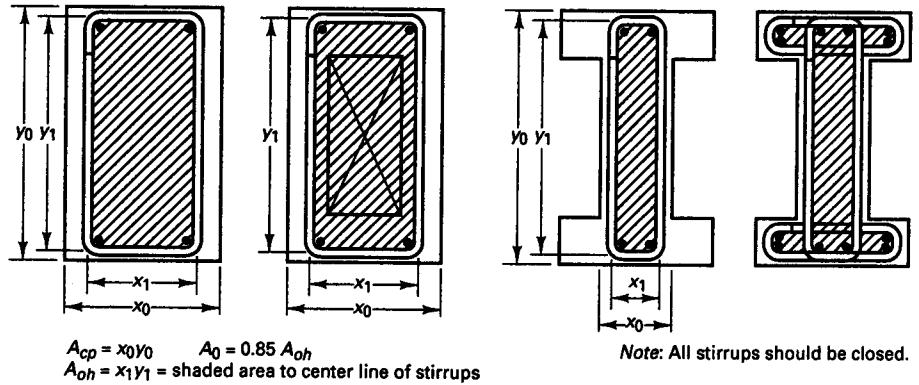


Figure 5.45 Torsional geometric parameters.

The wall thickness  $t$  is the thickness where stresses are being checked.

$$\begin{aligned}
 V_c &= \left( 0.6\lambda \sqrt{f'_c} + 700 \frac{V_u d_p}{M_u} \right) b_w d_p; & \frac{V_u d_p}{M_u} &\leq 1.0 \\
 &\geq 1.7\lambda \sqrt{f'_c} b_w d_p & & \\
 &\leq 5.0\lambda \sqrt{f'_c} b_w d_p & &
 \end{aligned}
 \tag{5.83}$$

where  $f_{pe} > 0.4f_{pu}$ .

**5.17.5.4 Torsional web reinforcement.** As indicated in Section 5.17.3, meaningful additional torsional strength due to the addition of torsional reinforcement can be achieved only by using both stirrups and longitudinal bars. Ideally, *equal* volumes of steel in both the closed stirrups and the longitudinal bars should be used so that both participate equally in resisting the twisting moments. This principle is the basis of the ACI expressions for proportioning the torsional web steel. If  $s$  is the spacing of the stirrups,  $A_l$  is the total cross-sectional area of the longitudinal bars, and  $A_t$  is the cross section of one stirrup leg, the transverse reinforcement for torsion has to be based on the full external torsional moment strength value  $T_m$ , namely,  $(T_u/\phi)$  where

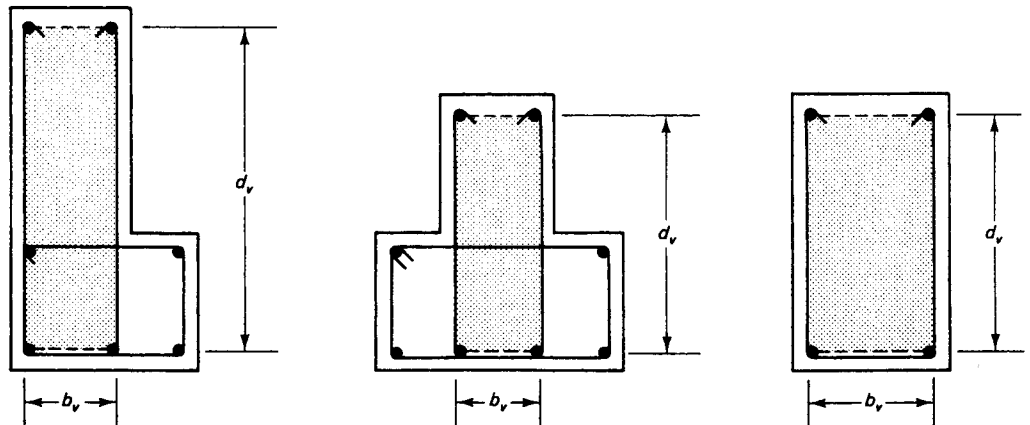
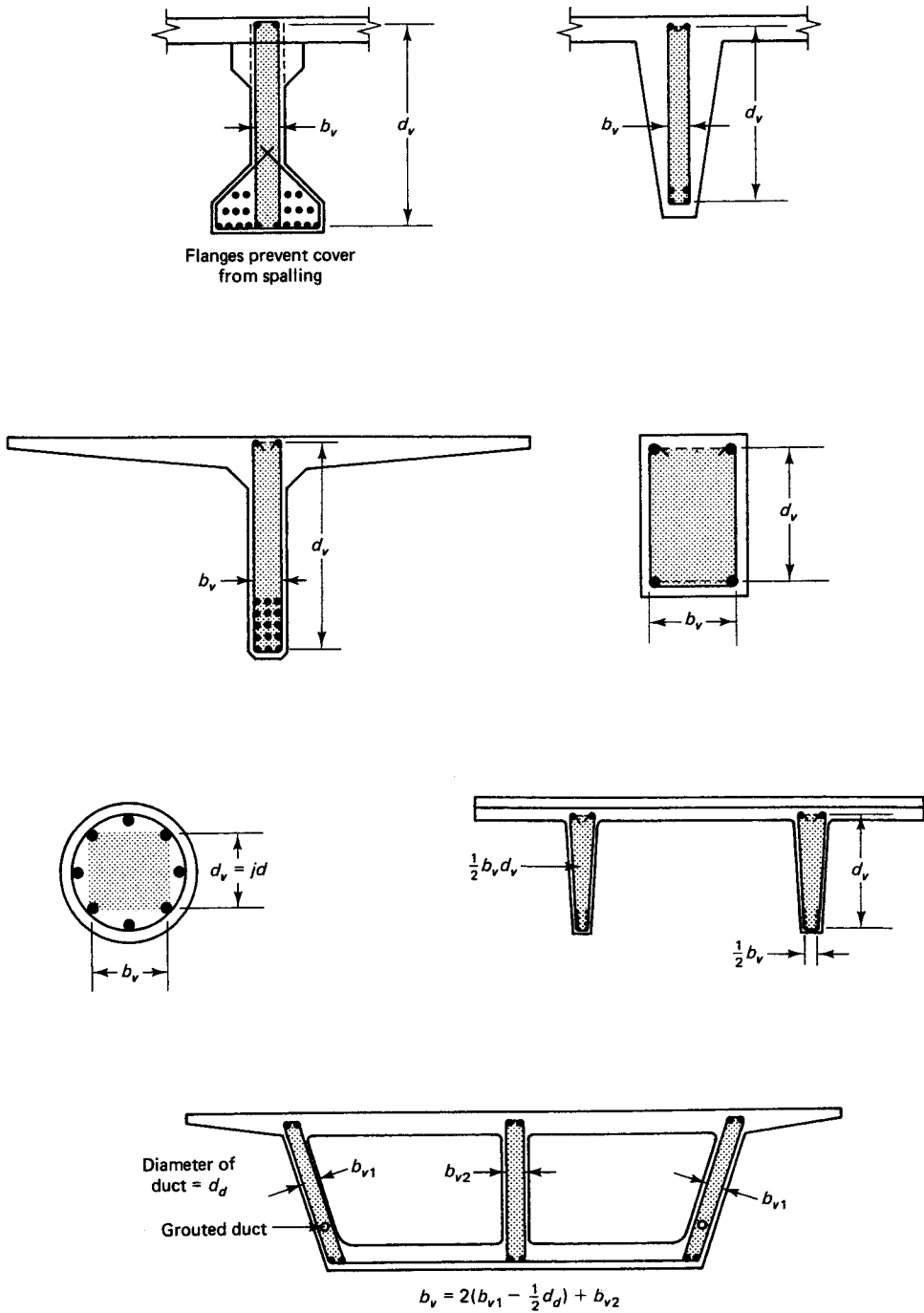
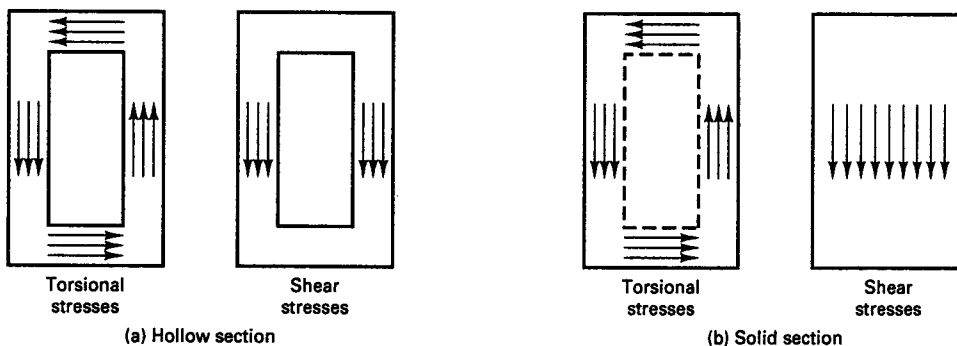


Figure 5.46 Shear-flow geometry and effective shear area.



**Figure 5.77** Effective shear width and depth of typical prestressed concrete sections.





**Figure 5.48** Superposition of torsional and shear stresses. (a) Directly additive occurring in the left wall of the box (Equation 7.30b). (b) Torsion acts on “tubular” outer-wall section while shear stress acts on the full width of solid section: stresses combined using square root of sum of squares (Equation 7.30b).

$$T_n = \frac{2A_0 A_t f_{yt}}{s} \cot \theta \quad (5.84a)$$

(See the derivation of Equation 5.72)

$A_0$  = gross area enclosed by the shear flow path, sq. in.

$A_t$  = cross-sectional area of one leg of the transverse closed stirrups, sq. in.

$f_{yt}$  = yield strength of closed transverse torsional reinforcement not to exceed 60,000 psi.

$\theta$  = angle of the compression diagonals (struts) in the space truss analogy for torsion (See Figure 5.39).

Transposing terms in Equation 5.84b, the transverse reinforcement area becomes

$$\frac{A_t}{s} = \frac{T_n}{2A_0 f_{yt} \cot \theta} \quad (5.84b)$$

The area  $A_0$  has to be determined by analysis (Ref. 7.14 and 7.15) except that the ACI 318 Code permits taking  $A_0 = 0.85A_{oh}$  in lieu of the analysis.

As discussed in Section 5.17.3, the factored torsional resistance  $\phi T_n$  must equal or exceed the factored external torsional moment  $T_u$ . All the torsional moment is assumed in the ACI 318 code to be resisted by the closed stirrups and the longitudinal steel with the torsional resistance,  $T_c$ , of the concrete disregarded, namely  $T_c = 0$ . The shear  $V_c$  resisted by the concrete is assumed to be unchanged by the presence of torsion (see Section 5.17.3.2).

The angle  $\theta$  subtended by the concrete compression diagonals (struts) should not be taken smaller than  $30^\circ$  nor larger than  $60^\circ$ . It can be obtained by analysis as detailed in Ref. 5.17 and 5.18 by Hsu. The additional longitudinal reinforcement for torsion should not be less than

$$A_l = \frac{A_t}{s} p_h \left( \frac{f_{yt}}{f_y} \right) \cot^2 \theta \quad (5.85)$$

where  $f_{yt}$  = yield strength of the longitudinal torsional reinforcement, not to exceed 60,000 psi.

The same angle  $\theta$  should be used in both Equations 5.84 and 5.85. It should be noted that as  $\theta$  gets smaller, the amount of stirrups required by Equation 5.84 decreases. At the same time the amount of longitudinal steel required by Equation 5.85 increases.

In lieu of determining the angle  $\theta$  by analysis, the ACI Code allows a value of  $\theta$  equal to

- (i)  $45^\circ$  for non-prestressed members or members with less prestress than in (ii),
- (ii)  $37.5^\circ$  for prestressed members with an effective prestressing force larger than 40 percent of the tensile strength of the longitudinal reinforcement.

The PCI (Ref. 5.12) recommends computing the value of  $\theta$  from the expression:

$$\cot \theta = \frac{T_u/\phi}{1.7A_{oh}(A_t/s)f_{yt}} \quad (5.86)$$

**5.17.5.5 Minimum torsional reinforcement.** It is necessary to provide a minimum area of torsional reinforcement in all regions where the factored torsional moment  $T_u$  exceeds the value given by Equation 5.80. In such a case, the minimum area of the required transverse closed stirrups is

$$A_v + 2A_t \geq \frac{50b_ws}{f_{yt}} \quad (5.87)$$

The maximum spacing should not exceed the smaller of  $p_n/8$  or 12 in.

The minimum total area of the additional longitudinal torsional reinforcement should be determined by

$$A_{t,\min} = \frac{5\sqrt{f'_c}A_{cp}}{f_y} - \left(\frac{A_t}{s}\right)p_h \frac{f_{yt}}{f_y} \quad (5.88)$$

where  $A_t/s$  should not be taken less than  $25b_w/f_{yt}$ . The additional longitudinal reinforcement required for torsion should be distributed around the perimeter of the closed stirrups with a maximum spacing of 12 in. The longitudinal bars or tendons should be placed inside the closed stirrups and at least one longitudinal bar or tendon in each corner of the stirrup. The bar diameter should be at least  $\frac{1}{16}$  of the stirrup spacing but not less than a No. 3 bar. Also, the torsional reinforcement should extend for a minimum distance of  $(b_t + d)$  beyond the point theoretically required for torsion because torsional diagonal cracks develop in a helical form extending beyond the cracks caused by shear and flexure.  $b_t$  is the width of that part of cross section containing the stirrups resisting torsion. The critical section in beams is at a distance  $d$  from the face of the support for reinforced concrete elements and at  $h/2$  for prestressed concrete elements,  $d$  being the effective depth and  $h$  the total depth of the section.

### 5.17.6 SI-Metric Expressions for Torsion Equations

In order to design for combined torsion and shear using the SI (System International) method, the following equations replace the corresponding expressions in the PI (Pound-Inch) method

$$T_u \leq \frac{\phi\sqrt{f'_c}}{3} \left(\frac{A_{cp}^2}{p_{cp}}\right) \sqrt{1 + \frac{3f'_c}{\sqrt{f'_c}}} \quad (5.79)$$

$$T_u \leq \frac{\phi \sqrt{f'_c} \left( \frac{A_{cp}^2}{p_{cp}} \right) \sqrt{1 + \frac{3f'_c}{\sqrt{f'_c}}}}{12} \quad (5.80)$$

$$\sqrt{\left( \frac{V_u}{b_w d} \right)^2 + \left( \frac{T_u p_h}{1.7 A_{0h}^2} \right)^2} \leq \phi \left( \frac{V_c}{b_w d} + \frac{8 \sqrt{f'_c}}{12} \right) \quad (5.81)$$

$$\left( \frac{V_u}{b_w d} \right) + \left( \frac{T_u p_h}{1.7 A_{0h}^2} \right) \leq \phi \left( \frac{V_c}{b_w d} + \frac{8 \sqrt{f'_c}}{12} \right) \quad (5.82)$$

$$\begin{aligned} V_c &= \left( \lambda \sqrt{f'_c} / 20 + \frac{5 V_u d}{M_u} \right) b_w d \\ &\geq (0.17 \lambda \sqrt{f'_c}) b_w d \\ &\leq (0.4 \lambda \sqrt{f'_c}) b_w d \end{aligned} \quad (5.83)$$

and

$$\begin{aligned} V_u d_p / M_u &\leq 1.0 \\ T_n &= \frac{2 A_0 A_t f_{yt}}{s} \cot \theta \end{aligned} \quad (5.84a)$$

where  $f_{yv}$  is in MPa,  $s$  in millimeter,  $A_0$ ,  $A_t$  in  $\text{mm}^2$  and  $T_n$  in kN-m.

$$\frac{A_t}{s} = \frac{T_n}{2 A_0 f_{yt} \cot \theta} \quad (5.84b)$$

$$A_t = \frac{A_t}{s} p_h \left( \frac{f_{yt}}{f_y} \right) \cot^2 \theta \quad (5.85)$$

where  $f_{yv}$  and  $f_{yt}$  are in MPa,  $p_h$  and  $s$  in millimeters and  $A_p$ ,  $A_t$  in  $\text{mm}^2$ .

$$A_v = \frac{0.35 b_w s}{f_{yt}} \quad (5.87)$$

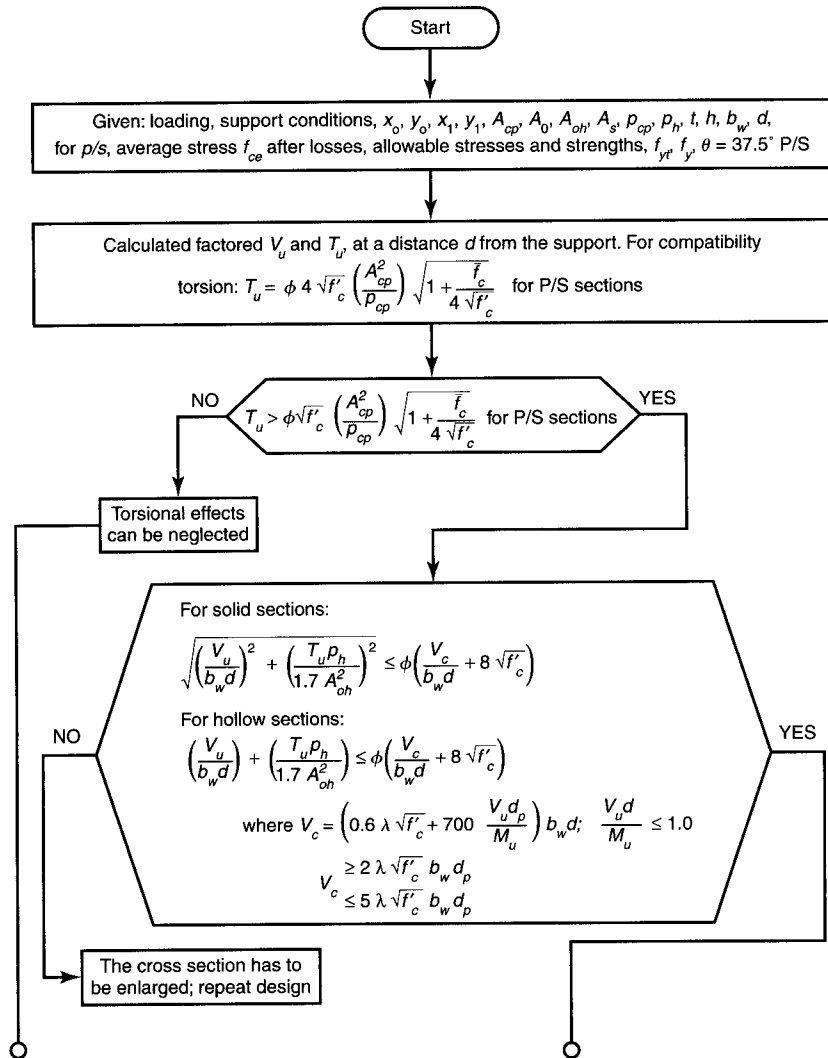
$$A_{l,\min} = \frac{5 \sqrt{f'_c} A_{cp}}{12 f_y} - \left( \frac{A_t}{s} \right) p_h \left( \frac{f_{yt}}{f_y} \right) \quad (5.88)$$

where  $A_t/s$  should not be taken less than  $0.175 b_w/f_{yt}$ . Maximum allowable spacing of transverse stirrups is the smaller of  $\frac{1}{8} P_h$  or 300 mm, and bars should have a diameter of at least  $\frac{1}{16}$  of the stirrups spacing but not less than No. 10 M bar size. Max.  $f_{yt}$  or  $f_y$  should not exceed 400 MPa. Min.  $A_{vt}$  the smaller of

$$\begin{aligned} \frac{A_{vt}}{s} &\geq \frac{0.35 b_w}{f_{yt}} \text{ or } \frac{A_{vt}}{s} = \frac{1}{16} \sqrt{f'_c} \left( \frac{b_w}{f_{yt}} \right) \text{ whichever is larger, where } b_w, d_p \text{ and } s \text{ are in millimeters} \\ &\geq \frac{A_{ps} f_{pu}}{80 f_{yt} d_p} \sqrt{\frac{d_p}{b_w}}. \text{ Use the lesser of the two sets.} \end{aligned}$$

## 5.18 DESIGN PROCEDURE FOR COMBINED TORSION AND SHEAR

The following is a summary of the recommended sequence of design steps. A flowchart describing the sequence of operations in graphical form is shown in Figure 5.49.



**Figure 5.49** Flowchart for the design reinforcement for combined shear and torsion: (a) torsional web steel, (b) shear web steel.

1. Classify whether the applied torsion is equilibrium or compatibility torsion. Determine the critical section and compute the factored torsional moment  $T_u$ . The critical section is taken at  $h/2$  from the face of the support in prestressed concrete beams. If  $T_u$  is less than  $\phi \sqrt{f'_c} (A_{cp}^2 / p_{cp}) \sqrt{1 + \bar{f}_c / 4 \sqrt{f'_c}}$  for prestressed members, torsional effects are neglected.  $f'_c$  is the compressive stress in the concrete after prestress losses at the centroid of the section resisting externally applied loads (termed as  $f_{pc}$  in the ACI Code).
2. Check whether the factored torsional moment  $T_u$  causes equilibrium or compatibility torsion. For compatibility torsion, limit the design torsional moment to the lesser of the actual moment  $T_u$  or  $T_u = \phi 4 \sqrt{f'_c} (A_{cp}^2 / p_{cp}) \sqrt{1 + \bar{f}_c / 4 \sqrt{f'_c}}$  for prestressed concrete members. The value of the design nominal strength  $T_n$  has to be at least equivalent to the factored  $T_u / \phi$ , proportioning the section such that

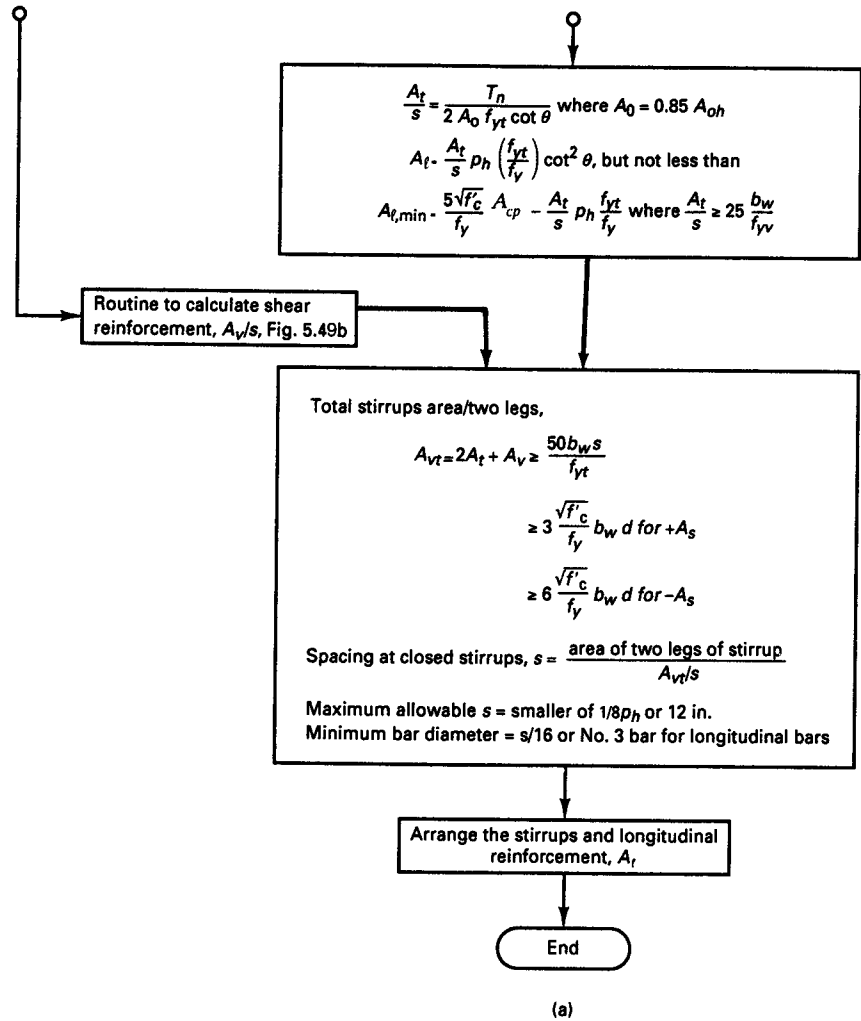


Figure 5.49 Continued

(a) for solid sections:

$$\sqrt{\left(\frac{V_u}{b_w d}\right)^2 + \left(\frac{T_u p_h}{1.7 A_{0h}^2}\right)^2} \leq \phi \left( \frac{V_c}{b_w d} + 8\sqrt{f'_c} \right)$$

(b) for hollow sections:

$$\left(\frac{V_u}{b_w d}\right) + \left(\frac{T_u p_h}{1.7 A_{0h}^2}\right) \leq \phi \left( \frac{V_c}{b_w d} + 8\sqrt{f'_c} \right)$$

If the wall thickness is less than  $A_{0h}/p_h$ , the second term should be taken as  $T_u/1.7A_{0h}t$ .

$$V_c = \left( 0.6\lambda\sqrt{f'_c} + 700 \frac{V_u d_p}{M_u} \right) b_w d_p; \quad \frac{V_u d_p}{M_u} \leq 1.0$$

$$\geq 2.0\lambda\sqrt{f'_c} b_w d_p$$

$$\leq 5.0\lambda\sqrt{f'_c} b_w d_p \quad \text{and} \quad f_{pe} \geq 0.4f_{pu}$$

Sub-routine

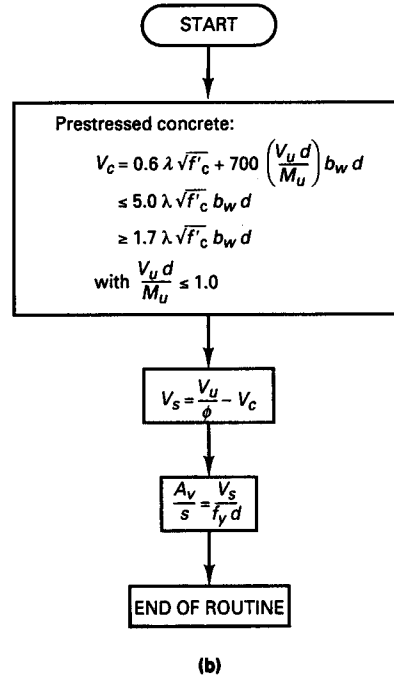


Figure 5.49 Continued

3. Select the required *torsional* closed stirrups to be used as transverse reinforcement, using a maximum yield strength of 60,000 psi, such that

$$\frac{A_t}{s} = \frac{T_n}{2A_0 f_{yv} \cot \theta}$$

Unless using  $A_0$  and  $\theta$  values obtained from analysis (Ref. 5.18) or from Equation 5.86, use  $A_0 = 0.85A_{0h}$  and  $\theta = 45^\circ$  for non-prestressed members and  $37.5^\circ$  for prestressed members with an effective prestress not less than the tensile strength of the longitudinal reinforcement. The additional longitudinal reinforcement should be

$$A_l = \left( \frac{A_t}{s} \right) p_h \left( \frac{f_{yt}}{f_y} \right) \cot^2 \theta$$

but not less than

$$A_{l,\min} = \frac{5\sqrt{f'_c} A_{cp}}{f_y} - \left( \frac{A_t}{s} \right) p_h \frac{f_{yt}}{f_y}$$

where  $A_t/s$  shall not be less than  $25b_w/f_{yt}$ .

Maximum allowable spacing of transverse stirrups in the smaller of  $\frac{1}{8}p_h$  or 12 in., and bars should have a diameter of at least  $\frac{1}{16}$  of the stirrup spacing but not less than a No. 3 bar size.

4. Calculate the required *shear* reinforcement  $A_v$  per unit spacing in a transverse section.  $V_u$  is the factored external shear force at the critical section,  $V_c$  is the nominal

shear resistance of the concrete in the web, and  $V_s$  is the shearing force to be resisted by the stirrups:

$$\frac{A_v}{s} = \frac{V_s}{f_y d}$$

where  $V_s = V_n - V_c$  and

$$V_c = \left( 0.6\lambda\sqrt{f'_c} + \frac{700V_u d}{M_u} \right) b_w d$$

$$V_c \geq 2.0\lambda\sqrt{f'_c} b_w d \leq 5.0\lambda\sqrt{f'_c} b_w d; \quad \frac{V_u d}{M_u} \leq 1.0$$

$\lambda = 1.0$  for normal-weight concrete

$= 0.85$  for sand lightweight concrete

$= 0.75$  for all lightweight concrete

The value of  $V_n$  has to be at least equal to the factored  $V_u/\phi$ .

5. Obtain the total  $A_{vt}$ , the area of closed stirrups for torsion and shear, and design the stirrups such that

$$\frac{A_{vt}}{s} = \frac{2A_t}{s} + \frac{A_v}{s}$$

$$\geq \text{the lesser of } \frac{50b_w}{f_{yt}} \quad \text{and} \quad A_v = 0.75\sqrt{f'_c} \frac{b_w s}{f_{yt}} \quad \text{or} \quad \frac{A_{ps} f_{pu}}{80f_{yt} d_p} \sqrt{\frac{d_p}{b_w}}$$

Extend the stirrups a distance  $(b_t + d_p)$  beyond the point theoretically no longer required, where  $b_t$  = width of the cross-section containing the closed stirrup resisting torsion.

## 5.19 DESIGN OF WEB REINFORCEMENT FOR COMBINED TORSION AND SHEAR IN PRESTRESSED BEAMS

### Example 5.9

A parking garage floor for medium-size cars has the prestressed concrete flooring system shown in Figure 5.50. The floor panels are 36 ft  $\times$  54 ft (11m  $\times$  16.5 m) on centers, and 54 ft (16.5m) span precast double-T's are supported by typical precast prestressed concrete spandrel L-beams spanning 36 ft (11m) on centers (Figures 5.50(a) and (b)). The spandrel beams are torsionally restrained by their connections to the supporting columns. The floor is subjected to a service superimposed dead load due to the double-T's of  $W_{SD} = 77$  psf (3,687 Pa) and a service live load of  $W_L = 60$  psf (2873 Pa). The depth of the L-beam is chosen as 6'-3" so as to provide a parapet wall for the roof on top of the double-Tee beams.

Design the spandrel beam web reinforcement to resist the combined torsion and shear to which it is subjected. Given data are the following:

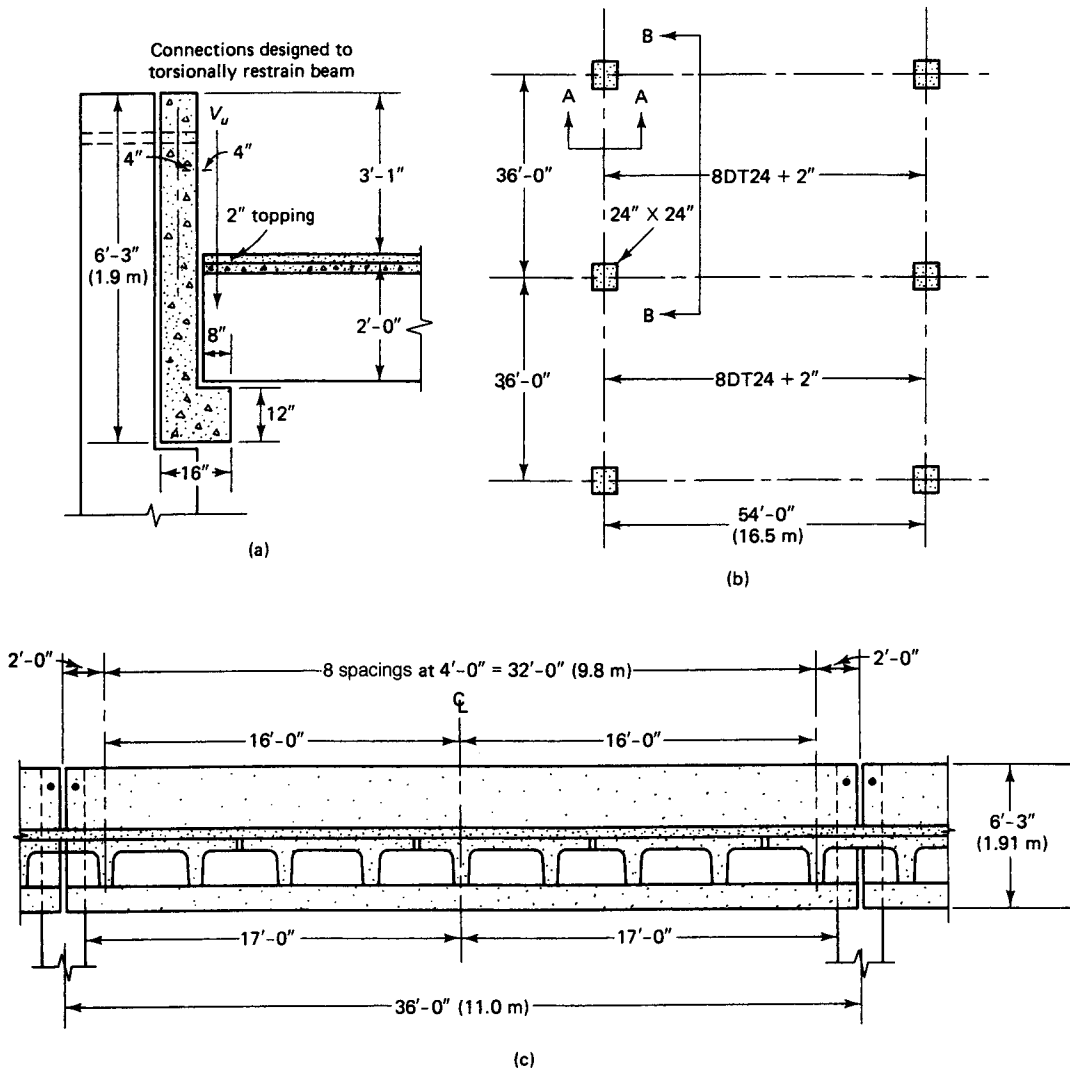
#### Beam Properties

$$A_c = 696 \text{ in.}^2 \text{ (4,491 cm}^2\text{)}$$

$$I_c = 364,520 \text{ in.}^4 \text{ (93.3} \times 10^6 \text{ cm}^4\text{)}$$

$$c_b = 33.2 \text{ in. (84.3 cm)}$$

$$c_t = 41.8 \text{ in. (106 cm)}$$



**Figure 5.50** Geometrical details of structure in Example 5.9. (a) Section A-A. (b) Partial plan. (c) Section B-B.

$$S' = 8,720 \text{ in.}^3 \text{ (142,895 cm}^3\text{)}$$

$$S_b = 10,990 \text{ in.}^3 \text{ (180,094 cm}^3\text{)}$$

$$W_D = 725 \text{ plf (10.6 kN.m)}$$

$$f'_c = 5,000 \text{ psi (34.5 MPa), normal-weight concrete}$$

$$f_y = f_{yt} = 60,000 \text{ psi (418 MPa) for stirrups}$$

#### **Prestressing**

$$A_{ps} = \text{six } \frac{1}{2} \text{ in. dia, 270 K stress-relieved strands}$$

$$f_{pu} = 270,000 \text{ psi (1,862 MPa)}$$

$$f_{ps} = 255,000 \text{ psi (1,758 MPa)}$$

$$f_{pe} = 155,000 \text{ psi (1,069 MPa)}$$



$$E_{ps} = 28 \times 10^6 \text{ psi } (193 \times 10^3 \text{ MPa})$$

$$d_p = 71.5 \text{ in. } (190 \text{ cm})$$

$$e = 71.5 - 41.8 = 29.7 \text{ in. } (75 \text{ cm}), \text{ straight tendon}$$

Disregard the effects of winds or earthquake.

**Solution:**

1. Calculate  $T_u$ ,  $V_u$ ,  $M_u$ ,  $T_{SL}$ ,  $V_{SL}$  acting on L-beam (step 1)  
 (a) Service load

$$W_D = 725 \text{ plf } (10.6 \text{ kN/m})$$

$$W_{SD} = \frac{77 \times 54}{2} \times 4 \text{ ft} = 8316 \text{ lb/stem } (37.0 \text{ kN})$$

$$W_L = \frac{60 \times 54}{2} \times 4 \text{ ft} = 6480 \text{ lb/stem } (28.0 \text{ kN})$$

$$\text{Total } P_{SL} \text{ per stem} = 8,316 + 6480 = 14,796 \text{ lb } (65.7 \text{ kN})$$

- (b) Factored loads

$$W_{Du} = 1.2 \times 725 = 870 \text{ plf } (12.7 \text{ kN/m})$$

$$W_{SDu} = 1.2 \times 8,316 = 9979 \text{ lb/stem } (44.4 \text{ kN/m})$$

$$W_{Lu} = 1.6 \times 6480 = 10,368 \text{ lb/stem } (46.1 \text{ kN})$$

$$\text{Total } P_u \text{ per stem} = 9979 + 10,368 = 20,347 \text{ lb } (90.5 \text{ kN})$$

$$T_u \text{ at face of support} = \frac{1}{2} P_u \times \text{arm} \times \text{no. of stems}$$

$$= \frac{20,347}{2} \times \frac{8}{12} \times 9 = 61,041 \text{ ft-lb } (82.8 \text{ kN-m})$$

$$T_{SL} \text{ at face of support} = \frac{14,796}{20,347} \times 61,041 = 44,388 \text{ ft-lb } (60.2 \text{ kN-m})$$

$$V_u \text{ at face of support} = \frac{1}{2} (P_u \times \text{no. of stems} + \text{factored } W_D \times \text{span})$$

$$= \frac{1}{2} (20,347 \times 9 + 870 \times 34) = 106,352 \text{ lb } (474 \text{ kN})$$

$$V_{SL} \text{ at face of support} = \frac{1}{2} (14,796 \times 9 + 725 \times 34) = 78,907 \text{ lb } (351 \text{ kN})$$

$$M_u \text{ at face of support} = 0$$

Similarly, calculate the values of  $T_u$ ,  $V_u$ , and  $M_u$ , and the corresponding service-load values at each transverse stem contact point along the span of the L-beam, and construct the torsion, shear, and moment diagrams as shown in Figure 5.51.

$$A_{ps} = 6 \times 0.153 = 0.918 \text{ in.}^2$$

$$P_e = A_{ps} f_{pe} = 0.918 \times 155,000 = 142,290 \text{ lb } (633 \text{ kN})$$

2. L-Beam torsional geometrical details (Step 1)

$$A_{cp} = \text{area enclosed by outside perimeter of concrete cross section} = 8 \times 75 = 600 \text{ in.}^2$$

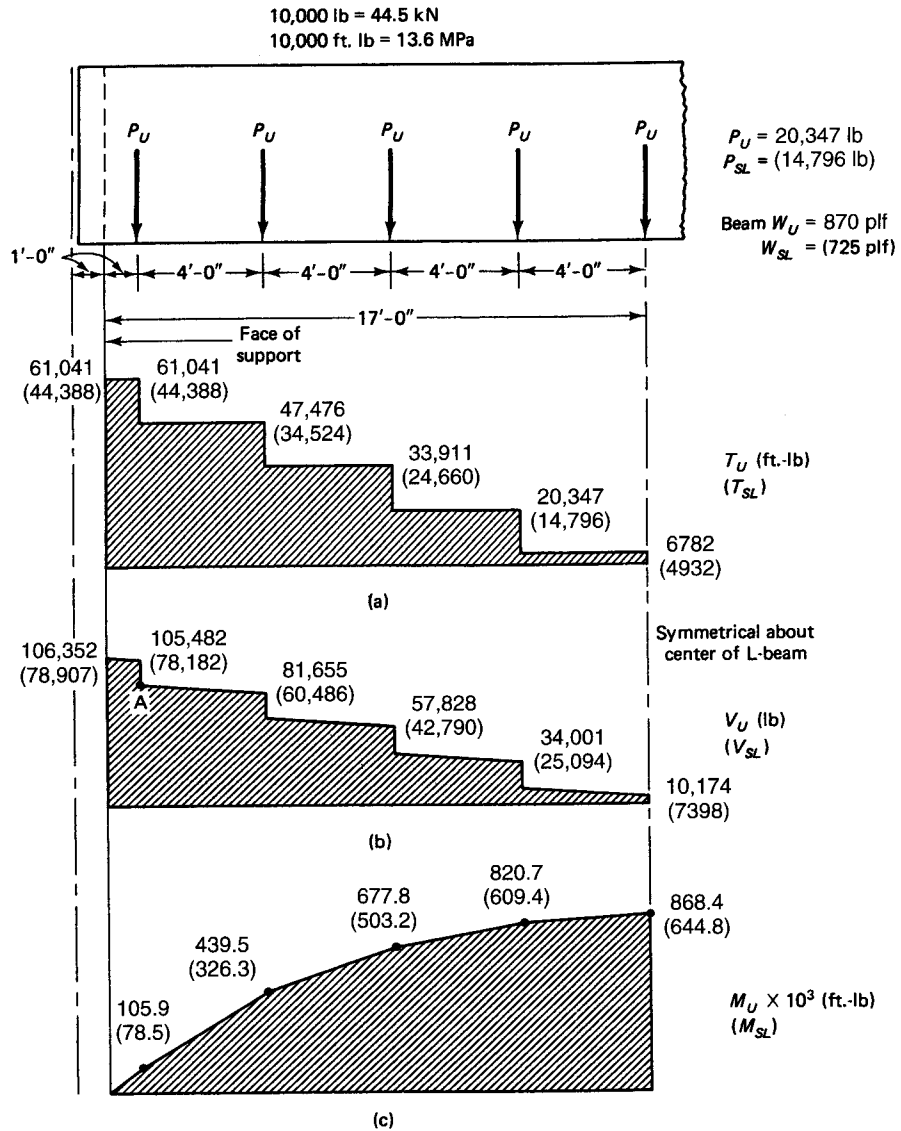
$$(3871 \text{ cm}^2)$$

$$p_{cp} = \text{outside perimeter of concrete cross section} = 2(8 + 75) = 166 \text{ in. } (422 \text{ cm})$$

$$x_1 = \text{smaller dimension to center of tie}$$

$$= 8 - 2(1.5 + 0.25) = 4.5 \text{ in. } (11.4 \text{ cm})$$

$$y_1 = 75 - 2(1.5 + 0.25) = 71.5 \text{ in. } (181.6 \text{ cm})$$



**Figure 5.51** Force and moment diagrams for beams in Example 5.9. (a) Torsional moment. (b) Shear. (c) Flexural moment. Bracketed values are for service-load level.

$$h = \text{total depth} = 75 \text{ in. (191 cm)}$$

$$b_w = \text{web width} = 8 \text{ in. (20.3 cm)}$$

$$p_h = \text{perimeter of center line of outermost closed transverse torsional reinforcement} \\ = 2(x_1 + y_1) = 2(4.5 + 71.5) = 152 \text{ in.}$$

$$d_p = \text{effective depth} = 75 - (1.5 + 0.5 + 0.5 + 1.0) = 71.5 \text{ in. (182 cm)}$$

$$A_{oh} = \text{area enclosed by centerline of the outermost closed transverse torsional ties} \\ = (x_1)(y_1) = 4.5 \times 71.5 = 322 \text{ in.}^2 \text{ (2077 cm}^2\text{)}$$

$$A_0 = \text{gross area enclosed by shear flow path} \\ = 0.85A_{oh} = 0.85 \times 322 = 274 \text{ in.}^2 \text{ (1766 cm}^2\text{)}$$

$\theta$  = angle of compression diagonals in truss analogy for torsion  $\cong 37.5^\circ$  for pre-stressed beams.

$$\cot \theta = 1.3$$

### 3. Cracking moment capacity (Step 1)

$$f_d = \text{unfactored dead load stress}$$

From Figure 5.51 and  $w_D = 725 \text{ lb/ft}$

$$f_d = \frac{M_D}{S_b} = \frac{725(36)^2}{8} \times 12 \times \frac{1}{10,990} = 128 \text{ psi (0.9 MPa)}$$

At the extreme fibers of the section,

$$\begin{aligned} f_{ce} &= -\left(\frac{P_e}{A_c} + \frac{P_e e}{S_b}\right) = -\left(\frac{142,290}{696} + \frac{142,290 \times 29.7}{10,990}\right) \\ &= -(204.4 + 384.5) = 588.9 \text{ psi say } 589 \text{ psi (C) (4.1 MPa)} \end{aligned}$$

At the centroid of the section,  $\bar{f}_c = -204.4 \text{ psi}$

$$\begin{aligned} M_{cr} &= S_b(6\lambda\sqrt{f'_c} + f_{ce} - f_d) \\ &= 10,990(6 \times 1.0\sqrt{5000} + 589 - 128) \\ &= 9.73 \times 10^6 \text{ in.-lb (1,100 kN-m)} \end{aligned}$$

$$1.2M_{cr} = 1.2 \times 9.73 \times 10^6 = 11.7 \times 10^6 \text{ in.-lb}$$

$$a = \frac{A_{ps} f_{ps}}{0.85 f'_c b} = \frac{0.918 \times 255,000}{0.85 \times 5000 \times 8} = 6.9 \text{ in. (175 mm)}$$

$$\begin{aligned} M_n &= A_{ps} f_{ps} \left(d_p - \frac{a}{2}\right) = 0.918 \times 255,000 \times \left(71.5 - \frac{6.9}{2}\right) \\ &= 15,930,000 = 15.9 \times 10^6 \text{ in.-lb (1800 kN-m)} \\ &> 1.2M_{cr} = 11.7 \times 10^6 \text{ in.-lb} \end{aligned}$$

hence, minimum flexural reinforcement is satisfied for flexure.

### 4. Verify whether torsional reinforcement is needed (Step 2)

From Equation 5.80,

$$\begin{aligned} \text{Min. for disregarding torsion } T_u &\leq \phi \sqrt{f'_c} \left(\frac{A_{cp}^2}{p_{cp}}\right) \sqrt{1 + \frac{f_c}{4\sqrt{f'_c}}} \\ &= 0.75 \sqrt{5000} \left(\frac{600^2}{166}\right) \sqrt{1 + \frac{204.4}{4\sqrt{5000}}} \\ &= 150,953 \text{ in.-lb (17.0 kN-m)} \end{aligned}$$

Considering section at  $h/2$  from support face in Figure 5.51, namely at 3 ft from the face of the support,

$$\begin{aligned} \text{Rqd. } T_u &= \frac{1}{2} (61,041 + 47,476) \times 12 \\ &= 651,102 \text{ in.-lb (73 kN-m)} > 150,953 \text{ in.-lb} \end{aligned}$$

The average value was used instead of 47,476 ft.-lb as a conservative value of the torsional moment.

Hence, torsion has to be considered and appropriate torsional reinforcement provided. The garage elements are all precast. Thus, assume equilibrium torsion con-

dition and no redistribution of moment, using the total applied factored  $T_u = 651,102$  in.-lb (Equation 5.79 is therefore inapplicable).

5. Check adequacy of section for torsion

- (a) Determine  $V_c$  as the smaller value obtained for  $V_{ci}$  from Equation 5.11 and  $V_{cw}$  from Equation 5.15.

From Fig. 5.51 for section at  $h/2 = 3$  ft from face of support,

$$\text{Rqd. } V_u = \frac{1}{2}(105,482 + 81,655) = 93,569 \text{ lb (417 kN)}$$

$$\begin{aligned} \text{Rqd. } M_u &= \frac{1}{2}(105.9 + 439.5)12 \times 1000 \text{ in.-lb} \\ &= 3,272,400 \text{ in.-lb (370 kN-m)} \end{aligned}$$

$$V_{ci} = \left[ 0.6\lambda\sqrt{f'_c}b_wd_p + V_d + V_i \frac{M_{cr}}{M_{\max}} \right]$$

$$\geq 1.7\sqrt{f'_c}b_wd_p$$

$$\leq 5.0\sqrt{f'_c}b_wd_p$$

$V_d$  = shear at section due to unfactored dead load

$$V_d \text{ at face of support} = \frac{1}{2}(8316 \times 9 + 725 \times 34) = 49,747 \text{ lb}$$

$$V_d \text{ at point A in Figure 5.51} = 49,747 - 725 \times 1 \text{ ft} - 8316 = 40,706 \text{ lb}$$

$$V_d \text{ at 5 ft. from support} = 40,706 - 725 \times 5 - 8316 = 28,765 \text{ lb}$$

At the required section at  $h/2$  from face of support,

$$V_d = \frac{1}{2}(40,706 + 28,765) = 34,736 \text{ lb (154.5 kN)}$$

$V_i$  = factored shear force at section due to externally applied loads occurring simultaneously with  $M_{\max}$

$$= \frac{20,347 \text{ per stem}}{20,347 + 870 \times 4 \text{ per stem}} \times 93,569$$

$$= 79,902 \text{ lb}$$

$M_{\max}$  = maximum factored moment at section due to externally applied load, namely due to live load and superimposed dead load

Factored  $M_u$  at point A in Figure 5.51 due to the live load and

$$SDL = \frac{1}{2}(20,347 \times 9) = 91,562 \text{ ft-lb}$$

Factored  $M_u$  at 5 ft from face

$$= \frac{1}{2}(20,347 \times 9)5 - 20,347 \times 4 = 376,420 \text{ ft-lb}$$

Hence

$M_{\max}$  at  $h/2 = 3$  ft from face of support

$$= \frac{1}{2}(91,562 + 376,420)12 = 2.81 \times 10^6 \text{ in.-lb}$$

$M_{cr} = 9.73 \times 10^6 \text{ in.-lb}$  from before

hence,

$$\begin{aligned} V_{ci} &= \left[ 0.6 \times 1.0\sqrt{5000} \times 8 \times 71.5 + 34,738 + 79,902 \frac{9.73 \times 10^6}{2.81 \times 10^6} \right] \\ &= 24,268 + 34,738 + 276,671 = 335,677 \text{ lb} \end{aligned}$$

$$v_{ci} = \frac{335,667}{8 \times 71.5} = 587 \text{ psi (3.46 MPa)}$$

$$1.7\lambda\sqrt{f'_c} = 1.7\sqrt{5000} = 120 \text{ psi} < 587 \text{ psi}$$

$$5\lambda\sqrt{f'_c} = 5.0\sqrt{5000} = 354 \text{ psi} < 587 \text{ psi}$$

Use  $v_{ci} = 354 \text{ psi (2.4 MPa)}$

From Equation 5.15,

$$V_{cw} = (3.5\sqrt{f'_c} + 0.3\bar{f}_c)b_wd + V_p$$

$V_p = 0$  since tendons are straight, hence

$$V_{cw} = 3.5\sqrt{5000} + 0.3\left(\frac{142,290}{696}\right) = 310 \text{ psi} < v_{ci} = 354 \text{ psi (controls)}$$

Use  $v_c = 310 \text{ psi}$  in this solution

$$V_c = v_cb_wd = 310 \times 8 \times 71.5 = 177,320 \text{ lb (788 kN)}$$

**(b) Alternate method for evaluating  $V_c$**

If  $f_{pe} > 0.4f_{pu}$ , the ACI allows using a more conservative expression as in Equation 5.16

$$V_c = \left(0.6\lambda\sqrt{f'_c} + 700\frac{V_u d_p}{M_u}\right)b_wd_p$$

$$\geq 2\lambda\sqrt{f'_c}b_wd$$

$$\leq 5\lambda\sqrt{f'_c}b_wd$$

$$\frac{V_u d_p}{M_u} = \frac{93,569 \times 71.5}{3,272,400} = 2.04 > 1.0,$$

$$\text{use } \frac{V_u d}{M_u} = 1.0$$

$$v_c = \frac{V_c}{b_wd} = (0.6 \times 1.0\sqrt{5000} + 700 \times 1.0) = 742 \text{ psi (5.1 MPa)}$$

$$> 5\sqrt{f'_c} = 354 \text{ psi}$$

$$v_c = 354 \text{ psi (2.4 MPa)}$$

**(c) Check section adequacy**

$v_c$  in solution (a) will be used in this check = 310 psi (2.1 MPa). From Equation 5.81 for solid sections,

$$\sqrt{\left(\frac{V_u}{b_wd}\right)^2 + \left(\frac{T_u p_h}{1.7A_{oh}^2}\right)^2} = \sqrt{\left(\frac{93,569}{8 \times 71.5}\right)^2 + \left(\frac{651,102 \times 152}{1.77 \times (322)^2}\right)^2}$$

$$\sqrt{26,759 + 290,814} = 564 \text{ psi (3.9 MPa)}$$

$$\phi\left(\frac{V_c}{b_wd} + 8\sqrt{f'_c}\right) = 0.75(310 + 8\sqrt{5000})$$

$$= 656 \text{ psi (4.5 MPa) available}$$

$$> 564 \text{ psi (3.8 MPa) actual,}$$

hence section is adequate.

**6. Torsional reinforcement (Step 3)**

$$T_n = T_u/\phi = 651,102/0.75 = 868,137 \text{ in.-lb (96 kN-m)}$$

From Equation 5.38b,

$$\begin{aligned}\frac{A_t}{s} &= \frac{T_n}{2A_0f_{yt} \cot \theta} = \frac{868,137}{2 \times 274 \times 60,000 \times 1.3} \\ &= 0.0203 \text{ in.}^2/\text{in.}/\text{one leg} \text{ (} 0.046 \text{ cm}^2/\text{cm}/\text{one leg})\end{aligned}$$

Using the PCI method in which  $\cot \theta$  is computed,

$$\cot \theta = \frac{T_u/\phi}{1.7A_{0h}(A_t/s)f_{yt}} = \frac{868,137}{1.7(322)(0.0203) \times 60,000} = 1.30$$

by assuming a value of  $s$ , finding  $(A_t/s)$  for the tie size chosen and entering the value of  $(A_t/s)$  into the expression.

#### 7. Shear reinforcement (Step 4)

$$V_c = 310 \times 8 \times 71.5 = 177,320 \text{ lb (788 kN)}$$

$$V_n = \frac{V_u}{\phi} = \frac{93,569}{0.75} = 124,757 \text{ lb (555 kN)}$$

$$V_s = (V_n - V_c); \quad \text{but } V_n < V_c$$

Use minimum shear web reinforcement.

$$\begin{aligned}\frac{A_v}{s} &= \frac{50b_w}{f_{yt}} = \frac{50 \times 8}{60,000} \\ &= 0.0067 \text{ in.}^2/\text{in.}/\text{two legs} \text{ (} 0.017 \text{ cm}^2/\text{cm}/\text{two legs}) \\ \frac{A_{vt}}{s} &= 2 \left( \frac{A_t}{s} \right) + \frac{A_v}{s} = 2 \times 0.0203 + 0.0067 \\ &= 0.0473 \text{ in.}^2/\text{in.}/\text{two legs} \text{ (} 0.110 \text{ cm}^2/\text{cm}/\text{two legs})\end{aligned}$$

Assuming No. 4 closed ties (12.7 mm diameter),  $A_v = 2 \times 0.20 = 0.40 \text{ in.}^2$

$$s = \frac{\text{cross-sectional tie area}}{A_{vt}/s} = \frac{0.40}{0.0473} = 8.5 \text{ in.}$$

Maximum allowable spacing  $s_{\max} = p_h/8$  or 12 in. = 152/8 = 19 in. or 12 in.

$$\text{Min. } \frac{A_v}{s} = \text{lesser of } \frac{50b_w}{f_{yt}} \quad \text{or} \quad \frac{A_{ps}f_{pu}}{80f_{yt}d} \sqrt{\frac{d}{b_w}}$$

$$0.75\sqrt{f'_c} = 0.75\sqrt{5000} = 53$$

$$\begin{aligned}\frac{A_v}{s} &= \frac{53b_w}{f_{yt}} = \frac{53 \times 8}{60,000} \\ &= 0.0071 \text{ in.}^2/\text{in.}/\text{two legs} \text{ (} 0.017 \text{ cm}^2/\text{cm}/\text{two legs})\end{aligned}$$

$$\begin{aligned}\frac{A_v}{s} &= \frac{A_{ps}f_{pu}}{80f_{yt}d} \sqrt{\frac{d}{b_w}} = \frac{0.918 \times 270,000}{80 \times 60,000 \times 71.5} \sqrt{\frac{71.5}{8}} \\ &= 0.0022 \text{ in.}^2/\text{in.}/\text{two legs} \text{ (} 0.006 \text{ cm}^2/\text{cm}/\text{two legs}), \text{ controls.}\end{aligned}$$

Available  $\frac{A_v}{s} = 0.0473 > 0.0022$ , O.K.

Minimum bar diameter =  $s/16$  or No. 3 bar =  $8.5/16 = 0.53 \text{ in.} > 0.5 \text{ in.}$  for No. 4 bar, use No. 5 closed stirrups.  $A_v = 0.31 \times 2 = 0.62 \text{ in.}^2$

$$s = \frac{0.62}{0.0473} = 13.1 \text{ in.} > 12 \text{ in.}$$

Another alternative for the transverse reinforcement is to use No. 4 bars but reduce the computed spacing of 8.5 in. to  $8.5 \times (0.50/0.53) \approx 8.0 \text{ in.}$  This gives No. 4 closed stir-

rups spaced at 8 in. center to center instead of No. 5 at 12 in. center to center. Using No. 4 closed stirrups at 8 in. center to center is more preferable as it is easier to bend them than the No. 5 bars. Therefore, for this design, use closed No. 4 stirrups (12.7 mm diameter) at 8 in. center to center for transverse shear + torsion web reinforcement.

8. *Longitudinal reinforcement (Steps 5–6)*

From Equation 5.85,

$$\begin{aligned} A_t &= \frac{A_t}{s} p_h \left( \frac{f_{yt}}{f_y} \right) \cot^2 \theta \\ &= 0.0203 \times 152 \left( \frac{60,000}{60,000} \right) (1.3)^2 = 5.21 \text{ in.}^2 \text{ (30 cm}^2\text{)} \end{aligned}$$

From Equation 5.88,

$$\begin{aligned} A_{t,\min} &= \frac{5\sqrt{f'_c} A_{cp}}{f_y} - \left( \frac{A_t}{s} \right) p_h \frac{f_{yt}}{f_y} \\ &= \frac{5\sqrt{5000} \times 600}{60,000} - 0.0203 \times 152 \times \frac{60,000}{60,000} \\ &= 0.50 \text{ in.}^2 \text{ (5.2 cm}^2\text{); } A_t = 5.21 \text{ in.}^2 \text{ controls} \end{aligned}$$

Using No. 4 longitudinal bars = 0.20 in.<sup>2</sup>

$$\text{No. of bars} = \frac{5.21}{0.20} = 26.05 \text{ bars}$$

Use 12 No. 4 bars on each face equally spaced (12 bars 12.7 mm diameter/face) and add another 4 bars for reinforcing the ledge to give a total of 28 No. 4 bars. Note that maximum allowable spacing = 12 in. In this case  $s \approx 6.5$  in. c. to c., O.K. Adopt the design. Details of reinforcement and cross-sectional geometry of the L-beam are given in Fig. 5.52.

For the reinforcing details to be complete, a design of the ledge and hanger reinforcement would be required, as well as details of the anchorage of the longitudinal reinforcement at the supports. Chapter 10 on the design of connections provides these details.

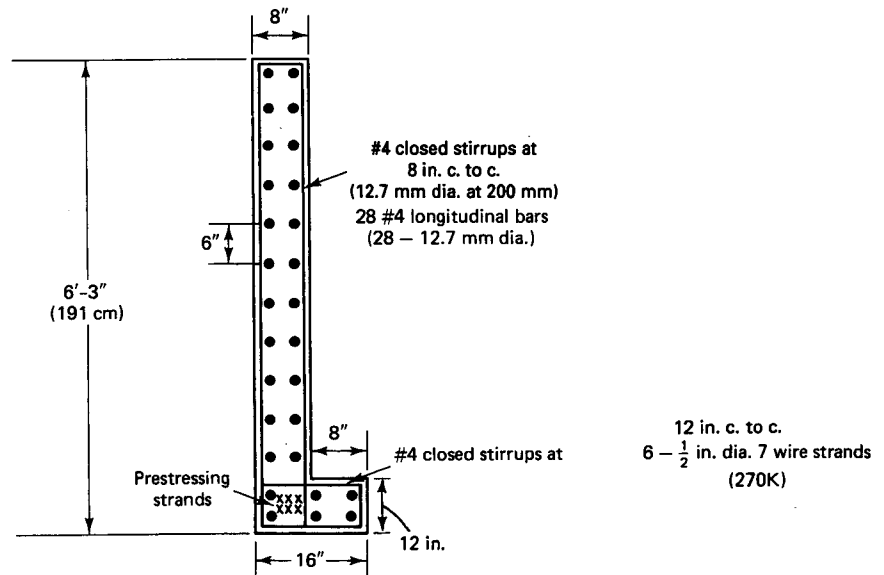


Figure 5.52 Reinforcement details of beam in Example 5.9.

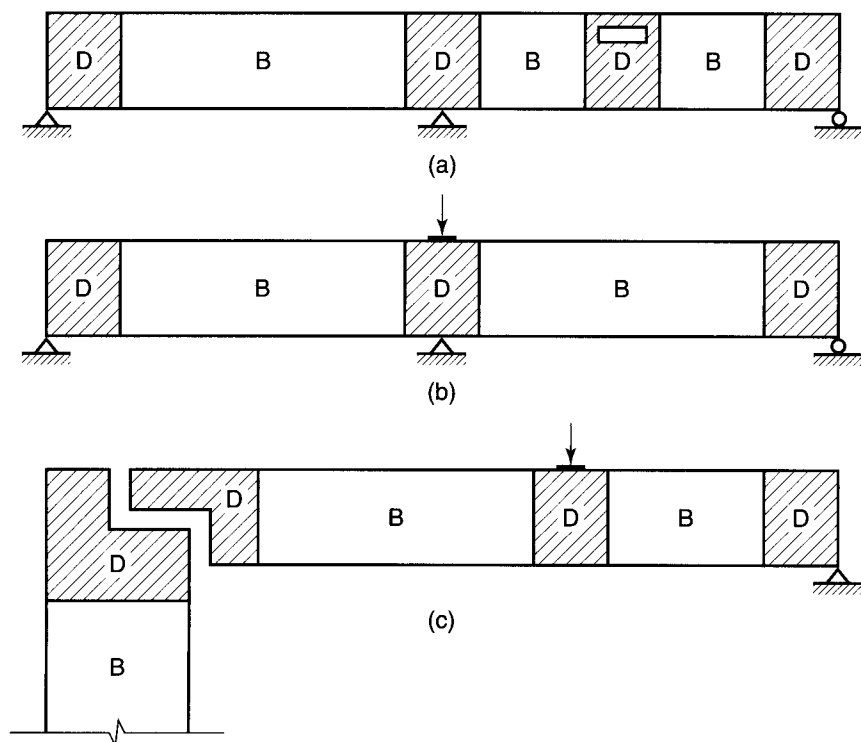
## 5.20 STRUT-AND-TIE MODEL ANALYSIS AND DESIGN OF CONCRETE ELEMENTS

### 5.20.1 Introduction

As an alternative to the usual approach for plane sections before bending remaining plane after bending, the strut-and-tie model is applied effectively in regions of discontinuity. These regions could be the support sections in a beam, the zones of load application, the discontinuity caused by abrupt changes in a section, such as brackets, beam daps, pile caps cast with column sections, portal frames, and others. Consequently, structural elements can be divided into segments called *B-regions*, where the standard beam theory applies, with the assumption of linear strains, and the others as *D-regions*, where the plane sections hypothesis is no longer applicable. Figure 5.53 (adapted from Ref. 5.1) demonstrates the locations of B and D regions.

The analysis essentially follows the truss analogy approach, where parallel *inclined* cracks are assumed and expected to form in the regions of high shear. The concrete between the *inclined* cracks carries inclined compressive forces such as in Fig. 5.11(a) and (b), acting as diagonal struts. Thus, provision of transverse stirrups along the beam span, as in Fig. (5.11c), results in truss-like action in which the longitudinal steel provides the tension chord of the truss as a tie, hence the “strut-and-tie” expression.

Strut-and-tie modeling has been introduced in some codes including ACI 318-08 Appendix A. Simplifying assumptions in design have to be made when applying this approach to different structural systems. These simplifications are necessitated because of the wide range of alternatives in the selection of the path of forces, which represent the compressive struts and the tension ties intersecting at the “nodal” points, and the choice of locations where the corresponding reinforcement is to be placed.



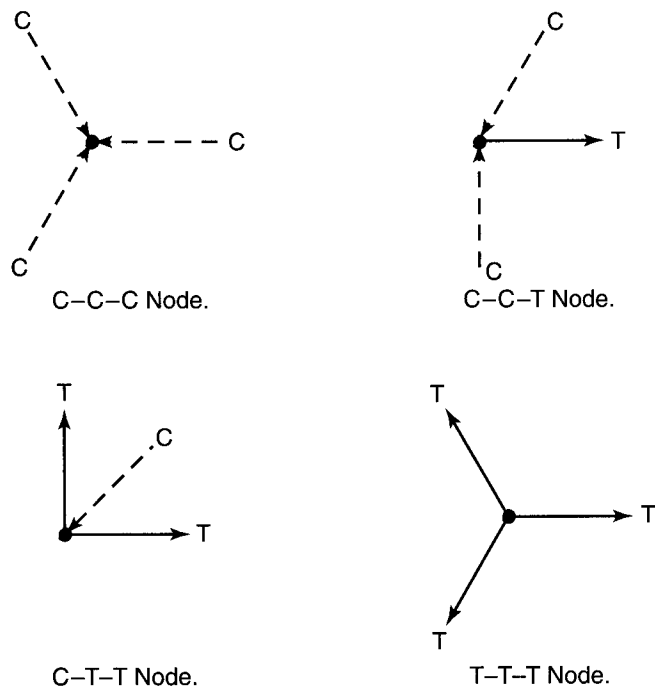
**Figure 5.53** B-regions and D-regions in beams: (a) continuous beam; (b) beam with concentrated load; (c) dapper-ended beam on column support.



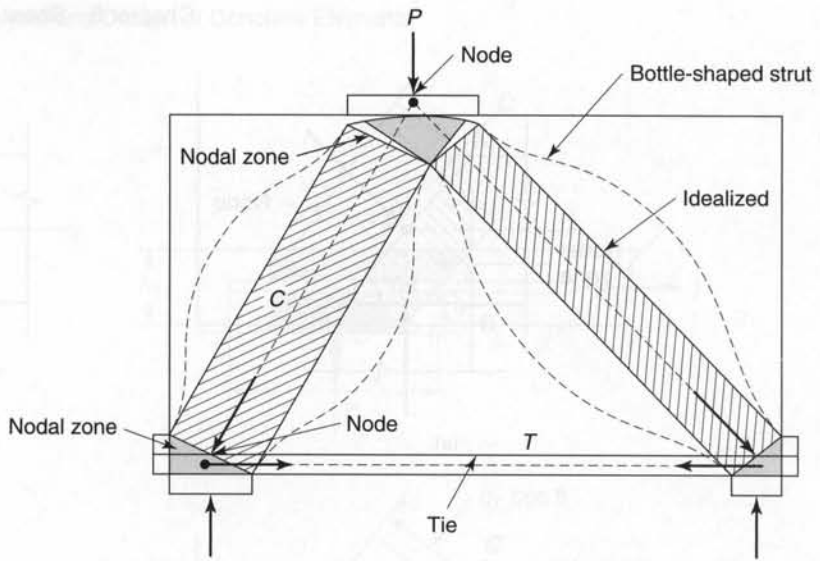
Therefore, depending on the interpretation of the designer, simplifications of the paths of forces that are chosen to represent the real structure can considerably differ. Since this load-path modeling method is a plastic method with stress concentration conditions and load concentration, it does not provide a check for the serviceability levels inherent in the semi-plastic methods, but represents strength-limit states at the critical sections. Thus, after excessive deformation and cracking, the idealizations made in the choice of the force paths render this method less accurate for design purposes, particularly because no unique design solutions are possible. This approach is *more an art than an engineering science* in the selection of the models. Significant overdesign is, therefore, required and extensive full-scale tests needed for different structural systems. Such extensive tests were conducted in the case of anchor blocks in post-tensioned beams, as discussed by the author in Section 4.5.3.3. It should be thus emphasized that this approach is a design method that enables analyzing *non-flexural regions*, particularly as affected by shear and torsion, with infinite possible configurations for identifying load paths in structural systems (Ref. 6.21 and Ref. 6.27) and that it does not provide a check on serviceability, as it principally deals with high-overload conditions and with load-carrying capacity.

### 5.20.2 Strut-and-Tie Mechanism

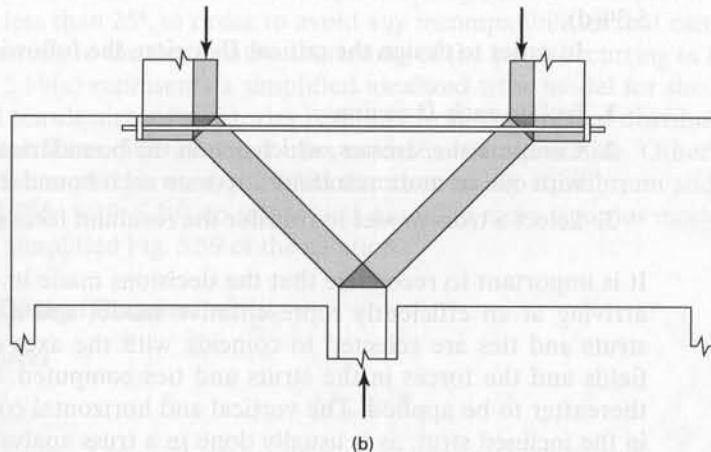
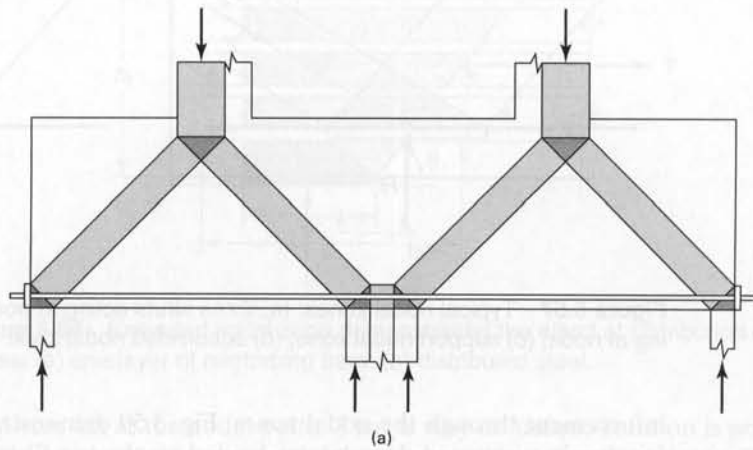
For equilibrium, at least three forces have to act at a joint, termed as the *node*, as in Figure 5.54, where  $C$  = compression vector and  $T$  = tension vector. The nodes are classified in accordance with the sense of the forces intersecting at the nodal point. As an example, a  $C-C-T$  node resists one tensile force and two compressive forces. A typical representation of the strut-and-tie model of a simply supported deep beam is shown in Figure 5.55, and for a continuous beam in Fig. 5.56. A  $C-C-T$  nodal zone can be represented as a hydrostatic nodal zone if the tie is assumed to extend through the node and anchored by a plate on the far end of the node (Ref. 5.1, Appendix A). Typical nodal zones are shown in Figs. 5.57 and 5.58 (Ref. 5.1), including the possible distribution of the steel re-



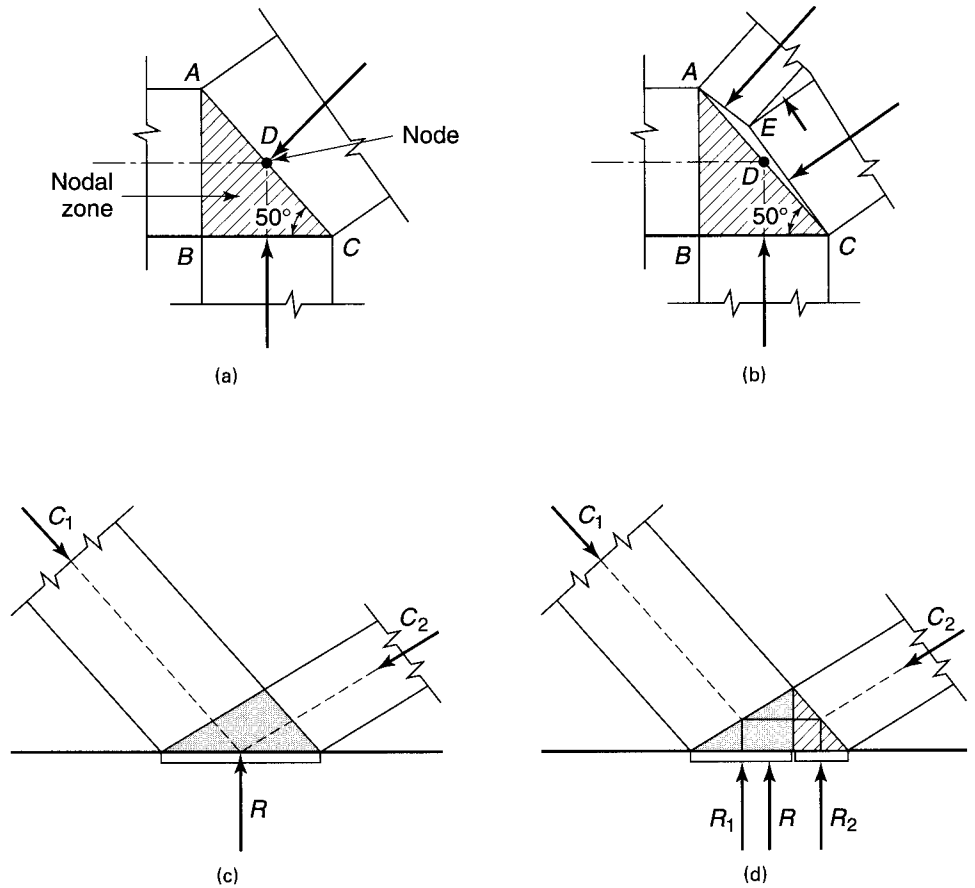
**Figure 5.54** Classifications of strut-and-tie nodes.



**Figure 5.55** Strut-and-tie model of a simply supported deep beam subjected to concentrated load on top.



**Figure 5.56** Typical strut-and-tie model for continuous beams subjected to concentrated loads on top: (a) positive moment truss; (b) negative moment truss.



**Figure 5.57** Typical nodal zones: (a) three struts acting at node; (b) two struts AE and CE acting at node; (c) support nodal zone; (d) subdivided nodal zone.

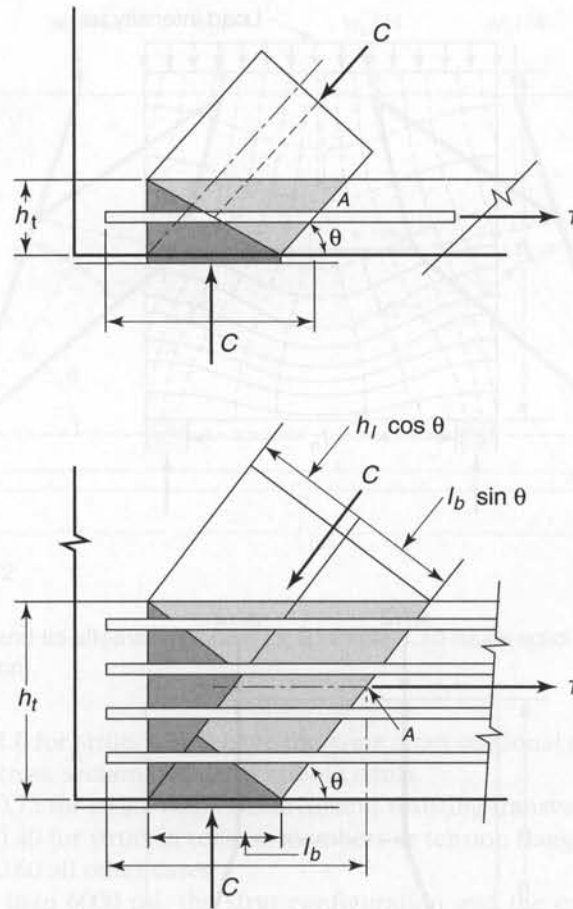
inforcement through the nodal zones. Fig. 5.59 demonstrates the simplified truss model for simply supported deep beams loaded on the top fibers. Note that nodes A and B at the beam support are compressive nodes as seen by the crushing of the concrete in Fig. 5.39(d).

In order to design the critical  $D$ -region, the following steps need to be taken:

1. Isolate each  $D$ -region
2. Compute the stresses, which act on the boundaries of the  $D$ -region, replacing them with one or more resultant forces on each boundary.
3. Select a truss model to transfer the resultant forces *across* the  $D$ -region.

It is important to recognize that the decisions made in steps 2 and 3 are very critical in arriving at an efficiently representative model and a safe structure. The axes of the struts and ties are selected to coincide with the axes of the compression and tension fields and the forces in the struts and ties computed. Serviceability limit checks have thereafter to be applied. The vertical and horizontal components equilibrate the forces in the inclined strut, as is usually done in a truss analysis (see Fig. 5.59) of the forces in the nodal zones.

If more than three forces act at a nodal point as shown in Fig. 5.57 (b), it becomes necessary to exercise engineering judgment in resolving the system of forces such that



**Figure 5.58** Extended nodal zone demonstrating the effect of distribution of forces: (a) one layer of reinforcing bars; (b) distributed steel.

only three forces act at the nodal point. That is why no unique solution is possible, as assumptions based on significant idealizations can widely differ (Ref. 5.22). The angle between the axes of struts and ties that intersect through the node should not be too small, namely, not less than  $25^\circ$ , in order to avoid any incompatibilities that can result because of the lengthening of the ties and the shortening of the struts occurring in the same direction. Figure 5.59(c) represents a simplified idealized truss model for the principal compressive and tensile stress trajectories resulting from the applied distributed load at the top deep beam fibers. The assumed truss model is one alternative. Other possible alternative models can also be used, provided that they satisfy equilibrium and compatibility. Figure 5.60 (Refs. 5.19, 5.20), to follow, is a modified more rigorous model for Example 6.7, than the simplified Fig. 5.59 of the solution.

### 5.20.3 ACI Design Requirements

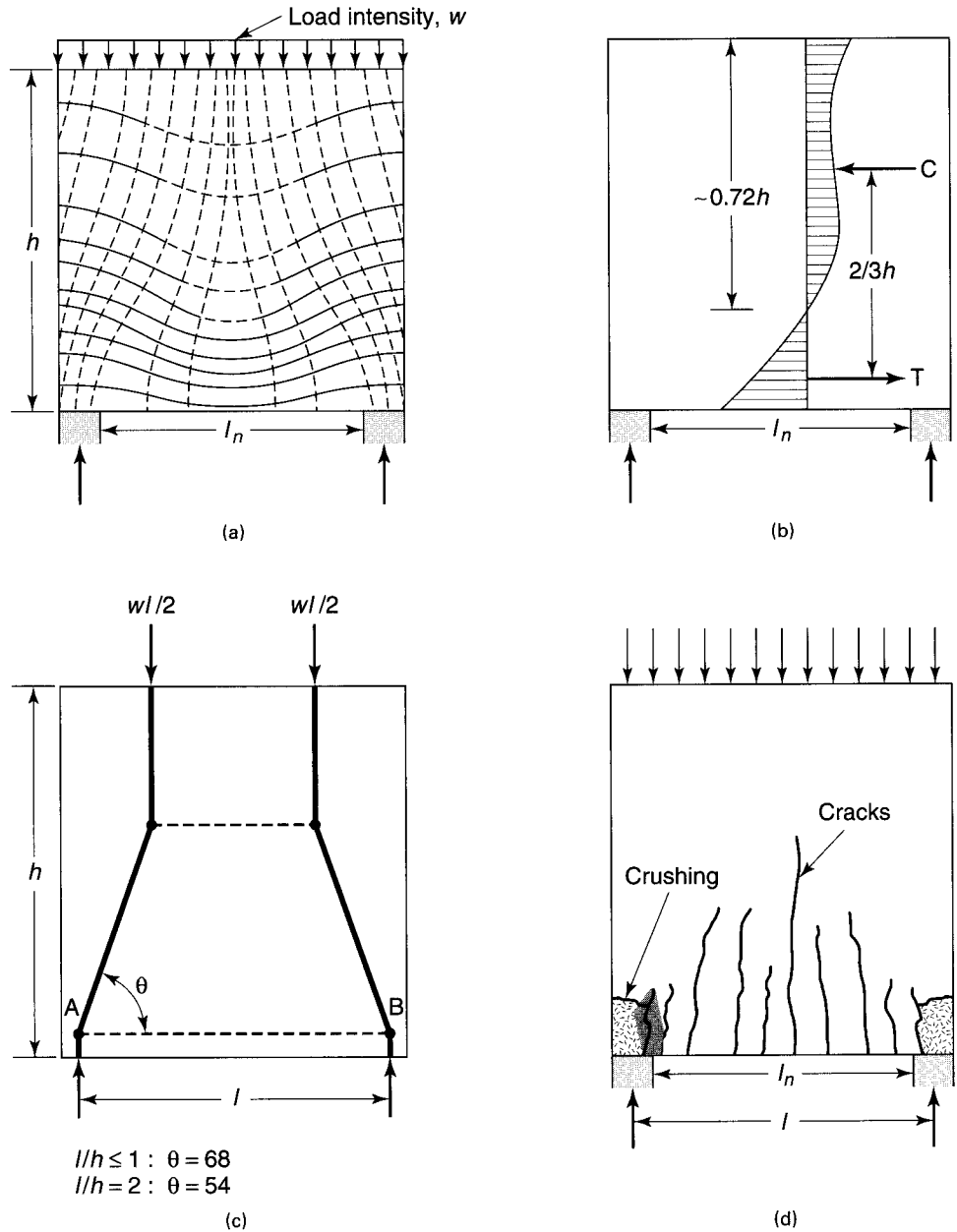
#### (1) Nodal Forces

$$\phi F_{ns} \geq F_{us} \quad (5.88)$$

where,  $F_{ns}$  = nominal strength of a strut, tie, or nodal zone, lb.

$F_{us}$  = factored force acting on a strut, tie, bearing area, or nodal zone, lb.

where  $\phi = 0.75$  for both struts and ties (similar to the strength reduction for shear)



**Figure 5.59** Truss model and stress distribution in simply supported deep beams: (a) lines of principal stress trajectories for beams loaded on top; (b) elastic stress distribution across beam depth; (c) idealized truss model (adapted from Refs. 5.19, 5.20); (d) cracking pattern.

(2) Strength of Struts

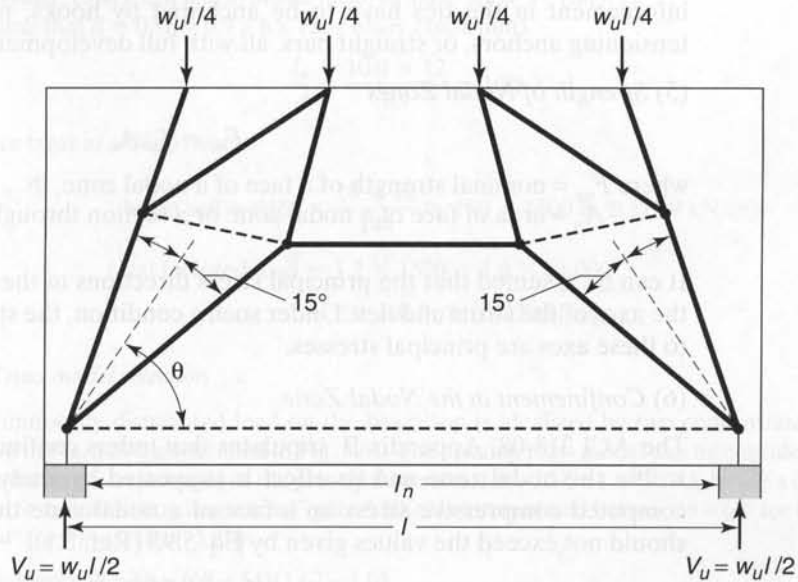
$$F_{ns} = f_{ce} A_c \tag{5.89}$$

where  $F_{ns}$  = nominal strength of strut,  $lb$

$A_c$  = effective cross-sectional area at one end of a strut, taken perpendicular to the axis of the strut,  $in.^2$

$f_{ce}$  = effective compressive strength of the concrete in a strut or nodal zone,  $psi$

$$f_{ce} = 0.85 \beta_s f'_c \tag{5.90}$$



**Figure 5.60** Strut-and-tie alternative model for Example 5.10 (truss solid lines = compression; dashed lines = tension).

where

- $\beta_s = 1.0$  for struts which have the same cross-sectional area of the midstrut cross-section in case of bubble struts.
- $= 0.75$  for struts with reinforcement resisting transverse tensile forces
- $= 0.40$  for struts in tension members or tension flanges
- $= 0.60$  all other cases

For  $f'_c$  not greater than 6000 psi, the strut configuration and the compressive forces in the strut can be satisfied if  $\sum \frac{A_{si}}{b_{si}} \sin \gamma_i \geq 0.003$ , where  $A_{si}$  is the total area of reinforcement at spacing  $s_i$  in a layer of reinforcement with bars at an angle  $\alpha_i$  to the axis of the strut.

#### (3) Longitudinal Reinforcement

$$F_{ns} = f_{ce} A_c + A'_s f'_s \quad (5.91)$$

where  $A'_s$  = area of compression reinforcement in a strut, in.<sup>2</sup>

$f'_s$  = stress in compression reinforcement, in.<sup>2</sup>

#### (4) Strength of Ties

$$F_{nt} = A_{st} f_y + A_{ps} (f_{pe} + \Delta f_{ps}) \quad (5.92)$$

where  $F_{nt}$  = nominal strength of tie, lb.

$A_{st}$  = area of non-prestressed reinforcement in a tie, in.<sup>2</sup>

$A_{ps}$  = area of prestressing reinforcement, in.<sup>2</sup>

$f_{pe}$  = effective stress after losses in prestressing reinforcement

$\Delta f_{ps}$  = increase in prestressing stress beyond the service load level

$(f_{pe} + \Delta f_{ps})$  should not exceed  $f_{py}$ . When no prestressing reinforcement is used,  $A_{ps} = 0$  in Equation 5.92.

$$h_{t,max} = F_{nt} / f_{ce} \quad (5.93)$$

where  $h_{t,max}$  = maximum effective height of concrete concentric with the tie, used to dimension nodal zone, in.

If the bars in the tie are in one layer, the effective height of the tie can be taken as the diameter of the bars in the tie plus twice the cover to the surface of the bars. The re-

inforcement in the ties have to be anchored by hooks, mechanical anchorages, post-tensioning anchors, or straight bars, all with full development length.

(5) *Strength of Nodal Zones*

$$F_{nn} = f_{ce} A_n \quad (5.94)$$

where  $F_{nn}$  = nominal strength of a face of a nodal zone, lb.

$A_n$  = area of face of a nodal zone or a section through a nodal zone, in.<sup>2</sup>

It can be assumed that the principal stress directions in the struts and ties act parallel to the axes of the struts and ties. Under such a condition, the stresses on faces perpendicular to these axes are principal stresses.

(6) *Confinement in the Nodal Zone*

The ACI 318-08, Appendix B, stipulates that unless confining reinforcement is provided within the nodal zone and its effect is supported by analysis and experimentation, the computed compressive stress on a face of a nodal zone due to the strut and tie forces should not exceed the values given by Eq. 5.95 (Ref. 5.1):

$$f_{ce} = 0.85 \beta_n f'_c \quad (5.95)$$

where  $\beta_n = 1.0$  in nodal zones bounded by struts or bearing stresses

$= 0.8$  in nodal zones anchoring one tie

$= 0.6$  in nodal zones anchoring two or more ties

The following are two examples of the use of the strut-and-tie method for the design of short span/depth ratio concrete elements: (a) deep beams; (b) corbels. While deep beams are most likely designed as reinforced concrete members, and not prestressed, the design of a deep beam illustrates the application of the discussed principles in the forgoing sections.

(7) *Orthogonal Shear Reinforcements that Cross the Compression Struts*

$A_v$  = total area of vertical reinforcement spaced at  $s_v$  in the horizontal direction at both faces of the beam

$A_{vh}$  = total area of horizontal reinforcement spaced at  $s_h$  in the vertical direction at both faces of the beam

$$\text{maximum } s_v \leq \frac{d}{5} \leq 12 \text{ in.}$$

$$\text{maximum } s_h \leq \frac{d}{5} \leq 12 \text{ in.}$$

and

$$\text{minimum } A_{vh} = 0.0015 b s_h \quad (5.96a)$$

$$\text{minimum } A_v = 0.0025 b s_v \quad (5.96b)$$

The shear reinforcement required at the critical section must be provided throughout the deep beams.

### 5.20.4 Example 5.10: Design of Deep Beam by Strut-and-Tie Method

A simply supported deep beam having a clear span  $l_n = 10$  ft (3.05 m) is subjected to a uniformly distributed live load of 81,000 lb/ft (1182 kN/m) on the top. The height  $h$  of the beam is 6 ft (1.83 m) and its thickness  $b$  is 20 in. (508 mm).

$$f'_c = 4000 \text{ psi (27.6 MPa)}$$

$$f_y = 60,000 \text{ psi (414 MPa)}$$

Design the beam reinforcement for this beam by the strut-and-tie method.

**Solution:** Check  $l_n/d$  and evaluate factored shear force  $V_u$  (Step 1)  
Assume that  $d \approx 0.9h = 0.9 \times 6 \times 12 \approx 65$  in. (1651 mm).

$$\frac{l_n}{d} = \frac{10.0 \times 12}{65} = 1.85 < 4$$

Hence treat as a deep beam.

$$\text{beam self-weight} = \frac{20 \times 72}{144} \times 150 = 1500 \text{ lb/ft (21.9 kN/m)}$$

$$\begin{aligned} \text{total factored load} &= 1.2 \times 1500 + 1.6 \times 81,000 \\ &= 131,400 \text{ lb/ft (1942 kN/m)} \end{aligned}$$

(1) *Truss model selection*

The uniformly distributed load on the beam top is idealized by two concentrated loads as shown in Fig. 5.59 and detailed in Fig. 5.61. The ensuing truss model can be considered to simulate the stress trajectories of the principal stresses.  $l/h = 10/6 = 1.67 < 2.5$ , hence a deep beam.

Strut inclination angle  $\theta$  in Figure 5.59(c) is interpolated between  $\theta = 68^\circ$  for  $l/h \leq 1$  and  $\theta = 54^\circ$  for  $l/h = 2$  (Ref. 5.20).

$$\begin{aligned} \text{Hence, } \theta &= 68 - (68 - 54)(1.67 - 1.0) \\ &= 68 - 0.67 \times 14 = 58.62^\circ \end{aligned}$$

Assume supports center line span = 11 ft 5 in.

Assume  $d_c$  = cover to centroid of tensile reinforcement = 7 in.

Vertical distance of node C in Figure 5.61(a) from the centroid of the tensile reinforcement =

$$= \frac{2h}{3} = \frac{2 \times 6}{3} = 4' - 0''$$

$$\begin{aligned} \text{Length } CD &= 11' - 5'' - 2 \left( 4' - \frac{7''}{12} \right) \cot 58.62^\circ \\ &= 11.42 - 4.17 = 7.25 \text{ ft.} \end{aligned}$$

Intensity of total factored distributed load is  $w_u = 131,400$  lb/ft.

Idealized equivalent concentrated load is

$$P_u = \frac{w_u l}{2} = \frac{131,400 \times 10}{2} = 657,000 \text{ lb./strut (see Fig. 5.61)}$$

$$V_n = \frac{P_u}{\phi} = \frac{657,000}{0.75} = 876,000 \text{ lb.}$$

Compressive forces in each of the compressive struts  $EC$  and  $FD = 876,000$  lb.

(2) *Vertical and horizontal components of forces in the truss model*

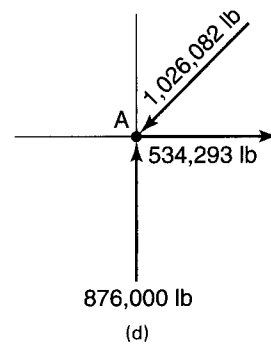
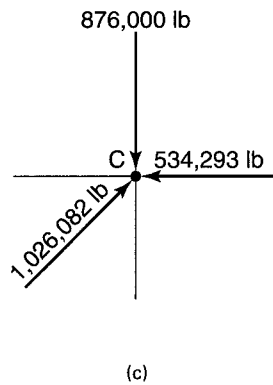
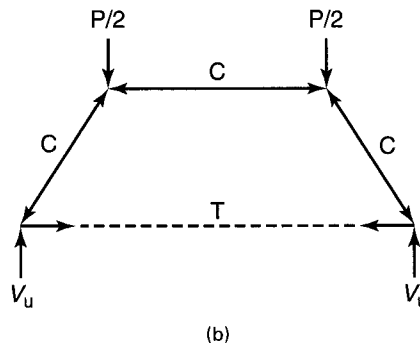
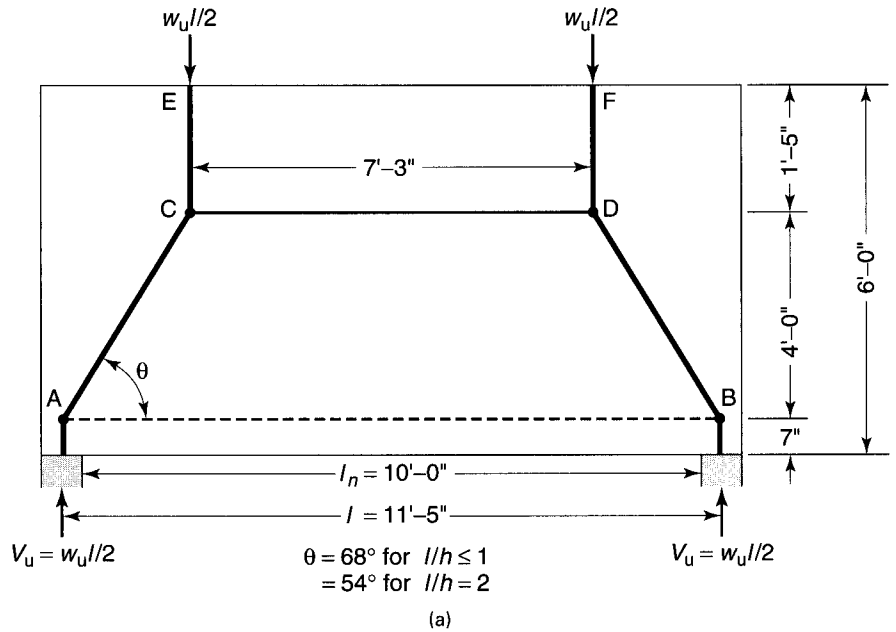
The compressive forces in the truss shown in Figure 5.61(b) are computed in the usual manner, as the vector sine and cosine components of the inclined struts at the assumed  $\theta = 58.62^\circ$ . Figure 5.61(c) gives the intersecting nodal forces in the  $D$ -region of node  $C$ , giving a strut force in  $CA = 1,026,082$  lb. ( $C-C-C$  node). Figure 5.61(d) gives the intersecting forces in the  $D$ -region of node  $A$ , giving a tie force in truss member  $AB = 534,293$  lb. ( $C-C-T$  node).

Evidently, idealizing the distributed load into four or six equivalent concentrated loads would have reduced the compressive forces in the struts and the tensile forces in the ties, leading to reduced reinforcement areas (see Ref. 5.2 by Nawy).

(3) *Vertical and horizontal reinforcement across depth of beam web*

Horizontal web requirement is not required as part of the truss. However, in order to control cracking, ACI-318 Code requires an area  $A_{vh} \geq 0.0015 b_w s_h$  for horizontal shear reinforcement and  $A_v \geq 0.0025 b_w s_h$  for vertical reinforcement, Eqs. 5.96 a, b.





**Figure 5.61** Truss-and-tie model in Example 5.10: (a) idealized truss model; (b) truss forces (*C* = compression, *T* = tension); (c) forces on joint *C* (*C-C-C* node); (d) forces on joint *A* (*C-C-T* node).

Assuming a spacing of 12 in. on centers,

$$\text{Min } A_{vh} = 0.0015 b_w s_h = 0.0015 \times 20 \times 12 = 0.36 \text{ in.}^2$$

Use No. 4 bars at 12 in. on centers as horizontal reinforcement in both faces of the deep beam (= 0.40 in.<sup>2</sup>).

*Vertical web requirement* to control cracking: assume a spacing of 8 in. on centers,

$$\text{From Eq. 5.96(b), Min } A_v = 0.0025 b_w s_v = 0.0025 \times 20 \times 8 = 0.40 \text{ in.}^2$$

Use No. 4 bars at 8 in. on centers as vertical reinforcement in each of the two faces of the deep beam.

(4) *Check of orthogonal shear reinforcement crossing compression strut*

As given in Sec. 5.20.3, the minimum reinforcement crossing the struts for

$$f'_c \leq \pm 6000 \text{ psi} = \Sigma \frac{A_{si}}{b_s s_i} \sin \gamma_i \geq 0.003.$$

$\gamma_1$  = inclination of vertical reinforcement to the strut = 31.38° where  $\sin \gamma_1 = 0.521$

$\gamma_2$  = inclination of horizontal reinforcement to the strut = 58.62° where  $\sin \gamma_2 = 0.854$

$$\Sigma \frac{A_{si}}{b_s s_i} \sin \gamma_i = \frac{0.60 \times 0.521}{20 \times 8} + \frac{0.40 \times 0.854}{20 \times 12} = 0.0020 + 0.0014 = 0.0034 > 0.003, \text{ O.K.}$$

Hence, adopt the reinforcement in item (3), namely, No. 4 bars at 8 in. c/c for vertical reinforcement and No. 4 bars at 12 in. c/c for horizontal reinforcement for both faces of the deep beam.

(5) *Strength of struts*

From Equation 5.90, compressive strength of concrete in a strut or nodal zone is

$$\begin{aligned} f_{ce} &= 0.85 \beta_s f'_c \text{ where } \beta_s = 0.75 \\ &= 0.85 \times 0.75 \times 4,000 = 2,550 \text{ psi.} \end{aligned}$$

Required strength of struts *CA*, *DB* is

$$F_{ns} = 1,026,082 \text{ lb.}$$

From Equation 5.89,

$$F_{ns} = f_{ce} A_c \text{ or } 1,026,082 = 2,550 A_c \text{ hence } A_c = \frac{1,026,082}{2,550} = 402 \text{ in.}^2$$

Width of *CA*, *DB* =  $\frac{402}{20} = 20.1$  in., which is within the available area of the deep beam, hence, O.K.

Similarly, for struts *EC* and *FD*,  $A_{cs} = 876,000/2550 = 344 \text{ in.}^2$ ; minimum required strut width =  $344/20 = 17.2$  in., which is available within the beam area, hence OK.

(6) *Strength of ties*

Required strength  $F_{nt} = 534,293 \text{ lb.}$

From Equation 5.92,

$$F_{nt} = A_{st} f_y + A_{ps} (f_{pe} + \Delta f_{ps})$$

or  $534,293 = A_{st} \times 60,000$

$$A_{st} = \frac{534,293}{60,000} = 8.9 \text{ in.}^2$$

$$\text{Trying No. 10 bars, } n = \frac{8.9}{1.27} = 7.0$$

Use 8 No. 10 bars in 4 layers of two bars at 3 in. on centers.

$d_c = 2.15$  in. cover + 3 + 1.5  $\cong 7$  in. assumed in constructing the truss model dimensions.

From Equation 5.93, the maximum height of concrete concentric with the tie for dimensioning the nodal zone is

$$h_{t,\max} = F_{nt}/f_{ce} = \frac{534,293}{2,550} = 210 \text{ in.}$$

Actual tie height =  $2.15 + 3 + 3 + 3 + 2.15 = 13.3$ , say 14 in., accept.

Anchor the 8 No. 10 bars using hooks at bar ends with full development length. Check the development length.

(7) *Strength of nodal zones*

From Equation 5.59,

Maximum allowable concrete strength in the nodal zone anchoring two or more ties is  $f_{cu} = 0.85 \beta_n f'_c$ , where  $\beta_n = 0.6$

or  $f_{cu} = 0.85 \times 0.6 \times 4,000 = 2,040$  psi.

Surface area of node perpendicular to CA:

$$A_n = 20 \left( \frac{14}{\cos \theta} \right) = \frac{20 \times 14}{0.521} = 537 \text{ in.}$$

From Equation 5.58, the nominal strength of the nodal force is

$$F_n = f_{ce} A_n = 2,040 \times 537 = 1,095,480 \text{ lb.} > 1,026,082 \text{ lb., O.K.}$$

Confinement of the nodal zone is not required, since the stress in the concrete in the nodal zone did not exceed the calculated permissible  $f_{ce} = 2,040$  psi.

Hence, adopt the design.

Another truss model simulating the uniformly distributed load on the top of the beam by four concentrated loads instead of two could have reduced the amount of the horizontal reinforcement. Such a truss model could have the form shown in Fig. 5.60 (Ref. 5.19) in idealizing the stress trajectories of the principal stresses in the deep beam. Careful engineering judgment has to be exercised in the selection of the path of forces on the basis of the principles outlined in Section 5.20.1 to determine whether the resulting reinforcement is excessive or relatively efficient. Principles of equilibrium and compatibility have to be maintained in any chosen model (Ref. 5.22).

### 5.20.5 Example 5.11: Design of Corbel by the Strut-and-Tie Method

Design the corbel in Example 5.7 to support a factored vertical load  $V_u = 80,000$  lb (160 kN) acting at a distance  $a_v = 5$  in. (127 mm) from the face of the column. It has a width  $b = 10$  in. (254 mm), a total depth  $h = 18$  in. (457 mm), and an effective depth  $d = 14$  in. (356 mm). Given:

$$f'_c = 5000 \text{ psi (34.5 MPa), normal weight concrete}$$

$$f_y = f_{yt} = 60,000 \text{ psi (414 MPa)}$$

The supporting column size is  $12 \times 14$  in.

Assume the corbel to be monolithically cast with the column, and neglect the weight of the corbel in the computations.

**Solution:**

1. Assume the corbel is monolithically cast with the column. The total depth  $h = 18$  in. and effective depth  $d = 14$  in. are based on the requirement that the vertical dimension of the corbel outside the bearing area is at least *one half* the column face width of 14 in. (column size:  $12 \times 14$  in.)

Select a simple strut-and-tie model as shown in Fig. 5.62, assuming that the center of tie AB is located at a distance of 4 in. below the top extreme corbel fibers, using one layer of reinforcing bars. Also assume that horizontal tie DC lies on a horizontal line passing at the re-entrant corner C of the corbel. The solid lines in Fig. 5.62 denote tension tie action (T), and the dashed lines denote compression strut action (C). The nodal points A, B, C, D result from the selected strut-and-tie model. Note that the entire corbel is a D-region structure because of the existing statical discontinuities in the geometry of the corbel and the vertical and horizontal loads.

2. *Strut-and-Tie Truss Forces*

$$N_{ue} = 0.20 V_u = 16,000 \text{ lb}$$

The following are the truss member forces calculated from statics in Fig. 5.62.

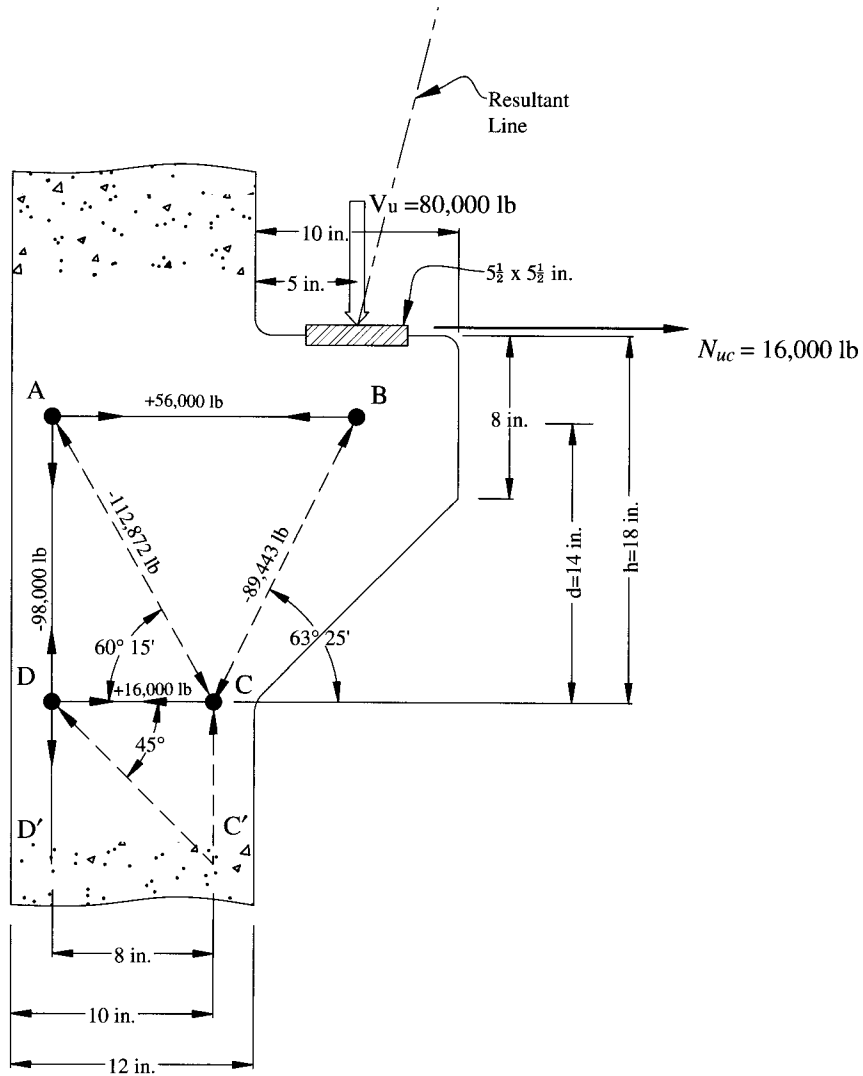


Figure 5.62 Strut-and-Tie Model in Example 5.11.

a) *Compression strut BC:*

$$\text{Length } BC = \sqrt{(7)^2 + (14)^2} = 15.652 \text{ in.}$$

$$F_{BC} = 80,000 \times \frac{15.652}{14} = 89,443 \text{ lb.}$$

b) *Tension tie BA:*

$$F_{BA} = 80,000 \times \frac{7}{14} + 16,000 = 56,000 \text{ lb.}$$

c) *Compression strut AC:*

$$F_{AC} = \frac{56,000 \sqrt{(8)^2 + (14)^2}}{8} = 112,872 \text{ lb.}$$

d) *Tension tie AD:*

$$F_{AD} = \frac{112,872 \times 14}{\sqrt{(8)^2 + (14)^2}} = 98,000 \text{ lb.}$$

e) *Compression strut CC'*:

$$F_{CC'} = 80,000 + 98,000 = 178,000 \text{ lb.}$$

f) *Tension tie CD*:

$$F_{CD} = 56,000 - 40,000 = 16,000 \text{ lb}$$

### 3. Steel Bearing Plate Design

$f_{cu} = \phi(0.85f'_c)$  where  $\phi = 0.75$  for bearing in strut-and-tie models

$$\begin{aligned} \text{Area of plate is } A_1 &= \frac{80,000}{0.75(0.85f'_c)} = \\ &= \frac{80,000}{0.75 \times 0.85 \times 5000} = 25.10 \text{ in.}^2 \end{aligned}$$

Use  $5\frac{1}{2} \times 5\frac{1}{2}$  in. plate and select a thickness to produce a rigid plate.

### 4. Tie Reinforcement Design

$$A_{ts,AB} = \frac{56,000}{\phi f_y} = \frac{56,000}{0.75 \times 60,000} = 1.25 \text{ in.}^2$$

Use 3 # 6 bars = 1.32 in.<sup>2</sup>, or, conservatively,

3 # 7 bars = 1.80 in.<sup>2</sup> as in Example 5.7.

These top bars in one layer have to be fully developed along the longitudinal column reinforcement.

$$A_{ts,CD} = \frac{16,000}{0.75 \times 60,000} = 0.36 \text{ in.}^2$$

Use 2 # 6 tie bars = 0.88 in.<sup>2</sup> to form part of the cage shown in Fig. 5.63.

### 5. Horizontal Reinforcement $A_h$ for Crack Control of Shear Cracks

$$A_h = 0.50(A_{ts} - A_n)$$

Where  $A_n$  = reinforcement resisting the frictional force  $N_{ue}$

$$A_n = \frac{N_{ue}}{\phi f_y} = \frac{16,000}{0.75 \times 60,000} = 0.36 \text{ in.}^2$$

Hence,  $A_h = 0.50(1.25 - 0.36) = 0.45 \text{ in.}^2$

Try 3 # 3 closed ties evenly spaced vertically as shown in Fig. 5.63, giving  $A_h = 3(2 \times 0.11) = 0.66 \text{ in.}^2 > 0.45 \text{ in.}^2$ , O.K.

Because  $\beta_s = 0.75$  is used for calculating the effective concrete compressive strength in the struts in the following section, where  $f_{cu} = 0.85\beta_s f'_c$ , the minimum reinforcement provided has also to satisfy:

$$\begin{aligned} \Sigma \frac{A_h / \text{tie}}{bs_t} \sin \alpha_t &\geq 0.003 \\ &= \frac{2(0.11)}{14 \times 3.0} \sin 60^\circ 15' = 0.0045 > 0.003 \text{ O.K.} \end{aligned}$$

Hence adopt 3 # 3 closed ties at 3.0 in. c. to c. spacing.

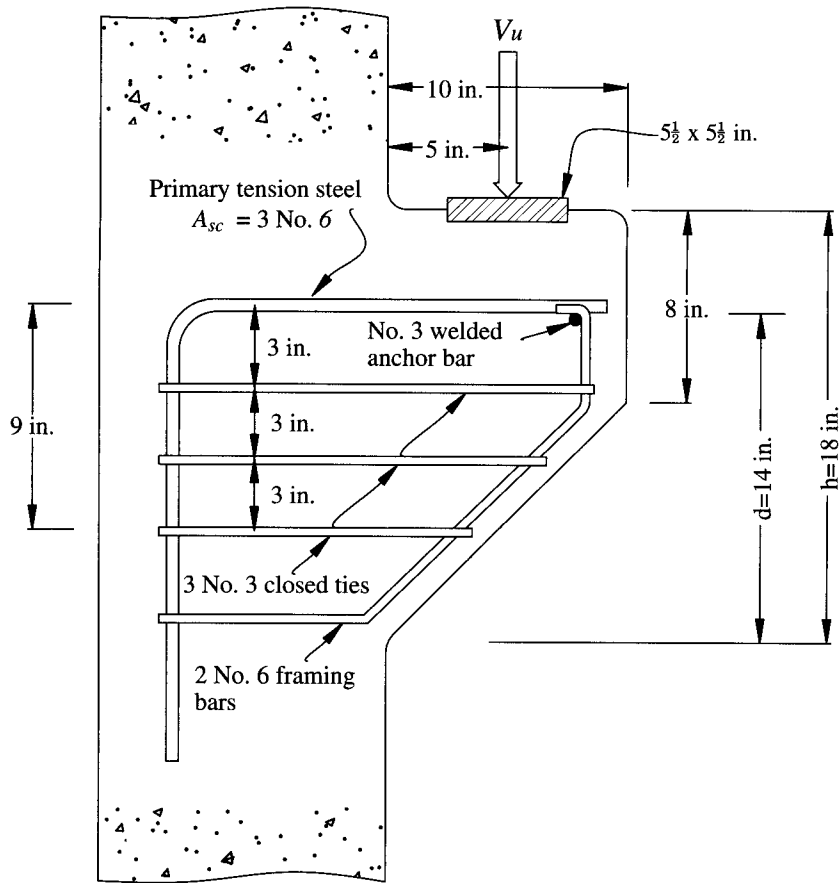
### 6. Strut Capacity Evaluation

(i) *Strut CC'*

The width  $w_s$  of nodal zone C has to satisfy the allowable stress limit on the nodal zones, namely, node B below the bearing plate and node C in the re-entrant corner to the column. Both nodes are CCT nodes and considered unconfined.

$$F_{u,CC'} \left(10 - \frac{w_s}{2}\right) = 80^k(5 + 10) + 16^k \times 18 \text{ to give } \frac{w_s}{2} = 1.64 \text{ in.,}$$

hence, strut width  $w_s = 3.28$  in. fits within the available concrete dimension about the strut center line.



**Figure 5.63** Corbel reinforcement details (Ex. 5.11).

**(ii) Strut BC**

Nominal strength is limited to  $F_{ns} = f_{cu} A_{cs}$ , where  $f_{cu} = 0.85\beta_s f'_c$   
 $f_{cu} = 0.85 \times 0.75 \times 5000 = 3188 \text{ psi} = 3.188 \text{ ksi}$

$A_{cs}$  is the smaller strut cross-sectional area at the two ends of the strut, namely, at node C, while at node B, the node width can be assumed equal to the steel plate width of 5.50 in.

$$A_{cs} \text{ at node } C = 14 \times 3.28 = 45.92 \text{ in.}^2$$

$$\text{Available factored } F_{us,C} = \phi F_{ns,C}$$

$$= 0.75 \times 3.188 \times 45.92 = 109.8 \text{ kip} > \text{required } F_{BC} = 89.4 \text{ kip, OK}$$

**(iii) Strut AC**

Required width,  $w_s$ , of strut AC

$$= \frac{F_{u,AC}}{\phi f_{ce} b} = \frac{112.87 \text{ kip}}{0.75 \times 3.188 \times 14} = 3.37 \text{ in.}$$

Examination of the corbel and column depth of 12 in., shows there is a minimum clear cover of 2.0 in. from the outer concrete surface. Hence the widths,  $w_s$ , of all struts fit within the corbel geometry.

Adopt the design as shown in Fig. 5.63.

## 5.21 SI COMBINED TORSION AND SHEAR DESIGN OF PRESTRESSED BEAM

### Example 5.12

Solve Example 5.9 using the SI procedure and ACI Shear value obtained from Equation 5.16 in Example 5.9.

#### Solution:

1. See calculation step 1 in Example 5.9.
2. See calculation step 2 in Example 5.9.
3. *L-Beam torsional geometrical details*

$$\begin{array}{lll}
 A_{cp} = 3870 \text{ cm}^2 & p_{cp} = 422 \text{ cm} & \\
 x_1 = 11.7 \text{ cm} & y_1 = 181.6 \text{ cm} & p_h = 2(x_1 + y_1) = 386 \text{ cm} \\
 h = 191 \text{ cm} & b_w = 20.3 \text{ cm} & d = 182 \text{ cm} \\
 A_{0h} = 2077 \text{ cm}^2 & A_0 = 0.85A_{0h} = 1766 \text{ cm}^2 & \\
 \theta = 37.5^\circ & \cot \theta = 1.3 & \cot^2 \theta = 1.69
 \end{array}$$

From Figure 5.51

$$\text{factored } T_u = 73 \text{ kN-m}$$

$$\text{factored } V_u = 417 \text{ kN}$$

$$\text{factored } M_u = 370 \text{ kN-m}$$

$$\frac{V_u d}{M_u} = \frac{417 \times 182 \text{ cm}}{37,000 \text{ kN-m}} = 2.05 > 1.0, \text{ use } \frac{V_u d}{M_u} = 1.0$$

$$P_e = 142,290 \text{ lb} = 633 \text{ kN} \quad e = 29.7 \text{ in.} = 75.4 \text{ cm}$$

$$A_c = 696 \text{ in}^2 = 4490 \text{ cm}^2$$

$$c = 26.2 \text{ in.} = 66.5 \text{ cm}$$

$$S_b = 10,990 \text{ in}^3 = 180,094 \text{ cm}^3$$

$$f'_c = 34.5 \text{ MPa} \quad f_{pu} = 1860 \text{ MPa}$$

$$E_s = 200,000 \text{ MPa} \quad f_y = 414 \text{ MPa} \quad f_{ps} = 1760 \text{ MPa}$$

$$A_{ps} = 6 \text{ tendons } 12.7 \text{ mm diameter} = 5.92 \text{ cm}^2$$

$$\phi \text{ for shear and torsion} = 0.85$$

$$1 \text{ Pa} = \text{N/m}^2$$

#### 4. Cracking moment capacity

$$S_b = 180,094 \text{ cm}^2$$

$$\bar{f}_c = \frac{P_e}{A_c} = \frac{633,000}{4490 \times 10^2} = 1.41 \text{ MPa}$$

$$f_{ce} = \frac{P_e}{A_c} \pm \frac{P_e e}{S_b} = 1.41 + \frac{633,000 \times 75.4}{180,094 \times 10^2}$$

$$= 1.41 + 2.65 = 4.06 \text{ say } 4.1 \text{ MPa}$$

From Example 5.9,  $\bar{f}_c = 1.14 \text{ MPa}$

$$f_d = \text{unfactored dead load stress} = 289 \text{ psi} = 2.0 \text{ MPa}$$

$$\begin{aligned} M_{cr} &= S_b \left( \frac{1}{2} \sqrt{f'_c} + f_{ce} - f_d \right) \\ &= 180,094 \left( \frac{\sqrt{34.5}}{2} + 4.06 - 2.0 \right) \times 10^{-3} = 900 \text{ kN-m} \end{aligned}$$

$$1.2M_{cr} = 1.2 \times 900 = 1080 \text{ kN-m}$$

$$a = \frac{A_{ps} f_{ps}}{0.85 f'_c} = \frac{5.9 \text{ cm}^2 \times 1760}{0.85 \times 34.5 \times 20.3} = 17.5 \text{ cm}$$

Nominal moment strength,

$$\begin{aligned} M_n &= A_{ps} f_{ps} \left( d_p - \frac{a}{2} \right) \\ &= 5.92 \times 1760 \left( 182 - \frac{17.5}{2} \right) \text{ N-m} = 1800 \text{ kN-m} \\ &> 1.2M_{cr} = 1080 \text{ kN-m} \end{aligned}$$

hence flexural reinforcement is satisfied for flexure.

**5. Verify whether torsional reinforcement is needed**

From Equation 5.80,

$$\begin{aligned} T_u &\leq \frac{\phi \sqrt{f'_c} \left( \frac{A_{cp}^2}{p_{cp}} \right) \sqrt{1 + \frac{3f_c}{\sqrt{f'_c}}}}{12} \\ T_u &= \frac{0.85 \sqrt{34.5}}{12} \left( \frac{(3870)^2}{422} \right) \sqrt{1 + \frac{3 \times 1.14}{\sqrt{34.5}}} \times 10^{-3} \text{ kN-m} \\ &= 18.6 \text{ kN-m} \end{aligned}$$

From Figure 5.51 and the acting torsional moment value from Example 5.9,  $T_u = 73 \text{ kN-m} > 18.6 \text{ kN-m}$ . Hence, torsional reinforcement is required. The garage elements are all precast; assume equilibrium torsion condition with no redistribution of torsional moment using the total applied factored  $T_u = 73 \text{ kN-m}$ .

**6. Check adequacy of section for torsion**

From Figure 5.51 at  $h/2$  from face of support and values computed in Example 5.9,  $V_u = 434 \text{ kN}$ ,  $M_u = 385 \text{ kN-m}$ .

From Equation 5.80 for  $f_{pe} > 0.4f_{pu}$

$$v_c = \frac{V_c}{b_w d} = \left( \frac{\sqrt{f'_c}}{20} + 5 \frac{V_u d}{M_u} \right), \quad \frac{V_u d}{M_u} \leq 1.0$$

where  $f'_c$  is in MPa

$$\frac{V_u d}{M_u} = \frac{417 \times 1.82}{370} = 2.05 > 1.0, \text{ use } 1.0$$

$$v_c = \frac{V_c}{b_w d} = \left( \frac{\sqrt{34.5}}{20} + 5 \times 1.0 \right) = 5.3 \text{ MPa}$$

$$\text{Max. allow. } v_c = 0.4 \sqrt{f'_c} = 0.4 \sqrt{34.5} = 2.4 \text{ MPa controls.}$$

From Equation 5.81 for solid section,



$$\begin{aligned} \sqrt{\left(\frac{V_u}{b_w d}\right)^2 + \left(\frac{T_u p_h}{1.7 A_{oh}^2}\right)^2} &\leq \phi \left(\frac{V_c}{b_w d} + \frac{8\sqrt{f'_c}}{12}\right) \\ \sqrt{\left(\frac{V_u}{b_w d}\right)^2 + \left(\frac{T_u p_h}{1.7 A_{oh}^2}\right)^2} &= \sqrt{\left(\frac{417 \times 10^3}{0.2 \times 1.82}\right)^2 + \left(\frac{73 \times 10^3 \times 3.86}{1.7 \times 0.208^2}\right)^2} \\ &= \sqrt{1422 \times 10^6 + 15.5 \times 10^{12}} \text{ N/m}^2 = 4.0 \text{ MPa} \\ \phi \left(\frac{V_c}{b_w d} + \frac{8\sqrt{f'_c}}{12}\right) &= 0.75 \left(2.4 + \frac{8\sqrt{34.5}}{12}\right) = 4.8 \text{ MPa} \end{aligned}$$

available > 4.0 MPa actual, hence section is adequate.

### 7. Torsional reinforcement

$$T_n = T_u / \phi = 73 / 0.75 = 97 \text{ kN-m}$$

From Equation 5.84b,

$$\begin{aligned} \frac{A_t}{s} &= \frac{T_n}{2A_0 f_{yt} \cot \theta} = \frac{97 \times 10^3}{2 \times 1766 \times 414 \times 1.3} \\ &= 0.051 \text{ cm}^2/\text{cm}/\text{one leg} \end{aligned}$$

### 8. Shear reinforcement

From Example 5.9,

$V_c = 1796 \text{ kN} > V_n = 556 \text{ kN}$ , hence provide only minimum reinforcement for shear.

$$\frac{A_v}{s} = \frac{0.35b_w}{f_{yt}} = \frac{0.35 \times 20.3}{414} = 0.017 \text{ cm}^2/\text{cm}/\text{two legs}$$

$$\frac{A_{vt}}{s} = 2 \left(\frac{A_t}{s}\right) + \frac{A_v}{s} = 2 \times 0.051 + 0.017 = 0.119 \text{ cm}^2/\text{cm}/\text{two legs}$$

Assuming No. 10 M closed stirrups are used

$$\begin{aligned} A_v &= 2 \times 100 = 200 \text{ mm}^2 = 2.0 \text{ cm}^2 \\ s &= \frac{\text{cross-sectional area}}{A_{vt}/s} = \frac{2.0}{0.119} = 17 \text{ cm (6.8 in. c. to c.)} \end{aligned}$$

Maximum allowable  $s = p_h/8$  or  $30 \text{ cm} = p_h/8 = 386/8 = 48 \text{ cm}$

$$\text{Min. } \frac{A_v}{s} = \text{lesser of } \frac{0.35b_w}{f_{yt}} \text{ or } \frac{A_{ps} f_{pu}}{80f_{yt}d} \sqrt{\frac{d}{d_p}}$$

where  $b_w$ ,  $d$ , and  $s$  are in millimeters

$$\begin{aligned} \frac{0.35b_w}{f_{yt}} &= \frac{0.35 \times 203}{414} = 0.17 \text{ mm}^2/\text{mm}/\text{two legs} \\ &= 0.017 \text{ cm}^2/\text{cm}/\text{two legs} \end{aligned}$$

$$\frac{1}{16} \sqrt{f'_c} \left(\frac{b_w}{f_{yt}}\right) = \frac{1}{16} \sqrt{34.5} \left(\frac{20.3}{414}\right) = 0.018 \text{ mm}^2/\text{mm}/\text{two Pegs}$$

$$\begin{aligned} \frac{A_{ps} f_{pc}}{80f_{yt}d} \sqrt{\frac{d}{b_w}} &= \frac{592 \times 1860}{80 \times 414 \times 1820} \sqrt{\frac{1820}{203}} \\ &= 0.06 \text{ mm}^2/\text{mm}/\text{two legs} \\ &= 0.006 \text{ cm}^2/\text{cm}/\text{two legs controls} \end{aligned}$$

Available  $A_v = 0.17 > 0.06$ , O.K.

Minimum bar diameter =  $s/16$  or No. 10 M bar =  $(18/16) \times 10 \text{ mm} = 11.3 \text{ mm} =$  available No. 10 M bars (11.3 mm), O.K.

Use No. 10 bars at 18 cm c. to c.

### 9. Longitudinal reinforcement

From Equation 5.85,

$$\begin{aligned} A_l &= \frac{A_t}{s} p_h \left( \frac{f_{yt}}{f_y} \right) \cot^2 \theta \\ &= 0.051 \times 386 \left( \frac{414}{414} \right) (1.3)^2 = 33.3 \text{ cm}^2 \end{aligned}$$

From Equation 5.88,

$$\begin{aligned} A_{l,\min} &= \frac{5\sqrt{f'_c} A_{cp}}{12f_{yt}} - \frac{A_t}{s} p_h \left( \frac{f_{yv}}{f_{yt}} \right) \\ &= \frac{5\sqrt{34.5} \times 3870}{12 \times 414} - 0.046 \times 386 \left( \frac{414}{414} \right) \\ &= 22.9 - 17.7 = 5.2 \text{ cm}^2 \\ A_l &= 33.3 \text{ cm}^2 \text{ controls} \end{aligned}$$

Using No. 10 M bars,  $A_s = 1.0 \text{ cm}^2$

No. of bars =  $33.3/1.0 = 33.3$  bars

Use 17 No. 10 M bars on each face of the L-beam equally spaced.

Note that maximum allowable spacing  $s = 30 \text{ cm}$

In this case  $s = \frac{191 - 2(1.5)}{15} \approx 12 \text{ cm}$  O.K.

Adopt the design.

For the reinforcing details to be complete, a design of the ledge and hanger reinforcement would be required, as well as details of the anchorage of the longitudinal reinforcement at the supports. Chapter 10 on the design of connections provides these details.

## SELECTED REFERENCES

- 5.1 ACI Committee 318. *Building Code Requirements for Structural Concrete*, (ACI 318-08), and *Commentary to the Building Code Requirements for Reinforced Concrete* (ACI 318R-08) American Concrete Institute, Farmington Hills, MI: 2008, 465 pp.
- 5.2 Nawy, E. G. *Reinforced Concrete—A Fundamental Approach*, 6th Ed., Upper Saddle River, N.J.: Prentice Hall, 2009, pp. 936.
- 5.3 Mattock, A. H., Chen, K. C., and Soogswang, K. "The Behavior of Reinforced Concrete Corbels." *Journal of the Prestressed Concrete Institute* 21 (1976): 52-77.
- 5.4 Nawy, E. G. *Simplified Reinforced Concrete*. Upper Saddle River, NJ: Prentice Hall, 1986.
- 5.5 Sozen, M. A., Zwoyer, E. M., and Siess, C. P. Strength in Shear of Beams without Web Reinforcement. Urbana, Illinois: Bulletin No. 452, Engineering Experiment Station, University of Illinois, April 1959.

- 5.6 ACI Committee 318. *Building Code Requirements for Reinforced Concrete*, 318–63, and *Commentary on the Building Code Requirements for Reinforced Concrete*, 318–63. Farmington Hills, MI: American Concrete Institute, 1963.
- 5.7 Nawy, E. G., and Ukadike, M. M. “Shear Transfer in Concrete and Polymer Modified Concrete Members Subjected to Shear Load.” *Journal of the American Society for Testing and Materials*, March 1983, pp. 83–97.
- 5.8 Prestressed Concrete Institute. *Manual of Design and Detailing of Precast and Prestressed Connections*. Chicago: Prestressed Concrete Institute, 1994.
- 5.9 Hsu, T. T. C. *Torsion in Reinforced Concrete*. Van Nostrand Reinhold, New York, 1983.
- 5.10 Hsu, T. T. C. “Torsion in Structural Concrete—Uniformly Prestressed Members without Web Reinforcement.” *Journal of the Prestressed Concrete Institute* 13 (1968): 34–44.
- 5.11 Collins, M. P., and Mitchell, D. “Shear and Torsion Design of Prestressed and Non-Prestressed Concrete Beams.” *Journal of the Prestressed Concrete Institute* 25 (1980): 32–100.
- 5.12 Prestressed Concrete Institute. *PCI Design Handbook* 6th Ed. Prestressed Concrete Institute, Chicago, 2006.
- 5.13 Rabbat, B. G. and Collins, M. P. “A Variable Angle Space Truss Model For Structural Concrete Members Subjected to Complex Loading,” SP 55–22, American Concrete Institute, Farmington Hills, 1978, pp 547–587.
- 5.14 McGee, W. D., and Zia, P. “Prestressed Concrete Members under Torsion, Shear and Bending.” *Journal of the American Concrete Institute* 73 (1976): 26–32.
- 5.15 Zia, P., and Hsu, T. T. C. *Design for Torsion and Shear in Prestressed Concrete*. ASCE Annual Convention, Reprint No. 3423, 1979.
- 5.16 Abeles, P. W., and Bardhan-Roy, B. K. *Prestressed Concrete Designer’s Handbook*. 3d Ed. Viewpoint Publications, London, 1981.
- 5.17 Hsu, T. T. C. “Shear Flow Zone in Torsion of Reinforced Concrete,” Vol. 116 No. 11, Journ. of Structural Division, ASCE, New York, Nov. 1990, pp. 3206–3225.
- 5.18 Hsu, T. T. C. *Unified Theory of Reinforced Concrete*, CRC Press, Boca Raton, 1993, pp. 313.
- 5.19 Schlaich, J., Schaeffer, K., and Jennewein, M., 1987, “Toward a Consistent Design of Structural Concrete,” *PCI Journal*, v. 32, No. 3, May–June, pp. 74–150.
- 5.20 Schlaich, J., Weischede, D., “Detailing of Concrete Structures (in German),” Bulletin d’Information 150, Comité Euro-International du Béton, Paris, March 1982, 163 pp.
- 5.21 Bergmeister, K., Breen, J. E., and Jirsa, J. O., “Dimensioning of the Nodes and Development of Reinforcement,” *IABSE Colloquim Stuttgart 1991*, International Association for Bridge and Structural Engineering, Zurich, 1991, pp. 551–556.
- 5.22 Nawy, E. G., “Discussion of Appendix A of ACI 318-02, on the Strut and Tie Method,” *Concrete International Journal*, Vol. 24, No. 1, American Concrete Institute, Farmington Hills, MI, January 2002, pp. 122–124.
- 5.23 Nawy, E. G., “ACI 318-02 Shear Provision on the Design of Deep Beams,” *Concrete International Journal (CI)*, American Concrete Institute, Farmington Hills, MI, 2002.
- 5.24 Tjhin, Tin, and Kuchma, D.A., *Corbel at Column*, ACI SP-208 on Strut and Tie Models, Ed. K. H. Reineck, American Concrete Institute, Farmington Hill, MI, 2003, pp. 105–115.
- 5.25 Nawy, E. G., “Concrete—The Sustainable Infrastructure Material for the 21st Century,” Keynote Address Paper, No. E-C103, Transportation Research Board, National Research Council, Washington, D.C., September 2006, pp 1–23.
- 5.26 Nawy, E. G., “Concrete—The Sustainable Infrastructure Material for the 21st Century,” Keynote Address Paper, Proceedings, The First International Conference on Recent Advances in Concrete Technology, Crystal City, Washington, D.C., September 19, 2007, pp. 1–24.

## PROBLEMS

- 5.1 A post-tensioned bonded prestressed beam has the cross section shown in Figure P5.1. It has a span of 75 ft (22.9 m) and is subjected to a service superimposed dead load  $W_{SD} = 450$  plf (6.6 kN/m) and a superimposed service live load  $W_L = 2,300$  plf (33.6 kN/m). Design the web reinforcement necessary to prevent shear cracking (a) by the detailed design method and (b) by the alternative method at a section 15 ft (4.6 m) from the face of the support. The profile of the prestressing tendon is parabolic. Use #3 stirrups in your design, and detail the section. The following data are given:

$$A_c = 876 \text{ in.}^2 (5,652 \text{ cm}^2)$$

$$I_c = 433,350 \text{ in.}^4 (18.03 \times 10^6 \text{ cm}^4)$$

$$r^2 = 495 \text{ in.}^2 (3,194 \text{ cm}^2)$$

$$c_t = 25 \text{ in. (63.5 cm)}$$

$$S' = 17,300 \text{ in.}^3 (2.83 \times 10^5 \text{ cm}^3)$$

$$c_b = 38 \text{ in. (96.5 cm)}$$

$$S_b = 11,400 \text{ in.}^3 (1.86 \times 10^5 \text{ cm}^3)$$

$$W_d = 910 \text{ plf (13.3 kN/m)}$$

$$e_c = 32 \text{ in. (81.3 cm)}$$

$$e_e = 2 \text{ in. (5 cm)}$$

$$f'_c = 5,000 \text{ psi (44.5 MPa), normal-weight concrete}$$

$$f'_{ci} = 3,500 \text{ psi (24.1 MPa)}$$

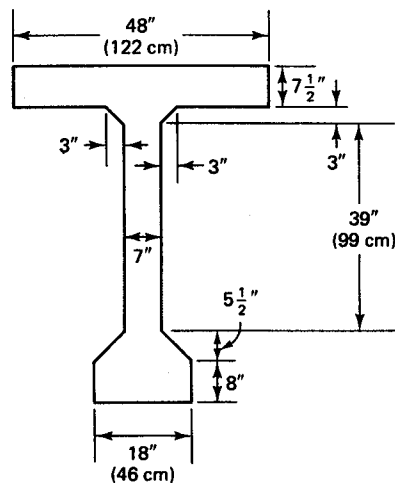


Figure P5.1.

$$f_{yt} \text{ for stirrups} = 60,000 \text{ psi (41.8 MPa)}$$

$$f_{pu} = 270,000 \text{ psi (1,862 MPa) low-relaxation strands}$$

$$f_{ps} = 243,000 \text{ psi (1,675 MPa)}$$

$$f_{pe} = 157,500 \text{ psi (1,086 MPa)}$$

$$A_{ps} = \text{twenty-four } \frac{1}{2}\text{-in. dia (12.7 mm dia) 7-wire tendons}$$

- 5.2** Find the shear strengths  $V_c$ ,  $V_{ci}$ , and  $V_{cw}$  for the beam in Problem 5.1 at 1/10 span intervals along the entire span, and plot the variations in their values along the span in a manner similar to the plot in Figure 5.13.
- 5.3** Assume that a 4 in. (10 cm) topping of width  $b = 8 \text{ ft } 6 \text{ in. (2.6 m)}$  is situ cast on the precast section of Problem 5.1. If the top surface of the precast section is unroughened, design the necessary dowel reinforcement to ensure full composite action. Use the ACI coefficient of friction for determining the area and spacing of the shear-friction reinforcement, and use  $f'_c = 3,000 \text{ psi (20.7 MPa)}$  for the topping. Compare the results with those obtained using the PCI coefficient of friction.
- 5.4** A 14 in. (35.6 cm) standard PCI double-T simply supported beam is shown in Figure P5.4. It has a span of 40 ft (12.2 m) and is subjected to a service dead load  $W_{SD} = 25 \text{ psf (1,197 Pa)}$  plus self-weight  $W_D = 31 \text{ psf (1,484 Pa)}$  and a service live load  $W_L = 45 \text{ psf (2,155 Pa)}$ . Design the web-shear reinforcement at  $\frac{1}{2}d_p$  from the support and at quarter span by (a) the detailed method and (b) the alternative method, and then compare the two designs. The tendon is harped at midspan. Given data are as follows:

$$f'_c \text{ (precast)} = 5,000 \text{ psi, lightweight concrete}$$

$$f'_{ci} = 3,500 \text{ psi}$$

$$f'_c \text{ (topping)} = 3,000 \text{ psi, normal weight}$$

$$f_{pu} = 270,000 \text{ psi, low-relaxation strand}$$

$$f_{ps} = 189,000 \text{ psi (1,303 MPa)}$$

$$f_{pe} = 156,000 \text{ psi (1,076 MPa)}$$

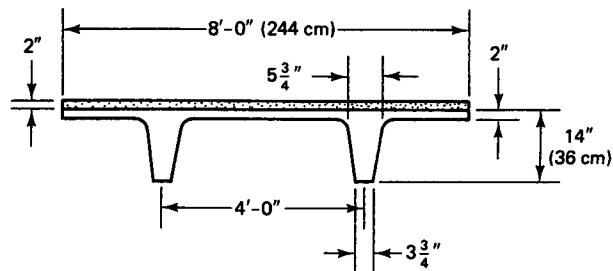
$$\text{Stirrups } f_y = 60,000 \text{ psi (41.8 MPa)}$$

$$A_{ps} = \text{six } \frac{1}{2}\text{-in. (12.7 mm) dia 7-wire strands}$$

$$e_c = 8.01 \text{ in. (20.3 cm)}$$

$$e_e = 4.51 \text{ in. (11.5 cm)}$$

Use  $d_p = 10 \text{ in.}$  in the solution. The values of the section properties are as follows:



**Figure P5.4.**

Section properties	Untopped	Topped
$A_c$	306 in. <sup>2</sup>	
$I_c$	4,508 in. <sup>4</sup>	7,173 in. <sup>4</sup>
$c_b$	10.51 in.	12.40 in.
$c_t$	3.49 in.	3.60 in.
$S_b$	429 in. <sup>3</sup>	578 in. <sup>3</sup>
$S_t$	1,292 in. <sup>3</sup>	1,992 in. <sup>3</sup>
$W_D$	31 psf	56 psf

- 5.5** Design a bracket to support a concentrated factored load  $V_u = 125,000$  lb (556 kN) acting at a lever arm  $a = 4$  in. (101.6 mm) from the column face. The horizontal factored force  $N_{uc} = 40,000$  lb (177.9 kN). Given data are:

$$b = 14 \text{ in. (355.6 mm)}$$

$$f'_c = 5,000 \text{ psi (34.47 MPa), normal-weight concrete}$$

$$f_y = f_{yt} = 60,000 \text{ psi (413.7 MPa)}$$

Solve by both the shear-friction approach and the strut-and-tie method.

Assume that the bracket was cast after the supporting column cured, and that the column surface at the bracket location was not roughened before casting the bracket. Detail the reinforcing arrangements for the bracket.

- 5.6** Solve Problem 5.5 if the structural system was made from monolithic sand-lightweight concrete in which the corbel or bracket was cast simultaneously with the supporting column.

Use both the strut-and-tie method and the shear friction approach in your solution.

- 5.7** A simply supported deep beam has a clear span  $l_n = 10$  ft (3.1 m) and an effective center-to-center span  $l = 11$  ft 6 in. (3.5 m). The total depth of the beam is  $h = 8$  ft 10 in. (2.7 m). It is subjected to a uniform factored load on the top fibers of intensity  $w = 120,000$  lb/ft (1601.8 kN/m), including its self-weight. Design the beam for flexure and shear by the strut-and-tie approach.

$$\text{Given: } f'_c = 4500 \text{ psi (31.0 MPa), normal-weight concrete}$$

$$f_y = f_{yt} = 60,000 \text{ psi (413.7 MPa)}$$

- 5.8** Design the transverse and longitudinal reinforcement in Example 5.9 for combined torsion and shear assuming that the L-beam concrete is made of sand-lightweight concrete.
- 5.9** Design the web reinforcement for the beam in Example 5.9 for combined shear and torsion assuming that the centerline dimensions of the interior floor panels are 30 ft x 56 ft (9.1 m x 17.1 m). The floor is subjected to a service superimposed dead load due to the double T's of  $W_{SD} = 77$  psf (3,687 Ma) and a service live load of 60 psf (2,873 MPa).

# 6



## INDETERMINATE PRESTRESSED CONCRETE STRUCTURES

### 6.1 INTRODUCTION

As in reinforced concrete and other structural materials, continuity can be achieved at intermediate supports and knees of portal frames. The reduction of moments and stresses at midspans through the design of continuous systems results in shallower members that are stiffer than simply supported members of equal span and of comparable loading and are of lesser deflection.

Consequently, lighter structures with lighter foundations reduce the cost of materials and construction. In addition, the structural stability and resistance to longitudinal and lateral loads are usually improved. As a result, the span-to-depth ratio is also improved, depending on the type of continuous system being considered. For continuous flat plates, a ratio of 40 to 45 is reasonable, while in box girders this ratio can be 25 to 30.

An additional advantage of continuity is the elimination of anchorages at intermediate supports through continuous post-tensioning over several spans, thereby reducing further the cost of materials and labor.

Continuous prestressed concrete is widely applied in the United States in the construction of flat plates for floors and roofs with continuity in one or both directions and with prestressing in one or both directions. Also, continuity is widely used in long-span

Lincoln Executive Plaza, Arlington Heights, Illinois. (Courtesy, Prestressed Concrete Institute.)

prestressed concrete bridges, particularly situ-cast post-tensioned spans. Cantilevered box girder bridges, widely used in Europe as segmental bridges, are increasingly being used in the United States for very large spans, and cable-stayed bridges with prestressed decks are increasingly built as well.

The success of prestressed concrete construction is largely due to the economy of using precast elements, with the associated high-quality control during fabrication. This desirable feature has been widely achieved by imposing continuity on the precast elements through placement of situ-cast reinforced concrete at the intermediate supports. The situ-cast concrete tends to resist the superimposed dead load and the live load that act on the spans after the concrete hardens. Note that forming, shoring, and reshoring can also be avoided in this type of construction, thereby reducing the costs further as compared with the costs of reinforced concrete.

## 6.2 DISADVANTAGES OF CONTINUITY IN PRESTRESSING

There are several disadvantages to having continuously prestressed elements:

1. Higher frictional losses due to the larger number of bends and longer tendons.
2. Concurrence of moment and shear at the support sections, which reduces the moment strength of those sections.
3. Excessive lateral forces and moments in the supporting columns, particularly if they are rigidly connected to the beams. These forces are caused by the elastic shortening of the long-span beams under prestress.
4. Effects of higher secondary stresses due to shrinkage, creep temperature variations, and settlement of the supports.
5. Secondary moments due to induced reactions at the supporting columns caused by the prestressing force (to be subsequently discussed).
6. Possible serious reversal of moments due to alternate loading of spans.
7. Moment values at the interior supports that require additional reinforcement at these supports, which might otherwise not be needed in simply supported beams.

All these factors can be accounted for through appropriate design and construction of the final system, including special provisions for bearings at the supporting columns.

## 6.3 TENDON LAYOUT FOR CONTINUOUS BEAMS

The construction system used, the length of the adjacent spans, and the engineering judgment and ingenuity of the design engineer determine the type of layout and method of framing to be used for achieving continuity. Basically, there are two categories of continuity in beams:

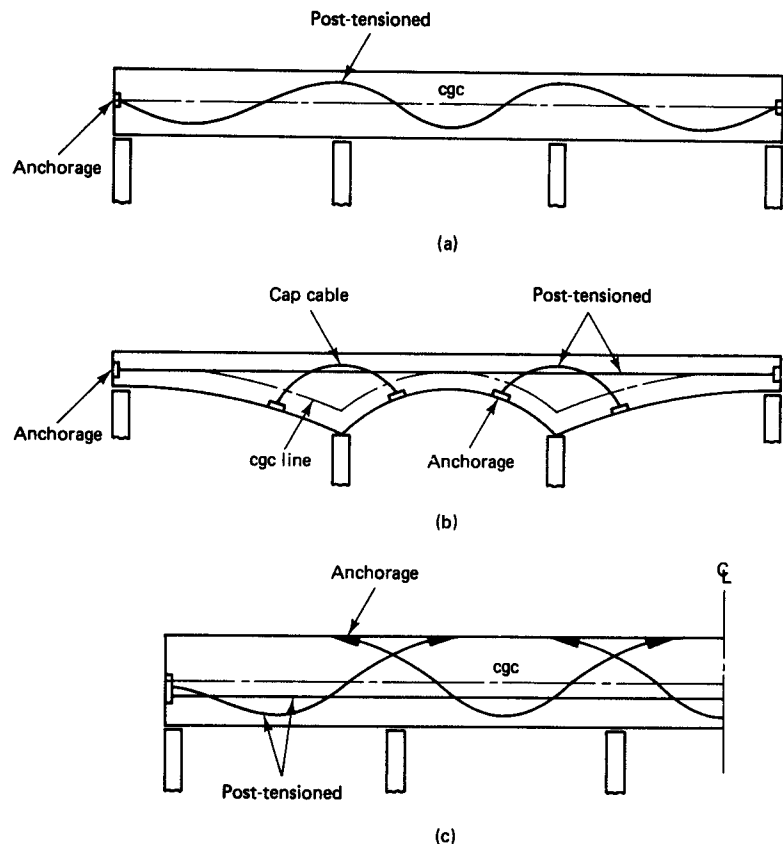
1. Monolithic continuity, where all the tendons are generally continuous throughout all or most of the spans and all tendons are prestressed at the site. Such prestressing is accomplished by post-tensioning.
2. Nonmonolithic continuity, where precast elements are used as simple beams on which continuity is imposed at the support sections through situ-cast reinforced concrete which provides the desired level of continuity to resist the superimposed dead load and live load after the concrete hardens.



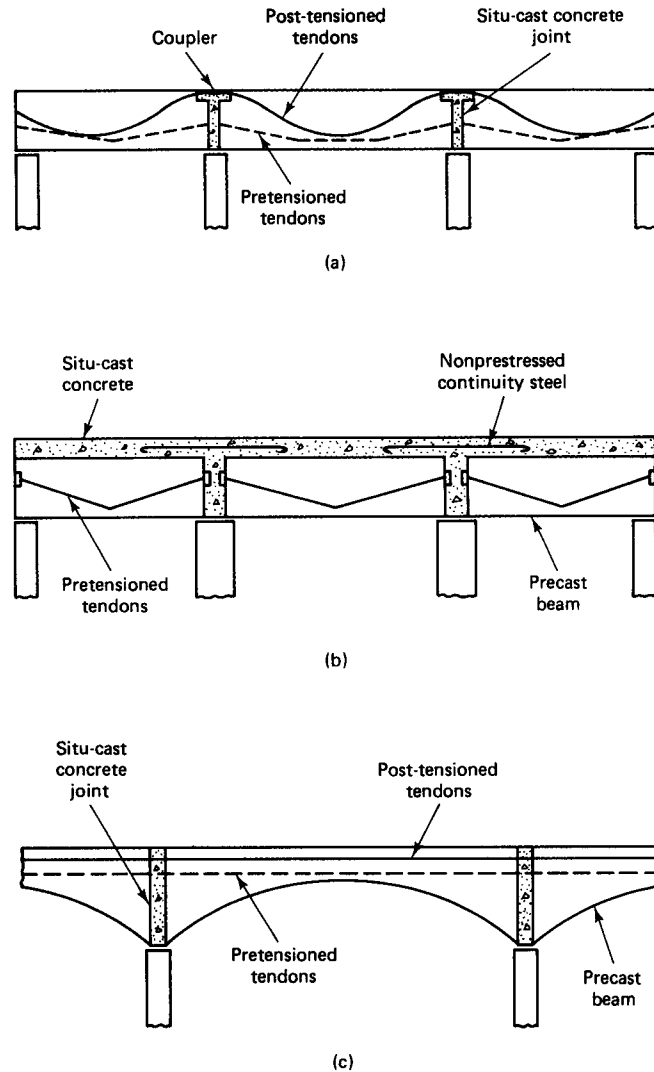
Figure 6.1 schematically demonstrates the various systems and combinations of systems to achieve monolithic continuity. Figure 6.2 illustrates how continuity is achieved in nonmonolithic construction. Figure 6.1(a) presents a simple continuity system in which all the spans are situ cast and post-tensioning is accomplished after the concrete hardens. Problems are encountered, however, in the accurate evaluation of frictional losses due to the large number of bends. The system shown in Figure 6.1(b), using variable-depth beams, namely, nonprismatic sections, can add to the cost of formwork.

Frictional losses in the post-tensioned straight cables are easier to evaluate accurately. Additional costs are incurred due to the necessity of several anchorages. The system shown in Figure 6.1(a) has the advantage on that of Figure 6.1(b) in that the cost of formwork will in general be less because the continuous beam has a constant depth, although architectural considerations sometimes require nonprismatic continuous sections.

Continuity achieved through the use of precast pretensioned beams with situ-cast concrete connecting joints can in many cases be easier to erect, and considerable savings may accrue since formwork and shoring at the site are generally not needed. Figures 6.2(a) and (c) are essentially comparable in the degree of their accuracy in estimating frictional and other losses.



**Figure 6.1** Tendon geometry in beams with monolithic continuity. (a) Beam with constant depth. (b) Nonprismatic beam with overlapping tendons. (c) Prismatic beam with overlapping tendons.



**Figure 6.2** Continuity using precast prestressed beams. (a) Post-tensioned continuity using couplers. (b) Continuity using nonprestressed steel. (c) Continuity in post-tensioning for nonprismatic beams.

The system illustrated in Figure 6.2(b) is probably the simplest for achieving continuity in prestressed concrete composite construction. The precast prestressed elements are designed to carry the prestressing and self-weight moments, while the nonprestressed steel at the negative moment region at the support is designed to resist the additional superimposed dead load and the applied live load moments. If design for continuity due to the total dead load is to be achieved, the precast beams have to be shored before placing the composite concrete topping.

In general, precast elements, including those shown in Figures 6.2(a) and (c), are designed to resist their own weight as well as handling and transportation stresses by the strength provided in pretensioning. Post-tensioning or the use of nonprestressed steel at the supports provides the strength required to resist the live load and superimposed load stresses, and no shoring is used in the construction process.

## 6.4 ELASTIC ANALYSIS FOR PRESTRESS CONTINUITY

### 6.4.1 Introduction

Reinforced concrete structures are usually statically indeterminate due to the continuity provided by monolithic construction. Advantageously, the bending moments are always smaller than those of comparable statically determinate beams, leading to shallower, more economical sections. Deformations due to axial loads are usually ignored except in very stiff members, and the settlement of the supports is also rarely considered since creep and shrinkage do not cause major stresses.

In prestressed concrete, continuity also leads to reduced bending moments. However, the bending moments due to the eccentric prestressing forces cause *secondary reactions* and secondary bending moments. These secondary forces and moments increase or decrease the primary effect of the eccentric prestressing forces. Also, the effects of elastic shortening, shrinkage, and creep become considerable as compared to those in reinforced concrete continuous structures.

Because prestressed elements, including those that are partially prestressed, have very limited flexural cracking as compared with reinforced concrete elements, the elastic theory for indeterminate structures can be applied with sufficient accuracy at the limit state of service load. In other words, the prestressed elements can be essentially considered homogenous elastic material because of the limited cracking level, whereas in reinforced concrete it would not be rational to make such an assumption since flexural cracks start to generate at almost 5 to 10 percent of the failure load.

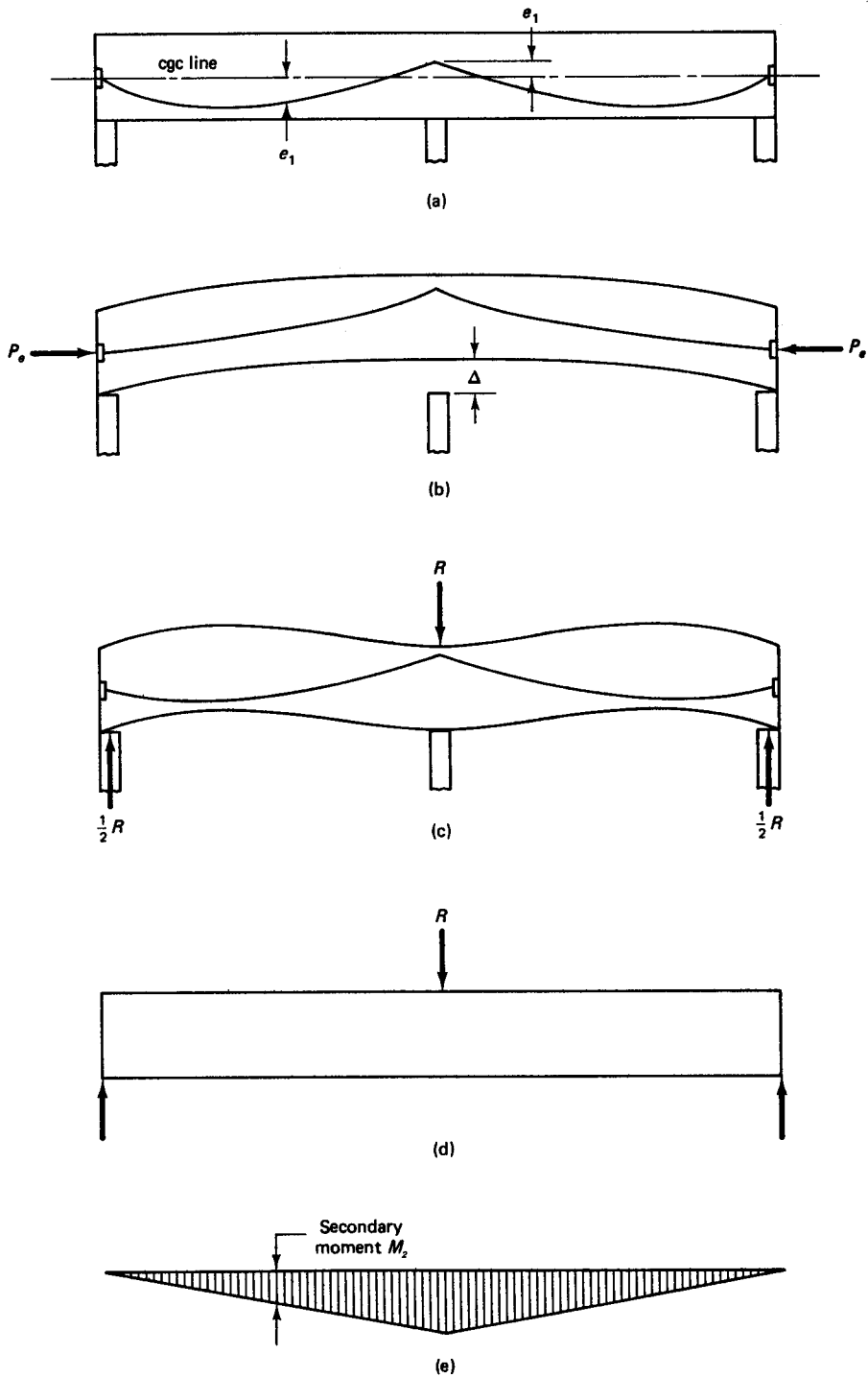
### 6.4.2 Support Displacement Method

Figure 6.3(a) shows a two-span continuous prestressed concrete beam. In part (b), the central support is assumed to have been removed. Because of the induced *secondary* force or reaction  $R$  at the internal support caused by the eccentric prestress, the original moments due to prestressing, namely,  $M_1 = P_e e_1$ , will be called *primary moments*, and the moments  $M_2$  caused by the induced reactions will be called *secondary moments*. The effect of the secondary moment is to shift the location of the line of thrust, the C-line, at the intermediate supports of the continuous structure, and to return the beam section at the support to its original position before prestressing [see Figure 6.3(c)]. The line of thrust is the center line of compressive force acting along the beam span. The secondary reaction  $R$  causes the camber  $\Delta$  to be neutralized and the beam to be held down at the intermediate support by an equal but opposite reaction  $R$ , provided that the C-line at the intermediate support is above the cgc line. If the two lines coincide, the reaction  $R$  will be zero, as explained in Section 6.6

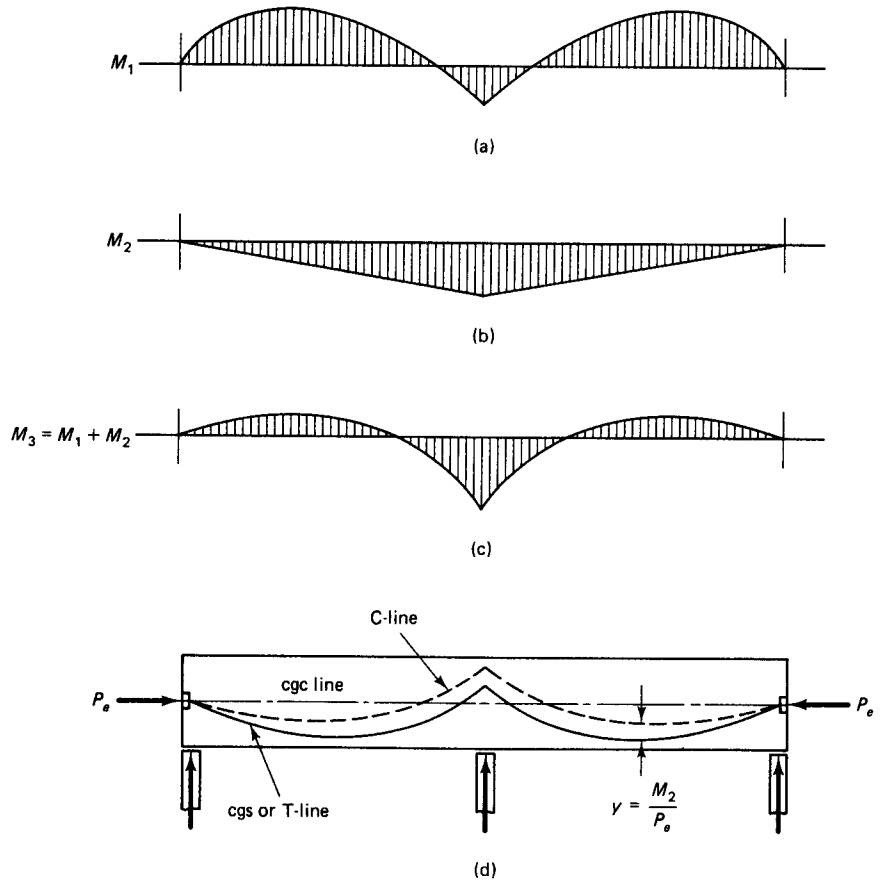
The primary structure bending moment diagram  $M_1$  due to the prestressing force is shown in Figure 6.4(a). If it is superimposed on the secondary moment diagram  $M_2$  in Figure 6.4(b), a resulting moment diagram  $M_3 = (M_1 + M_2)$  [Figure 6.4(c)] is generated due to the prestressing force for the condition where the beam lower fibers just touch the intermediate support, with the thrust line (C-line) moving a distance  $y$  from the tendon cgs profile, i.e., the T-line [Figure 6.4(d)]. As a sign convention, the bending moments diagrams are drawn on the *tension* side of the columns. Such a convention can help eliminate errors in superposition in the analysis of portal frames and other systems whose vertical members are subjected to moments.

The deviation of the C-line from the cgs line is

$$y = \frac{M_2}{P_e} \quad (6.1)$$



**Figure 6.3** Secondary moments in continuous prestressed beams. (a) Tendon profile prior to prestressing. (b) Profile after prestressing if beam is not restrained by central support. (c) Secondary reaction to eliminate uplift or camber. (d) Reaction  $R$  on theoretically simply supported beam. (e) Secondary moment diagram due to  $R$ .



**Figure 6.4** Superposition of secondary moments due only to prestress and transformation of the thrust C-line. (a) Primary moments  $M_1$ . (b) Secondary moments  $M_2$ . (c) Superposition of (b) on (a) to give resulting moment  $M_3$ . (d) Transformation of the C-line from the T-line.

and the new location of the tendon profile cgs is determined from the net moment  $M_3 = M_1 + M_2$  using the appropriate moment sign, positive (+) above and negative (-) below the base line. The resulting limit eccentricity of the C-line is

$$e' = e_3 = \frac{M_3}{P_e} \tag{6.2}$$

where  $P_e$  is the effective prestressing force after losses. Note that  $e'$  is negative when the thrust line is *above* the neutral axis, as is the case for the intermediate support section. The concrete fiber stresses due to prestress only at an intermediate support become, from Equations 1.4a and b,

$$f^t = -\frac{P_e}{A_c} \left( 1 + \frac{e'_e c_t}{r^2} \right) \tag{6.3a}$$

and

$$f_b = -\frac{P_e}{A_c} \left( 1 - \frac{e'_e c_b}{r^2} \right) \tag{6.3b}$$

The concrete fiber stresses at the support due to prestressing and the self-weight support moment are

$$f^t = -\frac{P_e}{A_c} \left( 1 + \frac{e'_e c_t}{r^2} \right) + \frac{M_D}{S^t} \quad (6.4a)$$

and

$$f_b = -\frac{P_e}{A_c} \left( 1 - \frac{e'_e c_t}{r^2} \right) - \frac{M_D}{S_b} \quad (6.4b)$$

Alternatively, using the  $M_3$  moment values in Equations 6.4a and b, the net moment at the section is  $M_4 = M_3 - M_D$ , and the concrete fiber stresses at the support where the tendons are above the neutral axis are evaluated from

$$f^t = -\frac{P_e}{A_c} - \frac{M_4}{S^t} \quad (6.5a)$$

and

$$f_b = -\frac{P_e}{A_c} + \frac{M_4}{S_b} \quad (6.5b)$$

Both Equations 6.4 and 6.5 should give the same results whether applied to support, midspan sections, or any other sections along the span provided that the appropriate sign convention is maintained.

### 6.4.3 Equivalent Load Method

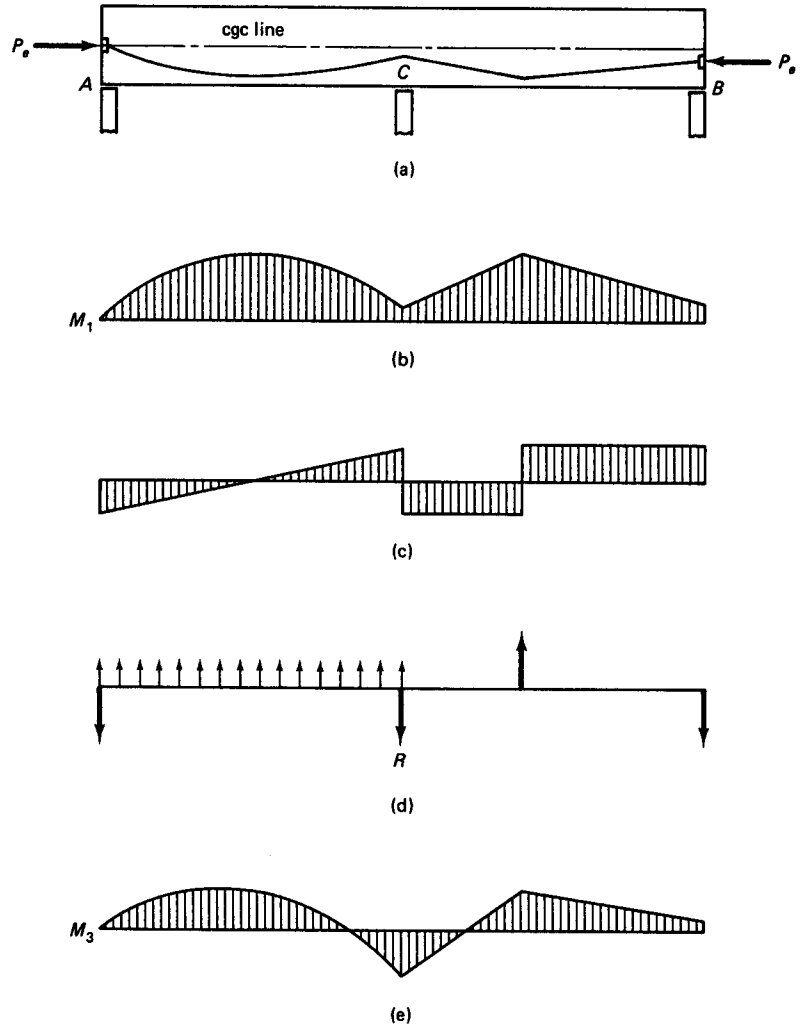
The equivalent load method is based on theoretically replacing the effects of the prestressing force by equivalent loads produced by the prestressing moments profile along the span due to the primary moment  $M_1$  in Figure 6.5(b). If the shear diagram causing moments  $M_1$  is constructed as in Figure 6.5(c), and the load producing this shear is evaluated as in Figure 6.5(d), the reaction  $R$  is the same as the displacement reaction  $R$  in the method described in Section 6.4.1. Calculation of the moment distribution due to the loading on the continuous beam in Figure 6.5(d) produces the moment diagram of moment  $M_3$  in part (e) of the figure. This moment is the same as the net moment  $M_3$  in Section 6.4.1, so that the resulting limit eccentricity of the cgs line will be  $e_3 = M_3/P_e$ . The prestress interior support reaction  $R$  is obtained from Figure 6.5(d) in order to determine the secondary moment  $M_2$  caused by a load  $R$  acting at point  $c$  of a simple span AB. The deviation of the C-line from the cgs line is then  $y = M_2/P_e$ , as in the previous method.

## 6.5 EXAMPLES INVOLVING CONTINUITY

### 6.5.1 Effect of Continuity on Transformation of C-Line for Draped Tendons

#### Example 6.1

A bonded post-tensioned prestressed prismatic beam is continuous on three supports. It has two equal spans of 90 ft (27.4 m), and the tendon profile is shown in Figure 6.6. The effective prestressing force  $P_e$  after losses is 300,000 lb (1,334 kN). The beam overall dimensions are  $b = 12$  in. (30 cm) and  $h = 34$  in. (86 cm). Compute the primary and secondary moments due to prestressing, and find the concrete fiber stresses at the intermediate support C due to the prestressing force. Use both the support displacement method and the equivalent load method; assume that the variation in tension force along the beam can be neglected.

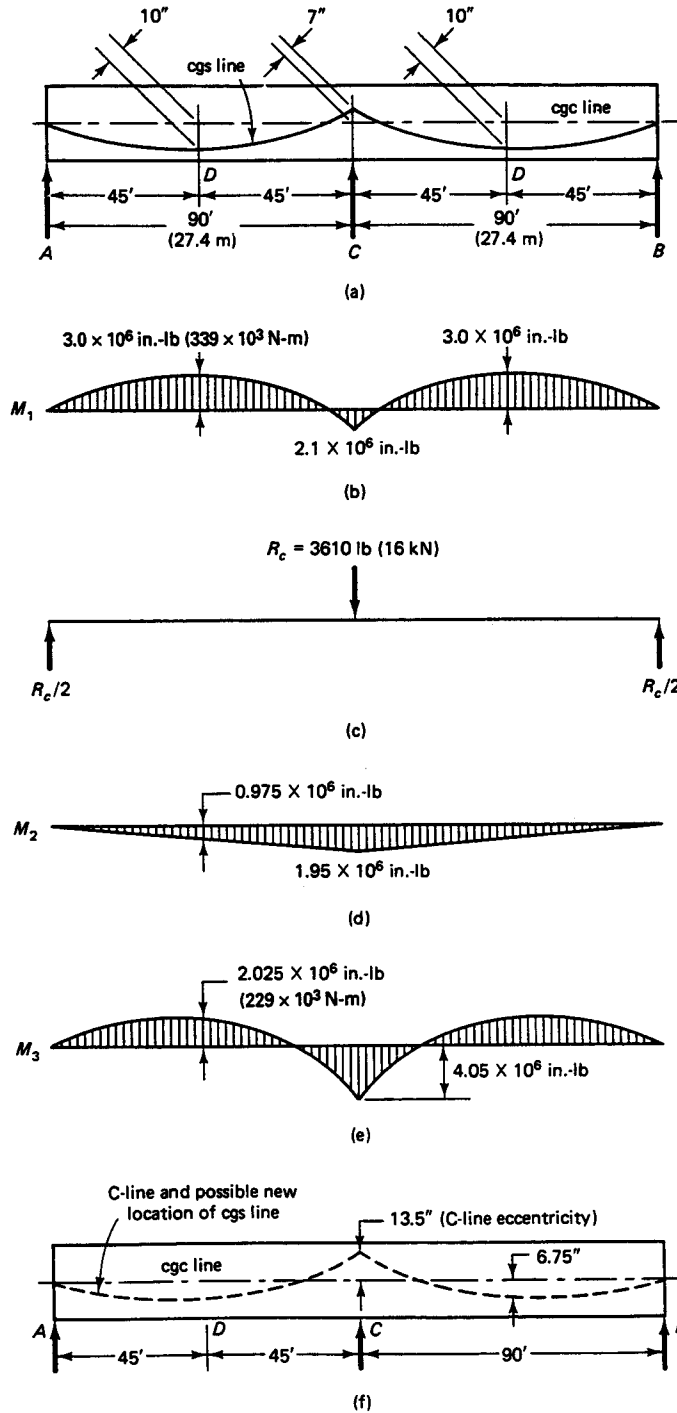


**Figure 6.5** Equivalent load method of C-line transformation. (a) Primary structure after prestressing. (b) Primary moment  $M_1$  due to prestressing. (c) Shear diagram for moments  $M_1$ . (d) Load-causing moment in (b) and shear in (c). (e) Moment diagram for loads in (d) after moment distributions.

**Solution (a):**

**Support Displacement Method.** The primary moment  $M_1$  due to prestressing causes upward *camber* or deflection at the intermediate support C. This camber,  $\Delta_c$ , can be readily obtained from basic mechanics by the moment area method, taking the moments of areas AEC and ADC about point A in Figure 6.7(a) to get the tangential deviation of the elastic curve at A from the horizontal at C as the displacement at C. From the figure,

$$\begin{aligned}
 EI\Delta_c &= \left[ (3.0 \times 10^6 + 1.05 \times 10^6) \frac{90 \times 2}{3} \right] \frac{90}{2} \times 144 \\
 &\quad - \left( \frac{2.1 \times 10^6 \times 90}{2} \right) \frac{90 \times 2}{3} \times 144 \\
 &= 7.58 \times 10^{11} \text{ in}^3\text{-lb}
 \end{aligned}$$



**Figure 6.6** Transformation of thrust line in Example 6.1 due to continuity. (a) Tendon geometry: one possible location. (b) Primary moment  $M_1$  due to prestress  $P_e$ . (c) Reaction  $R$  on theoretically simple beam. (d) Secondary moment  $M_2$  due to  $R$ . (e) Final moment  $M_3 = M_1 + M_2$ . (f) New location of C-line and possible cgs line.



Similarly, from Figure 6.7(c),

$$EI\Delta_c = \frac{45R \times 12 \times 90}{2} \times \frac{90 \times 2}{3} \times 144 = 2.1 \times 10^8 R \text{ in.}^3\text{-lb}$$

Equating the right sides of these equations to each other yields

$$7.58 \times 10^{11} = 2.1 \times 10^8 R$$

Then

$$R_c = \frac{7.58 \times 10^{11}}{2.1 \times 10^8} = 3,610 \text{ lb } \downarrow (16 \text{ kN})$$

$$R_A = R_B = 1,805 \text{ lb } \uparrow (8 \text{ kN})$$

The secondary moment  $M_2$  due to concentrated load  $R_c$  varies linearly from interior support C to end supports A and B in Figures 6.6(d) and 6.7(c). From Figure 6.6(c),

$$M_2 = \frac{R_c}{2} \times 90 \times 12 = \frac{3,610}{2} \times 90 \times 12 = 1.95 \times 10^6 \text{ in.-lb}$$

The total moment  $M_3$  at C due to prestress continuity is

$$M_1 + M_2 = 2.1 \times 10^6 + 1.95 \times 10^6 = 4.05 \times 10^6 \text{ in.-lb}$$

From Equation 6.1, the distance through which the C-line has to be transformed upwards at support C is

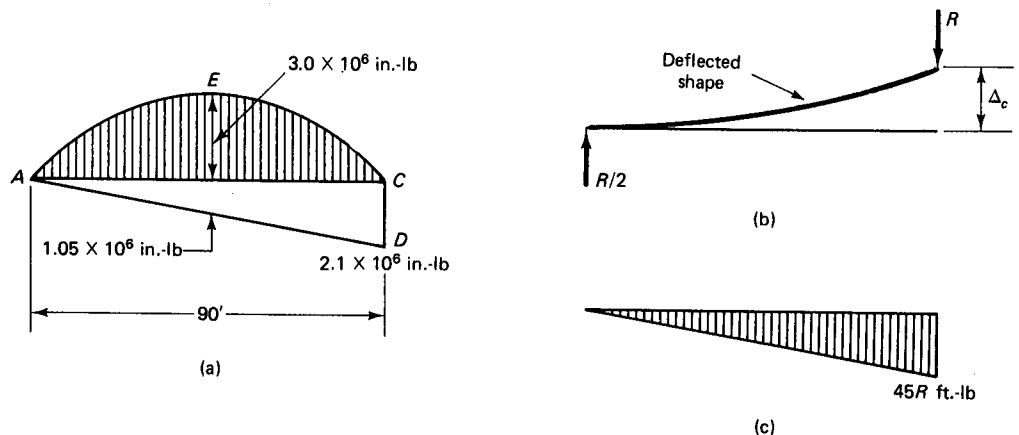
$$y_c = \frac{M_2}{P_e} = \frac{1.95 \times 10^6}{300,000} = 6.5 \text{ in. (16.5 cm)}$$

From Equation 6.2, the distance of the C-line above the cgc line, i.e., the eccentricity of the C-line above the cgc line at interior support C, is

$$e_c = \frac{M_3}{P_e} = \frac{4.05 \times 10^6}{300,000} = 13.5 \text{ in. (34.3 cm)}$$

The midspan total moment is

$$\begin{aligned} M_3 &= 3.0 \times 10^6 - \frac{1}{2} \times 1.95 \times 10^6 \\ &= 2.025 \times 10^6 \text{ in.-lb} \end{aligned}$$



**Figure 6.7** Camber  $\Delta_c$  due to  $M_1$ . (a) Primary moment  $M_1$ . (b) Deflected shape due to  $R$ . (c) Secondary moment  $M_2$  due to  $R$ .

and the C-line eccentricity is

$$e_D = \frac{2.025 \times 10^6}{300,000} = 6.75 \text{ in. (17.1 cm)}$$

*Concrete Fiber Stresses at Interior Support C due to Prestress Only*

$$c_t = c_b = \frac{34}{2} = 17 \text{ in.}$$

$$e_c = 13.5 \text{ in.}$$

$$A_c = bh = 12 \times 34 = 408 \text{ in.}^2$$

$$I_c = \frac{bh^3}{12} = \frac{12(34)^3}{12} = 39,304 \text{ in.}^4$$

$$r^2 = \frac{I_c}{A_c} = \frac{39,304}{408} = 96.33 \text{ in.}^2$$

From Equations 6.3a and b, the top concrete fiber stress is

$$\begin{aligned} f^t &= -\frac{P_e}{A_c} \left( 1 + \frac{ec_t}{r^2} \right) \\ &= -\frac{300,000}{408} \left( 1 + \frac{13.5 \times 17}{96.33} \right) \\ &= -2,487 \text{ psi (C) (17.1 MPa)} \end{aligned}$$

and the bottom concrete fiber stress is

$$\begin{aligned} f_b &= -\frac{P_e}{A_c} \left( 1 - \frac{ec_b}{r^2} \right) \\ &= -\frac{300,000}{408} \left( 1 - \frac{13.5 \times 17}{96.33} \right) \\ &= +1,016 \text{ psi (T) (7.0 MPa)} \end{aligned}$$

Although the bottom fiber stress in tension is higher and well beyond the maximum allowable, it is only due to prestress. Once self-weight is considered, it diminishes considerably.

**Solution (b):**

**Equivalent Load Method.** From Equation 1.16 for load balancing,

$$W_b = \frac{8Pa}{l^2}$$

where  $a$  is the eccentricity of the tendon from the cgc line. So

$$W_b = \frac{8 \times 300,000 \times 13.5}{(90)^2 \times 12} = 333.3 \text{ lb/ft}$$

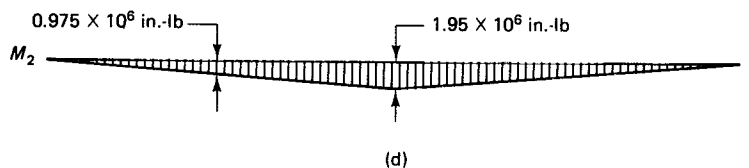
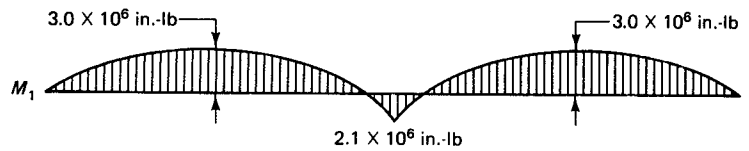
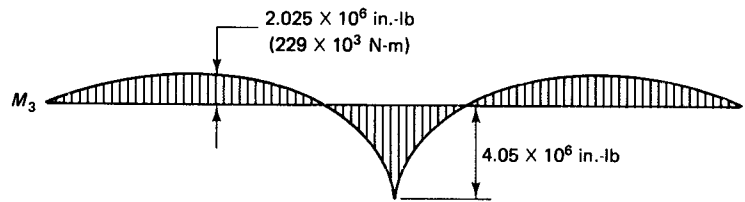
$$\text{FEM} = \frac{W_b l^2}{12} = \frac{333.3(90)^2}{12} = 224,978 \text{ ft-lb}$$

From the moment distribution operation in Figure 6.8, the final moment at the interior support C is  $M_3 = M_1 + M_2 = 337,467 \text{ ft-lb} = 4.05 \times 10^6 \text{ in.-lb}$ , which is the same value as solution (a).

Since the  $M_1$  diagram is the primary moment diagram as in Figure 6.6(b), the diagram for the secondary moment  $M_2$  can be constructed from  $M_3 - M_1$  as shown in Figure 6.8(b), which is identical to Figure 6.6(d). Thereafter, all other steps for calculation of fiber stresses and location of both fiber stresses and the C-line are identical and give the same results as solution (a).

	$W_b$ 333.3 lb/ft (4.87 kN/m)			
	A	D	C	B
	45'	45'	45'	45'
Dist. factor	1.00	0.50		1.00
FEM (ft-lb)	+224,978	-224,978	+224,978	-224,978
	-224,978	-112,489	+112,489	+224,978
$M_3$	0	-337,467	+337,467 ft-lb ( $4.05 \times 10^6$ in.-lb)	0

(a)



**Figure 6.8** Equivalent load method for continuous beam analysis. (a) Equivalent load and moment distribution. (b) Total moment  $M_3$ . (c) Primary moment  $M_1$ . (d) Secondary moment  $M_2$ .

**6.5.2 Effect of Continuity on Transformation of C-line for Harped Tendons**

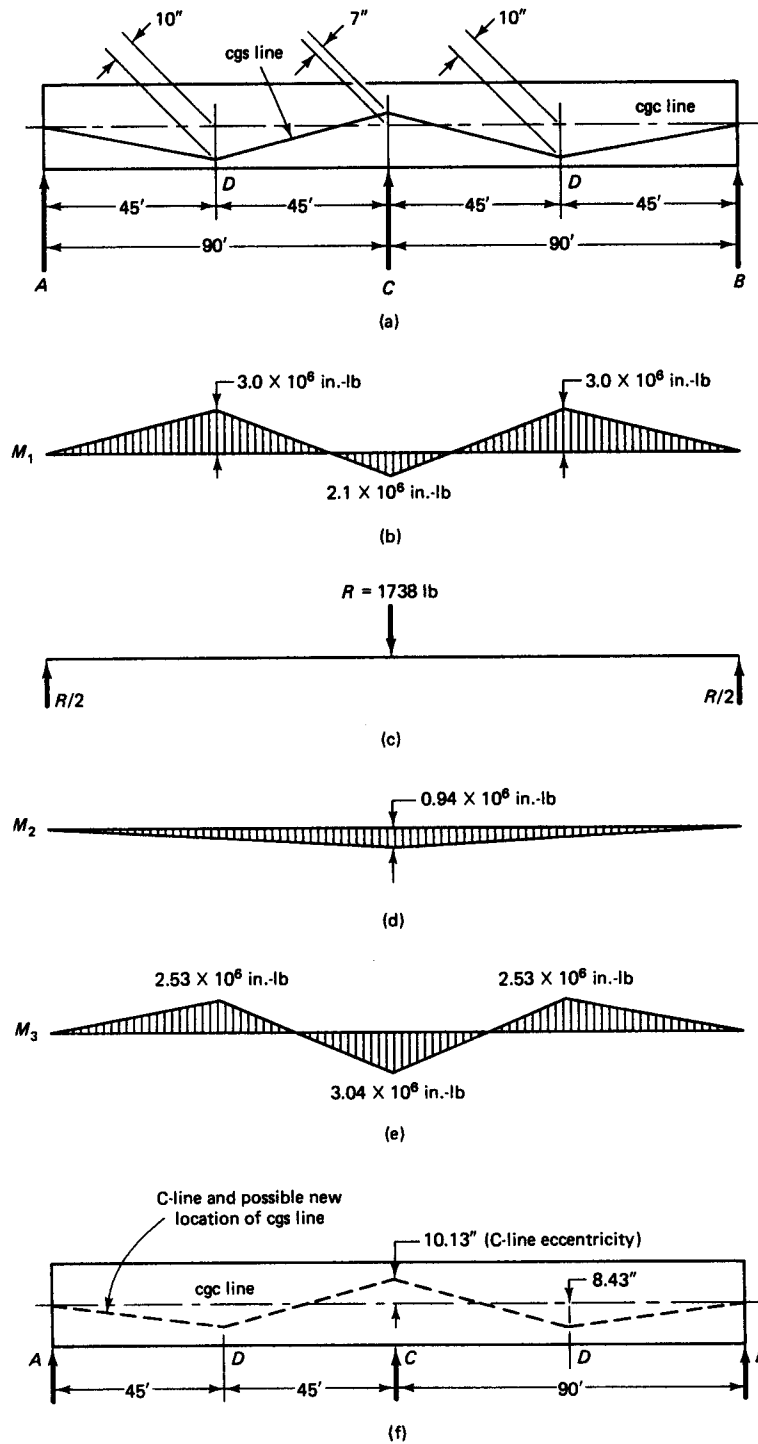
**Example 6.2**

Solve Example 6.1 assuming that the prestressing tendon is harped at the midspan of both adjacent spans. Use the support displacement method in your solution.

**Solution:** Construct the primary and secondary moment diagram shown in Figure 6.9. Then

$$EI\Delta_c = (3.0 \times 10^6 + 1.05 \times 10^6)90 \times \frac{1}{2} \times \frac{90}{2} \times 144 - \frac{2.1 \times 10^6 \times 90}{2} \times \frac{90 \times 2}{3} \times 144 = 3.65 \times 10^{11} \text{ in.}^3\text{-lb}$$

From Figure 6.7 (c),



**Figure 6.9** Transformation of thrust line in Example 6.2 due to continuity. (a) Tendon geometry: one possible location. (b) Primary moment  $M_1$  due to prestress  $P_e$ . (c) Reaction  $R$  on theoretically simple beam. (d) Secondary moment  $M_2$  due to  $R$ . (e) Final moment  $M_3 = M_1 + M_2$ . (f) New location of C-line and possible cgs line.

$$EI\Delta_c = 2.1 \times 10^8 R_c$$

$$R_c = \frac{3.65 \times 10^{11}}{2.1 \times 10^8} = 1,738 \text{ lb} \downarrow$$

The secondary moment ordinate at interior support C is

$$M_2 = \frac{R}{2} \times 90 \times 12 = \frac{1,738}{2} \times 90 \times 12 = 0.94 \times 10^6 \text{ in.-lb}$$

Thus, the total moment  $M_3 = 2.1 \times 10^6 + 0.94 \times 10^6 = 3.04 \times 10^6 \text{ in.-lb}$  ( $344 \times 10^3 \text{ N-m}$ ).

From Equation 6.1, the distance through which the C-line has to be transformed upwards at support C is

$$y_c = \frac{M_2}{P_e} = \frac{0.94 \times 10^6}{300,000} = 3.13 \text{ in. (8 cm)}$$

From Equation 6.2, the distance of the C-line above the cgc line, i.e., the eccentricity of the C-line above the cgc line at interior support C, is

$$e_c = \frac{M_3}{P_e} = \frac{3.04 \times 10^6}{300,000} = 10.13 \text{ in. (25.7 cm)}$$

So the midspan total moment is

$$M_3 = 3.0 \times 10^6 - \frac{0.94 \times 10^6}{2} = 2.53 \times 10^6 \text{ in.-lb}$$

and the C-line eccentricity is

$$e_D = \frac{2.53 \times 10^6}{300,000} = 8.43 \text{ in. (21.4 cm)}$$

**Concrete Fiber Stresses at Interior Support C Due to Prestress Only.**  $e_c = 10.13 \text{ in.}$  for the C-line or thrust line. So the top concrete fiber stress is

$$\begin{aligned} f^t &= -\frac{P_e}{A_c} \left( 1 + \frac{ec_t}{r^2} \right) \\ &= -\frac{300,000}{408} \left( 1 + \frac{10.13 \times 17}{96.33} \right) \\ &= -2,049 \text{ psi (C) (14.1 MPa)} \end{aligned}$$

and the bottom concrete fiber stress is

$$\begin{aligned} f_b &= -\frac{P_e}{A_c} \left( 1 - \frac{ec_b}{r^2} \right) \\ &= -\frac{300,000}{408} \left( 1 - \frac{10.13 \times 17}{96.33} \right) \\ &= +579 \text{ psi (T) (4.0 MPa)} \end{aligned}$$

Comparing the results of the harped tendon case of this example to the draped parabolic tendon of Example 6.1 reveals that smaller total continuity moments  $M_3$  resulted at the intermediate support since the triangular area of the moment diagram is one-half the product of the span and the moment ordinate while the parabolic area is two-thirds of that same product. Consequently, the concrete fiber stresses are lower.

## 6.6 LINEAR TRANSFORMATION AND CONCORDANCE OF TENDONS

It can be recognized from the discussion in Section 6.4 that the profile of the line of thrust (the C-line) follows the profile of the prestressing tendon (the cgs line). This is to be expected since the C-line ordinates are the moment ordinates resulting from the product of

the prestressing force  $P_e$  and the tendon eccentricity from the cgc line varying along the span. The deflection behavior of any beam is a function of the variation in moment along the span, and the shape of the moment diagram is a function of the type of load, namely, concentrated or distributed. Consequently, tendon profiles are often draped for distributed loads, while they are harped for concentrated loads, as illustrated in Chapters 1 and 4.

Examples 6.1 and 6.2 show that in a continuous beam, the deviation of the C-line from the cgc line is directly proportional to the secondary moment  $M_2$ . Since the  $M_2$  diagram varies *linearly* with the distance from the support, it is possible to *linearly* transform the C-line by raising or lowering its position at the *interior* support while preferably maintaining its original position at the exterior simple supports. The profile of the C-line remains the same because of the linearity of the transformation. Consequently, it is possible to linearly transform the cgs line, i.e., the prestressing tendon profile along the beam span, without changing the profile positions of the C-line. This flexibility has major practical significance in the design of continuous prestressed concrete beams.

Example 6.3 demonstrates such a flexibility. Compare the tendon profile it presents with that of Example 6.1, and note that the C-line in Figure 6.6(f) is the same as the C-line in Figures 6.10(f) and 6.11(f), although the cgs line locations along the span are not the same as those in Figures 6.6(a), 6.10(a), and 6.11(a). Also, note that in solution b, where the tendon profile coincides with the C-line profile, the reaction  $R = 0$  and the secondary moment  $M_2 = 0$ . This means that when the cgs line *coincides* with C-line, the beam just touches the intermediate support and behaves like a simply supported beam. Such a beam is called a *concordant beam*, and the prestressing tendon is called a *concordant tendon*.

### 6.6.1 Verification of Tendon Linear Transformation Theorem

#### Example 6.3

The continuous beam of Example 6.1 has a new tendon profile as shown in

- (a) Figure 6.10(a) with eccentricities  $e_c = 0$  and an eccentricity  $e_D = 13.5$  in. (24.3 cm) at midspan similar to the intermediate support eccentricity in Example 6.1, and
- (b) Figure 6.11(a) with eccentricities  $e_c = 13.5$  in. (24.3 cm) and  $e_D = 6.75$  in. (17.1 cm) that are the same C-line eccentricities as in Example 6.1.

Verify that the profile and alignment of the C-line in (a) and (b) are the same as the C-line geometry in Example 6.1 and Figure 6.6(f). The total moment at the intermediate support C in both cases is  $M_3 = 4.05 \times 10^6$  in.-lb, and at midspan D the moment is  $M_3 = 2.025 \times 10^6$  in.-lb, as in Example 6.1.

**Solution (a):** The secondary moment is

$$M_2 = 4.05 \times 10^6 \text{ in.-lb} (458 \times 10^3 \text{ N-m})$$

Also,

$$\frac{R_c}{2} \times 90 \times 12 = 4.05 \times 10^6$$

$$R_c = \frac{4.05 \times 10^6 \times 2}{90 \times 12} = 7,500 \text{ lb} (33.4 \text{ kN}) \downarrow$$

$$R_A = R_B = 3,750 \text{ lb} (16.7 \text{ kN}) \uparrow$$

**Solution (b):** Both  $M_2 = 0$  and  $R = 0$ .

It can be seen from both solution (a) in Figure 6.10 and solution (b) in Figure 6.11 that the C-line coordinates are the same and close to the values obtained in Example 6.1. The

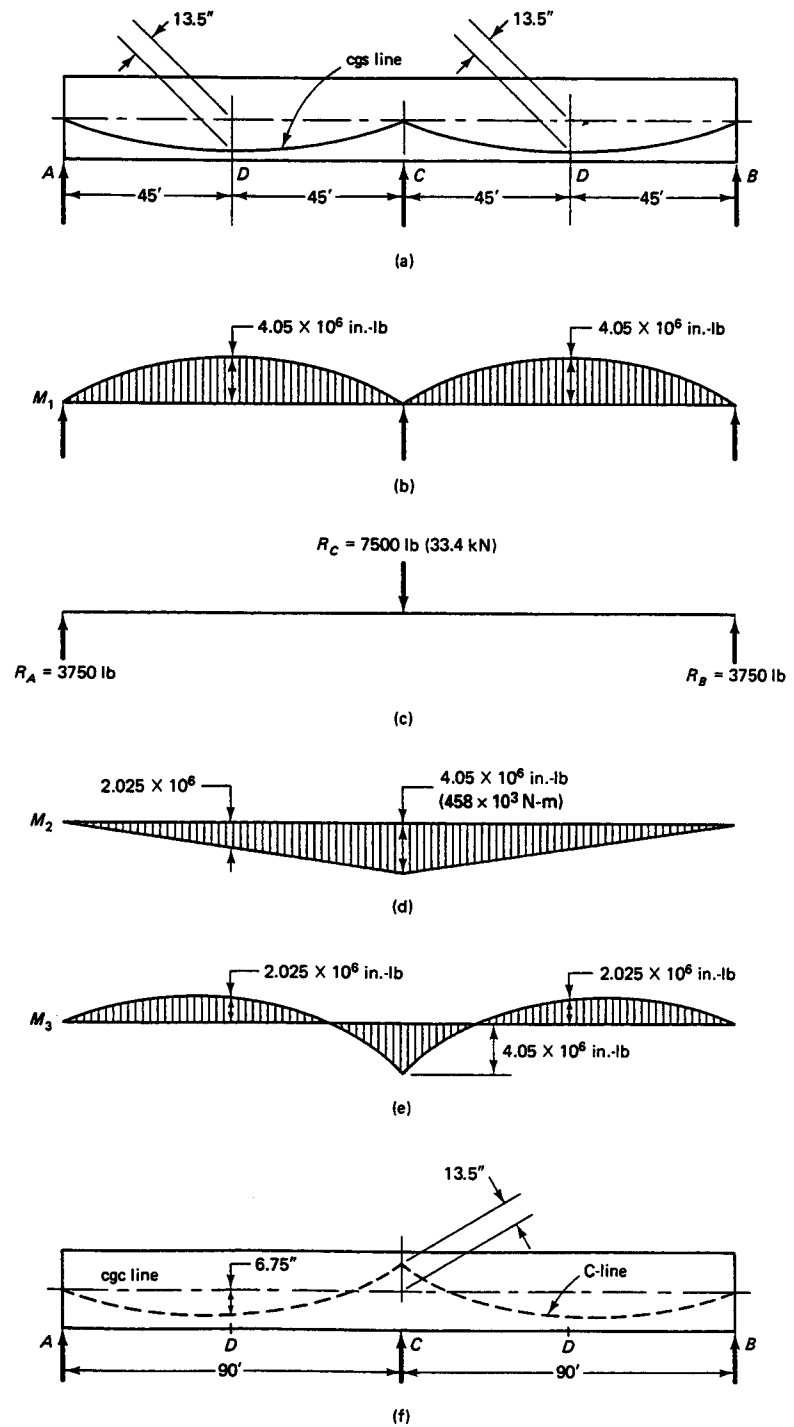


Figure 6.10 Tendon transformation in Example 6.3 (alternative a).

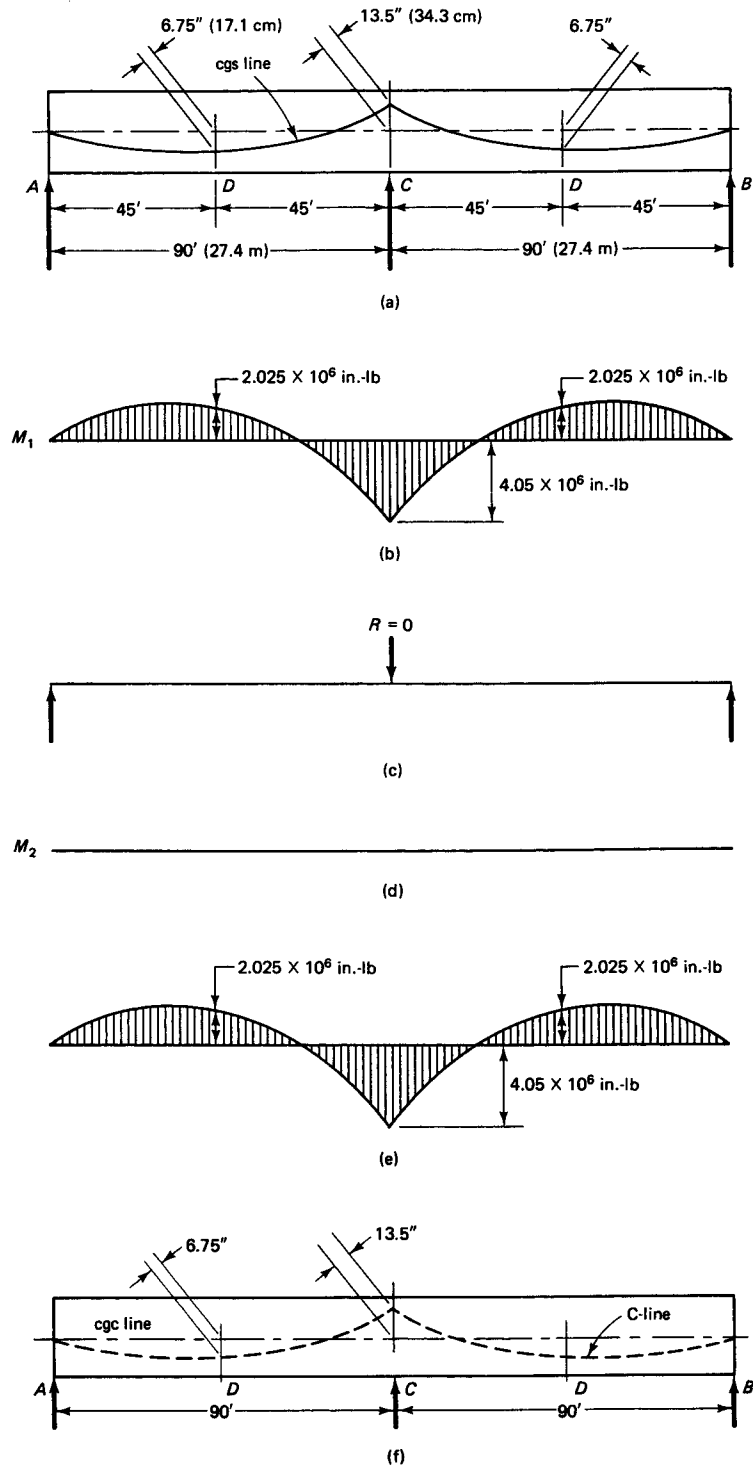


Figure 6.11 Tendon transformation in Example 6.3 (alternative b).



fiber stresses are also the same, viz.,  $f^t = -2,487$  psi (C) (17.1 MPa) and  $f_b = +1,016$  psi (T) (7.0 MPa).

### 6.6.2 Concordance Hypotheses

The following list summarizes the hypotheses defining the transformation and concordance of tendons in continuous prestressed beams:

1. Any tendon profile can be linearly transformed without affecting the C-line position.
2. A beam with a concordant tendon is a continuous beam whose C-line coincides with its cgs line.
3. A concordant tendon induces no reactions on intermediate supports.
4. The eccentricity of any concordant tendon measured from the cgc line produces a moment diagram representing a profile similar in form to the moment profile due to the superimposed load.
5. Any line of thrust (C-line) is a profile for a concordant tendon.
6. Superposition of several concordant tendons produces a concordant tendon, but superposition of concordant and nonconcordant tendons produces a nonconcordant tendon.
7. A change in eccentricity at one or both *end* supports results in a shift of the C-line, but a change in eccentricity at *intermediate* supports does not affect the position of the C-line.
8. The choice of concordance or nonconcordance is determined by concrete cover and efficiency in beam depth selection. Bending moments and shear diagrams for superposition of transverse loads on continuous beams is shown in Figure 6.12.

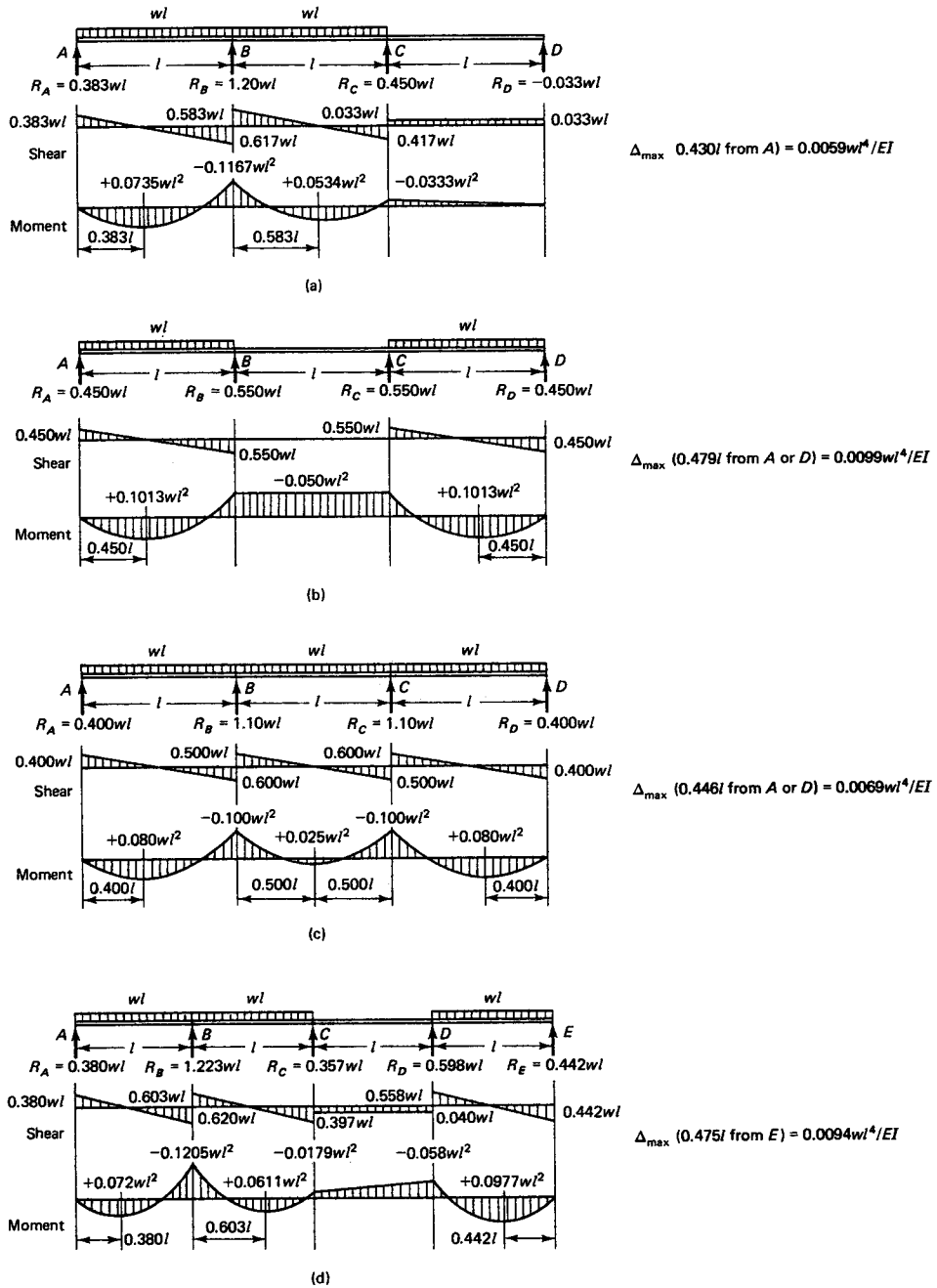
It is advisable to start a design assuming concordance in order to eliminate the need for calculating the secondary moment  $M_2$ . By trial and adjustment, one can arrive at the final beam section depth that fulfills the design requirements with the cgs location either concordant or nonconcordant, as the final design dictates.

## 6.7 ULTIMATE STRENGTH AND LIMIT STATE AT FAILURE OF CONTINUOUS BEAMS

### 6.7.1 General Considerations

The service-load design of continuous prestressed beams assumes *elastic* behavior of the material up to the limit of allowable tensile stress in the concrete due to all loads. This limit in tensile stress is based on allowing some limited cracking beyond the first cracking load as determined by the modulus of rupture of concrete. As cracking becomes more effective during overload conditions, internal plastic deformation at the critical regions of maximum or peak moments and plastic redistribution of elastic moments from the negative to the positive moment regions are generated. At this stage of overload and beyond, up to the limit state at failure, plastic hinging develops at the most highly stressed regions in the continuous beam.

Total redistribution and full development of plastic hinges at the continuous supports of a fully bonded prestressed beam render the beam statically determinate, as if concordance of tendons were present with zero moments at the supports. Theoretically, in such cases the secondary moments  $M_2$  can be disregarded beyond the first cracking load. However, such an assumption can result in an unsafe design unless a concordant tendon is assumed from the beginning and is executed in the final design with no overload conditions permitted. Otherwise, it is important to consider the secondary moment



**Figure 6.12** Bending moments and shear diagrams for continuous beams. (a) Continuous beam, three equal spans, one end span unloaded. (b) Continuous beam, three equal spans, end spans loaded. (c) Continuous beam, three equal spans, all spans loaded. (d) Continuous beam, four equal spans, third span unloaded. (e) Continuous beam, four equal spans, first and third spans loaded. (f) Continuous beam, four equal spans, all spans loaded. (g) Continuous beam, two equal spans, concentrated load at center of one span. (h) Continuous beam, two equal spans, concentrated load at any point.

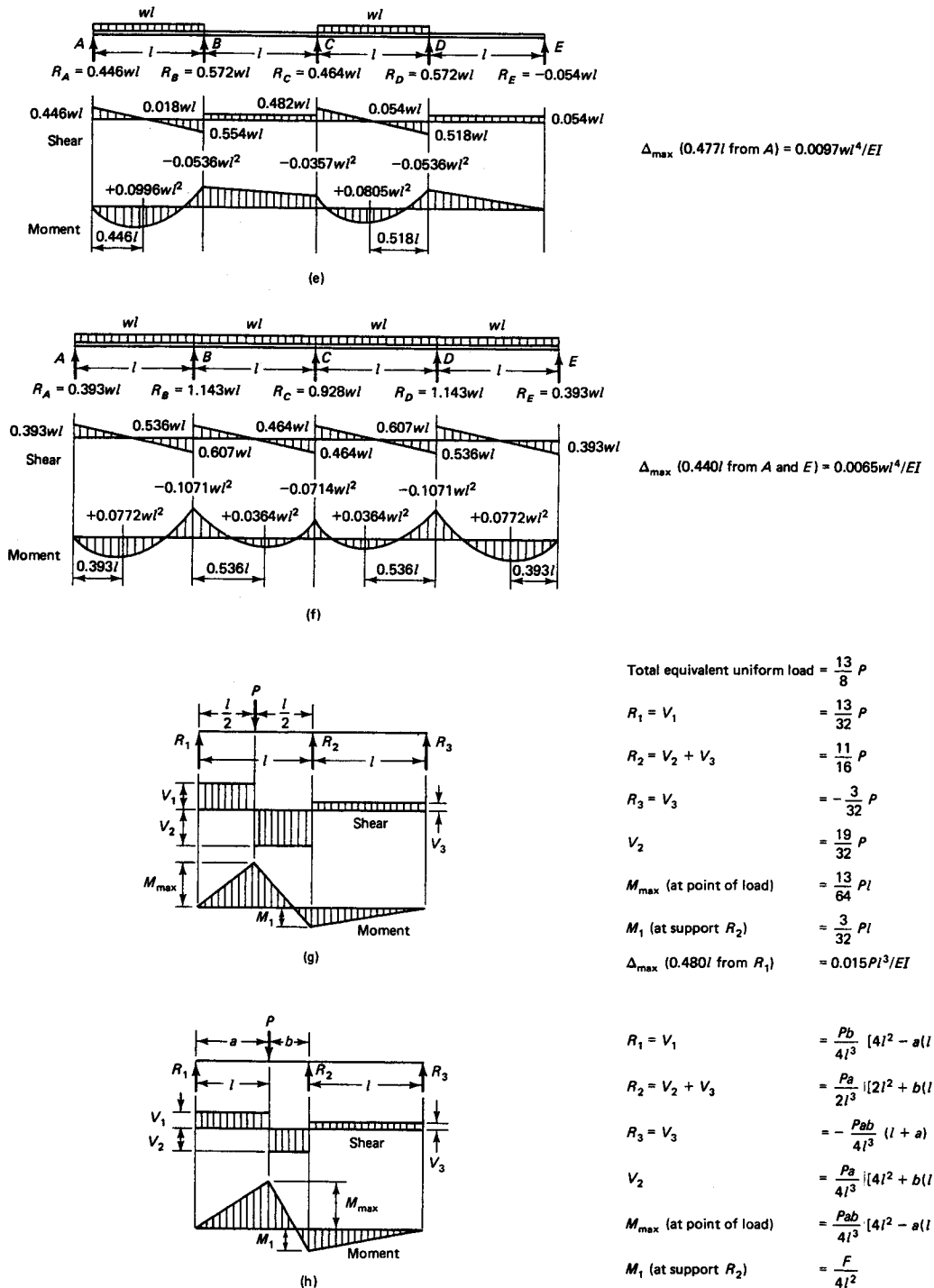


Figure 6.12 Continued



**Photo 6.1** Seven Mile Bridge, Florida Keys. (Courtesy, Post-Tensioning Institute.)

$M_2$  due to prestressing up to the limit state of the failure load, but with a load factor of 1.0. Considering the secondary moments is mandated by the fact that the elastic deformation caused by the nonconcordant tendons changes the amount of *inelastic* rotation required to obtain a given amount of redistribution. Conversely, for a beam with a given elastic rotational capacity, the amount by which the moment at the support may be varied is changed by an amount equal to the secondary moment at the support due to prestressing (Ref. 6.2).

In order to determine the moments to be used in the design, the following sequence of steps is recommended:

1. Determine the moments due to the dead and live loads at factored load level.
2. Modify by algebraic addition of secondary moments  $M_2$  due to prestressing.
3. Redistribute as permitted. A positive secondary moment at the support caused by transforming a tendon downwards from a concordant profile will therefore *reduce* the negative moments near the supports and *increase* the positive moment in the midspan region. A tendon that is transformed upwards will have a reverse effect.

### 6.7.2 Moment Redistribution

The ultimate analysis and design of prestressed concrete members follows the strain limits approach detailed in Section 4.12.3. The net tensile strain limits for compression- and tension-controlled sections shown in Figure 4.5 are equally applicable to prestressed concrete sections. They replace the maximum reinforcement limits used in code provisions prior to the 2002 ACI-318 Code. The net tensile strain for tension-controlled sections, may still be stated in terms of the reinforcement index,  $\omega_p$ , embodied in Equation 4.38b, where the maximum reinforcement index

$$\left[ \omega_p + \frac{d}{d_p} (\omega - \omega') \right]$$

not to exceed  $0.24\beta_1$  for prestressed sections, with a *limit inelastic moment redistribution factor of 1000  $\epsilon_r$* . See Section 4.12.4 for a detailed discussion.

It should be noted that the total amount of prestressed and non-prestressed reinforcement should be adequate to develop a factored load of at least 1.2 times the cracking load computed on the basis of the modulus of rupture  $f_r$ . This provision in ACI 318

Code is permitted to be waived for (a) Two-way, unbonded post-tensioned slabs; and (b) Flexural members with shear and flexural strength at least twice the load level causing the first cracking moment  $M_{cr}$ .

## 6.8 TENDON PROFILE ENVELOPE AND MODIFICATIONS

The envelope for limiting tendon eccentricities for continuous beams can be constructed in the same manner as discussed in Section 4.4.3 for simply supported beams. A determination has to be made as to whether tension is to be allowed in the design in order to establish the limiting maximum and minimum ordinates of the upper and lower envelopes relative to the top and bottom kerns.

The tendon profile at the intermediate supports cannot have the same peak configuration as that of the negative bending moment diagram, due to both design and practical considerations. These considerations include the magnitude of frictional losses that increase with the decrease in the radius of curvature, the high level of compressive stress concentration in cases of abrupt changes in the tendon, and the additional difficulties that can be encountered in post-tensioning. Consequently, it is advisable to modify the tendon profile at the support so as to have a curvilinear transition at the support zone. Such modification has to be accounted for by modifying the primary moment  $M_1$  diagram and the total moment  $M_3$  diagram.

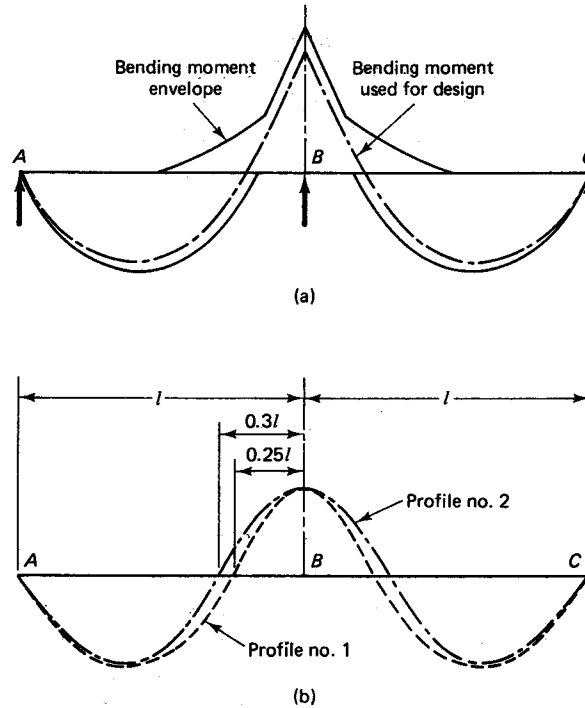
Typical tendon alternative profiles with equal upper and lower eccentricities at the peak moment sections are shown in Figure 6.13, where the chain-dotted line gives the average bending moments used in the service-load design. Selection of the tendon profile should be based on the following considerations:

1. The eccentricity should be as large as possible at the point where the largest bending moment develops at the limit state at failure.
2. Where possible, the total prestressing moment at any section should be sufficient to counteract the average service-load bending moment at that section. The test for this condition should be based on the resulting stress values rather than moment values, since the prestressing force causes axial load stress as well as bending moment stress.
3. A tendon profile alternative that produces the *least* frictional losses should be chosen in the design.
4. It is essential to consider the ultimate-load requirements when selecting the tendon profile; a tendon chosen only on the basis of linear transformation and concordance is not necessarily satisfactory, as it might neither totally fulfill the service-load stress requirements nor fully satisfy the ultimate-load requirements at both the midspan and interior supports.
5. A decrease in eccentricities at the intermediate supports through additional tendon transformation decreases the service-load compressive stresses and can result in allowing additional live-load moments, and hence more live load, *provided* that the midspan profile eccentricity and moments produce satisfactory concrete stresses.

## 6.9 TENDON AND C-LINE LOCATION IN CONTINUOUS BEAMS

### Example 6.4

Design the tendon profile in the beam of Example 4.7, assuming the unshored beam to be continuous over three spans 64 ft (19.5 m) each, with only uniformly distributed live load  $w_L = 1,514$  plf (22.1 kN/m). Consider the post-tensioned prestressing tendon to be continuous



**Figure 6.13** Tendon profile modification. (a) Bending moment diagram for continuous beam. (b) Tendon profile alternatives.

throughout the structure and fully grouted. Disregard tension force variation due to frictional losses in the bends, and assume that a maximum allowable concrete compressive fiber stress  $f_c = 0.45f'_c = 2,250$  psi (15.5 MPa) is reached at the extreme top fibers of the composite section when the live load acts on the section. Use a modified effective width  $b_m = 65$  in. (165 cm) for the compression flange to account for the modular ratio of the topping and precast concrete.

**Solution:**

1. Input data from Example 4.7

(a) Stress data

Precast  $f'_c = 5,000$  psi (34.5 MPa), normal-weight concrete

Topping  $f'_c = 3,000$  psi (20.7 MPa), normal-weight concrete

$$f'_{ci} = 4,000 \text{ psi (27.6 MPa)}$$

$$f_{pu} = 270,000 \text{ psi (1,862 MPa)}$$

$$f_{py} = 243,000 \text{ psi (1,655 MPa)}$$

$$f_{pi} = 189,000 \text{ psi (1,303 MPa)}$$

$$f_{pe} = 0.8(0.7f_{pu}) = 151,200 \text{ psi (1,043 MPa)}$$

$$\gamma = 0.8$$

$$\text{Midspan } f_t = 12\sqrt{f'_c} = 12\sqrt{5,000} = 849 \text{ psi (5.85 MPa)}$$

$$\text{Support } f_t = 6\sqrt{f'_c} = 425 \text{ psi (2.93 MPa)}$$

**(b) Load data**

$$W_D = 583 \text{ plf (8.5 kN/m)}$$

$$W_{SD} = (1\frac{3}{4}/12) \times 7 \text{ ft} \times 150 = 153 \text{ plf (2.2 kN/m) for } 1\frac{3}{4} \text{ in. precast slab formwork}$$

$$W_{CSD} = (4/12) \times 7 \text{ ft} \times 150 = 350 \text{ plf (5.1 kN/m) for 4 in. situ-cast topping}$$

$$W_L = 1,514 \text{ plf (22.1 kN/m) (obtained from } M_L = 9,300,000 \text{ in.-lb)}$$

$$\text{Span} = 64 \text{ ft (19.5 cm)}$$

**(c) Section properties****AASHTO Type III**

Property	Precast	Composite
$A_c$ , in. <sup>2</sup>	560	934
$I_c$ , in. <sup>4</sup>	125,390	297,045
$r^2$ , in. <sup>2</sup>	223.9	318.1
$c_b$ , in.	20.27	31.32
$c_t$ , in.	24.73	13.86
$S_b$ , in. <sup>3</sup>	6,186	9,490
$S_t$ , in. <sup>3</sup>	5,070	21,174
$S_{cbs}$ , in. <sup>3</sup> (bottom of slab)		19,251
$S_{cst}$ , in. <sup>3</sup> (top of slab)		15,288

$$n = E_c (\text{topping}) / E_c (\text{precast}) = 0.77$$

$$\text{Precast } h = 45 \text{ in. (114.3 cm)}$$

$$\text{Transformed } b = 65 \text{ in. (165 cm)}$$

$$\text{Situ-cast } h_f = 5.75 \text{ in. (14.6 cm)}$$

**(d) Prestressing steel**

Twenty-two  $\frac{1}{2}$ -in. dia (12.7 mm dia) 7-wire low-relaxation strands

$$A_{ps} = 22 \times 0.153 = 3.366 \text{ in.}^2 (21.7 \text{ cm}^2)$$

**2. Assume a trial tendon profile location as shown in Figure 6.14**

The prestressing force after losses is

$$P_e = 3.366 \times 151,200 = 508,940 \text{ lb (2,264 kN)}$$

while the primary moment at support B is

$$M_B = P_e \times e_B = 508,940 \times 15 = 7.63 \times 10^6 \text{ in.-lb (862} \times 10^3 \text{ N-m)}$$

The primary moment at midspan  $E_1$  is

$$M_{E_1} = 508,940 \times 9 = 4.58 \times 10^6 \text{ in.-lb}$$

For simplification, the tangential deviation used for computing  $\Delta_B$  is based on assuming the tangent to the elastic curve at B as horizontal.

Taking moments of areas about A in Figure 6.15 yields

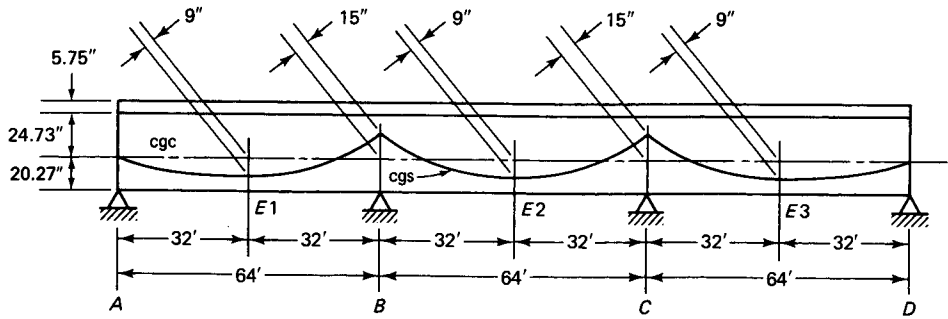


Figure 6.14 Trial profile of the prestressing tendon.

$$\begin{aligned}
 E_c I_c \Delta_B = E_c I_c \Delta_c &= \left[ \left( \frac{7.63}{2} + 4.58 \right) 10^6 \times \frac{64 \times 2}{3} \right] \times \frac{64}{2} \times 144 \\
 &\quad - \left[ \frac{7.63 \times 10^6 \times 64}{2} \right] \times \frac{64 \times 2}{3} \times 144 \\
 &= 15.0 \times 10^{10} \text{ in.-lb}
 \end{aligned}$$

Also,

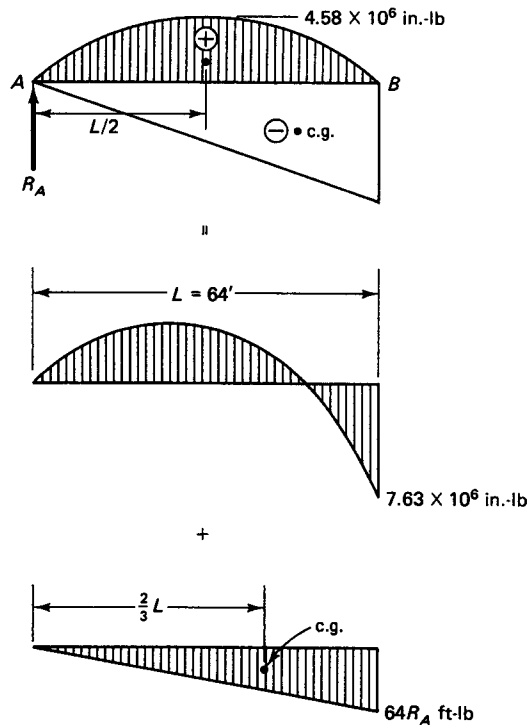


Figure 6.15 Computation of displacement by taking moments of area about support A.



$$E_c I_c \Delta_B = (R_A \times 64 \times 12) \left( \frac{64 \times 12}{2} \right) \left( \frac{64 \times 12 \times 2}{3} \right)$$

$$= 151 \times 10^6 R_B \text{ in.}^3\text{-lb}$$

$$R_A = R_D = \frac{15.0 \times 10^{10}}{151 \times 10^6} = 994 \text{ lb } \uparrow \text{ (By exact calculation = 798 lb)}$$

The secondary moment  $M_2$  at support B is

$$R_A \times 64 \times 12 = 994 \times 64 \times 12 = 0.76 \times 10^6 \text{ in.-lb}$$

The total moment at support B due to prestressing only is

$$\text{Support } M_3 = (7.63 + 0.76) \times 10^6 = 8.39 \times 10^6 \text{ in.-lb (see Figure 6.16)}$$

The C-line eccentricity is

$$e'_B = -\frac{8.39 \times 10^6}{508,940} = -16.49 \text{ in. (41.9 cm)}$$

(The eccentricity  $e'$  of the C-line when it is above the neutral axis is considered negative in order to conform to Equations 6.3a and b.) Finally, the total moment at midspans,  $E_1$ ,  $E_2$ , and  $E_3$  due to prestressing only is

$$\text{Midspan } M_3 = (4.58 - 0.38)10^6 = 4.20 \times 10^6 \text{ in.-lb}$$

and the C-line eccentricity is

$$e'_{E_1} = +\frac{4.20 \times 10^6}{508,940} = +8.25 \text{ in. (21.0 cm)}$$

### 3. Concrete fiber stresses due to prestress and self-weight (583 plf)

Using the moment factors and reaction factors from Figure 6.12, we have

$$M_D \text{ at } B = M_{B1} = 0.10 \times 583(64)^2 \times 12 = 2.87 \times 10^6 \text{ in.-lb}$$

(see Figure 6.17)

$$P_e = A_{ps} f_{pe} = 3.366 \times 151,200 = 508,940 \text{ lb}$$

$$M_D \text{ at } E_1 = 2.12 \times 10^6 \text{ in.-lb (Max. } + M \text{ is not at midspan; hence, calculate } M_{E1} \text{ from the area of the shear diagram)}$$

$$\text{Net } R_B = 1.1W \uparrow - 994 = 1.1 \times 583 \times 64 - 994 = 40,048 \text{ lb}$$

The total support B moment due to prestressing and self-weight is, then,

$$M_4 = M_3 - 2.87 \times 10^6 = (8.39 - 2.87)10^6$$

$$= 5.52 \times 10^6 \text{ in.-lb (624} \times 10^3 \text{ N-m)}$$

#### (i) Support section B or C

The construction process in this stage involves mounting the precast I-beams and prestressing them. The fiber stresses due to prestressing and self-weight, from Equations 6.5a and b, are as follows:

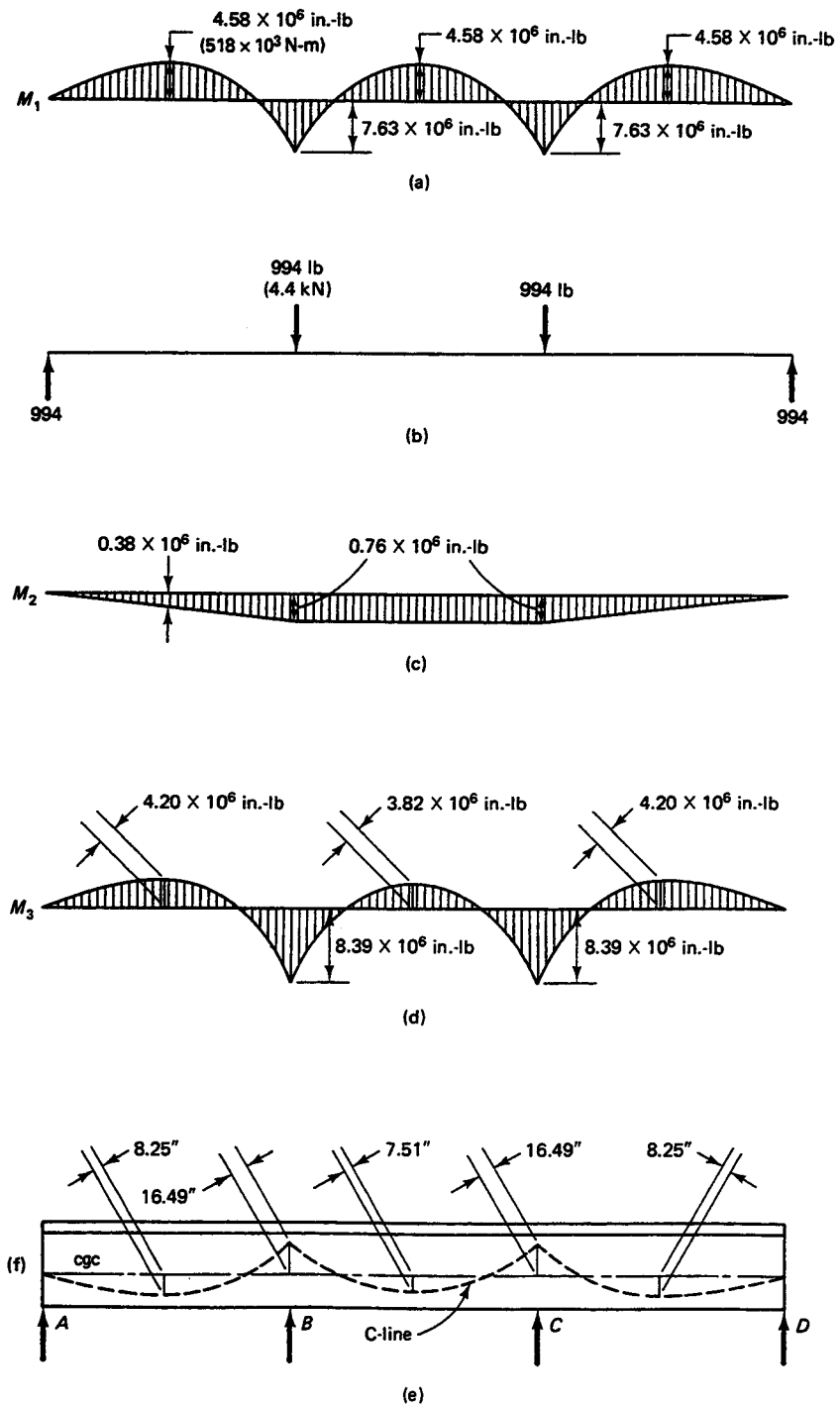


Figure 6.16 Tendon C-line profile in continuous beam of Example 6.4.

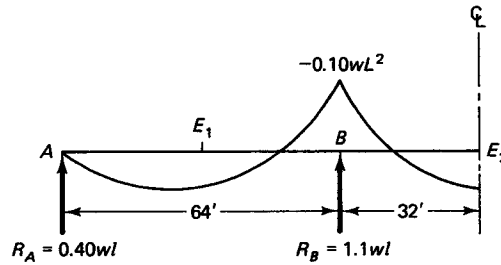


Figure 6.17 Moment diagram due to external load.

$$f'_1 = -\frac{P_e}{A_c} - \frac{M_4}{S^t} = -\frac{508,940}{560} - \frac{5.52 \times 10^6}{5,070} = -908.8 - 1,088.8$$

$$= -1997.6 \text{ psi (C) (13.8 MPa) } < 2,250 \text{ psi, O.K.}$$

$$f_{1b} = -\frac{P_e}{A_c} + \frac{M_4}{S_b} = -\frac{508,940}{560} + \frac{5.52 \times 10^6}{6,186} = -908.8 + 892.3$$

$$= -16.5 \text{ psi (C), no tension, O.K.}$$

Alternatively, the concrete fiber stresses at the support can be computed from Equations 4.1a and b or Equations 6.4a and b using the C-line eccentricities  $e'_e = -16.49$  in. We obtain

$$f'_1 = -\frac{P_e}{A_c} \left( 1 + \frac{e'_e c_t}{r^2} \right) + \frac{M_D}{S^t}$$

$$= -\frac{508,940}{560} \left( 1 + \frac{16.49 \times 24.73}{223.9} \right) + \frac{2.87 \times 10^6}{5,070}$$

$$= -2,564.1 + 566.1 = -1,998 \text{ psi (C) (13.8 MPa)}$$

$$f'_{1b} = -\frac{P_e}{A_c} \left( 1 - \frac{e'_e c_b}{r^2} \right) - \frac{M_D}{S_b}$$

$$= -\frac{508,940}{560} \left( 1 - \frac{16.49 \times 20.27}{223.91} \right) - \frac{2.87 \times 10^6}{6,186}$$

$$= +447.9 - 463.9 = -16.0 \text{ psi (C)}$$

(ii) *Outer span midspan  $E_1$*

The eccentricity at the midspan is  $e'_{E1} = +8.25$  in. Hence,

$$f'_1 = -\frac{P_e}{A_c} + \frac{M_4}{S^t}$$

$$f_{1b} = -\frac{P_e}{A_c} - \frac{M_4}{S_b}$$

Total moment  $M_4$  at  $E_1 = (4.20 - 2.12)10^6 = 2.08 \times 10^6$  in.-lb

$$f'_1 = -\frac{P_e}{A_c} + \frac{M_4}{S^t} = -\frac{508,940}{560} + \frac{2.08 \times 10^6}{5,070}$$

$$= -908.8 + 410.3 = -498.5 \text{ psi (C) (3.4 MPa), O.K.}$$

$$f_{1b} = -908.8 - \frac{2.08 \times 10^6}{6,186} = -1,245 \text{ psi (C) (8.6 MPa), O.K.}$$

Figure 6.16 gives the moments, eccentricities, and C-line geometry of the continuous beam in this example.

4. *Effect of adding the superimposed dead loads on support sections B and C* At this stage of the construction process the 1 $\frac{3}{4}$  in. thick precast slabs ( $W_{SD}$ ) are erected, followed by placing the 4 in. thick layer of wet concrete ( $W_{SD}$ ). Thus,  $W_{SD} = 153 + 350 = 503$  plf (7.3 kN/m). The support moment due to superimposed load is

$$M_{B2} = 0.1wl^2 = 0.1 \times 503(64)^2 \times 12 = -2.47 \times 10^6 \text{ in.-lb}$$

Also,

$$f_2^t = -\frac{P_e}{A_c} - \frac{M_5}{S^t}$$

$$f_{2b} = -\frac{P_e}{A_c} + \frac{M_5}{S_b}$$

$$M_5 = (M_4 - 2.47 \times 10^6) \text{ in.-lb} = 3.05 \times 10^6 \text{ in.-lb}$$

Hence,

$$f_2^t = -908.8 - \frac{3.05 \times 10^6}{5,070} = -1,510.4 \text{ psi (C)}$$

$$f_{2b} = -908.8 + \frac{3.05 \times 10^6}{6,186} = -415.8 \text{ psi (C)}$$

5. *Effects of adding the superimposed live load on support sections B and C* After the concrete cures, resulting in full composite action for supporting the total service live load, the section moduli for the precast beam become

$$S_c^t = 21,714 \text{ in.}^3$$

and

$$S_{cb} = 9,490 \text{ in.}^3$$

The loading combination which causes the highest stress condition is when the load acts on only two *adjacent* spans AB and BC. We have

$$W_L = 1,514 \text{ plf (22.1 kN/m)}$$

including  $W_{CSD}$ . From Figure 6.12, the support moments due to live load on *two adjacent* spans is

$$M_{B3} = 0.1167W_L l^2 = 0.1167 \times 1,514(64)^2 \times 12 = -8.68 \times 10^6 \text{ in.-lb}$$

The live-load moment causes tension at the top, and compression at the bottom fibers of the support section. The resulting total fiber stresses in the precast section at the support due to all loads become

$$f_T^t = f_2^t + \frac{M_{B3}}{S_c^t}$$

and

$$f_{bT} = f_{2b} - \frac{M_{B3}}{S_{cb}}$$

Hence,

$$f_T^t = -1,510.4 + \frac{8.68 \times 10^6}{21,714}$$

$$\cong -1,111 \text{ psi (C) (7.7 MPa)} < 2,250 \text{ psi, O.K.}$$

$$f_{bT} = -414.3 - \frac{8.68 \times 10^6}{9,490} = -1,329 \text{ psi (9.2 MPa)} < 2,250 \text{ psi, O.K.}$$

Alternative one-step solution using Equations 4.19a and b

$$f_T^t = -\frac{P_e}{A_c} \left( 1 - \frac{ec_t}{r^2} \right) - \frac{M_D + M_{SD}}{S^t} - \frac{M_{CSD} + M_L}{S_c^t}, \text{ where } S_c^t \text{ is at the top of the precast section}$$

$$f_{bT} = -\frac{P_e}{A_c} \left( 1 + \frac{ec_b}{r^2} \right) + \frac{M_D + M_{SD}}{S_b} + \frac{M_{CSD} + M_L}{S_{cb}}$$

where  $e = e'_B = M_3/P_e$  and  $M_{CSD}$  is the additional superimposed dead load at service after erection, assumed zero here.

From before, the C-line eccentricity is  $e'_B = M_3/P_e = -8.39 \times 10^6/508,940 = -16.49$  in. (41.9 cm). Also, the support moments, using the appropriate signs, are

$$M_D = -2.87 \times 10^6 \text{ in.-lb}$$

$$M_{SD} = -2.47 \times 10^6 \text{ in.-lb}$$

and

$$M_L = -8.68 \times 10^6 \text{ in.-lb (including } M_{CSD})$$

Hence, at top of the precast section,

$$\begin{aligned} f_T^t &= -\frac{508,940}{560} \left[ 1 - \frac{(-16.49) \times 24.73}{223.91} \right] \\ &\quad + \frac{(2.87 + 2.47) \times 10^6}{5,070} + \frac{8.68 \times 10^6}{21,714} \\ &= -2,560 + 1,053.2 + 399.7 = -1,111 \text{ psi (C)} \end{aligned}$$

$$\begin{aligned} f_{bT} &= -\frac{508,940}{560} \left[ 1 + \frac{(-16.49) \times 20.27}{223.91} \right] \\ &\quad - \frac{(2.87 + 2.47) \times 10^6}{6,186} - \frac{8.68 \times 10^6}{9,490} \\ &= +447.9 - 863.2 - 914.6 \\ &= -1,330 \text{ psi (C) (9.2 MPa) } < 2,250 \text{ psi, O.K.} \end{aligned}$$

Stresses at top and bottom fibers of the situ-cast 4 in. slab

From Equations 4.20a and b, the maximum fiber stresses at the top and bottom fibers on the composite slab at the support section are evaluated using section moduli  $S'_{CS}$  and  $S_{bCS}$ , where

$$f'_{CS} = +\frac{M_L}{S'_{CS}} \times \text{modular ratio } n = 0.77$$

$$f_{bCS} = +\frac{M_L}{S_{bCS}} \times n$$

Hence,

$$f'_{CS} = \frac{8.68 \times 10^6}{15,288} \times 0.77 \cong +437 \text{ psi (T) (3 MPa) } \cong 425 \text{ psi, O.K.}$$

$$f_{bCS} = +\frac{8.68 \times 10^6}{19,251} \times 0.77 \cong +347 \text{ psi (T) (2.4 MPa) } < 425 \text{ psi, O.K.}$$

Superposition of the tensile stress at the bottom fibers of the slab and the compressive stress of  $-1,111$  psi at the extreme top fibers of the precast section can result in a net compressive stress at the bottom of the slab =  $-1,111 + 347 = -764$  psi.

The fiber stress at the extreme lower fibers of the precast section at support B or C is

$$f_{bT} = -414.3 - \frac{8.68 \times 10^6}{9,490} \cong -1,329 \text{ psi (9.2 MPa)}$$

The final distribution of stress is shown in Figure 6.18.

Note that the concrete fiber stresses are considerably below the maximum allowable stresses at service load for the same live load and spans as the simply supported beam of Example 4.7. Consequently, the selected continuous tendon profile is not the most efficient in this example, since the superimposed live load is the same in both cases and the section is the same for the span lengths used. Example 6.5 demonstrates preferable modifications.

6. *Limit state at failure*

(a) *Degree of ductility for moment redistribution*

$$h = 45 + 5.75 = 50.75 \text{ in.}$$

$$d = 50.75 - (1.5 + 0.5 \text{ for stirrup} + 0.25) \cong 48.5 \text{ in.}$$

$$\begin{aligned} \text{Support } d_p &= c_b + e_B = 20.27 + 16.49 \text{ from bottom fibers} \\ &= 36.76 \text{ in. (89.6 cm)} \end{aligned}$$

Since the width of the compression flange at support  $b = 22$  in., try two #4 bars as compression steel and four #4 bars at tension steel. We obtain

$$\omega' = \frac{A'_s f_y}{bd f'_c} = \frac{2 \times 0.20}{22 \times 48.5} \times \frac{60,000}{5,000} = 0.0045$$

$$\omega = \frac{4 \times 0.2}{22 \times 48.5} \times \frac{60,000}{5,000} = 0.0090$$

$$\omega_p = \frac{A_{ps} f_{ps}}{bd_p f'_c} = \frac{3.366 \times 240,000}{22 \times 36.76 \times 5,000} = 0.20$$

$$\beta_1 = 0.80 \text{ for 5,000 psi concrete}$$

$$\frac{d}{d_p} (\omega - \omega') = \frac{48.5}{35.27} (0.0090 - 0.0045) = 0.0062$$

$$\omega_p + \frac{d}{d_p} (\omega - \omega') = 0.20 + 0.0062 = 0.2062$$

$$0.24\beta_1 = 0.24 \times 0.80 = 0.19 < 0.2062 \text{ at the support}$$

$0.24 \beta_1$  is comparable to  $\epsilon_t = 0.005$  so that the actual strain for total  $\omega$  is  $\cong 0.0054$

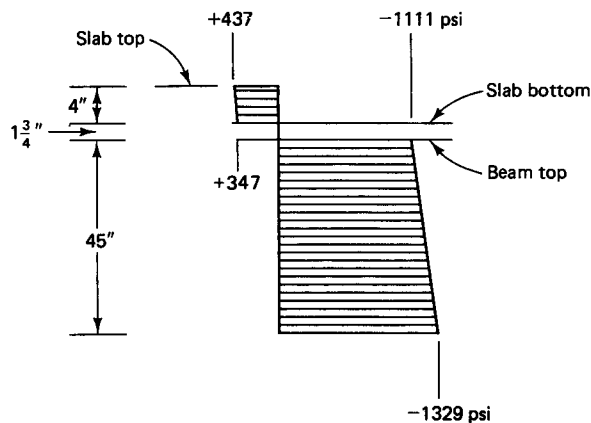


Figure 6.18 Stress distribution in the concrete at service load.

Hence, strain  $\epsilon_t$  is less than 0.0075, precluding application of moment redistribution. A test using the 1000  $\epsilon_t$  percent code provision for redistribution factor, would have allowed moment redistribution in this case, however. For maximum allowable  $\omega_T$ ,  $0.36\beta_1 = 0.36 \times 0.80 = 0.45 > 0.2062$ , O.K.

Alternatively by the ACI Code,  $c/d_t = a/\beta_1 d_t = 8.9/(0.80 \times 48.5) = 0.232 < 0.375$ .

Hence, the beam is in the tensile zone of Fig. 4.45 and did not exceed the maximum permissible reinforcement, allowing  $\phi = 0.90$  for determining the design moment  $M_u$ , and thus OK for the chosen reinforcement.

**(b) Flexural moments modifications**

It is advisable to apply the redistribution modifications separately to the dead and live loads since alternate span loading for live load has to be considered for worst loading conditions while dead load acts simultaneously on all spans. Since no redistribution is used here, the elastic moments at support are

$$M_D + M_{SD} = (2.87 + 2.47)10^6 = 5.34 \times 10^6 \text{ in.-lb}$$

and

$$M_L = 8.68 \times 10^6 \text{ in.-lb}$$

**(c) Nominal moment strength**

The support section factored  $M_u$  is

$$1.2 \times 5.34 \times 10^6 + 1.6 \times 8.68 \times 10^6 = 20.3 \times 10^6 \text{ in.-lb}$$

From step 2, the factored elastic secondary moment induced by reactions due to prestress, using a load factor of 1.0 as stipulated in the ACI code, is  $M_2 = 0.76 \times 10^6$  in.-lb, and the total factored moment  $M_u = (20.3 - 0.76) \times 10^6$  in.-lb =  $19.54 \times 10^6$  in.-lb (2.20 kN-m). Also, the required nominal moment strength  $M_n = M_u/\phi = 19.54 \times 10^6/0.90 = 21.71 \times 10^6$  in.-lb (2.46 kN-m). If  $A'_s$  yielded,  $f_y = f'_s = 60,000$  psi, width  $b$  at bottom = 22 in. So

$$\begin{aligned} a &= \frac{A_{ps}f_{ps} + A_s f_y - A'_s f_y}{0.85f'_c b} \\ &= \frac{3.366 \times 240,000 + 0.8 \times 60,000 - 0.4 \times 60,000}{0.85 \times 5,000 \times 22} \\ &= 8.90 \text{ in. (22.6 cm)} \end{aligned}$$

The depth of the flange up to the 7-in.-wide web section at support is

$$7 + 7.5/2 = 10.8 \text{ in.} > 8.90 \text{ in.}$$

The neutral axis is inside the flange, and the section behaves like a rectangular section.

From Equation 4.44,

$$\begin{aligned} \text{Available } M_n &= A_{ps}f_{ps} \left( d_p - \frac{a}{2} \right) + A_s f_y \left( d - \frac{a}{2} \right) + A'_s f_y \left( \frac{a}{2} - d' \right) \\ &= 3.366 \times 240,000 \left( 36.76 - \frac{8.90}{2} \right) \\ &\quad + 0.80 \times 60,000 \left( 48.5 - \frac{8.9}{2} \right) + 0.40 \times 60,000 \left( \frac{8.9}{2} - 3 \right) \\ &= 28.25 \times 10^6 \text{ in.-lb (3.1} \times 10^3 \text{ kN-m)} > 21.71 \times 10^6 \text{ in.-lb} \end{aligned}$$

The factored moment is at least 1.2  $M_{cr}$ , as the code requires. Hence, the section is safe, but not efficient. Figure 6.19 shows the load and moment distributions. It could be reduced in size by either changing the tendon eccentricities or enlarging the span or allowing a higher live load with new tendon eccentricities.

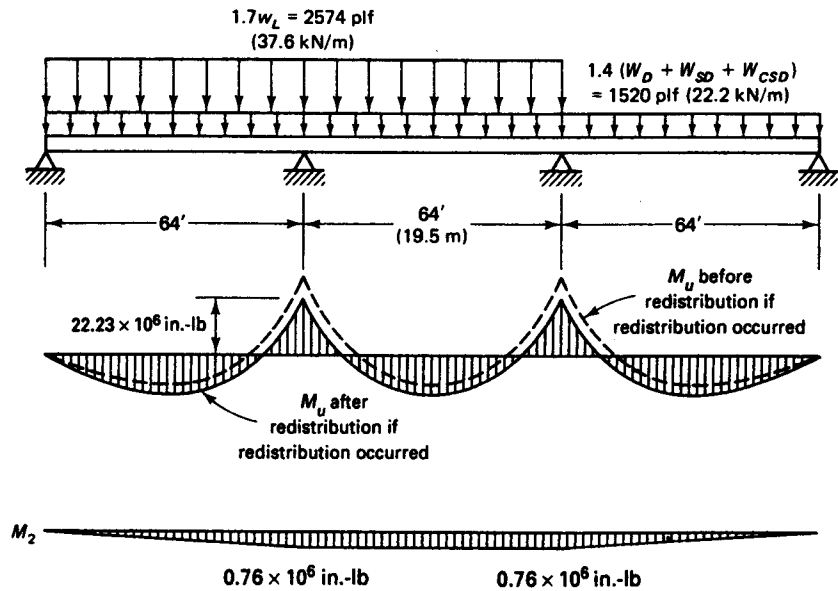


Figure 6.19 Loading and factored moment in Example 6.4.

## 6.10 TENDON TRANSFORMATION TO UTILIZE ADVANTAGES OF CONTINUITY

### Example 6.5

Linearly transform the prestressing tendon in the continuous prestressed beam in Example 6.4 such that the superimposed live load  $W_L$  on the 64 ft (19.8 m) spans can be increased by at least 50 percent.

#### Solution:

##### 1. Transformation of tendon

The tendon eccentricity at support B in Example 6.4 produces compressive fiber stress at the support precast section due to all loads of 1,111 psi at the top, and 1,329 psi at the bottom fibers. These are lower than the maximum allowable  $f_c = -2,250$  psi. Therefore, the beam can sustain more load if the concrete compressive stress capacity is to be utilized. In order to allow the beam to carry more live load, more compressive stress at the midspan bottom fibers due to prestress needs to be developed through an increase in the tendon eccentricity.

Accordingly, assume that the tendon is linearly transformed throughout all the spans such that  $e_B = e_C = 11.5$  in. (27.9 cm), as shown in Figure 6.20. Then the transformation vertical distance =  $16.5 - 11.5 = 5$  in. (10 cm), the midspan eccentricity  $e_{E1} = 8.25 + 5 = 13.25$  in. (34 cm), and the primary support B moment  $M_1 = 508,940 \times 11.5 = 5.85 \times 10^6$  in.-lb ( $0.63 \times 10^3$  kN-m). Also, the primary midspan  $E_1$  moment  $M_1 = 508,940 \times 13.25 = 6.74 \times 10^6$  in.-lb ( $0.75 \times 10^3$  kN-m), and we have

$$E_c I_c \Delta_B = \left[ \left( \frac{5.85}{2} + 6.73 \right) 10^6 \times \frac{64 \times 2}{3} \right] \times \frac{64}{2} \times 144$$

$$- \left[ \frac{5.85 \times 10^6 \times 64}{2} \right] \times \frac{64 \times 2}{3} \times 144 = 75.0 \times 10^{10}$$

Also,



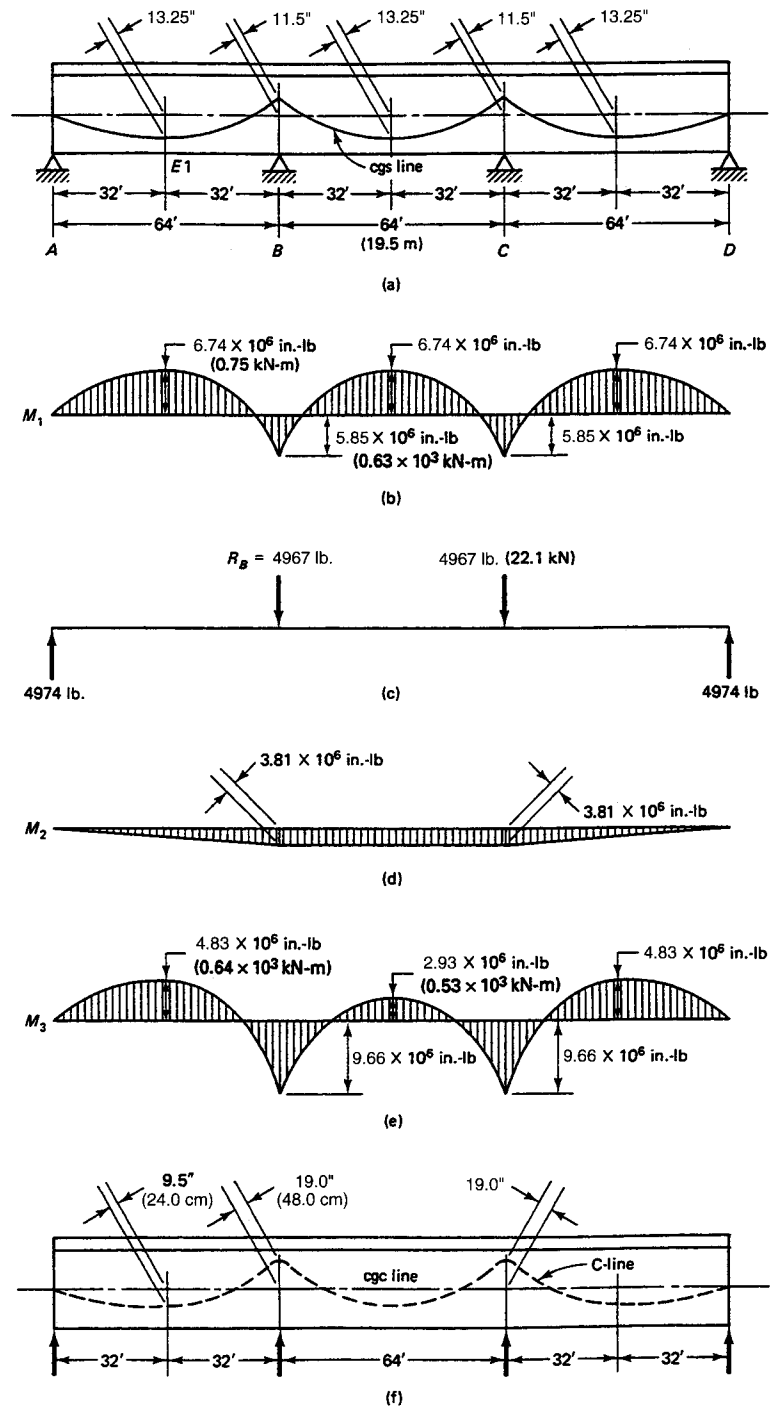


Figure 6.20 Tendon transformation in continuous beam of Example 6.5.

$$E_c I_c \Delta_c = \left[ 64R_A \times 12 \times \frac{64 \times 12}{2} \right] \frac{64 \times 2}{3} \times 12$$

$$= 15.1 \times 10^7 R_A \text{ in.-lb}$$

$$R_A = R_B = \frac{75.0 \times 10^{10}}{15.1 \times 10^7} = 4967 \text{ lb}$$

$$M_2 = R_A \times 64 \times 12 = 4,974 \times 64 \times 12$$

$$= 3.81 \times 10^6 \text{ in.-lb (} 0.44 \times 10^3 \text{ kN-m)}$$

$$\text{Support } M_3 = (5.85 + 3.81) \times 10^6 = 9.66 \times 10^6 \text{ in.-lb (see Figure 6.20)}$$

$$\text{Midspan } M_3 = \left( 6.74 - \frac{1}{2} \times 3.81 \right) 10^6 = 4.83 \times 10^6 \text{ in.-lb}$$

From Example 6.4,  $P_e = 508,940$  lb. So calculate the final C-line eccentricities  $= M_3/P_e$  as shown in Figure 6.20(f).

**2. Concrete fiber stresses due to prestress and self-weight (583 plf)**

From step 3 of the solution to Example 6.4, the moment due to self-weight is  $2.87 \times 10^6$  in.-lb so the total moment  $M_4 = M_3 - 2.87 \times 10^6 = (9.66 - 2.87) 10^6 = 6.79 \times 10^6$  in.-lb.

**(i) Support section B or C**

$$f^t = -\frac{P_e}{A_c} - \frac{M_4}{S^t} = -\frac{508,940}{560} - \frac{6.79 \times 10^6}{5,070}$$

$$= -908.8 - 1339$$

$$= -2248 \text{ psi (C) (15.2 MPa) } < 2,250 \text{ psi, O.K.}$$

$$f_b = -908.8 + \frac{6.79 \times 10^6}{6,186} = -908.8 + 1098$$

$$= +189 \text{ psi (T), O.K.}$$

**(ii) Outer span midspan section  $E_1$**

From Example 6.4,  $M_D = 2.12 \times 10^6$  in.-lb. So the net moment  $M_4 = M_3 - 2.12 \times 10^6 = (4.83 - 2.12) 10^6 = 2.71 \times 10^6$  in.-lb ( $0.4 \times 10^3$  kN-m), and

$$f^t = -908.8 + \frac{2.71 \times 10^6}{5,070} = -347 \text{ psi (C) (2.7 MPa), O.K.}$$

$$f_b = -908.8 - \frac{2.71 \times 10^6}{6,186}$$

$$= -1347 \text{ psi (C) (9.2 MPa), no tension, O.K.}$$

**3. Determination of live-load intensity for new tendon profile for unshored construction**

$$f^t = -\frac{P_e}{A_c} \left( 1 - \frac{e'_B c_t}{r^2} \right) - \frac{M_D + M_{SD}}{S^t} - \frac{M_{CSD} + M_L}{S^t_c}$$

$$f_{bT} = -\frac{P_e}{A_c} \left( 1 + \frac{e'_B c_b}{r^2} \right) + \frac{M_D + M_{SD}}{S_b} + \frac{M_{CSD} + M_L}{S_{cb}}$$

**(i) Support section (at B or C)**

From Figure 6.20(e),  $M_3 = -9.66 \times 10^6$  in.-lb Hence,

$$e'_B = -\frac{9.66 \times 10^6}{508,940} = -19 \text{ in. (47.0 cm)}$$

From Example 6.4,  $M_D + M_{SD} = -(2.87 + 2.47)10^6 = -5.34 \times 10^6$  in.-lb. Also, from Figure 6.12, the live-load moment for a three-span beam with one span unloaded is

$$\begin{aligned} M_L &= -0.1167W_L l^2 = -0.1167W_L (64)^2 (12) \\ &= -5,736W_L \text{ in.-lb, including } M_{CSD} \end{aligned}$$

The maximum allowable tensile stress  $f_t = +849$  psi at midspan and  $f_t = +425$  psi at support.

$$\begin{aligned} f_t^s = +425 &= -\frac{508,940}{560} \left( 1 - \frac{(-19) \times 24.73}{223.91} \right) \\ &+ \frac{5.34 \times 10^6}{5,070} + \frac{5,736W_L}{21,714} \end{aligned}$$

giving  $W_L = 8,092$  plf.

(ii) *Midspan section (at  $E_1$ )*

Since  $W_D = 583$  plf, by proportioning we obtain

$$M_D + M_{SD} = +(2.12 + 1.83)10^6 = +3.95 \times 10^6 \text{ in.-lb}$$

$$M_L = 0.0735W_L(64)^2 \times 12 = 3613W_L \text{ in.-lb}$$

$$\begin{aligned} f_t^s = -2,250 &= -\frac{508,940}{560} \left( 1 - \frac{9.5 \times 24.73}{223.91} \right) \\ &- \frac{3.95 \times 10^6}{5,070} - \frac{3613W_L}{21,714} \end{aligned}$$

$$\frac{3613W_L}{21,714} = 44.8 - 779 + 2,250$$

$$W_L = 9109 \text{ plf}$$

$$\begin{aligned} f_{bT} = 849 &= -\frac{508,940}{560} \left( 1 + \frac{9.5 \times 20.27}{223.91} \right) \\ &+ \frac{3.95 \times 10^6}{6,186} + \frac{3613W_L}{9,490} \end{aligned}$$

$$\frac{3613W_L}{9,490} = 849 + 1691 - 638.5$$

$$W_L = 4995 \text{ plf}$$

Hence,  $W_L = 4995$  plf controls for service load levels, to be verified by checking the ultimate moment strength available.

4. *Available nominal moment strength*

$$A_{ps} = 3.366 \text{ in.}^2$$

$$\text{Support } d_p = 11.5 + 20.27 = 31.77 \text{ in.}$$

Assume that  $A_s$  at supports B and C is increased to four #6 bars in order to facilitate an increased live load. Then

$$A_s = 4 \times 0.44 = 1.76 \text{ in.}^2$$

$$\omega = \frac{1.76}{22 \times 48.5} \times \frac{60,000}{5,000} = 0.020$$

$$\begin{aligned}\omega_p + \frac{d}{d_p}(\omega - \omega') &= 0.2312 + \frac{48.5}{31.77}(0.02 - 0.0045) \\ &= 0.255 > 0.24\beta_1 = 0.19\end{aligned}$$

Hence, strain  $\epsilon_t$  is less than 0.0075, precluding application of moment redistribution. A test using the 1000  $\epsilon_t$  percent code provision for redistribution factor, would have allowed moment redistribution in this case, however.

Now, from before, the elastic  $M_2 = 3.82 \times 10^6$  in.-lb and we have

$$M_u = 1.2(M_D + M_{SD}) + 1.6M_L - M_2$$

or

$$\begin{aligned}M_u &= 1.2 \times 5.34 \times 10^6 + 1.6M_L - 3.82 \times 10^6 \\ &= 2.59 \times 10^6 + 1.6M_L\end{aligned}$$

Next,

$$\begin{aligned}\text{Required } M_n &= \frac{M_u}{\phi} = \frac{2.59 \times 10^6}{0.9} + 1.6M_L = 2.88 \times 10^6 + 1.78M_L \\ a &= \frac{A_{ps}f_{ps} + A_s f_y - A'_s f_y}{0.85f'_c b}\end{aligned}$$

If  $A'_s$  yielded  $f_y = f'_s = 60,000$  psi, then

$$a = \frac{3.366 \times 240,000 + (1.76 - 0.40)60,000}{0.85 \times 5,000 \times 22} = 9.51 \text{ in. (24.2 cm)}$$

which is less than the flange depth up to the 7-in.-wide web section. Hence, the neutral axis is inside the flange, and the section behaves like a rectangular section. Accordingly, we have

$$\begin{aligned}\text{Available } M_n &= A_{ps}f_{ps}\left(d_p - \frac{a}{2}\right) + A_s f_y\left(d - \frac{a}{2}\right) + A'_s f_y\left(\frac{a}{2} - d'\right) \\ &= 3.366 \times 240,000\left(31.77 - \frac{9.51}{2}\right) + 1.76 \\ &\quad \times 60,000\left(48.5 - \frac{9.51}{2}\right) + 0.40 \times 60,000\left(\frac{9.51}{2} - 3\right) \\ &= 26.49 \times 10^6 \text{ in.-lb} - 2.89 \times 10^6 + 1.78M_L\end{aligned}$$

Hence,

$$M_L = \frac{(26.49 - 2.89) \times 10^6}{1.78} = 13.26 \times 10^6 \text{ in.-lb}$$

If  $M_L = 0.1167W_L l^2$ , then

$$13.26 \times 10^6 = 0.1167W_L(64)^2 \times 12$$

So  $W_L = 2312$  plf  $< W_L = 4995$  plf from the service-load analysis. Hence,  $W_L = 2312$  plf controls, and the percent increase in live load is

$$\frac{(2312 - 1,514)}{1,514} \times 100 = 52.7\% \cong 50\%, \text{ O.K.}$$

Thus, we can adopt the new profile of the tendon with four #6 bars at the support top fibers in the situ-cast slab and two #4 bars at the bottom precast section fibers. Note that if the mild steel is changed from 4 #6 to 4 #8, the increase in  $W_L$  would have been 70%.

## 6.11 DESIGN FOR CONTINUITY USING NONPRESTRESSED STEEL AT SUPPORT

### Example 6.6

Design the beam in Example 6.5 such that the section and tendon profile of the AASHTO type-III bridge beam used in Example 4.7 is made continuous through the use of nonprestressed mild steel reinforcement to carry the superimposed service dead load  $W_{SD} = 503$  plf and service live load  $W_L = 2,290$  plf (33.4 kN/m). Assume that the tendon profile in the precast simply supported section is the same as the one in Example 4.7, namely, with midspan eccentricity  $e_c = 16.27$  in. (41.3 cm) and end eccentricity  $e_e = 10.0$  in. (25.4 cm). Sketch the prestressing tendon and other reinforcement details if the maximum allowable concrete compressive fiber stress at service load is  $f_c = 2,250$  psi (15.5 MPa).

### Solution:

#### 1. Data for strength design at support

Because continuity is obtained in this case through the use of reinforced concrete at the supports, it is suggested that the topping concrete also be of  $f'_c = 5,000$  psi compressive strength. Thus, we have

$$f'_c = 5,000 \text{ psi (34.5 MPa), normal weight}$$

$$f_y = 60,000 \text{ psi (413.7 MPa)}$$

Design the continuity to resist the superimposed dead and live loads only, and *not* the self-weight:

$$\begin{aligned} d &= 50.75 - (1.5 \text{ in. cover} + 0.5 \text{ in. for stirrup} + 0.5 \text{ in. for half-bar dia}) \\ &= 48.25 \text{ in. (123 cm)} \end{aligned}$$

$$b_b = 22 \text{ in. at bottom}$$

$$b_t = 84 \text{ in. at top (modified } b_m = 65 \text{ in.)}$$

#### 2. Nominal moment strength

From Example 6.5, the required moment strength due to  $(W_{SD} + W_L)$  at support B is  $M_u = 1.2 \times 2.47 \times 10^6 + 1.6 \times 13.03 \times 10^6 = 23.81 \times 10^6$  in.-lb. The bonded prestressed steel does not extend through the supports; hence, consider  $\omega_p = 0$  for calculating the moment redistribution factor. Assume

$$A_s = 9.0 \text{ in.}^2$$

$$\omega = \frac{9.0}{22 \times 48.25} \times \frac{60,000}{5,000} = 0.1012$$

$$A'_s = \text{two \#4} = 0.40 \text{ in.}^2$$

and

$$\omega' = 0.0961 \times \frac{0.4}{8.5} = 0.0045$$

Then from Example 6.4,  $d_p = 35.87$  in.,  $d = 48.25$  in.,  $\omega_p + [d/d_p](\omega - \omega') = 0 + [48.25/35.87](0.1012 - 0.0045) = 0.1300 < 0.24\beta_1 = 0.192$ . Hence, redistribution is possible, based on elastic moment analysis giving  $M_u = 23.81 \times 10^6$  in.-lb.

Using the ACI Code redistribution test, the tensile strain at the extreme tensile steel reinforcement is  $\epsilon_t = 0.003 \left( \frac{d_t}{c} - 1 \right)$ .

$$c = \left( \frac{a}{\beta_1} \right) = \frac{9.51}{0.80} = 11.89 \text{ in.}; d_t = 48.5 \text{ in.}$$

$$\epsilon_t = 0.003 \left( \frac{48.5}{11.89} - 1 \right) = 0.0092; \text{ hence, redistribution percentage} = 1000\epsilon_t = 9.2\%.$$

Use 9% redistribution, reducing the negative moment by this amount, and increasing the positive midspan moment by the same magnitude. A  $\phi$  factor of 0.90 is to be used since  $\epsilon_t > 0.005$ .

So use a distribution factor of 0.09:

$$\text{Rqd. } M_u = (1 - 0.09) \times 23.81 \times 10^6 = 21.67 \times 10^6 \text{ in.-lb } (2.0 \times 10^6 \text{ kN-m})$$

$$\text{Using } M_n = \frac{M_u}{\phi} = \frac{21.67 \times 10^6}{0.9} = 24.07 \times 10^6 \text{ in.-lb}$$

$$M_n = A_s f_y \left( d - \frac{a}{2} \right)$$

Assume for the first trial that  $d - a/2 \cong 0.9d$ . Then

$$24.07 \times 10^6 = A_s \times 60,000 \times 0.9(48.25)$$

$$A_s = \frac{24.07 \times 10^6}{60,000 \times 0.9 \times 48.25} = 9.24 \text{ in.}^2 (58 \text{ cm}^2)$$

$$a = \frac{A_s f_y}{0.85 f'_c b} = \frac{9.24 \times 60,000}{0.85 \times 5,000 \times 22} = 5.93 \text{ in.}$$

The depth of the flange to the web is  $5.75 + 7 + 4.5/2$  for the AASHTO type-3 section = 15 in.  $> 5.80/0.9 = 6.44$  in. The neutral axis is inside the flange, and the section behaves like a rectangular section. Therefore,

$$A_s = \frac{M_n}{f_y (d - a/2)} = \frac{24.07 \times 10^6}{60,000(48.25 - 5.93/2)} = 8.86 \text{ in.}^2 (55 \text{ cm}^2)$$

Since the assumed  $A_s = 9.0 \text{ in.}^2$  is very close to  $8.86 \text{ in.}^2$ , the moment distribution factor is satisfactory.

The area  $A_s$  is to be distributed over the total actual flange width of 84 in.  $A_s$  per ft width =  $(8.86/84) \times 12 = 1.26 \text{ in.}^2/12 \text{ in.}$  Using #6 bars,  $A_s$  per bar =  $0.44 \text{ in.}^2 (2.82 \text{ cm}^2)$ , and the spacing is

$$s = \frac{\text{Bar } A_s}{\text{Rqd. } A_s/12 \text{ in.}} = \frac{0.44}{1.26/12} = 4.19 \text{ in.}$$

Thus, use #6 bars at 4 in. center to center over the 84-in. width (19.1 mm dia. bars at 10.8 cm). The total number of bars over the 84-in.-width flange is

$$\frac{84 - (2 \times 1.5\text{-in. cover})}{4.25} + 1 \cong 20$$

so that we have

$$\text{Total } A_s = 20 \times 0.44 = 8.80 \text{ in.}^2, \text{ O.K.}$$

Accordingly, adopt the design for flexure. Note that the complete design would involve dowel design for composite action, stirrup design for web shear, end block design, and design for serviceability requirements in deflection and crack control as detailed in earlier examples. Note also that continuity on three spans in this example using mild steel only at the supports allowed a 50% increase in the live-load intensity from 1,514 plf to 2,329 plf.

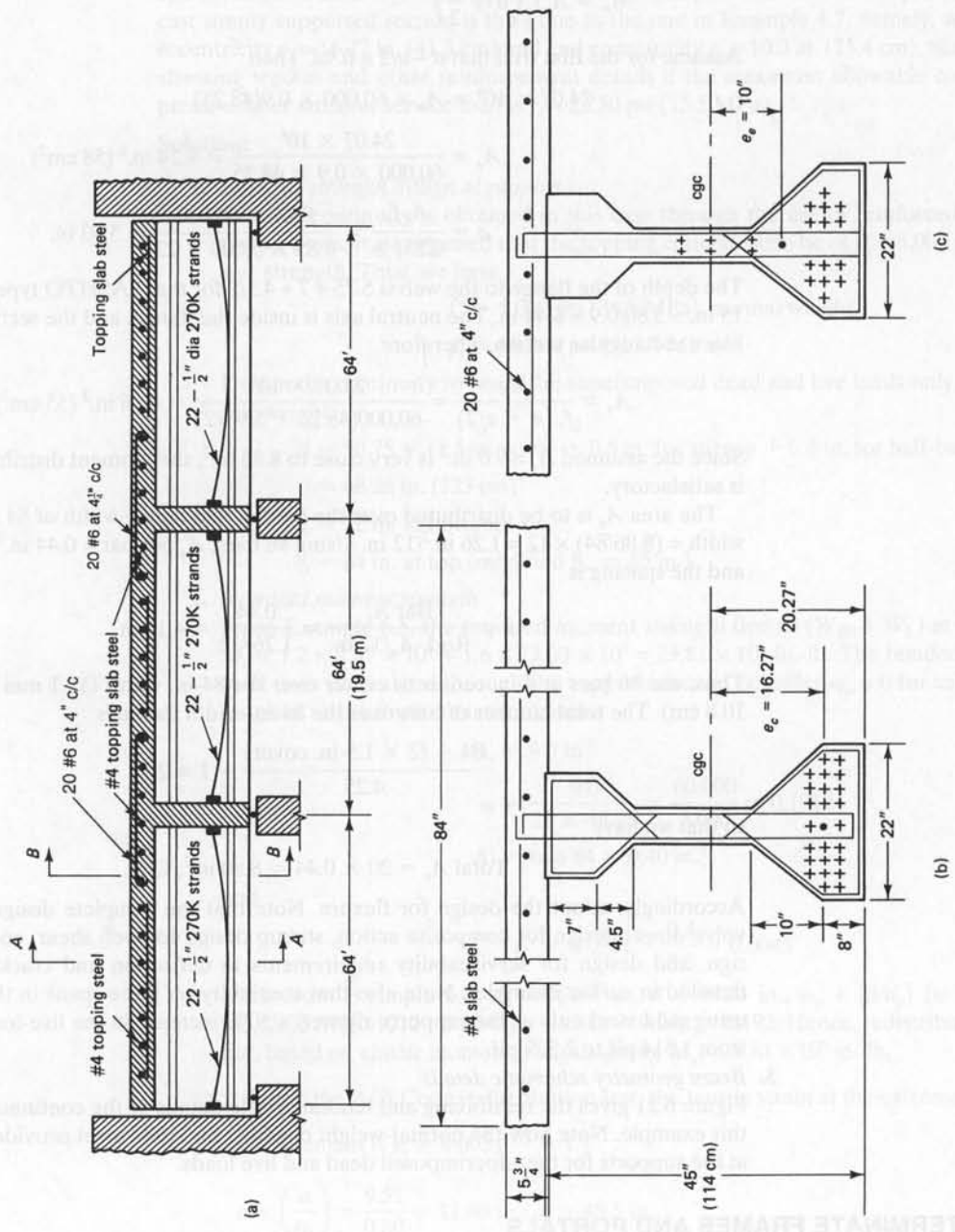
### 3. Beam geometry schematic details

Figure 6.21 gives the reinforcing and tendon profile details of the continuous beam of this example. Note how the normal-weight concrete and mild steel provide continuity at the supports for the superimposed dead and live loads.

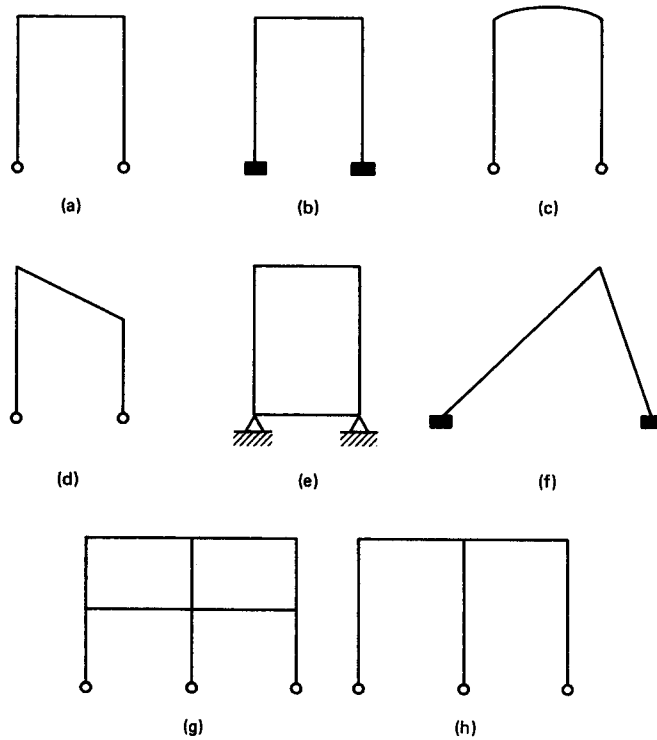
## 6.12 INDETERMINATE FRAMES AND PORTALS

### 6.12.1 General Properties

Concrete frames are indeterminate structures consisting of horizontal, vertical, or inclined members joined in such a manner that the connection can withstand the stresses and bending moments that act on it. The degree of indeterminacy depends upon the



**Figure 6.21** Schematic geometry details of continuous beam in Example 6.6 (see also Example 4.7). (a) Longitudinal section of bridge beam (not to scale). (b) Midspan section A-A. (c) Support section B-B.



**Figure 6.22** Typical structure frames.

number of spans, the number of vertical members, and the type of end reactions. Typical frame configurations are shown in Figure 6.22. If  $n$  is the number of joints,  $b$  the number of members,  $r$  the number of reactions, and  $s$  the number of indeterminacies, the degree of indeterminacy is determined from the following inequalities:

$$3n + s > 3b + r \quad (\text{unstable}) \quad (6.7a)$$

$$3n + s = 3b + r \quad (\text{statically determinate}) \quad (6.7b)$$

$$3n + s < 3b + r \quad (\text{statically indeterminate}) \quad (6.7c)$$

The degree of indeterminacy is

$$s = 3b + r - 3n \quad (6.9)$$

where  $3n$  equations of static equilibrium are always available and the total number of unknowns is  $3b + r$ . As an example, the degree of indeterminacy of the frame in Figure 6.22(a) is

$$s = 3 \times 3 + 2 \times 2 - 3 \times 4 = 1$$

and for the frame in part (g) of the same figure it is

$$s = 3 \times 10 + 2 \times 3 - 3 \times 9 = 9$$

Note that in order for a frame to perform satisfactorily, the following conditions have to be satisfied:

1. The design must be based on the most unfavorable moment and shear combinations. If moment reversal is possible due to reversal of live-load direction, the highest values of positive and negative bending moments have to be considered in the design.



2. Proper foundation support for horizontal thrust has to be provided. If the frame is designed as hinged, an expensive construction procedure, an actual hinge system has to be provided.

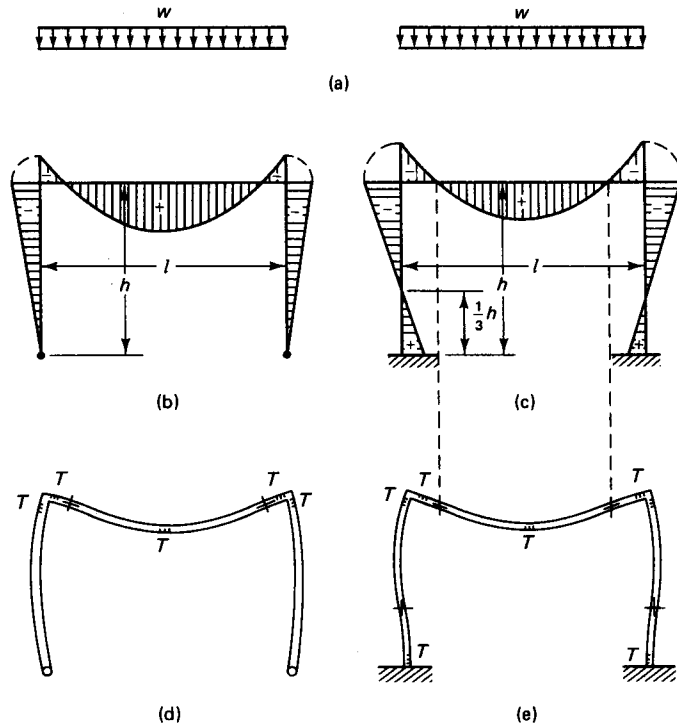
**6.12.2 Forces and Moments in Portal Frames**

The behavior of concrete frames before cracking can be considered reasonably elastic, as was done in the case of a continuous beam at service-load and slight-overload conditions. Consequently, well before the development of plastic hinges, the bending moment diagrams shown in Figures 6.23 and 6.24 will be used in the design of indeterminate prestressed concrete frames. The usual methods of analyses of indeterminate structures including frames, such as virtual work, stiffness matrix, and flexibility matrix procedures, as well as the clapeyron three- or four-moment equations, are assumed familiar in this text, so that only the minimum guidelines and simplifications are presented.

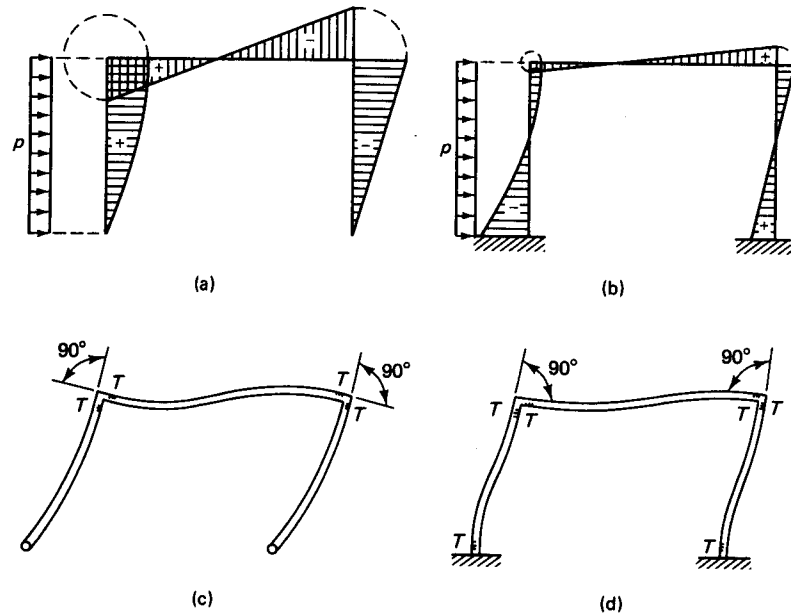
**6.12.2.1 Uniform Gravity Loading on Single-Bay Portal.** Suppose that the moments of inertia  $I_c$  of the vertical columns and  $I_b$  of the horizontal beam of the portal in Figure 6.25(a) are not equal. The following values of the moments and thrusts can be inferred:

*End Shear in Beam*

$$V_B = V_C = \frac{1}{2} wl \tag{6.9a}$$



**Figure 6.23** Right-angled portal frame loaded with gravity load intensity  $w$  ( $T$  indicates tension fibers). (a) Load intensity. (b) Bending moment (hinged-base frame). (c) Bending moment (fixed-base frame). (d) Deformation of frame in (b). (e) Deformation of frame in (c).



**Figure 6.24** Right-angled portal frame loaded with wind load intensity  $p$  ( $T$  indicates tension fibers). (a) Bending moment (hinged-base frame). (b) Bending moment (fixed-base frame). (c) Deformation of frame in (a). (d) Deformation of frame in (b).

### Horizontal Thrust

$$H = \frac{1}{h} C_1 w l^2 \quad (6.9b)$$

where

$$C_1 = \frac{1}{12 \left( \frac{2 I_b h}{3 I_c l} + 1 \right)} \quad (6.9c)$$

### Maximum Negative Moment at Corner

$$M_B = M_c = -Hh = -C_1 w l^2 \quad (6.9d)$$

### Maximum Positive Moment at Midspan

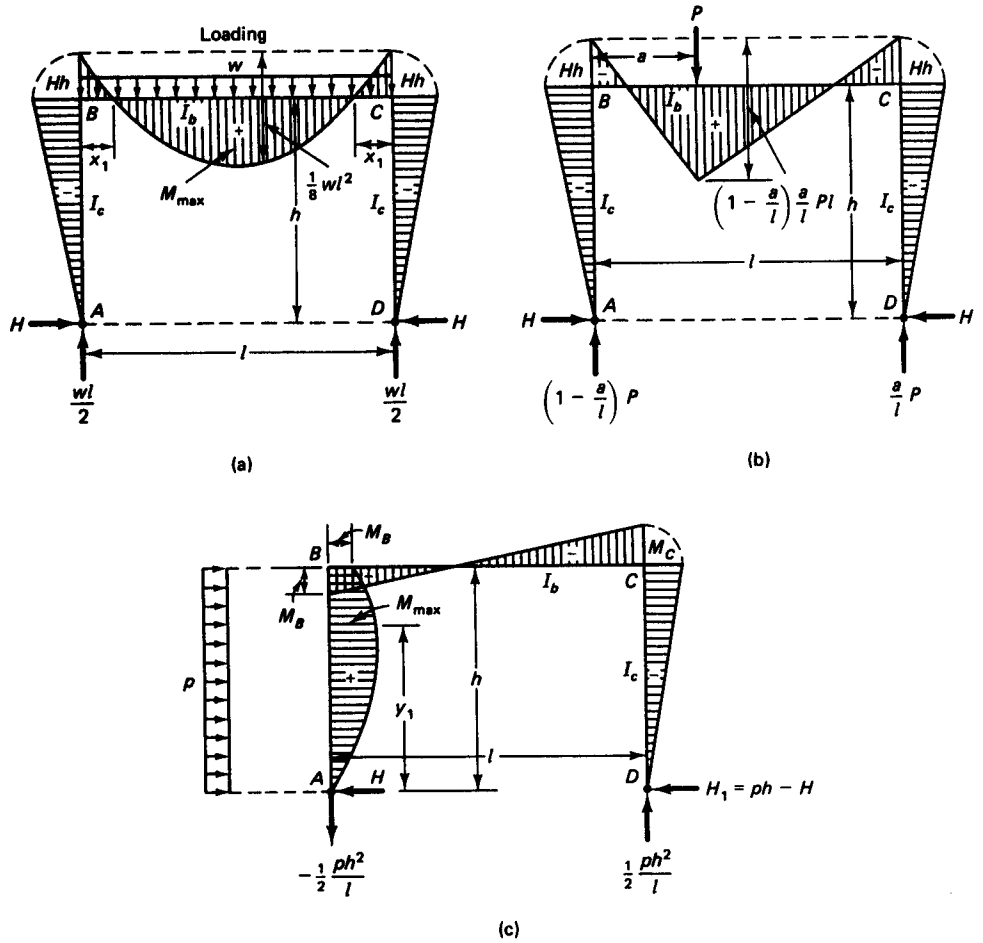
$$M_{\max} = \frac{1}{8} w l^2 - Hh = \left( \frac{1}{8} - C_1 \right) w l^2 \quad (6.9e)$$

### Bending Moments at Any Point $x$

$$M_x = \frac{1}{2} x(l-x)w - C_1 w l^2 \quad (6.9f)$$

where the points of contraflexure from either corner of the portal are

$$x_1 = \frac{1}{2} (1 - \sqrt{1 - 8C_1}) l = C_2 l \quad (6.9g)$$



**Figure 6.25** Bending moment ordinates in single-bay frame. (a) Uniform gravity loading. (b) Concentrated gravity loading. (c) Uniform horizontal pressure.

and

$$C_2 = \frac{1}{2}(1 - \sqrt{1 - 8C_1}) \tag{6.9h}$$

**6.12.2.2 Concentrated Gravity Loading on Single-Bay Portal.** Since the concentrated load  $P$  does not have to act at midspan, nonsymmetry of shears results. From Figure 6.25(b), the end shear are

$$V_B = \left(1 - \frac{a}{l}\right)P$$

and

$$V_C = \frac{a}{l}P \tag{6.10a}$$

**Horizontal Thrust**

$$H = C_3 \frac{a}{l} \left(1 - \frac{a}{l}\right)P \frac{l}{h} \tag{6.10b}$$

where

$$C_3 = \frac{1}{2\left(\frac{2}{3}\frac{I_b}{I_c}\frac{h}{l} + 1\right)} \quad (6.10c)$$

**Bending Moments at Corners**

$$M_B = M_c = -Hh = -C_3 \frac{a}{l} \left(1 - \frac{a}{l}\right) Pl \quad (6.10d)$$

**Bending Moments at Any Point along BC.** For  $x < a$ ,

$$M_x = \left(1 - \frac{a}{l}\right) \left(\frac{x}{l} - \frac{a}{l} C_3\right) Pl \quad (6.10e)$$

For  $x > a$ ,

$$M_x = \frac{a}{l} \left[1 - \frac{x}{l} - \left(1 - \frac{a}{l}\right)\right] C_3 Pl \quad (6.10f)$$

**Maximum Positive Moment at  $x = a$**

$$M_{\max} = \frac{a}{l} \left(1 - \frac{a}{l}\right) Pl - Hh = (1 - C_3) \frac{a}{l} \left(1 - \frac{a}{l}\right) Pl \quad (6.10g)$$

**Horizontal Thrust for Several Concentrated Gravity Loads**

$$H = \frac{1}{h} C_3 \left[ P_1 \frac{a_1}{l} \left(1 - \frac{a_1}{l}\right) + P_2 \frac{a_2}{l} \left(1 - \frac{a_2}{l}\right) + \dots \right] \quad (6.10h)$$

or

$$H = \frac{1}{h} C_3 \sum P \frac{a}{l} \left(1 - \frac{a}{l}\right) \quad (6.10i)$$

**6.12.2.3 Uniform Horizontal Pressure on Single-Bay Portal.** From Figure 6.25(c), we have the following:

**Vertical Reactions at Supports**

$$R_A = -\frac{1}{2} ph \frac{h}{l}$$

and

$$R_D = +\frac{1}{2} ph \frac{h}{l} \quad (6.11a)$$

**Horizontal Reactions.** For windward hinge A,

$$H_A = \frac{1}{8} \frac{11\frac{I_b}{I_c}\frac{h}{l} + 18}{2\frac{I_b}{I_c}\frac{h}{l} + 3} ph = C_4 ph \quad (6.11b)$$

where

$$C_4 = \frac{1}{8} \frac{11 \frac{I_b h}{I_c l} + 18}{2 \frac{I_b h}{I_c l} + 3} \quad (6.11c)$$

For leeward hinge  $D$ ,

$$H_D = ph - H_A = (1 - C_4)ph \quad (6.11d)$$

The bending moments at any point  $y$  along the column height due to horizontal pressure, with  $y$  being measured from the *bottom*, are

$$M_y = H_A y - \frac{1}{2} p y^2 \quad (6.11e)$$

#### **Maximum Moment at Windward Column**

$$M_{\max} = \frac{1}{2} \left( \frac{1}{8} \frac{11 \frac{I_b h}{I_c l} + 18}{2 \frac{I_b h}{I_c l} + 3} \right) p h^2 = \frac{1}{2} C_4 p h^2 \quad (6.11f)$$

#### **Point of Maximum Bending Moment above Support A**

$$y_1 = \frac{1}{8} \left( \frac{11 \frac{I_b h}{I_c l} + 18}{2 \frac{I_b h}{I_c l} + 3} \right) h = C_4 h \quad (6.11g)$$

#### **Bending Moments in Corners of Portal**

$$\begin{aligned} M_B &= H_A h - \frac{1}{2} p h^2 = \frac{3}{8} \frac{\frac{I_b h}{I_c l} + 2}{2 \frac{I_b h}{I_c l} + 3} p h^2 \\ &= (C_4 - 0.5) p h^2 \end{aligned} \quad (6.11h)$$

$$M_c = -H_D h = -(1 - C_4) p h^2 \quad (6.11i)$$

The constants  $C_1$ ,  $C_2$ ,  $C_3$ , and  $C_4$  in Equations 6.9, 6.10, and 6.11 can be graphically represented as shown in Figure 6.26. Canned computer programs for the analysis of indeterminate beams and frames render the use of charts such as this unnecessary except for a quick check of numerical values.

### **6.12.3 Application to Prestressed Concrete Frames**

As with continuous beams, a tendon profile has to be assumed at the start in order to determine the secondary bending moments  $M_2$  for the portal frame horizontal beam and vertical legs. A concordant tendon is assumed for the horizontal beam for symmetrical

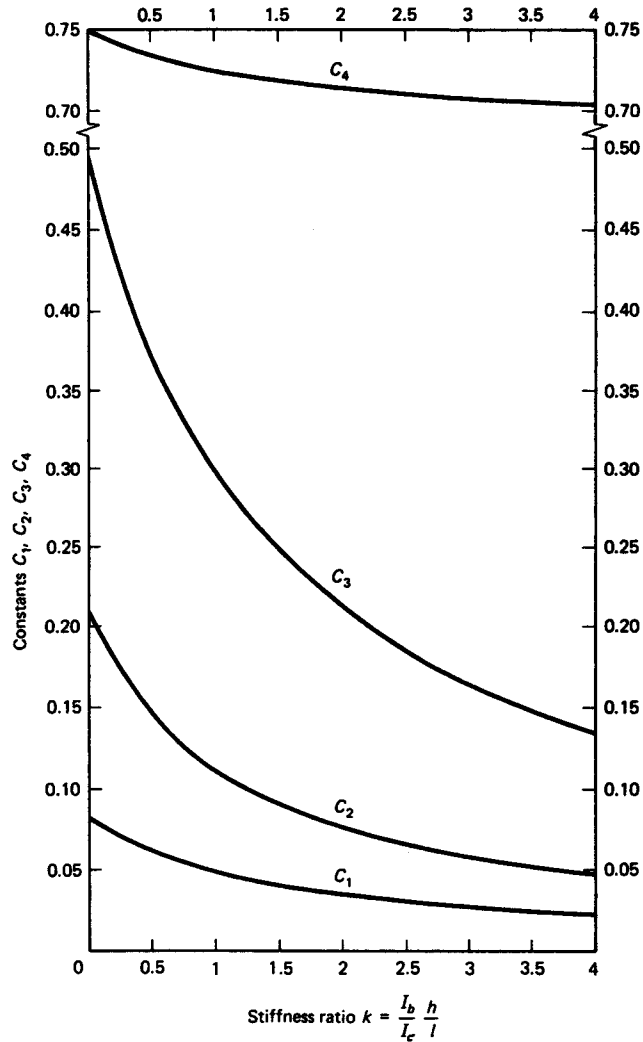


Figure 6.26 Constants  $C_1$  through  $C_4$  in Equations 6.9, 6.10, and 6.11.

gravity loading, and the vertical columns or legs are proportioned to resist the horizontal pressure and the extra moment caused by the shortening of the beam.

Longitudinal shortening of the horizontal beam caused by the prestressing force results in tensile stresses at the outside face of the frame columns. The prestressing vertical tendon should be designed to resist these stresses as well as others. The longitudinal shortening also results in horizontal reactions at the column's supports. Consequently, in order to obtain a prestressing force  $P$  in the longitudinal member, a force  $P + \Delta P$  has to be applied to the frame. The incremental force  $\Delta P$  can be evaluated by means of the following expressions.

**Frame with Two Hinges at Supports**

$$\Delta P = \frac{M_B}{h} = \frac{3}{2k + 3} \frac{E_c I_c}{h^2} \epsilon_{BC} \quad (6.12)$$

where  $k = (I_b/I_c)(h/l)$  and  $\epsilon_{BC}$  is the total strain due to elastic shortening and movement due to shrinkage and creep. The subscripts  $B$  and  $C$  denote the member extremities of the frame in Figures 6.25 and 6.27.

### Frame with Fixed Supports

$$\begin{aligned}\Delta P &= \frac{M_B - M_A}{h} = \frac{E_c I_c}{h} \left( \frac{3}{k+2} + \frac{k+3}{k(k+2)} \right) \\ &= \frac{3(2k+1) E I_c}{k(k+2) h^2}\end{aligned}\quad (6.13)$$

Figure 6.27 shows the axial deformation due to the strain  $\epsilon_{BC} = \Delta l/l$  caused by shortening, creep, and shrinkage.

The *tributary* moments  $M_A$  and  $M_B$  due to the longitudinal shortening of member  $BC$  in Figure 6.27 are as follows.

### Frame with Two Hinges at Supports

$$M_B = \frac{6}{2k+3} \frac{E_c I_b \theta}{l} = \frac{3}{2k+3} \frac{E_c I_c}{h} \epsilon_{BC} \quad (6.14)$$

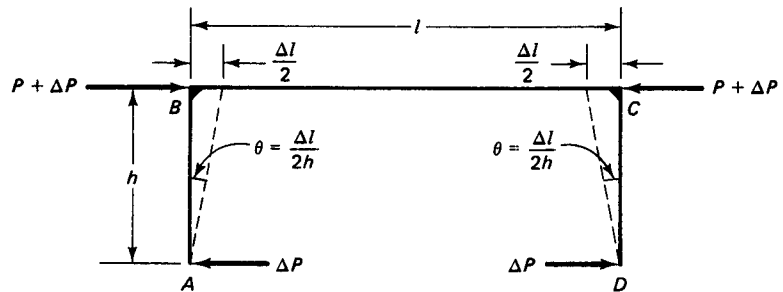
as  $k \rightarrow 0$ ,  $M_B \rightarrow \frac{E I_c}{h} \epsilon_{BC}$ .

### Frame with Fixed Supports

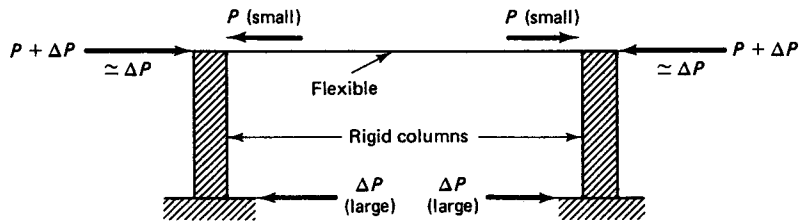
$$M_B = \frac{6}{k+2} \frac{E_c I_c \theta}{h} = \frac{3}{k+2} \frac{E_c I_c}{h} \epsilon_{BC} \quad (6.15)$$

as  $k \rightarrow 0$ ,  $M_B \rightarrow \frac{1.5 E_c I_c}{h} \epsilon_{BC}$  and  $M_A \rightarrow \infty$ .

The reason for the drastic change in moment values  $M_B$  and  $M_A$  is that as  $k$  approaches zero,  $\Delta P$  approaches infinity. In such a case, the stiffness of the vertical members relative to the horizontal member approaches infinity, and the horizontal member becomes very flexible, as shown in Figure 6.28. The effects of the horizontal reactions on



**Figure 6.27** Longitudinal deformation of beam BC due to elastic shortening, creep, and shrinkage.



**Figure 6.28** Effect of tributary moments due to elastic shortening.

the prestressing force are schematically shown in Figure 6.29 for both hinged-base and fixed-base frames.

Note that the discussion here and in the previous section applies equally to continuously cast and precast prestressed composite frames. Continuity at the corner of the frames has to be accomplished in the construction process. A typical prestressing tendon profile for a frame is shown in Figure 6.30. The prestressing force  $P_1$  is assumed to be less than  $P_2$  in order to allow for the frictional losses in prestress.

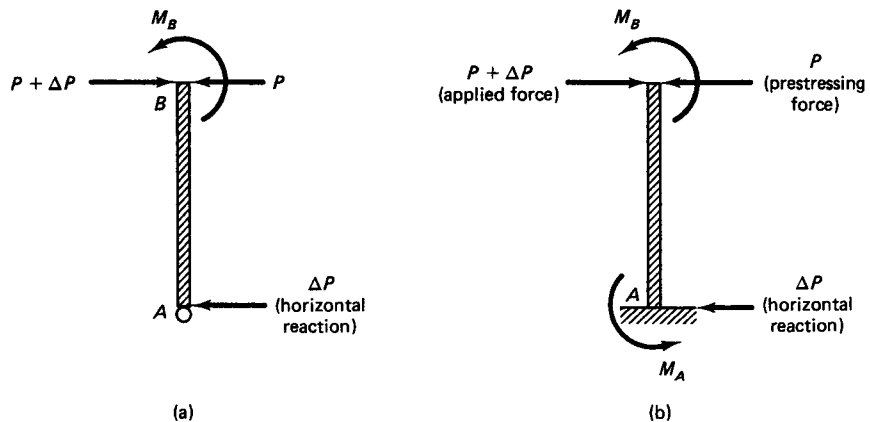
#### 6.12.4 Design of Prestressed Concrete Bonded Frame

##### Example 6.7

A warehouse structure is made of a prestressed single-bay hinged-base portal frame made of standard double-T-sections for both the horizontal beam and the two vertical columns. The units are 8-ft. wide (2.44 m). The frame has a clear span of 80 ft (24.4 m) and is subjected to a uniform gravity live-load intensity  $W_L = 240$  plf (3.5 kN/m) and a uniform horizontal wind pressure of intensity  $p_w = 65$  plf (0.95 kN/m) at the windward side and a suction of intensity  $p_L = 40$  plf (0.58 kN/m) at the leeward side, as shown in Figure 6.31. Design the frame, the profile, and the location of the prestressing tendons for service-load and ultimate load conditions given the following data:

$$f_{pu} = 270,000 \text{ psi (1,862 MPa) for low-relaxation tendons}$$

$$f_{ps} = 235,000 \text{ psi (1,620 MPa)}$$



**Figure 6.29** Horizontal reaction effect on prestressing force. (a) Hinged-base frame. (b) Fixed-base frame.



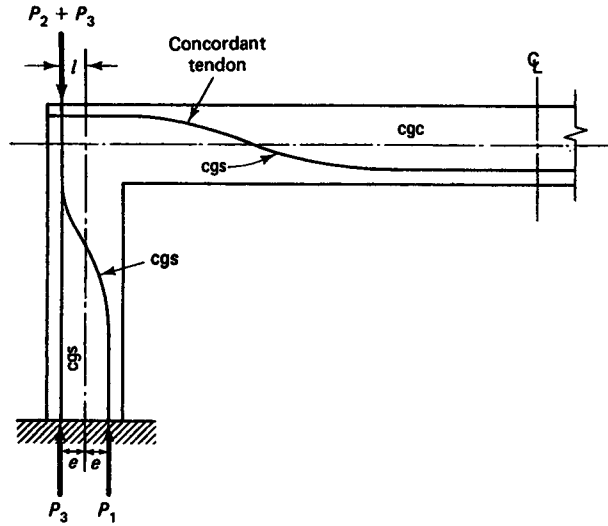


Figure 6.30 Tendon profile in a prestressed frame.

$$f_{pi} = 189,000 \text{ psi (1,303 MPa)}$$

Total losses = 21%, losses after one month of prestressing = 17%

$$f_{pe} \text{ (one month)} = (1 - 0.17)189,000 = 156,870 \text{ psi (1,082 MPa)}$$

$$f_{pe} \text{ (final)} = (1 - 0.21)189,000 = 149,310 \text{ psi (1,029 MPa)}$$

$$f'_c = 5,000 \text{ psi (34.5 MPa)}$$

$$f_c = 0.45f'_c = 2,250 \text{ psi (15.5 MPa)}$$

$$f'_{ci} \cong 0.70f'_c = 3,500 \text{ psi (24.1 MPa)}$$

$$f_{ci} = 0.6f'_{ci} = 2,100 \text{ psi (14.5 MPa)}$$

$$f_u \text{ (midspan)} = 3\sqrt{f'_{ci}} = 177 \text{ psi}$$

$$f_u \text{ (support)} = 6\sqrt{f'_{ci}} = 355 \text{ psi}$$

$$f_t = 6\sqrt{f'_c} \text{ to } 12\sqrt{f'_c} = 425 \text{ to } 849 \text{ psi (5.85 MPa)}$$

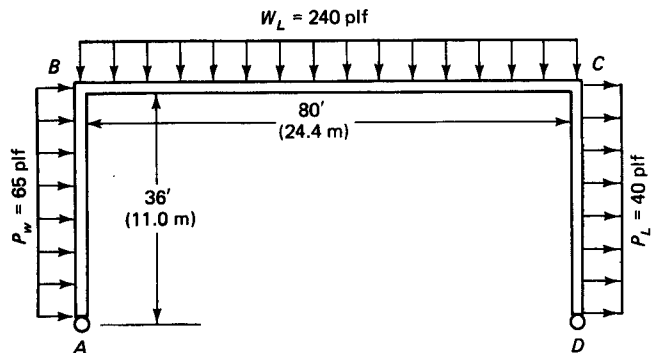


Figure 6.31 Portal frame in Example 6.7.

**Solution:**

**Frame Horizontal Beam BC**

*Preliminary Analysis.* Assume that self-weight  $W_D = 600$  plf (8.8 kN/m). Then from Equation 6.9c, the stiffness coefficient is

$$C_1 = \frac{1}{12\left(\frac{2}{3}k + 1\right)}$$

where

$$k = \frac{I_b h}{I_c l}$$

Assume at this stage that  $I_b = I_c$ , where  $I_b$  is the moment of inertia of the beam  $BC$  and  $I_c$  is the moment of inertia of the column  $AB$  or  $DC$ . Then

$$k = \frac{h}{l} \times 1.0 = \frac{36}{80} = 0.45$$

From the chart for  $C_1$  in Figure 6.26,  $C_1 = 0.064$ . So given total losses = 21%, it follows that  $\gamma = 0.79$ .

Now, assume 2 in. of concrete topping ( $f'_c = 3,000$  psi lightweight), 5 psf insulation, and a waterproofing width of the segment = 8 ft. Then

$$W_{SD} = \left(\frac{2}{12} \times 110 + 5\right) 8 \text{ ft} = 187 \text{ plf}$$

Beam  $BC$  is to be designed as a concordant cable, i.e., it is to behave as a simply supported beam for self-weight  $W_D$ . But it would be considered continuous for the superimposed dead load  $W_{SD}$  and live load  $W_L$  as part of the rigid portal frame. The C-line would then coincide with the cgs line due to concordance. Accordingly, if  $W_D \equiv 600$  plf, then from Equation 6.9e, the *midspan* moment is

$$M = \left(\frac{1}{8} - C_1\right) wl^2$$

so that

$$M_D = \frac{wl^2}{8} = \frac{600(80)^2}{8} \times 12 = 5.760 \times 10^6 \text{ in.-lb}$$

$$M_{SD} = \left(\frac{1}{8} - 0.064\right) 187(80)^2 \times 12 = 0.876 \times 10^6 \text{ in.-lb}$$

$$M_L = \left(\frac{1}{8} - 0.064\right) 240(80)^2 \times 12 = 1.124 \times 10^6 \text{ in.-lb}$$

Assume  $f_t = 0$ . Then from Equation 4.4b, the minimum section modulus at the bottom fibers for an efficient section is given by

$$S_b \geq \frac{(1 - \gamma)M_D + M_{SD} + M_L}{f_t - \gamma f_{ci}}$$

or

$$S_b = \frac{(1 - 0.79)5.760 \times 10^6 + 0.876 \times 10^6 + 1.124 \times 10^6}{0 - 0.79(-2,100)} = 1,935 \text{ in.}^3$$

The closest section is PCI 8DT32 + 2 Double-T type 168-D1 with 2 in. concrete topping (Ref. 6.15).

*Properties of Preliminary Section*

Property	Untopped	Topped
$A_c$ (in. <sup>2</sup> )	567	759
$I_c$ (in. <sup>4</sup> )	55,464	71,886
$r^2 = I_c/A_c$ (in. <sup>2</sup> )	97.8	94.7
$c_b$ (in.)	21.21	23.66
$c_t$ (in.)	10.79	10.34
$S^t$ (in. <sup>3</sup> )	5,140	6,952
$S_b$ (in. <sup>3</sup> )	2,615	3,038
$W_D$ (plf)	591	738

$$e_e = 8.21 \text{ in. (20.9 cm)}$$

$$e_c = 17.46 \text{ in. (44.3 cm)}$$

sixteen  $\frac{1}{2}$ -in. dia (12.7-mm dia) 270-K low relaxation strands

$$A_{ps} = 16 \times 0.153 = 2.45 \text{ in.}^2 (15.8 \text{ cm}^2)$$

**Analysis of Section at Transfer**

(a) *Midspan Section* ( $e_c = 17.46$  in.)

$$M_D = 5.760 \times 10^6 \times \frac{591}{600} = 5.673 \times 10^6 \text{ in.-lb}$$

where

$$591 = \frac{567}{12 \times 12} \times 150 \text{ plf}$$

From Equation 4.1a,

$$f^t = -\frac{P_i}{A_c} \left( 1 - \frac{ec_t}{r^2} \right) - \frac{M_D}{S^t} \leq f_{ti}$$

$$P_i = A_{ps} f_{pi} = 2.45 \times 189,000 = 463,050 \text{ lb}$$

$$\begin{aligned} f^t &= -\frac{463,050}{567} \left( 1 - \frac{17.46 \times 10.79}{97.8} \right) - \frac{5.673 \times 10^6}{5,140} \\ &= -347 \text{ psi (C), no tension, O.K.} \end{aligned}$$

Provide nonprestressed steel at the top fibers at midspan to account for any possible tensile stresses. Then, from Equation 4.1b,

$$\begin{aligned} f_b &= -\frac{P_i}{A_c} \left( 1 + \frac{ec_b}{r^2} \right) + \frac{M_D}{S_b} \\ &= -\frac{463,050}{567} \left( 1 + \frac{17.46 \times 21.21}{97.8} \right) + \frac{5.673 \times 10^6}{2,615} \\ &= -1,740 \text{ psi (C)} < f_{ci} = 2,100 \text{ psi, O.K.} \end{aligned}$$

(b) *Support Section* ( $e_e = 8.21$  in.)

$$\begin{aligned} f^t &= -\frac{463,050}{567} \left( 1 - \frac{8.21 \times 10.79}{97.8} \right) - 0 \\ &= -76.9 \text{ psi (C), no tension, O.K.} \end{aligned}$$

$$f_b = \frac{463,050}{567} \left( 1 + \frac{8.21 \times 21.21}{97.8} \right) + 0$$

$$= -2,271 \text{ psi (C) (15.7 MPa)} > f_{ci} = 2,100 \text{ psi, unsatisfactory}$$

Hence, lower the magnitude of the prestressing force by *debonding* some strands over a length of 15% of span from the support face, or change the eccentricity of the tendon. If the former technique is employed, debond four strands over a length =  $0.15 \times 80 \text{ ft} = 12 \text{ ft}$  (366 m) from the support, releasing the anchorage of the four grouted strands. We obtain

$$A_{ps} = (16 - 4)0.153 = 1.836 \text{ in.}^2$$

$$P_i = 1.836 \times 189,000 = 347,004 \text{ lb (1,543 kN)}$$

$$f_b = -\frac{347,004}{567} \left( 1 + \frac{8.21 \times 21.21}{97.8} \right) + 0$$

$$= -1702 \text{ psi} < 2,100 \text{ psi, O.K.}$$

**Frame Vertical Column Analysis.** Choose a double-T as walls for the frame and suppose that  $e_b$  and  $S_b$  refer to the outer face and that  $e_i$  and  $S_i$  refer to the inner face of the vertical T-section. Since it was assumed, in calculating the stiffness coefficient  $k$  in the previous section, that  $I_b = I_c$ , choose also 8DT32, hinged at the base. This vertical member will act as a compression member subject to large axial load and bending. The bending moments are caused by wind load and moments from the frame horizontal beam  $BC$ . In such a case it is preferable to spread the tendon across the section, as shown in Figure 6.32 comparing the beam section and the column section.

Assume that the center of gravity of the prestressing strands coincides with the cgc line, and design the distribution of the strands according to

$$e_c = e_e = 0$$

Try using twenty  $\frac{1}{2}$ -in. dia 270-K low-relaxation strands:

$$A_{ps} = 20 \times 0.153 = 3.06 \text{ in.}^2$$

$$P_i = A_{ps} f_{pi} = 3.06 \times 189,000 = 578,340 \text{ lb}$$

$$f^t = f_b = -\frac{P_i}{A_c} \pm 0 = -\frac{578,340}{567} = -1,020 \text{ psi (C)} < f_{ci} = 2,100 \text{ psi, O.K.}$$

### Frame Moments and Reactions at Service-Load Level

#### Horizontal Portal Beam BC

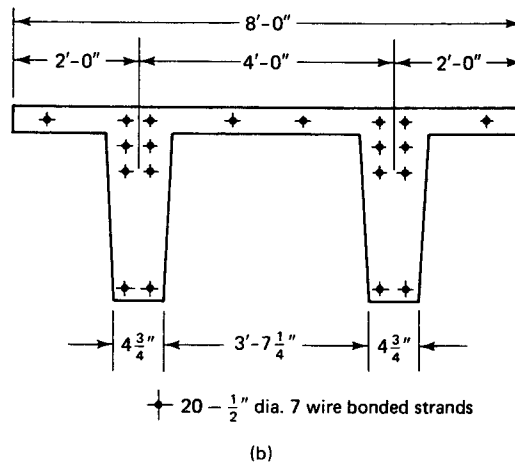
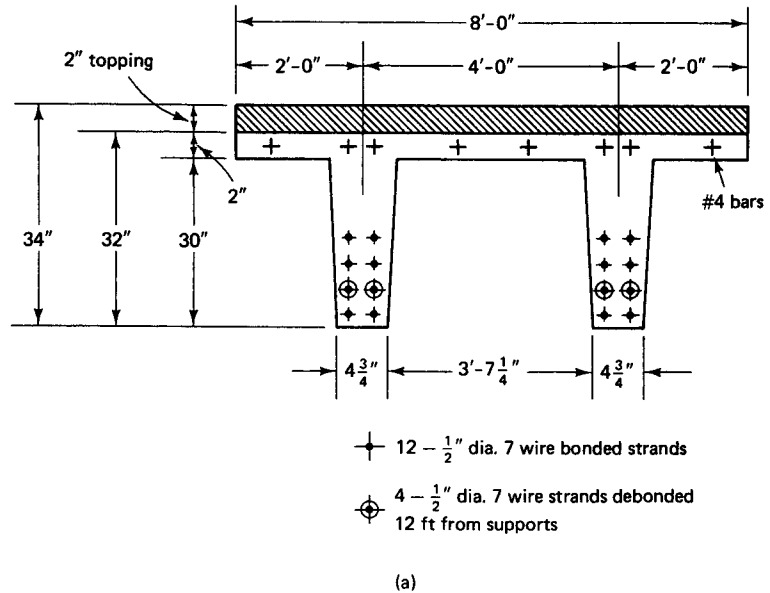
**Free Support  $W_D$  Stage.** Assume that the length of precast beams is  $80 - 1.3 = 78.7 \text{ ft}$ . Then the midspan moment  $M_E = wl^2/8 = [591(78.7)^2/8] \times 12 = 5.491 \times 10^6 \text{ in.-lb}$  and the reaction at the column-wall bracket support is  $R_D = 591 \times 78.7/2 = 23,256 \text{ lb}$ .

**Composite Topping  $W_{SD}$  Stage.** From before, the midspan moment is  $M_{SD} = 0.876 \times 10^6 \text{ in.-lb}$ . The support moment is then

$$M_B = M_c = \frac{wl^2}{8} - 0.876 \times 10^6$$

$$= \frac{187(80)^2 \times 12}{8} - 0.876 \times 10^6 = 0.919 \times 10^6 \text{ in.-lb}$$

**Redistribution of Moments.** The maximum distribution percentage is



**Figure 6.32** Details of beam and wall double-T's in Example 6.7. (a) Horizontal beam standard PCI section 8DT32 + 2 (168-D1). (b) Vertical wall section 8DT32 with twenty  $\frac{1}{2}$ -in. dia. strands with  $e_c = e_e = 0$ .

$$d = 32 + 2 - 2.5 \cong 31.5 \text{ in.}$$

$$\text{compression side } b = 2 \times 4.75 = 9.50 \text{ in.}$$

$d_p = c_b + e_e = 21.21 + 8.21 = 29.42 \text{ in.}$  or  $d_p = 0.8h = 0.8 \times 32 = 25.6 \text{ in.}$  whichever is larger. Use  $d_p = 29.42 \text{ in.}$ , and assume two #5 bars per rib at the compression side and two #7 bars per rib at the tension side of both the horizontal roof beams and the vertical wall beams. We obtain

$$A'_s = 4 \times 0.305 = 1.22 \text{ in.}^2$$

$$\omega' = \frac{A'_s f_y}{bd f'_c} = \frac{1.22}{9.5 \times 31.5} \times \frac{60,000}{5,000} = 0.0489$$

$$A_s = 4 \times 0.60 = 2.40 \text{ in.}^2$$

$$\omega = \frac{A_s f_y}{bd f'_c} = \frac{2.40}{9.5 \times 31.5} \times \frac{60,000}{5,000} = 0.0962$$

Use  $\omega_p = (A_{ps}/bd_p)(f_{ps}/f'_c) = 0$  since the prestressing steel is not continuous over corners of the portal frame. Then  $\omega_p + (d/d_p)(\omega - \omega') = 0 + (31.5/29.42) \times (0.0962 - 0.0489) = 0.0506$ . Also,  $0.24\beta_1 = 0.24 \times 0.80 = 0.192 > 0.0506$ . Hence,  $\epsilon_t$  is larger than 0.0075.

$$a = \frac{A_s f_y}{0.85 f'_c b} = \frac{4 \times 0.60 \times 60,000}{0.85 \times 5000 \times 9.5} = 3.57 \text{ in.}; \quad c = \frac{3.57}{0.80} = 4.46 \text{ in.}$$

$$\epsilon_t = 0.003 \left( \frac{d_t}{c} - 1 \right) = 0.003 \left( \frac{31.5}{4.46} - 1 \right) = 0.0181$$

$$1000 \epsilon_t = 1000 \times 0.0181 = 18.1\% < 20\% \text{ allowable limit, O.K.}$$

Because of the possible large rotations at the composite joint of this frame, use a reduced redistribution percentage of 12 percent in the horizontal member of the frame.

Accordingly, use a moment distribution factor of 0.12 for transferring 12% of the moment from the frame corners  $B$  and  $C$  to midspan  $BC$ . Also, rigid connecting steel plates should be used at the portal upper joints and be so designed to provide a moment connection capable of transferring at least 12% of the support moment to the midspan. Then the adjusted  $M_B = M_C = (1 - 0.12)0.919 \times 10^6 = 0.809 \times 10^6$  in.-lb, the adjusted midspan moment  $M_E = 0.876 \times 10^6 \times 1.12 = 0.981 \times 10^6$  in.-lb, and the superimposed dead-load reaction  $R_{SD}$  at the support  $= (187 \times 80)/2 = 7,480$  lb.

*Live-load  $W_L$  Stage.* From before, the midspan is  $M_L = 1.124 \times 10^6$  in.-lb. So the support moment is

$$\begin{aligned} M_B = M_C &= \frac{240(80)^2 \times 12}{8} - 1.124 \times 10^6 \\ &= 1.180 \times 10^6 \text{ in.-lb} \end{aligned}$$

The adjusted elastic moment  $= M_c = (1 - 0.12) \times 1.180 \times 10^6 = 1.038 \times 10^6$  in.-lb, and the adjusted midspan  $M_L = 1.124 \times 10^6 \times 1.12 = 1.259 \times 10^6$  in.-lb. The live-load reaction at the vertical support is

$$R_L = \frac{240 \times 80}{2} = 9,600 \text{ lb}$$

*Wind Pressure Stage.* From Equations 6.11h and i,

$$M_B = (C_4 - 0.5)ph^2$$

$$M_C = -(1 - C_4)ph^2$$

From before,

$$k = \frac{I_b h}{I_c l} = 0.45 \text{ for } I_b = I_c$$

From the chart for  $C_4$  in Figure 6.26,  $C_4 = 0.73$ .

*Windward side moment  $M_B$*

$$M_{B1} = (0.73 - 0.5)65(36)^2 \times 12 = 232,502 \text{ in.-lb}$$

$$M_{B2} = (1 - 0.73)40(36)^2 \times 12 = 167,961 \text{ in.-lb}$$

$$\text{Total } M_B = 232,502 + 167,961 = 400,463 \text{ in.-lb}$$

*Leeward side moment  $M_c$*

$$M_{c1} = -(1 - 0.73)65(36)^2 \times 12 = -272,938 \text{ in.-lb}$$

$$M_{c2} = -(0.73 - 0.5)40(36)^2 \times 12 = -143,078 \text{ in.-lb}$$

$$\text{Total } M_c = -272,938 - 143,078 = -416,016 \text{ in.-lb}$$

The controlling wind moment  $M_w = 416,016$  in.-lb, since wind can blow from either the left or the right.

From Equation 6.11a, the vertical reactions at  $A$  and  $D$  due to wind are

$$R_{WA} = -\frac{1}{2}ph \frac{h}{l} = -\frac{(65 + 40)(36)^2}{2 \times 80} = -851 \text{ lb}$$

$$R_{WD} = +\frac{1}{2}ph \frac{h}{l} = +851 \text{ lb}$$

### **Loads and Moments Due to Long-Term Effects**

*Moments to Restrain End Rotations at  $B$  and  $C$  Due to Long-Term Prestress Losses.* Figure 6.33 shows the moment distributions on horizontal member  $BC$ . One month after prestressing we have:

$$f_{pe1} = 156,870 \text{ psi}$$

$$\text{Midspan } P_e = 16 \times 0.153 \times 156,870 = 384,018 \text{ lb}$$

$$\text{Support } P_e = (16 - 4) \times 0.153 \times 156,870 = 288,013 \text{ lb}$$

$$\text{Midspan moment } M_E = 384,018 \times 17.46 = 6.705 \times 10^6 \text{ in.-lb}$$

$$\text{Support moment } M_B = 288,013 \times 8.21 = 2.364 \times 10^6 \text{ in.-lb}$$

The eccentricity at section  $F$ , where four strands were debonded, is

$$e_F = (17.46 - 8.21) \frac{12}{40} + 8.21 = 10.99 \text{ in.}$$

and the moment at section  $F$  is

$$M_F = 384,018 \times 10.99 = 4.220 \times 10^6 \text{ in.-lb}$$

The reduced  $M_F$  due to debonding is  $288,013 \times 10.99 = 3.165 \times 10^6$  in.-lb.

The service load after all losses have occurred is as follows:

$$f_{pe} = 149,310 \text{ psi}$$

$$f_{pe}/f_{pe1} = \frac{149,310}{156,870} = 0.952$$

$$M_E = 6.705 \times 10^6 \times 0.952 = 6.383 \times 10^6 \text{ in.-lb}$$

$$M_F = 4.220 \times 10^6 \times 0.952 = 4.017 \times 10^6 \text{ in.-lb}$$

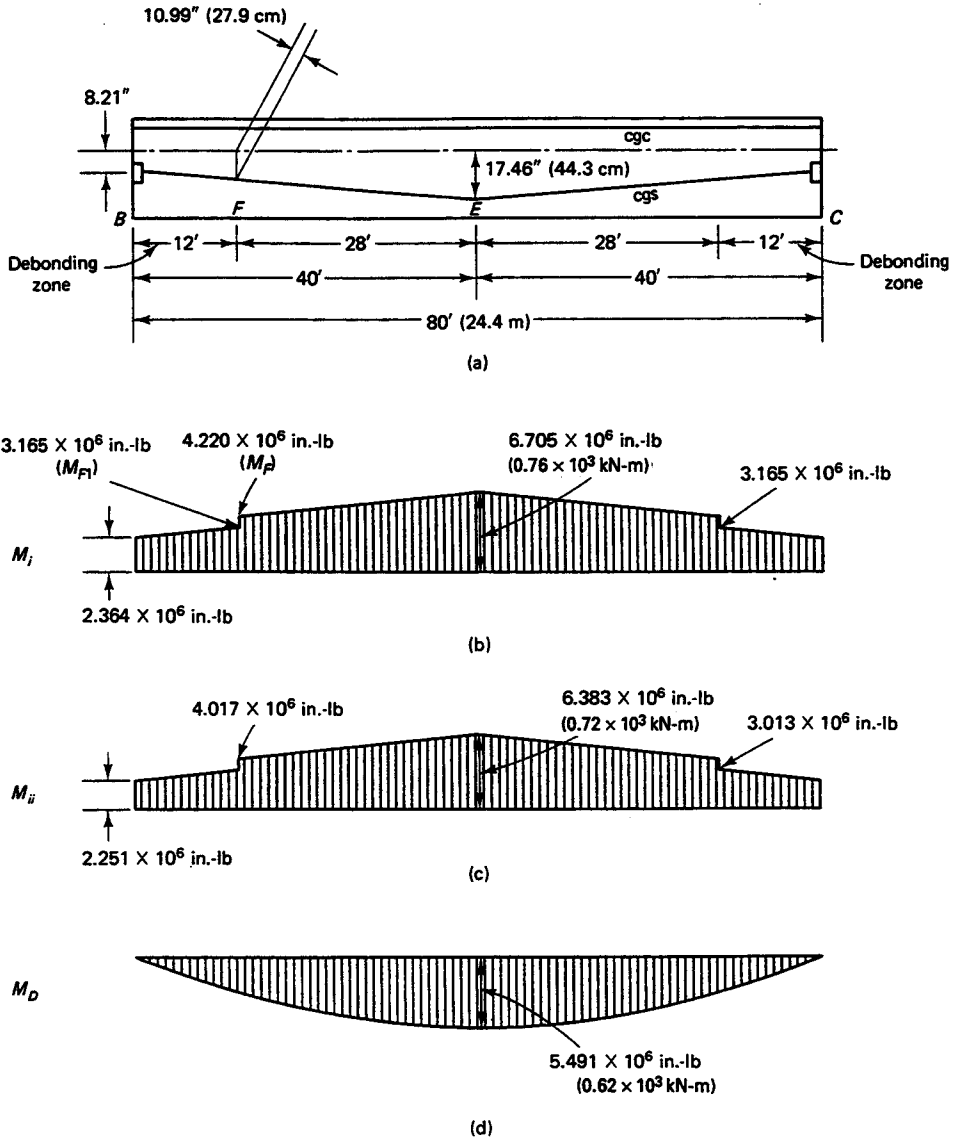
$$M_{F1} = 3.165 \times 10^6 \times 0.952 = 3.013 \times 10^6 \text{ in.-lb}$$

$$M_B = M_C = 2.364 \times 10^6 \times 0.952 = 2.251 \times 10^6 \text{ in.-lb}$$

*Slopes at  $B$  and  $C$  at Beam Erection One Month After Prestressing*

$$\text{Slope } \theta = \frac{1}{E_c I_b} [MI]$$

To find the areas of the moment diagrams for half the span due to symmetry, (i) add half of Figure 6.33(b) to half of Figure 6.33(d), and (ii) add half of Figure 6.33(c) to half of Figure 6.33(d). Then subtract (ii) from (i) to get the rotation of the beam at  $B$  or



**Figure 6.33** Bending moment diagrams for primary and self-weight moments for beam BC. (a) Tendon profile. (b) Prestressing moments one month after initial prestress. (c) Effective prestressing moment after all losses. (d) Beam BC self-weight moments.

$C$  that would have to be restrained by a welded connection to develop continuity at the portal frame corners  $B$  and  $C$ . We have:

(i)

$$\begin{aligned}
 \theta E_c I_b \times 10^{-6} &= M_{(i)} l \text{ at beam erection} \\
 &= 2.364 \times 12 \times 12 + (3.165 - 2.364) \times 12 \times 12 \times \frac{1}{2} \\
 &\quad + 4.220 \times 28 \times 12 + (6.705 - 4.220) \times 28 \times 12 \times \frac{1}{2}
 \end{aligned}$$



$$- 5.491 \times 40 \times 12 \times \frac{2}{3} = 2,233.49 - 1,757.12 = 476.7$$

(ii)

$$\begin{aligned} \theta E_c I_b \times 10^{-6} &= M_{(ii)} l \text{ at service load} \\ &= 2.251 \times 12 \times 12 + (3.013 - 2.251) \times 12 \times 12 \times \frac{1}{2} \\ &\quad + 4.017 \times 28 \times 12 + (6.383 - 4.017) \times 28 \times 12 \times \frac{1}{2} \\ &\quad - 5.491 \times 40 \times 12 \times \frac{2}{3} = 2,126.21 - 1,757.12 = 369.4 \end{aligned}$$

The rotational angle  $\theta$  at  $B$  or  $C$  caused by the reduction in the prestressing force due to long-term losses is

$$\frac{1}{E_c I_b} (476.7 - 369.4) 10^6 = \frac{107.3 \times 10^6}{E_c I_b}$$

If  $M_r$  is the resisting moment at the connection weld to restrain the member against this rotation,

$$\text{Slope } \theta = \frac{M_r l/2}{E_c I_b} = \frac{M_r \times 480}{E_c I_b}$$

Equating the right sides of the preceding equations yields

$$\begin{aligned} \frac{107.3 \times 10^6}{E_c I_b} &= \frac{480 M_r}{E_c I_b} \\ M_r &= \frac{107.3 \times 10^6}{480} = 0.224 \times 10^6 \text{ in.-lb} \end{aligned}$$

#### Moments Resulting from Creep and Shrinkage Long-Term Losses

(a) Creep

$$P_i = 463,050 \text{ lb}$$

$$P_e \text{ at erection} = 384,018 \text{ lb}$$

It is reasonable to take the creep force as the average of  $P_i$  and  $P_e$ . Thus,

$$\epsilon_{CR} = \frac{1}{A_c E_c} \left[ \left( \frac{P_i + P_e}{2} \right) C_u \right]$$

Use the creep coefficient  $C_u = 2.25$ :

$$\begin{aligned} E_c &= 57,000 \sqrt{f'_c} = 57,000 \sqrt{5,000} = 4.03 \times 10^6 \text{ psi} \\ \epsilon_{CR} &= \frac{1}{567 \times 4.03 \times 10^6} \left( \frac{463,050 + 384,018}{2} \times 2.25 \right) \\ &= 417 \times 10^{-6} \text{ in./in.} \end{aligned}$$

(b) Shrinkage

From Equation 3.14, the shrinkage strain from the time of erection (30 days after prestressing) to one year later is

$$\epsilon_{SH} = 8.2 \times 10^{-6} K_{SH} \left( 1 - 0.06 \frac{V}{S} \right) (100 - RH)$$

Now,  $V/S = 1.79$ , and if we assume that  $RH = 75\%$ , then, from Table 3.6, which states that after 30 days to within one year  $K_{SH} = 0.45$ , we have

$$\begin{aligned}\epsilon_{SH} &= 8.2 \times 10^{-6} \times 0.45(1 - 0.06 \times 1.79)(100 - 75) \\ &= 82.3 \times 10^{-6} \text{ in./in.}\end{aligned}$$

So the total deformation strain due to creep and shrinkage is  $(417 + 82.3)10^{-6} = 499.3 \times 10^{-6}$  in./in.

From Equation 6.14,

$$M_B = M_C = \frac{3}{(2k + 3)} \frac{E_c I_c}{h} \epsilon_{BC}$$

From before, the stiffness coefficient  $k = 0.45$ , and  $E_c = 4.03 \times 10^6$  psi. Also, precast  $I_c = 55,464$  in.<sup>4</sup> Consequently,

$$\begin{aligned}M_B = M_C &= \frac{3}{(2 \times 0.45 + 3)} \times \frac{4.03 \times 10^6 \times 55,464}{36 \times 12} \times 499.3 \times 10^{-6} \\ &= 198,724 \text{ in.-lb} = 0.199 \times 10^6 \text{ in.-lb}\end{aligned}$$

These moments due to long-term effects will produce tensile stresses at the inside face of the vertical member and bottom face of the horizontal member. Elastic shortening should also be considered often for accuracy.

### ***Final Moments and Stresses in the Horizontal Beam BC***

*Midspan Section ( $e_c = 17.46$  in.)*

$$M_D = 5.491 \times 10^6 \text{ in.-lb} \quad (0.62 \times 10^3 \text{ kN-m})$$

$$M_{SD} = 0.981 \times 10^6 \text{ in.-lb}$$

$$M_L = 1.259 \times 10^6 \text{ in.-lb}$$

$$M_r = 0.224 \times 10^6 \text{ in.-lb}$$

$$M_{CR+SH} = 0.199 \times 10^6 \text{ in.-lb}$$

$$P_e \text{ after all losses} = 2.45 \times 149,310 = 365,810 \text{ lb}$$

The total superimposed moments are

$$\begin{aligned}M_T &= M_{SD} + M_L + M_r + M_{CR+SH} \\ &= (0.981 + 1.259 + 0.244 + 0.199) \times 10^6 \\ &= 2.663 \times 10^6 \text{ in.-lb}\end{aligned}$$

$$\begin{aligned}f_b &= -\frac{P_e}{A_c} \left( 1 + \frac{e_c c_b}{r^2} \right) + \frac{M_D}{S_b} + \frac{M_T}{S_{bc}} \\ &= -\frac{365,810}{567} \left( 1 + \frac{17.46 \times 21.21}{97.8} \right) + \frac{5.491 \times 10^6}{2,615} + \frac{2.663 \times 10^6}{3,038} \\ &= -112 \text{ psi (C), no tension, O.K.}\end{aligned}$$

$$\begin{aligned}f' &= -\frac{P_e}{A_c} \left( 1 - \frac{e_c c_t}{r^2} \right) - \frac{M_D}{S'} - \frac{M_T}{S'_c} \\ &= -\frac{365,810}{567} \left( 1 - \frac{17.46 \times 10.79}{97.8} \right) - \frac{5.491 \times 10^6}{5,140} - \frac{2.663 \times 10^6}{6,952} \\ &= -854 \text{ psi (C)} < f_c = 2,250 \text{ psi, O.K.}\end{aligned}$$

*Support Section ( $e_e = 8.21$  in.)*

$$M_D = 0$$

$$M_{SD} = 0.809 \times 10^6 \text{ in.-lb}$$

$$M_L = 1.038 \times 10^6 \text{ in.-lb}$$

$$M_W = 0.416 \times 10^6 \text{ in.-lb}$$

Not including the relief moments due to rotation, creep, and shrinkage, which cause compressive stresses, the total negative moments at supports B or C are

$$-M_T = (0.809 + 1.038 + 0.416)10^6 = 2.26 \times 10^6 \text{ in.-lb}$$

The sections at supports B and C are virtually reinforced concrete.  $P_e$  for 12 strands at either support after all losses = 274,133 lb, and

$$f'_t = -\frac{274,133}{567} \left( 1 - \frac{8.21 \times 10.79}{97.8} \right) + 0 + \frac{2.26 \times 10^6}{6,952}$$

$$= +280 \text{ psi } (T) < f_t = 12\sqrt{f'_c} = 849 \text{ psi, O.K.}$$

Provide nonprestressed steel to accommodate all the tensile stress. Also,

$$f_b = -\frac{274,133}{567} \left( 1 + \frac{8.21 \times 21.21}{97.8} \right) - 0 - \frac{2.26 \times 10^6}{3,038}$$

$$= -2,088 \text{ psi } (C) < f_c = 2,250 \text{ psi, O.K.}$$

From Eq. 4.31d,

$$M_u = 1.2 \times 0.809 \times 10^6 + 1.6(1.038 \times 10^6) + 1.0(0.416 \times 10^6)$$

$$= 3.05 \times 10^6 \text{ in.-lb}$$

$$\text{Rqd. } M_n = \frac{M_u}{\phi} = \frac{3.05 \times 10^6}{0.90} = 3.39 \times 10^6 \text{ in.-lb}$$

$$M_n = A_s f_y \left( d - \frac{a}{2} \right)$$

Assume a moment arm  $d - a/2 \cong 0.9d = 0.9 \times 31.5 = 28.35$  in. Then

$$3.39 \times 10^6 = A_s \times 60,000 \times 28.35$$

$$A_s = \frac{3.39 \times 10^6}{60,000 \times 28.35} = 1.99 \text{ in}^2 \text{ (12.0 cm}^2\text{)}$$

$$a = \frac{A_s f_y}{0.85 f'_c b} = \frac{1.99 \times 60,000}{0.85 \times 5,000 \times 96}$$

$$= 0.29 \text{ in. (0.81 cm)} < h_f = 4 \text{ in.}$$

Hence, treat as a rectangular section:

$$d - \frac{a}{2} = 31.5 - \frac{0.29}{2} = 31.3 \text{ in. (79.5 cm)}$$

$$A_s = \frac{3.39 \times 10^6}{60,000 \times 31.3} = 1.81 \text{ in}^2 \text{ (12.3 cm}^2\text{)}$$

Use two #7 bars (22-mm dia) in each rib. Then

$$A_s = 4 \times 0.60 = 2.40 \text{ in}^2 > 1.81 \text{ in}^2, \text{ O.K.}$$

**Final Moments and Stresses in the Vertical Column Walls AB and DC.** The direct load on the column is

$$R_D + R_{SD} + R_L + R_W = 23,256 + 7,480 + 9,600 + 851 = 41,187 \text{ lb (183 kN)}$$

Assuming 15 in eccentricity, the moment  $M_D$  becomes

$$M_D = 41,187 \times 15 = 0.617 \times 10^6 \text{ in.-lb}$$

$$M_{SD} = 0.809 \times 10^6$$

$$M_L = 1.038 \times 10^6$$

$$M_W = 0.416 \times 10^6$$

The total moment is

$$\begin{aligned} M_T &= (0.617 + 0.809 + 1.038 + 0.416)10^6 \\ &= 2.880 \times 10^6 \text{ in.-lb } (0.33 \times 10^3 \text{ kN-m}) \end{aligned}$$

For 20 strands in the wall units,

$$P_e = A_{ps} f_{pe} = 3.06 \times 149,310 = 456,887 \text{ lb } (2,032 \text{ kN})$$

$$\begin{aligned} f_b (\text{outer face}) &= -\frac{P_e}{A_c} - \frac{P}{A_c} + \frac{M_T}{S_b} \\ &= -\frac{456,887}{567} - \frac{41,187}{567} + \frac{2.880 \times 10^6}{2,615} \\ &= +223 \text{ psi } (T) \leq 849 \text{ psi, O.K.} \end{aligned}$$

$$\begin{aligned} f_i (\text{innerface}) &= -\frac{P_e}{A_c} - \frac{P}{A_c} - \frac{M_T}{S^i} \\ &= -\frac{456,887}{567} - \frac{41,187}{567} - \frac{2.880 \times 10^6}{5,140} \\ &= -1,439 \text{ psi } (C) (9.9 \text{ MPa}) < f_c = 2,250 \text{ psi } (15.5 \text{ MPa}) \end{aligned}$$

Consequently, adopt the double-T section 8DT32 for the walls with twenty  $\frac{1}{2}$ -in. dia 7-wire 270-K low-relaxation strands arranged as shown in Figure 6.32. Also, adopt the double-T section 8DT32 + 2(168 - D1) for the horizontal top beam BC with sixteen  $\frac{1}{2}$ -in. dia 7-wire 270-K low-relaxation strands with four strands debonded 12 ft (3.66 m) from the face of the supports.

Figure 6.34 gives a schematic of the configuration details of the prestressed concrete portal frame. The total design would involve designing the vertical wall brackets, shear strength, flexural strength, and serviceability checks as well as detailing the welded connections between the horizontal beam and the supporting wall columns.

## 6.13 LIMIT DESIGN (ANALYSIS) OF INDETERMINATE BEAMS AND FRAMES

The discussions presented so far deal with proportioning the controlling sections in the design process, such as the midspan and support sections, with redistribution factors  $p_D$  for continuity empirically provided by the code. The continuity factors assume that adequate longitudinal reinforcement is provided at the critical continuity zones to properly control the cracking levels of those zones.

Such a procedure does not necessarily give the most efficient solution to a statically indeterminate continuous beam or frame, since full redistribution at ultimate load is not considered. As the applied load is gradually increased until the structure as a whole reaches its limit capacity, the critical sections, such as the supports or corners of frames, develop severe cracking, and the rotation becomes so large that, for all practical purposes, rotating *plastic hinges* have developed. If the number of plastic hinges that develop equals the number of indeterminacies, the structure becomes determinate, as *full redistribution* of moments would have taken place throughout it. With the development of an additional hinge, the structure becomes a mechanism tending toward collapse.

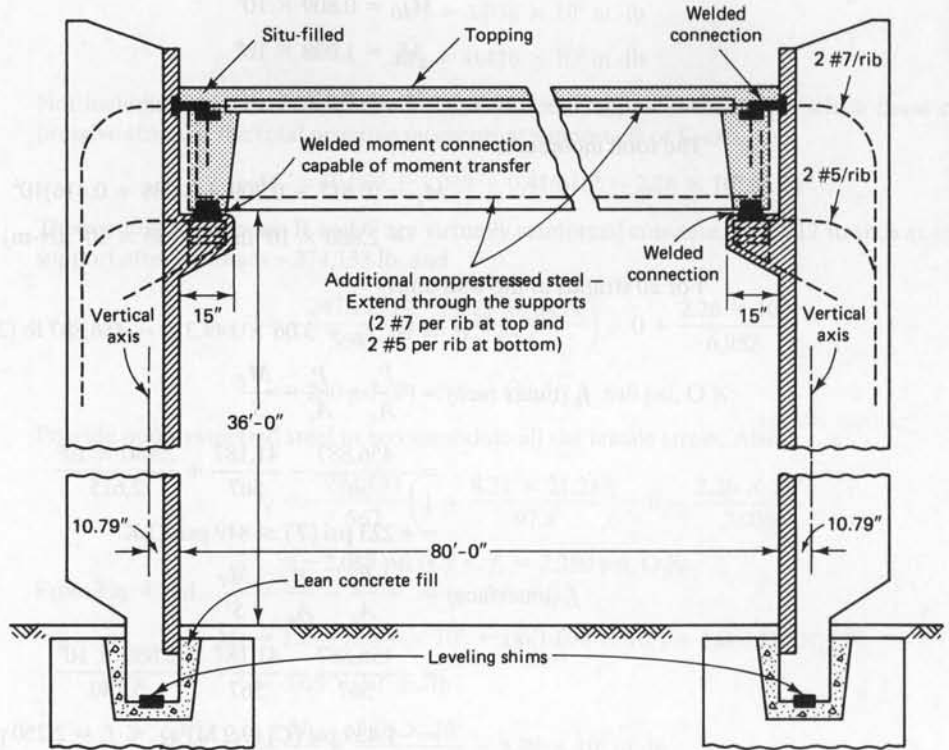


Figure 6.34 Sectional elevation and connection details of frame in Example 6.7.

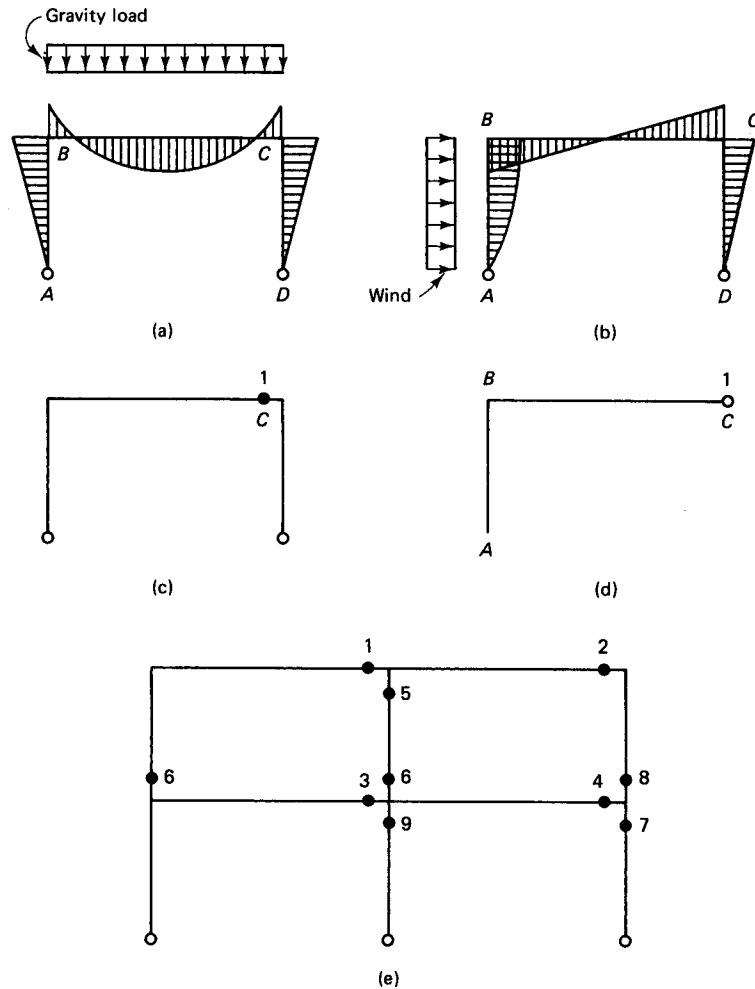
Analysis of the structure at *full* moment redistribution is termed as *plastic* or *limit* analysis. Since concrete cracks severely at high overloads, it is possible for the designer to *impose* the desirable locations of the plastic hinges by making the concrete member fail or making it adequately strong at any section by decreasing or increasing the reinforcement percentage without appreciably altering the stiffness of the member. This flexibility in proportioning is not available in the plastic design of steel structures, where the resulting locations of the plastic hinges are obtained from mechanisms determined by upper and lower bound solutions. Details of Baker's *theory of imposed rotations* are presented in Refs. 6.5, 6.6, and 6.7.

### 6.13.1 Method of Imposed Rotations

The imposed locations of the plastic hinges coincide with the locations of the maximum elastic moments for combined gravity loads and horizontal wind loads. These locations occur at the intermediate supports of continuous beams and beam-column corners of frames, as seen in the portal frame of Figure 6.35. By superposing part (a) on part (b), one plainly sees that the maximum elastic moment occurs at corner C. Since plastic moments are a magnification of the elastic moments, the natural location for the development of a plastic hinge is at that corner.

Because the structure is indeterminate to the first degree, only one hinge develops, resulting in a *basic* frame ABC, which is the fundamental frame for the imposed hinges seen in Figure 6.35(e), numbered in the order in which they are expected to form.

The structure in Figure 6.35(e) has nine indeterminacies; hence, nine plastic hinges are formed. A tenth hinge reduces the structure to a mechanism resulting in collapse. Note that no plastic hinges are permitted to form at midspan of the horizontal members.



**Figure 6.35** Imposed plastic hinges in concrete frames. (a) Gravity-load elastic moment. (b) Wind-load intensity moments. (c) Hinge 1 at C reducing frame to statically determinate. (d) Basic plastic frame. (e) Succession of plastic hinges in two-span, two-level frame.

The plastic moments resulting in hinges 1,2,3, . . . , $n$  are denoted  $\bar{X}_1, \bar{X}_2, \bar{X}_3, \dots, \bar{X}_n$  and are assumed to remain constant throughout the progressive deformation of the structure. Hence, the derivative of the total strain energy  $U$  with respect to the assumed plastic moments  $\bar{X}_i$  at any hinge  $i$  is set equal to the plastic rotation at the hinge, i.e.,

$$\frac{\delta U}{\delta \bar{X}_i} = -\theta_i \tag{6.16}$$

If  $\delta_{ik}$  is assumed to represent the relative rotation of the  $i$ th hinge due to a unit moment at the  $k$ th hinge,  $\delta_{ik} = \delta_{ki}$  from Maxwell's reciprocal theorem. The coefficients  $\delta_{ik}$  are called *influence coefficients*, because they represent the displacement or rotation at a particular section due to a unit moment at *another* section, i.e.,  $\delta_{ik} = -\theta_i$ .

From the principle of virtual work,

$$\delta_{ik} = \sum \int_0^l \frac{M_i M_k}{E_c I} ds \tag{6.17}$$

Consequently,

$$\Sigma \int_0^l \frac{M_i M_k}{E_c I} ds = -\theta_i \quad (6.18)$$

The left-hand side of Equation 6.18 represents the integration of the products of the areas of the  $M_i$  diagrams and the ordinates of  $M_k$  diagrams at their centroids along the horizontal distance  $s$  along the span. Substituting  $\delta_{i0}$  and  $\delta_{ik}$  for  $M_k$ , we obtain

$$\delta_{i0} + \sum_{k=1}^{k=n} \delta_{ik} \bar{X}_k = -\theta_i \quad (6.19)$$

This is a structure having  $n$  plastic hinges to reduce it to statically determinate:

$$\begin{aligned} \delta_{i0} + \delta_{i1} \bar{X}_1 + \delta_{i2} \bar{X}_2 + \cdots + \delta_{in} \bar{X}_n &= -\theta_i \\ \delta_{20} + \delta_{21} \bar{X}_1 + \delta_{22} \bar{X}_2 + \cdots + \delta_{2n} \bar{X}_n &= -\theta_2 \\ \delta_{n0} + \delta_{n1} \bar{X}_1 + \delta_{n2} \bar{X}_2 + \cdots + \delta_{nn} \bar{X}_n &= -\theta_n \end{aligned} \quad (6.20)$$

The number of equations is equal to the number of redundancies or indeterminacies. By trial and adjustment of the redundant plastic moments  $\bar{X}_1, \dots, \bar{X}_n$  in the solution of Equations 6.20 for controlled maximum allowable rotation of the largest rotating hinge  $\theta_1$ , the plastic moments at the beam supports and column ends are obtained for the plastic design of the concrete structure. The arbitrary plastic moment values  $\bar{X}_1, \bar{X}_2, \dots, \bar{X}_n$  are chosen to result in plastic rotations  $\theta_1, \theta_2, \dots, \theta_n$  that give *full redistribution* of moments throughout the structure.

It can be proven that the influence coefficient  $\delta_{ik}$  in Equations 6.20 is

$$\delta_{ik} = \frac{A_i}{E_i} \eta \quad (6.21)$$

where  $A_i$  is the area under the primary  $M_i$  bending moment diagram and  $\eta$  is the ordinate of the  $M_k$  moment diagram under the centroid of the  $M_i$  diagram (Ref. 6.5). As an example, in Figure 6.36 the influence coefficient  $\delta_{01}$  is obtained by superposing the moment diagram  $M_0$  of the primary structure on the diagram  $\bar{X}_1$  of the redundant structure created by the development of hinge 1. We have

$$A_i = \frac{2}{3} la$$

and  $\eta$  under the centroid of the  $M_0$  diagram =  $c/2$ , resulting in

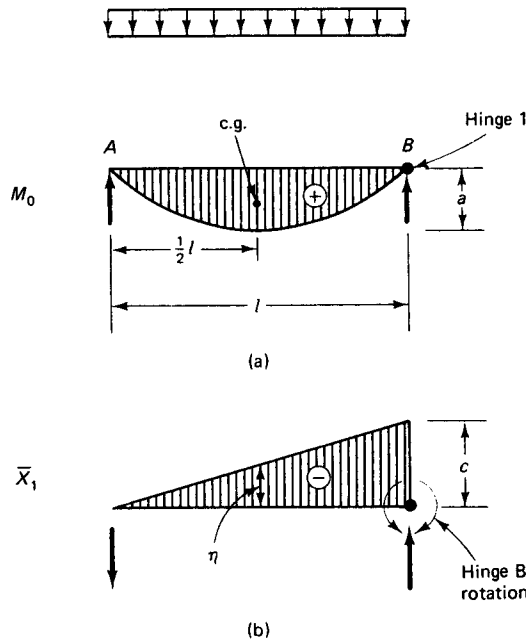
$$\delta_{01} = -\frac{1}{EI} \left( \frac{2}{3} la \right) \left( \frac{c}{2} \right) = \frac{1}{3EI} lac$$

$\delta_{11}$  is obtained by superposing the redundant structure  $\bar{X}_1$  on itself:

$$A_i = \frac{1}{2} la$$

$$\eta = \frac{2}{3} c$$

$$\delta_{11} = -\frac{1}{EI} \left( \frac{1}{2} la \times \frac{2}{3} c \right) = -\frac{1}{3EI} lac$$



**Figure 6.36** Influence coefficient determination from superposing  $M_0$  and  $\bar{X}_1$ . (a) Primary structure moment. (b) Redundant structure moment.

Table 6.1 gives the values  $\int M_i M_k ds$  for evaluating the influence coefficient values  $\delta_{ik}$  for various combinations of primary and redundant moment diagrams. It can aid the designer in easily forming and solving sets of Equations 6.20 for any indeterminate structural system.

### 6.13.2 Determination of Plastic Hinge Rotations in Continuous Beams

#### Example 6.8

Determine the required plastic hinge rotation in the four-span beam of Figure 6.37. The beam is subjected to simple-span plastic moment  $M_0$  so that the midspan moment is equal to the support moment  $= \frac{1}{2} M_0$  before full rotation of the hinges and full moment redistribution take place.

**Solution:** The structure is statically indeterminate to the third degree, so that three hinges will develop at the plastic limit. Assume the maximum ordinate  $c$  of the redundant moment at hinge location to be unity. Then, from Table 6.1 and Figure 6.38,

$$EI\delta_{10} = -\frac{2}{3} M_0 l$$

$$\delta_{11} = \frac{2}{3} l$$

$$\delta_{12} = \frac{1}{6} l$$

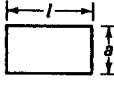


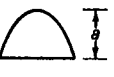
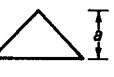

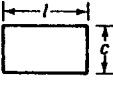
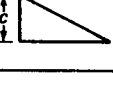
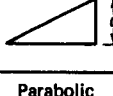

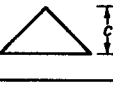

$$\delta_{13} = 0$$

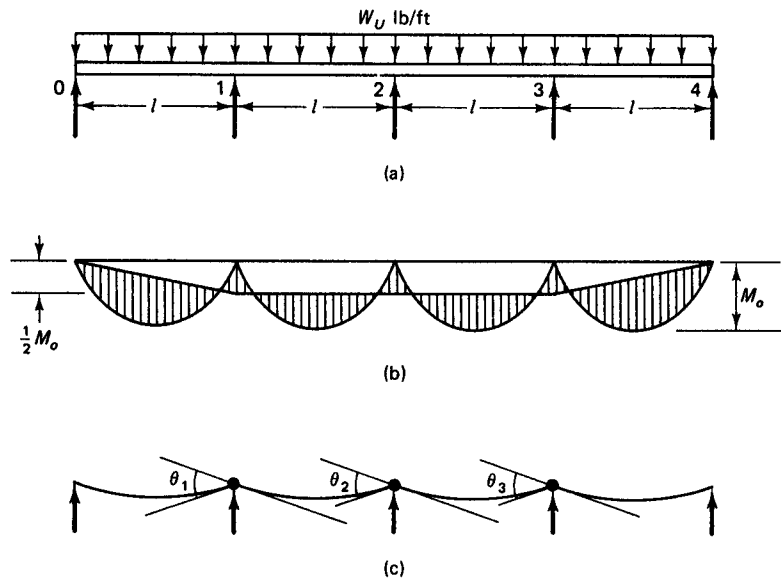
From Equation 6.19,

$$-\delta_1 = \delta_{10} + \delta_{11}\bar{X}_1 + \delta_{12}\bar{X}_2 + \delta_{13}\bar{X}_3$$

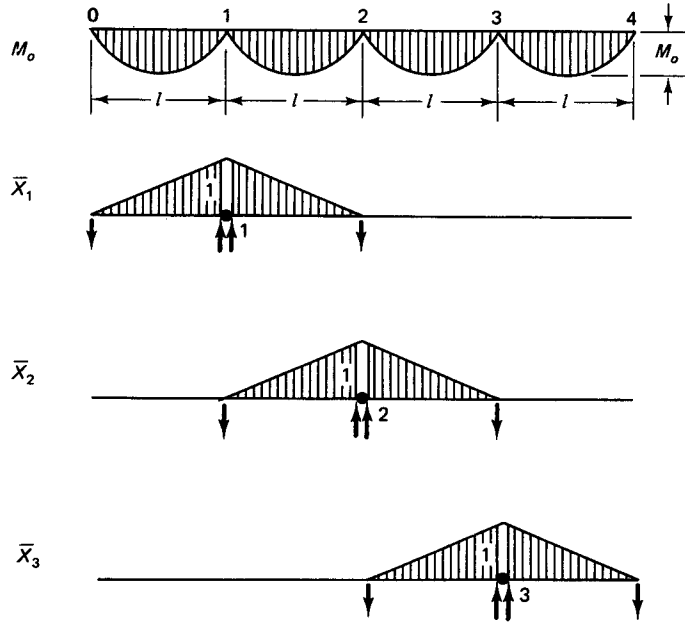


**Table 6.1** Product Integral Values  $\int M_i M_k ds$  for Various Moment Combinations  $EI \delta_{ik}$

$M_i \backslash M_k$						
	$lac$	$\frac{1}{2} lac$	$\frac{1}{2} lac$	$\frac{2}{3} lac$	$\frac{1}{2} lac$	$\frac{1}{2} l (a + b)c$
	$\frac{1}{2} lac$	$\frac{1}{3} lac$	$\frac{1}{6} lac$	$\frac{1}{3} lac$	$\frac{1}{4} lac$	$\frac{1}{6} l (2a + b)c$
	$\frac{1}{2} lac$	$\frac{1}{6} lac$	$\frac{1}{3} lac$	$\frac{1}{3} lac$	$\frac{1}{4} lac$	$\frac{1}{6} l (a + 2b)c$
	$\frac{2}{3} lac$	$\frac{1}{3} lac$	$\frac{1}{3} lac$	$\frac{8}{16} lac$	$\frac{5}{12} lac$	$\frac{1}{3} l (a + b)c$
	$\frac{1}{2} lac$	$\frac{1}{4} lac$	$\frac{1}{4} lac$	$\frac{5}{12} lac$	$\frac{1}{3} lac$	$\frac{1}{4} l (a + b)c$
	$\frac{1}{2} la (c + d)$	$\frac{1}{6} la (2c + d)$	$\frac{1}{6} la (c + 2d)$	$\frac{1}{3} la (c + d)$	$\frac{1}{4} la (c + d)$	$\frac{1}{6} l [a(2c + d) + b(2d + c)]$



**Figure 6.37** Primary moments and plastic hinge rotations in Example 6.8.



**Figure 6.38** Primary and redundant moments in Example 6.8.

$$-EI\theta_1 = -\frac{2}{3}M_0l + 0.5M_0\left(\frac{2l}{3}\right) + 0.5M_0\left(\frac{l}{6}\right) + 0 = -\frac{M_0l}{4}$$

Also, again from Table 6.1 and Figure 6.38,

$$EI\delta_{20} = \frac{2}{3}M_0l\left(-\frac{1}{2}\right) + \frac{2}{3}M_0l\left(-\frac{1}{2}\right) = -\frac{2}{3}M_0l$$

$$EI\delta_{21} = \left(-\frac{l}{2}\right)\left(-\frac{1}{3}\right) = +\frac{l}{6}$$

$$EI\delta_{22} = 2\left(-\frac{l}{2}\right)\left(-\frac{2}{3}\right) = +\frac{2l}{3}$$

$$EI\delta_{23} = \left(-\frac{l}{2}\right)\left(-\frac{1}{3}\right) = +\frac{l}{6}$$

From Equation 6.19,

$$-\theta_2 = \delta_{20} + \delta_{21}\bar{X}_1 + \delta_{22}\bar{X}_2 + \delta_{23}\bar{X}_3$$

$$-EI\theta_2 = -\frac{2}{3}M_0l + 0.5M_0\left(+\frac{l}{6}\right) + 0.5M_0\left(+\frac{2}{3}l\right) + 0.5M_0\left(+\frac{l}{6}\right) = -\frac{M_0l}{6}$$

From symmetry,  $\theta_3 = \theta_1$ . Therefore, the required plastic hinge rotations at the support are

$$\theta_1 = \frac{M_0l}{4EI} = \theta_3$$

and

$$\theta_2 = \frac{M_0l}{6EI}$$

Since  $\theta_2 < \theta_1$ , the first hinge to develop, and the controlling one in the design, is  $\theta_1 = M_0l/4EI$ .

Note that the procedure used in Example 6.8 can be used in the limit design of any continuous beam or multistory frame. Also, it is important to maintain the correct sign convention by drawing all moments at the *tension* side of the member, as noted earlier.

The preceding discussion gives the basic *imposed rotations approach* embodied in Baker's theory. Other modified approaches have been proposed by Cohn (Ref. 6.17), Sawyer (Ref. 6.18), and Furlong (Ref. 6.19). Cohn's method is based on the requirements of limit equilibrium and serviceability, with a subsequent check of rotational compatibility. Sawyer's method is based on the simultaneous requirements of limit equilibrium and rotational compatibility, with a subsequent check of serviceability.

Furlong's method is based on assigning ultimate moments for various loading patterns on the continuous spans that would satisfy serviceability and limit equilibrium for the worst case. The sections are reinforced in such a manner that the ultimate moment strengths for each span are equal to or greater than the *product* of the maximum ultimate moment  $M_o$  in the span when the ends are free to rotate and a moment coefficient  $k_1$  for various boundary conditions as listed in Table 6.2.

### 6.13.3 Rotational Capacity of Plastic Hinges

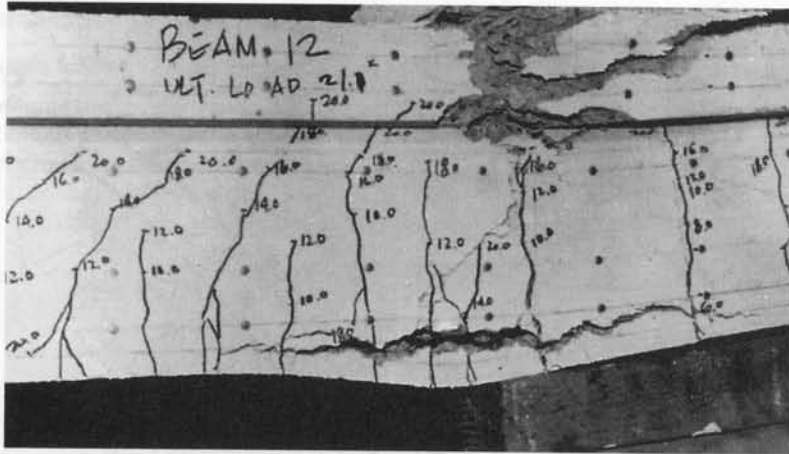
Rotation is the *total* change in slope along the short plasticity length concentrated at the hinge zone. It can also be described as the angle of discontinuity between the plastic parts of the member on either side of the plastic hinge. As Figure 6.39 shows, there are two types of hinges—tensile and compressive. In order that the first hinge that develops in the structure, usually the critical hinge, can rotate without rupture until the  $n$ th hinge develops, the concrete section at the first hinge has to be made ductile enough through section core confinement to be able to sustain the necessary rotation. This is equally applicable to both tension and compression hinges, where confinement of the concrete core is obtained through concentration of closed stirrups at the supports and column ends. A typical plot showing increase in rotation through increase in confining reinforcement is shown in Figure 6.40 (Ref. 6.14).

The plasticity length  $l_p$  determines the extent of severe cracking and the magnitude of rotation of the hinge. Therefore, it is important to limit the magnitude of  $l_p$  through the use of *closely spaced* ties or closed stirrups. In this manner, the strain capacity of the concrete at the confined section can be significantly increased, as experimentally demonstrated by several investigators, including Nawy (Refs. 6.12, 6.13, and 6.14). Several empirical expressions have been developed; see, for example, Baker (Ref. 6.5), Corley (Ref. 6.11), Nawy (Ref. 6.14), Sawyer (Ref. 6.18), and Mattock (Ref. 6.20). Two of them, for the plasticity length  $l_p$  and the concrete strain  $\epsilon_c$  (Ref. 6.20), are

$$l_p = 0.5d + 0.5Z \quad (6.22)$$

**Table 6.2** Beam Moment Coefficients for Assigned Moments

Boundary condition	Moment type	Beam loaded by one concentrated load at midspan	
			All other beams
Span with ends restrained	Negative	0.37	0.50
	Positive	0.42	0.33
Span with one end restrained	Negative	0.56	0.75
	Positive	0.50	0.46



**Photo 6.2** Pretensioned T-beam with rectangular confining reinforcement at failure (Nawy, Potyondy).

and

$$\epsilon_c = 0.003 + 0.02 \frac{b}{Z} + 0.2\rho_s \quad (6.23)$$

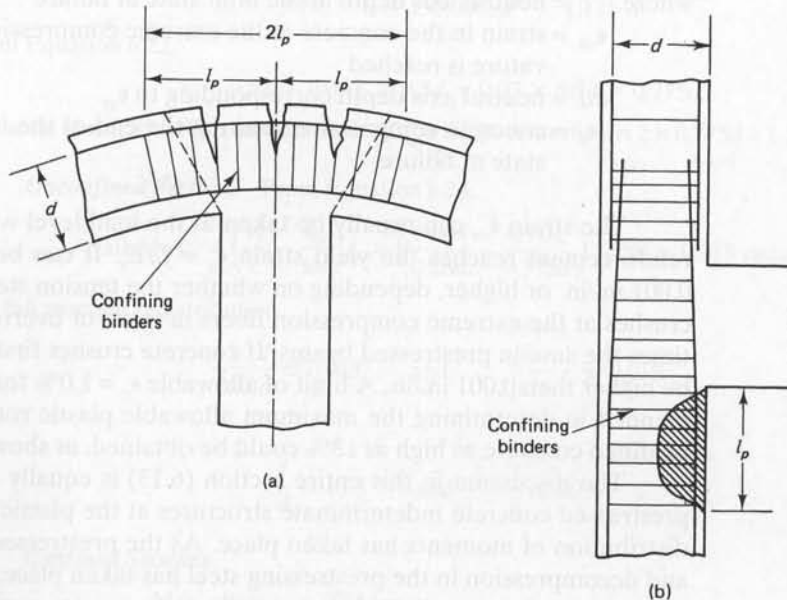
where  $d$  = effective depth of the beam (in.)

$Z$  = distance from the critical section to the point of contraflexure

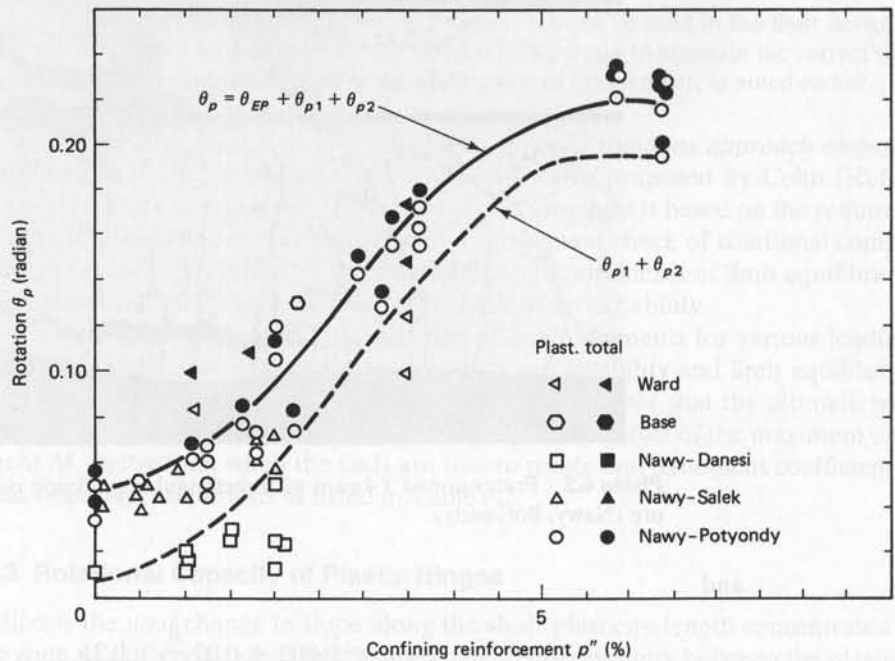
$\rho_s$  = ratio of volume of confining binder steel (including the compression steel) to the volume of the concrete core

$l_p$  = half the plasticity length on each side of the centerline of plastic hinge.

Equation 6.22 can be more conservative for high values of  $\rho_s$ .



**Figure 6.39** Plasticity zones  $l_p$  in plastic hinges. (a) Tensile hinge. (b) Compressive hinge.



**Figure 6.40** Comparison of plastic rotation with results of other authors.

Once the concrete strain  $\epsilon_c$  is determined, the angle of rotation of the plastic hinge is readily determined from the expression

$$\theta_p = \left( \frac{\epsilon_c}{c} - \frac{\epsilon_{ce}}{kd} \right) l_p \quad (6.24)$$

where  $c$  = neutral axis depth at the limit state at failure

$\epsilon_{ce}$  = strain in the concrete at the extreme compression fibers when the yield curvature is reached

$kd$  = neutral axis depth corresponding to  $\epsilon_{ce}$

$\epsilon_c$  = concrete compressive strain at the end of the inelastic range or at the limit state at failure.

The strain  $\epsilon_{ce}$  can usually be taken at the load level when the strain in the tension reinforcement reaches the yield strain  $\epsilon_y = f_y/E_s$ . It can be taken to be approximately 0.001 in./in. or higher, depending on whether the tension steel yields before the concrete crushes at the extreme compression fibers in cases of overreinforced beams, as is sometimes the case in prestressed beams. If concrete crushes first, the value of  $\epsilon_{ce}$  will have to be higher than 0.001 in./in. A limit of allowable  $\epsilon_c = 1.0\%$  for confined concrete is recommended in determining the maximum allowable plastic rotation  $\theta_p$ , although strains of confined concrete as high as 13% could be obtained, as shown in Ref. 6.14.

The discussion in this entire section (6.13) is equally applicable to reinforced and prestressed concrete indeterminate structures at the plastic loading range where full redistribution of moments has taken place. As the prestressed concrete section is cracked and decompression in the prestressing steel has taken place, the structural system gradually starts to behave similarly to a reinforced concrete system. As the load reaches the limit state at failure, the flexural behavior of the prestressed concrete elements is expected to closely resemble that of reinforced concrete elements.

### 6.13.4 Calculation of Available Rotational Capacity

#### Example 6.9

Determine the required and available rotational capacities of the critical plastic hinges in the continuous prestressed concrete beam in Example 6.8 for both confined and unconfined concrete. Given data are as follows:

$$M_u = \frac{1}{2} M_0 = 400bd^2$$

$$c = 0.28d$$

$$kd = 0.375d$$

$$\epsilon_{ce} = 0.001 \text{ in./in. at end of the elastic range}$$

$$\epsilon_c = 0.004 \text{ in./in. at end of the inelastic range for unconfined sections}$$

$$\text{Max. allowable } \epsilon_c = 0.01 \text{ in./in. for confined sections}$$

$$E_c I_c = 150,000bd^3 \text{ in.}^3\text{-lb}$$

$$\frac{Z}{d} = 5.5$$

$$f'_c = 5,000 \text{ psi}$$

$$f_y = 60,000 \text{ psi for the mild steel}$$

Also, calculate the maximum allowable span-to-depth ratio  $l/d$  for the beam if full redistribution of moments is to occur at the limit state at failure.

#### Solution:

$$M_0 = 2 \times 400bd^2 = 800bd^2$$

From Example 6.8,

$$\text{Required } \theta_1 = \theta_3 = \frac{M_0 l}{4E_c I_c} = \frac{800bd^2 l}{4 \times 150,000bd^3} = \frac{1}{750} \frac{l}{d} \text{ radian}$$

$$\text{Required } \theta_2 = \frac{M_0 l}{6EI} = \frac{800bd^2 l}{6 \times 150,000bd^3} = \frac{1}{1,125} \frac{l}{d} \text{ radian}$$

From Equation 6.22,

$$l_p = 0.5d + 0.05Z = 0.5d + 0.05 \times 5.5d = 0.775d$$

The total plasticity length on both sides of the hinge centerline is  $2 \times 0.775d = 1.55d$ .

**Unconfined Section.** From Equation 6.24,

$$\text{Available } \theta_p = \left( \frac{\epsilon_c}{c} - \frac{\epsilon_{ce}}{kd} \right) l_p = \left( \frac{0.004}{0.28d} - \frac{0.001}{0.375d} \right) 1.55d = 0.018 \text{ radian}$$

For full moment redistribution,

$$\frac{1}{750} \frac{l}{d} \leq 0.018 \quad \text{and} \quad \frac{1}{1,125} \frac{l}{d} \leq 0.018$$

or

$$\frac{l}{d} \leq 13.5 \quad \text{and} \quad \frac{l}{d} \leq 20.3$$

#### Confined Sections

Max. allow  $\epsilon_c = 0.01 \text{ in./in.}$

$$\text{Available } \theta_p = \left( \frac{0.01}{0.28d} - \frac{0.001}{0.375d} \right) 1.55d = 0.51 \text{ radian}$$

For full moment redistribution,

$$\frac{1}{750} \frac{l}{d} \leq 0.051 \quad \text{and} \quad \frac{1}{1,125} \frac{l}{d} \leq 0.051$$

or

$$\frac{l}{d} \leq 38.3 \quad \text{and} \quad \frac{l}{d} = 57.4$$

Comparing the results of the unconfined sections in the first case to the confined sections in the second case, one sees that confinement of the concrete at the plastic hinging zone permits more slender sections for full plasticity and, hence, a more economical indeterminate structural system.

### 6.13.5 Check for Plastic Rotation Serviceability

#### Example 6.10

If closed-stirrup binders are used in Example 6.9 with binder ratio  $\rho_s = 0.025$  and  $l/d = 35$  with  $c$  at failure  $= 0.25d$ , verify whether the continuous beam satisfies the rotation serviceability criteria given that  $b = \frac{1}{2}d$ .

**Solution:**

$$\frac{Z}{d} = 5.5$$

Hence,

$$\frac{b}{Z} = \frac{1}{11}$$

Also,

$$\begin{aligned} \text{Available } \epsilon_c &= 0.003 + 0.02 \frac{b}{Z} + 0.2\rho_s \\ &= 0.003 + 0.02 \times \frac{1}{11} + 0.2 \times 0.025 = 0.0098, \text{ say } 0.01 \text{ in./in.} \end{aligned}$$

The maximum allowable to be utilized is  $\epsilon_c = 0.01$  in./in. So use, for  $\epsilon_c = 0.01$ , the corresponding available plastic rotation:

$$\theta_p = \left( \frac{0.01}{0.25d} - \frac{0.001}{0.375d} \right) 1.55d = 0.058 \text{ radian}$$

$$\text{Rqd. } \theta_1 = \frac{1}{750} \frac{l}{d} = \frac{35}{750} = 0.046 \text{ radian}$$

$$\text{Rqd. } \theta_2 = \frac{1}{1,125} \frac{l}{d} = \frac{35}{1,125} = 0.031 \text{ radian}$$

Available  $\theta_p = 0.058$  radian  $>$  required  $\theta = 0.046$  radian. Thus, the beam satisfies the serviceability criteria for plastic rotation.

The foregoing discussion for the limit design of reinforced and prestressed concrete indeterminate beams and frames permits the design engineer to provide ductile connections at beam-column supports and generate full moment redistribution throughout the structure, resulting in full utilization of the strength of the prestressed system. Also, continuity in both pretensioned and post-tensioned systems to withstand seismic loading can be effectively utilized through the appropriate confinement of the connecting zones by means of the procedures presented in this section.

### 6.13.6 Transverse Confining Reinforcement for Seismic Design

Transverse reinforcement in the form of closely spaced hoops (ties) or spirals has to be adequately provided for concrete frame structural elements in seismic regions. The aim is to produce *adequate rotational capacity* within the plastic hinges that may develop as a result of the seismic forces. The Uniform Building Code, the International Building Code (IBC2000), and the ACI Code on seismic design require design and detailing of closed ties at the beam-column connection zones and in shear walls to be governed by the following (See Chapter 15 of Ref. 6.8 by the author and Chapter 13 to follow):

1. For column spirals, the minimum volumetric ratio of the spiral hoops needed for the concrete core confinement is

$$\rho_s \geq \frac{0.12f'_c}{f_{yh}} \quad (6.25)$$

or

$$\rho_s \geq 0.45 \left( \frac{A_g}{A_{ch}} - 1 \right) \frac{f'_c}{f_{yt}} \quad (6.26)$$

whichever is greater, where

$\rho_s$  = ratio of volume of spiral reinforcement to the core volume measured out to out.

$A_g$  = gross area of the column section.

$A_{ch}$  = core area of section measured to the outside of the transverse reinforcement (sq. in.).

$f_{yt}$  = specified yield of transverse reinforcement, psi.

2. For column rectangular hoops, the total cross-sectional area within spacing  $s$  is

$$A_{sh} \geq 0.09sh_c \frac{f'_c}{f_{yt}} \quad (6.27)$$

or

$$A_{sh} \geq 0.3sh_c \left( \frac{A_g}{A_{ch}} - 1 \right) \frac{f'_c}{f_{yt}} \quad (6.28)$$

whichever is greater, where

$A_{sh}$  = total cross-sectional area of transverse reinforcement (including cross ties) within spacing  $s$  and perpendicular to dimension  $h_c$ .

$h_c$  = cross-sectional dimension of column core measured center to center of confining reinforcement, in.

$A_{ch}$  = cross-sectional area of structural member, measured out-to-out of transverse reinforcement.

$s$  = spacing of transverse reinforcement measured along the longitudinal axis of the member, in.

$s_{\max}$  =  $\frac{1}{4}$  of the smallest cross-sectional dimension of the member or 4 in., whichever is smaller (IBC requires 4 in.).



3. The confining transverse reinforcement in *columns* should be placed on *both* sides of a potential hinge over a distance  $l_0$ . The largest of the following three conditions govern:
  - (a) depth of member at joint face
  - (b)  $\frac{1}{6}$  of the clear span
  - (c) 18 in.
4. For beam confinement, the confining transverse reinforcement at *beam* ends should be placed over a length equal to *twice* the member depth  $h$  from the face of the joint on either side or of any other location where plastic hinges can develop. The maximum hoop spacing should be the smallest of the following four conditions:
  - (a)  $\frac{1}{4}$  effective depth  $d$ .
  - (b)  $8 \times$  diameter of longitudinal bars.
  - (c)  $24 \times$  diameter of the hoop.
  - (d) 12 in. (300 mm).

Figure 6.41 from Reference 6.8 gives a typical detailing example of confining reinforcement at a joint to resist seismic forces.

5. Reduction in confinement at joints: A 50% reduction in confinement and an increase in the minimum tie spacing to 6 in. are allowed by the ACI Code if a joint is confined on all *four* faces by adjoining beams with each beam wide enough to cover three quarters of the adjoining face.

### 6.13.7 Selection of Confining Reinforcement

#### Example 6.11

Design the confining reinforcement in the column at the beam-column joint of Figure 6.41. Given:

$$\text{column size} = 15 \times 24 \text{ in. (380} \times \text{610 mm)}$$

$$f'_c = 4,000 \text{ psi (27.6 MPa), normal weight}$$

$$f_{yt} = 60,000 \text{ psi (414 MPa)}$$

$$\text{clear cover} = 1\frac{1}{2} \text{ in. (38 mm)}$$

**Solution:** From Equations 6.27 and 6.28, whichever is greater,

$$A_{sh} \geq 0.09sh_c \frac{f'_c}{f_{yt}}$$

or

$$A_{sh} \geq 0.3sh_c \left( \frac{A_g}{A_{ch}} - 1 \right) \frac{f'_c}{F_{yt}}$$

$$h_c = \text{column core dimension} = 24 - 2(1.5 + 0.5) = 20 \text{ in.}$$

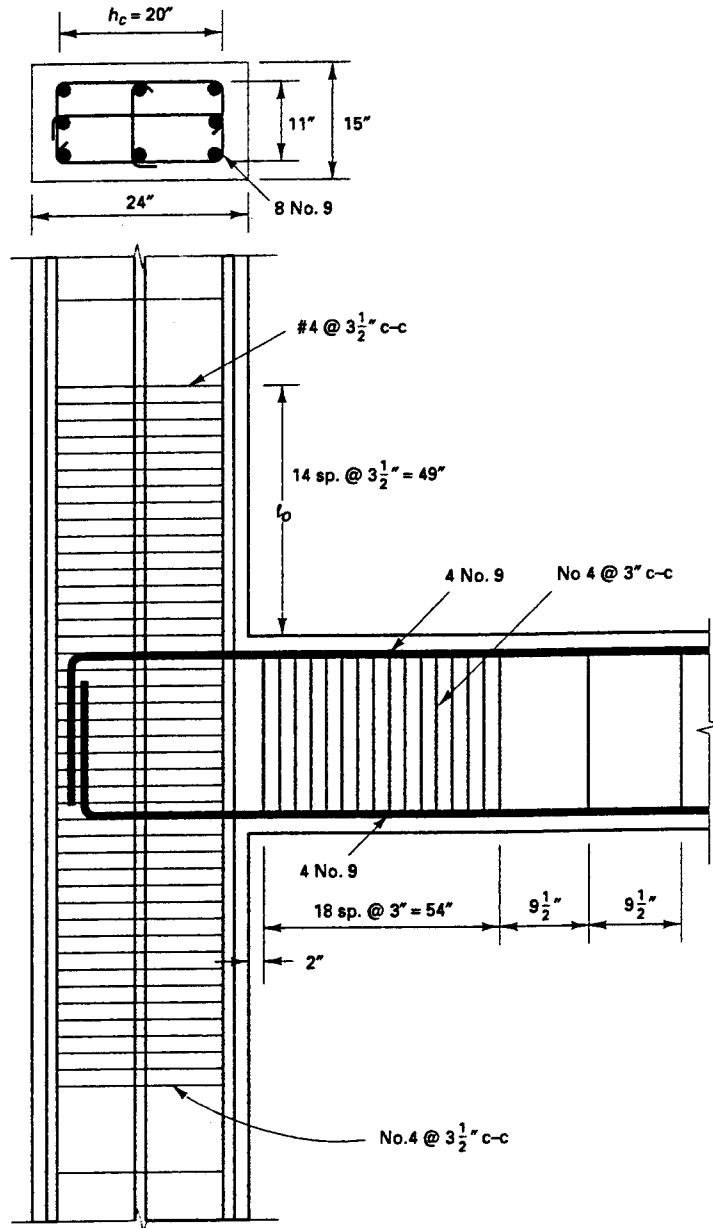
$$A_{sh} = 0.09 \times 3.5 \times 20 \left( \frac{4,000}{60,000} \right) = 0.42 \text{ in.}^2$$

$$A_{sh} = 0.3 \times 3.5 \times 20 \left( \frac{15 \times 24}{11 \times 20} - 1 \right) \left( \frac{4,000}{60,000} \right) = 0.89 \text{ in.}^2 \text{ controls}$$

Trying  $s = 3\frac{1}{2}$  in., maximum allowance  $s = \frac{1}{4}$  smallest column dimension or 4 in.,  $b/4 = 0.25 \times 15 = 3.75$  in.

Use No. 4 hoops plus two No. 4 crossties at  $3\frac{1}{2}$  in. center to center. Place the confining hoops in the column on both sides of potential hinge over a distance  $l_0$  being the largest of

- (a) depth of member = 24 in. (610 mm)
- (b)  $\frac{1}{6} \times$  clear span =  $(24 \times 12)/6 = 48$  in. (1220 mm)
- (c) 18 in. (450 mm)



**Figure 6.41** Confining reinforcement for seismic resistance (Example 6.11).

Use  $l_0 = 48$  in. (1220 mm), spacing the No. 4 hoops and cross ties at 3.5 in. center to center over this distance (12.7-mm dia. bars at 89 mm center to center) as shown in Figure 6.41.

## SELECTED REFERENCES

- 6.1** ACI Committee 318. *Building Code Requirements for Structural Concrete (ACI 318-08) and Commentary (ACI 318 R-08)*. Farmington Hills, MI: American Concrete Institute, 2008, pp. 465.

- 6.2 Gerwick, B. C., *Construction of Prestressed Concrete Structures*, 3rd ed., CRC Press, Boca Raton, FL, 2007.
- 6.3 Taylor, F. W., Thompson, S. E., and Smulski, E. *Concrete Plain and Reinforced*, vol. 2. John Wiley & Sons, New York, 1947.
- 6.4 Abeles, P. W., and Bardhan-Roy, B. K. *Prestressed Concrete Designer's Handbook*, 3d ed. Viewpoint Publications, London, 1981.
- 6.5 Baker, A. L. L. *The Ultimate Load Theory Applied to the Design of Reinforced and Prestressed Concrete Frames*. Concrete Publications Ltd., London, 1956.
- 6.6 Baker, A. L. L. *Limit State Design of Reinforced Concrete*. London: Cement and Concrete Association, 1970.
- 6.7 Ramakrishnan, V., and Arthur, P. D. *Ultimate Strength Design of Structural Concrete*. London: Wheeler, 1977.
- 6.8 Nawy, E. G. *Reinforced Concrete—A Fundamental Approach*, 6th ed. Prentice Hall, Upper Saddle River, NJ, 2009, pp. 936.
- 6.9 Lin, T. Y., and Thornton, K. "Secondary Moments and Moment Redistribution in Continuous Prestressed Concrete Beams." *Journal of the Prestressed Concrete Institute*, January–February 1972, pp. 8–20.
- 6.10 Nilson, A. H. *Design of Prestressed Concrete*. New York: John Wiley & Sons, 1987.
- 6.11 Corley, W. G. "Rotational Capacity of Reinforced Concrete Beams." *Journal of the Structural Division, ASCE* 92 (1966): 121–146.
- 6.12 Nawy, E. G., and Salek, F. "Moment-Rotation Relationships of Non-Bonded Prestressed Flanged Sections Confined with Rectangular Spirals." *Journal of the Prestressed Concrete Institute*, August 1968, pp. 40–55.
- 6.13 Nawy, E. G., Danesi, R., and Grosco, J. "Rectangular Spiral Binders Effect on the Rotation Capacity of Plastic Hinges in Reinforced Concrete Beams." *Journal of the American Concrete Institute*, Farmington Hills, MI, December 1968, pp. 1001–1010.
- 6.14 Nawy, E. G., and Potyondy, J. G. "Moment Rotation, Cracking and Deflection of Spirally Bound Pretensioned Prestressed Concrete Beams." *Engineering Research Bulletin No. 51*, N.J.: Bureau of Engineering Research, Rutgers University, New Brunswick, 1970, pp. 1–97.
- 6.15 Prestressed Concrete Institute. *PCI Design Handbook*. Chicago: Prestressed Concrete Institute, 5th ed., 1999.
- 6.16 Park, R., and Paulay, J. *Reinforced Concrete Structures*. John Wiley & Sons, New York, 1975.
- 6.17 Cohn, M. Z., "Rotational Compatibility in the Limit Design of Reinforced Concrete Beams." *Proceedings of the International Symposium on the Flexural Mechanics of Reinforced Concrete*, ASCE-ACI. Miami, Nov. 1964, pp. 359–382.
- 6.18 Sawyer, H. A. "Design of Concrete Frames for Two Failure Stages." *Proceedings of the International Symposium on the Flexural Mechanics of Reinforced Concrete*, ASCE-ACI. Miami, Nov. 1964, pp. 405–431.
- 6.19 Furlong, R. W. "Design of Concrete Frames by Assigned Limit Moments." *Journal of the American Concrete Institute* 67, Farmington Hills, MI, 1970, 341–353.
- 6.20 Mattock, A. H. "Discussion of Rotational Capacity of Reinforced Concrete Beams by W. G. Corley." *Journal of the Structural Division, ASCE* 93, 1967, 519–522.
- 6.21 International Conference of Building Officials, *Uniform Building Code (UBC)*, Vol. 2, ICBO, Whittier, California, 1997.
- 6.22 International Code Council, *International Building Code 2000 (IBC)*, Joint UBC, BOCA, SBCCI, Whittier, California, 2000.
- 6.23 Nawy, E. G., *Concrete Construction Engineering Handbook*, CRC Press, Boca Raton, FL, 1998, 1250 pp.
- 6.24 Nawy, E. G., *Fundamentals of High Performance Concrete*, 2nd ed., John Wiley and Sons, New York, NY, 2001, 452 pp.

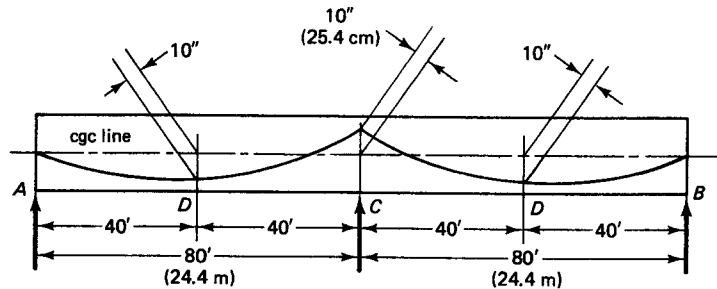


Figure P6.1.

## PROBLEMS

- 6.1 A two-span continuous beam has a parabolic tendon profile shown in Figure P6.1. The prestressing force  $P_e$  after all losses is 450,000 lb (2,002 kN). The beam has a rectangular section 15-in. (38.1 cm) wide.
- Find the final profile of the thrust C-line and the beam reactions at all supports.
  - Design the beam depth such that the concrete fiber stresses due only to prestressing do not exceed the maximum allowable for normal-weight concrete having cylinder strength  $f'_c = 6,000$  psi (41.4 MPa).
  - Determine the shape of the concordant tendon, and draw a beam elevation of the tendon profile.
- 6.2 Solve Problem 6.1 for a tendon profile harped at midspan points D, but having the same eccentricities. Compare the results with those of Problem 6.1.
- 6.3 Solve Problem 6.1 for a tendon profile which has eccentricities  $e_A = e_B = 3$  in. (7.6 cm) at the exterior supports above the cgc line.
- 6.4 Develop the tendon profile for the continuous beam in Example 6.4 if the beam is continuous over two equal spans of 64 ft (19.4 m).
- 6.5 Solve Problem 6.4 if the beam is continuous over four equal spans of 64 ft (19.4 m).
- 6.6 Design, for service loading, the frame in Example 6.7 using the same loading conditions if the span of the horizontal beam is 90 ft (27.4 m) and the height of the portal is 25 ft (7.6 m).
- 6.7 Design the portal frame of an aircraft hangar having the dimensions and the loading shown in Figure P6.7. Detail the connections and the configuration of the prestressing tendons of the horizontal member. Use the same allowable stresses as in Example 6.7.

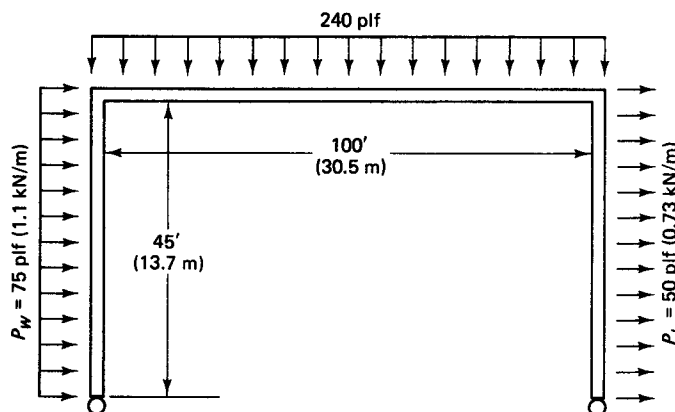
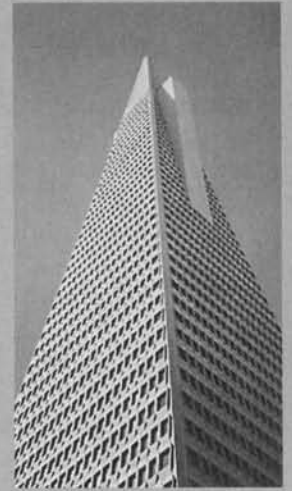


Figure P6.7.

# 7



## CAMBER, DEFLECTION, AND CRACK CONTROL

### 7.1 INTRODUCTION

Serviceability of prestressed concrete members in their deflection and cracking behavior is at least as important a criterion in design as serviceability of reinforced concrete elements. The fact that prestressed concrete elements are more slender than their counterparts in reinforced concrete, and their behavior more affected by flexural cracking, makes it more critical to control their deflection and cracking. The primary design involves proportioning the structural member for the limit state of flexural stresses at service load and for limit states of failure in flexure, shear, and torsion, including anchorage development strength. Such a design can only become complete if the magnitudes of long-term deflection, camber (reverse deflection), and crack width are determined to be within allowable serviceability values.

Prestressed concrete members are continuously subjected to sustained eccentric compression due to the prestressing force, which seriously affects their long-term creep deformation performance. Failure to predict and control such deformations can lead to high reverse deflection, i.e., camber, which can produce convex surfaces detrimental to proper drainage of roofs of buildings, to uncomfortable ride characteristics in bridges and aqueducts, and to cracking of partitions in apartment buildings, including misalignment of windows and doors.

Transamerica Pyramid, San Francisco, California.

The difficulty of predicting very accurately the total long-term prestress losses makes it more difficult to give a precise estimate of the magnitude of expected camber. Accuracy is even more difficult in partially prestressed concrete systems, where limited cracking is allowed through the use of additional nonprestressed reinforcement. Creep strain in the concrete increases camber, as it causes a negative increase in curvature which is usually more dominant than the decrease produced by the decrease in prestress losses due to creep, shrinkage, and stress relaxation. A best estimate of camber increase should be based on accumulated experience, span-to-depth ratio code limitations, and a correct choice of the modulus  $E_c$  of the concrete. Calculation of the moment-curvature relationships at the major incremental stages of loading up to the limit state at failure would also assist in giving a more accurate evaluation of the stress-related load deflection of the structural element.

The cracking aspect of serviceability behavior in prestressed concrete is also critical. Allowance for limited cracking in “partial prestressing” through the additional use of nonprestressed steel is prevalent. Because of the high stress levels in the prestressing steel, corrosion due to cracking can become detrimental to the service life of the structure. Therefore, limitations on the magnitudes of crack widths and their spacing have to be placed, and proper crack width evaluation procedures used. The presented discussion of the state of the art emphasizes the extensive work of the author on cracking in pretensioned and post-tensioned prestressed beams.

Prestressed concrete flexural members are classified into three classes in the new ACI 318 Code.

$$(a) \quad \text{Class U:} \quad f_t \leq 7.5\sqrt{f'_c} \quad (7.1a)$$

In this class, the gross section is used for section properties when both stress computations at service loads, and deflection computations are made. No skin reinforcement needs to be used in the vertical faces.

$$(b) \quad \text{Class T:} \quad 7.5\sqrt{f'_c} \leq f_t \leq 12\sqrt{f'_c} \quad (7.1b)$$

This class is a transition between uncracked and cracked sections. For stress computations at service loads, the gross section is used. The cracked bi-linear section is used in the deflection computations. No skin reinforcement needs to be used in the vertical faces.

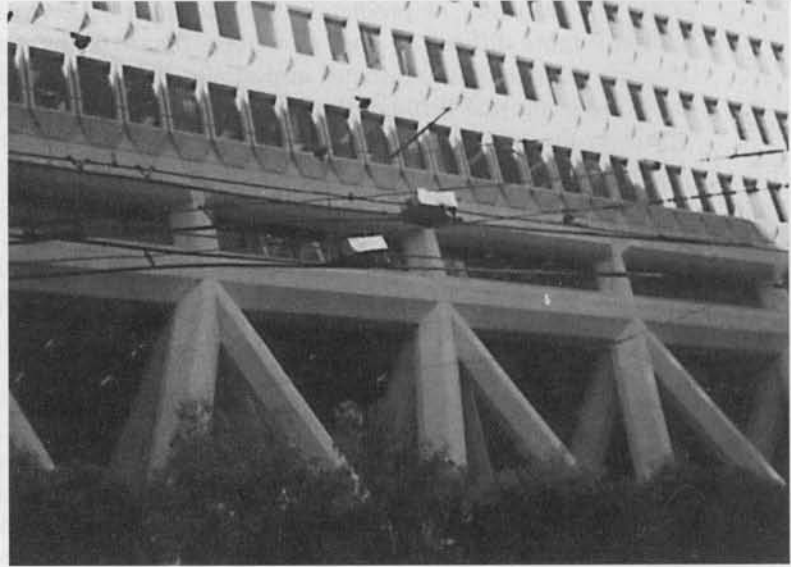
$$(c) \quad \text{Class C:} \quad f_t > 12\sqrt{f'_c} \quad (7.1c)$$

This class denotes cracked sections. Hence, a cracked section analysis has to be made for evaluation of the stress level at service, and for deflection. Computation of  $\Delta f_{ps}$  or  $f_s$  for crack control is necessary, where  $\Delta f_{ps}$  = stress increase beyond the decompression state, and  $f_s$  = stress in the mild reinforcement when mild steel reinforcement is also used. Prestressed two-way slab systems are to be designed as Class U.

## 7.2 BASIC ASSUMPTIONS IN DEFLECTION CALCULATIONS

Deflection calculations can be made either from the moment diagrams of the prestressing force and the external transverse loading, or from the moment-curvature relationships. In either case, the following basic assumptions have to be made:

1. The concrete gross cross-sectional area is accurate enough to compute the moment of inertia except when refined computations are necessary.
2. The modulus of concrete  $E_c = 33w^{1.5}\sqrt{f'_c}$ , where the value of  $f'_c$  corresponds to the cylinder compressive strength of concrete at the age at which  $E_c$  is to be evaluated.
3. The principle of superposition applies in calculating deflections due to transverse load and camber due to prestressing.



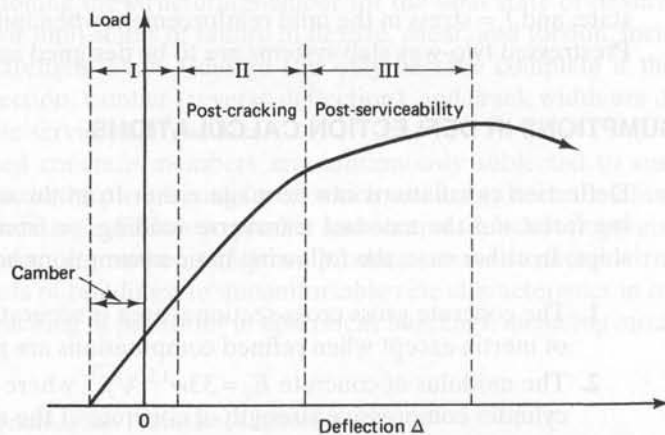
**Photo 7.1** Supporting base of the Transamerica Pyramid, San Francisco, California.

4. All computations of deflection can be based on the center of gravity of the prestressing strands (cgs), where the strands are treated as a single tendon.
5. Deflections due to shear deformations are disregarded.
6. Sections can be treated as *totally elastic* up to the decompression load. Thereafter, the cracked moment of inertia  $I_{cr}$  can give a more accurate determination of deflection and camber.

### 7.3 SHORT-TERM (INSTANTANEOUS) DEFLECTION OF UNCRACKED AND CRACKED MEMBERS

#### 7.3.1 Load-Deflection Relationship

Short-term deflections in prestressed concrete members are calculated on the assumption that the sections are homogeneous, isotropic, and elastic. Such an assumption is an approximation of actual behavior, particularly that the modulus  $E_c$  of concrete varies



**Figure 7.1** Beam load-deflection relationship. Region I, precracking stage; region II, postcracking stage; region III, postserviceability stage.

with the age of the concrete and the moment of inertia varies with the stage of loading, i.e., whether the section is uncracked or cracked.

Ideally, the load-deflection relationship is trilinear, as shown in Figure 7.1. The three regions prior to rupture are:

*Region I.* Precracking stage, where a structural member is crack free.

*Region II.* Postcracking stage, where the structural member develops acceptable controlled cracking in both distribution and width.

*Region III.* Postserviceability cracking stage, where the stress in the tensile reinforcement reaches the limit state of yielding.

**7.3.1.1 Precracking stage: region I.** The precracking segment of the load-deflection curve is essentially a straight line defining full elastic behavior, as in Figure 7.1. The maximum tensile stress in the beam in this region is less than its tensile strength in flexure, i.e., it is less than the modulus of rupture  $f_r$  of concrete. The flexural stiffness  $EI$  of the beam can be estimated using Young's modulus  $E_c$  of concrete and the moment of inertia of the uncracked concrete cross section. The load-deflection behavior significantly depends on the stress-strain relationship of the concrete. A typical stress-strain diagram of concrete is shown in Figure 7.2.

The value of  $E_c$  can be estimated using the ACI empirical expression given in Chapter 2, viz.,

$$E_c = 33w^{1.5}\sqrt{f'_c} \quad (7.2a)$$

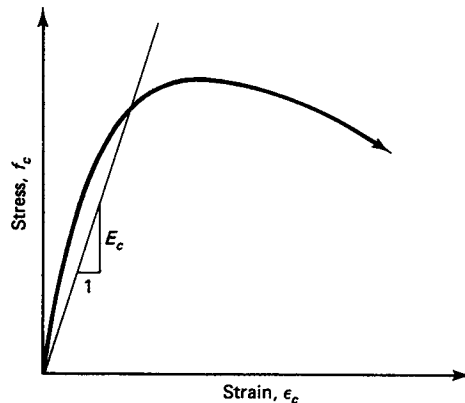
or

$$E_c = 57,000\sqrt{f'_c} \quad \text{for normal-weight concrete}$$

The precracking region stops at the initiation of the first flexural crack, when the concrete stress reaches its modulus of rupture strength  $f_r$ . Similarly to the direct tensile splitting strength, the modulus of rupture of concrete is proportional to the square root of its compressive strength. For design purposes, the value of the modulus of rupture for concrete may be taken as

$$f_r = 7.5\lambda \sqrt{f'_c} \quad (7.2b)$$

where  $\lambda = 1.0$  for normal-weight concrete. If all-lightweight concrete is used, then  $\lambda = 0.75$ , and if sand-lightweight concrete is used,  $\lambda = 0.85$ .



**Figure 7.2** Stress-strain diagram of concrete.



If one equates the modulus of rupture  $f_r$  to the stress produced by the cracking moment  $M_{cr}$  (decompression moment), then

$$f_b = f_r = -\frac{P_e}{A_c} \left( 1 + \frac{ec_b}{r^2} \right) + \frac{M_{cr}}{S_b} \quad (7.3a)$$

where subscript  $b$  stands for the bottom fibers at midspan of a simply supported beam. If the distance of the extreme *tension* fibers of concrete from the center of gravity of the concrete section is  $y_t$ , then the cracking moment is given by

$$M_{cr} = \frac{I_g}{y_t} \left[ \frac{P_e}{A_c} \left( 1 + \frac{ec_b}{r^2} \right) + 7.5\lambda\sqrt{f'_c} \right] \quad (7.3b)$$

or

$$M_{cr} = S_b \left[ 7.5\lambda\sqrt{f'_c} + \frac{P_e}{A_c} \left( 1 + \frac{ec_b}{r^2} \right) \right] \quad (7.3c)$$

where  $S_b$  = section modulus at the bottom fibers. More conservatively, from Equation 5.12, the cracking moment due to that portion of the applied *live load* that causes cracking is

$$M_{cr} = S_b [6.0\lambda\sqrt{f'_c} + f_{ce} - f_d] \quad (7.4a)$$

where  $f_{ce}$  = compressive stress at the center of gravity of concrete section due to effective prestress *only* after losses when tensile stress is caused by applied external load

$f_d$  = concrete stress at extreme tensile fibers due to unfactored *dead* load when tensile stresses and cracking are caused by the external load.

A factor 7.5 can also be used instead of 6.0 for deflection purposes for beams. Equation 7.3a can be transformed to the PCI format (Ref. 7.7) giving identical results:

$$\frac{M_{cr}}{M_a} = 1 - \left( \frac{f_{il} - f_r}{f_L} \right) \quad (7.4b)$$

where  $M_a$  = maximum service unfactored live load moment

$f_{il}$  = final calculated total service load concrete stress in the member

$f_r$  = modulus of rupture

$f_L$  = service live load of concrete stress in the member.

### 7.3.1.2 Calculation of cracking moment $M_{cr}$

#### Example 7.1

Compute the cracking moment  $M_{cr}$  for a prestressed rectangular beam section having a width  $b = 12$  in. (305 mm) and a total depth  $h = 24$  in. (610 mm), given that  $f'_c = 4,000$  psi (27.6 MPa). The concrete stress  $f_b$  due to eccentric prestressing is 1,850 psi (12.8 MPa) in compression. Use a modulus of rupture value of  $7.5\sqrt{f'_c}$ .

**Solution:** The modulus of rupture  $f_r = 7.5\sqrt{f'_c} = 7.5\sqrt{4,000} = 474$  psi (3.27 MPa). Also,  $I_g = bh^3/12 = 12(24)^3/12 = 13,824$  in<sup>4</sup> (575,400 cm<sup>4</sup>);  $y_t = 24/2 = 12$  in. (305 mm) to the tension fibers; and  $S_b = I_g/y_t = 13,824/12 = 1,152$  in<sup>3</sup> (18,878 cm<sup>3</sup>).

$$\begin{aligned} M_{cr} &= S_b \left[ 7.5\lambda\sqrt{f'_c} + \frac{P_e}{A_c} \left( 1 + \frac{ec_b}{r^2} \right) \right] = 1,152[474 + 1850] \\ &= 2.68 \times 10^6 \text{ in.-lb (302.9 kN-m)} \end{aligned}$$

If the beam were not prestressed, the moment would be  $M_{cr} = f_r I_g / y_t = 474 \times 13,824 / 12 = 0.546 \times 10^6$  in.-lb (61.7 kN-m).

**7.3.1.3 Postcracking service-load stage: region II.** The precracking region ends at the initiation of the first crack and moves into region II of the load-deflection diagram of Figure 7.1. Most beams lie in this region at service loads. A beam undergoes varying degrees of cracking along the span corresponding to the stress and deflection levels at each section. Hence, cracks are wider and deeper at midspan, whereas only narrow, minor cracks develop near the supports in a simple beam.

When flexural cracking develops, the contribution of the concrete in the tension area diminishes substantially. Hence, the flexural rigidity of the section is reduced, making the load-deflection curve less steep in this region than in the precracking stage segment. As the magnitude of cracking increases, stiffness continues to decrease, reaching a lower bound value corresponding to the reduced moment of inertia of the cracked section. The moment of inertia  $I_{cr}$  of the cracked section can be calculated from the basic principles of mechanics.

**7.3.1.4 Postserviceability cracking stage and limit state of deflection behavior at failure: region III.** The load-deflection diagram of Figure 7.1 is considerably flatter in region III than in the preceding regions. This is due to substantial loss in stiffness of the section because of extensive cracking and considerable widening of the stabilized cracks throughout the span. As the load continues to increase, the strain  $\epsilon_s$  in the steel at the tension side continues to increase beyond the yield strain  $\epsilon_y$  with no additional stress. The beam is considered at this stage to have structurally failed by initial yielding of the tension steel. It continues to deflect without additional loading, the cracks continue to open, and the neutral axis continues to rise toward the outer compression fibers. Finally, a secondary compression failure develops, leading to total crushing of the concrete in the maximum moment region followed by rupture.

## 7.3.2 Uncracked Sections

**7.3.2.1 Deflection calculations.** Deflection calculations for uncracked prestressed sections tend to be more accurate than those for cracked sections since the assumptions of elastic behavior are more applicable. The use of the moment of inertia of the gross section rather than the transformed section does not appreciably affect the accuracy sought in the calculations.

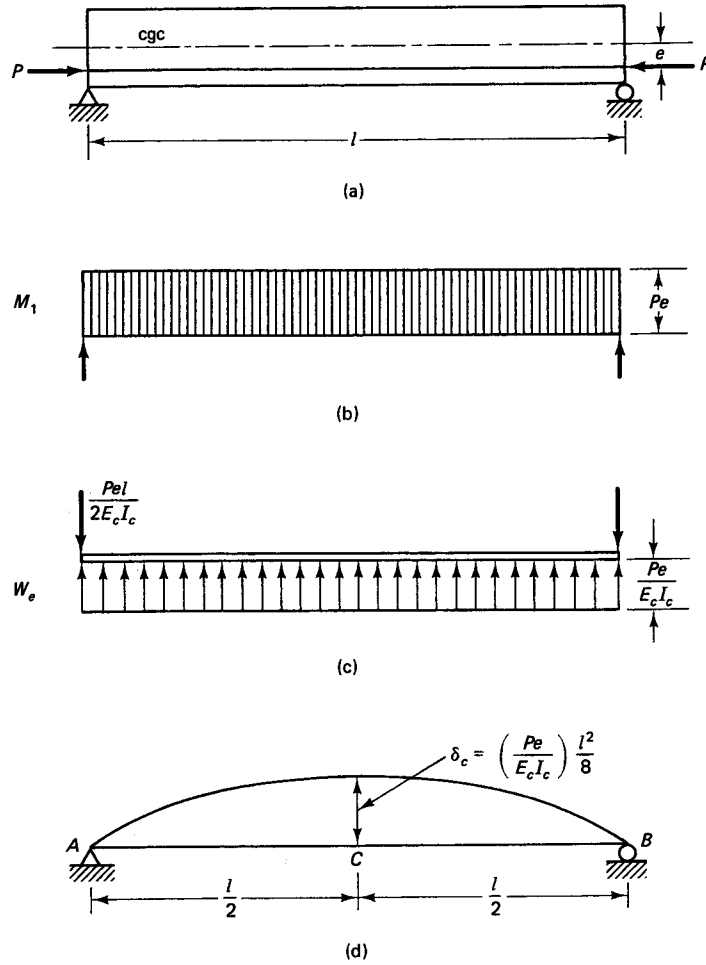
Suppose a beam is prestressed with a constant eccentricity tendon as shown in Figure 7.3. Use the sign convention of plotting the primary moment diagram on the tension side of the beam, and employ the elastic weight method by converting the moment diagram ordinates to elastic weights  $M_1 / (E_c I_c)$  on a beam span  $l$ . Then the moment of the weight intensity  $(Pe) / E_c I_c$  of the half-span AC in Figure 7.3(c) about the midspan point C gives

$$\delta_c = \frac{Pel}{2E_c I_c} \left( \frac{l}{2} \right) - \frac{Pe}{E_c I_c} \left( \frac{l}{2} \times \frac{l}{4} \right) = \frac{Pel^2}{8E_c I_c} \quad (7.5)$$

Notice that the deflection diagram in Figure 7.3(d) is drawn *above* the base line, as the beam cambers upwards due to prestressing.

Similar computations can be performed for any tendon profile and any type of transverse loading regardless of whether the tendon geometry or loading is symmetrical or not. The final camber or deflection is the superposition of the deflections due to prestressing on the deflections due to external loads.

**7.3.2.2 Strain and curvature evaluation.** The distribution of strain across the depth of the section at the controlling stages of loading is linear, as is shown in Figure 7.4, with



**Figure 7.3** Calculation of deflection by elastic weight or moment-area method. (a) Prestressing force. (b) Primary moment  $M_1$ . (c) Elastic weight  $W_e = M/E_c I_c$ . (d) Deflection.

the angle of curvature dependent on the top and bottom concrete extreme fiber strains  $\epsilon_{ct}$  and  $\epsilon_{cb}$ . From the strain distributions, the curvature at the various stages of loading can be expressed as follows:

(1) Initial prestress:

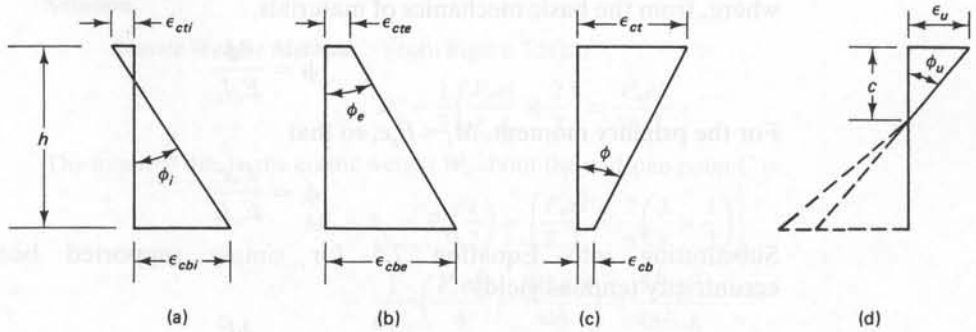
$$\phi_i = \frac{\epsilon_{cbi} - \epsilon_{cti}}{h} \tag{7.6a}$$

(2) Effective prestress after losses:

$$\phi_e = \frac{\epsilon_{cbe} - \epsilon_{cte}}{h} \tag{7.6b}$$

(3) Service load:

$$\phi = \frac{\epsilon_{ct} - \epsilon_{cb}}{h} \tag{7.6c}$$



**Figure 7.4** Strain distribution and curvature at controlling stages. (a) Initial prestress,  $\phi_i = (\epsilon_{cbl} - \epsilon_{cti})/h$ . (b) Effective prestress after losses,  $\phi_e = (\epsilon_{cbe} - \epsilon_{cte})/h$ . (c) Service load,  $\phi = (\epsilon_{ct} - \epsilon_{cb})/h$ . (d) Failure,  $\phi_u = \epsilon_u/c$ .

**(4) Failure:**

$$\phi_u = \frac{\epsilon_u}{c} \quad (7.6d)$$

Use a *plus* sign for tensile strain and a *minus* sign for compressive strain. Figure 7.4c denotes the stress distribution for uncracked section. It has to be modified to show tensile stress at the bottom fibers if the section is cracked.

The effective curvature  $\phi_e$  in Figure 7.4(b) after losses is the sum, using the appropriate sign, of the initial curvature  $\phi_i$ , the change in curvature  $d\phi_1$  due to loss of prestress from creep, relaxation, and shrinkage, and the change in curvature  $d\phi_2$  due to creep of concrete under sustained prestressing force, i.e.,

$$\phi_e = \phi_i + d\phi_1 + d\phi_2 \quad (7.7)$$



**Photo 7.2** Priest Point Park Bridge in Olympia, Washington, a cast-in-place prestressed concrete structure. (Courtesy, Arvid Grant and Associates, Inc.)

where, from the basic mechanics of materials,

$$\phi = \frac{M}{E_c I_c} \tag{7.8a}$$

For the primary moment,  $M_1 = P_e e$ , so that

$$\phi = \frac{P_e e}{E_c I_c} \tag{7.8b}$$

Substituting into Equation 7.5 for simply supported beams with constant-eccentricity tendons yields

$$\delta_c = \frac{\phi l^2}{8} \tag{7.9a}$$

The general expression for deflection in terms of curvature as proposed by Tadros in Ref. 7.4 gives

$$\delta = \phi_c \frac{l^2}{8} - (\phi_e - \phi_c) \frac{a^2}{6} \tag{7.9b}$$

where  $\phi_c$  = curvature at midspan

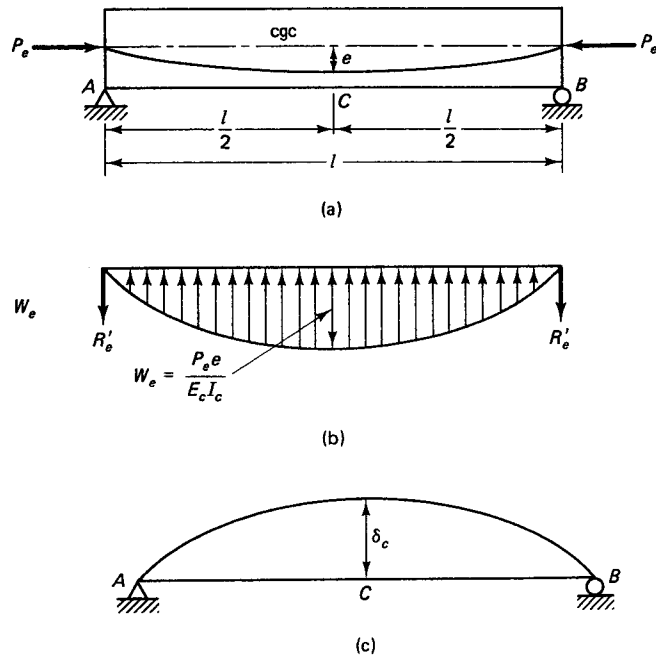
$\phi_e$  = curvature at the support

$a$  = length parameter as a function of the tendon profile.

### 7.3.2.3 Immediate deflection of simply supported beam prestressed with parabolic tendon

#### Example 7.2

Find the immediate midspan deflection of the beam shown in Figure 7.5 prestressed by a parabolic tendon with maximum eccentricity  $e$  at midspan and effective prestressing force  $P_e$ . Use both the elastic weight method and the equivalent weight method. The span of the beam is  $l$  ft, and its stiffness is  $E_c I_c$ .



**Figure 7.5** Deflection of beam in Example 7.2. (a) Tendon profile. (b) Elastic weight  $M/E_c I_c$ . (c) Deflection.

**Solution:**

**Elastic Weight Method.** From Figure 7.5(b),

$$R'_e = \frac{1}{2} \left( \frac{P_e e l}{E_c I_c} \times \frac{2}{3} \right) = \frac{P_e e l}{3 E_c I_c}$$

The moment due to the elastic weight  $W_e$  about the midspan point C is

$$\begin{aligned} M_C = \delta_c &= R'_e \left( \frac{l}{2} \right) - \left[ \frac{P_e e l}{E_c I_c} \times \frac{2}{6} \left( \frac{3}{8} \times \frac{l}{2} \right) \right] \\ &= \frac{1}{E_c I_c} \left( \frac{P_e e l^2}{6} - \frac{3 P_e e l^2}{48} \right) = \frac{5 P_e e l^2}{48 E_c I_c} \end{aligned}$$

Then

$$\delta_c = \frac{5 P_e e l^2}{48 E_c I_c} \quad (a)$$

**Equivalent Weight Method.** From Chapter 1, the equivalent balancing load intensity  $W$  resulting from the pressure of the parabolic tendon on the concrete is

$$W = \frac{8 P_e e}{l^2}$$

Also, from the basic mechanics of materials, the midspan deflection of a uniformly loaded simply supported beam is

$$\delta_c = \frac{5 w l^4}{384 E_c I_c} \quad (b)$$

Substituting for the load intensity  $W$  from the previous equation into this one yields

$$\delta_c = \frac{5 P_e e l^2}{48 E_c I_c} \quad (c)$$

As expected, Equation (c) is identical to Equation (a) for the midspan deflection of the beam.

Figure 7.6 shows typical midspan deflection expressions for simply supported beams, complementing the shear and moment expressions for continuous beams given earlier in Figure 6.12.

### 7.3.3 Cracked Sections

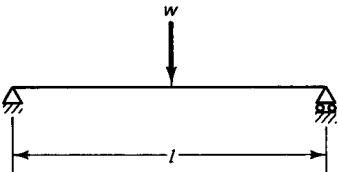
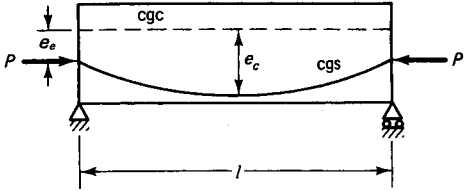
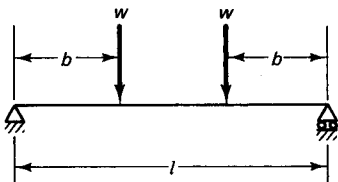
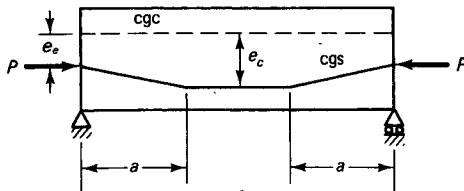
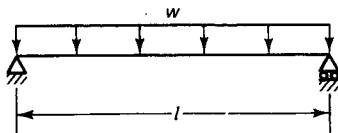
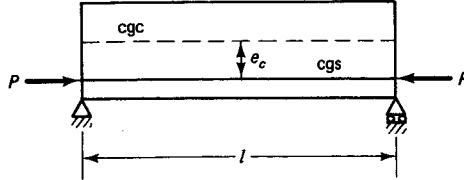
**7.3.3.1 Effective-moment-of-inertia computation method.** As the prestressed element is overloaded, or in the case of partial prestressing where limited controlled cracking is allowed, the use of the gross moment of inertia  $I_g$  underestimates the camber or deflection of the prestressed beam. Theoretically, the cracked moment of inertia  $I_{cr}$  should be used for the section across which the cracks develop while the gross moment of inertia  $I_g$  should be used for the beam sections between the cracks. However, such refinement in the numerical summation of the deflection increases along the beam span is sometimes unwarranted because of the accuracy difficulty of deflection evaluation. Consequently, an effective moment of inertia  $I_e$  can be used as an average value along the span of a simply supported bonded tendon beam, a method developed by Branson in Refs. 7.5 and 7.6. According to this method,

$$I_e = I_{cr} + \left( \frac{M_{cr}}{M_a} \right)^3 (I_g - I_{cr}) \leq I_g \quad (7.10a)$$

Equation 7.10a can also be written in the form

$$I_e = \left( \frac{M_{cr}}{M_a} \right)^3 I_g + \left[ 1 - \left( \frac{M_{cr}}{M_a} \right)^3 \right] I_{cr} \leq I_g \quad (7.10b)$$

The ratio  $(M_{cr}/M_a)$  from Equation 7.4b can be substituted into Equations 7.10a and b to get the effective moment of inertia

Load deflection	Prestress camber
 $\delta = \frac{wl^3}{48EI} = \phi_c \frac{l^2}{12}$	 $\delta = -\frac{Pl^2}{8EI} \left[ e_e + \frac{5}{6}(e_c - e_e) \right]$ $= \phi_c \frac{l^2}{8} + (\phi_e - \phi_c) \frac{l^2}{48}$
 $\delta = \frac{wb}{24EI} (3l^2 - 4b^2)$ $= \phi_c \frac{3l^2 - 4b^2}{24}$	 $\delta = -\frac{Pl^2}{8EI} \left[ e_c + (e_e - e_c) \frac{4}{3} \frac{a^2}{l^2} \right]$ $= \phi_c \frac{l^2}{8} + (\phi_e - \phi_c) \frac{a^2}{6}$
 $\delta = \frac{5wl^4}{384EI} = \phi_c \frac{5l^2}{48}$	 $\delta = -\frac{Pe_c l^2}{8EI} = \phi_c \frac{l^2}{8}$

**Figure 7.6** Short-term deflection in prestressed beams. Subscript *c* indicates midspan; subscript *e* indicates support.

$$\frac{M_{cr}}{M_a} = 1 - \left( \frac{f_{tl} - f_r}{f_L} \right) \quad (7.11)$$

where  $I_{cr}$  = moment of inertia of the cracked section, from Equation 7.13 to follow  
 $I_g$  = gross moment of inertia

Note that both  $M_{cr}$  and  $M_a$  are the unfactored moments due to *live load only* such that  $M_{cr}$  is taken as that portion of the live load moment which causes cracking. The effective moment of inertia  $I_e$  in Equations 7.10a and b thus depends on the maximum moment  $M_a$  along the span in relation to the cracking moment capacity  $M_{cr}$  of the section.

In the case of uncracked continuous beams with both ends continuous,

$$\text{Avg. } I_e = 0.70I_m + 0.15(I_{e1} + I_{e2}) \quad (7.12a)$$

and for continuous uncracked beams with one end continuous,

$$\text{Avg. } I_e = 0.85I_m + 0.15(I_{\text{cont. end}}) \quad (7.12b)$$

where  $I_m$  is the midspan section moment of inertia and  $I_{e1}$  and  $I_{e2}$  are the end-section moments of inertia.

**7.3.3.2 Bilinear computation method.** In graphical form, the bilinear moment-deflection relationship follows stages I and II described in Section 7.3.1 in accordance with ACI code. The idealized diagram for the  $I_g$  and  $I_{cr}$  zones is shown in Figure 7.7. Branson's effective  $I_e$  gives the average total *immediate* deflection  $\delta_{\text{tot}} = \delta_e + \delta_{cr}$  described in the previous section.

The ACI code requires that computation of deflection in the cracked zone in the bonded tendon beams be based on the transformed section whenever the tensile stress  $f_t$  in the concrete exceeds  $6\sqrt{f'_c}$ . Hence,  $\delta_{cr}$  in Figure 7.7 is evaluated using the transformed  $I_{cr}$  utilizing the contribution of the reinforcement in the bilinear method of deflection computation. The cracking moment of inertia can be calculated by the PCI approach (Ref. 7.8) for fully prestressed members by means of the equation

$$I_{cr} = n_p A_{ps} d_p^2 (1 - 1.6\sqrt{n_p \rho_p}) \quad (7.13a)$$

where  $n_p = E_{ps}/E_c$ . If nonprestressed reinforcement is used to carry tensile stresses, namely, in "partial prestressing," Equation 7.13 can be modified to give

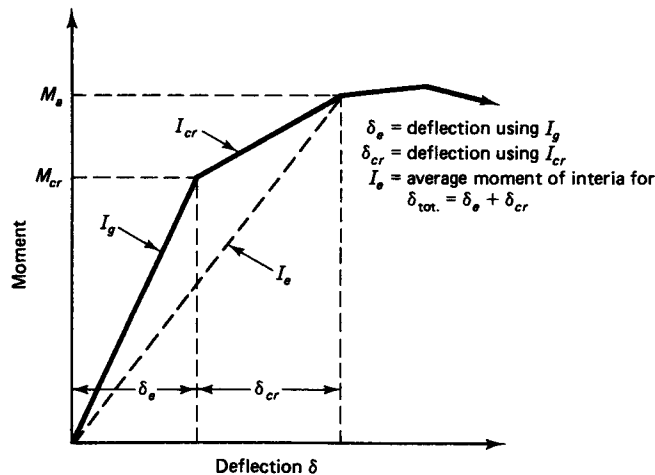


Figure 7.7 Moment-deflection relationship.



$$I_{cr} = (n_p A_{ps} d_p^2 + n_s A_s d^2)(1 - 1.6\sqrt{n_p \rho_p + n_s \rho}) \quad (7.13b)$$

where  $n_s = E_s/E_c$  for the nonprestressed steel,  $d$  = effective depth to center of mild steel or nonprestressed strand steel.

**7.3.3.3 Incremental moment-curvature method.** The cracked moment of inertia can be calculated more accurately from the moment-curvature relationship along the beam span and from the stress and, consequently, strain distribution across the depth of the critical sections. As shown in Figure 7.4(d) for strain  $\epsilon_{cr}$  at first cracking,

$$\phi_{cr} = \frac{\epsilon_{cr}}{c} = \frac{M}{E_c I_{cr}} \quad (7.14)$$

where  $\epsilon_{cr}$  is the strain at the extreme concrete compression fibers and  $M$  is the total moment, including the prestressing primary moment  $M_1$ , about the centroid cgc of the section under consideration. Equation 7.14 can be rewritten to give

$$I_{cr} = \frac{Mc}{E_c \epsilon_{cr}} = \frac{Mc}{f} \quad (7.15)$$

where  $f$  is the concrete stress at the extreme compressive fibers of the section.

A flowchart for instantaneous deflection calculation and construction of the moment-curvature diagram in step-by-step increments is given in Figure 7.8.

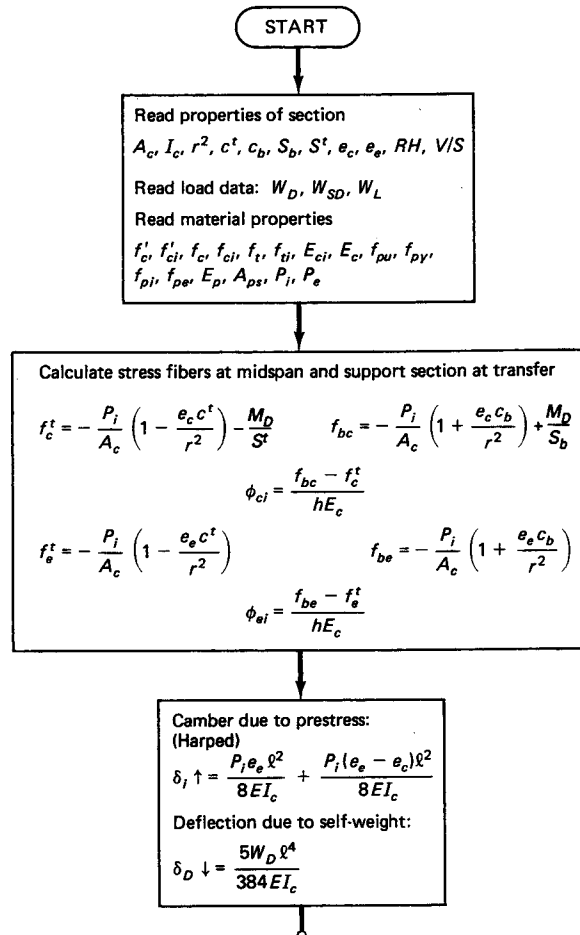
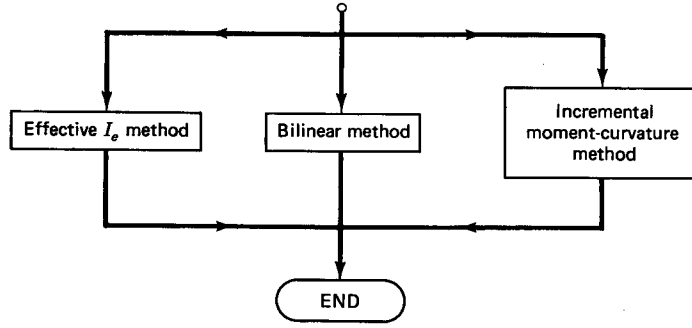
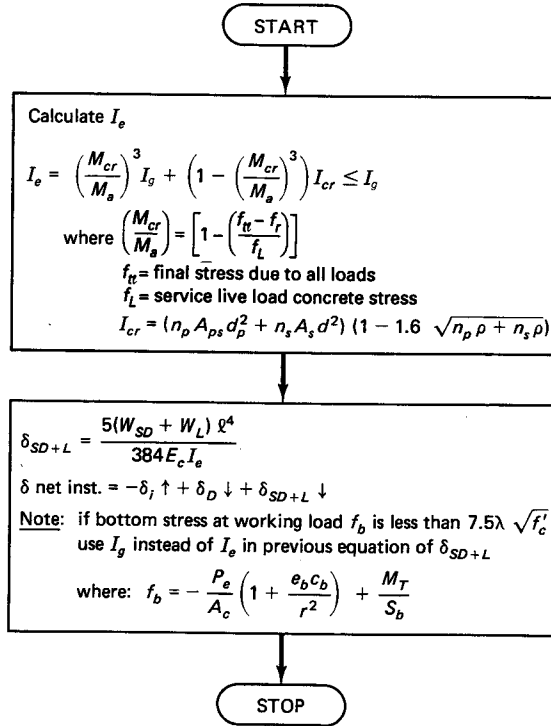


Figure 7.8 Flowchart for immediate moment-curvature camber and deflection.



(a)

Subroutine for  $I_e$  method



(b)

Subroutine for bilinear method

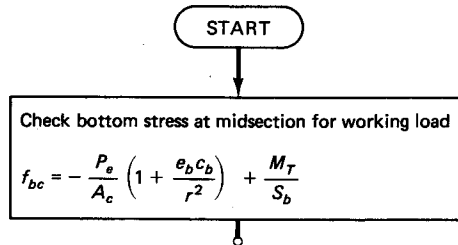
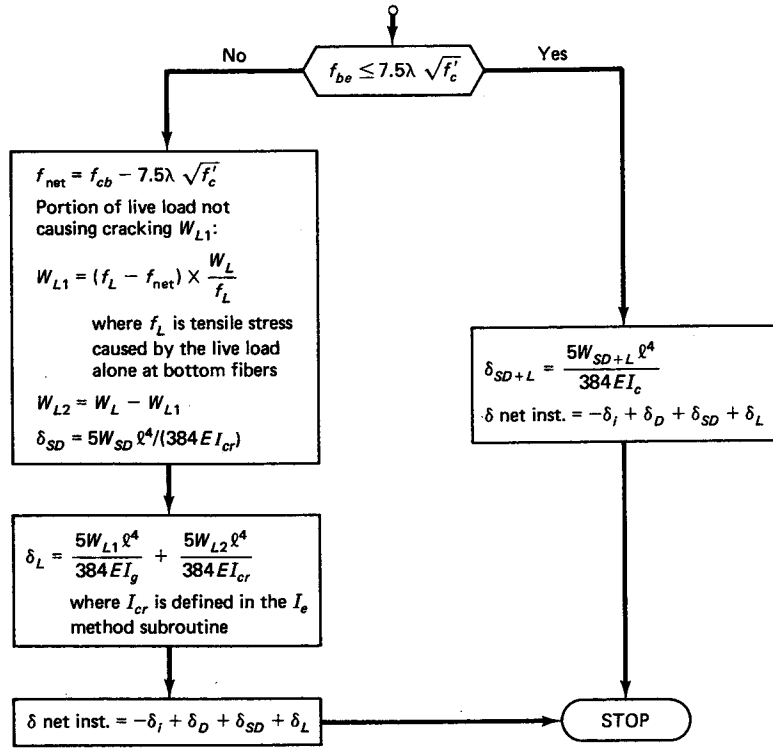


Figure 7.8 Continued



(c)

Subroutine for incremental moment-curvature method

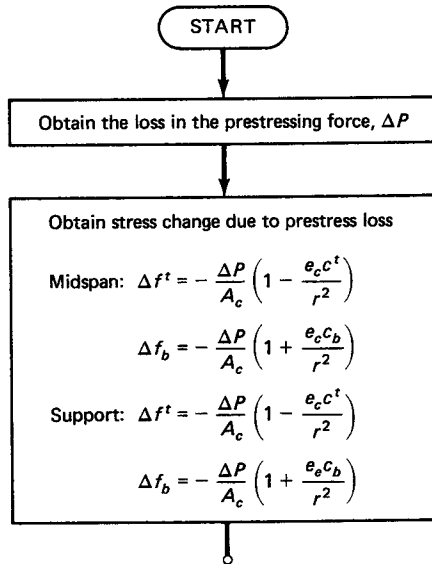


Figure 7.8 Continued

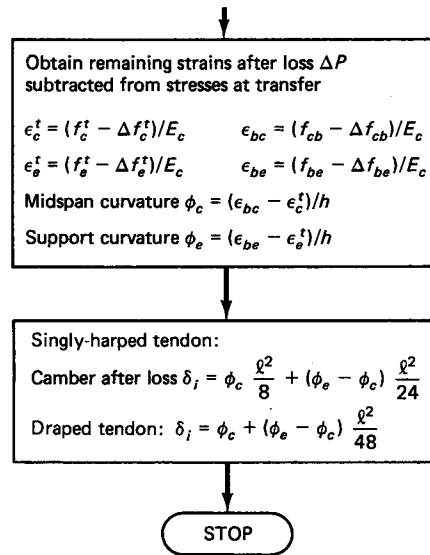


Figure 7.8 Continued

## 7.4 SHORT-TERM DEFLECTION AT SERVICE LOAD

### 7.4.1 Example 7.3 Non-Composite Uncracked Double T-Beam Deflection

Evaluate the total short-term (immediate) elastic deflection of the 12 DT 34 beam in Example 4.1 using (a) applicable moment of inertia  $I_g$  or  $I_e$  method, (b) incremental moment-curvature method. The beam carries a superimposed service live load of 1,100 plf (16.1 kN/m) and superimposed dead load of 100 plf (1.5 kN/m). It is bonded pretensioned, with  $A_{ps}$  = sixteen  $\frac{1}{2}$ -in. diameter 7-wire 270-ksi ( $f_{pu} = 270$  ksi = 1,862 MPa) stress-relieved strands = 2.448 in.<sup>2</sup> Disregard the contribution of the nonprestressed steel in calculating the moment of inertia in this example. Assume that strands are jacked to  $0.70f_{pu}$  resulting in the initial prestress  $P_i = 462,672$  lb. The effective prestress  $P_e = 379,391$  lb occurs at the first load application 30 days after erection and does not include all the time-dependent losses.

#### Data

##### (a) Geometrical Properties (Fig. 7.9)

$$A_c = 978 \text{ in.}^2 (6,310 \text{ cm}^2)$$

$$I_c = 86,072 \text{ in.}^4 (3.59 \times 10^6 \text{ cm}^4)$$

$$S_b = 3,340 \text{ in.}^3 (5.47 \times 10^4 \text{ cm}^3)$$

$$S^t = 10,458 \text{ in.}^3$$

$$W_D = 1,019 \text{ plf, self-weight}$$

$$W_{SD} = 100 \text{ plf (1.46 kN/m)}$$

$$W_L = 1,100 \text{ plf (16.05 kN/m)}$$

$$e_c = 22.02 \text{ in.}$$

$$e_e = 12.77 \text{ in.}$$

$$c_b = 25.77 \text{ in.}$$

$$c_t = 8.23 \text{ in.}$$

$$A_{ps} = 16 \times 0.153 = 2.448 \text{ in.}^2 (15.3 \text{ cm}^2)$$

$$P_i = 462,672 (2,058 \text{ kN}) \text{ at transfer}$$

$$P_e = 379,391 \text{ lb (1,688 kN)}$$

##### (b) Material Properties

$$V/S = 2.39 \text{ in}$$

$$RH = 70\%$$

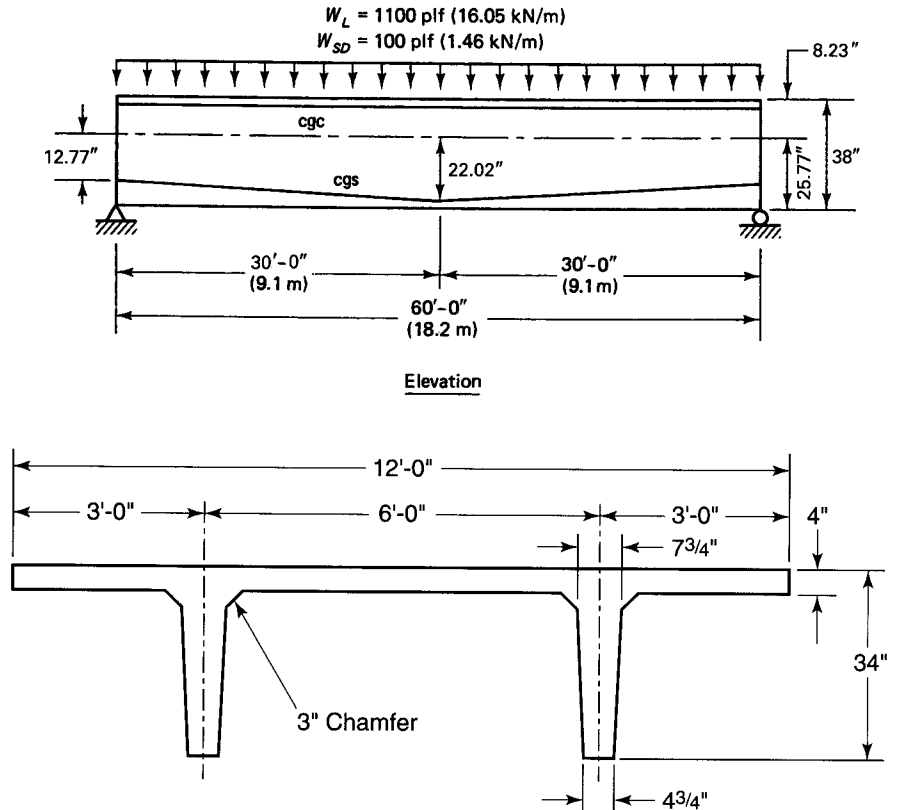


Figure 7.9 Beam geometry of Example 4.1.

$$\begin{aligned}
 f'_c &= 5,000 \text{ psi} \\
 f'_{ci} &= 3,750 \text{ psi} \\
 f_{pu} &= 270,000 \text{ psi (1,862 MPa)} \\
 f_{pi} &= 189,000 \text{ psi (1,303 MPa)} \\
 f_{pe} &= 154,980 \text{ psi (1,067 MPa)} \\
 f_{py} &= 230,000 \text{ psi} \\
 E_{ps} &= 28.5 \times 10^6 \text{ psi (196 GPa)}
 \end{aligned}$$

**(c) Allowable Stresses**

$$\begin{aligned}
 f_{ci} &= 2,250 \text{ psi} \\
 f_c &= 2,250 \text{ psi} \\
 f_{ti} &= 184 \text{ psi (midspan)} \\
 f_t &= 849 \text{ psi (midspan)}
 \end{aligned}$$

**Solution: (a)**

**1. Midspan Section Stresses**

$$e_c = 22.02 \text{ in. (559 mm)}$$

Maximum self-weight moment

$$M_D = \frac{1,019(60)^2}{8} \times 12 = 5,502,600 \text{ in.-lb}$$

**(a)** At transfer, calculated fiber stresses are  
From Equation 4.1a,

$$\begin{aligned}
 f' &= -\frac{P_i}{A_c} \left( 1 - \frac{e_c c_t}{r^2} \right) - \frac{M_D}{S'} \\
 &= -\frac{462,672}{978} \left( 1 - \frac{22.02 \times 8.73}{88.0} \right) - \frac{5,502,600}{10,458} \\
 &= +501 - 526 = -25 \text{ psi (C)} < f_t = +184 \text{ psi (T), O.K.}
 \end{aligned}$$

$$\begin{aligned}
 f_b &= -\frac{P_i}{A_c} \left( 1 + \frac{e_c c_b}{r^2} \right) + \frac{M_D}{S_b} \\
 &= -\frac{462,672}{978} \left( 1 + \frac{22.02 \times 25.77}{88.0} \right) + \frac{5,502,600}{3,340} \\
 &= -3,524 + 1,647 = -1,877 \text{ psi (C)} < -2,250 \text{ psi, O.K.}
 \end{aligned}$$

(b) At service load

$$M_{SD} = \frac{100(60)^2 12}{8} = 540,000 \text{ in.-lb (61 kN-m)}$$

$$M_L = \frac{1,100(60)^2 12}{8} = 5,940,000 \text{ in.-lb (672 kN-m)}$$

$$\text{Live-load } f' = \frac{5,940,000}{10,458} = -568 \text{ psi (C)}$$

$$\text{Live-load } f_b = \frac{5,940,000}{3,340} = 1,778 \text{ psi (T)}$$

Total Moment  $M_T = M_D + M_{SD} + M_L = 5,502,600 + 6,480,000 = 11,982,600$  in.-lb (1,354 kN-m).

From Equation 4.3a,

$$\begin{aligned}
 f' &= -\frac{P_e}{A_c} \left( 1 - \frac{e c_t}{r^2} \right) - \frac{M_T}{S'} \\
 &= -\frac{379,391}{978} \left( 1 - \frac{22.02 \times 8.23}{88.0} \right) - \frac{11,982,600}{10,458} \\
 f' &= +411 - 1146 = -735 \text{ psi} < f_c = -2,250 \text{ psi, O.K.}
 \end{aligned}$$

From Equation 4.3b,

$$\begin{aligned}
 f_b &= -\frac{P_e}{A_c} \left( 1 + \frac{e c_b}{r^2} \right) + \frac{M_T}{S_b} \\
 &= -\frac{379,391}{978} \left( 1 + \frac{22.02 \times 25.77}{88.0} \right) + \frac{11,982,600}{3,340} \\
 &= -2,689 + 3,587 = +698 \text{ psi (T)} < 849 \text{ psi, O.K.}
 \end{aligned}$$

Allow using the gross moment of inertia  $I_g$  for deflection calculations. In such a case, the effective moment of inertia  $I_e$  can be taken as  $I_g$ . If compared with the modulus of rupture  $f_r = 7.5\sqrt{f'_c} = 7.5\sqrt{5000} = 530$  psi, minor cracking is expected and allowed as the 7.5 factor is conservative.

## 2. Support Section Stresses

From Example 4.1,

$$f_{ii} = 6\sqrt{f'_{ci}} = 6\sqrt{3,750} = 367 \text{ psi}$$

$$f_i = 12\sqrt{f'_c} = 12\sqrt{5,000} = 849 \text{ psi}$$

$$e_e = 12.77 \text{ in.}$$

Follow the same steps as in the midspan section, with the moment  $M = 0$  in the above steps. A check of support section stresses at transfer gave stresses below the allowable, hence O.K.

*Summary of Fiber Stresses (psi)*

	Midspan		Support	
	$f^t$	$f_b$	$f^t$	$f_b$
Prestress $P_i$ only	+501	-3,524	+92	-2,242
At transfer and $W_d$	-25	-1,877	+92	-2,242
Live load $W_L$ only	-568	+1,778	0	0
At service load	-735	+698	+75	-1,839

(1 psi = 6.895 kPa)

**3. Deflection and Camber Calculation at Transfer**

From basic mechanics or from Figure 7.6, for  $a = l/2$ , the camber at midspan due to a single harp or depression of the prestressing tendon is

$$\delta \uparrow = \frac{P_e l^2}{8EI} + \frac{P(e_e - e_c)l^2}{24EI}$$

So

$$E_{ci} = 57,000\sqrt{f'_{ci}} = 57,000\sqrt{3,750} = 3.49 \times 10^6 \text{ psi (24.1 MPa)}$$

$$E_c = 57,000\sqrt{f'_c} = 57,000\sqrt{5,000} = 4.03 \times 10^6 \text{ psi (27.8 MPa)}$$

$$\begin{aligned} \delta_{pi} \uparrow &= \frac{462,672 \times 22.02 \times (60 \times 12)^2}{8 \times 3.49 \times 10^6 \times 86,702} \\ &+ \frac{462,672 \times (12.77 - 22.02)(60 \times 12)^2}{24 \times 3.49 \times 10^6 \times 86,072} \\ &= -2.20 + 0.31 = -1.89 \text{ in. (48 mm)} \uparrow \end{aligned}$$

This upward deflection (camber) is due to prestress only. The self-weight per inch is  $1,019/12 = 84.9 \text{ lb/in.}$ , and the deflection caused by self-weight is  $\delta_D \downarrow = 5wl^4/384EI$ ,

$$\delta_D = 5 \times 84.9 (60 \times 12)^4 / 384 \times 3.49 \times 10^6 \times 86,072 = 0.99 \text{ in.} \downarrow$$

Thus, the net camber at transfer is  $-1.89 \uparrow + 0.99 \downarrow = -0.90 \text{ in.} \uparrow$  (25 mm).

**4. Total Immediate Deflection at Service Load of Uncracked Beam**

(a) Superimposed dead load deflection, using  $E_c = 4.03 \times 10^6 \text{ psi}$

$$\delta_{SD} = 0.99 \frac{E_{ci}}{E_c} \left( \frac{100}{1,019} \right) = 0.99 \left( \frac{3.49}{4.03} \right) \left( \frac{100}{1,019} \right) = 0.08 \text{ in. (2.0 mm)} \downarrow$$

(b) Live load deflection

$$\delta_L = \frac{5wl^4}{384E_c I_c} = \frac{5(1100)(60 \times 12)^4}{384 \times 4.03 \times 10^6 \times 86,072} \times \frac{1}{12} = 0.93 \text{ in.} \downarrow$$

A summary of the short-term cambers and deflections at service load is as follows:

- Camber due to initial prestress = 1.89 in. (48 mm)  $\uparrow$
- Deflections due to self-weight = 0.99 in. (25 mm)  $\downarrow$
- Deflection due to superimposed dead load = 0.08 in. (2 mm)  $\downarrow$
- Deflection due to live load = 0.93 in. (23 mm)  $\downarrow$
- Net deflection at transfer =  $-1.89 + 0.99 = -0.90 \text{ in.} \uparrow$

If deflection due to prestress loss from the transfer stage to erection at 30 days is considered, reduced camber is

$$= 1.89 \left( \frac{462,672 - 379,391}{462,672} \right)$$

$$= 1.89 \left( \frac{83,281}{462,672} \right) = 0.34 \text{ in. } \downarrow$$

**Solution: (b)****Alternate Solution by Incremental Moment Curvature Method**

$P_e$  at 30 days after transfer is 379,391 lb. So 30 days' prestress loss

$$\Delta P = P_i - P_e = 462,672 - 379,391 = 83,281 \text{ lb (370 kN)}$$

**Strains at Transfer Due to Prestressing**

$$E_{ci} \text{ at 7 days} = 3.49 \times 10^6 \text{ psi}$$

**(i) Due to prestressing force ( $P_i$ )**

Midspan :

$$f^t = +501 \text{ psi}$$

$$f_b = -3,524 \text{ psi}$$

$$\epsilon_c^t = \frac{+501}{3.49 \times 10^6} = +144 \times 10^{-6} \text{ in./in.}$$

$$\epsilon_{cb} = -1,010 \times 10^{-6} \text{ in./in.}$$

Support:

$$f^t = +92 \text{ psi}$$

$$f_b = -2,242 \text{ psi}$$

$$\epsilon_c^t = 26 \times 10^{-6} \text{ in./in.}$$

$$\epsilon_{cb} = -642 \times 10^{-6} \text{ in./in.}$$

$$(1 \text{ psi} = 6.895 \text{ KPa})$$

**(ii) Due to prestressing force and self-weight ( $P_i + W_D$ )**

Midspan:

$$f^t = -25 \text{ psi} \quad \epsilon_c^t = -7.2 \times 10^{-6} \text{ in./in.}$$

$$f_b = -1,877 \text{ psi} \quad \epsilon_{cb} = -537.8 \times 10^{-6} \text{ in./in.}$$

Support: same as in (i)

Strain change due to prestress loss

$$-\Delta P = 83,281 \text{ lb.}$$

$$E_{ci} = 3.49 \times 10^6 \text{ psi}$$

**Midspan Section**

$$\Delta f^t = -\frac{(-\Delta P)}{A_c} \left( 1 - \frac{ec_t}{r^2} \right) = +\frac{83,281}{978} \left( 1 - \frac{22.02 \times 8.23}{88.0} \right)$$

$$= -90 \text{ psi (C)}$$

$$\Delta \epsilon_c^t = \frac{-90}{3.49 \times 10^6} = -26 \times 10^{-6} \text{ in./in.}$$

$$\Delta f_b = -\frac{(-\Delta P)}{A_c} \left( 1 + \frac{ec_b}{r^2} \right) = +\frac{83,281}{978} \left( 1 + \frac{22.02 \times 25.77}{88.0} \right) = +634 \text{ psi (T)}$$



$$\Delta\epsilon_{cb} = \frac{634}{3.49 \times 10^6} = +182 \times 10^{-6} \text{ in./in.}$$

**Support Section**

$$\Delta f'_t = -\frac{(-\Delta P)}{A_c} \left(1 - \frac{ec_t}{r^2}\right) = +\frac{83,281}{978} \left(1 - \frac{12.77 \times 8.23}{88.0}\right) = -16.5 \text{ psi (C)}$$

$$\Delta\epsilon'_e = \frac{-16.5}{3.49 \times 10^6} = -5 \times 10^{-6} \text{ in./in.}$$

$$\Delta f_b = -\frac{(-\Delta P)}{A_c} \left(1 + \frac{ec_b}{r^2}\right) = +\frac{83,281}{978} \left(1 + \frac{12.77 \times 25.77}{88.0}\right) = 404 \text{ psi (T)}$$

$$\Delta\epsilon_{be} = \frac{+404}{3.49 \times 10^6} = +116 \times 10^{-6} \text{ in./in.}$$

Superimposing the strain at transfer on the strain due to prestress loss gives the strain distributions at service load after prestress *due to prestress only*, as shown in Figure 7.10.

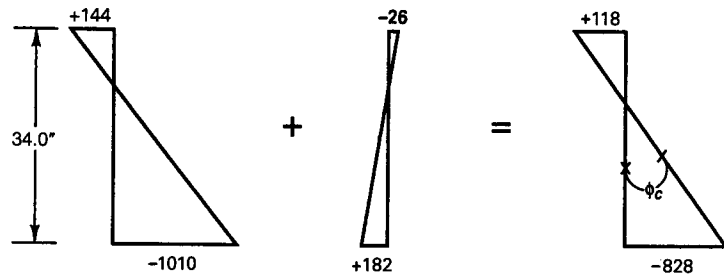
From Figure 7.10

Midspan curvature

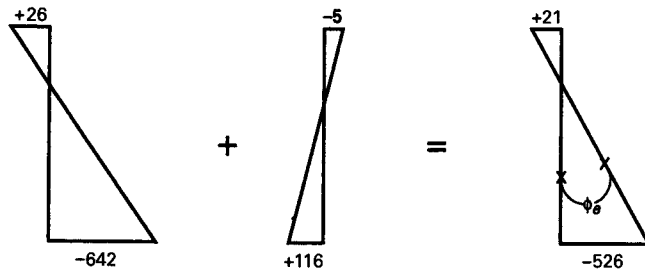
$$\phi_c = \frac{-828 - 118}{34} \times 10^{-6} = -27.82 \times 10^{-6} \text{ rad/in.}$$

Support curvature

$$\phi_e = \frac{-526 - 21}{34} \times 10^{-6} = -16.09 \times 10^{-6} \text{ rad/in.}$$



(a) Midspan section strains  $\epsilon_c \times 10^{-6}$  in./in.



(b) Support section strains  $\epsilon_e \times 10^{-6}$  in./in.

**Figure 7.10** Strain distribution across section depth at prestress transfer in Example 7.4.

From Figure 7.6 for  $a = l/2$ , the beam camber after losses due only to  $P_e$  is

$$\begin{aligned}\delta_e \uparrow &= \phi_c \left( \frac{l^2}{8} \right) + (\phi_e - \phi_c) \frac{l^2}{24} \\ &= -27.82 \times 10^{-6} \frac{(60 \times 12)^2}{8} + (-16.09 + 27.82) \\ &\quad \times 10^{-6} \frac{(60 \times 12)^2}{24} = -1.80 + 0.25 \\ &= -1.55 \text{ in. } \uparrow (39 \text{ mm}) \text{ (camber)}\end{aligned}$$

which is identical to  $(-1.89 + 0.34) = -1.55 \text{ in. } \uparrow$  after losses in the previous solution. The deflections due to self-weight  $W_D$ , superimposed dead load  $W_{SD}$  and live load  $W_L$  are the same as in the previous solution.

Note that the computed deflection values can differ by 20 to 40 percent from the actual values because of the several parameters which affect the modulus of concrete. Hence, all computational values in the various steps of the solution can be rounded to three significant figures without appreciably affecting the final results.

## 7.5 SHORT-TERM DEFLECTION OF CRACKED PRESTRESSED BEAMS

### 7.5.1 Short-Term Deflection of the Beam in Example 7.3 If Cracked

#### Example 7.4

Solve Example 7.3 by (a) the bilinear method, (b) the effective moment of inertia method for a condition of tensile stress  $f_b = 750 \text{ psi}$  at midspan bottom fibers at service load, i.e., the tensile stress exceeds the modulus of rupture  $f_r = 7.5\sqrt{f'_c} = 530 \text{ psi}$  for crack formation. Assume that the net beam camber due to prestress and self-weight is  $\delta = 0.95 \text{ in.}$

**Solution:** The net tensile stress beyond the first cracking load at the modulus of rupture is  $f_{net} = f_b - f_r = 750 - 530 = +220 \text{ psi } (T)$ . From Example 7.3, the tensile stress caused by the live load alone at the bottom fibers is  $+1,778 \text{ psi}$ . Now, since  $W_L = 1,100 \text{ plf}$ , the portion of the load that would not result in tensile stress at the bottom fibers is

$$\begin{aligned}w_1 &= \frac{(1,778 - 220)}{(1,778)} \times 1,100 = 964 \text{ plf} \\ &= \frac{964}{12} = 80 \text{ lb/in.}\end{aligned}$$

The deflection determined by the uncracked  $I_g$  is

$$\delta_g = \frac{5w_1l^4}{384E_cI_g} = \frac{5 \times 80(60 \times 12)^4}{384 \times 4.03 \times 10^6 \times 86,072} = 0.8 \text{ in. } \downarrow (20 \text{ mm})$$

#### (a) Bilinear Method

$$I_{cr} = n_p A_{ps} d_p^2 (1 - 1.6\sqrt{n_p \rho_p})$$

$$n_p = \frac{E_{ps}}{E_c} = \frac{28.5 \times 10^6}{4.03 \times 10^6} = 7.07$$

$$d_p = e_c + c_t = 22.02 + 8.23 = 30.25 \text{ in. } > 0.8h = 27.2 \text{ in.}$$

Used  $d_p = 30.25 \text{ in.}$  and  $A_{ps} = 2.448 \text{ in.}^2$  Then

$$\rho_p = \frac{A_{ps}}{bd_p} = \frac{2.448}{144 \times 30.25} = 0.0006$$

$$I_{cr} = 7.07 \times 2.448 (30.25)^2 (1 - 1.6\sqrt{7.07 \times 0.0006}) \\ = 14,187 \text{ in.}^4 (5.9 \times 10^5 \text{ cm}^4)$$

Balance of the total load that results in cracking of the section is

$$w_2 = \frac{1,100 - 964}{1,100 \times 12} = 11.3 \text{ lb/in.}$$

$$\delta_{cr} = \frac{5w_2l^4}{384E_cI_{cr}} = \frac{5 \times 11.3(60 \times 12)^4}{384 \times 4.03 \times 10^6 \times 14,187} \\ = 0.69 \text{ in.} \downarrow (17 \text{ mm})$$

Thus, the total deflection due to live load

$$\delta_L = 0.80 + 0.69 = +1.49 \text{ in.} \downarrow (38 \text{ mm})$$

**(b) Effective Moment of Inertia Method  $I_e$  Method:**

From Equation 7.10b,

$$I_e = \left(\frac{M_{cr}}{M_a}\right)^3 I_g + \left[1 - \left(\frac{M_{cr}}{M_a}\right)^3\right] I_{cr} \leq I_g$$

From Equation 7.11,

$$\left(\frac{M_{cr}}{M_a}\right) = 1 - \left(\frac{f_{il} - f_r}{f_L}\right)$$

$f_{il}$  = final total stress = +750 psi ( $T$ )

$f_r$  = modulus of rupture = 530 psi from before

$f_L$  = live load stress = 1778 psi

$$\left(\frac{M_{cr}}{M_a}\right) = 1 - \left(\frac{750 - 530}{1,778}\right) = 1 - 0.124 = 0.876$$

$$\left(\frac{M_{cr}}{M_a}\right)^3 = 0.67$$

$$I_e = 0.67 \times 86,072 + (1 - 0.67)14,187 \\ = 62,350 \text{ in.}^4$$

Total live-load intensity =  $1,100/12 = 92 \text{ lb/in.}$

Deflection due to live load

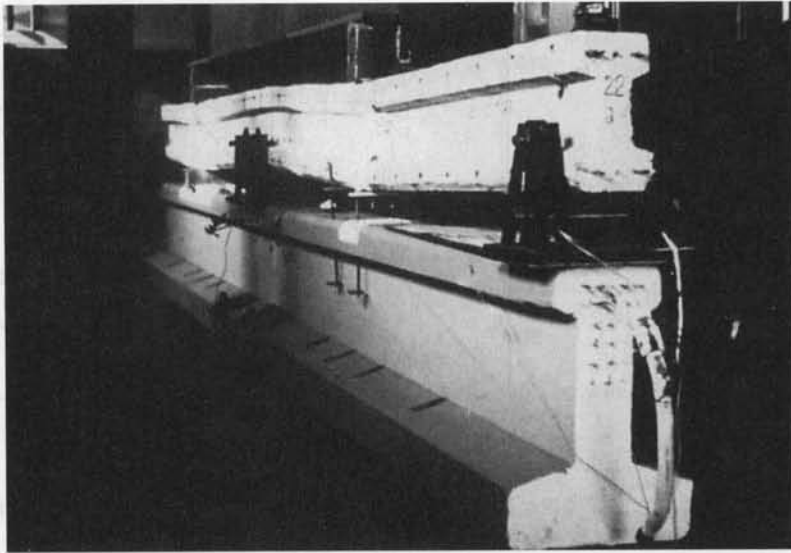
$$\delta_L = \frac{5 \times 92(60 \times 12)^4}{384 \times 4.03 \times 10^6 \times 62,350} = 1.28 \text{ in.} \downarrow (33 \text{ mm})$$

as compared to 1.49 in. in Solution (a). Choose  $\delta_L = +1.49 \text{ in.} \downarrow$ . Use this value for the final net long-term deflection after losses as tabulated in Example 7.6.

## 7.6 CONSTRUCTION OF MOMENT-CURVATURE DIAGRAM

### Example 7.5

Construct the moment-curvature diagram for the midspan section of the bonded double-T beam in Example 7.3 for the following incremental strain steps:



**Photo 7.3** Deflection of continuous beam (Nawy et al.).

1. Strain at transfer  $f_{pi} = 189,000$  psi due to  $P_i$  only.
2. Strain at  $f_{pe} = 154,980$  psi prior to gravity loads.
3. Decompression at tendon cgs level.
4. Modulus of rupture level.
5. Cracked section, strain  $\epsilon_{ct}$  at top = 0.001 in./in.
6. Cracked section, strain  $\epsilon_{ct}$  at top = 0.003 in./in.

**Solution:**

1. *Prestress Transfer Stage*

From the data for Example 7.3, the midspan stresses due only to prestress  $P_i$  are as follows:

$$f_t = +501 \text{ psi}$$

$$f_b = -3,524 \text{ psi}$$

$$\epsilon'_c = \frac{+501}{3.49 \times 10^6} = +144 \times 10^{-6} \text{ in./in.}$$

$$\epsilon_{cb} = \frac{-3524}{3.49 \times 10^6} = -1,010 \times 10^{-6} \text{ in./in.}$$

$$\phi_i = \frac{(\epsilon_{cb} - \epsilon'_c)}{h} = \frac{(-1010 - 144)}{34} \times 10^{-6} = -33.94 \times 10^{-6} \text{ rad/in.}$$

From Example 7.3, the corresponding moments due to  $P_i + M_D$  are  $M_i = -462,672 \times 22.02 + 5,502,600 = -4.69 \times 10^6$  in.-lb.

2. *Prestress Stage after Losses*

In the subsequent decompression stage a moment value  $M_g$  due to gravity loads has to be found which would reduce the stress in the prestressing steel to zero. From Example 4.1,  $P_e = 379,391$  lb. Hence,

$$\frac{P_e}{P_i} = \frac{379,391}{462,672} = 0.82$$

The stresses and strains at midspan at transfer prestress  $P_i$  are

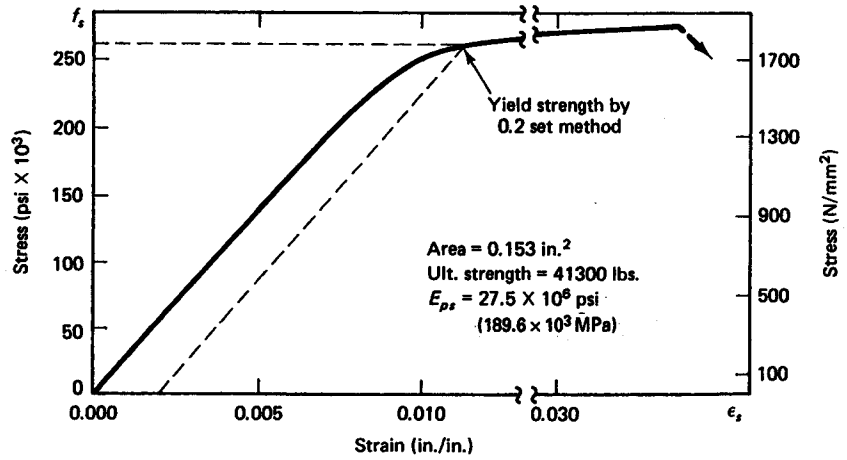


Figure 7.11 Stress-strain diagram for 1/2 in. (12.7 mm) dia prestressing tendons.

$$f'_c = +501 \text{ psi}$$

$$f_{cb} = -3,524 \text{ psi}$$

$$\epsilon'_c = +144 \times 10^{-6} \text{ in./in.}$$

$$\epsilon_{cb} = -1,010 \times 10^{-6} \text{ in./in.}$$

Reduce the strains up to the  $P_e$  stage as follows:

$$\epsilon'_c = 0.82(+144 \times 10^{-6}) = +118 \times 10^{-6} \text{ in./in.}$$

$$\epsilon_{cb} = 0.82(-1010 \times 10^{-6}) = -828 \times 10^{-6} \text{ in./in.}$$

The strain distribution becomes, as shown in Figure 7.13,

$$\phi_2 = \frac{(\epsilon_{cb} - \epsilon'_c)}{h} = \frac{(-828 - 118)10^{-6}}{34} = -27.82 \times 10^{-6} \text{ rad/in.}$$

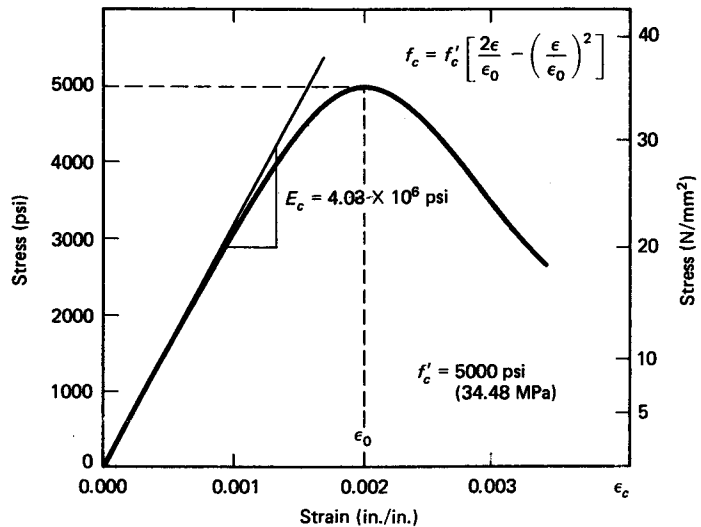


Figure 7.12 Stress-strain diagram for  $f'_c = 5,000$  psi concrete.

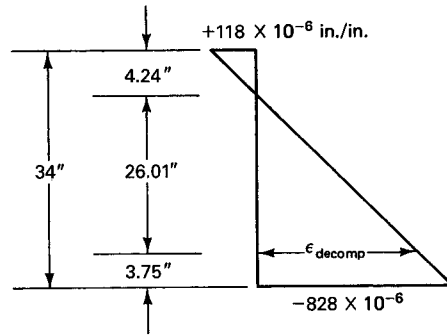


Figure 7.13 Strain distribution due only to prestress  $P_e$ .

The corresponding gravity-load moment  $M_g = 0$ .

Note the strain distribution in Figure 7.13 due to the prestressing force  $P_e$ . Use the stress-strain diagram of Figure 7.11 for the prestressing steel and that of Figure 7.12 for the concrete to determine the actual stresses through strain compatibility.

### 3. Decompression Stage with Zero Concrete Stress at Tendon cgs

From Figure 7.11, the decompression strain at the cgs level is

$$\epsilon_{\text{decomp.}} = -828 \times 10^{-6} \times \frac{26.01}{26.01 + 3.75} = 723 \times 10^{-6} \text{ in./in.}$$

and

$$\epsilon_{pe} = \frac{f_{pe}}{E_{ps}} = \frac{154,980}{27.5 \times 10^6} = 5,636 \times 10^{-6} \text{ in./in.}$$

Compatibility of strain requires that the prestressing tendons in the *bonded* beam undergo the same change in strain as the surrounding concrete, *increasing* the tensile strain in the tendon in order to reduce the compressive stress in the concrete at the cgs level to zero. Thus,

$$\text{Total } \epsilon_{pe} = 5,636 \times 10^{-6} + 723 \times 10^{-6} = 6,359 \times 10^{-6} \text{ in./in.}$$

From the stress-strain diagram in Figure 7.11 the corresponding stress  $f_{pe} = 177,000$  psi. Consequently, we have

$$\text{Adjusted } P_e = 177,000 \times 0.153 \times 16 = 433,296$$

$$\text{Adjusted } f^t = -\frac{433,296}{978} \left( 1 - \frac{22.02 \times 8.23}{88.0} \right) \cong +469 \text{ psi (T)}$$

$$\epsilon_c^t = -\frac{+469}{4.03 \times 10^6} = 116 \times 10^{-6} \text{ in./in.}$$

$$\text{Adjusted } f_b = -\frac{433,296}{978} \left( 1 + \frac{22.02 \times 25.77}{88.0} \right) \cong -3,300 \text{ psi (C)}$$

$$\epsilon_{cb} = \frac{-3,300}{4.03 \times 10^6} = -819 \times 10^{-6} \text{ in./in.}$$

$$f_{\text{decomp.}} = \frac{M_{\text{decomp.}} \times y}{I_c} = \frac{M_{\text{decomp.}} \times 22.02}{86,072} = 2,884 \text{ psi}$$

$$M_{\text{decomp.}} = \frac{2,884 \times 86,072}{22.02} = 11.27 \times 10^6 \text{ in.-lb (} 1.27 \times 10^6 \text{ N-m)}$$

$$f^t = \frac{M_{\text{decomp.}}}{S^t} = \frac{11.27 \times 10^6}{10,458} = -1,078 \text{ psi (C)}$$

Net stress  $f^t = -1,078 + 469 = -609 \text{ psi (C)}$  (4.16 MPa)

$$\epsilon_c^t = \frac{-609}{4.03 \times 10^6} = -151.1 \times 10^{-6} \text{ in./in.}$$

$$f_b = \frac{11.27 \times 10^6}{S_b} = \frac{11.27 \times 10^6}{3,340} = +3,374 \text{ psi (T)}$$

Net stress  $f_b = +3,374 - 3,300 = +74 \text{ psi (T)}$

$$\epsilon_{cb} = \frac{+74}{4.03 \times 10^6} = +18.4 \times 10^{-6} \text{ in./in.}$$

$$\phi_{\text{decomp.}} = \frac{(\epsilon_{cb} - \epsilon_c^t)}{h} = \frac{(18.4 + 151.1)}{34} = 10^{-6} = +4.99 \times 10^{-6} \text{ rad/in.}$$

Corresponding  $M = 11.27 \times 10^6 \text{ in.-lb}$

Figure 7.14 gives the stress and strain distributions in this beam at the decompression state.

4. Modulus of Rupture Stage

$$f_r = 7.5\lambda\sqrt{f_c'} = 7.5\sqrt{5,000} = 530 \text{ psi}$$

$$M_{cr} = S_b \left[ 7.5\lambda\sqrt{f_c'} + \frac{P_e}{A_c} \left( 1 + \frac{ec_b}{r^2} \right) \right]$$

From before, the second part of the above expression for moment gives a stress of 3,300 psi.

Therefore  $M_{cr} = 3,340(530 + 3,300) = 12.8 \times 10^6 \text{ in.-lb}$

Net bottom concrete stress = modulus of rupture  $f_r$  for this stage = +530 psi (T)

$$\epsilon_{cb} = \frac{+530}{4.03 \times 10^6} = +132 \times 10^{-6} \text{ in./in.}$$

$$f^t = \frac{12.8 \times 10^6}{10,458} = -1,224 \text{ psi (C)}$$

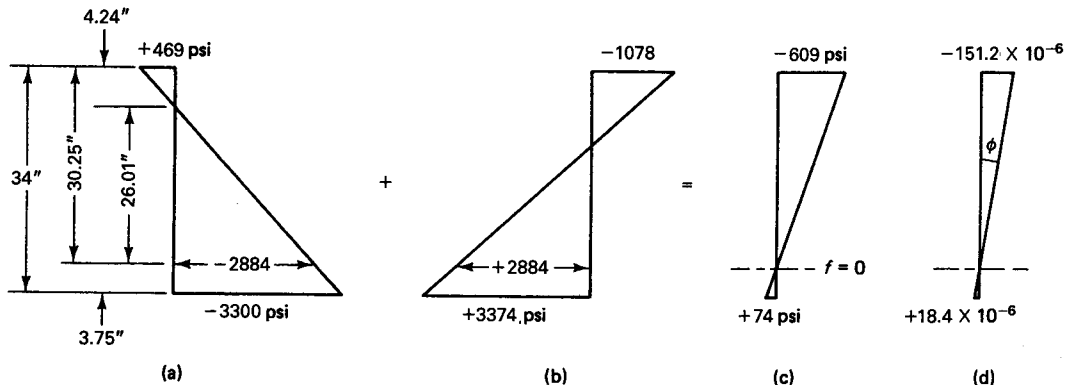
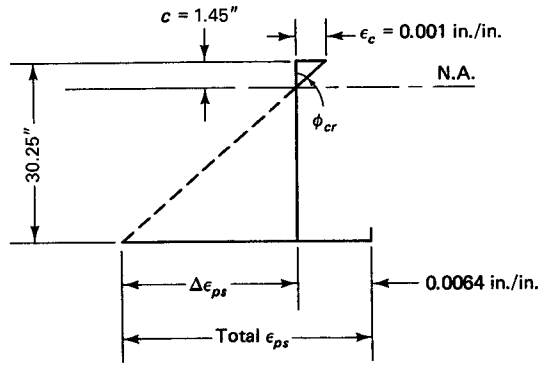


Figure 7.14 Stress distribution at decompression in Example 7.6. (a) Loading stress. (b) Decompression stress. (c) Final stress. (d) Unit strain.



**Figure 7.15** Strain distribution at  $\epsilon_c = 0.001$  in./in. in Example 7.5.

$$\text{Net stress } f^t = -1,224 + 469 = -755 \text{ psi (C)}$$

$$\epsilon_c^t = \frac{-755}{4.03 \times 10^6} = -187 \times 10^{-6} \text{ in./in.}$$

$$\begin{aligned} \phi_4 &= \frac{(\epsilon_{cb} - \epsilon_c^t)}{h} = \frac{(132 + 187)}{34} \times 10^{-6} \\ &= +9.38 \times 10^{-6} \text{ rad./in.} \end{aligned}$$

**5. Cracked Section Stage,  $\epsilon_c = 0.001$  in./in.**

From before,  $\epsilon_{pe} = 6,359 \times 10^{-6} = 0.0064$  in./in. By trial and adjustment, assume a neutral axis depth  $c = 1.5$  in. below the top fibers of the flange. Then  $\Delta\epsilon_{ps}$  is the additional strain in bonded prestressing strands due to  $\epsilon_c = 0.001$  in./in. at the top fibers, and from similar triangles in Figure 7.15,

$$\Delta\epsilon_{ps} = \frac{(30.25 - 1.5)}{1.5} \times 0.001 = 0.0192 \text{ in./in.}$$

So the total  $\epsilon_{ps} = 0.0192 + 0.0064 = 0.0256$  in./in.

From the stress-diagram of the prestressing steel in Figure 7.11, the corresponding stress is

$$f_{ps} \cong 260,000 \text{ psi}$$

and

$$A_{ps} = 16 \times 0.153 = 2.448 \text{ in.}^2$$

Thus, the tensile force  $T_p = 260,000 \times 2.448 = 636,480$  lb.

From Figure 7.12,  $f_c = 3,000$  psi corresponds to  $\epsilon_c = 0.001$  in./in. The compressive force is then  $C_c = (12 \times 12 \times 1.5)3000 = 648,000 > T = 636,480$  lb.

Hence, the neutral axis depth should be reduced.

**Second Trial**

Assume  $c_c = 1.45$  in. Then

$$\Delta\epsilon_{ps} = \frac{(30.25 - 1.45)}{1.45} \times 0.001 = 0.0199 \text{ in./in.}$$

and

$$\text{Total } \epsilon_{ps} = 0.0199 + 0.0064 = 0.0263 \text{ in./in.}$$

From Figure 7.12,  $f_{ps} \cong 255,000$  psi,  $T_p = 255,000 \times 2.448 = 624,240$  lb., and  $C_c = (12 \times 12 \times 1.45)3000 = 624,400$  lb  $\cong T_p$ . Hence, assumed  $c = 1.45$  in., O.K.

$$a = 0.80 \quad c = 1.16 \text{ in.}$$

$$\text{Moment } M_n = 624,240 \left( 30.25 - \frac{1.16}{2} \right) = 18.9 \times 10^6 \text{ in.-lb}$$



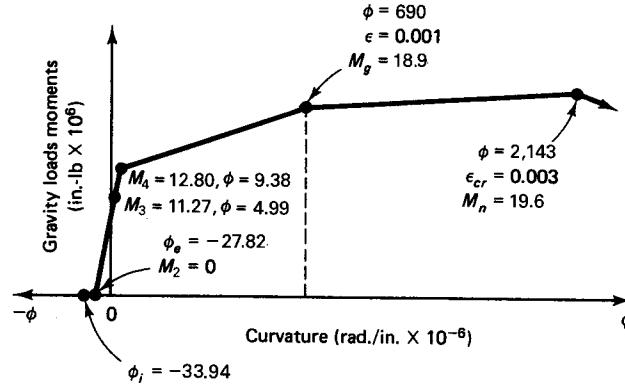


Figure 7.16 Moment-curvature diagram of Example 7.6.

and from Equation 7.5 d,

$$\phi_u = \frac{\epsilon_u}{c} = \frac{0.001}{1.45} = 690 \times 10^{-6} \text{ rad/in.}$$

6. Fully Cracked Section Stage,  $\epsilon_c = 0.003$  in./in. (Ultimate Load)  
 $\epsilon_c = 0.003$  in./in. is the maximum unit strain allowed by the ACI Code at ultimate load. Assume  $f_{ps} = 263,000$  psi. Then

$$a = \frac{A_{ps} f_{ps}}{0.85 f'_c b} = \frac{2.448 \times 263,000}{0.85 \times 5,000 \times 144} = 1.1 \text{ in.}$$

$$c = \frac{a}{\beta_1} = \frac{1.1}{0.80} = 1.38 \text{ in.}$$

From Figure 7.15,

$$\epsilon_{ps} = \frac{30.25 - 1.38}{1.38} \times 0.003 = 0.0628 \text{ in./in.}$$

$$\text{Total } \epsilon_{ps} = 0.0628 + 0.0064 = 0.0692 \text{ in./in.}$$

From the stress diagram in Figure 7.12,  $f_{ps} \cong f_{pu} = 270,000$  psi. So use  $a \cong 1.1$  in., giving

$$\begin{aligned} M_n &= A_{ps} f_{ps} \left( d_p - \frac{a}{2} \right) = 2.448 \times 270,000 \left( 30.25 - \frac{1.1}{2} \right) \\ &= 19.6 \times 10^6 \text{ in.-lb} \end{aligned}$$

Use  $c \cong 1.4$  in.

$$\phi_u = \frac{\epsilon_u}{c} = \frac{0.003}{1.4} = 2,143 \times 10^{-6} \text{ rad/in.}$$

A schematic plot of the moment-curvature diagram is shown in Figure 7.16. The load-deflection diagram has the same form and can be inferred from the moment-curvature diagram.

## 7.7 LONG-TERM EFFECTS ON DEFLECTION AND CAMBER

### 7.7.1 PCI Multipliers Method

The ACI Code provides the following equation for estimating the time-dependent factor for deflection of nonprestressed concrete members:

$$\lambda = \frac{\xi}{1 + 50\rho'} \quad (7.16)$$

where  $\xi$  = time-dependent factor for sustained load  
 $\rho'$  = compressive reinforcement ratio  
 $\lambda$  = multiplier for *additional* long-term deflection

In a similar manner, the PCI multipliers method provides a multiplier  $C_1$  which takes account of long-term effects in prestressed concrete members,  $C_1$  differs from  $\lambda$  in Equation 7.16, because the determination of long-term cambers and deflections in prestressed members is more complex due to the following factors:

1. The long-term effect of the prestressing force and the prestress losses.
2. The increase in strength of the concrete after release of prestress due to losses.
3. The camber and deflection effect during erection.

Because of these factors, Equation 7.16 cannot be readily used.

Table 7.1, based on Refs. 7.8 and 7.9, can provide reasonable multipliers of immediate deflection and camber provided that the upward and downward components of the initial calculated camber are separated in order to take into account the effects of loss of prestress, *which only apply to the upward component*.

Shaikh and Branson, in Ref. 7.7, propose that substantial reduction can be achieved in long-term camber by the addition of nonprestressed steel. In that case, a reduced multiplier  $C_2$  can be used given by

$$C_2 = \frac{C_1 + A_s/A_{ps}}{1 + A_s/A_{ps}} \quad (7.17)$$

**Table 7.1**  $C_1$  Multipliers for Long-Term Camber and Deflection

	Without composite topping	With composite topping
<i>At erection:</i>		
(1) Deflection (downward) component—apply to the elastic deflection due to the member weight at release of prestress	1.85	1.85
(2) Camber (upward) component—apply to the elastic camber due to prestress at the time of release of prestress	1.80	1.80
<i>Final:</i>		
(3) Deflection (downward) component—apply to the elastic deflection due to the member weight at release of prestress	2.70	2.40
(4) Camber (upward) component—apply to the elastic camber due to prestress at the time of release of prestress	2.45	2.20
(5) Deflection (downward)—apply to the elastic deflection due to the superimposed dead load only	3.00	3.00
(6) Deflection (downward)—apply to the elastic deflection caused by the composite topping	—	2.30

where  $C_1$  = multiplier from Table 7.1  
 $A_s$  = area of nonprestressed reinforcement  
 $A_{ps}$  = area of prestressed strands.

### 7.7.2 Incremental Time-Steps Method

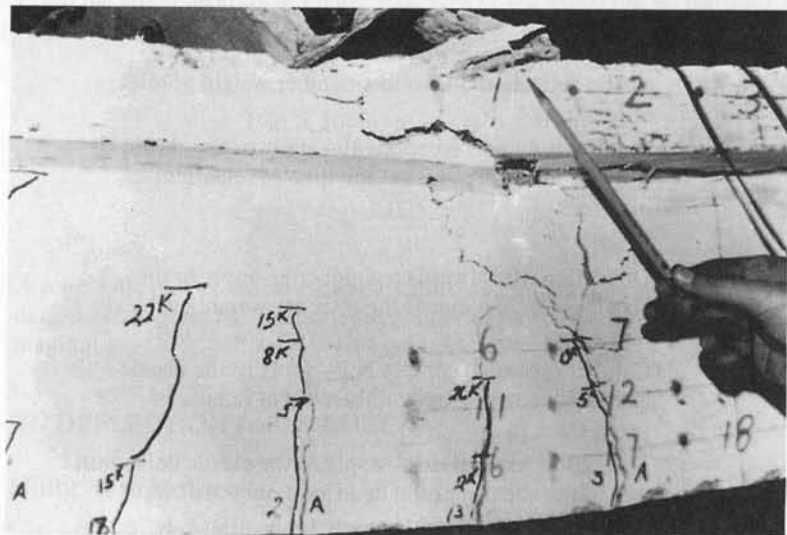
The incremental time-steps method is based on combining the computations of deflections with those of prestress losses due to time-dependent creep, shrinkage, and relaxation. The design life of the structure is divided into several time intervals selected on the basis of specific concrete strain limits, such as unit strain levels  $\epsilon_{c1} = 0.001$  and  $0.002$  in./in., and ultimate allowable strain  $\epsilon_c = 0.003$  in./in. The strain distributions, curvatures, and prestressing forces are calculated for each interval together with the incremental shrinkage, creep, and relaxation strain losses during the particular time interval. The procedure is repeated for all subsequent incremental intervals, and an integration or summation of the incremental steps is made to give the total time-dependent deflection at the particular section along the span. These calculations should be made for a sufficient number of points along the span, such as midspan and quarter-span points, to be able to determine with sufficient accuracy the form of the moment-curvature diagram.

The general expression for the total rotation at the end of a time interval can be expressed as

$$\phi_t = -\frac{P_i e_x}{E_c I_c} + \sum_0^t (P_{n-1} - P_n) \frac{e_x}{E_c I_c} - \sum_0^t (C_n - C_{n-1}) P_{n-1} \frac{e_x}{E_c I_c} \quad (7.18a)$$

where  $P_i$  = initial prestress before losses  
 $e_x$  = eccentricity of tendon at any section along the span  
 Subscript  $n - 1$  = beginning of a particular time step  
 Subscript  $n$  = end of the aforementioned time step  
 $C_{n-1}, C_n$  = creep coefficients at beginning and end, respectively, of a particular time step  
 $P_n - P_{n-1}$  = prestress loss at a particular time interval from all causes.

Obviously, this elaborate procedure is justified only in the evaluation of deflection and camber of very large-span bridge systems such as segmental bridges, where the errec-



**Photo 7.4** Prestressed I-beam at the limit state of failure load (Nawy et al.).

tion and assembly of the segments require a relatively accurate estimate of deflections. From Equation 7.18a, the total deflection at a particular section is

$$\delta_x = \phi_l k l^2 \quad (7.18b)$$

Now, suppose that the following strains from subsequent Example 7.7 are used to illustrate calculation of incremental and total rotations:

$\epsilon'_{n-1}$  = gross strain due only to prestress at the top fibers, e.g.,  $\epsilon'_c = +144 \times 10^{-6}$  in./in. (Figure 7.19)

$\epsilon'_{b,n-1}$  = gross strain due only to prestress at the bottom fibers, e.g.,  $\epsilon'_{cb} = -1010 \times 10^{-6}$  in./in. (Figure 7.19)

$\Delta\epsilon'_{CR,n}$  = gross creep incremental strain at the top fibers, e.g.,  $\Delta\epsilon'_{CRc} = +127 \times 10^{-6}$  in./in. (Figure 7.20)

$\Delta\epsilon'_{CRb,n}$  = gross creep incremental strain at the bottom fibers, e.g.,  $\Delta\epsilon'_{CRcb} = -895 \times 10^{-6}$  in./in. (Figure 7.20)

$\Delta\epsilon'_{ps,n}$  = strain reduction due to prestress loss caused by creep force  $\Delta P$ ,  $n$  (such as  $169 \times 10^{-6}$  in./in., as seen from Figure 7.20)

Then the net incremental creep strain that will result in incremental rotation  $\phi_n$  is

$$\Delta\epsilon'_{CR,net} = (\Delta\epsilon'_{CR,n} - \Delta\epsilon'_{ps,n}) \quad (7.19a)$$

for the top fibers and

$$\Delta\epsilon'_{CRb,net} = (\Delta\epsilon'_{CRb,n} - \Delta\epsilon'_{psb,n}) \quad (7.19b)$$

for the bottom fibers.

The incremental rotation is, then,

$$\Delta\phi_n = \frac{\Delta\epsilon'_{CR,net} - \Delta\epsilon'_{CRb,net}}{h} \quad (7.19c)$$

and the total rotation becomes

$$\phi_T = \phi_{n-1} + \Delta\phi_n \quad (7.20)$$

A schematic of the changes in strains and rotations from time step  $n - 1$  to time step  $n$  is shown in Figure 7.17.

The selection of the time intervals depends on the refinement level desired in the computation of cambers. For each time step, the incremental creep and shrinkage strains and relaxation loss in prestress are computed as shown in Example 7.7 to give a curvature increment  $\Delta\phi$ . Thereafter, new values of stress, strain, and curvature are obtained at the end of the time interval, adding the curvature increment  $\Delta\phi_n$  to the total curvature  $\phi_{n-1}$  at the beginning of the desired intervals, as given in Equation 7.18. Clearly, the incremental time-step procedure is lengthy and, hence, justified only in evaluation and assembly of segments requiring relatively accurate estimates of deformations.

The total camber ( $\uparrow$ ) or deflection ( $\downarrow$ ) due to the prestressing force can be obtained from Equation 7.20 as

$$\delta_T = \phi_T k l^2 \quad (7.21)$$

where  $k$  is a function of the span and geometry of the section and the prestressing tendon.

Several investigators have proposed different formats for estimating the additional time-dependent deflection  $\Delta\delta$  from the moment-curvature relationship  $\phi$  modified for creep. Both Tadros and Dilger recommend integrating the modified curvature along the beam span, while Naaman expresses the long-term deflection in terms of midspan and support curvatures at a time interval  $t$  (Refs. 7.11, 7.12, 7.13). As an example, Naaman's expression gives, for a parabolic tendon,

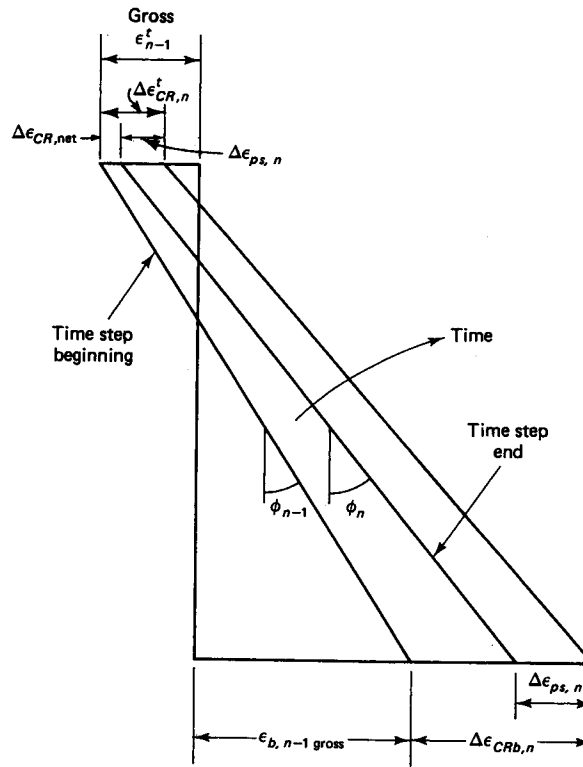


Figure 7.17 Strain changes and rotations at step  $n$ .

$$\Delta\delta(t) = \phi_1(t) \frac{l^2}{8} + [\phi_2(t) - \phi_1(t)] \frac{l^2}{48}$$

where  $\phi_1(t)$  = midspan curvature at time  $t$

$\phi_2(t)$  = support curvature at time  $t$

in which

$$\phi(t) = \frac{M}{E_{ce}(t)I_c}$$

where  $E_{ce}(t)$  = time adjusted modulus

$$= \frac{E_c(t_1)}{1 + KC_c(t)}$$

in which  $E_c(t_1)$  = modulus of concrete at start of interval

$C_c(t)$  = creep coefficient at end of time interval.

### 7.7.3 Approximate Time-Steps Method

The approximate time-steps method is based on a simplified form of summation of constituent deflections due to the various time-dependent factors. If  $C_u$  is the long-term creep coefficient, the curvature at effective prestress  $P_e$  can be defined as

$$\phi_e = \frac{P_i e_x}{E_c I_c} + (P_i - P_e) \frac{e_x}{E_c I_c} - \left( \frac{P_i + P_e}{2} \right) \frac{e_x}{E_c I_c} C_u \quad (7.22)$$

The final deflection under  $P_e$  is

$$\delta_{et} = -\delta_i + (\delta_i - \delta_e) - \left(\frac{\delta_i + \delta_e}{2}\right)C_u \quad (7.23a)$$

or

$$\delta_{et} = -\delta_e - \left(\frac{\delta_i + \delta_e}{2}\right)C_u \quad (7.23b)$$

Adding the deflection due to self-weight  $\delta_D$  and superimposed dead load  $\delta_{SD}$ , which are affected by creep gives the final time-dependent *increase* in deflection due to prestressing and sustained loads as

$$\Delta\delta = -\delta_e - \left(\frac{\delta_i + \delta_e}{2}\right)C_u + (\delta_D + \delta_{SD})(1 + C_c) \quad (7.24a)$$

and the final total *net* deflection including live-load deflection is

$$\delta_T = -\delta_e - \left(\frac{\delta_i + \delta_e}{2}\right)C_u + (\delta_D + \delta_{SD})(1 + C_u) + \delta_L \quad (7.24b)$$

Intermediate deflections are found by substituting  $C_t$  for  $C_u$  in Equations 7.24a and b, where

$$C_t = \frac{t^{0.60}}{10 + t^{0.60}}C_u \quad (7.25)$$

in which  $t^{0.60}/(10 + t^{0.60})$  is the creep ratio  $\alpha$ .

Branson et al., in Refs. 7.5 to 7.7, proposed the following expression for predicting the time-dependent increase in deflection  $\Delta\delta$  of Equation 7.24a:

$$\Delta\delta = -\left[\eta + \frac{(1 + \eta)}{2}k_r C_t\right]\delta_{i(P)} + k_r C_t \delta_{i(D)} + K_a k_r C_t \delta_{i(SD)} \quad (7.26)$$

where  $\eta = P_e/P_i$

$C_t$  = creep coefficient at time  $t$

$K_a$  = factor corresponding to age of concrete at superimposed load application

=  $1.25t^{-0.118}$  for moist-cured concrete

=  $1.13t^{-0.095}$  for steam-cured concrete

$t$  = age, in days, at loading

$k_r = 1/(1 + A_s/A_{ps})$  when  $A_s/A_{ps} \ll 1.0$

$\cong 1$  for all practical purposes.

For the final deflection increment,  $C_u$  is used in place of  $C_t$  in Equation 7.26.

For noncomposite beams, the total deflection  $\delta_{T,t}$  becomes (Ref. 7.9)

$$\delta_{T,t} = -\delta_{pi}\left[1 - \frac{\Delta P}{P_0} + \lambda(k_r C_t)\right] + \delta_D[1 + k_r C_t] + \delta_{SD}[1 + K_a k_r C_t] + \delta_L \quad (7.27)$$

where  $\delta_p$  = deflection due to prestressing

$\Delta P$  = total loss of prestress excluding initial elastic loss

$\lambda = 1 - \Delta P/2P_0$

in which  $P_0$  = prestress force at transfer after elastic loss

=  $P_i$  less elastic loss.

For composite beams, the total deflection is

$$\begin{aligned}
\delta_T = & -\delta_{pi} \left[ 1 - \frac{\Delta P}{P_0} + K_a k_r C_u \lambda \right] + \delta_D [1 + K_a k_r C_u] \\
& + \delta_{pi} \frac{I_e}{I_{comp.}} \left[ 1 - \frac{\Delta P - \Delta P_c}{P_0} + k_r C_u (\lambda - \alpha \lambda') \right] \\
& + (1 - \alpha) k_r C_u \delta_D \frac{I_c}{I_{comp}} + \delta_D \left[ 1 + \alpha k_r C_u \frac{I_c}{I_{comp.}} \right] \\
& + \delta_{df} + \delta_L
\end{aligned} \tag{7.28}$$

where  $\lambda' = 1 - (\Delta P_c / 2P_0)$

$\Delta P_c$  = loss of prestress at time composite topping slab is cast, excluding initial elastic loss

$I_{comp.}$  = moment of inertia of composite section

$\delta_{df}$  = deflection due to differential shrinkage and creep between precast section and composite topping slab

=  $F y_{cs}^2 / 8 E_{cc} I_{comp.}$  for simply supported beams (for continuous beams, use the appropriate factor in the denominator)

$y_{cs}$  = distance from centroid of composite section to centroid of slab topping

$F$  = force resulting from differential shrinkage and creep

$E_{cc}$  = modulus of composite section

$\alpha$  = creep strain at time  $t$  divided by ultimate creep strain

=  $t^{0.60} / (10 + t^{0.60})$ .

In sum, comparing the relative rigor involved in applying the three methods of Sections 7.7.1, 7.7.2, and 7.7.3, it is important to recognize that the degree of spread can be very large. Engineering judgment has to be exercised in determining a reasonable accurate concrete modulus  $E_c$  value at the various loading stages and in achieving values of creep coefficients that are neither under- nor overestimated.

#### 7.7.4 Computer Methods for Deflection Evaluation

Several computer approaches and canned programs are available for deflection calculations. They lend themselves handily for such more refined methods as the time-step method in Section 7.7.2. Keep in mind, however, that the deflection under short and long-term loading is governed by a variety of possible conditions too numerous to be covered by a single set of rules for calculating deflections. These conditions are related to all properties of the concrete constituent materials which affect deflection, particularly long-term deflection. Hence, except in cases of very large span bridges such as cable-stayed bridges, deflection calculation procedures and methods should be viewed within a  $\pm 40$  percent variability, if not more. The material properties input to any computer program should be carefully scrutinized based on laboratory tests if large span structures are involved.

#### 7.7.5 Deflection of Composite Beams

Computing deflections for composite prestressed beams is similar to that for noncomposite sections. The process becomes more rigorous if the incremental time-steps method is used. The additional steps at the various construction stages of the precast element and the situ-cast top slab require consideration of the changes in the moments of inertia from the precast to the composite values at the appropriate stages. Moreover, the difference in the shrinkage characteristics and time-step increments due to the difference in shrinkage values of the precast section and the added concrete topping increase the rigor

of the computational process. Fortunately, the use of computer programs facilitates speedy evaluation of camber and deflection in composite elements.

## 7.8 PERMISSIBLE LIMITS OF CALCULATED DEFLECTION

The ACI Code requires that the calculated deflection has to satisfy the serviceability requirement of maximum permissible deflection for the various structural conditions listed in Table 7.2. Note that long-term effects cause measurable increases in deflection and camber with time and result in excessive overstress in the concrete and the reinforcement, *requiring* computation of deflection and camber.

AASHTO permissible deflection requirements, shown in Table 7.3, are more rigorous because of the dynamic impact of moving loads on bridge spans.

Following is a step-by-step procedure for computing deflection:

1. Determine the properties of the concrete, including the concrete modulus  $E_c$ , concrete creep, and the shrinkage and prestress relationship at the various loading stages.
2. Choose the time increments to be used in the deflection calculations.
3. Compute the concrete fiber stresses at the top and bottom extreme fibers due to all loads.
4. Compute the initial strains  $\epsilon_{ci}$  at the top and bottom fibers and the corresponding rotations, as well as subsequent strains and rotations. Use the equations

**Table 7.2** ACI Minimum Permissible Ratios of Span ( $l$ ) to Deflection ( $\delta$ )  
( $l$  = Longer Span)

Type of member	Deflection $\delta$ to be considered	$(l/\delta)_{\min}$
Flat roofs not supporting and not attached to nonstructural elements likely to be damaged by large deflections	Immediate deflection due to live load $L$	180 <sup>a</sup>
Floors not supporting and not attached to nonstructural elements likely to be damaged by large deflections	Immediate deflection due to live load $L$	360
Roof or floor construction supporting or attached to nonstructural elements likely to be damaged by large deflections	That part of total deflection occurring after attachment of nonstructural elements; sum of long-term deflection due to all sustained loads (dead load plus any sustained portion of live load) and immediate deflection due to any additional live load <sup>b</sup>	480 <sup>c</sup>
Roof or floor construction supporting or attached to nonstructural elements not likely to be damaged by large deflections	That part of total deflection occurring after attachment of nonstructural elements; sum of long-term deflection due to all sustained loads (dead load plus any sustained portion of live load) and immediate deflection due to any additional live load <sup>b</sup>	240

<sup>a</sup>Limit not intended to safeguard against ponding. Ponding should be checked by suitably calculating deflection, including added deflections due to ponded water, and considering long-term effects of all sustained loads, camber, construction tolerances, and reliability of provisions for drainage.

<sup>b</sup>Long-term deflection has to be determined, but may be reduced by the amount of deflection calculated to occur before attachment of nonstructural elements. This reduction is made on the basis of accepted engineering data relating to time-deflection characteristics of members similar to those being considered.

<sup>c</sup>Ratio limit may be lower if adequate measures are taken to prevent damage to supported or attached elements, but should not be lower than tolerance of nonstructural elements.



**Table 7.3** AASHTO Maximum Permissible Deflection ( $l$  = Longer Span)

Type of member	Deflection considered	Maximum permissible deflection	
		Vehicular traffic only	Vehicular and pedestrian traffic
Simple or continuous spans	Instantaneous due to service live load plus impact	$\frac{l}{800}$	$\frac{l}{1000}$
Cantilever arms		$\frac{l}{300}$	$\frac{l}{375}$

$$\phi_i = \frac{\epsilon_{cbi} - \epsilon_{ci}^t}{h}$$

$$\phi_e = \frac{\epsilon_{cbe} - \epsilon_{cte}}{h}$$

$$\phi = \frac{\epsilon_c^t - \epsilon_{cb}}{h}$$

$$\phi_u = \frac{\epsilon_u}{c}$$

Also, compute the strains at the cgs line and compute the relaxation of the strands during the first time interval.

5. Compute the total change of stress in the prestressing steel due to creep, shrinkage, and relaxation acting as a force  $F$  at the cgs. Then compute the concrete fiber stresses at the cgs level due to  $F$ .
6. Add the result of step 5 to the result of step 3.
7. Repeat the same procedure for all time intervals, and add the effect of superimposed dead loads.
8. Add the deflections due to live load to get the total deflection  $\delta_T$ .
9. Verify whether the computed  $\delta_T$  is within the permissible limits. If not, change the section.

Figure 7.18 presents a flowchart for computation of deflection by the approximate time-step method.

## 7.9 LONG-TERM CAMBER AND DEFLECTION CALCULATION BY THE PCI MULTIPLIERS METHOD

### Example 7.6

Given  $f_{pi} = 189,000$  psi, evaluate the long-term camber and deflection of the bonded double T-beam in Example 7.3 by the PCI multipliers method, and verify whether the deflection values satisfy the ACI permissible limits. If the beam were to be post-tensioned, assume that  $f_{pi}$  would be equal to 189,000 psi after anchorage losses and after eliminating frictional losses by jacking from both beam ends and then re-jacking so as to maintain the net  $f_{pi} = 189,000$  psi prior to erection. Also, assume that the nonstructural elements attached to the structure will not be damaged by deflections and that live load is transient. Use  $E_c = 4.03 \times 10^6$  psi for all loads in the solution.

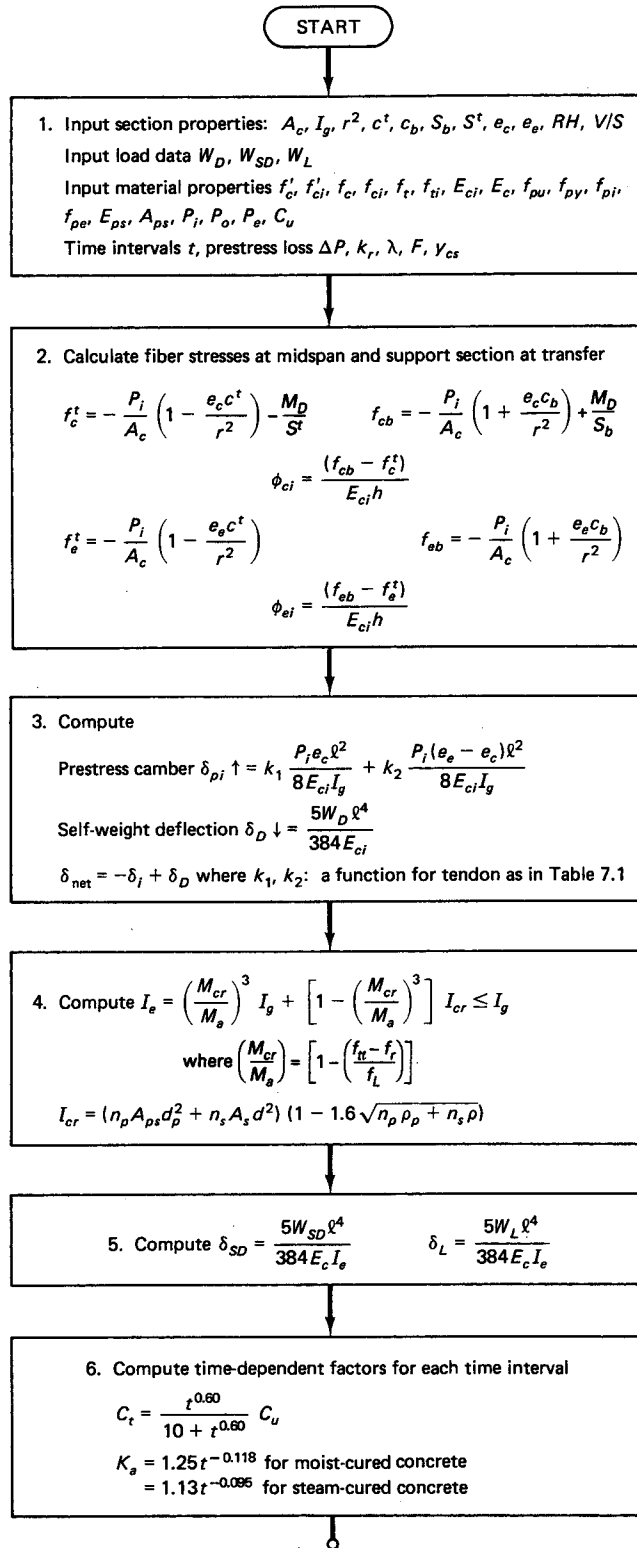


Figure 7.18 Flowchart for computation of deflection.

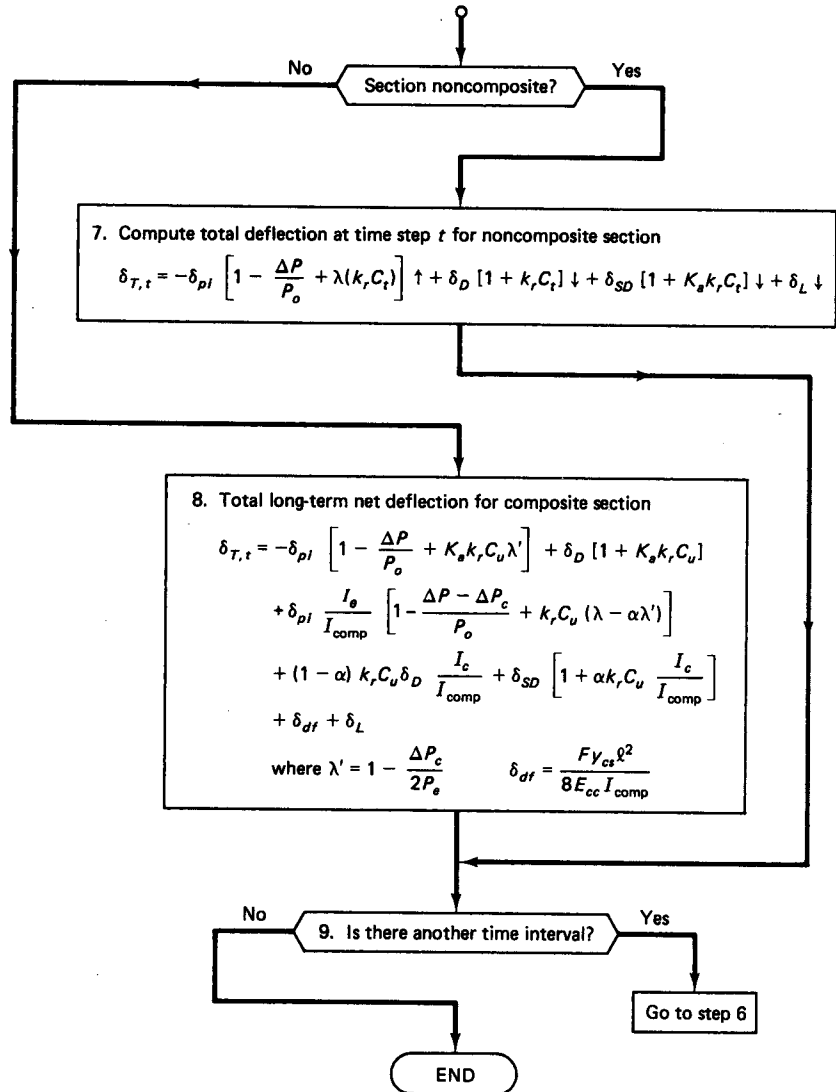


Figure 7.18 Continued

**Solution:**

$$I_g = 86,072 \text{ in.}^4$$

$$W_D = 1,019 \text{ plf} = 84.9 \text{ lb/in.}$$

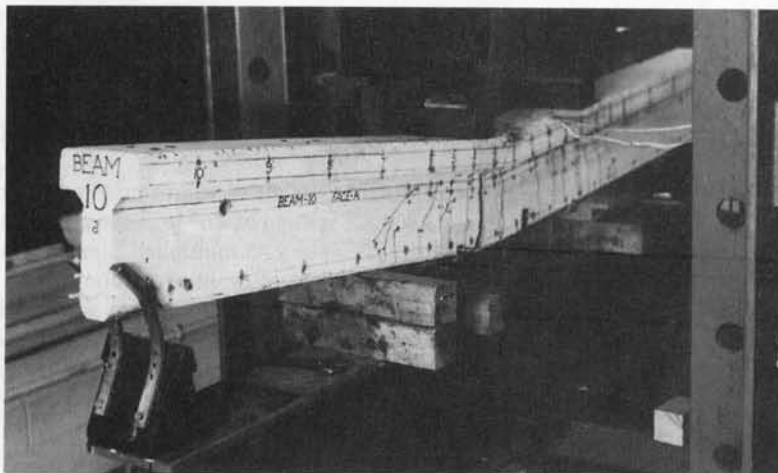
$$\delta_D = \frac{5Wl^4}{384E_c I_g} = \frac{5 \times 84.9 (60 \times 12)^4}{384 \times 3.49 \times 10^6 \times 86,072} = 0.99 \text{ in.} \downarrow (14 \text{ mm})$$

$$W_{SD} = 100 \text{ plf} = 8.3 \text{ lb/in.}$$

$$\delta_{SD} = \frac{5 \times 8.3 (60 \times 12)^4}{384 \times 4.03 \times 10^6 \times 86,072} = 0.08 \text{ in.} \downarrow (2.0 \text{ mm})$$

$$W_L = 1,100 \text{ plf} = 91.7 \text{ lb/in.}$$

the section did not crack (See Example 7.3)



**Photo 7.5** Typical deflection prior to limit state at failure (Nawy et al.).

$$I_e = I_g = 86,072 \text{ in.}^4 \text{ (max. } f_t < f_r = 530 \text{ psi)}$$

$$\delta_L = \frac{5 \times 91.7 (60 \times 12)^4}{384 \times 4.03 \times 10^6 \times 86,072} = 0.93 \text{ in. } \downarrow (24 \text{ mm})$$

If the section were cracked, the effective  $I_e$  would have had to be used instead of  $I_g$ . Using the PCI multipliers method for calculating deflection at construction erection time (30 days) and at the final service-load deflection (5 years), the following are the tabulated values of long-term deflection and camber obtained using the applicable PCI multipliers from Table 7.1. If the section is composite after erection,  $I_{\text{comp}}$  has to be used in calculating  $\delta_L$  and  $\delta_{SD}$  if the beam is shored during placement of concrete topping. If mild steel reinforcement  $A_s$  was also used in this prestressed beam, the reduced multiplier would be used. The  $C_1$  multiplier is reduced by the factor  $C_2$  where

$$C_2 = \frac{C_1 + A_s/A_{ps}}{1 + A_s/A_{ps}}$$

**Table 7.4** Long-Term Camber and Deflection Values in Example 7.6 by PCI Multipliers Method

Load	Transfer $\delta_p$	Erection $\delta_{er}$ (in.)		
		Multiplier	Multiplier (noncomposite)	Final $\delta_{net}$ (in.)
	(1)	(2)	(3)	(3)
Prestress	1.89in. $\uparrow$	1.80	3.40 in. $\uparrow$	4.63 in. $\uparrow$
$W_D$	0.99 in. $\downarrow$	1.85	1.83 in. $\downarrow$	2.67 in. $\downarrow$
Net $\delta$	0.90 in. $\uparrow$		1.57 in. $\uparrow$	1.96 in. $\uparrow$
$W_{SD}$			0.08 in. $\downarrow$	0.24 in. $\downarrow$
Net $\delta$			1.49 in. $\uparrow$	1.72 in. $\uparrow$
$W_L$				0.93 in. $\downarrow$
Final $\delta$	0.90 in. $\uparrow$		1.49 in. $\uparrow$	0.79 in. $\uparrow$

due to the mild steel reinforcement controlling propagation or widening of the flexural cracks at long-term loading, hence enhancing stiffness. As an example, assume three No. 5 bars were also used in the prestressed beam,

$$\frac{A_s}{A_{ps}} = \frac{3 \times 0.31}{2.142} = 0.43 \quad \text{giving } C_2 = 2.01$$

As an example of the adjustment of values previously tabulated, the value of the original camber becomes 3.80 in. ↑ instead of 4.63 in. ↑ shown in the table as a multiplier value of 2.01 is used instead of the previous 2.45 multiplier. Similar adjustment for all deflection components can be made applying the relevant correction factor.

From Table 7.4 the camber after erection and installation of the superimposed dead load at 30 days = 1.49 in. ↑ (38 mm). Also, the final net camber after 5 years = 0.79 in. ↑ (20 mm), the live-load deflection = 0.93 in. ↓ (24 mm), and the allowable deflection =  $l/240 = (60 \times 12)/240 = 3.0$  in. (76 mm) > 0.79 in. camber if the live load is assumed all transient in this case, which is satisfactory.

## 7.10 LONG-TERM CAMBER AND DEFLECTION CALCULATION BY THE INCREMENTAL TIME-STEPS METHOD

### Example 7.7

Solve Example 7.6 by the incremental time-steps method assuming that  $f_{pi} = 189,000$  psi and that prestress losses are incrementally evaluated at prestressing (7 days after casting), 30 days after transfer (completion of erection and application of the superimposed dead load), 90 days, and 5 years. Assume that the ultimate creep coefficient  $C_u = 2.35$  for the concrete and  $f_{py} = 230,000$  psi for the prestressing steel used in the beam. Plot the camber-time and deflection-time relationships for the beam, using  $E_c = 4.03 \times 10^6$  for all incremental steps in this solution, except at transfer, where  $f'_{ci} = 3,750$  psi. Assume the beam to be post-tensioned. Use  $E_{ps} = 27.5 \times 10^6$  psi.

### Solution:

#### *Instantaneous Stresses, Strains, and Deflections*

$$E_{ci} = 57,000\sqrt{3,750} = 3.49 \times 10^6 \text{ psi}$$

From Example 7.3 and Figure 7.9, the initial fiber stresses (psi) and strains (in./in.) for the beam at transfer due to prestress force  $P_i$  and  $P_i + W_D$  are as follows:

*Prestress Force  $P_i$*

Midspan:

$$f^t = +501 \text{ psi (3.1 MPa)}$$

$$f_b = -3,524 \text{ psi (24.3 MPa)}$$

$$\epsilon_c^t = \frac{+501}{3.49 \times 10^6} = +144 \times 10^{-6} \text{ in./in.}$$

$$\epsilon_{cb} = -1,010 \times 10^{-6} \text{ in./in.}$$

Support:

$$f^t = +92 \text{ psi (0.7 MPa)}$$

$$f_b = -2,242 \text{ psi (15.5 MPa)}$$

$$\epsilon_c^t = +26 \times 10^{-6} \text{ in./in.}$$

$$\epsilon_{cb} = -642 \times 10^{-6} \text{ in./in.}$$

Note that unless otherwise stated, the modulus  $E_c$  of concrete should be calculated for the time change at each incremental time stop.

Continuing, we have

$$\text{Midspan } \phi_{ei} = \frac{-1010 - 144}{34} \times 10^{-6} = -33.94 \times 10^{-6} \text{ rad/in.}$$

$$\text{Support } \phi_{ei} = \frac{-642 - 26}{34} \times 10^{-6} = -19.65 \times 10^{-6} \text{ rad/in.}$$

From Figure 7.6,

$$\delta_i \uparrow = \phi_c \left( \frac{l^2}{8} \right) + (\phi_e - \phi_c) \frac{l^2}{24}$$

$$\delta_i \uparrow = -33.94 \times 10^{-6} \frac{(60 \times 12)^2}{8} + (-19.65 + 33.94) \times 10^{-6} \times \frac{(60 \times 12)^2}{24}$$

$$= \frac{(60 \times 12)^2}{24} \times 10^{-6} (-33.94 \times 2 - 19.65)$$

$$= -1.89 \text{ in. } \uparrow (48 \text{ mm})$$

Notice that this value is the same as that obtained by the moment expression in Example 7.3.

Finally,

$$\text{Self-wt. } \delta_D = + \frac{5wl^4}{384E_c I_g} = \frac{5 \times \left( \frac{1019}{12} \right) (60 \times 12)^4}{384 \times 3.49 \times 10^6 \times 86,072} = +0.99 \text{ in. } \downarrow (25 \text{ mm})$$

$$\text{Net camber at transfer} = -1.89 \uparrow + 0.99 \downarrow = -0.90 \text{ in. } \uparrow (23 \text{ mm})$$

### Time Dependent Factors

(a) *Creep.* From Equation 3.10,

$$\epsilon_{CR} = \frac{C_t}{E_c} (f_{cs}) = C_1 \epsilon_{cs}$$

where  $f_{cs}$  = concrete stress at cgs level

$\epsilon_{cs}$  = concrete strain at cgs level

$\epsilon_{CR}$  = unit creep strain per unit stress at ultimate creep =  $C_u/E_c$

$$= 2.35 / 4.03 \times 10^6 = 0.583 \times 10^{-6} \text{ in./in. per unit stress.}$$

Note that creep strain has to be calculated at the centroid of the reinforcement in order to calculate the creep loss in prestress.

From Equation 3.9b, the creep coefficient at any time, in days, is

$$C_t = \frac{t^{0.60}}{10 + t^{0.60}} C_u$$

As an example, at 30 days after transfer

$$\begin{aligned} \epsilon'_{CR,t} &= \epsilon'_{CR} \left( \frac{t^{0.60}}{10 + t^{0.60}} \right) = 0.583 \times 10^{-6} \left( \frac{30^{0.60}}{10 + 30^{0.60}} \right) \\ &= 0.254 \times 10^{-6} \text{ in./in. per unit stress} \end{aligned}$$

Creep strains at other time intervals are similarly computed.

(b) *Shrinkage of Concrete.* From Equation 3.15a for moist-cured concrete,

$$\epsilon_{SH,t} = \frac{t}{t + 35} \epsilon_{SH}$$

where  $\epsilon_{SH} = 800 \times 10^{-6}$  in./in. for moist-cured concrete

Thirty days after transfer, the shrinkage time  $t = 30$  days if the beam is post-tensioned and  $t = 30 + 7 = 37$  days if it is pretensioned. Hence,

$$\epsilon_{SH,30} = \frac{30}{30 + 35} \times 800 \times 10^{-6} = 369 \times 10^{-6} \text{ in./in.}$$

In a similar manner,  $\epsilon_{SH}$  may be calculated for all other steps tabulated in Table 7.5.

(c) *Relaxation of Strands.* From Equation 3.6,

$$\frac{f_{pR}}{f_{pi}} = 1 - \left( \frac{\log t_2 - \log t_1}{10} \right) \left( \frac{f_{pi}}{f_{py}} - 0.55 \right)$$

where  $\log t$ , in hours, is to the base 10,  $f_{pi}/f_{py}$  exceeds 0.55, and  $f_{pR}$  is the remaining stress in the steel after relaxation for 30 days = 720 hr after prestressing. If the relaxation loss ratio is

$$R = 1 - \frac{f_{pR}}{f_{pi}} = \left( \frac{\log 720 - 0}{10} \right) \left( \frac{189,000}{230,000} - 0.55 \right) = 0.078$$

we must find the  $R$  values for all time-steps using  $t_1 = 0$  as a base.

Table 7.5 gives the incremental time-dependent parameters for prestress loss factors in this example for time steps 7, 30, 90, and 365 days, and 5 years after prestressing.

**Table 7.5** Time-Dependent Incremental Prestress Loss Factors in Example 7.7

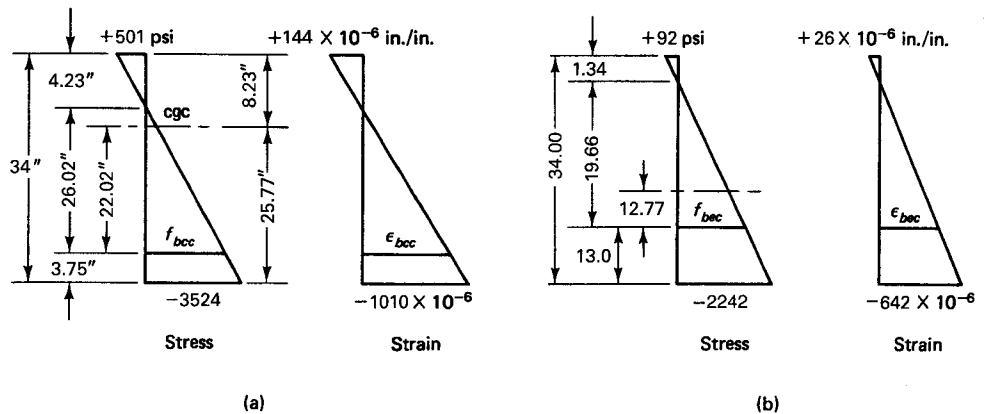
Time	Creep $\times 10^{-6}$		Shrinkage $\times 10^{-6}$		Relaxation	
Days	$\epsilon'_{CR,t}$	$\Delta\epsilon'_{CR}$	$\epsilon_{SH,t}$	$\Delta\epsilon_{SH}$	$R$	$\Delta R$
(1)	(2)	(3)	(4)	(5)	(6)	(7)
P/S (7 day)	0	—	133	133	0	—
30	0.254	0.254	369	236	0.0776	0.0776
90	0.349	0.095	576	207	0.0906	0.0130
365	0.452	0.103	730	154	0.1071	0.0165
5 yrs	0.525	0.073	785	55	0.1261	0.0190

$\Delta$  = Incremental increase. Columns 2, 4, and 6 give cumulative values.

**Transfer to Erection (Step end = 30 days)**

(a) *Concrete Fiber Stresses at the cgs Level for Calculation of Creep*

The tendon eccentricities are  $e_c = 22.02$  in. and  $e_e = 12.77$  in. Figure 7.19 gives the instantaneous stresses and the corresponding gross strains before losses due to prestress. From the figure,



**Figure 7.19** Stress and strain at transfer due only to prestress before losses in Example 7.7. (a) Midspan section. (b) Support section.

$$f_{bcc} = -3,524 \times \frac{26.02}{26.02 + 3.75} = -3,080 \text{ psi (C) (21.2 MPa)}$$

$$\epsilon_{bcc} = \frac{-3,080}{4.03 \times 10^6} = -764 \times 10^{-6} \text{ in./in.}$$

$$f_{bec} = -2,242 \times \frac{19.66}{19.66 + 13.00} = -1,350 \text{ psi (C) (9.3 MPa)}$$

$$\epsilon_{bec} = \frac{-1,350}{4.03 \times 10^6} = -335 \times 10^{-6} \text{ in./in.}$$

**Creep Incremental Strain**

$$\Delta\epsilon_{CR} = \Delta\epsilon'_{CR} \times \text{stress } f \text{ at cgs}$$

From Table 7.5  $\Delta\epsilon'_{CR} = 0.254 \times 10^{-6}$  in./in. per unit stress. So

$$\text{Midspan } \Delta\epsilon_{CR} = \Delta\epsilon'_{CR} \times f_{bcc} = 0.254 \times 10^{-6} (-3,080) = -782 \times 10^{-6} \text{ in./in.}$$

$$\text{Support } \Delta\epsilon_{CR} = \Delta\epsilon'_{CR} \times f_{bec} = 0.254 \times 10^{-6} (-1,350) = -343 \times 10^{-6} \text{ in./in.}$$

**Shrinkage Incremental Strain**

$$\Delta\epsilon_{SH} = -236 \times 10^{-6} \text{ in./in.}$$

**Relaxation Stress Loss**

$$\Delta f_{R30} = 0.0776 \times 189,000 = 14,666 \text{ psi (101.0 MPa)}$$

**Total Steel Stress Loss**

$$\Delta f_T = (\Delta\epsilon_{CR} + \Delta\epsilon_{SH})E_{ps} + \Delta f_R$$

$$\text{Midspan } \Delta f_{T30} = (782 + 236) \times 10^{-6} \times 27.5 \times 10^6 + 14,666 = 42,661 \text{ psi}$$

$$\text{Support } \Delta f_{T30} = (343 + 236) \times 10^{-6} \times 27.5 \times 10^6 + 14,666 = 30,589 \text{ psi}$$

Hence, use an average  $\Delta f_{T30} = \frac{1}{2} (42,661 + 30,589) = 36,625$  psi (253 MPa).

- (b) **Corresponding Change in Concrete Fiber Stresses and Strains** Prestress force loss  $\Delta P_{30} = \Delta f_{T30} A_{ps} = 36,625 \times 2.448 = 89,658$  lb. (399 kN)

- (i) **Midspan Section** (1 psi =  $6.895 \times 10^{-3}$  MPa)

$$\Delta f^t = -\frac{\Delta P_{30}}{A_c} \left(1 - \frac{ec_t}{r^2}\right) = -\frac{89,658}{978} \left(1 - \frac{22.02 \times 8.23}{88.0}\right)$$

$$= +97 \text{ psi (T)}$$

$$\Delta\epsilon_c^t = \frac{+97}{4.03 \times 10^6} = +24 \times 10^{-6} \text{ in./in.}$$

$$\Delta f_b = -\frac{\Delta P_{30}}{A_c} \left(1 + \frac{ec_b}{r^2}\right) = -\frac{89,658}{978} \left(1 + \frac{22.02 \times 25.77}{88.0}\right) = -683 \text{ psi (C)}$$

$$\Delta\epsilon_{cb} = \frac{-683}{4.03 \times 10^6} = -169 \times 10^{-6} \text{ in./in.}$$

- (ii) **Support Section**

$$\Delta f^t = -\frac{89,658}{978} \left(1 - \frac{12.77 \times 8.23}{88.0}\right) = +18 \text{ psi (T)}$$

$$\Delta\epsilon_c^t = \frac{+18}{4.03 \times 10^6} = +4 \times 10^{-6} \text{ in./in.}$$

$$\Delta f_b = -\frac{89,658}{978} \left(1 + \frac{12.77 \times 25.77}{88.0}\right) = -435 \text{ psi (C)}$$



$$\Delta\epsilon_{eb} = \frac{-435}{4.03 \times 10^6} = -108 \times 10^{-6} \text{ in./in.}$$

(c) *Net Strains, Resulting Curvatures, and Camber*  
*Net creep strain (in./in.)*

(i) *Fiber gross strain*  
*Midspan*

$$\Delta\epsilon'_{CRc} = f'_7 \times \Delta\epsilon'_{CR} = +501 \times 0.254 \times 10^{-6} = +127 \times 10^{-6} \text{ in./in.}$$

$$\Delta\epsilon_{CRcb} = f_{7b} \times \Delta\epsilon'_{CR} = -3,524 \times 0.254 \times 10^{-6} = -895 \times 10^{-6} \text{ in./in.}$$

*Support*

$$\Delta\epsilon'_{CRe} = +92 \times 0.254 \times 10^{-6} = +23 \times 10^{-6} \text{ in./in.}$$

$$\Delta\epsilon_{CReb} = -2,242 \times 0.254 \times 10^{-6} = -569 \times 10^{-6} \text{ in./in.}$$

*Net strains (in./in.)*

$$\Delta_{\text{net}}\epsilon_{CR} = \Delta\epsilon_{CR} - \Delta\epsilon_{ps}$$

where  $\Delta\epsilon_{ps}$  is the strain loss due to prestress loss  $\Delta f$  in part (b) of the solution. From Figure 7.20, we have the following:

*Midspan*

$$\Delta\epsilon'_{CRc,\text{net}} = \Delta\epsilon'_{CRc} - \Delta\epsilon'_{psc} = (+127 - 24)10^{-6} \text{ in./in.} = +103 \times 10^{-6}$$

$$\Delta\epsilon_{CRcb,\text{net}} = \Delta\epsilon_{CRcb} - \Delta\epsilon_{pscb} = (-895 + 169)10^{-6} \text{ in./in.} = -726 \times 10^{-6}$$

*Support*

$$\Delta\epsilon'_{CReb,\text{net}} = \Delta\epsilon'_{CRe} - \Delta\epsilon'_{pse} = (+23 - 4)10^{-6} \text{ in./in.} = +19 \times 10^{-6}$$

$$\Delta\epsilon_{CRe,\text{net}} = \Delta\epsilon_{CReb} - \Delta\epsilon_{pseb} = (-569 + 108)10^{-6} \text{ in./in.} = -461 \times 10^{-6}$$

(ii) *Curvatures (rad/in.)*

$\Delta\phi_{30}$  is the added curvature due to losses at the end of 30 days after transfer based on the adjusted net strains, in other words the curvature increment for this step.

*Midspan*

$$\Delta\phi_{c30} = \frac{\Delta\epsilon_{CRcb,\text{net}} - \Delta\epsilon'_{CRc,\text{net}}}{h} = \frac{(-726 - 103)10^{-6}}{34}$$

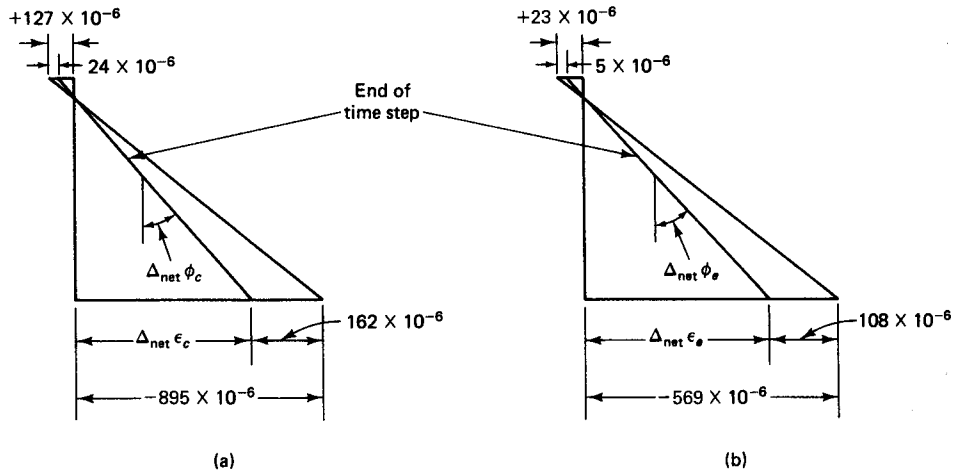


Figure 7.20 Creep incremental strains at 30 days in Example 7.7.

$$= -24.38 \times 10^{-6} \text{ rad/in. } (0.96 \times 10^{-6} \text{ rad/mm})$$

*Support*

$$\begin{aligned} \Delta\phi_{e30} &= \frac{\Delta\epsilon_{\text{CRe } b, \text{net}} - \Delta\epsilon_{\text{CRe } t, \text{net}}}{h} = \frac{(-461 - 19)10^{-6}}{34} \\ &= -14.12 \times 10^{-6} \text{ rad/in. } (0.54 \times 10^{-6} \text{ rad/mm}) \end{aligned}$$

**(iii) Total Curvature (rad/in.) and camber**

From before,  $\phi_{ci} = -33.94 \times 10^{-6}$  rad/in. and  $\phi_{ei} = -19.65 \times 10^{-6}$  rad/in. So the total curvature at 30 days after transfer is

$$\phi_T = \phi_i + \Delta\phi_{30}$$

*Midspan*

$$\phi_{Tc30} = (-33.94 - 24.38) \times 10^{-6} \text{ rad/in. } = -58.32 \times 10^{-6} (2.30 \times 10^{-6} \text{ rad/mm})$$

*Support*

$$\phi_{Te30} = (-19.65 - 14.12) \times 10^{-6} = -33.77 \times 10^{-6} (1.33 \times 10^{-6} \text{ rad/mm})$$

From Figure 7.6, the camber due to prestress at the end of 30 days for singly harped tendon beam is

$$\begin{aligned} \delta_{P30} \uparrow &= \phi_{Tc30} \left( \frac{l^2}{8} \right) + (\phi_{Te30} - \phi_{Tc30}) \frac{l^2}{24} \\ &= -58.32 \times 10^{-6} \frac{(60 \times 12)^2}{8} + (-33.77 - 58.32) 10^{-6} \times \frac{(60 \times 12)^2}{24} \end{aligned}$$

namely,

$$\begin{aligned} \delta_{30(\text{cambr.})} \uparrow &= \frac{(60 \times 12)^2}{24} (-58.32 \times 2 + 33.77) \times 10^{-6} \\ &= -3.24 \text{ in. } \uparrow (82 \text{ mm}) \end{aligned}$$

**(d) Long-term Deflections Due to Gravity Loads at 30 Days after Transfer.** Assume  $E_c = 4.03 \times 10^6$  psi as a reasonable value for the modulus of concrete for the rest of the example. We have  $W_D = 1019$  plf = 84.9 lb/in. Also,

$$\text{Self-weight deflection } \delta_D = \frac{5Wl^4}{384E_c I_g} = +0.99 \text{ in. } \downarrow (25 \text{ mm}) \text{ from before}$$

$$W_{SD} = 100 \text{ plf}$$

$$\begin{aligned} \delta_{SD} &= \frac{5 \times \frac{100}{12} (60 \times 12)^4}{384 \times 4.03 \times 10^6 \times 169,020} \\ &= +0.08 \text{ in. } \downarrow (1.5 \text{ mm}) \end{aligned}$$

$$C_t = \frac{t^{0.60}}{10 + t^{0.60}} C_u = \frac{30^{0.60}}{10 + 30^{0.60}} \times 2.35 = 1.02$$

( $C_t$  for  $W_{SD}$  at  $\sim 15$  days = 0.80)

$$\delta_{D30} = 0.99(1 + 1.02) = +2.00 \text{ in. } \downarrow (51 \text{ mm})$$

$$\delta_{SD30} = 0.08(1 + 0.80) = +0.14 \text{ in. } \downarrow (4 \text{ mm})$$

$$\delta_L = 0 \text{ (building occupied at 90 days)}$$

Total gravity load deflections = 2.00 + 0.14 + 0 = +2.14 in.  $\downarrow$  (31 mm)

$$\delta_{\text{net}30} = -3.24 \uparrow + 2.14 \downarrow = -1.10 \text{ in. } \uparrow (28 \text{ mm}) \text{ (cambr.)}$$

**Service-Load Step—90 Days after Transfer**

- (a) *New Reduced Concrete Fiber Stresses and Strains Due to Prestress Losses in the Previous Stage*

Prestressing force change =  $\Delta P_e$

- (i) *Midspan*

$$f^t = +501 - 97 = +404 \text{ psi}$$

$$f_b = -3,524 + 683 = -2,841 \text{ psi}$$

$$\epsilon_c^t = \frac{+404}{4.03 \times 10^6} = +100 \times 10^{-6} \text{ in./in.}$$

$$\epsilon_{cb} = -705 \times 10^{-6} \text{ in./in.}$$

- (ii) *Support*

$$f^t = +92 - 18 = +74 \text{ psi}$$

$$f_b = -2,242 + 435 = -1,807 \text{ psi}$$

$$\epsilon_c^t = +18 \times 10^{-6} \text{ in./in.}$$

$$\epsilon_{eb} = -448 \times 10^{-6} \text{ in./in.}$$

From Figure 7.21,

$$f_{bcc} = -2,841 \times \frac{26.02}{26.02 + 3.75} = -2,483 \text{ psi}$$

$$\epsilon_{bcc} = -616 \times 10^{-6} \text{ in./in.}$$

$$f_{bec} = -1,807 \times \frac{19.66}{19.66 + 13.0} = -1,088 \text{ psi}$$

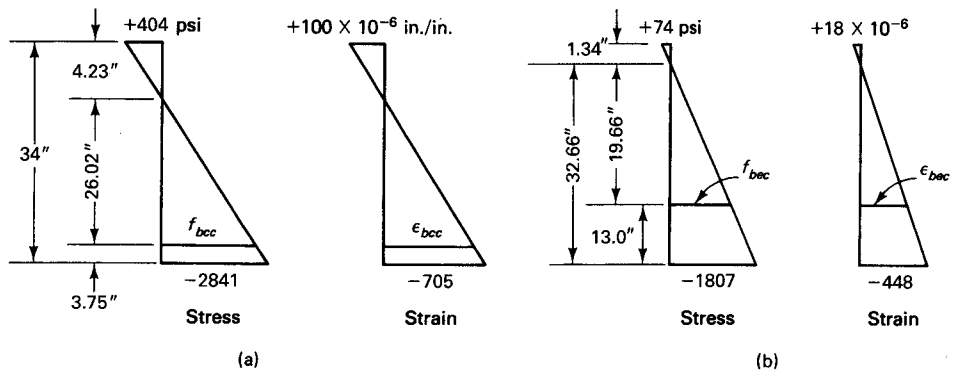
$$\epsilon_{bec} = -270 \times 10^{-6} \text{ in./in.}$$

*Creep Incremental Strain*

$$\Delta\epsilon'_{CR} = 0.095 \times 10^{-6} \text{ in./in. per unit stress (Table 7.5)}$$

$$\text{Midspan } \Delta\epsilon_{CR} = \Delta\epsilon'_{CR} f_{bcc} = 0.095 \times 10^{-6} (-2,483) = -236 \times 10^{-6} \text{ in./in.}$$

$$\text{Support } \Delta\epsilon_{CR} = \Delta\epsilon'_{CR} f_{bec} = 0.095 \times 10^{-6} (-1,088) = -103 \times 10^{-6} \text{ in./in.}$$



**Figure 7.21** Adjusted stress and strain at 30 days due to prestress only in Example 7.7. (a) Midspan section. (b) Support section.

*Shrinkage Incremental Strain*

$$\Delta\epsilon_{SH} = -207 \times 10^{-6} \text{ in./in.}$$

*Relaxation Stress Loss*

$$\Delta f_R = 0.0130(189,000 - 36,625) = 1,981 \text{ psi}$$

*Total Steel Stress Loss*

$$\Delta f_T = (\Delta\epsilon_{CR} + \Delta\epsilon_{SH})E_{ps} + \Delta f_R$$

$$\text{Midspan } \Delta f_{T90} = (236 + 207) \times 10^{-6} \times 27.5 \times 10^6 + 1,981 = 14,164 \text{ psi}$$

$$\text{Support } \Delta f_{T90} = (103 + 207) \times 10^{-6} \times 27.5 \times 10^6 + 1,981 = 10,506 \text{ psi}$$

Hence, use an average  $\Delta f_{T90} = \frac{1}{2}(14,164 + 10,506) = 12,335 \text{ psi}$

**(b) Corresponding Change in Concrete Fiber Stresses and Strains.** Prestress force loss  $\Delta P_{90} = \Delta f_{T90} A_{ps} = 12,335 \times 2.448 = 30,196 \text{ lb (134 kN)}$

**(i) Midspan Section** (1 psi =  $6.895 \times 10^{-3} \text{ MPa}$ )

$$\Delta f^t = +97 \times \frac{30,196}{89,658} = +33 \text{ psi}$$

$$\Delta f_b = -230 \text{ psi}$$

$$\Delta\epsilon_c^t = +8 \times 10^{-6} \text{ in./in.}$$

$$\Delta\epsilon_{cb} = -57 \times 10^{-6} \text{ in./in.}$$

**(ii) Support Section**

$$\Delta f^t = +6 \text{ psi}$$

$$\Delta f_b = -147 \text{ psi}$$

$$\Delta\epsilon_c^t = +2 \times 10^{-6} \text{ in./in.}$$

$$\Delta\epsilon_{cb} = -36 \times 10^{-6} \text{ in./in.}$$

**(c) Net Strains, Resulting Curvatures, and Camber**

**(i) Net creep strain (in./in.)**

*Fiber gross strain*

*Midspan*

$$\Delta\epsilon'_{CRc} = f_{30}^t \times \Delta\epsilon'_{CR} = +404 \times 0.095 \times 10^{-6} = +38 \times 10^{-6} \text{ in./in.}$$

$$\Delta\epsilon'_{CRcb} = f_{30b} \times \Delta\epsilon'_{CR} = -2,841 \times 0.095 \times 10^{-6} = -270 \times 10^{-6} \text{ in./in.}$$

*Support*

$$\Delta\epsilon'_{CRe} = +74 \times 0.095 \times 10^{-6} = +7 \times 10^{-6} \text{ in./in.}$$

$$\Delta\epsilon'_{CReb} = -1,807 \times 0.095 \times 10^{-6} = -172 \times 10^{-6} \text{ in./in.}$$

*Net strains (in./in.)*

*Midspan*

$$\Delta\epsilon'_{CRc,net} = \Delta\epsilon'_{CRc} - \Delta\epsilon'_{psc} = (+38 - 8) \times 10^{-6} = +30 \times 10^{-6}$$

$$\Delta\epsilon'_{CRcb,net} = \Delta\epsilon'_{CRcb} - \Delta\epsilon'_{psc} = (-270 + 57) \times 10^{-6} = -213 \times 10^{-6}$$

*Support*

$$\Delta\epsilon'_{CRe,net} = \Delta\epsilon'_{CRe} - \Delta\epsilon'_{pse} = (+7 - 2) \times 10^{-6} = +5 \times 10^{-6}$$

$$\Delta\epsilon'_{CReb,net} = \Delta\epsilon'_{CReb} - \Delta\epsilon'_{pseb} = (-172 + 36) \times 10^{-6} = -136 \times 10^{-6}$$

(ii) *Curvature (rad/in.)*  
*Midspan*

$$\begin{aligned}\Delta\phi_{e90} &= \frac{\Delta\epsilon_{Cr,net} - \Delta\epsilon_{cRcb,net}^t}{h} = \frac{(-213 - 30) \times 10^{-6}}{34} \\ &= -7.15 \times 10^{-6} \text{ rad/in.}\end{aligned}$$

*Support*

$$\begin{aligned}\Delta\phi_{e90} &= \frac{\Delta\epsilon_{CReb,net} - \Delta\epsilon_{CRe,net}^t}{h} = \frac{(-136 - 5)10^{-6}}{34} \\ &= -4.15 \times 10^{-6} \text{ rad/in.}\end{aligned}$$

(iii) *Total Curvature (rad/in.) and camber*

From before,  $\phi_{c30} = -58.32 \times 10^{-6}$  rad/in. and  $\phi_{e30} = -33.77 \times 10^{-6}$ . So the total curvature is

$$\phi_T = \Delta\phi_{30} + \Delta\phi_{90}$$

and we also have the following:

$$\text{Midspan } \phi_{Tc90} = (-58.32 - 7.15) \times 10^{-6} = -65.47 \times 10^{-6} \text{ (1.72 rad/mm)}$$

$$\text{Support } \phi_{Te90} = (-33.77 - 4.15) \times 10^{-6} = -37.92 \times 10^{-6} \text{ (1.04 rad/mm)}$$

$$\begin{aligned}\delta_{P90} \text{ (camber)} \uparrow &= \phi_{Tc90} \left( \frac{l^2}{8} \right) + (\phi_{Te90} - \phi_{Tc90}) \frac{l^2}{24} \\ &= -65.47 \times 10^{-6} \frac{(60 \times 12)^2}{8} + (-37.92 + 65.47) \times 10^{-6} \times \frac{(60 \times 12)^2}{24} \\ &= \frac{(60 \times 12)^2}{24} (-65.47 \times 2 + 37.92) \times 10^{-6} \\ &= -3.65 \text{ in. } \uparrow \text{ (93 mm)}\end{aligned}$$

(d) *Long-term Deflections Due to Gravity Loads at 90 Days after Transfer*

$$t = 90 \text{ days}$$

$$C_t = \frac{t^{0.60}}{10 + t^{0.60}} C_u = \frac{90^{0.60}}{10 + 90^{0.60}} \times 2.35 = 1.41$$

$$(C_t = 1.27 \text{ for } t = 60 \text{ days})$$

$$\delta_{D90} = \delta_i(1 + C_t) = 0.99(1 + 1.41) = +2.39 \text{ in. } \downarrow \text{ (51 mm)}$$

$$\delta_{SD90} = 0.08(1 + 1.27) = +0.17 \text{ in. } \downarrow$$

$$\delta_L \text{ (from Example 7.6)} = +0.93 \text{ in. } \downarrow$$

So the total deflection at 90 days due to gravity loads is

$$\delta_g = +2.39 + 0.18 + 0.93 = +3.50 \text{ in. } \downarrow \text{ (89 mm)}$$

and the net deflection is

$$\text{Net } \delta_{\text{net},90} = -3.65 \uparrow + 3.5 \downarrow = -0.51 \text{ in. } \uparrow \text{ (4 mm) (camber)}$$

**Service-Load Deflection at 5 Years**

The same steps as the previous give the results tabulated in Tables 7.6 and 7.7, while a plot of the cambers and deflections as a function of time is shown in Figure 7.22. The deflection-time relationship becomes almost asymptotic.

From Table 7.7, the final net deflection (camber) at five years is 0.87 in., which is much less than the maximum allowable deflection or camber. From Table 7.2,  $\delta_T = l/240 = 60 \times 12 /$

**Table 7.6** Long-Term Stress and Strain Changes in Example 7.7

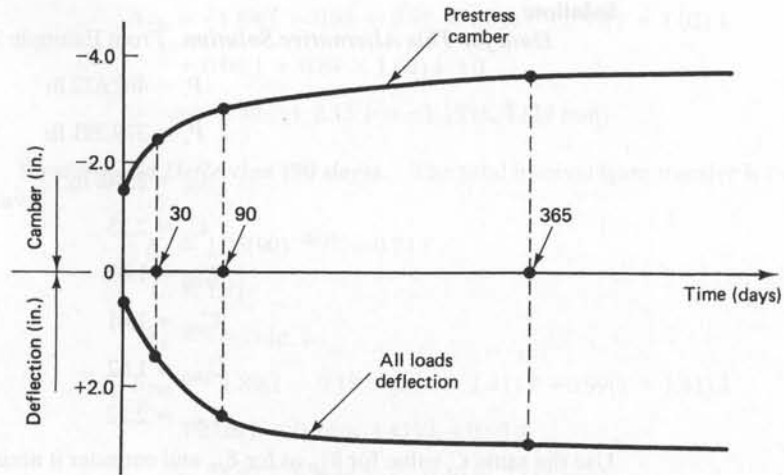
Time at step end	Gross fiber stress in concrete at start of time increment		Creep strain increment $\times 10^{-6}$ in./in. per unit stress	Shrinkage strain increment $\times 10^{-6}$ in./in.	Steel relaxation increment psi	Total steel stress loss increment psi	Concrete stress change due to losses psi		Concrete strain change due to losses $\times 10^{-6}$ in./in.		
	Midspan	End					Midspan	End	Midspan	End	
Days	$f_b$	$f_t$	$\Delta\epsilon_{CRc}$	$\Delta\epsilon_{SH}$	$\Delta f_R$	$\Delta f_{r,t}$	$\Delta f_t$	$\Delta f_b$	$\Delta\epsilon'_c$	$\Delta\epsilon'_{cb}$	$\Delta\epsilon'_e$
(1)	(2)	(3)	(4)	(5)	(6)	(7)	(8)	(9)	(10)	(11)	(11)
P/S*	0	0	0	133	—	—	—	—	—	—	—
30	+501	+92	-782	236	14,666	36,625	+97	+18	+24	+4	+4
	-3524	-2242	-343				-683	-435	-169	-108	-108
90	+404	+74	-236	207	1,981	12,335	+33	+6	+8	+2	+2
	-2841	-1807	-103				-230	-147	-57	-36	-36
365	+371	+68	-235	154	2,311	11,194	+30	+6	+7	+2	+2
	-2611	-1660	-103				-209	-133	-52	-33	-33
5 yr	+341	+62	-153	55	2,448	6,986	+19	+4	+5	+1	+1
	-2402	-1527	-67				-130	-83	-32	-21	-21

\*P/S = step at transfer of prestress at 7 days after concrete is cast; 1,000 psi = 6,895 MPa.

Table 7.7 Long-Term Curvatures and Deflections in Example 7.7

Time at step end	Net creep strain increment $\times 10^{-6}$ in./in.		Curvature increment $\times 10^{-6}$ rad/in.		Total cumulative curvature $\times 10^{-6}$ rad/in.		Deflection		
	Midspan	End	Midspan	End	Midspan	End	Prestress camber force $P$ in.	Gravity loads $W_D + W_{SD} + W_L$ in.	Net in.
Days	$\Delta \epsilon_{CR,net}^t$		$\Delta \phi_c$		$\Sigma \phi_c$		$\delta_{p,t}$	$\delta_g$	$\delta_{net,t}$
(1)	(2)	(3)	(4)	(5)	(6)	(7)	(8)	(9)	(10)
P/S*	0	0	-33.94	-19.65	-33.94	-19.65	-1.89	+0.99	-0.90↑
30	+103	+19	-24.38	-14.12	-58.92	-34.07	-3.24	+2.14	-1.14↑
90	-726	-461	-7.15	-4.15	-66.07	-38.22	-3.65	+3.50	-0.16↑
365	+38	+7	-7.29	-4.21	-73.36	-42.43	-4.09	+3.93	-0.16↑
5 yr	-270	-172	-4.79	-2.76	-78.15	45.19	-4.35	+4.26	-0.09↑
	+31	+5							
	-217	-138							
	+20	+4							
	-143	-90							

\*P/S = step at transfer of prestress at 7 days after concrete is cast; 1 in. = 25.4 mm.



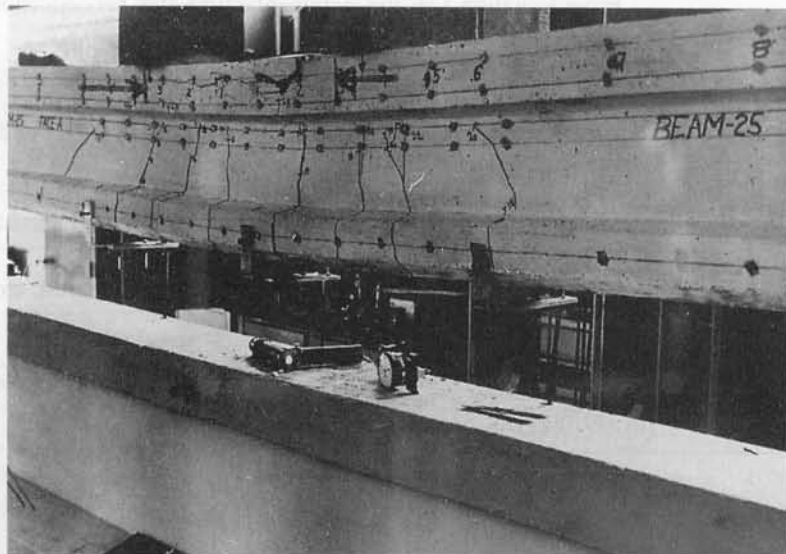
**Figure 7.22** Prestressed camber and load deflections vs. time in Example 7.7.

$240 = 3.09 \text{ in.} \gg 0.09 \text{ in.}$  Hence, the beam satisfies the serviceability requirements for time-dependent deflection. Note that long-term creep losses can be considerably reduced by the addition of nonprestressed reinforcement to the section at the compression side.

## 7.11 LONG-TERM CAMBER AND DEFLECTION CALCULATION BY THE APPROXIMATE TIME-STEPS METHOD

### Example 7.8

Solve Example 7.6 by the approximate time-steps method using the same allowable steel and concrete stresses. Compare this solution with those of Examples 7.6 and 7.7.



**Photo 7.6** Deflection at failure of prestressed T-beam with confining reinforcement (Nawy, Potyondy).



**Solution:**

**Data for This Alternative Solution.** From Example 7.7,

$$P_i = 462,672 \text{ lb}$$

$$P_e = 379,391 \text{ lb}$$

$$A_{ps} = 2.448 \text{ in.}^2$$

$$C_u = 2.35$$

$$C_{t30} = 1.02$$

$$C_{t90} = 1.41$$

$$C_{t365} = 1.82$$

$$C_{t5yr} = 2.12$$

Use the same  $C_t$  value for  $\delta_{SD}$  as for  $\delta_D$ , and consider it accurate enough. Then

$$K_a = 1.25t^{-0.118} \text{ for moist-cured concrete}$$

$$t = \text{age at loading, in days} = 30, 90, 365, 5 \text{ yr}$$

$$k_r = \frac{1}{1 + A_s/A_{ps}}$$

where  $A_s/A_{ps} \ll 1.0$  under normal conditions

Use  $k_r \cong 1$  as accurate enough for practical purposes, since usually  $A_s/A_{ps} \ll 1$ .

**Instantaneous Camber and Deflections.** From Example 7.3,

$$\delta_{i(P)} = \delta_{pi} = \text{instantaneous initial prestress camber} = -1.89 \text{ in. } \uparrow$$

$$\delta_{i(D)} = \text{instantaneous dead-load deflection} = +0.99 \text{ in. } \downarrow$$

$$\delta_{i(SD)} = \text{instantaneous superimposed dead-load deflection} = +0.08 \text{ in. } \downarrow$$

$$\delta_L = \text{live-load deflection} = +0.93 \text{ in. } \downarrow$$

From Equation 7.26, the incremental time-step *net* deflection is

$$\Delta\delta_T = -\left[\eta + \left(\frac{1 + \eta}{2}\right)k_r C_u\right]\delta_{i(P)} \uparrow + k_r C_t \delta_{i(D)} \downarrow + K_a k_r C_t \delta_{i(SD)} \downarrow$$

$\delta_p$  is the deflection (camber) due to prestressing =  $\delta_{i(P)}$  and  $\eta = P_e/P_i$ . From Equation 7.27, the total *net* deflection due to loads is

$$\delta_T = -\delta_p \left[1 - \frac{\Delta P}{P_o} + \lambda(k_r C_t)\right] \uparrow + \delta_D [1 + k_r C_t] \downarrow + \delta_{SD} [1 + K_a k_r C_t] \downarrow + \delta_L \downarrow$$

where  $\Delta P = (P_o - P_e)$  is the total loss of prestress excluding any initial elastic loss,  $\lambda = 1 - \Delta P/2P_o$ , and  $\delta_p$  and  $\eta$  are as before.

**Transfer to Erection (30 days).** Assume  $P_o \cong P_i$ . Then  $\Delta P = P_i - P_e = 462,672 - 379,391 = 83,281$  lb, and  $\Delta P/P_i = 83,281/462,672 = 0.18$ . So

$$\lambda = 1 - \frac{83,281}{2 \times 462,672} = 0.91$$

$$k_r = 1$$

$$K_a = 1.25(30)^{-0.118} = 0.84$$

$$C_t = 1.02$$

$$\begin{aligned}\delta_{730} &= -1.89(1 - 0.81 + 0.91 \times 1.02) \uparrow + 0.99(1 + 1.02) \downarrow \\ &\quad + 0.08(1 + 0.84 \times 1.02) \downarrow + 0 \\ &= -3.30 \uparrow + 2.15 \downarrow = -1.15 \text{ in. } \uparrow (29 \text{ mm})\end{aligned}$$

**Service-Load Deflection (90 days).** The total interval from transfer is  $t = 90$  days. So we have

$$\begin{aligned}K_a &= 1.25(90)^{-0.118} = 0.74 \\ C_t &= 1.41 \\ \delta_L &= +0.93 \text{ in. } \downarrow \\ \delta_{790} &= -1.89(1 - 0.18 + 0.91 \times 1.41) \uparrow + 0.99(1 + 1.41) \downarrow \\ &\quad + 0.08(1 + 0.74 \times 1.41) \downarrow + 0.93 \downarrow \\ &= -3.97 \uparrow + 3.48 \downarrow = -0.49 \text{ in. } \uparrow (12 \text{ mm})\end{aligned}$$

**Service-Load Deflection at 365 days**

$$\begin{aligned}K_a &= 1.25(365)^{-0.118} = 0.62 \\ C_t &= 1.82 \\ \delta_{7365} &= -1.89(1 - 0.18 + 0.91 \times 1.82) \uparrow + 0.99(1 + 1.82) \downarrow \\ &\quad + 0.08(1 + 0.62 \times 1.82) \downarrow + 0.93 \downarrow \\ &= -4.68 \uparrow + 3.89 \downarrow = -0.79 \text{ in. } \uparrow (20 \text{ mm})\end{aligned}$$

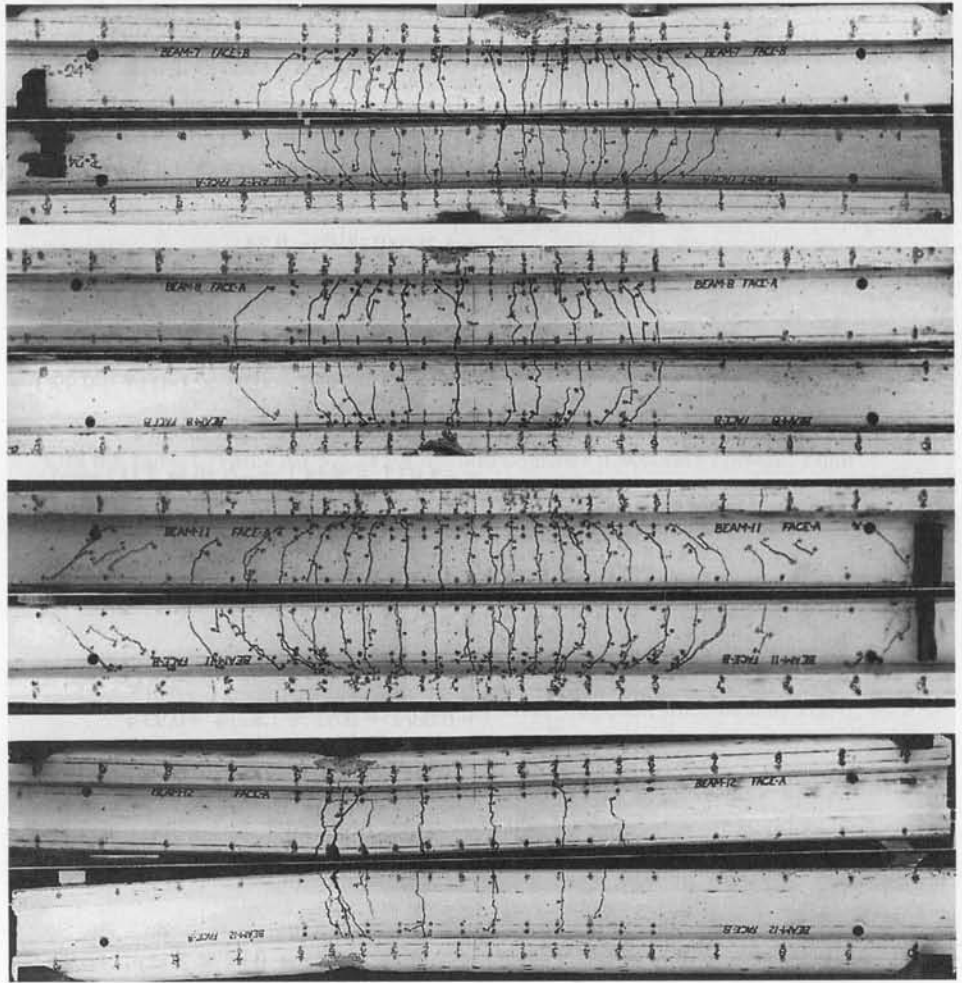
**Service-Load Deflections at 5 Years**

$$\begin{aligned}K_a &= 1.25(1,825)^{-0.118} = 0.52 \\ C_t &= 2.12 \\ \delta_{75\text{yr}} &= -1.89(1 - 0.18 + 0.91 \times 2.12) \uparrow + 0.99(1 + 2.12) \downarrow \\ &\quad + 0.08(1 + 0.52 \times 2.12) \downarrow + 0.93 \downarrow \\ &= -5.20 \uparrow + 4.19 \downarrow = -1.01 \text{ in. } \uparrow (26 \text{ mm})\end{aligned}$$

*Comparison of Deflection Calculations by the Three Methods.* Table 7.8 gives the calculated values of camber and deflection using the three methods in Examples 7.6, 7.7, and 7.8. The minus sign (-) indicates upward camber  $\uparrow$ , and the plus sign (+) indicates downward

**Table 7.8** Camber and Deflection Comparisons ( $\delta$  Inch)

Time at step end, days	Methods								
	PCI multipliers			Incremental time-step			Approximate time-step		
	Camber	$\delta_g$	$\delta_{\text{net}}$	Camber	$\delta_g$	$\delta_{\text{net}}$	Camber	$\delta_g$	$\delta_{\text{net}}$
(1)	(2)	(3)	(4)	(5)	(6)	(7)	(8)	(9)	(10)
7	-1.89	+0.99	-0.90	-1.89	+0.99	-0.90	-1.89	+0.99	-0.90
30	-3.40	+1.91	-1.49	-3.24	+2.14	-1.10	-3.30	+2.15	-1.15
90				-3.65	+3.50	-0.15	-3.97	+3.48	-0.49
365				-4.09	+3.93	-0.16	-4.68	+3.89	-0.79
5 yrs	-4.63	+3.84	-0.79	-4.35	+4.26	-0.09	-5.20	+4.19	-1.01



**Photo 7.7** Typical cracking propagation in prestressed concrete beams (Nawy et al.).

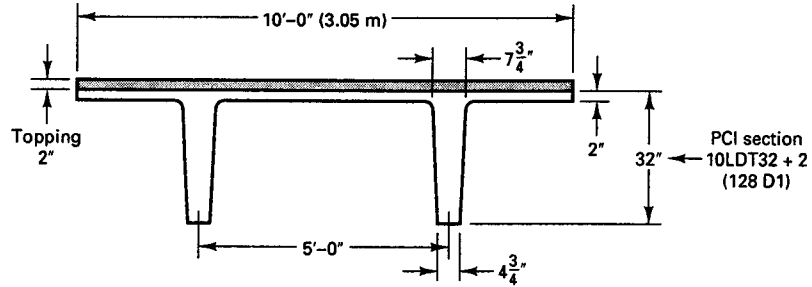
deflection  $\downarrow$ . The camber is the upward deflection due to the prestress force *less* the reduction in deflection due to self-weight.

Comparison of the net deflections shows that the multipliers method and the approximate time-steps method give essentially comparable results, while the incremental time-steps method gives slightly lower camber values (approximately  $\frac{3}{4}$ -in. difference). This variation is expected because incremental prestress losses are determined at each step rather than as a single lump-sum loss taken at the final stage. The incremental time step method is time-consuming, and use of computers is necessary to justify its use. A large number of incremental time steps need to be investigated in large-span major structures such as segmental or cable-stayed bridges where accuracy of deflection and computations of camber are of a major concern.

## 7.12 LONG-TERM DEFLECTION OF COMPOSITE DOUBLE-T CRACKED BEAM

### Example 7.9

A 72-ft (21.9 m) span simply supported roof normal weight concrete double-T-beam (Figure 7.23) is subjected to a superimposed topping load  $W_{SD} = 250$  plf (3.65 kN/m) and a service live load  $W_L = 280$  plf (4.08 kN/m). Calculate the short-term (immediate) camber and deflection of this beam by (a) the  $I_e$  method, (b) the bilinear method as well as the time-dependent



**Figure 7.23** Double-T composite beam in Example 7.9.

deflections after 2-in. topping is cast (30 days) and the final deflection (5 years), using the PCI multipliers method. Given prestress losses 18%.

	Noncomposite	Composite
$A_c$ , in. <sup>2</sup>	615 (3,968 cm <sup>2</sup> )	855 (5,516 cm <sup>2</sup> )
$I_c$ , in. <sup>4</sup>	59,720 (24.9 × 10 <sup>5</sup> cm <sup>4</sup> )	77,118 (32.1 × 10 <sup>5</sup> cm <sup>4</sup> )
$r^2$ , in. <sup>2</sup>	97 (625 cm <sup>2</sup> )	90 (580 cm <sup>2</sup> )
$c_b$ , in.	21.98 (558 mm)	24.54 (623 mm)
$c_r$ , in.	10.02 (255 mm)	9.46 (240 mm)
$S_b$ , in. <sup>3</sup>	2,717 (4.5 × 10 <sup>4</sup> cm <sup>3</sup> )	3,142 (5.1 × 10 <sup>4</sup> cm <sup>3</sup> )
$S_r$ , in. <sup>3</sup>	5,960 (9.8 × 10 <sup>4</sup> cm <sup>3</sup> )	8,152 (13.4 × 10 <sup>4</sup> cm <sup>3</sup> )
$W_d$ , plf	641 (9.34 kN/m)	891 (13.0 kN/m)

$$V/S = 615/364 = 1.69 \text{ in. (43 mm)}$$

$$RH = 75\%$$

$$e_c = 18.73 \text{ in. (476 mm)}$$

$$e_e = 12.81 \text{ in. (325 mm)}$$

$$f'_c = 5,000 \text{ psi (34.5 MPa)}$$

$$f'_{ci} = 3,750 \text{ psi (25.9 MPa)}$$

$$\text{topping } f'_c = 3,000 \text{ psi (20.7 MPa)}$$

$$f_t \text{ at bottom fibers} = 12\sqrt{f'_c} = 849 \text{ psi (5.9 MPa)}$$

$A_{ps}$  = twelve 1/2-in. dia low-relaxation prestressing steel depressed at midspan only

$$f_{pu} = 270,000 \text{ psi (1,862 MPa), low relaxation}$$

$$f_{pi} = 189,000 \text{ psi (1,303 MPa)}$$

$$f_{pj} = 200,000 \text{ psi (1,380 MPa)}$$

$$f_{py} = 260,000 \text{ psi (1,793 MPa)}$$

$$E_{ps} = 28.5 \times 10^6 \text{ psi (19.65} \times 10^4 \text{ MPa)}$$

### Solution by the $I_e$ Method

#### 1. Midspan Section Stresses

$$f_{pj} = 200,000 \text{ psi at Jacking}$$

$$f_{pi} \text{ assumed} = 0.945f_{pj} = 189,000 \text{ psi at transfer}$$

$$e_c = 18.73 \text{ in. (475 mm)}$$

$$P_i = 12 \times 0.153 \times 189,000 = 347,004 \text{ lbs (1,540 kN)}$$

## Self-Weight Moment

$$M_D = \frac{641(72)^2}{8} \times 12 = 4,984,416 \text{ in.-lb}$$

**(a) At Transfer**

From Equation 4.1a,

$$\begin{aligned} f^t &= -\frac{P_i}{A_c} \left( 1 - \frac{e_c c_t}{r^2} \right) - \frac{M_D}{S^t} \\ &= -\frac{347,004}{615} \left( 1 - \frac{18.73 \times 10.02}{97} \right) - \frac{4,984,416}{5,960} \\ &= +527.44 - 836.31 \\ &= -308.87 \text{ psi (C), say } 310 \text{ psi (C) (2.1 MPa)} < 0.60f'_{ci} = 0.60(3,750) \\ &= 2,250 \text{ psi, O.K.} \end{aligned}$$

From Equation 4.1b,

$$\begin{aligned} f_b &= -\frac{P_i}{A_c} \left( 1 + \frac{e_c c_b}{r^2} \right) + \frac{M_D}{S_b} \\ &= -\frac{347,004}{615} \left( 1 + \frac{18.73 \times 21.98}{97} \right) + \frac{4,984,416}{2,717} \\ &= -2,958.95 + 1,834.53 \\ &= -1,124.42 \text{ psi (C), say } 1,125 \text{ psi (C)} < -2,250 \text{ psi, O.K.} \end{aligned}$$

**(b) After Slab Is Cast**

At this load level assume 18 percent prestress loss

$$f_{pe} = 0.82f_{pi} = 0.82 \times 189,000 = 154,980 \text{ psi}$$

$$P_e = 12 \times 0.153 \times 154,980 = 284,543 \text{ lb}$$

For the 2-in. slab,

$$W_{SD} = \frac{2}{12} \times 10 \text{ ft} \times 150 = 250 \text{ plf (3.6 kN/m)}$$

$$M_{SD} = \frac{250(72)^2}{8} \times 12 = 1,944,000 \text{ in.-lb}$$

$$M_D + M_{SD} = 4,984,416 + 1,944,000 = 6,928,416 \text{ in.-lb (783 kN-m)}$$

From Equation 4.18a,

$$\begin{aligned} f^t &= -\frac{P_e}{A_c} \left( 1 - \frac{e_c c_t}{r^2} \right) - \frac{M_D + M_{SD}}{S^t} \\ &= -\frac{284,543}{615} \left( 1 - \frac{18.73 \times 10.02}{97} \right) - \frac{6,928,416}{5,960} \\ &= +432.5 - 1,162.5 = -730 \text{ psi (5.0 MPa)} < 0.45f'_c = -2,250 \text{ psi, O.K.} \end{aligned}$$

From Equation 4.18b,

$$\begin{aligned} f_b &= -\frac{P_e}{A_c} \left( 1 + \frac{e_c c_b}{r^2} \right) + \frac{M_D + M_{SD}}{S_b} \\ &= -\frac{284,543}{615} \left( 1 + \frac{18.73 \times 21.98}{97} \right) + \frac{6,928,416}{2,717} \end{aligned}$$

$$= -2,426.33 + 2,550.02 = +123.7 \text{ (0.85 MPa), say 124 psi (T), O.K.}$$

This is a very low tensile stress when the unshored slab is cast and before the service load is applied,  $\ll 12\sqrt{f'_c} = 849$  psi.

**(c) At Service Load for the Precast Section**

Section modulus for composite section at the top of the precast section is

$$S'_c = \frac{77,118}{9.46 - 2} = 10,337 \text{ in}^3$$

$$M_L = \frac{280(72)^2}{8} \times 12 = 2,177,288 \text{ in.-lb (246 kN-m)}$$

from Equation 4.19a,

$$f' = -\frac{P_e}{A_c} \left( 1 - \frac{e_c c_t}{r^2} \right) - \frac{M_D + M_{SD}}{S'} - \frac{M_{CSD} + M_L}{S'_c}$$

$M_{CSD}$  = superimposed dead load = 0 in this case

$$f' = -730 - \frac{2,177,288}{10,337}$$

$$= -730 - 210 = -940 \text{ psi (6.5 MPa) (C), O.K.}$$

from Equation 4.19b,

$$f_b = +123.7 + \frac{2,177,288}{3,142} = +123.7 + 693.0$$

$$= +816.7, \text{ say 817 psi (T) (5.4 MPa) } < f_t = 849 \text{ psi, O.K.}$$

**(d) Composite Slab Stresses**

Precast double-T concrete modulus is

$$E_c = 57,000\sqrt{f'_c} = 57,000\sqrt{5,000} = 4.03 \times 10^6 \text{ psi (} 2.8 \times 10^4 \text{ MPa)}$$

Situ-cast slab concrete modulus is

$$E_c = 57,000\sqrt{3,000} = 3.12 \times 10^6 \text{ psi (} 2.2 \times 10^4 \text{ MPa)}$$

Modular ratio

$$n_p = \frac{3.12 \times 10^6}{4.03 \times 10^6} = 0.77$$

$S'_c$  for 2-in. slab top fibers = 8,152 in.<sup>3</sup> from data.

$S_{cb}$  for 2-in. slab bottom fibers = 10,337 in.<sup>3</sup> from before for top of precast section.

$$\text{Stress } f'_{cs} \text{ at top slab fibers} = n \frac{M_L}{S'_c}$$

$$= -0.77 \times \frac{2,177,288}{8,152} = -207 \text{ psi (1.4 MPa) (C)}$$

Stress  $f'_{csb}$  at bottom slab fibers

$$= -0.77 \times \frac{2,177,288}{10,337} = -162 \text{ psi (1.1 MPa) (C)}$$

**2. Support Section Stresses**

Check is made at the support face (a slightly less conservative check can be made at  $50d_b$  from end).

$$e_c = 12.81 \text{ in.}$$

**(a) At Transfer**

$$\begin{aligned}
 f^t &= -\frac{347,004}{615} \left( 1 - \frac{12.81 \times 10.02}{97} \right) - 0 \\
 &= +182. \text{ psi } (T) \text{ (1.26 MPa)} \ll -2,250 \text{ psi, O.K.} \\
 f_b &= -\frac{347,004}{615} \left( 1 + \frac{12.81 \times 21.98}{97} \right) + 0 \\
 &= -2,202 \text{ psi } (C) \text{ (15.2 MPa)} < 0.60f'_{ci} = -2,250 \text{ psi, O.K.}
 \end{aligned}$$

- (b)** After slab is cast and at service load, the support section stresses both at top and bottom extreme fibers were found to be below the allowable, hence, O.K.

## Summary of Midspan Stresses (psi)

	$f^t$	$f_b$
Transfer $P_e$ only	+433	-2,426
$W_D$ at transfer	-1,163	+2,550
Net at transfer	-730	+124
External load ( $W_L$ )	-210	+693
Net total at service	-940	+817

**3. Camber and Deflection Calculation***At Transfer*

Initial

$$E_{ci} = 57,000\sqrt{3,570} = 3.49 \times 10^6 \text{ psi } (2.2 \times 10^4 \text{ MPa})$$

From before, 28 days

$$E_c = 4.03 \times 10^6 \text{ psi } (2.8 \times 10^4 \text{ MPa})$$

Due to initial prestress only, from Figure 7.6

$$\begin{aligned}
 \delta_i &= \frac{P_i e_c l^2}{8E_{ci} I_g} + \frac{P_i (e_e - e_c) l^2}{24E_{ci} I_g} \\
 &= \frac{(-347,004)(18.73)(72 \times 12)^2}{8(3.49 \times 10^6)59,720} \\
 &\quad + \frac{(-347,004)(12.81 - 18.73)(72 \times 12)^2}{24(3.49 \times 10^6)59,720} \\
 &= -2.90 + 0.30 = -2.6 \text{ in. (66 mm)} \uparrow
 \end{aligned}$$

Self-weight intensity  $w = 641/12 = 53.42 \text{ lb/in.}$ 

$$\begin{aligned}
 \text{Self-weight } \delta_D &= \frac{5wl^4}{384E_{ci} I_g} \text{ for uncracked section} \\
 &= \frac{5 \times 53.42(72 \times 12)^4}{384(3.49 \times 10^6)59,720} = 1.86 \text{ in. (47 mm)} \downarrow
 \end{aligned}$$

Thus the net camber at transfer

$$= -2.6 + 1.86 = -0.74 \text{ in. (19 mm)} \uparrow$$

## 4. Immediate Service Load Deflection

(a) Effective  $I_e$  Method

Modulus of Rupture

$$f_r = 7.5\sqrt{f'_c} = 7.5\sqrt{5,000} = 530 \text{ psi}$$

$f_b$  at service load = 817 psi (5.4 MPa) in tension (from before). Hence, the section is cracked and the effective  $I_e$  from Eqs. 3.19(a) or (b) should be used.

$$d_p = 18.73 + 10.02 + 2 \text{ (topping)} = 30.75 \text{ in. (780 mm)}$$

$$\rho_p = \frac{A_{ps}}{bd_p} = \frac{12(0.153)}{120 \times 30.75} = 4.98 \times 10^{-4}$$

From Equation 7.13,

$$I_{cr} = n_p A_{ps} d_p^2 (1 - 1.6\sqrt{n_p \rho_p})$$

$$n_p = 28.5 \times 10^6 / 4.03 \times 10^6 = 7 \text{ to be used in Equation 7.13}$$

Equation 7.13 gives  $I_{cr} = 11,110 \text{ in.}^4 (4.63 \times 10^5 \text{ cm}^4)$ , use.

From Equation 7.3a and the stress  $f_{pe}$  and  $f_d$  values already calculated for the bottom fibers at midspan with  $f_r = 7.5\sqrt{f'_c} = 530 \text{ psi}$ .

Moment  $M_{cr}$  due to that portion of live load that causes cracking is

$$\begin{aligned} M_{cr} &= S_b(7.5\sqrt{f'_c} + f_{ce} - f_d) \\ &= 3,142(530 + 2,426 - 2,550) \\ &= 1,275,652 \text{ in.-lb} \end{aligned}$$

$M_a$ , unfactored maximum live load moment = 2,177,288 in.-lb

$$\frac{M_{cr}}{M_a} = \frac{1,275,652}{2,177,288} = 0.586$$

where  $M_{cr}$  is the moment due to that portion of the *live load* that causes cracking and  $M_a$  is the maximum service *unfactored live load*.

Using the preferable PCI expression of  $(M_{cr}/M_a)$  from Equation 7.11, and the stress values previously tabulated,

$$\begin{aligned} \frac{M_{cr}}{M_a} &= 1 - \frac{f_u - f_r}{f_L} = 1 - \left( \frac{817 - 530}{693} \right) = 0.586 \\ \left( \frac{M_{cr}}{M_a} \right)^3 &= (0.586)^3 = 0.20 \end{aligned}$$

Hence, from Equation 7.10b,

$$I_e = \left( \frac{M_{cr}}{M_a} \right)^3 I_g + \left[ 1 - \left( \frac{M_{cr}}{M_a} \right)^3 \right] I_{cr} \leq I_g$$

$$\begin{aligned} I_e &= 0.2(77,118) + (1 - 0.2)11,110 \\ &= 15,424 + 8,888 = 24,312 \text{ in}^4 \end{aligned}$$

$$w_{SD} = \frac{1}{12} (891 - 641) = 20.83 \text{ lb/in.}$$

$$w_L = \frac{1}{12} \times 280 = 23.33 \text{ lb/in.}$$



$$\begin{aligned}\delta_L &= \frac{5wl^4}{384E_cI_e} = \frac{5 \times 23.33(72 \times 12)^4}{384(4.03 \times 10^6)24,312} \\ &= +1.73 \text{ in. (45 mm)} \downarrow \text{(as an average value)}\end{aligned}$$

When the concrete 2-in. topping is placed on the precast section, the resulting topping deflection with  $I_g = 59,720 \text{ in.}^4$

$$\delta_{SD} = \frac{5 \times 20.83(72 \times 12)^4}{384(4.03 \times 10^6)59,720} = +0.63 \text{ in.} \downarrow$$

#### **Solution by Bilinear Method**

$$\begin{aligned}f_{\text{net}} &= f_{cb} - 7.5\lambda\sqrt{f'_c} = 817 - 530 \\ &= +287 \text{ psi (T) causing cracking}\end{aligned}$$

$$\begin{aligned}f_L &= \text{tensile stress caused by live load alone} \\ &= +693 \text{ psi (T)}\end{aligned}$$

$w_{L1}$  = Portion of live load not causing cracking

$$\begin{aligned}&= (f_L - f_{\text{net}}) \frac{w_L}{f_L} = \frac{693 - 287}{693} \times 280 \text{ plf} \\ &= 0.586 \times 280 = 164.1 \text{ plf} = 13.68 \text{ lb/in.}\end{aligned}$$

$\delta_{L1}$  due to uncracked  $I_g$

$$\begin{aligned}\delta_{L1} &= \frac{5w_{L1}l^4}{384E_cI_g} = \frac{5 \times 13.68(72 \times 12)^4}{384(4.03 \times 10^6)77,118} \\ &= 0.32 \text{ in.} \downarrow\end{aligned}$$

$$w_{L2} = w_L - w_{L1} = \frac{1}{12} (280 - 164.1) = 9.66 \text{ lb/in.}$$

$\delta_{L2}$  due to cracked  $I_{cr}$

$$\begin{aligned}\delta_{cr} &= \frac{5w_{L2}l^4}{384E_cI_{cr}} = \frac{5 \times 9.66(72 \times 12)^4}{384(4.03 \times 10^6)11,110} \\ &= 1.57 \text{ in.} \downarrow\end{aligned}$$

Total live-load deflection prior to prestress losses

$$= \delta_{L1} + \delta_{cr} = 0.32 + 1.57 = 1.89 \text{ in.} \downarrow$$

versus 1.73 in.  $\downarrow$  obtained by the  $I_e$  method.

From before,  $\delta_i = -0.74 \uparrow$

Net short-term deflection prior to prestress loss is

$$\delta_{\text{Total}} = -0.74 + 1.89 = 1.15 \text{ in.} \downarrow$$

#### **5. Long-term Deflection (Camber) by PCI Multipliers**

When the 2-in. concrete topping is placed on the precast section, the resulting topping deflection with  $I_g = 59,720 \text{ in.}^4$  is

$$\delta_{SD} = \frac{5 \times 20.83(72 \times 12)^4}{384(4.03 \times 10^6)59,720} = +0.63 \text{ in. (16 mm)}$$

Using PCI multipliers at slab topping completion stage (30 days) and at the final service load (5 years), the following are the tabulated deflection values:

Load	Transfer $\delta_p$ in.	PCI Multipliers	$\delta_{30}$ in.	PCI Multiplier (Composite)	$\delta_{\text{Final}}$ in.
	(1)		(2)		(3)
Prestress	-2.60	1.80	-4.68	2.20	-5.71 ↑
$w_D$	+1.86	1.85	+3.44	2.40	+4.46 ↓
	-0.74 ↑		-1.24 ↑		-1.25 ↑
$w_{SD}$			+0.63 ↓	2.30	+1.45 ↓
$w_L$			+1.89 ↓		+1.89 ↓
Final $\delta$	-0.74 ↑		+1.28 ↓		+2.09 ↓

Hence, final deflection  $\approx 2.1$  in. (53 mm) ↓

$$\text{Allowable deflection} = \text{span}/180 = \frac{72 \times 12}{180} = 4.8 \text{ in.} > 2.1 \text{ in., O.K.}$$

## 7.13 CRACKING BEHAVIOR AND CRACK CONTROL IN PRESTRESSED BEAMS

### 7.13.1 Introduction

The increased use of partial prestressing, allowing limited tensile stresses in the concrete under service-load and overload conditions while allowing nonprestressed steel to carry the tensile stresses, is becoming prevalent due to practicality and economy. Consequently, an evaluation of the flexural crack widths and spacing and control of their development become essential. Work in this area is relatively limited because of the various factors affecting crack width development in prestressed concrete. However, experimental investigations support the hypothesis that the major controlling parameter is the reinforcement stress change beyond the decompression stage. Nawy, et al., have undertaken extensive research since the 1960s on the cracking behavior of prestressed pretensioned and post-tensioned beams and slabs because of the great vulnerability of the highly stressed prestressing steel to corrosion and other environmental effects and the resulting premature loss of prestress (Refs. 7.13–7.17). Serviceability behavior under service and overload conditions can be controlled by the design engineer through the application of the criteria presented in this section.

### 7.13.2 Mathematical Model Formulation for Serviceability Evaluation

**Crack Spacing.** Primary cracks form in the region of maximum bending moment when the external load reaches the cracking load. As loading is increased, additional cracks will form and the number of cracks will be stabilized when the stress in the concrete no longer exceeds its tensile strength at further locations regardless of load increase. This condition essentially produces the absolute minimum crack spacing that can occur at high steel stresses, here termed *stabilized minimum crack spacing*. The maximum possible crack spacing under this stabilized condition is twice the minimum and is termed the *stabilized maximum crack spacing*. Hence, the stabilized mean crack spacing  $a_{cs}$  is the mean value of the two extremes.

The total tensile force  $T$  transferred from the steel to the concrete over the stabilized mean crack spacing can be defined as

$$T = \gamma a_{cs} \mu \Sigma o \quad (7.29)$$

where  $\gamma$  is a factor reflecting the distribution of bond stress,  $\mu$  is the maximum bond stress which is a function of  $\sqrt{f'_c}$ , and  $\Sigma o$  is the sum of the reinforcing elements' circum-

ferences. The resistance  $R$  of the concrete area in tension,  $A_t$ , can be defined (see Figure 7.24) as

$$R = A_t f'_t \quad (7.30)$$

By equating Equations 7.29 and 7.30, the following expression for  $a_{cs}$  is obtained, where  $c$  is a constant to be developed from the tests:

$$a_{cs} = c \frac{A_t f'_t}{\Sigma o \sqrt{f'_c}} \quad (7.31)$$

From extensive tests (see Refs. 7.13, 7.14, and 7.15),  $cf'_t/\sqrt{f'_c}$  is found to have an average value of 1.2 for pretensioned, and 1.54 for post-tensioned prestressed beams.

**Crack Width.** If  $\Delta f_s$  is the net stress in the prestressed tendon or the magnitude of the tensile stress in the normal steel at any crack width load level in which the decompression load (decompression here means  $f_c = 0$  at the level of the reinforcing steel) is taken as the reference point, then for the prestressed tendon

$$\Delta f_s = f_{nt} - f_d \text{ ksi } (= 1,000 \text{ psi}) \quad (7.32)$$

where  $f_{nt}$  is the stress in the prestressing steel at any load level beyond the decompression load and  $f_d$  is the stress in the prestressing steel corresponding to the decompression load.

The unit strain  $\epsilon_s = \Delta f_s / E_s$ . Because it is logical to disregard as insignificant the unit strains in the concrete due to the effects of temperature, shrinkage, and elastic shortening, the maximum crack width can be defined as

$$w_{\max} = k a_{cs} \epsilon_s^\alpha \quad (7.33)$$

or

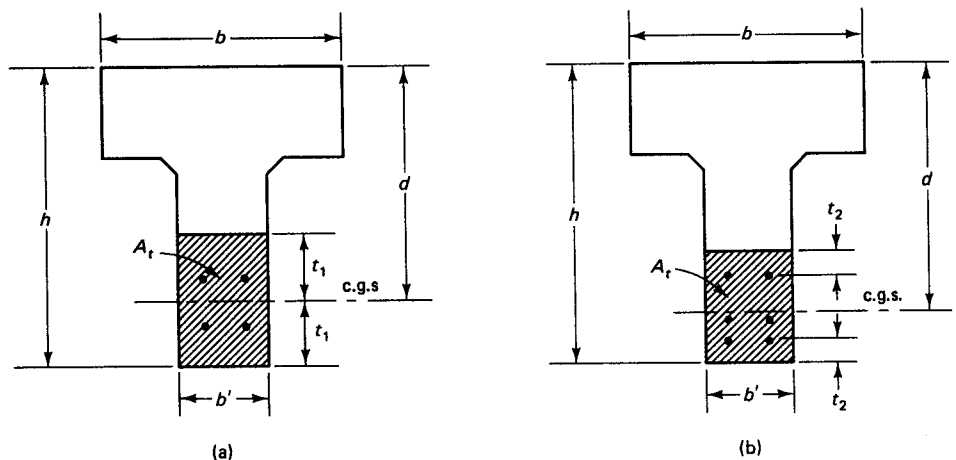
$$w_{\max} = k' a_{cs} (\Delta f_s)^\alpha \quad (7.34)$$

where  $k$  and  $\alpha$  are constants to be established by tests.

### 7.13.3 Expressions for Pretensioned Beams

Equation 7.34 is rewritten in terms of  $\Delta f_s$  so that the following expression at the reinforcement level is obtained based on large numbers of tests:

$$w_{\max} = 1.4 \times 10^{-5} a_{cs} (\Delta f_s)^{1.31} \quad (7.35)$$



**Figure 7.24** Effective concrete area in tension. (a) For even distribution of reinforcement in concrete. (b) For noneven distribution of reinforcement in concrete.

A 40-percent band of scatter envelops all the data for the expression in Equation 7.35 for  $\Delta f_s = 20$  to 80 ksi.

Linearizing Equation 7.35 for easier use by the design engineer leads to the simplified expression

$$w_{\max} = 5.85 \times 10^{-5} \frac{A_t}{\Sigma o} (\Delta f_s) \quad (7.36a)$$

of maximum crack width at the reinforcing steel level, and a maximum crack width (in.) at the tensile face of the concrete of

$$w'_{\max} = 5.85 \times 10^{-5} R_i \frac{A_t}{\Sigma o} (\Delta f_s) \quad (7.36b)$$

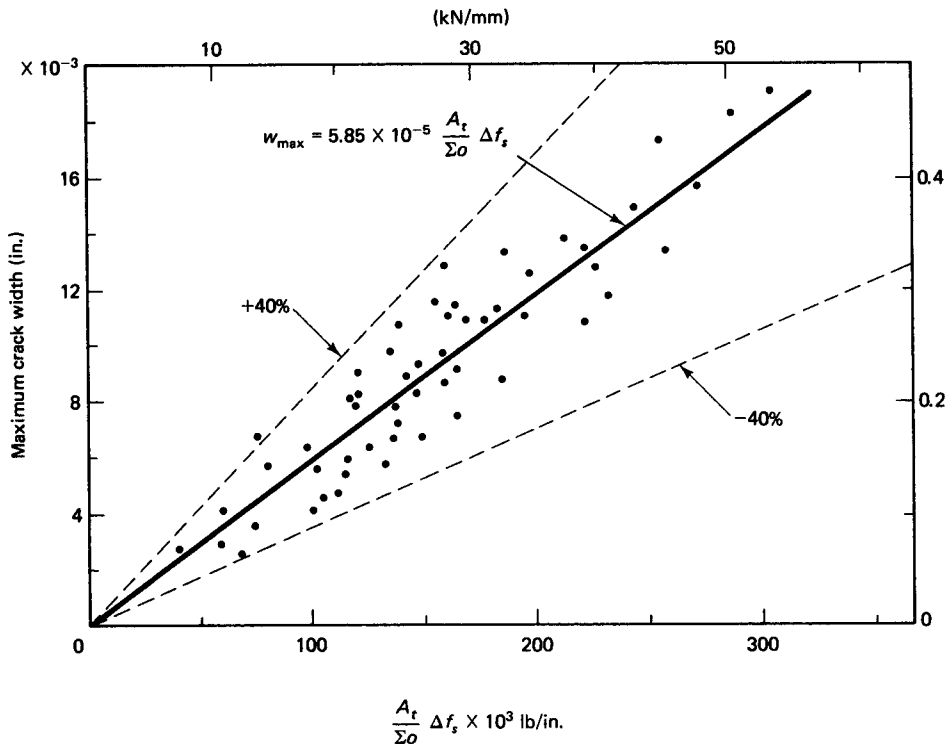
where  $R_i$  is the ratio of distance from neutral axis to tension face to the distance from neutral axis to centroid of reinforcement.

A plot of the data and the best-fit expression for Equation 7.36a is given in Figure 7.25 with a 40-percent spread, which is reasonable in view of the randomness of crack development and the linearization of the original expression (Equation 7.35).

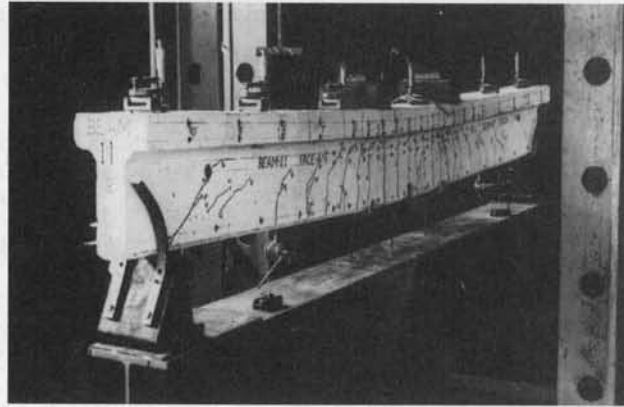
#### 7.13.4 Expressions for Post-Tensioned Beams

The expression developed for the crack width in post-tensioned bonded beams which contain mild steel reinforcement is

$$w_{\max} = 6.51 \times 10^{-5} \frac{A_t}{\Sigma o} (\Delta f_s) \quad (7.37a)$$



**Figure 7.25** Linearized maximum crack width versus  $(A_t/\Sigma o)\Delta f_s$ , pretensioned beams.



**Photo 7.8** Flexural cracking propagation in pretensioned prestressed T-beam (Nawy et al.).

for the width at the reinforcement level closest to the tensile face, and

$$w'_{\max} = 6.51 \times 10^{-5} R_i \frac{A_t}{\Sigma o} (\Delta f_s) \quad (7.37b)$$

at the tensile face of the concrete lower fibers.

For nonbonded beams, the factor 6.51 in Equations 7.37a and 7.37b becomes 6.83. Figure 7.26 gives a regression plot of Equation 7.37a that shows a scatter band of  $\pm 40$  percent, which is not unexpected in flexural cracking behavior. The crack spacing stabilizes itself beyond an incremental stress  $\Delta f_s$  of 30,000 psi to 35,000 psi, as shown in Figure 7.27, depending on the *total* reinforcement percent  $\rho_T$  of both the prestressed and the nonprestressed steel.

Recent work by Nawy et al., on the cracking performance of high strength prestressed concrete beams, both pretensioned and post-tensioned has shown that the factor 5.85 in Equation 7.36a is considerably reduced. For concrete strengths in the range of 9,000 to 14,000 psi (60 to 100 MPa), this factor reduces to 2.75, so that the expression for the maximum crack width at the reinforcement level (inch) becomes

$$w_{\max} = 2.75 \times 10^{-5} \frac{A_t}{\Sigma o} (\Delta f_s) \quad (7.38a)$$

In SI units, the expression is

$$w_{\max} = 4.0 \times 10^{-5} \frac{A_t}{\Sigma o} (\Delta f_s) \quad (7.38b)$$

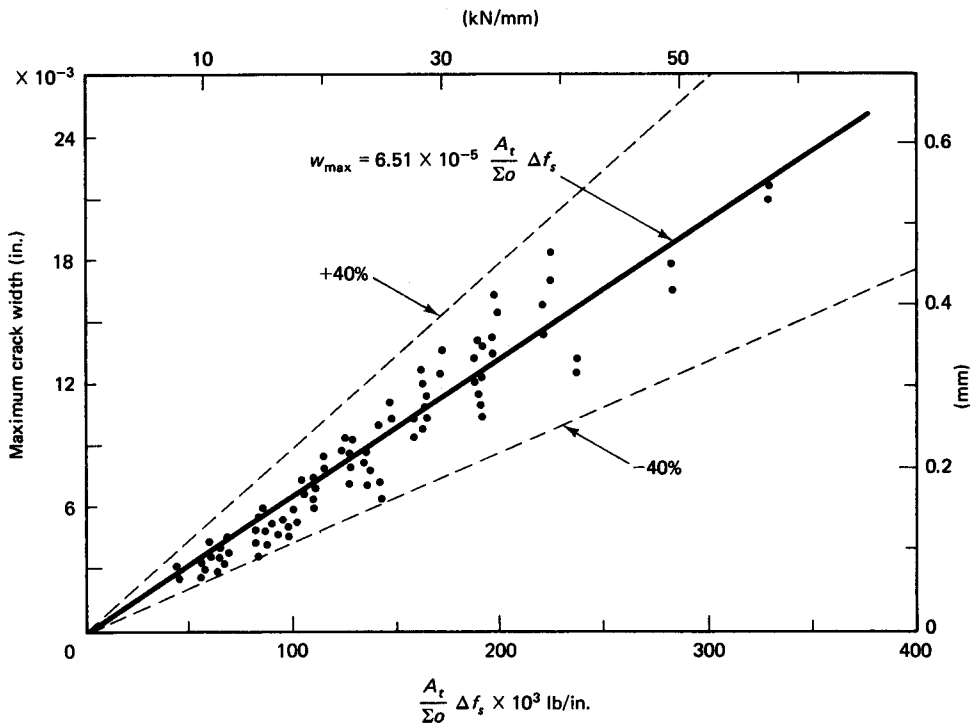
where  $A_t$ ,  $\text{cm}^2$ ;  $\Sigma o$ , cm;  $\Delta f_s$ , MPa.

For more refined values in cases where the concrete cylinder compressive strength ranges between 6,000 psi and 12,000 psi or higher, a modifying factor for particular  $f'_c$  values can be obtained from the following expressions:

$$\lambda_r = \frac{2}{\left(0.75 + 0.06\sqrt{f'_c}\right)\sqrt{f'_c}} \quad (7.39a)$$

For post-tensioned beams, the reduction multiplier  $\lambda_0$  is

$$\lambda_0 = \frac{1}{0.75 + 0.06\sqrt{f'_c}} \quad (7.39b)$$

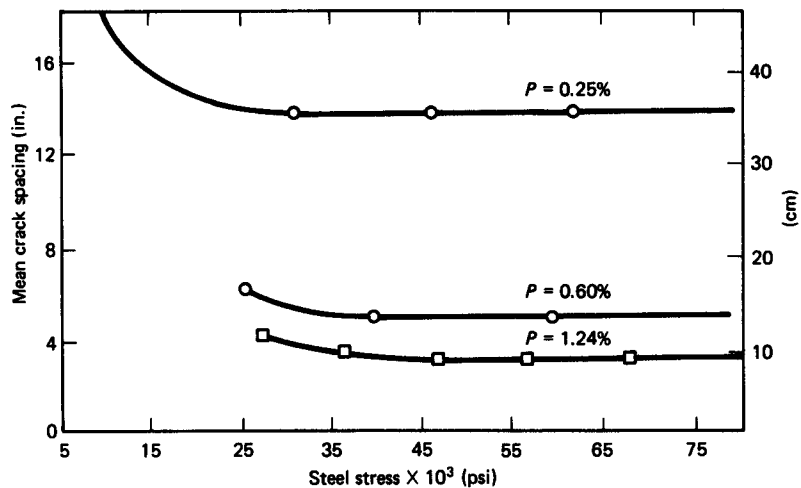


**Figure 7.26** Linearized maximum crack width versus  $(A_t/\Sigma\sigma_o)\Delta f_s$ , post-tensioned beams.

where  $f'_c$  and the reinforcement stress are in ksi.

### 7.13.5 ACI New Code Provisions

The provisions used for crack control in reinforced concrete through bar spacing is extended to prestressed concrete bonded beams, on the assumption of the desirability of a “seamless transition” between serviceability requirements for non-prestressed members



**Figure 7.27** Reinforcement percentage effect on the relationship between crack spacing and incremental reinforcement stress.

and fully prestressed members. The mechanism of crack generation differs in the prestressed beam from that in reinforced concrete due to initially imposed precompression. Also, effects of environmental conditions are considerably more serious in the case of prestressed concrete elements due to the corrosion risks to the tendons. These provisions stipulate that the spacing of the bonded tendons should not exceed 2/3 of the maximum spacing permitted for non-prestressed reinforcement. The expression for prestressed members becomes

$$s = 10 \left( \frac{40,000}{f_s} \right) - 2.5 c_c \quad (7.40)$$

but not to exceed  $8(40,000/\Delta f_s)$ .

In SI units, the expression becomes

$$s = 250 \left( \frac{280}{f_y} \right) - 2.5 c_c \quad (7.41)$$

but not to exceed  $200(280/\Delta f_s)$ , where  $\Delta f_s$  is in MPa and  $c_c$  is in mm units.

$\Delta f_s$  = difference between the stress computed in the prestressing tendon at service load based on cracked section analysis, and the decompression stress  $f_{dc}$  in the prestressing tendon. The code permits using the effective prestress  $f_{pe}$  in lieu of  $f_{dc}$ , ksi. A limit  $\Delta f_s = 36$  ksi, and no check needed if  $\Delta f_s$  is less than 20 ksi.

$c_c$  = clear cover from the nearest surface in tension to the flexural tension reinforcement, in.

While the code follows the author's definition of  $\Delta f_s$  given in Section 7.13.2 (Refs. 7.15, 7.17, 7.18, 7.26), Equations 7.40 and 7.41 still lack the practicability of use as a crack control measure and the 2/3 factor used to change the multiplier 15 to 10 in Eq. 7.40 and correspondingly in Eq. 7.41 for maximum tolerable spacing, is arbitrary and not substantiated by test results. It should be emphasized that beams have finite web widths. Such spacing provisions as presented in the Code are essentially unworkable, since actual spacing of the tendons in almost all practical cases is *less* than the code equation limits, hence almost all beams satisfy the code, though cracking levels may be detrimental in bridge decks, liquid containment vessels and other prestressed concrete structures in severe environment or subject to overload. They require additional mild steel reinforcement to control the crack width. Therefore, the expressions presented in Sections 7.13.3 and 7.13.4 in conjunction with Table 7.9 from ACI 224 Report (Refs. 7.3, 7.18), should be used for safe mitigation of cracking in prestressed concrete members.

### 7.13.6 Long-Term Effects on Crack-Width Development

Limited studies on crack-width development and increase with time show that both sustained and cyclic loadings increase the amount of microcracking in the concrete. Also, microcracks formed at service-load levels in partially prestressed beams do not seem to have a recognizable effect on the strength or serviceability of the concrete element. Macroscopic cracks, however, do have a detrimental effect, particularly in terms of corrosion of the reinforcement and appearance. Hence, an increase of crack width due to sustained loading significantly affects the durability of the prestressed member regardless of whether prestressing is circular, such as in tanks, or linear, such as in beams. Information obtained from sustained load tests of up to two years and fatigue tests of up to one million cycles indicates that a *doubling* of crack width with time can be expected. Therefore, engineering judgment has to be exercised as regards the extent of tolerable crack width under long-term loading conditions.

**Table 7.9** Maximum Tolerable Flexural Crack Widths

Exposure condition	Crack width	
	in.	mm
Dry air or protective membrane	0.016	0.41
Humidity, moist air, soil	0.012	0.30
De-icing chemicals	0.007	0.18
Seawater and seawater spray; wetting and drying	0.006	0.15
Water-retaining structures (excluding nonpressure pipes)	0.004	0.10

### 7.13.7 Tolerable Crack Widths

The maximum crack width that a structural element should tolerate depends on the particular function of the element and the environmental conditions to which the structure is liable to be subjected. Table 7.9 from the ACI Committee 224 report on cracking serves as a reasonable guide on the acceptable crack widths in concrete structures under the various environmental conditions encountered.

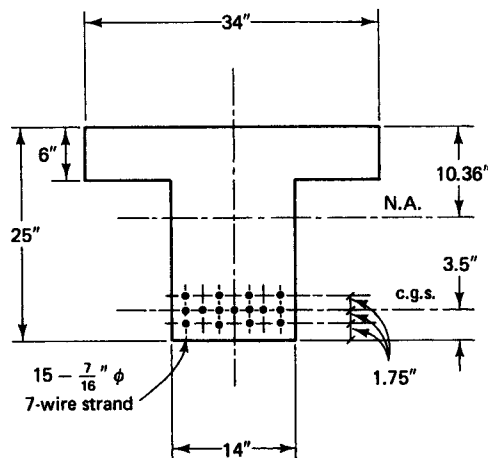
## 7.14 CRACK WIDTH AND SPACING EVALUATION IN PRETENSIONED T-BEAM WITHOUT MILD STEEL

### Example 7.10

A pretensioned prestressed concrete beam has a T-section as shown in Figure 7.28. It is prestressed with fifteen  $\frac{7}{16}$ -in. dia 7-wire strand 270-K grade. The locations of the neutral axis and center of gravity of steel are shown in the figure.  $f'_c = 5,000$  psi,  $E_c = 57,000\sqrt{f'_c}$ , and  $E_s = 28 \times 10^6$  psi. Find the mean stabilized crack spacing and the crack widths at the steel level as well as at the tensile face of the beam at  $\Delta f_s = 30 \times 10^3$  psi. Assume that no failure in shear or bond takes place.

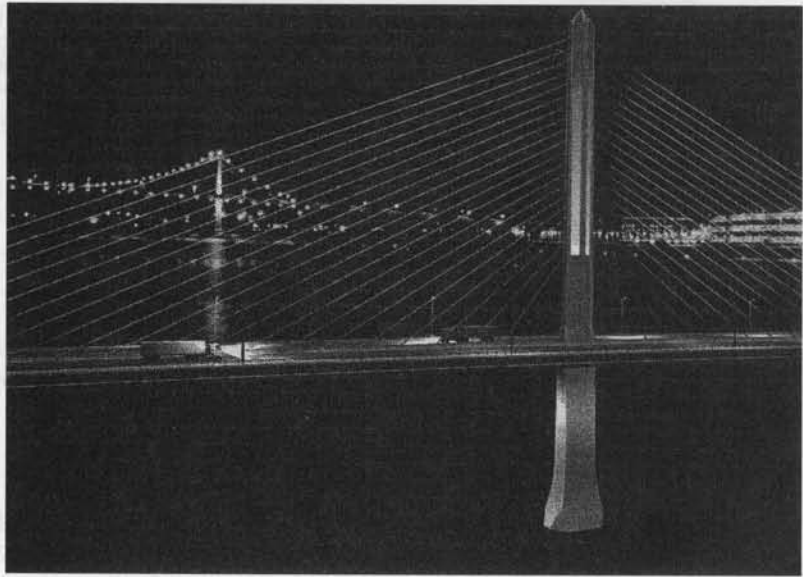
### Solution:

$$\Delta f_s = 30,000 \text{ psi} = 30 \text{ ksi}$$



**Figure 7.28** Beam cross section in Example 7.10.





**Photo 7.9** New Maumee River Cable-Stayed Bridge, Toledo, Ohio night rendering. The design includes a unique single pylon clad with glass emitting LED arrays at night, single plane of stays, and a main span of 612 feet in both direction. Courtesy of the designer, the Figg Engineering Group of Tallahassee, Florida (see Photo 1.18 also)

#### *Mean Stabilized Crack Spacing*

$$A_t = 7 \times 14 = 98 \text{ sq in.}$$

$$\Sigma o = 15\pi D = 15\pi \left( \frac{7}{16} \right) = 20.62 \text{ in.}$$

$$a_{cs} = 1.2 \left( \frac{A_t}{\Sigma o} \right) = 1.2 \left( \frac{98}{20.62} \right) = 5.7 \text{ in. (145 mm)}$$

#### *Maximum Crack Width at Steel Level*

$$\begin{aligned} w_{\max} &= 5.85 \times 10^{-5} \left( \frac{A_t}{\Sigma o} \right) \Delta f_s = 5.85 \times 10^{-5} \left( \frac{98}{20.62} \right) 30 \\ &= 834.1 \times 10^{-5} \text{ in.} \cong 0.0083 \text{ in. (0.21 mm)} \end{aligned}$$

#### *Maximum Crack Width at Tensile Face of Beam*

$$R_i = \frac{25 - 10.36}{25 - 10.36 - 3.5} = 1.31$$

$$w'_{\max} = w_{\max} R_i = 0.0083 \times 1.31 = 0.011 \text{ in. (0.28 mm)}$$

## 7.15 CRACK WIDTH AND SPACING EVALUATION IN PRETENSIONED T-BEAM CONTAINING NONPRESTRESSED STEEL

### **Example 7.11**

The beam in Example 7.10 also contains three #6 nonprestressed mild steel bars as shown in Figure 7.29. Find the crack spacing and width for an incremental steel stress  $\Delta f_s = 30,000 \text{ psi} = 30 \text{ ksi (207 MPa)}$

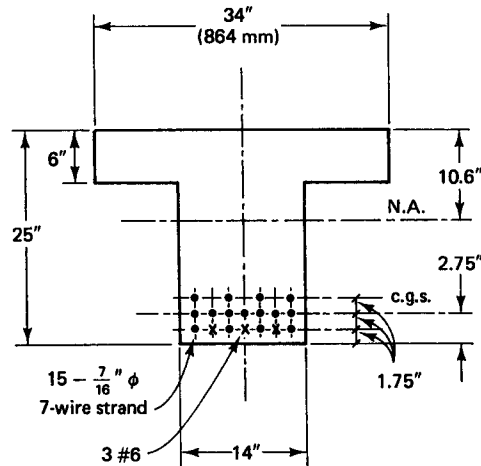


Figure 7.29 Beam cross section in Example 7.11.

**Solution:**

**Mean Stabilized Crack Spacing**

$$A_t = 14(3 \times 1.75 + \frac{1}{2} \times \frac{7}{16} + 1\frac{3}{8}) = 14 \times 6.84 = 95.8 \text{ in.}^2$$

$$\Sigma o = 20.62 + 3 \times 2.36 = 27.70 \text{ in.}$$

$$a_{cs} = 1.2 \left( \frac{A_t}{\Sigma o} \right) = 1.2 \left( \frac{95.8}{27.7} \right) = 4.15 \text{ in. (105 mm)}$$

**Maximum Crack Width at Steel Level**

$$\begin{aligned} w_{\max} &= 5.85 \times 10^{-5} \left( \frac{A_t}{\Sigma o} \right) \Delta f_s = 5.85 \times 10^{-5} \left( \frac{95.8}{27.7} \right) 30 \\ &= 606.9 \times 10^{-5} \cong 0.0061 \text{ in. (0.15 mm)} \end{aligned}$$

**Maximum Crack Width at Tensile Face of Beam**

$$R_i = \frac{25 - 10.6}{25 - 10.6 - 2.75} = 1.24$$

$$w'_{\max} = w_{\max} R_i = 0.0061 \times 1.24 = 0.007 \text{ in. (0.18 mm)}$$

## 7.16 CRACK WIDTH AND SPACING EVALUATION IN PRETENSIONED I-BEAM CONTAINING NONPRESTRESSED MILD STEEL

**Example 7.12**

A pretensioned prestressed concrete I-beam has the geometry shown in Figure 7.30. It is prestressed with twenty  $\frac{7}{16}$ -in. dia 7-wire 270-K grade low-relaxation strands and four #7 mild steel bars having yield strength  $f_y = 60,000$  psi. Find the mean stabilized crack spacing and the crack widths at the steel level as well as at the tensile face of the beam at incremental steel stress  $\Delta f_s = 20,000$  psi (138 MPa). Assume that no failure in shear or bond takes place, and check whether the crack widths that develop satisfy the crack control criteria for deicing chemicals.

**Solution:**  $\Delta f_s = 20,000$  psi = 20 ksi (138 MPa)

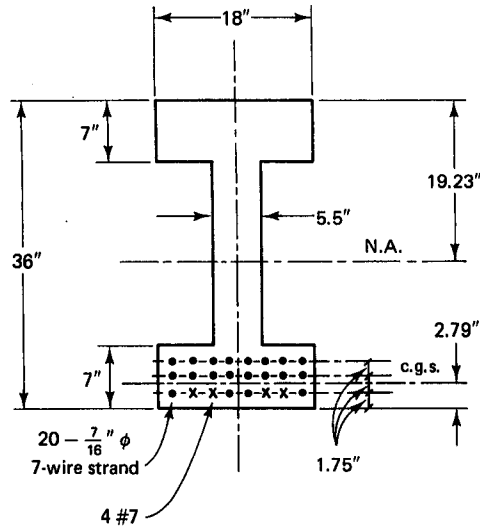


Figure 7.30 Beam cross section in Example 7.12.

#### Mean Stabilized Crack Spacing

$$A_t = 18 \times \left( 3 \times 1.75 + \frac{1}{2} \times \frac{7}{16} + 1 \frac{5}{16} \right) = 122.06 \text{ in.}^2$$

$$\Sigma o = 20\pi D + 4 \times 2.75 = 20\pi \times \frac{7}{16} + 4 \times 2.75 = 38.49 \text{ in.}$$

$$a_{cs} = 1.2 \left( \frac{A_t}{\Sigma o} \right) = 1.2 \left( \frac{122.06}{38.49} \right) = 3.8 \text{ in. (97 mm)}$$

#### Maximum Crack Width at Steel Level

$$\begin{aligned} w_{\max} &= 5.85 \times 10^{-5} \left( \frac{A_t}{\Sigma o} \right) \Delta f_s = 5.85 \times 10^{-5} \left( \frac{122.06}{38.49} \right) 20 \\ &= 371.0 \times 10^{-5} \cong 0.0037 \text{ in. (0.1 mm)} \end{aligned}$$

#### Maximum Crack Width at Tensile Face of Beam

$$R_i = \frac{36 - 19.23}{36 - 19.23 - 2.79} = 1.2$$

$$w'_{\max} = w_{\max} R_i = 0.0037 \times 1.2 = 0.004 \text{ in. (0.1 mm)}$$

**Maximum Allowable Crack Width for Deicing.** From Table 7.9, the maximum tolerable crack width for deicing is  $W_{\max} = 0.007 > 0.004$  in. (0.1 mm). Hence, serviceability requirement is satisfied.

## 7.17 CRACK WIDTH AND SPACING EVALUATION FOR POST-TENSIONED T-BEAM CONTAINING NONPRESTRESSED STEEL

### Example 7.13

A post-tensioned prestressed concrete beam has a T-section as shown in Figure 7.31. It is prestressed with twelve  $\frac{7}{16}$ -in. dia 7-wire strands of 270-K grade and additionally reinforced with four #6 nonprestressed steel bars. The locations of the neutral axis and center of gravity

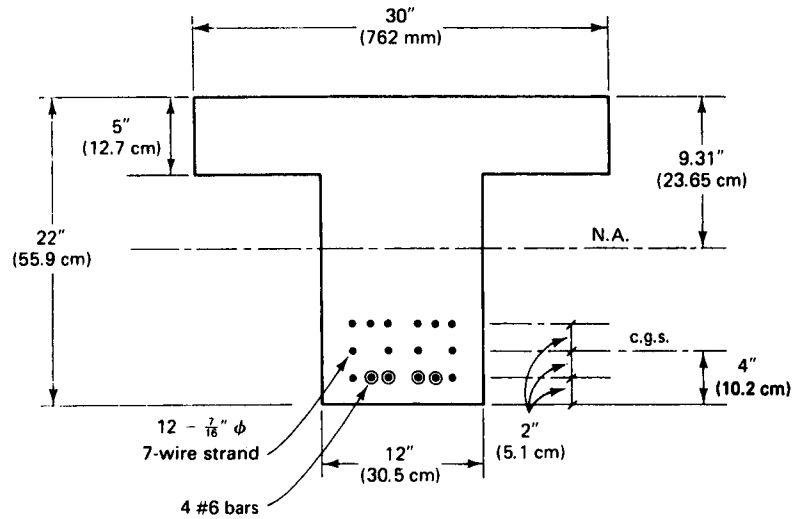


Figure 7.31 Beam cross section in Example 7.13.

of steel are shown in the figure. Assume that  $f'_c = 5,000$  psi,  $E_c = 57,000\sqrt{f'_c}$  psi, and  $E_s = 28,000$  ksi. Find the mean stabilized crack spacing and the crack widths at the steel level as well as at the tensile face of the beam at  $\Delta f_s = 30,000$  psi, assuming there is no failure in shear or bond. Then determine whether the beam satisfies the serviceability criteria for crack control for humidity and moist air.

**Solution:**

$$\Delta f_s = 30,000 \text{ psi} = 30 \text{ ksi}$$

**Mean Stabilized Crack Spacing**

$$A_t = 8 \times 12 = 96 \text{ in.}^2$$

$$\Sigma O = 12 \times \pi \times \frac{7}{16} + 4 \times 2.36 = 25.93 \text{ in.}$$

$$a_{cs} = 1.54 \frac{A_t}{\Sigma O} = 1.54 \times \frac{96}{25.93} = 5.70 \text{ in. (145 mm)}$$

**Maximum Crack Width at Steel Level**

$$\begin{aligned} w_{\max} &= 6.51 \times 10^{-5} \frac{A_t}{\Sigma O} (\Delta f_s) = 6.51 \times 10^{-5} \times \frac{96}{25.93} \times 30 \\ &= 0.0072 \text{ in. (0.18 mm)} \end{aligned}$$

**Maximum Crack Width at Tensile Face of Beam**

$$R_i = \frac{22 - 9.31}{22 - 9.31 - 4} = 1.46$$

$$w'_{\max} = w_{\max} R_i = 0.007 \times 1.46 = 0.0102 \text{ in. (0.26 mm)}$$

**Maximum Tolerable Crack Width for Humidity.** From Table 7.9, the maximum tolerable crack width for the stated humidity conditions is 0.012 in. (0.3 mm) > 0.0102 in. (0.26 mm), which is satisfactory.

## 7.18 CRACK CONTROL BY ACI CODE PROVISIONS

### Example 7.14

Solve Example 7.10 by the ACI 318 code provisions for crack control.

#### Solution:

$$\Delta f_s = 30 \text{ ksi}$$

$$c_c = 1.5 \text{ in.}$$

From Eq. 7.40,

$$s = 10 \left( \frac{40,000}{30,000} \right) - 2 \times 1.5 = 10.3 \text{ in.}$$

$$\text{Max. allowable} = 8 \left( \frac{40,000}{30,000} \right) = 10.7 \text{ in.} < 12.0 \text{ in., O.K.}$$

From this solution, it is evident that every prestressed concrete beam would satisfy the ACI code requirements for crack control regardless of the loading conditions and/or overloading, or environmental conditions. It is rare that prestressed or mild steel reinforcement would ever be spaced within a flange that can violate the code spacing requirements. Hence the code provisions are not effective, and probably rarely would they be effective for crack control even in two-way prestressed concrete plates.

## 7.19 SI DEFLECTION AND CRACKING EXPRESSIONS

$$E_c = w_c^{1.5} 0.043 \sqrt{f'_c} \text{ MPa} \quad (7.2a)$$

where  $f'_c$  is in MPa units and  $w_c$  is in  $\text{Kg/m}^3$  ranging between 1,500 to 2,500  $\text{Kg/m}^3$ .

For  $f'_c > 35 \text{ MPa}$ ,  $< 80 \text{ MPa}$

$$E_c = 3.32 \sqrt{f'_c} + 6,895 \left( \frac{w_c}{2,320} \right)^{1.5} \text{ MPa}$$

For normal-weight concrete,  $E_c = 3.32 \sqrt{f'_c} + 6,895 \text{ MPa}$

$$f_r = 0.62 \sqrt{f'_c} \quad (7.2b)$$

$$I_e = \left( \frac{M_{cr}}{M_a} \right)^3 I_g + \left[ 1 - \left( \frac{M_{cr}}{M_a} \right)^3 \right] I_{cr} \quad (7.10b)$$

$$\left( \frac{M_{cr}}{M_a} \right) = \left[ 1 - \left( \frac{f_{tl} - f_r}{f_L} \right) \right] \quad (7.11)$$

$$I_{cr} = n_p A_{ps} d_p^2 (1 - 1.6 \sqrt{n_p \rho_p}) \quad (7.13a)$$

$$I_{cr} = (n_p A_{ps} d_p^2 + n_s A_s d^2) (1 - 1.6 \sqrt{n_p \rho_p + n_s \rho}) \quad (7.13b)$$

$$\lambda = \frac{\xi}{1 + 50 \rho'} \quad (7.16)$$

Equations 7.36 and 7.37 on crack control

$$w_{\max} = \alpha_w \times 10^{-5} \frac{A_t}{\Sigma O} (\Delta f_s), \text{ millimeters}$$

where  $A_t$ ,  $\text{cm}^2$ ,  $\Sigma O$ ,  $\text{cm}$ ;  $\Delta f_s$ ,  $\text{MPa}$

$$\begin{aligned}\alpha_w &= 8.48 \times 10^{-5} \text{ for pretensioned} \\ &= 9.44 \times 10^{-5} \text{ for post-tensioned} \\ &= 4.0 \times 10^{-5} \text{ for concretes with } f'_c > 70 \text{ MPa}\end{aligned}$$

$$\text{MPa} = \text{N/mm}^2$$

$$(\text{psi}) 0.006895 = \text{MPa}$$

$$(\text{lb/ft}) 14.593 = \text{N/m}$$

$$(\text{in.-lb}) 0.113 = \text{N-m}$$

## 7.20 SI DEFLECTION CONTROL

### Example 7.15

Solve Example 7.9 for short-term deflection using the SI procedure.

*Data*

(a) Section Geometry	Noncomposite	Composite
$A_c, \text{cm}^2$	3,968	5,516
$I_c, \text{cm}^4$	$24.9 \times 10^5$	$32.2 \times 10^5$
$r^2, \text{cm}^2$	626	581
$c_b, \text{cm}$	55.8	62.3
$c_t, \text{cm}$	25.5	24.0
$e_c, \text{cm}$	47.5	
$e_e, \text{cm}$	32.5	
$S_b, \text{cm}^3$	$4.5 \times 10^4$	$5.2 \times 10^4$
$S_t, \text{cm}^3$	$9.8 \times 10^4$	$13.4 \times 10^4$
$w_D, \text{kN/m}$	9.34	13.0
$l = 21.95 \text{ m}$	topping $t = 5 \text{ cm}$	flange width $b = 3.05 \text{ m}$
$w_L = 4.09 \text{ kN/m}$		

### (b) Material properties

$$V/S = 615/364 = 0.43 \text{ cm}$$

$$RH = 75\%$$

$$f'_c = 34.5 \text{ MPa, normal weight (2,370 kg/m}^3\text{)}$$

$$f_c = 0.45f'_c = 15.5 \text{ MPa}$$

$$f'_{ci} = 25.9 \text{ MPa}$$

$$f_{ci} = 0.6 \times 25.9 = 15.5 \text{ MPa}$$

$$\text{topping } f'_c = 20.7 \text{ MPa}$$

$$f_t \text{ at bottom fibers} = \sqrt{f'_c} = 5.9 \text{ MPa at service load}$$

$$f_t \text{ allowable before unshored slab cast} = 1.4 \text{ MPa } (\frac{1}{4}\sqrt{f'_c})$$

$$A_{ps} = \text{twelve tendons, 12.7-mm diameter, low-relaxation (0.99 mm}^2\text{/tendon)}$$

$$f_{pu} = 1,860 \text{ MPa, low-relaxation}$$

$$f_{pi} = 1,300 \text{ MPa}$$

$$f_{PJ} = 1,380 \text{ MPa}$$

$$f_{py} = 1,790 \text{ MPa}$$

$$E_{ps} = 19.7 \times 10^4 \text{ MPa}$$

**Solution:****1. Midspan section stresses**

$$f_{pj} = 1,380 \text{ MPa}$$

$$f_{pi} \text{ assumed} = 0.945f_{pj} = 1,300 \text{ MPa at transfer}$$

$$e_c = 47.5 \text{ cm}$$

$$P_i = 12 \times 99 \times 1,300 \text{ MPa} = 1.54 \times 10^6 \text{ N} = 1,540 \text{ kN}$$

$$\text{self-weight moment } M_D = \frac{9,340(21.95)^2}{8} = 562,500 \text{ N-m}$$

From Equation 4.1a,

$$\begin{aligned} f^t &= -\frac{P_i}{A_c} \left( 1 - \frac{e_c c_t}{r^2} \right) - \frac{M_D}{S^t} \\ &= -\frac{1,540,000}{3,968 \times 100} \left( 1 - \frac{47.5 \times 25.5}{626} \right) - \frac{562,500}{9.8 \times 10^4} \\ &= 3.6 - 5.7 = -2.1 \text{ MPa (C)} \end{aligned}$$

From Equation 4.1b,

$$\begin{aligned} f_b &= -\frac{P_i}{A_c} \left( 1 + \frac{e_c c_b}{r^2} \right) + \frac{M_D}{S_b} \\ &= -\frac{1,540,000}{3,968 \times 100} \left( 1 + \frac{47.5 \times 55.8}{626} \right) + \frac{562,500}{4.5 \times 210^4} \\ &= -20.3 + 12.5 = -7.8 \text{ MPa (C)} < \text{allow. } 15.5 \text{ MPa, O.K.} \end{aligned}$$

**2. After unshored slab is cast**

At this load level, assume 18% prestress losses.

$$f_{pe} = 0.82f_{pi} = 0.82 \times 1,300 = 1,066 \text{ MPa}$$

$$P_e = 12 \times 99 \times 1,066 = 1,266 \text{ kN}$$

For the 5 cm topping,

$$\begin{aligned} \text{concrete weight} &= 2,370 \text{ kg/m} = 2,370 \times 9.81 \text{ N/m}^3 \\ &= 23.3 \text{ kN/m}^3 \end{aligned}$$

For 5 cm slab,  $w_{SD} = 0.05 \times 3.05 \times 23.3 = 3.6 \text{ kN/m}$

$$M_{SD} = \frac{3,600(21.95)^2}{8} = 216,800 \text{ N-m}$$

$$M_D + M_{SD} = 562,500 + 216,800 = 780,000 \text{ N-m}$$

(In Example 7.9,  $M_D + M_{SD} = 782 \text{ kN-m}$  since 2 in. topping is slightly more than 5 cm.)

For unshored case, from Equation 4.18a,

$$\begin{aligned} f^t &= -\frac{P_e}{A_c} \left( 1 - \frac{e_c c_t}{r^2} \right) - \frac{M_D + M_{SD}}{S^t} \\ &= -\frac{1,266,000}{3,968 \times 100} \left( 1 - \frac{47.5 \times 25.5}{626} \right) - \frac{780,000}{9.8 \times 10^4} \\ &= +2.96 - 7.96 = -5.0 \text{ MPa (C)} < \text{allow. } f_c = 15.5 \text{ MPa, O.K.} \end{aligned}$$

From Equation 4.18b,

$$\begin{aligned}
 f_b &= -\frac{P_e}{A_c} \left( 1 + \frac{e_c c_b}{r^2} \right) + \frac{M_D + M_{SD}}{S_b} \\
 &= -\frac{1,266,000}{3,968 \times 100} \left( 1 + \frac{47.5 \times 55.8}{626} \right) + \frac{780,000}{4.5 \times 10^4} \\
 &= -16.61 + 17.34 = 0.64 \text{ MPa (T)} < \text{allow. } f_t = 1.4 \text{ MPa, O.K.}
 \end{aligned}$$

### 3. At service load for precast section

Section modulus at top of precast section is

$$\begin{aligned}
 S'_c &= \frac{32.2 \times 10^5}{25.5 - 5.0} = 15.7 \times 10^4 \text{ cm}^3 \\
 M_L &= \frac{4,090(21.95)^2}{8} = 246,320 \text{ N-m}
 \end{aligned}$$

From Equation 4.19a,

$$f'_t = -\frac{P_e}{A_c} \left( 1 - \frac{e_c c'_t}{r^2} \right) - \frac{M_D + M_{SD}}{S'_t} - \frac{M_{CSD} + M_L}{S'_c}$$

$M_{SD}$  = superimposed dead load = 0 in this case

$$f'_t = -5.0 - \frac{246,320}{15.7 \times 10^4} = -5.0 - 1.57 = -6.57 \text{ MPa (C), O.K.}$$

From Equation 4.19b,

$$\begin{aligned}
 f_b &= +0.64 + \frac{246,320}{5.2 \times 10^4} = +0.74 + 4.74 \\
 &= +5.38 \text{ MPa (T)} \approx \text{allow. } f_t = +5.9 \text{ MPa, O.K.}
 \end{aligned}$$

### 4. Composite slab stresses

Precast double-T concrete modulus

$$\begin{aligned}
 E_c &= w_c^{1.5} 0.043 \sqrt{f'_c}, \quad w_c = 2,370 \text{ Kg/m}^3 \\
 E_c &= 2,370^{1.5} \times 0.043 \sqrt{34.5} = 2.91 \times 10^4 \text{ MPa}
 \end{aligned}$$

Situ-cast slab concrete modulus

$$E_c = 2,370^{1.5} \times 0.043 \sqrt{20.7} = 2.25 \times 10^4 \text{ MPa}$$

Modular ratio

$$n_p = \frac{2.25 \times 10^4}{2.91 \times 10^4} = 0.77$$

$S'_c$  for 5 cm slab top fiber =  $13.4 \times 10^4 \text{ cm}^3$

$S_{cb}$  for 5 cm slab bottom fiber =  $15.7 \times 10^4 \text{ cm}^3$  from before for top of precast section.

$$\text{Stress } f'_{cs} \text{ at top slab fiber} = n \frac{M_L}{S'_c} = -0.77 \times \frac{246,320}{13.4 \times 10^4} = 1.4 \text{ MPa (C)}$$

$$\text{Stress } f_{csb} \text{ at bottom slab fibers} = -0.77 \times \frac{246,320}{15.7 \times 10^4} = -1.2 \text{ MPa (C)}$$

### 5. Support section stresses

Check is made at the support face (a slightly less conservative check can be made at  $50d_b$  from end).

$$e_e = 32.5 \text{ cm}$$



At transfer

$$f^t = \frac{1,540,000}{3,968 \times 100} \left( 1 - \frac{32.5 \times 25.5}{626} \right) - 0$$

$$= -1.26 \text{ MPa (C)} < \text{allow. } f_c = 15.5 \text{ MPa, O.K.}$$

$$f_b = -\frac{1,540,000}{3,968 \times 100} \left( 1 + \frac{32.5 \times 55.8}{626} \right) + 0$$

$$= -15.2 \text{ MPa (C)} < \text{allow. } f_c = 15.5 \text{ MPa, O.K.}$$

After the unshored slab was cast and at service load, the support section stresses both at top and bottom extreme fibers were found to be below the allowable, hence O.K.

Summary of Midspan Stresses (MPa)

Load Stage	$f^t$	$f_b$
Transfer $P_e$ only	+2.96	-16.60
$w_D$ at transfer	-7.96	+17.34
Net at transfer	-5.00	+0.74
External load $w_L$	-1.57	+4.74
Net total at service	-6.57	+5.48

## 6. Short-term (immediate) deflection

### (a) Deflection at transfer

$$\text{Initial } E_{ci} = w_c^{1.5} 0.043 \sqrt{f'_c}$$

$$= (2,370)^{1.5} \times 0.043 \sqrt{25.9} = 2.52 \times 10^4 \text{ MPa}$$

from before, 28 days  $E_c = 2.80 \times 10^4 \text{ MPa}$

From Figure 7.6, deflection due to initial prestress only.

$$\delta_i = \frac{P_i e_c l^2}{8 E_{ci} I_g} + \frac{P_i (e_e - e_c) l^2}{24 E_{ci} I_g}$$

$$= 10^3 \left[ \frac{-1,540,000 \times 47.5 (21.95)^2}{8 (2.52 \times 10^4) (24.9 \times 10^5)} \right]$$

$$+ 10^3 \left[ \frac{-1,540,000 (32.5 - 47.5) (21.95)^2}{24 (2.52 \times 10^4) (24.9 \times 10^5)} \right]$$

$$= -70.2 + 7.3 = -62.9 \text{ say } 65 \text{ mm } \uparrow$$

$$\text{Self-weight } \delta_D = \frac{5 w_D l^4}{384 E_{ci} I_g}$$

$$= \frac{5 \times 9,340 (21.95)^4 \times 10^5}{384 (2.52 \times 10^4) (24.9 \times 10^5)} = 45 \text{ mm } \downarrow$$

Thus, net camber at transfer =  $-(65 - 45) = -20 \text{ mm } \uparrow$ .

### (b) Immediate service load deflection

From Equation 7.13,

$$I_{cr} = n_p A_{ps} d_p^2 (1 - 1.6 \sqrt{n_p \rho_p})$$

$$d_p = e_c + c_t + 5 \text{ cm (topping)}$$

$$= 47.5 + 25.5 + 5 = 78 \text{ cm}$$

$$A_p = 12 \times 99 = 1,188 \text{ mm}^2$$

$$\rho_p = \frac{A_p}{b d_p} = \frac{11.88 \text{ cm}^2}{305 \times 78} = 0.0047$$

$$n_p = \frac{E_{ps}}{E_c} = \frac{19.7 \times 10^4}{2.91 \times 10^4} = 6.8$$

$$I_{cr} = 6.8 \times 11.88 (78)^2 (1 - 1.6 \sqrt{6.8 \times 4.94 \times 10^{-4}})$$

$$= 4.03 \times 10^5 \text{ cm}^4$$

From Equation 7.11,

$$\frac{M_{cr}}{M_a} = 1 - \left( \frac{f_{il} - f_r}{f_L} \right)$$

$$f_r = 0.62 \sqrt{f'_c} = 0.62 \times \sqrt{3.45} = 3.64 \text{ MPa}$$

$$f_{il} = +5.48 \text{ MPa (T)} \quad f_L = +4.74 \text{ (T)}$$

$$\left( \frac{M_{cr}}{M_a} \right) = 1 - \frac{(5.48 - 3.64)}{4.74} = 0.6$$

$$\left( \frac{M_{cr}}{M_a} \right)^3 = 0.216$$

from Equation 7.10b,

$$I_e = \left( \frac{M_{cr}}{M_a} \right) I_g + \left[ 1 - \left( \frac{M_{cr}}{M_a} \right)^3 \right] I_{cr} \leq I_g$$

$$= 0.216 (24.9 \times 10^5) + (1 - 0.216) (4.03 \times 10^5)$$

$$= 5.378 \times 10^5 + 3.160 \times 10^5 = 8.54 \times 10^5 \text{ cm}^4$$

$$w_L = 4,090 \text{ N/m}$$

$$\delta_L = \frac{5 w_L l^4}{384 E_c I_e} = \frac{5 (4,090) (21.95)^4 \times 10^5}{384 (2.91 \times 10^4) (8.54 \times 10^5)} = +50 \text{ mm} \downarrow$$

When the concrete 5 cm topping is placed on the precast section, the resulting topping deflection with  $I_g = 24.9 \times 10^5$ ,  $w_{SD} = 3,600 \text{ N/m}$ .

$$\delta_{SD} = \frac{5 \times 3,600 (21.95)^4 \times 10^5}{384 (2.91 \times 10^4) (24.9 \times 10^5)} = +15 \text{ mm} \downarrow$$

(c) *Summary of short-term deflections*

$$\text{Prestress Camber } \delta_i = 65 \text{ mm} \uparrow$$

$$\text{Dead Load } \delta_D = 45 \text{ mm} \downarrow$$

$$\text{Live Load } \delta_L = 50 \text{ mm} \downarrow$$

$$\text{5 cm topping Load } \delta_{SD} = 15 \text{ mm} \downarrow$$

## 7.21 SI CRACK CONTROL

### Example 7.15

Solve Example 7.11 using SI procedure

*Data*

$$\Delta f_s = 207 \text{ MPa}$$

$$A_t = 618 \text{ cm}^2$$

$$\Sigma o = 70.4 \text{ cm}$$

(a) *Steel level*

$$\begin{aligned} w_{\max} &= 8.48 \times 10^{-5} \left( \frac{A_t}{\Sigma o} \right) \Delta f_s \\ &= 8.48 \times 10^{-5} \left( \frac{618}{70.4} \right) 207 = 0.15 \text{ mm} \end{aligned}$$

(b) *Tensile beam face*

$$R_t = 1.24 \text{ from Example 7.11}$$

$$w_{\max} = 1.24 \times 0.15 = 0.19 \text{ say } 0.2 \text{ mm}$$

## SELECTED REFERENCES

- 7.1 ACI Committee 318. *Building Code Requirements for Structured Concrete (ACI 318-08 and Commentary 318R-08)*, American Concrete Institute, Farmington Hills, MI, 2008, pp. 465.
- 7.2 ACI Committee 435. *Control of Deflection in Concrete Structures*, Committee Report ACI 435R-95, Chairman, E. G. Nawy. American Concrete Institute, Farmington Hills, MI, 2000, 1995, p. 77.
- 7.3 ACI Committee 224. *Control of Cracking in Concrete Structures*, Committee Report ACI 224R-99, American Concrete Institute, Farmington Hills, MI, 1972, 2001, pp. 65.
- 7.4 Tadros, M. K. "Designing for Deflection." Paper presented at CIP Seminar on Advanced Design Concepts in Precast Prestressed Concrete, Prestressed Concrete Institute Convention, Dallas, October 1979.
- 7.5 Branson, D. E. *Deformation of Concrete Structures*. McGraw Hill, New York, 1977.
- 7.6 Branson, D. E. "The Deformation of Non-Composite and Composite Prestressed Concrete Members." In *Deflection of Concrete Structures*, ACI Special Publication SP-43. American Concrete Institute, Farmington Hills, MI, 1974, pp. 83-127.
- 7.7 Shaikh, A. F., and Branson, D. E. "Non-Tensioned Steel in Prestressed Concrete Beams." *Journal of the Prestressed Concrete Institute* 15, 1970, 14-36.
- 7.8 Prestressed Concrete Institute. *PCI Design Handbook*. 6th ed. Prestressed Concrete Institute, Chicago, 2006.
- 7.9 Martin, L. D. "A Rational Method of Estimating Camber and Deflections of Precast, Prestressed Concrete Members." *Journal of the Prestressed Concrete Institute* 22 (1977): 100-108.
- 7.10 Nilson, A. H. *Design of Prestressed Concrete*. John Wiley & Sons, New York, 1987.
- 7.11 Tadros, M. K., Ghali, A., and Dilger, W. H. "Effect of Non-Prestressed Steel on Prestress Loss and Deflection." *Journal of the Prestressed Concrete Institute* 22, 1977, 50-63.
- 7.12 Tadros, M. K. "Expedient Service Load Analysis of Cracked Prestressed Concrete Sections." *Journal of the Prestressed Concrete Institute* 27, 86-111, 1982, also Discussions and Author's Closure, 28 (1983): 137-158.

- 7.13 Naaman, A. E. "Partially Prestressed Concrete: Review and Recommendations." *Journal of the Prestressed Concrete Institute* 30, 1985, 30–71.
- 7.14 Nawy, E. G., and Potyondy, J. G. "Flexural Cracking Behavior of Pretensioned Prestressed Concrete I- and T-Beams." *Journal of the American Concrete Institute* 65, Farmington Hills, MI, 1971, 335–360.
- 7.15 Nawy, E. G., and Huang, P. T. "Crack and Deflection Control of Pretensioned Prestressed Beams." *Journal of the Prestressed Concrete Institute* 22, 1977, 30–47.
- 7.16 Nawy, E. G., and Chiang, J. Y. "Serviceability Behavior of Post-Tensioned Beams." *Journal of the Prestressed Concrete Institute* 25, 1980, 74–95.
- 7.17 Cohn, M. Z. "Partial Prestressing From Theory to Practice." *NATO-ASI Applied Science Series*, Vols. I and II, Publ. Martinus Nijhoff Publishers, in Cooperation with NATO Scientific Affairs Division, Dordrecht, 1986, Vol. 1, p. 405; Vol. II, p. 425.
- 7.18 Nawy, E. G. "Flexural Cracking Behavior of Pretensioned and Post-Tensioned Beams: The State of the Art." *Journal of the American Concrete Institute*, Farmington Hills, MI, December 1985, pp. 890–900.
- 7.19 Nawy, E. G. "Flexural Cracking Behavior and Crack Control of Pretensioned and Post-Tensioned Prestressed Beams." *Proceedings of the NATO-NSF Advanced Research Workshop*, vol. 2. Dordrecht-Boston: Martinus Nijhoff, 1986, pp. 137–156.
- 7.20 Neville, A. M. *Properties of Concrete*. 4th ed., Addison Wesley Longman, London, UK, 1996.
- 7.21 Bazant, Z. P. "Prediction of Creep Effects Using Age Adjusted Effective Modulus Method." *Journal of the American Concrete Institute*, Farmington Hills, MI, April 1972, pp. 212–217.
- 7.22 Libby, J. R. *Modern Prestressed Concrete*. Van Nostrand Reinhold, New York, 1984.
- 7.23 Nawy, E. G., *High Performance Concrete*, 2nd Ed., John Wiley and Sons, New York, 2001, 440 p.
- 7.24 Nawy, E. G., editor-in-chief, *Concrete Construction Engineering Handbook*, 2nd ed., CRC Press, Boca Raton, FL, 2008, 1560 pp.
- 7.25 PCI, *Prestressed Concrete Bridge Design Handbook*, Precast/Prestressed Concrete Institute, Chicago, 1998.
- 7.26 AASHTO, *Standard Specifications for Highway Bridges*, 18th ed. and 2009, American Association of State Highway and Transportation Officials, Washington, D.C., 2009.

## PROBLEMS

- 7.1 Calculate the instantaneous and long-term cambers and deflections of the AASHTO beam of Example 4.2 for 7, 30, 180, and 365 days, and 5 years by (a) the PCI multipliers method, (b) the incremental time-steps method, and (c) the approximate time-steps method. Then tabulate and compare the results. Are the deflections within the AASHTO permissible limits on deflection? Given  $f'_c = 6,000$  psi.
- 7.2 A 68-ft (20.7-m) span simply supported lightweight concrete double-T-beam is subjected to a superimposed topping load  $W_{SD} = 250$  plf (3.65 kN/m) and a service live load  $W_L = 300$  plf (4.38

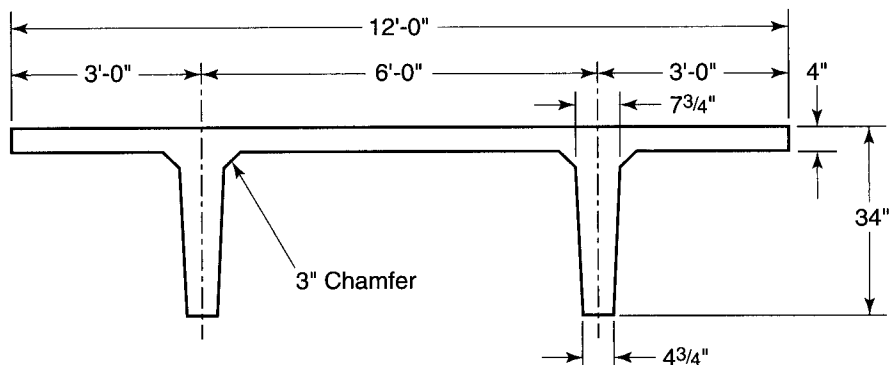


Figure P7.2

kN/m). Calculate the immediate camber and deflection of this beam by the bilinear method and the time-dependent deflections at intervals of 7, 30, 90, and 365 days using the PCI multipliers method and verify whether they are within the permissible ACI limits on deflection for the conditions where nonstructural elements are not likely to be damaged by large deflections. Use Figure P7.2 and the following data.

	Noncomposite	Composite
$A_c$ , in. <sup>2</sup>	615 (3,968 cm <sup>2</sup> )	855
$I_c$ , in. <sup>4</sup>	59,720 (24.9 × 10 <sup>5</sup> cm <sup>4</sup> )	82,723
$r^2$ , in. <sup>2</sup>	97	97
$c_b$ , in.	21.98 (558 mm)	25.37
$c_p$ , in.	10.02 (255 mm)	8.63
$S_b$ , in. <sup>3</sup>	2,717 (4.5 × 10 <sup>4</sup> )	3,261
$S'$ , in. <sup>3</sup>	5,960 (9.8 × 10 <sup>4</sup> )	9,587
$W_d$ , plf	491 (7.15 kN/m)	741

$$V/S = 615/346 = 1.69 \text{ in. (4.3 cm)}$$

$$RH = 75\%$$

$$e_c = 18.73 \text{ in. (476 mm)}$$

$$e_e = 12.81 \text{ in. (325 mm)}$$

$$f'_c = 5,000 \text{ psi (34.5 MPa) (lightweight)}$$

$$f'_{ci} = 3,750 \text{ psi (25.7 MPa)}$$

$$f_t \text{ at bottom fibers} = 12\sqrt{f'_c} = 849 \text{ psi (5.6 MPa)}$$

$$A_{ps} = \text{twelve } \frac{1}{2}\text{-in. dia low-relaxation steel depressed at midspan only}$$

$$f_{pu} = 270,000 \text{ psi (1,862 MPa)}$$

$$f_{pi} = 189,000 \text{ psi (1,303 MPa)}$$

$$f_{py} = 260,000 \text{ psi (1,793 MPa)}$$

$$E_{ps} = 28.5 \times 10^6 \text{ psi (196 GPa)}$$

- 7.3** Determine the crack width and stabilized mean crack spacing in the double-T beam of Problem 7.2 for an incremental stress of 15,000 psi (103 MPa) beyond the decompression state. Also, determine whether the maximum crack width obtained satisfies the serviceability requirement for crack control for a humid and moist environment.
- 7.4** A simply supported bonded double-T beam has a 50-ft span and is subjected to a uniform live load of 1,250 plf and a superimposed dead load of 200 plf. Its geometrical properties and maximum allowable stresses are as follows:

$$A_c = 615 \text{ in.}^2$$

$$I_c = 59,720 \text{ in.}^4 (77,118 \text{ in.}^4)$$

$$S_b = 2,717 \text{ in.}^3 (3,142 \text{ in.}^3)$$

$$S' = 5,960 \text{ in.}^3 (8,150 \text{ in.}^3)$$

$$W_D = 641 \text{ plf (491 plf)}$$

$$V/S = 1.69 \text{ in.}$$

$$f'_c = 5,000 \text{ psi (normal weight)}$$

$$f_c = 2,250 \text{ psi}$$

$$f'_{ci} = 3,750 \text{ psi}$$

$$f_{ii} = 184 \text{ psi}$$

$$f_{pu} = 270,000 \text{ psi}$$

$$f_{py} = 235,000 \text{ psi}$$

$$f_{pi} = 195,000 \text{ psi}$$

$$E_{ps} = 28 \times 10^6 \text{ psi}$$

$$c_b = 21.98 \text{ in. (24.54 in.)}$$

$$c_t = 10.02 \text{ in. (9.46 in.)}$$

$$RH = 70\%$$

$$f_{ci} = 2,250 \text{ psi}$$

$$f_t = 849 \text{ psi}$$

$$f_{pe} = 150,000 \text{ psi}$$

$$f_y = 60,000 \text{ psi}$$

$$A_{ps} = \text{sixteen } \frac{1}{2}\text{-in. dia 7-wire low-relaxation strands}$$

Bracketed values are for the composite section due to 2-in. topping.

- (a) Find the eccentricities  $e_c$  and  $e_e$  that would result in a tensile stress  $f_t = 750$  psi at the lower fiber at midspan *at service load*, and tensile stresses within the allowable limits at the support section both at initial prestress and at service load. Use *nonprestressed* reinforcement where necessary.
  - (b) Find the long-term camber and deflection of the beam by the *approximate time-step procedure* for  $t = 7$  days and  $t = 180$  days, assuming that the ultimate creep coefficient  $C_u = 2.35$ . Use the moment-curvature approach to determine the initial camber at transfer. Are the values within the allowable ACI limits?
  - (c) Calculate the flexural crack width at service load for a stress increment  $\Delta f_s = 15,000$  psi beyond the decompression stress.
- 7.5** Find the long-term camber and deflection in Example 7.9 by the incremental time-steps method, assuming that twelve  $\frac{1}{2}$ -in. dia 7-wire 270 K stress-relieved strands are used for prestressing the beam section. Calculate the flexural crack width at service load for a stress increment  $\Delta f_s = 15,000$  psi beyond the decompression stress.

# 8



## PRESTRESSED COMPRESSION AND TENSION MEMBERS

### 8.1 INTRODUCTION

Although prestressing is predominantly used in flexural members such as beams and slabs, it is also used in axially loaded members such as long columns (compression members) and ties for arches and truss elements (tension members). Yet another use is in pre-tensioned and post-tensioned prestressed piles and masts.

The theory, analysis, and design of prestressed compression members are similar to those of reinforced concrete members. The internal axial prestressing force in the *bonded* tendon produces no column action; hence, no buckling can result as long as the prestressing steel and the surrounding concrete are in direct contact along the total length of the element. As such, the bending tendency of the concrete at midlength is neutralized by the stretching effect of the axially embedded prestressing strands.

Columns are normally subjected to bending in addition to axial load, since external loads are rarely concentric. As a result, the concrete section is subjected to tension at the side farthest from the line of action of the longitudinal load. Cracking develops, but it can be prevented through the use of prestress in the columns. If the applied load is concen-

The George Moscone Convention Center, San Francisco, California, design by T.Y. Lin International. (Courtesy, Post-Tensioning Institute.)

tric, prestressing is inconsequential if not altogether disadvantageous, as the compressive stress on the concrete section is needlessly increased.

A compression member can be considered fully prestressed throughout its length if no loss in development of prestressing occurs at its ends. If partial loss occurs, the reinforcement segment in the development zone is considered nonprestressed and the section at the end zone is treated as a reinforced concrete eccentrically loaded section.

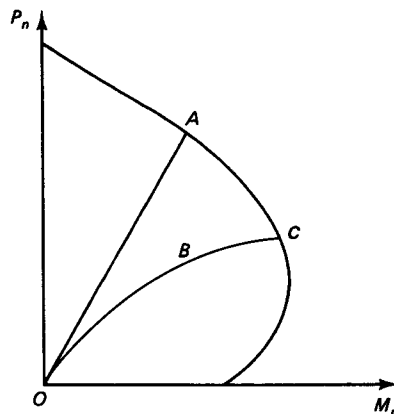
Tension members are normally subjected to direct tension only. These elements are mostly linear, as for example, railroad ties, restraining ties for arch bridges, tension members in trusses, and foundation anchorages for earthwork retaining structures. Tension members can also be circular or parabolic in shape, as witness prestressed circular containers or catenary-shaped bridge elements. The fundamental function of the pure tension members is to prevent their cracking at service load and to enable them to sustain all the necessary deformation needed to develop full resistance to the external service loads and overloads. Being crack-free would fully protect the reinforcement from corrosion and other environmental conditions.

## 8.2 PRESTRESSED COMPRESSION MEMBERS: LOAD–MOMENT INTERACTION IN COLUMNS AND PILES

In order to evaluate the nominal strength of a column at various eccentric load levels, it is necessary to evaluate all possible combinations of ultimate nominal loads  $P_n$  and ultimate nominal moments  $M_n$  given by

$$M_n = P_n e_i \quad (8.1)$$

where  $e_i$  is the eccentricity of the load at the various load–moment combinations. A plot of the relationship between  $P_n$  and  $M_n$  is shown in the interaction diagram of Figure 8.1 for both nonslender columns (material failure) and slender columns (stability failure). In the nonslender column, failure occurs as the load reaches the value A along path OA, and the concrete arches at the compression side. In the slender column, the maximum load is reached at B along the path OBC, which intersects the interaction diagram at C. Instability occurs once the critical load is reached. A quantitative definition of slender and nonslender columns is given later.

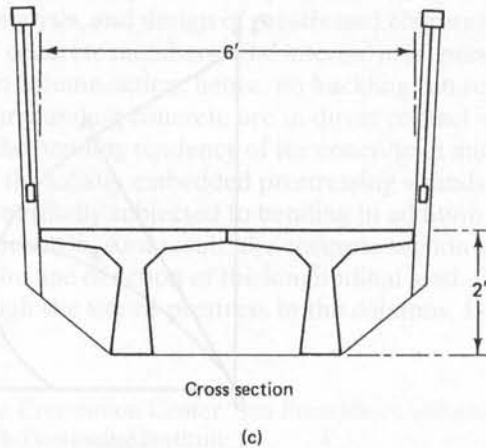
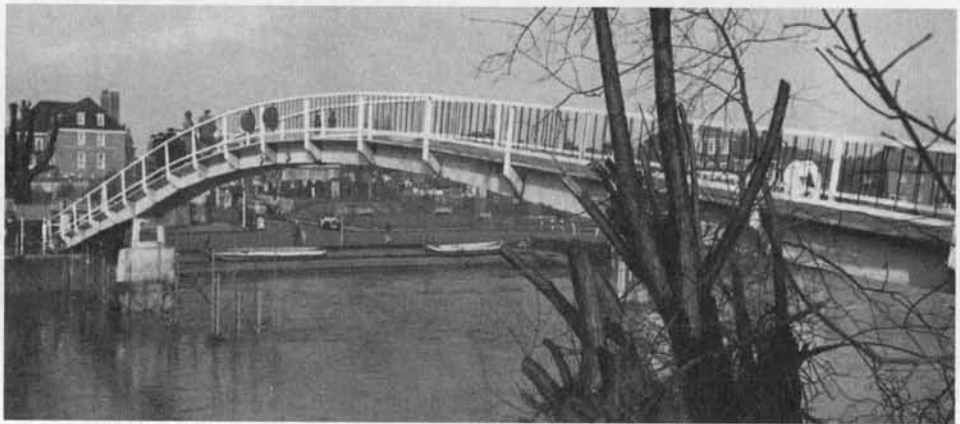
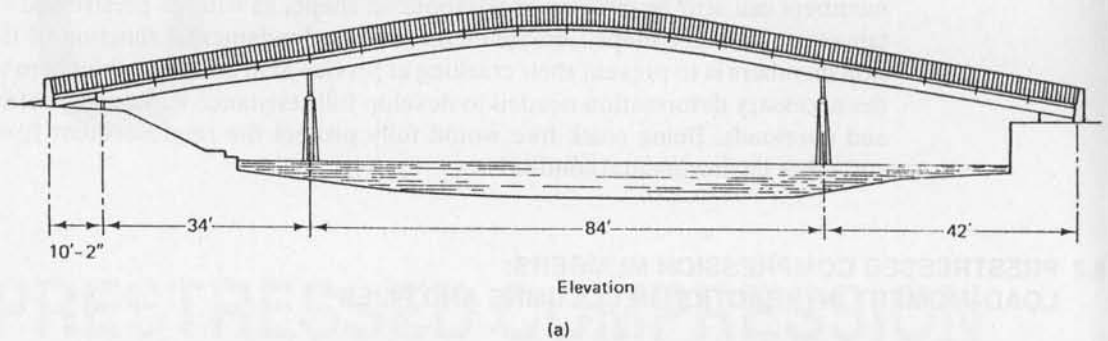


**Figure 8.1** Basic interaction diagram for columns. (a) Path OA for material failure in nonslender column. (b) Path OBC for buckling failure of slender column.



The basic assumptions made in regard to prestressed concrete, similar to those made in regard to reinforced concrete columns, are as follows:

1. The strain distribution in the concrete varies linearly with depth.
2. The stress distribution in the compression zone is parabolic and is replaced in analysis and design by an equivalent rectangular block.



**Photo 8.1** Eel Pie Island, Twickenham, England, prestressed concrete footbridge.

3. The stress-strain diagrams of the concrete and the prestressing steel are known.
4. The crushing strain of the concrete in combined bending and axial load at the extreme fibers is  $\epsilon_c = 0.003$  in./in., and the average crushing strain at mid-depth of a concrete section subjected mainly to axial load is  $\epsilon_0 = 0.002$  in./in.
5. The section is considered to have failed when the strain in the concrete at the extreme compression fibers reaches  $\epsilon_c = 0.003$  in./in. or  $\epsilon_0 = 0.002$  in./in. at mid-depth. Note that  $\epsilon_c = 0.003$  is the value used in the ACI Code, whereas other codes use a higher value of 0.0035 or 0.0038.
6. Compatibility of strain is postulated between the concrete and the prestressing steel.

The modes of failure are also similar to those of reinforced concrete columns:

1. *Initial compression failure, small eccentricity.* This failure mode develops when the strain in the concrete at the loaded side reaches  $\epsilon_{cu} = 0.003$  in./in. while the strain in the prestressing steel at the far side is below the yield strain. The eccentricity  $e$  of the axial load is smaller than the balanced eccentricity  $e_b$ .
2. *Initial tension failure, large eccentricity.* This failure mode is the reverse of the preceding one. The steel at the far side yields prior to the crushing of the concrete at the loaded side. The eccentricity  $e$  of the axial load is larger than the balanced eccentricity  $e_b$ .
3. *Balanced state of strain,  $\epsilon_t = 0.002$  in./in., balanced eccentricity.* This mode defines the condition of maximum moment value  $M_{nb}$  on the interaction curve corresponding to a maximum tensile strain in the tension layers equal to a strain increment  $\Delta\epsilon_{ps} = 0.0012$  to 0.0020 in./in. beyond the service load level. The eccentricity of the axial load is defined as the balanced eccentricity  $e_b$ .

It should be noted that if  $P_n = 0.10 f'_c A_g$  or less, the column essentially behaves as a flexural beam because of the low level of axial force, resulting in a large eccentricity and a strain value greater than 0.004 as a minimum value for beams in the transition zone.

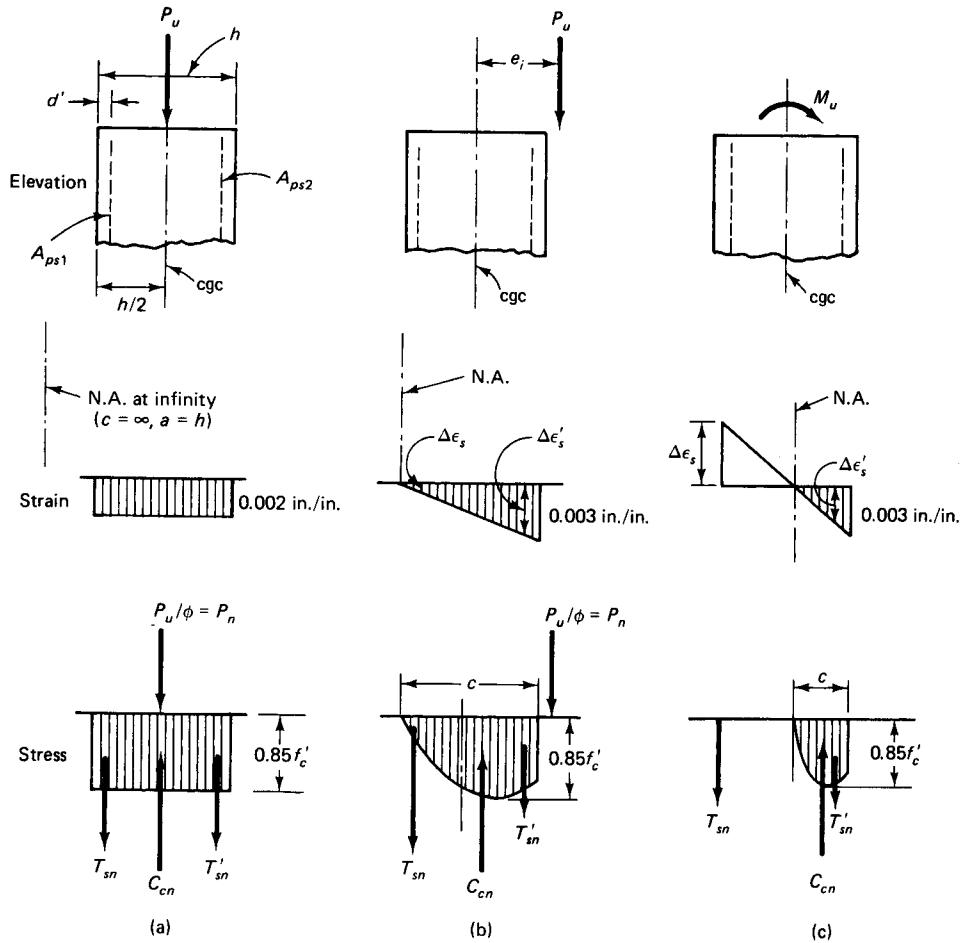
The three major controlling points on the interaction diagram are:

1.  $M_u = 0$ , corresponding to  $\epsilon_0 = 0.002$  in./in. at failure due to the concentric load  $P_u$ . The neutral axis position is at infinity.
2. No tension at the extreme concrete tensile fibers and  $\epsilon_{cu} = 0.003$  in./in. at the extreme concrete compression fibers. The neutral axis position is at the extreme tension fibers.
3.  $P_u = 0$  and  $\epsilon_{cu} = 0.003$  in./in. at the extreme compression fibers. The neutral axis is inside the section and is determined by trial and adjustment, assuming a depth  $c$  and then testing the assumption.

Figure 8.2 shows the strain and stress distribution for these three cases.

The remaining points on the interaction diagram are for cases that lie between stages (a), (b), and (c) of Figure 8.2, namely, from concentric loading to pure bending. In the case of columns, pure bending defines the state where the ratio of the factored axial load  $P_u$  to the factored flexural moment  $M_u$  is negligible. The parabolic distribution of stress for cases (b) and (c) is replaced by the equivalent rectangular block, where the block depth  $a = \beta_1 c$ , as is done in the case of flexural beams.

The typical case of a compression member lies between stages (b) and (c) of Figure 8.2. The strains, stresses, and forces for such a case are shown in Figure 8.3 for the critical section at the limit state of ultimate load by material failure. Cutting the free-body diagram at the column midheight above section 1–1, the cross-section of the member is shown in part (b) of the figure, and the strain and stress at failure in parts (c) and (d), re-



**Figure 8.2** Strain and stress distribution alternatives across concrete section depth. (a)  $M_u = 0$ . (b)  $\epsilon_c = 0.003 \text{ in./in.}$ , and zero tension at the extreme tensile fibers. (c)  $P_u = 0$  and  $\epsilon_c = 0.003 \text{ in./in.}$  at the extreme compressive fibers.

spectively. The strain  $\epsilon_{ce}$  is the *uniform* strain in the concrete under effective prestress after creep, shrinkage, and relaxation losses given respectively by

$$C_{cn} = 0.85f'_c ba \tag{8.2a}$$

$$T'_{sn} = A'_{ps} f'_{ps} \tag{8.2b}$$

and

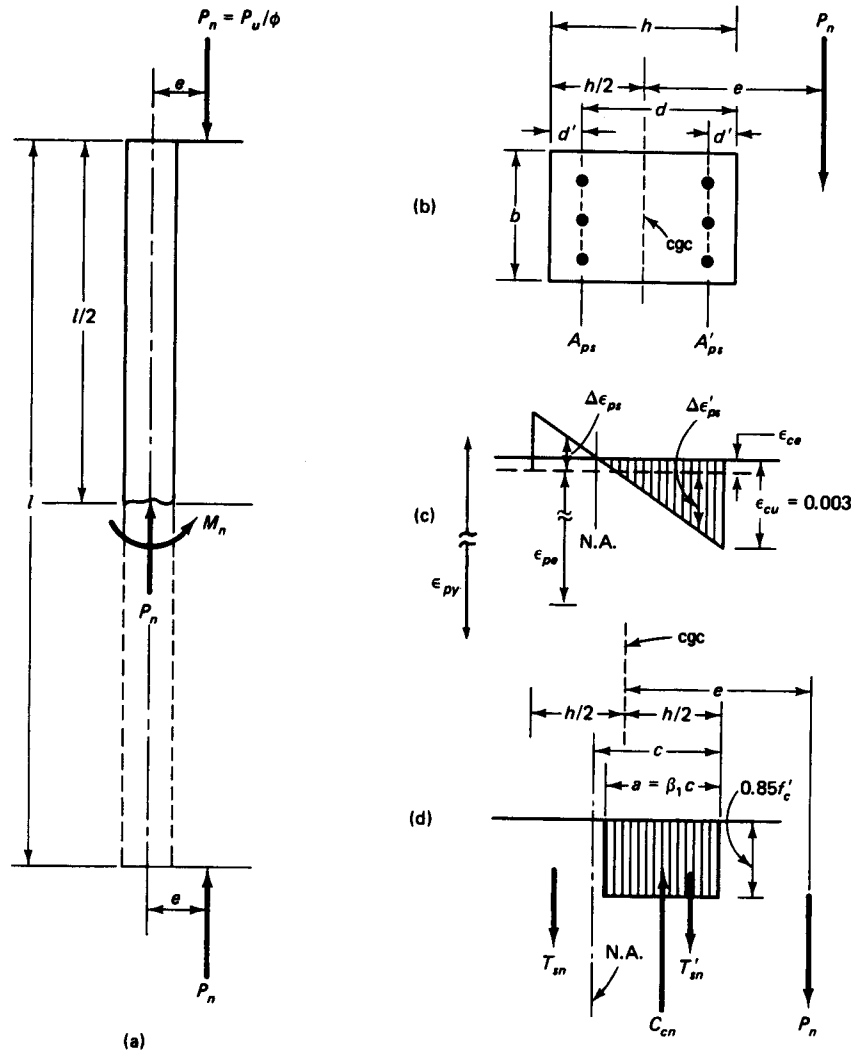
$$T_{sn} = f_{ps} A_{ps1} \tag{8.2c}$$

Equilibrium of forces then gives

$$P_n = C_{cn} - T'_{sn} - T_{sn} \tag{8.3}$$

If the effective prestressing force after all losses is  $P_e$ , the corresponding strain in the tendons prior to the application of the external load is

$$\epsilon_{pe} = \frac{f_{pe}}{E_{ps}} = \frac{P_e}{(A_{ps} + A'_{ps})E_{ps}} \tag{8.4a}$$



**Figure 8.3** Stresses and forces in typical eccentrically loaded nonslender column. (a) Elevation. (b) Cross section. (c) Strain distribution. (d) Stresses and forces.

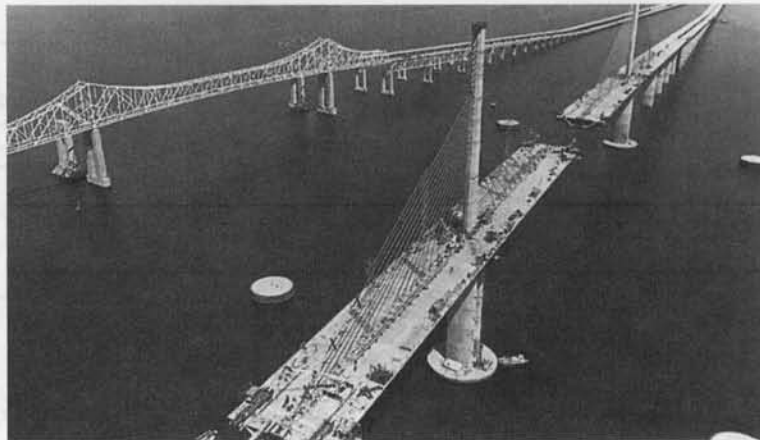
The change in strain in the prestressing steel area  $A'_{ps}$  as the compression member passes from the effective prestressing stage to the ultimate load can be defined as

$$\Delta\epsilon'_{ps} = \epsilon_{cu} \left( \frac{c - d'}{c} \right) - \epsilon_{ce} \quad (8.4b)$$

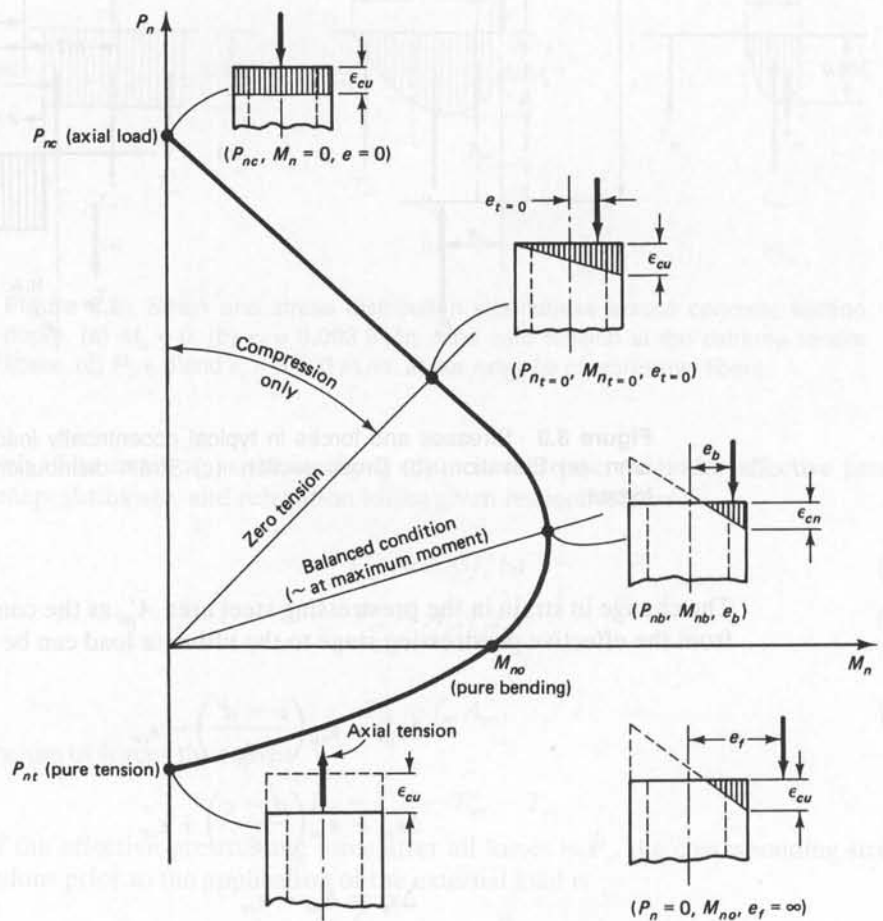
$$\Delta\epsilon_{ps} = \epsilon_{cu} \left( \frac{d - c}{c} \right) + \epsilon_{ce} \quad (8.4c)$$

$$\Delta\epsilon_p = \Delta\epsilon_{ps} - \epsilon_{ce} \quad (8.4d)$$

$$T'_{sn} = A'_{ps} f'_{ps} = A'_{ps} E_{ps} (\epsilon_{pe} - \Delta\epsilon'_{ps})$$



**Photo 8.2** Cable-stayed Sunshine Skyway Bridge, Tampa, Florida. (Courtesy, Figg Engineering Group Tallahassee, FL.)



**Figure 8.4** Load-moment interaction diagram controlling eccentricities.

or

$$T'_{sn} = A'_{ps} E_{ps} \left[ \epsilon_{pe} - \epsilon_{cu} \left( \frac{c - d'}{c} \right) + \epsilon_{ce} \right] \quad (8.5)$$

Similarly,

$$T_{sn} = A_{ps} f_{ps} = A_{ps} E_{ps} (\epsilon_{pe} + \Delta\epsilon_{ps})$$

or

$$T_{sn} = A_{ps} E_{ps} \left[ \epsilon_{pe} + \epsilon_{cu} \left( \frac{d - c}{c} \right) + \epsilon_{ce} \right] \quad (8.6)$$

Taking moments about the geometric centroid cgc of the section gives

$$M_n = P_n \bar{e} = C_{cn} \left( \frac{h}{2} - \frac{a}{2} \right) \curvearrowright - T'_{sn} \left( \frac{h}{2} - d' \right) \curvearrowright + T_{sn} \left( d - \frac{h}{2} \right) \curvearrowright \quad (8.7)$$

From Equations 8.2a, 8.5, 8.6, and 8.7, the nominal strengths  $P_n$  and  $M_n$  for several eccentricities  $e_i$  can be evaluated in order to construct the P–M interaction diagram for any section or develop nondimensional series of P–M interaction diagrams for various concrete strength levels. The design strengths are evaluated from the nominal strength values as

$$\text{Design } P_u = \phi P_n$$

and

$$\text{Design } M_u = \phi M_n = \phi P_n e$$

where  $\phi$  is the strength reduction factor for compression members. Note that the *design*  $P_u$  and  $M_u$  have to have a value close to, but not less than, the *factored* values  $P_u$  and  $M_u$ . The load-moment interaction diagram for the controlling eccentricities is shown in Figure 8.4.

### 8.3 STRENGTH REDUCTION FACTOR $\phi$

For members subject to flexure and relatively small axial loads, failure is initiated by yielding of the tension reinforcement and takes place in an increasingly ductile manner. Hence, for small axial loads it is reasonable to permit an increase in the  $\phi$  factor from that required for pure compression members. When the axial load vanishes, the member is subjected to pure flexure, and the strength reduction factor  $\phi$  becomes 0.90.

Figure 4.45 shows the transition zone in which the strength reduction factor,  $\phi$ , can be increased from 0.65 for tied columns and 0.70 for spirally reinforced columns to 0.90 for pure flexure in the strain limits approach. The balanced limit strain for the compression-controlled state is denoted by limiting strain  $\epsilon_t = 0.002$  in./in., or a neutral axis depth ratio  $c/d_t = 0.60$  for compression members. The value  $\phi P_n = 0.10 f'_c A_g$  can be considered as a design axial load below which the  $\phi$  factor can safely be increased for most compression members, within the limitations of the transition zone of Figure 4.45. To recapitulate, interpolation of the  $\phi$  values for the transition zone from the limit strain state in compression ( $\epsilon_t = 0.002$ ) to the limit strain state in tension ( $\epsilon_t = 0.005$ ), as in Equations 4.35 (a) and 4.35 (b), can be made from the following expressions:

(a)  $\phi$  as a function of strain,

Tied Sections:

$$0.65 \leq \left[ \phi = 0.65 + (\epsilon_t - 0.002) \left( \frac{250}{3} \right) \right] \leq 0.90 \quad (8.8a)$$

Spirally-reinforced sections:

$$0.75 \leq \left[ \phi = 0.75 + (\epsilon_t - 0.002) \left( \frac{200}{3} \right) \right] \leq 0.90 \quad (8.8b)$$

(b)  $\phi$  as a function of the neutral axis depth ratio, from Eqs. 4.36(a) and (b),  
Tied sections:

$$0.65 \leq \left( \phi = 0.65 + 0.25 \left[ \frac{1}{c/d_t} - \frac{5}{3} \right] \right) \leq 0.90 \quad (8.9a)$$

Spirally-reinforced sections:

$$0.75 \leq \left( \text{Spiral: } \phi = 0.75 + 0.15 \left[ \frac{1}{c/d_t} - \frac{5}{3} \right] \right) \leq 0.90 \quad (8.9b)$$

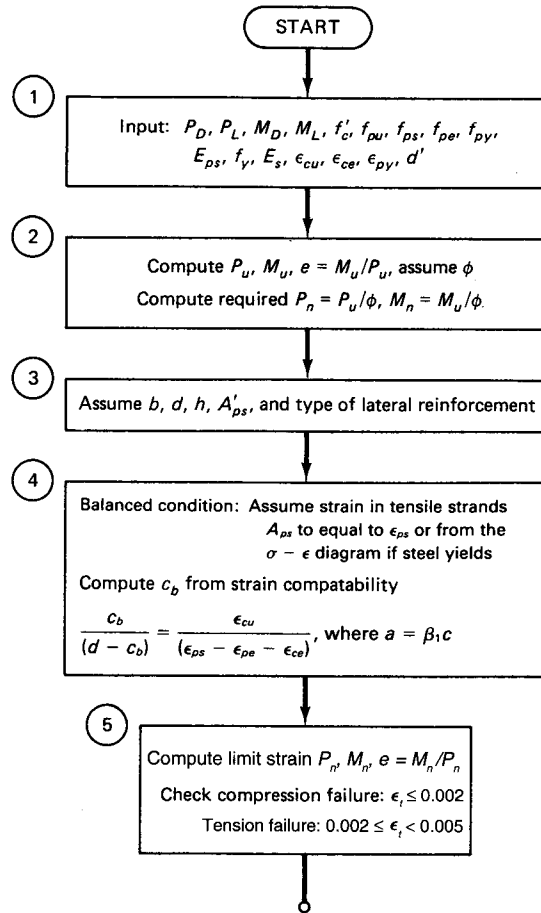
Note that the balanced strain condition in *prestressed concrete* compression members is highly indeterminate. A reasonable approximation can be made by assuming, in trial and adjustment, a value  $\Delta_{ps} = 0.0012$  to  $0.0020$  in./in. beyond the service load level and computing the stress block depth “a” of the concrete section accordingly. This assumption has to be verified, and the nominal moment for the limit strain condition  $\epsilon_t = 0.002$  adjusted after the interaction diagram is plotted. In this manner, it becomes possible to refine the maximum moment ordinate value for the balanced strain limit state in compression represented by the neutral axis depth  $c_b$  if needed.

#### 8.4 OPERATIONAL PROCEDURE FOR THE DESIGN OF NONSLENDER PRESTRESSED COMPRESSION MEMBERS

The following steps can be carried out for the design of nonslender (short) columns where the behavior is controlled by material failure:

1. Evaluate the factored external axial load  $P_u$  and the factored moment  $M_u$ . Compute the applied eccentricity  $e = M_u/P_u$ .
2. Assume a cross section and type of lateral reinforcement to be used, namely, tied or spiral. Avoid fractional quantities in selecting sectional dimensions.
3. Assume the number and size of strands.
4. Assume that the strain in the extreme tensile fibers is equal to an assumed strain  $\epsilon_{ps}$  of the prestressing steel, and then proceed to compute the balanced limit strain axial load  $P_{nb}$  and the corresponding moment  $M_{nb}$  at limit strain  $\epsilon_t = 0.002$ . This step also enables one to verify the value of the strength reduction factor. The moment  $M_{nb}$  results from an  $\epsilon_{ps}$  strain value which gives a maximum moment in the interaction diagram.
5. Assume a neutral axis depth  $c$ , and find the corresponding  $P_n$  and  $M_n$ . Then check for the adequacy of the assumed section, i.e., whether  $\phi P_n > P_u$  and  $\phi M_n > M_u$ . If the section cannot support the factored load or is oversized and hence uneconomical, revise the cross section and the reinforcement through trial and adjustment by repeating steps 4 and 5 as necessary, including the construction of an interaction diagram.
6. Design the lateral reinforcement.

Figure 8.5 presents a flowchart of the trial-and-adjustment sequences of the design or analysis procedure.



**Figure 8.5** Flowchart for design or analysis of prestressed concrete nonslender compression members.

## 8.5 CONSTRUCTION OF NOMINAL LOAD–MOMENT ( $P_n-M_n$ ) AND DESIGN ( $P_u-M_u$ ) INTERACTION DIAGRAMS

### Example 8.1

Construct the nominal load–moment interaction diagram for a prestressed concrete compression member 14-in. (356 mm) wide and 14-in. deep. The member is reinforced with eight  $\frac{1}{2}$ -in. (12.7 mm) dia 7-wire stress-relieved 270-K strands, half on each side of the two faces parallel to the neutral axis as shown in Figure 8.6. The stress-strain diagram for the strands is shown in Figure 8.7. The effective prestress after all losses is  $f_{pe} = 150,000$  psi (1,034 MPa). Additionally, draw the design interaction diagram using the appropriate strength reduction factor values. Consider the strands fully developed throughout the length of the member. Given data are as follows:

$$f'_c = 6,000 \text{ psi (47.5 MPa), normal-weight concrete}$$

$$E_{ps} = 29 \times 10^6 \text{ psi (200} \times 10^3 \text{ MPa)}$$

$$f_{ps} = 240,000 \text{ psi (1,655 MPa)}$$



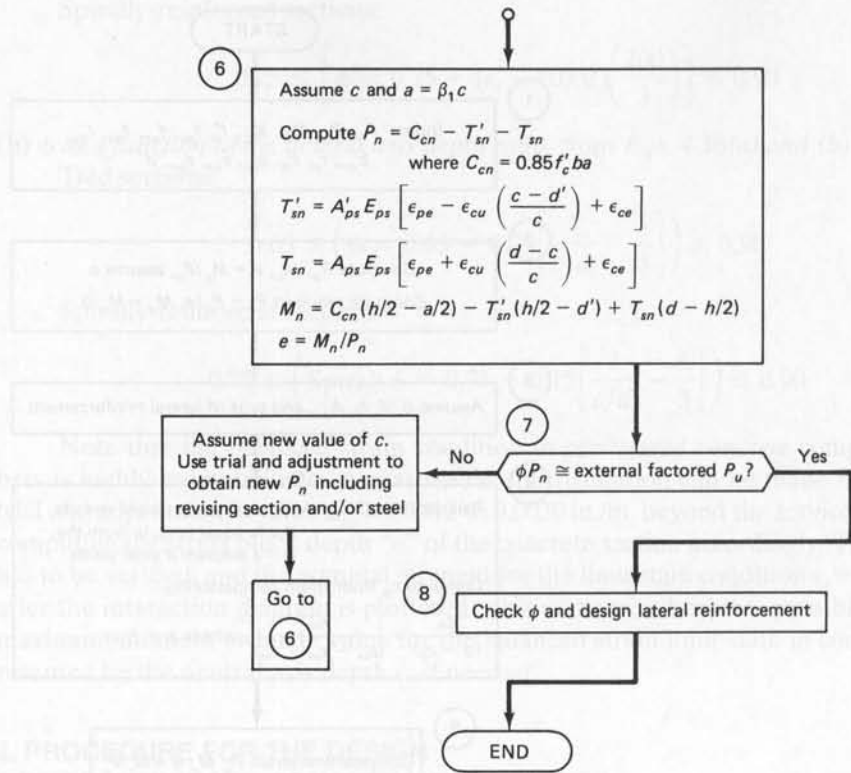


Figure 8.5 Continued

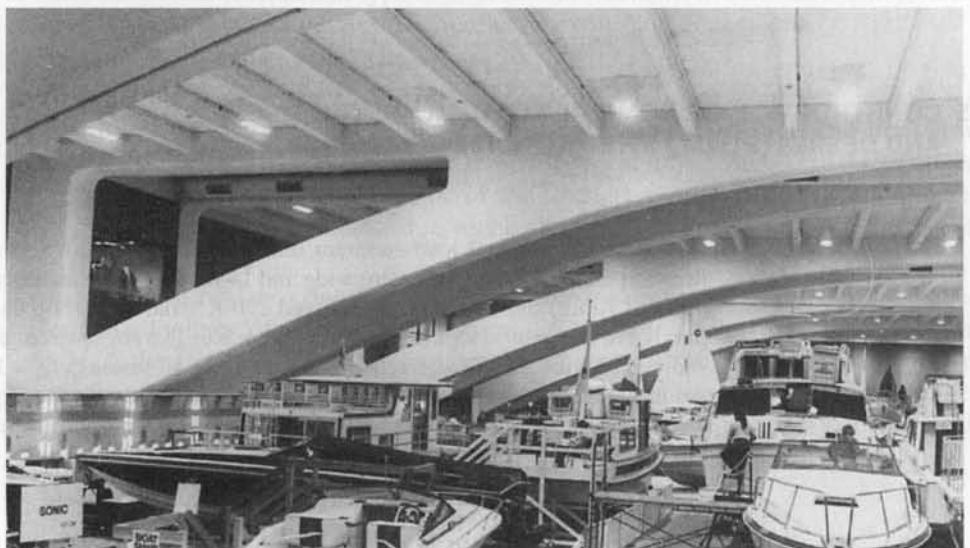


Photo 8.3 Interior of the George Moscone Convention Center, San Francisco, California, design by T. Y. Lin International. (Courtesy, Post-Tensioning Institute.)

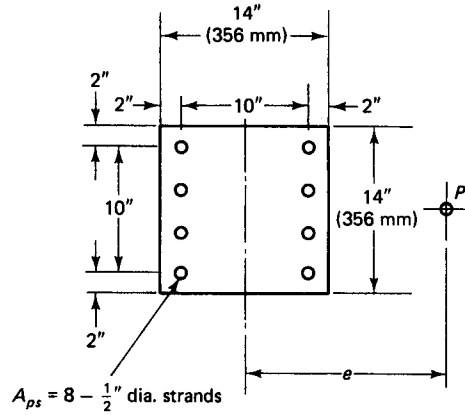


Figure 8.6 Section geometry.

$$\epsilon_{cu} = 0.003 \text{ in./in. at failure}$$

$$\epsilon_{ce} = 0.0005 \text{ in./in. when } P_e \text{ acts on the section} = \frac{P_e}{A_c E_c} \left( 1 + \frac{e^2}{r^2} \right)$$

$$\epsilon_{py} = \text{strand yield strain} \cong 0.012 \text{ in./in. from Figure 8.9}$$

Assume a reasonable value of  $\epsilon_p$  and adjust as necessary.

### Solution:

#### Nominal Strength $P_n$ – $M_n$ Diagram

1. Axial Compression:  $M_u = 0$ ,  $c = \infty$  (Use  $\epsilon_{cu} = 0.003$  since perfect axial compression is impossible.)

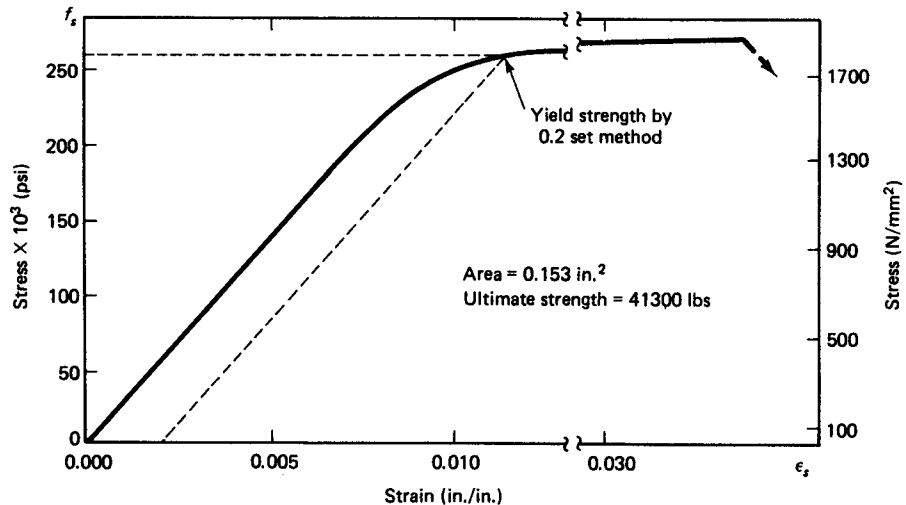


Figure 8.7 Stress-strain diagram for  $\frac{1}{2}$ -in. (12.7 mm) dia 270-K prestressing tendon.

The compressive block depth  $a = 14$  in. (356 mm), and the effective depth  $d = 14 - 2 = 12$  in. (305 mm). So we have  $C_{cn} = 0.85f'_c ba = 0.85 \times 6000 \times 14 \times 14 = 999,600$  lb (4,446 kN).

From Equation 8.5,

$$T'_{sn} = A'_{ps} E_{ps} \left[ \epsilon_{pe} - \epsilon_{cu} \left( \frac{c - d'}{c} \right) + \epsilon_{ce} \right]$$

$$A'_{ps} = 4 \times 0.153 = 0.612 \text{ in.}^2 (3.95 \text{ cm}^2)$$

From Figure 8.7, for  $E_{ps} = 29 \times 10^6$  psi ( $200 \times 10^3$  MPa),  $\epsilon_{pe} = 0.0052$  in./in. and  $\epsilon_{cu} = 0.003$  in./in. Thus,

$$\begin{aligned} T'_{sn} &= 0.612 \times 29 \times 10^6 \left[ 0.0052 - 0.003 \left( \frac{\infty - 2}{\infty} \right) + 0.0005 \right] \\ &= 0.612 \times 29 \times 10^6 (0.0052 - 0.003 + 0.0005) \\ &= 47,920 \text{ lb (213 kN)} \end{aligned}$$

From Equation 8.6,

$$\begin{aligned} T_{sn} &= A_{ps} E_{ps} \left[ \epsilon_{pe} + \epsilon_{cu} \left( \frac{d - c}{c} \right) + \epsilon_{ce} \right] \\ &= 0.612 \times 29 \times 10^6 \left[ 0.0052 + 0.003 \left( \frac{12 - \infty}{\infty} \right) + 0.0005 \right] \\ &= 47,920 \text{ lb (213 kN)} \end{aligned}$$

From Equation 8.2,

$$\begin{aligned} P_n &= C_{cn} - T'_{sn} - T_{sn} = 999,600 - 47,920 - 47,920 \\ &= 903,760 \text{ lb (4,020 kN)} \end{aligned}$$

From Equation 8.7,

$$\begin{aligned} M_n &= C_{cn} \left( \frac{h}{2} - \frac{a}{2} \right) - T'_{sn} \left( \frac{h}{2} - d' \right) + T_{sn} \left( d - \frac{h}{2} \right) \\ &= 999,600 \left( \frac{14}{2} - \frac{14}{2} \right) - 47,920 \left( \frac{14}{2} - 2 \right) + 47,920 \left( 12 - \frac{14}{2} \right) \\ &= 0 \\ e_1 &= \frac{M_n}{P_n} = 0 \end{aligned}$$

**2. Zero Tension at Tension Face,  $c = 14$  in.**

$$\beta_1 = 0.85 - \frac{0.05(f'_c - 4,000)}{1,000} = 0.75$$

$$a = \beta_1 c = 0.75 \times 14 = 10.5 \text{ in. (267 mm)}$$

$$C_{cn} = 0.85 \times 6,000 \times 14 \times 10.5 = 749,700 \text{ lb (3,335 kN)}$$

$$\begin{aligned} T'_{sn} &= 0.612 \times 29 \times 10^6 \left[ 0.0052 - 0.003 \left( \frac{14 - 2}{14} \right) + 0.0005 \right] \\ &= 55,526 \text{ lb (247 kN)} \end{aligned}$$

$$\begin{aligned} T_{sn} &= 0.612 \times 29 \times 10^6 \left[ 0.0052 + 0.003 \left( \frac{12 - 14}{14} \right) + 0.0005 \right] \\ &= 93,557 \text{ lb (416 kN)} \end{aligned}$$

$$P_n = C_{cn} - T'_{sn} - T_{sn} = 749,700 - 55,526 - 93,557$$

$$\begin{aligned}
 &= 600,617 \text{ lb (2,672 kN)} \\
 M_n &= 749,700 \left( \frac{14}{2} - \frac{10.5}{2} \right) \curvearrow - 55,526 \left( \frac{14}{2} - 2 \right) \curvearrow + 93,557 \left( 12 - \frac{14}{2} \right) \curvearrow \\
 &= 1,502,130 \text{ in.-lb (170 kN-m)} \\
 e_2 &= \frac{1,502,130}{600,617} = 2.50 \text{ in. (63.5 mm)}
 \end{aligned}$$

### 3. Pure Bending: $P_u = 0$

Neglecting the effect of the compression steel  $A'_{ps}$ , we have

$$a = \frac{A_{ps} f_{ps}}{0.85 f'_c b} = \frac{0.612 \times 240,000}{0.85 \times 6,000 \times 14} = 2.06 \text{ in. (52.3 mm)}$$

$$c = \frac{2.06}{0.75} = 2.75 \text{ in. (69.9 mm)}$$

$$M_n = A_{ps} f_{ps} \left( d - \frac{a}{2} \right) = 0.612 \times 240,000 \left( 12 - \frac{2.06}{2} \right)$$

$$= 1,611,274 \text{ in.-lb}$$

$$e_3 = \frac{1,611,274}{0} = \infty$$

### 4. Limit Strain Condition: $P_n, M_n, e$

Assume the strain in the tensile strands  $A_{ps}$  to be equal to the incremental strain  $\Delta\epsilon_p$  beyond the service-load level  $P_e$ . Taking a value  $\Delta\epsilon_p \cong 0.0014$  to be modified by trial and adjustment, and from Figure 8.8, similar triangles give

$$\frac{c}{(d - c)} = \frac{\epsilon_{cu}}{\Delta\epsilon_p} = \frac{0.003}{0.0014}$$

Hence  $c = 8.15 \text{ in. (207 mm)}$ . So

$$a = \beta_1 c = 0.75 \times 8.15 = 6.11 \text{ in. (155 mm)}$$

$$C_{cn} = 0.85 \times 6,000 \times 6.10 \times 14 = 435,540 \text{ lb (1,937 kN)}$$

$$T'_{sn} = 0.612 \times 29 \times 10^6 \left[ 0.0052 - 0.003 \left( \frac{8.13 - 2}{8.13} \right) + 0.0005 \right]$$

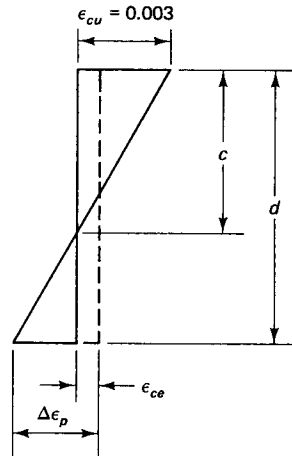


Figure 8.8 Strain distribution.

$$\begin{aligned}
 &= 61,018 \text{ lb (271 kN)} \\
 T_{sn} &= 0.612 \times 29 \times 10^6 \left[ 0.0052 + 0.003 \left( \frac{12 - 8.13}{8.13} \right) + 0.0005 \right] \\
 &= 126,509 \text{ lb (563 kN)}
 \end{aligned}$$

The *limit* strain state for  $P_n$ ,  $M_n$ , and  $e$  are as follows:

$$\begin{aligned}
 P_n &= 435,540 - 61,018 - 126,509 = 248,013 \text{ lb (1,103 kN)} \\
 M_n &= 435,540 \left( \frac{14}{2} - \frac{6.10}{2} \right) - 61,018 \left( \frac{14}{2} - 2 \right) + 126,509 \left( 12 - \frac{14}{2} \right) \\
 &= 2,047,838 \text{ in.-lb (272 kN-m)} \\
 e_4 = e &= \frac{2,047,838}{248,013} = 8.26 \text{ in. (210 mm)}
 \end{aligned}$$

The coordinates for the preceding four cases are the controlling points on the  $P_n$ - $M_n$  interaction diagram. Other points need to be computed as well, in order to develop an accurate diagram to cover the entire loading range. For example, additional points between the coordinates of the second and third cases have to be determined, assuming additional values of the neutral axis depth  $c$  and computing  $P_n$ ,  $M_n$ , and  $e$  for the  $c$ -values assumed. Table 8.1 summarizes the values of the coordinates used for plotting the  $P_n$ - $M_n$  interaction diagram as well as the  $P_u$ - $M_u$  design diagram. From the diagram, it is seen that the maximum moment ordinate seems to have a value close to  $M_n = 2,047,838$  in.-lb. Hence, an assumption of  $c_b = 8.15$  in. is verified.

**Design Load-Moment ( $P_u$ - $M_u$ ) Diagram.** From Section 8.3. Construct the  $P$ - $M$  interaction diagram for the coordinates listed in Table 8.1. For step 7 in the diagram, the column is in the transition zone, as  $c/d_t = 6.0/12.0 = 0.50 < 0.60$  for the limit balanced strain in compression.

From Equation 8.9 (a),

$$\begin{aligned}
 \phi &= 0.65 + 0.25 \left[ \frac{1}{c/d_t} - \frac{5}{3} \right] \\
 &= 0.65 + 0.25 \left( \frac{1}{0.50} - \frac{5}{3} \right) = 0.73
 \end{aligned}$$

$$\begin{aligned}
 \text{Hence, } P_u &= 101.2 \times 10^3 \times 0.73 = 73.7 \times 10^3 \text{ lb,} \\
 M_u &= 1969.9 \times 10^3 \times 0.73 = 1438.0 \times 10^3 \text{ in.-lb.}
 \end{aligned}$$

**Table 8.1** Summary of  $P$ - $M$  Interaction Diagram Coordinates in Example 8.1

Point	$c$ in.	$a$ in.	$P_n \times 10^3$ lb	$M_n \times 10^3$ in.-lb	$\phi$	$P_u \times 10^3$ lb	$M_u \times 10^3$ in.-lb	$e$ in.
1	$\infty$	14	903.8	0	0.65	587.5	0	0
5	18	13.5	826.6	388.9	0.65	537.3	252.8	0.5
2	14	10.5	600.6	1,502.1	0.65	390.4	976.4	2.5
6	10	7.5	365.1	2,005.6	0.65	237.3	1303.6	5.5
4	8.15	6.1	248	2,047.9	0.65	161.2	1331.1	8.3
7	6	4.5	101.2	1,969.9	0.73	73.9	1438.0	19.5
3	2.75	2.1	0	1,611.3	0.90	0	1,450.1	$\infty$

\*Max  $P_u$  allowed by the code for tied columns =  $0.80\phi P_n = 469.6 \times 10^3$  lb (2090 kN). Also,

1,000 lb = 4.448 kN

1,000 in.-lb = 1.1130 kN-m

1 in. = 25.4 mm.

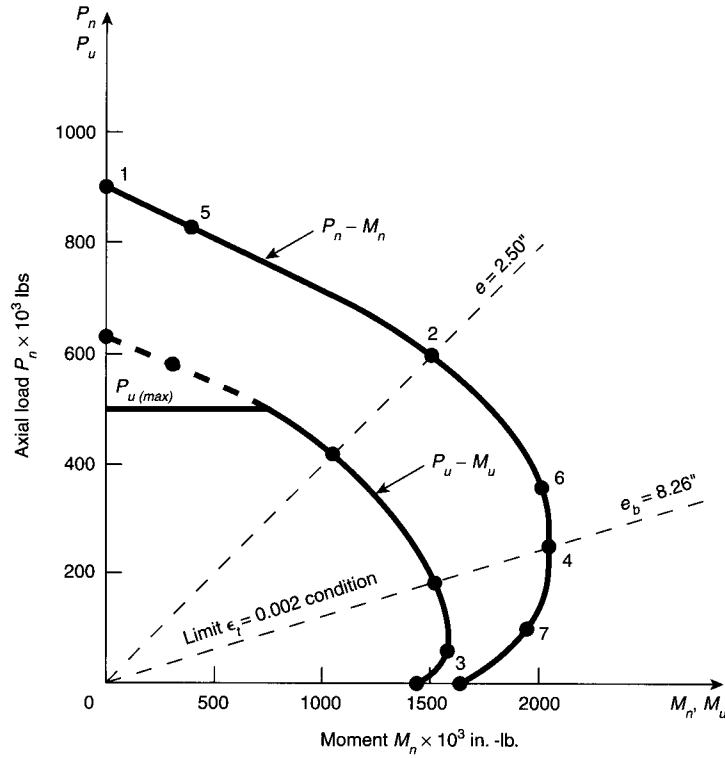


Figure 8.9 Load-moment interaction plots in Example 8.1.

$$M_{u3} \text{ for pure bending} = \phi M_{n3} = 0.90 \times 1,611,274 = 1,450,147 \text{ in.-lb (164 kN-m)}$$

$$P_{u1} = \phi P_n = 0.65 \times 903,760 = 587,444 \text{ lb (not usable)}$$

The ACI Code requires that the maximum design axial load strength  $\phi P_n$  for tied prestressed columns should not exceed  $0.80\phi P_n$ , and for spirally reinforced prestressed columns should not exceed  $0.85\phi P_n$ . We thus have

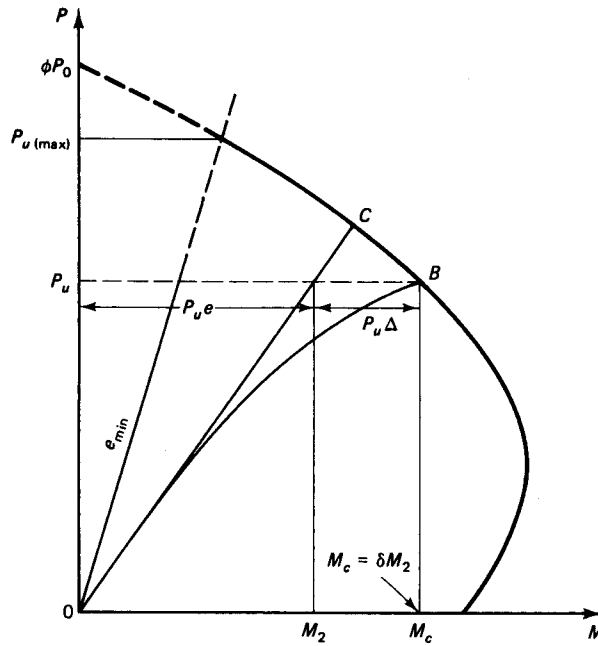
$$\begin{aligned} \text{Max } P_u &= 0.8\phi P_n = 0.8 \times 587,444 \\ &= 469,955 \text{ lb (2090 kN)} \end{aligned}$$

$$P_{u5} = 0.65 \times 826,648 = 537,321 \text{ (2,574 kN)}$$

The remaining values of the coordinates are summarized in Table 8.1. Plots of the interaction diagrams for the nominal strength ( $P_n - M_n$ ) and the design strength ( $P_u - M_u$ ) are shown in Figure 8.9.

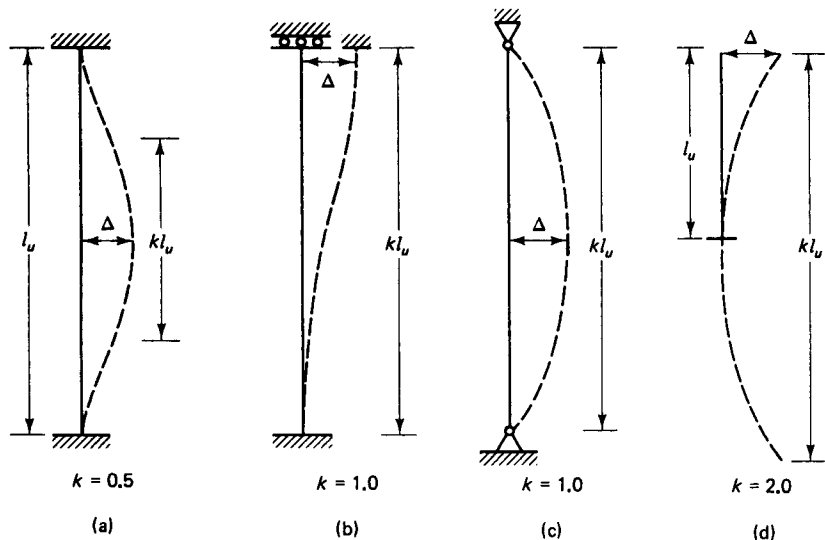
### 8.6 LIMIT STATE AT BUCKLING FAILURE OF SLENDER (LONG) PRESTRESSED COLUMNS

Considerable literature exists on the behavior of columns subjected to stability testing. If the column slenderness ratio exceeds the limits for short columns, the compression member will buckle prior to reaching its limit state of material failure. The strain in the com-



**Figure 8.10** Loading moment ( $P$ - $M$ ) magnification interaction diagram.

pression face of the concrete at buckling load will then be less than the 0.003 in./in. shown in Figure 8.10. Such a column would be a slender member subjected to combined axial load and bending, deforming laterally and developing additional moment due to the  $P\Delta$  effect, where  $P$  is the axial load and  $\Delta$  is the deflection of the column's buckled shape at the section being considered.



**Figure 8.11** Values of column length factor  $k$  for typical end conditions. (a) Fixed-fixed. (b) Fixed-fixed with lateral motion. (c) Pinned. (d) Fixed-free.

Consider a slender column subjected to axial load  $P_u$  at an eccentricity  $e$ . The buckling effect produces an additional moment of  $P_u \Delta$ . This moment reduces the load capacity from point  $C$  to point  $B$  in the interaction diagram of Figure 8.10. The total moment  $P_u e + P_u \Delta$  is represented by point  $B$  in the diagram, and the column can be designed for a larger or magnified moment  $M_c$  as a nonslender column.

The effective length  $kl_u$  shown in Figure 8.11 is used as the modified length of the column to account for end restraints other than being pinned.  $kl_u$  represents the length of an auxiliary pin-ended column which has an Euler buckling load equal to that of the column under consideration. Alternatively, it is the distance between the points of contraflexure of the member in its buckled form.

The value of the end restraint effective length factor  $k$  varies between 0.5 and 2.0 according to the nature of the restraint as follows:

Both column ends pinned, no lateral motion	$k = 1.0$
Both column ends fixed	$k = 0.5$
One end fixed, other end free	$k = 2.0$
Both column ends fixed, lateral motion exists	$k = 1.0$

Typical cases illustrating the buckled shape of the column for several end conditions and the corresponding length factors  $k$  are shown in Figure 8.11.

For members in a structural frame, the end restraint lies between the hinged and fixed conditions. The actual  $k$  value can be determined from the Jackson and Moreland alignment charts in Figure 8.12. In lieu of these charts, the following equations suggested in the ACI Code commentary can also be used for computing  $k$ :

1. *Braced compression members.* An upper bound to the effective length factor may be taken as the smaller of the expressions

$$k = 0.7 + 0.05(\psi_A + \psi_B) \leq 1.0 \quad (8.10a)$$

and

$$k = 0.85 + 0.05\psi_{\min} \leq 1.0 \quad (8.10b)$$

where  $\psi_A$  and  $\psi_B$  are the values of  $\psi$  at the two ends of the column and  $\psi_{\min}$  is the smaller of the two values.  $\psi$  is the ratio of the stiffness of all compression members to the stiffness of all flexural members in a plane at one end of the column. That is,

$$\psi = \frac{\sum EI/l_u \text{ columns}}{\sum EI/l_n \text{ beams}} \quad (8.11)$$

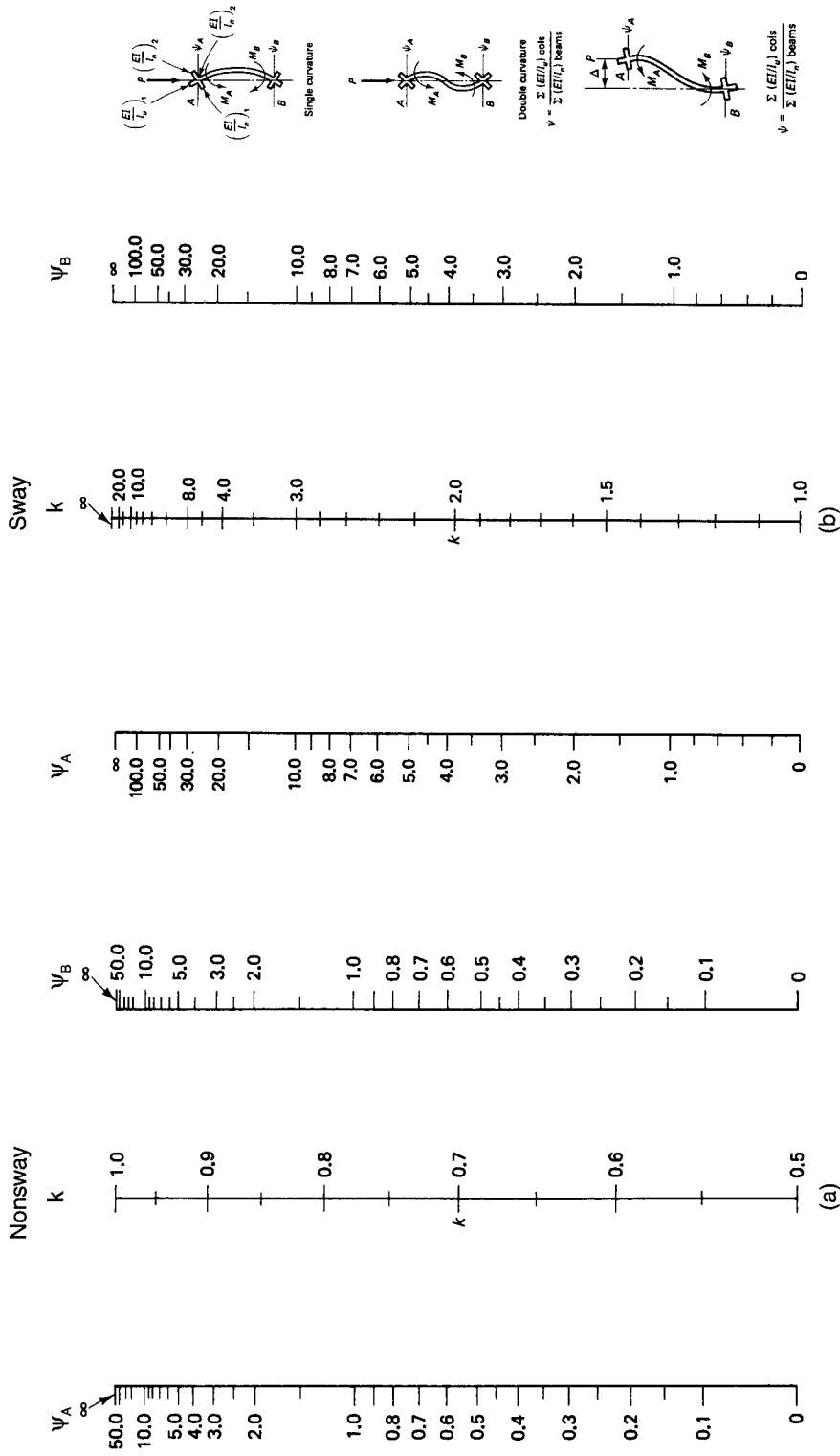
where  $l_u$  is the unsupported length of the column and  $l_n$  is the clear beam span.

2. *Unbraced compression members restrained at both ends.* The effective length may be taken as follows:

For  $\psi_m < 2$ ,

$$k = \frac{20 - \psi_m}{20} \sqrt{1 + \psi_m} \quad (8.12a)$$





$\psi$  = ratio of  $\sum(EI/\ell_0)$  of compression members to  $\sum(EI/\ell)$  of flexural members in a plane at one end of a compression member  
 $\ell$  = span length of flexural member measured center to center of joints

**Figure 8.12** Jackson and Moreland effective length factor  $k$  for (a) Nonsway (braced) frames and (b) Sway (nonbraced) frames.

For  $\psi_m \geq 2$ ,

$$k = 0.9\sqrt{1 + \psi_m} \quad (8.12b)$$

where  $\psi_m$  is the average of the  $\psi$  values at the two ends of the compression member.

3. *Unbraced compression members hinged at one end.* The effective length factor may be taken as

$$k = 2.0 + 0.3\psi \quad (8.13)$$

where  $\psi$  is the value at the restrained end.

The radius of gyration  $r = \sqrt{I_g/A_g}$  can be taken as  $r = 0.3h$  for rectangular sections, where  $h$  is the column dimension perpendicular to the axis of bending. For circular sections,  $r$  is taken as  $0.25h$ .

### 8.6.1 Buckling Considerations

Frames that do not have lateral bracing such as shear walls, diaphragms, or diagonal coupling beams are more flexible than those which are braced laterally. Lateral flexibility can cause the mass of a structure to sufficiently displace horizontally above the foundations that significant additional overturning moments can result leading to loss of stability of the structure. This behavior is particularly critical when nonslender columns support the floors.

The ACI 318 Code stipulates three methods for determining the forces on slender columns and members in frames that resist lateral forces in addition to the vertical gravity loads. However, for gravity loading *without* side-sway, a first-order analysis using moment magnification factors,  $\delta_{ns}$ , is adequate. For combined gravity and side-sway forces causing the  $P$ - $\Delta$  effect, the three code methods are:

- (a) Computer programs using a second-order analysis that determines iteratively the magnitudes of the additional overturning moments in a frame.
- (b) Moment magnification factors  $\delta_s$  are computed on the basis of first-order lateral displacements and the mass above each level.
- (c) Moment magnification relationship similar in form to those required for computing the no-sway magnifier,  $\delta_{ns}$ , for columns in braced frames using a stability index,  $Q$ . Horizontal displacement in this method need not be evaluated but moments that resist lateral forces have to be computed. This method is too cumbersome and least accurate. While the most accurate is the method in (a) using computer programs such as PCA's Frame Program, STAAD Pro, CSI Sap2008, RISA, and others.

Consider a slender column subjected to axial load  $P_u$  at an eccentricity  $e$ . The buckling effect produces an additional moment  $P_u \Delta$  where  $\Delta$  is the maximum lateral displacement of the compression member between its two ends from the vertical "plumb" position. This additional moment reduces the load capacity from point  $C$  to point  $B$  in the interaction diagram, Figure 8.10. The total moment ( $P_u e + P_u \Delta$ ) is represented by point  $B$  in the diagram and the column should be designed for a larger magnified moment  $M_c$  as a non-slender column by the usual *first-order analysis*.

In such an analysis, the moments and axial forces in a frame are obtained by the classical elastic procedures. These procedures do not consider the effects of the lateral displacement  $\Delta$  on the axial force  $P_u$  and the bending moment  $M_c$ . Consequently the re-

sulting load-deflection and load-moment relationships are linear. If the  $P-\Delta$  effect is taken into account, a second-order analysis becomes necessary with a resulting nonlinear relationship of the load to the lateral displacement (deflection) and the moment. The ACI 381-02 Code permits using either a first- or a second-order analysis for columns of intermediate slenderness and requires a second-order analysis for long columns having a slenderness ratio of 100 or more. One ACI Code method where the  $P-\Delta$  effect is ignored is termed the moment magnification method presented in Section 8.7.

## 8.7 MOMENT MAGNIFICATION METHOD: FIRST-ORDER ANALYSIS

The factored axial forces,  $P_u$ , the factored moments  $M_1$  and  $M_2$  at the column ends, and, where required, the relative story deflections, are computed in this method using an elastic first-order analysis with the section properties determined taking into account the influence of axial loads, the presence of cracked regions along the length of the member and the effects of duration of the load.

As discussed in Section 8.6 in conjunction with Figure 8.10, the moment  $M_2$  is magnified by a magnification factor  $\delta$ . The column is subjected to moments  $M_1$  and  $M_2$  at its ends where  $M_2$  is considered larger than  $M_1$ . The factored axial force,  $P_u$ , and the factored moments,  $M_1$  and  $M_2$ , are resisted by analytically chosen sectional properties taking into account the cracked regions along the compression member's length or height and the load duration. In lieu of these computations, the ACI 318 Code allows using the following average values for properties of members in a structure:

- (a) Modulus of elasticity  $E_c = 33w_c^{1.5} f'_c$  and for concrete strength  $f'_c > 5000$  psi  $< 12,000$  psi  $E_c = (40,000 + 1 \times 10^6) (w_c/145)^{1.5}$
- (b) Moment of Inertia

Beams:	$0.35I_g$
Columns	$0.70I_g$
Walls—Uncracked	$0.70I_g$
—Cracked	$0.35I_g$
Flat plates and flat slabs:	$0.25I_g$

- (c) Area:  $1.0A_g$
- (d) Radius of gyration  $r = 0.30h$  for rectangular members where  $h$  is in the direction stability is being considered, or  $r = 0.25D$  for circular members where  $D$  is the diameter of the compression member.

The moments of inertia should be divided by  $(1 + \beta_d)$  when sustained lateral loads act, or for stability checks where  $\beta_d$  is a creep factor, thus

$$\beta_d = \frac{\text{maximum factored sustained axial load}}{\text{total factored axial load}}$$

Hence, for *non-sway* frames,  $\beta_d$  is the ratio of maximum factored *sustained* axial load to maximum factored axial load associated with the same load combination. For *sway* frames, as load combinations involve lateral loads, the strength and stability of the structure as a whole under factored gravity loads should be considered, with  $\beta_d$  as the ratio of maximum factored *sustained* shear within a story to the maximum factored shear in that story.

The column load is assumed to act at an eccentricity  $(e + \Delta)$  in Figure 8.10 to produce a moment  $M_c$ . The ratio  $M_c/M_2$  is termed the magnification factor  $\delta$ . The degree of magnification is dependent on the slenderness ratio  $kl_u/r$  where  $k$  is the effective length

factor for compression members, a function of the relative stiffnesses at the joint of each end of the member.

The magnification factor is controlled by the type of the magnified moments  $\delta M_2$  and  $\delta M_1$  acting at the respective ends 2 and 1 of a column, namely, whether side-sway of the structural frame occurs or not. It should be noted that in the case of compression members subjected to bending about both principal axes, the moment about each axis should be *separately* considered based on the restraint condition corresponding to that axis.

### 8.7.1 Moment Magnification in Non-Sway Frames

In the case of compression members in non-sway frames, namely, braced frames, the effective length factor  $k$  can be taken as 1.0, unless analysis gives a lower value. In such a case,  $k$  values are computed on the basis of the  $EI$  values tabulated in Section 8.7 and the monograms in Figure 8.12.

The slenderness effects can be disregarded if

$$\frac{kl_u}{r} \leq 34 - 12 \left( \frac{M_1}{M_2} \right) \quad (8.14)$$

$kl_u$  = effective length between points of inflection and  $[34 - 12 (M_1/M_2)]$  cannot be taken greater than the limit of Eq. 8.14. The term  $(M_1/M_2)$  is positive if the member is bent in a single curvature so that the two terms subtract in Equation 8.12 and negative in double curvature so that the two terms add (see Figure 8.12a). If the non-sway magnification factor is  $\delta_{ns}$  and the sway factor  $\delta_s = 0$ , the magnified moment becomes

$$M_c = \delta_{ns} M_2 \quad (8.15)$$

where

$$\delta_{ns} = \frac{C_m}{1 - \frac{P_u}{0.75P_c}} \geq 1.0 \quad (8.16a)$$

$$P_c = \frac{\pi^2 EI}{(kl_u)^2} \quad (8.16b)$$

where  $P_c$  is the Euler buckling load for pin-ended columns. Stiffness  $EI$  is to be taken as

$$EI = \frac{0.2E_c I_g + E_s I_{se}}{1 + \beta_d} \quad (8.16c)$$

or conservatively as

$$EI = \frac{0.4E_c I_g}{1 + \beta_d}$$

$C_m$  = a factor relating the actual moment diagram to an equivalent uniform moment diagram. For members without transverse loads, namely, subjected to end loads only,

$$C_m = 0.6 + \frac{M_1}{M_2} \geq 0.4 \quad (8.17)$$

where  $M_2 \leq M_1$  and  $M_1/M_2 > 0$  if no inflection point exists between the column ends, Figure 8.12a (single curvature). For other conditions, such as members with transverse loads between supports,  $C_m = 1.0$ .

The minimum allowed value of  $M_2$  is

$$M_{2,\min} = P_u(0.6 + 0.03h) \quad (8.18)$$

where  $h$  is in inches. In SI units  $M_{2,\min} = P_u (15 + 0.03h)$  where  $h$  is in millimeters. In other words, the minimum eccentricity in the slender columns is  $e_{\min} = 0.6 + 0.03h$ . If  $M_{2,\min}$  ex-

ceeds the applied moment  $M_2$ , the value of  $C_m$  in Equation 8.17 should either be taken as 1.0 or be based on the actual computed end moments  $M_1$  and  $M_2$ .

Frames braced against side-sway or braced with shear walls, would normally have a lateral deflection less than total height  $h_s/1500$ . Once this ratio is exceeded, appropriate measures have to be taken to minimize the additional moments caused by side sway and hence reduce lateral drift of the frame and its constituent columns.

### 8.7.2 Moment Magnification in Sway Frames

For compression members not braced against side-sway, the effective length factor  $k$  can also be determined from the  $EI$  values presented in Section 8.7, but its value should not exceed 1.0. The slenderness effects can be disregarded if

$$\frac{kl_u}{r} < 22 \quad (8.19)$$

The end moments  $M_1$  and  $M_2$  should be magnified as follows:

$$\begin{aligned} M_1 &= M_{1ns} + \delta_s M_{1s} \\ M_2 &= M_{2ns} + \delta_s M_{2s} \end{aligned} \quad (8.20)$$

On the assumption that  $M_2 > M_1$ , the design moment should be

$$M_c = M_{2ns} + \delta_s M_{2s} \quad (8.21)$$

where  $M_{2ns}$  = factored end moment at the end of the compression member due to loads that cause no appreciable side-sway, computed using a first-order elastic frame analysis.  $M_{2s}$  = factored end moment at the end of the compression members due to loads that cause appreciable side-sway, computed using a first-order elastic frame analysis.

$$\delta_s M_s = \frac{M_s}{1 - \frac{\Sigma P_u}{0.75 \Sigma P_c}} \geq M_s \leq 2.5 \quad (8.22)$$

where  $\Sigma P_u$  is the summation for all the vertical loads in a story and  $\Sigma P_c$  is the summation of the Euler buckling loads,  $P_c$ , for pin-ended columns for all sway resisting columns in a story [ $P_c = \pi^2 EI / (kl_u)^2$ ] from Equation 8.16b) with the  $EI$  values obtained from Equations 8.16c or d.

In the case of an individual compression member having

$$\frac{l_u}{r} > \frac{35}{\sqrt{P_u / f'_c A_g}}$$

the member has to be designed for a factored axial load,  $P_u$ , and magnified moment  $M_c = \delta_{ns} M_2$  where  $M_2$  in this case is  $M_2 = \delta_{ns} M_{2ns} + \delta_s M_{2s}$ . This condition can develop in slender columns with high axial loads when the maximum moment may develop *between* the ends of the column so that the end moments might not necessarily be the maximum moments.

**8.7.2.1 Moment magnification in sway frames using a stability index,  $Q$ .** In this method (method c in Section 8.6.1), the code permits assuming a column in a braced structure as non-sway if the increase in column loads and moments due to second-order effects does not exceed 5 percent of the first-order end moments. A story within a structure can be considered non-sway if a stability index,  $Q$ , in the following expression does *not* exceed a value of 0.05:

$$Q = \frac{\Sigma P_u \Delta_o}{V_u l_c} \quad (8.23a)$$

where,

$\Sigma P_u$  = total vertical load at a story

$V_u$  = story shear

$\Delta_o$  = first-order relative deflection between the top and bottom of a particular story due to shear  $V_u$

$l_c$  = length of compression member in a frame measured from centers of joints.

The non-sway magnification factor in terms of  $Q$  is:

$$\delta_s = \frac{1}{1 - Q} \geq 1.0 \quad (8.23b)$$

When  $Q$  exceeds a value of 0.05, one has to proceed to a second-order analysis through computer program usage. Such a computer analysis would make it possible to efficiently compute the iterating values of moments and  $\Delta_o$  sway values due to the  $P-\Delta$  effect in a reasonably accurate and speedy manner.

It should be noted that the stability index  $Q$  method, while relatively adaptable to hand computations, is too cumbersome and least accurate for effective evaluation of the  $P-\Delta$  effect on moments at the column joints in braced frames.

It is important to summarize that the moment magnification method, originally developed for prismatic columns, should work well for columns of slenderness ratio  $kl_u/r$  less than 100, particularly if the frame is braced. In the case of unbraced frames of comparable slenderness ratios, taking into account the  $P-\Delta$  effect on the moments and deflections through a second-order analysis should be used so as to give more accurate results. Such an analysis can be either

1. Execute several applications of the first-order analysis where the lateral load (from  $h_i$  in Figure 8.13 to follow) is incremented by  $\Sigma P_u \Delta_i$  in each cycle, and consider the final result a second-order result, or
2. Use a real second-order analysis computer program in which the reduction in the relative side-sway resistance is used in a global stiffness matrix for the elements involved.

## 8.8 SECOND-ORDER FRAMES ANALYSIS AND THE $P - \Delta$ EFFECTS

A second-order analysis is a frame analysis which includes the internal force effects resulting from lateral displacement (deflection) of a column. When such an analysis is performed in order to evaluate  $\delta_s M_s$  in a non-braced frame, the deflections must be computed on the basis of fully cracked sections with reduced  $EI$  stiffness values. Approximations such as the use of several first-order analysis cycles and idealizations of non-prismatic sections can be made in the analysis. But the analysis should verify that the predicted strength of the compression members of a structural frame are in good agreement within a 15-percent range with results for columns in indeterminate reinforced concrete structures. The structure being analyzed should result in geometry of members similar to the geometry of the sections to be built. If the members in the final structure have cross-sectional dimensions differing by more than 10 percent from those assumed in the analysis, a new computation cycle has to be performed.

A second-order analysis is an iterative procedure of the  $P - \Delta$  effects on the slender column, including shear deformations. Hence, it is reasonable to expect that canned computer programs have to be used rather than long-hand computations in the design of the slender columns of a frame structure. An attempt will be made here to illustrate the iteration procedure involved in the use of several cycles of lateral load increments to the  $P - \Delta$  values. It must be stated, however, that the large majority of columns in concrete

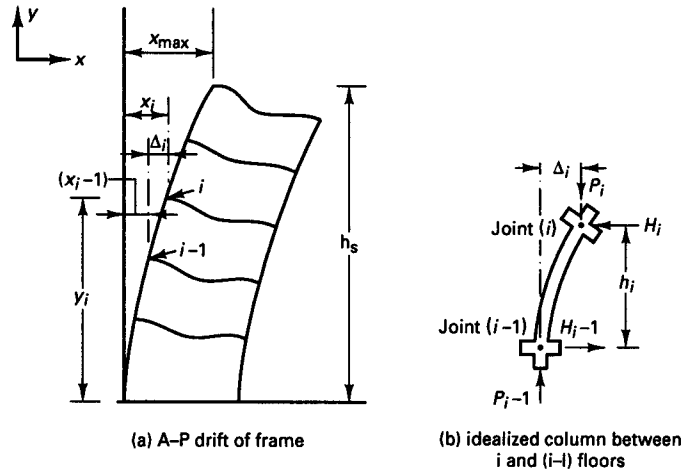


Figure 8.13 Second-order frame parameters.

building frames do not necessitate such an analysis since the  $(kl_u/r)$  ratio is in most cases below 100.

Consider the column between the two floors  $(i-1)$  and  $(i)$  in the frame shown in Figure 8.13. Assume that the maximum lateral displacement or drift at the upper end of the top column in the frame is  $x_{\max}$  and that the total height of the building is  $h_s$ . A large drift, or lateral displacement of the building upper floors results in cracking of the masonry and interior finishes. Unless precautions are taken to permit movement of interior partitions without damage, the maximum lateral deflection limitation should be  $h_s/500$ . Hence, a good assumption is to choose  $x_{\max}$  in the range of  $h_s/350$  to  $h_s/500$ , considering that a *fully braced* frame has normally a ratio of maximum drift  $x_{\max}$  to frame height  $h_s$  less than  $1/1,500$ .

If  $x_i$  is the drift at floor level  $i$ , and  $y_i$  is the height of the column between floors  $(i-1)$  and  $(i)$  in Figure 8.13a, it can be assumed that the proportional horizontal drift for a particular floor is directly proportional to the square of the ratio of the height  $h_i$  of the floor and the total height  $h_s$  of the entire frame. Hence,

$$x_i = x_{\max}(h_i/h_s)^2 \quad (8.24)$$

The procedure can be summarized as follows:

1. Choose geometrical sections of the frame and its columns and their stiffness  $EI$  by approximate procedures.
2. Compute the drifts, namely, the lateral deflections  $\Delta_i$ , and the corresponding ultimate loads  $P_{u,i}$  at joints  $i = 1, \dots, n$  (Figure 8.13).
3. Find the equivalent horizontal forces  $H_i$  from  $H_i = P_i \Delta_i/h_i$  (Figure 8.13b).
4. Add the values obtained in step 3 to the actual lateral loads acting on the frame.
5. Perform a frame analysis using the appropriate computer program.
6. The iterative computer program, using the stiffnesses,  $EI$ , chosen for the input data, gives  $\Delta_i$  results that have to be compared with the  $x_i$  values allowed.
7. If all  $\Delta_i$  values are  $\leq$  all the  $x_i$  values, accept the solution and the design as a second order solution. If not, run additional computer cycles with modified stiffnesses until the desired results are achieved.

Any of several computer programs can be used to account for the  $P$ - $\Delta$  effects in frame side-sways. Strudel, PCA Frame, STAAD Pro, or CSI Sap 2000 are examples of such general-purpose programs.

## 8.9 OPERATIONAL PROCEDURE AND FLOWCHART FOR THE DESIGN OF SLENDER COLUMNS

1. Determine whether the frame has an appreciable side-sway. If it does, use the magnification factors  $\delta_{ns}$  and  $\delta_s$ . If the side-sway is negligible, assume that  $\delta_s = 0$ . Then assume a cross section, compute the eccentricity, using the greater of the end moments, and check whether it is more than the minimum allowable eccentricity, that is,

$$\frac{M_2}{P_u} \geq (0.6 + 0.03h) \text{ in.}$$

If the given eccentricity is less than the specified minimum, use the minimum value.

2. Compute  $\psi_A$  and  $\psi_B$  using Equation 8.12 or 8.13, and then obtain  $k$  using Figure 8.12 or Equations 8.13. Compute  $kl_u/r$ , and determine whether the column is a short or long column. If the column is slender and  $kl_u/r$  is less than 100, compute the magnified moment  $M_c$ . Then, using the value obtained, compute the equivalent eccentricity to be used if the column is to be designed as a short column. If  $kl_u/r$  is greater than 100, perform a second-order analysis.
3. Design the equivalent non-slender column. The flowchart in Figure 8.14 presents the sequence of calculations. The necessary equations are provided in Section 8.2 and in the flowchart.

## 8.10 DESIGN OF SLENDER (LONG) PRESTRESSED COLUMN

### Example 8.2

A square tied prestressed bonded column is part of a  $5 \times 3$  bays frame building subjected to uniaxial bending. Its clear height is  $l_u = 15$  ft (4.54 in.), and it is not braced against sidesway. The factored external load  $P_u = 300,000$  lb (1,334 kN), and the factored end moments are  $M_1 = 425,000$  in.-lb (48.0 kN-m) and  $M_2 = 750,000$  in.-lb (84.8 kN-m). Design the column section and the reinforcement necessary for the following two conditions:

1. Consider gravity loads only, assuming negligible lateral sidesway due to wind.
2. Suppose sidesway wind effects cause a factored  $P_u = 24,000$  lb (107 kN) and a factored  $M_u = 220,000$  in.-lb (24.9 kN-m). The loads per floor of all columns at that level are  $\Sigma P_u = 4.5 \times 10^6$  lb ( $20 \times 10^3$  kN) and  $\Sigma P_c = 31.0 \times 10^6$  lb ( $138 \times 10^3$  kN).

Use  $\frac{1}{2}$ -in. dia 270-K stress-relieved prestressing strands. Given data are as follows:

$$\beta_d = 0.4$$

$$\psi_A = 1.0$$

$$\psi_B = 2.0$$

$$f'_c = 6,000 \text{ psi (41.4 MPa)}$$

$$f_{pu} = 270,000 \text{ psi (1,862 MPa)}$$

$$f_{ps} = 240,000 \text{ psi (1,655 MPa)}$$

$$f_{pe} = 150,000 \text{ psi (1,034 MPa)}$$

$$E_{ps} = 28 \times 10^6 \text{ psi (200} \times 10^3 \text{ MPa)}$$



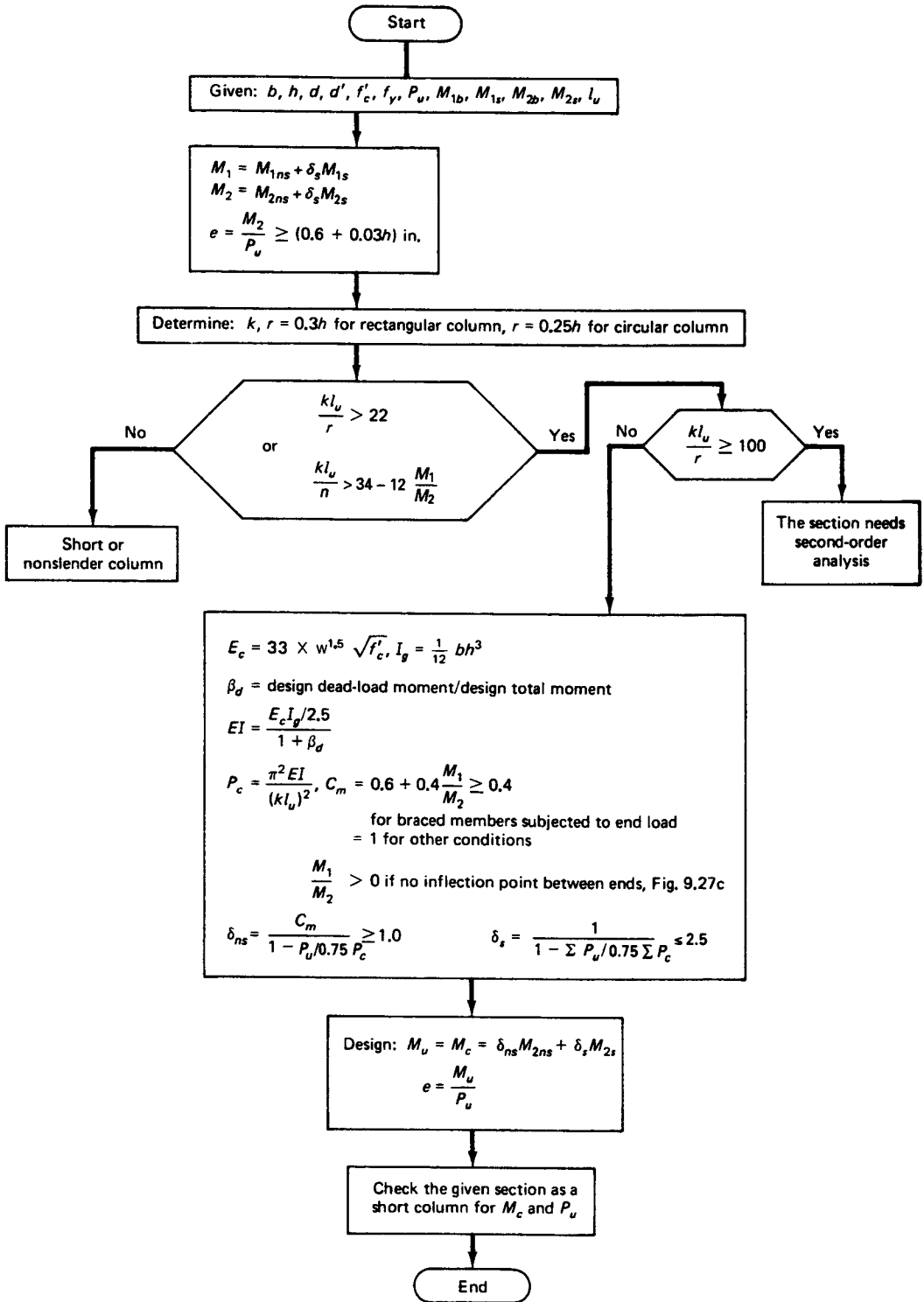


Figure 8.14 Flowchart for design of slender columns.

$$\epsilon_{cu} \text{ at failure} = 0.003 \text{ in./in.}$$

$$\epsilon_{ce} = 0.0005 \text{ in./in. when } P_e \text{ acts on the section}$$

$$d' = 2 \text{ in. (50.8 mm)}$$

$$\text{Ties } f_y = 60,000 \text{ psi (414 MPa)}$$

The stress-strain diagram of the prestressing steel is as in Figure 8.7.

**Solution:**  $\epsilon_{pe} = 0.0052 \text{ in./in.}$  from the stress-strain diagram of Figure 8.7, corresponding to  $f_{pe} = 150,000 \text{ psi}$ . Similarly,  $\epsilon_{py} \cong 0.012 \text{ in./in.}$  from the same figure, corresponding to  $f_{py} = 260,000 \text{ psi}$ .

### 1. Gravity Loads Only

*Check for No Sidesway and Minimum Eccentricity (Step 1).* Since the frame has no appreciable sidesway, the entire  $M_2$  is taken to be  $M_{2ns}$  and the magnification factor for sidesway,  $\delta_s$ , is taken to be equal to zero in Equation 8.15. By trial and adjustment, a column section is assumed and analyzed. Accordingly, we try a section 15 in.  $\times$  15 in. (381 mm  $\times$  381 mm) as shown in Figure 8.15(a) and obtain

$$\text{Actual eccentricity} = \frac{M_{2ns}}{P_u} = \frac{750,000}{300,000} = 2.50 \text{ in. (63.5 mm)}$$

$$\begin{aligned} \text{Minimum allowable eccentricity} &= 0.6 + 0.03h = 0.6 + 0.03 \times 15 \\ &= 1.05 \text{ in. (2.67 mm)} < 2.50 \text{ in.} \end{aligned}$$

Hence, use  $M_{2ns} = 750,000 \text{ in.-lb}$  as the larger of the moments  $M_1$  and  $M_2$  on the column.

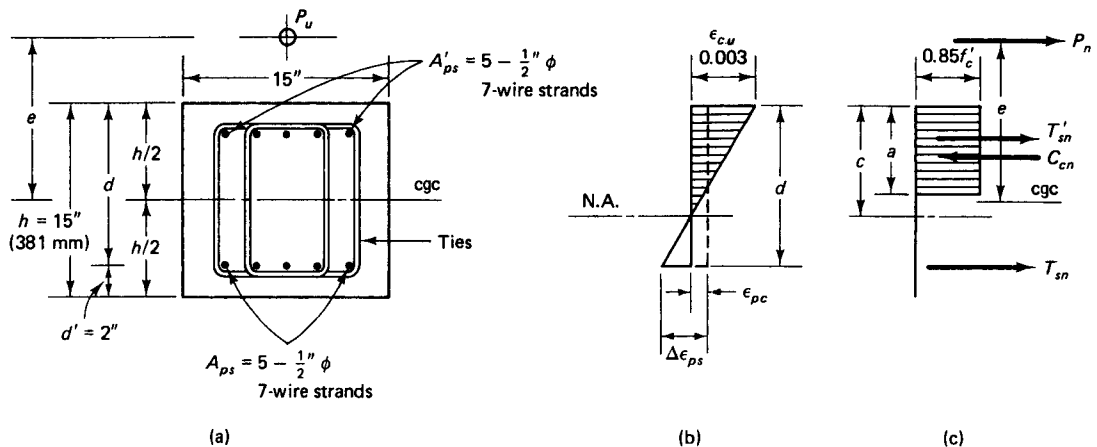
*Compute the Eccentricity to Be Used for Equivalent Short Column (Step 2).* From the chart in Figure 8.12(b),  $k = 1.45$  and the slenderness ratio is

$$\frac{kl_u}{r} = \frac{1.45 \times 15 \times 12}{0.3 \times 15} = 58.0$$

Since  $58.0 > 22$  and  $< 100$ , use the moment magnification method. We obtain

$$E_c = 33w^{1.5}\sqrt{f'_c} = 33 \times 145^{1.5}\sqrt{6,000} = 4.46 \times 10^6 \text{ psi (} 32 \times 10^3 \text{ MPa)}$$

$$I_g = \frac{15(15)^3}{12} = 4,218.8 \text{ in.}^4$$



**Figure 8.15** Proposed column section geometry in Example 8.2. (a) Cross-sectional details. (b) Strain distribution. (c) Stress block and forces.

$$EI = \frac{E_c I_g / 2.5}{1 + \beta_d} = \frac{4.46 \times 10^6 \times 4,218.3}{2.5} \times \frac{1}{1 + 0.4}$$

$$= 5.34 \times 10^9 \text{ lb.-in.}^2$$

$$(kl_u)^2 = (1.45 \times 15 \times 12)^2 = 68.1 \times 10^3 \text{ in.}^2$$

Hence,

$$P_c = \text{Euler buckling load} = \frac{\pi^2 EI}{(kl_u)^2} = \frac{\pi^2 \times 5.34 \times 10^9}{68.1 \times 10^3}$$

$$= 773,132 \text{ lb} = 773.1 \text{ Kips (3,439 kN)}$$

Now,  $C_m = 1.0$  for a nonbraced column. Assume  $\phi = 0.65$ . Then we have

$$\text{Moment magnifier } \delta_{ns} = \frac{C_m}{1 - P_u / 0.75 P_c} = \frac{1.0}{1 - \frac{300,000}{0.75 \times 773,132}} = 2.07$$

$$\text{Design moment } M_c = \delta_{ns} M_{2ns} = 2.07 \times 750,000$$

$$= 1,552,500 \text{ in.-lb (184 kN-m)}$$

$$\text{Required } P_n = \frac{P_u}{\phi} = \frac{300,000}{0.65} = 461,538 \text{ lb (2053 kN)}$$

$$\text{Required } M_n = \frac{1,552,500}{0.65} = 2,388,462 \text{ in.-lb (291 kN-m)}$$

$$\text{Eccentricity } e = \frac{2,388,462}{461,538} = 5.18 \text{ in. (131 mm)}$$

*Design of an Equivalent Nonslender Column (Step 3).* The equivalent column has to carry a minimum nominal axial load  $P_n = 461,538 \text{ lb}$  and a minimum nominal uniaxial moment  $M_n = 2,388,462 \text{ in.-lb}$ .

To design the equivalent nonslender column, we analyze the assumed 15 in.  $\times$  15 in. column section assuming five  $\frac{1}{2}$ -in. dia. 7-wire stress-relieved strands on each of the two faces parallel to the neutral axis, as in Example 8.1. Then

$$A_{ps} = A'_{ps} = 5 \times 0.153 = 0.765 \text{ in.}^2 (4.94 \text{ cm}^2)$$

#### Balanced Limit Strain Failure Condition

$$d = h - 2 = 15 - 2 = 13 \text{ in. (330 mm)}$$

Comparing with Example 8.1 and using trial and adjustment, a reasonable assumption of the neutral axis depth for the balanced condition would be a value of  $c_b = 8.3 \text{ in. (211 mm)}$ . Then  $a_b = \beta_1 \times c_b = 0.75 \times 8.3 = 6.23 \text{ in. (158 mm)}$ .

Next, from Figure 8.3,

$$C_{cn} = 0.85 \times 6,000 \times 15 \times 6.23 = 476,595 \text{ lb (2,119 kN)}$$

From Equation 8.5,

$$T'_{sn} = 0.765 \times 28 \times 10^6 \left[ 0.0052 - 0.003 \left( \frac{8.3 - 2}{8.3} \right) + 0.0005 \right]$$

$$= 73,318 \text{ lb (385 kN)}$$

From Equation 8.6,

$$T_{sn} = 0.765 \times 28 \times 10^6 \left[ 0.0052 + 0.003 \left( \frac{13 - 8.3}{8.3} \right) + 0.0005 \right]$$

$$= 158,482 \text{ lb (704 kN)}$$

From Equation 8.2, for the “balanced” strain limit case ( $c/d_t = 0.60$ ):

$$\begin{aligned} P_{nb} &= C_{cn} - T'_{sn} - T_{sn} \\ &= 476,595 - 73,318 - 158,482 \\ &= 229,310 \text{ lb (1,020 kN)} \end{aligned}$$

From Equation 8.7, for the “balanced” strain limit case ( $c/d_t = 0.60$ )

$$\begin{aligned} M_{nb} &= 476,595 \left( \frac{15}{2} - \frac{6.23}{2} \right) = 73,318 \left( \frac{15}{2} - 2 \right) + 158,482 \left( 13 - \frac{15}{2} \right) \\ &= 2,103,124 \text{ in.}\cdot\text{lb (237.7 kN}\cdot\text{m)} \\ e_b &= \frac{M_{nb}}{P_{nb}} = \frac{2,103,124}{229,310} = 9.17 \text{ in. (233 mm)} > \text{actual } e = 5.18 \text{ in.} \end{aligned}$$

The prestressed column load has small eccentricity, and initial failure would be in compression. Also,  $\phi = 0.65$ , as assumed.

*Assume Neutral Axis Depth  $c = 12$  in.*

$$a = \beta_1 c = 0.75 \times 12 = 9.0 \text{ in.}$$

From Equation 8.1a,

$$C_{cn} = 0.85 f'_c b a = 0.85 \times 6,000 \times 15 \times 9 = 688,500 \text{ lb}$$

From Equation 8.5,

$$\begin{aligned} T'_{sn} &= A'_{ps} E_{ps} \left[ \epsilon_{pe} - \epsilon_{cu} \left( \frac{c - d'}{c} \right) + \epsilon_{ce} \right] \\ &= 0.765 \times 28 \times 10^6 \left[ 0.0052 - 0.003 \left( \frac{12 - 2}{12} \right) + 0.0005 \right] \\ &= 68,544 \text{ lb} \end{aligned}$$

From Equation 8.6,

$$\begin{aligned} T_{sn} &= A_{ps} E_{ps} \left[ \epsilon_{pe} + \epsilon_{cu} \left( \frac{d - c}{c} \right) + \epsilon_{ce} \right] \\ &= 0.765 \times 28 \times 10^6 \left[ 0.0052 + 0.003 \left( \frac{13 - 12}{12} \right) + 0.0005 \right] \\ &= 127,449 \text{ lb} \end{aligned}$$

From Equation 8.2,

$$\begin{aligned} P_n &= C_{cn} - T'_{sn} - T_{sn} \\ \text{Available } P_n &= 688,500 - 68,544 - 127,449 \\ &= 492,507 \text{ lb} > \text{required } P_n = 461,538 \text{ lb} \end{aligned}$$

Accordingly, we go on to a second trial-and-adjustment cycle.

*Assume Neutral Axis Depth  $c = 11.2$  in.*

$$a = \beta_1 c = 0.75 \times 11.2 = 8.4 \text{ in.}$$

$$C_{cn} = 0.85 f'_c b a = 0.85 \times 6,000 \times 15 \times 8.4 = 642,600 \text{ lb}$$

$$\begin{aligned} T'_{sn} &= 0.765 \times 28 \times 10^6 \left[ 0.0052 - 0.003 \left( \frac{11.2 - 2}{11.2} \right) + 0.0005 \right] \\ &= 69,309 \text{ lb} \end{aligned}$$

$$T_{sn} = 0.765 \times 28 \times 10^6 \left[ 0.0052 + 0.003 \left( \frac{13 - 11.2}{11.2} \right) + 0.0005 \right]$$

$$\begin{aligned}
 &= 132,421 \text{ lb} \\
 \text{Available } P_n &= 642,600 - 6,309 - 132,421 \\
 &= 440,870 \text{ lb while required } P_n = 461,538 \text{ lb, O.K.,}
 \end{aligned}$$

as the moment capacity is larger than required  $M_n$ . A very slight increase in section depth would overcome the small difference between the required and available  $P_n$ .

From Equation 8.7,

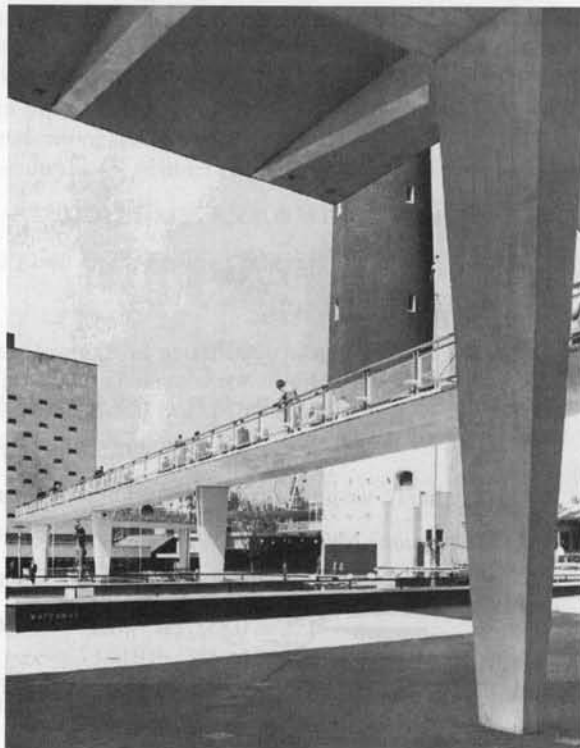
$$\begin{aligned}
 M_n &= C_{cn} \left( \frac{h}{2} - \frac{a}{2} \right) \overleftarrow{\curvearrowright} - T_{sn} \left( \frac{h}{2} - d' \right) \overrightarrow{\curvearrowright} + T_{sn} \left( d - \frac{h}{2} \right) \overleftarrow{\curvearrowright} \\
 &= 642,600 \left( \frac{15}{2} - \frac{8.4}{2} \right) - 69,309 \left( \frac{15}{2} - 2 \right) + 132,421 \left( 13 - \frac{15}{2} \right) \\
 &= 2,467,696 \text{ in.-lb} > 2,338,462 \text{ in.-lb} (278.8 \text{ kN-m} > 250 \text{ kN-m), O.K.} \\
 e &= \frac{2,467,696}{448,870} = 5.5 \approx \text{actual } e = 5.18 \text{ in., accept.}
 \end{aligned}$$

Consequently, adopt a section 15 in.  $\times$  15 in. with five  $\frac{1}{2}$ -in. dia. 7-wire stress-relieved 270-K strands at each of the two faces parallel to the neutral axis. Then design the necessary transverse ties.

**2. Gravity and Wind Loading (Sidesway).** From part 1,  $P_c = 773,132 \text{ lb}$  and  $U = (1.2D + 1.0L + 1.6W)$ . Also,  $U = 0.9D + 1.6W$  (did not control),  $P_u = (300,000 + 24,000) = 324,000 \text{ lb}$ ,  $M_{2b} = 750,000 \text{ in.-lb}$ , and  $M_{2s} = 220,000 \text{ in.-lb}$ .

Check if the gravity moment needs to be magnified:

$$\frac{35}{\sqrt{P_u/f'_c A_g}} = \frac{35}{\sqrt{324,000/6,000 \times 225}} = 71.4 > \frac{l_u}{r} = 40; \text{ hence, gravity moment } M_{2b} \text{ is not magnified}$$



**Photo 8.4** One of the earliest prestressed concrete footbridges in England at the Festival of Britain, London, 1951.

From Equation 8.16(b),

$$\delta_s = \frac{1.0}{1 - \frac{\Sigma P_u}{0.75 \Sigma P_c}} = \frac{1.0}{1 - \frac{4.5 \times 10^6}{0.75 \times 31.0 \times 10^6}} = 1.24$$

From Equation 8.15,

$$M_c = M_{2ns} + \delta_s M_{2s} = 750,000 + 1.24 \times 220,000 = 1,022,800 \text{ in.-lb}$$

$$\text{Required } P_n = \frac{324,000}{0.65} = 498,462 \text{ lb}$$

$$\text{Required } M_n = \frac{1,022,800}{0.65} = 1,573,538 \text{ in.-lb}$$

$$\text{Eccentricity } e = \frac{1,573,538}{498,462} = 3.16 \text{ in.} < e_b = 9.17 \text{ in.} < \text{actual } e = 5.18 \text{ in.}$$

Hence, initial compression failure occurs. Also  $M_n = 1,573,538 \text{ in.-lb} < M_n = 2,388,462 \text{ in.-lb}$  of case 1.

The conditions for case 2 with sidesway do not control, since failure is still in compression, the required  $M_n$  is less than that for case 1 and the eccentricity is smaller than in case 1. Accordingly, adopt the same 15 in.  $\times$  15 in. section of case 1, with five  $\frac{1}{2}$ -in. dia 270-K-stress-relieved prestressing strands on each of the two faces parallel to the neutral axis.

## 8.11 COMPRESSION MEMBERS IN BIAxIAL BENDING

### 8.11.1 Exact Method of Analysis

Columns in corners of buildings are compression members subjected to biaxial bending about both the  $x$  and the  $y$  axes as shown in Figure 8.16. Also, biaxial bending occurs due to imbalance of loads in adjacent spans and almost always in bridge piers. Such columns are subjected to moment  $M_{xx}$  about the  $x$  axis creating a load eccentricity  $e_y$ , and a moment  $M_{yy}$  about the  $y$  axis creating a load eccentricity  $e_x$ . Thus, the neutral axis is inclined at an angle  $\theta$  to the horizontal.

The angle  $\theta$  depends on the interaction of the bending moments about both axes and the magnitude of the total  $P_u$ . The compressive area in the column section can have one of the alternative shapes shown in Figure 8.16(c). Since such a column has to be designed from first principles, the trial-and-adjustment procedure has to be followed where compatibility of strain has to be maintained at all levels of the reinforcing bars. Additional computational effort is also needed, because of the position of the inclined neutral-axis plane and the four different possible forms of the concrete compression area.

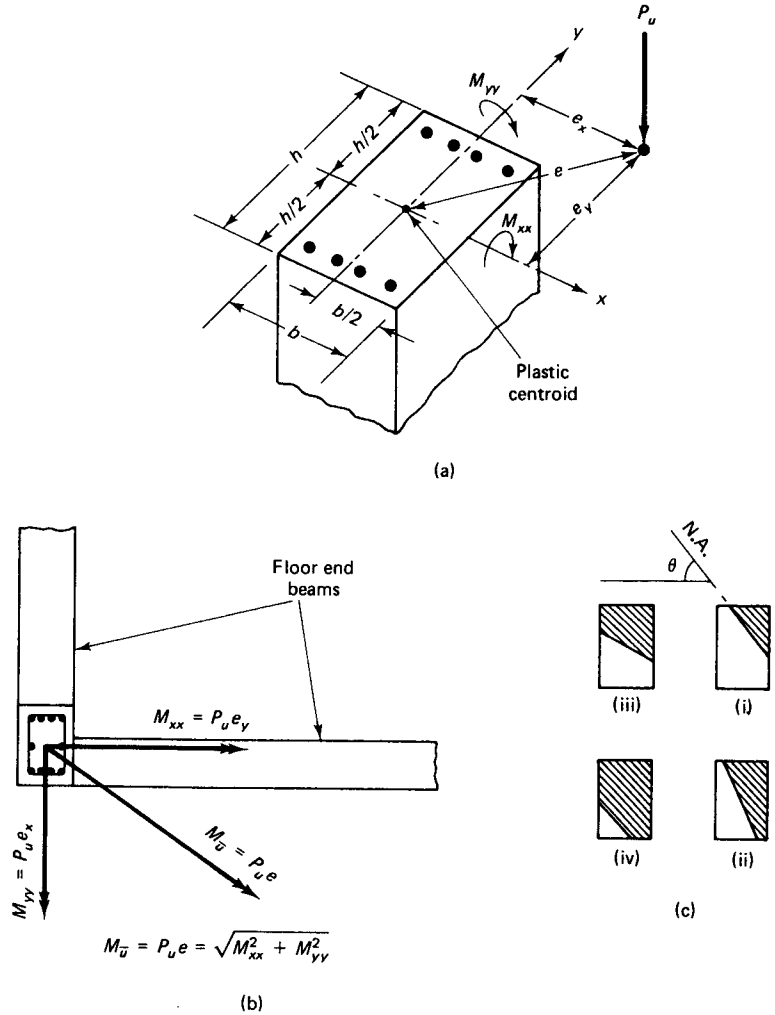
Figure 8.17 shows the strain distribution and forces on a biaxially loaded rectangular column cross section.  $G_c$  is the center of gravity of the concrete compression area, having coordinates  $x_c$  and  $y_c$  from the neutral axis in the  $x$  and  $y$  directions, respectively.  $G_{sc}$  is the resultant position of the steel forces in the compression area having coordinates  $x_{sc}$  and  $y_{sc}$  from the neutral axis in the  $x$  and  $y$  directions, respectively.  $G_{st}$  is the resultant position of the steel forces in the tension area having coordinates  $x_{st}$  and  $y_{st}$  from the neutral axis in the  $x$  and  $y$  directions, respectively. From equilibrium of internal and external forces,

$$P_n = 0.85f'_c A_c + F_{sc} - F_{st} \quad (8.25)$$

where  $A_c$  = area of the compression zone covered by the rectangular stress block

$F_{sc}$  = resultant steel compressive forces ( $\Sigma A'_s f_{sc}$ )

$F_{st}$  = resultant steel tensile force ( $\Sigma A_s f_{st}$ )



**Figure 8.16** Corner column subjected to axial load. (a) Biaxially stressed column cross section. (b) Vector moments  $M_{xx}$  and  $M_{yy}$  in column plan. (c) Neutral axis direction.

Also, from equilibrium of internal and external moments,

$$P_n e_x = 0.85f'_c A_c x_c + F_{sc} x_{sc} + F_{st} x_{st} \tag{8.26a}$$

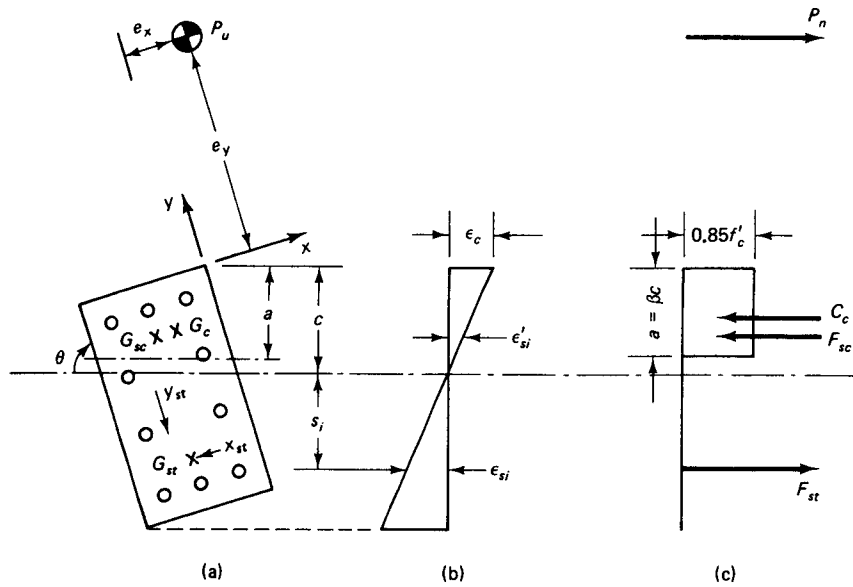
$$P_n e_y = 0.85f'_c A_c y_c + F_{sc} y_{sc} + F_{st} y_{st} \tag{8.26b}$$

The position of the neutral axis has to be assumed in each trial and the stress computed in *each* bar using

$$f_{si} = E_s \epsilon_{si} = E_c \epsilon_c \frac{S_i}{c} < f_y \tag{8.27}$$

**8.11.2 Load Contour Method of Analysis**

One method of arriving at a rapid solution is to design the column for the vector sum of  $M_{xx}$  and  $M_{yy}$  and use a circular reinforcing cage in a square section for the corner column. However, such a procedure cannot be economically justified in most cases. Another de-



**Figure 8.17** Strain compatibility and forces in biaxially loaded rectangular columns. (a) Cross section. (b) Strain. (c) Forces.

sign approach well proven by experimental verification is to transform the biaxial moments into an equivalent uniaxial moment and an equivalent uniaxial eccentricity. The section can then be designed for uniaxial bending, as previously discussed in this chapter, to resist the actual factored biaxial bending moments.

Such a method considers a failure surface instead of failure planes and is generally termed the *Bresler-Parme contour method*. The method involves cutting the three-dimensional failure surfaces in Figure 8.18 at a constant value  $P_n$  to give an interaction plane relating  $M_{nx}$  and  $M_{ny}$ . In other words, the contour surface  $S$  can be viewed as a curvilinear surface which includes a family of curves, termed the *load contours*.

The general nondimensional equation for the load contour at a constant load  $P_n$  may be expressed as

$$\left(\frac{M_{nx}}{M_{ox}}\right)^{\alpha_1} + \left(\frac{M_{ny}}{M_{oy}}\right)^{\alpha_2} = 1.0 \quad (8.28)$$

where  $M_{nx} = P_n e_y$   
 $M_{ny} = P_n e_x$   
 $M_{ox} = M_{nx}$  at an axial load  $P_n$  such that  $M_{ny}$  or  $e_x = 0$   
 $M_{oy} = M_{ny}$  at an axial load  $P_n$  such that  $M_{nx}$  or  $e_y = 0$

The moments  $M_{ox}$  and  $M_{oy}$  are the *required* equivalent resisting moment strengths about the  $x$  and  $y$  axes, respectively, while  $\alpha_1$  and  $\alpha_2$  are exponents that depend on the cross-sectional geometry and the steel percentage and its location and material stress  $f'_c$  and  $f_y$ .

Equation 8.28 can be simplified using a common exponent and introducing a factor  $\beta$  for one particular axial load value  $P_n$  such that the ratio  $M_{nx}/M_{ny}$  would have the same value as the ratio  $M_{ox}/M_{oy}$  as detailed by Parme and associates. Such simplification leads to

$$\left(\frac{M_{nx}}{M_{ox}}\right)^{\alpha} + \left(\frac{M_{ny}}{M_{oy}}\right)^{\alpha} = 1.0 \quad (8.29)$$



$$\text{where } M_{nx} = P_n e_y$$

$$M_{ny} = P_n e_x$$

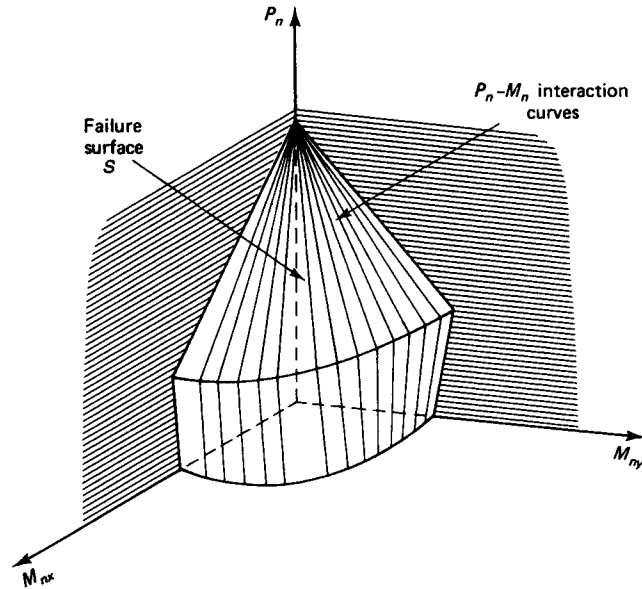


Figure 8.18 Failure interaction surface for biaxial column bending.

where  $\alpha = \log 0.5 / \log \beta$ . Figure 8.19 gives a contour plot  $ABC$  from Equation 8.27.

For design purposes, the contour is approximated by two straight lines  $BA$  and  $BC$ , and Equation 8.29 can be simplified to two conditions:

1. For  $AB$  when  $M_{ny}/M_{oy} < M_{nx}/M_{ox}$ ,

$$\frac{M_{nx}}{M_{ox}} + \frac{M_{ny}}{M_{oy}} \left[ \frac{1 - \beta}{\beta} \right] = 1.0 \quad (8.30a)$$

2. For  $BC$  when  $M_{ny}/M_{oy} > M_{nx}/M_{ox}$ ,

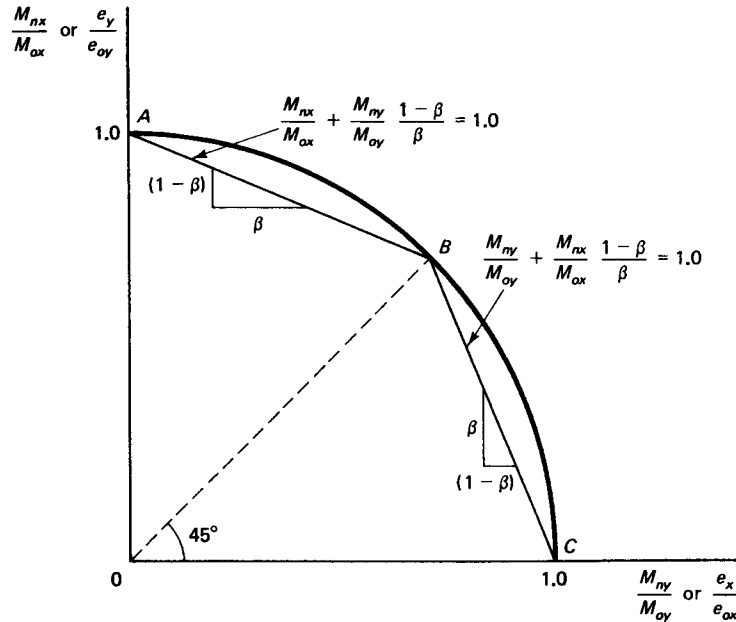
$$\frac{M_{ny}}{M_{oy}} + \frac{M_{nx}}{M_{ox}} \left[ \frac{1 - \beta}{\beta} \right] = 1.0 \quad (8.30b)$$

In both of these equations, the *actual* controlling equivalent uniaxial moment strength  $M_{oxn}$  or  $M_{oyn}$  should be at least equivalent to the *required* controlling moment strength  $M_{ox}$  or  $M_{oy}$  of the chosen column section.

For rectangular sections where the reinforcement is evenly distributed along all the column faces, the ratio  $M_{oy}/M_{ox}$  can be taken to be approximately equal to  $b/h$ . In that case, Equations 8.30 can be modified as follows:

1. For  $\frac{M_{ny}}{M_{nx}} > b/h$ ,

$$M_{ny} + M_{nx} \frac{b}{h} \frac{1 - \beta}{\beta} \cong M_{oy} \quad (8.31a)$$



**Figure 8.19** Modified interaction contour plot of constant  $P_n$  for biaxially loaded column.

2. For  $\frac{M_{ny}}{M_{nx}} \leq b/h$ ,

$$M_{nx} = M_{ny} \frac{h}{b} \frac{1 - \beta}{\beta} \cong M_{ox} \quad (8.31b)$$

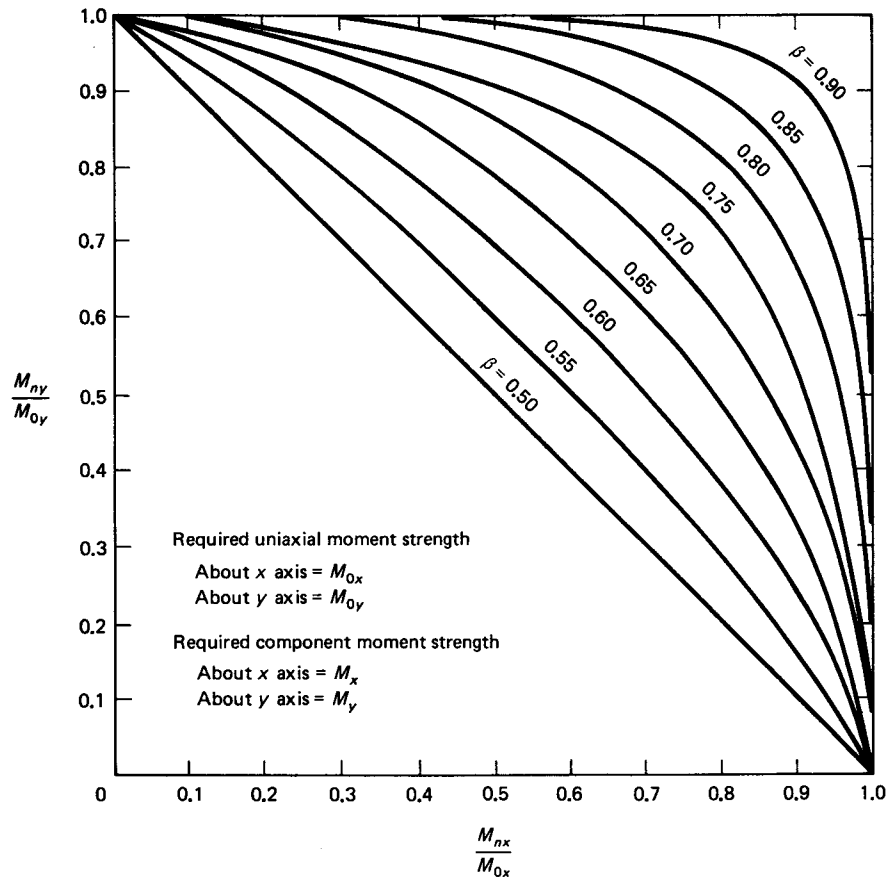
The controlling required moment strength  $M_{ox}$  or  $M_{oy}$  for designing the section is the larger of the two values as determined from Equations 8.31.

Plots like those of Figure 8.20 are used in the selection of  $\beta$  in the analysis and design of the columns just described. In effect, the modified load-contour method can be summarized in Equation 8.31 as a method for finding equivalent required moment strengths  $M_{ox}$  and  $M_{oy}$  for designing the columns as if they were uniaxially loaded.

### 8.11.3 Step-by-Step Operational Procedure for the Design of Biaxially Loaded Columns

The following steps can be used as a guideline for the design of columns subjected to bending in both the  $x$  and  $y$  directions. The procedure assumes an equal area of reinforcement on all four faces.

1. Compute the uniaxial bending moments assuming an equal number of bars on each column face. Assume a value of an interaction contour  $\beta$  factor between 0.50 and 0.70 and a ratio of  $h/b$ . This ratio can be approximated to  $M_{nx}/M_{ny}$ . Using Equations 8.31 determine the equivalent required uniaxial moment  $M_{ox}$  or  $M_{oy}$ . If  $M_{nx}$  is larger than  $M_{ny}$ , use  $M_{ox}$  for the design and vice versa.
2. Assume a cross section for the column and a reinforcement ratio  $\rho = \rho' \cong 0.01$  to 0.02 on each of the two faces parallel to the axis of bending of the larger equivalent

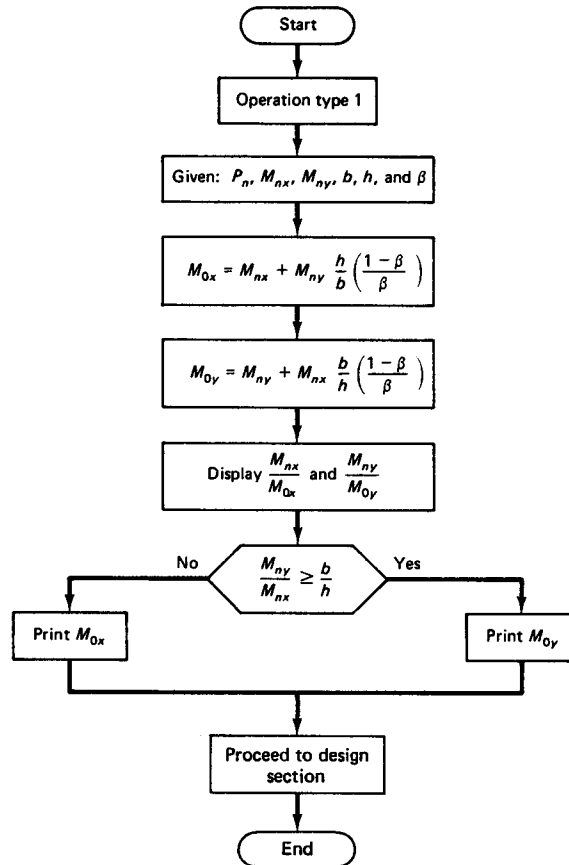


**Figure 8.20** Contour  $\beta$ -factor chart for rectangular columns in biaxial bending.

moment. Then make a preliminary selection of the steel bars, and verify the capacity  $P_n$  of the assumed column cross section. In the completed design, the same amount of longitudinal steel should be used on all four faces.

3. Compute the *actual* nominal moment strength  $M_{oxn}$  for equivalent uniaxial bending about the  $x$  axis when  $M_{ox} = 0$ . Its value has to be at least equivalent to the *required* moment strength  $M_{ox}$ .
4. Compute the actual nominal moment strength  $M_{oy n}$  for the equivalent uniaxial bending moment about the  $y$  axis when  $M_{oy} = 0$ .
5. Find  $M_{ny}$  by entering  $M_{nx}/M_{oxn}$  and the trial  $\beta$  value into the  $\beta$  factor contour plots of Figure 8.20.
6. Make a second trial and adjustment, increasing the assumed  $\beta$  value if the  $M_{ny}$  value obtained from entering the chart is less than the required  $M_{ny}$ . Repeat this step until the two values of  $M_{ny}$  converge, either through changing  $\beta$  or changing the section.
7. Design the lateral ties and detail the section.

A flowchart for the primary steps in evaluating the controlling moment values in biaxially loaded columns is given in Figure 8.21. A detailed computational example, together with a discussion of biaxially loaded columns, is presented in Ref. 8.2.



**Figure 8.21** Flowchart for evaluation of controlling moment values in biaxially loaded columns.

## 8.12 PRACTICAL DESIGN CONSIDERATIONS

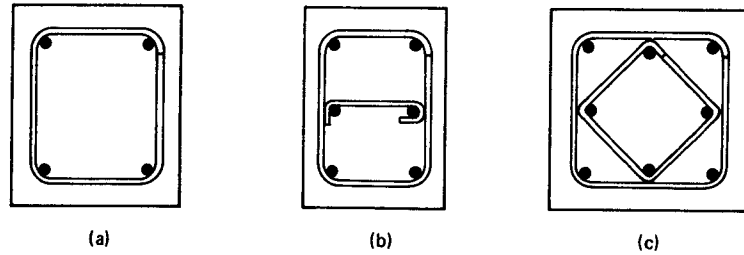
The following guidelines are presented for the design and arrangement of reinforcement to arrive at a practical design.

### 8.12.1 Longitudinal or Main Reinforcement

The average effective prestress in the concrete in prestressed compression members should not be less than 225 psi (1.55 MPa). This code requirement sets a minimum reinforcement ratio such that compressive members with lower prestress values will have a minimum nonprestressed reinforcement ratio of one percent.

### 8.12.2 Lateral Reinforcement for Columns

**8.12.2.1 Lateral Ties.** Lateral reinforcement is required to prevent spalling of the concrete cover or local buckling of the longitudinal bars. The reinforcement could be in the form of ties evenly distributed along the height of the column at specified intervals. Longitudinal bars spaced more than 6 in. apart should be supported by lateral ties, as shown in Figure 8.22.



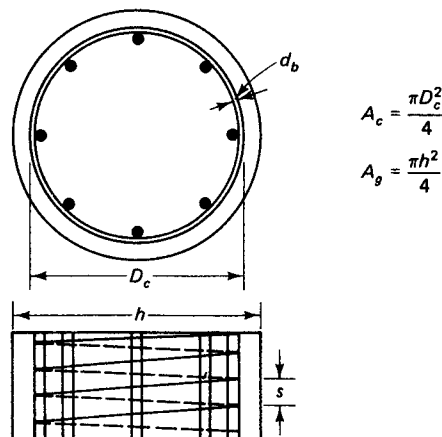
**Figure 8.22** Typical arrangement of ties for four, six, and eight longitudinal bars in a column. (a) One tie. (b) Two ties. (c) Two ties.

The following guidelines are to be followed for the selection of the size and spacing of ties.

1. The size of the tie should not be less than a #3 (9.5 mm) bar.
2. The vertical spacing of the ties must not exceed
  - (a) Forty-eight times the diameter of the tie
  - (b) Sixteen times the diameter of the longitudinal bar
  - (c) The least lateral dimension of the column

Figure 8.22 shows a typical arrangement of ties for four, six, and eight longitudinal bars in a column cross section.

**8.12.2.2 Spirals.** The other type of lateral reinforcement is spirals or helical lateral reinforcement, as shown in Figure 8.23. Spirals are particularly useful in increasing ductility or member toughness, and hence are mandatory in high-earthquake-risk regions. Normally, concrete outside the confined core of the spirally reinforced column can totally spall under unusual and sudden lateral forces such as earthquake-induced forces. The columns have to be able to sustain most of the load even after the spalling of the cover in order to prevent the collapse of the building. Hence, the spacing and size of spirals are designed to maintain most of the load-carrying capacity of the column, even under such severe load conditions.



**Figure 8.23** Helical or spiral reinforcement for columns.

Closely spaced spiral reinforcement increases the ultimate-load capacity of columns. The spacing or pitch of the spiral is so chosen that the load capacity due to the confining spiral action compensates for the loss due to spalling of the concrete cover.

Equating the increase in strength due to confinement to the loss of capacity in spalling, and incorporating a safety factor of 1.2, we obtain the minimum spiral reinforcement ratio

$$\rho_s = 0.45 \left( \frac{A_g}{A_c} - 1 \right) \frac{f'_c}{f_{yt}} \quad (8.32)$$

where  $\rho_s = \frac{\text{volume of the spiral steel per one revolution}}{\text{volume of concrete core contained in one revolution}}$

$$A_c = \frac{\pi D_c^2}{4} \quad (8.33a)$$

$$A_g = \frac{\pi h^2}{4} \quad (8.33b)$$

$h$  = diameter of the column

$a_s$  = cross-sectional area of the spiral

$d_b$  = nominal diameter of the spiral wire

$D_c$  = diameter of the concrete core out-to-out of the spiral

and  $f_{yt}$  = yield strength of the spiral reinforcement

To determine the pitch  $s$  of the spiral, compute  $\rho_s$  using Equation 8.33, choose a bar diameter  $d_b$  for the spiral, compute  $a_s$ , and then obtain pitch  $b$  using Equation 8.35b below.

The spiral reinforcement ratio  $\rho_s$  can be written

$$\rho_s = \frac{a_s \pi (D_c - d_b)}{(\pi/4) D_c^2 s} \quad (8.34)$$

Therefore, the pitch is given by

$$s = \frac{a_s \pi (D_c - d_b)}{(\pi/4) D_c^2 \rho_s} \quad (8.35a)$$

or

$$s = \frac{4a_s(D_c - d_b)}{D_c^2 \rho_s} \quad (8.35b)$$

The spacing or pitch of spirals is limited to a range of 1 to 3 in. (25.4 to 76.2 mm), and the diameter should be at least  $\frac{3}{8}$  in. (9.53 mm). The spiral should be well anchored by providing at least  $1\frac{1}{2}$  extra turns when splicing of spirals rather than welding is used.

### 8.12.2.3 Design of Spiral Lateral Reinforcement

#### Example 8.3

Design the lateral spiral reinforcement for a circular prestressed concrete column  $h = 20$  in. (508 mm) and clear cover  $d_c = 1.5$  in. (38 mm) given that  $f_y = 60,000$  psi (414 MPa).

**Solution:** Using Equation 8.32,

$$\text{required } \rho_s = 0.45 \left( \frac{A_g}{A_c} - 1 \right) \frac{f'_c}{f_{yt}}$$

Using #3 spirals with a yield strength  $f_y = 60,000$  psi, we obtain

Clear concrete cover  $d_c = 1.5$  in. (38 mm)

$$f_{yt} = 60,000 \text{ psi}$$

$$D_c = h - 2d_c = 20.0 - 2 \times 1.5 = 17.0 \text{ in. (432 mm)}$$

$$A_c = \frac{\pi(17.0)^2}{4} = 226.98 \text{ in.}^2$$

$$A_g = 314.0 \text{ in.}^2$$

$$\rho_s = 0.45 \left( \frac{314.0}{226.98} - 1 \right) \frac{4,000}{60,000} = 0.0115$$

For #3 spirals,  $a_s = 0.11$  in.<sup>2</sup> So using Equation 8.35b, we get

$$\text{pitch } s = \frac{4a_s(D_c - d_b)}{D_c^2 \rho_s} = \frac{4 \times 0.11(17.0 - 0.375)}{(17.0)^2 \times 0.0115} = 2.20 \text{ in. (56 mm)}$$

Accordingly, provide #3 spirals at  $2\frac{1}{4}$  in. pitch (9.53 mm dia spiral at 54.0 mm pitch).

### 8.13 RECIPROCAL LOAD METHOD FOR BIAXIAL BENDING

This method developed by Bressler relates the desired axial force  $P_u$  value to three other values on a reciprocal of the failure surface (Ref. 8.2). Assume  $S_1$  denotes the coordinates on the failure surface in Figure 8.18 such that the values of the load and eccentricities as  $P_u$ ,  $e_x$  and  $e_y$ . If  $S_2$  is a point on the compatible reciprocal surface to that in Fig. 8.18, then  $S_2$  would define the coordinates of that point as  $1/P_u$ ,  $e_x$  and  $e_y$ , where  $P_u = \phi P_n$ , which is the factored (design) load.

If the desired axial load  $P_u$  under biaxial loading about the  $x$  and  $y$  axes is related to the  $P_u$  values devoted by  $P_{uy}$ ,  $P_{ux}$ , and  $P_{uo}$ , then

$$\frac{1}{P_u} = \frac{1}{P_{ux}} + \frac{1}{P_{uy}} - \frac{1}{P_{uo}} \quad (8.36a)$$

or

$$\frac{1}{\phi P_n} = \frac{1}{\phi P_{n_{xo}}} + \frac{1}{\phi P_{n_{yo}}} - \frac{1}{\phi P_{n_o}} \quad (8.36b)$$

where,  $P_{ux} = \phi P_{n_{xo}}$  = design strength of the column having eccentricity  $e_x$ , provided  $e_y = 0$

$P_{uy} = \phi P_{n_{yo}}$  = design strength of the same column having eccentricity  $e_y$ , provided  $e_x = 0$

$P_{uo} = \phi P_{n_o}$  = theoretical axial load design strength for the same column having eccentricity  $e_y = e_x = 0$

$M_{ux}$  = moment about the  $x$ -axis =  $P_u e_y$

$M_{uy}$  = moment about the  $y$ -axis =  $P_u e_x$

$e_x$  = eccentricity measured parallel to the  $y$ -axis as in Figure 8.24 a, namely

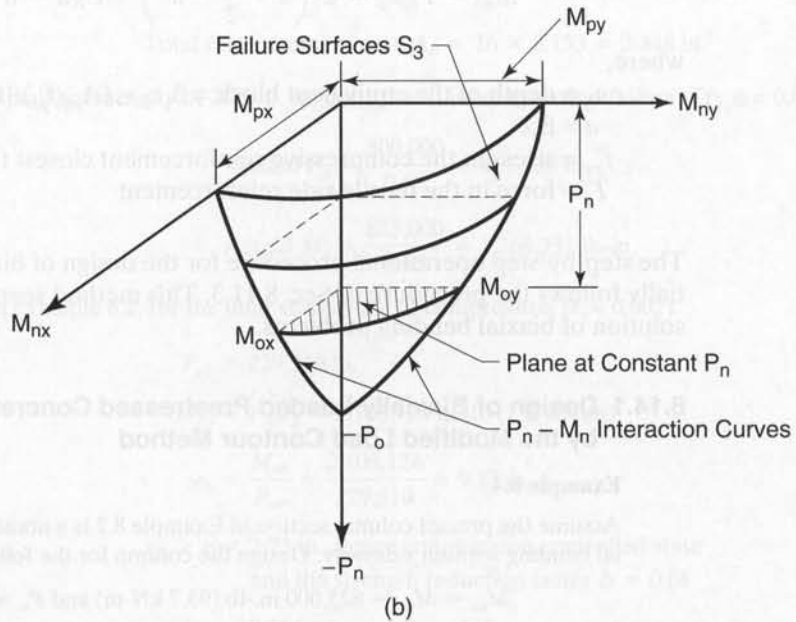
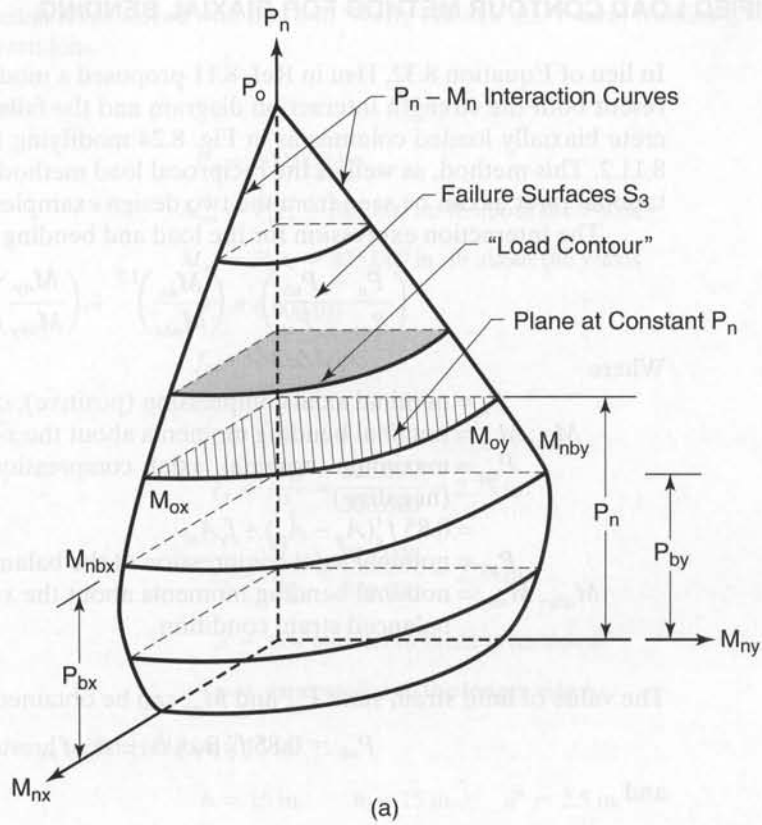
$$e_x = (M_{uy}/P_u) = (P_u e_x/P_u)$$

$e_y$  = eccentricity measured parallel to the  $x$ -axis =  $(P_u e_y/P_u)$

$x$  = column cross-section dimension parallel to the  $x$ -axis

$y$  = column cross-section dimension parallel to the  $y$ -axis

The step-by-step operational procedure essentially follows the logic in the steps presented in Sec. 8.11.3.



**Figure 8.24** Failure Surface Interaction Diagram (Ref. 8.11) (a) Biaxial Bending and Compression, (b) Biaxial Bending and Tension.



### 8.14 MODIFIED LOAD CONTOUR METHOD FOR BIAXIAL BENDING

In lieu of Equation 8.32, Hsu in Ref. 8.11 proposed a modified expression which can represent both the strength interaction diagram and the failure surface of a reinforced concrete biaxially loaded columns as in Fig. 8.24 modifying the approach presented in Sec. 8.11.2. This method, as well as the reciprocal load method, seems to demand less computational rigor as can be seen from the two design examples to follow.

The interaction expression for the load and bending moments about the two axes is

$$\left(\frac{P_n - P_{nb}}{P_{no} - P_{nb}}\right) + \left(\frac{M_{nx}}{M_{nbx}}\right)^{1.5} + \left(\frac{M_{ny}}{M_{nby}}\right)^{1.5} = 1.0 \quad (8.37)$$

Where

$$\begin{aligned} P_n &= \text{nominal axial compression (positive), or tension (negative)} \\ M_{nx}, M_{ny} &= \text{nominal bending moments about the } x\text{- and } y\text{-axis respectively} \\ P_{no} &= \text{maximum nominal axial compression (positive) or axial tension} \\ &\quad \text{(negative)} \\ &= 0.85 f'_c (A_g - A_{st}) + f_y A_{st} \\ P_{nb} &= \text{nominal axial compression at the balanced strain condition} \\ M_{nbx}, M_{nby} &= \text{nominal bending moments about the } x\text{- and } y\text{-axis respectively, at the} \\ &\quad \text{balanced strain condition} \end{aligned}$$

The value of limit strain state  $P_{nb}$  and  $M_{nb}$  can be obtained from:

$$P_{nb} = 0.85 f'_c \beta_1 c_b b + A_{ps} f'_{ps} - A_{ps} f_{ps} \quad (8.38a)$$

and

$$M_{nb} = P_{nb} e_b = C_c \left( d - \frac{a}{2} - d'' \right) + C_s (d - d' - d'') + T_s d'' \quad (8.38b)$$

where,

$$\begin{aligned} a_b &= \text{depth of the equivalent block} = \beta_1 c_b = (A_{ps} f_{ps}) / (0.85 f'_c b) \\ a &= \beta_1 c \\ f'_{ps} &= \text{stress in the compressive reinforcement closest to the load} = f_{py} \text{ if } f_{ps} \geq f_{py} \\ T_s &= \text{force in the tensile side reinforcement} \end{aligned}$$

The step-by-step operational procedure for the design of biaxially loaded columns essentially follows the procedure of Sec. 8.11.3. This method seems to require less effort in the solution of biaxial bending problems.

#### 8.14.1 Design of Biaxially Loaded Prestressed Concrete Column by the Modified Load Contour Method

##### Example 8.4

Assume the precast column section in Example 8.2 is a nonslender column subjected to biaxial bending without sidesway. Design the column for the following bending moments:

$$M_{ux} = M_{uy} = 825,000 \text{ in.-lb (93.7 kN-m) and } P_u = 300,000 \text{ lb (1334 kN)}$$

Given:

$$f'_c = 6,000 \text{ psi (41.4 MPa) normal weight concrete}$$

$$f_{pu} = 270,000 \text{ psi (1863 MPa)}$$

$$f_{ps} = 240,000 \text{ psi (1565 MPa)}$$

The section is reinforced with five  $\frac{1}{2}$ -in. 7-wire (12-mm dia. 7 wire) tendons giving a total of sixteen tendons.

**Solution:**

$$P_u = 300,000 \text{ lbs}$$

$$M_{ux} = P_u e_y = 825,000 \text{ in.-lb about the } x\text{-axis}$$

$$M_{uy} = P_u e_x = 825,000 \text{ in.-lb about the } y\text{-axis}$$

$$f'_c = 6,000 \text{ psi}$$

$$f_{ps} = 240,000 \text{ psi}$$

Hence:

$$e_x = \frac{M_{ux}}{P_u} = \frac{825,000}{300,000} = 2.75 \text{ in.}$$

$$e_y = \frac{M_{uy}}{P_u} = \frac{825,000}{300,000} = 2.75 \text{ in.}$$

$x$  = axis parallel to the shorter side  $b$ .

$y$  = axis parallel to the longer side  $h$ .

The column section is 15 in.  $\times$  15 in.

$$b = 15 \text{ in.} \quad h = 15 \text{ in.} \quad d' = 2.5 \text{ in.}$$

On each face  $A_s = (\text{five } \frac{1}{2}\text{-in. dia. 7-wire tendons}) = 5 \times 0.153 = 0.765 \text{ in.}^2$

$$\text{Total reinforcement area } A_{st} = 16 \times 0.153 = 2.448 \text{ in.}^2$$

The small eccentricity of 2.75 in. suggests that it is compression failure. Try  $\phi = 0.65$ .

$$\text{Actual } P_n = \frac{300,000}{0.65} = 461,538 \text{ lb}$$

$$\text{Actual } M_n = \frac{825,000}{0.65} = 1,269,231 \text{ lb-in.}$$

From example 8.2, for the limit strain state in compression ( $\epsilon_t = 0.002$ )

$$P_{nb} = 229,310 \text{ lb.}$$

$$M_{nb} = P_{nb} e_b = 2,103,124 \text{ in.-lb (237 kN-m)}$$

$$e_b = \frac{M_{nb}}{P_{nb}} = \frac{2,103,124}{229,310} = 9.17 \text{ in.}$$

$e_b > e = 2.75 \text{ in.}$ , hence compression controlled state and the strength reduction factor  $\phi = 0.65$

$$\begin{aligned} P_{no} &= 0.85f'_c(A_g - A_{st}) + A_{st}f_{ps} \\ &= 0.85 \times 6,000 (225 - 2.448) + 1.53 \times 240,000 \\ &= 1,502,205 \text{ lb.} \end{aligned}$$

Using the interaction surface expression for biaxial bending in equation 8.37,

$$\begin{aligned} & \left( \frac{P_n - P_{nb}}{P_{no} - P_{nb}} \right) + \left( \frac{M_{nx}}{M_{nbx}} \right)^{1.5} + \left( \frac{M_{ny}}{M_{nby}} \right)^{1.5} \\ &= \frac{461,538 - 229,310}{1,502,205 - 229,310} + \left( \frac{1,269,231}{2,103,124} \right)^{1.5} + \left( \frac{1,269,231}{2,103,124} \right)^{1.5} \\ &= 0.182 + 0.468 + 0.468 = 1.118 > 1.0 \\ & \text{(this section is very slightly oversized)} \end{aligned}$$

Accept the design, namely,

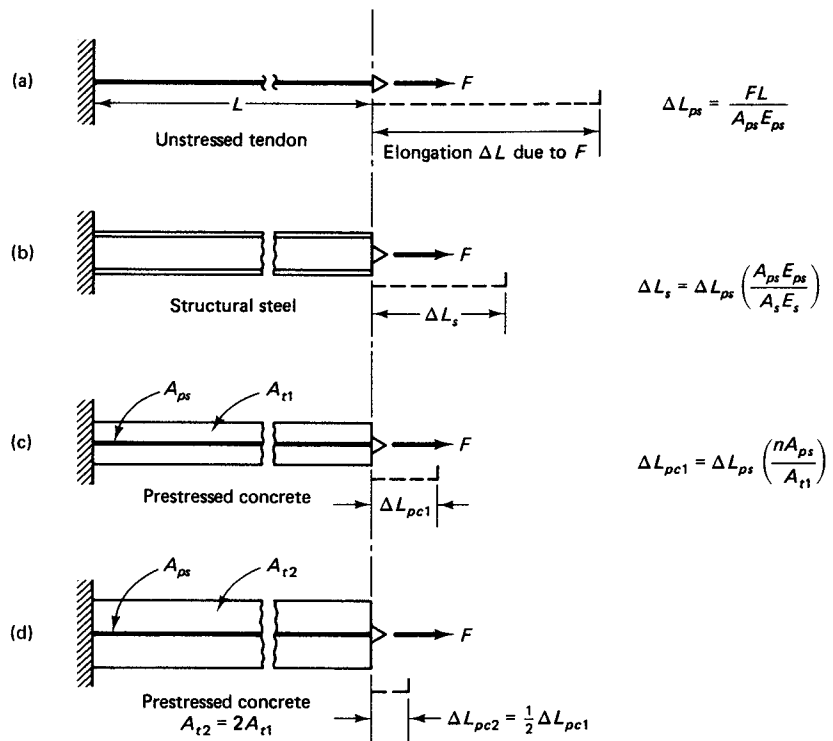
$b = 15$  in.     $h = 15$  in.     $d = 12.5$  in.

$A_s =$  five  $\frac{1}{2}$ -in. dia. 7-wire strand tendons *on each face* as in Figure 8.15 giving a total of sixteen tendons.

### 8.15 PRESTRESSED TENSION MEMBERS

#### 8.15.1 Service-Load Stresses

Tension elements and systems such as railroad ties, bridge truss tension members, foundation anchors for retaining walls, and ties in walls of liquid-retaining tanks combine the high strength of the prestressing strands with the stiffness of the concrete. As such, they provide tensile resistance and reduced deformations that could not be provided if the member were made of an all-steel section to carry the same load. The limited and controlled deformation of the prestressed tension member in spite of its slenderness makes it especially useful as a tie or as part of an overall structural system.



**Figure 8.25** Relative elongation of tension members. (a) Unstressed tendon. (b) Structural steel. (c) Prestressed concrete, area  $A_{t1} = A_g + (n - 1)A_{ps}$ . (d) Prestressed concrete, area  $A_{t2} = 2A_{t1}$ .

Figure 8.25 compares the elongation of a prestressed concrete member in direct tension with a structural steel member of similar capacity. The elongation of the tension tie results from application of the external force  $F$ , while the elongation of the unstressed tendon in part (a) due to force  $F$  is, from basic mechanics,

$$\Delta L_{ps} = \frac{FL}{A_{ps}E_{ps}} \quad (8.39)$$

If the tendon is replaced by a rolled structural member, the change in the properties of the section results in a deformation

$$\Delta L_s = \Delta L_{ps} \left( \frac{A_{ps}E_{ps}}{A_sE_s} \right) \quad (8.40)$$

where  $A_s$  is considerably larger than  $A_{ps}$ . Hence, a considerably reduced elongation is seen as shown in Figure 8.25b. The transformed area of concrete in Figure 8.25c is

$$A_{t1} = A_g + (n_p - 1)A_{ps} \quad (8.41)$$

and if the change in stress in the concrete is

$$\Delta f_c = \frac{F}{A_{t1}} \quad (8.42)$$

the corresponding change in stress in the prestressing steel is

$$\Delta f_{ps} = \frac{n_p F}{A_{t1}} \quad (8.43)$$

where  $n_p$  is the modular ratio  $E_{ps}/E_c$ . Therefore,

$$\Delta L_{pc1} = \Delta L_{ps} \left( \frac{n_p A_{ps}}{A_{t1}} \right) \quad (8.44)$$

or

$$\Delta L = \frac{n_p FL}{A_t E_{ps}} = \frac{FL}{A_t E_c} \quad (8.45)$$

Equation 8.45 gives the elongation of the tension tie due to the external load  $F$  at service load. It is readily seen that if the area of concrete is doubled, the elongation is halved for the same tensile force  $F$ . In sum, through a judicious choice of the geometry of the section, it is possible to reduce the elongation of prestressed tension members considerably.

Shortening of the tension tie occurs due to both the prestressing force and the long-term effects. The stress in the concrete due to initial prestress after transfer is

$$f_{ci} = -\frac{P_i}{A_c} \quad (8.46)$$

where  $A_c$  is the net area of concrete in the section. The reduced stress in the concrete that results in an effective prestressing force  $P_e$  after all time-dependent losses have occurred is

$$f_{ce} = -\frac{P_e}{A_c} \quad (8.47a)$$

while the effective stress in the prestressing steel is

$$f_{pe} = -\frac{P_e}{A_{ps}} \quad (8.47b)$$

Superimposing Equation 8.42 on Equation 8.47a for the total effect of the external tensile force  $F$  and the prestressing force  $P_e$ , we have, for the total stress in the concrete,

$$f_c = -\frac{P_e}{A_c} + \frac{F}{A_t} \quad (8.48)$$

The corresponding stress in the tendon is

$$f_{ps} = f_{pe} + \frac{nF}{A_t} \quad (8.49)$$

If cracking is not allowed in the tension member, the change in length  $\Delta L_{pc}$  (elongation) at service load, from Equation 8.49, is essentially equivalent to the reduction in length  $\Delta P$  due to the effective prestressing force  $P_e$  (see next).

### 8.15.2 Deformation Behavior

Evaluation of the deformation of the tension member is critical to the overall design of the entire structure. Changes in the length of the member can induce severe stresses in the adjoining members, which could lead to structural failure. If the member is post-tensioned and fully bonded, then the reduction in length due to the initial prestress  $P_i$  alone is

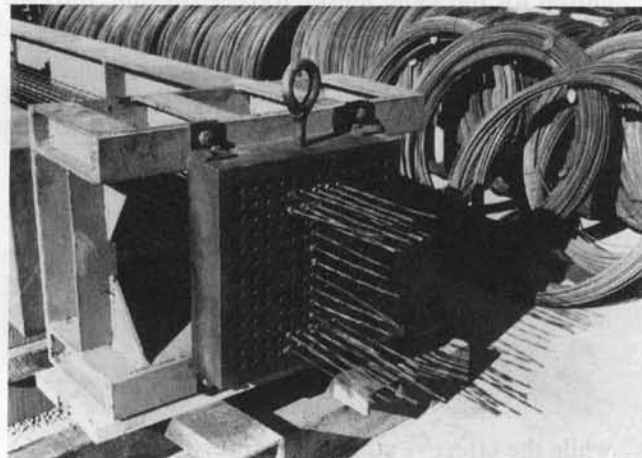
$$\Delta_i = -\frac{P_i L}{A_c E_c} \quad (8.50a)$$

and the elastic reduction in length after losses is

$$\Delta P = -\frac{P_e L}{A_c E_c} \quad (8.50b)$$

Due to creep, the initial prestressing force  $P_i$  reduces to the effective force  $P_e$ . So using a creep coefficient  $C_u$  and assuming, as in Chapter 7, an average force  $(P_i + P_e)/2$  as sufficiently accurate for evaluating creep loss, the change in length due to creep is

$$\Delta_{CR} = -\frac{L}{A_c E_c} \left[ C_u \left( \frac{P_i + P_e}{2} \right) \right] \quad (8.51)$$



**Photo 8.5** Laboratory prestressing bed. (Courtesy, Building Research Establishment, Garston, Watford, England.)

To account for shrinkage, the change in length is

$$\Delta_{SH} = \epsilon_{SH}L \quad (8.52)$$

so that the total effective reduction in length becomes

$$\Delta_e = -\left\{ \frac{L}{A_c E_c} \left[ P_e + C_u \left( \frac{P_i + P_e}{2} \right) \right] + \epsilon_{SH}L \right\} \quad (8.53)$$

Conversely, the loss in tension due to creep and shrinkage alone, from Equations 8.51 and 8.52, is

$$\Delta P = \frac{\Delta_{CR} + \Delta_{SH}}{L} E_{ps} A_{ps} \quad (8.54)$$

### 8.15.3 Decompression and Cracking

In considering decompression and cracking, it has to be assumed that no cracking is allowed at service load. If the probability of cracking exists due to a possible overload, an additional prestressing force and the addition of nonprestressed reinforcement become necessary to control cracking.

Assuming that only prestressed steel is provided, the tensile stress in the concrete at the *first cracking load*  $F_{cr}$  should not exceed the direct tensile strength of the concrete, ranging between  $f'_t = 3\lambda \sqrt{f'_c}$  and  $f'_t = 5\lambda \sqrt{f'_c}$ , where  $\lambda = 1, 0.85,$  and  $0.75$  for normal-weight, sand-lightweight and all-lightweight concrete, respectively. The cracking load  $F_{cr}$  can be evaluated from Equation 8.48 using the appropriate value of  $f'_t$ , viz.,

$$f'_t = -\frac{P_e}{A_c} + \frac{F_{cr}}{A_t} \quad (8.55)$$

Any overload beyond  $F_{cr}$  is expected to cause a dynamic increase in cracking such that all the applied load starts to be carried by the prestressing steel alone, with a consequent failure of the member. Therefore, provision of an adequate level of residual compressive stress in the concrete becomes necessary in major tension members.

A *decompression load*, namely, the load at  $f'_t = 0$  in Equation 8.55, should be the maximum allowable service load to which the member can be subjected. Equation 8.55 then becomes

$$f'_t = 0 = -\frac{P_e}{A_c} + \frac{F_{dec}}{A_t} \quad (8.56)$$

### 8.15.4 Limit State at Failure and Safety Factors

After cracking, the entire tension in the member is assumed to be carried by the prestressing tendon. Consequently, the nominal strength of the linear tension member is

$$F_n = A_{ps} f_{pu} \quad (8.57)$$

and the design ultimate load is

$$F_u = \phi_n F_n = \phi A_{ps} f_{pu} \quad (8.58)$$

It is important to provide a minimum safety factor of 1.5 for the decompression load  $F_{dec}$ . The safety factor level is determined by the importance of the tension member in the structure, the importance of the structure itself, and the negative effects of long-term reductions in length of the tension member on the integrity of the overall structure. It is not unreasonable under certain conditions to use a safety factor of 2.0 or more in a particular design.

### 8.16 SUGGESTED STEP-BY-STEP PROCEDURE FOR THE DESIGN OF TENSION MEMBERS

1. Determine the factored load  $F_u$  and the corresponding required nominal strength  $F_n = F_u/\phi$ .
2. Choose a uniform concrete compressive stress value at service load due to  $P_e$  to range between  $f_c = 0.20 f'_c$  and  $f_c = 0.30 f'_c$ . Select the area  $A_{ps}$  and the size of the prestressing strands, and then compute the net concrete area  $A_c = A_g - A_{duct}$  and the transformed area  $A_t = A_g + (n - 1)A_{ps}$ .
3. Compute the maximum allowable external force  $F$  based on decompression stress  $f'_t = 0$ , i.e., find  $F_{dec}$ . Then compute the first cracking load  $F_{cr}$ .
4. Find the factors of safety due to forces  $F$ ,  $F_{dec}$ , and  $F_{cr}$  to verify that they exceed the value 1.5.
5. Compute the length-shortening deformations due to creep and shrinkage (Equation 8.53):

$$\Delta_e = - \left\{ \frac{L}{A_c E_c} \left[ P_e + C_u \left( \frac{P_i + P_e}{2} \right) \right] + \epsilon_{SH} L \right\}$$

Then check whether the value obtained causes excessive stress in adjoining members. Next, compute the elongation

$$\Delta_L = \frac{FL}{A_t E_c}$$

due to external load (Equation 8.45) and verify whether the value obtained is within the specified limits of the design.

6. Adopt the design if all requirements are satisfied; otherwise, proceed through another trial-and-adjustment cycle.

A flowchart for the step-by-step trial-and-adjustment procedure that can be used for the design and/or analysis of linear tension members is presented in Figure 8.26.

### 8.17 DESIGN OF LINEAR TENSION MEMBERS

#### Example 8.4

A linear post-tensioned fully grouted direct-tension tie for an underground shelter shown in Figure 8.29 has a length  $L = 130$  ft (39.6 m). The tie is to be designed for a net horizontal roof and earthfill dead load of thrust  $F_d = 115,000$  lb (512 kN) and live load of thrust  $F_L = 55,000$  lb (245 kN). Design the tie with a safety factor not less than 1.5 against cracking and 1.2 against failure, using  $\frac{1}{2}$ -in. (12.7-mm) dia 270-K prestressing strands. The maximum allowable elongation due to external load is  $\frac{1}{2}$ -in., and given data are as follows:

$$f'_c = 6,000 \text{ psi, (41.4 MPa), normal weight}$$

$$f'_{ci} = 4,000 \text{ psi (31.0 MPa)}$$

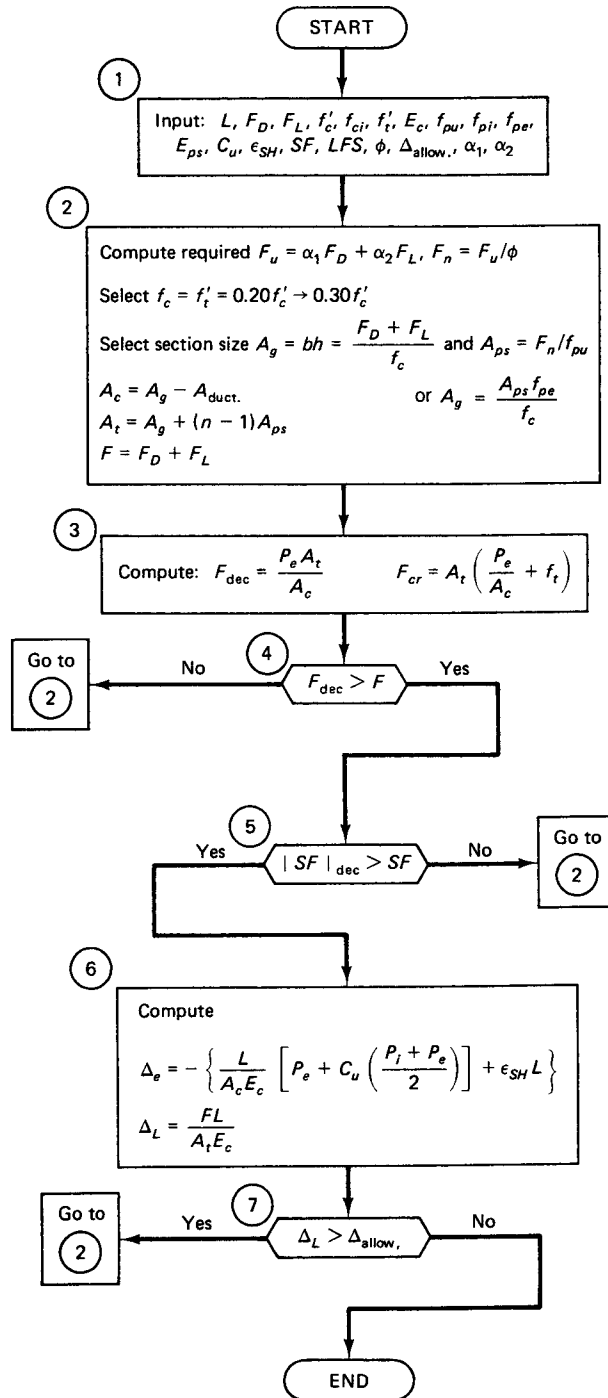
$$f'_t = 4\sqrt{f'_c} = 310 \text{ psi (2.14 MPa)}$$

$$E_{ci} = 4.06 \times 10^6 \text{ psi (28 MPa)}$$

$$E_c = 4.69 \times 10^6 \text{ psi (32.2 MPa)}$$

$$f_{pu} = 270,000 \text{ psi (1,862 MPa)}$$

$$f_{pi} = 190,000 \text{ psi (1,310 MPa)}$$



**Figure 8.26** Flowchart for the design (analysis) of linear prestressed tension members.



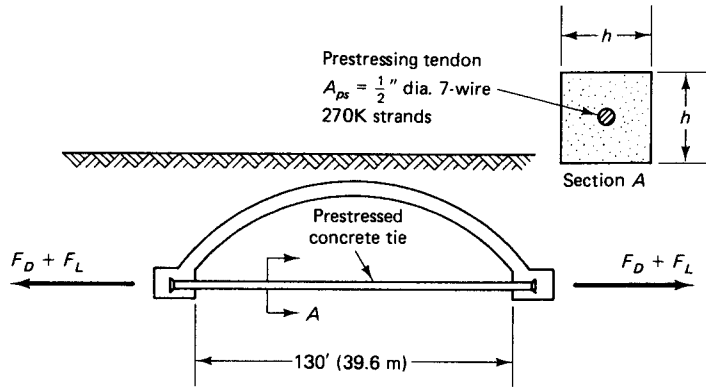


Figure 8.27 Prestressed concrete tie in Example 8.3.

$$f_{pe} = 150,000 \text{ psi (1,034 MPa)}$$

$$E_{ps} = 29 \times 10^6 \text{ psi (200} \times 10^3 \text{ MPa)}$$

$$n_p = E_{ps}/E_c = 29 \times 10^6/4.69 \times 10^6 = 6.18$$

$$C_u = 2.35$$

$$\epsilon_{SH} = 700 \times 10^{-6} \text{ in./in.}$$

The stress-strain diagram of the strands is given in Figure 8.7. Use a load factor of 1.2 for  $F_D$  and 1.6 for  $F_L$ .

**Solution:**

**Factored Loads and Choice of Strands (Steps 1 and 2).** The factored load is  $F_u = 1.2F_D + 1.6F_L = 1.2 \times 115,000 + 1.6 \times 55,000 = 226,000 \text{ lb (1005 kN)}$ , and the required nominal strength is  $F_n = F_u / \phi = 226,000/0.9 = 251,111 \text{ lb (1116 kN)}$ . So  $A_{ps} = F_n/f_{pu} = 251,111/270,000 = 0.93 \text{ in.}^2 \text{ (6.77 cm}^2\text{)}$ . Hence, trying  $\frac{1}{2}$ -in. (12.7-mm) dia 7-wire strands, we find that the number of strands =  $0.93/0.153 = 6.08$ . So we use seven tendons and obtain  $A_{ps} = 7 \times 0.153 = 1.07 \text{ in.}^2 \text{ (6.9 cm}^2\text{)}$ . Then the available nominal strength is  $F_n = 1.07 \times 270,000 = 288,900 \text{ lb (1,285 kN)}$ .

Now, assume that the uniform compressive stress that is caused by the prestressing force  $P_e$  is  $f_c = 0.25f'_c$ . Then  $P_e = 1.07 \times 150,000 = 160,500 \text{ lb}$  and  $A_g = 160,500/(0.25 \times 6,000) = 107 \text{ in.}^2$ . Accordingly, we try a tie rod section 11 in.  $\times$  11 in. (279 mm  $\times$  279 mm) and obtain  $A_g = 121 \text{ in.}^2$ . Then, assuming the tendon duct has a 2-in. diameter.

$$A_c = A_g - \frac{\pi(2)^2}{4} = 117.86 \text{ in.}^2 \text{ (760 cm}^2\text{)}$$

From Equation 8.41, the transformed concrete area is

$$A_t = A_g + (n - 1)A_{ps} = 121 + (6.18 - 1)1.07 = 126.54 \text{ in.}^2 \text{ (816.4 cm}^2\text{)}$$

**Check of Forces  $F$ ,  $F_{dec}$ , and  $F_{cr}$  (Steps 3 and 4).** From Equation 8.56,

$$f'_t = 0 = -\frac{P_e}{A_c} + \frac{F_{dec}}{A_t}$$

or

$$0 = -\frac{160,500}{117.86} + \frac{F_{dec}}{126.54}$$

So the maximum allowable  $F_{dec}$  is

$$\frac{160,500}{117.86} \times 126.54 = 172,320 \text{ lb (766 kN)}$$

and the actual  $F = F_D + F_L = 115,000 + 55,000 = 170,000 \text{ lb} < 172,320 \text{ lb}$ , which is satisfactory.

The first cracking load  $F_{cr}$  is obtained from Equation 8.55. Assume that the maximum tensile stress in the concrete at the first cracking load is  $4\lambda \sqrt{f'_c} = 4 \times 1.0 \times \sqrt{6,000} = 310 \text{ psi}$ . Then

$$f'_t = -\frac{P_e}{A_c} + \frac{F_{cr}}{A_t}$$

or

$$310 = -\frac{160,500}{117.86} + \frac{F_{cr}}{126.54}$$

$$F_{cr} = 211,548 \text{ lb}$$

From before, the available nominal strength is  $F_n = 288,900 \text{ lb}$ . So the design strength is  $F_u = \phi F_n = 0.9 \times 288,900 = 260,010 \text{ lb} > \text{required } F_u = 226,000 \text{ lb}$ , which is satisfactory. The cracking SF is  $F_u/F_{cr} = 260,010/211,548 = 1.23$ . This is close to 1.2, indicating that once the member is cracked it almost reaches its limit state at failure. Finally, the decompression SF is  $F_u/F_{dec} = 260,010/172,320 = 1.51$  and the actual SF is  $\phi F_n/F = 260,010/170,000 = 1.53$ . Thus, the available SF is greater than the required SF = 1.5, which is satisfactory.

**Deformation Check (Step 5).** We know that  $P_i = f_{pi}A_{ps} = 190,000 \times 1.07 = 203,300 \text{ lb}$  (904 kN). From Equation 8.50(a), the initial shortening at prestress transfer is

$$\Delta_i = -\frac{P_i L}{A_c E_c} = -\frac{203,300 \times 130 \times 12}{117.86 \times 4.69 \times 10^6} = -0.57 \text{ in. (15 mm)}$$

From Equation 8.53, the effective prestress shortening and long-term shortening due to creep and shrinkage is

$$\begin{aligned} \Delta_e &= -\left\{ \frac{L}{A_c E_c} \left[ P_e + C_u \left( \frac{P_i + P_e}{2} \right) \right] + \epsilon_{SH} L \right\} \\ &= -\left\{ \frac{130 \times 12 \times 10^3}{117.86 \times 4.69 \times 10^6} \left[ 160.5 + 2.35 \left( \frac{203.3 + 160.5}{2} \right) \right] \right. \\ &\quad \left. + 700 \times 10^{-6} (130 \times 12) \right\} \\ &= -2.75 \text{ in. (70 mm)} \end{aligned}$$

From Equation 8.45, the elongation due to external load is

$$\Delta_L = \frac{FL}{A_t E_c} = \frac{170,000(130 \times 12)}{126.54 \times 4.69 \times 10^6} = 0.45 \text{ in. (12 mm)}$$

which is satisfactory since the allowable  $\Delta$  is  $\frac{1}{2}$  in. So the net shortening is  $-2.75 + 0.45 - 0.57 = -2.87 \text{ in. (72 mm)}$ . Thus, a deformation of this magnitude has to be imposed on the adjoining elements in order to determine whether the resulting stresses are within the allowable limits. Assuming they are, we can adopt the design of an 11 in.  $\times$  11 in. tie prestressed with seven  $\frac{1}{2}$ -in. 7-wire 270-K straight tendons.

## SELECTED REFERENCES

- 8.1 ACI Committee 318. *Building Code Requirements for Structural Concrete (ACI 318-08)* (ACI 318R-08), American Concrete Institute, Farmington Hills, MI, 2008, 465 pp.

- 8.2 Nawy, E. G., *Reinforced Concrete—A Fundamental Approach*, 6th ed. (1st ed., 1985). Upper Saddle River, NJ: Prentice Hall, 2009, 936 pp.
- 8.3 Prestressed Concrete Institute. *PCI Design Handbook*, 5th ed. Prestressed Concrete Institute, Chicago, 1999.
- 8.4 Post-Tensioning Institute. *Post-Tensioning Manual*. 5th ed. Post-Tensioning Institute, Phoenix, 1991.
- 8.5 Lin, T. Y., and Lakhwara, T. R. "Ultimate Strength of Eccentrically Loaded Partially Prestressed Columns." *PCI Journal* 11 (1986): 37–49.
- 8.6 Gerwick, B. C., Jr. *Construction of Prestressed Concrete Structures*. Wiley-Interscience, New York, 1993.
- 8.7 Zia, P., and Moriadith, F. L. "Ultimate Load Capacity of Prestressed Concrete Columns." *Journal of the American Concrete Institute* 63 (1986): 767–788.
- 8.8 Gerwick, B. C., Jr. "Prestressed Concrete Developments in Japan." *Journal of the Prestressed Concrete Institute* 23 (1978): 66–76.
- 8.9 Wheen, R. J. "Prestressed Concrete Members in Direct Tension." *Journal of the Structural Division, American Society of Civil Engineers*, 105 (1979): 1471–1487.
- 8.10 Wilhelm, W. J., and Zia, P. "Effects of Creep and Shrinkage on Prestressed Concrete Columns." *Journal of the Structural Division, American Society of Civil Engineers*, Reston, Va, 96, 1970, 2103–2123.
- 8.11 Hsu, C. T. T., "Analysis and Design of Square and Rectangular Columns by Equation of Failure Surface," *ACI Struct. J.*, March–April 1988, American Concrete Institute, Farmington Hills, MI, March–April, 1988, pp. 167–189.
- 8.12 Nawy, E. G., editor-in-chief, *Concrete Construction Engineering Handbook*, 2nd ed., CRC Press, Boca Raton, FL, 2008, 1560 p.
- 8.13 Nawy, E. G., *Fundamentals of High Performance Concrete*, 2nd ed., John Wiley and Sons, New York, 2001, 440 p.
- 8.14 Nawy, E. G., "Concrete—The Sustainable Infrastructure Material for the 21 st. Century," Keynote Address Paper, No. E-C103, Transportation Research Board, National Research Council, Washington, D.C., September 2006, pp. 1–23.
- 8.15 Nawy, E. G., "Concrete—The Sustainable Infrastructure Material for the 21 st. Century," Keynote Address Paper, Proceedings, The First International Conference on Recent Advances in Concrete Technology, Crystal City, Washington, D.C., September 19, 2007, pp. 1–24.

## PROBLEMS

- 8.1 Compute the nominal strengths  $P_n$  and  $M_n$  of the precast prestressed tied concrete nonslender column having the cross section shown in Figure P8.1 and an eccentricity  $e = 9$  in. The column is prestressed with six  $\frac{1}{2}$ -in. dia 7-wire 270-K stress-relieved prestressing strands having the stress-strain properties shown in figure 8.9. Determine the type of initial failure of the column, and design the size and spacing of the necessary ties. Given data are as follows:

$$f'_c = 7,000 \text{ psi (48.6 MPa), normal-weight concrete}$$

$$f'_{ci} = 4,900 \text{ psi (33.8 MPa)}$$

$$f_{pu} = 270,000 \text{ psi (1,862 MPa)}$$

$$f_{py} = 255,000 \text{ psi (1,758 MPa)}$$

$$f_{pe} = 150,000 \text{ psi (1,034 MPa)}$$

$$\epsilon_{cu} = 0.0038 \text{ in./in.}$$

$$\epsilon_{ce} = 0.0008 \text{ in./in.}$$

$$E_{ps} = 29 \times 10^6 \text{ psi (200} \times 10^3 \text{ MPa)}$$

$$d' = 2 \text{ in. (50.8 mm)}$$

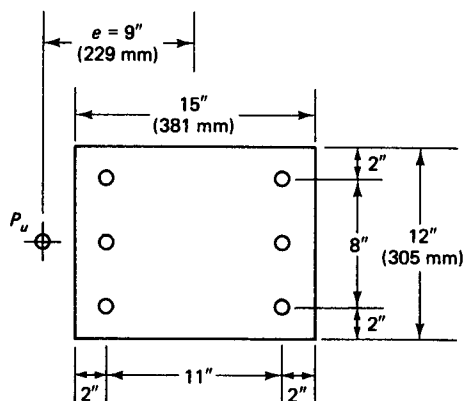


Figure P8.1 Column section.

- 8.2** Construct the nominal load–moment  $P_n - M_n$  and the design  $P_u - M_u$  diagrams for the prestressed concrete columns in Example 8.1 if the overall sectional dimensions of the column are 20 in. (508 mm)  $\times$  20 in. (508 mm) and the prestressing reinforcement is twelve  $\frac{1}{2}$ -in. dia 7-wire 270-K, half of which are placed at each face parallel to the neutral axis.
- 8.3** Design a square tied prestressed bonded slender column having a clear height  $l_u = 20$  ft (6.10 m) and which is not braced against sidesway. The column is loaded with the same magnitudes of loads and moments and is constructed of the same properties as the materials used in Example 8.2. The design should cover the following two loading conditions:
1. Gravity loading only, assuming that lateral sidesway due to wind is negligible.
  2. Sidesway of the force and moment magnitudes of Example 8.2.
- Compare the size needed in Problem 8.2 for  $l_u = 20$  ft to the size of the column in Example 8.2 with  $l_u = 15$  ft (4.57 m).
- 8.4** Design the column in Problem 8.3 as a biaxially loaded non-slender braced column subjected to factored moments  $M_{ux} = M_{uy} = 1,100,000$  in.-lb. Use the Modified Load Contour Method in the solution.
- 8.5** Design the prestressed tension member in Example 8.4 if its length  $L = 90$  ft (27.4 m), and compare the section obtained with the section of the 130-ft (39.6-m)-long tie in the example.

# 9



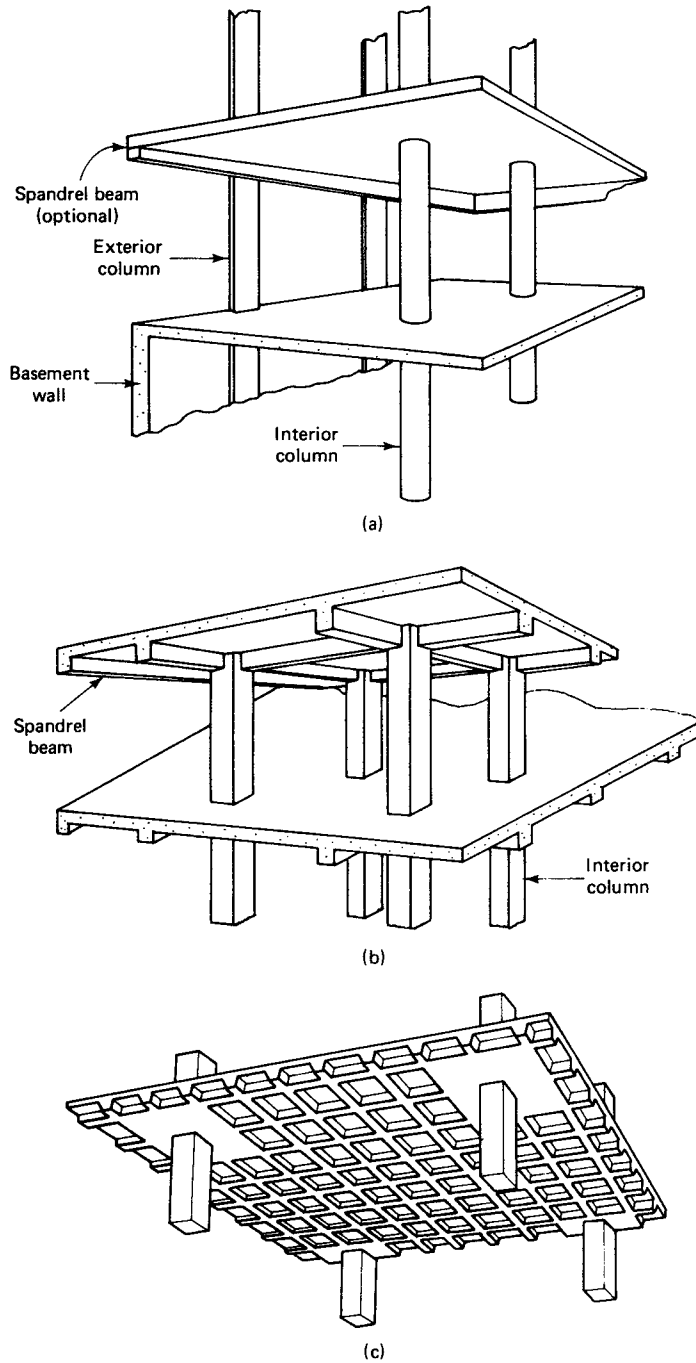
## TWO-WAY PRESTRESSED CONCRETE FLOOR SYSTEMS

### 9.1 INTRODUCTION: REVIEW OF METHODS

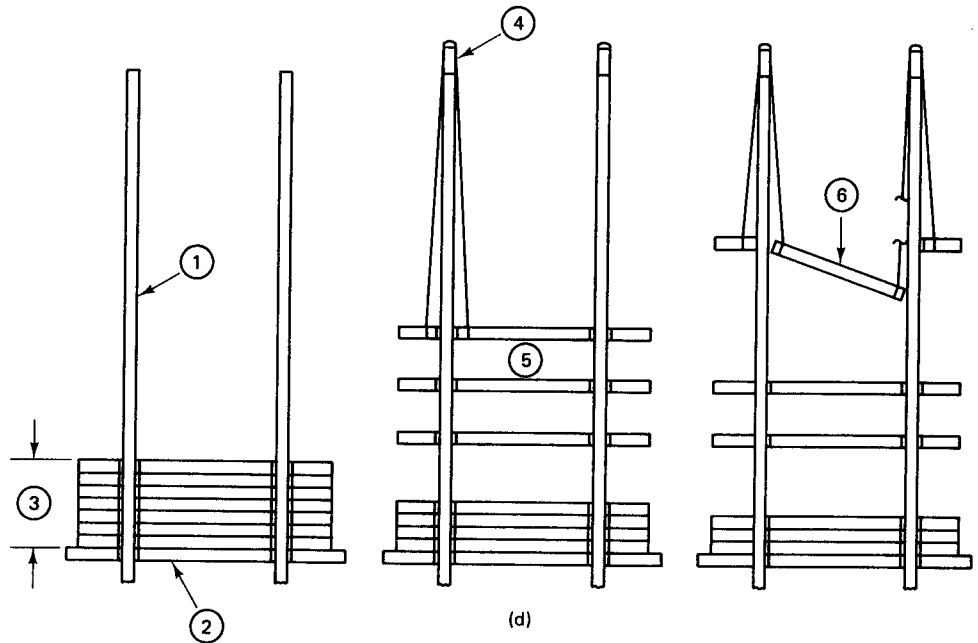
Supported floor systems are usually constructed of reinforced concrete cast in place. Two-way slabs and plates are those panels in which the dimensional ratio of length to width is less than 2. The analysis and design of framed floor slab systems represented in Figure 9.1 encompasses more than one aspect of such systems. The present state of knowledge permits reasonable evaluation of (1) the moment capacity, (2) the slab-column shear capacity, and (3) serviceability behavior, as determined by deflection control and crack control. Note that flat plates are slabs supported directly on columns without beams, as shown in part (a) of the figure, compared to part (b) for slabs on beams, and part (c) for waffle slab floors.

Essentially the same principles are used in the analysis of continuous two-way prestressed concrete flat plate systems as in the analysis of reinforced concrete plate systems. The techniques of construction differ, however, and it is often unlikely that economic considerations alone can justify using prestressed two-way floor systems of the types shown in Figures 9.1(b) and (c). The prestressing is normally post-tensioned after the two-way plate is cast. Sometimes, on-site precast two-way slabs, called *lift slabs*, are used

University of Wyoming, addition. (Courtesy, Prestressed Concrete Institute.)



**Figure 9.1** Two-way-action floor systems. (a) Two-way flat-plate floor. (b) Two-way slab floor on beams. (c) Waffle slab floor.



- ① Support columns are set in place.
- ② Ground-floor slab is cast.
- ③ Slabs for succeeding floors are cast and layered atop each other, separated by a membrane.
- ④ Jacks are fastened on top of support columns.
- ⑤ Slabs are raised, starting with the top one, and are gradually worked up one at a time.
- ⑥ Jack failure could cause slab to become unlevel and fall, causing slabs below and beside also to fall.

Figure 9.1 Continued (d) Lift-slab installation technique.

as a distinct structural system that is fast to construct and perhaps more economical than cast-in-place prestressed two-way slabs. However, the construction technique in lift slabs and the absence of the expertise required for such construction can create hazardous conditions which may result in loss of stability and structural collapse.

The technique for producing lift slabs involves casting a ground-level slab which can double as a casting bed over which all the other floor slabs are cast and stacked, separated by a membrane or sprayed parting agent. The columns, which can be steel or concrete, are built prior to the casting of the basic bottom slab extending to the building's height. All the other slabs are cast around the columns, with steel collars having sufficient clearance to permit *lifting* (jacking) of the slab or plate to the appropriate floor level, as shown in Figure 9.1(d). Lifting is accomplished through the use of jacks placed on top of the columns and connected to threaded rods extending down the faces of the columns to the lifting collars embedded in the slabs. Simultaneous activation of all the jacks is essential in order to maintain the slab in a totally horizontal state to avoid imbalance.

The analysis of slab behavior in flexure up to the 1940s and early 1950s followed the classical theory of elasticity, particularly in the United States. The small-deflections theory of plates, assuming the material to be homogeneous and isotropic, formed the basis of ACI Code recommendations with moment coefficient tables. The work, principally by Westergaard, which empirically allowed limited moment redistribution, guided the

thinking of the code writers. Hence, the elastic solutions, complicated even for simple shapes and boundary conditions when no computers were available, made it mandatory to idealize, and sometimes render empirical, conditions beyond economic bounds.

In 1943, Johansen presented his yield-line theory for evaluating the collapse capacity of slabs. Since that time, extensive research into the ultimate behavior of reinforced concrete slabs has been undertaken. Studies by many investigators, such as those of Ockleston, Mansfield, Rzhantsyn, Powell, Wood, Sawczuk, Gamble-Sozen-Siess, and Park, contributed immensely to a further understanding of the limit-state behavior of slabs and plates at failure as well as at serviceable load levels.

The various methods that are used for the analysis and design of two-way action slabs and plates are summarized in the following subsections.

### 9.1.1 The Semielastic ACI Code Approach

The ACI approach gives two alternatives for the analysis and design of a framed two-way action slab or plate system: the direct design method and the equivalent frame method. Both methods are discussed in more detail in Section 9.3. The equivalent frame method will be used in the design and analysis of prestressed slabs and plates.

### 9.1.2 The Yield-Line Theory

Whereas the semielastic code approach applies to standard cases and shapes and has an inherent excessively large safety factor with respect to capacity, the yield-line theory is a plastic theory easy to apply to irregular shapes and boundary conditions. Provided that serviceability constraints are applied, Johansen's yield-line theory represents the true behavior of concrete slabs and plates, permitting evaluation of the bending moments from an assumed collapse mechanism which is a function of the type of external load and the shape of the floor panel. This topic will be discussed in more detail in Section 9.14.

### 9.1.3 The Limit Theory of Plates

The interest in developing a limit solution became necessary due to the possibility of finding a variation in the collapse field which could give a lower failure load. Hence, an upper bound solution requiring a valid mechanism when applying the work equation was sought, as well as a lower bound solution requiring that the stress field satisfy everywhere the differential equation of equilibrium, that is,

$$\frac{\partial^2 M_x}{\partial x^2} - 2 \frac{\partial^2 M_{xy}}{\partial x \partial y} + \frac{\partial^2 M_y}{\partial y^2} = -w \quad (9.1)$$

where  $M_x$ ,  $M_y$ , and  $M_{xy}$  are the bending moments and  $w$  is the unit intensity of load. Variable reinforcement permits the lower bound solution still to be valid. Wood, Park, and other researchers have given more accurate semiexact predictions of the collapse load.

For limit-state solutions, the slab is assumed to be completely rigid until collapse. Further work at Rutgers by Nawy incorporated the deflection effect at high load levels as well as the compressive membrane force effects in predicting the collapse load.

### 9.1.4 The Strip Method

The strip method was proposed by Hillerborg, in attempting to fit the reinforcement to the strip fields. Since practical considerations require the reinforcement to be placed in orthogonal directions, Hillerborg set twisting moments equal to zero and transformed the slab into intersecting beam strips, hence the name "strip method."



Except for Johansen's yield-line theory, most of the other solutions are lower bound. Johansen's upper-bound solution can give the highest collapse load as long as a valid failure mechanism is used in predicting the collapse load.

### 9.1.5 Summary

The equivalent frame method will be the chief method discussed, because of the limitations of the use of the direct design method in its applicability to two-way prestressed floor systems and the need for more refined determination of the stiffnesses at the column-slab joints in the design process. The yield-line theory for the limit state at failure evaluation of slabs and plates will also be concisely presented.

## 9.2 FLEXURAL BEHAVIOR OF TWO-WAY SLABS AND PLATES

### 9.2.1 Two-Way Action

Consider a single rectangular panel supported on all four sides by unyielding supports such as shear walls or stiff beams. We seek to visualize the physical behavior of the panel under gravity load. The panel will deflect in a dishlike form under the external load, and its corners will lift if it is not monolithically cast with the supports. The contours shown in Figure 9.2(a) indicate that the curvatures and consequently the moments at the central area  $C$  are more severe in the shorter direction  $y$  with its steep contours than in the longer direction  $x$ .

Evaluation of the division of moments in the  $x$  and  $y$  directions is extremely complex, as the behavior is highly statically indeterminate. The simple case of the panel in part (a) of Figure 9.2 is expounded by taking strips  $AB$  and  $DE$  at midspan, as in part (b), such that the deflection of both strips at the central point  $C$  is the same.

The deflection of a simply supported uniformly loaded beam is  $5wl^4/384EI$ , i.e.,  $\Delta = kwl^4$ , where  $k$  is a constant. If the thickness of the two strips is the same, the deflection of strip  $AB$  is  $kw_{AB}L^4$  and the deflection of strip  $DE$  is  $kw_{DE}S^4$ , where  $w_{AB}$  and  $w_{DE}$  are the portions of the total load intensity  $w$  transferred to strips  $AB$  and  $DE$ , respectively, i.e.,  $w = w_{AB} + w_{DE}$ . Equating the deflections of the two strips at the central point  $C$ , we get

$$w_{AB} = \frac{wS^4}{L^4 + S^4} \quad (9.2a)$$

and

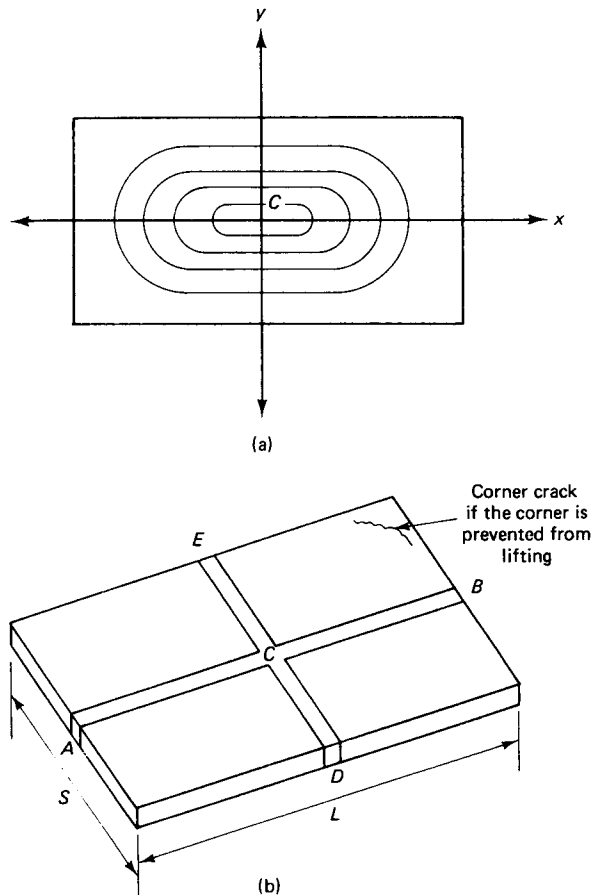
$$w_{DE} = \frac{wL^4}{L^4 + S^4} \quad (9.2b)$$

It is seen from these equations that the shorter span  $S$  of strip  $DE$  carries the heavier portion of the load. Hence, the shorter span of such a slab panel on unyielding supports is subjected to the larger moment, supporting the foregoing discussion of the steepness of the curvature contours in Figure 9.2(a).

Note that while the ACI 318 Code proposes using "q" for the unit intensity of load for two-way slabs, it is preferable to continue the traditional practice of identifying the load intensity as "w," as is done in this chapter.

### 9.2.2 Relative Stiffness Effects

Alternatively, one has to consider a slab panel supported by flexible supports such as beams and columns, or flat plates supported by a grid of columns. In either case, the distribution of moments in the short and long directions is considerably more complex. This complexity arises from the fact that the degree of stiffness of the yielding supports determines the intensity of steepness of the curvature contours in Figure 9.2(a) in both the  $x$  and  $y$  directions and the redistribution of moments.



**Figure 9.2** Deflection of panels and strips. (a) Curvature and deflection contours in a floor panel. (b) Central slips in a two-way slab panel.

The ratio of the stiffness of the beam supports to the slab stiffness can result in curvatures and moments in the long direction larger than those in the short direction, as the total floor behaves as an orthotropic *plate* supported on a grid of columns without beams. If the long span  $L$  in such floor systems of slab panels without beams is considerably larger than the short span  $S$ , the maximum moment at the center of a plate panel would approximate the moment at the middle of a uniformly loaded strip of span  $L$  that is clamped at both ends.

In sum, as slabs are flexible and highly underreinforced, redistribution of moments in both the long and short directions depends on the relative stiffnesses of the supports and the supported panels. Overstress in one region is reduced by such redistribution of moments to the lesser stressed regions.

## 9.3 THE EQUIVALENT FRAME METHOD

### 9.3.1 Introduction

The following discussion of the equivalent frame method of analysis for two-way systems summarizes the ACI Code approach to the evaluation and distribution of the total moments in a two-way slab panel. The Code assumes that vertical panels cut through an en-

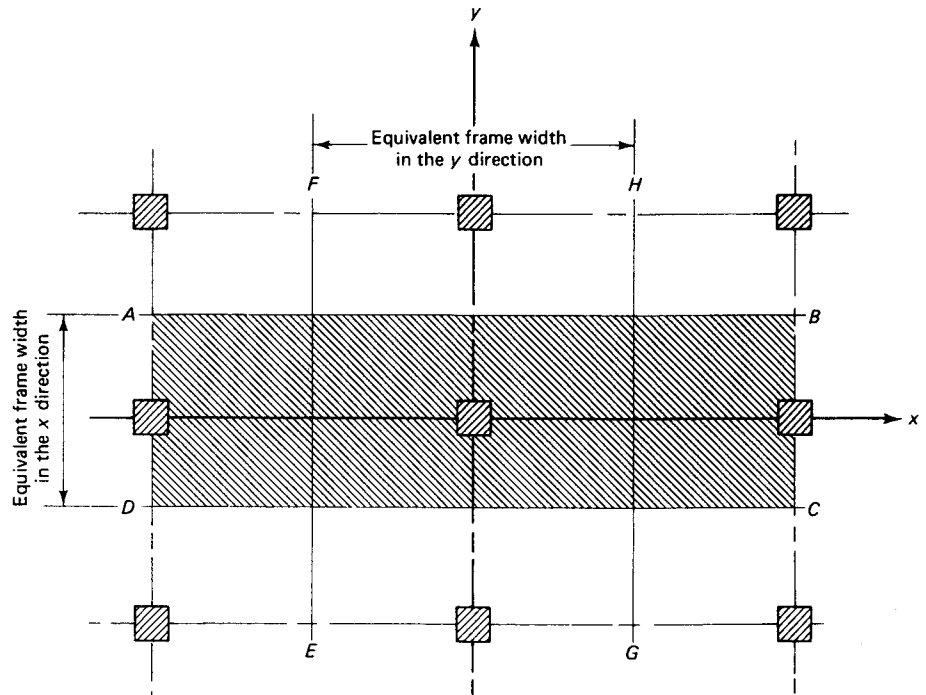
ture rectangularly planned multistory building along lines  $AB$  and  $CD$  in Figure 9.3 midway between columns. A rigid frame results in the  $x$  direction. Similarly, vertical planes  $EF$  and  $HG$  result in a rigid frame in the  $y$  direction. A solution of such an idealized frame consisting of horizontal beams or equivalent slabs and supporting columns enables the design of the slab as the beam part of the frame. The equivalent frame method thus treats the idealized frame in a manner similar to an actual frame, and hence is more exact and has fewer limitations than the direct design method. Basically, it involves a full moment distribution of many cycles as compared to the direct design method, which involves a one-cycle moment distribution approximation.

### 9.3.2 Limitations of the Direct Design Method

The following are the limitations of the direct design method:

1. There is a minimum of three continuous spans in each direction.
2. The ratio of the longer to the shorter span within a panel should not exceed 2.0.
3. Successive span lengths in each direction should not differ by more than one-third the length of the longer span.
4. Columns may be offset a maximum of 10 percent of the span in the direction of the offset from either axis between the center lines of successive columns.
5. All loads shall be due to gravity only and uniformly distributed over the entire panel. The live load shall not exceed three times the dead load.
6. If the panel is supported by beams on all sides, the relative stiffness of the beams in two perpendicular directions shall not be less than 0.2 or greater than 5.0.

Given these limitations, for prestressed concrete floor slabs, it is necessary to use the equivalent frame method.



**Figure 9.3** Floor plan with equivalent frame (shaded area in  $x$  direction).

### 9.3.3 Determination of the Statical Moment $M_0$

There are basically four major steps in the design of the floor panels:

1. Determine the total statical moment in each of the two perpendicular directions.
2. Distribute the total moment for the design of sections for negative and positive moment.
3. Distribute the negative and positive moments to the column and middle strips and to the panel beams, if any. A column strip is a width that is 25 percent of the equivalent frame width on each side of the column center line, and whose middle strip is the balance of the equivalent frame width.
4. Proportion the size and distribution of the reinforcement in the two perpendicular directions.

Given the above, correct determination of the values of the distributed moments becomes a principal objective. Consider typical interior panels having center line dimensions  $l_1$  in the direction of the moments being considered and dimensions  $l_2$  in the direction perpendicular to  $l_1$ , as shown in Figure 9.4. The clear span  $l_n$  extends from face to face of columns, capitals, or walls. Its value should not be less than  $0.65l_1$ , and circular supports shall be treated as square supports having the same cross-sectional area. The total statical moment of a uniformly loaded simply supported beam as a one-dimensional member is  $M_0 = wl^2/8$ . In a two-way slab panel as a two-dimensional member, the idealization of the structure through conversion to an equivalent frame makes it possible to compute  $M_0$  once in the  $x$  direction and again in the orthogonal  $y$  direction. If one takes as a free-body diagram the typical interior panel shown in Figure 9.5(a), symmetry reduces the shears and twisting moments to zero along the edges of the cut segment. If no restraint existed at ends  $A$  and  $B$ , the panel would be considered simply supported in the span  $l_n$  direction. If one cuts at midspan, as in Figure 9.5(b), and considers half the panel as a free-body diagram, the moment  $M_0$  at midspan would be

$$M_0 = \frac{wl_2 l_{n1}}{2} \frac{l_{n1}}{2} - \frac{wl_2 l_{n1}}{2} \frac{l_{n1}}{4}$$

or

$$M_0 = \frac{wl_2(l_{n1})^2}{8} \quad (9.3)$$

Due to the existence of restraint at the supports,  $M_0$  in the  $x$  direction would be distributed to the supports and midspan such that

$$M_0 = M_C + \frac{1}{2}(M_A + M_B) \quad (9.4a)$$

The distribution would depend on the degree of stiffness of the support. In a similar manner,  $M_0$  in the  $y$  direction would be the sum of the moments at midspan and the average of the moments at the supports in that direction.

In the orthogonal direction, Equation 9.4a becomes

$$M'_0 = M'_C + \frac{1}{2}(M'_A + M'_B) \quad (9.4b)$$

where  $M'_0$ ,  $M'_A$ ,  $M'_B$ , and  $M'_C$  are at 90 degrees to  $M_0$ ,  $M_A$ ,  $M_B$ , and  $M_C$ , respectively. Also, in an analogous manner to Equation 9.3,

$$M'_0 = \frac{Wl_1(l_{n2})^2}{8} \quad (9.5)$$

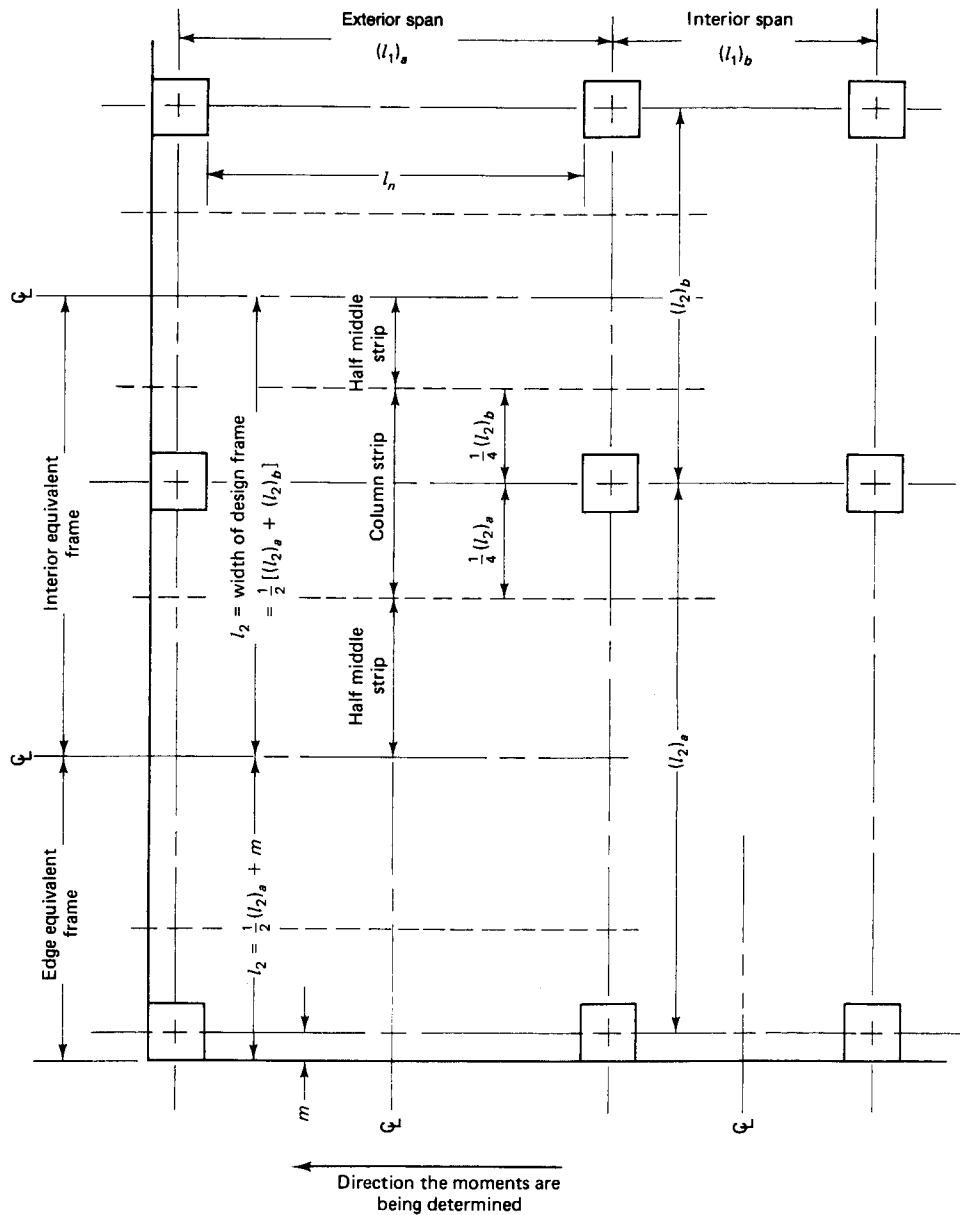
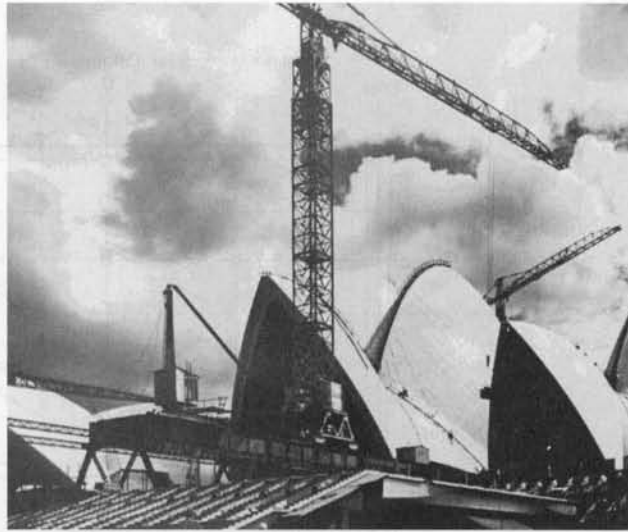


Figure 9.4 Column and middle strips of the equivalent frame (y direction).

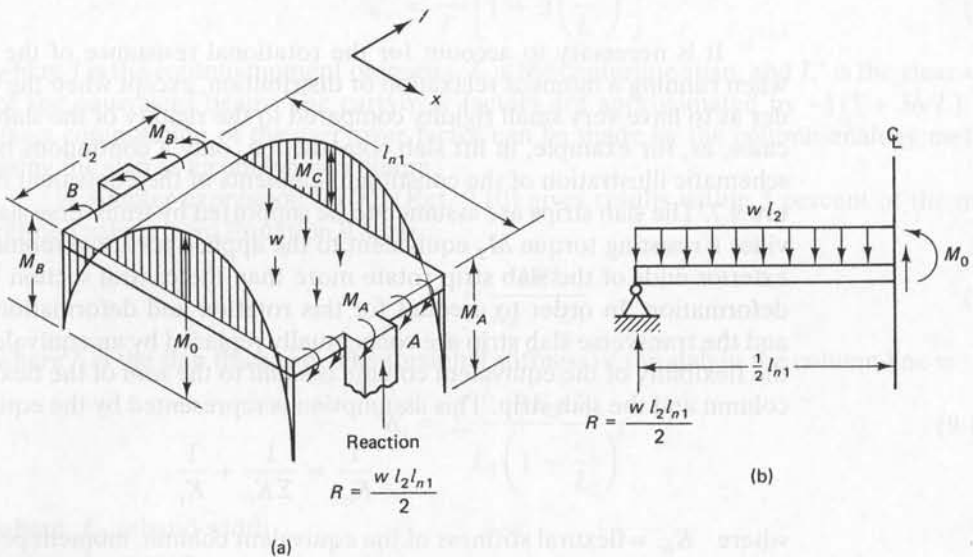


**Photo 9.1** Sydney Opera House during construction.

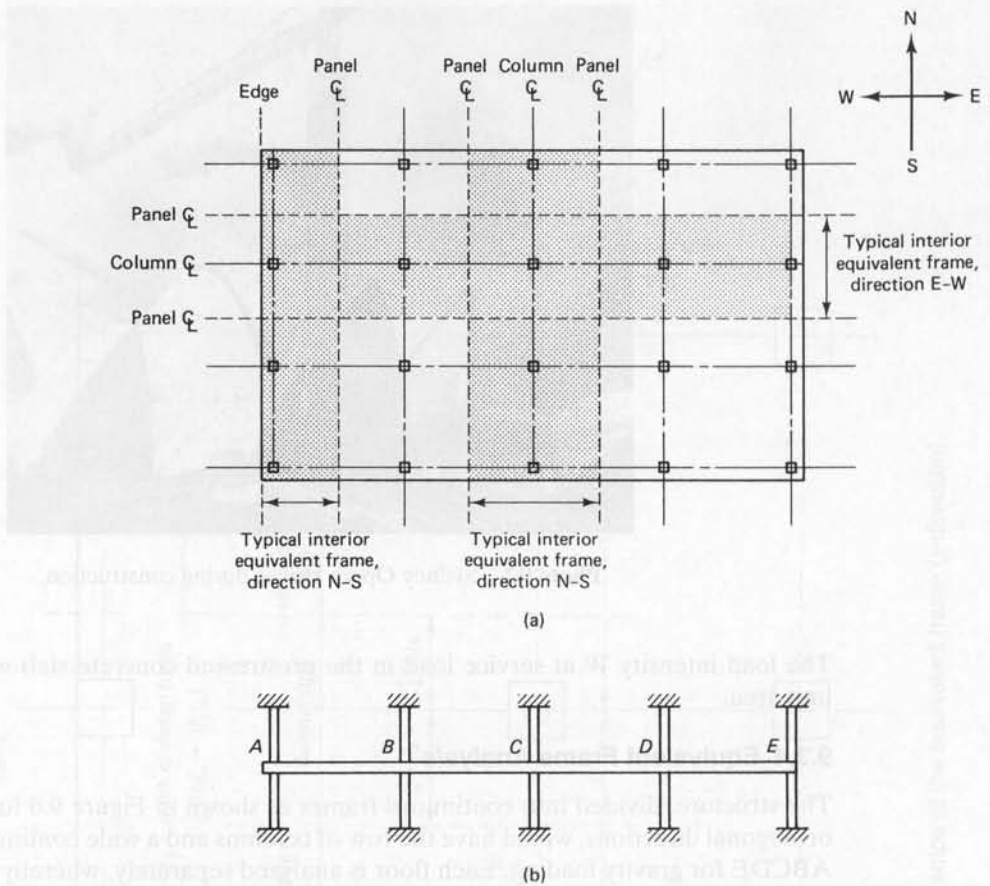
The load intensity  $W$  at service load in the prestressed concrete slab would be  $W_w$  per unit area.

### 9.3.4 Equivalent Frame Analysis

The structure, divided into continuous frames as shown in Figure 9.6 for frames in both orthogonal directions, would have the row of columns and a wide continuous beam (slab) ABCDE for gravity loading. Each floor is analyzed separately, whereby the columns are assumed fixed at the floors above and below. To satisfy statical and equilibrium considerations, each equivalent frame must carry the total applied load; alternate span loading has to be used for the worst live-load condition.



**Figure 9.5** Simple moment  $M_0$  acting on an interior two-way slab panel in  $x$ -direction. (a) Moment on panel. (b) Free-body diagram.

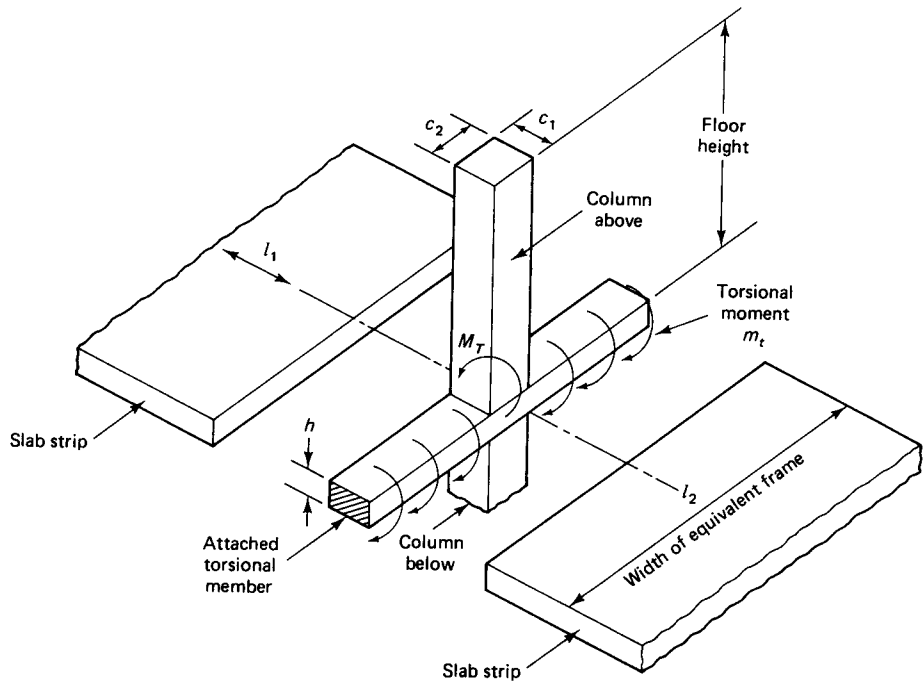


**Figure 9.6** Idealized structure divided into equivalent frames. (a) Plan. (b) Section in E-W direction.

It is necessary to account for the rotational resistance of the column at the joint when running a moment relaxation or distribution, except when the columns are so slender as to have very small rigidity compared to the rigidity of the slab at the joint. In such cases, as, for example, in lift slab construction, only a continuous beam is necessary. A schematic illustration of the constituent elements of the equivalent frame is given in Figure 9.7. The slab strips are assumed to be supported by transverse slabs. The column provides a resisting torque  $M_T$  equivalent to the applied torsional moment intensity  $m_t$ . The exterior ends of the slab strip rotate more than the central section because of torsional deformation. In order to account for this rotation and deformation, the actual column and the transverse slab strip are conceptually replaced by an equivalent column such that the flexibility of the equivalent column is *equal* to the *sum* of the flexibilities of the actual column and the slab strip. This assumption is represented by the equation

$$\frac{1}{K_{ec}} = \frac{1}{\Sigma K_c} + \frac{1}{K_t} \quad (9.6)$$

where  $K_{ec}$  = flexural stiffness of the equivalent column, moment per unit rotation  
 $\Sigma K_c$  = sum of flexural stiffnesses of the upper and lower columns at the joint, moment per unit rotation  
 $K_t$  = torsional stiffness of the torsional beam, moment per unit rotation.



**Figure 9.7** Constituent elements of the equivalent frame.

Alternatively, Equation 9.6 can be written as the stiffness equation

$$K_{ec} = \frac{\sum K_c}{1 + \frac{\sum K_c}{K_t}} \quad (9.7)$$

and the column stiffness for an equivalent frame (Ref. 9.9) can be defined as

$$K_c = \frac{EI}{l'} \left[ 1 + 3 \left( \frac{L}{L'} \right)^2 \right] \quad (9.8)$$

where  $I$  is the column moment of inertia,  $L$  is the centerline span, and  $L'$  is the clear span of the equivalent beam. The carryover factors are approximated by  $-\frac{1}{2}(1 + 3h/L)$ . An exact computation of the carryover factor can be made by the column-analogy method using the slab as an analogous column.

A simpler expression for  $K_c$  (Ref. 9.10) gives results within 5 percent of the more refined values from Equation 9.8, viz.,

$$K_c = \frac{4EI}{L_n - 2h} \quad (9.9)$$

where  $h$  is the slab thickness. The torsional stiffness of the slab in the column line is

$$K_t = \sum \frac{9E_{cs}C}{L_2 \left( 1 - \frac{c_2}{L_2} \right)^3} \quad (9.10a)$$

where  $L_2 =$  band width

$L_n =$  span

$c_2 =$  column dimensions in the direction parallel to the torsional beam and the torsional constant is



$$C = \Sigma(1 - 0.63x/y)x^3 y/3 \tag{9.10b}$$

in which  $x$  = shorter dimension of the rectangular part of the cross section at the column junction (such as the slab depth)

$y$  = longer dimension of the rectangular part of the cross section at the column junction (such as the column width).

It should be noted that the torsional stiffness  $K_t = \frac{9E_s C}{L_2[1 - (c_2/L_2)]^3}$  denotes the value of only the part of the torsional beam at *one* side of the equivalent frame column. The summation in Equation 9.10a gives the value for the total length of the torsional beam. Hence, if the adjacent spans are equal, then  $\Sigma K_t$  = twice the value obtained from the above expression.

The slab stiffness is given by the equation

$$K_s = \frac{4E_{cs} I_s}{L_n - c_1/2} \tag{9.11}$$

As the effective stiffness  $K_{ec}$  of the column and the slab stiffness  $K_s$  are established, the analysis of the equivalent frame can be performed by any applicable methods, such as relaxation or moment distribution.

The distribution factor for the fixed-end moment *FEM* is

$$DF = \frac{K_s}{\Sigma K} \tag{9.12}$$

where  $\Sigma K = K_{ec} + K_{s(left)} + K_{s(right)}$ . A carryover factor of  $COF \cong \frac{1}{2}$  can be used without loss of accuracy since the nonprismatic section causes only very small effects on fixed-end moments and carryover factors. The fixed-end moment *FEM* for a uniformly distributed load is  $wl_2(l_n)^2/12$  at the supports, such that after moment redistribution the sum of the negative distributed moment at the support and the midspan moment is always equal to the static moment  $M_0 = wl_2(l_n)^2/8$ .

### 9.3.5 Pattern Loading of Spans

Loading all spans simultaneously does not necessarily produce the maximum positive and negative flexural stresses. Consequently, it is advisable to analyze the multispan frame using alternative span loading patterns for the *live* load. For a three-span frame, the suggested patterns for the live load are shown in Figure 9.8.

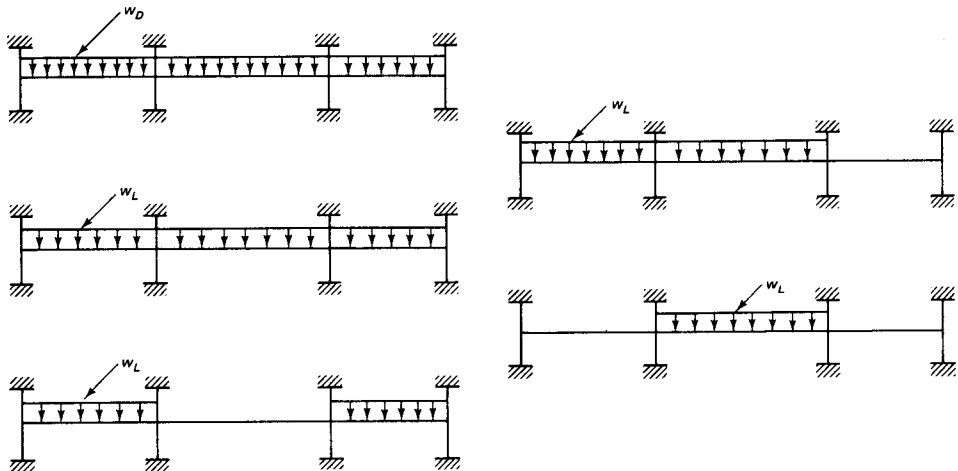


Figure 9.8 Loading patterns for live load.

## 9.4 TWO-DIRECTIONAL LOAD BALANCING

As mentioned in Chapter 1, load balancing represents the forces counteracting the external gravity load. These forces are produced by the transverse component of the longitudinal prestressing force in a parabolic or harped tendon. The load  $w$  in Equations 9.3 to 9.5 represents the *downward* external transverse load intensity, which can be either the working load intensity  $w_w$  or the factored load intensity  $w_u$ . The *upward* load intensity in the slab field due to the transverse component of the prestressing force, also mentioned in Chapter 1, would reduce the effect of  $w_w$  and can be chosen so as to *exactly balance* a particular downward load intensity. Under such a condition, the two-way slab would be subjected to neither bending nor twisting moments, and the analysis would be considerably simplified.

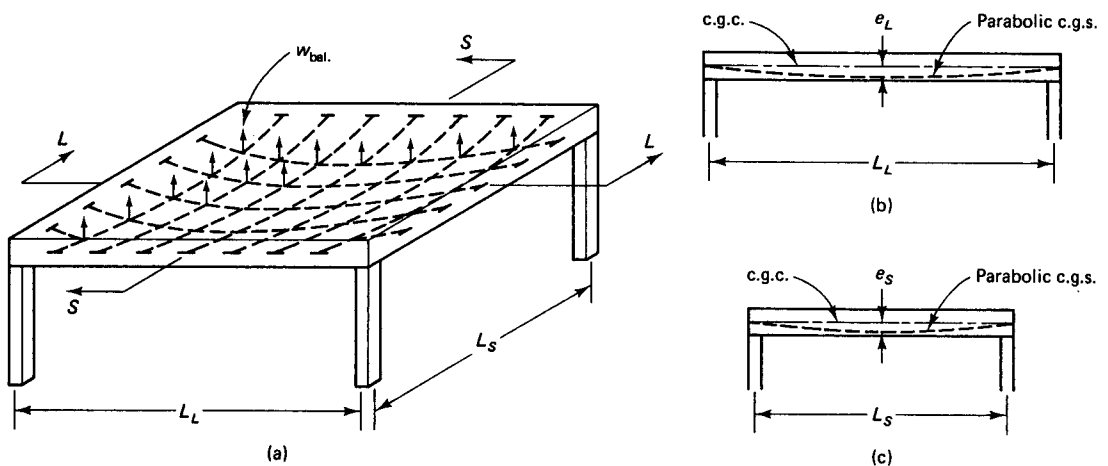
Two-directional load balancing in two-way slabs is different from one-directional load balancing in beams. The balancing load produced by the tendons in one direction either increases or decreases the balancing load produced by the tendons in the perpendicular direction. Hence, the prestressing forces and tendon profiles in the two orthogonal directions are totally *interrelated*, fully maintaining the basic principles of statics. The ultimate benefit of load balancing is in the creation of a design of a structural prestressed floor such that the upward component of the prestressing force results in a load intensity distribution in each direction that is equivalent to the downward external load intensity. Such a design is called a pure *balanced design*. Any deviation from the balanced condition should be analyzed as a load acting on the slab without being affected by the transverse upward component of prestress.

If a two-way slab on rigid supports such as walls is prestressed in both orthogonal directions having spans  $L_S$  and  $L_L$  in the short and long directions, respectively, as shown in Figure 9.9, the intensity of the upward balancing load required to produce balanced design loads is given, from Equation 1.15a, by the equations

$$W_{\text{bal}(S)} = \frac{8P_S e_S}{L_S^2} \quad (9.13a)$$

and

$$W_{\text{bal}(L)} = \frac{8P_L e_L}{L_L^2} \quad (9.13b)$$



**Figure 9.9** Balancing loads in two-way prestressed panel. (a) Three-dimensional view. (b) Section L-L in the long direction. (c) Section S-S in the short direction.

where  $P_S$  and  $P_L$  are the effective prestressing forces after losses in the short and long directions  $L_S$  and  $L_L$ , respectively, *per unit width of slab*, and  $e_S$  and  $e_L$  are the corresponding maximum eccentricities of the prestressing tendons. The total balancing load per unit width then becomes

$$W_{\text{bal}} = W_{\text{bal}(S)} + W_{\text{bal}(L)} = \frac{8P_S e_S}{L_S^2} + \frac{8P_L e_L}{L_L^2} \quad (9.14)$$

The designer would select the level of  $W_{\text{bal}}$  and determine the values of the prestressing forces  $P_S$  and  $P_L$  accordingly. Many combinations of  $P_S$  and  $P_L$  can satisfy the statics Equation 9.14. If the slab panels were supported on beams, or if simple panels were supported on a wall, the most economical design would be to carry the load  $W$  only in the short direction, or to carry  $\frac{1}{2} W$  in each direction in the case of a square slab panel. The slab panel loaded by  $W_{\text{bal}}$  and stressed by prestressing forces  $P_S$  and  $P_L$  would be subjected to a uniform stress distribution  $P_S/h$  and  $P_L/h$  in the respective directions,  $h$  being the slab thickness. The slab panel would be totally level, with no deflection or cambers. Any deviation of the applied load from  $W_{\text{bal}}$  would require the use of the usual elastic theory for the analysis of two-way plates.

As prestressed post-tensioned two-way slabs are usually flat plates supported directly on columns, all of the load has to be carried in both directions using either uniformly distributed prestressing tendons or banded tendons, with a concentration of tendons at the column strips of the two-way plate panels.

Uniform stress distribution and zero deflection/camber are not mandatory for proportioning the floor system. If they were, load balancing would not necessarily be the most economical way of determining the prestressing forces. Instead, the designer would often use a partial balancing load  $W_{\text{bal}} < W_D + W_L$  for a multipanel floor system, as will be seen in Example 9.2. If the load intensity  $W_w = W_D + W_L$  is larger than the balanced load  $W_{\text{bal}}$  from Equation 9.14, then unit moments  $M_S$  and  $M_L$  will result in the directions  $S$  and  $L$ , respectively.

The unit stress in the concrete in the short and long directions due to the unbalanced loading is obtained by superimposing the uniform compression due to balanced loading on the flexural stress in the concrete caused by the bending moments  $M_S$  and  $M_L$  that result from the unbalanced load  $W_w - M_{\text{bal}}$ . The resulting concrete stresses at the top and bottom fibers in each direction are given as follows:

*Short direction*

$$f^t = -\frac{P_S}{bh} - \frac{M_S c}{I_s} \quad (9.15a)$$

$$f_b = -\frac{P_S}{bh} + \frac{M_S c}{I_s} \quad (9.15b)$$

*Long direction*

$$f^t = -\frac{P_L}{bh} - \frac{M_L c}{I_L} \quad (9.16a)$$

$$f_b = -\frac{P_L}{bh} + \frac{M_L c}{I_L} \quad (9.16b)$$

In these equations, superscript  $t$  represents the top of the slab, subscript  $b$  represents the bottom of the slab,  $c = \frac{1}{2}h$ , width  $b = 12$  in., and

$$P_s = \frac{\text{total } P_S}{L}$$



**Photo 9.2** Kishwaukee River segmental bridge during construction. Winnebago County, Illinois. The first bridge in the U.S. constructed with launching gantry and the only precast segmental bridge post-tensioned totally with Dywidag bars. (Courtesy, H. Wilden & Associates, Macungie, Pennsylvania and the Prestressed Concrete Institute.)

and

$$P_L = \frac{\text{total } P_L}{S}$$

are the unit prestress forces. The service-load moment coefficient for evaluating  $M_S$  and  $M_L$  can be obtained from the chart in Figure 9.10 for any boundary condition (Ref. 9.13–CP 114). The bending moment coefficients there are for the maximum positive and negative bending moments, where  $\beta x_2$  and  $\beta x'_2$  apply to  $+M$  and  $-M$ , respectively, on the short span  $L_x$ . Similarly,  $\beta y_2$  and  $\beta y'_2$  apply to the maximum positive and negative bending moments, respectively, on the long span  $L_y$ . In an analogous fashion, the charts in Figure 9.11 give a rapid method for the evaluation of the ultimate bending moment coefficients (Ref. 9.13–CP 110) in continuous two-way-action concrete plates.

## 9.5 FLEXURAL STRENGTH OF PRESTRESSED PLATES

### 9.5.1 Design Moments $M_u$

The design moments for statically indeterminate prestressed bonded members are determined by combining the frame distributed moments  $M_u$  due to the *factored* dead plus live loads with the secondary moments  $M_s$  induced into the frame by the tendons. The load balancing approach discussed in the previous section directly includes both the primary moments  $M_1$  and the secondary moments  $M_s$ . Hence, for service-load intensity values, only the net loads  $M_{\text{net}}$  need to be considered in the calculation of the fixed-end factored moments, while  $W_{\text{bal}}$  needs to be considered for flexural strength analysis.

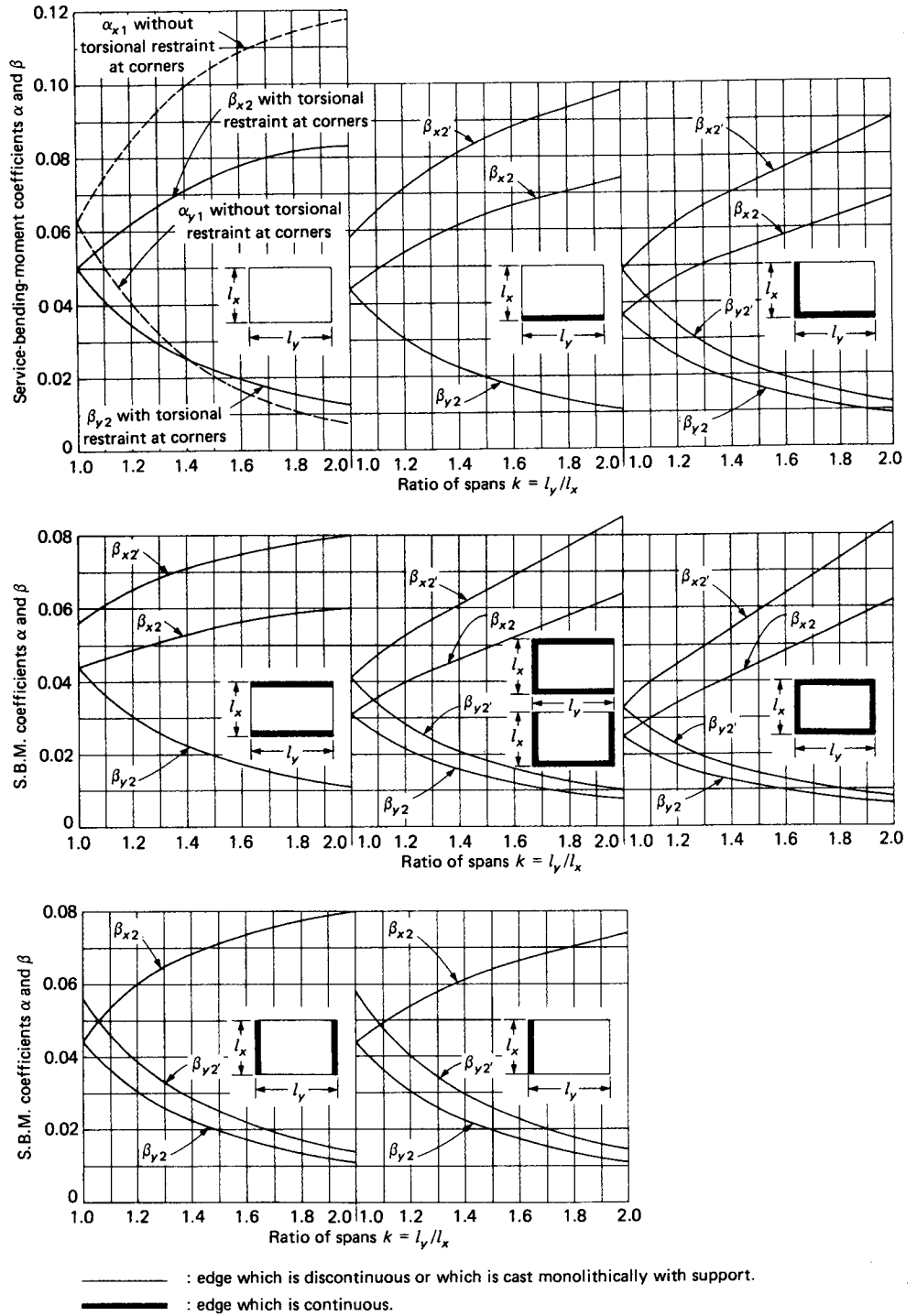
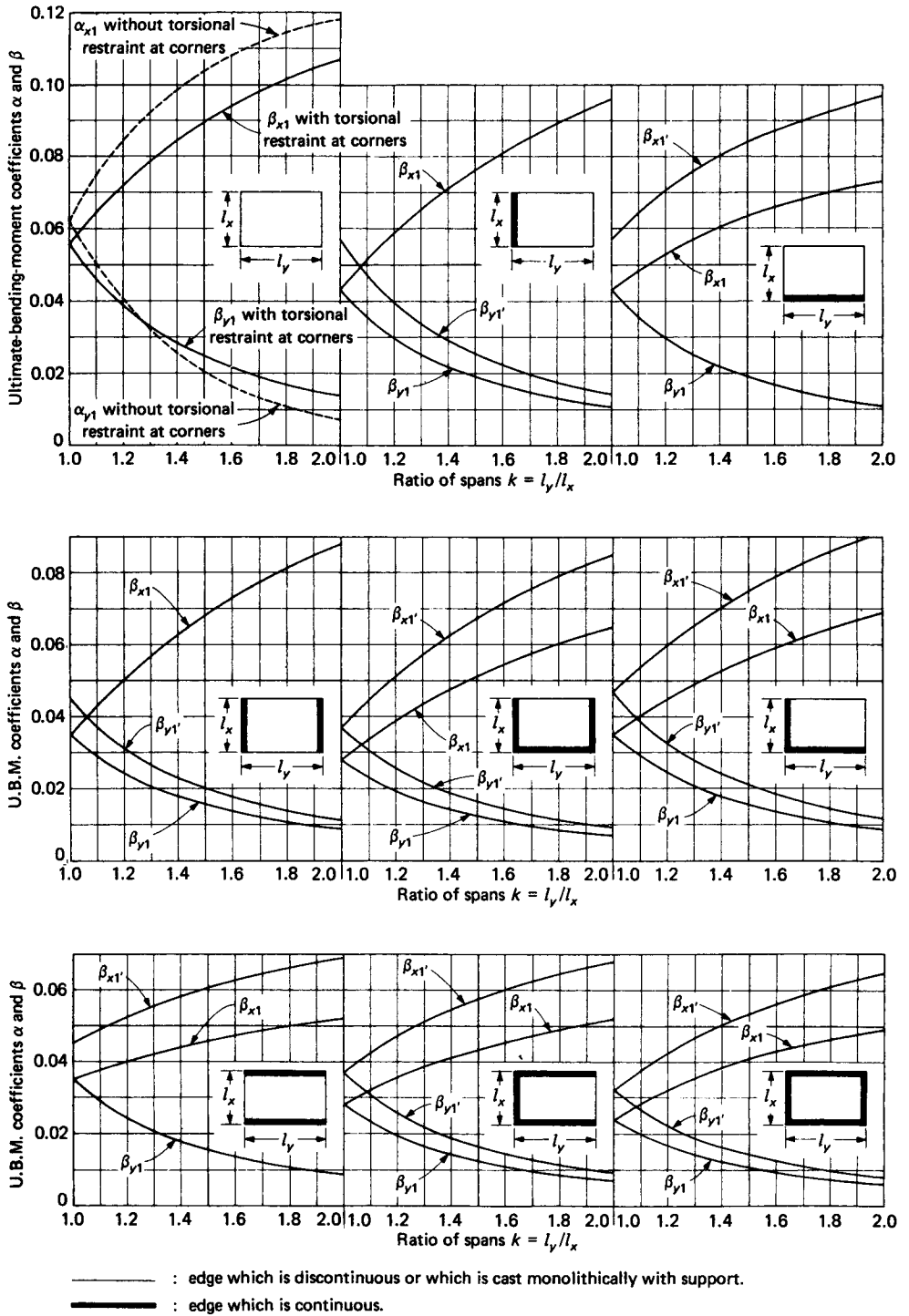


Figure 9.10 Service-load moment coefficients in two-way action slabs and plates (Ref. 9.13).



**Figure 9.11** Ultimate-load moment coefficients in two-way action slabs and plates (Ref. 9.13).

*Fixed-end  $M_u$  for moment distribution*

If  $M_1 = P_e e = Fe$  is the primary moment,  $M_{bal}$  is the balanced moment due to  $W_{bal}$ ,  $M_S =$  distributed  $M_{bal} - M_1$  is the secondary moment, and  $\bar{M}_u$  is the fixed-end factored moment due to the factored load intensity  $W_u$ , then the design ultimate moment would be at least

$$\text{Design } M_u = \text{distributed } \bar{M}_u - M_S \quad (9.17)$$

and the available moment strength would be

$$M_n = \frac{M_u}{\phi} \quad (9.18)$$

Inelastic redistribution of moments due to continuity would be applied to the available moment strength  $M_n$  at the support towards the required  $M_n$  at midspan.

Where bonded reinforcement is provided at the supports with minimum nonprestressed steel provided in accordance with Equations 9.19 and 9.20, negative moments computed by the elastic theory for any assumed loading arrangement may be increased or decreased by not more than the percentage given by the inelastic moment redistribution factor described in Sections 4.12.2 and 6.7.2.

The modified negative moment should be used for computing moments at sections within spans, viz., the positive moments, for the same loading arrangement. Inelastic moment redistribution of the negative moments can be made only when the section at which the moment is reduced is so designed that  $\omega_p$  or  $\omega_p + (d/d_p)(\omega - \omega')$  is not greater than  $0.24\beta_1$ , and the redistribution factor not to exceed  $1000 \epsilon_r$ .

Example 9.2 illustrates in detail the equivalent frame analysis procedure both for service-load and ultimate-load conditions, and the inelastic moment redistribution due to continuity that is utilized in the strength analysis.

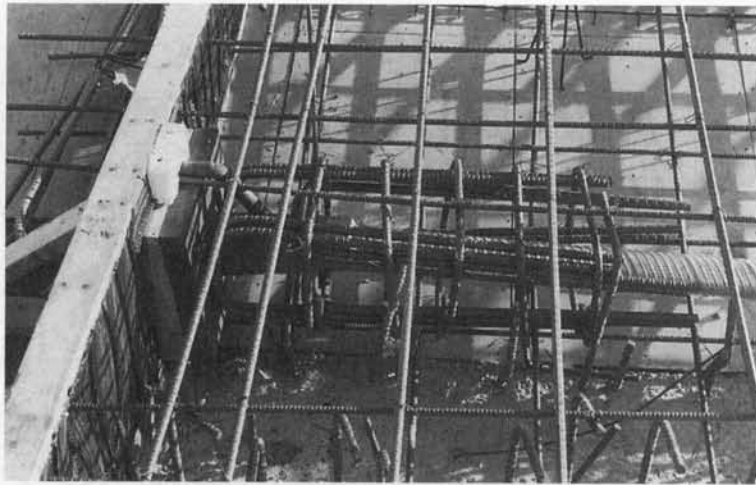
## 9.6 BANDING OF PRESTRESSING TENDONS AND LIMITING CONCRETE STRESSES

### 9.6.1 Distribution of Prestressing Tendons

Each plate panel is assumed to be supported continuously along the transverse column center lines. The assumption is also made, as previously stated, that the slab panel behaves as an orthogonal panel of two wide beams whose width is equal to the panel width and which is supported along the column centerlines. Consequently, 100 percent of the load to be balanced is considered to be supported by the wide beam in *each* of the two perpendicular directions.

It is also known that the lateral distribution of moments is *not uniform* across the width of the panel, but tends to be more concentrated in the column strips. Consequently, it is not unreasonable to concentrate a large percentage of the tendons in the column strip, as defined in Figure 9.4, and to spread the remaining tendons in the middle strip. For continuous spans, 65 to 75 percent of the moment in each direction is carried by the respective column strip, while the total area and number of tendons required by the total applied moment are maintained.

The width of half the column strip on either side of the column is one-fourth of the *smaller* of the two panel dimensions. The middle strip is the slab band bound by the two column strips. Accordingly, the distribution or banding of the prestressing tendons follows the percentage distribution of the moment between the column and middle strips. Consequently, if 70 percent of the tendons are concentrated in the column strip, it is rea-



**Photo 9.3** Bridge deck prestressing reinforcement.

sonable to expect that the column strip will carry *essentially* 70 percent, and the middle strip will carry the remaining 30 percent, of the total moment.

Since tendons exert downward loads at the high points which join adjacent parabolic profiles, the accompanying downward reactions should, as nearly as practicable, be resisted by columns, walls and/or upward tendon loads to achieve minimum deflections and maximum shear capacity. Consequently, a logical statical distribution of tendons can be one in which all tendons in one direction are placed through or immediately adjacent to the columns, and the tendons in the perpendicular direction are spaced uniformly across the bay width.

Figure 9.12 shows the resulting distribution of prestressing tendons in the two orthogonal directions. As a general guideline, the recommended spacing of the tendons in the column strip is about three to four times the slab thickness, while the maximum spacing of the tendons in the middle strip should not exceed six times the slab thickness. An average compressive stress in the concrete in each direction should be at least about 125 psi (0.90 MPa).

Investigations have verified (Ref. 9.4), through testing of the four-panel prestressed plates shown in Figure 9.13, that variation of distribution of prestressing strands does not alter the deflection behavior or magnitude and capacity for the *same* total prestressing steel percentage. Banding of the prestressing tendons as shown in part (b) of the figure, with about 65 to 75 percent of the tendons in the column strip, seems to be the most effective, particularly in enhancing the shear-moment transfer capacity at the column support section of the two-way slab.

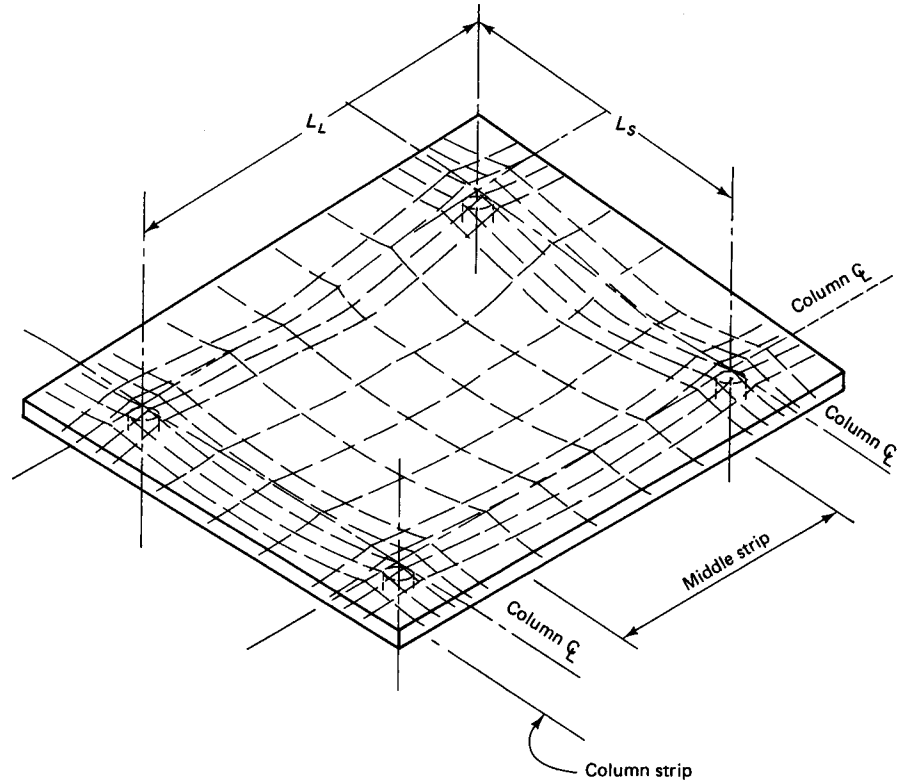
## 9.6.2 Limiting Concrete Tensile Stresses at Service Load

**9.6.2.1 Flexure.** The ACI 318 Code limits the tensile stresses in the concrete for prestressed elements in order to control flexural cracking development. The following tabulated values give the maximum permissible tensile stress in the prestressed elements for the various moment regions.

1. Negative moment area with the addition of nonprestressed reinforcement

$$6\sqrt{f'_c}$$





**Figure 9.12** Bending of prestressing tendons in two-way-action panels.

- |  |                  |
|--|------------------|
| 2. Negative moment area without the addition of nonprestressed reinforcement     | 0                |
| 3. Positive moment area with the addition of nonprestressed reinforcement        | $2\sqrt{f'_c}$   |
| 4. Positive moment area without the addition of nonprestressed reinforcement     | 0                |
| 5. Compressive stress in the concrete<br>(Under certain conditions, $0.60f'_c$ ) | $f_c = 0.45f'_c$ |

**9.6.2.2 Reinforcement.** The minimum area of bonded reinforcement, except as required by Equation 9.20 below, is

$$A_s = 0.004 A \tag{9.19a}$$

where  $A$  is the area in square inches of that part of the cross section between the flexural tension face and the center of gravity of the gross section. In positive-moment areas where the computed tensile stress in the concrete at service load exceeds  $2\sqrt{f'_c}$ , the minimum area of bonded reinforcement has to be computed from

$$A_s = \frac{N_c}{0.5f_y} \tag{9.19b}$$

where  $N_c$  is the tensile force in the concrete due to the unfactored dead plus live load, and  $f_y = 60,000$  psi. In negative-moment areas at column supports, the minimum area of bonded reinforcement in each direction has to be determined from

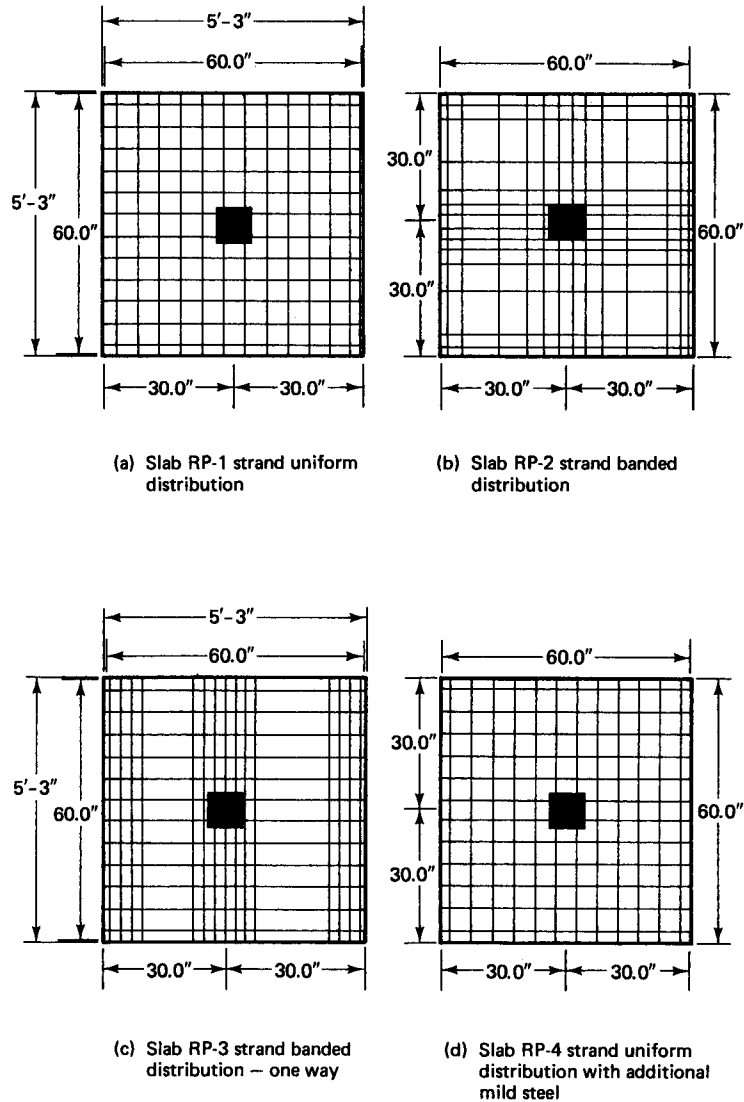


Figure 9.13 Various alternatives of tendon distribution (Ref. 9.4).

$$A_s = 0.00075hL \tag{9.20}$$

where  $L$  = span length in the direction parallel to the reinforcement being determined  
 $h$  = slab thickness.

The reinforcement obtained from Equation 9.20 has to be distributed within a slab band width between the lines that are  $1.5h$  outside opposite faces of the column support. At least four bars or wires should be provided in both directions.

The minimum length of bonded reinforcement in the *positive* area should be *one-third* the clear span, centered in the positive-moment area. The minimum length of bonded reinforcement in the *negative* area should extend *one-sixth* the clear span on each side of the support, placed at the *top* fibers. The stress  $f_{ps}$  in the prestressing reinforcement at nominal strength, as required by the ACI 318 Code, is governed by the following requirements.

**Bonded Tendons.** For bonded tendons,

$$f_{ps} = f_{pu} \left( 1 - \frac{\gamma_p}{\beta_1} \left[ \rho_p \frac{f_{pu}}{f'_c} + \frac{d}{d_p} (\omega - \omega') \right] \right) \quad (9.21)$$

where  $\omega' = \rho' = f_y / f'_c$

$$\begin{aligned} \text{and } \gamma_p &= 0.40 \text{ for } f_{py}/f_{pu} \geq 0.85 \\ &= 0.28 \text{ for } f_{py}/f_{pu} \geq 0.90. \end{aligned}$$

If any compression reinforcement is considered, the term  $[\rho_p f_{pu} / f'_c + (d/d_p)(\omega - \omega')]$  in Equation 9.21 shall be taken not less than 0.17, and  $d'$  shall be no greater than  $0.15d_p$ .

**Nonbonded Tendons.** For nonbonded tendons with a slab span-to-depth ratio  $\leq 35$ ,

$$f_{ps} = f_{pe} + 10,000 + \frac{f'_c}{100\rho_p} \quad (9.22)$$

where  $f_{ps} \leq f_{py} \leq f_{pe} + 60,000$ .

For nonbonded tendons with a slab span-to-depth ratio  $> 35$ ,

$$f_{ps} = f_{pe} + 10,000 + \frac{f'_c}{300\rho_p} \quad (9.23)$$

where  $f_{ps} \leq f_{py} \leq f_{pe} + 30,000$ .

### 9.6.2.3 Shear

**Column Support Sections in Flat Plates.** The nominal shear strength provided by the concrete at the column junctions of two-way prestressed slabs is given by

$$V_c = (\beta_p \sqrt{f'_c} + 0.3\bar{f}_c) b_o d + V_p \quad (9.24a)$$

or the nominal unit shearing strength is

$$v_c = \beta_p \sqrt{f'_c} + 0.3\bar{f}_c + \frac{V_p}{b_o d} \quad (9.24b)$$

where  $b_o$  = perimeter of the critical shear section at distance  $d/2$  from face of support

$f'_c$  = average value of the effective compressive stress in the concrete due to externally applied load for the two orthogonal directions computed at the section centroid after all prestress losses (termed  $f_{pc}$  by the ACI Code)

$V_p$  = vertical component of all effective prestressing forces crossing the critical section

$\beta_p$  = the smaller of the two values 3.5 or  $(\alpha_s d/b_o + 1.5)$ , where  $\alpha_s$  is 40 for interior columns, 30 for edge columns, and 20 for corner columns.

In slabs with distributed tendons, the term  $V_p$  can be conservatively disregarded; otherwise it becomes necessary to use the actual reverse curvature tendon geometry in the calculations in order to assess the shear carried by the tendons crossing the critical section. According to the ACI 318 Code, no portion of the column cross section shall be closer to a discontinuous edge than four times the slab thickness,  $f'_c$  in Equations 9.24 shall not exceed 5,000 psi, and  $f_c$  in each direction shall be neither less than 125 psi nor greater than 500 psi.

If these requirements are not satisfied,  $V_c$  shall be computed by the smaller of the values obtained from the expressions

$$(i) V_c = \left(2 + \frac{4}{\beta}\right) \sqrt{f'_c} b_o d \quad (9.25a)$$

$$(ii) V_c = \left(\frac{\alpha_s d}{b_o} + 2\right) \sqrt{f'_c} b_o d \quad (9.25b)$$

$$(iii) V_c = 4 \sqrt{f'_c} b_o d \quad (9.25c)$$

where  $\beta_c$  = ratio of long to short side of the column or concentrated load area.

Equations 9.25(a) and (b) are the results of tests which indicate that as the ratio  $b_o/d$  increases, the available nominal shear strength  $V_c$  decreases so that in such situations Equation 9.25(c) would not control as it becomes unsafe.

**Continuous Edge Support.** For distributed load and continuous edge support such as supporting beams or wall support, if the effective prestress is not less than 40 percent of the tensile strength of the reinforcement, the maximum allowable shear stress is

$$V_c = \left[0.60 \sqrt{f'_c} + 700 \frac{V_u d}{M_u}\right] b_w d_p \geq 2 \sqrt{f'_c} b_w d$$

$$< 5 \sqrt{f'_c} b_w d \quad (9.26)$$

where  $b_w$  is taken as the strip width and  $V_u d/M_u$  at a distance  $d_p/2$  from the face of the support,  $d_p \geq 0.80h_c$ .

Values of  $\sqrt{f'_c}$  in all the above equations are to be multiplied by a factor  $\lambda = 1.0$  for normal-weight concrete,  $\lambda = 0.85$  for sand-lightweight concrete, and  $\lambda = 0.75$  for all-lightweight concrete.

**Shear Force Coefficients.** The maximum shear force at the edge of a two-way slab panel carrying uniformly distributed load and supported along the length of its perimeters can be approximated as follows

$$V = \frac{1}{3} w L_s \text{ (short edge)} \quad (9.27a)$$

$$V = k w L_s / (2k + 1) \text{ (long edge)} \quad (9.27b)$$

where  $k$  is the ratio of the long span  $L_L$  to the short span  $L_s$ . The same values are applicable to a panel that is fixed or continuous along all four edges. For other conditions, the distribution of shearing forces, the stresses due to which are rarely critical, have to be adjusted on the basis that the shearing force is slightly larger at a continuous edge than at a simply supported edge.

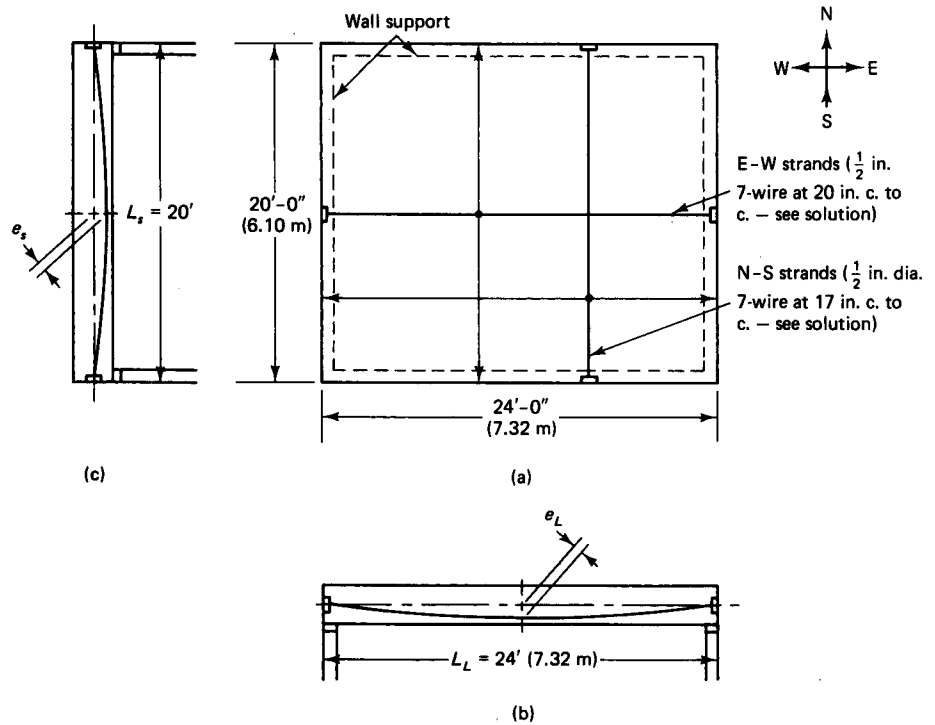
The ACI Code allows a 15 percent increase in the shear force at the first interior continuous support for one-way action.

## 9.7 LOAD-BALANCING DESIGN OF A SINGLE-PANEL TWO-WAY FLOOR SLAB

### Example 9.1

A two-way single-panel prestressed warehouse lift slab 20 ft  $\times$  24 ft (6.10 m  $\times$  7.32 m) has the plan shown in Figure 9.14. It is supported on masonry walls on all sides, with negligible rotational restraint at these boundaries but that the corners are held down. The slab has to carry a superimposed service dead load of 15 psf (0.72 kPa) in addition to its self-weight and a service live load of 75 psf (3.59 kPa). No deflection is allowed under full dead load.

Design the slab as a post-tensioned nonbonded prestressed two-way floor using  $\frac{1}{2}$ -in. dia 7-wire 270-K strands (12.7-mm dia strands). Given data are as follows:



**Figure 9.14** Two-way prestressed panel in Example 9.1. (a) Plan. (b) Section in longitudinal E-W direction. (c) Section in transverse N-S direction.

$f'_c = 5,000$  psi (34.5 MPa), normal weight

$f'_{ci} = 3,750$  psi (25.9 MPa)

E-W max.  $f_c$  due to net prestress after losses = 200 psi

N-S max.  $f_c$  due to net prestress after losses not to exceed 350 psi (ACI allows up to 500 psi)

Max.  $f_c$  due to combined stresses =  $0.45f'_c$

$E_c = 57,000\sqrt{f'_c} = 4.03 \times 10^6$  psi ( $27.8 \times 10^6$  MPa)

$f_{ps} \leq 0.70f_{pu} = 189,000$  psi (1,303 MPa), as required by the ACI Code

$f_{py} = 240,000$  psi (1,655 MPa)

$f_{pe} = 159,000$  psi (1,096 MPa)

$E_{ps} = 29 \times 10^6$  psi ( $200 \times 10^3$  MPa)

$f_y = 60,000$  psi (414 MPa)

$E_s = 29 \times 10^6$  psi ( $200 \times 10^3$  MPa)

**Solution:**

$$e_s = e_L = \frac{6}{2} - 1 = 2.0 \text{ in. (51 mm)}$$

Choose a trial slab thickness on the basis of a span-to-depth ratio  $\cong 45$ :

$$h = \frac{(20 + 24) \times 12}{2} \times \frac{1}{45} = 5.87 \text{ in.}$$

So try a 6-in. (152-mm)-thick slab assuming a duct diameter  $\cong 0.5$  in. and an effective depth  $d_p = 6.0 - (0.5/2 + \frac{3}{4}) = 5.0$  in. (127 mm).

### Balancing Load

$$W_D = 15 \text{ psf} + \frac{6}{12} \times 150 = 90 \text{ psf (4.31 kPa)}$$

Since a balancing load is required for zero deflection or camber due to dead load, assume that  $W_{\text{bal}} = W_D = 90$  psf (4.31 kPa). Also, since  $f_c$  due to prestressing = 200 psi (given), assume this to be the stress in the E–W direction. Then the effective prestressing force in the E–W direction is  $P_L = 200 \times 6 \times 12 = 14,400$  lb per strip, and from Equation 9.13b,

$$W_{\text{bal}(L)} = \frac{8P_L e_L}{L_L^2} = \frac{8 \times 14,400 \times 2}{(24)^2 \times 12} \cong 33 \text{ psf (1.58 kPa)}$$

The uplift to be provided by the tendons in the short direction (preferably the load is to be carried by the short-direction span) becomes  $W_{\text{bal}(S)} = W_D - W_{\text{bal}(L)} = 90 - 33 = 57$  psf (2.73 kPa). Then, from Equation 9.13a,

$$P_S = \frac{W_{\text{bal}(S)} L_S^2}{8e_S} = \frac{57 \times (20)^2 \times 12}{8 \times 2}$$

= 17,100 lb/ft (249.7 kN/m) after losses, and the compression in the concrete after losses in prestress in the N–S direction is

$$f_c = \frac{P_S}{bh} = \frac{17,100}{12 \times 6} = 238 \text{ psi} < 350 \text{ psi}$$

which is satisfactory. Hence, use  $\frac{1}{2}$ -in. dia 7-wire 270-K strands with effective prestressing force  $P_e = 159,000 \times 0.153 = 24,327$  lb (108.2 kN).

*Required Spacing in the N–S Direction.* The required spacing in the N–S direction is

$$s_S = \frac{24,327}{17,100} = 1.42 \text{ ft} = 17 \text{ in. (432 mm)}$$

*Required Spacing in the E–W Direction.* The required spacing in the E–W direction is

$$s_L = \frac{24,327}{14,400} = 1.69 \text{ ft} \cong 20 \text{ in. (508 mm)}$$

Note that both spacings correspond to the recommended spacing of 3 to 5 times the slab thickness. As an additional measure, to prevent splitting of the concrete in the anchorage zones at the wall, add two #4 nonprestressed mild steel bars (12.7-mm dia) along the anchorage line on the slab perimeter.

**Service-load Stresses.** The service live load  $W_L = 75$  psf (3.59 kPa), and the aspect ratio  $k = L_L/L_S = 24/20 = 1.20$ . From Figure 9.10, the moment coefficients for the maximum midspan moments in the short and long directions are  $\alpha_{N-S} = 0.062$  and  $\alpha_{E-W} = 0.035$ , respectively, assuming that the corners of the two-way slab are held down, i.e., torsionally restrained.

We assume an effective  $L_S = 19.5$  ft and  $L_L = 23.5$  ft.

*Live-load Moments.* The live-load moments are

$$M_S = 0.062 \times 75 \times (19.5)^2 \times 12 = 21,218 \text{ in.-lb/ft}$$

and

$$M_L = 0.035 \times 75 \times (23.5)^2 \times 12 = 17,396 \text{ in.-lb/ft}$$

The moment of inertia is

$$I_s = \frac{12(6)^3}{12} = 216 \text{ in}^4$$

*Concrete Stresses Due to Live Load.* In the short direction, we have

$$f = \frac{Mc}{I_s} = \frac{21,218 \times 3}{216} = 295 \text{ psi (2.03 MPa)}$$

while in the long direction,

$$f = \frac{17,396 \times 3}{216} = 242 \text{ psi (1.67 MPa)}$$

The combined axial stresses due to the balanced load and the flexural stresses due to the live load, from Equations 9.15 and 9.16, become, in the short direction (N-S),

$$f' = -\frac{P_S}{bh} - \frac{M_S c}{I_s} = -238 - 295 = -533 \text{ psi (C) (3.68 MPa)}$$

and

$$f_b = -238 + 295 = +57 \text{ psi (T) (very small and, hence, negligible)}$$

and in the long direction (E-W),

$$f' = -200 - 242 = -442 \text{ psi (C) (3.05 MPa)}$$

and

$$f_b = -200 + 242 = +42 \text{ psi (T) (again negligible)}$$

The ACI allowable compressive stress is  $f_c = 0.45 \times 5,000 = 2,250$  psi, which is well above the actual stress and, hence, satisfactory. These low stress levels can justify making the slab thinner than 6 in., provided that the deflection due to live load is acceptable. Note that the slab develops zero deflection or camber under dead load in this example, due to the load balancing.

**Deflection Check.** Only the deflection due to live load is checked. From principles of mechanics, we have

$$\Delta = \frac{5}{48} \frac{ML^2}{E_c I_s}$$

$$I_s = 216 \text{ in}^4$$

$$E_c = 4.03 \times 10^6 \text{ psi}$$

$$\Delta_{E-W} = \frac{5}{48} \frac{17,396(24 \times 12)^2}{4.03 \times 10^6 \times 216} = 0.17 \text{ in.}$$

$$\Delta_{N-S} = \frac{5}{48} \frac{21,218(20 \times 12)^2}{4.03 \times 10^6 \times 216} = 0.15 \text{ in.}$$

$$\text{Avg. midspan deflection } \Delta = \frac{0.17 + 0.15}{2} = 0.16 \text{ in. (4.1 mm)}$$

$$\text{Acceptable deflection} = \frac{L_s}{360} = \frac{20 \times 12}{360} = 0.67 \text{ in. (17 mm)} \gg 0.16 \text{ in.}$$

Consequently, a second cycle reducing the slab thickness to  $5\frac{1}{2}$  in. could also be used, provided that the resulting slab nominal moment strengths are adequate to carry the load. In this case,  $h = 5\frac{1}{2}$  in. is not adequate for nominal moment strength, as the next part of the solution indicates.

**Nominal Moment Strength**

$$W_u = 1.2 \times 90 + 1.6 \times 75 = 228 \text{ psf (11.0 kPa)}$$

Also,

$$\text{Effective } L_S = 19.5 \text{ ft}$$

$$L_L = 23.5 \text{ ft}$$

From Figure 9.11, the moment coefficients for maximum factored moment are

$$\alpha_{N-S} = 0.072$$

and

$$\alpha_{E-W} = 0.038$$

*N-S Direction.* In the N-S direction, we have

$$\text{Factored } M_u = 0.072 \times 228 (19.5)^2 \times 12 = 74,906 \text{ in.-lb/ft}$$

$$\text{Required } M_n = \frac{M_u}{\phi} = \frac{74,906}{0.9} = 83,229 \text{ in.-lb/ft}$$

The value of  $\phi$  has to be verified in accordance with Figure 4.45.

Note that prestressing forces in this structure do not produce any secondary moments  $M_s$  since there is no continuity at the slab boundaries. We have  $A_{ps} = 0.153 \text{ in.}^2$  on 1.42 ft center to center (from before), and  $A_{ps}/\text{ft} = 0.153/1.42 = 0.11 \text{ in.}^2/\text{ft}$ . Also, the effective  $f_{pe} = 159,000 \text{ psi}$ . So in cases where the  $A_{ps}$  used exceeds  $P_e/\text{initial } A_{ps}$ , reduce  $f_{pe}$  accordingly.

We have, further,

$$\rho_{N-S} = \frac{0.11}{12 \times 5} = 0.0018$$

$$\text{Slab span-to-depth ratio} = \frac{20 \times 12}{6} = 40$$

From Equation 9.23b,

$$f_{ps} = f_{pe} + 10,000 + \frac{f'_c}{300\rho_p} \leq f_{py} \leq f_{pe} + 30,000$$

$$f_{ps} = 159,000 + 10,000 + \frac{5,000}{300 \times 0.0018} = 178,259 \text{ psi}$$

$$< f_{py} = 240,000 \text{ psi} < f_{pe} + 30,000 = 189,000 \text{ psi}$$

$$< \text{limit } f_{ps} = 189,000 \text{ psi, O.K.}$$

$$a = \frac{A_{ps} f_{ps}}{0.85 f'_c b} = \frac{0.11 \times 178,259}{0.85 \times 5,000 \times 12} = 0.38 \text{ in.}$$

Check for the value of  $\phi$ :

$$c = a/\beta_1 = 0.38/0.80 = 0.48$$

$$c/d_t = 0.48/5.0 = 0.096 \ll 0.375 \text{ in Figure 4.45.}$$

Hence, the section is tension controlled, and  $\phi = 0.90$ .

$$\begin{aligned} \text{Available } M_n &= A_{ps} f_{ps} \left( d - \frac{a}{2} \right) = 0.11 \times 178,259 \left( 5 - \frac{0.38}{2} \right) \\ &= 94,316 \text{ in.-lb/ft} > \text{req } M_n = 83,229 \text{ in.-lb, O.K.} \end{aligned}$$

*E-W Direction.* In the E-W direction, we have

$$\text{Factored } M_u = 0.038 \times 228 (23.5)^2 \times 12 = 57,417 \text{ in.-lb/ft}$$

$$\text{Required } M_n = \frac{M_u}{\phi} = \frac{57,417}{0.90} = 63,797 \text{ in.-lb/ft}$$



$$A_{ps} = 0.153 \text{ in.}^2 \text{ per 1.69 ft center to center (from before)}$$

$$A_{ps}/\text{ft} = \frac{0.153}{1.69} = 0.09 \text{ in}^2/\text{ft}$$

$$\rho_{E-W} = \frac{0.09}{12 \times 5} = 0.0015$$

$$f_{ps} = 159,000 + 10,000 + \frac{5,000}{300 \times 0.0015} = 180,111 \text{ psi, O.K.}$$

$$a = \frac{0.09 \times 180,111}{0.85 \times 5,000 \times 12} = 0.32 \text{ in.}$$

$$\begin{aligned} \text{Available } M_n &= 0.09 \times 180,111 \left( 5 - \frac{0.32}{2} \right) \\ &= 78,456 \text{ in.-lb/ft} > \text{Req. } M_n \text{ of } 63,797 \text{ in.-lb/ft, O.K.} \\ &(29.1 \text{ kN-m/m} > 23.6 \text{ kNm/m}) \end{aligned}$$

**Shear Strength.** From before, the aspect ratio  $k = 1.2$ , and from Equations 9.27,

$$V_u = \frac{1}{3} w_u L_S = \frac{1}{3} \times 228 \times 19.5 = 1482 \text{ lb/ft} \quad (\text{N-S})$$

$$\begin{aligned} V_u &= \frac{k w_u L_S}{2k + 1} \quad (\text{E-W}) \\ &= 1.2 \times 228 \times \frac{19.5}{2 \times 1.2 + 1} = 1569 \text{ lb/ft (22.9 kN/m)} \end{aligned}$$

From Equation 9.26,

$$2\sqrt{f'_c} b_w d_p \leq V_c = \left( 0.6\sqrt{f'_c} + 700 \frac{V_u d}{M_u} \right) b_w d_p \leq 5\sqrt{f'_c} b_w d_p$$

Consider  $700 (V_u d)/(M_u) \approx 0$  at the boundaries of the single-panel wall-supported slab in this example. In such a case,

$$V_c = 0.6\sqrt{5,000} \times 12 \times 5 = 2,546 \text{ lb/ft (37.2 kN/m)} \gg 1569 \text{ lb/ft}$$

which is satisfactory. Hence, adopt the following design:

$$h = 6 \text{ in. (152 mm)}$$

$$d_p = 5 \text{ in. (127 mm)}$$

Use  $\frac{1}{2}$ -in. dia 7-wire 270-K strands spaced 17 in. (432 mm) center-to-center in the N-S direction, and 20 in. (508 mm) center-to-center in the E-W direction. Also, use two #4 bars (12.7-mm dia) along the anchorage zone line around all the slab perimeter.

## 9.8 ONE-WAY SLAB SYSTEMS

One-way prestressed slabs behave similarly to beams regardless of whether they are simply supported or continuous over several supports. A one-way slab is therefore designed as a 12-in.-wide beam. The main prestressing strands are placed in the direction of the slab length, namely, spanning the continuous spans. The aspect ratio, the ratio of the span to the width of the slab band, has to have a value of 2 or greater in order for the slab to be considered one-way.

The same design and analysis procedures and examples as in Chapter 6 are to be used for the analysis and design of continuous one-way-action prestressed floor systems.

## 9.9 SHEAR-MOMENT TRANSFER TO COLUMNS SUPPORTING FLAT PLATES

### 9.9.1 Shear Strength

The shear behavior of two-way slabs and plates is a three-dimensional stress problem. The critical shear failure plane follows the perimeter of the loaded area and is located at a distance that gives a minimum shear perimeter  $b_0$ . Based on extensive analytical and experimental verification, the shear plane should not be closer than a distance  $d/2$  from the concentrated load or reaction area.

If no special shear reinforcement is provided, the nominal shear strength  $V_c$ , as required by the ACI, is defined in Equations 9.24, 9.25, and 9.26. The coefficients for evaluating the factored external shear force  $V_u$  in a continuous two-way slab supported all along the panel perimeters can be evaluated approximately from Equations 9.27.

### 9.9.2 Shear-Moment Transfer

The unbalanced moment at the column face support of a slab without beams is one of the more critical design considerations in proportioning a flat plate or a flat slab. To ensure adequate shear strength requires moment transfer to the column by flexure across the perimeter of the column and by eccentric shearing stress such that approximately 60 percent is transferred by flexure and 40 percent by shear.

The fraction  $\gamma_v$  of the moment transferred by eccentricity of the shear stress decreases as the width of the face of the critical section resisting the moment increases in such a manner that

$$\gamma_v = 1 - \frac{1}{1 + \frac{2}{3}\sqrt{\frac{b_1}{b_2}}} \quad (9.28)$$

where  $b_2 = c_2 + d$  is the width of the face of the critical section resisting the moment and  $b_1 = c_1 + d$  is the width of the face at right angles to  $b_2$ .

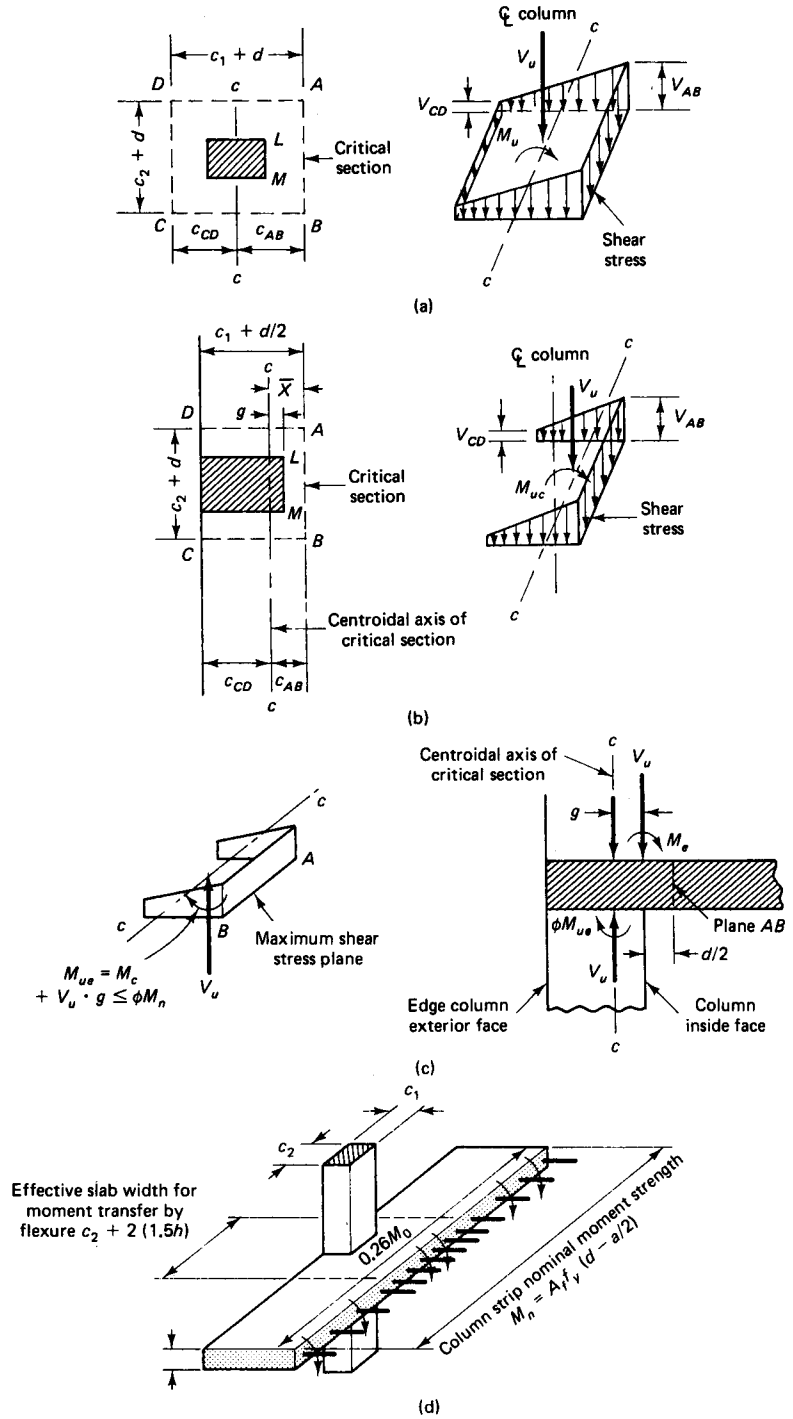
The remaining portion  $\gamma_f$  of the unbalanced moment transferred by flexure is given by and acting on an effective slab width between lines that are  $1\frac{1}{2}$  times the total slab thickness  $h$  on both sides of the column support.

$$\gamma_f = \frac{1}{1 + \frac{2}{3}\sqrt{\frac{b_1}{b_2}}} = 1 - \gamma_v \quad (9.29)$$

For exterior columns,  $b_1 = c_1 + \frac{1}{2}d$ . The value of  $\gamma_f$  can be increased to 1.0 provided that  $V_u$  is less than  $0.75\phi V_c$ . At interior supports,  $\gamma_f$  can be increased by 25 percent provided that  $V_u \leq 0.4\phi V_c$  and  $\rho \leq 0.375\rho_b$ .

The distribution of shear stresses around the column edges is as shown in Figure 9.15. It is considered to vary linearly about the centroid of the critical section. The factored shear force  $V_u$  and the unbalanced factored moment  $M_u$ , both assumed to be acting at the column face, have to be transferred to the centroidal axis  $c-c$  of the critical section. Thus, the axis position has to be located, thereby obtaining the shear force arm  $g$  (the distance from the column face to the centroidal axis plane) of the critical section  $c-c$  for the shear moment transfer.

For computing the maximum shear stress sustained by the plate in the edge column region, the ACI Code requires using the full nominal moment strength  $M_n$  provided by the column strip in Equations 9.30 to follow as the unbalanced moment, multiplied by the transfer fraction factor  $\gamma_v$ . This unbalanced moment  $M_n \geq M_{ue}/\phi$  is composed of two parts: the negative end panel moment  $M_{ne} = M_c/\phi$  at the face of the column, and the mo-



**Figure 9.15** Shear stress distribution around column edge. (a) Interior column. (b) End column. (c) Critical surface. (d) Transfer nominal moment strength  $M_n$ .

ment  $(V_u/\phi)g$  due to the eccentric factored perimetric shear force  $V_u$ . The limiting value of the shear stress intensity is expressed as

$$\frac{v_{u(AB)}}{\phi} = \frac{V_u}{\phi A_c} + \frac{\gamma_v M_{ue} c_{AB}}{\phi J_c} \quad (9.30a)$$

$$\frac{v_{u(CD)}}{\phi} = \frac{V_u}{\phi A_c} - \frac{\gamma_v M_{ue} c_{CD}}{\phi J_c} \quad (9.30b)$$

where the nominal shear strength intensity is

$$v_n = \frac{v_u}{\phi} \quad (9.30c)$$

and where  $A_c$  = area of concrete of assumed critical section

=  $2d(c_1 + c_2 + 2d)$  for an interior column

and  $J_c$  = property of assumed critical section analogous to polar moment of inertia.

The value of  $J_c$  for an interior column is

$$J_c = \frac{d(c_1 + d)^3}{6} + \frac{d^3(c_1 + d)}{6} + \frac{d(c_2 + d)(c_1 + d)^2}{2}$$

and the value of  $J_c$  for an edge column with bending parallel to the edge is

$$J_c = \frac{(c_1 + d/2)(d)^3}{6} + \frac{2(d)}{3}(c_{AB}^3 + c_{CD}^3) + (c_2 + d)(d)(c_{AB})^2$$

From basic principles of the mechanics of materials, the shearing stress is

$$v_u = \frac{V_u}{A_c} + \gamma_v \frac{Mc}{J}$$

where the second term on the right-hand side is the shearing stress resulting from the torsional moment at the column face.

If the nominal moment strength  $M_n$  of the shear moment transfer zone after the design of the reinforcement results in a larger value than  $M_{ue}/\phi$ , this value of  $M_n$  should be used in Equations 9.30a and b in lieu of  $M_{ue}/\phi$ . In such a case, where the moment strength value  $M_n = M_{ne} + (V_u/\phi)g$  is increased because of the use of flexural reinforcement in excess of what is needed to resist  $M_{ue}/\phi$ , the slab stiffness is raised, thereby increasing the transferred shear stress  $v_u$  computed from Equations 9.30a and b for development of full moment transfer. Consequently, it is advisable to maintain a design moment  $M_{ue}$  with a value close to the factored moment value  $M_{ue}$  if an increase in the shear stress due to additional moment transfer needs to be avoided and a resulting need for additional increase in the plate design thickness prevented.

Example 9.2 illustrates the procedure for computing the limit perimeter shear stress in the plate at the edge column region.

A higher perimetric shearing stress  $v_u$  can occur than that evaluated by Equation 9.30a or b when adjoining spans are unequal or unequally loaded in the case of an interior column. The ACI Code stipulates, in the slab section pertaining to factored moments in columns and walls, that the supporting element such as a column or a wall has to resist an unbalanced moment

$$M' = 0.07[(w_{nd} + 0.5w_{nl})l_2 l_{n2} - w'_{nd} l'_2 (l'_n)^2] \quad (9.31)$$

where  $w'_{nd}$ ,  $l'_2$ , and  $l'_n$  refer to the shorter span. Hence, an additional term is added to Equation 9.30a or b in such cases so that

$$v_u = \frac{V_u}{A_c} + \frac{\gamma_v M_u c_{AB}}{J_c} + \frac{\gamma_v M'c}{J'_c} \quad (9.32)$$

where  $J'_c$  is the polar moment of inertia with moment areas taken in a direction perpendicular to that used for  $J_c$ .

### 9.9.3 Deflection Requirements for Minimum Thickness: An Indirect Approach

For a preliminary estimate of the two-way slab thickness, it is necessary to use some approximate guidelines in order to expeditiously select a trial depth. Span-to-depth ratios in prestressed slabs are expected to be higher than those in reinforced concrete slabs if the advantages of prestressing are not to be economically lost.

Service live loads rather than total dead plus live loads should be used to evaluate deflection. Load balancing from the transverse component of the prestressing force would have to be used to neutralize the dead-load deflection or even produce camber if the live load is excessively high. An approximate guideline of a span-to-depth ratio of 16 to 25 for solid cantilever slabs and 40 to 50 for two-way continuous slabs is not unreasonable to use. For waffle slabs, a lower value of 35 to 40 is recommended. For simply supported spans and for single- and double-T's, use 90 percent of these values for the first trial.

The ACI requires that the minimum span-to-deflection ratio be restricted depending on the type of loading and conditions of use. This limitation is obviated by the need to prevent cracking of plaster in the ceilings and damage to sensitive supported equipment as well as cracking of partitions and ponding of water in roofs. Table 9.1 gives recommended values of span-to-deflection ratios for deflection control.

**Table 9.1** Minimum Permissible Ratios of Span ( $l$ ) to Deflection ( $a$ ) ( $l$  = longer span)

Type of member	Deflection $a$ to be considered	$(l/a)_{\min}$
Flat roofs not supporting and not attached to non-structural elements likely to be damaged by large deflections	Immediate deflection due to live load $L$	180 <sup>a</sup>
Floors not supporting and not attached to non-structural elements likely to be damaged by large deflections	Immediate deflection due to live load $L$	360
Roof or floor construction supporting or attached to nonstructural elements likely to be damaged by large deflections	That part of total deflection occurring after attachment of nonstructural elements: sum of long-time deflection due to all sustained loads (dead load plus any sustained portion of live load) and immediate deflection due to any additional live load <sup>b</sup>	480 <sup>c</sup>
Roof or floor construction supporting or attached to nonstructural elements not likely to be damaged by large deflections		240 <sup>c</sup>

<sup>a</sup>Limit not intended to safeguard against ponding. Ponding should be checked by suitable computations of deflection, including added deflections due to ponded water, and considering long-term effects of all sustained loads, camber, construction tolerances, and reliability of provisions for drainage.

<sup>b</sup>Long-term deflection has to be determined, but may be reduced by the amount of deflection computed to occur before attachment of nonstructural elements. This reduction is made on the basis of accepted engineering data relating to time-deflection characteristics of members similar to those being considered.

<sup>c</sup>Ratio limit may be lower if adequate measures are taken to prevent damage to supported or attached elements, but should not be lower than tolerance of nonstructural elements.

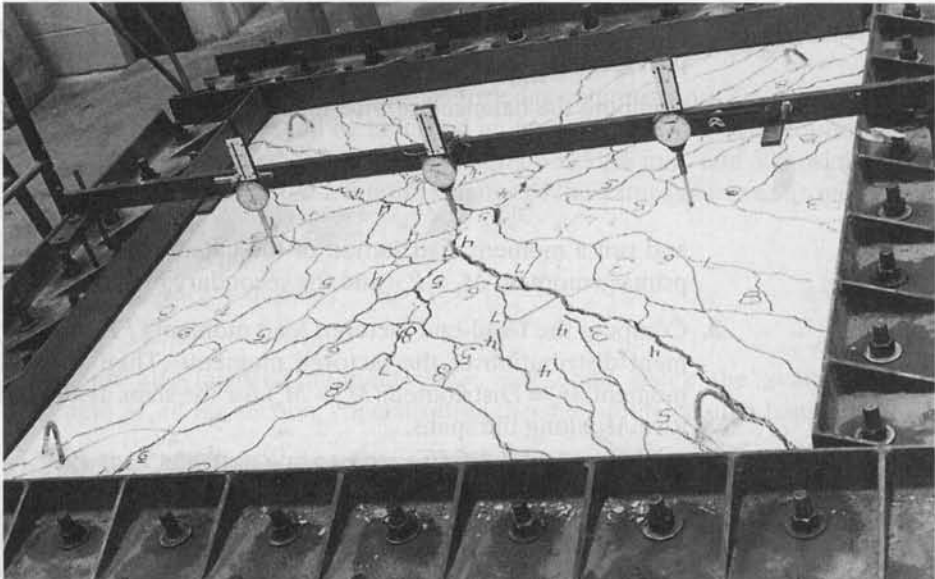
A more accurate evaluation of the deflection/camber of reinforced concrete and prestressed concrete two-way-action slabs and plates is presented in Section 9.12. This approach utilizes the stiffnesses of the interconnecting members using the equivalent frame method in the deflection analysis. It is both logical and expedient to use, particularly since the stiffness factors of the various elements have already been computed in the flexural analysis of the equivalent continuous frames.

### 9.10 STEP-BY-STEP TRIAL-AND-ADJUSTMENT PROCEDURE FOR THE DESIGN OF A TWO-WAY PRESTRESSED SLAB AND PLATE SYSTEM

The following sequence of steps is suggested for the design or analysis of two-way action prestressed slabs:

1. Determine whether the slab geometry and loading require a two-way analysis by the equivalent frame method.
2. Select a trial slab thickness for the maximum of either the longitudinal  $h = L/45$  or the transverse  $h = L/45$ . Compute the total service dead and live loads and the factored loads.
3. Assume a tendon profile across the continuous spans in both the E-W and N-S directions, and determine the prestressing force  $F$ , the concrete stress  $f_c = F/A_c$ , and the number of strands in a span. Compute the balancing load intensity  $W_{bal} = 8Fa/L^2$  and the net load  $W_{net \downarrow} = W_{w \downarrow} - W_{bal \uparrow}$ .
4. Determine, by the equivalent frame method, the equivalent frame characteristics and the flexural and torsional stiffnesses of the slab given by

$$K_c \cong \frac{4EI}{L_n - 2h}$$



**Photo 9.4** Flexural cracking in a restrained one-panel reinforced concrete slab. (Tests by Nawy et al.)

and

$$K_t = \Sigma \frac{9E_{cs} C}{L_2 \left(1 - \frac{c_2}{L_2}\right)^3}$$

where  $C = \Sigma(1 - 0.63x/y)x^3 y/3$ . Then determine

$$K_{ec} = \left(\frac{1}{K_c} + \frac{1}{K_t}\right)^{-1}$$

for the exterior and interior columns, and the slab stiffness

$$K_s \cong \frac{4EI}{L_1 - c_1/2}$$

where  $L_1$  is the centerline span and  $c_1$  is the column depth for each slab-column joint.

- From the values of  $K_{ec}$  and  $K_s$  obtained at each joint, determine the moment distribution factors

$$DF = \frac{K_s}{\Sigma K}$$

for the slabs, where  $\Sigma K = K_{ec} + K_{S(\text{left})} + K_{S(\text{right})}$ . Then compute the fixed-end moments  $FEM$  at the joints for the net loads given by  $FEM = WL^2/12$  for a distributed load.

- Run a moment distribution for the net load moment  $M_{\text{net}}$ , and adjust the redistributed moments to obtain the net moment values at the face of the supports; the equation is  $M_n = \text{centerline } M_n - Vc/3$ . Then verify that the concrete stresses

$$f_t = -\frac{P}{A} + \frac{M_{\text{net}}}{S}$$

resulting from these moments are below the maximum allowable  $f_t = 6\sqrt{f'_c}$  for support sections and  $f_t = 2\sqrt{f'_c}$  for midspan sections.

- Compute the balanced service-load fixed-end moments

$$FEM_{\text{bal}} = \frac{w_{\text{bal}}L^2}{12}$$

and run a moment distribution of the balanced load moments  $M_{\text{bal}}$ . Then find the primary moment  $M_1 = P_e e$  and the secondary moment  $M_s = \text{Distributed } (M_{\text{bal}} - M_1)$ .

- Compute the fixed-end factored load moments  $FEM_u^- = (w_u L^2)/(12)$  and run a moment distribution of the factored moments. Then determine the required design moment  $M_u = \text{Distributed } (M_u^- - M_s)$  for the slabs at all joints and at maximum positive  $M_u$  along the spans.
- Determine the required nominal moment strengths  $M_n = M_u/\phi$  for the negative support moments  $-M_n$  and the positive span moments  $+M_n$ . Then check whether the available  $-M_n$  and  $+M_n$  for the slab and the prestressing steel are adequate. Next, determine the *inelastic* moment redistribution  $\Delta M_R$  from the procedure outlined in Sections 4.12.4 and 6.7.2.

where  $\Delta M_R = \rho_D$  (support  $M_u$ ). Add mild steel to the support and midspan where necessary, recalling that the minimum nonprestressed steel  $A_s = 0.00075hL$ .

- 10.** Check the nominal shear strength of the slab at the exterior and interior supports, and compute the shear-moment transfer and the flexure-moment transfer to the columns. The moment shear factor is

$$\gamma_v = 1 - \frac{1}{1 + \frac{2}{3}\sqrt{b_1/b_2}}$$

and the moment flexure factor is

$$\gamma_f = \frac{1}{1 + \frac{2}{3}\sqrt{b_1/b_2}}$$

where  $b_1 = c_1 + d/2$  for an exterior column

$b_1 = c_1 + d$  for an interior column

$b_2 = c_2 + d$

The value of  $\gamma_f$  can be increased by 25 percent at the interior supports and can be also increased to 1.0 at other supports as indicated in the discussion of Equation 9.29. Then compute  $c_{AB}$  and  $c_{CD}$  for exterior columns, as well as the total nominal unbalanced moment strength  $M_n = M_{ue} + V_u g$ .

- 11.** Compute the shear ultimate stress due to perimeter shear and effect of  $\gamma_v M_n$ :

$$v_n = \frac{V_u}{\phi_v A_c} + \frac{\gamma_v c_{AB} M_n}{J_c} \leq \text{max. allowable } v_c \text{ where}$$

$$\text{max. allowable shear stress } v_c = \beta_p \sqrt{f'_c} + 0.3\bar{f}_c + \frac{V_p}{b_o d}$$

$$\beta_p = \text{the smaller of the two values of } 3.5 \text{ or } (\alpha_s d/b_o + 1.5)$$

$$\phi = 0.75 \text{ for shear and torsion}$$

where  $\alpha_s$  is 40 for interior columns, 30 for edge columns, and 20 for corner columns.

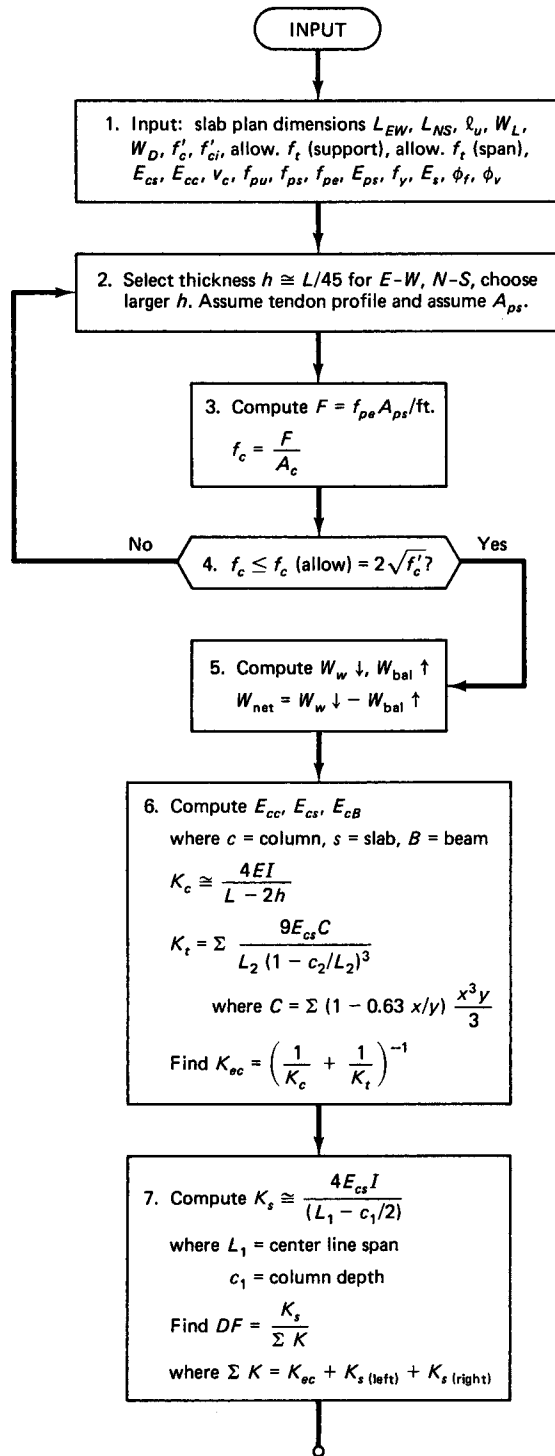
Column section shall be at least 4 in. from the face of the discontinuous edge, and  $f'_c$  shall not exceed 5000 psi and  $f$  shall be 125 psi min. and 500 psi max.; otherwise  $v_c$  shall be computed from the smaller of the values obtained from the following expressions.

$$v_c = (2 + 4/\beta) \sqrt{f'_c} \quad \text{or} \quad v_c = \left( \frac{\alpha_s d}{b_o} + 2 \right) \sqrt{f'_c} \quad \text{or} \quad v_c = 4 \sqrt{f'_c}$$

- 12.** Compute the factored moment value  $\gamma_f M_n$ , and check the available moment strength  $M_n$  of the section, concentrating the steel in the column band  $[c + 2(1.5h)]$ .
- 13.** Check the deflection and camber serviceability behavior of the critical slab panels.
- 14.** Adopt the design if it satisfied all the preceding criteria. Then perform the operations for the E-W and N-S directions of the floor system.

Figure 9.16 gives a flowchart for the design or analysis of two-way action prestressed concrete floor slabs and plates.





**Figure 9.16** Flowchart for the design (analysis) of prestressed concrete two-way slabs and plates in flexure and shear.

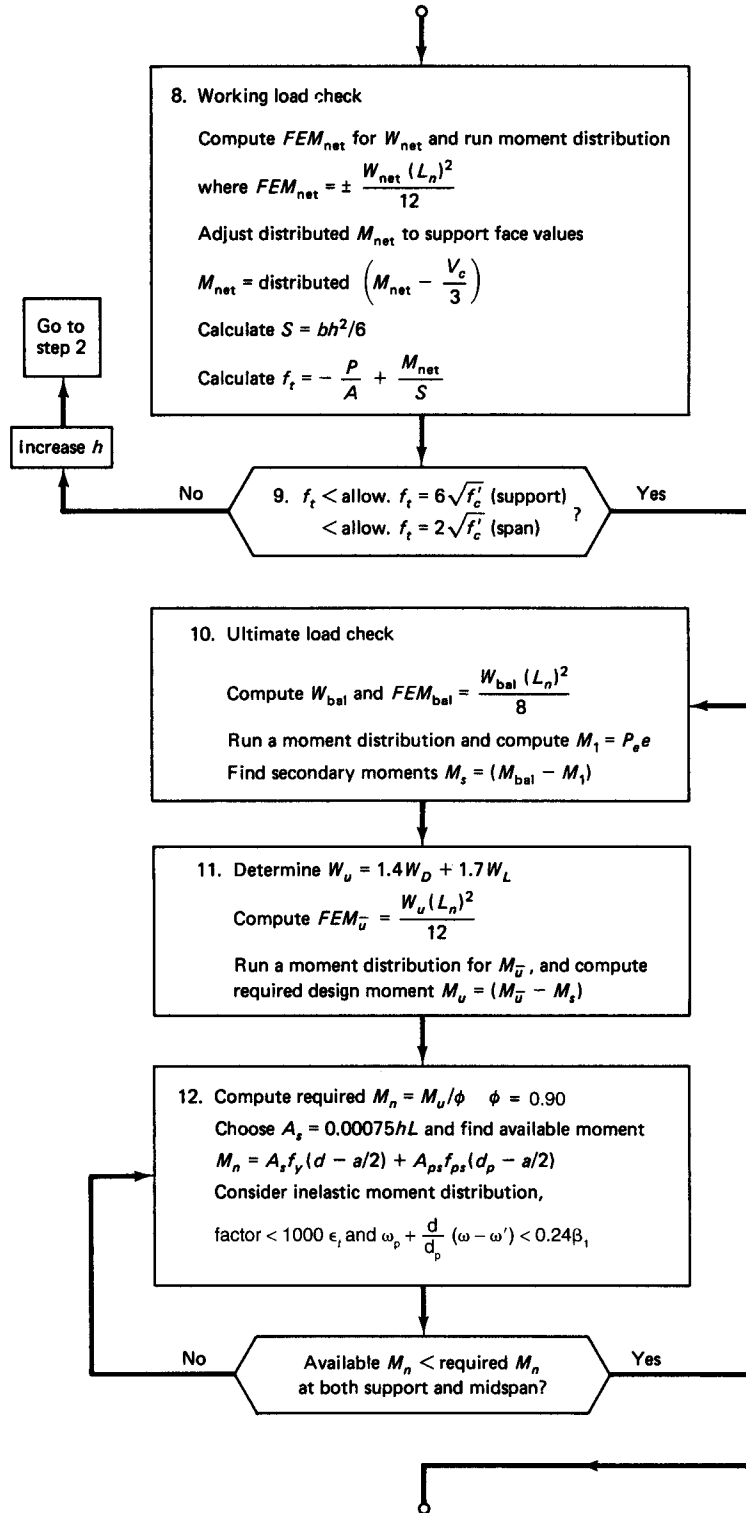


Figure 9.16 Continued

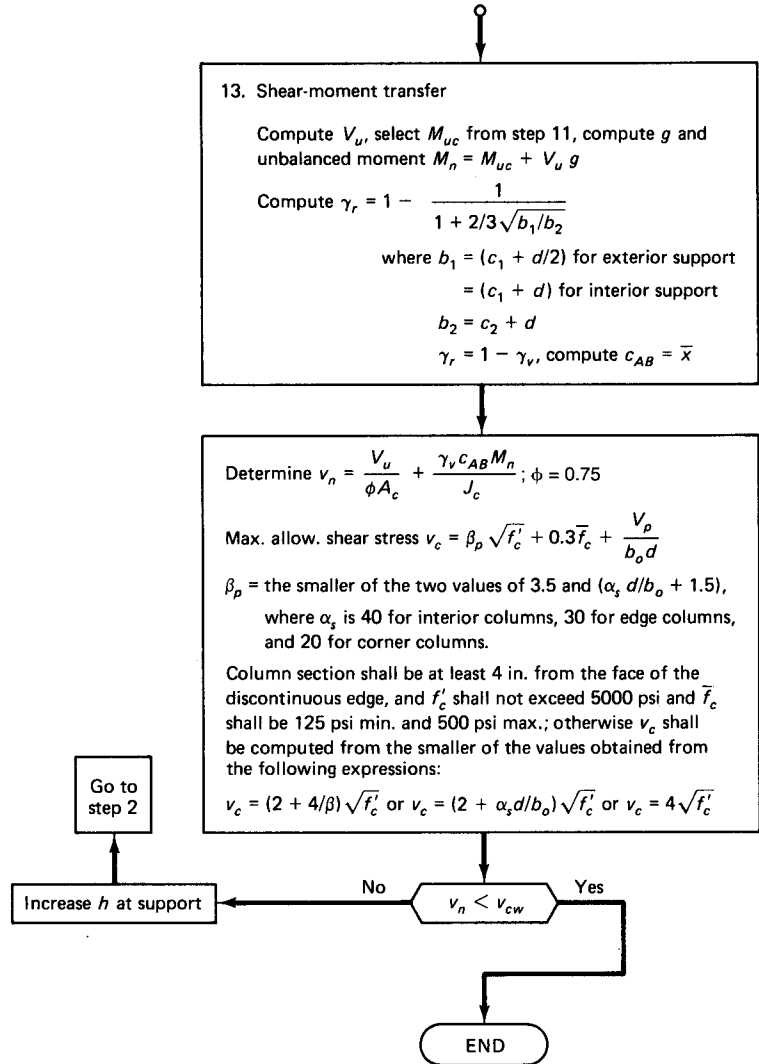
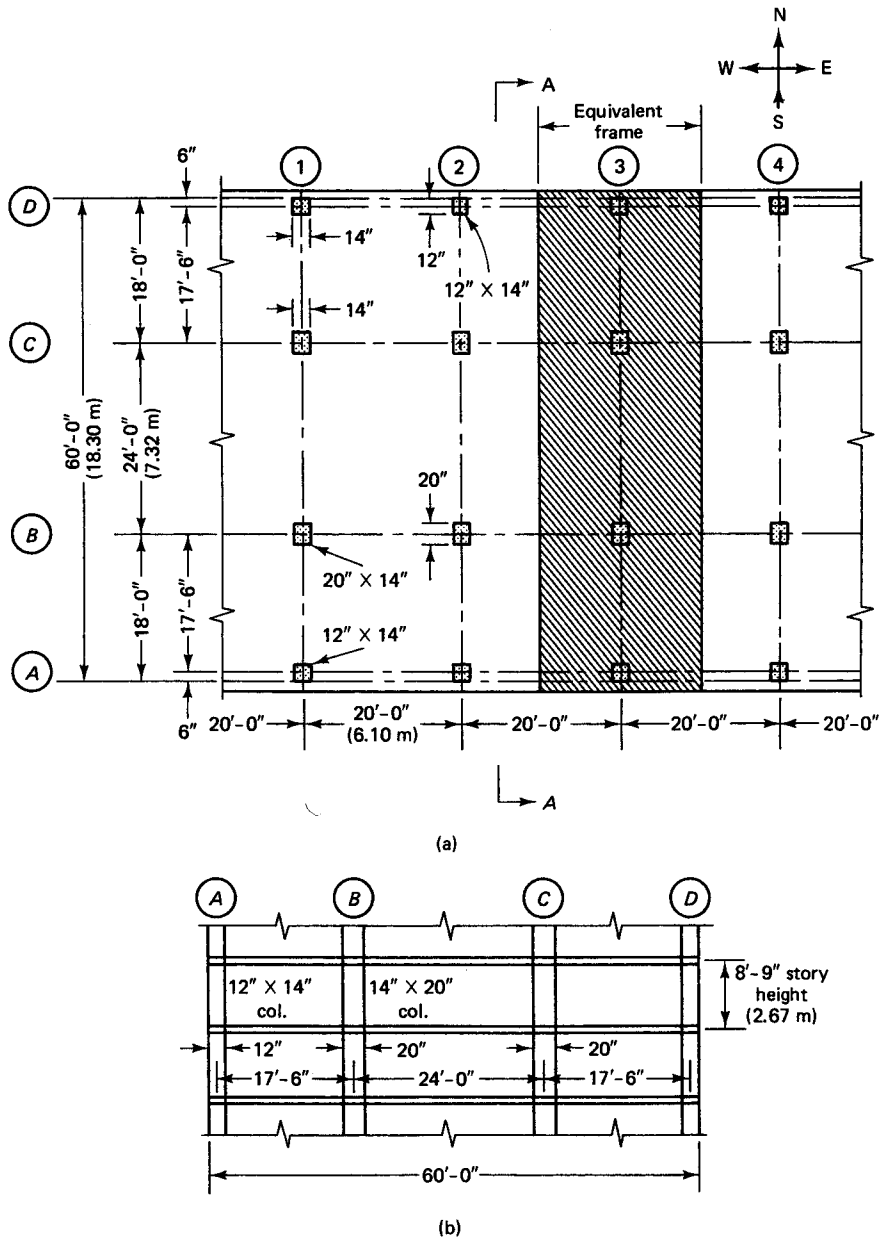


Figure 9.16 Continued

**9.11 DESIGN OF PRESTRESSED POST-TENSIONED FLAT-PLATE FLOOR SYSTEM**

**Example 9.2**

A post-tensioned prestressed nonbonded flat-plate floor system for an apartment complex is shown in Figure 9.17. The end-panel centerline dimensions are 17 ft, 6 in.  $\times$  20 ft, 0 in. (5.33 m  $\times$  6.10 m), and the interior panel dimensions are 24 ft, 0 in.  $\times$  20 ft, 0 in. (7.32 m  $\times$  6.10 m). The heights  $l_u$  of the intermediate floors are typically 8 ft, 9 in. (2.67 m). Design a typical floor panel to withstand a working live load  $W_L = 40$  psf (1.92 kPa) and a superimposed dead load  $W_{SD} = 20$  psf (0.96 kPa) due to partitions and flooring. Assume in your solution that all panels are simultaneously loaded by the live load, and verify the shear-moment transfer capacity of the floor at the column supports. Use  $\frac{1}{2}$ -in. dia 7-wire 270-K prestressing strands and the equivalent frame method to arrive at your solution. Given data are as follows:



**Figure 9.17** Flat-plate apartment structure in Example 9.1. (a) Plan. (b) Section A-A, N-S.

$$f'_c = 4,000 \text{ psi (27.6 MPa), normal weight}$$

$$f'_{ct} = 3,000 \text{ psi (20.7 MPa)}$$

$$\text{Support } f_t = 6\sqrt{f'_c} = 380 \text{ psi (2.62 MPa)}$$

$$\text{Midspan } f_t = 2\sqrt{f'_c} = 127 \text{ psi (0.88 MPa)}$$

Max.  $v_c$  required by the ACI Code

$$f_{pu} = 270,000 \text{ psi (1,862 MPa)}$$

$f_{ps}$  not to exceed 185,000 psi (1,276 MPa)

$f_{py} = 243,000$  psi (1,675 MPa)

$f_{pe} = 159,000$  psi (1,096 MPa)

$E_{ps} = 29 \times 10^6$  psi ( $200 \times 10^3$  MPa)

$f_y = 60,000$  psi (414 MPa)

**Solution:**

***N-S Direction***

**I. Service Load Analysis**

**1. Loads**

For deflection control, assume that the slab thickness  $h \cong L/45$ . Then the longitudinal direction  $h = 20 \times 12/45 = 5.33$  in. and the transverse direction  $h = 24 \times 12/45 = 6.40$  in. So try  $h = 6\frac{1}{2}$  in. (165-mm) slabs = 81 psf. The superimposed dead load = 20 psf, and we have

$$\text{Total } W_D = 101 \text{ psf}$$

$$W_L = 40 \text{ psf}$$

$$\text{Total } W_w = W_{D+L} = 141 \text{ psf (6.75 kPa)}$$

$$W_u = 1.2W_D + 1.6W_L = 1.2 \times 101 + 1.6 \times 40 \cong 186 \text{ psf (8.9 kPa)}$$

$$L_n = \text{bay span (N-S for this part of the solution)}$$

$$L_2 = \text{band width (E-W direction)} = 20 \text{ ft (240 in.)}$$

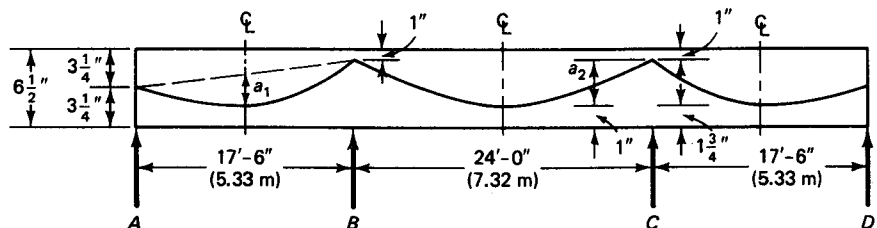
**2. Load Balancing and Tendon Profile**

In order to make a preliminary estimate of the balanced load, assume an average intensity of compressive stress on the concrete due to load balancing of  $f_c = 170$  psi (1.17 MPa). Then the unit  $F = 170 \times 6.5 \times 12 = 13,260$  lb/ft (193.6 kN/m). So, trying  $\frac{1}{2}$ -in. dia 270-K seven-wire strands, we find that the effective force  $P_e$  per strand =  $A_{ps} f_{pe} = 0.153 \times 159,000 = 24,327$  lb. For the  $L = 20$ -ft bay along the longitudinal direction of the structure, the total force is  $F_e = FL = 13,260 \times 20 = 265,200$  lb (1,180 kN).

The number of strands per bay is  $F_e/P_e = 265,200/24,327 \cong 11$  strands, and the total  $P_e = F_e = 24,327 \times 11 = 267,597$  lb. The actual unit force  $F = 267,597/20 = 13,380$  lb/ft (195.3 kN/m), and the actual  $f_c = F/A = 13,380/(6.5 \times 12) \cong 172$  psi  $\cong 170$  psi, which is satisfactory. Consequently, use  $f_c = 172$  psi due to load balancing, and assume a parabolic tendon profile as shown in Figure 9.18.

***Outside Spans AB or CD at Midspan***

$$a_1 = a_3 = \frac{3.25 + 5.50}{2} - 1.75 = 2.625 \text{ in.}$$



**Figure 9.18** Tendon profile in N-S direction in Example 9.2.

From Equation 1.16 for a parabolic tendon,

$$W = \frac{8Fa}{L_n^2}$$

$$W_{\text{bal}} = \frac{8 \times 13,380 \times 2.625/12}{(18)^2} \cong 72 \text{ psf}$$

The net load intensity producing bending is

$$W_{\text{net}} = W_w - W_{\text{bal}} = 141 - 72 = 69 \text{ psf (3.30 kPa)}$$

*Interior Span BC*

$$a_2 = 6.5 - 1 - 1 = 4.5 \text{ in.}$$

$$W_{\text{bal}} = \frac{8Fa}{L_n^2} = \frac{8 \times 13,380 \times 4.5/12}{(24)^2} \cong 70 \text{ psf}$$

$$W_{\text{net}} = 141 - 70 = 71 \text{ psf (3.40 kPa)}$$

### 3. Equivalent Frame Characteristics

Take the equivalent frame in the N-S direction whose plan is shown in the shaded portion of Figure 9.17. The approximate flexural stiffness of the column above and below the floor joint (the moment per unit rotation), from Ref. 9.10 and Equation 9.9, is

$$K_c = \frac{4E_c I_c}{L_n - 2h}$$

where  $L_n = l_u = 8 \text{ ft, } 9 \text{ in.} = 105 \text{ in.}$

#### (a) Exterior column (14 in. × 12 in.) stiffness

For the exterior columns,  $b = 14 \text{ in.}$ , so  $I_c = 14(12)^3/12 = 2,016 \text{ in.}^4$ . Assume that  $E_{\text{col}}/E_{\text{slab}} = E_{\text{cc}}/E_{\text{cs}} = 1.0$ , and use  $E_{\text{cc}} = E_{\text{cs}} = 1.0$  in the calculations as  $E_{\text{cs}}$  drops out in the equation for  $K_{\text{ec}}$ . Then we obtain

$$\text{Total } K_c = \frac{4 \times 1 \times 2,016}{105 - (2 \times 6.5)} \times 2 \text{ (for top and bottom columns)}$$

$$= 175.3 \text{ in.-lb/rad}/E_{\text{cc}}$$

From Equation 9.10b, the torsional constant is

$$C = \Sigma \left( 1 - 0.63 \frac{x}{y} \right) \frac{x^3 y}{3}$$

$$= \left( 1 - 0.63 \times \frac{6.5}{12} \right) 6.5^3 \times \frac{12}{3} = 724$$

The torsional stiffness of the slab at the column line is

$$K_t = \Sigma \frac{9E_{\text{cs}} C}{L_2 \left( 1 - \frac{c_2}{L_2} \right)^3}$$

$$= \frac{9 \times 1 \times 724}{20 \times 12 \left( 1 - 14/(12 \times 20) \right)^3} + \frac{9 \times 1 \times 724}{20 \times 12 \left( 1 - 14/(12 \times 20) \right)^3}$$

$$= 65.0 \text{ in.-lb/rad}/E_{\text{cc}}$$

From Equation 9.7, the equivalent column stiffness is  $K_{\text{ec}} = (1/K_c + 1/K_t)^{-1} = (1/175.3 + 1/65)^{-1} = 47 \text{ in.-lb/rad}/E_{\text{cc}}$ .

**(b) Interior column (14 in. × 20 in.) stiffness**

For the interior columns,  $b = 14$  in., so  $I = 14(20)^3/12 = 9,333$  in.<sup>4</sup> Hence, we have

$$\text{Total } K_c = \frac{4 \times 1 \times 9,333}{105 - 2 \times 6.5} \times 2 = 812 \text{ in.-lb/rad}/E_{cc}$$

$$C = \left(1 - 0.63 \times \frac{6.5}{20}\right) \times (6.5)^3 \times \frac{20}{3} = 1,456$$

$$K_t = \frac{9 \times 1,456}{20 \times 12(1 - 14/(12 \times 20))^3} + \frac{9 \times 1,456}{20 \times 12(1 - 14/(12 \times 20))^3} = 131 \text{ in.-lb/rad}/E_{cs}$$

$$K_{ec} = (1/812 + 1/131)^{-1} = 113 \text{ in.-lb/rad}/E_{cc}$$

**(c) Slab stiffness**

From Equation 9.9 and Ref. 9.10,

$$K_s = \frac{4E_{cs} I_s}{L_n - \frac{c_1}{2}}$$

where  $L_n$  is the centerline span and  $c_1$  the column depth. The slab band width in the E-W direction is  $20/2 + 20/2 = 20$  ft. Thus,  $I_s = 20 \times 12(6.5)^3/12 = 5,493$  in.<sup>4</sup>, and for the slab at the right of exterior column A,

$$K_s = \frac{4 \times 1 \times 20(6.5)^3}{12 \times 17.5 - 12/2} = 108 \text{ in.-lb/rad}/E_{cs}$$

while for the slab at the left of interior column B,

$$K_s = \frac{4 \times 1 \times 20(6.5)^3}{12 \times 17.5 - 20/2} = 110 \text{ in.-lb/rad}/E_{cs}$$

and for the slab at the right of interior column B,

$$K_s = \frac{4 \times 1 \times 20(6.5)^3}{12 \times 24 - 20/2} = 79 \text{ in.-lb/rad}/E_{cs}$$

From Equation 9.12, the slab distribution factor at the joints is  $DF = K_s/\Sigma K$ , where  $\Sigma K = K_{ec} + K_{s(left)} + K_{s(right)}$ . So for the outer joint A slab,  $DF = 108/(47 + 108) = 0.697$ ; for the left joint B slab,  $DF = 110/(113 + 110 + 79) = 0.364$ ; and for the right joint B slab,  $DF = 79/(113 + 110 + 79) = 0.262$ .

**4. Design Service-load Moments and Stresses***Design net load moments*

For the exterior spans AB and CD,  $W_{net} = 69$  psf. So the fixed-end moment is

$$FEM = \frac{WL_n^2}{12} = \frac{69 \times (17.5)^2}{12} \times 12 = 21.1 \times 10^3 \text{ in.-lb}$$

Similarly, for the interior span BC,  $W_{net} = 71$  psf. So the fixed-end moment is

$$FEM = \frac{71(24)^2}{12} \times 12 = 40.9 \times 10^3 \text{ in.-lb}$$

By running a moment distribution analysis as shown in Table 9.2, a carryover factor  $COF = \frac{1}{2}$  can be used for all spans. Such an assumption is justified, as the effect of non-prismatic sections would be negligible on the fixed-end moments and carryover factors. It can also be assumed in multispan frames that the frame at a joint two spans away from the left joint (joint C) can be considered fixed in the distribution of the moments.

**Table 9.2** Moment Distribution of Net Load Moments  $M_{net}$ 

	(A)	(B)	∅	(C)
<i>DF</i>	0.697	0.364	0.262	0.262
<i>COF</i>	0.5	0.5	0.5	0.5
$FEM_{net}$ $\times 10^3$ in.-lb	-21.1	21.1	-40.9	40.9
Dist.	+14.71	7.21	5.19	-5.19
<i>CO</i>	3.61	7.36	-2.60	
Dist.	-2.52	-1.73	-1.25	
Final $M_{net}$ $\times 10^3$ per ft	-5.30	33.94	-39.56	

*Slab concrete tensile stress at support*

The net moment at the interior face of column B is the difference of the centerline moment and  $Vc/3$ , i.e.,

$$M_{net,max} = 39.56 \times 10^3 - \frac{20}{3} \left( \frac{71 \times 24}{2} \right) = 33,880 \text{ in.-lb/ft}$$

The slab section modulus  $S = bh^2/6 = 12(6.5)^2/6 = 84.5 \text{ in.}^3$ , and we have, for the support concrete stress,

$$f_t = -\frac{P}{A} + \frac{M}{S} = -172 + \frac{33,880}{84.5} = +229 \text{ psi (1.63 MPa) (T)}$$

So the allowable  $f_t = 6\sqrt{f'_c} = 380 \text{ psi} > 229 \text{ psi}$ , which is satisfactory.

*Slab concrete tensile stress at midspan*

The net midspan maximum moment is  $WL^2/8 - 39.56 \times 10^3$ , or

$$M_{net,max} = \frac{71(24)^2}{8} \times 12 - 39.56 \times 10^3 = 21,784 \text{ in.-lb/ft (7.85 kN/m)}$$

Also,

$$\text{Midspan } f_t = -\frac{P}{A} + \frac{M}{S} = -172 + \frac{21,784}{84.5} = +86 \text{ psi (0.545 MPa) (T)}$$

So the allowable  $f_t = 2\sqrt{f'_c} = 127 \text{ psi} > 86 \text{ psi}$ , which is satisfactory.

If  $f_t$  were to exceed the allowable  $f_t$ , the entire tensile force would have to be taken by mild steel reinforcement at a stress  $f_s = \frac{1}{2} f_y$ .

**Ultimate Flexural Strength Analysis****II. Design Moments  $M_u$ .****1. Balanced moments  $M_{bal}$** 

The secondary moment is given by  $M_s = M_{bal} - M_1$ , where  $M_{bal}$  is the balanced moment and  $M_1$  is the primary moment  $= P_e e = Fe$ . For the span AB or CD,

$$FEM_{bal} = \frac{72(17.5)^2}{12} \times 12 = 22,050 \text{ in.-lb/ft}$$

and for the span BC,

$$FEM_{bal} = \frac{70(24)^2}{12} \times 12 = 40,320 \text{ in.-lb/ft}$$



**Table 9.3** Moment Distribution of Balanced Load Moments  $M_{bal}$ 

	Ⓐ		Ⓑ	Ⓒ	Ⓓ
<i>DF</i>	0.697	0.364	0.262	0.262	0.364
<i>COF</i>	0.5	0.5	0.5	0.5	0.5
<i>FEM</i> <sub>bal</sub> × 10 <sup>3</sup> in.-lb	-22.05	22.05	-40.32	40.3	-22.05
Dist.	+15.37	+6.65	+4.79	-4.79	-6.65
<i>CO</i> Dist.	3.33 -2.32	7.69 -1.93	-2.40 -1.39		
Final <i>M</i> <sub>bal</sub> × 10 <sup>3</sup> per ft	-5.67	34.46	-39.32		

Running a moment distribution as in Table 9.3 will determine the maximum  $M_{bal}$  for the exterior column joints.

## 2. Secondary moments $M_s$ and factored load moment $M_u$

### Span AB

From the tendon profile of Figure 9.18,  $e = 0$ . So we have:

$$\text{Primary moment } M_1/\text{ft at } A = P_e e = 0$$

$$M_{bal} = 5,670 \text{ in.-lb/ft (from Table 9.3)}$$

$$M_s = M_{bal} - M_1 = 5,670 - 0 = 5.67 \times 10^3 = 5,670 \text{ in.-lb/ft}$$

$$\text{Factored load } FEM_u = \frac{W_u l^2}{12} = \frac{186(17.5)^2}{12} \times 12 = 56,963 \text{ in.-lb/ft}$$

### Span BA

From the tendon profile in Figure 9.18,  $e = 6.5/2 - 1 = 2.25$  in. So we have:

$$M_1 = 13,380 \times 2.25 = 30,105 \text{ in.-lb/ft (11.16 kN-m)}$$

$$M_{bal} = 34,460 \text{ in.-lb/ft (from Table 9.3)}$$

$$M_s = 34,460 - 30,105$$

$$= 4,355 \text{ in.-lb/ft (1.61 kN-m/m)}$$

$$\text{Factored load } FEM_u = 56,963 \text{ in.-lb/ft (21.1 kN-m/m)}$$

### Span BC

$$e = 2.25 \text{ in.}$$

$$M_1 = 30,105 \text{ in.-lb/ft}$$

$$M_{bal} = 39,320 \text{ in.-lb/ft (from Table 9.3)}$$

$$M_s = 39,320 - 30,105 = 9,215 \text{ in.-lb/ft (3.4 kN-m/m)}$$

$$\text{Factored load } FEM_u = \frac{186(24)^2}{12} \times 12 = 107,136 \text{ in.-lb/ft (39.7 kN-m/m)}$$

Run a moment distribution for the factored moments as in Table 9.4. Analysis of pattern loading of alternate spans should also be made to determine the worst conditions of service-load and factored-load moments.

**Table 9.4** Moment Distribution of Factored Loads

	Ⓐ		Ⓑ	∅	Ⓒ	
<i>DF</i>	0.697	0.364		0.262	0.262	0.364
<i>COF</i>	0.5	0.5		0.5	0.5	0.5
<i>FEM<sub>u</sub><sup>-</sup></i> × 10 <sup>3</sup> in.-lb per ft Dist.	-56.96	+56.96		-107.14	107.14	-56.96
<i>CO</i> Dist.	+39.70	+18.27		+13.15	-13.15	-18.27
<i>CO</i> Dist.	+9.14	+19.85		-6.58		
	-6.37	-4.83		-3.48		
Final <i>M<sub>u</sub><sup>-</sup></i> × 10 <sup>3</sup> per ft	-14.49	+90.25		-104.05		

**3. Design moment  $M_u$** 

The design moments  $M_u$  are the difference between the factored-load moments  $M_u^-$  and the secondary moments  $M_s$ , i.e.,  $M_u = M_u^- - M_s$  (from Equation 9.17).

**Joint A (span AB) moment  $-M_u$** 

For the joint A (span AB) moment,  $M_s = 5,670$  in.-lb/ft (from before), and so the centerline  $M_u = 14,490 - 5,670 = 8,820$  in.-lb/ft. The moment reduction to the column face of support A =  $Vc/3$ . Thus,

$$V_{AB} = \frac{W_u L}{2} - \frac{M_{u@B}^- - M_{u@A}^-}{L_n} = \frac{186 \times 17.5}{2} - \frac{10^3(90.25 - 14.49)}{17.5 \times 12}$$

$$= 1627.5 - 360.8 = 1266.7 \text{ lb/ft}$$

$$c = 12 \text{ in.}$$

$$\text{Centerline } M_u = 14,490 - 5,670 = 8,820 \text{ in.-lb/ft}$$

$$\text{Req column face } M_u = 8,820 - \frac{1266.7 \times 12}{3}$$

$$= 8,820 - 4,924 = 3,753 \text{ in.-lb/ft (1.39 kN-m/m)}$$

$$\text{Req } -M_n = \frac{M_u}{\phi} = \frac{3,753}{0.9} = 4,170 \text{ in.-lb/ft (1.55 kN-m/m)}$$

**Joint B (span BA) moment  $-M_u$** 

For the joint B (span BA) moment,  $M_s = 4,355$  in.-lb/ft (from before), and so the centerline  $M_u = 90,250 - 4,355 = 85,895$  in.-lb/ft. Thus,

$$V_{BA} = 1,627.5 + 360.8 = 1,988.3 \text{ lb/ft.}$$

$$c = 20 \text{ in.}$$

$$\text{Req. column face } M_u = 85,895 - \frac{1,988.3 \times 20}{3}$$

$$= 85,895 - 13,255 = 72,604 \text{ in.-lb/ft (26.8 kN-m/m)}$$

$$\text{Req } -M_n = \frac{M_u}{\phi} = \frac{72,604}{0.9} = 80,671 \text{ in.-lb/ft (30 kN-m/m)}$$

**Table 9.5** Summary of Shear  $V_u$  and Secondary Moment  $M_s$  for Ultimate Load Evaluation

Factored Shear $V_u$ (lb/ft)	Secondary Moment $M_s$ (in.-lb/ft)
$V_{AB} = 1266.7$	$M_{s,AB} = 5670$
$V_{BA} = 1988.3$	$M_{s,BA} = 4335$
$V_{BC} = 2232.0$	$M_{s,BC} = 9215$

Joint B (span BC) moment  $-M_u$

For the joint B (span BC) moment,  $M_s = 9,215$  in.-lb/ft, and so the centerline  $M_u = 104,050 - 9,215 = 94,835$  in.-lb/ft. Thus,

$$V_{BC} = \frac{186 \times 24}{2} = 2,232 \text{ lb/ft}$$

$$\text{Req. column face } -M_u = 94,835 - \frac{2,232 \times 20}{3} = 94,835 - 14,880$$

$$= 79,955 \text{ in.-lb/ft (28 kN-m/m)}$$

$$\text{Req } -M_n = \frac{M_u}{\phi} = \frac{79,955}{0.9}$$

$$= 88,839 \text{ in.-lb/ft (35 kN-m/m)}$$

Span AB maximum positive moment  $+M_u$

Assume that the point of zero shear and maximum moment is  $x$  ft from face A. Then  $x = V_{AB}/W_u = 1266.7/186 = 6.81$  ft. Also, from Table 9.4, the end  $M_u^-$  at A = 12,310 in.-lb/ft., and from before,  $M_s = \frac{1}{2}(5,670 + 4,355) = 5,013$  in.-lb/ft. So we have

$$\begin{aligned} \text{Max. } +M_u &= V_{AB}x - \frac{W_u x^2}{2} - M_u^- + M_s \\ &= 1266.7 \times 6.81 \times 12 - \frac{186(6.81)^2}{2} \times 12 - 14,490 + 5,013 \end{aligned}$$

$$= 103,515 - 51,756 - 14,490 + 5,013$$

$$= 42,282 \text{ in.-lb/ft (15.7 kN-m/m) at 6.81 ft from A}$$

$$\text{Req } +M_n = \frac{M_u}{\phi} = \frac{42,282}{0.9} = 46,980 \text{ in.-lb/ft (17.4 kN-m/m)}$$

Span BC maximum positive moment  $+M_u$

From before,  $V_{BC} = 2,232$  lb/ft and  $x = L_n/2 = 24/2 = 12$  ft. The simple span midspan moment is, then,

$$M_u = V_{BC} \times \frac{L_n}{2} - \left( W_u \times \frac{L}{2} \right) \frac{(L)}{4}$$

$$= 2232 \times \frac{24}{2} - \frac{186(24)^2}{8} = 13,392 \text{ ft.-lb/ft} = 160,704 \text{ in.-lb/ft}$$

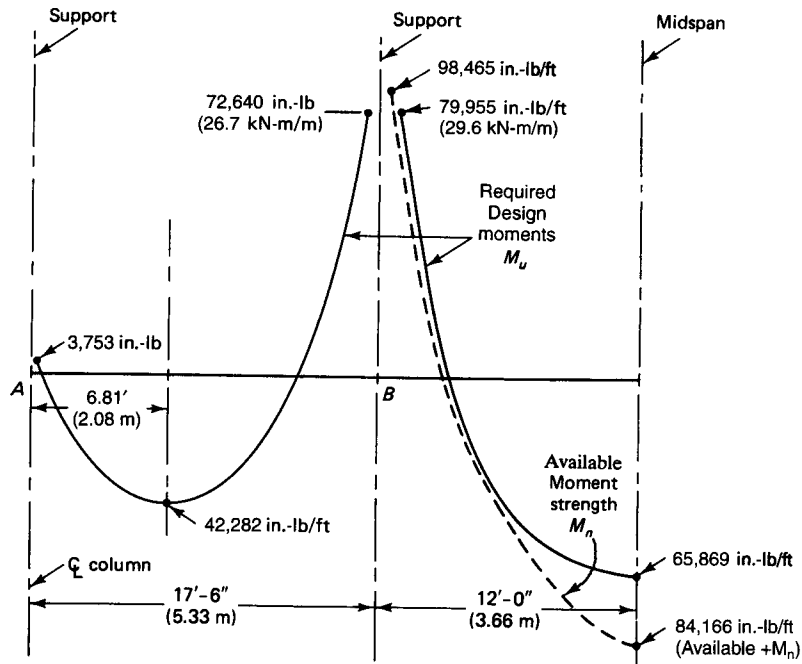
Alternatively, the simple span moment is

$$M = \frac{W_u L^2}{8} = \frac{186(24)^2}{8} \times 12$$

$$= 160,704 \text{ in.-lb/ft}$$

Now,  $+M_u = M - M_u^- + M_s$ . From Table 9.4,  $M_u^- = -104,050$  in.-lb/ft, and  $M_s = 9,215$  in.-lb/ft. So the required maximum  $+M_u = 160,704 - 104,050 + 9,215 = 65,869$  in.-lb/ft (24.42 kN-m/m) at midspan. And the required  $+M_n = M_u/\phi = 65,869/0.9 = 73,188$  in.-lb/ft (27.13 kN-m/m).

Figure 9.19 gives a plot of the required design moments  $M_u$  across the continuous spans and the peak values of the moments.



**Figure 9.19** Maximum required design moments  $M_u$  and available nominal moment strengths  $M_n$  in Example 9.2, after redistribution.

**III. Flexural Strength  $M_n$  (Nominal Moment Strength).** The ACI Code requires a minimum amount of nonprestressed reinforcement. From Equation 9.20,

$$A_s = 0.00075hL_n$$

**1. Interior support section at B**

For the interior support section at B, the controlling required  $M_n = 88,839$  in.-lb/ft.

Hence, the minimum area of non-prestressed steel reinforcement in each direction in the negative moment areas of slabs at column supports as in Equation 4.55(b) is  $A_s = 0.00075hl$ , where  $h$  = total slab thickness and  $l$  = span length in the direction parallel to that of the reinforcement being determined, Section 4.12.5.3.

$$A_s = 0.00075 \times 6.5 \left( \frac{18 + 24}{2} \right) \times 12 = 1.23 \text{ in}^2 (7.93 \text{ cm}^2)$$

Hence, try six #4 bars of 11-ft length, and space the bars at a maximum of 6 in. (152 mm) center-to-center so that they are concentrated over the column on a band width equal to the column width plus  $1\frac{1}{2}$ -slab thicknesses on each side of the column. Then

$$A_s = 6 \times 0.20 = 1.20 \text{ in}^2 \cong \text{required } 1.23 \text{ in}^2, \text{ O.K.}$$

$$\text{Panel width} = 20 \text{ ft}$$

$$A_s/\text{ft} = \frac{1.2}{20} = 0.06 \text{ in}^2$$

From Equation 9.23b, the design stress in the tendon is

$$f_{ps} = f_{pe} + \frac{f'_c}{300\rho_p} + 10,000 \text{ psi}$$

and

$$\rho_p = \frac{A_{ps}}{bd} = \frac{11 \times 0.153}{(20 \times 12)5.5} = 0.0013$$

$$f_{pe} = 159,000 \text{ psi}$$

$$f_{ps} = 159,000 + \frac{4,000}{300 \times 0.0013} + 10,000 = 179,256 \text{ psi (1,236 MPa)}$$

$$F_{ps} = \frac{179,256 \times 0.153 \times 11}{20} = 15,084 \text{ lb/ft}$$

$$F_s = 60,000 \times A_s/\text{ft} = 60,000 \times 0.06 = 3,600 \text{ lb/ft}$$

The total force  $F/\text{ft} = F_{ps} + F_s = 15,084 + 3,600 = 18,684 \text{ lb/ft}$ , and we also have

$$\begin{aligned} \text{Compression block depth } a &= \frac{A_s f_y + A_{ps} f_{ps}}{0.85 f'_c b} \\ &= \frac{18,684}{0.85 \times 4,000 \times 12} = 0.46 \text{ in. (11.7 mm)} \end{aligned}$$

The bars and tendons are to be placed at the same level  $d = 6.5 - 1 = 5.5 \text{ in.}$  Also,  $M_n = (A_s f_y + A_{ps} f_{ps})(d - a/2)$ , the available  $-M_n = 18,684 \times (5.5 - 0.46/2) = 98,465 \text{ in.-lb/ft (36.5 MPa)}$ , and the required  $M_n = 88,839 \text{ in.-lb/ft} < 98,465$ . Thus, no additional moment strength is needed.

No inelastic negative moment redistribution (reduction) is essential in this case, provided that the available positive moment reinforcement is adequate. If redistribution is applied, from Figure 4.46:

$$\epsilon_t = 0.003 \left( \frac{d_t}{c} - 1 \right) = 0.003 \left( \frac{5.5}{0.46/0.85} - 1 \right) = 0.027 \text{ in./in.} > 0.0075 \text{ in./in., O.K.}$$

It is desirable to cause a moment redistribution from the support to midspan, maximum moment redistribution value =  $1000 \epsilon_t \leq 20 \%$

Actual redistribution factor =  $1000 \times 0.027 = 27 \%$ , exceeds the maximum allowable.

Apply a 15 % redistribution factor to the positive midspan moment.

Hence, required  $+M_n = 1.15 \times 73,188 = 84,166 \text{ in.-lb/ft}$ .

A corresponding reduction in the area of mild steel reinforcement for the negative moment is warranted, provided that the minimum is satisfied.

## 2. Midspan section at span BC

From before,  $F_{ps} = A_{ps} f_{ps} = 15,084 \text{ lb/ft}$ , and

$$a = \frac{A_{ps} f_{ps}}{0.85 f'_c b} = \frac{15,084}{0.85 \times 4,000 \times 12} = 0.37 \text{ in.}$$

So the available  $-M_n = A_{ps} f_{ps}(d - a/2) = 15,084(5.5 - 0.37/2) = 80,171 \text{ in.-lb/ft}$ , and the required  $+M_n$  after redistribution =  $+84,166 \text{ in.-lb/ft} > 80,171 \text{ in.-lb/ft}$ , and hence is unsatisfactory. Accordingly, add two #4 bars at midspan over a 20-ft width to get

$$A_s = 2 \times 0.20 = 0.40 \text{ in.}^2$$

$$A_s f_y = \frac{0.40 \times 60,000}{20} = 1200 \text{ lb/ft}$$

$$a = \frac{(15,084 + 1200)}{0.85 \times 4,000 \times 12} = 0.40 \text{ in.}$$

$$\begin{aligned} \text{Available } +M_n &= (A_s f_y + A_{ps} f_{ps}) \left( d - \frac{a}{2} \right) \\ &= (15,084 + 1200) \left( 5.5 - \frac{0.40}{2} \right) = 86,305 \text{ in.-lb/ft} \\ &> \text{req } +M_n = 84,116 \text{ in.-lb/ft, O.K.} \end{aligned}$$

Verify value of  $\phi = 0.90$  used:

$$c = a/\beta_1 = 0.40/0.85 = 0.47; c/d_t = 0.47/(6.25 - 2.75)$$

= 0.10  $\ll$  0.375 in Fig. 4.45, hence section is tension controlled, and  $\phi = 0.90$  O.K.

**Reinforcement Summary**

After moment redistribution, use two #4 (12.7-mm dia) nonprestressed mild steel bars at the bottom fibers at midspan in addition to the continuous prestressing tendon in the 20-ft segment. Also, use six #4 nonprestressed mild steel bars at the top fibers at the support, centered through the column at 6 in. center-to-center spacing (six 12.7-mm dia bars at 152 mm center-to-center) as minimum reinforcement, to be verified for shear-moment transfer.

The midspan sections of spans AB and CD would have more than adequate positive nominal moment strength to resist the positive factored moments. The nominal negative moment strength of the sections at the exterior supports A and D are governed by the moment-shear transfer stresses.

**3. Banding the reinforcement at the column region**

There are eleven  $\frac{1}{2}$ -in. dia strands, and the width of a column strip =  $2(\frac{1}{4} \times 20 \times 12) = 120$  in. Assume that 70 percent of the tendons are concentrated in the column strip. Then the number of strands =  $0.7 \times 11 = 7.7$ . Accordingly, concentrate seven strands in the column strip, three of which are to pass through and be centered on the column section.

There are  $11 - 7 = 4$  strands in the middle strip. On this basis, it can be reasonably assumed that the percentage distribution of moments between the column strip and the middle strip would be approximately as follows:

$$\text{Column strip moment factor} = 7/11 = 0.64$$

$$\text{Middle strip moment factor} = 0.36$$

$$\text{Max total } -M \text{ at column face B} = 33,880 \text{ in.-lb/ft (see Table 9.2)}$$

$$\text{Max total } +M \text{ at midspan} = 21,784 \text{ in.-lb/ft}$$

Consequently, distribute the prestressing tendons between the column strips and middle strips as shown subsequently.

**IV. Nominal Shear Strength****1. Exterior columns A and D****(a) Geometry and external load**

From before,  $V_{AB} = 1266.7$  lb/ft, and the total shear is  $V_B = 1266.7 \times 20 = 25,334$  lb. Assume an exterior wall and glass averaging a load of 500 plf:

$$\text{Wall } V_u = 1.2 \times 500 \times 20 = 12,000 \text{ lb}$$

$$\text{Slab } V_u = 25,334 \text{ lb}$$

$$\text{Total factored } V_{uA} = 25,334 + 12,000 = 37,334 \text{ lb (166.1 kN)}$$

The critical shear section is taken at  $d/2$  from the face of the column, as shown in Figure 9.20. We have

$$d = 6.5 - 1.0 = 5.5 \text{ in.}$$

$$\text{Max } d_p = d_v = 0.8h = 0.8 \times 6.5 = 5.2 \text{ in. (132 mm)}$$

$$c_1 = 12 \text{ in.}$$

$$c_2 = 14 \text{ in.}$$

$$b_1 = c_1 + \frac{d}{2} = 12 + \frac{5.2}{2} = 14.6 \text{ in.}$$

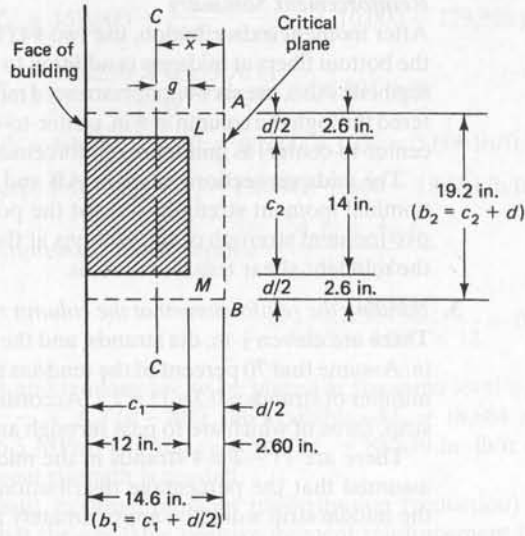
$$b_2 = c_2 + d = 14 + 5.2 = 19.2 \text{ in.}$$

$$A_c = b_0 d = 5.2(2 \times 14.6 + 19.2) = 252 \text{ in.}^2$$

From the figure,

$$d(2c_1 + c_2 + 2d)\bar{x} = d\left(c_1 + \frac{d}{2}\right)^2$$

or



**Figure 9.20** Critical planes for shear moment transfer in end column of Example 9.2 (line A, Figure 9.17).

$$5.2(2 \times 12 + 14 + 2 \times 5.2)\bar{x} = 5.2(14.6)^2$$

$$\bar{x} = c_{AB} = 4.40 \text{ in.}$$

$$g = \bar{x} - \frac{d}{2} = 4.4 - \frac{5.2}{2} = 1.8 \text{ in.}$$

Alternatively,

$$c_{AB} = \frac{b_1^2 d}{A_c} = \frac{(14.6)^2 \times 5.2}{252} = 4.4$$

$$c_{CD} = b_1 - c_{AB} = 14.6 - 4.4 = 10.2 \text{ in.}$$



**Photo 9.5** Placing concrete in a post-tensioned prestressed concrete slab.

From the geometrical properties of the exterior column shown in Figure 9.20, and from Equations 9.28 and 9.29,

$$\begin{aligned}\gamma_v &= 1 - \frac{1}{1 + \frac{2}{3}\sqrt{b_1/b_2}} = 1 - \frac{1}{1 + \frac{2}{3}\sqrt{14.6/19.2}} \\ &= 1 - 0.63 = 0.37 \\ \gamma_f &= \frac{1}{1 + \frac{2}{3}\sqrt{b_1/b_2}} = 0.63\end{aligned}$$

Using  $d_v$  for  $d$ , the polar moment of inertia is

$$\begin{aligned}J_c &= \frac{(c_1 + d/2)d^3}{6} + \frac{2d}{3}(c_{AB}^3 + c_{CD}^3) + (c_2 + d)(d)(c_{AB})^2 \\ &= \frac{14.6(5.2)^3}{6} + \frac{2 \times 5.2}{3}(4.4^3 + 10.2^3) + 19.2 \times 5.2(4.4)^2 \\ &= 342 + 3,974 + 1,933 = 6,249 \text{ in}^4\end{aligned}$$

From before, the unit  $-M_u = 8820 \text{ in.-lb/ft}$  at the column centerline. So the total bay moment at the column centerline is  $-M_c = 8820 \times 20 = 176,400 \text{ in.-lb}$ . Now assume that the resultant  $V_u$  acts at the face of the column for shear-moment transfer. Then the shear moment transferred by eccentricity is  $V_u g = -25,334 \times 1.8 = 45,601 \text{ in.-lb}$ , the total external factored moment  $M_{ue} = 176,400 + 45,601 = 222,001 \text{ in.-lb}$ , and the total required unbalanced moment strength  $M_n = M_{ue}/\phi = 222,001 = 246,668 \text{ in.-lb}$ .

**(b) Shear-moment transfer**

The fraction of the nominal moment strength to be transferred by shear is  $\gamma_v M_n = 0.37 \times 246,668 = 91,267 \text{ in.-lb}$ . From Equation 9.30a, the shearing stress due to perimeter shear, the effect of  $\gamma_v M_n$  and the weight of the wall, is

$$\begin{aligned}v_n &= \frac{V_u}{\phi A_c} + \frac{\gamma_v c_{AB} M_n}{J_c} \\ &= \frac{37,334}{0.75 \times 252} + \frac{0.37 \times 4.4 \times 246,668}{6,249} \\ &= 197.5 + 64.3 \cong 262 \text{ psi}\end{aligned}$$

From the load balancing part of the solution, the average compressive stress in the concrete at the cross-section centroid due to externally applied load  $P_e$  is  $f_c = P_e/A_c = 172 \text{ psi}$ .

From Equations 9.24 and 9.25 and disregarding the effect of the vertical component  $V_p$  of the prestressing force, the maximum allowable shear strength becomes

$$v_c = \beta_p \sqrt{f'_c} + 0.3\bar{f}_c$$

where the factor  $\beta_p$  is the smaller of  $(\alpha_s d/b_0 + 1.5)$  and 3.5, and  $\alpha_s = 30$  for end column support. From Figure 9.20,  $b_0 = 2 \times 14.6 + 19.2 = 48.2 \text{ in.}$ , and

$$\frac{\alpha_s d}{b_0} + 1.5 = \frac{30 \times 5.5}{48.2} + 1.5 = 4.92 > 3.5.$$

Hence use  $\beta_p = 3.5$ .

$$\begin{aligned}\text{Max allowable } v_c &= 3.5\sqrt{4,000} + 0.3 \times 172 \\ &= 221 + 52 = 273 \text{ psi} > \text{actual } v_n = 262 \text{ psi, O.K.}\end{aligned}$$



If  $V_p$  were accounted for, the maximum allowable  $v_c$  would have been higher than 273 psi.

(c) *Flexure moment transfer*

The fraction of nominal moment strength to be transferred by flexure is  $M_n = 0.63 \times 246,668 = 155,401$  in.-lb. From Equation 9.20,  $\text{Min}A_s = 0.00075hL = 0.00075 \times 6.5 \times 17.5 \times 12 = 1.02$  in<sup>2</sup>. So use six #4 bars  $\times 6$  ft, including the standard hook, yielding  $A_s = 6 \times 0.2 = 1.2$  in<sup>2</sup>. The stress in the tendon strands is computed from Equation 9.23 assuming that three strands pass the column at the exterior support at  $e = 0$ . We have  $d_p = 6.5/2 = 3.25$  in., and the effective concrete width  $b = c_2 + 2(1.5 \times h) = 14 + 2(1.5 \times 6.5) = 33.5$  in. Also,

$$\rho_p = \frac{A_{ps}}{bd_p} = \frac{3 \times 0.153}{33.5 \times 3.25} = 0.0042$$

$$f_{ps} = f_{pe} + 10,000 + \frac{f'_c}{300\rho_p}$$

$$= 159,000 + 10,000 + \frac{4,000}{300 \times 0.0042}$$

$$= 172,174 \text{ psi}$$

$$A_{ps} = 3 \times 0.153 = 0.459 \text{ in.}$$

$$a = \frac{A_s f_y + A_{ps} f_{ps}}{0.85 f'_c b} = \frac{1.20 \times 60,000 + 0.459 \times 172,174}{0.85 \times 4,000 \times 33.5}$$

$$= 1.33 \text{ in.}$$

$$\begin{aligned} \text{Available } M_n \text{ in the column zone} &= A_s f_y \left( d - \frac{a}{2} \right) + A_{ps} f_{ps} \left( d_p - \frac{a}{2} \right) \\ &= 1.2 \times 60,000 \left( 5.5 - \frac{1.33}{2} \right) + 0.459 \times 172,101 \left( 3.25 - \frac{1.33}{2} \right) \\ &= 347,400 + 203,410 = 550,810 \text{ in.-lb} \\ &\gg \gamma_f M_n = 155,401 \text{ in.-lb} \end{aligned}$$

The available nominal moment strength is thus considerably larger than the moment being transferred by flexure. Figure 9.21 shows one scheme for banding both the prestressed and nonprestressed reinforcement to provide for shear-moment transfer at the exterior column zone.

A similar check as in Sec. III will show that the  $c/d_t$  value is  $\ll 0.375$  in Figure 4.45. Hence, the section is tension controlled, and the value of  $\phi = 0.90$  is validated.

## 2. Interior columns B and C

(a) *Geometry and external load*

From before,  $V_{BA} + V_{BC} = 1988.3 + 2232 \cong 4220$  plf. The total shear is  $V_{uB} = 4220 \times 20 = 84,400$  lb (375 kN), and also,  $c_1 = 20$  in.,  $c_2 = 14$  in., and  $d = 6.5 - 1 = 5.5$  in.

Assume that  $d_v = 0.8h \cong 5.2$  in.; compute  $g = \frac{1}{2}c_1 = 20/2 = 10$  in.

$$b_1 = c_1 + d = 20 + 5.2 = 25.2 \text{ in.}$$

$$b_2 = c_2 + d = 14 + 5.2 = 19.2 \text{ in.}$$

$$A_c = b_0 d = 2(25.2 \times 5.2 + 19.2 \times 5.2) = 462 \text{ in}^2$$

Using  $d_v$  for  $d$ , the polar moment of inertia is

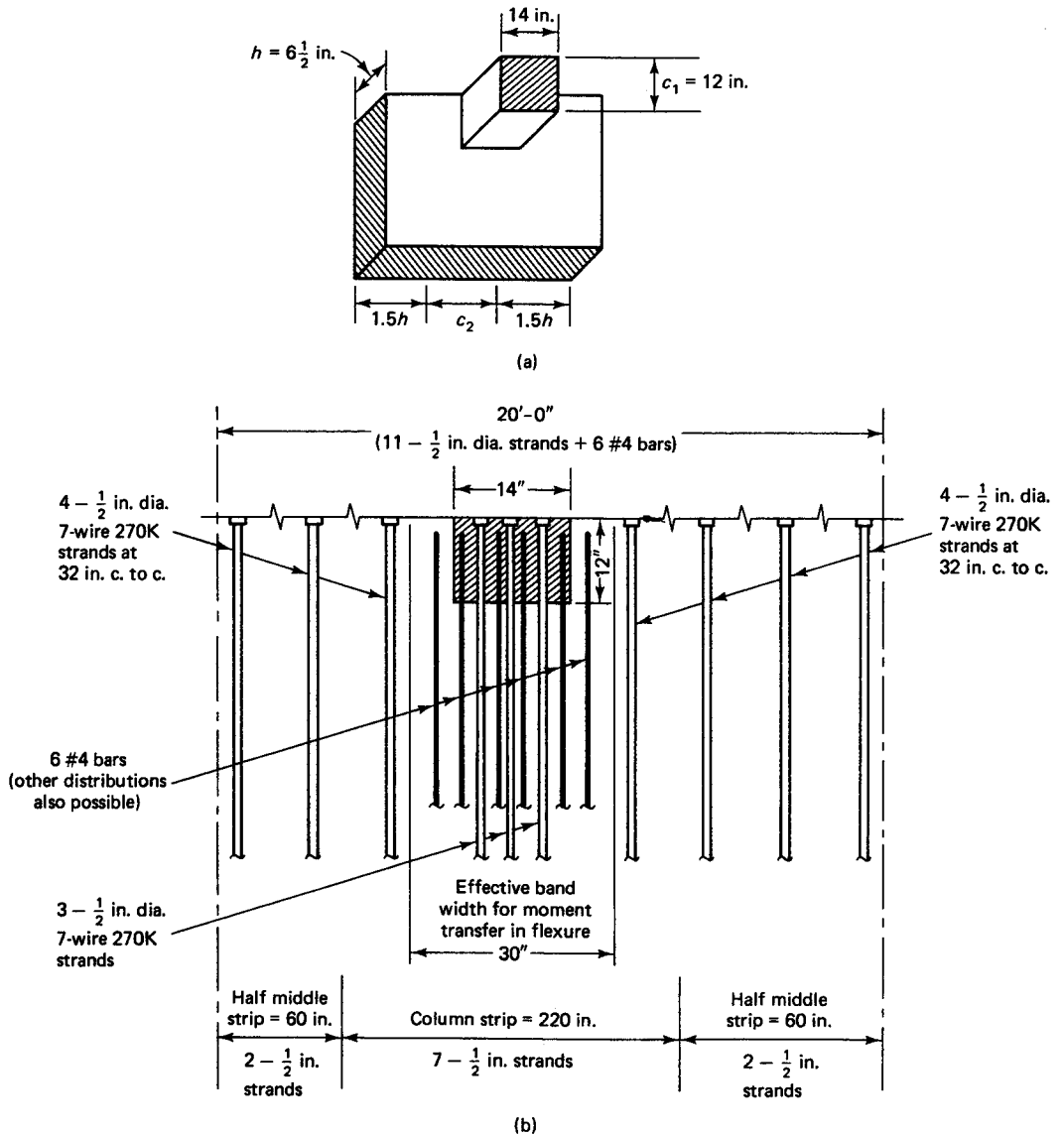
$$\begin{aligned} J_c &= \frac{d(c_1 + d)^3}{6} + \frac{d^3(c_1 + d)}{6} + \frac{d(c_2 + d)(c_1 + d)^2}{2} \\ &= \frac{5.2(25.2)^3}{6} + \frac{(5.2)^3(25.2)}{6} + \frac{5.2(19.2)(25.2)^2}{2} \\ &= 46,161 \text{ in}^4 \end{aligned}$$

Figure 9.22 shows the geometrical properties of the *interior columns*:

$$\gamma_v = 1 - \frac{1}{1 + \frac{2}{3}\sqrt{25.2/19.2}} = 0.433$$

$$\gamma_f = 1 - 0.433 = 0.567$$

The moment  $M_{ue} = M_e$  for each interior column, and the net unit moment  $M_e = 79,955 - 72,640 = 7315$  in.-lb. The unbalanced shear moment is equal to the net  $V_u \times g = 10(2,232 - 1988.3) = 2437$  in.-lb. Finally, the total moment is:



**Figure 9.21** Shear-moment transfer zone and reinforcement distribution in Example 9.2. (a) Column zone band (33.5 in. wide). (b) Reinforcement distribution plan.

$M_{ue} = 7315 \times 20 + 2437 = 148,737$  in.-lb, and the total required unbalanced moment strength is  $M_n = M_{ue}/\phi = 148,737/0.9 = 165,263$  in.-lb.

**(b) Shear-moment transfer**

The fraction of nominal moment strength to be transferred by shear is  $\gamma_v M_n = 0.433 \times 165,263 = 71,559$  in.-lb, and  $c_{AB} = \frac{1}{2}(c_1 + d) = \frac{1}{2}b_1 = 25.2/2 = 12.6$  in.

From Equation 9.30a, the shear stress due to perimeter shear and the effect of  $M_n$  is

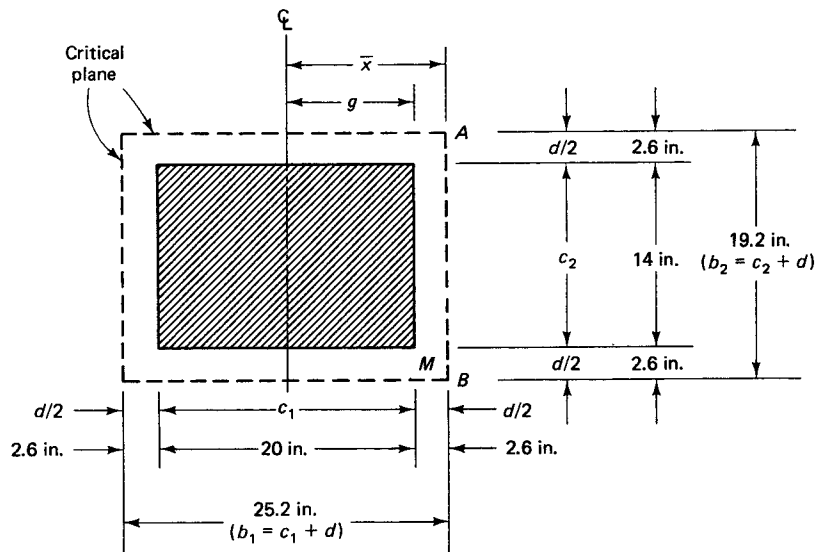
$$\begin{aligned} v_n &= \frac{V_u}{\phi A_c} + \frac{\gamma_v c_{AB} M_n}{J_c} \\ &= \frac{84,400}{0.75 \times 462} + \frac{0.433 \times 165,263 \times 12.6}{46,161} = 243.5 + 19.5 = 263 \text{ psi (180 MPa)} \\ &< \text{allowable } v_c = 273 \text{ psi, O.K.} \end{aligned}$$

**(c) Flexure moment transfer**

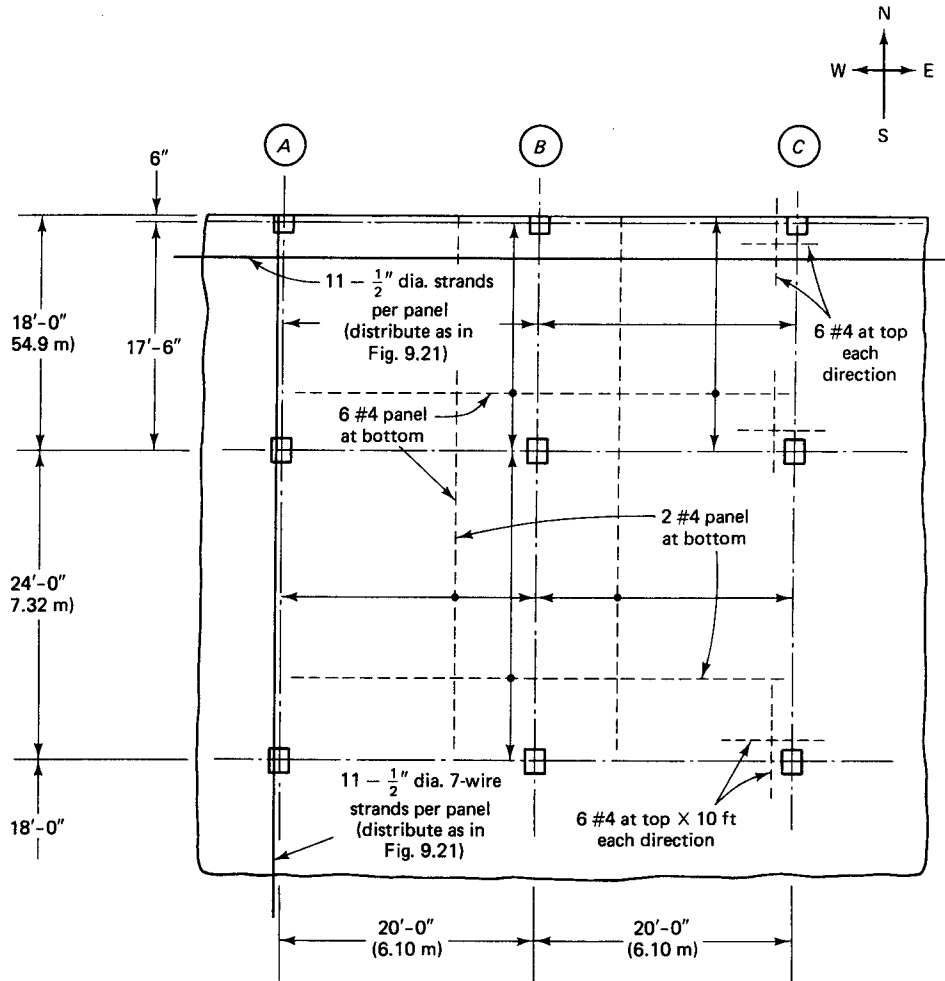
The fraction of nominal moment strength to be transferred by flexure is  $\gamma_f M_n = 0.567 \times 165,263 = 93,704$  in.-lb, and  $b = c_2 + 2(1.5 \times h) = 14 + 2(1.5 \times 6.5) = 33$  in., the same as for exterior column A. Assume, as in the case of exterior columns, that three strands pass the interior columns B and C. We have

$$\begin{aligned} d_p &= 6.5 - 1 = 5.5 \\ \rho_p &= \frac{A_{ps}}{bd_p} = \frac{3 \times 0.153}{33.5 \times 5.5} = 0.0025 \\ f_{ps} &= f_{pe} + 10,000 + \frac{f'_c}{300\rho_p} \\ &= 159,000 + 10,000 + \frac{4,000}{300 \times 0.0025} = 174,333 \text{ psi} \end{aligned}$$

which is very close to  $f_{ps}$  for column A. Accordingly, using six #4 bars  $\times$  12 ft as minimum mild steel, as for the exterior columns,  $a \cong 1.48$  in. and the available moment capacity in the column is:



**Figure 9.22** Critical plane for shear transfer in interior column of Example 9.2 (line B or C, Figure 9.17).



**Figure 9.23** Schematic reinforcement distribution, partial floor plan for Example 9.2.

$M_n = 1.2 \times 60,000(5.5 - 1.33/2) + 0.459 \times 174,333(5.5 - 1.33/2) = 348,120 + 386,891 = 735,011 \text{ in.-lb} \gg$  required  $M_n = 165,263 \text{ in.-lb}$ , and hence satisfactory.

Figure 9.23 shows a schematic layout of the reinforcement in the continuous flat plate. The three  $\frac{1}{2}$ -in. dia strands in each direction should pass through the critical shear perimeter of the supporting columns. Of course, serviceability requirements for deflection should be checked, as in Section 9.13.

From the analysis made, we adopt the design and use the same pattern of reinforcement for both the N-S and E-W directions of the floor system, as the spans dimensions in both directions are very close in value.

It is important to note that the contribution of the prestressing reinforcement to the available moment strength of the slab at the column zone is valid only if the strands are placed straight through the column, as shown in Figure 9.21. In many designs, the prestressing strands are diverted around the column section at a shallow slope, so that only the mild steel reinforcement develops the moment capacity to resist the unbalanced moment. Even in such cases, the available moment strength developed from the mild steel reinforcement concentrated through the column section is still considerably higher than the required moment, as the computations in this example show.

## 9.12 DIRECT METHOD OF DEFLECTION EVALUATION

### 9.12.1. The Equivalent Frame Approach

As in the equivalent frame method for flexural analysis detailed in the preceding sections, the structure is divided into continuous frames centered on the column lines in each of the two perpendicular directions. Each frame is composed of a row of columns and a *broad* band of slab together with column line beams, if any, between panel centerlines.

By the requirement of statics, the applied load must be accounted for in each of the two perpendicular (orthogonal) directions. In order to account for the torsional deformations of the support beams, an *equivalent* column is used whose flexibility is the *sum* of the flexibilities of the actual column and the torsional flexibility of the transverse beam or slab strips (stiffness is the inverse of flexibility). In other words,

$$\frac{1}{K_{ec}} = \frac{1}{\Sigma K_c} + \frac{1}{K_t} \quad (9.33)$$

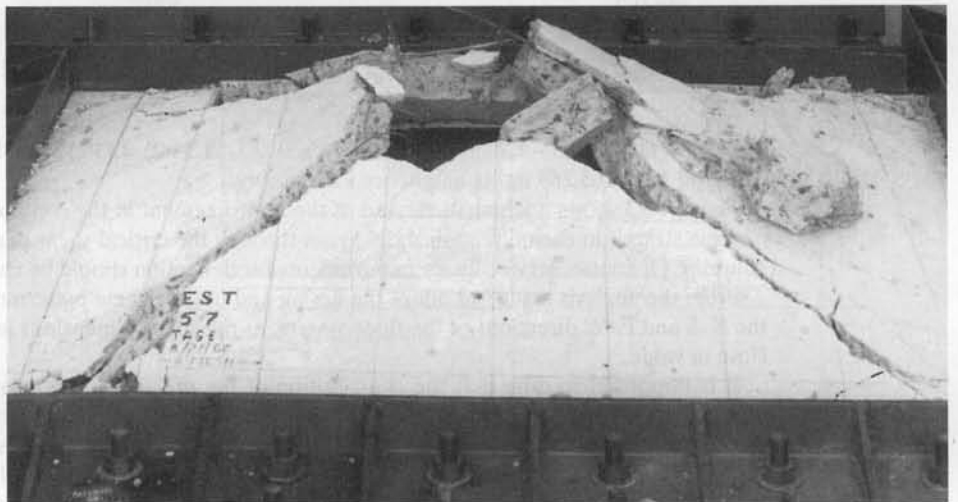
where  $K_{ec}$  = flexural stiffness of the equivalent column, bending moment per unit rotation

$\Sigma K_c$  = sum of flexural stiffnesses of upper and lower columns, bending moment per unit rotation

$K_t$  = torsional stiffness of the transverse beam or slab strip, torsional moment per unit rotation.

The value of  $K_{ec}$  would thus have to be known in order to compute the deflection by this procedure.

The slab-beam strips are considered supported *not* on the columns, but on *transverse* slab-beam strips on the column centerlines. Figure 9.24(a) illustrates this point. Deformation of a typical panel is considered in *one direction at a time*. Thereafter, the



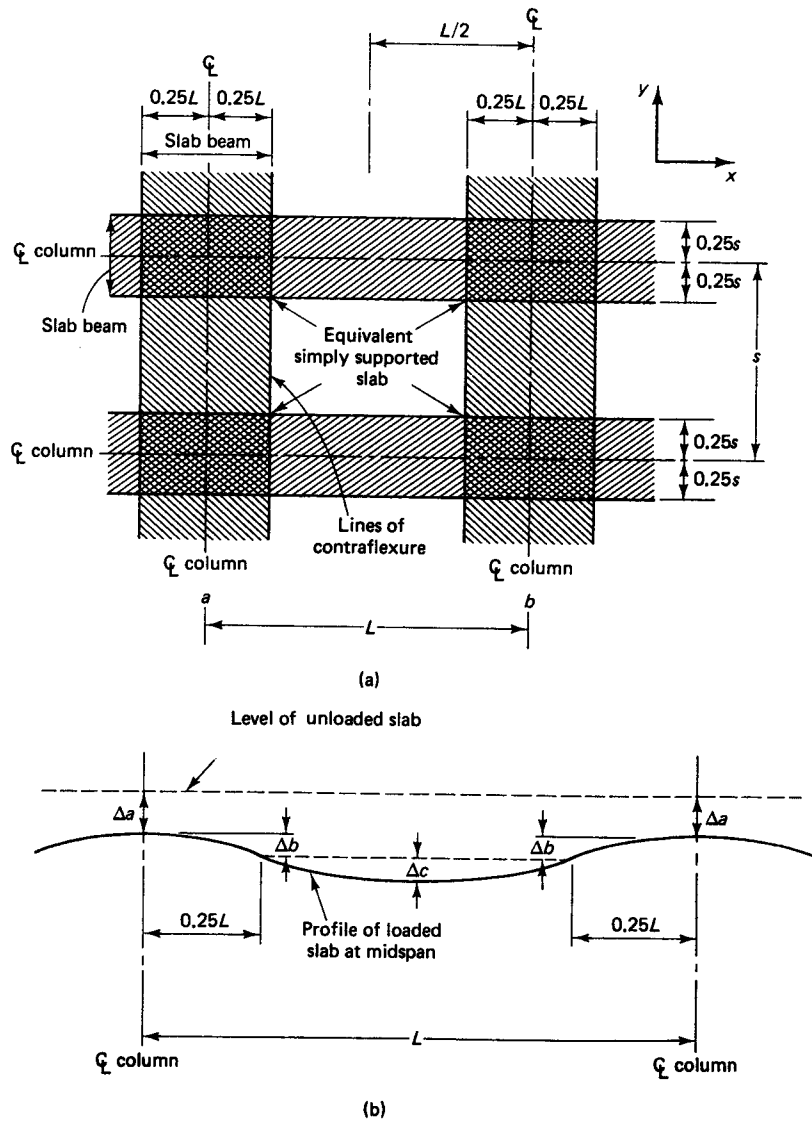
**Photo 9.6** Rectangular concrete slab at rupture. (Tests by Nawy et al.)

contributions in each of the two directions,  $x$  and  $y$ , are added to obtain the total deflection at any point in the slab or plate.

First, the deflection due to bending in the  $x$  direction is computed [Figure 9.24(b)]. Then the deflection due to bending in the  $y$  direction is found. The midpanel deflection can now be obtained as the sum of the center-span deflections of the column strip in one direction and that of the middle strip in the orthogonal direction [Figure 9.24(c)].

### 9.12.2 Column and Middle Strip Deflections

The deflection of each panel can be considered the sum of three components:



**Figure 9.24** Equivalent frame method for deflection analysis. (a) Plate panel transferred into equivalent frames. (b) Profile of deflected shape at centerline. (c) Deflected shape of panel.

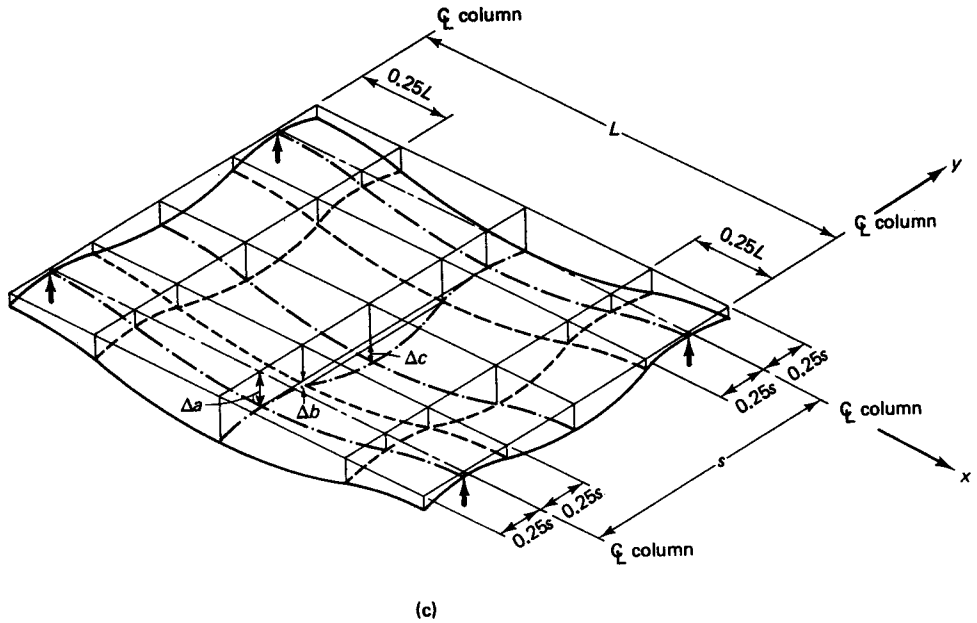


Figure 9.24 Continued

1. The basic midspan deflection of the panel, assumed fixed at both ends, given by

$$\delta' = \frac{wL^4}{384E_c I_{\text{frame}}} \tag{9.34}$$

This has to be proportioned to separate deflections  $\delta_c$  of the column strip and  $\delta_s$  of the middle strip, such that

$$\delta_c = \delta' \frac{M_{\text{col strip}}}{M_{\text{frame}}} \frac{E_c I_{cs}}{E_c I_c} \tag{9.35a}$$

and

$$\delta_s = \delta' \frac{M_{\text{slap strip}}}{M_{\text{frame}}} \frac{E_c I_{cs}}{E_c I_s} \tag{9.35b}$$

where  $I_{cs}$  is the moment of inertia of the total frame,  $I_c$  the moment of inertia of the column strip, and  $I_s$  the moment of inertia of the middle slab strip.

2. The center deflection,  $\delta''_{\theta L} = \frac{1}{8}\theta L$ , due to rotation at the left end while the right end is considered fixed, where  $\theta L$  is the left  $M_{net}/K_{ec}$  and  $K_{ec}$  is the flexural stiffness of the equivalent column (moment per unit rotation).
3. The center deflection,  $\delta''_{\theta R} = \frac{1}{8}\theta L$  due to rotation at the right end while the left end is considered fixed, where  $\theta L$  is the right  $M_{net}/K_{ec}$ . Hence,

$$\delta_{cx} \text{ or } \delta_{cy} = \delta_c + \delta''_{\theta L} + \delta''_{\theta R} \tag{9.36a}$$

$$\delta_{sx} \text{ or } \delta_{sy} = \delta_s + \delta''_{\theta L} + \delta''_{\theta R} \quad (9.36b)$$

In Equations 9.36a and 9.36b, use the values of  $\delta_c$ ,  $\delta''_{\theta L}$ , and  $\delta''_{\theta R}$  which correspond to the applicable span directions. From Figures 9.24(b) and (c), the total deflection is

$$\Delta = \delta_{sx} + \delta_{cy} = \delta_{sy} + \delta_{cx} \quad (9.37)$$

### 9.13 DEFLECTION EVALUATION OF TWO-WAY PRESTRESSED CONCRETE FLOOR SLABS

#### Example 9.3

Compute the central deflection of the exterior panels of the two-way post-tensioned prestressed concrete floor designed in Example 9.2 for both short-term and long-term loading. Assume that the maximum allowable deflection is 1/480 of the span.

#### Solution:

**Structural Data.** From Example 9.2, we have the following data:

Plate thickness  $h = 6\frac{1}{2}$  in. (165 mm)

Loads:  $W_d = 101$  psf (4.84 kPa)

$W_L = 40$  psf (1.92 kPa)

Span AB  $W_{bal} = 72$  psf (3.45 kPa)

$W_{net} = W_D + W_L - W_{bal} = 101 + 40 - 72 = 69$  psf (3.3 kPa)

Span BC  $W_{bal} = 70$  psf (3.35 kPa)

$W_{net} = 141 - 70 = 71$  psf (3.4 kPa)

The floor plan is shown in Figure 9.25, and the overall details and vertical section of the building are presented in Figure 9.17. The distributed bending moments in the N-S direction taken from the flexural analysis for  $W_{net}$  in Table 9.2 are shown in Figure 9.26.

**Stiffness Factors and Strip Moments** *N-S Direction (Span 18 ft).* The column stiffness factor  $K_{ec}$  values were computed in Example 9.2, with the following results:

Exterior column A:  $K_{ec} = 47E_c$  in.-lb/rad

Interior column B:  $K_{ec} = 113E_c$  in.-lb/rad

Net Frame  $M_A = 5.30 \times 10^3$  in.-lb/ft

Net Frame  $M_B = (39.56 - 33.94)10^3 = 5.62 \times 10^3$  in.-lb/ft

As discussed in Example 9.2, the column strip takes 64 percent of the moment and the middle strip takes 36 percent of the moment. The frame total  $I_{cs} = bh^3/12 = 20 \times 12(6.5)^3/12 = 5,493$  in.<sup>4</sup>, while the column strip  $I_c =$  the middle strip  $I_c = 5,493/2 = 2,747$  in.<sup>4</sup>

From Equation 9.34, the basic midspan deflection in the N-S direction at central point O in Figure 9.27, assuming both ends of the panel fixed, is

$$\delta' = \frac{WL^4}{384E_c I_{cs}} = \frac{69 \times 20(18)^4(12)^3}{384 \times 4.03 \times 10^6 \times 5,493} = 0.029 \text{ in.}$$

This deflection has to be proportioned to separate deflections  $\delta_c$  of the column strip and  $\delta_s$  of the middle strip:

$$\delta_c = \delta' \frac{M_{col. \text{ strip}}}{M_{frame}} \frac{E_c I_{cs}}{E_c I_c}$$

from Example 9.2,  $M_{col. \text{ strip}}/M_{frame} = 0.64$ , so N-S  $\delta_c = 0.029 \times 0.64 \times 2 = 0.037$  in., N-S  $\delta_s = 0.029 \times 0.36 \times 2 = 0.021$  in., and the rotation at end A is



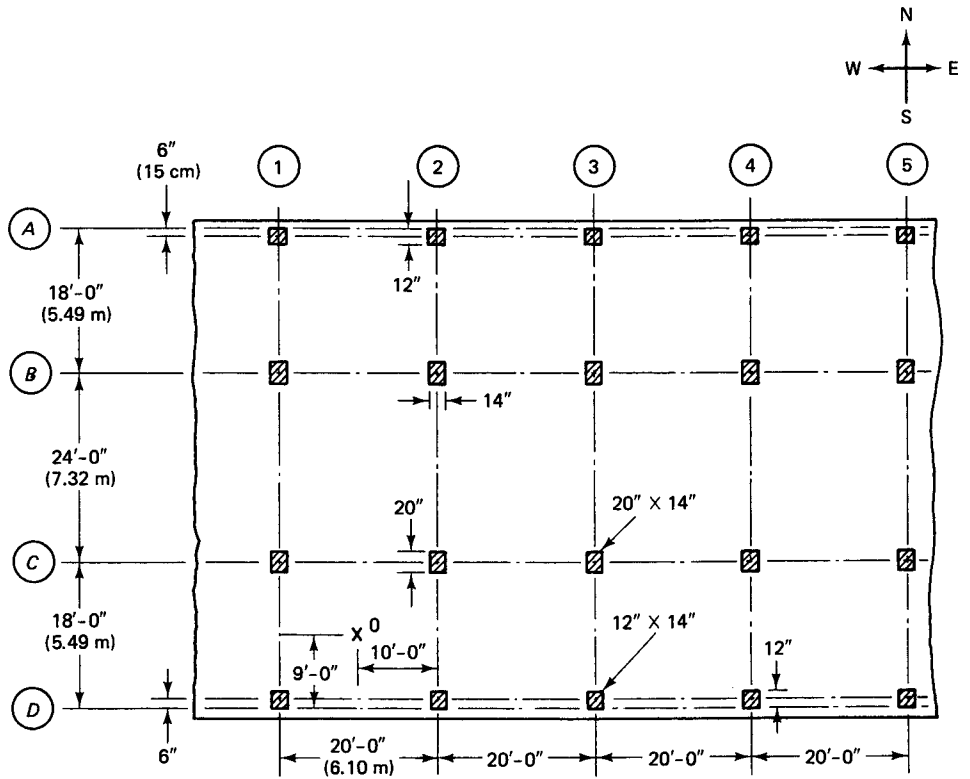


Figure 9.25 Two-way post-tensioned floor plan in Example 9.3

$$\theta_A = \frac{M_A}{K_{ec}} = \frac{5.30 \times 10^3 \times 20}{47 \times 4.03 \times 10^6} = 5.6 \times 10^{-4} \text{ rad}$$

$$\theta_B = \frac{M_B}{K_{ec}} = \frac{5.62 \times 10^3 \times 20}{113 \times 4.03 \times 10^6} = 2.5 \times 10^{-4} \text{ rad}$$

$$\delta'' = \frac{\theta l}{8} = \frac{(5.6 + 2.5)10^{-4}(18 \times 12)}{8} = 0.022 \text{ in.}$$

Therefore, N-S net  $\delta_{cy} = 0.037 + 0.022 = 0.059 \text{ in.}$  and N-S net  $\delta_{sy} = 0.021 + 0.022 = 0.043 \text{ in.}$

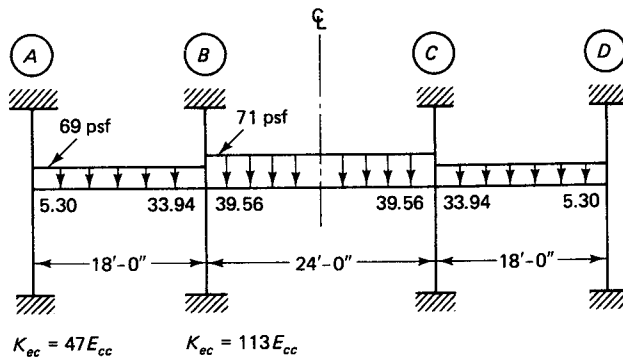
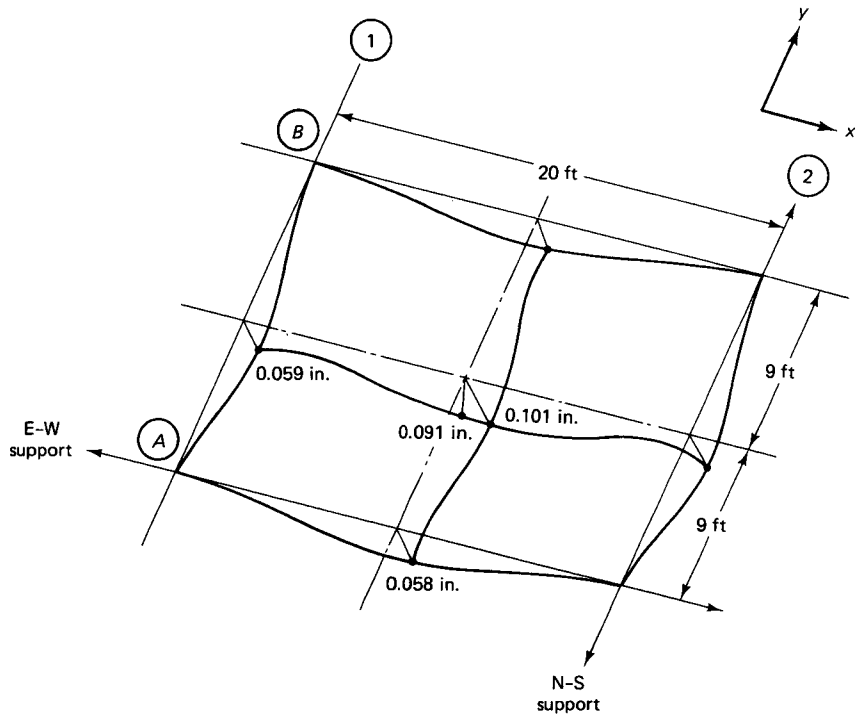


Figure 9.26 Service net load moments  $\times 10^{-3}$  in.-lb in the N-S direction in Example 9.3.



**Figure 9.27** Column and middle strips immediate deflections in Example 9.3.

*E-W Direction (Span 20 ft).* For the E-W direction, the width  $b$  of an equivalent frame =  $\frac{1}{2}(18 + 24) = 21.0$  ft. The frame total  $I_{cs}$  is

$$\frac{bh^3}{12} = \frac{21 \times 12(6.5)^3}{12} = 5,767 \text{ in}^4$$

and the column strip  $I_c$  = the middle strip  $I_s = 5,767/2 = 2,884 \text{ in}^4$

From Equation 9.34, the fixed-end central deflection at O is

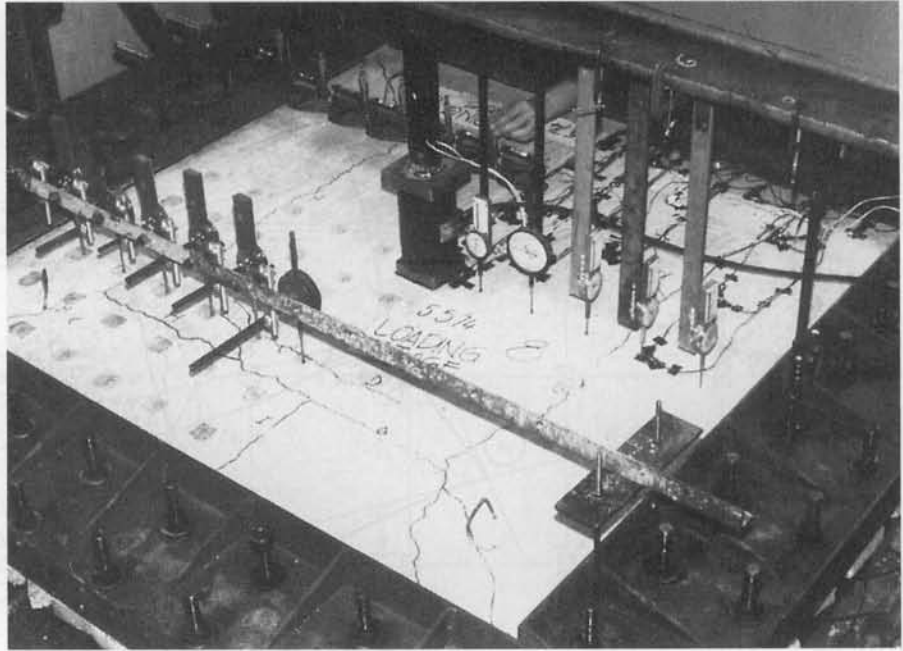
$$\delta' = \frac{WL^4}{384E_c I_{cs}} = \frac{69 \times 21(20)^4(12)^3}{384 \times 4.03 \times 10^6 \times 5,767} = 0.045 \text{ in.}$$

If the same distribution of moments is assumed to exist between the column and middle strips, then E-W  $\delta_c = 0.045 \times 0.64 \times 2 = 0.058$  in. and E-W  $\delta_s = 0.045 \times 0.36 \times 2 = 0.032$  in.

For the case of all panels loaded in this example, the net moments at each column due to the difference in negative moments from the spans to the left and to the right of the column are zero. Hence, consider the net rotation  $\theta = 0$ , and use E-W net  $\delta_{cx} = 0.058$  in. and E-W net  $\delta_{sx} = 0.032$  in.

Figure 9.27 gives the column and middle strip deflections in both the N-S and E-W directions.

**Total Immediate Central Deflection.** The total central deflection  $\Delta = \delta_{xs} + \delta_{cy} = \delta_{sy} + \delta_{cx}$ ; therefore  $\Delta_{N-S} = \delta_{sy} + \delta_{cx} = 0.043 + 0.058 = 0.101$  in. and  $\Delta_{E-W} = \delta_{sx} + \delta_{cy} = 0.032 + 0.059 = 0.091$  in. Hence, the average immediate deflection due to the net load is  $\Delta_{net} = \frac{1}{2}(\Delta_{N-S} + \Delta_{E-W}) = \frac{1}{2}(0.101 + 0.091) = 0.096$  in. (2.44 mm).



**Photo 9.7** Testing setup of four-panel prestressed concrete floor. (Tests by Nawy et al.)

**Long-Term Deflection.** For the long-term deflection,  $W_{\text{net}} = 69$  psf and the live load  $W_L = 40$  psf. Assuming that 65 percent of the live load is sustained, the total sustained load intensity is  $W_{\text{sust.}} = (69 - 40) + 0.65 \times 40 = 55$  psf. Assuming further a total creep factor of 2, we have

$$\text{Long-term deflection} = \frac{55}{69} \times 0.096 \times 2 = 0.153 \text{ in. (4.09 mm)}$$

$$\text{Total deflection} = 0.096 + 0.153 = 0.249 \text{ in. (6.33 mm)}$$

The maximum allowable deflection in this structure is

$$\Delta_{\text{allow.}} = \frac{L}{480} = \frac{20 \times 12}{480} = 0.50 \text{ in. (12.7 mm)} > \text{actual } \Delta = 0.249 \text{ in., O.K.}$$

## 9.14 YIELD-LINE THEORY FOR TWO-WAY-ACTION PLATES

A study of the hinge-field mechanism in a slab or plate at loads close to failure aids the engineering student in developing a feel for the two-way-action behavior of plates. Hinge fields are successions of hinge bands which are idealized by lines; hence the name *yield-line theory* by K. W. Johansen.

To do justice to this subject, an extensive discussion over several chapters or a whole textbook is necessary. The intention of this chapter is only to introduce the reader to the fundamentals of the yield-line theory and its application.

The yield-line theory is an upper-bound solution to the plate problem. This means that the predicted moment capacity of the slab has the highest expected value in comparison with test results. Additionally, the theory assumes a totally rigid-plastic behavior, namely, that the plate stays plane at collapse. Consequently, deflection is not accounted for, nor are the compressive membrane forces that will act in the plane of the slab or plate considered. The plates are assumed to be considerably underreinforced, in such a

manner that the maximum reinforcement percentage  $\rho$  does not exceed  $\frac{1}{2}$  percent of the section  $bd$ .

Since the solutions are upper bound, the slab thickness obtained by this process is in many instances thinner than what is obtained by the lower bound solutions, such as the equivalent frame method. Consequently, it is important to apply rigorously the serviceability requirements for deflection control and for crack control in conjunction with the use of the yield-line theory.

One distinct advantage of this theory is that solutions are possible for any shape of plate, whereas most other approaches are applicable only to the rectangular shapes with rigorous computations for boundary effects. The engineer can, with ease, find the moment capacity for a triangular, trapezoidal, rectangular, circular, or any other conceivable shape, provided that the failure mechanism is known or predictable. Since most failure patterns are presently identifiable, solutions can be readily obtained.

### 9.14.1 Fundamental Concepts of Hinge-Field Failure Mechanisms in Flexure

Under action of a two-dimensional system of bending moments, yielding of a rigid-plastic plate occurs when the principal moments satisfy Johansen's square yield criterion as shown in Figure 9.28. According to this criterion, yielding is considered to have occurred when the numerically greater of the principal moments reaches the value of  $\pm M$  at the yield-line cracks. The directions of the principal curvature rates are considered to coincide with the curvatures of the principal moments. The idealized moment-curvature relationship is shown as the solid line in Figure 9.29. Line  $OA$  is considered almost vertical at point  $O$ , and strain hardening is neglected.

If one considers the simplest case of a square slab with supports, with degree of fixity  $i$  varying from  $i = 0$  for simply supported to  $i = 1.0$  for fully restrained on all four sides, the failure mechanism would be as shown in Figure 9.30 when a uniformly distributed load is applied.

Consider the simply supported case (a). The yield-line moments along the yield lines are the principal moments. Hence, the twisting moments are zero in the yield lines and in most cases the shearing forces are also zero. Consequently, only the moment  $M$  per unit length of the yield line acts about the lines  $AD$  and  $BE$  in Figure 9.31. The total moments can be represented by a vector in the direction of the yield line whose value is the product of  $M$  and the length of the yield line, that is,  $M(a/2 \cos \theta)$  in Figure 9.31(c). The virtual work of the yield moments of the shaded triangular segment  $ABO$  is the

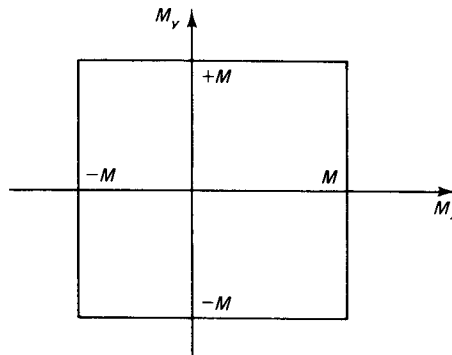


Figure 9.28 Johansen's square yield criterion.

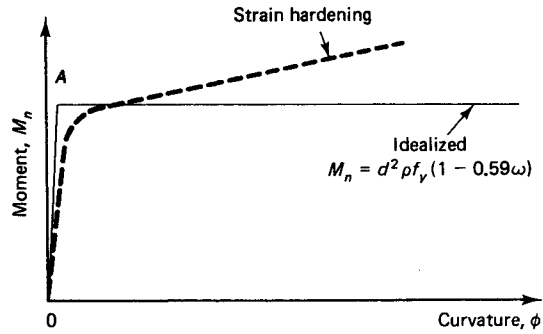


Figure 9.29 Moment-curvature relationship.

scalar product of the two moment vectors  $Ma/2 \cos \theta$  on fracture lines  $AO$  and  $BO$  and rotation  $\theta$ . In other words, the internal work is

$$E_I = \Sigma \bar{M} \bar{\theta}$$

If the displacement of the shaded segment at its center of gravity  $c$  is  $\delta$ , the external work is

$$E_E = \text{force} \times \text{displacement} = \Sigma \iint w_u dx dy \delta$$

where  $w_u$  is the intensity of external load per unit area. But  $E_I = E_E$ ; hence,

$$\Sigma \bar{M} \bar{\theta} = \Sigma \iint w_u dx dy \delta \tag{9.38}$$

Applying Equation 9.38 to the case under discussion gives us

$$\bar{M} \bar{\theta} = Ma \frac{\Delta}{a/2}$$

since angle  $\theta$  in Figure 9.31(b) is small  $[(\theta = \Delta/(a/2))]$ .

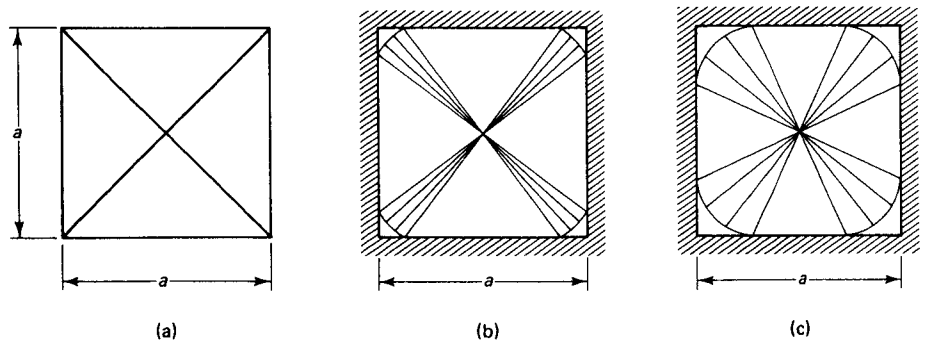


Figure 9.30 Failure mechanism of a square slab. (a)  $i = 0$ . (b)  $i = 0.5$ . (c)  $i = 1.0$ .

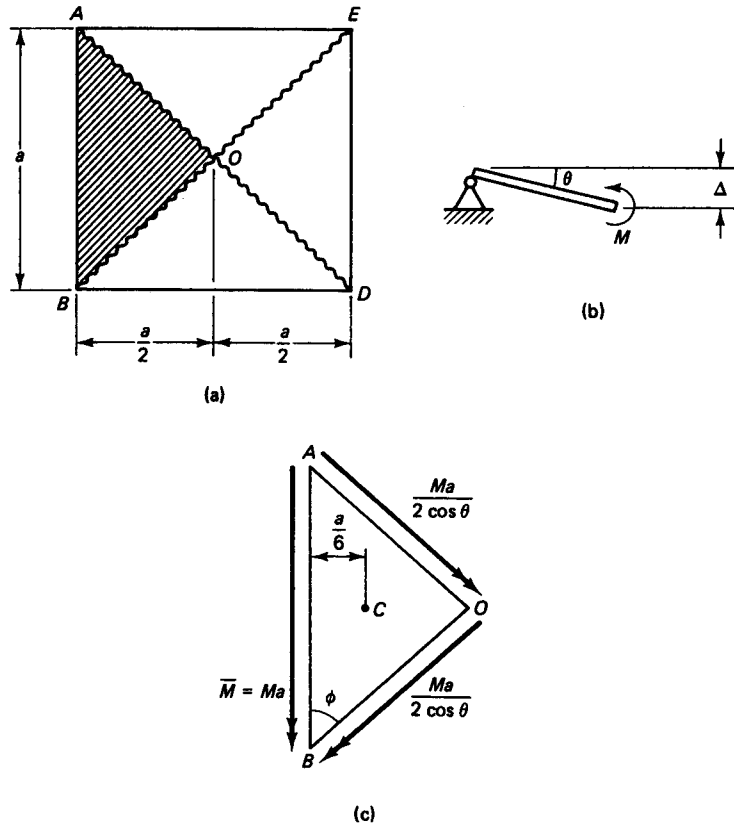


Figure 9.31 Vector moments on slab segment at failure.

The work per triangular segment is

$$E_I = \bar{M} \bar{\theta} = 2M \Delta$$

$$E_E = \frac{w_u a^2}{4} \times \frac{\Delta}{3}$$

where the deflection at the center of gravity of the triangle is  $\Delta/3$ . Therefore,

$$4(2M \Delta) = 4 \left( \frac{w_u a^2}{12} \Delta \right)$$

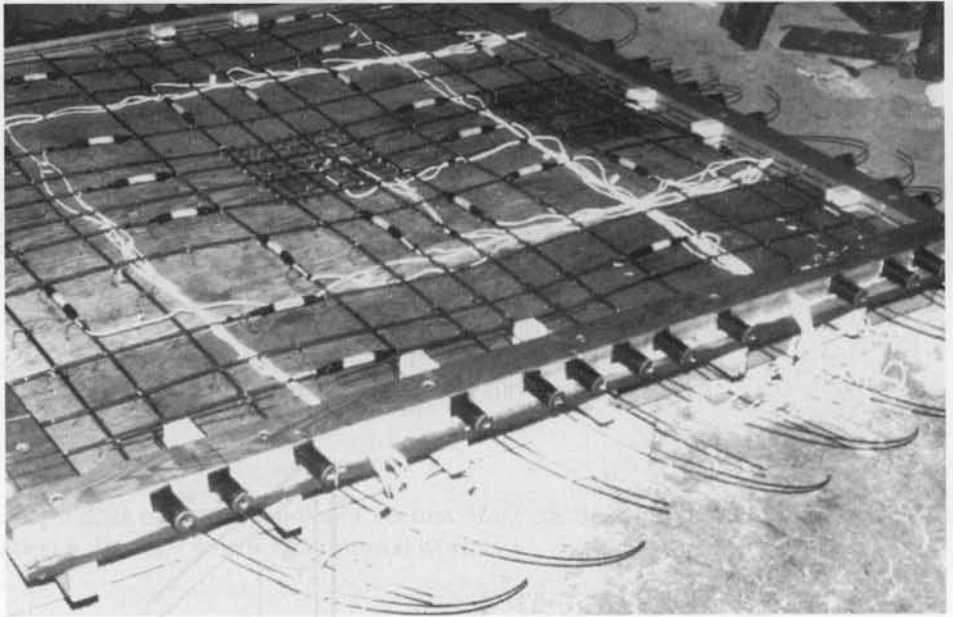
and

$$\text{unit } M = \frac{w_u a^2}{24} \tag{9.39}$$

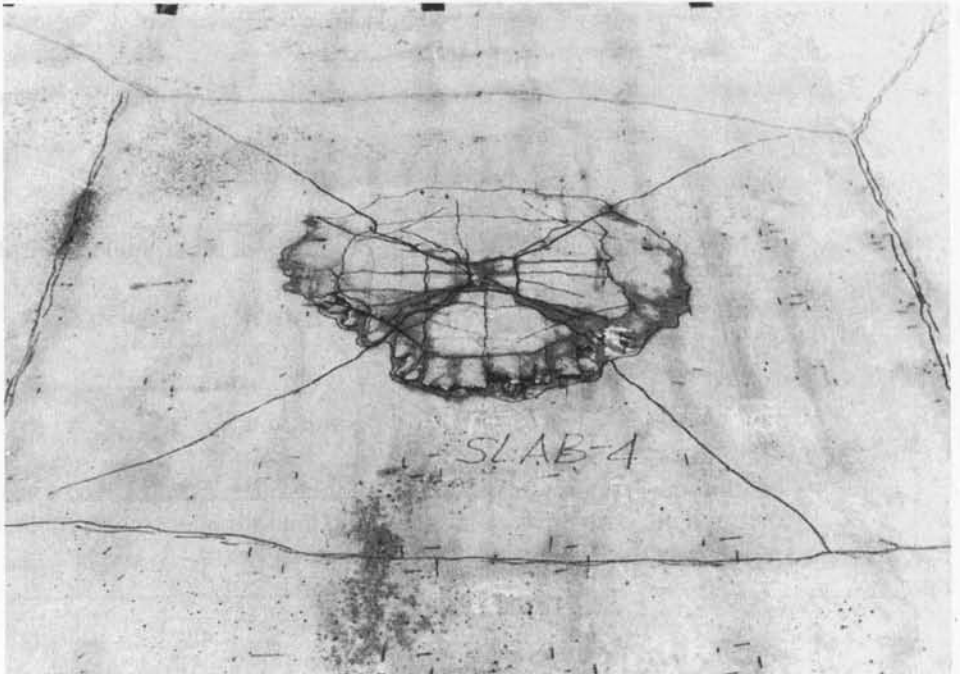
If the square slab is fully fixed on all four sides,  $E_I = 4(4M \Delta)$  since fracture lines develop around not only the diagonals but also the four edges, as shown in Figure 9.30(c). Hence, for a fully fixed square slab,

$$\text{unit } M = \frac{w_u a^2}{48} \tag{9.40}$$

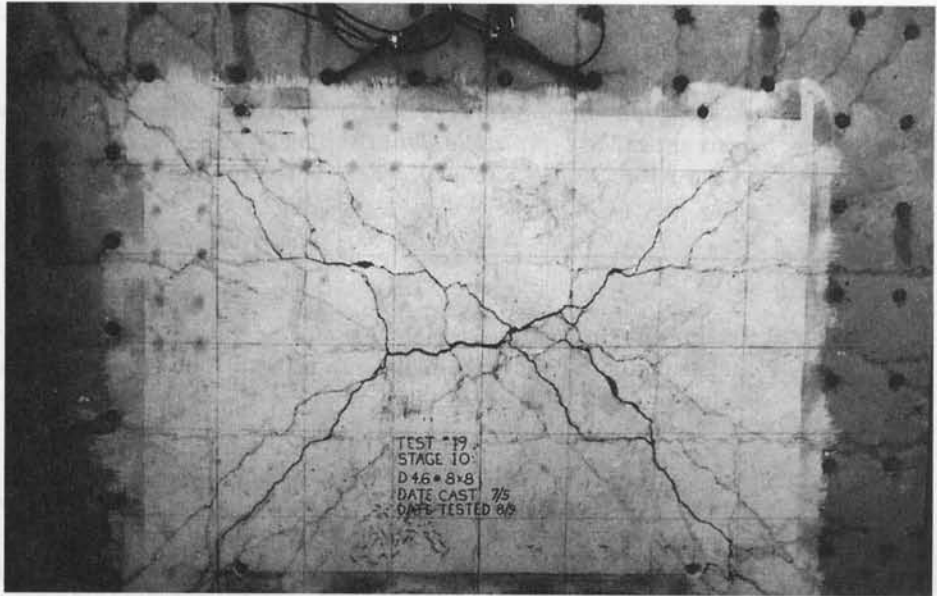
Observe that a lower-bound solution as proposed by Mansfield's failure pattern in Figure 9.30(c) gives a value  $M = w_u a^2/42.88$ . Hence, for a uniformly loaded square slab with load intensity  $w_u$  per unit area and degree of support fixity  $i$  on all sides,



**Photo 9.8** Preparing prestressing tendons in the forms for a four-panel continuous prestressed two-way-action plate (Nawy, Chakrabarti et al.).



**Photo 9.9** Yield-line pattern at failure at column reaction and panel boundaries of a two-way multipanel floor. (Tests by Nawy, Chakrabarti et al.)



**Photo 9.10** Yield-line patterns at failure at tensions face of rectangular restrained panel. (Tests by Nawy et al.)

$$w_u a^2 = M[24(1 + i)] \tag{9.41}$$

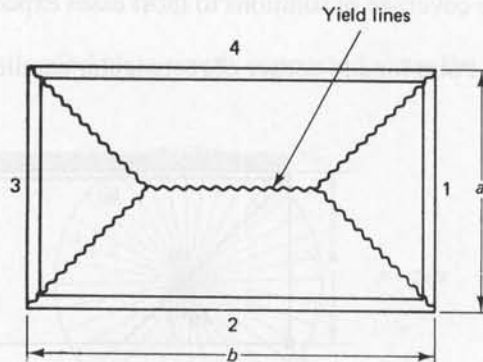
The general equation for the yield-line moment capacity of a rectangular isotropic slab on beams and having dimensions  $a \times b$  as shown in Figure 9.32, with side  $a$  being the shorter dimension, is

$$\text{unit } M \frac{\text{ft-lb}}{\text{ft}} = \frac{w_u d_r^2}{24} \left[ \sqrt{3 + \left(\frac{a_r}{b_r}\right)^2} - \frac{a_r}{b_r} \right]^2 \tag{9.42}$$

$$\text{where } a_r = \frac{2a}{\sqrt{1 + i_2} + \sqrt{1 + i_4}}$$

$$b_r = \frac{2b}{\sqrt{1 + i_1} + \sqrt{1 + i_3}}$$

$i$  = degree of restraint, depending on stiffness ratios as discussed in Section 9.2.



**Figure 9.32** Rectangular slab. Note sequence of side numbers.



Note that Equation 9.42 reduces to the simplified form of Equation 9.40 or 9.41 for the case of a square slab restrained on all four sides ( $i = 1.0$ ).

**Affine Slabs.** Slabs that are reinforced differently in the two perpendicular directions are called *orthotropic slabs* (or *plates*). The moment in the  $x$  direction equals  $M$  and in the  $y$  direction equals  $\mu M$ , where  $\mu$  is a measure of the degree of orthotropy, or the ratio

$$\frac{M_y}{M_x} = \frac{(A_s)_y}{(A_s)_x}$$

To simplify the analysis, the slab should be converted to an *affine* (isotropic) slab, where the strength and reinforcement area in both the  $x$  and  $y$  directions are the same. Such conversion can be made as follows:

1. Divide the linear dimension in the  $M$  direction by  $\sqrt{\mu}$  for a slab to be reinforced for a moment  $M$  in both directions using the same unit load intensity  $w_u$  per unit area.
2. In the case of concentrated loads or total loads, also divide such loads by  $\sqrt{\mu}$ .
3. In the case of line loads, the line load has to be divided by  $\sqrt{\mu \cos^2 \theta + \sin^2 \theta}$ , where  $\theta$  is the angle between the line load and the  $M$  direction.

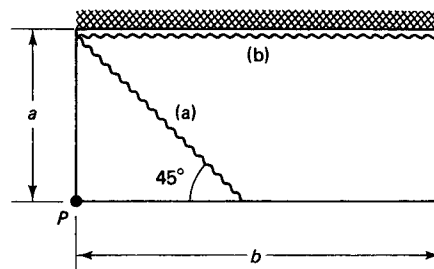
If the slab is to be analyzed as an affine slab with the moment  $\mu M$  in both directions, the dimension in the  $\mu M$  direction has to be multiplied by  $\sqrt{\mu}$ . In either case, the result is of course the same.

### 9.14.2 Failure Mechanisms and Moment Capacities of Slabs of Various Shapes Subjected to Distributed or Concentrated Loads

The preceding concise introduction to the virtual-work method of yield-line moment evaluation should facilitate a good understanding of the mathematical procedures of most standard rectangular shapes subjected to uniform loading. More complicated slab shapes and other types of symmetrical and nonsymmetrical loading require more advanced knowledge of the subject. Also, the assumed failure shape and minimization energy principles can give values for particular cases that differ slightly from one experimenter to another depending on the mathematical assumptions made with respect to the failure shape.

The following summary of failure patterns and the respective moment capacities in terms of load, many of them due to Mansfield (Ref. 9.14), should give the reader adequate coverage of solutions to most cases expected in today's and tomorrow's structures.

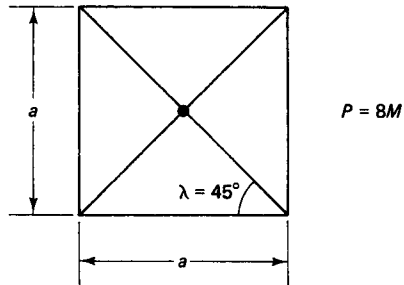
1. Point load to corner of rectangular cantilever plates:



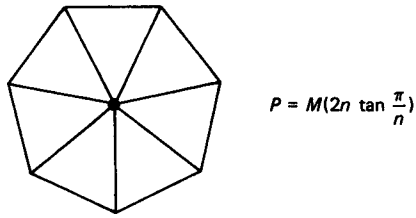
Case (a)  $P = 2M$

Case (b)  $P = \frac{b}{a} (M)$

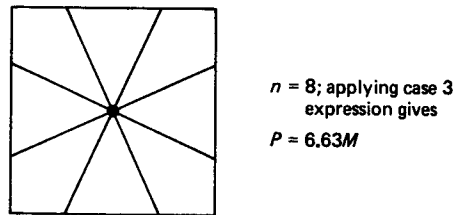
2. Square plate centrally loaded and having boundaries simply supported against both downward and upward movements:



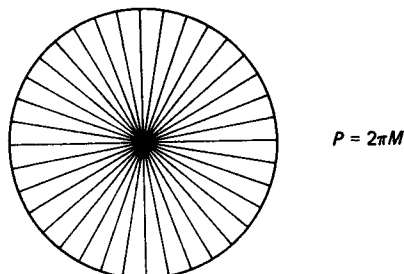
3. Regular  $n$ -sided plate with simply supported edges and centrally loaded ( $n > 4$ ):



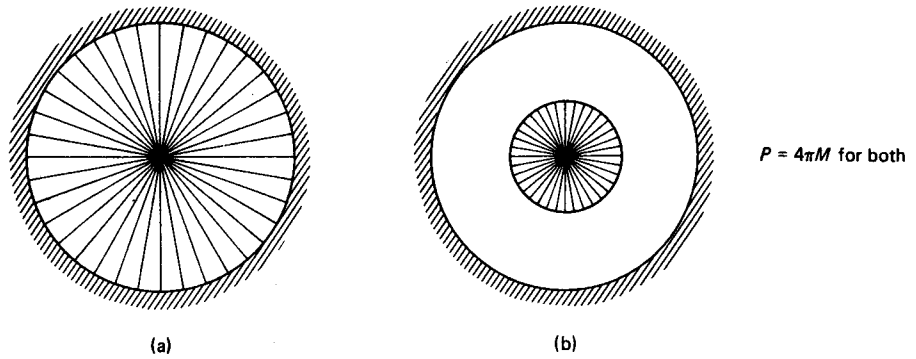
4. Square plates centrally loaded and having boundaries simply supported against downward movement, but free for upward movement:



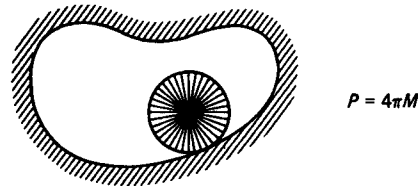
5. Circular centrally loaded plate simply supported along the edges:



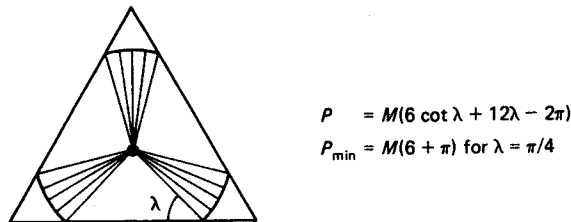
6. Circular plate with fully restricted edges and centrally loaded by point load  $P$ :



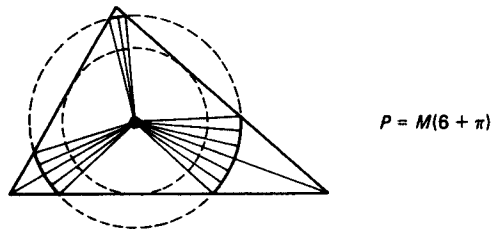
7. Point load  $P$  applied anywhere in arbitrarily shaped plate fully restrained on all boundaries:



8. Equilateral triangular plate with simply supported edges and centrally loaded by point load  $P$ :



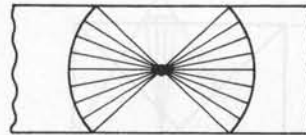
9. Acute-angled triangular plate on simply supported edges loaded with point load  $P$  at the center of the inscribed circle:



10. Obtuse-angled triangular plate with simply supported edges and load  $P$  at the center of the inscribed circle:

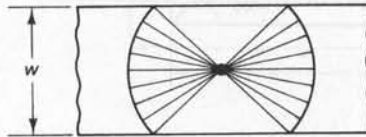


11. Long strip simply supported along the edges and loaded with point  $P$  midway between the edges:



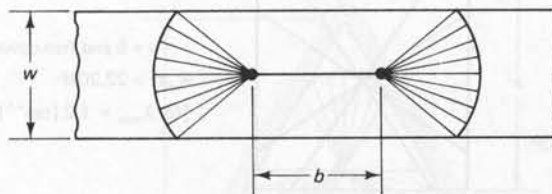
$$P = M(4 + 2\pi)$$

12. Simply supported strip with equal loads  $P$  between the edges:



- (a) Loads  $P$  sufficiently far apart; hence no mutual interaction between the two loads

$$P = M(4 + 2\pi)$$



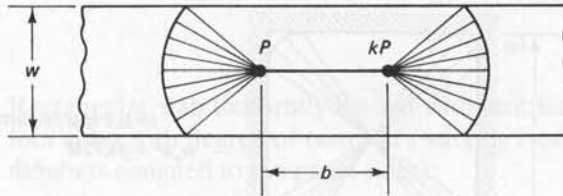
- (b) Loads  $P$  sufficiently close

$$P = M[\pi + 2(1 + b/w)]$$

Limiting spacing  $b$  between the two loads is

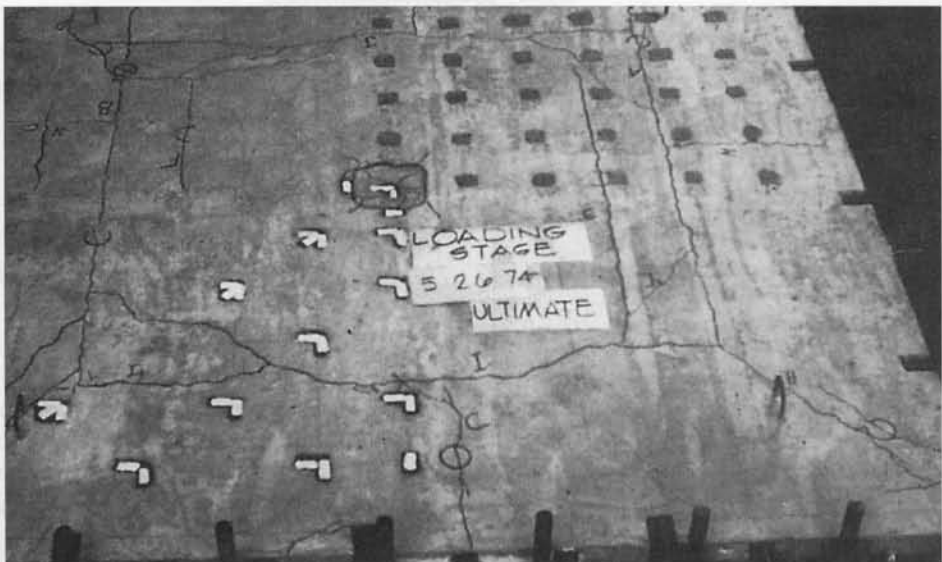
$$b_{lim} = (1 + 1/2\pi)w$$

13. Simply supported strip with unequal loads  $P$  and  $kP$  midway between the edges, where  $k < 1.0$  and the loads are sufficiently apart:

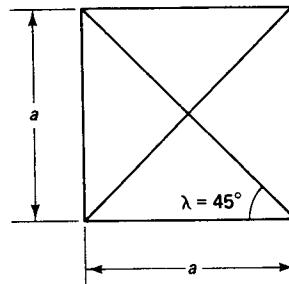


$$P = M \left\{ \frac{2}{1+k} \left[ \pi + 2 \left( 1 + \frac{b}{w} \right) \right] \right\}$$

where  $k$  is less than 1

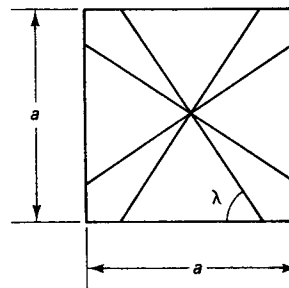


**Photo 9.11** Four-panel slab at failure showing the yield-line patterns at the negative compression face of the supports. (Tests by Nawy and Chakrabarti.)

14. Uniformly loaded square slab with degree of fixity  $i$  varying between zero and 1.0:

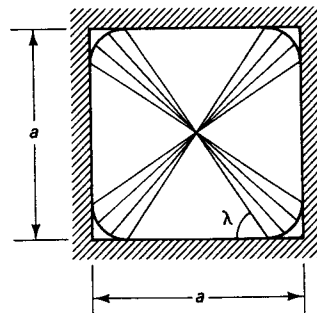
$i = 0$  and no upward movement  
 $w_u a^2 = 24M$

(a)



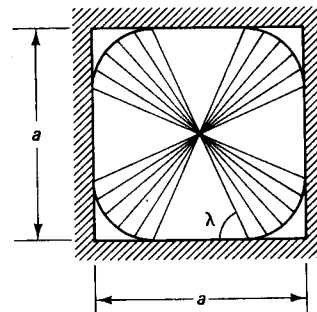
$i = 0$  and free upward movement  
 $w_u a^2 = 22.20M$   
 [for  $\lambda_{\min} = 1/2 [\tan^{-1}(3)]$ ]

(b)



$i = 0.5$  (partial restraint)  
 $w_u a^2 = 34.72M$

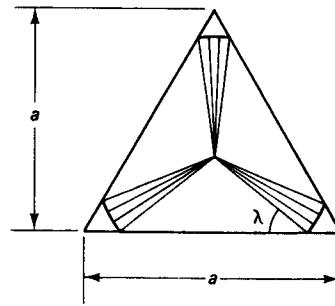
(c)



$i = 1.0$  (full restraint)  
 $w_u a^2 = 48M$  (upper bound)

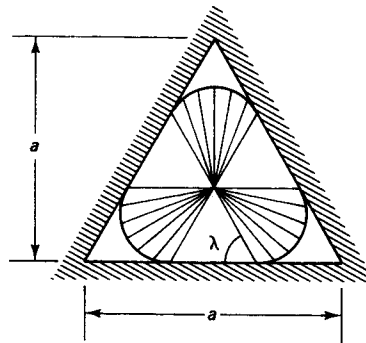
(d)

15. Equilateral triangular plate ( $\lambda = 60^\circ$ ) uniformly loaded:



$i = 0$  (simple support)  
 $w_u a^2 = 50.85M$

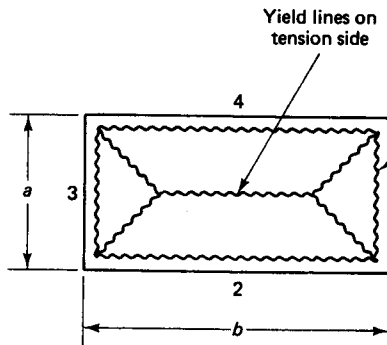
(a)



$i = 1.0$  (full restraint)  
 $w_u a^2 = 86.85M$

(b)

16. Rectangular slab uniformly loaded with unit load of intensity  $w_u$  supported on all four sides with degree of restraint  $i$  varying from zero to 1.0 (note the sequence of numbers assigned to the panel sides):



Yield lines on tension side

Yield lines on compression side

$$M = \frac{w_u a_r^2}{24} \left[ \sqrt{3 + \left(\frac{a_r}{b_r}\right)^2} - \frac{a_r}{b_r} \right]^2$$

where  $a_r = \frac{2a}{\sqrt{1+i_2} + \sqrt{1+i_4}}$

$b_r = \frac{2b}{\sqrt{1+i_1} + \sqrt{1+i_3}}$

As a general note, in the foregoing equations relating the load  $P$  to the moment  $M$ , load  $P$  is assumed to act at a point. To adjust for the fact that  $P$  acts on a finite area, assume that it acts over a circular area of radius  $\rho$ . For a slab fully restrained on all boundaries, the hinge field would be bound by a circle touching the slab boundary (circle radius =  $r$ ). In such a case,

$$M + M' = \frac{P}{2\pi} \left( 1 - \frac{2\rho}{3r} \right) \tag{9.43}$$

where  $M$  is the positive unit moment and  $M'$  the negative unit moment.

The reaction of columns supporting flat plates can be similarly considered for analyzing the flexural local capacity of the plate in the column area. For rectangular supports, an approximation to an equivalent circular support can be made in the use of Equation 9.43.

### 9.15 YIELD-LINE MOMENT STRENGTH OF A TWO-WAY PRESTRESSED CONCRETE PLATE

#### Example 9.4

Find the nominal moment strength of the two-way prestressed concrete plate in Example 9.2, assuming that the prestressing strands are bonded.

#### Solution:

**Loads.** The total load intensity at the limit state of failure, from Example 9.2, is  $W_u = 1.2W_D + 1.6W_L = 186$  psf. Assuming that the column reaction is an inverted concentrated load in the continuous plate field, the required moment strength  $M_n$  can be defined from case 7 of subsection 9.14.2 as follows:

$$P_A = 4\pi M_n$$

$$\text{Factored } P_u = 186 \times 20 \left( \frac{24 + 18}{2} \right) = 78,120 \text{ lb (348 kN)}$$

(the column weight is negligible)

$$\text{Req } P_n = \frac{P_u}{\phi} = \frac{78,120}{0.9} = 86,800 \text{ lb (38.6 kN)}$$

$$\text{Req Unit } M_n \text{ for point load} = \frac{P_n}{4\pi} = \frac{86,800}{4 \times 3.14} = 6910 \text{ lb (30.7 kN)}$$

$$\text{Equivalent } \rho = \frac{20 \times 14}{\pi^2} = 28.4 \text{ in.}$$

Assume  $r \cong 17.5 \text{ ft} = 210 \text{ in.}$  and  $M' = M$ . Then

$$M_n = \frac{P_n}{4\pi} \left( 1 - \frac{2\rho}{3r} \right) = 6910 \left( 1 - \frac{2 \times 28.4}{3 \times 210} \right) = 6287 \text{ lb (28 kN)}$$

**Available Moment Strength  $M_n$**  The available column area slab reinforcement is determined as follows.

#### Prestressing Steel

$$A_{ps} = \text{three } \frac{1}{2}\text{-in. dia 7-wire 270 K strands} = 3 \times 0.153 = 0.459 \text{ in.}^2$$

$$f_{py} = 243,000 \text{ psi (1,675 MPa)}$$

$$f_{ps} = 179,256 \text{ psi at interior column}$$

$$f'_c = 4,000 \text{ psi (27.58 MPa)}$$

Accordingly, use  $f_{py}$  at the limit state of failure.

#### Nonprestressed Steel

$$A_s = \text{six #4 bars} = 6 \times 0.2 = 1.20 \text{ in.}^2$$

$$f_y = 60,000 \text{ psi}$$

*Moment Strength  $M_n$* 

$$d_p = d = 6.5 - 1 = 5.5 \text{ in.}$$

$$b = 33.5 \text{ in. (from Example 9.2)}$$

$$a = \frac{A_s f_y + A_{ps} f_{py}}{0.85 f'_c b} = \frac{1.2 \times 60,000 + 0.459 \times 243,000}{0.85 \times 4,000 \times 33.5} = 1.61 \text{ in. (40.9 mm)}$$

$$\begin{aligned} \text{Available } M_n &= A_s f_y \left( d - \frac{a}{2} \right) + A_{ps} f_{py} \left( d_p - \frac{a}{2} \right) \\ &= 1.2 \times 60,000 \left( 5.5 - \frac{1.61}{2} \right) + 0.459 \times 243,000 \left( 5.5 - \frac{1.61}{2} \right) \\ &= 338,040 + 523,666 = 861,706 \text{ in.-lb} \end{aligned}$$

$$\text{Unit } M_n = \frac{861,706 \text{ in.-lb}}{33.5 \text{ in.}} = 25,723 \text{ in.-lb/in.} = 25,723 \text{ lb}$$

**Check  $M_n$  For the Entire Panel Width**

$$\text{N-S slab band width} = \frac{18 + 24}{2} = 21 \text{ ft (6.4 m)}$$

$$\text{E-W slab band width} = 20 \text{ ft}$$

So use  $b = 21 \text{ ft} = 252 \text{ in.}$  Then the total  $A_{ps}$  = eleven  $\frac{1}{2}$ -in. (12.7 mm) dia 7-wire strands. Since the top prestressed steel is only in the column zone, disregarding it would be on the safe side. We then have

$$\text{Unit } A_{ps} = \frac{11 \times 0.153}{252} = 0.0067 \text{ in.}^2/\text{in.}$$

$$a = \frac{0.0067 \times 243,000}{0.86 \times 4,000 \times 1} = 0.48 \text{ in.}$$

$$\begin{aligned} \text{Unit } M_n &= 0.0067 \times 243,000 \left( 5.5 - \frac{0.48}{2} \right) = 8,564 \text{ in.-lb/in.} \\ &= 8,564 \text{ lb (38.09 kN), use} \end{aligned}$$

$$\text{Req } M_n = 6287 \text{ lb} < \text{available } M_n = 8,564 \text{ lb, O.K.}$$

Plainly, from this *limit theory* solution, quick analysis of a prestressed plate can be performed. Such an analysis, however, should also include an evaluation of yield-line shear strength at the support (Ref. 9.15) and serviceability checks for crack control and deflection control. The designer can easily choose the moment values for the applicable failure mechanism as presented in subsection 9.14.2. A serviceability check for crack control can be easily made using the criteria based on the extensive research reported in Refs. 9.19 to 9.21 and the discussion in Section 11.9 in this text on crack control in walls of large prestressed concrete tanks.

**SELECTED REFERENCES**

- 9.1 Post-Tensioning Institute. *Post-Tensioning Manual*. 6th ed. Phoenix: Post-Tensioning Institute, 2006.
- 9.2 ACI Committee 318. *Building Code Requirements for Structural Concrete (ACI 318-08) and Commentary (ACI 318R-08)*, American Concrete Institute, Farmington Hills, MI, 2008, pp. 465.
- 9.3 Nawy, E. G. *Reinforced Concrete—A Fundamental Approach*. 6th ed. Prentice Hall, Upper Saddle River, NJ, 2009, pp. 936.



- 9.4 Nawy, E. G., and Chakrabarti, P. "Deflection of Prestressed Concrete Flat Plates." *Journal of the Prestressed Concrete Institute* 21 (1976): 86–102.
- 9.5 Lin, T. Y. "Load-Balancing Method for Design and Analysis of Prestressed Concrete Structures." *Journal of the American Concrete Institute* 60 (1963): Farmington Hills, MI 719–742.
- 9.6 Burns, N. H., and Hemabom, R. "Test of Scale Model Post-Tensioned Flat Plate." *Journal of the Structural Division, American Society of Civil Engineers* 103 (1977): 1237–1255.
- 9.7 Nilson, A. H. *Design of Prestressed Concrete*. John Wiley & Sons, New York, 1987.
- 9.8 Scordelis, A. C., Lin, T. Y., and Itaya, R. "Behavior of a Continuous Slab Prestressed in Two Directions." *Journal of the American Concrete Institute* 56, Farmington Hills, MI (1959): 441–459.
- 9.9 Cross, H., and Morgan, N. *Continuous Frames of Reinforced Concrete*. John Wiley & Sons, New York, 1954.
- 9.10 Rice, P. F., Hoffman, E. S., Gustafson, D. P., and Gouwens, A. J. *Structural Design Guide to the ACI Building Code*. 3d ed. Van Nostrand Reinhold, New York, 1985.
- 9.11 Nawy, E. G. "Strength, Serviceability, and Ductility." In *Handbook of Structural Concrete*, pp. 12-1 to 12-88. McGraw Hill, New York, 1983.
- 9.12 Lin, T. Y., and Burns, N. H. *Design of Prestressed Concrete Structures*. 3d ed. John Wiley & Sons, New York, 1981.
- 9.13 Reynolds, C. E., and Steedman, J. C. *Reinforced Concrete Designer's Handbook*. 9th ed. Viewpoint Publications, London, 1981.
- 9.14 Mansfield, E. H. "Studies in Collapse Analysis of Rigid-Plastic Plates with a Square Yield Diagram." *Proceedings of the Royal Society* 241 (1957): 225–261.
- 9.15 Gesund, H., and Dikshit, O. P. "Yield Line Analysis of Punching Problem at Slab Column Intersections," *International Symposium on Cracking, Deflection, and Ultimate Load of Concrete Slab Systems*, pp. 177–203. American Concrete Institute, Farmington Hills, MI, 1971.
- 9.16 Hung, T. Y., and Nawy E. G. "Limit Strength and Serviceability Factors in Uniformly Loaded, Isotropically Reinforced Two-Way Slabs," *International Symposium on Cracking, Deflection, and Ultimate Load of Concrete Slab Systems*, pp. 1–41. American Concrete Institute, Farmington Hills, MI, 1971.
- 9.17 Nilson, A. H., and Walters, D. B. "Deflection of Two-Way Floor Systems by the Equivalent Frame Method." *Journal of the American Concrete Institute* 72, Farmington Hills, MI, (1975): 210–218.
- 9.18 Nawy, E. G., and Chakrabarti, P. "Serviceability Deflection Behavior of Two-Way Action Prestressed Concrete Plates." In *International Conference on Prestressed Concrete*, Concrete Institute of Australia, Sydney, Australia, 1976, pp. 1–10.
- 9.19 Nawy, E. G. "Crack Control Through Reinforcement Distribution in Two-Way Acting Slabs and Plates." *Journal of the American Concrete Institute* 69, Farmington Hills, MI, (1972): 217–219.
- 9.20 Nawy, E. G., and Blair, K. *Further Studies of Flexural Crack Control in Structural Slab Systems*. American Concrete Institute, Farmington Hills, MI, 1971.
- 9.21 Vessey, J. V., and Preston, R. L. *A Critical Review of Code Requirements for Prestressed Concrete Reservoirs*. Paris: F. I. P., 1978.
- 9.22 Cohn, M. Z. "Partial Prestressing, From Theory to Practice." In *NATO—ASI Applied Science Series*, Vol. 1, p. 405, and Vol. 2, p. 425. Martinus Nijhoff, in Cooperation with NATO Scientific Affairs Division, Dordrecht, Netherlands, 1986.
- 9.23 Nawy, E. G., editor-in-chief, *Concrete Construction Engineering Handbook* 2nd ed., CRC Press, Boca Raton, FL: 2008, 1560 pp.
- 9.24 Nawy, E. G., *Fundamentals of High Performance Concrete*, 2nd ed. John Wiley & Sons, New York, 2001, 440 p.

## PROBLEMS

- 9.1 Design the two-way prestressed floor in Example 9.2 by the equivalent frame method if the spacing of the columns in the E-W direction is changed to 24 ft (7.32 m) center to center. Analyze the floor

for flexure and shear, and find the maximum long-term deflection of both the central and the end floor panels and compare it with the maximum allowable deflection if the floor carries equipment that is sensitive to excessive deflection.

- 9.2 Design the flat plate in Problem 9.1 considering it as a lift slab supported on steel columns as shown in Figure P9.2. Assume that no negative moments are transferred from the slab panels to the supporting columns, and check for deflections accordingly.

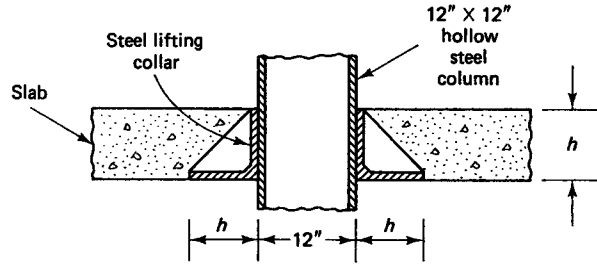


Figure P9.2 Lift slab at column support.

- 9.3 Analyze the flat plate in Problem 9.1 by the yield-line theory, and compare the design results with the equivalent frame design used in Problem 9.1.

# 10



## CONNECTIONS FOR PRESTRESSED CONCRETE ELEMENTS

### 10.1 INTRODUCTION

The function of a connection is to economically transmit loads and stresses from one part of a structure to an adjoining part and provide stability to the structural system. The forces acting at the connection or joint are produced not only by gravity loads but by winds, seismic effects, volumetric changes due to long-term creep and shrinkage, differential movement of panels, and temperature effects.

Since a connection is the weakest link in the overall structural system, it has to be designed for nominal strength higher than the elements it connects. An additional load factor of at least 1.3 should be used in the design of connections, except in the case of insensitive connections, such as pads for column bases, where such an additional load factor is not necessary. All connections should be designed for a minimum horizontal tensile force of 0.2 times the vertical dead load, unless properly designed bearing pads are used.

The factors that have to be considered in design of a connection for strength are as follows:

1. The load transfer mechanism
2. Load factors

Gulf Life Center, Jacksonville, Florida. (Courtesy, Prestressed Concrete Institute.)

3. Volumetric changes
4. Ductility
5. Durability
6. Fire resistance
7. Required tolerances and clearances
8. Erection-related considerations
9. Considerations regarding hot weather and cold weather
10. The economics of the details of the connection

## 10.2 TOLERANCES

Clearances between elements must be realistically assessed. Where large tolerances are allowed in a supporting structure, or where no tolerances are specified, the clearances have to be increased to account for these factors. The following are recommended tolerances from Ref. 10.2 for deviations from idealized dimensions in beams, columns, and spandrel panels:

1. Variation in plan from specified location in plan:  $\pm\frac{1}{2}$  in., any column or beam, any locations.
2. Deviation in plan from straight lines parallel to specified linear building lines:  $\frac{1}{40}$  in. per ft, any beam less than 20 ft, or adjacent columns less than 20 ft apart;  $\frac{1}{2}$  in., adjacent columns 20 ft or more apart.
3. Difference in relative position of adjacent columns from specified relative position:  $\frac{1}{2}$  in. at any deck level.
4. Deviation from plumb:  $\frac{1}{4}$  in. for every 10 ft of height; 1 in. maximum for the entire height.
5. Variation in elevation of bearing surfaces from specified elevation:  $\pm\frac{1}{2}$  in., any column or beam, any location.
6. Deviation of top of spandrel from specified elevation:  $\frac{1}{2}$  in., any spandrel.
7. Deviation in elevation of bearing surfaces from lines parallel to specified grade lines:  $\frac{1}{40}$  in. per ft, any beam less than 20 ft or adjacent columns less than 20 ft apart;  $\frac{1}{2}$  in. maximum, any beam 20 ft or more in length or adjacent columns 20 ft or more apart.
8. Variation from specified bearing length on support:  $\pm\frac{3}{4}$  in.
9. Variation from specified bearing width on support:  $\pm\frac{1}{2}$  in.
10. Jog in alignment of matching edges:  $\frac{1}{4}$  in.

Table 10.1 gives tolerances applicable to connections.

## 10.3 COMPOSITE MEMBERS

As discussed in detail in Chapter 5 Sections 5.7 through 5.11, full transfer of horizontal shear forces must be assured at the interface of the precast member and the situ-cast topping. Figure 5.14 presents the interacting forces, and the flowchart of Section 5.8.2 gives the operational step-by-step design procedure and the applicable design equations. Figure 5.18 of Example 5.3 and the accompanying design give the size and spacing of the

**Table 10.1** Tolerances for Connections

Item	Recommended tolerances* in.
Field-placed anchor bolts (transit or template)	$\pm\frac{1}{2}$
Elevation of field cast footings and piers	$\pm 1$
<i>Structural Precast Concrete</i>	
Position of plates	$\pm 1$
Location of inserts	$\pm\frac{1}{2}$
Location of bearing plates	$\pm\frac{3}{4}$
Location of blockouts	$\pm\frac{1}{2}$
Length	$\pm\frac{3}{4}$
Overall depth	$\pm\frac{1}{4}$
Width of stem	$\pm\frac{1}{8}$
Overall width	$\pm\frac{1}{4}$
Horizontal deviation of ends from square	$\pm\frac{1}{2}$
Vertical deviation of ends from square	$\pm\frac{1}{8}$ per ft of height
Bearing deviation from plane	$\pm\frac{3}{16}$
Position of post-tensioning ducts in precast members	$\pm\frac{1}{2}$
<i>Architectural Precast Concrete</i>	
Length or width	$\pm\frac{1}{16}$ per 10 ft, but not less than $\pm\frac{1}{8}$
Thickness	$+\frac{1}{4}-\frac{1}{8}$
Location of blackouts	$\pm\frac{1}{2}$
Location of anchors and inserts	$\pm\frac{3}{8}$
Warpage or squareness	$\pm\frac{1}{8}$ in 6 ft
Joint widths	
—specified	$\frac{3}{8}-\frac{5}{8}$
—min. and max. dimensions	$\frac{1}{4}$ and $\frac{3}{4}$

\*Other construction materials may control tolerances selected.

dowels necessary to effect the full transfer of the horizontal shear forces between the interconnected elements.

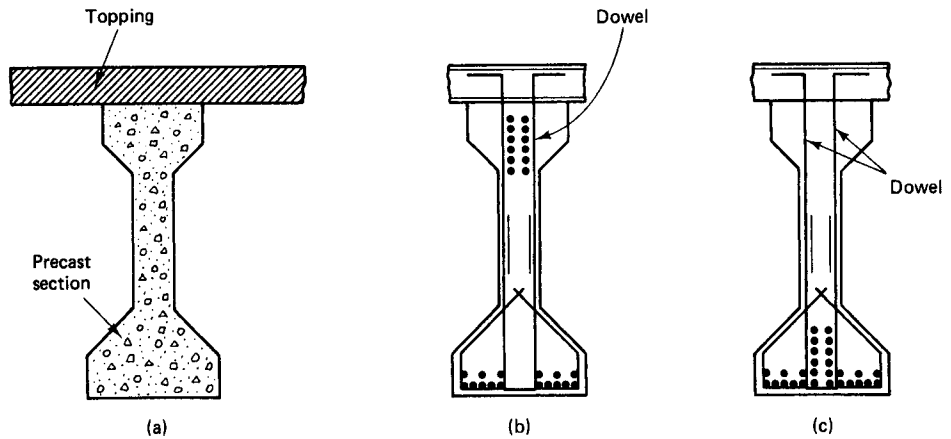
## 10.4 REINFORCED CONCRETE BEARING IN COMPOSITE MEMBERS

A typical composite-action dowel reinforcement is shown in Figure 10.1. In order to prevent the concrete that is in direct bearing contact in such reinforcements from crushing due to excess direct compressive load, the external load has to be applied to an adequate bearing area size such that the resulting limit-state stresses do not exceed the compressive strength of concrete. The nominal bearing strength of *plain* concrete can be defined as

$$V_n = C_r(0.85f'_c A_1) \sqrt{A_2/A_1} \leq 1.2f'_c A_1 \quad (10.1)$$

where  $C_r = 1.0$  when reinforcement is provided in the direction of the horizontal frictional force  $N_u$  shown in Figure 10.2 or when  $N_u$  is taken to be zero.  $C_r$  can be defined as  $(S \times W/200)^{N_u/V_u}$ , where the area  $S \times W$ , shown in Figure 10.3, should not exceed 9.0 in.<sup>2</sup>

$A_1$  = direct bearing area



**Figure 10.1** Typical dowel-action reinforcement. (a) Situ-cast topping on precast section. (b) Support section. (c) Midspan section.

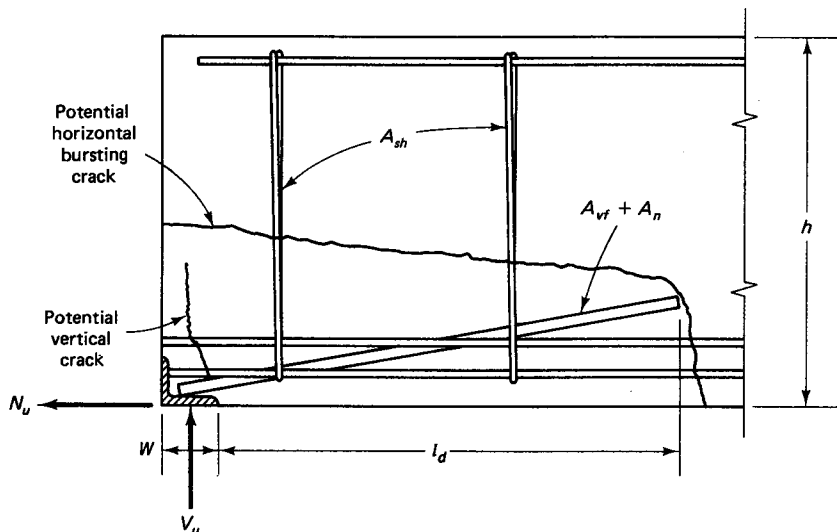
$A_2$  = maximum area of the portion of the supporting surface that is geometrically similar to and concentric with the loaded area shown in Figure 10.3.

The design bearing strength is

$$V_u = \phi V_n$$

where  $\phi = 0.70$ . In order to avoid accidental cracking or spalling at the ends of thin-stemmed members, a minimum reinforcement equal to  $N_u/\phi f_y$ , but not less than one #3 bar (9.52 mm dia), is recommended when the bearing area is less than 2 in.<sup>2</sup> (12.9 cm<sup>2</sup>).

If the applied factored load  $V_u$  exceeds the *design* bearing strength  $V_u = \phi V_n$  as computed from Equation 10.1, reinforcement is required in the bearing area. This reinforcement can be designed by the shear-friction theory presented in Chapter 5. *All* precast members ought to be designed for reinforced bearing except solid and hollow-core slabs,



**Figure 10.2** Reinforced bearing end in beam.

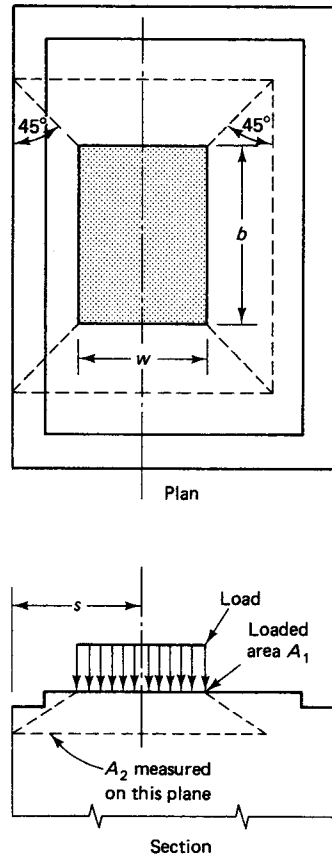


Figure 10.3 Bearing area on a concrete pad.

as recommended in Ref. 10.2, in order to prevent horizontal and vertical cracks from forming at the beam's extreme ties at the supports. The inclination of the end crack can be safely assumed to be approximately 20 degrees, as in Figure 10.2. Also, if  $V_u$  is equal to the applied factored shear force, in pounds, parallel to the assumed crack plane, it should be limited by the values given in Table 10.2 for the indicated maximum effective shear-friction coefficients  $\mu_e$ .

The reinforcement area nominally perpendicular to the assumed crack plane can be found from

Table 10.2 Maximum Applied Factored Force  $V_u$ , lb

Crack Interface Condition	Recommended $\mu$	Maximum $\mu_e$	Maximum $V_u$ , lb
1. Concrete to concrete, cast monolithically	$1.4\lambda$	3.4	$0.30\lambda^2 f'_c A_{cr} \leq 1,000 \lambda^2 A_{cr}$
2. Concrete to hardened concrete with roughened surface	$1.0\lambda$	2.9	$0.25\lambda^2 f'_c A_{cr} \leq 1,000 \lambda^2 A_{cr}$
3. Concrete to concrete	$0.6\lambda$	2.2	$0.20\lambda^2 f'_c A_{cr} \leq 800 \lambda^2 A_{cr}$
4. Concrete to steel	$0.7\lambda$	2.4	$0.20\lambda^2 f'_c A_{cr} \leq 800 \lambda^2 A_{cr}$

$$A_{vf} = \frac{V_{up}}{\phi \mu_e f_y} \tag{10.2}$$

where  $V_u/\phi$  = nominal strength  $V_N$

$f_y$  = yield strength of  $A_{vf}$ , psi

$V_{up}$  = applied factored shear force, limited by the values given in Table 10.2 and

$$\mu_e = \frac{1,000\lambda A_{cr} \mu}{V_{up}} \tag{10.3}$$

in which  $\lambda = 1.0$  for normal-weight, 0.85 for sand-lightweight, and 0.75 for all-lightweight concrete

$A_{cr}$  = area of the crack plane interface (in.<sup>2</sup>), which can be taken as  $l_d b$ , where  $l_d$  is the development length of the  $A_{vf}$  bars (in.) and  $b$  is the average member width (in.).

Table 10.3 gives the development length  $l_d$  for various bar sizes. The vertical reinforcement  $A_{sh}$  across potential horizontal cracks can be determined from

$$A_{sh} = \frac{(A_{vf} + A_n) f_y}{\mu_e' f_{ys}} \tag{10.4}$$

**Table 10.3** Tension Reinforcement and Development Length (Inches) For  $f'_c = 4,000^{**}$  psi concrete  $f_y = 60,000$  psi Steel ( $\alpha, \beta, \lambda = 1.0, \gamma = 0.8$  for #6 Bars or Smaller and = 1.0 for #7 Bars and Larger)

Bar Size	Cross-Sectional Area (in. <sup>2</sup> )	Bar Diameter (in.)	Development length, $l_d^{+++}$ (in.)	
			$s \geq 2d_b$ or $*d_b$	Other
			$\leq \#6: l_d = 38d_b$ $\geq \#7: l_d = 48d_b$	$\geq \#6: l_d = 57d_b$ $\geq \#7: l_d = 72d_b$
(1)	(2)	(3)	(4)	(5)
3	0.11	0.375	15	21
4	0.20	0.500	19	29
5	0.31	0.625	24	36
6	0.44	0.750	29	43
7	0.60	0.875	42	63
8	0.79	1.000	48	72
9	1.00	1.128	54	81
10	1.27	1.270	61	92
11	1.56	1.410	68	102
14	2.25	1.693	82	122
18	4.00	2.257	108	163

\*Confined

\*\*For  $f'_c$  values different from 4000 psi, multiply table values by  $(\sqrt{4,000/f'_c})$ . For  $f_y = 40,000$  psi, multiply by  $\frac{2}{3}$ ;  $\sqrt{f'_c}$  should not exceed 100.

†For Compression development length,  $l_d = \lambda l_{db}$  where  $l_{db} = 0.02d_b f_y / \sqrt{f'_c} \geq 0.0003d_b f_y$  and  $\lambda_s$  = Required  $A_s$ /Provided  $A_s$  or  $\lambda_{s1} = 0.75$  for spirally confined reinforcement.

‡Multiply table values by:

$\alpha = 1.3$  for top reinforcement

$\lambda = 1.3$  for lightweight aggregate

$\beta = 1.5$  for epoxy-coated bars with cover less than  $3d_b$  or clear spacing less than  $6d_b$  and  $\beta$



where

$$\mu'_e = \frac{1,000\lambda A_{cr} \mu}{(A_{vf} + A_n)f_y} \quad (10.5)$$

and  $f_{ys}$  = yield strength of  $A_{sh}$ , psi

$A_n$  = area of reinforcement to resist axial tension  $N_u$  in Figure 10.2, defined as

$$A_n = N_u/(\phi f_y) \quad (10.6)$$

in which  $N_u$  = factored applied horizontal tensile force nominally perpendicular to the assumed crack plane

$\phi$  = strength reduction factor = 0.75.

Note that all reinforcement on either side of the assumed crack plane should be properly anchored by development length or welding to angles, plates, or hooks in order to develop the computed resisting force.

### 10.4.1 Reinforced Bearing Design

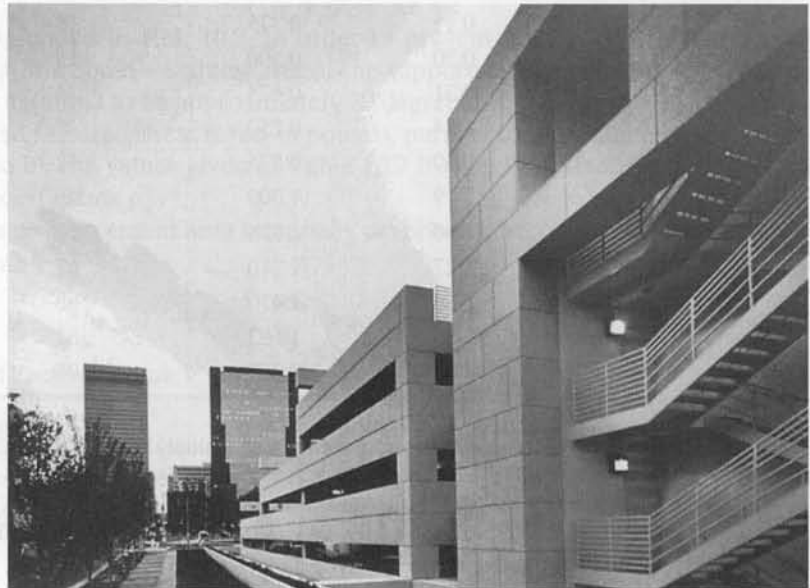
#### Example 10.1

A PCI standard 16RB28 rectangular prestressed beam is subjected to a vertical factored end shear force  $V_u = 90,000$  lb (400 kN) and a horizontal tensile force  $N_u = 21,000$  lb (93.4 kN). The beam is supported on a teflon pad of size 4 in.  $\times$  4 in. (10 cm  $\times$  10 cm). Design the end reinforcement in the beam that can prevent the development of vertical or horizontal bearing cracks, given the following data:

$f'_c = 5,000$  psi (34.47 MPa), normal-weight concrete

$f_y = 60,000$  psi for all mild reinforcement (413.7 MPa)

$\theta = 20$  degrees



**Photo 10.1** Charlotte-Mecklenburg Government Center Parking Structure. (Courtesy, Prestressed Concrete Institute.)

**Solution:**

**Horizontal Reinforcement ( $A_{vf} + A_n$ ).** For the determination of the horizontal reinforcement, try No. 6 bars.

$$\text{Beam depth } h = 28 \text{ in.}, \quad b = 16 \text{ in.}$$

From Table 10.3,  $l_d = 29 \text{ in.}$

$$A_{cr} = l_d b = 29 \times 16 = 464 \text{ in.}^2$$

From Table 10.2,  $\mu = 1.4$ , and from Equation 10.3,

$$\mu_e = \frac{1,000\lambda A_{cr} \mu}{V_{up}} = \frac{1,000 \times 1.0 \times 464 \times 1.4}{90,000} = 10.61 > \text{allowable } \mu_e = 3.4$$

Thus, use  $\mu_e = 3.4$ .

From Equation 10.2,

$$A_{vf} = \frac{V_{up}}{\phi f_y \mu_e} = \frac{90,000}{0.75 \times 60,000 \times 3.4} = 0.59 \text{ in.}^2 (3.4 \text{ cm}^2)$$

$$N_u = 21,000 \text{ lb}$$

$$\frac{N_u}{V_u} = \frac{21,000}{90,000} = 0.23 > \text{minimum } 0.20$$

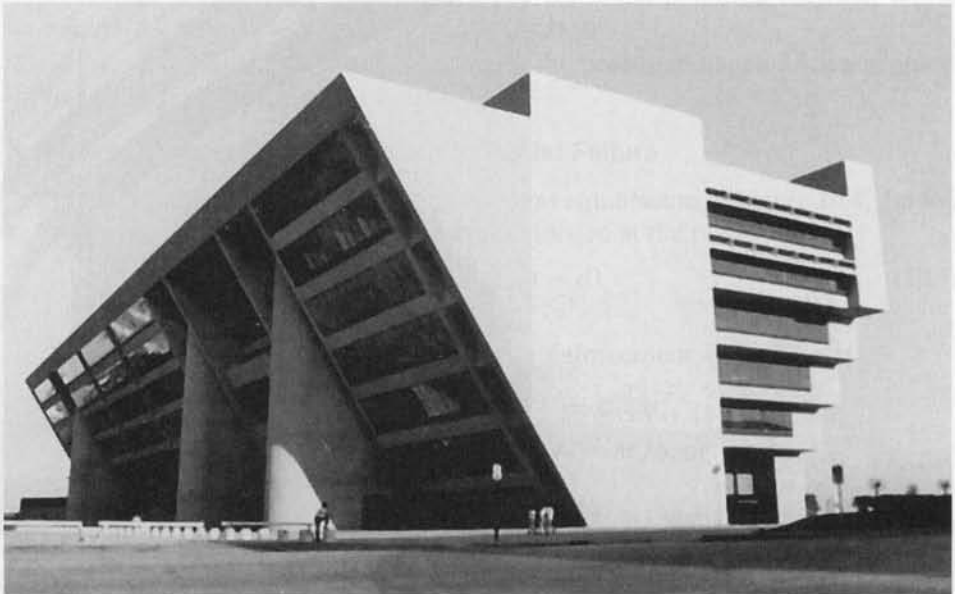
Hence, use  $N_u = 21,000 \text{ lb}$ .

$$\text{From Equation 10.6, } A_n = N_u / \phi f_y = 21,000 / (0.75 \times 60,000) = 0.47 \text{ in.}^2 (2.94 \text{ cm}^2)$$

**Total Steel**

$$A_s = A_{vf} + A_n = 0.59 + 0.47 = 1.06 \text{ in.}^2 (6.63 \text{ cm}^2)$$

So use three #6 bars = 1.32 in.<sup>2</sup> (8.52 cm<sup>2</sup>).



**Photo 10.2** Dallas Municipal Center, Dallas, Texas. (Courtesy, Post-Tensioning Institute.)

**Vertical Reinforcement ( $A_{sh}$ ).** From Table 10.3,  $l_d$  = development length of #6 bars = 29 in. (74 cm) and  $A_{cr} = l_d b = 29 \times 16 = 464 \text{ in.}^2$  (3,159  $\text{cm}^2$ ). From Equation 10.5,

$$\mu'_e = \frac{1,000 \lambda A_{cr} \mu}{(A_{vf} + A_n) f_y} = \frac{1,000 \times 1.0 \times 464 \times 1.4}{0.93 \times 60,000} = 11.64 > \text{allowable } \mu_e = 3.4$$

So use  $\mu'_e = 3.4$ . Then, from Equation 10.4,

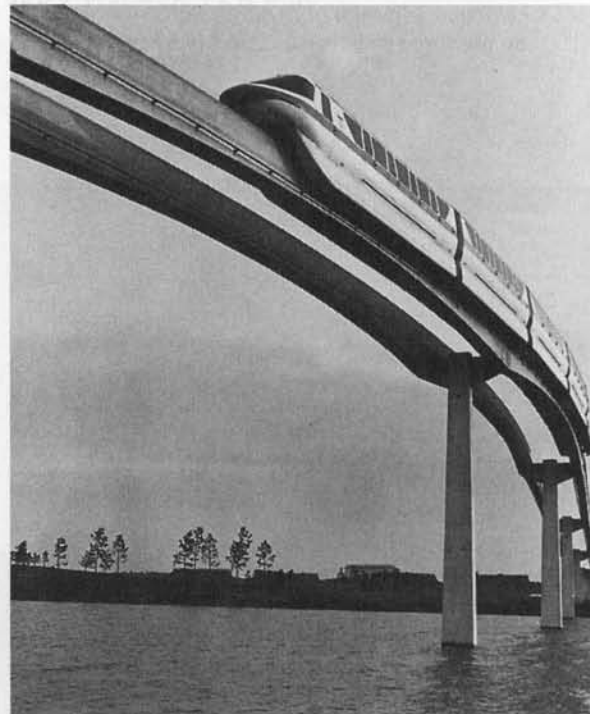
$$A_{sh} = \frac{(A_{vf} + A_n) f_y}{\mu'_e f_{ys}} = \frac{0.93 \times 60,000}{3.4 \times 60,000} = 0.27 \text{ in.}^2 (1.74 \text{ cm}^2)$$

Accordingly, use three #3 stirrups = 0.66  $\text{in.}^2$  (4.26  $\text{cm}^2$ ).

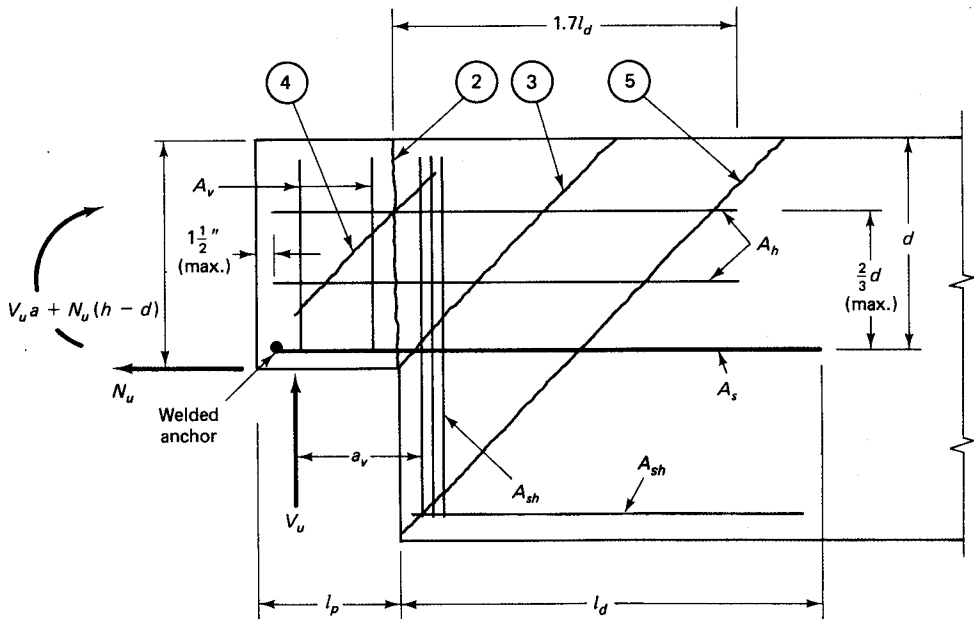
## 10.5 DAPPED-END BEAM CONNECTIONS

A dapped-end beam is a structural element with abruptly reduced depth at its ends in order to provide the necessary seating or bearing on corbels or brackets without loss of clear height between floors. A typical dapped end in a prestressed beam is shown in Figure 10.4. Two types of cracks can develop: crack 2 is a direct shear crack, while cracks 3, 4, and 5 are diagonal tension cracks caused by flexure and axial tension in the extended reduced depth and the stress concentration at the reentrant corner. Therefore, the following types of reinforcement, as shown in the figure, have to be provided:

1. Flexural reinforcement  $A_f$  plus axial tension reinforcement  $A_n$ , where  $A_s = A_f + A_n$ , to resist the cantilever bending stresses.



**Photo 10.3** Walt Disney World Monorail, Orlando, Florida, a series of hollow precast prestressed concrete 100-box girders that are individually post-tensioned to provide a six-span continuous structure, design by ABAM Engineers. (Courtesy, Walt Disney World Co.)



**Figure 10.4** Cracking and reinforcement in dapped-end beam connections.

2. Shear-friction reinforcement  $A_f + A_n$ , plus axial tension reinforcement  $A_n$ , to resist the direct vertical shear force at the junction of the dapped and the undapped portion of the beam causing crack 2.
3. Shear reinforcement  $A_{sh}$ , to resist the diagonal tension generated at the reentrant corner causing crack 3.
4. Diagonal tension reinforcement  $A_h + A_v$ , to resist the potential diagonal tension crack 4 in the extended dapped portion of the beam.
5. Development length of  $A_s = A_f + A_n$ , to resist the potential diagonal tension crack 5 in the undapped portion of the beam.

### 10.5.1 Determination of Reinforcement to Resist Failure

**10.5.1.1 Flexure and axial tension.** For moment equilibrium in Figure 10.4, the total factored moment acting on the cantilever dapped portion at the plane of  $A_s$  is

$$M_u = V_u a_v + N_u (h - d) \quad (10.7a)$$

where  $h$  = depth of member above the dap

$d$  = effective depth of the dap to center of reinforcement  $A_s$

$a$  = shear span.

$M_u$  has to be resisted by a nominal moment strength  $M_n = M_u / \phi$ , or

$$M_n = \frac{V_u a_v + N_u (h - d)}{\phi} \quad (10.7b)$$

Assuming that the moment arm  $jd \cong 0.9d$ ,

$$F_n = \frac{V_u a_v + N_u (h - d)}{0.9\phi d} \quad (10.8)$$

where  $\phi = 0.90$  for flexure. Since  $0.9\phi \cong 0.81$ , for simplification use a value of  $\phi = 0.85$  in Equation 10.8 to obtain

$$F_n = \frac{V_u a_v + N_u (h - d)}{\phi d} \quad (10.9a)$$

or

$$F_n = \frac{V_u}{\phi} \left( \frac{a_v}{d} \right) + \frac{N_u}{\phi} \left( \frac{h - d}{d} \right) \quad (10.9b)$$

The flexural reinforcement is then

$$A_f = \frac{F_n}{f_y} = \frac{V_u a_v + N_u (h - d)}{\phi f_y d} \quad (10.10)$$

and the direct tension reinforcement due to the tensile force  $N_u$  is

$$A_n = \frac{N_u}{\phi f_y} \quad (10.11)$$

The total area of the flexural and direct tension reinforcement then becomes, from Equations 10.10 and 10.11,

$$A_s = A_f + A_n = \frac{1}{\phi f_y} \left[ V_u \left( \frac{a_v}{d} \right) + N_u \left( \frac{h}{d} \right) \right] \quad (10.12)$$

where, again, the adjusted  $\phi = 0.85$ .

**10.5.1.2 Direct Vertical Shear.** The potential direct shear crack 2 is resisted by the combination of reinforcements  $A_s$  and  $A_h$  in Figure 10.4. The horizontal reinforcement  $A_h$  needed to resist the direct shear can be evaluated as

$$A_h = 0.5(A_s - A_n) \quad (10.13)$$

where

$$A_s = \frac{2V_u}{3\phi f_y \mu_e} + A_n \quad (10.14a)$$

$$A_n = \frac{N_u}{\phi F_y} \quad (10.14b)$$

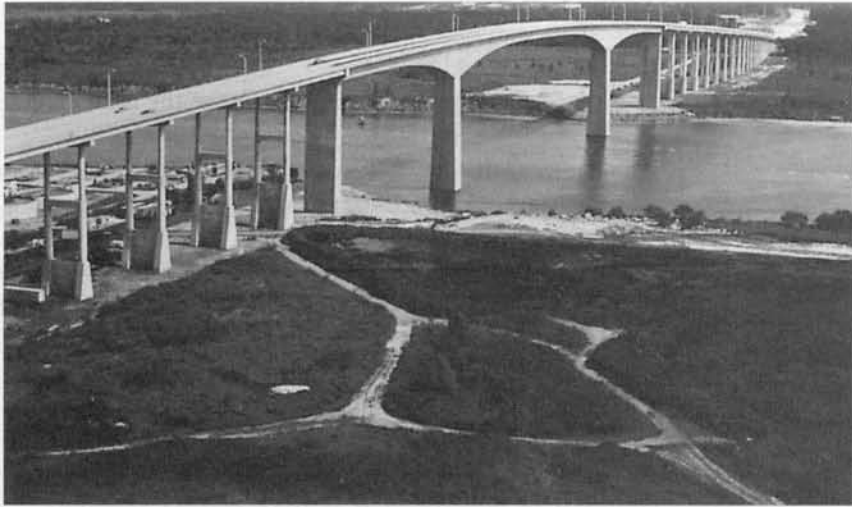
$$\mu_e = \frac{1,000\lambda b h \mu}{V_u} \quad (10.14c)$$

with  $\phi = 0.85$  and  $\mu_e$  the same as in Equation 10.3. Hence,

$$A_s = \frac{1}{\phi f_y} \left( \frac{2V_u}{3\mu_e} + N_u \right) \quad (10.15)$$

The value of  $A_s$  used in Equation 10.13 should be the greater of the two values obtained from Equations 10.12 and 10.15.

The reinforcement  $A_s$  should be extended a minimum of  $1.7l_d$  past the end of the dap, or  $l_d$  past crack 5, and anchored at the end of the beam by welding to cross bars, angles, or plates. Horizontal bars  $A_h$  should be similarly extended, and vertical bars  $A_{sh}$  and vertical or inclined bars  $A_v$  should be well anchored by hooks as required by the ACI Code.



**Photo 10.4** Jesse H. Jones Memorial Bridge, Houston, Texas. (Courtesy, Post-Tensioning Institute.)

The nominal shear strength of the dapped end is limited to

$$V_n \leq 0.30f'_c bd \leq 1,000bd \quad (10.16a)$$

for normal-weight concrete, and

$$V_n \leq \left(0.20 - \frac{0.07a}{d}\right) f'_c bd \quad (10.16b)$$

or

$$V_n \leq \left(800 - \frac{280a}{d}\right) bd \quad (10.16c)$$

whichever is smaller, for sand-lightweight or all-lightweight concrete, where  $a$  is the shear span and  $d$  the effective depth of the beam.

**10.5.1.3 Diagonal Tension at Reentrant Corner.** The reinforcement needed to resist the inclined diagonal tension cracking propagating from the center of stress concentration at the reentrant corner towards the undapped portion can be obtained from the expression

$$A_{sh} = \frac{V_u}{\phi f_y} \quad (10.17)$$

where  $\phi = 0.85$  and  $f_y$  is the yield strength of the  $A_{sh}$  reinforcement.

**10.5.1.4 Diagonal Tension in the Dapped End.** In order to resist the potential diagonal crack 4 in the dapped end, additional reinforcement  $A_y$  has to be provided such that the total nominal shear strength  $V_n$  satisfies the equation

$$V_n = \frac{V_u}{\phi} = A_v f_y + A_h f_y + 2\lambda bd \sqrt{f'_c} \quad (10.18)$$

At least half of the reinforcement in this area has to be placed vertically, so that Equation 10.18 gives

$$\text{Min } A_v = \frac{1}{2f_y} \left( \frac{V_u}{\phi} - 2\lambda b d \sqrt{f'_c} \right) \quad (10.19)$$

Note that performance considerations require the following:

1. The depth of the dapped end should be at least one-half the beam depth, unless the beam is significantly deeper than required by design for other than structural considerations.
2. If the flexural stress computed for the full depth of the section using factored loads and gross section properties exceeds  $6\sqrt{f'_c}$  immediately beyond the dap, additional longitudinal reinforcement should be placed in the beam in order to develop the required flexural strength.
3. The diagonal tension reinforcement  $A_{sh}$  should be placed as closely as practicable to the reentrant corner. This reinforcement is in addition to the design shear reinforcement required for the full-depth beam section.

### 10.5.2 Dapped-End Beam Connection Design

#### Example 10.2

A PCI standard 16RB28 prestressed beam dapped at the end for bearing on a column corbel is subjected to a factored gravity end shear  $V_u = 110,000$  lb (489 kN) and a horizontal axial tension  $N_u = 20,000$  lb (97.9 kN). Design the flexural, direct shear, and diagonal tension reinforcements  $A_s$ ,  $A_h$ ,  $A_{sh}$ , and  $A_v$  required to prevent potential cracking due to dapping the beam ends. Given data are  $f'_c = 5,000$  psi (34.5 MPa), normal weight, and  $f_y = f_{yt} = 60,000$  psi (414 MPa). Use bars for the reinforcement.

**Solution:** Assume that the shear span  $a = 6$  in. (152 mm), the dapped-end effective  $d = 16$  in. (406 mm), and  $h = 18$  in. (457 mm).

#### *Flexure and Axial Tension Reinforcement $A_s$*

$$\frac{N_u}{V_u} = \frac{20,000}{110,000} = 0.18 < 0.20$$

Hence,  $N_u = 0.20 \times 110,000 = 22,000$  lb (97.9 kN). Thus,

$$\begin{aligned} A_s &= \frac{1}{\phi f_y} \left[ V_u \left( \frac{a}{d} \right) + N_u \left( \frac{h}{d} \right) \right] \\ &= \frac{1}{0.75 \times 60,000} \left[ 110,000 \times \frac{6}{16} + 22,000 \times \frac{18}{16} \right] = 1.46 \text{ in.}^2 \end{aligned}$$

**Direct Shear Reinforcement  $A_s$  and  $A_h$ .** From Table 10.2  $\mu = 1.4\lambda$  where  $\lambda = 1.0$ . Then, from Equation 10.14c, where  $b$  for the 16RB28 section is 16 in.,

$$\mu_e = \frac{1,000\lambda b h \mu}{V_u} = \frac{1,000 \times 1.0 \times 16 \times 18 \times 1.4}{110,000} = 3.67$$

> max allowable  $\mu_e = 3.4$

Thus, use  $\mu_e = 3.4$ . Then, from Equation 10.5,

$$\begin{aligned} A_s &= \frac{1}{\phi f_y} \left( \frac{2V_u}{3\mu_e} + N_u \right) = \frac{1}{0.75 \times 60,000} \left( \frac{2 \times 110,000}{3 \times 3.4} + 22,000 \right) \\ &= 0.96 \text{ in.}^2 < A_s = 1.46 \text{ in.}^2 \text{ from before} \end{aligned}$$

Hence, use  $A_s = 1.46 \text{ in.}^2$  ( $9.1 \text{ cm}^2$ ). Then three #7 bars =  $1.80 \text{ in.}^2$ , which is satisfactory.

From Equation 10.4b,

$$A_n = \frac{N_u}{\phi f_y} = \frac{22,000}{0.75 \times 60,000} = 0.49 \text{ in.}^2 (3.0 \text{ cm}^2)$$

From Equation 10.13, the horizontal shear reinforcement across the depth of the beam is  $A_h = 0.5(A_s - A_n) = 0.5(1.29 - 0.43) = 0.43 \text{ in.}^2$  ( $2.77 \text{ cm}^2$ ). So try two #3 U bars =  $2(2 \times 0.11) = 0.44 \text{ in.}^2$  ( $2.84 \text{ cm}^2$ ), which will be verified subsequently. As a check, the nominal shear strength, from Equation 10.16a, is

$$\text{Available } V_n = 800bd = 800 \times 16 \times 16 = 204,800 \text{ lb}$$

$$\text{Required } V_n = \frac{V_u}{\phi} = \frac{110,000}{0.75} = 146,667 \text{ lb} < 204,800 \text{ lb, O.K.}$$

**Diagonal Tension Vertical Reinforcement at Reentrant Corner.** From Equation 10.17,

$$A_{sh} = \frac{V_u}{\phi f_{yt}} = \frac{110,000}{0.75 \times 60,000} = 2.45 \text{ in.}^2 (15.3 \text{ cm}^2)$$

So trying #4 closed ties,  $A_s = 2 \times 0.20 = 0.40 \text{ in.}^2$ . The number of ties =  $2.16/0.4 = 5.4$ ; hence, use six #4 ties, concentrated close to the reentrant corner.

**Diagonal Tension Reinforcement  $A_v$  in the Dapped End.** From Equation 10.19,

$$A_v = \frac{1}{2f_{yt}} \left( \frac{V_u}{\phi} - 2\lambda bd\sqrt{f'_c} \right)$$

The nominal shear strength of the *plain concrete* is

$$2\lambda bd\sqrt{f'_c} = 2 \times 1.0 \times 16 \times 16\sqrt{5,000} = 36,204 \text{ lb}$$

Then

$$A_v = \frac{1}{2 \times 60,000} \left( \frac{110,000}{0.75} - 36,204 \right) = 0.92 \text{ in.}^2$$

Try four #4 U stirrups =  $4(2 \times 0.20) = 1.60 \text{ in.}^2$ . From before,  $A_h = 0.44 \text{ in.}^2$ . So the total nominal shear strength of the section, from Equation 10.18, is

$$\begin{aligned} \text{Available } V_n &= A_v f_{yt} + A_h f_{yt} + 2\lambda bd\sqrt{f'_c} \\ &= 1.60 \times 60,000 + 0.44 \times 60,000 + 36,034 \\ &= 158,434 \text{ lb} > \frac{V_u}{\phi} = 146,667 \text{ lb O.K.} \end{aligned}$$

**Check Development Length Requirements for Anchorage.** The reinforcement  $A_s$  is three #7 bars. From Table 10.3 for #7 bars,  $f'_c = 5,000 \text{ psi}$  and  $l_d = 42 \text{ in.}$  Also, the undapped beam depth =  $2 \text{ ft}, 4 \text{ in.} = 28 \text{ in.}$ , and the total development length =  $28 - d + l_d = 28 - 16 + 42 = 54 \text{ in.}$  Since the minimum  $l_d = 42 \text{ in.}$ , use  $54 \text{ in.} = 4 \text{ ft}, 6 \text{ in.}$  ( $108 \text{ cm}$ ).

The reinforcement  $A_h$  is #4 U bars. So from Table 10.3,  $1.7l_d = 32 \text{ in.}$  ( $81 \text{ cm}$ ) beyond the beam dap. Figure 10.5 gives the reinforcement details for the dapped beam connection.



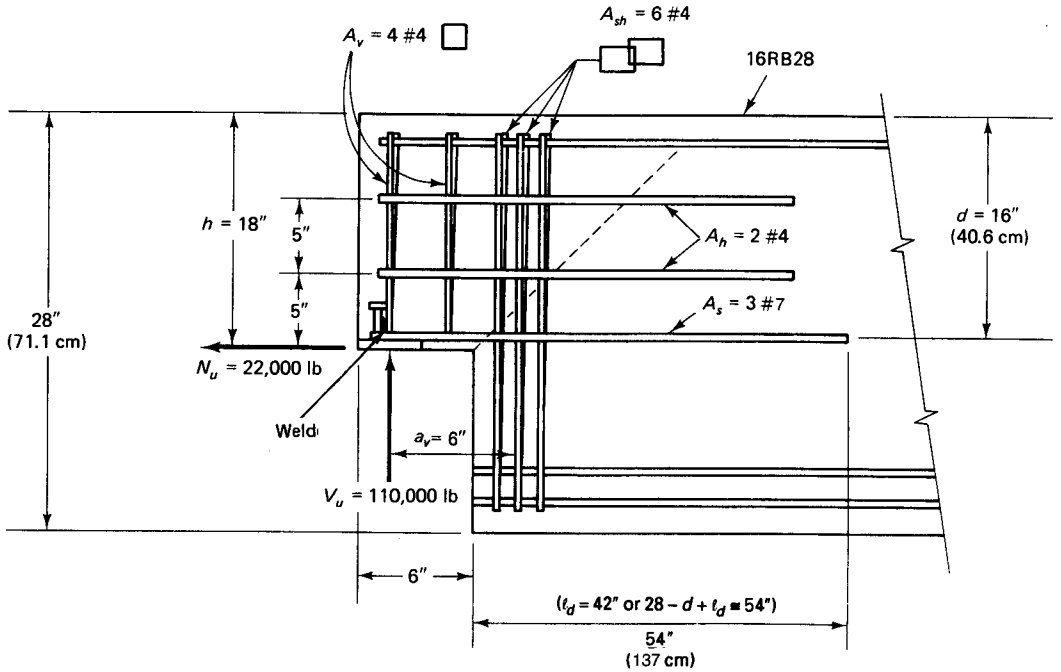


Figure 10.5 Reinforcing details for dapped-end beam connection in Example 10.2.

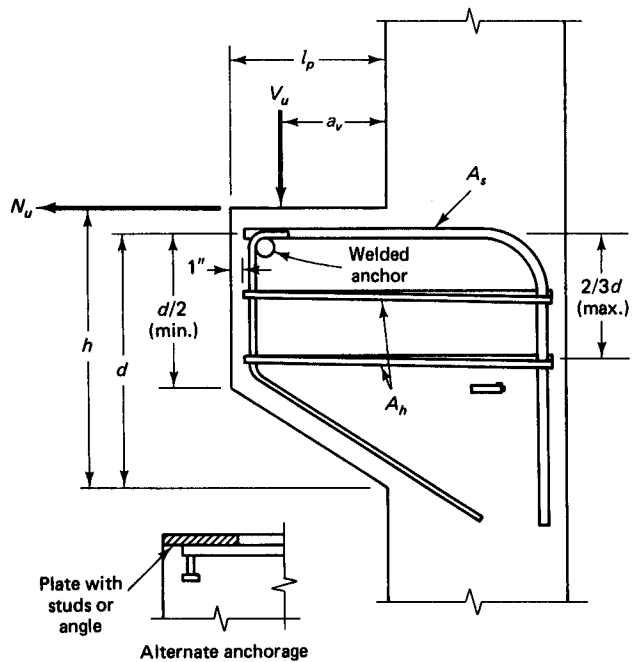


Figure 10.6 Typical corbel reinforcing details (see also Example 5.7.).

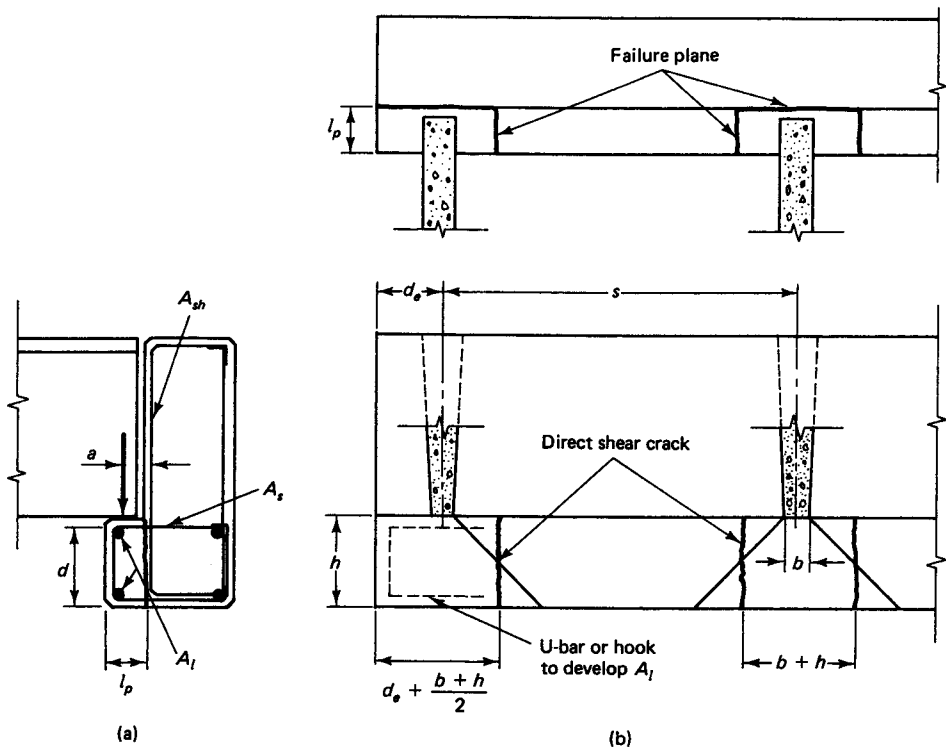
## 10.6 REINFORCED CONCRETE BRACKETS AND CORBELS

Corbels are short cantilevers whose shear span-to-depth ratio  $a/d$  does not exceed a value of 1.0. They are subjected to a direct shear  $V_u$  and a horizontal tension  $N_u$ . Section 5.14 in Chapter 5, the design flowchart in Sec. 5.14.4 and the detailed design example 5.7 give a comprehensive discussion and application of the shear-friction theory in the design of corbels. Working out the details of reinforcement of the connection is of major significance in the success of the design of a corbel as regards its ability to resist applied loads. Typical corbel reinforcing details are shown in Figure 10.6.

## 10.7 CONCRETE BEAM LEDGES

Beam ledges are used to support transverse precast prestressed beam-end concentrated loads in a manner similar to the way corbels operate. Direct shear acting on the ledge can cause vertical cracks as shown in Figure 10.7. If the load is noncontinuous and comes from one side, the ledge beam in L-shaped form acts like a spandrel beam and is subjected to torsional moment in addition to direct shear. The design of the ledge beam itself follows the procedures and examples in Chapter 5. The discussion presented here covers the design of the shear reinforcement for the cantilevering ledge, which often has a shear span-to-depth ratio  $l_p/d$  of  $\frac{1}{2}$  or less.

The nominal shear strength of the ledge at the reentrant corner can be determined by the lesser of the two values obtained from the following expressions under the given conditions:



**Figure 10.7** Connection design for beam ledges. (a) Ledge beam cross section. (b) Plan and elevation.

1.  $s > b + h$ 

$$V_n = 3h\lambda\sqrt{f'_c}(2l_p + b + h) \quad (10.20a)$$

$$V_n = h\lambda\sqrt{f'_c}(2l_p + b + h + 2d_e) \quad (10.20b)$$

2.  $s < b + h$ , and equal concentrated loads

$$V_n = 1.5h\lambda\sqrt{f'_c}(2l_p + b + h + s) \quad (10.21a)$$

$$V_n = h\lambda\sqrt{f'_c}\left(l_p + \frac{b + h}{2} + d_e + s\right) \quad (10.21b)$$

where  $l_p$  = ledge projection, in.  
 $b$  = width of bearing area, in.  
 $h$  = depth of beam ledge, in.  
 $s$  = spacing of concentrated loads, in.  
 $d_e$  = distance from center of load to end of beam, in.

If the ledge supports a continuous load or closely spaced concentrated loads, the nominal shear strength of the ledge section has to be evaluated from

$$V_n = 24h\lambda\sqrt{f'_c} \quad (10.22)$$

where  $V_n$  is in lb per ft of length. The design strength  $V_u$  has to be at least equal to the factored force  $V_u = \phi V_n$  for  $\phi = 0.85$ . If the applied factored load  $V_u$  exceeds the design strength as determined from Equation 10.20, 10.21, or 10.22, special reinforcement has to be provided in a design similar to the reinforcement required in a dapped beam end as discussed in Section 10.5. In such a case, the flexural reinforcement  $A_s$  is determined from Equation 10.12, the vertical diagonal tension “hanger” reinforcement  $A_{sh}$  from Equation



**Photo 10.5** Hoisting double-T prestressed roof element at the Civil Engineering Laboratory, Rutgers University.

10.17, and the longitudinal reinforcement  $A_l$  placed at the top and bottom fibers of the ledge from

$$A_l = \frac{200l_p d}{f_y} \quad (10.23)$$

where  $A_l$  is the area of the longitudinal reinforcement in the ledge. The reinforcement  $A_{sh}$  can be uniformly spaced over a width  $6h$  on either side of the bearing, but not to exceed half the distance to the next load. The bar spacing should not exceed the ledge depth  $h$  or 18 in., and the  $A_{sh}$  designed for the ledge need not be additive to the shear and torsional reinforcement of the total ledge beam.

### 10.7.1 Design of Ledge Beam Connection

#### Example 10.3

A garage floor structure is composed of 10-ft-wide double-T's supported at the exterior end by standard L-beam sections. The layout of the double-T's is such that a stem can be placed at any point on the ledge. The vertical factored end shear  $V_u = 24,000$  lb (107 kN) per stem, and the horizontal tensile force  $N_u = 5,000$  lb (22.4 kN) per stem. Compute the nominal shear strength of the ledge and design the reinforcement if necessary, given that

$$b = 4 \text{ in.}$$

$$h = 12 \text{ in.}$$

$$d = 10.5 \text{ in.}$$

$$l_p = 6 \text{ in. (15 cm)}$$

$$s = 48 \text{ in. (122 cm)}$$

$$f'_c = 5,000 \text{ psi (34.5 MPa), normal weight}$$

$$f_y = f_{yt} = 60,000 \text{ psi (414 MPa)}$$



**Photo 10.6** Mariners Island Office Building, San Mateo, California (Courtesy, Robert Englekirk Consulting Structural Engineers and W2MH Group Architects, Los Angeles, California. Photo by Dixie Carillo.).

**Solution:**

$$V_u = 24,000 \text{ lb}$$

$$N_u = 5,000 \text{ lb}$$

$$s = 48 \text{ in.}$$

$$b + h = 4 + 12 = 16 \text{ in.}$$

$$\text{Min. } d_e = \frac{1}{2} b = 2 \text{ in.}$$

$$2l_p + b + h = 2 \times 6 + 4 + 12 = 28 \text{ in.}$$

Since  $s > b + h$ , and  $d_e < 2l_p + b + h$ , Equation 10.20b applies, and the available  $V_n = h\lambda \sqrt{f'_c} (2l_p + b + h + 2d_e) = 12 \times 1.0 \sqrt{5,000} (2 \times 6 + 4 + 12 + 2 \times 2) = 27,153 \text{ lb}$  (120.8 kN). So the design  $V_u = \phi V_n = 0.75 \times 27,153 = 20,365 \text{ lb} < \text{Factored } V_u = 24,000 \text{ lb}$ , and we have to use dapped section reinforcement design.

**Flexural Reinforcement  $A_s$ .** The shear span  $a \cong 3l_p/4 + 1.5 = 3 \times 6/4 + 1.5 = 6 \text{ in.}$  (15 cm). Since  $N_u/V_u = 5,000/24,000 = 0.21 > 20\%$ , use  $N_u = 5,000 \text{ lb}$ . Then, from Equation 10.12,

$$A_s = \left[ \frac{1}{\phi f_y} \left[ V_u \left( \frac{a_v}{d} \right) + N_u \left( \frac{h}{d} \right) \right] \right]$$

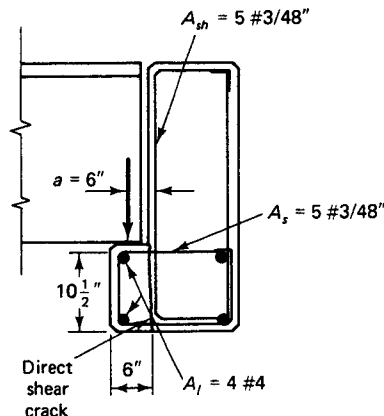
$$= \frac{1}{0.85 \times 60,000} \left[ 24,000 \frac{6}{10.5} + 5,000 \frac{12}{10.5} \right] = 0.38 \text{ in}^2 (2.45 \text{ cm}^2)$$

Since  $6h = 6 \times 12 > s/2 = 24 \text{ in.}$ , distribute the reinforcement  $s/2 = 24 \text{ in.}$  on each side of the load.

The width of the band for placement of flexural reinforcement  $A_s = 2 \times 24 = 48 \text{ in.}$ , and the maximum bar spacing  $= h = 12 \text{ in.}$  So use four #3 bars in each 48-in. band width  $= 0.44 \text{ in.}^2 > \text{required } 0.38 \text{ in.}^2$  Accordingly, place two additional bars at the beam end in order to provide equivalent reinforcement for the stem placed near the end.

**Diagonal Tension Vertical Reinforcement  $A_{st}$**  From Equation 10.17,

$$A_{sh} = \frac{V_u}{\phi f_{yt}} = \frac{24,000}{0.75 \times 60,000} = 0.53 \text{ in.}^2 (3.42 \text{ cm}^2)$$



**Figure 10.8** Ledge connection reinforcement in Example 10.3.

over a 48-in.-width band. Thus,  $A_{sh}/ft = 0.47/4 = 0.12 \text{ in.}^2/\text{ft}$ , or #3 bars @ 11 in. Consequently, use five #3 bars in each 48-in. band width =  $0.55 \text{ in.}^2 >$  required  $0.53 \text{ in.}^2$ . Then, for practical considerations, use the same number and spacing for both the  $A_s$  and  $A_{sh}$  steel, namely, five #3 closed hoops. Note that only one leg of the hanger steel hoop  $A_{sh}$  is accounted for in the selection of the five #3 bars in order to provide for the required concentration of the steel near the reentrant corner.

**Longitudinal Reinforcement  $A_l$ .** From Equation 10.23,

$$A_l = \frac{200l_p d}{f_y} = \frac{200 \times 6 \times 10.5}{60,000} = 0.21 \text{ in.}^2$$

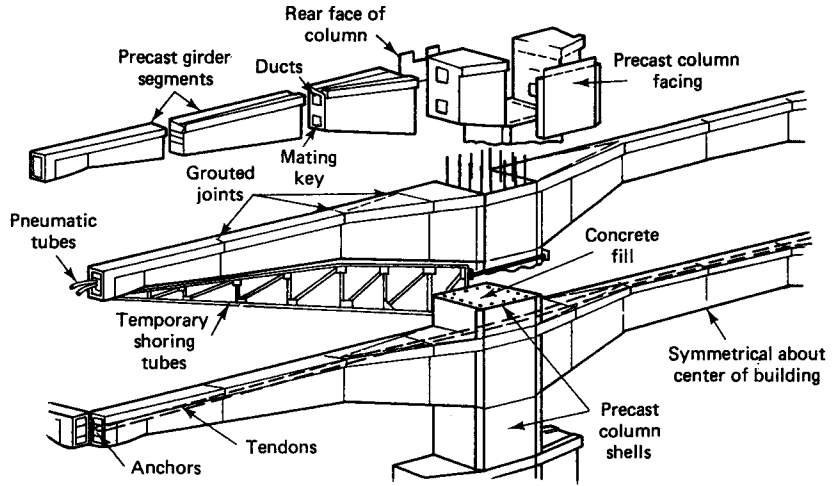
For practical field considerations, use #4 bars, one on each corner of the ledge, giving four #4 bars =  $0.80 \text{ in.}^2$  (12.7 mm dia)  $> 0.21 \text{ in.}^2$ , O.K.

The complete design of the ledge beam, of course, would require shear and torsional analysis of the total section to resist the total shear transmitted by all the double-T supported stems and the torsional moment caused by the application of the *eccentric* load from the supported stems. The designed ledge reinforcement area discussed in this example is in addition to the shear and torsional reinforcement required for the total beam.

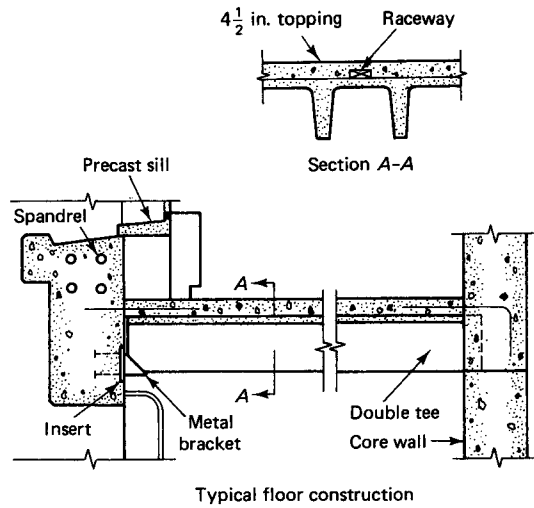
Figure 10.8 gives the details of the ledge connection reinforcement, but does not include the shear and torsional reinforcement that has to be designed for the entire L-beam.

## 10.8 SELECTED CONNECTION DETAILS

As discussed in Section 10.1, connections are the major links in the overall structural system whose performance determines whether the structure will be safe and stable. Consequently, the design engineer has to be particularly cautious in the design and selection of the appropriate section for reasons of both safety and economy. Details of the design of numerous types of connections are given in Refs. 10.1 and 10.2, and Figures 10.9 through 10.16 show typical details of selected connections from these two references. The diagrams illustrate the application of the theories presented in this chapter.



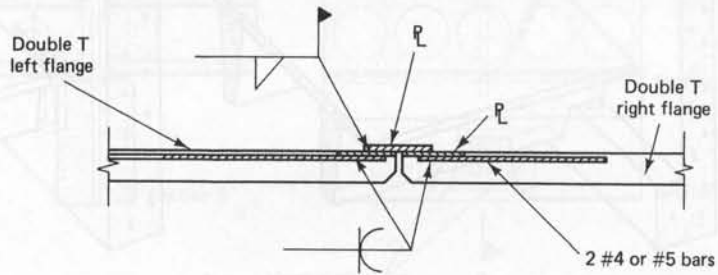
Beam assembly showing precast elements, temporary truss and prestressing



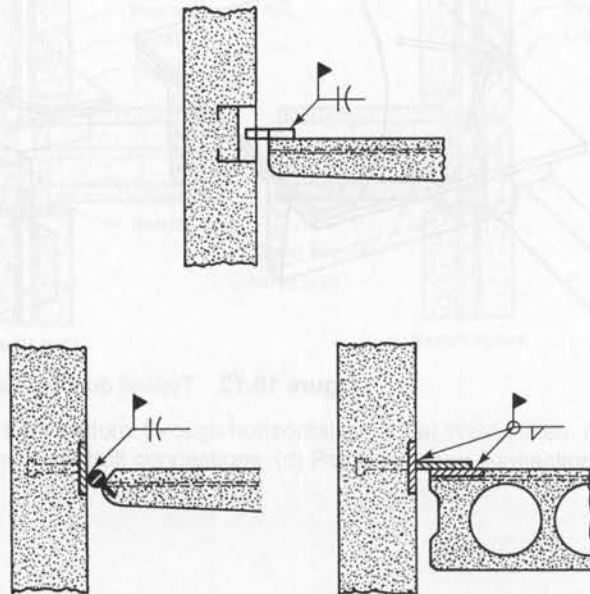
**Figure 10.9** Construction method and typical joint details in Gulf Life Prestressed Building, Jacksonville, Florida.



**Photo 10.7** Installation of prestressed double-T elements at the rod-suspended support, Civil Engineering Laboratory, Rutgers University.



**Figure 10.10** Connection of double-T flanges if no composite-action concrete topping is used.



**Figure 10.11** Typical precast floor-to-wall connections.



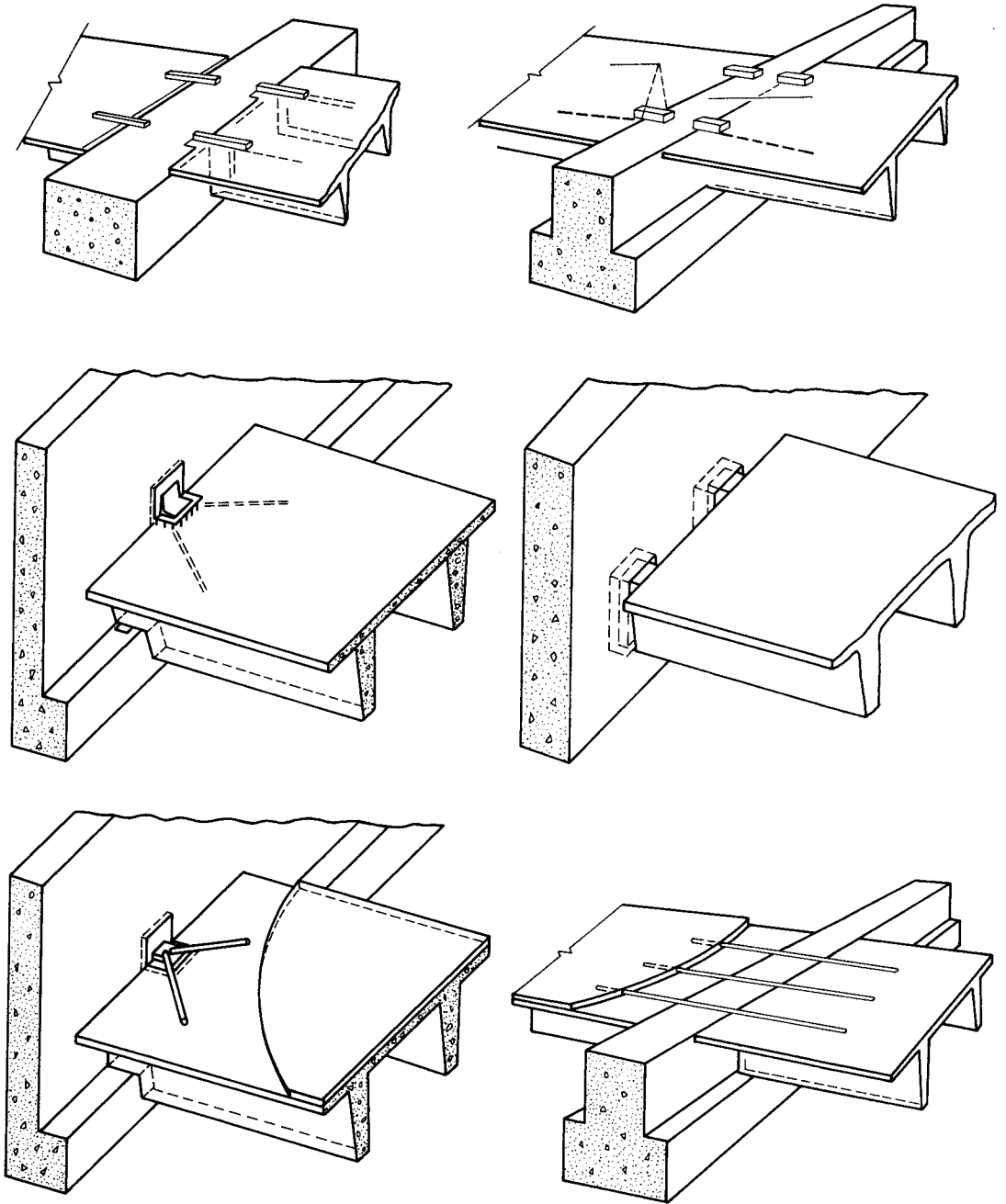
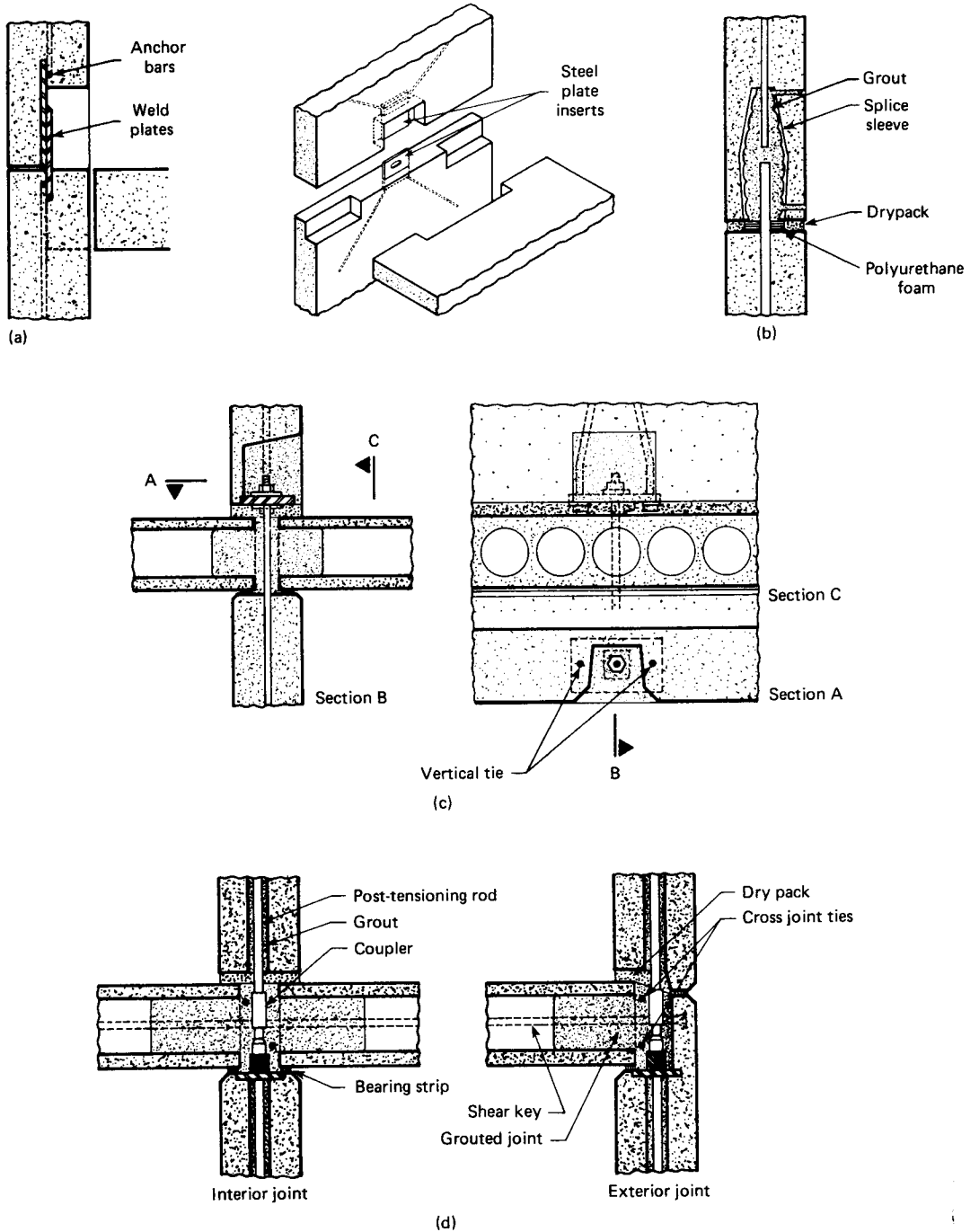


Figure 10.12 Typical double-T connections.



**Figure 10.13** Connections through horizontal joints. (a) Weld plates. (b) Grouted splice sleeve. (c) Plate-bolt connections. (d) Post-tensioned connection.

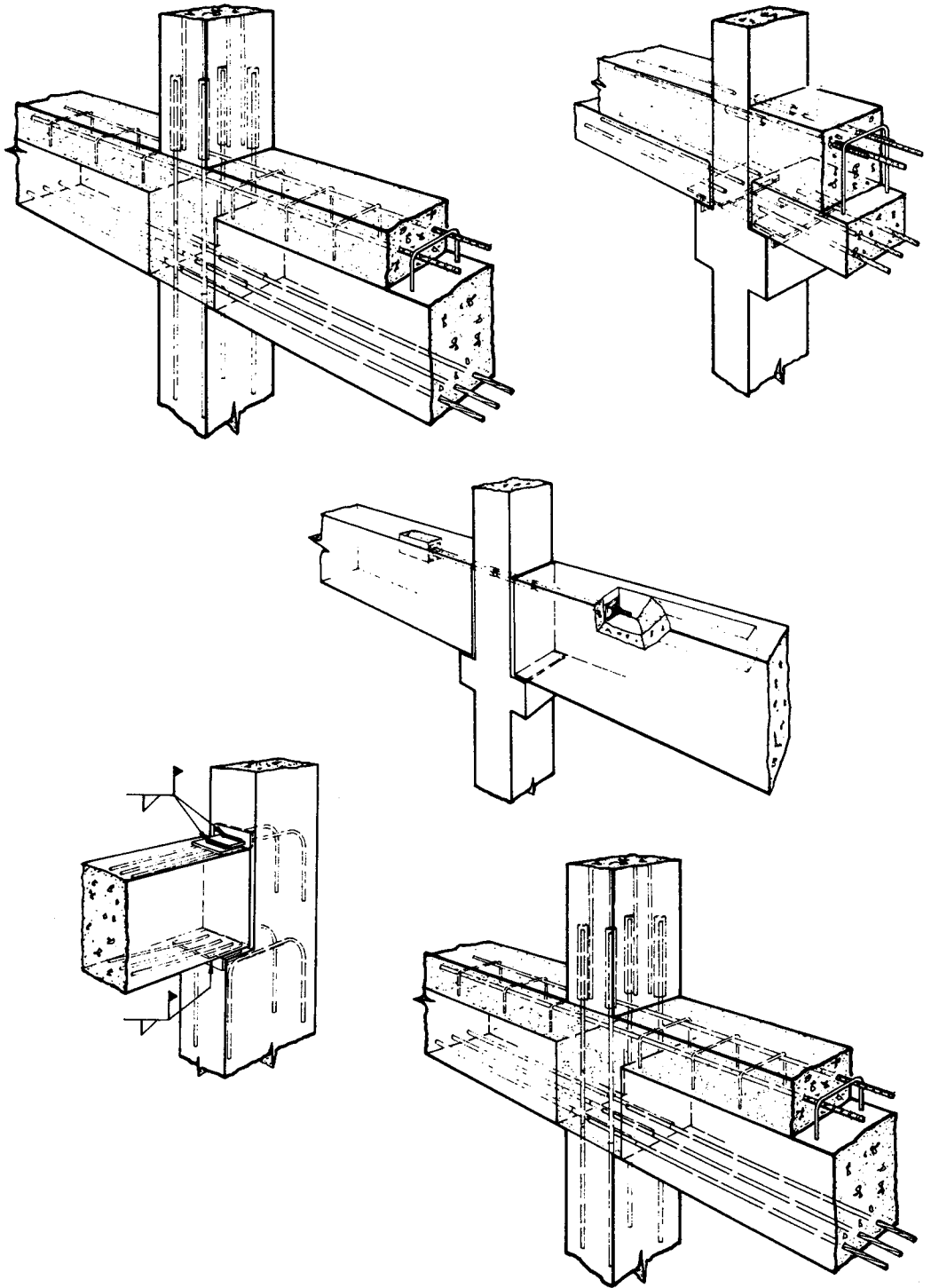


Figure 10.14 Moment connections.

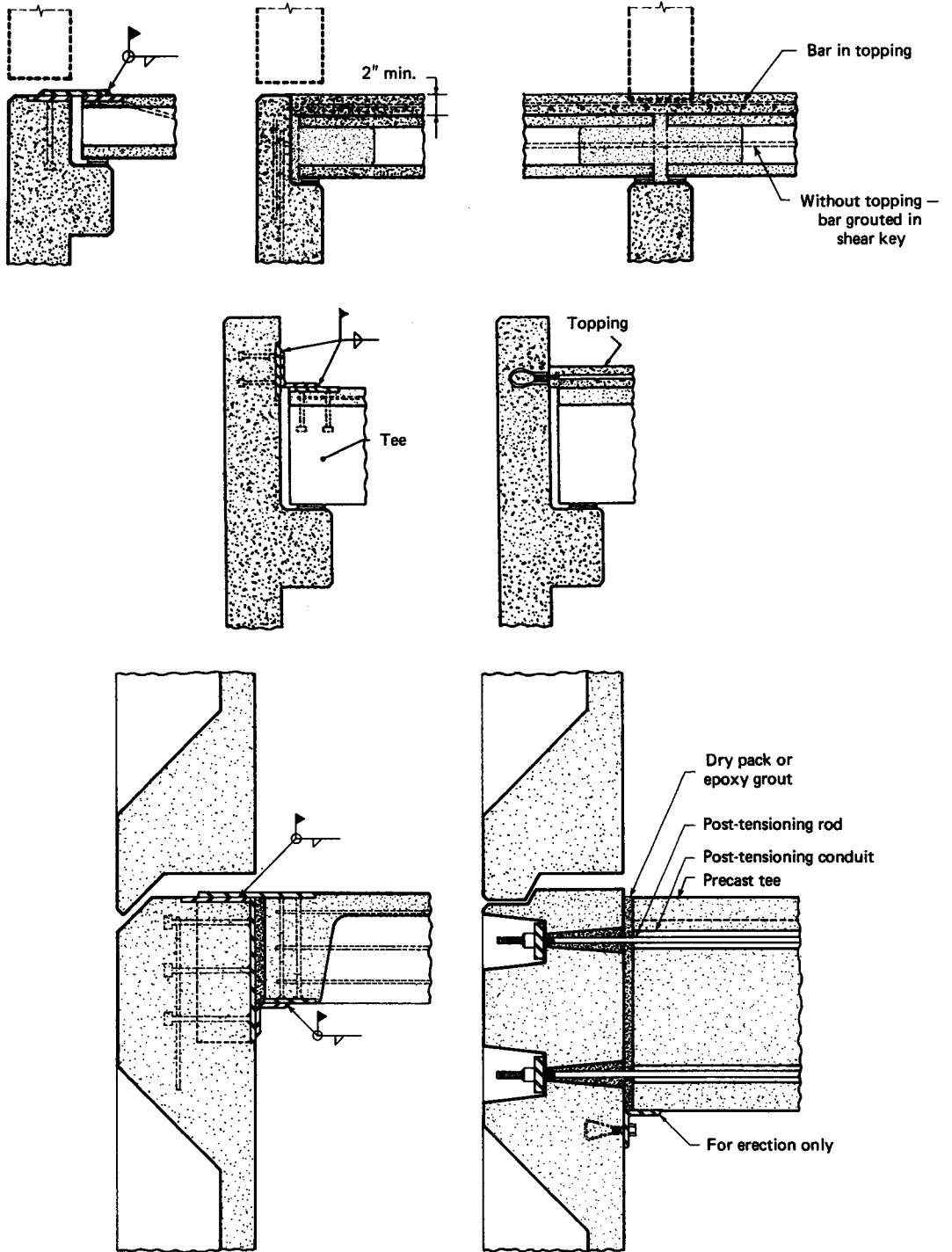
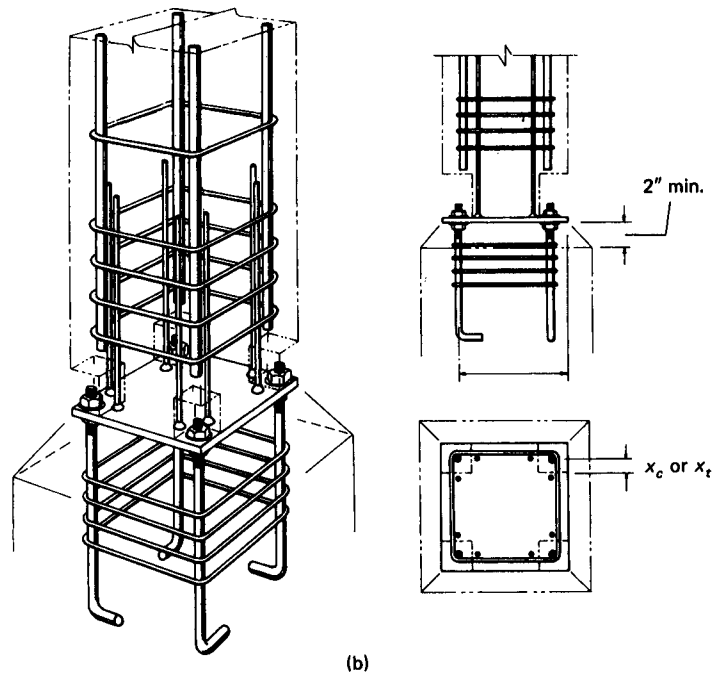
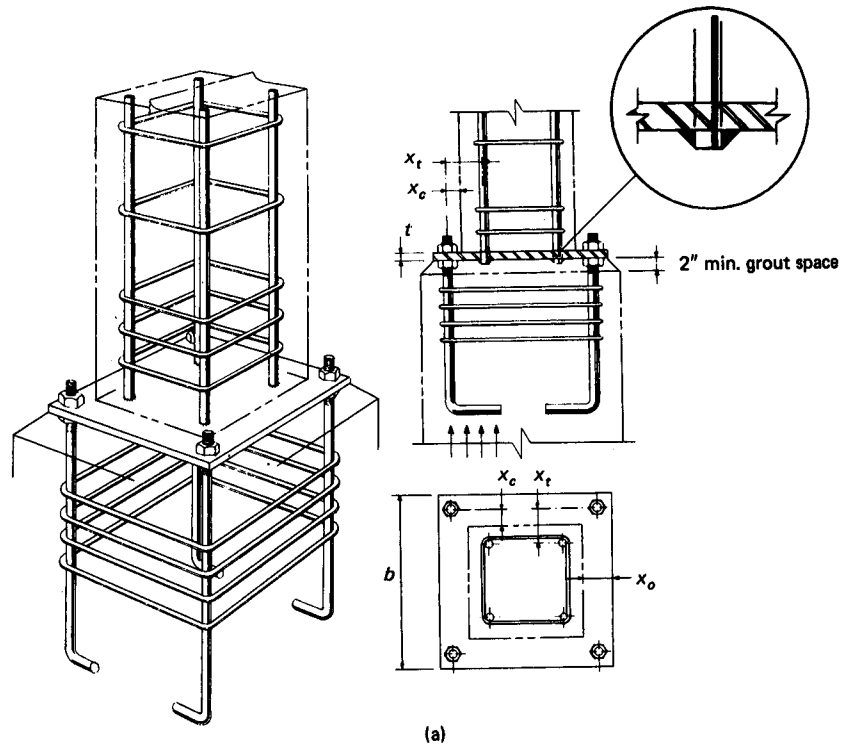


Figure 10.15 Floor-to-bearing wall connections.



**Figure 10.16** Column base connections. (a) Base plate larger than column. (b) Flush base plate.

**SELECTED REFERENCES**

- 10.1** Prestressed Concrete Institute. *PCI Design Handbook—Precast and Prestressed Concrete*. 6th ed. Prestressed Concrete Institute, Chicago, 2004.
- 10.2** PCI Committee on Connection Details. *Manual on Design and Detailing of Connections for Precast and Prestressed Concrete*. Prestressed Concrete Institute, Chicago, 1988.
- 10.3** Post-Tensioning Institute. *Post-Tensioning Manual*. 6th ed. Post-Tensioning Institute, Phoenix, 2006, pp. 354.
- 10.4** Shaikh, A. F., and Yi, W. “In-Place Strength of Welded Headed Studs.” *Journal of the Prestressed Concrete Institute* 30, 1985, 56–81.
- 10.5** Mattock, A. H., and Chan, T. C. “Design and Behavior of Dapped-End Beams.” *Journal of the Prestressed Concrete Institute* 30, 1985, 28–45.
- 10.6** Mirza, S. A., and Furlong, R. W. “Serviceability Behavior of Concrete Inverted T-Beam Bridge Bent Caps.” *Journal of the American Concrete Institute* 80, 1983, 294–304.
- 10.7** Clough, D. P. “Design of Connections for Precast Prestressed Concrete Buildings for the Effect of Earthquake.” *PCI Technical Report No. 5*. Prestressed Concrete Institute, Chicago, 1985.
- 10.8** PCI Erectors Committee. *Recommended Practice for Erection of Precast Concrete*. Prestressed Concrete Institute, Chicago, 1985, pp. 1–198.

**PROBLEMS**

- 10.1** Design the end reinforcement required to resist the bearing stresses caused by an end vertical shear  $V_u = 125,000$  lb (556 kN) and a horizontal tensile force  $N_u = 24,000$  lb (107 kN) in a PCI 16RB28 rectangular beam supported at its ends on 5 in.  $\times$  5 in. pads. Take  $f'_c = 5,000$  psi (34.47 MPa), normal weight, and  $f_y = 60,000$  psi (413.7 MPa).
- 10.2** If the beam in Problem 10.1 is dapped at its ends and rests on concrete corbels, design the flexure and direct shear reinforcement for the dapped ends in order to prevent potential shear cracking and failure.
- 10.3** Solve Example 10.3 for factored loads  $V_u = 29,000$  lb (128 kN) and factored  $N_u = 2,500$  lb (11.1 kN).

# 11



## PRESTRESSED CONCRETE CIRCULAR STORAGE TANKS AND SHELL ROOFS

### 11.1 INTRODUCTION

Prestressed concrete circular tanks are usually the best combination of structural form and material for the storage of liquids and solids. Their performance over the past half-century indicates that, when designed with reasonable skill and care, they can function for 50 years or more without significant maintenance problems.

The first effort to introduce circumferential prestressing into circular structures was that of W. S. Hewett, who applied the tie rod and turnbuckle principle in the early 1920s (Ref. 11.6). But the reinforcing steel available at that time had very low yield strength, limiting the applied tension to not more than 30,000 to 35,000 psi (206.9 to 241.3 MPa). Indeed, significant long-term losses due to concrete creep, shrinkage, and steel relaxation almost neutralized the prestressing force. As higher strength steel wires became available, J. M. Crom, Sr., in the 1940s, successfully developed the principle of winding high-tensile wires around the circular walls of prestressed tanks. Since that time, over 3,000 circular storage structures have been built of various dimensions up to diameters in excess of 300 feet (92 m).

Two 583,000-bbl (92,500-m<sup>3</sup>) double-wall prestressed concrete tanks for liquefied natural gas storage, Philadelphia. (Courtesy, N.A. Legatos, Preload Technology, Inc., New York.)

The major advantage in performance and economy of using circular prestressing in concrete tanks over regular reinforcement is the requirement that no cracking be allowed. The circumferential “hugging” hoop stress in compression provided by external winding of the prestressing wires around the tank shell is the natural technique for eliminating cracking in the exterior walls due to the internal liquid, solid, or gaseous loads that the tank holds. Other techniques of circumferential prestressing using *individual* tendons which are anchored to buttresses have been more widely used in Europe than in North America for reasons of local economy and technological status.

Containment vessels utilizing circumferential prestressing, which can be either situ-cast or precast in segments, include water storage tanks, wastewater tanks and effluent clarifiers, silos, chemical and oil storage tanks, offshore oil platform structures, cryogenic vessels, and nuclear reactor pressure vessels. All these structures are considered thin shells because of the exceedingly small ratio of the container thickness to its diameter. Because no cracking at working-load levels is permitted, the shells are expected to behave elastically under working-load and overload conditions.

## 11.2 DESIGN PRINCIPLES AND PROCEDURES

### 11.2.1 Internal Loads

Considering the behavior of circular tanks involves examining both the interior pressure due to the material contained therein acting on a thin-walled cylindrical shell cross section and the exterior radial and sometimes vertical prestressing forces balancing the interior forces. The interior pressure is horizontally radial, but varies vertically depending on the type of material contained in the tank. If the material is water or a similar liquid, the vertical pressure distribution against the tank walls is *triangular*, with maximum intensity at the base of the wall. Other liquids which are accompanied by gas would give a *constant* horizontal pressure throughout the height of the wall. The vertical pressure distribution in tanks used for storage of granular material such as grain or coal would be essentially similar to the gas pressure distribution, with a constant value along most of the depth of the material contained. Figure 11.1 shows the pressure distributions for these three cases of loading.

The basic elastic theory of cylindrical shells applies to the analysis and design of the walls of prestressed tanks. A ring force causes ring tension in the thin cylindrical walls, assumed unrestrained at the ends at each horizontal section. The magnitude of the force is proportional to the internally applied pressure, and *no* vertical moment is produced along the height of the walls. If the wall ends are restrained, the magnitude of the ring force changes and a bending moment is induced in the vertical section of the tank wall. The magnitudes of the ring forces and vertical moments are thus a function of the degree of restraint of the cylindrical shell at its boundaries and are computed from the elastic shell theory and its simplifications and idealizations to be discussed subsequently.

**Liquid Load and Freely Sliding Base.** From basic mechanics, the ring force is

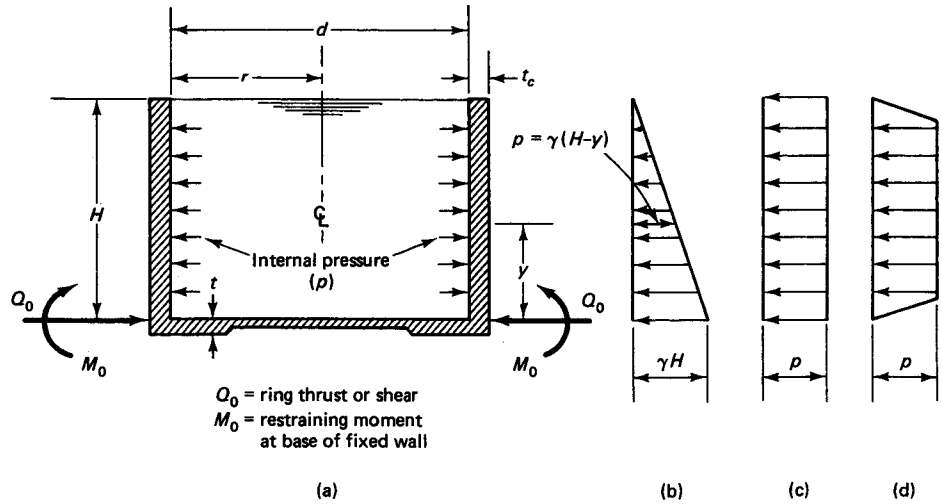
$$F = \frac{pd}{2} = pr \quad (11.1a)$$

and the ring stress is

$$f_R = \frac{pd}{2t} = \frac{pr}{t} \quad (11.1b)$$

where  $d$  = diameter of cylinder  
 $r$  = radius of cylinder





**Figure 11.1** Tank internal pressure diagrams. (a) Tank cross section, showing radial shear  $Q_0$  and restraining moment  $M_0$  at base for fixed-base walls. (b) Liquid pressure, triangular load. (c) Gaseous pressure, rectangular load. (d) Granular pressure, trapezoidal load.

$t$  = thickness of wall core

$p$  = unit internal pressure at wall base =  $\gamma H$

$\gamma$  = unit weight of material contained in vessel.

The tensile ring stress *at any point below the surface* of the material contained in the vessel becomes

$$f_R = \gamma(H - y) \frac{d}{2t} = \gamma(H - y) \frac{r}{t} \quad (11.2a)$$

where  $H$  is the height of the liquid contained and  $y$  is the distance *above* the base. The corresponding ring force is

$$F = \gamma(H - y)r \quad (11.2b)$$

The maximum tensile ring stress at the base of the freely sliding tank wall for  $y = 0$  becomes, as in Equation 11.1b,

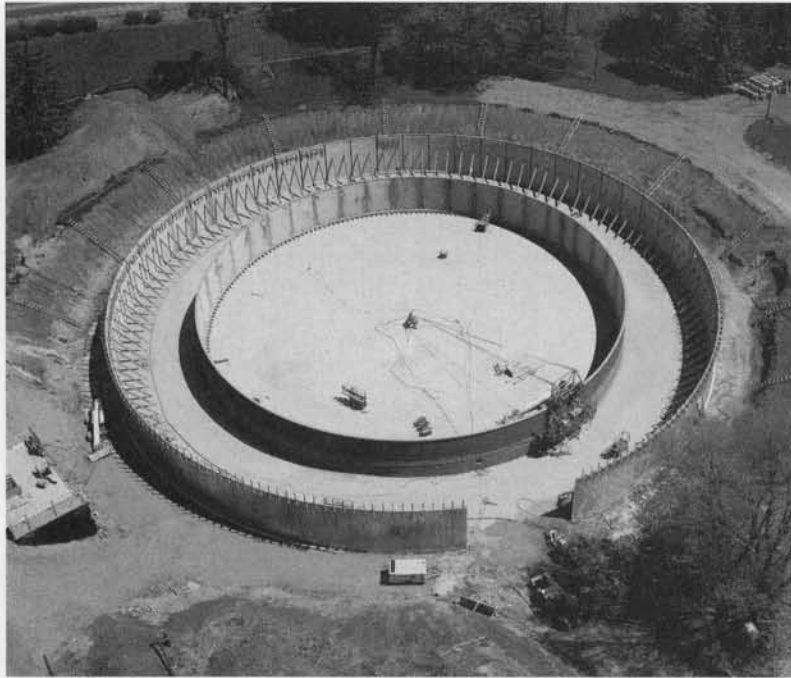
$$f_{R(\max)} = \frac{\gamma H d}{2t} = \frac{\gamma h r}{t} \quad (11.2c)$$

**Gaseous Load on Freely Sliding Base.** Again from basic principles of mechanics, the constant tensile ring stress is

$$f_R = \frac{pd}{2t} = \frac{pr}{t} \quad (11.3)$$

Note that while theoretically the centerline diameter dimension is more accurate to use, the ratio  $t/d$  is so small that the use of the internal diameter  $d$  is appropriate.

**Liquid and Gaseous Load on a Restrained Wall Base.** If the base of the wall is fixed or pinned, the ring tension at the base vanishes. Because of the restraint imposed



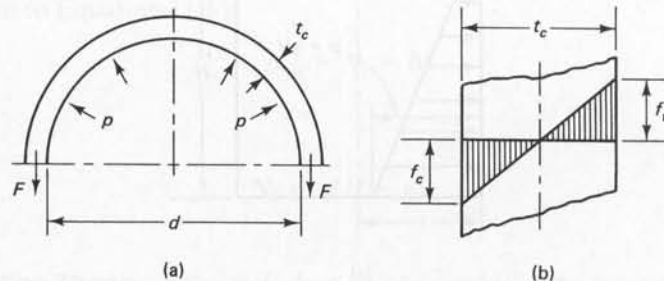
**Photo 11.1** 4.0 Million Gallon Preload Tank, City of Troy, Ohio. (Courtesy, N.A. Legatos, Preload Inc., Garden City, New York.)

on the base, the simple membrane theory of shells is then no longer applicable, due to the imposed deformations of the restraining force at the wall base. Instead, bending modifications to the membrane stresses become necessary (see Refs. 11.2 and 11.6), and the deviation of the ring tension at intermediate planes along the wall height must be approximated as in Ref. 11.2 and the discussion in Sec. 11.3.

If the vertical bending moment in the horizontal plane of the wall at any height is  $M_y$ , the flexural stress in compression or tension in the concrete becomes

$$f_t = f_c = \frac{M_y}{S} = \frac{6M_y}{t^2} \text{ per unit height} \quad (11.4)$$

The distribution of the flexural stress across the thickness of the tank wall is shown in Figure 11.2.



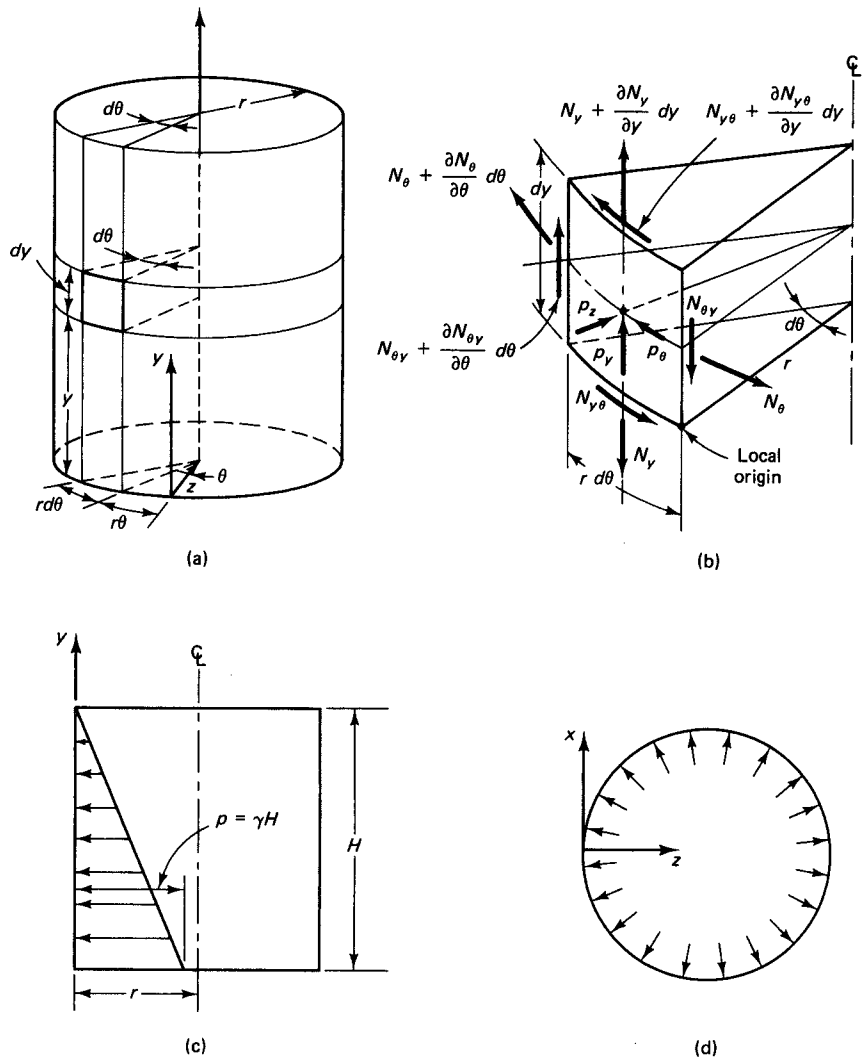
**Figure 11.2** Ring tension and flexural stresses. (a) Ring tension internal force  $F$  in the horizontal section. (b) Flexural stress due to bending moment  $M$  in the wall thickness of the vertical section.

### 11.2.2 Restraining Moment $M_0$ and Radial Shear Force $Q_0$ at Freely Sliding Wall Base Due to Liquid Pressure

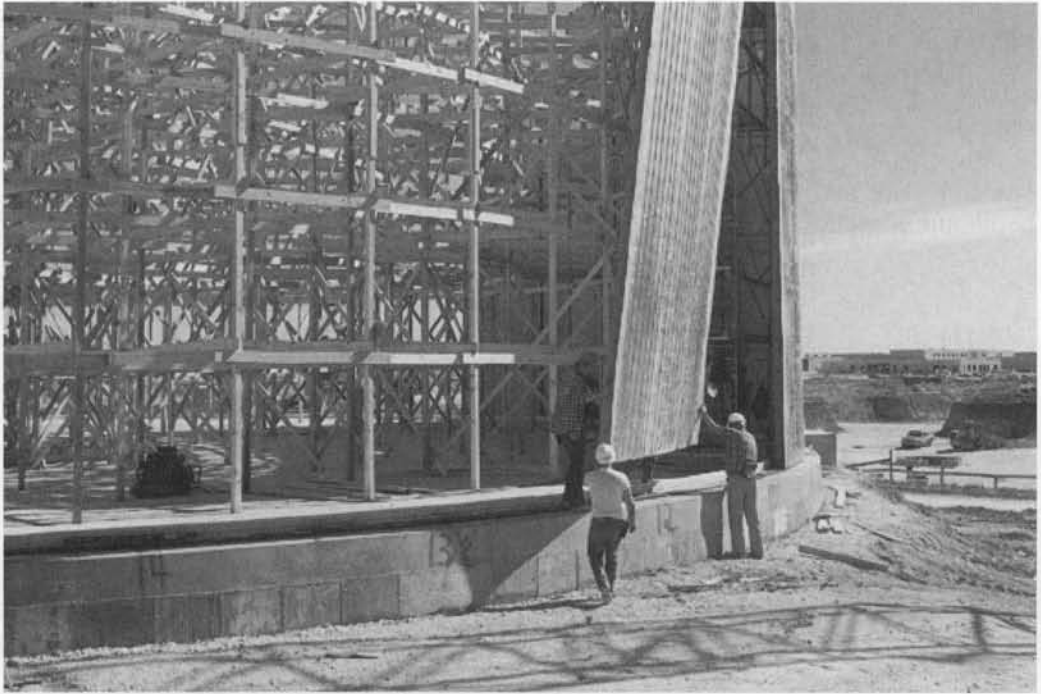
**11.2.2.1 Membrane Theory.** The study of forces and stresses in a circular uncracked tank wall is an elasticity problem in cylindrical shell analysis. If the shell is free to deform under the influence of the internal liquid pressure, the basic membrane equations of equilibrium apply. The longitudinal unit force  $N_y$ , the “hugging” circumferential unit force  $N_\theta$ , and the central unit shears  $N_{y\theta}$  and  $N_{\theta y}$  are shown in the differential element of Figure 11.3(b). Note that these *four* unknowns all act in the plane of the shell.

The basic three equations of equilibrium for these four unknown unit forces are

$$\frac{\partial N_\theta}{\partial \theta} + r \frac{\partial N_{y\theta}}{\partial y} + p_\theta r = 0 \tag{11.5a}$$



**Figure 11.3** Membrane forces in cylindrical tank. (a) Tank shell geometry. (b) Shell membrane forces. (c) Liquid-filled tank elevation. (d) Axisymmetrical internal pressure at any horizontal plane.



**Photo 11.2** Panel Being Lifted in a Preload Prestressed Tank (Courtesy, N.A. Legatos, Preload Inc., Garden City, New York.)

$$r \frac{\partial N_y}{\partial y} + \frac{\partial N_{\theta y}}{\partial \theta} + p_y r = 0 \quad (11.5b)$$

$$\frac{N_{\theta}}{r} = +p_z = 0 \quad (11.5c)$$

where  $\partial N_{y\theta} = \partial N_{\theta y}$  due to loading symmetry. The unknowns are thus reduced to three, representing a statically *determinate* structure subjected to direct forces only.

For axisymmetrical loading as in Figure 11.3(c),  $p_{\theta} = p_y = 0$  and  $p_z = p \cdot f(y)$ , independent of  $\theta$ . Hence,

$$p_z = -\gamma(H - y) \quad (11.6)$$

and the solution to Equation 11.5 is

$$N_{y\theta} = N_y = 0$$

and

$$N_{\theta} = \gamma(H - y)r \quad (11.7)$$

**11.2.2.2 Bending Theory.** The introduction of restraint at the boundary of the vessel induces radial ring horizontal shear and vertical moments in the shell. Consequently, the membrane force equations presented in the previous section have to be modified by superimposing these additional moments and shears. The modified expressions are de-

noted the *bending theory of circular shells*; the theory accounts for strain compatibility requirements in the induced deformations caused by the induced shears and moments.

The bending moments and central shears in the axisymmetrically loaded cylindrical shell are shown by force and moment vectors in Figure 11.4. The infinitesimal element  $ABCD$  shows the points of application and sense of the unit moments  $M_y$  about the  $x$ -axis and  $M_\theta$  about the  $y$ -axis, the circumferential unit moments  $M_{y\theta}$  and  $M_{\theta y}$ , the unit normal shear  $Q_y$  acting in the plane of the vertical shell generator and perpendicularly to the shell axis, and the unit radial shear  $Q_\theta$  acting through the shell radius in the plane of the shell parallels.

Superposition of the moments and shears in Figure 11.4 on the forces in Figure 11.3(b) results in the following equilibrium equations:

$$\frac{\partial N_\theta}{\partial \theta} + \frac{\partial N_{y\theta}}{\partial y} - Q_\theta + p_\theta r = 0 \quad (11.8a)$$

$$\frac{\partial N_y}{\partial y} r + \frac{\partial N_{\theta y}}{\partial \theta} + p_y r = 0 \quad (11.8b)$$

$$\frac{\partial Q_\theta}{\partial \theta} + \frac{\partial Q_y}{\partial y} r + N_\theta + p_z r = 0 \quad (11.8c)$$

$$-\frac{\partial M_y}{\partial y} r + \frac{\partial M_{y\theta}}{\partial y} + Q_y r = 0 \quad (11.8d)$$

$$\frac{\partial M_\theta}{\partial \theta} + \frac{\partial M_{y\theta}}{\partial y} r - Q_\theta r = 0 \quad (11.8e)$$

Due to symmetry of loading,  $N_{y\theta} = N_{\theta y} = M_{y\theta} = M_{\theta y} = 0$ , and  $dQ_\theta$  can be disregarded, reducing the partial differential equations 11.8 to the set of the ordinary differential equations

$$\frac{dN_y}{dy} r + p_y r = 0 \quad (11.9a)$$

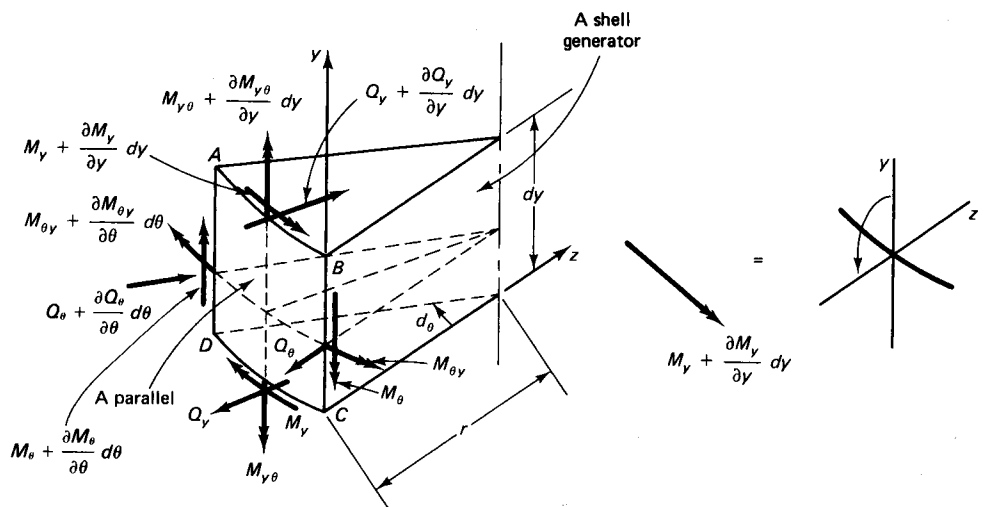


Figure 11.4 Bending moments and normal shears in a cylindrical shell wall.

$$\frac{dQ_y}{dy} r + N_\theta + p_z r = 0 \quad (11.9b)$$

$$-\frac{dM_y}{dy} r + Q_y r = 0 \quad (11.9c)$$

With the central membrane forces  $N_y$  constant and taken to be zero (see Refs. 11.1 and 11.3), the remaining equations 11.9b and 11.9c can be written in the following simplified form having the three unknowns  $N_\theta$ ,  $Q_y$ , and  $M_y$ :

$$\frac{dQ_y}{dy} + \frac{1}{r} N_\theta = -p_z \quad (11.10a)$$

$$\frac{dM_y}{dy} - Q_y = 0 \quad (11.10b)$$

In order to solve these equations, displacements have to be considered and equations of geometry developed.

**Force Equations.** If  $v$  and  $w$  are the displacements in the  $y$  and  $z$  directions, then the unit strains in these directions are, respectively,

$$\epsilon_y = \frac{dv}{dy}$$

and

$$\epsilon_\theta = -\frac{w}{r}$$

which give

$$N_y = \frac{Et}{1 - \mu^2} (\epsilon_y + \mu \epsilon_\theta) = \frac{Et}{1 - \mu^2} \left( \frac{dv}{dy} - \mu \frac{w}{r} \right) = 0 \quad (11.11a)$$



**Photo 11.3** 250,000-bbl (39,750-m<sup>3</sup>) prestressed concrete propane gas storage container, Winnipeg, Manitoba, Canada. (Courtesy, N.A. Legatos, Preload Technology, Inc., New York.)

and

$$N_{\theta} = \frac{Et}{1 - \mu^2} (\epsilon_{\theta} + \mu \epsilon_y) = \frac{Et}{1 - \mu^2} \left( -\frac{w}{r} + \mu \frac{dv}{dy} \right) \quad (11.11b)$$

where  $\mu$  = Poisson's ratio

$t$  = thickness of the wall core.

From Equation 11.11a,

$$\frac{dv}{dy} = \mu \frac{w}{r} \quad (11.12a)$$

From Equation 11.11b,

$$N_{\theta} = -Et \frac{w}{r} \quad (11.12b)$$

**Moment Equations.** Due to symmetry, there is no change in curvature in the circumferential direction; hence, the curvature in the  $y$  direction has to be equal to  $-d^2 v/dy^2$ . Using the same moment expressions for thin elastic plates results in

$$M_{\theta} = \mu M_y \quad (11.13a)$$

$$M_y = -D \frac{d^2 w}{dy^2} \quad (11.13b)$$

where  $D = Et^3/12(1 - \mu^2)$  is the shell or plate flexural rigidity.

Introducing Equations 11.12 and 11.13 into Equations 11.10 results in

$$\frac{d^2}{dx^2} \left( D \frac{d^2 w}{dy^2} \right) + \frac{Et}{r^2} w = p_z \quad (11.14)$$

If the wall thickness  $t$  is constant, Equation 11.14 becomes

$$D \frac{d^4 w}{dy^4} + \frac{Et}{r^2} w = p_z \quad (11.15)$$

Letting

$$\beta^4 = \frac{Et}{4r^2 D} = \frac{3(1 - \mu^2)}{(rt)^2}$$

Equation 11.15 becomes

$$\frac{d^4 w}{dy^4} + 4\beta^4 w = \frac{p_z}{D} \quad (11.16)$$

Equation 11.16 is the same as is obtained for a prismatic bar with flexural rigidity  $D$  supported by a continuous elastic foundation and subject to the action of a unit load intensity  $p_z$ . The general solution to this equation (Ref. 11.1) for the *radial* displacement in the  $z$ -direction is

$$w = e^{\beta y} (C_1 \cos \beta y + C_2 \sin \beta y) + e^{-\beta y} (C_3 \cos \beta y + C_4 \sin \beta y) + f(y) \quad (11.17)$$

where  $f(y)$  is the particular solution of Equation 11.16 as a membrane solution giving displacement

$$w = \frac{p_z r^2}{Et}$$

### 11.2.3 General Equations of Forces and Displacements

Solving Equation 11.17 and introducing the notation

$$\Phi(\beta y) = e^{-\beta y}(\cos \beta y + \sin \beta y)$$

$$\Psi(\beta y) = e^{-\beta y}(\cos \beta y - \sin \beta y)$$

$$\theta(\beta y) = e^{-\beta y} \cos \beta y$$

$$\zeta(\beta y) = e^{-\beta y} \sin \beta y$$

the expression for radial deformation in the  $z$  direction and its consecutive derivatives at any height  $y$  above the wall base can be evaluated from the following simplified expressions as a function of the wall base unit moments  $M_0$  and unit radial shears  $Q_0$ :

$$\text{Deflection } w = -\frac{1}{2\beta^3 D} [\beta M_0 \psi(\beta y) + Q_0 \theta(\beta y)] \quad (11.18a)$$

$$\text{Rotation } \frac{dw}{dy} = \frac{1}{2\beta^2 D} [2\beta M_0 \theta(\beta y) + Q_0 \Phi(\beta y)] \quad (11.18b)$$

$$\frac{d^2 w}{dy^2} = -\frac{1}{2\beta D} [2\beta M_0 \Phi(\beta y) + 2Q_0 \zeta(\beta y)] \quad (11.18c)$$

$$\frac{d^3 w}{dy^3} = \frac{1}{D} [2\beta M_0 \zeta(\beta y) - Q_0 \Psi(\beta y)] \quad (11.18d)$$

The shell functions  $\Phi(\beta y)$ ,  $\psi(\beta y)$ ,  $\theta(\beta y)$ , and  $\zeta(\beta y)$  are given in the standard influence coefficients of Table 11.1 (Ref. 11.1), for a range  $0 \leq \beta y \leq 3.9$ .

The maximum radial displacement or deflection at the restrained wall base, from Equation 11.18a, is

$$(w)_{y=0} = -\frac{1}{2\beta^3 D} (\beta M_0 + Q_0) \quad (11.19a)$$

and the maximum rotation of the wall at the base, from Equation 11.18b, becomes

$$\left(\frac{dw}{dy}\right)_{y=0} = \frac{1}{2\beta^2 D} (2\beta M_0 + Q_0) \quad (11.19b)$$

where  $M_0$  and  $Q_0$  are respectively the restraining moment and the ring shear at the base shown in Figure 11.1.

For tanks with constant wall thickness, the unit forces along the wall height are as follows:

$$N_\theta = -\frac{Etw}{r} \quad (11.20a)$$

$$Q_y = -D \frac{d^3 w}{dy^3} \quad (11.20b)$$

$$M_\theta = \mu M_y \quad (11.20c)$$

$$M_y = -D \frac{d^2 w}{dy^2} \quad (11.20d)$$



**Table 11.1** Table of Functions  $\Phi$ ,  $\psi$ ,  $\theta$ , and  $\zeta$ 

$\beta y$	$\Phi$	$\psi$	$\theta$	$\zeta$
0	1.0000	1.0000	1.0000	0
0.1	0.9907	0.8100	0.9003	0.0903
0.2	0.9651	0.6398	0.8024	0.1627
0.3	0.9267	0.4888	0.7077	0.2189
0.4	0.8784	0.3564	0.6174	0.2610
0.5	0.8231	0.2415	0.5323	0.2908
0.6	0.7628	0.1431	0.4530	0.3099
0.7	0.6997	0.0599	0.3798	0.3199
0.8	0.6354	-0.0093	0.3131	0.3223
0.9	0.5712	-0.0657	0.2527	0.3185
1.0	0.5083	-0.1108	0.1988	0.3096
1.1	0.4476	-0.1457	0.1510	0.2967
1.2	0.3899	-0.1716	0.1091	0.2807
1.3	0.3355	-0.1897	0.0729	0.2626
1.4	0.2849	-0.2011	0.0419	0.2430
1.5	0.2384	-0.2068	0.0158	0.2226
1.6	0.1959	-0.2077	-0.0059	0.2018
1.7	0.1576	-0.2047	-0.0235	0.1812
1.8	0.1234	-0.1985	-0.0376	0.1610
1.9	0.0932	-0.1899	-0.0484	0.1415
2.0	0.0667	-0.1794	-0.0563	0.1230
2.1	0.0439	-0.1675	-0.0618	0.1057
2.2	0.0244	-0.1548	-0.0652	0.0895
2.3	0.0080	-0.1416	-0.0668	0.0748
2.4	-0.0056	-0.1282	-0.0669	0.0613
2.5	-0.0166	-0.1149	-0.0658	0.0492
2.6	-0.0254	-0.1019	-0.0636	0.0383
2.7	-0.0320	-0.0895	-0.0608	0.0287
2.8	-0.0369	-0.0777	-0.0573	0.0204
2.9	-0.0403	-0.0666	-0.0534	0.0132
3.0	-0.0423	-0.0563	-0.0493	0.0071
3.1	-0.0431	-0.0469	-0.0450	0.0019
3.2	-0.0431	-0.0383	-0.0407	-0.0024
3.3	-0.0422	-0.0306	-0.0364	-0.0058
3.4	-0.0408	-0.0237	-0.0323	-0.0085
3.5	-0.0389	-0.0177	-0.0283	-0.0106
3.6	-0.0366	-0.0124	-0.0245	-0.0121
3.7	-0.0341	-0.0079	-0.0210	-0.0131
3.8	-0.0314	-0.0040	-0.0177	-0.0137
3.9	-0.0286	-0.0008	-0.0147	-0.0140

From Equations 11.18c, 11.18d, 11.20b, and 11.20d, the expressions for vertical moments and horizontal radial shears at the base of the wall, where  $y$  is zero, become (Ref. 11.1)

$$(M_y)_{y=0} = M_0 = \left(1 - \frac{1}{\beta H}\right) \frac{\gamma H r t}{\sqrt{12(1 - \mu^2)}} \quad (11.21a)$$

$$(Q_y)_{y=0} = Q_0 = - (2\beta H - 1) \frac{\gamma r t}{\sqrt{12(1 - \mu^2)}} \quad (11.21b)$$

The expression for the vertical moment at any level  $y$  above the wall base can be obtained from

$$M_y = -\frac{1}{\beta} [\beta M_0 \Phi(\beta y) + Q_0 \zeta(\beta y)] \quad (11.22)$$

The *offset* ring shear force  $\Delta Q_y$  corresponds to a radial displacement  $w_y$  of the wall at a height  $y$  above the base when the tank is *empty* and the values of  $Q_0$  and  $M_0$  due to a full liquid or full gas load are *induced*, as shown in Figure 11.5. This force can be expressed as either

$$\Delta Q_y = + \frac{E t}{r} (w_y)$$

or

$$\Delta Q_y = \frac{E t}{2r\beta^3 D} [\beta M_0 \psi(\beta y) + Q_0 \theta(\beta y)]$$

or

$$\Delta Q_y = + \frac{6(1 - \mu^2)}{\beta^3 r t^2} [\beta M_0 \psi(\beta y) + Q_0 \theta(\beta y)] \quad (11.23)$$

The ring shear  $Q_y$  at a plane  $y$  above the base would be equal to the difference between the ring force for a freely sliding base and  $\Delta Q_y$ :

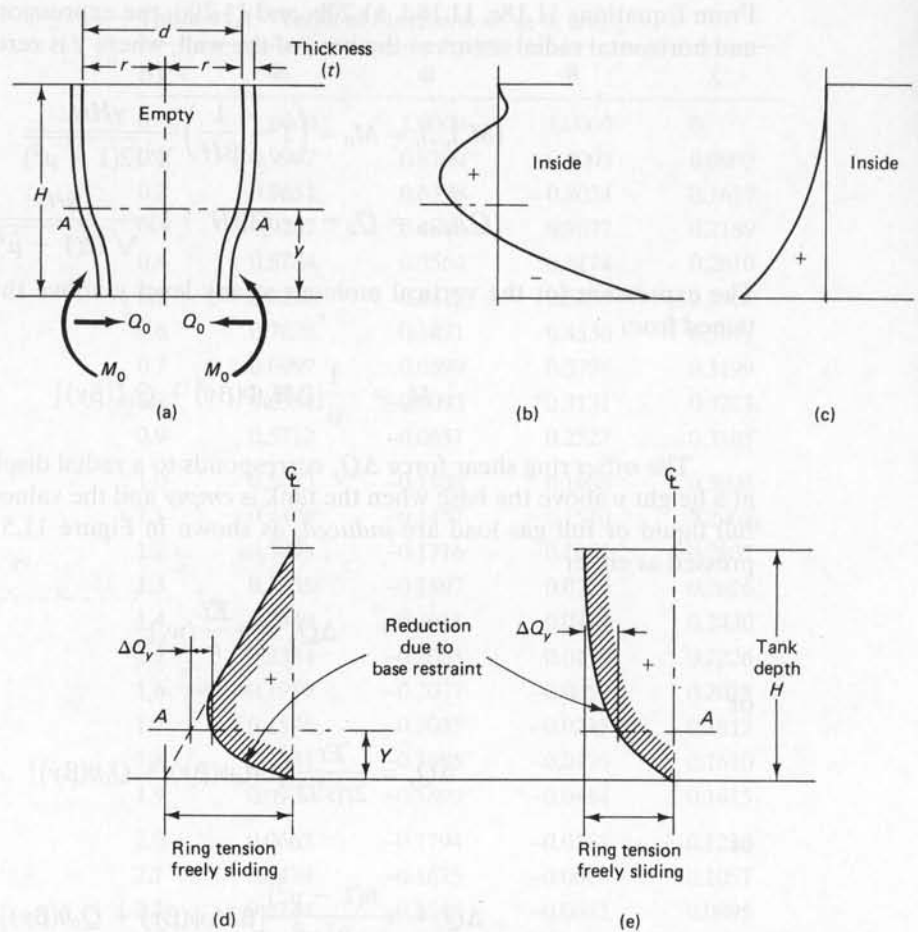
$$Q_y = F - \Delta Q_y \quad (11.24)$$

It is important to be consistent in the sign convention used throughout a solution. The easiest approach is to draw the deflected shape of the wall and use a positive (+) notation for the following conditions:

1. Moment causing tension on the outside extreme fibers.
2. Ring tension radial forces.
3. Thrust inwards toward the vertical axis. Here, the same sense is used as for ring tension forces in order to draw the diagram for the balancing prestressing forces on the same side as the ring tension forces for comparison.
4. Lateral wall movement *inwards* toward the vertical axis.
5. Anticlockwise rotation.

***Pinned Wall Base, Liquid Pressure.*** When the wall base is *pinned* and carrying a liquid load moment  $M_0 = 0$  at the base,

$$Q_0 = + \frac{2\beta^3 \gamma H (r t)^2}{12(1 - \mu^2)}$$



**Figure 11.5** Wall base restraint in empty tank inducing  $M_o$  and  $Q_o$  for full liquid or gas pressure. (a) Deformed walls of empty tank. (b) Moment along vertical section (+ represents tension on outside). (c) Ring tension force  $F$  in horizontal section (always positive). (d) Offset  $\Delta Q_v$  for liquid pressure. (e) Offset  $\Delta Q_v$  for gas pressure.

or

$$Q_o = + \frac{\gamma H}{[12(1 - \mu^2)]^{1/4}} \left( \frac{rt}{2} \right)^{1/2} \quad (11.25)$$

The value of the shell constants  $\beta$ ,  $\beta^2$ , and  $\beta^4$  for use in the preceding equations can easily be computed from the expression for  $\beta^4$  as follows:

$$\beta^4 = \frac{Et}{4r^2 D} = \frac{3(1 - \mu^2)}{(rt)^2} \quad (11.26a)$$

$$\beta^3 = \frac{[3(1 - \mu^2)]^{3/4}}{(rt)^{3/2}} \quad (11.26b)$$

$$\beta^2 = \frac{[3(1 - \mu^2)]^{1/2}}{(rt)} \quad (11.26c)$$



**Photo 11.4** Wire Winding Operation (Courtesy, N.A. Legatos, Preload Inc., Garden City, New York.)

$$\beta = \frac{[3(1 - \mu^2)]^{1/4}}{(rt)^{1/2}} \quad (11.26d)$$

#### 11.2.4 Ring Shear $Q_0$ and Moment $M_0$ Gas Containment

If the edges of the shell are free at the wall base, the internal pressure produces only hoop stress  $f_R = pr/t$  and the radius of the cylinder increases by the amount

$$w = \frac{rf_R}{E} = \frac{pr^2}{Et} \quad (11.27)$$

Also, for full restraint at the wall base,

$$(w)_{y=0} = \frac{1}{2\beta^3 D}(\beta M_0 + Q_0) \quad (11.28a)$$

and

$$\left(\frac{dw}{dy}\right)_{y=0} = \frac{1}{2\beta^2 D}(2\beta M_0 + Q_0) = 0 \quad (11.28b)$$

Solving for  $M_0$  and  $Q_0$  gives

$$M_0 = -2\beta^2 D w = -\frac{p}{2\beta^2} = -\frac{prt}{\sqrt{12(1 - \mu^2)}} \quad (11.29a)$$

and

$$Q_0 = +4\beta^3 D w = +\frac{p}{\beta} = +\frac{p(2rt)^{1/2}}{[12(1 - \mu^2)]^{1/4}} \quad (11.29b)$$

**Table 11.2** Equations for Liquid-Retaining Tanks

Parameter	Equation	Number
Flexural rigidity, $D$	$Et^3/[12(1 - \mu^2)]$	
Ring stress, $f_R$	$\gamma(H - Y)rt$	11.2 a
Ring force, $F$	$\gamma(H - y)r$	11.2 b
Pressure, $P_z$	$\gamma(H - y)$	11.2 b
Radial deflection, $w$	$\frac{1}{2\beta^2 D} [\beta M_0 \psi(\beta y) + Q_0 \theta(\beta y)]$	11.18 a
Rotation $\frac{dw}{dy}$	$\frac{1}{2\beta^3 D} [2\beta M_0 \theta(\beta y) + Q_0 \Phi(\beta y)]$	11.18 b
Maximum deflection, $(w)_{y=0}$	$\frac{1}{2\beta^3 D} (\beta M_0 + Q_0)$	11.19 a
Maximum rotation $\left(\frac{dw}{dy}\right)_{y=0}$	$\frac{1}{2\beta^3 D} (2\beta M_0 + Q_0) = 0$	11.19 b
$M_0 = (M_y)_{y=0}$	$-\left(1 - \frac{1}{\beta H}\right) \frac{\gamma H r t}{\sqrt{12(1 - \mu^2)}}$	11.21 a
$Q_0 = (Q_y)_{y=0}$	$+ (2\beta H - 1) \frac{\gamma r t}{\sqrt{12(1 - \mu^2)}}$	11.21 b
$M_y$	$+ \frac{1}{\beta} [\beta M_0 \Phi(\beta y) + Q_0 \zeta(\beta y)]$	11.22
Empty tank offset, $\Delta Q_y$	$+ \frac{6(1 - \mu)^2}{\beta^3 r t^2} [\beta M_0 \psi(\beta y) + (Q_0(\beta y))]$	11.23
$Q_y$	$+ (F - \Delta Q_y)$	11.24
$Q_0$ when $M_0 = 0$ (Pinned base)	$+ \frac{\gamma H \sqrt{rt/2}}{[12(1 - \mu^2)]^{1/4}}$	11.25
Tank Constants: $\beta^3$	$[3(1 - \mu^2)]^{3/4}/(rt)^{3/2}$	11.26 b
$\beta^2$	$[3(1 - \mu^2)]^{1/2}/rt$	11.26 c
$\beta$	$[3(1 - \mu^2)]^{1/4}/(rt)^{1/2}$	11.26 d

**Pinned Wall Base, Gas Pressure.** If the wall base is *pinned* and carrying a gas load moment  $M_0 = 0$  at the base,

$$Q_0 = 2\beta^3 D \left( \frac{pr^2}{Et} \right)$$

or

$$Q_0 = \frac{p}{[12(1 - \mu^2)]^{1/4}} \left( \frac{rt}{2} \right)^{1/2} \quad (11.30)$$

Table 11.2 presents a summary of the design equations for liquid-retaining tanks, and Table 11.3 gives a similar summary for gas-retaining tanks.

### 11.3 MOMENT $M_0$ AND RING FORCE $Q_0$ IN LIQUID RETAINING TANK

#### Example 11.1

A prestressed concrete circular tank is fully restrained at the wall base. It has an interior diameter  $d = 125$  ft (38.1 m) and retains water having height  $H = 25$  ft (7.62 m). The wall thick-

**Table 11.3** Equations for Gas-Retaining Tanks

Parameter	Equation	Number
Maximum deflection $(w)_{y=0}$	$\frac{1}{2\beta^3 D} (\beta M_0 + Q_0)$	11.28 a
Maximum rotation $\left(\frac{dw}{dy}\right)_{y=0}$	$\frac{1}{2\beta^2 D} (2\beta M_0 + Q_0) = 0$	11.28 b
$M_0 = (M_y)_{y=0}$	$-\frac{prt}{\sqrt{12(1-\mu^2)}}$	11.29 a
$Q_0 = (Q_y)_{y=0}$	$+\frac{p\sqrt{2}rt}{[12(1-\mu^2)]^{1/4}}$	11.29 b
$Q_0$ when $M_0 = 0$ (Pinned base)	$+\frac{p\sqrt{rt/2}}{[12(1-\mu^2)]^{1/4}}$	11.30

Note: Values of  $\beta$ ,  $\beta^2$ , and  $\beta^3$  constants as in Table 11.2.

ness  $t = 10$  in. (25 cm). Compute (a) the unit vertical moment  $M_0$  and the radial ring force  $Q_0$  at the base of the wall, and (b) the unit vertical moment  $M_y$  at  $7\frac{1}{2}$  ft (2.29 m) above the base. Use Poisson's ratio  $\mu = 0.2$  and unit water weight  $\gamma = 62.4$  lb/ft<sup>3</sup> (1,000 kg/m<sup>3</sup>).

**Solution:****(a) At Wall Base**

$$r = \frac{1}{2} \times 125 = 62.5 \text{ ft (19 m)}$$

$$t = 10 \text{ in.} = 0.83 \text{ ft (.25 m)}$$

From Equation 11.26d,

$$\beta = \frac{[3(1-\mu^2)]^{1/4}}{(rt)^{1/2}} = \frac{[3(1-0.2 \times 0.2)]^{1/4}}{(62.5 \times 0.83)^{1/2}} = 0.181$$

From Equation 11.21a,

$$\begin{aligned} M_0 &= -\left(1 - \frac{1}{\beta H}\right) \frac{\gamma H r t}{\sqrt{12(1-\mu^2)}} \\ &= -\left(1 - \frac{1}{0.181 \times 25}\right) \times \frac{62.4 \times 25 \times 62.5 \times 0.83}{\sqrt{12(1-0.04)}} \\ &= -18,574 \text{ ft-lb/ft (7.68 kN-m/m) of circumference} \end{aligned}$$

From Equation 11.21b,

$$\begin{aligned} Q_0 &= +(2\beta H - 1) \frac{\gamma r t}{\sqrt{12(1-\mu^2)}} \\ &= +(2 \times 0.181 \times 25 - 1) \frac{62.4 \times 62.5 \times 0.83}{\sqrt{12(1-0.04)}} \\ &= +7,677 \text{ lb/ft (112 kN/m) of circumference} \end{aligned}$$

**(b)  $7\frac{1}{2}$  ft above Wall Base**

$$y = 7.5 \text{ ft}$$

$$\text{Water height} = (H - y) = 25 - 7.5 = 17.5 \text{ ft (5.33 m)}$$

$$\text{Height ratio} = \left(1 - \frac{y}{H}\right) = 1 - \frac{7.5}{25} = 0.7$$

$$\beta y = 0.181 \times 7.5 = 1.36$$

From Equation 11.22,

$$M_y = +\frac{1}{\beta}[\beta M_0 \Phi(\beta y) + Q_0 \zeta(\beta y)]$$

From Table 11.1 for  $\beta y = 1.36$ ,

$$\Phi = 0.311$$

$$\zeta = 0.252$$

$$\begin{aligned} M_y &= +\frac{1}{0.181}(-0.181 \times 18,574 \times 0.311 + 7,677 \times 0.252) \\ &= +4,912 \text{ ft-lb/ft of circumference} \end{aligned}$$

## 11.4 RING FORCE $Q_y$ AT INTERMEDIATE HEIGHTS OF WALL

### Example 11.2

Compute the radial ring force  $Q_y$  in Example 11.1 at (a)  $y = 7\frac{1}{2}$  ft (2.29 m) and (b)  $y = 10$  ft (3.05 m) above the wall base, for freely sliding wall.

**Solution:** The freely sliding base ring force  $F = \gamma H r = 62.4 \times 25 \times 62.5 = 97,500$  lb/ft (1,423 kN/m). From Equation 11.23, the ring force offset is

$$\Delta Q_y = +\frac{6(1 - \mu^2)}{\beta^3 r t^2}[\beta M_0 \psi(\beta y) + Q_0 \theta(\beta y)]$$

From Example 11.1,  $\beta = 0.181$ ; hence,  $\beta^3 = 0.0059$ ,

(a)  $Q_y$  at 7.5 ft above Wall Base

$$\beta y = 0.181 \times 7.5 = 1.36$$

From Table 11.1 for  $\beta y = 1.36$ ,

$$\psi = -0.1965$$

$$\theta = +0.0543$$

$$\begin{aligned} \Delta Q_y &= +\frac{6(1 - 0.04)}{0.0059 \times 62.5(0.83)^2} \\ &\quad \times [0.181(-18,574)(-0.1965) + 7,677(+0.0543)] \\ &= 24,431 \text{ lb/ft (356 kN/m)} \end{aligned}$$

From Equation 11.2b, the ring force  $F = \gamma(H - y)r = 62.4 \times (25 \times 7.5) \times 62.5 = 68,250$  lb/ft. So  $Q_{7.5} = F - \Delta Q_y = 68,250 - 24,431 = 43,819$  lb/ft (705 kN/m) of circumference, as shown in Figure 11.6(a): (a) At  $7\frac{1}{2}$  ft above the base; (b) At 10 ft above the base.

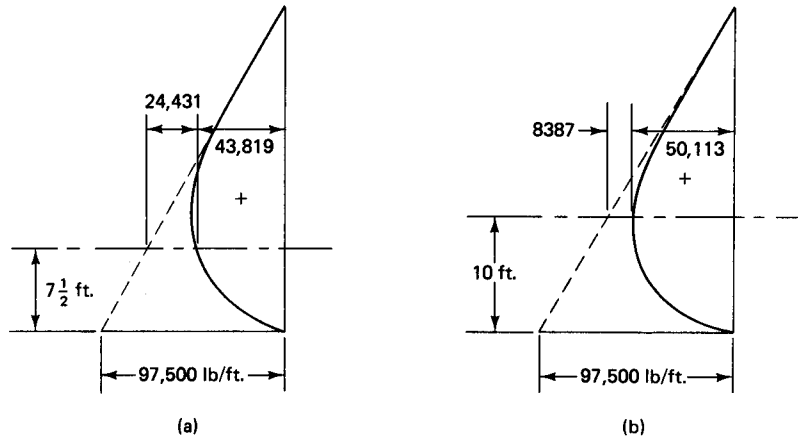
(b)  $Q_y$  at 10.0 ft above Wall Base

$$\beta y = 0.181 \times 10 = 1.81$$

From Table 11.1 for  $\beta y = 1.81$ ,

$$\psi = -0.1984$$

$$\theta = -0.0387$$



**Figure 11.6** Radial ring force profile. (a) At 7½ ft above the base. (b) At 10 ft above the base in Ex. 11.1.

$$\Delta Q_y = \frac{6(1 - 0.04)}{0.0059 \times 62.50(0.83)^2} \times [0.181(-18,574)(-0.1984) + 7,677(-0.0387)] = 8,387 \text{ lb/ft}$$

The ring force  $F = \gamma(H - y)r = 62.4(25 - 10)62.5 = 58,500 \text{ lb/ft}$ . So  $Q_{10} = F - \Delta Q_y = 58,500 - 8,387 = 50,113 \text{ lb/ft}$  (731 kN/m) of circumference, as shown in Figure 11.6(b). Compare how close this value is to  $Q = 50,115 \text{ lb/ft}$  obtained by using membrane coefficients in Example 11.3.

### 11.5 CYLINDRICAL SHELL MEMBRANE COEFFICIENTS

The bending moment at any level along the height above the base of a cylindrical tank can be computed from the bending moment expression for a cantilever beam. This is accomplished by multiplying the cantilever moment values by coefficients whose magnitudes are functions of the geometrical dimensions of the tank and which are termed *membrane coefficients*. The basic moment expressions developed in Section 11.2 for the circular container can be rearranged into a factor  $H^2/dt$  denoting *geometry* and a factor  $\gamma H^3$  or  $pH^2$  denoting *cantilever effect*, for liquid and gaseous loading, respectively (Ref. 11.2).

The tank constant  $\beta$  in Equation 11.26d is a function of  $rt$  or  $dt$ , where  $d$  is the tank diameter. Using Poisson's ratio  $\mu \cong 0.2$  for concrete, we have

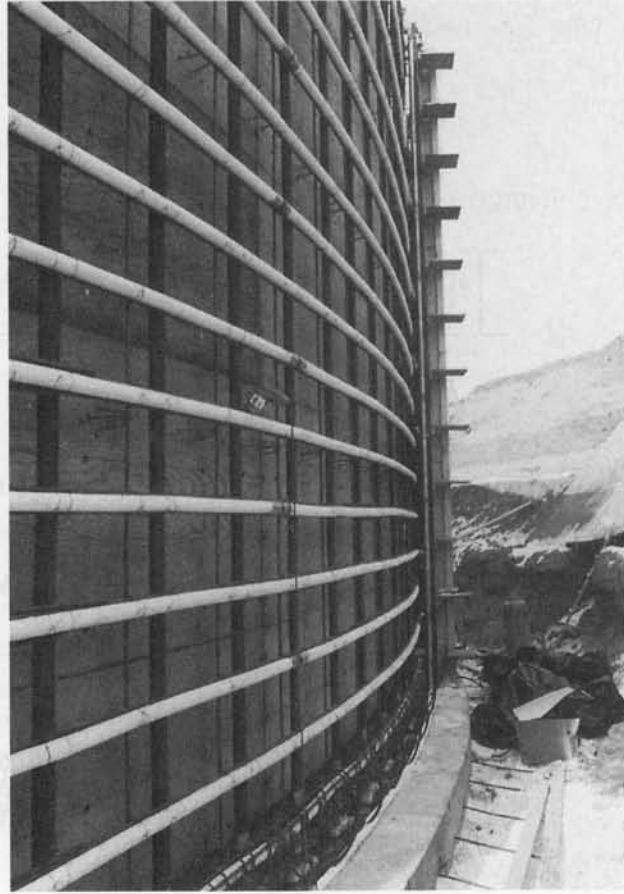
$$\beta = \frac{[3(1 - \mu^2)]^{1/4}}{(rt)^{1/2}} = \frac{1.30}{(rt)^{1/2}} = \frac{1.84}{(dt)^{1/2}}$$

The factor  $1/\beta H$  used in the basic bending expressions of Section 11.2 can be rewritten in terms of  $(dt/H^2)^{1/2}$  since  $\beta = 1.84/(dt)^{1/2}$ . The product  $\beta_y$  can also be rewritten in terms of  $\lambda(H^2/dt)^{1/2}$  using  $y = \lambda H$ , where  $y$  is the height above the base.

Consequently, the moment  $M_y$  of Equation 11.22 in a wall section a distance  $y$  above the base can be represented in terms of the form factor  $H^2/dt$  and the cantilever factor  $\gamma H^3$  or  $pH^2$  as follows:

$$M_y = \text{numerical variant} \times \text{form factor} \times \text{cantilever factor}$$





**Photo 11.5** Two-and-a-half-million-gallon tendon prestressed concrete tank with the horizontal and vertical tendons utilizing plastic sheathing to protect the prestressing steel from seepage through the wall. (Courtesy, Jorgenson, Hendrickson and Close, Denver, Colorado.)

or

$$M_y = \left[ \text{variant} \times \frac{H^2}{dt} \right] \times [\gamma H^3 \text{ or } pH^2] \quad (11.31)$$

The form factor  $H^2/dt$  is constant for the particular structure being designed. Hence, the product of the variant and the form factor produces the membrane coefficient  $C$ , so that Equation 11.31 becomes

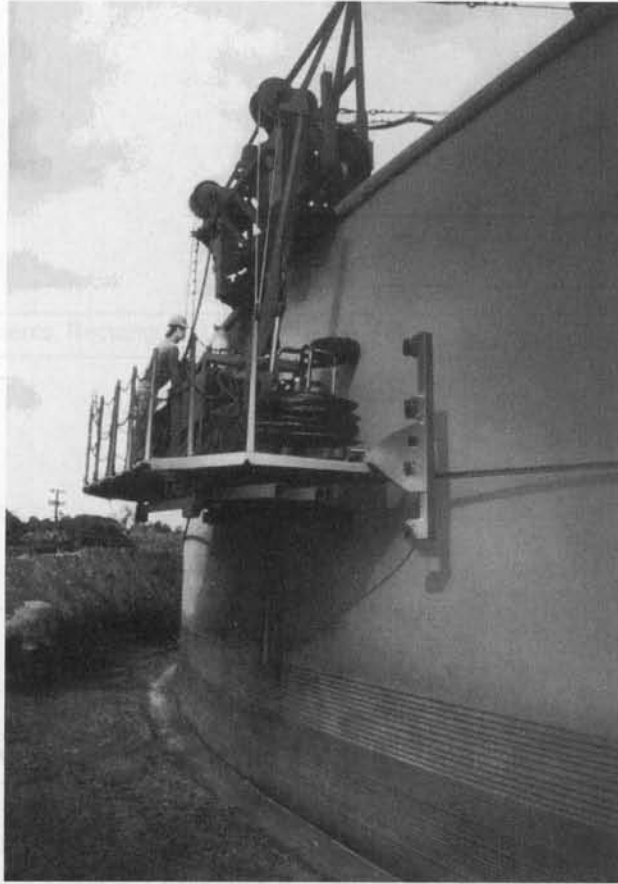
$$M_y = C\gamma H^3 \quad (11.32a)$$

for a liquid load and

$$M_y = CpH^2 \quad (11.32b)$$

for a gaseous load.

Tables 11.4 to 11.16 from Ref. 11.5 give the membrane coefficients  $C$  for various form factors  $H^2/dt$  and most expected boundary and load conditions. They significantly reduce the computational efforts normally required in the design and analysis of shells, without loss of accuracy in the results. Using the membrane coefficients for the solution



**Photo 11.6** Prestressing preload circular tank wall with wire winder. (Courtesy, N.A. Legatos, Preload Technology, Inc., New York.)

of the circular tank forces and moments should give results reasonably close to those obtained from the bending solutions presented in Section 11.2 and the sets of equations listed in Tables 11.2 and 11.3.

### 11.6 PRESTRESSING EFFECTS ON WALL STRESSES FOR FULLY HINGED, PARTIALLY SLIDING AND HINGED, FULLY FIXED, AND PARTIALLY FIXED BASES

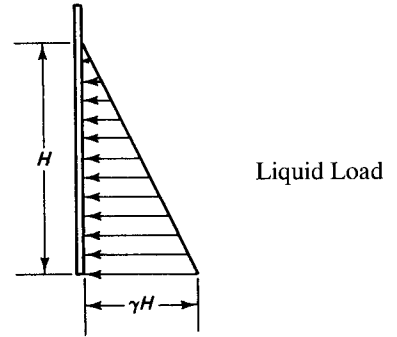
The liquid or gas contained in a cylindrical tank exerts *outward* radial pressure  $\gamma h$  or  $p$  on the tank walls, inducing ring tensions in each horizontal section of wall along its height. This ring tension in turn causes tensile stresses in the concrete at the *outside* extreme wall fibers, resulting in impermissible cracking. To eliminate this cracking that causes leaks and structural deterioration, external *horizontal* prestressing is applied which induces *inward* radial thrust that can balance the outward radial tension. Additionally, in order to prevent the development of cracks in the inside walls when the tank is empty, *vertical* prestressing is induced to reduce the residual tension within the range of the modulus of rupture of the concrete and with an adequate safety factor.

In order to ensure against the development of cracking at the outside face of the tank wall, it is good practice to apply somewhat larger horizontal prestressing forces than

(text continues on page 694)

**Table 11.4** Moment Influence Coefficients, Triangular Load

Moments in Cylindrical Wall  
 Triangular Load  
 Fixed Base, Free Top  
 Mom. = coef.  $\times \gamma H^2$  ft. lb. per ft.  
 Positive sign indicates tension in the outside



$\frac{H^2}{dt}$	Coefficients at Point									
	0.1H	0.2H	0.3H	0.4H	0.5H	0.6H	0.7H	0.8H	0.9H	1.0H
0.4	+0.005	+0.0014	+0.0021	+0.0007	-0.0042	-0.0150	-0.0302	-0.0529	-0.0816	-0.1205
0.8	+0.0011	+0.0037	+0.0063	+0.0080	+0.0070	+0.0023	-0.0068	-0.0224	-0.0465	-0.0795
1.2	+0.0012	+0.0042	+0.0077	+0.0103	+0.0112	+0.0090	+0.0022	-0.0108	-0.0311	-0.0602
1.6	+0.0011	+0.0041	+0.0075	+0.0107	+0.0121	+0.0111	+0.0058	-0.0051	-0.0232	-0.0505
2.0	+0.0010	+0.0035	+0.0068	+0.0099	+0.0120	+0.0115	+0.0075	-0.0021	-0.0185	-0.0436
3.0	+0.0006	+0.0024	+0.0047	+0.0071	+0.0090	+0.0097	+0.0077	+0.0012	-0.0119	-0.0333
4.0	+0.0003	+0.0015	+0.0028	+0.0047	+0.0066	+0.0077	+0.0069	+0.0023	-0.0080	-0.0268
5.0	+0.0002	+0.0008	+0.0016	+0.0029	+0.0046	+0.0059	+0.0059	+0.0028	-0.0058	-0.0222
6.0	+0.0001	+0.0003	+0.0008	+0.0019	+0.0032	+0.0046	+0.0051	+0.0029	-0.0041	-0.0187
8.0	.0000	+0.0001	+0.0002	+0.0008	+0.0016	+0.0028	+0.0038	+0.0029	-0.0022	-0.0146
10.0	.0000	.0000	+0.0001	+0.0004	+0.0007	+0.0019	+0.0029	+0.0028	-0.0012	-0.0122
12.0	.0000	-0.0001	+0.0001	+0.0002	+0.0003	+0.0013	+0.0023	+0.0026	-0.0005	-0.0104
14.0	.0000	.0000	.0000	.0000	+0.0001	+0.0008	+0.0019	+0.0023	-0.0001	-0.0090
16.0	.0000	.0000	-0.0001	-0.0002	-0.0001	+0.0004	+0.0013	+0.0019	+0.0001	-0.0079

Notes: 1-Tables 11.4 to 11.16 Adapted from Ref. 11.5.

2-0.0H is the top and 1.0H is the bottom of the wall, except if wall is fixed at top and with shear and moment at top.

3-Shear acting inwards is positive; moment applied at an edge is positive when outward rotation results at that edge.

**Table 11.5** Moment Influence Coefficients, Rectangular Load

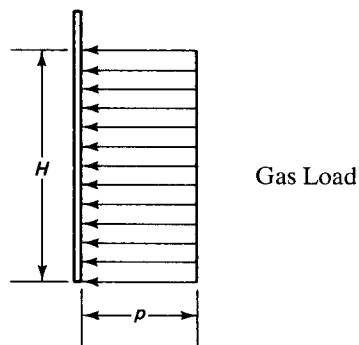
Moments in Cylindrical Wall

Rectangular Load

Fixed Base, Free Top

Mom. = coef.  $\times$   $pH^2$  ft. lb. per ft.

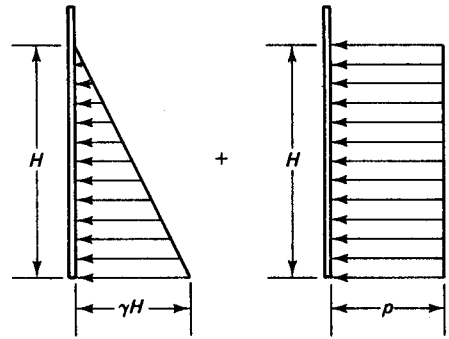
Positive sign indicates tension in the outside



$\frac{H^2}{dt}$	Coefficients at Point									
	0.1H	0.2H	0.3H	0.4H	0.5H	0.6H	0.7H	0.8H	0.9H	1.0H
0.4	-.0023	-.0093	-.0227	-.0439	-.0710	-.1018	-.1455	-.2000	-.2593	-.3310
0.8	.0000	-.0006	-.0025	-.0083	-.0185	-.0362	-.0594	-.0917	-.1325	-.1835
1.2	+.0008	+.0026	+.0037	+.0029	-.0009	-.0089	-.0227	-.0468	-.0815	-.1178
1.6	+.0011	+.0036	+.0062	+.0077	+.0068	+.0011	-.0093	-.0670	-.0529	-.0876
2.0	+.0010	+.0036	+.0066	+.0088	+.0089	+.0059	-.0019	-.0167	-.0389	-.0719
3.0	+.0007	+.0026	+.0051	+.0074	+.0091	+.0083	+.0042	-.0053	+.0223	-.0483
4.0	+.0004	+.0015	+.0033	+.0052	+.0068	+.0075	+.0053	-.0013	-.0145	-.0365
5.0	+.0002	+.0008	+.0019	+.0035	+.0051	+.0061	+.0052	+.0007	-.0101	-.0293
6.0	+.0001	+.0004	+.0011	+.0022	+.0036	+.0049	+.0048	+.0017	-.0073	-.0242
8.0	+.0000	+.0001	+.0003	+.0008	+.0018	+.0031	+.0038	+.0024	-.0040	-.0184
10.0	.0000	-.0001	.0000	+.0002	+.0009	+.0021	+.0030	+.0026	-.0022	-.0147
12.0	.0000	.0000	-.0001	.0000	+.0004	+.0014	+.0024	+.0022	-.0012	-.0123
14.0	.0000	.0000	.0000	.0000	+.0002	+.0010	+.0018	+.0021	-.0007	-.0105
16.0	.0000	.0000	.0000	-.0001	+.0001	+.0006	+.0012	+.0020	-.0005	-.0091

**Table 11.6** Moment Influence Coefficients, Trapezoidal Load

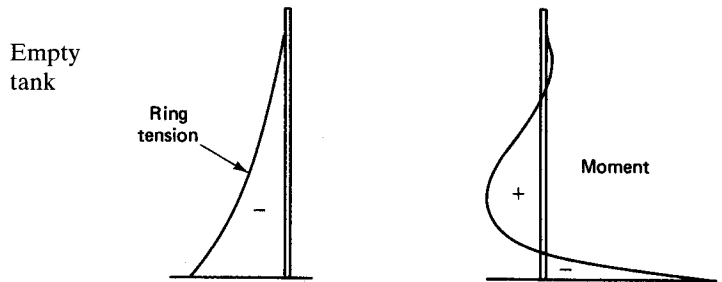
Moments in Cylindrical Wall  
 Trapezoidal Load  
 Hinged Base, Free Top  
 Mom. = coef.  $\times (\gamma H^2 + p H^2)$  ft. lb. per ft.  
 Positive sign indicates tension in the outside



$\frac{H^2}{dt}$	Coefficients at Point									
	0.1H	0.2H	0.3H	0.4H	0.5H	0.6H	0.7H	0.8H	0.9H	1.0H
0.4	+0.0020	+0.0072	+0.0151	+0.0230	+0.0301	+0.0348	+0.0357	+0.0312	+0.0197	0
0.3	+0.0019	+0.0064	+0.0133	+0.0207	+0.0271	+0.0319	+0.0329	+0.0292	+0.0187	0
1.2	+0.0016	+0.0058	+0.0111	+0.0177	+0.0237	+0.0280	+0.0296	+0.0263	+0.0171	0
1.6	+0.0012	+0.0044	+0.0091	+0.0145	+0.0195	+0.0236	+0.0255	+0.0232	+0.0155	0
2.0	+0.0009	+0.0033	+0.0073	+0.0114	+0.0158	+0.0199	+0.0219	+0.0205	+0.0145	0
3.0	+0.0004	+0.0015	+0.0040	+0.0063	+0.0092	+0.0127	+0.0152	+0.0153	+0.0111	0
4.0	+0.0001	+0.0007	+0.0016	+0.0033	+0.0057	+0.0083	+0.0109	+0.0118	+0.0092	0
5.0	.0000	+0.0001	+0.0006	+0.0016	+0.0034	+0.0057	+0.0080	+0.0094	+0.0078	0
6.0	.0000	.0000	+0.0002	+0.0008	+0.0019	+0.0039	+0.0062	+0.0078	+0.0068	0
8.0	.0000	.0000	-.0002	.0000	+0.0007	+0.0020	+0.0038	+0.0057	+0.0054	0
10.0	.0000	.0000	-.0002	-.0001	+0.0002	+0.0011	+0.0025	+0.0043	+0.0045	0
12.0	.0000	.0000	-.0001	-.0002	.0000	+0.0005	+0.0017	+0.0032	+0.0039	0
14.0	.0000	.0000	-.0001	-.0001	-.0001	.0000	+0.0012	+0.0026	+0.0033	0
16.0	.0000	.0000	.0000	-.0001	-.0002	-.0004	+0.0008	+0.0022	+0.0029	0

**Table 11.7** Moment Influence Coefficients, Empty Tank (Shear Applied at Top Base Fixed)

Moments in Cylindrical Wall  
 Shear Per Ft.,  $Q$ , Applied at Top  
 Fixed Base, Free Top  
 Mom. = coef.  $\times$   $VH$  ft. lb. per ft.  
 Positive sign indicates tension in the outside

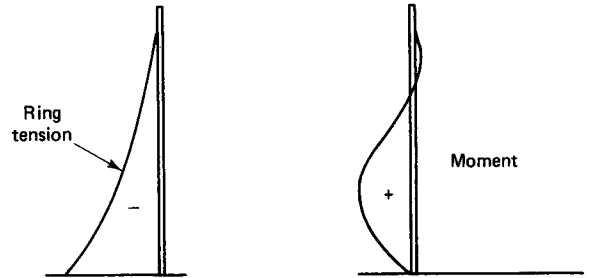


$\frac{H^2}{dt}$	Coefficients at Point									
	0.1H	0.2H	0.3H	0.4H	0.5H	0.6H	0.7H	0.8H	0.9H	1.0H
0.4	+0.093	+0.172	+0.240	+0.300	+0.354	+0.402	+0.448	+0.492	+0.535	+0.578
0.8	+0.085	+0.145	+0.185	+0.208	+0.220	+0.224	+0.223	+0.219	+0.214	+0.208
1.2	+0.082	+0.132	+0.157	+0.164	+0.159	+0.145	+0.127	+0.106	+0.084	+0.062
1.6	+0.079	+0.122	+0.139	+0.138	+0.125	+0.105	+0.081	+0.056	+0.030	+0.004
2.0	+0.077	+0.115	+0.126	+0.119	+0.103	+0.080	+0.056	+0.031	+0.006	+0.019
3.0	+0.072	+0.100	+0.100	+0.086	+0.066	+0.044	+0.025	+0.006	-0.010	-0.024
4.0	+0.068	+0.088	+0.081	+0.063	+0.043	+0.025	+0.010	-0.001	-0.010	-0.019
5.0	+0.064	+0.078	+0.067	+0.047	+0.028	+0.013	+0.003	-0.003	-0.007	-0.011
6.0	+0.062	+0.070	+0.056	+0.036	+0.018	+0.006	0.000	-0.003	-0.005	-0.006
8.0	+0.057	+0.058	+0.041	+0.021	+0.007	0.000	-0.002	-0.003	-0.002	-0.001
10.0	+0.053	+0.049	+0.029	+0.012	+0.002	-0.002	-0.002	-0.002	-0.001	-0.000
12.0	+0.049	+0.042	+0.022	+0.007	0.000	-0.002	-0.002	-0.001	0.000	0.000
14.0	+0.046	+0.036	+0.017	+0.004	-0.001	-0.002	-0.001	-0.001	0.000	0.000
16.0	+0.044	+0.031	+0.012	+0.001	-0.002	-0.002	-0.001	0.000	0.000	0.000

**Table 11.8** Moment Influence Coefficients, Empty Tank (Shear Applied at Top Hinged Base)

Moments in Cylindrical Wall  
 Moment Per Ft.,  $M$ , Applied at Base  
 Hinged Base, Free Top  
 Mom. = coef.  $\times M$  ft. lb. per ft.  
 Positive sign indicates tension in the outside

Empty Tank



$\frac{H^2}{dt}$	Coefficients at Point									
	0.1H	0.2H	0.3H	0.4H	0.5H	0.6H	0.7H	0.8H	0.9H	1.0H
0.4	+0.013	+0.051	+0.109	+0.196	+0.296	+0.414	+0.547	+0.692	+0.843	+1.000
0.8	+0.009	+0.040	+0.090	+0.164	+0.253	+0.375	+0.503	+0.659	+0.824	+1.000
1.2	+0.006	+0.027	+0.063	+0.125	+0.206	+0.316	+0.454	+0.616	+0.802	+1.000
1.6	+0.003	+0.011	+0.035	+0.078	+0.152	+0.253	+0.393	+0.570	+0.775	+1.000
2.0	-0.002	-0.002	+0.012	+0.034	+0.096	+0.193	+0.340	+0.519	+0.748	+1.000
3.0	-0.007	-0.022	-0.030	-0.029	+0.010	+0.087	+0.227	+0.426	+0.692	+1.000
4.0	-0.008	-0.026	-0.044	-0.051	-0.034	+0.023	0.150	+0.354	+0.645	+1.000
5.0	-0.007	-0.024	-0.045	-0.061	-0.057	-0.015	+0.095	+0.296	0.606	+1.000
6.0	-0.005	-0.018	-0.040	-0.058	-0.065	-0.037	+0.057	+0.252	+0.572	+1.000
8.0	-0.001	-0.009	-0.022	-0.044	-0.068	-0.062	+0.002	+0.178	+0.515	+1.000
10.0	0.000	-0.002	-0.009	-0.028	-0.053	-0.067	-0.031	+0.123	+0.467	+1.000
12.0	0.000	0.000	-0.003	-0.016	-0.040	-0.064	-0.049	+0.081	+0.424	+1.000
14.0	0.000	0.000	0.000	-0.008	-0.029	-0.059	-0.060	+0.048	+0.387	+1.000
16.0	0.000	0.000	+0.002	-0.003	-0.021	-0.051	-0.066	+0.025	+0.354	+1.000

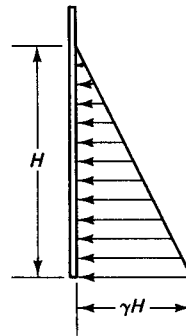
**Table 11.9** Shear  $Q$  Influence Coefficients

Shear at Base of Cylindrical Wall			
$Q = \text{coef.} \times \begin{cases} \gamma H^2 \text{ lb. (triangular)} \\ p H \text{ lb. (rectangular)} \\ M/H \text{ lb. (mom. at base)} \end{cases}$			
Positive sign indicates shear acting inward			
$\frac{H^2}{dt}$	Triangular load, fixed base	Rectangular load, fixed base	Triangular or rectangular load, hinged base
0.4	0.436	0.755	0.245
0.8	0.374	0.552	0.234
1.2	0.339	0.460	0.220
1.6	0.317	0.407	0.204
2.0	0.299	0.370	0.189
3.0	0.262	0.310	0.158
4.0	0.236	0.271	0.137
5.0	0.213	0.243	0.121
6.0	0.197	0.222	0.110
8.0	0.174	0.193	0.096
10.0	0.158	0.172	0.087
12.0	0.145	0.158	0.079
14.0	0.135	0.147	0.073
16.0	0.127	0.137	0.068



**Table 11.10** Ring Tension Influence Coefficients, Triangular Load (Fixed Base)

Tension in Circular Rings  
 Triangular Load  
 Fixed base, Free Top  
 $F = \text{coef.} \times \gamma HR$  lb. per ft.  
 Positive sign indicates tension

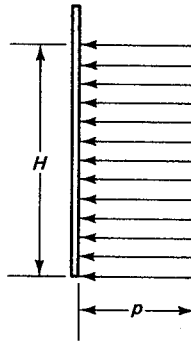


'Liquid Load'—Fixed

$\frac{H^2}{dt}$	Coefficients at Point									
	0.0H	0.1H	0.2H	0.3H	0.4H	0.5H	0.6H	0.7H	0.8H	0.9H
0.4	+0.149	+0.134	+0.120	+0.101	+0.082	+0.066	+0.049	+0.029	+0.014	+0.004
0.8	+0.263	+0.239	+0.215	+0.190	+0.160	+0.130	+0.096	+0.063	+0.034	+0.010
1.2	+0.283	+0.271	+0.254	+0.234	+0.209	+0.180	+0.142	+0.099	+0.045	+0.016
1.6	+0.265	+0.268	+0.268	+0.266	+0.250	+0.266	+0.185	+0.134	+0.075	+0.023
2.0	+0.234	+0.251	+0.273	+0.285	+0.285	+0.274	+0.232	+0.172	+0.104	+0.031
3.0	+0.134	+0.203	+0.267	+0.322	+0.357	+0.362	+0.330	+0.262	+0.157	+0.052
4.0	+0.067	+0.164	+0.256	+0.339	+0.403	+0.429	+0.409	+0.334	+0.210	+0.073
5.0	+0.025	+0.137	+0.245	+0.346	+0.428	+0.477	+0.469	+0.398	+0.259	+0.092
6.0	+0.018	+0.119	+0.234	+0.344	+0.441	+0.504	+0.514	+0.447	+0.301	+0.112
8.0	+0.011	+0.104	+0.218	+0.335	+0.443	+0.534	+0.575	+0.530	+0.381	+0.151
10.0	-0.011	+0.098	+0.208	+0.323	+0.437	+0.542	+0.608	+0.589	+0.440	+0.179
12.0	-0.005	+0.097	+0.202	+0.312	+0.429	+0.543	+0.628	+0.633	+0.494	+0.211
14.0	-0.002	+0.098	+0.200	+0.306	+0.420	+0.539	+0.639	+0.666	+0.541	+0.241
16.0	0.000	+0.099	+0.199	+0.304	+0.412	+0.531	+0.641	+0.687	+0.582	+0.265

**Table 11.11** Ring Tension Influence Coefficients, Rectangular Load (Fixed Base)

Tension in Circular Rings  
 Rectangular Load  
 Fixed Base, Free Top  
 $F = \text{coef.} \times pR$  lb. per ft.  
 Positive sign indicates tension

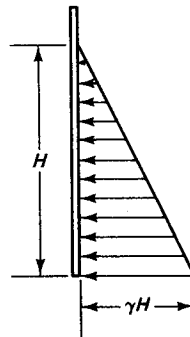


'Gas' Load—Fixed

$\frac{H^2}{dt}$	Coefficients at Point									
	0.0H	0.1H	0.2H	0.3H	0.4H	0.5H	0.6H	0.7H	0.8H	0.9H
0.4	+0.582	+0.505	+0.431	+0.353	+0.277	+0.206	+0.145	+0.092	+0.046	+0.013
0.8	+1.052	+0.921	+0.796	+0.669	+0.542	+0.415	+0.289	+0.179	+0.089	+0.024
1.2	+1.218	+1.078	+0.946	+0.808	+0.665	+0.519	+0.378	+0.246	+0.127	+0.034
1.6	+1.257	+1.141	+1.009	+0.881	+0.742	+0.600	+0.449	+0.294	+0.153	+0.045
2.0	+1.253	+1.144	+1.041	+0.929	+0.806	+0.667	+0.514	+0.345	+0.186	+0.055
3.0	+1.160	+1.112	+1.061	+0.998	+0.912	+0.796	+0.646	+0.459	+0.258	+0.081
4.0	+1.085	+1.073	+1.057	+1.029	+0.997	+0.887	+0.746	+0.553	+0.322	+0.105
5.0	+1.037	+1.044	+1.047	+1.042	+1.015	+0.949	+0.825	+0.629	+0.379	+0.128
6.0	+1.010	+1.024	+1.038	+1.045	+1.034	+0.986	+0.879	+0.694	+0.430	+0.149
8.0	+0.989	+1.005	+1.022	+1.036	+1.044	+1.026	+0.953	+0.788	+0.519	+0.189
10.0	+0.989	+0.998	+1.010	+1.023	+1.039	+1.040	+0.996	+0.859	+0.591	+0.226
12.0	+0.994	+0.997	+1.003	+1.014	+1.031	+1.043	+1.022	+0.911	+0.652	+0.262
14.0	+0.997	+0.998	+1.000	+1.007	+1.022	+1.040	+1.035	+0.949	+0.705	+0.294
16.0	+1.000	+0.999	+0.999	+1.003	+1.015	+1.032	+1.040	+0.975	+0.750	+0.321

**Table 11.12** Ring Tension Influence Coefficients, Triangular Load (Pinned Base)

Tension in Circular Rings  
 Triangular Load  
 Hinged Base, Free Top  
 $F = \text{coef.} \times \gamma HR$  lb. per ft.  
 Positive sign indicates tension

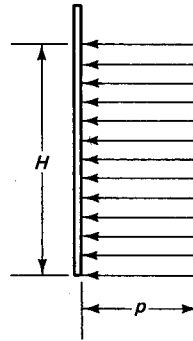


'Liquid Load'—Pinned

$\frac{H^2}{dt}$	Coefficients at Point									
	0.0H	0.1H	0.2H	0.3H	0.4H	0.5H	0.6H	0.7H	0.8H	0.9H
0.4	+0.474	+0.440	+0.395	+0.352	+0.308	+0.264	+0.215	+0.165	+0.111	+0.057
0.8	+0.423	+0.402	+0.381	+0.358	+0.330	+0.297	+0.249	+0.202	+0.145	+0.076
1.2	+0.350	+0.355	+0.361	+0.362	+0.358	+0.343	+0.309	+0.256	+0.186	+0.098
1.6	+0.271	+0.303	+0.341	+0.369	+0.385	+0.385	+0.362	+0.314	+0.233	+0.124
2.0	+0.205	+0.260	+0.321	+0.373	+0.411	+0.434	+0.419	+0.369	+0.280	+0.151
3.0	+0.074	+0.179	+0.281	+0.375	+0.449	+0.506	+0.519	+0.479	+0.375	+0.210
4.0	+0.017	+0.137	+0.253	+0.367	+0.469	+0.545	+0.579	+0.553	+0.447	+0.256
5.0	-0.008	+0.114	+0.235	+0.356	+0.469	+0.562	+0.617	+0.606	+0.503	+0.294
6.0	-0.011	+0.103	+0.223	+0.343	+0.463	+0.566	+0.639	+0.643	+0.547	+0.327
8.0	-0.015	+0.096	+0.208	+0.324	+0.443	+0.564	+0.661	+0.697	+0.621	+0.386
10.0	-0.008	+0.095	+0.200	+0.311	+0.428	+0.552	+0.666	+0.730	+0.678	+0.433
12.0	-0.002	+0.097	+0.197	+0.302	+0.417	+0.541	+0.664	+0.750	+0.720	+0.477
14.0	0.000	+0.098	+0.197	+0.299	+0.408	+0.531	+0.659	+0.761	+0.752	+0.513
16.0	+0.002	+0.100	+0.198	+0.299	+0.403	+0.521	+0.650	+0.764	+0.776	+0.543

**Table 11.13** Ring Tension Influence Coefficients, Rectangular Load (Hinged Base)

Tension in Circular Rings  
 Rectangular Load  
 Hinged Base, Free Top  
 $F = \text{coef.} \times pR$  lb. per ft.  
 Positive sign indicates tension

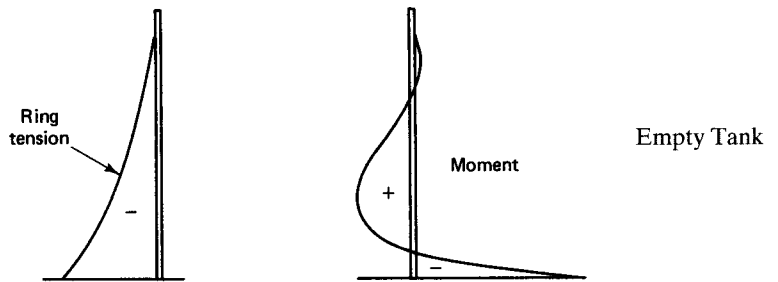


'Gas' Load—Pinned

$\frac{H^2}{dt}$	Coefficients at Point									
	0.0H	0.1H	0.2H	0.3H	0.4H	0.5H	0.6H	0.7H	0.8H	0.9H
0.4	+1.474	-1.340	+1.195	+1.052	+0.903	+0.764	+0.615	+0.465	+0.311	+0.154
0.8	+1.423	+1.302	+1.181	+1.058	+0.930	+0.797	+0.649	+0.502	+0.345	+0.166
1.2	+1.350	+1.255	+1.161	+1.062	+0.958	+0.843	+0.709	+0.556	+0.386	+0.198
1.6	+1.271	+1.203	+1.141	+1.069	+0.985	+0.885	+0.756	+0.614	+0.433	+0.224
2.0	+1.205	+1.160	+1.121	+1.173	+1.011	+0.934	+0.819	+0.669	+0.480	+0.251
3.0	+1.074	+1.079	+1.081	+1.075	+1.049	+1.006	+0.919	+0.779	+0.575	+0.310
4.0	+1.017	+1.037	+1.053	+1.067	+1.069	+1.045	+0.979	+0.853	+0.647	+0.356
5.0	+0.992	+1.014	+1.035	+1.056	+1.069	+1.062	+1.017	+1.906	+0.703	+0.394
6.0	+0.989	+1.003	+1.023	+1.043	+1.063	+1.066	+1.039	+0.943	+0.747	+0.427
8.0	+0.985	+0.996	+1.008	+1.024	+1.043	+1.064	+1.061	+0.997	+0.821	+0.486
10.0	+0.992	+0.995	+1.000	+1.011	+1.028	+1.052	+1.066	+1.030	+0.878	+0.523
12.0	+0.998	+0.997	+0.997	+1.002	+1.017	+1.041	+1.064	+1.050	+0.920	+0.577
14.0	+1.000	+0.998	+0.997	+0.999	+1.008	+1.031	+1.059	+1.061	+0.952	+0.613
16.0	+1.002	+1.000	+0.998	+0.999	+1.003	+1.021	+1.050	+1.064	+0.976	+0.543

**Table 11.14** Empty Tank Ring Tension Influence Coefficients, Fixed Base

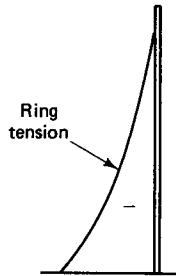
Tension in Circular Rings  
 Shear per Ft.,  $Q$ , Applied at Top  
 Fixed Base, Free Top  
 $F = \text{coef.} \times VR/H$  lb. per ft.  
 Positive sign indicates tension



$\frac{H^2}{dt}$	Coefficients at Point									
	0.0H	0.1H	0.2H	0.3H	0.4H	0.5H	0.6H	0.7H	0.8H	0.9H
0.4	-1.57	-1.32	-1.08	-0.86	-0.65	-0.47	-0.31	-0.18	-0.08	-0.02
0.8	-3.09	-2.55	-2.04	-1.57	-1.15	-0.80	-0.51	-0.28	-0.13	-0.03
1.2	-3.95	-3.17	-2.44	-1.79	-1.25	-0.81	-0.48	-0.25	-0.10	-0.02
1.6	-4.57	-3.54	-2.60	-1.80	-1.17	-0.69	-0.36	-0.16	-0.05	-0.01
2.0	-5.12	-3.83	-2.68	-1.74	-1.02	-0.52	-0.21	-0.05	+0.01	+0.01
3.0	-6.32	-4.37	-2.70	-1.43	-0.58	-0.02	-0.15	+0.19	+0.13	+0.04
4.0	-7.34	-4.73	-2.60	-1.10	-0.19	+0.26	+0.38	+0.33	+0.19	+0.06
5.0	-8.22	-4.99	-2.45	-0.79	+0.11	+0.47	+0.50	+0.37	+0.20	+0.06
6.0	-9.02	-5.17	-2.27	-0.50	+0.34	+0.59	+0.53	+0.35	+0.17	+0.01
8.0	-10.42	-5.36	-1.85	-0.02	+0.63	+0.66	+0.46	+0.24	+0.09	+0.01
10.0	-11.67	-5.43	-1.43	+0.36	+0.78	+0.62	+0.33	+0.12	+0.02	0.00
12.0	-12.76	-5.41	-1.03	+0.63	+0.83	+0.52	+0.21	+0.04	-0.02	0.00
14.0	-13.77	-5.34	-0.68	+0.80	+0.81	+0.42	+0.13	0.00	-0.03	-0.01
16.0	-14.74	-5.22	-0.33	+0.96	+0.76	+0.32	+0.05	-0.04	-0.05	-0.02

**Table 11.15** Empty Tank Ring Tension Influence Coefficients, Hinged Base

Tension in Circular Rings  
 Moment per Ft.,  $M$ , Applied at Base  
 Hinged Base, Free Top  
 $F = \text{coef.} \times MR/H^2$  lb. per ft.  
 Positive sign indicates tension



Empty Tank

$\frac{H^2}{dt}$	Coefficients at Point									
	0.0H	0.1H	0.2H	0.3H	0.4H	0.5H	0.6H	0.7H	0.8H	0.9H
0.4	+2.70	+2.50	+2.30	+2.12	+1.91	+1.69	+1.41	+1.13	+0.80	+0.44
0.8	+2.02	+2.06	+2.10	+2.14	+2.10	+2.02	+1.95	+1.75	+1.39	+0.80
1.2	+1.06	+1.42	+1.79	+2.03	+2.46	+2.65	+2.80	+2.60	+2.22	+1.37
1.6	+0.12	+0.79	+1.43	+2.04	+2.72	+3.25	+3.56	+3.59	+3.13	+2.01
2.0	-0.68	+0.22	+1.10	+2.02	+2.90	+3.69	+4.30	+4.54	+4.08	+2.75
3.0	-1.78	-0.71	+0.43	+1.60	+2.95	+4.29	+5.66	+6.58	+6.55	+4.73
4.0	-1.87	-1.00	-0.08	+1.04	+2.47	+4.31	+6.34	+8.19	+8.82	+6.81
5.0	-1.54	-1.03	-0.42	+0.45	+1.86	+3.93	+6.60	+9.41	+11.03	+9.02
6.0	-1.04	-0.86	-0.59	-0.05	+1.21	+3.34	+6.54	+10.28	+13.08	+11.41
8.0	-0.24	-0.53	-0.73	-0.67	-0.02	+2.05	+5.87	+11.32	+16.52	+16.06
10.0	+0.21	-0.23	-0.64	-0.94	-0.73	+0.82	+4.79	+11.63	+19.48	+20.87
12.0	+0.32	-0.05	-0.46	-0.96	-1.15	-0.18	+3.52	+11.27	+21.80	+25.73
14.0	+0.26	+0.04	-0.28	-0.76	-1.29	-0.87	+2.29	+10.55	+23.50	+30.34
16.0	+0.22	+0.07	-0.08	-0.64	-1.28	-1.30	+1.12	+9.67	+24.53	+34.65

**Table 11.16** Supplementary Influence Coefficients for Values of  $H^2/dt$  Greater Than 16 for Tables 11.4–11.15**Table 11.4a**

$\frac{H^2}{dt}$	Coefficients at Point				
	.80H	.85H	.90H	.95H	1.00H
20	+0.0015	+0.0014	+0.0005	-.0018	-.0063
24	+0.0012	+0.0012	+0.0007	-.0013	-.0053
32	+0.0007	+0.0009	+0.0007	-.0008	-.0040
40	+0.0002	+0.0005	+0.0006	-.0005	-.0032
48	.0000	+0.0001	+0.0006	-.0003	-.0026
56	.0000	.0000	+0.0004	-.0001	-.0023

**Table 11.5a**

$\frac{H^2}{dt}$	Coefficients at Point				
	.80H	.85H	.90H	.95H	1.00H
20	+0.0015	+0.0013	+0.0002	-.0024	-.0073
24	+0.0012	+0.0012	+0.0004	-.0018	-.0061
32	+0.0008	+0.0009	+0.0006	-.0010	-.0046
40	+0.0005	+0.0007	+0.0007	-.0005	-.0037
48	+0.0004	+0.0006	+0.0006	-.0003	-.0031
56	+0.0002	+0.0004	+0.0005	-.0001	-.0026

**Table 11.6a**

$\frac{H^2}{dt}$	Coefficients at Point				
	.75H	.80H	.85H	.90H	.95H
20	+0.0008	+0.0014	+0.0020	+0.0024	+0.0020
24	+0.0005	+0.0010	+0.0015	+0.0020	+0.0017
32	.0000	+0.0005	+0.0009	+0.0014	+0.0013
40	.0000	+0.0003	+0.0006	+0.0011	+0.0011
48	.0000	+0.0001	+0.0004	+0.0008	+0.0010
56	.0000	.0000	+0.0003	+0.0007	+0.0008

**Table 11.7a**

$\frac{H^2}{dt}$	Coefficients at Point				
	.05H	.10H	.15H	.20H	.25H
20	+0.032	+0.039	+0.033	+0.023	+0.014
24	+0.031	+0.035	+0.028	+0.018	+0.009
32	+0.028	+0.029	+0.020	+0.011	+0.004
40	+0.026	+0.025	+0.015	+0.006	+0.001
48	+0.024	+0.021	+0.011	+0.003	0.000
56	+0.023	+0.018	+0.008	+0.002	0.000

**Table 11.8a**

$\frac{H^2}{dt}$	Coefficients at Point				
	.80H	.85H	.90H	.95H	1.00H
20	-0.015	+0.095	+0.296	+0.606	+1.000
24	-0.037	+0.057	+0.250	+0.572	+1.000
32	-0.062	+0.002	+0.178	+0.515	+1.000
40	-0.067	-0.031	+0.123	+0.467	+1.000
48	-0.064	-0.049	+0.081	+0.424	+1.000
56	-0.059	-0.060	+0.048	+0.387	+1.000

**Table 11.9a**

$\frac{H^2}{dt}$	Coefficients at Point		
	Tri. Fixed	Rect. Fixed	T. or R. Hinged
20	+0.114	+0.122	+0.062
24	+0.102	+0.111	+0.055
32	+0.089	+0.096	+0.048
40	+0.080	+0.086	+0.043
48	+0.072	+0.079	+0.039
56	+0.067	+0.074	+0.036

**Table 11.16** *Continued*

**Table 11.10a**

$\frac{H^2}{dt}$	Coefficients at Point				
	.75H	.80H	.85H	.90H	.95H
20	+0.716	+0.654	+0.520	+0.325	+0.115
24	+0.746	+0.702	+0.577	+0.372	+0.137
32	+0.782	+0.768	+0.663	+0.459	+0.182
40	+0.800	+0.805	+0.731	+0.530	+0.217
48	+0.791	+0.828	+0.785	+0.593	+0.254
56	+0.763	+0.838	+0.824	+0.636	+0.285

**Table 11.11a**

$\frac{H^2}{dt}$	Coefficients at Point				
	.75H	.80H	.85H	.90H	.95H
20	+0.949	+0.825	+0.629	+0.379	+0.128
24	+0.986	+0.879	+0.694	+0.430	+0.149
32	+1.026	+0.953	+0.788	+0.519	+0.189
40	+1.040	+0.996	+0.859	+0.591	+0.226
48	+1.043	+1.022	+0.911	+0.652	+0.262
56	+1.040	+1.035	+0.949	+0.705	+0.294

**Table 11.12a**

$\frac{H^2}{dt}$	Coefficients at Point				
	.75H	.80H	.85H	.90H	.95H
20	+0.812	+0.817	+0.756	+0.603	+0.344
24	+0.816	+0.839	+0.793	+0.647	+0.377
32	+0.814	+0.861	+0.847	+0.721	+0.436
40	+0.802	+0.866	+0.880	+0.778	+0.483
48	+0.791	+0.864	+0.900	+0.820	+0.527
56	+0.781	+0.859	+0.911	+0.852	+0.563

**Table 11.13a**

$\frac{H^2}{dt}$	Coefficients at Point				
	.75H	.80H	.85H	.90H	.95H
20	+1.062	+1.017	+0.906	+0.703	+0.394
24	+1.066	+1.039	+0.943	+0.747	+0.427
32	+1.064	+1.061	+0.997	+0.821	+0.486
40	+1.052	+1.066	+1.030	+0.878	+0.533
48	+1.041	+1.064	+1.050	+0.920	+0.577
56	+1.021	+1.059	+1.061	+0.952	+0.613

**Table 11.14a**

$\frac{H^2}{dt}$	Coefficients at Point				
	.00H	.05H	.10H	.15H	.20H
20	-16.44	- 9.98	-4.90	-1.59	+0.22
24	-18.04	-10.34	-4.54	-1.00	+0.68
32	-20.84	-10.72	-3.70	-0.04	+1.26
40	-23.34	-10.86	-2.86	+0.72	+1.56
48	-25.52	-10.82	-2.06	+0.26	+1.66
56	-27.54	-10.68	-1.36	+1.60	+1.62

**Table 11.15a**

$\frac{H^2}{dt}$	Coefficients at Point				
	.75H	.80H	.85H	.90H	.95H
20	+15.30	+25.9	+36.9	+43.3	+ 35.3
24	+13.20	+25.9	+40.7	+51.8	+ 45.3
32	+ 8.10	+23.2	+45.9	+65.4	+ 63.6
40	+ 3.28	+19.2	+46.5	+77.9	+ 83.5
48	- 0.70	+14.1	+45.1	+87.2	+103.0
56	- 3.40	+ 9.2	+42.2	+94.0	+121.0





**Photo 11.7** Shotcrete Application Covering the Wire (Courtesy, N.A. Legatos, Preload Inc., Garden City, New York.)

are required to neutralize or balance the outward radial forces caused by the internal liquid or gas, thereby producing *residual* compression in the tank when it is full (Ref. 11.2). Such an increase in circumferential prestressing forces through the use of additional horizontal prestressing steel, and sometimes mild vertical steel, also counteracts the effects of temperature and moisture gradients across the wall thickness in an adverse environment.

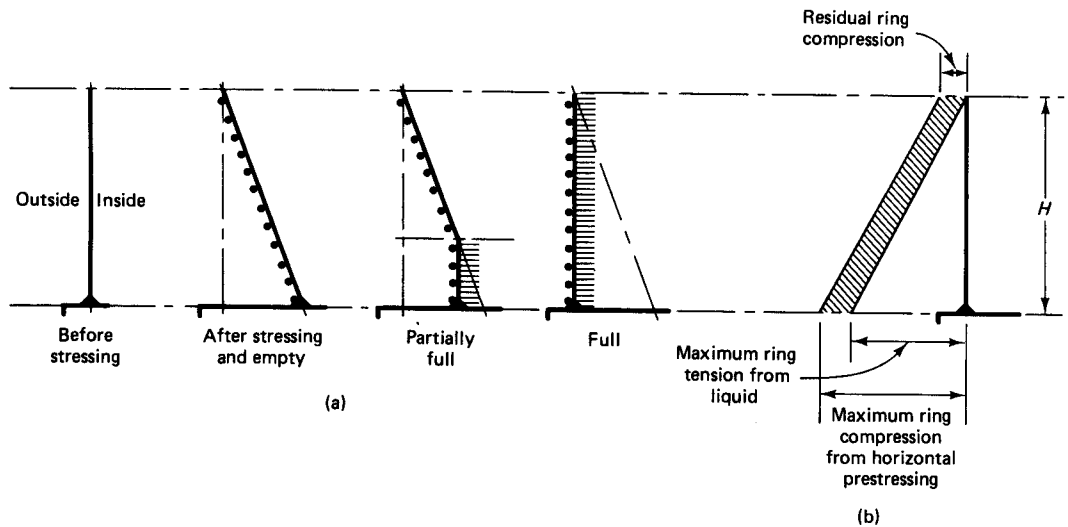
### 11.6.1 Freely Sliding Wall Base

When the boundary condition is such that the wall at its base can freely slide when the tank is internally loaded, there is no moment in the vertical wall due either to liquid load or to prestressing when the tank is totally filled to height  $H$ . Only a small nominal moment develops when the tank is partially filled, partially prestressed, or empty, and *no* vertical prestressing is necessary. The deflected shape of the freely sliding tank is shown in Figure 11.7.

While free sliding is an ideal condition that renders the structure statically determinate and hence most economical, it is difficult to achieve in practice. Frictional forces produced at the wall base after the tank becomes operational and the difficulty of achieving liquid tightness render this alternative essentially unimplementable.

### 11.6.2 Hinged Wall Base

For walls with a hinged connection to the base, the maximum radial forces due to the liquid retained and the prestressing at the critical section a distance  $y$  above the base are almost equal to those in the freely sliding case at height  $y$ . But vertical moments are introduced, and vertical prestressing becomes necessary to reduce the tensile stresses in the concrete at the outer wall face.



**Figure 11.7** Freely sliding tank. (a) Deflected shape. (b) Residual ring compression.

The deflected shape of the hinged wall is shown in Figure 11.8. Note that the critical section for ring forces is not necessarily at the same height as the moment critical section.

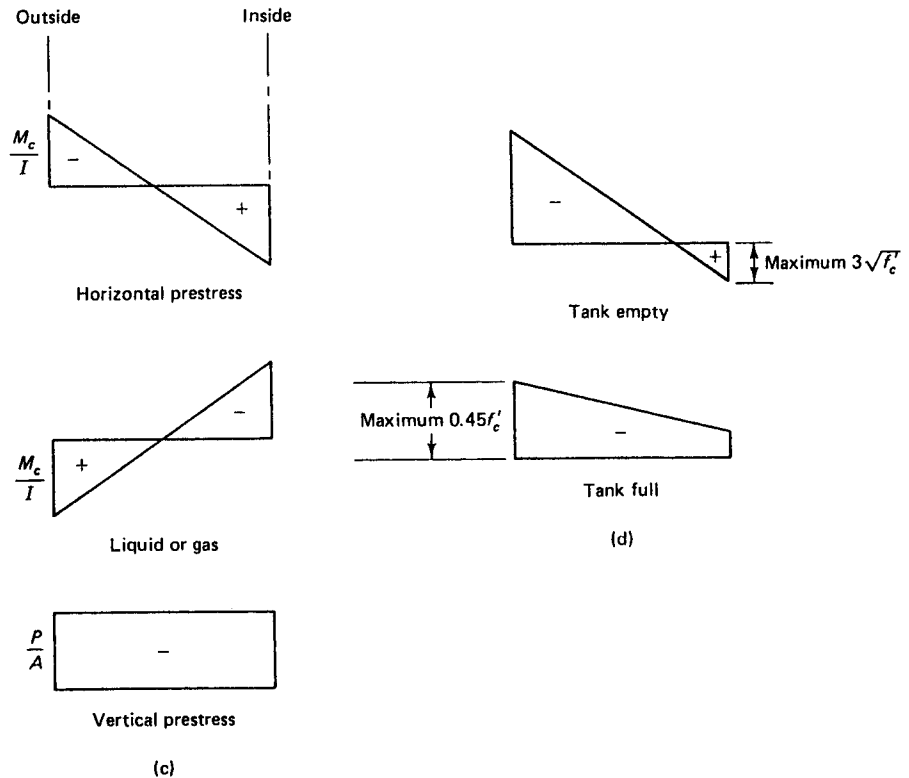
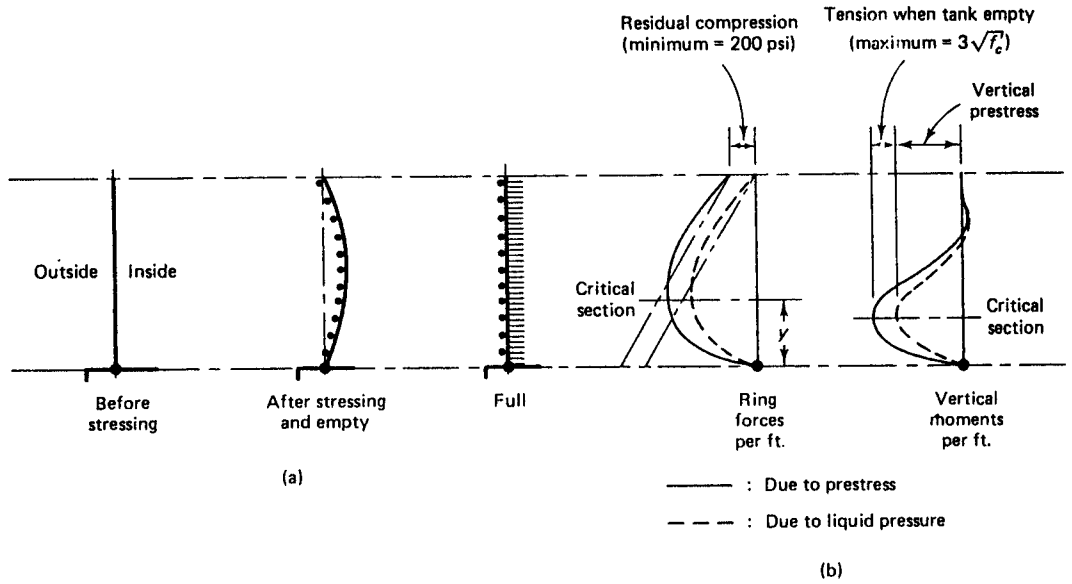
In order to minimize the possibility of cracking, a residual ring compression of a minimum value of 200 psi (1.38 MPa) is necessary for wire-wrapped prestressed tanks without diaphragms, and 100 psi (0.7 MPa) for tanks with a continuous metal diaphragm. The maximum tension at the inside face of the wall should not exceed  $3\sqrt{f'_c}$  at working-load level as given in Table 11.17 in a later section. The deflected shape of the tank walls and the stress variations in the concrete across the thickness of the section when the tank is empty and when it is full are shown in Figure 11.8. For tanks prestressed with pretensioned and post-tensioned tendons, the minimum residual compressive stress should be as stipulated in Section 11.10.

### 11.6.3 Partially Sliding and Hinged Wall Base

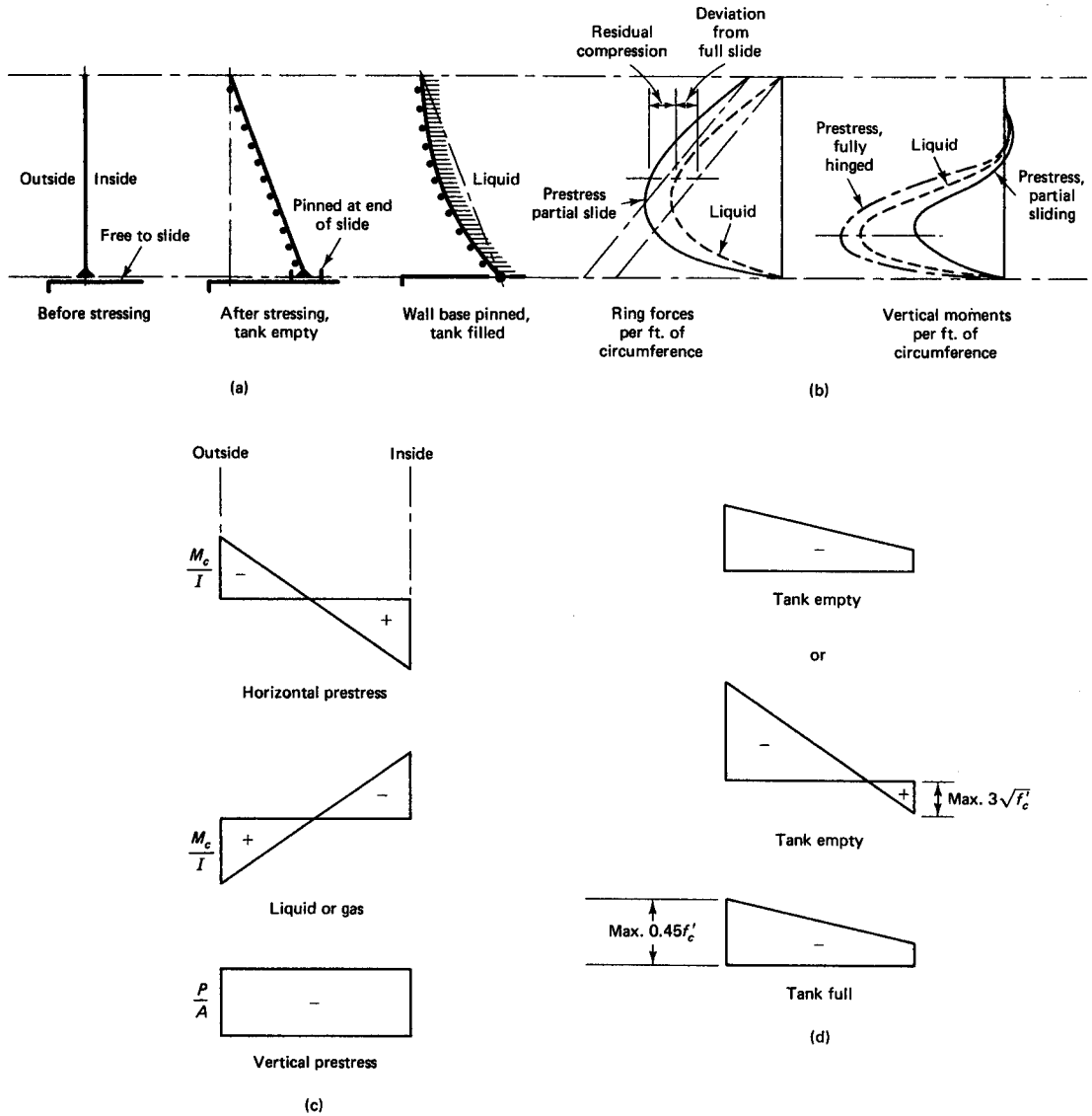
A partially sliding and hinged wall-base system is accomplished by providing a slot in the wall-base supporting slab such that the wall can slide within its base during the prestressing. After prestressing and all losses due to creep, shrinkage, and relaxation have taken place, the slot is sealed and the tank wall behaves as hinged under service-load conditions. The magnitude of sliding can be controlled such that either full or partial sliding is allowed before hinging is accomplished. A partial slide of about 50 percent of the full slide with hinging at the end of the wall movement has the structural advantages of both full sliding and hinging, and the sealing of the wall-base slab-pinned joint against leakage of liquids or gases is more dependable than if full sliding prior to anchorage is allowed. The deformed shape of the wall during the prestressing procedure, together with the ring forces, vertical moments, and concrete stress variations across the wall thickness, is shown in Figure 11.9. The vertical prestress needed for the partial slide-pinned case can be considerably smaller than the fully pinned case without sliding.

### 11.6.4 Fully Fixed Wall Base

Full fixity of the wall at its base means full restraint against rotation at the wall base. This condition can be accomplished if the lower segment of the wall is cast monolithically and is well anchored into a base slab of a similar stiffness. But such an indeterminate system

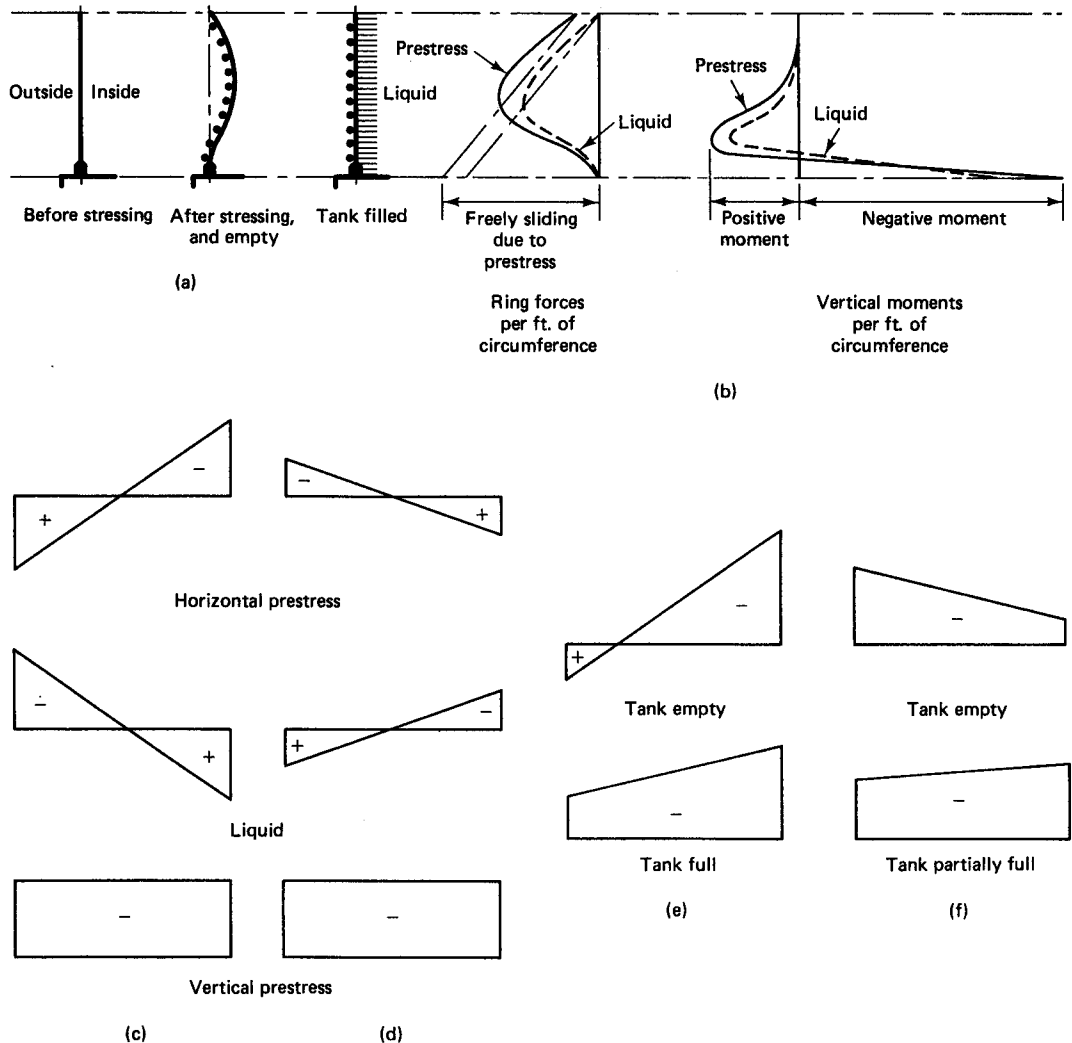


**Figure 11.8** Hinged-base tank. (a) Deflected shape of tank wall. (b) Horizontal ring forces and vertical moments. (c) Concrete stresses across wall thickness. (d) Resultant wall stresses.



**Figure 11.9** Partially sliding and hinged-base tank. (a) Deflected shape. (b) Horizontal ring forces and comparative vertical moments. (c) Concrete stresses across wall thickness. (d) Resultant wall stresses.

is difficult to fully achieve and is not economical as well, since a tank base area is very large and partial fixity becomes necessary (see shortly). The radial horizontal forces from both prestressing and the contained internal pressure are unchanged from the triangular form for liquid, rectangular for gas, and trapezoidal for granular contained material. The restraint imposed by the horizontal slab base, however, modifies the ring forces and introduces additional moment in the vertical section of the wall. Because of fixity at the base, no displacement takes place at either the bottom or the top of the wall, and a change in curvature along the height of the wall above the base takes place when the tank is empty, as is shown in Figure 11.10. Note that the wall should be designed to become essentially vertical, with a minimum residual compressive stress due to prestressing of 200



**Figure 11.10** Fully fixed-base tank. (a) Deflected wall shape. (b) Horizontal ring forces and vertical moments. (c) Concrete stresses across wall for full tank. (d) Concrete stresses across wall for partially full tank. (e) Resultant stresses, full tank. (f) Resultant stresses, partially full tank.

psi as in the previous cases. The vertical prestress needed for tanks with fully fixed wall bases is considerably greater than the vertical prestress needed for the other boundary conditions. This is necessary in order to offset the high tensile stresses in the wall base at the *outside* face caused by the large negative movement at the base [see Figure 11.10(a) and (b)] and the reverse curvature near it. It is sometimes more economical to use mild steel reinforcement at the lower portion of the wall in addition to prestressing, in order to be able to use lesser vertical prestressing and assign the excess negative moment to the nonprestressed reinforcement. The tensile stresses in the concrete can also be reduced by using *eccentric* vertical prestressing with the appropriate eccentricity achieved by trial and adjustment, as well as by using additional mild steel. Vertical prestressing in tanks is expensive, however, due to the required anchorages at the top and bottom of the tank wall. Thus, reducing the level of vertical prestress needed in the design adds to the economy of the total design of the system.

### 11.6.5 Partially Fixed Wall Base

**11.6.5.1 Rotational Restraint.** As indicated previously, full restraint against rotation at the wall base is difficult to achieve. The reasons are essentially threefold: (1) one has to provide the necessary stiffness in the tank floor slab at the wall junction for total fixity; (2) subsoil movement under the wall can cause rotation of the wall base; and (3) a concentration of anchorages is required, for both the vertical prestressing of the wall and the horizontal circumferential prestressing of the wall-base segment since the wall and base rings are separately prestressed.

Because the floor slab area is large, its restraining or stiffening influence is limited to the narrow peripheral toe cantilevering from the wall bottom. The choice of the correct width of the toe or base ring determines whether or not the assumed degree of fixity of the wall base gives the correct stiffness values in the design. Figure 11.11 schematically demonstrates the effect of the base ring width on the rotation of the wall and the deformation of the ring. Part (c) of the figure gives an equilibrium state where the tip of the ring is at the same level as the bottom of the wall, whereas the conditions represented in parts (a) and (b) involve deformations below the bottom of the wall and are consequently unsatisfactory.

The theoretical formulation of the solution to the critical ring base width can be attained through the use of the principle of superposition by combining the case of a freely rotating wall with that of a totally fixed wall as shown in Figure 11.12. Let

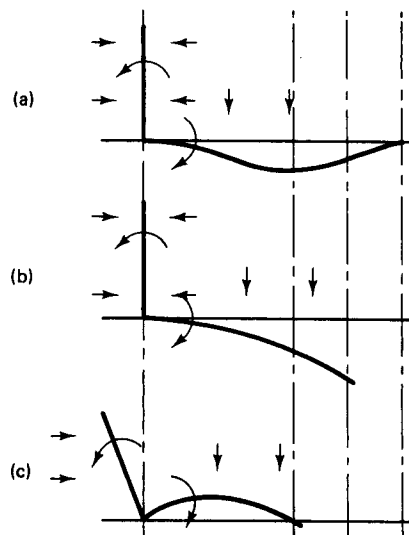
$M_0$  = theoretical fully fixed moment at the wall base

$M_p$  = partial moment at the wall base caused by the loaded cantilever toe

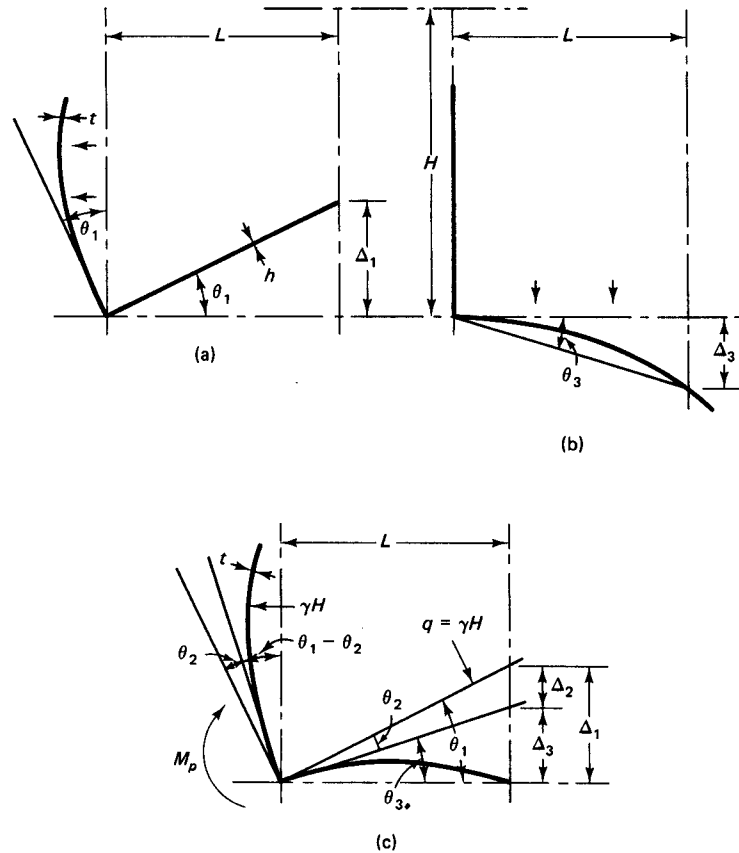
$\theta_1$  = free rotation of wall base when pinned only, corresponding to deflection  $\Delta_1$  of a stiff unloaded toe

$\theta_2$  = wall base rotation due to restraining moment  $M_p$ , corresponding to deflection  $\Delta_2$  of a straight unloaded toe

$\theta_3$  = rotation of the tip of the stiffening toe as a cantilever under vertical load, corresponding to deflection  $\Delta_3$  of the toe tip due to the vertical load



**Figure 11.11** Base ring effective width. (a) Full base slab. (b) Large cantilever. (c) Equilibrium condition.



**Figure 11.12** Deformation and rotation of wall base. (a) Fully free wall. (b) Fully fixed wall. (c) Superposition of (a) and (b).

$L$  = width of stiffening toe

$q$  = unit load applied to the stiffening toe =  $\gamma H$ , where  $H$  is the height of a tank whose diameter is  $d$ , whose wall thickness is  $t$ , and whose base slab thickness is  $h$ .

Then the unit rotation  $\theta$  of the wall at its base due to moment  $M_0$ , but without radial displacement, can be obtained from Equation 11.18a by setting  $w = 0$  to get  $Q = -\beta M$ . Equation 11.18b for unit rotation then becomes

$$\theta_1 = \frac{M_o}{2\beta D}, \quad \theta_2 = \frac{M_p}{2\beta D} \quad (11.33)$$

Hence, we have

$$\Delta_1 = \frac{LM_o}{2\beta D}, \quad \Delta_2 = \frac{LM_p}{2\beta D} \quad (11.34)$$

If the stiffening wall toe is considered a cantilever subjected to a transverse load  $\gamma H$ , the maximum cantilever moment  $M_p$  and the corresponding deflection  $\Delta_3$  are, respectively,

$$M_p = \frac{\gamma H L^2}{2}, \quad \Delta_3 = \frac{3\gamma H L^4}{2Eh^3} \quad (11.35)$$

The moment at the fixed wall base can be obtained using the membrane coefficient  $C$  from Table 11.4 for the applicable form factor  $H^2/dt$  and type of load. For liquid load,

$$M_o = C\gamma H^3 \quad (11.36)$$

The deflected form due to full load, from Figure 11.12(c), is

$$\Delta_1 = \Delta_2 + \Delta_3$$

As a reasonable approximation, assume

$$\mu = 0.2 \quad \text{and} \quad \beta = 2/\sqrt{dt}.$$

Substituting for  $\Delta_2$  and  $\Delta_3$  from Equation 11.34 into Equations 11.35 and 11.36 and rearranging terms gives

$$L^2 = \frac{2CH^2}{1 + \frac{(t/h)^3}{(dt)^{1/2}} (L = 1)} \quad (11.37)$$

and

$$M_o = \frac{\gamma HL^2}{2} \quad (11.38)$$

Now let the term

$$S = \frac{(t/h)^3}{(dt)^{1/2}} \quad (11.39)$$

in Equation 11.37 be designated a *modifying factor for partial fixity*. This factor is normally small and represents the difference between the total fixity moment  $M_o$  and the partial restraint moment  $M_p$ . Hence,

$$M_p = M_o(1 - S) \quad (11.40)$$

The value of  $L$  in the *denominator* of Eq. 11.37 is conservatively assumed = 1 for simplification in modifying the factor  $S$ .

If the value of  $S$  is very small, as is the case in large-diameter tanks (diameter larger than 125 to 150 ft), the expressions for  $L$  and  $M_p$  become expressions for full fixity, namely,

$$L^2 = 2CH^2$$

and

$$M_p = C\gamma H^3$$

**11.6.5.2 Base Radial Deformation.** The radial deformation  $\Delta_s$  of the base ring subjected to radial force in its plane can be obtained from the theory of circular plates with concentric holes. The expression for the deflection of the plate shown in Figure 11.13(a) is

$$\Delta_s = \frac{d_o Q}{2hE} \left( \frac{d_o^2 + d^2}{d_o^2 - d^2} - \mu \right) \quad (11.41)$$

where  $\mu$  = Poisson's ratio  $\sim 0.2$  for concrete and  $E$  is the modulus. The horizontal radial thrust per unit of circumference required to induce unit displacement in a solid circular slab is



$$Q_2 = \frac{2.5hE}{d_o} \quad (11.42)$$

and the corresponding value of the radiant thrust applied to the outer ring is

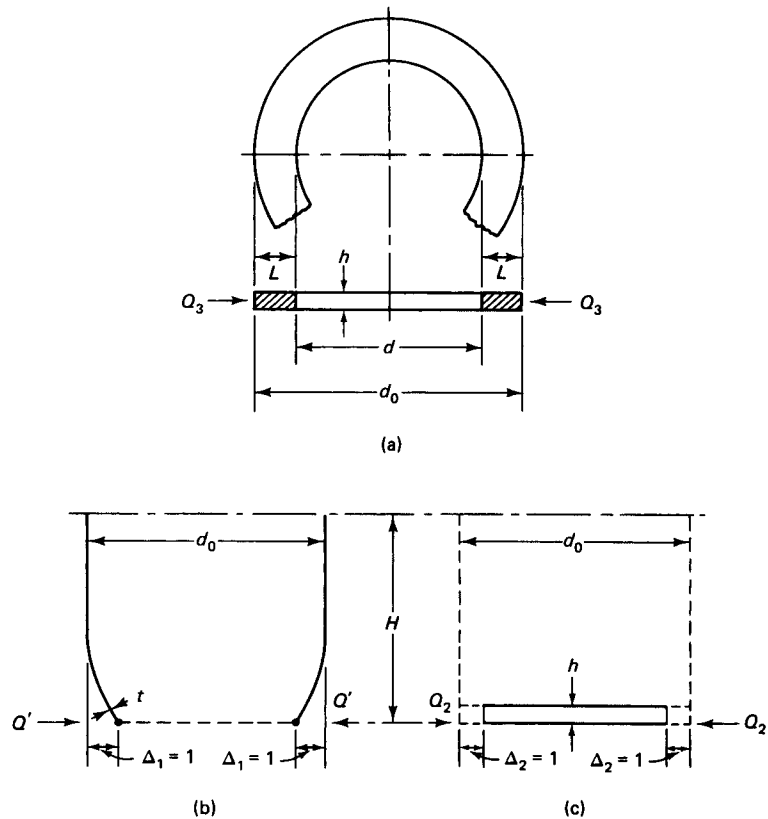
$$Q_3 = \frac{2hE}{d_o K} \quad (11.43)$$

where

$$K = \left( \frac{d_0^2 + d^2}{d_0^2 - d^2} - \mu \right)$$

and  $d$  = inside diameter of base ring =  $(d_o - 2L)$ .

The relative stiffness of the wall to the base is determined in terms of the force required to produce a *unit* deformation in the wall and the base slab from the principles of virtual work as shown in Figures 11.13(b) and (c). The distribution of the prestressing energy between the wall and base slab ring is a function of their relative radial stiffness; hence, determining the relative stiffness is necessary. In doing so, however, one must keep in mind that the stiffness response of the base ring in a prestressed tank to radial compression in its own plane is considerably larger than the response of the cylindrical wall of the tank under radial internal pressure. Thus, the loss of prestress from the differ-



**Figure 11.13** Deformation of circular wall base ring. (a) Ring plan and cross section. (b) Deflected wall bottom due to radial force  $Q'$ . (c) Deflected ring base due to radial force  $Q_2$ .

ence in stiffness is insignificant in large-diameter tanks (Ref. 11.2), but should be considered in small-diameter tanks.

The unit deformation  $\Delta$  due to the radial force  $Q'$  per unit of circumference *without rotation* at the foot base can be obtained from Equation 11.18b using  $2\beta M = -Q$  for rotation  $dw/dy = 0$ . The unit deflection  $\Delta$  in Equation 11.18a becomes

$$\Delta = \frac{Q_3}{4\beta^3 D}$$

or

$$\Delta = \frac{Q'}{4\beta^3 D} \quad (11.44)$$

where

$$D = \frac{Et^3}{12(1 - \mu^2)}$$

Using  $\mu \sim 0.2$ , Equation 11.44 for unit radial displacement of the wall at the wall base without rotation becomes

$$Q' = 2.2E \left( \frac{t}{d} \right)^{3/2} \quad (11.45)$$

where  $E$  is the modulus of concrete. From Equation 11.42, the radial force per unit of circumference required to produce unit radial displacement in the solid circular slab is

$$Q_2 = 2.5E \left( \frac{h}{d_o} \right) \quad (11.46)$$

By superimposing  $Q'$  on  $Q_2$ , the total force exerted at the wall-slab base junction is distributed to the wall and the slab base in proportion to the relative energy required to produce unit deformation in each.

The proportion of the total force  $Q' + Q_2$  to be carried by the wall is

$$R = \frac{Q'}{Q' + Q_2}$$

say

$$\frac{1}{1 + S_1}$$

Rearranging terms while combining Equations 11.45 and 11.46 results in

$$S_1 = \frac{2.5(h/d)}{2.2(t/d)^{3/2}}$$

assuming that  $d \sim d_o$ , or

$$S_1 = 1.1 \left( \frac{h}{t} \right) \times \left( \frac{d}{t} \right)^{1/2} \quad (11.47)$$

If  $S_1$  is small, the proportion of the horizontal force transferred from the slab base to the wall can be taken, with sufficient accuracy, to be

$$R = \frac{100}{S_1} \text{ percent} \quad (11.48)$$



**Photo 11.8** Six-million-gallon tendon-prestressed circular tank seen from inside with situ-cast walls. (Courtesy, Jorgensen, Hendrickson and Close, Inc., Denver, Colorado.)

When only the outer ring of the slab is compressed by radial thrust at the rim, the value of  $Q_2$  has to be modified from that obtained by Equation 11.42, and  $S_1$  in Equation 11.48 becomes

$$S_1 = \frac{1}{K} \left( \frac{h}{t} \right) \times \left( \frac{d}{t} \right)^{1/2} \quad (11.49)$$

where, from before,

$$K = \left( \frac{d_o^2 + d^2}{d_o^2 - d^2} - \mu \right)$$

in which  $d$  is the inner slab ring diameter  $= d_o = 2L$  and  $d_o$  is the outer diameter.

## 11.7 RECOMMENDED PRACTICE FOR SITU-CAST AND PRECAST PRESTRESSED CONCRETE CIRCULAR STORAGE TANKS

### 11.7.1 Stresses

General guidelines for situ-cast and precast prestressed concrete circular storage tanks are provided by the Prestressed Concrete Institute (Ref. 11.6), the American Concrete Institute (Refs. 11.7–11.9), and the Post-Tensioning Institute (Ref. 11.10) for choosing the applicable allowable stresses, dimensioning, minimum wall thickness, and construction and erection procedure. The allowable stresses in concrete and shotcrete are given in Table 11.17 (Ref. 11.7), with modifications to accommodate the recommended stresses in Ref. 11.6. Allowable stresses in the reinforcement are given in Table 11.18.

**Table 11.17** Allowable Concrete Stresses in Circular Tanks

Type and limit of stress	Concrete situ-cast and precast		Shotcrete situ-cast	
	Temporary <sup>a</sup> stresses $f_{ci}$ , psi	Service load stresses $f_c$ , psi	Temporary <sup>a</sup> stresses $f_{gi}$ , psi	Service load stresses $f_g$ , psi
Axial compression, $f_c$	$0.55f'_{ci}$	$0.45f'_c$	$0.45f'_{gi}$ but not more than 1,600 + $40t_c$ psi	$0.38f'_g$
Axial tension	0	0	0	0
Flexural compression, $f_c$	$0.55f'_{ci}$	$0.4f'_c$	$0.45f'_{gi}$	$0.38f'_g$
Maximum flexural tension <sup>b</sup> , $f_t$	$\approx 3\sqrt{f'_c}$	$3\sqrt{f'_c}$		
Minimum residual compression, $f_{cv}$	$200\left(\frac{f_{ci}}{f_c}\right)$	200 psi	$200\left(\frac{f_{ci}}{f_c}\right)$	200 psi

<sup>a</sup>Before creep and shrinkage losses.<sup>b</sup>Fiber stress in precomposed tension zone.**Table 11.18** Stresses in Reinforcement

Type of Stress	Max allowable stress*
Tendon jacking force	$0.94f_{py} \leq 0.85f_{pu}$
Immediately after prestress transfer	$0.82f_{py} \leq 0.75f_{pu}$
Post-tensioning tendons at anchorage and couplers, immediately after tendon anchorage	$0.70f_{pu}$
Service load stress, $f_{pe}$	$0.55f_{pu}$
Nonprestressed mild steel at initial prestressing, $f_{si}$	$f_y/1.6$
Final service load stress, $f_s$ (psi), potable water storage, 60 grade steel	24,000
corrosive storage	18,000
dry storage	$f_y/1.8$

\*1,000 psi = 6,895 Pa.

### 11.7.2 Required Strength Load Factors

The structure, together with its components and foundations, would have to be designed so that the design strength exceeds the effect of factored load combinations specified by ACI 318, ANSI/ASCE 7-95, or as justified by the engineer based on rational analysis, with the following exceptions:

Feature	Load factor
Initial liquid pressure	1.3
Internal lateral pressure from dry material	1.7
<i>Prestressing forces:</i>	
Final prestress after losses	1.7
Strength reduction factor for both reinforcement and concrete, $\phi$	0.9

The nominal moment strength equation  $M_n$  is similar to the one used for linear prestressing, i.e.,

$$M_n = A_{ps} f_{ps} \left( d_p - \frac{a}{2} \right) \quad (11.50a)$$

or

$$M_n = A_{ps} f_{ps} \left( d_p - \frac{a}{2} \right) + A_s f_y \left( d - \frac{a}{2} \right) \quad (11.50b)$$

when mild vertical steel  $A_s$  is used and

where  $A_{ps}$  = vertical prestressing steel per unit width of circumference, in<sup>2</sup>.

$f_{ps}$  = stress in prestressed reinforcement at nominal strength, psi

$f_y$  = yield strength of mild steel, psi

### 11.7.3 Minimum Wall-Design Requirements

#### 11.7.3.1 Circumferential Forces

##### *Liquid*

$$\text{Initial } F_i = \gamma r (H - y) \frac{f_{pi}}{f_{ps}} \text{ per foot of wall} \quad (11.51a)$$

##### *Backfill*

$$\text{Initial } F_{bi} = p(r + t) \quad (11.51b)$$

where  $t$  is the total wall thickness.

#### 11.7.3.2 Thickness and Stresses

##### *Core Wall Thickness*

$$t_{co} = \frac{F_i}{f_{ci}} \quad (11.52)$$

but not less than the minimum wall thickness to be set out in subsection 11.7.3.6.

##### *Final Stress Due to Backfill and Initial Prestress*

$$f = \frac{F_{bi}}{t} + \frac{F_i f_{pe}}{t_{co} f_{pi}} \quad (11.53)$$

**11.7.3.3 Deflections.** The unrestrained initial elastic radial deflection of the wall due to initial prestressing is

$$\Delta_i = \frac{F_i r}{t_{co} E_c} \quad (11.54)$$

where  $r$  = tank inner radius

$t_{co}$  = thickness of wall core at top or bottom of wall

$E_c$  = 57,000  $\sqrt{f'_c}$  psi for both normal-weight concrete and shotcrete.

The final radial deflection  $\Delta f$  may reach 1.5 to 3 times the initial unrestrained deflection. For normal conditions, the final permitted radial deflection can be taken as

$$\Delta f = 1.7 \Delta_i \quad (11.55)$$

**11.7.3.4 Restraint Effects*****Maximum Vertical Wall Bending Due to Radial Shear***

$$M_y = 0.24Q_0 \sqrt{rt_{co}} \quad (11.56a)$$

This moment occurs at a distance

$$y = 0.68\sqrt{rt_{co}} \quad (11.56b)$$

from the base or top edge.

***Radial Shear for Monolithic Base Details Which May be Assumed to Provide Hinged Connection***

$$Q_o = 0.38 F_i \sqrt{\frac{t_{co}}{r}} \quad (11.57)$$

This type of detail should be used only with situ-cast tanks which incorporate a diaphragm in their wall construction.

**11.7.3.5 Mild Steel for Base Anchorage.** If a diaphragm is used, extend the full area of the inside bars in a U-shape a distance

$$y_1 = 1.4\sqrt{rt_{co}} \quad (11.58a)$$

above the base. If no diaphragm is used, extend to

$$y_2 = 1.8\sqrt{rt_{co}} \quad (11.58b)$$

above the base. Note that anchorage length has to be added to  $y_1$  or  $y_2$ . The minimum area of nominal vertical steel at the base region is

$$A_s = 0.005t_{co} \quad (11.59)$$

and should be extended above the base a distance of 3 ft or

$$y_3 = 0.75\sqrt{rt_{co}} \quad (11.60)$$

whichever is greater.

**11.7.3.6 Minimum Wall Thickness*****Situ-Cast Walls***

Type of tank	Minimum wall thickness
Shotcrete-steel diaphragm tanks	3½ in.
Tanks without vertical prestressing	8 in.
Tanks with vertical prestressing	7 in.

***Precast Walls***

Type of tank	Minimum wall thickness
Tanks with vertical pretensioning and external circumferential prestress	5 in.
Tanks with vertical pretensioning and internal circumferential prestress	6 in.
Tanks with vertical post-tensioning and internal circumferential prestress	7 in.

It should be noted that for tanks prestressed with tendons, a thickness not less than 9 in. is advisable for practical considerations.

### 11.8 CRACK CONTROL IN WALLS OF CIRCULAR PRESTRESSED CONCRETE TANKS

Vessey and Preston in Ref. 11.14 recommend the following expression based on Nawy's work in Ref. 11.15 for the maximum crack width at the exterior surface of the prestressed tank wall:

$$w_{\max} = 4.1 \times 10^{-6} \epsilon_{ct} E_{ps} \sqrt{I_x} \quad (11.61)$$

where  $\epsilon_{ct}$  = tensile surface strain in the concrete

$$I_x = \text{grid index} = \frac{8}{\pi} \left( \frac{s_2 s_1 t_b}{\phi_1} \right)$$

$s_2$  = reinforcement spacing in direction "2"

$s_1$  = reinforcement spacing in perpendicular direction "1" (horizontal)

$t_b$  = concrete cover to center of steel

$\phi_1$  = diameter of steel in main direction "1."

The tensile strain can be computed from

$$\epsilon_{ct} = \frac{\alpha_t f_{pi}}{E_{ps}} \quad (11.62)$$

where  $\alpha_t$  = stress parameter  $\cong f_p/f_{pi}$

$f_p$  = actual stress in the prestressing steel

$f_{pi}$  = initial prestress before losses.

For liquid-retaining tanks, the maximum allowable crack width is 0.004 in.

### 11.9 TANK ROOF DESIGN

Roofs for storage tanks are constructed in the form of a shell dome or as flat roofs supported internally on columns. The cost of the roof is generally about one-third of the overall cost of the structure. In the case of flat roofs, whether precast or situ cast, the design follows the normal design principles of floor systems for reinforced or prestressed concrete one-way- or two-way-action floors as stipulated in the ACI 318 Code. If the roof is made out of precast prestressed elements, and the tank diameter is not exceedingly large, no interior columns are necessary. Otherwise, the added cost of interior columns and the accompanying footings would increase the cost of the overall structure.

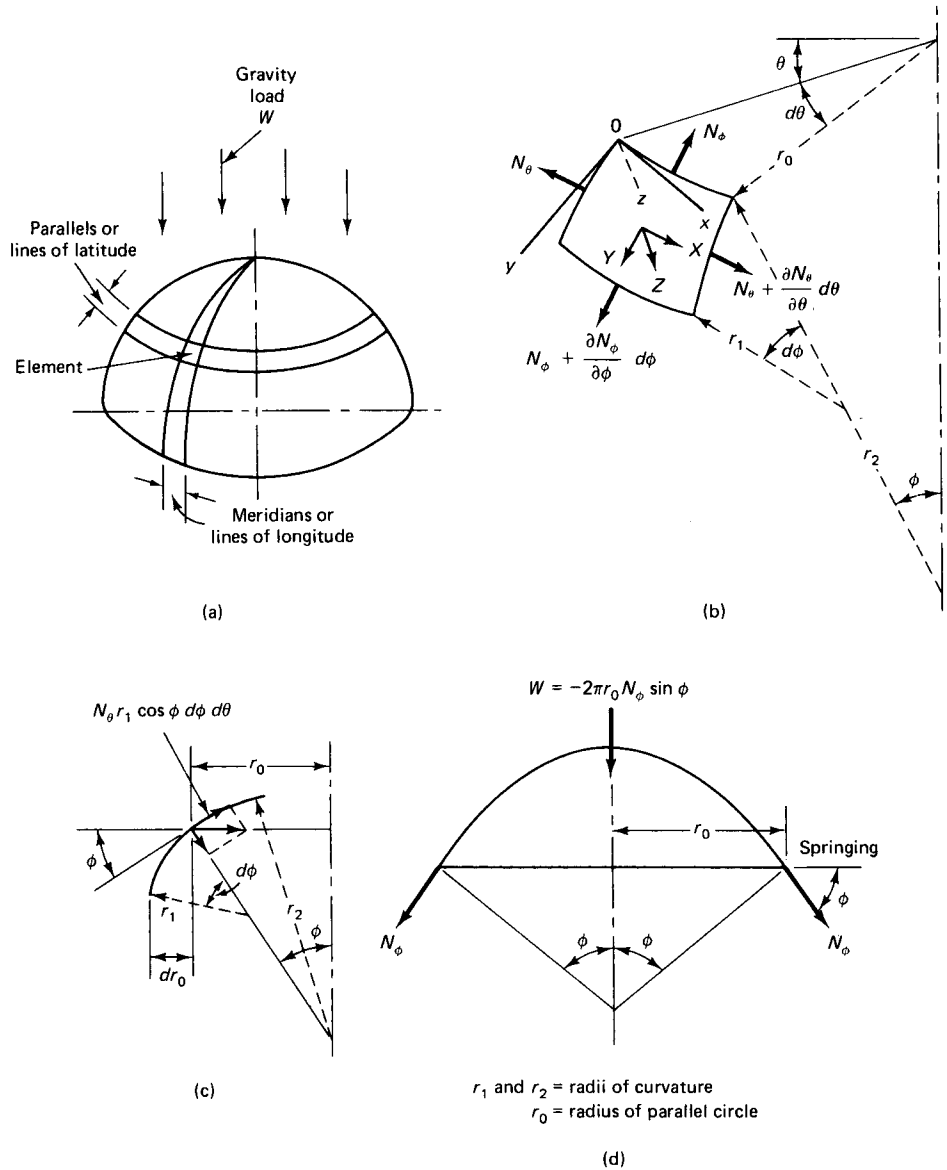
A shell roof in the form of a dome has distinct advantages for tanks not exceeding 150 ft. in diameter, namely, that the dome does not need supporting interior columns and can also be economical in underground storage tanks in withstanding backfill load. Hence, the shell form and the manner of its connection to the tank walls have a significant effect on cost. Preferably, the roof shell should be supported by tank walls with a completely *flexible* joint; otherwise the design of both the tank wall and the roof dome will have to be modified in relation to their degree of interrestraint and relative stiffness, with the concomitant added construction cost.

A spherical shell of low rise-to-diameter ratio  $h'/d$  of approximately  $\frac{1}{8}$  is reasonable to use. Such a flat dome or axisymmetrical shell introduces outward horizontal thrust at the springing, which has to be resisted by a properly designed prestressed ring beam at the support level. The type of support of the ring beam determines the extent to which redundant reactions and moments due to end restraint impose additional direct and bending stresses in the shell near the springing. In other words, the membrane solution

has to be adequately modified by superimposing on it the bending effects determined by the strain compatibility requirements of the bending theory.

### 11.9.1 Membrane Theory of Spherical Domes

**11.9.1.1 Shell of Revolution.** The basic membrane equations of equilibrium for the direct forces in a shell of revolution as shown in Figure 11.14 are used for defining the unit meridional forces  $N_\phi$ , unit tangential forces  $N_\theta$ , and unit central shears  $N_{\phi\theta}$  and  $N_{\theta\phi}$  in terms of the gravity loads  $p_\phi$ ,  $p_\theta$ , and  $p_z$ . These equations are as follows:



**Figure 11.14** Membrane forces in a shell of revolution. (a) Meridian and parallel lines. (b) Membrane forces on infinitesimal surface element. (c) Component of force  $N_\theta r_1 d\phi$  in the  $y$  direction needed to simplify the basic equation 11.63a. (d) Dome cross section with total gravity load  $W$ .



$$\text{Meridional: } \frac{\partial(N_\phi r_o)}{\partial\phi} - N_\theta \frac{\partial r}{\partial\phi} + \frac{\partial N_{\theta\phi}}{\partial\theta} r_1 + p_\phi r_o r_1 = 0 \quad (11.63a)$$

$$\text{Tangential: } \frac{\partial N_\theta}{\partial\theta} r_1 + N_{\theta\phi} \frac{\partial r_o}{\partial\phi} + \frac{\partial N_{\theta\phi}}{\partial\phi} r_1 + p_\theta r_o r_1 = 0 \quad (11.63b)$$

$$\text{z-direction: } \frac{N_\phi}{r_1} + \frac{N_\theta}{r_2} + p_z = 0 \quad (11.63c)$$

Because of loading symmetry, all terms involving  $\partial\theta$  vanish, and those involving  $\partial\theta$  can be rewritten as total differentials  $d\phi$  since nothing varies with respect to  $\theta$ . Also, the circumferential load component  $p_\theta = 0$ , as the shear resultants vanish along the meridional and parallel circles. Hence, Equations 11.63 can be rewritten as

$$\frac{d}{d\phi}(N_\phi r_o) - N_\theta r_1 \cos\phi + p_y r_1 r_o = 0 \quad (11.64a)$$

$$\frac{N_\phi}{r_1} + \frac{N_\theta}{r_2} + p_z = 0 \quad (11.64b)$$

### 11.9.1.2 Spherical Dome

*Membrane Analysis of the Equilibrium Forces.* The spherical dome has a uniform curvature. Consequently,  $r_1 = r_2 = r_o$ . Assuming that the radius of the sphere =  $a$ , then  $r_o = a \sin\phi$  in Figure 11.14(c), and, setting  $p_z = w_D$  for self-weight, the general equilibrium equations 11.64 become

$$N_\theta = aw_D \left( \frac{1}{1 + \cos\phi} - \cos\phi \right) \quad (11.65a)$$

and

$$N_\phi = -\frac{aw_D}{1 + \cos\phi} \quad (11.65b)$$

where  $w_D$  is the intensity of self-weight per unit area. It is plain from Equation 11.65b that the meridional force  $N_\phi$  is always negative. Therefore, *compression* develops along the meridians and increases as the angle  $\phi$  increases: when  $\phi = 0$ ,  $N_\phi = -\frac{1}{2} aw_D$ ; and when  $\phi = \pi/2$ ,  $N_\phi = -aw_D$ .

The tangential force  $N_\theta$  is negative, i.e., compressive, only for limited values of the angle  $\phi$ . Setting  $N_\theta = 0$  in Equation 11.65a,  $1/(1 + \cos\phi) - \cos\phi = 0$  gives  $\phi = 51^\circ 49'$ . This determination indicates that for  $\phi$  greater than  $51^\circ 49'$ , tensile stresses develop in the direction perpendicular to the meridians. The distribution of the meridional stresses  $N_\phi$  and the tangential stresses  $N_\theta$  for both the self-weight  $w_D$  and the external live load  $w_L$  is shown in Figure 11.15.

If the external load is uniform, such as snow, giving a projection intensity  $w_L$ , the meridional force  $N_\phi$  is obtained from free-body equilibrium by equating the external load to the internal meridional force, i.e.,  $-\pi(d/2)^2 w_L = 2\pi(a \sin\phi) N_\phi$ . Since  $d/2 = a \sin\phi$ , we obtain

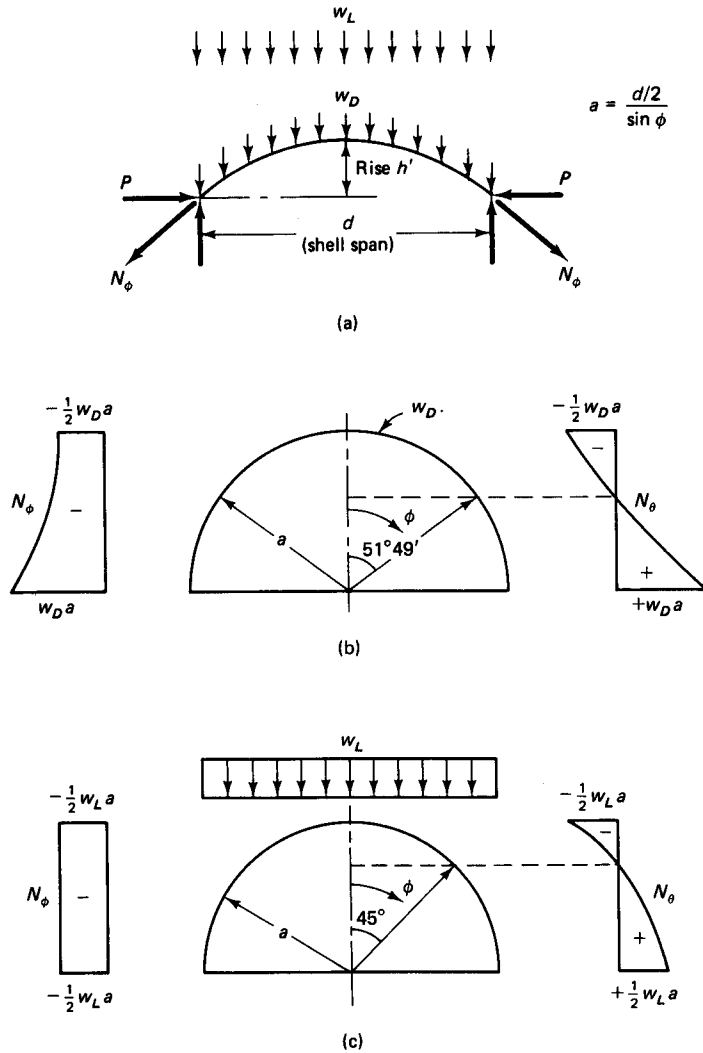
$$N_\phi = -\frac{w_L a}{2} \quad (11.66a)$$

Hence,  $N_\phi$  is constant throughout the shell depth, as is plain in Figure 11.15.

$N_\theta$  due to the live load  $w_L$  is

$$N_\theta = -aw_L \cos^2\phi + \frac{aw_L}{2} = aw_L \left( \frac{1}{2} - \cos^2\phi \right) = \frac{aw_L}{2} \cos 2\phi \quad (11.66b)$$

(-): Compression  
(+): Tension



**Figure 11.15** Gravity membrane force distribution in a spherical dome. (a) Flat dome segment of rise  $h'$ . (b) Membrane stresses due to self-weight  $w_D$  ( $N_\theta = 0$  for  $\phi = 51^\circ, 49'$ ). (c) Membrane stresses due to snow load  $w_L$  ( $N_\theta = 0$  for  $\phi = 45^\circ$ ).

For the case of  $N_\theta = 0$ , the shell angle  $\phi = 45^\circ$ . Consequently, shell stresses due to tangential forces  $N_\theta$  for  $\phi$  less than 45 degrees are compressive, eliminating cracking. From the distribution of the tangential forces  $N_\theta$ , it can be concluded that roofs of storage tanks should be flat, i.e., the ratio  $h'/d$  in Figure 11.15(b) should not exceed  $\frac{1}{8}$ , so that the concrete will be totally in compression due to both  $N_\phi$  and  $N_\theta$ , as angle  $\phi$  is less than  $51^\circ 49'$  for meridional forces and  $45^\circ$  for tangential forces.

As discussed at the outset, the support type at the springing level, if restrained, introduces indeterminate reactions that result in direct and bending stresses in the shell near the springing level. Accordingly, the bending theory, a rigorous procedure beyond the scope of this text, has to be applied. Refs. 11.1 and 11.3, on the subject of plates and shells, can be used for determining the resulting bending stresses. The following covers the design of the

prestressed ring beam at the springing level to counter the horizontal component of the meridional compressive thrust  $N_\phi$  which causes the edge of the dome to move inwards.

From Equations 11.65b and 11.66a, the meridional thrust,  $N_\phi$ , for self-weight  $w_D$  per unit surface area and uniform live load  $w_L$  per unit projected area can be written as

$$N_\phi = -a \left( \frac{w_D}{1 + \cos \phi} + \frac{w_L}{2} \right) \quad (11.67)$$

where  $a = d/2 \sin \phi$  is the radius of the shell.

Note that the thrust,  $N_\phi$ , becomes vertical at the springing ( $\phi = \pi/2$ ) of a hemispherical dome and is equal to  $W = a/2(2w_D + w_L)$  per unit width. At other values of  $\phi$ ,  $N_\phi$ , it is inclined and the value of its horizontal component is needed for the design of the prestressed ring beam at the springing level, namely, the shell rim. This horizontal component is  $p = N_\phi \cos \phi$ . If  $P$  is the prestressing force per beam height in the ring beam, then  $P = pd/2$  from Equation 11.1a, and

$$P = \frac{d}{2} (N_\phi \cos \phi) \quad (11.68)$$

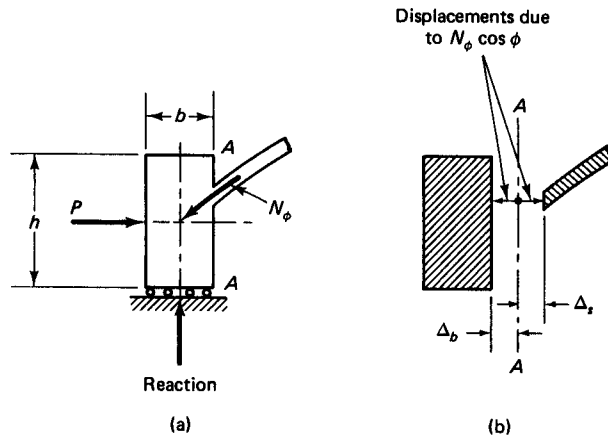
Evidently, if the force  $P$  could be applied directly to the dome rim, the stresses in the dome would be those defined by Equation 11.67. This is usually not feasible, since the large amount of prestressing steel needed due to  $P$  cannot be accommodated in the small thickness of the shell, and the stress in the concrete in the rim zone would be very high indeed. Thus, an edge beam has to be provided, transforming the shell into a statically determinate structure.

**Prestressing the Statically Indeterminate Flat Dome.** The simplest boundary condition is obtained when the edge beam reaction is vertical and without any support restraint, as shown in Figure 11.16, where the dome thrust  $N_\phi$  passes through the beam centroid. If an imaginary cut along line A-A is made, the horizontal thrust  $N_\phi \cos \phi$  causes the dome edge to move *inwards* a distance (Ref. 11.16)

$$\Delta_s = \frac{d}{2Et} (N_\phi - \mu N_\phi) \quad (11.69)$$

where  $\mu = \text{Poisson's ratio} \approx 0.2$  for concrete

$d = \text{shell span}$



**Figure 11.16** Ring beam effects. (a) Simply supported beam with thrust line passing through ring beam centroid. (b) Shell displacements at rim; rotations disregarded.

and the tangential unit force is obtained from Equation 11.65a as

$$N_{\theta} = \frac{w_D d}{2 \sin \phi} \left( \frac{1}{1 + \cos \phi} - \cos \phi \right) - \frac{w_L d}{4 \sin \phi} (\cos 2\phi) \quad (11.70)$$

Conversely, the meridional thrust  $N_{\phi}$  causes the ring beam to move *outwards* a distance

$$\Delta_b = \frac{N_{\phi}(\cos \phi)d^2}{4Ebh} \quad (11.71)$$

The prestressing force must therefore be sufficient to move the ring beam *inwards* a total distance

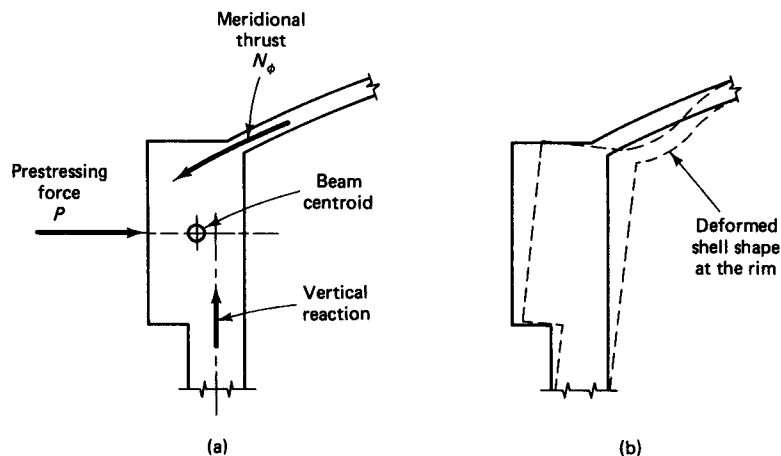
$$\Delta_T = \Delta_s + \Delta_b$$

so that the total force acting on the ring beam cross section is

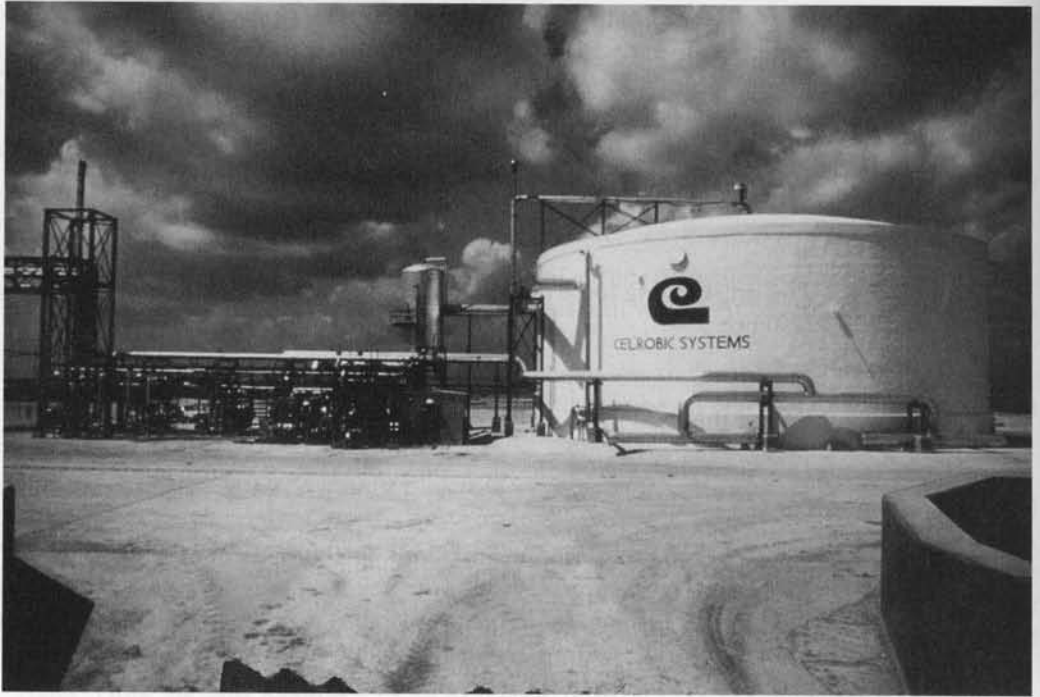
$$P = \frac{bh}{t} (N_{\theta} - \mu N_{\phi}) + \frac{d(N_{\phi} \cos \phi)}{2} \quad (11.72)$$

where  $h$  is the total ring beam depth. A comparison of Equations 11.72 and 11.68 shows that the effective prestressing force needed in the former is greater than that required in the latter. The magnitude of this increase is about 5 to 10 percent. The same conditions also hold true for domes in which the line of thrust from the dome does not pass through the centroid of the ring beam and the beam itself is rigidly attached to the wall as in Figure 11.17(a). The required prestressing force  $P$  can be obtained approximately by increasing the value of  $P$  in Equation 11.68 by 10 percent (Ref. 11.16). In such a case, the stresses in the shell itself at the springing level zone can significantly differ from those obtained in the membrane solution, and the bending solution modifications have to be made as in Ref. 11.1 or 11.3.

If the horizontal radial prestressing force in the ring beam is larger than required, excessive bending deformation develops in the shell rim, as is shown in Figure 11.17(b), with a significant increase in the value of the tangential force  $N_{\theta}$  as compared to the increase in the meridional force  $N_{\phi}$ . As a result, the bending stresses in the concrete in the affected zone could exceed the maximum allowable at service load. If the initial prestress before losses is  $P_i$ , the area of the beam cross section is



**Figure 11.17** Edge ring beam monolithic with tank wall. (a) Thrust  $N_{\phi}$  not passing through ring beam centroid—general case. (b) Shell deformed shape due to excessive prestressing.



**Photo 11.9** 1.55 Million Gallon Reactor Tank, Bishop Texas. (Courtesy, N.A. Legatos, Preload Inc., Garden City, New York.)

$$A_c = \frac{P_i}{f_c} \quad (11.73)$$

where  $P_i$  = initial prestressing force  $P/\bar{\gamma}$   
 $f_c$  = allowable compressive stress in the concrete  
 $\bar{\gamma}$  = residual stress percentage.

It is desirable to maintain a low value of  $f_c$ , about  $0.2f'_c$  and not exceeding 800 to 900 psi, in order to minimize any excessive strain that develops in the edge ring beam, which in turn could produce high stresses in the shell at the springing zone.

The area of the prestressing steel in the dome ring is

$$\text{Unit } A_{ps} = \frac{P_i}{f_{pi}} \quad (11.74a)$$

where  $f_{pi}$  is the allowable stress, in psi, in the prestressing reinforcement before losses. If accurate analysis to determine  $A_{ps}$  is not required, the steel area can be taken as

$$A_{ps} = \frac{W \cot \phi}{2\pi f_{pe}} \quad (11.74b)$$

where  $W$  = total dead and live load on the dome due to  $w_D + w_L$   
 $f_{pe}$  = effective steel prestress after losses, psi.

The minimum thickness of the dome required to withstand buckling (Ref. 11.7) may be taken to be

$$\text{Min } h_d = a \sqrt{\frac{1.5p_u}{\phi\beta_i\beta_c E_c}} \quad (11.75)$$

where  $a$  = radius of dome shell

$p_u$  = ultimate uniformly distributed design unit pressure due to dead load and live load =  $(1.2D + 1.6L)/144$

$\phi$  = strength reduction factor for material variability in compression = 0.65

$\beta_i$  = buckling reduction factor for deviations from true spherical surface due to imperfections

$\beta_i = (a/r_i)^2$ , where  $r_i \leq 1.4a$

$\beta_c$  = buckling reduction factor for creep, material nonlinearity, and cracking =  $0.44 + 0.003 W_L$ , but not to exceed 0.53

$E_c$  = initial modulus of concrete =  $57,000 \sqrt{f'_c}$  psi.

## 11.10 PRESTRESSED CONCRETE TANKS WITH CIRCUMFERENTIAL TENDONS

Instead of wrapping the prestressing wires or strands, as is done in the Preload System, internal or external horizontal tendons are used. These tendons are stressed after they are placed within or on the wall. Vertical post-tensioning is incorporated in the walls as part of the vertical reinforcement. The concrete walls are either cast in place or precast, and the core wall is considered to be the portion of the concrete wall that is circumferentially prestressed. No steel diaphragms are used in this type of construction as compared with wrapped-wire prestressing, where the tank walls can be either with or without steel diaphragms.

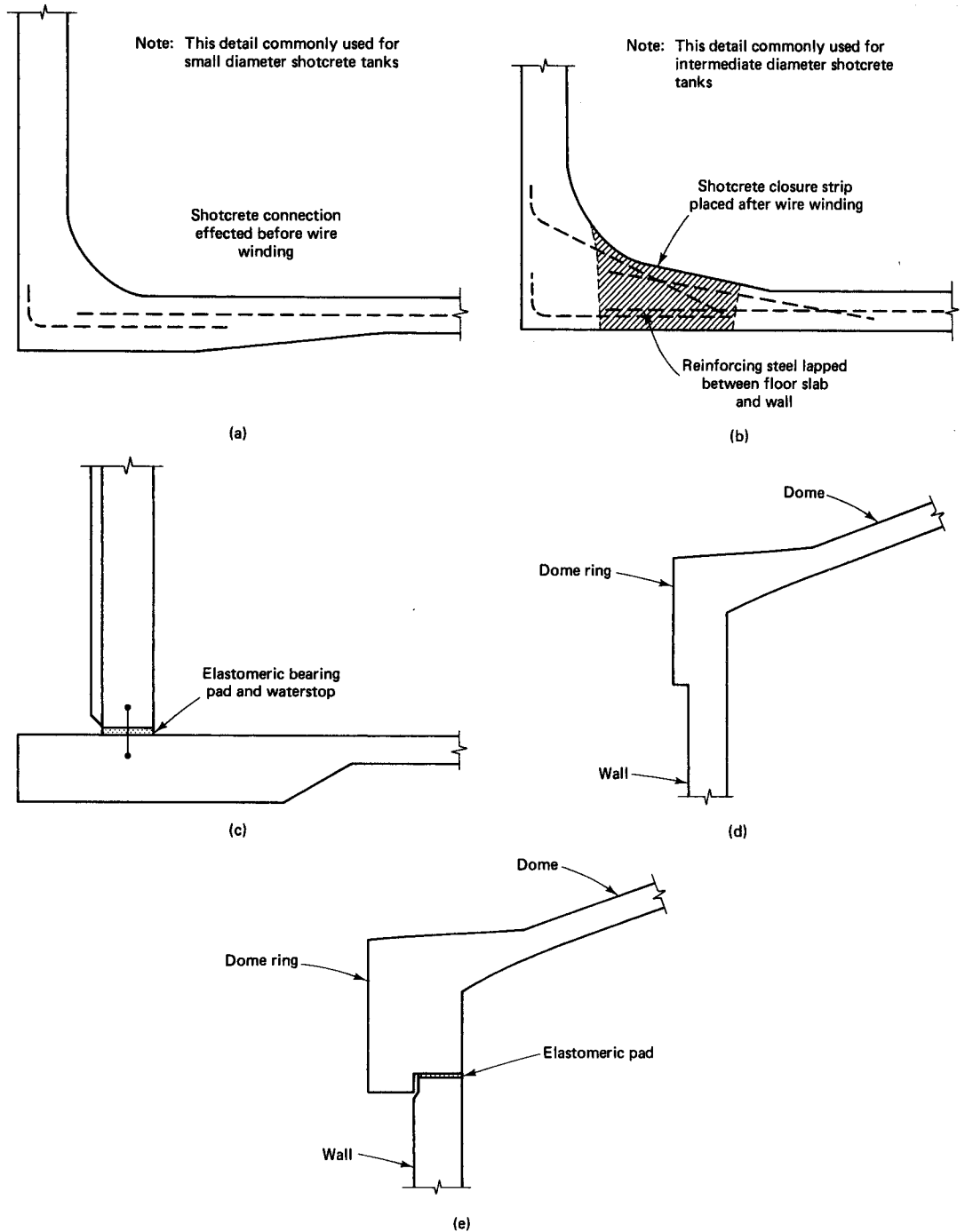
The internal prestressed reinforcement is protected by the concrete cover as required in ACI 318, and the ducts or sheathing have to be filled with corrosion-inhibiting materials or grouted. The bonded post-tensioned tendon reinforcement has to be protected by portland cement grout as required in the ACI 318 code, and external tendons should be protected by a shotcrete cover of 1-in. (25-mm) minimum thickness.

The wall design procedures are similar to those of circular tanks prestressed by wire or strand wrapping, and the same requirements for crack control and water or liquid tightness apply. A minimum residual compressive stress of 200 psi (1.4 MPa) in the concrete wall after all prestress losses has to be provided in the design when the tank is filled to the design level. If the tank is not covered, a residual compressive stress of 400 psi (2.8 MPa) has to be provided at the wall top, reducing linearly to not less than 200 psi at  $0.6\sqrt{Rh}$  from the top of the liquid level.

**Typical Wall Base and Dome Roof Connections.** From the foregoing discussions, it is clear that the boundary conditions at the base of the circular prestressed tank and at the ring beam support for the roof dome determine the practicality, economy, and success of the entire design. Consequently, accumulated experience in developing the connections at these boundary conditions is invaluable. A selection of connection details taken from Refs. 11.6 to 11.9 is given in Figures 11.18 through 11.22.

## 11.11 SEISMIC DESIGN OF LIQUID CONTAINMENT TANK STRUCTURES

Liquid containing tanks, including prestressed circular tanks, also have to be designed to resist earthquake loads in high seismic intensity zones. Such zones are in site classes C, D, E, and F, and seismic use groups II and III discussed in Sections 13.2.2 and 13.3.3 on the design of structures by IBC 2009. The scope of this book precludes extension of the detailed static design of prestressed circular tanks presented in the previous sections, to seismic design aspects. However, it is important to briefly bring to the reader's attention some highlights of this topic as they appear in the recent ACI 350 Report (Ref. 11.17).



**Figure 11.18** Cast-in-place tanks. (a) Monolithic base joint; monolithic and fully restrained against translation before and after wire winding. (b) Monolithic base joint; hinged with limited restraint against translation during wire winding, and monolithic and fully restrained against translation after wire winding. (c) Separated base joint, allows translation, rotation, or both (d) Monolithic dome-wall connection. (e) Separated dome-wall connection.

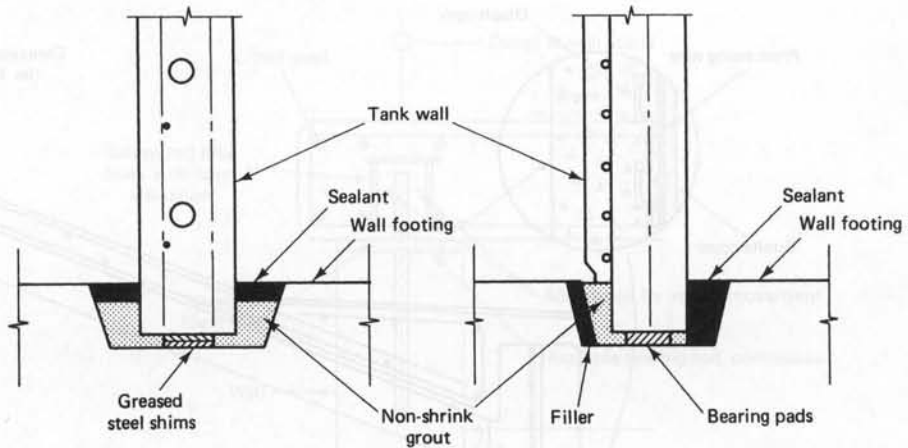


Figure 11.19 Wall base joints for precast tanks.

The general principles for ground motion in this Report are essentially similar to those of the IBC 2009. The walls of the liquid containment vessels have to be designed for the following dynamic forces in addition to the static pressures:

- (a) Lateral inertia wall force  $P_w$  and roof force  $P_r$ ,
- (b) Hydrodynamic impulsive pressure  $P_i$  from the contained liquid,
- (c) Hydrodynamic convective pressure  $P_c$  from the contained liquid,

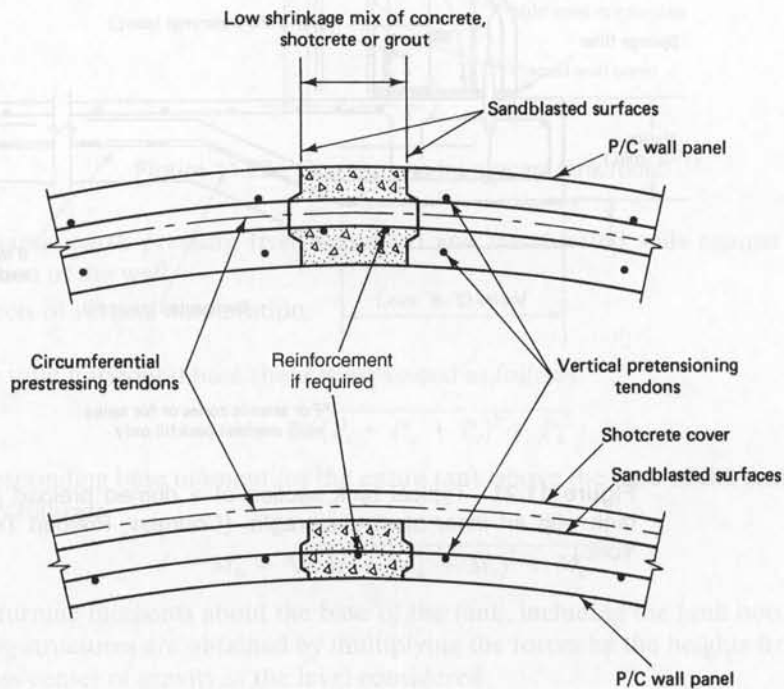
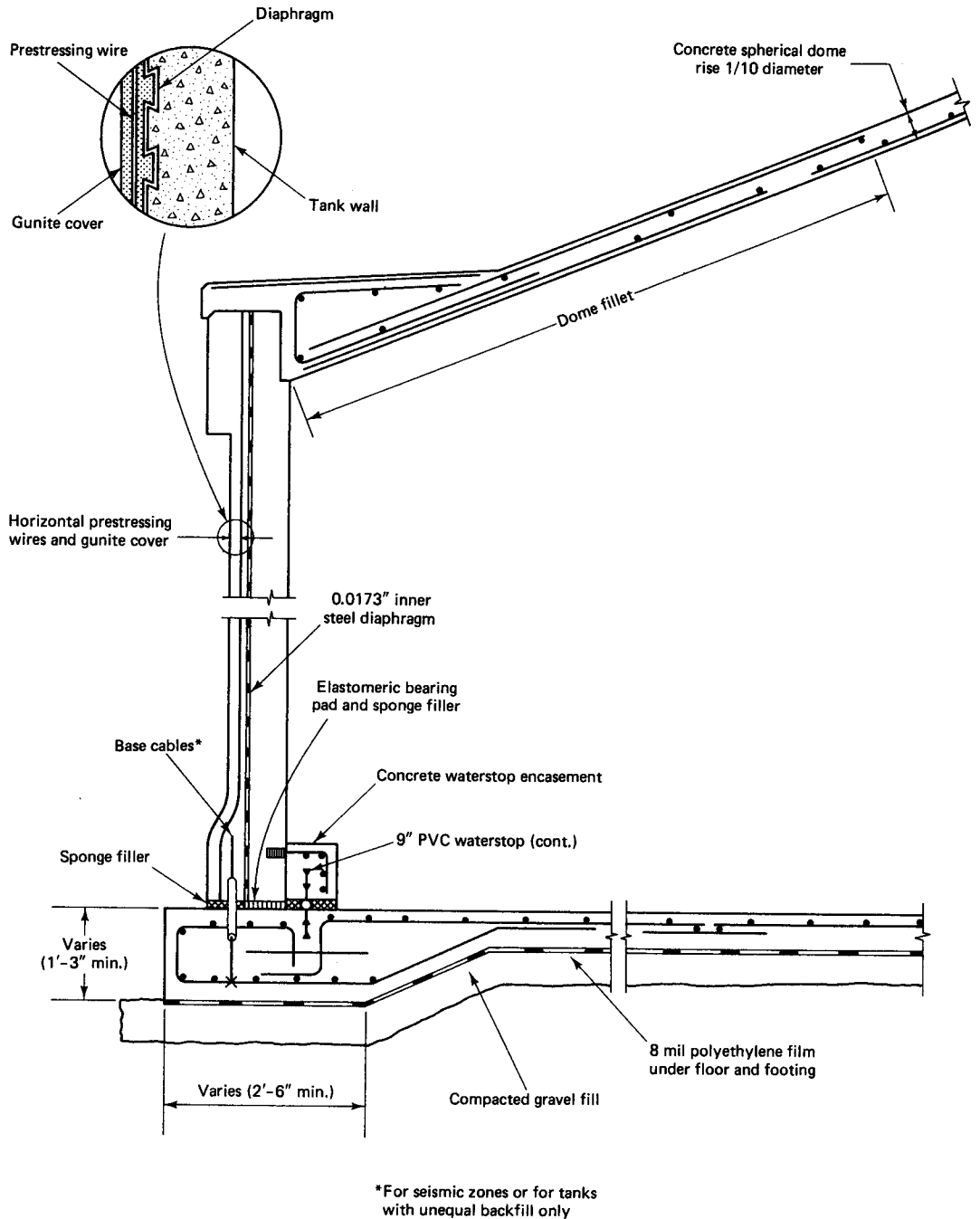
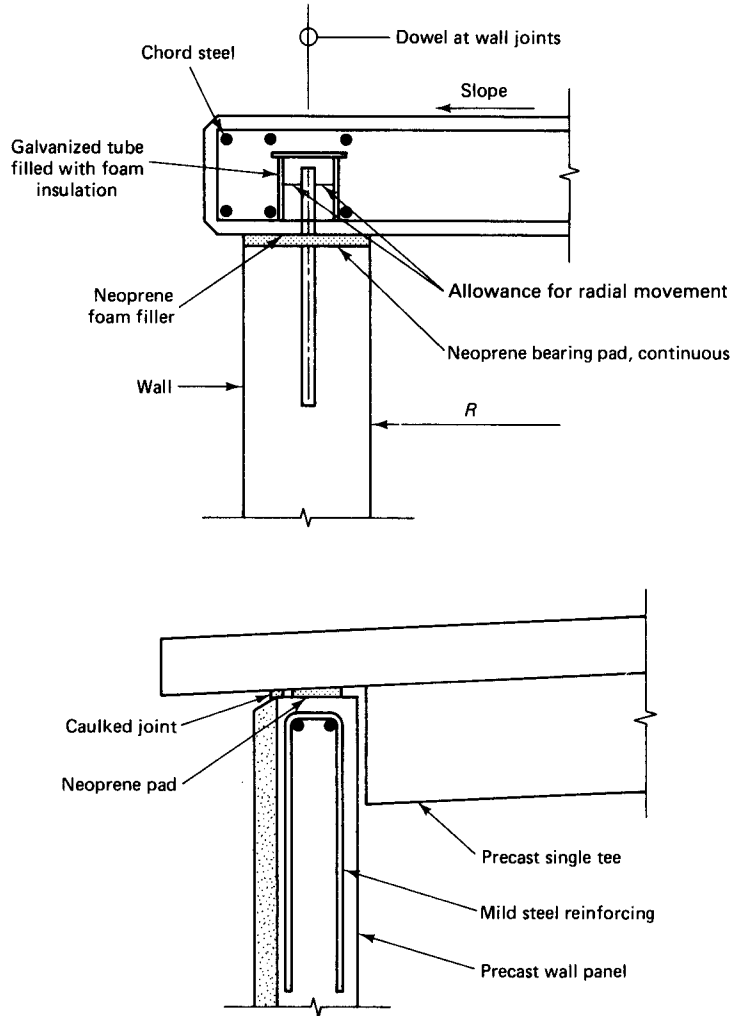


Figure 11.20 Vertical wall joints for precast tanks.





**Figure 11.21** Typical tank section of a domed preload prestressed concrete tank with an inner steel diaphragm. (Courtesy, Preload Technology, Inc., New York.)



**Figure 11.22** Connections for precast tank roofs.

- (d) Dynamic earth pressure from saturated and unsaturated soils against the buried portion of the wall,
- (e) Effects of vertical acceleration.

The total horizontal base shear is expressed as follows:

$$V = \sqrt{(P_i + P_w + P_r)^2 + P_c^2} \tag{11.76}$$

The corresponding base moment for the entire tank above the base of the tank wall is expressed as follows:

$$M_b = \sqrt{(M_i + M_w + M_r)^2 + M_c^2} \tag{11.77}$$

The overturning moments about the base of the tank, including the tank bottom and the supporting structures are obtained by multiplying the forces by the heights from the base to the mass center of gravity at the level considered.

Expressions for computing the various forces in Equation 11.76 and moments in Equation 11.77 are presented in ACI 350 Report. In addition, various factors and coeffi-

coefficients such as seismic zone factor, soil profile coefficient, importance factor, and response modification factor are presented, in a similar manner and often comparable in numerical values as those in the tables presented in Chapter 13.

### 11.12 STEP-BY-STEP PROCEDURE FOR THE DESIGN OF CIRCULAR PRESTRESSED CONCRETE TANKS AND DOME ROOFS

The following trial-and-adjustment procedure is recommended for designing a prestressed concrete circular tank and its roof shell:

1. Select the prestressing system, the type of prestressing wire, the concrete strength, and the type of restraint that can be accomplished under local conditions.
2. Determine the contained material pressure on the wall:  $\gamma H$  for liquid and  $p$  for gas. Use the trapezoidal distribution for granular or solid containment. Find the unit ring force  $F = \gamma(H - y)r$  for a completely sliding base, where  $r$  is the radius of the tank and  $y$  is the distance above the base.
3. Choose, from Tables 11.4 through 11.16, the applicable vertical moment coefficients for the particular load type and wall base restraint condition caused by liquid pressure

$$M_y = +\frac{1}{\beta}[\beta M_o \phi(\beta y) + Q_o \zeta(\beta y)]$$

and determine the corresponding horizontal radial ring tensions

$$Q_o = +(2\beta H - 1) \frac{\gamma r t}{\sqrt{12(1 - \mu^2)}}$$

and  $Q_y = (F - \Delta Q_y)$ , where the offset

$$\Delta Q_y = +\frac{6(1 - \mu^2)}{\beta^3 r t^2} (\beta M_o \psi(\beta y) + Q_o \theta(\beta y))$$

and

$$\beta = \frac{[3(1 - \mu^2)]^{1/4}}{(rt)^{1/2}}$$

where  $\mu \approx 0.20$  for concrete.

4. Find the applicable membrane coefficients  $C$  from Tables 11.4 through 11.16. Compute the applicable ring force  $F = C\gamma Hr$ .
5. Compute the critical vertical moments in the wall using the applicable membrane coefficient  $C$ . The equation for moment due to liquid load is

$$M_y = C(\gamma H^3 + p H^2)$$

or

$$M_y = CpH^2$$

due to gas load if applicable. Compute the moment at the base, where applicable, and at the critical  $y$  plane above the base.

6. Choose the level of vertical prestressing force.
7. Compute the concrete stresses across the thickness of the wall both for the condition when the tank is empty and for when it is totally full. Allow maximum residual

axial compressive stress  $f_{cv} = 200$  psi at service and a maximum tensile stress  $f_t = 3\sqrt{f'_c}$  as shown in Table 11.17.

8. Design both the horizontal and the vertical prestressing steel limiting stresses to those given in Table 11.18.
9. Compute the factored moment  $M_u$  using the applicable load factors given in subsection 11.7.2. The required  $M_n = M_u/\phi$ , where  $\phi = 0.9$ . Compute the available nominal moment strength  $M_n = A_{ps} f_{ps}(d_p - a/2)$ , or  $M_n = A_{ps} f_{ps}(d_p - a/2) + A_s f_y(d - a/2)$ . The available  $M_n$  has to be greater than or equal to the required  $M_n$ .
10. Design the length  $L$  of the annular ring at the base of the wall from the equation

$$L^2 = \frac{2CH^2}{1 + \frac{(t/h)^3}{(dt)^2}}$$

where  $t$  is the thickness of the wall and  $h$  the thickness of the base slab.

11. Compute the percentage of prestress in the base to be transferred to the wall from the formula

$$\text{Percentage } R = \frac{1}{1 + S}$$

where  $S = 1.1(h/t) \times (d/t)^{1/2}$ .

When only the outer rim of the slab ring is compressed by radial thrust at the rim, the value of  $S$  is modified to

$$S_1 = \frac{1}{K} \left( \frac{h}{t} \right) \left( \frac{d}{t} \right)^{1/2}$$

where

$$K = \left( \frac{d_o^2 + d^2}{d_o^2 - d^2} - \mu \right)$$

in which  $d_o$  = outer diameter

$d$  = inner slab ring diameter =  $d_o - 2L$ .

12. Check the minimum wall thickness requirements, and evaluate the unrestrained initial elastic radial deflection

$$\Delta_i = \frac{F_i r}{t_{co} E_c}$$

where  $E_c = 57,000\sqrt{f'_c}$

$t_{co}$  = thickness of wall core at top or bottom of wall

$r = \frac{1}{2}d$ .

The final radial deflection  $\Delta_f = 1.7\Delta_i$ .

13. Anchor the steel from the base to the wall such that the steel extends into the wall a distance  $y_2 = 1.8\sqrt{rt_{co}}$  or 3 ft, whichever is greater. Also, ensure that the minimum nominal vertical steel at the base region is

$$A_s = 0.005t_{co}$$

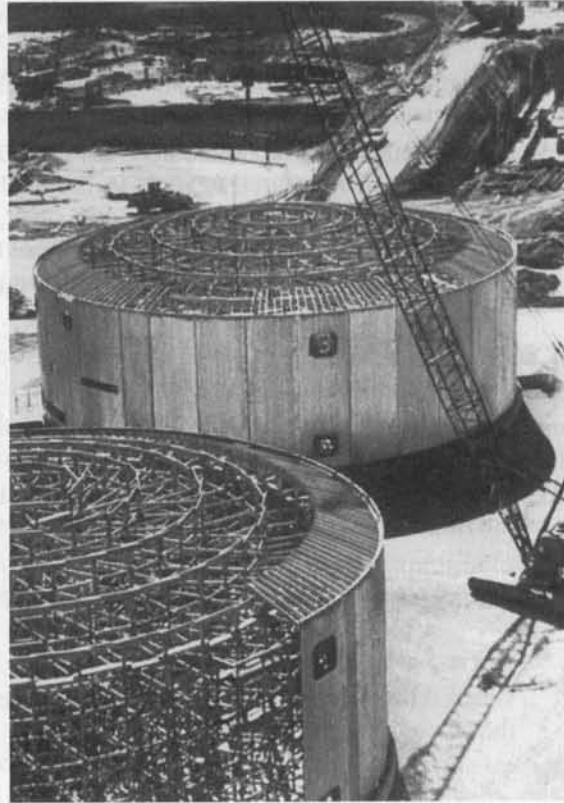
14. Verify the maximum crack width  $w_{\max} = 4.1 \times 10^{-6} \epsilon_{ct} E_{ps} \sqrt{I_x}$ ,

where  $\epsilon_{ct}$  = tensile surface strain in the concrete =  $(\lambda_t f_p)/(E_{ps})$

$f_p$  = actual stress in the steel

$f_{pi}$  = initial prestress before losses

$\lambda_t \sim f_p/f_{pi}$



**Photo 11.10** Two prestressed concrete anaerobic digester tanks during construction. (Courtesy, N.A. Legatos, Preload Technology, Inc., New York.)

$$I_x = \text{grid index} = \frac{8}{\pi} \left( \frac{s_2 s_1 t_b}{\phi_1} \right)$$

$s_1$  = spacing of reinforcement in direction "1"

$\phi_1$  = diameter of steel in direction "1"

$s_2$  = spacing of reinforcement in direction "2"

$t_b$  = concrete cover to center of steel, in.

Note that maximum allowable  $w_{\max} = 0.004$  in. for liquid-retaining tanks.

15. Design the roof cover dome after selecting the type of connection at the top of the tank wall. Limit the ratio of the rise  $h'$  of the dome to its base  $d$  such that  $h'/d$  does not exceed  $\frac{1}{3}$ .

Compute the required horizontal radial prestressing force  $P$  for the edge beam from the equation

$$P = \frac{bh}{t}(N_\theta - \mu N_\phi) + \frac{d(N_\phi \cos \phi)}{2}$$

where

$$N_\theta = \frac{w_D d}{2 \sin \phi} \left[ \frac{1}{1 + \cos \phi} - \cos \phi \right] - \frac{w_L d}{4 \sin \phi} (\cos 2\phi)$$

$$N_\phi = -a \left( \frac{w_D}{1 + \cos \phi} + \frac{w_L}{2} \right)$$

and

$h$  = total depth of rim beam

$b$  = ring beam width

$w_D$  = intensity of self-weight of shell per unit area (dead load)

$w_L$  = intensity of live-load projection.

**16.** Compute the ring-edge beam cross section

$$A_c = \frac{P_i}{f_c}$$

where  $P_i$  = initial prestressing force =  $P/\bar{\gamma}$

$\bar{\gamma}$  = residual stress percentage

$f_c$  = allowable compressive stress in the concrete, not to exceed  $0.2f'_c$ , but not more than 800–900 psi, in the edge beam.

**17.** Compute the area of the edge beam prestressing tendon

$$A_{ps} = \frac{P_i}{f_{si}}$$

where  $f_{si}$  is the allowable stress in the prestressing steel before losses, or

$$A_{ps} = \frac{W \cot \phi}{2\pi f_{pe}}$$

if accurate analysis is not performed. In the latter,  $W$  is the total dead and live load on the dome due to  $w_D + w_L$  and  $f_{pe}$  is the effective prestress after losses.

**18.** Check the minimum dome thickness required to withstand buckling, i.e.,

$$\text{Min. } h_d = a \sqrt{\frac{1.5p_u}{\phi\beta_i\beta_c E_c}}$$

where  $a$  = radius of dome shell

$P_u$  = ultimate uniformly distributed design unit pressure due to dead load and live load =  $(1.4D + 1.7L)/144$

$\phi$  = strength reduction factor for material variability = 0.7

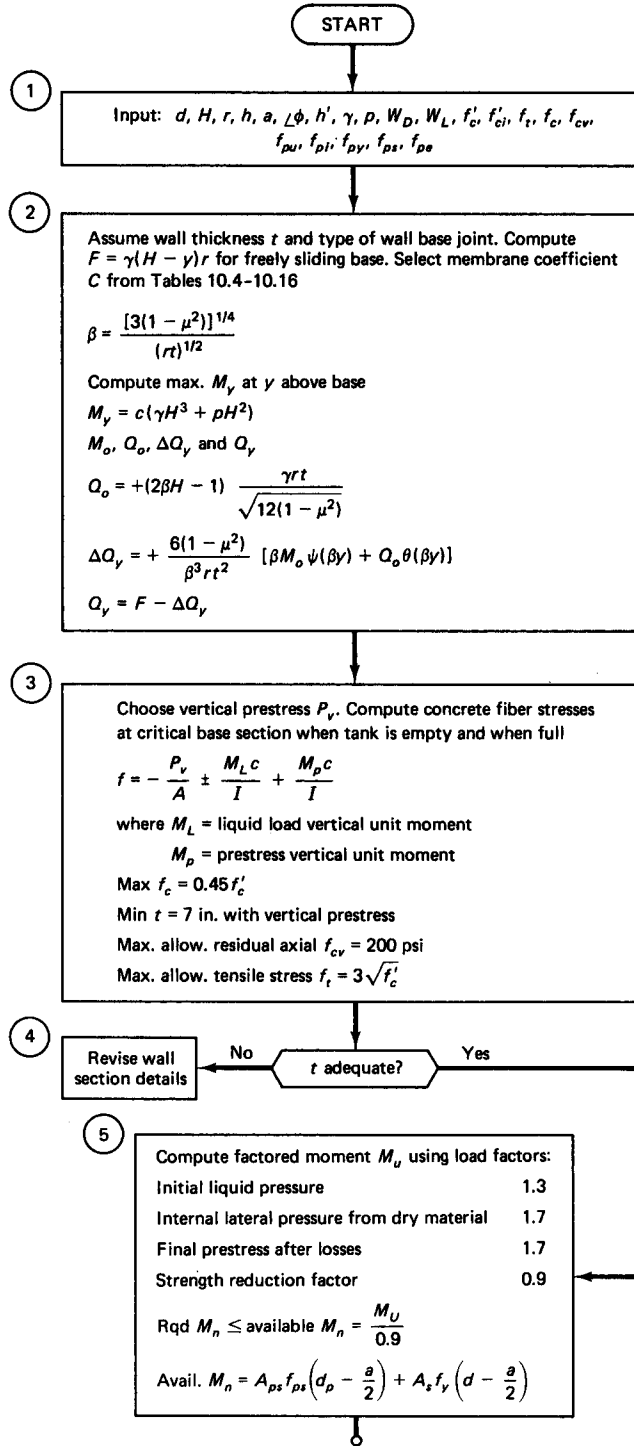
$\beta_i$  = buckling reduction factor for deviations from true spherical surface due to imperfections

$\beta_i = (a/r_i)^2$ , where  $r_i \leq 1.4a$

$\beta_c$  = buckling reduction factor for creep, material nonlinearity, and cracking =  $0.44 + 0.003W_L$ , but not to exceed 0.53

$E_c$  = initial modulus of concrete =  $57,000\sqrt{f'_c}$  psi.

Figure 11.23 gives a step-by-step flowchart for a recommended sequence of operations to be performed in the design of circular prestressed concrete tanks and their shell roofs.



**Figure 11.23** Flowchart for the design of circular prestressed tanks and their flat dome roofs.

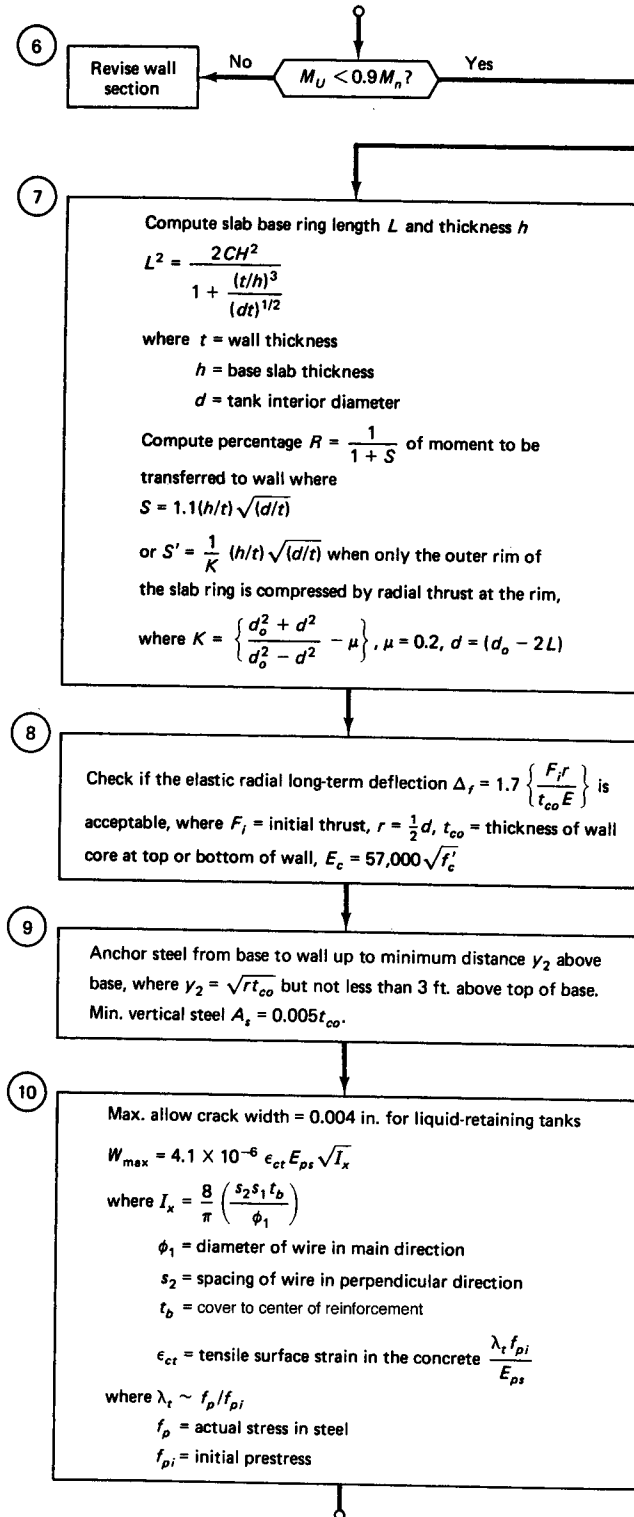


Figure 11.23 Continued



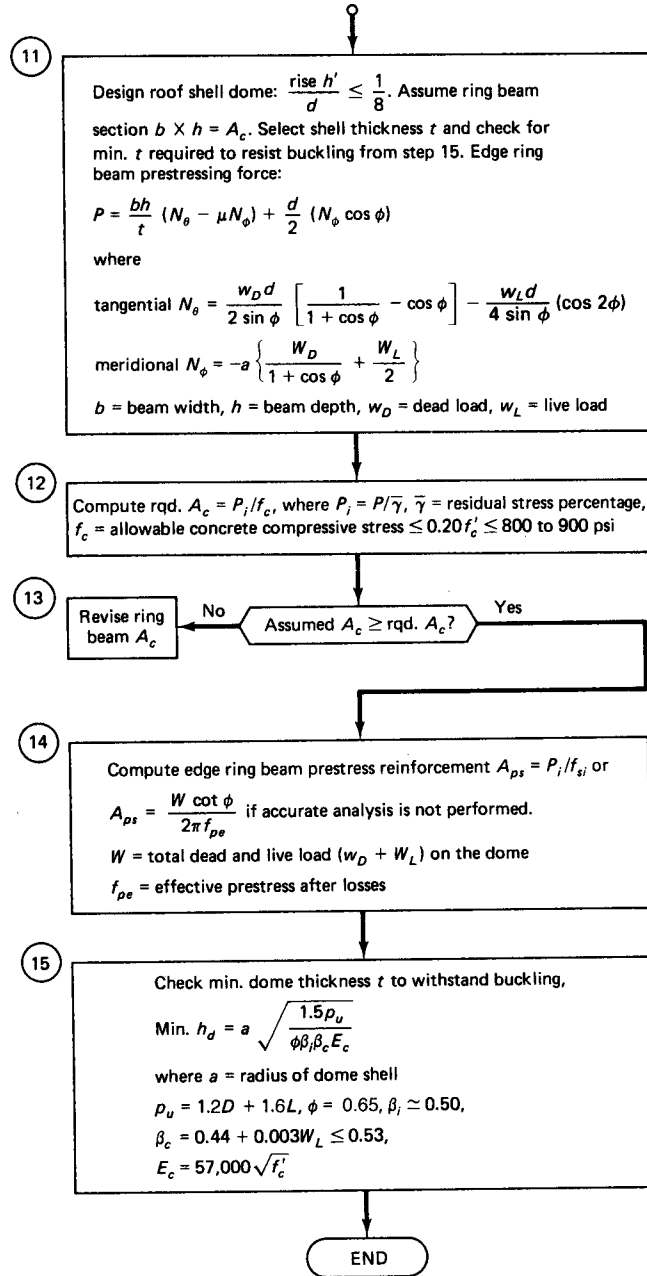


Figure 11.23 Continued

### 11.13 DESIGN OF CIRCULAR PRESTRESSED CONCRETE WATER-RETAINING TANK AND ITS DOMED ROOF

#### Example 11.3

Determine the maximum horizontal ring forces and vertical moments, and design the wall prestressing reinforcement, for a circular prestressed concrete tank whose diameter  $d = 125$  ft (38.1 m) and which retains a water height  $H = 25$  ft (7.62 m) for the following conditions of wall base support: (a) hinged, (b) fully fixed, (c) semisliding, and (d) partially fixed. Also, design the prestressed concrete ring edge beam for the domed roof shell assuming that the shell rise-span ratio  $h'/d = \frac{1}{8}$ . Use a flat shell roof having shell angle  $\phi = 36^\circ$ , and find the area of prestressing reinforcement for both wire-wrapped and tendon reinforced conditions. Given data are as follows:

$$f'_c = 5,000 \text{ psi (34.5 MPa), normal-weight concrete}$$

$$f'_{ci} = 3,750 \text{ psi (25.9 MPa)}$$

$$f_t = 212 \text{ psi (0.86 MPa)} \leq 3\sqrt{f'_c}$$

$$f_c = 0.45f'_c = 2,250 \text{ psi (15.5 MPa)}$$

$$\text{residual } f_{cv} = 225 \text{ psi (1.55 MPa)}$$

$$f_{pu} \text{ (wire)} = 250,000 \text{ psi (1,724 MPa)}$$

$$f_{pu} \text{ (strands and tendons)} = 250,000 \text{ psi (1,724 MPa)}$$

$$f_{pi} = 0.7f_{pu} = 175,000 \text{ psi (1,207 MPa)}$$

$$f_{ps} = 220,000 \text{ psi (1,517 MPa)}$$

$$w_L = 15 \text{ psf (718 Pa) for snow load on dome}$$

Assume 26 percent total loss in prestress for all long-term effects.

**Solution:** Disregard the weight of the wall and the roof dome effect as insignificant on the stresses as compared to the effect of the vertical prestress forces. Consider the water pressure distribution shown in Figure 11.24 on the tank wall giving

$$\gamma = 62.4 \text{ lb/ft}^3 \text{ (1,000 kg/m}^3\text{)}$$

$$r = \frac{d}{2} = \frac{125}{2} = 62.5 \text{ ft (19.1 m)}$$

Assume the wall thickness  $t = 10$  in. = 0.83 ft (25.4 cm). Then the form factor

$$\frac{H^2}{dt} = \frac{25 \times 25}{125 \times 0.83} = 6$$

and  $\gamma Hr = 62.4 \times 25 \times 62.5 = 97,500$  lb/ft of circumference.

**Basic Forces and Moments.** Tables 11.19 through 11.21 give the basic forces and moments in the tank wall.

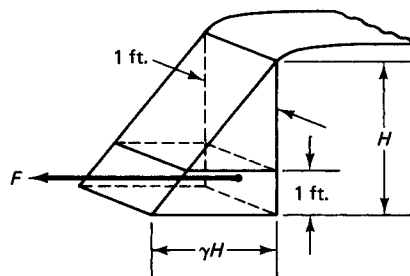
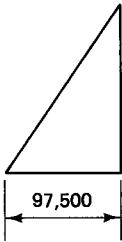
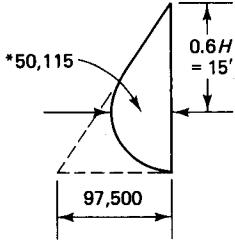
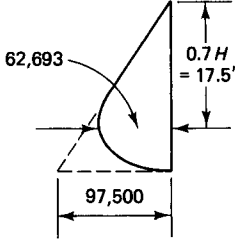


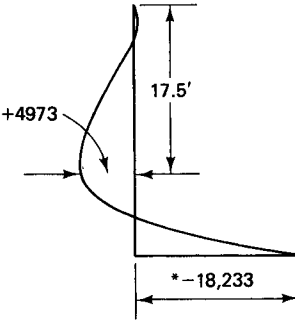
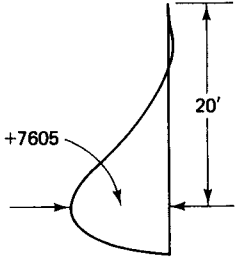
Figure 11.24 Liquid ring tension  $F$ , wall base freely sliding.

**Table 11.19** Maximum Ring Tension  $F = C(\gamma Hr)$  lb/ft Circumference, Example 11.3

Freely Sliding Wall Base	Fixed Base	Hinged Base
$C = 1$ $F = 97,500$	Table 11.10 for $\frac{H^2}{dt} = 6$ $C = 0.514$ $F = 0.514 \times 97,500 = 50,115$	Table 11.12 for $\frac{H^2}{dt} = 6$ $C = 0.643$ $F = 0.643 \times 97,500 = 62,693$
		

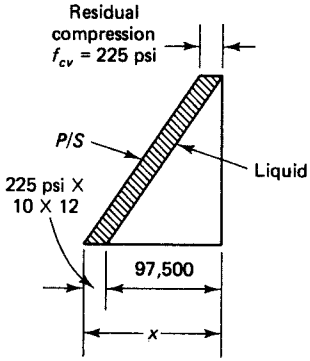
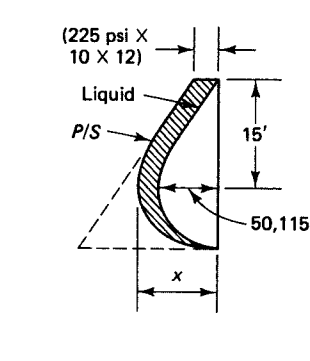
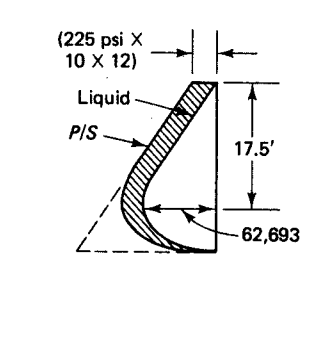
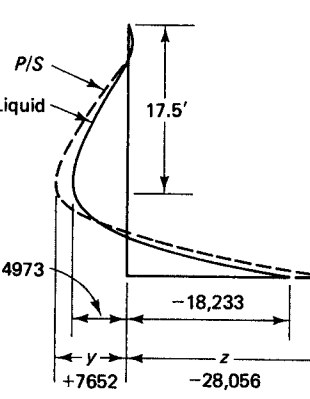
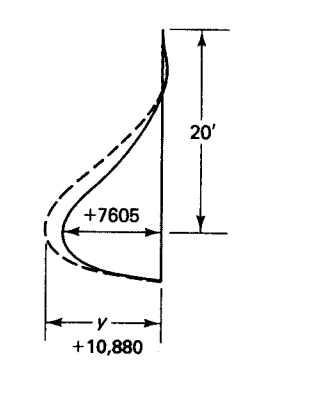
\*Compare with 50,113 lb/ft in the detailed method of Example 11.2.

**Table 11.20** Vertical Moments  $M = C(\gamma H^3)$  ft-lb/ft, Example 11.3. Positive (+) = Tension in Outside Face

Freely Sliding Base	Fixed Wall Base	Hinged Base
$M_v = M_o = 0$	Table 11.4 $C = +0.0051$ for $0.7H = 17.5$ ft $C = -0.0187$ for $1.0H = 25$ ft $M_v = +0.0051 \times 62.4(25)^3 = +4,973$ $M_o = -0.0187 \times 62.4(25)^3 = -18,233$	Table 11.6 $C = +0.0078$ for $0.8H = 20$ ft $C = 0$ for $1.0H$ , or full height $M_v = +0.0078 \times 62.4(25)^3 = +7,605$ $M_o = 0$
		

\*This moment value is very close to the value obtained by using the detailed method and the moment functions of Table 11.1 and Example 11.1 ( $M_o = -18,574$ ).

**Table 11.21** Prestressing Effects Using 225-psi Residual Radial Compression, Example 11.3. Ring Forces  $Q$  lb/ft, Vertical Moments  $M_y$  ft-lb/ft

Freely Sliding Base	Fixed Wall Base	Hinged Base
<p style="text-align: center;"><u>Ring Forces</u></p>  <p>Residual compression <math>f_{cv} = 225</math> psi</p> <p>P/S</p> <p>Liquid</p> <p>225 psi X 10 X 12</p> <p>97,500</p> <p>x</p> <p><math>x = 97,500 + [\text{Res. comp.} \times t \times 1 \text{ ft.}]</math>  <math>= 97,500 + [225 \times 10 \times 12]</math>  <math>= 124,500</math></p> <p style="text-align: center;"><u>Moments</u></p> <p><math>[M_y]_{y=0} = M_o = 0</math></p>	<p style="text-align: center;"><u>Ring Forces</u></p>  <p>(225 psi X 10 X 12)</p> <p>Liquid</p> <p>P/S</p> <p>15'</p> <p>50,115</p> <p>x</p> <p><math>x = 50,115 + [225 \times 10 \times 12]</math>  <math>= 77,115 = Q_{15}</math></p>	<p style="text-align: center;"><u>Ring Forces</u></p>  <p>(225 psi X 10 X 12)</p> <p>Liquid</p> <p>P/S</p> <p>17.5'</p> <p>62,693</p> <p><math>x = 62,693 + [225 \times 10 \times 12]</math>  <math>= 89,693 = Q_{17.5}</math></p>
	<p style="text-align: center;"><u>Moments</u></p>  <p>P/S</p> <p>Liquid</p> <p>17.5'</p> <p>*4973</p> <p>-18,233</p> <p>+7652</p> <p>-28,056</p> <p>y</p> <p>z</p> <p><math>y = 4,973 \times \frac{77,115}{50,115} = 7,652</math>  <math>= +M_y</math>  <math>M_o = -\frac{18,233 \times 77,115}{50,115}</math>  <math>= -28,056</math></p>	<p style="text-align: center;"><u>Moments</u></p>  <p>17.5'</p> <p>+7605</p> <p>+10,880</p> <p>y</p> <p><math>y = +7,605 \times \frac{89,693}{62,693}</math>  <math>= +10,880 = +M_y</math>  <math>M_o = 0</math></p>

\*Compare with the value  $M = +4,912$  ft-lb/ft obtained by the detailed method of Example 11.1.

**Wall Maximum Concrete Stresses at 20 ft from Top: Hinged Base.** By trial and adjustment, provide vertical concentric prestress  $P_v = 50,000$  lb/ft (730 kN/m) of circumference. Then for a wall thickness  $t = 10$  in. compute the resulting stresses as shown in Figure 11.25.

$$f_+ = \frac{M}{S} = \frac{10,880 \times 12}{\frac{12(10)^2}{6}} = \mp 653 \text{ psi}$$

$$f_+ = \frac{M}{S} = \frac{7,605 \times 12}{\frac{12(10)^2}{6}} = \pm 456 \text{ psi}$$

$$f_v = \frac{P_v}{A_c} = \frac{50,000}{12 \times 10} = -417 \text{ psi}$$

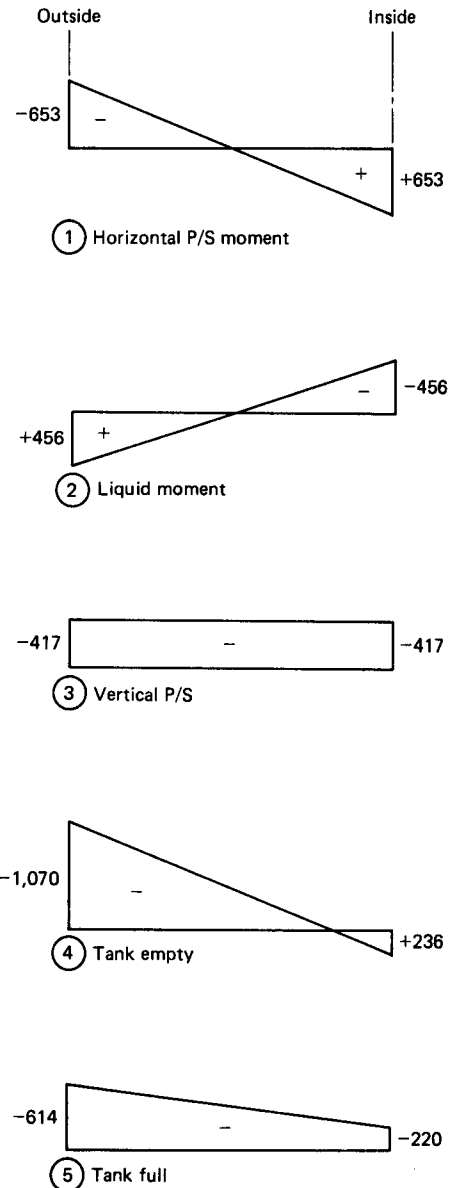
$$f_4 = \textcircled{1} + \textcircled{3}$$

$$\begin{aligned} \text{Max. } f_t &= 236 \text{ psi} \cong 3\sqrt{5,000} \\ &\cong 212 \text{ psi, O.K.} \end{aligned}$$

$$\text{Max. } f_c = -1,070 \text{ psi} < 0.45f'_c, \text{ O.K.}$$

$$f_5 = \textcircled{1} + \textcircled{2} + \textcircled{3}$$

$$\text{Max. } f_c = -614 \text{ psi} < 0.45f'_c, \text{ O.K.}$$



**Figure 11.25** Stress at maximum moment, 20 ft from top, psi. Negative (-) = compression, positive (+) = tension.

**Wall Maximum Concrete Stress at 17 ft 6 in. from Top: Fully Fixed Base.** The maximum positive moment  $M_y$  is at 17 ft 6 in. from the top of the wall. By trial and adjustment, use *eccentric* vertical prestressing  $P_v = 100,000$  lb/ft closer to the outer face [ $e = 1.05$  in. (26.7 mm)]. Then compute the resulting stresses in the wall as shown in Figure 11.26.

$$f_{\pm} = \frac{M}{S} = \frac{7,652 \times 12}{\frac{12(10)^2}{6}} = \mp 459 \text{ psi}$$

$$f_{\pm} = \frac{M}{S} = \frac{4,973 \times 12}{\frac{12(10)^2}{6}} = \pm 298 \text{ psi}$$

$$f_v = \frac{P_v}{A_c} = \frac{100,000}{12 \times 10} = -833 \text{ psi}$$

$$f_v = \frac{P_v e(c)}{I} = \frac{100,000 \times 1.05}{\frac{12(10)^2}{6}} = \mp 525 \text{ psi}$$

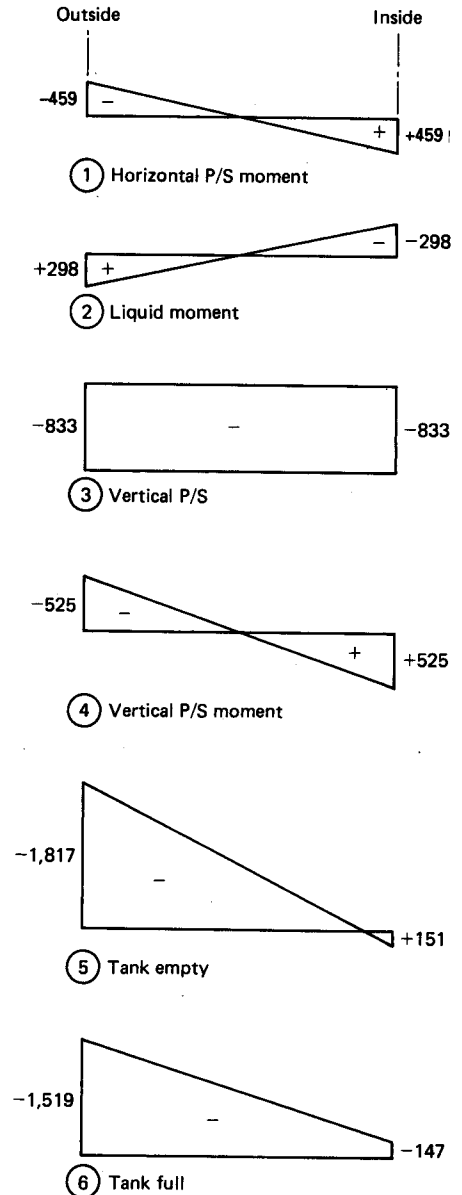
$$f_s = \textcircled{1} + \textcircled{3} + \textcircled{4}$$

$$\text{Max. } f_t = +151 \text{ psi} < 3\sqrt{f'_c} = 212, \text{ O.K.}$$

$$\text{Max. } f_c = -1,817 \text{ psi} < 0.45f'_c = -2,250 \text{ psi, O.K.}$$

$$f_6 = \textcircled{1} + \textcircled{2} + \textcircled{3} + \textcircled{4}$$

$$\text{Max. } f_c = -1,519 \text{ psi} < 0.45f'_c, \text{ O.K.}$$



**Figure 11.26** Stresses at maximum positive (+) moment, 17 ft, 6 in. from top, psi. Negative (-) = compression, positive (+) = tension.

**Wall Maximum Concrete Stress at Base: Fully Fixed Base.** Use eccentric vertical prestress  $P_v = 100,000$  lb closer to the outer face ( $e = 1.05$  in.). Then compute the resulting stresses in the wall as shown in Figure 11.27.

$$f_{\pm} = \frac{M}{S} = \frac{-28,056 \times 12}{\frac{12(10)^2}{6}} = \pm 1,683 \text{ psi}$$

$$f_{\pm} = \frac{M}{S} = \frac{-18,233 \times 12}{\frac{12(10)^2}{6}} = \mp 1,094 \text{ psi}$$

$$f_v = \frac{P_v}{A_c} = \frac{-100,000}{12 \times 10} = -833 \text{ psi}$$

$$f_v = \frac{P_v e(c)}{I} = \frac{100,000 \times 1.05}{\frac{12(10)^2}{6}} = \mp 525 \text{ psi}$$

$$f_5 = \textcircled{1} + \textcircled{3} + \textcircled{4}$$

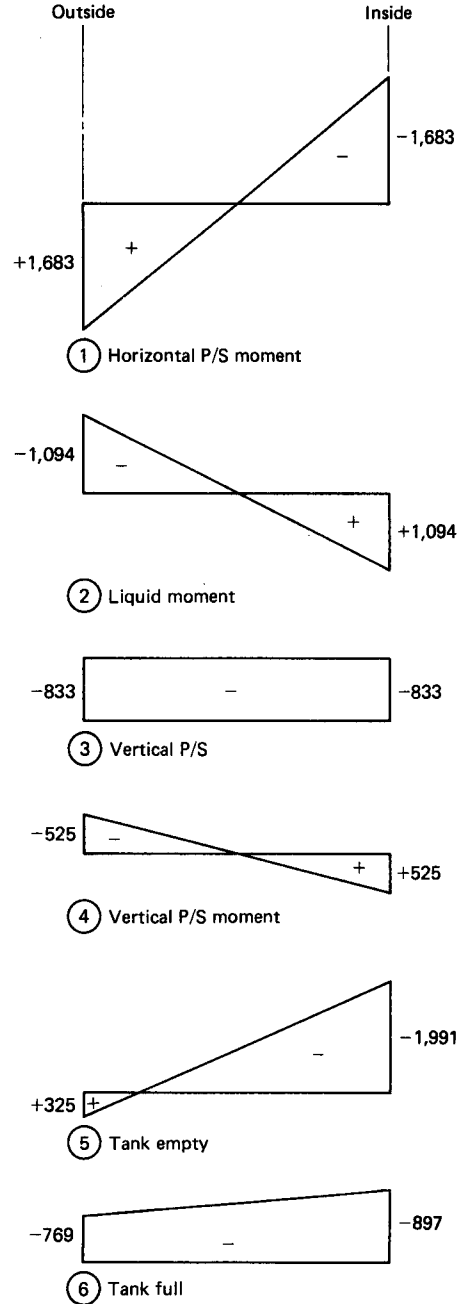
Max.  $f_c = -1,991$  psi <  $0.45 f'_c$ , O.K.

Max.  $f_t = +325$  psi at base when tank is empty.

This stress will rapidly decrease well below  $3\sqrt{f'_c}$  within one foot above base, hence O.K.

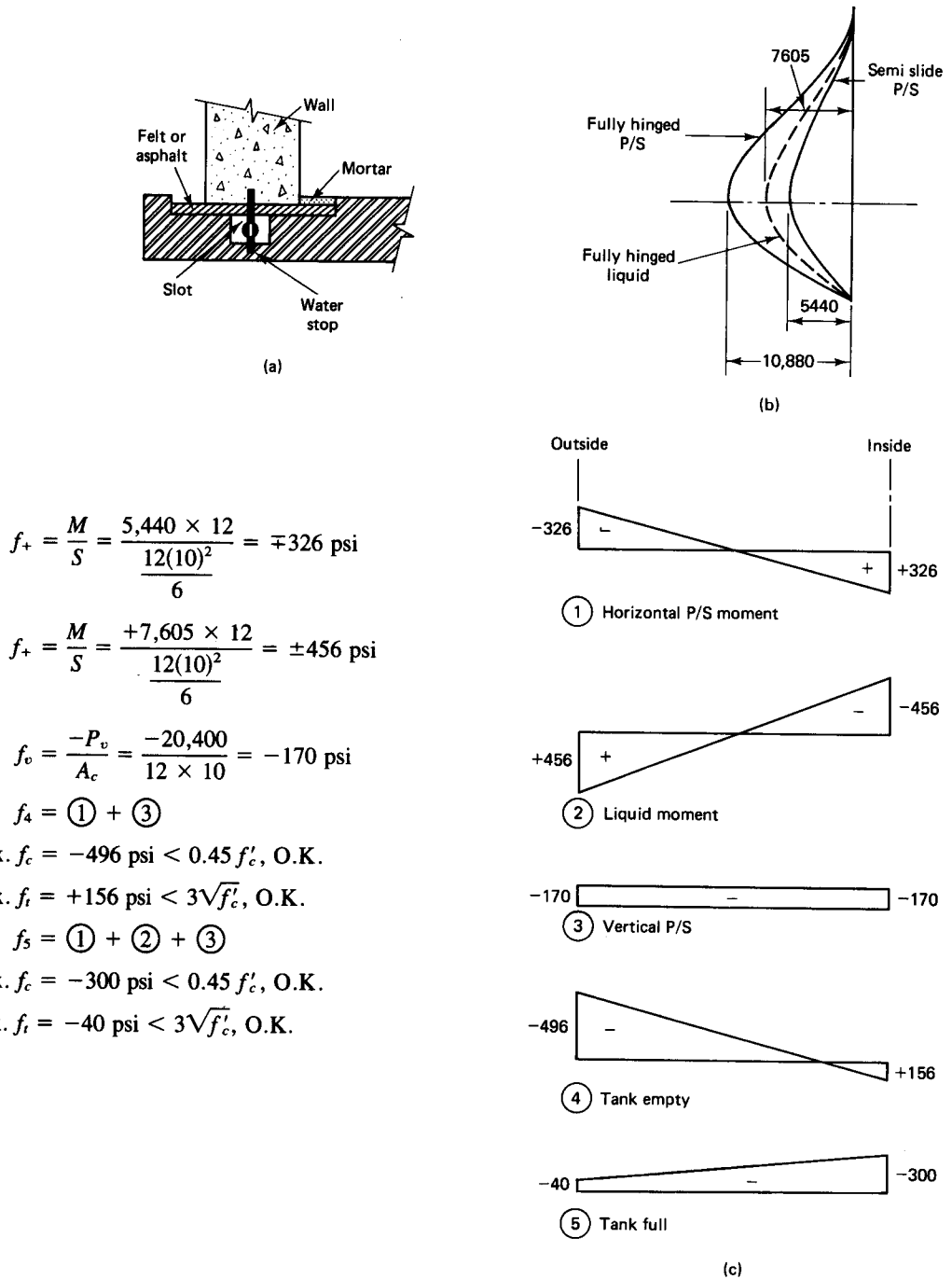
$$f_6 = \textcircled{1} + \textcircled{2} + \textcircled{3} + \textcircled{4}$$

Max.  $f_c = -897$  psi <  $0.45 f'_c$ , O.K.



**Figure 11.27** Stresses at maximum negative (-) moment at wall base, psi. Negative (-) = compression, positive (+) = tension.

**Wall Maximum Concrete Stress: Semisliding Base.** By trial and adjustment, use concentric vertical prestress  $P_v = 20,400$  lb/ft (297 kN/m). Then semislide  $M = \frac{1}{2} (+10,880) = 5,440$  ft-lb/ft, and compute the resulting stresses in the wall as shown in Figure 11.28.



$$f_+ = \frac{M}{S} = \frac{5,440 \times 12}{\frac{12(10)^2}{6}} = \mp 326 \text{ psi}$$

$$f_+ = \frac{M}{S} = \frac{+7,605 \times 12}{\frac{12(10)^2}{6}} = \pm 456 \text{ psi}$$

$$f_v = \frac{-P_v}{A_c} = \frac{-20,400}{12 \times 10} = -170 \text{ psi}$$

$$f_4 = \textcircled{1} + \textcircled{3}$$

Max.  $f_c = -496 \text{ psi} < 0.45 f'_c$ , O.K.

Max.  $f_t = +156 \text{ psi} < 3\sqrt{f'_c}$ , O.K.

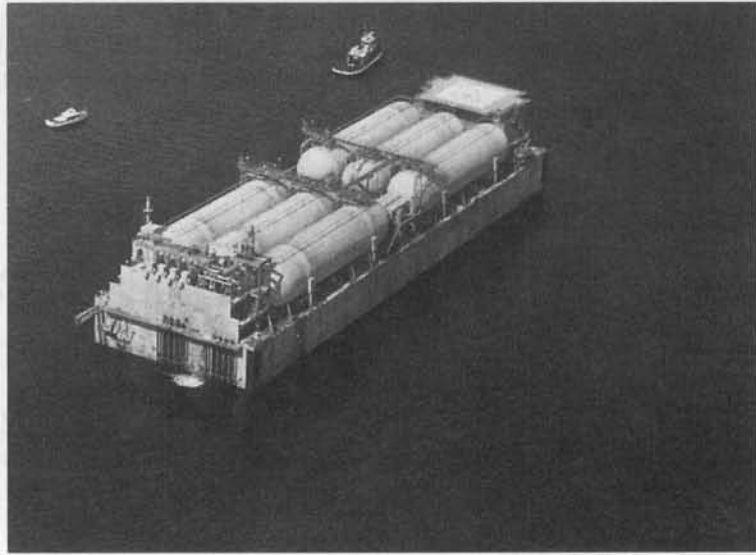
$$f_5 = \textcircled{1} + \textcircled{2} + \textcircled{3}$$

Max.  $f_c = -300 \text{ psi} < 0.45 f'_c$ , O.K.

Max.  $f_t = -40 \text{ psi} < 3\sqrt{f'_c}$ , O.K.

**Figure 11.28** Stresses at maximum positive (+) moment, psi. (a) Wall base details. (b) Semislide moment, ft-lb/ft. (c) Concrete stresses, psi.





**Photo 11.11** Arco Floating LPG Barge: ABAM-designed largest floating prestressed hull in the world. (Courtesy, ABAM Engineers, Tacoma, Washington.)

**Partial Fixity at the Wall Base.** The restraint moment  $M_p = M_o (1 - S)$ , where the full fixity moment  $M_o = 18,233$  ft-lb/ft. The modifying factor for partial fixity  $S = (t/h)^3 / (dt)^{1/2}$ .

Figure 11.29 shows the deformed shape of the base slab. If the base slab thickness  $h = 10$  in., then, from Equations 11.39 and 11.40,

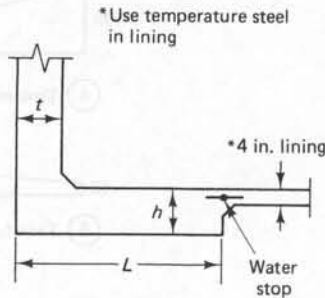
$$S = \frac{(10/10)^3}{(125 \times 0.83)^{1/2}} = 0.10$$

and

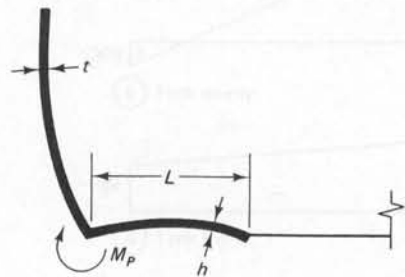
$$M_p = M_o(1 - S) = 18,233(1 - 0.1) = 16,410 \text{ ft-lb/ft.}$$

The moment loss due to partial fixity =  $18,233 - 16,410 = 1,823$  ft-lb/ft. From Equation 11.37 for the base ring width  $L$ ,

$$L^2 = \frac{2CH^2}{1 + S}$$



(a)



(b)

**Figure 11.29** Deformed shape of base slab. (a) Wall base. (b) Deformed section.

Also, from Table 11.4, the membrane coefficient at the base for form factor  $(H^2)/(dt) = 6$  is  $C = -0.0187$ . Thus, we have

$$L^2 = \frac{2 \times 0.0187(25)^2}{1 + 0.1} = 21.25$$

and it follows that

$$L = 4.61 \text{ ft} = 4 \text{ ft } 7\frac{1}{2} \text{ in.}$$

Accordingly, use a ring slab base width  $L = 4 \text{ ft } 9 \text{ in.}$  (145 cm). Since for large-diameter tanks  $S$  has a very small value, the degree of fixity, as the solution shows, is almost the same for both fully fixed and partially fixed wall bases.

From Equations 11.47 and 11.48, the percent  $R$  of prestress in the base that is transferred to wall  $= 100/S_1$ , where

$$S_1 = 1.1 \left( \frac{h}{t} \right) \left( \frac{d}{t} \right)^{1/2} = 1.1 \left( \frac{10}{10} \right) \left( \frac{125}{0.83} \right)^{1/2} = 13.50\%$$

Consequently,

$$R = \frac{100}{13.50} = 7.4\%$$

which means that the required design prestress for the wall can be slightly reduced, as some compression is available from the base ring.

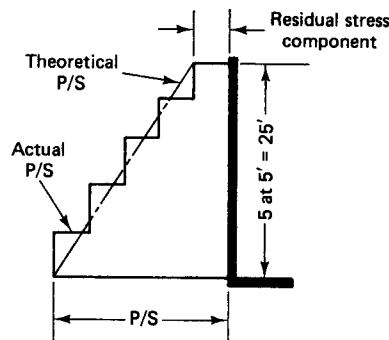
### ***Design of Prestressing Reinforcement***

**Horizontal Prestressing.** Use the same size wire to wrap the circular wall, varying the spacing of the wire hoops in 5-ft bands along the tank height. In the case of the freely sliding tank wall, the minimum spacing is in the lowest band at the base, as presented graphically in Figure 11.30.

In order to determine the variation of wire pitch throughout the height of the wall, additional computations of the horizontal ring thrust  $Q_y$  have to be made at the bottom of each band. Consequently, only one typical calculation of size and wire distribution will be made for purposes of illustration.

Taking the case of the fixed wall base from Table 11.21, the maximum  $Q_{15} = 77,115$  lb/ft of circumference per foot height of wall. So trying 0.192-in. dia (4.88 mm) prestressing 250-K wire, we obtain  $A_{ps} = 0.0289$  in.<sup>2</sup> per wire and  $f_{pi} = 0.7f_{pu} = 0.7 \times 250,000 = 175,000$  psi (1,207 MPa).

Now assume 26-percent prestress loss for elastic shortening, seating, creep, shrinkage, and steel relaxation. Then



**Figure 11.30** Horizontal-prestress wire distribution bands.

$$f_{pe} = 0.74 \times 175,000 = 129,500 \text{ psi (893 MPa)}$$

$$A_{ps} = \frac{77,115}{129,500} = 0.60 \text{ in.}^2 \text{ per 1 ft of wall height}$$

$$\text{No. of wire loops in 5-ft band} = \frac{0.60 \times 5}{0.0289} = 104$$

Hence, use 104 wire loops in the 5-ft wall band whose base is 15 ft below the top of the water level. Also, use 2-in. shotcrete to cover the wrapped horizontal 0.192-in. dia wires.

If the tank were prestressed with  $\frac{1}{2}$ -in. dia 250-K 7-wire strand tendons,  $A_{ps}$  would be 0.144 in.<sup>2</sup>/strand and the required number of strands in a 5-ft-height band would be  $0.60 \times 5/0.144 \cong 20$  strands.

**Vertical Prestressing.** For proportioning the vertical prestressing reinforcement,  $P_v = 100,000$  lb/ft at  $e = 1.05$  in. (1,459 N/m at  $e = 26.7$  mm) on the outer force side. Hence, try  $\frac{1}{2}$ -in. dia (17.7-mm dia) 7-wire 250-K strands. We obtain

$$A_{ps} = 0.144$$

$$f_{pu} = 250,000 \text{ psi (1,724 MPa)}$$

$$f_{pi} = 0.7f_{pu} = 0.7 \times 250,000 = 175,000 \text{ psi (1,207 MPa)}$$

Assume 26-percent total prestress loss. Then  $f_{pe} = 0.74 \times 175,000 = 129,500$  psi (889 MPa), the required  $A_{ps}$  per foot of circumference =  $100,000/129,500 = 0.772$  in.<sup>2</sup> (4.98 cm<sup>2</sup>), and the number of vertical strands per foot of circumference =  $0.772/0.144 = 5.36$ . Thus, use  $\frac{1}{2}$ -in. dia 7-wire 250-K strands for vertical prestressing at  $2\frac{1}{4}$  in. center-to-center spacing =  $0.769$  in.<sup>2</sup>  $\cong 0.772$  in.<sup>2</sup>, O.K.

**Nominal Moment Strength Check of Tank Wall.** The maximum wall vertical moment for a fixed-base wall, from Table 11.21, is  $M = 28,056$  ft-lb/ft or in.-lb/in. of circumference. We thus have:

$$\text{S.F.} = 1.3 \text{ (step 5 of flowchart)}$$

$$M_u = 1.3 \times 28,056 = 36,473 \text{ in.-lb/in.}$$

$$\text{Rqd } M_n = \frac{M_u}{0.9} = \frac{36,473}{0.9} = 40,525 \text{ in.-lb/in.}$$

$$d = \frac{10}{2} + 1.05 = 6.05 \text{ in. (15.37 cm)}$$

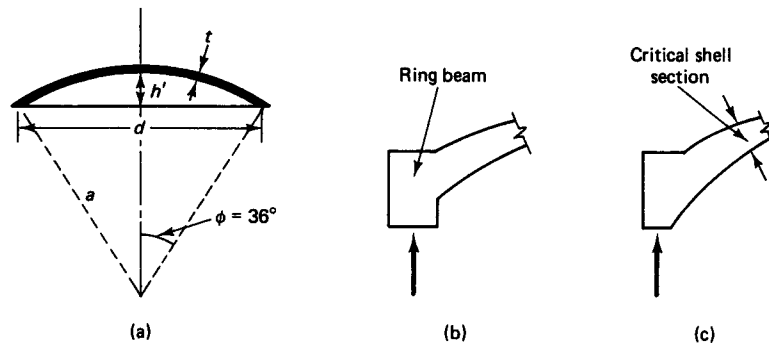
$$A_{ps} = \frac{0.144}{2.25} = 0.064 \text{ in.}^2/\text{in. width}$$

$$a = \frac{A_{ps} f_{ps}}{0.85 f'_c b} = \frac{0.064 \times 220,000}{0.85 \times 5,000 \times 1} = 3.31 \text{ in.}$$

$$\text{Available } M_n = A_{ps} f_{ps} \left( d - \frac{a}{2} \right) = 0.064 \times 220,000 \left( 6.05 - \frac{3.31}{2} \right)$$

$$= 61,882 \text{ in.-lb/in.} \gg \text{Rqd. } M_n = 40,525 \text{ in.-lb/in., O.K.}$$

The wall design should include a check of the deflection as described in step 8 of the flowchart. Also, a determination should be made of the anchor steel at the base of the wall as well as the crack width  $w_{\max}$  in step 9 of the flowchart. Finally, a check of temper-

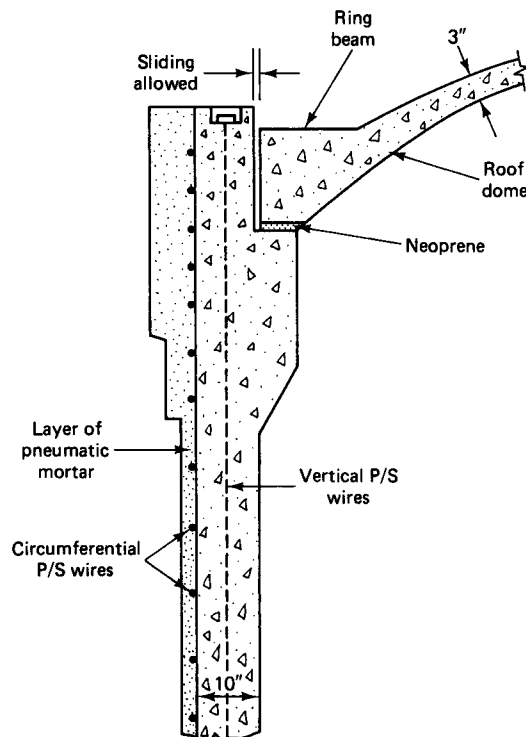


**Figure 11.31** Tank dome shell roof. (a) Geometry of dome. (b) Edge ring beam. (c) Equivalent ring beam.

ature and creep effects has to be made to ascertain whether any additional nonprestressed mild steel has to be added to the prestressed wall reinforcement.

**Design of Roof Dome Prestressed Edge Ring Beam.** Use a rise-span ratio  $h'/d = \frac{1}{8}$ . Also, choose a freely supporting reaction at the top of the tank wall, using a neoprene pad under the edge ring beam. The shell would then have the form shown in Figures 11.31 and 11.32.

Since  $d = 125$  ft.,  $h' = 125/8 = 15.63$  ft (4.76 m). Also, since  $\phi = 36^\circ$  is less than  $51^\circ 49'$ , the entire shell would be in compression, and only temperature reinforcement is needed.



**Figure 11.32** Dome prestressed ring beam support detail in Example 11.3.



**Photo 11.12** Olympic oval at the University of Calgary, Calgary, Canada. Structural engineers: Simpson, Lester, Goodrich; Calgary, Alberta, Canada. (Courtesy, Prestressed Concrete Institute.)

The shell radius is

$$a = \frac{d/2}{\sin \phi} = \frac{62.5}{0.588} = 106 \text{ ft (32.3 m)}$$

From Equation 11.75, the minimum shell thickness to withstand buckling is

$$h_d = a \sqrt{\frac{1.5P_u}{\phi\beta_i\beta_c E_c}}$$

Hence, assuming that  $t = 3.0$  in., we have

$$P_u = 1.2D + 1.6L = 1.2\left(\frac{3}{12} \times 150\right) + 1.6 \times 15 = 69 \text{ lb/ft}^2$$

$$\phi = 0.65$$

$$\beta_i = (a/r_i)^2 = \left(\frac{106}{1.4 \times 106}\right)^2 = 0.51$$

$$\beta_c = 0.44 + 0.003 \times 15 = 0.49 < 0.53, \text{ use } \beta_c = 0.49$$

$$E_c = 57,000\sqrt{5,000} = 4.03 \times 10^6 \text{ psi}$$

$$\begin{aligned} \text{Min } h &= a \sqrt{\frac{1.5p_u}{\phi\beta_i\beta_c E_c}} = 106 \sqrt{\frac{1.5 \times 69}{0.65 \times 0.51 \times 0.49 \times 4.03 \times 10^6}} \\ &= 1.33 \text{ in. (3.4 cm)} < 3 \text{ in., O.K.} \end{aligned}$$

So use a shell  $t = 3$  in. (7.6 cm). Then  $\sin \phi = \sin 36^\circ = 0.59$ ,  $\cos \phi = \cos 36^\circ = 0.81$ , and  $a =$  sphere radius = 106 ft.

From Equation 11.70, the tangential force per unit length of circumference is

$$\begin{aligned} N_{\theta} &= \frac{W_D d}{2 \sin \phi} \left[ \frac{1}{1 + \cos \phi} - \cos \phi \right] - \frac{W_L d}{4 \sin \phi} (\cos 2\phi) \\ &= \frac{37.5 \times 125}{2 \times 0.59} \left[ \frac{1}{1 + 0.81} - 0.81 \right] - \frac{15 \times 125}{4 \times 0.59} (0.31) \\ &= -1,269 \text{ lb/ft} \end{aligned}$$

From Equation 11.67, the meridional force per unit length of circumference, with  $a = 106$  ft, is

$$\begin{aligned} N_{\phi} &= -a \left( \frac{w_D}{1 + \cos \phi} + \frac{w_L}{2} \right) \\ &= -106 \left( \frac{37.5}{1.81} + \frac{15}{2} \right) = -2,991 \text{ lb/ft (43.6 kN/m)} \end{aligned}$$

From Equation 11.72, the radial prestressing force in the ring beam required to produce compatibility of deformation with the shell rim is

$$P = \frac{bh}{t} (N_{\theta} - \mu N_{\phi}) + \frac{d}{2} (N_{\phi} \cos \phi)$$

To determine the cross-sectional area  $bh$  of the ring beam, use  $P = (d/2)(N_{\phi} \cos \phi)$  for the first trial, since the first term of the equation has less than 10 percent of the total value of  $P$  (see the discussion accompanying Equation 11.62). We obtain

$$P = \frac{d}{2} (N_{\phi} \cos \phi) = \frac{125}{2} (-2,991 \times 0.81) = -151,149 \text{ lb per ft}$$

Given that the total prestress loss is 26 percent, it follows that

$$\bar{\gamma} = 1 - 0.26 = 0.74$$

and

$$P_i = \frac{151,149}{0.74} = 204,620 \text{ lb/ft}$$

Use a maximum concrete compressive stress  $f_c = 800$  psi (5.52 MPa) in order to minimize excess strain in the edge beam, which could produce high stresses in the shell rim. The required cross-sectional area of the prestressed ring beam is

$$A_c = bh = \frac{P_i}{f_c} = \frac{204,620}{800} = 256 \text{ in.}^2$$

Try  $b = 14$  in. and  $h = 20$  in. Then  $A_c = 280 \text{ in.}^2$  Substituting into Equation 11.72, we get

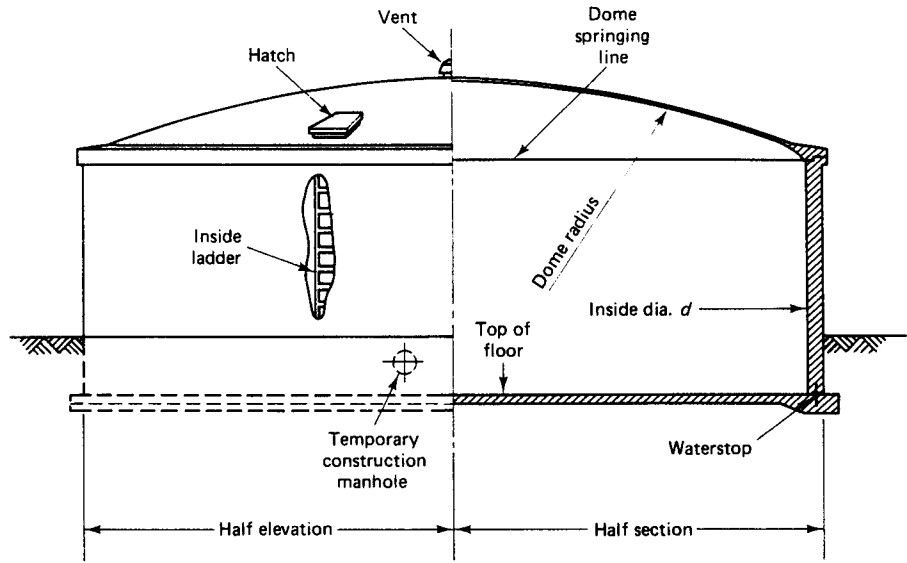
$$\begin{aligned} P &= \frac{280}{3.0} \left[ -\frac{1}{12} \times 1,269 - 0.2(-2,991) \right] + \frac{125}{2} (-2,991 \times 0.81) \\ &= -5,217 - 151,149 = -156,366 \text{ lb/ft} \end{aligned}$$

Use

$$P_i = \frac{156,366}{0.74} = 211,671 \text{ lb (717 kN)}$$

From before,

$$f_{pi} = 0.7f_{pu} = 175,000 \text{ psi}$$



**Figure 11.33** Typical elevation and section of a domed prestressed concrete circular tank.

so

$$A_{ps} = \frac{P_i}{f_{pi}} = \frac{211,671}{175,000} = 1.21 \text{ in}^2 (7.56 \text{ cm}^2)$$

Trying  $\frac{1}{2}$ -in. dia (12.7-mm) 7-wire 250-K strands, we obtain

$$A_{ps}/\text{strand} = 0.144 \text{ in.}^2$$

and

$$\text{No. of strands} = \frac{1.21}{0.144} = 8.4$$

If the prestress loss is slightly more than 26 percent, the number of strands should be approximately 9. Hence, use nine  $\frac{1}{2}$ -in. dia 7-wire strands to prestress the edge ring beam.

*Check the Concrete Stress in the Critical Section  $t = 3$  in. of the Shell Rim.* The meridional compression  $N_\phi = -2,991$  lb/ft of circumference, and the compressive stress  $f_c = 2,991/(12 \times 3) = 83$  psi only, which is satisfactory. The support details of the edge ring beam and the roof are shown in Figure 11.32. Note that the ring beam is supported vertically on a neoprene pad, which enables sliding. A typical elevation and section of a domed prestressed circular tank is shown in Figure 11.33.

## SELECTED REFERENCES

- 11.1 Timoshenko, S., and Woinowsky-Krieger, S. *Theory of Plates and Shells*. 2d ed. McGraw Hill, New York, 1959.
- 11.2 Creasy, L. R. *Prestressed Concrete Cylindrical Tanks*. John Wiley & Sons, New York, 1961.
- 11.3 Billington, D. P. *Thin Shell Concrete Structures*. 2d ed. McGraw Hill, New York, 1982.
- 11.4 Ghali, A. *Circular Storage Tanks and Silos*. E. & F. N. Spon Ltd., London, 1979.
- 11.5 PCA, "Circular Concrete Tanks without Prestressing," Concrete Information Series ST-57, Portland Cement Association, Skokie, Ill., 1957, 32 pp.

- 11.6** PCI Committee on Precast Prestressed Concrete Storage Tanks. "Recommended Practice for Precast Prestressed Concrete Circular Storage Tanks." Prestressed Concrete Institute, Chicago, 1987.
- 11.7** ACI Committee 344. *Design and Construction of Circular Prestressed Concrete Structures, ACI 344R*. American Concrete Institute, Farmington Hills, MI, 1970.
- 11.8** ACI Committee 344. *Design and Construction of Circular Wire and Strand Wrapped Prestressed Concrete Structures, ACI 344-R*, American Concrete Institute, Farmington Hills, MI, 1989.
- 11.9** ACI Committee 344. *Design and Construction of Circular Prestressed Concrete Structures with Circumferential Tendons, ACI 344.2R*, American Concrete Institute, Farmington Hills, MI, 1989.
- 11.10** Post-Tensioning Institute. *Post-Tensioning Manual*. 6th ed. Post-Tensioning Institute, Phoenix, 2006.
- 11.11** Prestressed Concrete Institute. *PCI Design Handbook*. 6th ed. Prestressed Concrete Institute, Chicago, 2004.
- 11.12** Tadros, M. K. "Expedient Service Load Analysis of Cracked Prestressed Concrete Sections." *Journal of the Prestressed Concrete Institute*, Vol. 27, No. 6, Nov-Dec, Chicago, 1983, 137-158.
- 11.13** Brondum-Nielsen, T. "Prestressed Tanks." *Journal of the American Concrete Institute*, Detroit, July-August 1985, pp. 500-509.
- 11.14** Vessey J.V., and Preston, R. L. *A Critical Review of Code Requirements for Circular Prestressed Concrete Reservoirs*. F.I.P., Paris, 1978.
- 11.15** Nawy, E. G., and Blair, H., *Further Studies of Flexural Crack Control in Structural Slab Systems*. American Concrete Institute, Farmington Hills, MI, SP-30, 1971.
- 11.16** Abeles, P. W., and Bardhan-Roy, B. K. *Prestressed Concrete Designer's Handbook*. 3d ed. Viewpoint Publications, London, 1981.
- 11.17** ACI Committee 350, *Seismic Design of Liquid-Containing Concrete Structures (ACI 350.3-01) and Commentary (350.3R-01)*, American Concrete Institute, Farmington Hills, MI, 2001.
- 11.18** Nawy, E. G., *Fundamentals of High Performance Concrete*, 2nd ed., John Wiley and Sons, New York, NY, 2001, 452 pp.
- 11.19** Nawy, E. G., *Concrete Construction Engineering Handbook*, 2nd ed., CRC Press, Boca Raton, FL, 2008, 1560 pp.

## PROBLEMS

- 11.1** Solve Example 11.3 if the tank diameter is 120 ft (36.6 m) and the water height is 30 ft (9.1 m). Assume that the total prestress loss is 20 percent, and use a rise-span ratio  $h'/d = \frac{1}{10}$  for the roof dome, assuming that half the shell angle is  $\phi = 45^\circ$ .
- 11.2** A circular prestressed concrete tank has an internal diameter  $d = 85$  ft (26 m) and retains water to a height  $H = 22$  ft (6.7 m). Determine the maximum horizontal ring forces and vertical moment, and design the prestressing reinforcement using both horizontal and vertical prestressing. Also, design a roof dome shell for the tank assuming a rise-span ratio  $h'/d = \frac{1}{8}$  and half shell angle  $\phi = 30^\circ$ . Solve for (a) hinged, (b) partially fixed, and (c) sliding wall base fixity, and design the prestressing reinforcement for both wire-wrapped and tendon prestressing conditions. Given data are:

$$f'_c = 6,000 \text{ psi (41.4 MPa), normal weight}$$

$$f'_{ci} = 4,250 \text{ psi (29.3 MPa)}$$

$$f_t \leq 3\sqrt{f'_c} = 230 \text{ psi (1.59 MPa)}$$

$$f_c = 0.45f'_c = 2,700 \text{ psi (18.6 MPa)}$$

$$f_{cv} = 250 \text{ psi (1.72 MPa)-residual compressive stress}$$

$$f_{pu} \text{ for both wire and strand or tendon} = 250,000 \text{ psi (1,724 Pa)}$$

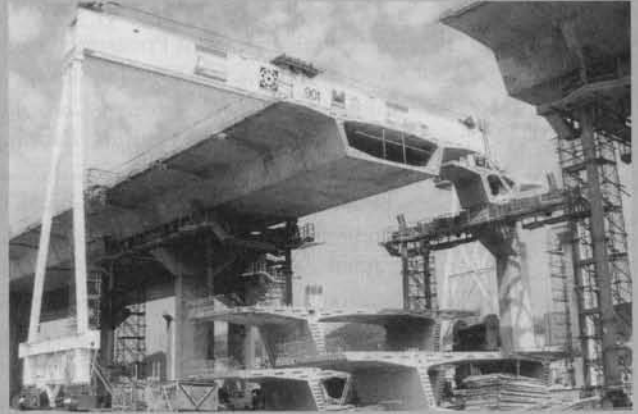
$$f_{pi} = 0.7f_{pu} = 175,000 \text{ psi (1,207 MPa)}$$

$$\text{Snow load intensity } w_L = 20 \text{ lb/ft}^2 \text{ (985 Pa)}$$

Assume 20-percent total loss in prestress.



# 12



## LRFD AND STANDARD AASHTO DESIGN OF CONCRETE BRIDGES

### 12.1 INTRODUCTION: SAFETY AND RELIABILITY

As discussed in Section 4.10.1, a load-resistance factor design method (LRFD) is a reliability-based approach for evaluating probability-based factored design criteria (Ref. 12.1). It is intended for proportioning structural members based on the load types such that the resisting strength levels are *greater* than the factored load or moment distributions.

Figures 12.1(a) and (b), as in Figure 4.36 of Chapter 4, show a plot of separate frequency distributions of the actual load  $W$  and the resistance  $R$  with mean value  $\bar{R}$ . Figure 12.1(c) gives the two distributions superimposed and intersecting at point  $C$  in the diagram.

The safety and reliable integrity of the structure can be expected to exist if the load effect  $W$  falls at a point to the left of intersection  $C$  on the resistance curve. Failure, on the other hand, would be expected to occur if the load effect on the resistance curve falls within the shaded area in Fig. 12.1(c). If  $\beta$  is a safety index, then:

$$\bar{\beta} = \frac{\bar{R} - \bar{W}}{\sqrt{\sigma_R^2 + \sigma_W^2}} \quad (12.1)$$

where,  $\sigma_R$  and  $\sigma_W$  are the standard deviations of the resistance and the load, respectively.

West Kowloon Expressway Viaduct, Hong Kong, 1997. A 4.2-Km dual 3-lane causeway connecting Western Harbor Crossing to new airport (Courtesy Institution of Civil Engineers, London)

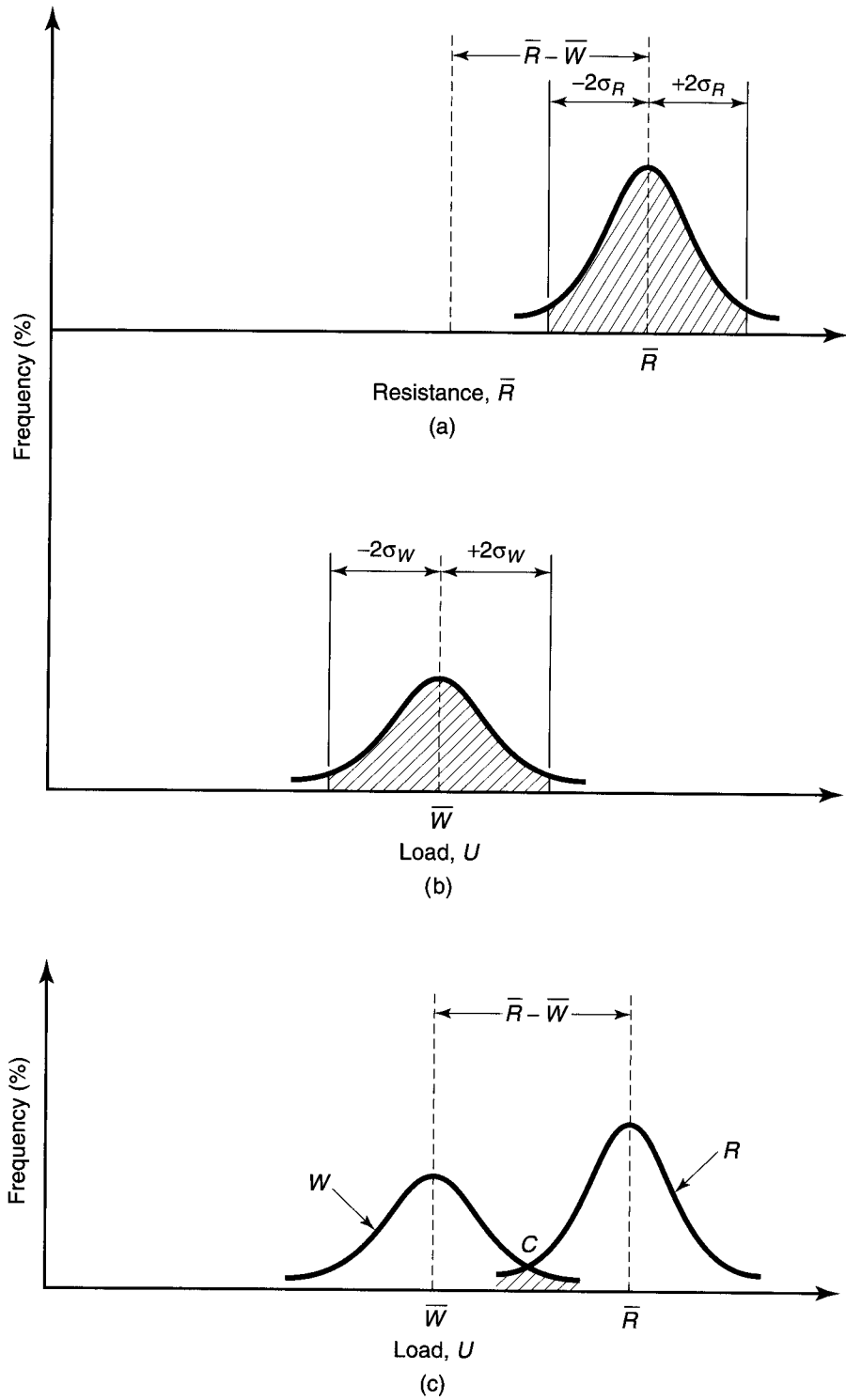


Figure 12.1 Frequency Distribution of Load vs. Resistance

**Table 12.1(a)** LRFD Resistance Factors  $\phi$ 

	$\phi$
Flexure and tension of reinforced concrete	0.90
Flexure and tension in prestressed concrete	1.00
Shear and torsion:	
normal density concrete	0.90
low-density concrete	0.70
Axial compression with spirals of ties	0.75
Bearing on concrete	0.70
Compression in strut and tie models	0.70
Compression in anchorage zones:	
normal density concrete	0.80
low-density concrete	0.65
Tension in steel in anchorage zones	1.00
For partially prestressed components in flexure with or without tension, where $PPR = A_{ps}f_{py}/(A_{ps}f_{py} + A_s f_y)$	$0.90 + 0.10(PPR)$

The different load combinations in Eq. 4.29, Chapter 4, are based on giving a reasonable difference between  $R$  and  $W$  as dictated by economical considerations.

The reliability of safe performance of the structure is, hence, controlled by the load-resistance considerations in the load factors used in the design.

AASHTO's LRFD approach (Ref. 12.2–12.3) is intended to extend the load-resistance considerations to the expressions for deformations and forces and modified load resistance factors  $\phi$  from those used by ACI 318 (Ref. 12.4) where necessary. Those LRFD  $\phi$  factors are listed in Table 12.1(a).

This chapter presents, and uses in design examples, the LRFD expressions where they differ from the standard AASHTO and ACI-318 expressions. Otherwise, the expressions used in the previous Chapters 3, 4, and 5 and the principles enunciated would apply. The student and the design engineer will easily recognize these expressions. Hence the need for redefining them becomes unnecessary.

It should be noted that most state DOTs have already mandated the use of the LRFD Design Method. However, other state DOTs and users of AASHTO standards in the United States and elsewhere still use the LFD Design Method. In addition, evaluation of bridge performance designed prior to 2008 by the LFD procedures requires use of the same criteria applied in the original design for comparison and conflict resolution. Hence, this chapter retains the LFD Design Method but fully presents the current AASHTO LRFD procedures.

## 12.2 AASHTO STANDARD (LFD) AND LRFD TRUCK LOAD SPECIFICATIONS

The design of prestressed concrete elements of a bridge is governed by requirements of the American Association of Highway and Transportation Officials (AASHTO). The traffic lanes and the loads they contain for the design of the bridge superstructure have to be chosen and placed in such numbers and positions on the roadway that they produce the maximum stress in the constituent members.

The bridge live loadings should consist of standard truck or lane loads that are equivalent to truck trains. For railway bridges, the requirements are set by the American Railway Engineering Association (AREA). Requirements for the structural proportioning of the supporting members usually follow the ACI and PCI standards.

**12.2.1 Loads**

There are four standard classes of highway loading: H 20, H 15, HS 20, and HS 15. Loading HS 15 is 75 percent of HS 20. If loadings other than these are to be considered, they should be obtained by proportionally adjusting the weights for the standard trucks and the corresponding lane loads. Bridges supporting interstate highways should be re-designed for HS 20-44 loading or an alternate military loading of two axles 4 ft apart, with each axle weighing 24,000 lb, whichever loading produces the larger stress value.

Figure 12.2 shows the standard H truck loading, while Figure 12.3 shows the standard HS truck loading giving wheel spacing and load distribution. Figure 12.4 gives the equivalent lane loading for both the H and HS 20-44 and the H and HS 15-44 categories (Ref. 12.1). Figure 12.5 gives an overview of the different bridge deck systems in common use.

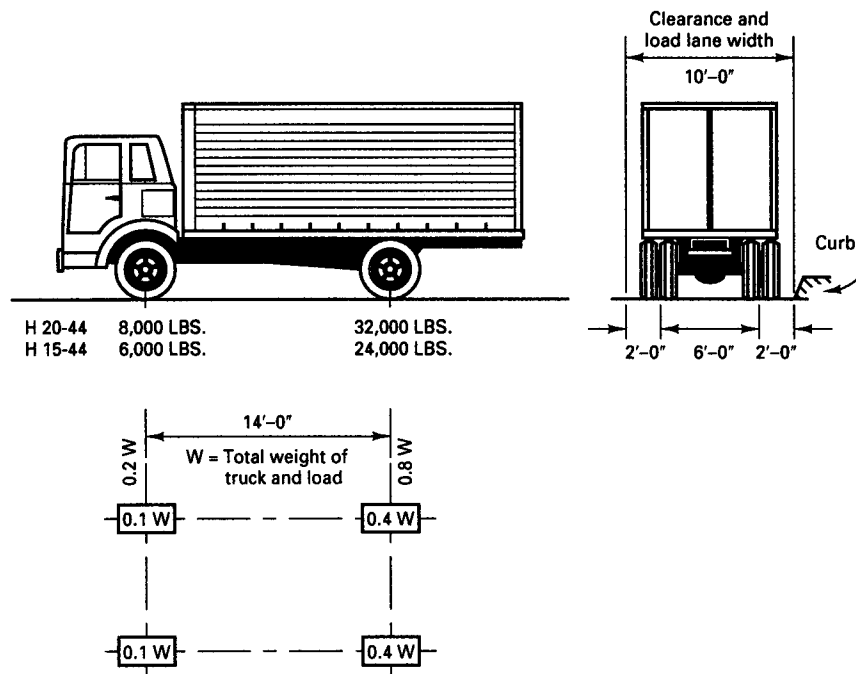
Figure 12.5 gives typical deck bridge structures.

**(i) Impact.** Movable loads require impact allowance as a fraction of the live load stress. It can be expressed by standard AASHTO (LFD):

$$I = \frac{50}{L + 125} \leq 30\% \tag{12.2}$$

where  $I$  = Impact fraction

$L$  = Length in feet of the portion of the span that is loaded resulting in maximum stress in that member.



**Figure 12.2** Wheel loads and geometry for H trucks

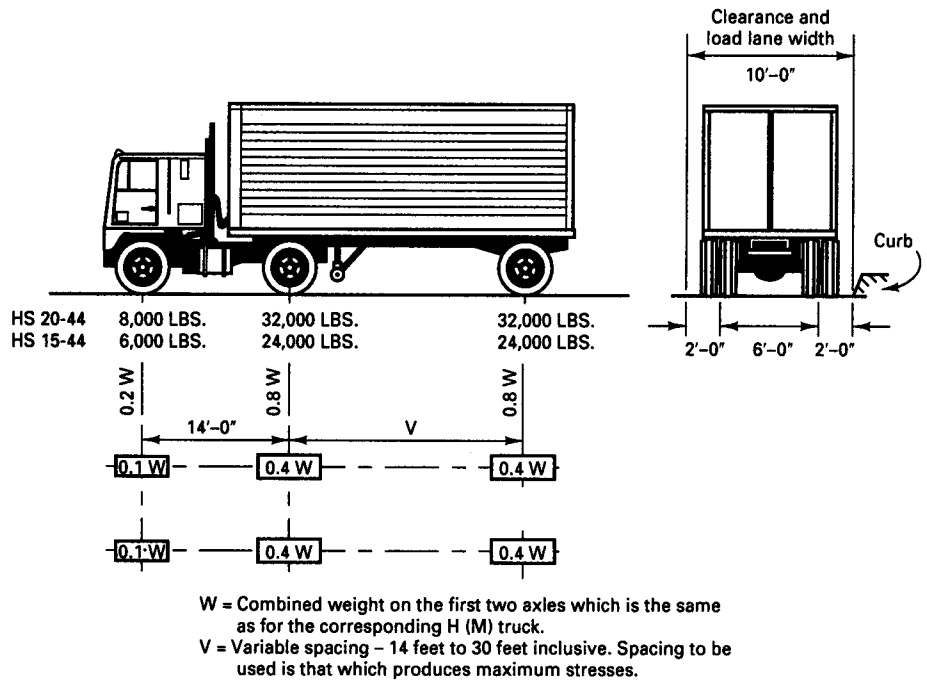


Figure 12.3 Wheel loads and geometry for HS trucks

The loaded length  $L$  for transverse members, such as floor beams, is the span length of the member center to center of the supports.

**(ii) Longitudinal Forces.** Provision should be made for the effect of a longitudinal force of 5 percent of the live load in all lanes carrying traffic headed in the same direction. All lanes should be loaded in the case of bridges which could likely become one-directional in the life of the structure. The load area, without impact, should be as follows:

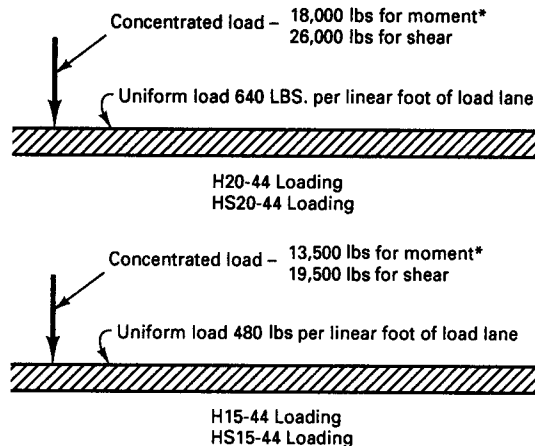


Figure 12.4 Equivalent lane loading for H and HS trucks

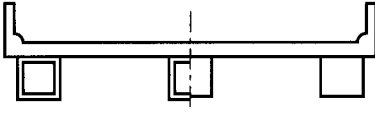
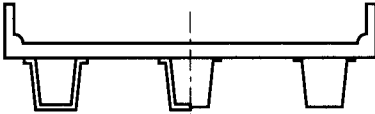
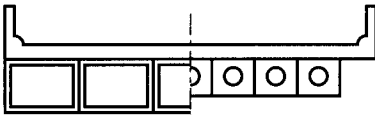
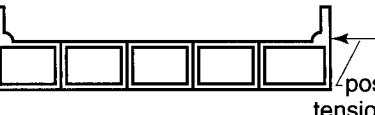
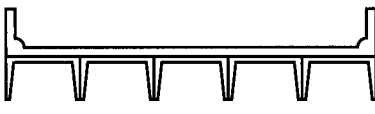
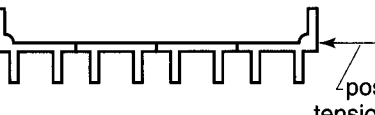
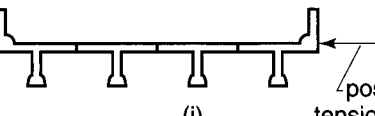
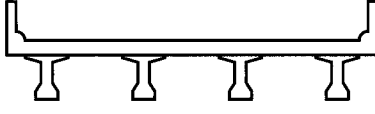
SUPPORTING COMPONENTS	TYPE OF DECK	TYPICAL CROSS-SECTION
Closed Steel or Precast Concrete Boxes	Cast-in-place concrete slab	 <p>(b)</p>
Open Steel or Precast Concrete Boxes	Cast-in-place concrete slab, precast concrete deck slab	 <p>(c)</p>
Precast Solid, Voided or Cellular Concrete Boxes with Shear Keys	Cast-in-place concrete overlay	 <p>(f)</p>
Precast Solid, Voided or Cellular Concrete Box with Shear Keys and with or without Transverse Post-Tensioning	Integral concrete	 <p>(g) post tension</p>
Precast Concrete Channel Sections with Shear Keys	Cast-in-place concrete overlay	 <p>(h)</p>
Precast Concrete Double Tee Section with Shear Keys and with or without Transverse Post-Tensioning	Integral concrete	 <p>(i) post tension</p>
Precast Concrete Tee Section with Shear Keys and with or without Transverse Post-Tensioning	Integral concrete	 <p>(j) post tension</p>
Precast Concrete I or Bulb-Tee Sections	Cast-in-place concrete, precast concrete	 <p>(k)</p>

Figure 12.5 Cross sections of Typical Bridge Deck Structures (Ref. 12.11)

Lane load + concentrated load so placed on the span as to produce maximum stress. The concentrated load and uniform load should be considered as uniformly distributed over a 10 foot width on a line normal to the centerline of the lane. The center of gravity of the longitudinal force is to be assumed located 6 feet above the floor slab.

A reduction factor should be applied when a number of traffic lanes are simultaneously loaded, as in Section (iv) to follow.

**(iii) Centrifugal Horizontal Force.** This force is produced by vehicle motion on curves. It is a percentage of the live load, without impact, as follows:

$$C = 0.00117S^2D = \frac{6.68S^2}{R} \quad (12.3)$$

where  $C$  = centrifugal force in percent of the live load without impact

$S$  = design speed in miles per hour

$D$  = degree of curve

$R$  = radius of curve in feet.

**(iv) Reduction in Load Intensity.** When maximum stresses are produced in any member by loading a number of traffic lanes simultaneously, a reduction in the live load intensity can be made as follows:

	<i>Percent</i>
One or two lanes	100
Three lanes	90
Four lanes or more	75

### 12.2.2 Wheel Load Distribution on Bridge Decks: Standard AASHTO Specifications (LFD)

**(i) Shear.** No longitudinal distribution of wheel loads can be made for wheel or axle load adjacent to the end when computing end shears and reactions in transverse or longitudinal beams.

**(ii) Bending Moments: Longitudinal Beams.** In computing bending moments in longitudinal beams or stringers, no longitudinal distribution of the wheel loads is permitted. In the case of interior stringers, the live load bending moment for each stringer should be determined by applying to the stringer a fraction of the wheel load as follows for prestressed concrete elements

	Bridge designed for one traffic lane	Bridge designed for two or more traffic lanes
Prestressed concrete girders	$S/7.0$ if $S > 6$ ft.*	$S/5.5$ if $S > 10$ .*
Non-attached Concrete Box girders	$S/8.0$ if $S > 12$ ft.*	$S/7.0$ if $S > 16$ ft.*

\*If  $S$  exceeds denominator, the load on the beam should be the reaction of the wheel loads assuming the flooring between beams to act as a simple beam.

$S$  = spacing of floor beams in feet.

**(iii) Side by Side Precast Beams in Multi-Beam Decks.**<sup>12.2</sup> A multi-beam bridge is constructed with precast reinforced or prestressed concrete beams that are placed *side by side* on the supports. The interaction between the beams is developed by continuous longitudinal shear keys used in combination with transverse tie assemblies which may, or

may not, be prestressed, such as bolts, rods, or prestressing strands, or other mechanical means. Full-depth rigid end diaphragms are needed to ensure proper load distribution for channel, single- and multi-stemmed tee beams.

In computing bending moments in multi-beam precast concrete bridges, conventional or prestressed, no longitudinal distribution of wheel load shall be assumed. The live load bending moment for each section is determined by applying to the beam the fraction of a wheel load (both front and rear) determined by the following equation:

$$\text{Load Fraction} = \frac{S}{D}$$

where,

$$\begin{aligned} S &= \text{width of precast member;} \\ D &= (5.75 - 0.5N_L) + 0.7N_L(1 - 0.2C)^2 \text{ when } C \leq 5 \\ D &= (5.75 - 0.5N_L) \text{ when } C > 5 \\ N_L &= \text{number of traffic lanes} \\ C &= K(W/L) \end{aligned}$$

where,

$$\begin{aligned} W &= \text{overall width of bridge measured perpendicular to the longitudinal girders in feet;} \\ L &= \text{span length measured parallel to longitudinal girders in feet; for girders with cast-in-place end diaphragms, use the length between end diaphragms;} \\ K &= \{(1 + \mu) I/J\}^{\frac{1}{2}} \end{aligned}$$

If the value of  $\sqrt{I/J}$  exceeds 5.0, the live load distribution should be determined using a more precise method, such as the Articulated Plate Theory or Grillage Analysis.

where,

$$\begin{aligned} I &= \text{moment of inertia;} \\ J &= \text{Saint-Venant torsion constant;} \\ \mu &= \text{Poisson's ratio for girders.} \end{aligned}$$

In lieu of more exact methods, "J" may be estimated using the following equations:

*For Non-voided Rectangular Beams, Channels, Tee Beams:*

$$J = \Sigma\{(1/3)bt^3(1 - 0.630t/b)\}$$

where,

$$\begin{aligned} b &= \text{the length of each rectangular component within the section,} \\ t &= \text{the thickness of each rectangular component within the section.} \end{aligned}$$

The flanges and stems of stemmed or channel sections are considered as separate rectangular components whose values are summed together to compute "J". Note that for "Rectangular Beams with Circular Voids" the value of "J" can usually be approximated by using the equation above for rectangular sections and neglecting the voids.

*For Box-Section Beams:*

$$J = \frac{2tt_f(b - t)^2(d - t_f)^2}{bt + dt_f - t^2 - t_f^2}$$



where

- $b$  = the overall width of the box,
- $d$  = the overall depth of the box,
- $t$  = the thickness of either web,
- $t_f$  = the thickness of either flange.

The formula assumes that both flanges are the same thickness and uses the thickness of only one flange. The same is true of the webs.

For preliminary design, the following values of  $K$  may be used:

Bridge type	Beam Type	K
Multi-beam	Non-voided rectangular beams	0.7
	Rectangular beams with circular voids	0.8
	Box section beams	1.0
	Channel, single- and multi-stemmed tee beams	2.2

#### (iv) Stresses in Concrete

Case I: *All Loads including Prestress ( $D + L + P/S$ )*

$$f_c = 0.60 f'_c$$

$$f_t = 6\sqrt{f'_c}$$

Case II: *Prestress + All Dead Loads ( $D + P/S$ )*

$$f_c = 0.40 f'_c$$

$$f_t = 6\sqrt{f'_c}$$

Case III:  *$\frac{1}{2}$ Prestress + Dead) + Live Load [ $0.5 (D + P/S) + L$ ]*

$$f_c = 0.40 f'_c$$

$$f_t = 6\sqrt{f'_c}$$

#### 12.2.3 Bending Moments in Bridge Deck Slabs: Standard AASHTO Specifications (LFD)

There are two categories for bending moment calculations: category A and category B for reinforcement perpendicular and parallel respectively to the traffic.

$S$  = effective span length in feet

$E$  = width of slab in feet over which a wheel load is distributed

$P$  = load on one rear wheel of truck ( $P_{15}$  or  $P_{20}$ )

$P_{15}$  = 12,000 lbs. for H 15 loading

$P_{20}$  = 16,000 lbs. for H 20 loading

##### (a) Case A—Main Reinforcement Perpendicular to Traffic (spans 2 to 24 feet)

The live load moments for simple spans are to be determined in accordance with the following expressions:

H 20 Loading,

$$M_L = \left( \frac{S + 2}{32} \right) P_{20} \quad (12.4a)$$

H 15 Loading,

$$M_L = \left( \frac{S + 2}{32} \right) P_{15} \quad (12.4b)$$

where  $M_L$  is in ft-lb/ft of slab width

In slabs continuous over three or more supports, a continuity factor of 0.8 should be applied to Equations 12.4(a) and 12.4(b)

**(b) Case B—Main Reinforcement Parallel to Traffic**

For wheel loads, the distribution width,  $E$ , should be  $= 4 + 0.06S \leq 7.0$  ft. Lane loads are distributed over a width  $2E$  as follows:

H 20 Loading

$$S \leq 50 \text{ ft:} \quad M_L = 900S \quad (12.4c)$$

$$S = 50 - 100 \text{ ft:} \quad M_L = 1000S \quad (12.4d)$$

where  $M_L$  is in ft-lb

For H 15 loading, reduce the values in Equations 12.4(c), and 12.4(d) by 25 percent.

### 12.2.4 Wind Loads

In accounting for the wind loads, the exposed area is equal to the sum of the areas of all members including floor system and railings as seen in an elevation 90 degrees to the longitudinal axis of the structure. Design should be based on a wind velocity  $V = 100$  miles per hour. The area may be reduced as stipulated in Ref. 12.2.

### 12.2.5 Seismic Forces

Both the equivalent static force method and the response spectrum method can be used for the design of structures with supporting members of approximately equal stiffnesses. Details are given in Ref. 12.2. Additional basic discussion of earthquake response, the fundamental period of vibration and the International Building Code (IBC 2009) are given in Ref. 12.5.

### 12.2.6 AASHTO LFD Load Combinations

The design should consider such a group of load combinations that results in the maximum stress condition in the member under consideration. There are ten groups of loadings under service load conditions:

Group I:  $D + (L + I) + CF + E + B + SF$

Group II:  $D + E + B + SF + W$

Group III:  $D + (L + I) + CF + E + B + SF + W + WL + LF$

Group IV:  $D + (L + I) + CF + E + SF + (R + S + T)$

Group V:  $D + E + B + SF + W + (R + S + T)$

Group VI:  $D + (L + I) + CF + E + B + SF + W + WL + LF + (R + S + T)$

Group VII:  $D + E + B + SF + EQ$

Group VIII:  $D + (L + I) + CF + E + B + SF + ICE$

Group IX:  $D + E + B + SF + W + ICE$

Group X:  $D + (L + I) + E$

where  $D$  = dead load

$L$  = live load

$I$  = live load impact

$E$  = earth pressure

$B$  = buoyancy

$W$  = wind load on the structure

$WL$  = wind load on live load – 100 lb./linear foot

$LF$  = longitudinal force from live load

$CF$  = centrifugal force

$R$  = rib shortening

$S$  = shrinkage

$T$  = temperature

$EQ$  = earthquake

$SF$  = stream flow pressure

$ICE$  = ice pressure

For load factor design, the proceeding parameters are multiplied by the load factors in Table 12.1(b)

For factor loads, the group value is

$$\begin{aligned} \text{Group number } (N) = & \gamma[\beta_D D + \beta_L(L + I) + \beta_C CF + \beta_E E \\ & + \beta_B B + \beta_S SF + \beta_W W + \beta_{WL} WL + \beta_L LF \\ & + \beta_R(R + S + T) + \beta_{EQ} EQ + \beta_{ICE} ICE] \end{aligned} \quad (12.5)$$

The load factors to be applied to any particular load combination are as follows:

$\beta_E = 0.7$  for vertical loads on reinforced concrete boxes.

= 1.00 for lateral loads on reinforced concrete boxes.

= 1.00 for vertical and lateral loads on all other culverts.

= 1.0 and 0.5 for lateral loads on rigid frames (check which loading governs for the particular group).

$\beta_E = 1.3$  for lateral earth pressure when checking positive moment in rigid frames, culverts or reinforced box culverts.

$\beta_D = 0.75$  when checking member for minimum axial load and maximum moment for maximum eccentricity for column design.

= 1.0 when checking for maximum axial load and minimum moment.

= 1.0 for flexural and tension members.

Table 12.1(b) gives the values of the  $\beta$  coefficients for the various load parameters in Equation 12.5 for Standard AASHTO Specifications.

**Table 12.1(b)**  $\beta$  Coefficients for LOAD Group Parameters: Standard AASHTO Specifications (Ref. 12.2)

Col. No.	1	2	3	3A	4	5	6	7	8	9	10	11	12	13	14
$\beta$ FACTORS															
GROUP	$\gamma$	D	$(L+I)_n$	$(L+I)_p$	CF	E	B	SF	W	WL	LF	R+S+T	EQ	ICE	%
<b>SERVICE LOAD</b>	I	1.0	1	1	0	1	$\beta_E$	1	1	0	0	0	0	0	100
	IA	1.0	1	2	0	0	0	0	0	0	0	0	0	0	150
	IB	1.0	1	0	1	1	$\beta_E$	1	1	0	0	0	0	0	**
	II	1.0	1	0	0	0	1	1	1	1	0	0	0	0	125
	III	1.0	1	1	0	1	$\beta_E$	1	1	0.3	1	1	0	0	125
	IV	1.0	1	1	0	1	$\beta_E$	1	1	0	0	0	1	0	125
	V	1.0	1	0	0	0	1	1	1	1	0	0	1	0	140
	VI	1.0	1	1	0	1	$\beta_E$	1	1	0.3	1	1	1	0	140
	VII	1.0	1	0	0	0	1	1	1	0	0	0	0	1	133
	VIII	1.0	1	1	0	1	1	1	1	0	0	0	0	1	140
	IX	1.0	1	0	0	0	1	1	1	1	0	0	0	0	150
X	1.0	1	1	0	0	$\beta_E$	0	0	0	0	0	0	0	100	
<b>LOAD FACTOR DESIGN</b>	I	1.3	$\beta_D$	1.67*	0	1.0	$\beta_E$	1	1	0	0	0	0	0	Not Applicable
	IA	1.3	$\beta_D$	2.20	0	0	0	0	0	0	0	0	0	0	
	IB	1.3	$\beta_D$	0	1	1.0	$\beta_E$	1	1	0	0	0	0	0	
	II	1.3	$\beta_D$	0	0	0	$\beta_E$	1	1	1	0	0	0	0	
	III	1.3	$\beta_D$	1	0	1	$\beta_E$	1	1	0.3	1	1	0	0	
	IV	1.3	$\beta_D$	1	0	1	$\beta_E$	1	1	0	0	0	1	0	
	V	1.25	$\beta_D$	0	0	0	$\beta_E$	1	1	1	0	0	1	0	
	VI	1.25	$\beta_D$	1	0	1	$\beta_E$	1	1	0.3	1	1	1	0	
	VII	1.3	$\beta_D$	0	0	0	$\beta_E$	1	1	0	0	0	0	1	
	VIII	1.3	$\beta_D$	1	0	1	$\beta_E$	1	1	0	0	0	0	1	
	IX	1.20	$\beta_D$	0	0	0	$\beta_E$	1	1	1	0	0	0	1	
X	1.30	1	1.67	0	0	$\beta_E$	0	0	0	0	0	0	0		

$(L + I)_n$  - Live load plus impact for AASHTO Standard Highway H or HS loading

$(L + I)_p$  - Live load plus impact consistent with the overload criteria of the operation agency.

### 12.2.7 LRFD Load Combinations

The load combinations using the LRFD specifications differ from the standard specifications. The following tables: 12.2 to 12.3, give the required load combinations, and Tables 12.4 to 12.7 the shear and moment expressions to be used in design. Section 12.1.1 gives the LRFD resistance factors,  $\phi$ , which differ from the standard reduction factor  $\phi$ . It should be noted that in the standard specifications, either the lane load or the truck load is used in the live-load calculations. The LRFD specifications require that the *combined* lane and truck loads be used in the live-load computations.

**Table 12.2(a)** LRFD Load Combinations and Load Factors

Load Combination  Limit State	DC DD DW EH EV ES	LL IM CE BR PL LS EL	WA	WS	WL	FR	TU CR SH	TG	SE	Use One of These at a Time			
										EQ	IC	CT	CV
STRENGTH-I*	$\gamma_P$	1.75	1.00	-	-	1.00	0.50/1.20	$\gamma_{TG}$	$\gamma_{SE}$	-	-	-	-
STRENGTH-II	$\gamma_P$	1.35	1.00	-	-	1.00	0.50/1.20	$\gamma_{TG}$	$\gamma_{SE}$	-	-	-	-
STRENGTH-III	$\gamma_P$	-	1.00	1.40	-	1.00	0.50/1.20	$\gamma_{TG}$	$\gamma_{SE}$	-	-	-	-
STRENGTH-IV EH, EV, ES, DW DC ONLY	$\gamma_P$ 1.5	-	1.00	-	-	1.00	0.50/1.20	-	-	-	-	-	-
STRENGTH-V	$\gamma_P$	1.35	1.00	1.00	0.40	1.00	0.50/1.20	$\gamma_{TG}$	$\gamma_{SE}$	-	-	-	-
EXTREME EVENT-I	$\gamma_P$	$\gamma_{EQ}$	1.00	-	-	1.00	-	-	-	1.00	-	-	-
EXTREME EVENT-II	$\gamma_P$	0.50	1.00	-	-	1.00	-	-	-	-	1.00	1.00	1.00
SERVICE-I	1.00	1.00	1.00	1.00	0.30	1.00	1.00/1.20	$\gamma_{TG}$	$\gamma_{SE}$	-	-	-	-
SERVICE-II	1.00	1.30	1.00	-	-	1.00	1.00/1.20	-	-	-	-	-	-
SERVICE-III	1.00	0.80	1.00	-	-	1.00	1.00/1.20	$\gamma_{TG}$	$\gamma_{SE}$	-	-	-	-
FATIGUE-LL, IM & CE ONLY	-	0.75	-	-	-	-	-	-	-	-	-	-	-

where:  $\gamma_p$  = Load factor for permanent loads

\*For load combinations,  
 Maximum  $Q = 1.25 DC + 1.50 DW + 1.75 (LL + IM)$   
 Minimum  $Q = 0.90 DC + 0.65 DW + 1.75 (LL + IM)$

**Permanent Loads**

- DD = downdrag
- DC = dead load of structural components and nonstructural attachments
- DW = dead load of wearing surfaces and utilities
- EH = horizontal earth pressure load
- ES = earth surcharge load
- EV = vertical pressure from dead load of earth fill
- EL = Locked-in erection stress
- Q = Factored Load

**Transient Loads**

- BR = vehicular braking force
- CE = vehicular centrifugal force
- CR = creep
- CT = vehicular collision force
- CV = vessel collision force
- EQ = earthquake
- FR = friction
- IC = ice load
- IM = vehicular dynamic load allowance
- LL = vehicular live load
- LS = live load surcharge
- PL = pedestrian live load
- SE = settlement
- SH = shrinkage
- TG = temperature gradient
- TU = uniform temperature
- WA = water load and stream pressure
- WL = wind on live load
- WS = snow load

Strength I: Basic load combination, no wind

Strength II: Load on bridge with owner-specified design, no wind

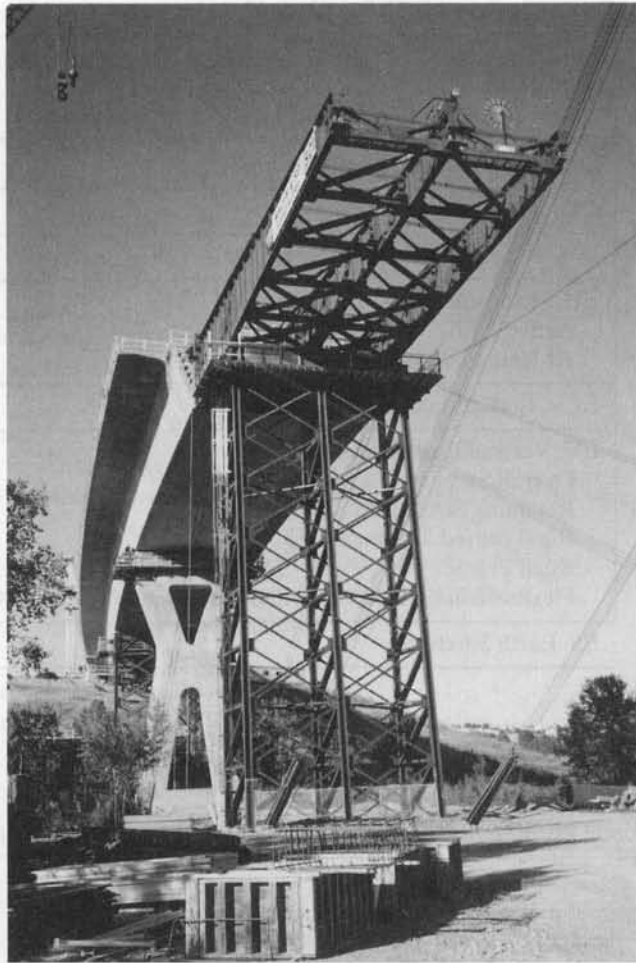
Strength III: Load includes wind

Strength IV: Very high ratio of dead to live load

Service I: Normal operational use load combinations with deflection and crack control

Service II: Load combinations with control of yielding of steel structures

Service III: Load combinations relating only to tension in prestressed concrete



**Photo 12.1** Stoney Trail Bow River segmental bridge, Calgary, Alberta, utilizing the incremental launch method—span 1562 ft, deck width 69 ft, and the deck rises 89 to 118 ft above the river valley (Courtesy James Skeet-Reid Crowther Engineering, Calgary)

The LRFD Resistance Factor  $\phi$  values are given in Table 12.1(a) to follow.

The following expressions in Table 12.4 and 12.5 (Ref. 12.2) may be used to compute the maximum bending moments and the maximum shear force per *lane* of any point in a span for HS20 truck, with the limitations indicated in the table. The computed values have to be halved in order to obtain the shear force and moment per *line* of wheels.

The expressions in the tables are limited to simply supported spans and do not include the impact factors.

The maximum bending moments and maximum shear forces per lane at any point on a span for a lane load of 0.64 kip/ft may be computed from the following simplified expressions:

**Table 12.2(b)** LRFD Permanent Loads

Type of Load	Load Factor	
	Maximum	Minimum
DC: Component and Attachments	1.25	0.90
DD: Downdrag	1.80	0.45
DW: Wearing surface and utilities	1.50	0.65
EH: Horizontal Earth Pressure	Active	0.90
	At-Rest	0.90
EL = Locked-in Earth Stresses	1.00	1.00
EV: Vertical Earth Pressure	Overall Stability	0.90
	Retaining Structure	1.00
	Rigid Buried Structure	0.90
	Rigid Frame	0.90
	Flexible Buried Structure other than Metal Box Culvert	0.90
ES: Earth Surcharge	1.50	0.75

$$\text{Maximum } V_{LL} = \frac{0.64}{2L} (L - x)^2 \text{ kip} \quad (12.6a)$$

$$\text{Maximum } M_{LL} = \frac{0.64(x)(L - x)}{2} \text{ ft-kip} \quad (12.6b)$$

where,  $x$  = distance from left support, ft  
 $L$  = beam span, ft  
 $LL$  = lane load

The LRFD specifications require a higher impact factor than the standard specifications. They also require consideration of the fatigue state limits. For fatigue, a special truck load is considered. It consists of a single design truck which has the same axle weight used in all other limit states, but with a constant spacing of 30 ft between the 32-kip axles. Table 12.6 gives the impact factor  $IM$  for the various types of limit states:

**Table 12.3(a)** Distribution of Live Load Per Lane for Shear in Interior Beams

Section	One Design Lane	Two or More Design Lanes
Concrete Box Beams in Multi-beam Decks	$\left(\frac{b}{130L}\right)^{0.15} \left(\frac{I}{J}\right)^{0.05}$	$\left(\frac{b}{156}\right)^{0.4} \left(\frac{b}{12L}\right)^{0.1} \left(\frac{I}{J}\right)^{0.05}$
Concrete Deck, I-, T- and Double-T Sections	$0.36 + \left(\frac{s}{25.0}\right)$	$0.20 + \left(\frac{s}{12}\right) - \left(\frac{s}{36}\right)^2$

1. Ranges for  $b$ ,  $d$ ,  $L$ ,  $s$ ,  $S$ ,  $t_s$ ,  $K_g$  are given in Ref. 12.3.

2. For exterior beams, see Ref. 12.3, Section 4.6.2

**Table 12.3(b)** Distribution of Live Load Per Lane For Moment in Interior Beams

Section	One Design Lane	Two or More Design Lanes
Concrete Box Beams in Multi-beam Decks	$k \left( \frac{b}{33.5L} \right)^{0.5} \left( \frac{I}{J} \right)^{0.25}$	$k \left( \frac{b}{305} \right)^{0.6} \left( \frac{b}{12L} \right)^{0.2} \left( \frac{I}{J} \right)^{0.06}$
Concrete Deck, I-, T- and Double-T Sections	$0.06 + \left( \frac{S}{14} \right)^{0.4} \left( \frac{S}{L} \right)^{0.3} \left( \frac{K_g}{12t_s^3 L} \right)^{0.1}$	$0.075 + \left( \frac{S}{9.5} \right)^{0.6} \left( \frac{S}{L} \right)^{0.2} \left( \frac{K_g}{12t_s^3 L} \right)^{0.1}$

1. Ranges for  $b, d, L, s, S, t, K_g$  are given in Ref. 12.3.

2. For exterior beams, see Ref. 12.3, Section 4.6.2

3. Notation:

$b$  = Beam width, in.

$J$  = St. Vincent's torsional constant, in<sup>4</sup> =  $4 A_0^2 / \sum s/t$

$K_g$  = Longitudinal Stiffness parameter distribution factor for multi-beam bridges, where

$$K_g = n(I + A_c e_g^2)$$

$e_g$  = distance between centers of gravity of members

$k = 2.5(N_b)^{-0.2}$  where  $N_b$  = number of beams

$A_c$  = cross-sectional area

$L$  = span, ft

$A_0$  = area enclosed by centerlines of the beam elements

$s$  = length of an element of box beam

**Table 12.4** Maximum Shear Force per Lane for HS20 Truck Load ( $V_{LT}$ )

Load Type	$x/L$	Formula for maximum shear, kips	Minimum		Maximum
			$x,^*$ ft	$L, ft$	$L, ft$
HS20 Truck	0-0.500	$\frac{72[(L-x) - 4.67]}{L} - 8$	14	28	42
	0-0.500	$\frac{72[(L-x) - 9.33]}{L}$	0	42	-

\* $x$  is the distance from left support to the section being considered, ft;  $LT$  = truck load

**Table 12.5** Maximum Bending Moment per Lane for HS20 Truck Load ( $M_{LT}$ )

Load Type	$x/L$	Formula for maximum bending moment, ft-kips	Minimum	
			$x,^*$ ft	$L,ft$
HS20 Truck	0-0.333	$\frac{72(x)[(L-x) - 9.33]}{L}$	14	28
	0.333-0.500	$\frac{72(x)[(L-x) - 4.67]}{L} - 112$	0	42

\* $x$  is the distance from left support to the section being considered, ft;  $LT$  = truck load



**Table 12.6** Impact Factors

Component	IM
<b>Deck Joints—All Limit States</b>	<b>15%</b>
All other Components	
Fatigue and Fracture Limit States	15%
All Other Limit States	33%

**Table 12.7** Fatigue Bending Moment per Lane

Load Type	$x/L$	Formula for maximum bending moment, ft-kips	Minimum	
			x, * ft	L, ft
Fatigue Truck Loading (LRFD)	0–0.241	$\frac{72(x)[(L-x) - 18.22]}{L}$	0	44
	0.241–0.500	$\frac{72(x)[L-x] - 11.78}{L} - 112$	14	28

\*x is the distance from left support to the section being considered, ft; LT = truck load

Table 12.7 (Ref 12.3) gives expressions for computing the maximum bending moments per lane due to HL-93 fatigue truck loading. The values obtained from the table have to be multiplied by a factor of  $\frac{1}{2}$  in order to obtain the values per line of wheels.

The LRFD design live load is an HL-93 truck configuration which consists of a combination of:

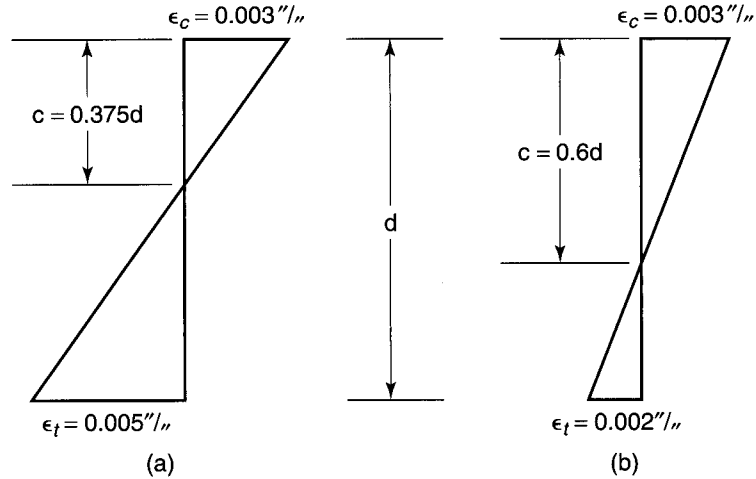
- (a) design truck or design tandem with dynamic allowance. The design truck is the same as the HS20 design truck specified in the Standard AASHTO specifications. The design tandem consists of a pair of 25 kip axles spaced at 4-ft apart.
- (b) design lane load of 0.64 kip/ft without dynamic allowance.

## 12.3 FLEXURAL DESIGN CONSIDERATIONS

### 12.3.1 Strain $\epsilon$ and Factor $\phi$ Variations: The Strain Limits Approach

For ductile behavior of sections, the reinforcement percentage has to be considerably smaller than the balanced limit strain in flexure percentage as detailed in Section 4.12.3. No upper limits on the amount of reinforcement needs to be used in a beam provided that the strain limit is not exceeded and the appropriate  $\phi$  factor is used. An upper limit tensile strain  $\epsilon_r = 0.005$  in./in. as the limiting strain is comparable to the 75% of the balanced reinforcement percentage in previous codes and is the basis of this approach (Figure 12.6). This limiting strain is considered at the extreme tensile steel reinforcement level, namely, at the centroid of the layer closest to the tensile face of the section. More precisely,  $\epsilon_r = 0.0041$  corresponds to  $f_y \approx 230,000$  psi in the prestressing steel.

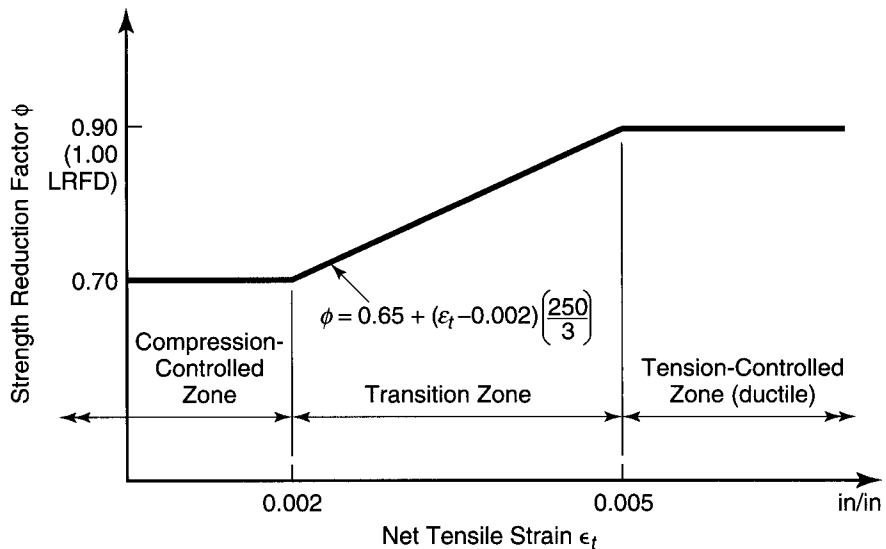
In the AASHTO LRFD procedure, a limiting value of the ratio of the neutral axis depth,  $c$ , to the effective beam depth,  $d_p$ , to the extreme tension reinforcement, is taken as 0.42 in this strain limits approach, invariably called as a unified approach (Refs.



**Figure 12.6** Strain Limits (a) Tension-Controlled, (b) Compression-Controlled

12.14–12.16). The approach is a rational way of assuring strain-compatibility using common strain and stress expressions regardless of whether the member is reinforced, prestressed or partially prestressed. The depth  $d_t$  in the ratio  $c/d_t$  becomes  $d_p$  if no mild steel reinforcement is used. Table 12.11 of section 12.8 presents a general comparison between the ACI and the LRFD procedures for determining the required reinforcement for flexure (Ref. 12.14).

A strain value  $\epsilon_t$ , considerably higher than 0.005 in./in. *has to be used*, such as 0.007 to 0.009 in./in. The limit compression-controlled state for beam-column sections is  $\epsilon_t = 0.002$  in./in. The  $\epsilon_t = 0.002$  is used as a basis for first yield strain.  $\epsilon_y = f_y/E_s = 0.002$ , although this value can vary depending on the type of reinforcement used. Fig. 12.7 gives on this basis the limits of strain for tension-controlled and compression-controlled concrete sections for all cases, reinforced and prestressed, where  $\epsilon_t = 0.003 (d_t/c - 1)$ .



**Figure 12.7** Variation of Strength Reduction Factor  $\phi$  with the Net Tensile Strain  $\epsilon_t$ .

When the net tensile strain in the extreme tension reinforcement is sufficiently large (equal to or greater than 0.005), the section is defined as tension-controlled where ample warning of failure with extensive deflection and cracking can occur. When the net tensile strain in the extreme tension reinforcement is small (less than or equal to the compression-controlled strain limit), a brittle failure condition is expected to develop, with little warning of impending failure.

A balanced strain condition develops at a section when the maximum strain at the extreme compression fibers just reaches 0.003 in./in. simultaneously with the first yield strain  $\epsilon_y = f_y/E_s$  in the tension reinforcement corresponding to a net tensile strain in the tension reinforcement set in this method at a value  $\epsilon_t = 0.002$  in./in.

This condition cannot be used in the flexural design of beams not subjected to compression. In such members, a strain  $\epsilon_t$  in the extreme tensile reinforcement should not exceed 0.0075 in./in. for practical purposes.

### 12.3.2 Factored Flexural Resistance

The factored flexural resisting moment,

$$M_r = \phi M_n \quad (12.7)$$

where the resistance factor  $\phi = 1.0$ .

It is recommended in strain compatibility analysis that  $\phi$  be reduced from a value  $\phi = 1.0$  for net tensile strain of 0.005 in./in. to  $\phi = 0.7$  for net tensile strain of 0.002 in./in. in the extreme tension steel, namely,

$$0.7 \leq \phi = 0.65 + 0.25 \left[ \frac{1}{c/d_{ext}} - \frac{5}{3} \right] \leq 1.0 \quad (12.8)$$

where  $d_{ext}$  is  $d_t$  of the extreme layer of reinforcement, namely the one closest to the extreme tension fibers of the prestressed concrete section.

### 12.3.3 Flexural Design Parameters

The expression for computing the nominal moment strength of the prestressed sections by the LRFD method are similar to the standard AASHTO and ACI 318 strength design procedures given in Section 4.11 of Chapter 4. The ultimate design strength,  $f_{ps}$ , of the reinforcement can be computed either by strain-compatibility procedures such as in Example 4.19 or by an approximate method using the following expression:

$$f_{ps} = f_{pu} \left( 1 - k \frac{c}{d_p} \right) \quad (12.9a)$$

where,

$$k = 2 \left( 1.04 - \frac{f_{py}}{f_{pu}} \right) \quad (12.9b)$$

= 0.28 for low relaxation steel

For unbonded tendons,

$$f_{ps} = f_{pe} + 900 \left( \frac{d_p - c}{l_e} \right) \quad (12.9c)$$

where  $l_e = 2 l_i / (2 + N_s)$ .

$l_e$  = embedment length,  $l_i$  = tendon length between anchorages;  $N_s$  = number of tendons

In the Standard AASHTO specifications a first estimate of the average stress in the prestressing steel may be made from the following:

$$f_{ps} = f_{pu} \left( 1 - \frac{\gamma}{\beta_1} \rho \frac{f_{pu}}{f'_c} \right) \quad (12.9c)$$

The depth,  $c$ , of the neutral axis is obtained from the following expressions:

**(a) Doubly reinforced sections:**

$$c = \frac{A_{ps}f_{pu} + A_s f_y - A'_s f'_y}{0.85f'_c \beta_1 + kA_{ps} \frac{f_{pu}}{d_p}} \quad (12.10)$$

where  $f'_y$  = yield strength of the compression reinforcement

**(b) Flanged Sections:**

$$c = \frac{A_{ps}f_{pu} + A_s f_y - A'_s f'_s - 0.85f'_c \beta_1 (b - b_w) h_f}{0.85f'_c \beta_1 b_w + kA_{ps} \frac{f_{pu}}{d_p}} \quad (12.11)$$

where  $b_w$  = web width

$d_p$  = distance from the extreme compression fiber to the centroid of the prestressing tendons.

### 12.3.4 Reinforcement Limits

**(a) Maximum reinforcement limit**

The maximum amount of prestressed and non-prestressed reinforcement should be such that,

$$\frac{c}{d_e} \leq 0.42 \quad (12.12a)$$

$$\text{where } d_e = \frac{A_{ps}f_{ps}d_p + A_s f_y d_s}{A_{ps}f_{ps} + A_s f_y} \quad (12.12b)$$

**(b) Minimum reinforcement**

At any section, the amount of prestressed and non-prestressed reinforcement should be adequate to develop a factored flexural resistance,  $M_r$ , at least equal to the lesser of  $1.2 M_{cr}$  determined on the basis of elastic analysis or 1.33 times the factored moment required by the applicable strength load combinations.

$$M_{cr} = (f_r + f_{ce})S_b - M_{dnc} \left[ \frac{S_{bc}}{S_b} - 1 \right] \quad (12.13)$$

where,

$M_{dnc}$  = moment due to non-composite dead loads

$S_b$  = non-composite section modulus

$S_{bc}$  = composite section modulus

$f_r$  = modulus of rupture =  $7.5 \sqrt{f'_c}$  psi =  $0.24 \sqrt{f'_c}$  ksi

$f_{ce}$  = compressive stress in the concrete due to effective prestress *only*, after losses, at the extreme tensile fibers of the section where tensile stresses are caused by external loads.

## 12.4 SHEAR DESIGN CONSIDERATIONS

### 12.4.1 The Modified Compression Field Theory

The compression field theory for both shear and shear combined with torsion is discussed in Section 5.17.3 of Chapter 5. When torsion exists, it assumes that concrete carries no tension after cracking and the field of diagonal compressive struts carries the torsional shear. The inclination angle  $\theta$  of these struts varies depending on the longitudinal, transverse, and principal strains (Ref. 12.6) in the web such that:

$$\tan^2 \theta = \frac{\epsilon_x - \epsilon_2}{\epsilon_t - \epsilon_2} \quad (12.14)$$

where  $\epsilon_x$  = longitudinal strain of web, tension positive  
 $\epsilon_t$  = transverse strain, tension positive  
 $\epsilon_2$  = principal compressive strain, negative

Figure 12.8 shows the stress field in the web of a non-prestressed beam before and after cracking. Before the beam cracks, the shear is equally carried by the diagonal tensile and diagonal compressive stresses acting at a  $45^\circ$  angle (Figure 12.8a). After cracking, the diagonal cracks from the tensile stresses in the concrete are considerably reduced (Ref. 12.6, 12.7; also the shear and torsion equilibrium theory by Hsu in Ref. 12.8, 12.9).

In the compression field theory, the assumption is made that the principal tensile stress,  $f_1$ , equals zero as in Figure 12-8(b) after the concrete has cracked. The modified compression field theory takes into account the contribution of the tensile stresses in the concrete between the cracks as in Figure 12.8(c). From Mohr's stress circle in Figure 5.2(b), in Chapter 5, in conjunction with Figure 12.8(c), the following expression can be obtained:

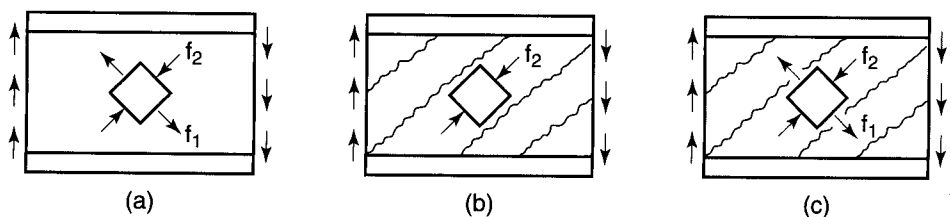
$$f_2 = (\tan\theta + \cot\theta)v - f_1 \quad (12.15a)$$

where the applied shear stress is:

$$v = \frac{V}{b_w j d} = \frac{(V_u - \theta V_p)}{\phi b_w d_v} \quad (12.15b)$$

$d_v = (d_p - a/2)$  and  $b_w$  = effective web width. The tension web reinforcement,  $A_v$ , required to balance the compressive stresses would have to be expressed as:

$$A_v f_v = (f_2 \sin^2 \theta - f_1 \cos^2 \theta) b_w s \quad (12.16)$$



**Figure 12.8** Stress fields in web of reinforced concrete beam (Ref. 12.6) (a) before cracking  $f_1 = f_2$ ,  $\theta = 45^\circ$ , (b) compression field theory,  $f_1 = 0$ , (c) modified compression field theory,  $f_1 \neq 0$ .

where  $A_v f_v$  is the vertical component of the balancing tensile force to close the diagonal crack inclined at angle  $\theta$  and  $f_v$  is the average stress in the vertical stirrups. Substituting for  $f_2$  in equation 12.15(a) into equation 12.16 gives:

$$V = f_1 b_w d_v \cot\theta + \frac{A_v f_v}{s} d_v \cot\theta \quad (12.17)$$

where  $V$  represents  $V_n$  and is equal to  $(V_c + V_s)$ ,  $V_s$  being the shear force taken by the vertical stirrups.

### 12.4.2 Design Expressions

As discussed in detail in Ref. 12.6, by making simplifying assumptions, the basic equations of the modified compression field theory can be rearranged so that the nominal shear resistance,  $V_n$ , in a prestressed beam can be evaluated, where:

$$V_n = V_c + V_s + V_p \quad (12.18)$$

where,  $V_c$  = nominal shear strength provided by the tensile stresses in the concrete

$V_s$  = nominal shear strength provided by the tensile stresses in the web reinforcement.

$V_p$  = nominal shear strength provided by the vertical component of the harped or draped longitudinal tendons.

**12.4.2.1 AASHTO Standard Specifications (LFD).** The AASHTO standard provisions, similar to the ACI-318 provision (Ref. 12.1–12.4) provide that  $V_c$  would be the smaller of the following two expressions presented and discussed in detail in Sections 5.5.1 and 5.5.2 of chapter 5:

**(a) Flexural shear:**

$$V_{ci} = 0.6\sqrt{f'_c} b_w d + \frac{V_i M_{cr}}{M_{\max}} \quad (12.19)$$

**(b) Web shear:**

$$V_{cw} = [3.5\sqrt{f'_c} + 0.3\bar{f}_c] b_w d + V_p \quad (12.20)$$

where, in AASHTO, the cracking moment is expressed as:

$$M_{cr} = S_i(6\sqrt{f'_c} + f_{pe} - f_d)$$

**12.4.2.2 LRFD Specifications.** The LRFD AASHTO provisions recognize two methods:

**(a)** Strut-and-tie model applicable to any section geometry with regular or discontinuity features

**(b)** Modified compression field model (Ref. 12.3, 12.6). This model is based on variable angle truss model in which the inclination of the diagonal compression field is allowed to vary. It differs from the LFD method where the angle  $\theta$  is always assumed as  $45^\circ$ , in that the plain concrete contribution,  $V_c$  is attributed to the tension carried across the compression diagonals as discussed in section 12.4.1.

The nominal resistance is taken as the lesser of:

$$V_n = V_c + V_s + V_p \quad (12.21)$$

or,

$$V_n = 0.25f'_c b_v d_v \quad (12.22)$$

where,  $b_v$  = effective web width

$d_v$  = effective shear depth  $\approx (d_p - a/2)$

$a$  = depth of the compressive block

This critical section for shear is located at distance  $d_v$  or  $(0.5d_v \cot \theta)$ , whichever is larger. The value of  $d_v$  is taken from midspan flexural capacity computations.

The nominal shear resistance of the plain concrete,  $V_c$ , in psi is:

$$V_c = \beta \sqrt{f'_c} b_v d_v \quad (12.23)$$

and in ksi,

$$V_c = 0.0316\beta \sqrt{f'_c} b_v d_v \quad (12.24)$$

The factor 0.0316 is  $1/\sqrt{1000}$ , which converts the expression from psi to ksi.

The contribution of the vertical web reinforcement is taken as:

$$V_s = \frac{A_v f_y d_v \cot \theta}{s} \quad (12.25)$$

except for slabs and footings.

Transverse shear reinforcement should always be provided when the factored shear,  $V_u$ , exceeds the plain concrete shear capacity, namely when

$$V_u > 0.5\phi(V_c + V_p) \quad (12.26)$$

The minimum area of transverse web shear reinforcement is

$$A_v \geq 0.036 \sqrt{f'_c} \frac{b_v s}{f_{yt}} \quad (12.27)$$

where  $b_v$  = width of web adjusted for presence of ducts (in.)

$f_{yt}$  = yield strength of transverse reinforcement (ksi)

$s$  = spacing of transverse reinforcement

where strength reduction factor  $\phi$  is taken from Table 12.1(a).

Additionally, when the beam reaction induces compression into the ends of the members as occurs in the majority of cases, the critical section for shear is taken as the larger of:  $0.5 d_v \cot \theta$  or  $d_v$ , measured from the face of the support.

In order to determine the nominal shear resistance of the prestressed member, the design engineer has to determine the values of  $\beta$  and  $\theta$  needed for computing  $V_c$  and  $V_s$  in equations 12.21 and 12.22. For non-prestressed concrete sections use  $\beta = 2.0$  and  $\theta = 45^\circ$ . For prestressed concrete sections, lower variable  $\beta$  values are to be used by trial and adjustment. AASHTO Table 12.8(a) gives values of  $\beta$  and  $\theta$  for values of  $\epsilon$  for sections containing *at least* minimum transverse reinforcement, and Table 12.8(b) containing *less* than the minimum.

#### 12.4.2.3 Longitudinal Strain $\epsilon_x$ in the Tension Reinforcement

1. If the section contains *at least* the minimum of transverse reinforcement, the initial value of longitudinal strain,  $\epsilon_x$ , should not be taken greater than 0.001 as in Equation 12.28(a) as follows:

$$\varepsilon_x = \frac{\left( \frac{M_u}{d_v} + 0.5 N_u + 0.5(V_u - V_p) \cot \theta - A_{ps} f_{po} \right)}{2(E_s A_s + E_p A_{ps})} \leq 0.001 \quad (12.28a)$$

2. If the section contains *less* than the minimum transverse reinforcement,

$$\varepsilon_x = \frac{\left( \frac{M_u}{d_v} + 0.5 N_u + 0.5(V_u - V_p) \cot \theta - A_{ps} f_{po} \right)}{E_s A_s + E_p A_{ps}} \leq 0.002 \quad (12.28b)$$

3. If the value of  $\varepsilon_x$  from Equations 12.28 (a) and (b) is *negative*, the longitudinal tensile strain is computed and applied to Table 12.8 from the following expression,

$$\varepsilon_x = \frac{\left( \frac{M_u}{d_v} + 0.5 N_u + 0.5(V_u - V_p) \cot \theta - A_{ps} f_{po} \right)}{2(E_c A_c + E_s A_s + E_p A_{ps})} \quad (12.28c)$$

where  $A_c$  = area of concrete on the flexural tension side of the member as shown in Figure 12.9 (in.<sup>2</sup>)

$A_{ps}$  = area of the prestressing steel on the flexural tension side of the member as in Figure 12.9 (in.<sup>2</sup>)

$A_s$  = area of non-prestressed steel on the flexural tension side of the member at the section under consideration shown in Figure 12.9 (in.<sup>2</sup>). In computing  $A_s$  in Equations 12.28 (a), (b), and (c), bars which are terminated at a distance less than their development length from the section under consideration have to be ignored.

$E_c$  = modulus of concrete (ksi)

$E_s$  = modulus of mild steel reinforcement (ksi)

$E_p$  = modulus of prestressing steel reinforcement (ksi)

$f_{po}$  = stress value primarily at jacking but taken as the modulus of elasticity of the prestressing tendon multiplied by the locked in difference in strain between the prestressing tendons and the surrounding concrete (ksi). It can be computed from the expression in Equation 12.29 below or a conservative average value of  $f_{po} = 0.70 f_{pu}$  is used.

$N_u$  = factored axial force, taken as positive if tensile and negative if compressive (kip)

$M_u$  = factored moment, taken as positive quantity (in.-kip), but not to be taken less than  $(V_u d_v)$ , namely,  $\left( \frac{V_u d_v}{M_u} \right) \leq 1.0$

$V_p$  = vertical component of harped or draped prestressing tendon (kip)

$V_u$  = factored shear forces, taken as positive quantity (kip)

The flexural tensile side of the member is taken as the half-depth containing the flexural tension zone as illustrated in Figure 12.9. The value of the stress  $f_{po}$  can be computed from the following expression as indicated in its definition previously stated and is applicable for both pretensioned and post-tensioned steel reinforcement:

$$f_{po} = f_{pe} + \frac{\bar{f}_{ce} E_p}{E_c} \quad (12.29)$$



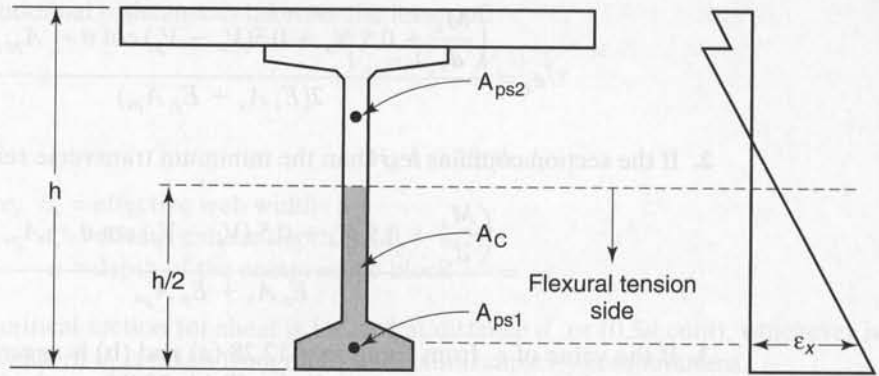


Figure 12.9 Strain distribution in prestressed flanged section

where  $\bar{f}_{ce}$  = concrete compressive stress at the centroid of the composite section resisting live load or at the junction of the web and the flange if it lies within the flange due to both prestress and the bending moment resisted by the precast section acting alone, namely prior to composite action (ksi)

$f_{pe}$  = effective stress in the prestressing steel reinforcement after all losses

The longitudinal reinforcement should be so proportioned that each beam section has to satisfy the following expression:

$$A_s f_s + A_{ps} f_{ps} \geq \frac{M_u}{d_v \phi_f} + 0.5 \frac{N_u}{\phi_c} + \left( \frac{V_u}{\phi_v} + 0.5 V_s + V_p \right) \cot \theta \quad (12.30)$$

where  $\phi_f$  = flexure  $\phi$  factor,  $\phi_c$  = compression  $\phi$  factor,  $\phi_v$  = shear  $\phi$  factor.

From the foregoing AASHTO expressions, the variable  $\beta$  is an essential determinant for evaluating the nominal shear resistance  $V_c$ , as in Equation 12.21. A plot of the values in Table 12.8, which is based on the compression field theory seems to indicate that the tabulated values are insensitive for ratios ( $v/f'_c$ ) in excess of 0.125 when the strain is less than 0.005 in./in. Hsu's discussion in Ref. 12.21 points to this difficulty, partly arising from assigning a numerical value to the crack shear stress,  $v_{ci}$ , namely, the ability of the crack interface to transmit a shear stress value dependant on the crack width,  $w$ , in the following expression:

$$v_{ci} \leq \frac{2.16 \sqrt{f'_c}}{0.3 + \frac{24w}{a + 0.63}} \text{ psi, } w(\text{in.}) \quad v_{ci} \leq \frac{0.18 \sqrt{f'_c}}{0.3 + \frac{24w}{a + 16}} \text{ MPa, } w(\text{mm})$$

Hsu's work (Ref. 12.21, 12.22) proposes using  $v_{ci} = 0$  in order to maintain equilibrium and compatibility. Also, the crack angle  $\theta$  in the  $V_s$  term of Equation 12.25 is the angle between the longitudinal steel and the principal compression stress (strain) of concrete. As such, the shear stress along the principal axis is zero. This discussion also applies to the LRFD provision for the case of combined shear and torsion. Future AASHTO modifications might become necessary in order to rectify the discrepancy.

**Table 12.8(a)** Values of  $\theta$  and  $\beta$  for Sections Containing at Least Minimum Transverse Reinforcement

$\frac{V}{f'_c}$	$\epsilon_x \times 1,000$								
	$\leq -0.20$	$\leq -0.10$	$\leq -0.05$	$\leq 0$	$\leq 0.125$	$\leq 0.25$	$\leq 0.50$	$\leq 0.75$	$\leq 1.00$
$\leq 0.075$	22.3 6.32	20.4 4.75	21.0 4.10	21.8 3.75	24.3 3.24	26.6 2.94	30.5 2.59	33.7 2.38	36.4 2.23
$\leq 0.100$	18.1 3.79	20.4 3.38	21.4 3.24	22.5 3.14	24.9 2.91	27.1 2.75	30.8 2.50	34.0 2.32	36.7 2.18
$\leq 0.125$	19.9 3.18	21.9 2.99	22.8 2.94	23.7 2.87	25.9 2.74	27.9 2.62	31.4 2.42	34.4 2.26	37.0 2.13
$\leq 0.150$	21.6 2.88	23.3 2.79	24.2 2.78	25.0 2.72	26.9 2.60	28.8 2.52	32.1 2.36	34.9 2.21	37.3 2.08
$\leq 0.175$	23.2 2.73	24.7 2.66	25.5 2.65	26.2 2.60	28.0 2.52	29.7 2.44	32.7 2.28	35.2 2.14	36.8 1.96
$\leq 0.200$	24.7 2.63	26.1 2.59	26.7 2.52	27.4 2.51	29.0 2.43	30.6 2.37	32.8 2.14	34.5 1.94	36.1 1.79
$\leq 0.225$	26.1 2.53	27.3 2.45	27.9 2.42	28.5 2.40	30.0 2.34	30.8 2.14	32.3 1.86	34.0 1.73	35.7 1.64
$\leq 0.250$	27.5 2.39	28.6 2.39	29.1 2.33	29.7 2.33	30.6 2.12	31.3 1.93	32.8 1.70	34.3 1.58	35.8 1.50

**Table 12.8(b)** Values of  $\theta$  and  $\beta$  for Sections Containing Less than Minimum Transverse Reinforcement

$s_{xe}^*$ (in.)	$\epsilon_x \times 1,000$										
	$\leq -0.20$	$\leq -0.10$	$\leq -0.05$	$\leq 0$	$\leq 0.125$	$\leq 0.25$	$\leq 0.50$	$\leq 0.75$	$\leq 1.00$	$\leq 1.50$	$\leq 2.00$
$\leq 5$	25.4 6.36	25.5 6.06	25.9 5.56	26.4 5.15	27.7 4.41	28.9 3.91	30.9 3.26	32.4 2.86	33.7 2.58	35.6 2.21	37.2 1.96
$\leq 10$	27.6 5.78	27.6 5.78	28.3 5.38	29.3 4.89	31.6 4.05	33.5 3.52	36.3 2.88	38.4 2.50	40.1 2.23	42.7 1.88	44.7 1.65
$\leq 15$	29.5 5.34	29.5 5.34	29.7 5.27	31.1 4.73	34.1 3.82	36.5 3.28	39.9 2.64	42.4 2.26	44.4 2.01	47.4 1.68	49.7 1.46
$\leq 20$	31.2 4.99	31.2 4.99	31.2 4.99	32.3 4.61	36.0 3.65	38.8 3.09	42.7 2.46	45.5 2.09	47.6 1.85	50.9 1.52	53.4 1.31
$\leq 30$	34.1 4.46	34.1 4.46	34.1 4.46	34.2 4.43	38.9 3.39	42.3 2.82	46.9 2.19	50.1 1.84	52.6 1.60	56.3 1.30	59.0 1.10
$\leq 40$	36.6 4.06	36.6 4.06	36.6 4.06	36.6 4.06	42.1 3.20	45.0 2.62	50.2 2.00	53.7 1.66	56.3 1.43	60.2 1.14	63.0 0.95
$\leq 60$	40.8 3.50	40.8 3.50	40.8 3.50	40.8 3.50	44.5 2.92	49.2 2.32	55.1 1.72	58.9 1.40	61.8 1.18	65.8 0.92	68.6 0.75
$\leq 80$	44.3 3.10	44.3 3.10	44.3 3.10	44.3 3.10	47.1 2.71	52.3 2.11	58.7 1.52	62.8 1.21	65.7 1.01	69.7 0.76	72.4 0.62

\* $s_{xe} = s_x [1.38/(a_g + 0.63)] \leq 80$  in. where  $a_g = \text{max. aggregate size (in.)}$  and  $s_x = \text{the lesser of either } d_v \text{, or the maximum distance between layers of longitudinal crack control reinforcement, where the area of the reinforcement in each layer is not less than } 0.003 b, s_x$  [Ref. AASHTO LRFD Bridge Design Specifications, 2004].

**12.4.2.4 Maximum Spacing of Web Transverse Reinforcement.** The maximum allowable spacing of transverse reinforcement is as follows:

- (a) If  $v_u < 0.125 f'_c$ ,  $s = 0.8 d_v \leq 24$  in.  
 (b) If  $v_u > 0.125 f'_c$ ,  $s = 0.4 d_v \leq 12$  in.

Note that the design yield strength of non-prestressed transverse reinforcement should not exceed 60.0 ksi. The design yield strength of prestressed transverse reinforcement should be taken as the effective prestress after allowing for all prestress losses plus 60.0 ksi, but not greater than  $f_{py}$ .

## 12.5 HORIZONTAL INTERFACE SHEAR

The principle of horizontal interface shear both at service and ultimate load levels are fully discussed in Chapter 5 Section 5.7, including illustrative examples in accordance with ACI 318 and PCI requirements. AASHTO Standard specifications requirements for the nominal horizontal shear strength,  $V_{nh}$ , are similar to those of ACI when no dowel reinforcement is used, namely, the maximum allowable stress is 80 psi. They differ when minimum dowel reinforcement is used in that the maximum allowable horizontal shear stress is 350 psi instead of the 500 psi allowed by the ACI.

Extensive investigations and tests by the author (Ref. 12.13) have shown that these are indeed very low allowable stresses. These tests demonstrate that even in early strength under sub-freezing temperature conditions, it is possible to obtain a strength at ultimate load in excess of 1200 psi (8.3 MPa) using vertical dowel reinforcement.

The standard AASHTO requirements are as follows (Ref. 12.2):

- (a) When no vertical ties are provided:

$$V_{nh} = 80b_v d \quad (12.31a)$$

- (b) When minimum vertical ties are provided:

$$V_{nh} = 500b_v d \quad (12.31b)$$

- (c) Required area of ties,  $A_{vh}$ , exceeds the minimum area:

$$V_{nh} = 500b_v d + 0.40A_{vh}f_y \frac{d_p}{s} \quad (12.31c)$$

where, factored vertical shear  $V_u = \phi V_{nh}$

$V_{nh}$  = nominal horizontal shear strength

$\phi = 0.90$

minimum  $A_{vh} = 50b_v s / f_y$

$b_v$  = width of cross-section at the contact surface being analyzed for horizontal shear

$b_p$  = distance from extreme compression fibers to centroid of prestressing steel, but not to be taken less than  $0.80h$

$s$  = maximum spacing of the dowels, but not to exceed four times the least-web width of the support element, nor 24 in.

The LRFD specifications do not give guidance for computing the horizontal shear  $V_{nh}$ . The following expression can be used:

$$v_{uh} = \frac{V_u}{b_v d_v} \quad (12.31d)$$

where

- $v_{nh}$  = horizontal factored shear stress
- $V_u$  = factored vertical shear
- $d_v$  = distance between resultants of tensile and compressive forces  
=  $(d - a/2)$
- $b_v$  = interface width

LRFD specifies that the nominal shear resistance of the interface surface,  $V_n$ , be computed using the following expression:

$$V_n = cA_{cv} + \mu[A_v f_y + P_c] \quad (12.32)$$

and that

$$v_{uh} A_{cv} \leq \phi V_n \quad (12.33)$$

where

- $c$  = cohesion factor
- $\mu$  = friction factor
- $A_{cv}$  = interface area of concrete engaged in shear transfer
- $A_{vf}$  = area of shear reinforcement crossing the shear plane within area  $A_c$
- $P_c$  = permanent net compressive force normal to the shear plane (may be conservatively neglected)
- $f_y = f_{yt}$  = yield strength of dowel reinforcement.

Typically, the top surface of the precast element is intentionally roughened to an amplitude of  $\frac{1}{4}$  in. as discussed in section 5.7. Hence, for normal weight concrete, LRFD recommends simplifying equations 12.32 and 12.33 as follows with units in ksi:

$$v_{uh} \leq \phi \left( 0.1 + \frac{A_{vf}}{A_{cv}} \right) \quad (12.34)$$

where the minimum

$$A_{vf} = \frac{(0.05b_v s)}{f_{yt}} \quad (12.35)$$

and the nominal shear resistance is to be taken as the lesser of

$$V_n \leq 0.20 f'_c A_{cv} \quad (12.36a)$$

or

$$V_n = 0.80 A_{cv} \quad (12.36b)$$

The cohesion factor  $c$  and the friction factor  $\mu$  in equation 12.32 have the following values for the particular conditions of the interacting surfaces:

**(a)** Monolithically placed concrete:

$$c = 145 \text{ psi} \quad \mu = 1.4 \lambda$$

**(b)** Concrete placed against clean, hardened concrete with surface intentionally roughened

$$c = 100 \text{ psi} \quad \mu = 1.0 \lambda$$

**(c)** Concrete placed against hardened concrete clean and free of laitance but not intentionally roughened

$$c = 75 \text{ psi} \quad \mu = 0.6 \lambda$$

- (d) Concrete anchored to as-rolled structural steel by headed studs or by reinforcing bars, where all steel in contact with the concrete is clean and free of paint

$$c = 25 \text{ psi} \quad \mu = 0.7 \lambda$$

where  $\lambda = 1.0$  for normal-density concrete  
 $= 0.85$  for sand-low-density concrete  
 $= 0.75$  all other low-density concrete.

While the LRFD AASHTO specifications require that minimum reinforcement is to be provided regardless of the stress level at the interface, designers may choose to limit this reinforcement to cases in which  $V_{uh}/\phi$  is greater than 100 psi (0.7 MPa). Doing so would be consistent with the ACI 318 code and the standard AASHTO specifications.

### 12.5.1 Maximum Spacing of Dowel Reinforcement

The maximum allowable spacing of the dowels is:

- (i) If  $V_u < 0.1 f'_c b_v d_v$ , maximum  $s \leq 0.8 d_v \leq 24$  in.  
(ii) If  $V_u > 0.1 f'_c b_v d_v$ , maximum  $s \leq 0.4 d_v \leq 12$  in.

## 12.6 COMBINED SHEAR AND TORSION

The discussion in Section 12.4.1 on the modified compression field theory in conjunction with Section 5.17.3 give an ample treatment of the strains, shear forces and the resisting diagonal compression struts. Figures 5.38, 5.39 and 5.40 illustrate the deformed shape of the critical section when subjected to torsional moments. The shear stresses due to torsion and shear are assumed in this hypothesis to add on one side of the section and counteract on the opposite side. The transverse closed tie reinforcement is designed for the side in which the combined shear and torsional effects are additive.

The external loading which causes the highest torsional moment is not the same as the loading that causes the highest shear at the critical section. The tendency by the designer is to combine the highest value of torsion and the highest value of shear in the design of the web reinforcement. This is, naturally, conservative. It is possible to utilize the fact that the two loads are different and thus design the transverse reinforcement for the highest torsion and its concurrent shear or the highest shear and its concurrent torsion, whichever leads to a higher resistance capacity. The LRFD uses the same nominal torsional resisting moment as the ACI:

$$T_n = \frac{2A_o A_t f_y \cot \theta}{s} \quad (12.37)$$

where

- $A_o$  = cross-section area enclosed by the shear flow path, including area of holes  
 $A_t$  = area of one leg of the enclosed transverse tension reinforcement  
 $\theta$  = variable angle of crack chosen by trial and adjustment using Table 12.8 (Ref. 12.3)

In order to determine the value of  $\theta$ , the strain,  $\epsilon_x$ , in the tensile reinforcement is obtained from equation 12.27, except that  $V_u$  should be replaced

$$V_u = \sqrt{V_u^2 + \left(\frac{P_h T_u}{2A_o}\right)^2} \quad (12.38)$$

The factored torsional moment is taken as  $T_u = \phi T_n$  and the factored shear force is taken as  $V_u = \phi V_n$ . For normal weight concrete elements where torsion exists, torsional effects have to be investigated if

$$T_u > 0.25 \phi T_{cr} \quad (12.39)$$

$$T_{cr} = 0.125 \sqrt{f'_c} \frac{A_{cp}}{p_{cp}} \sqrt{1 + \frac{f_{pe}}{0.125 \sqrt{f'_c}}} \quad (12.40)$$

where

$T_u$  = factored torsional moment (in.-kip)

$T_{cr}$  = torsional cracking moment (in.-kip)

$A_{cp}$  = total area enclosed by outside perimeter of concrete section (in.<sup>2</sup>)

$p_{cp}$  = length of outside perimeter of concrete section (in.)

$\bar{f}_{pe}$  = compressive stress in the concrete after prestress losses have occurred, either at the centroid of the cross-section resisting transient loads or at the junction of the web and flange where the centroid lies in flange (ksi)

$\phi$  = strength resistance factor:

flexure:  $\phi_f$

shear:  $\phi_v$

compression:  $\phi_c$

For lightweight concrete where the average tensile splitting strength of lightweight concrete,  $f_{cr}$ , is specified, the term  $\sqrt{f'_c}$  in Equation 12.40 is replaced by

$$4.7 f_{cr} \leq f'_c$$

If  $f_{cr}$  is not specified, the term  $0.75 \sqrt{f'_c}$  for all lightweight concrete and  $0.85 \sqrt{f'_c}$  for sand-lightweight concrete should be substituted for the term  $\sqrt{f'_c}$  in Equation 12.40.

The required amount of transverse reinforcement for shear is obtained from equations 12.21(a) in conjunction with equations 12.23(a) and 12.25, namely,

$$V_n = \beta \sqrt{f'_c} b_v d_v + \frac{A_w f_y d_v \cot \theta}{s} + V_p \quad (12.41)$$

so that for shear in lb units and stress in psi,

$$\frac{A_w}{s} = \frac{V_n - (\beta \sqrt{f'_c} b_v d_v + V_p)}{f_y d_v \cot \theta} \quad (12.42a)$$

If ksi units are used, multiply  $\beta$  by 0.0316 and for torsion, from equation 12.31,

$$\frac{A_t}{s} = \frac{T_n}{2A_0 f_{yt} \cot \theta} \quad (12.42b)$$

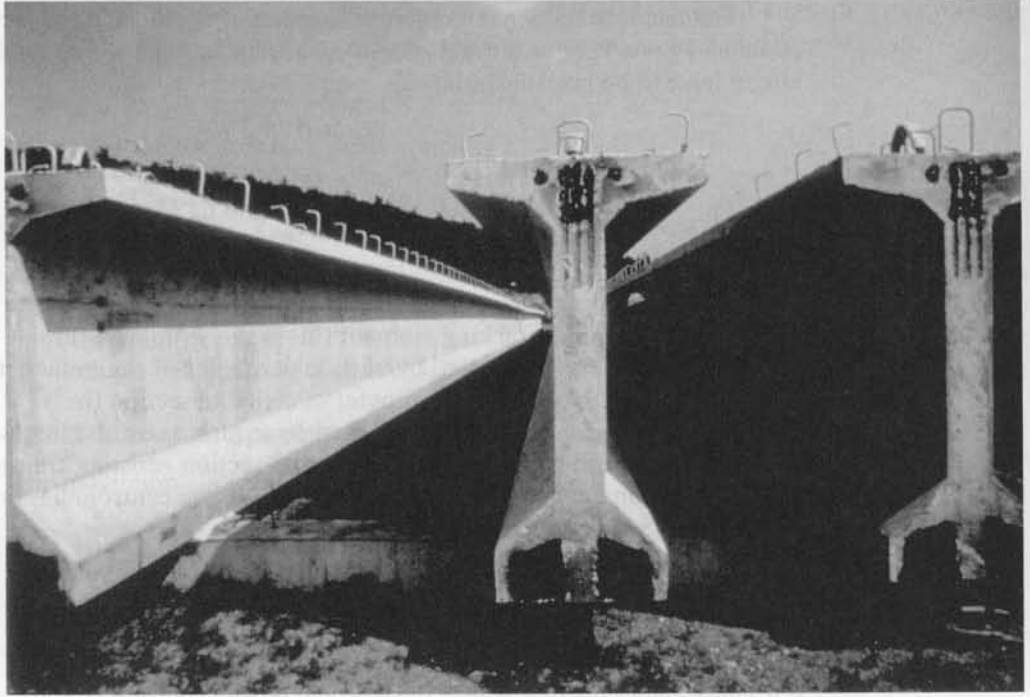
The total area of web reinforcement would be:

$$\frac{A_{vt}}{s} = \frac{A_w}{s} + 2 \frac{A_t}{s} \quad (12.42c)$$

The angle  $\theta$  is obtained from Tables 12.8(a) and 12.8(b) using shear,  $v$ , as follows:

(a) Box sections:

$$v_n = \frac{V_u - \phi V_p}{\phi_v b_v d_v} + \frac{T_u p_h}{\phi_v A_{oh}^2} \quad (12.43a)$$



**Photo 12.2** PCI bulb tee precast prestressed bridge deck beams (Courtesy Ms. Monica Schultese, Mid Atlantic Precast Concrete Association).

**(b) Other Sections:**

$$v_n = \sqrt{\left(\frac{V_u - \phi V_p}{\phi_v b_v d_v}\right)^2 + \left(\frac{T_u P_h}{\phi_v A_{oh}^2}\right)^2} \quad (12.43b)$$

where

$p_h$  = perimeter of the center line of the enclosed transverse torsion reinforcement

$A_{oh}$  = area enclosed by the center line of the outermost closed torsional reinforcement

$A_o$  = gross area enclosed by the shear flow path (see Figure 5.45 for graphical representation of  $A_o$  and  $A_{oh}$  where  $A_o \approx 0.85A_{oh}$ )

$T_u$  = factored torsional moment

$\phi$  = resistance factor  $\phi_f$ ,  $\phi_c$ ,  $\phi_v$  where applicable

The value of  $\beta$  in equation 12.41 for determining the shear capacity,  $V_c$ , of the plain concrete in the web is obtained from the chart in Table 12.8(a). In order to avoid yielding of the longitudinal reinforcement, a check has to be made that the flexural reinforcement on the tension face side of the member is so proportioned as to satisfy the following condition:

$$(A_s f_y + A_{ps} f_{ps}) \geq \frac{M_u}{d_v \phi_f} + \frac{0.5 N_u}{\phi_c} + \cot \theta \sqrt{\left(\frac{V_u}{\phi_v} - 0.5 V_s - V_p\right)^2 + \left(\frac{0.45 T_u P_o}{2 A_o \phi_v}\right)^2} \quad (12.44)$$

where  $p_0$  = Perimeter of the shear flow path  
 $N_u$  = Applied axial force, taken as positive if compressive

## 12.7 AASHTO-LRFD FLEXURAL-STRENGTH DESIGN SPECIFICATIONS VS. ACI CODE PROVISIONS

There are fundamental differences in the approaches of the AASHTO-LRFD flexural-strength design specifications and the ACI-318 code provisions. The LRFD approach is based on strain limit values as discussed in Section 12.3 and controlled by the ratio of the neutral axis depth,  $c$ , to the effective depth,  $d_e$  (Ref. 12.14–12.16). This approach is variably termed as a unified approach since it is applicable to reinforced, prestressed, and partially prestressed concrete ultimate limit state design. The ACI-318 code strength provisions have been applied for determining the ultimate design strength  $f_{ps}$  in several examples in other sections of the book such as sections 4.9 and 4.10. They have to be applied in the design of fully and partially prestressed concrete members in building structures. The current AASHTO standard specifications (Ref. 12.2) for proportioning prestressed concrete members in flexure generally follow the ACI code provisions. The LRFD alternative, which is a rational design approach, requires applying the strain limits unified procedure. It is useful to give a comparison summary showing the differences between the expressions specified in these two approaches as shown in Table 12.9 adapted from Ref. 12.15.



**Photo 12.3** Segmental bridge launching, (Courtesy Monica Schultese, MidAtlantic Precast Concrete Association)



**Table 12.9** LRFD and ACI Provisions for Ultimate Strength Flexural Design

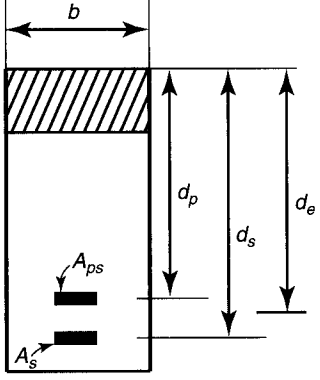
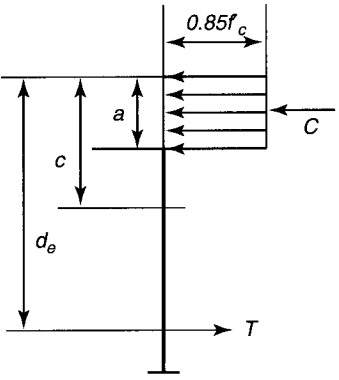
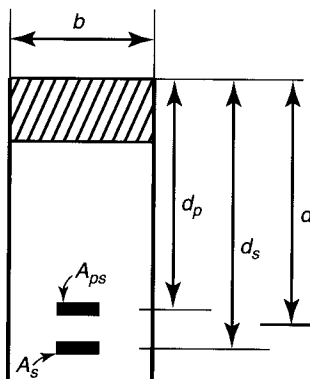
ACI Code	AASHTO-LRFD
<b>Notation</b>	
<p><math>d</math> to nonprestressed reinforcement</p> <p><math>d_p</math> to prestressed reinforcement</p> <p><math>d'</math> to compression steel</p> $\rho_p, \rho, \rho' \dots \rho = \frac{A_s}{bd}$ $\omega = \rho \frac{f_y}{f'_c} = \frac{A_s f_y}{b d f'_c}$ $\omega_p = \rho_p \frac{f_{ps}}{f'_c} = \frac{A_{ps} f_{ps}}{b d_p f'_c}$ $\omega_p + \frac{d}{d_p} (\omega - \omega')$	<p><math>d_s</math> to nonprestressed reinforcement</p> $d_e = \frac{A_{ps} f_{ps} d_p + A_s f_y d_s}{A_{ps} f_{ps} + A_s f_y}$ 
<b>Maximum Flexural Reinforcement</b>	
<p>Reinforced Concrete and Prestressed Concrete</p> <p>Maximum redistribution factor = <math>1000 \epsilon_t</math> percent, where <math>\epsilon_t = 0.003 \left( \frac{d_t}{c} - 1 \right)</math>.</p> <p>provided:</p> $\omega_p + \frac{d}{d_p} (\omega - \omega') \leq 0.24 \beta_1$ <p>for rectangular sections and:</p> $\omega_{pw} + \frac{d}{d_p} (\omega_w - \omega_w') < 0.24 \beta_1$ <p>for T-section behavior</p> <p>An alternative ACI Code check requires that <math>c/d_t</math> for the section is either tension controlled or in the transition zone of Fig. 4.45</p>	<p>All Cases - RC, PC, PPC Rectangular or T Section:</p> $20 \left( 1 - 2.36 \frac{c}{d_e} \right) \text{ in \%}$ <p>provided:</p> $\frac{c}{d_e} \leq 0.28 \text{ but never to exceed } 0.42$ <p>and <math>\phi</math> is based on Fig. 12.7.</p> 

Table 12.9 Continued

ACI Code	AASHTO-LRFD
<b>Minimum Reinforcement</b>	
Reinforced Concrete $\rho \geq \rho_{\min} \geq \frac{200}{f_y} \geq \frac{3.5\sqrt{f'_c}}{f_y}$ (For T-sections, $\rho$ is based on web only)	All Cases: $\phi M_n \geq 1.2 M_{cr}$ $\phi M_n \geq 1.33 M_u$
Prestressed and Partially Prestressed Concrete: $\phi P_n \geq 1.2 P_{cr}$	Particular result for reinforced concrete: $\rho \geq \rho_{\min} = \frac{0.03f'_c}{f_y}$ (For T-sections, $\rho$ is based on web only)
<b>Stress in Bonded Prestressing Steel at Ultimate Resistance in Bending</b>	
Prestressed and Partially Prestressed Concrete-Bonded Tendons $f_{ps} = f_{pu} \left[ 1 - \frac{\gamma_p}{\beta_1} \left\{ \rho_p \frac{f_{pu}}{f'_c} + \frac{d}{d_p} (\omega - \omega') \right\} \right]$ where: $\left[ \rho_p \frac{f_{pu}}{f'_c} + \frac{d}{d_p} (\omega - \omega') \right] \geq 0.17$ $d' < 0.15 d_p$ $\gamma_p = 0.28 \text{ for } f_{py} \geq 0.90 f_{pu} \text{ (Low Lax)}$ $0.40 \text{ for } f_{py} \geq 0.85 f_{pu} \text{ [normal]}$ $0.55 \text{ for } f_{py} \geq 0.80 f_{pu} \text{ (bars)}$ $\beta_1 = 0.85 \text{ for } f'_c \leq 4 \text{ ksi}$ $0.65 \text{ for } f'_c \geq 8 \text{ ksi}$ $0.85 - 0.05 (f'_c - 4) \text{ for } 4 \leq f'_c \leq 8 \text{ ksi}$	PC and PPC Bonded Tendons: $f_{ps} = f_{pu} \left( 1 - k \frac{c}{d_p} \right)$ $k = 2 \left( 1.04 - \frac{f_{py}}{f_{pu}} \right)$ 

## 12.8 STEP-BY-STEP DESIGN PROCEDURE (LRFD)

The following is a summary of a recommended sequence of design steps:

1. Determine whether or not partial prestressing is to be chosen.
2. Select the bending moments and shear forces from Table 12.2(a)&(b), Section 12.7.
3. Follow the step sequence for flexural design of the member outlined in steps 2 through 10 of Section 4.13 in Chapter 4 and the flowchart of Figure 12.10 when using the LRFD method for flexure. Generally,  $d_v = (d_e - a/2)$ .

4. Determine the factored shear force  $V_u$  due to all applied loads at the critical section located at a distance  $d_v$  or  $0.5 d_v \cot\theta$  from the face of the support, whichever is larger, where

$$\begin{aligned} d_e &= \text{effective depth as shown in Table 12.8(a) and (b)} \\ &= d_p \text{ if no mild steel is used.} \end{aligned}$$

5. Compute the tendon shear component  $V_p$ . The factored shear stress is:

$$v = \frac{V_u - \phi V_p}{\phi b_v d_v}$$

The nominal available shear stress  $v_c = v/h$ .

6. Compute the quantity  $v/f'_c$  and assume a value of  $\theta$ . A good initial assumption for prestressed beams is  $\theta = 25^\circ$
7. Compute the strain in the tensile reinforcement in order to enter Table 12.8 to obtain a trial value of  $\theta$  and  $\beta$  from Equations 12.28 (a), (b) or (c) that applies, namely,

Section contains *at least* the minimum transverse reinforcement:

$$\epsilon_x = \frac{\left( \frac{M_u}{d_v} + 0.5 N_u + 0.5(V_u - V_p) \cot\theta - A_{ps} f_{po} \right)}{2(E_s A_s + E_p A_{ps})} \leq 0.001$$

Section contains *less* than the minimum transverse reinforcement:

$$\epsilon_x = \frac{\left( \frac{M_u}{d_v} + 0.5 N_u + 0.5(V_u - V_p) \cot\theta - A_{ps} f_{po} \right)}{E_s A_s + E_p A_{ps}} \leq 0.002$$

If the value of  $\epsilon_x$  from Equations 12.28 (a) and (b) is *negative*, compute the longitudinal tensile strain from the following expression and enter it in Table 12.8(a) or Table 12.8(b) where applicable.

$$\epsilon_x = \frac{\left( \frac{M_u}{d_v} + 0.5 N_u + 0.5(V_u - V_p) \cot\theta - A_{ps} f_{po} \right)}{2(E_c A_c + E_s A_s + E_p A_{ps})}$$

$A_c$  = area of the concrete in the flexural tension side of the member.

8. Enter LRFD Figure 12.9 again, with the value of  $v/f'_c$  and strain  $\epsilon_x$  if the strut angle  $\theta$  is not close to the one assumed in the first trial, in order to obtain an adjusted value of  $\beta$ . Otherwise, compute  $V_c$  from Equation 12.23, namely  $V_c = \beta \sqrt{f'_c} b_v d_d$  (lb) or  $V_c = 0.0316\beta \sqrt{f'_c} b_v d_v$  (kip) using the  $\beta$  value obtained from the chart in Table 12.8(a). If Table 12.8(b) applies, enter the value of  $s_{xe}$  and  $\epsilon_x$  to determine the trial  $\theta$  and  $\beta$  values.
9. Compute  $V_s$  for the web reinforcement after the value of  $V_c$  has been determined. Find the corresponding shear reinforcement spacing from:

$$A_v = 0.036 \sqrt{f'_c} \frac{b_v s}{f_{yt}}$$

10. In regions of high shear stresses, ensure that the amount and development of the longitudinal reinforcement  $A_s$  and  $A_{ps}$  should satisfy the following expression:

$$A_s f_y + A_{ps} f_{ps} \geq \left[ \frac{M_u}{d_v \phi} + 0.5 \frac{N_u}{\phi} + \left( \frac{V_u}{\phi} - 0.5 V_s - V_p \right) \cot \theta \right]$$

It is recommended that this check be made at the face of the bearing which lies within the transfer length of the strands where the effective prestressing force is not fully developed.

11. When torsion exists combined with shear and flexure, the following steps need to be followed:

$$\text{nominal torsion } T_n = \frac{2A_0 A_t f_y \cot \theta}{s}$$

Obtain strain in tensile reinforcement from Equations 12.28 adjusted for torsion from Equation 12.38.

where  $f_{po} = 0.70 f_{pu}$

**Nominal shear resistance:**

$$V_n = V_c + V_s + V_p = \beta \sqrt{f'_c} b_v d_v + \frac{A_v f_y d_v \cot \theta}{s} + V_p$$

where  $d_v = (d_p - a/2)$

**Shear reinforcement:**

$$\frac{A_v}{s} = \frac{V_n - 0.0316 \beta \sqrt{f'_c} b_v d_v + V_p}{f_y d_v \cot \theta}$$

Forces are in kips and the stresses in ksi. For using lb and psi units, remove factor 0.0316.

**Torsion reinforcement:**

$$\frac{A_t}{s} = \frac{T_n}{2A_0 f_y \cot \theta}$$

**Total web closed ties reinforcement:**

$$\frac{A_{vt}}{s} = \frac{A_v}{s} + 2 \frac{A_t}{s}$$

Shear stress  $v$  for obtaining angle  $\theta$ :

(a) Box sections:

$$v = \frac{V_u - \phi V_p}{\phi_v b_v d_v} + \frac{TP_h}{\phi_v A_o h^2}$$

(b) Other sections

$$v = \sqrt{\left(\frac{V_u - \phi V_p}{\phi_v b_v d_v}\right)^2 + \left(\frac{TP_h}{\phi_v A_o h^2}\right)^2}$$

For avoiding yield of the longitudinal tensile reinforcement:

$$(A_s f_s + A_{ps} f_{ps}) \geq \frac{M_u}{d_v \phi_f} + \frac{0.5 N_u}{\phi_c} + \cot \theta \sqrt{(V_n - 0.5 V_s - V_p)^2 + \left(\frac{0.45 T_u P_h}{2 A_o \phi_v}\right)^2}$$

12. Check the horizontal interface shear:

$$v_n A_{cv} \leq \phi V_n$$

where

$$V_n = c A_{cv} + \mu (A_{vf} f_y)$$

$$v_{uh} \leq \phi \left(0.1 + \frac{A_{vf}}{A_{cv}}\right)$$

where

$$A_{vf} = \frac{0.05 b_v s}{f_{yt}}$$

( $f_y$  is in ksi)

Take the nominal shear resistance as the lesser of

$$V_n \leq 0.20 f'_c A_{cv}$$

or

$$V_n \leq 0.80 A_{cv}$$

$c$  = cohesion factor

$\mu$  = friction factor

$A_{cr}$  = concrete interface area =  $b_v l_v$

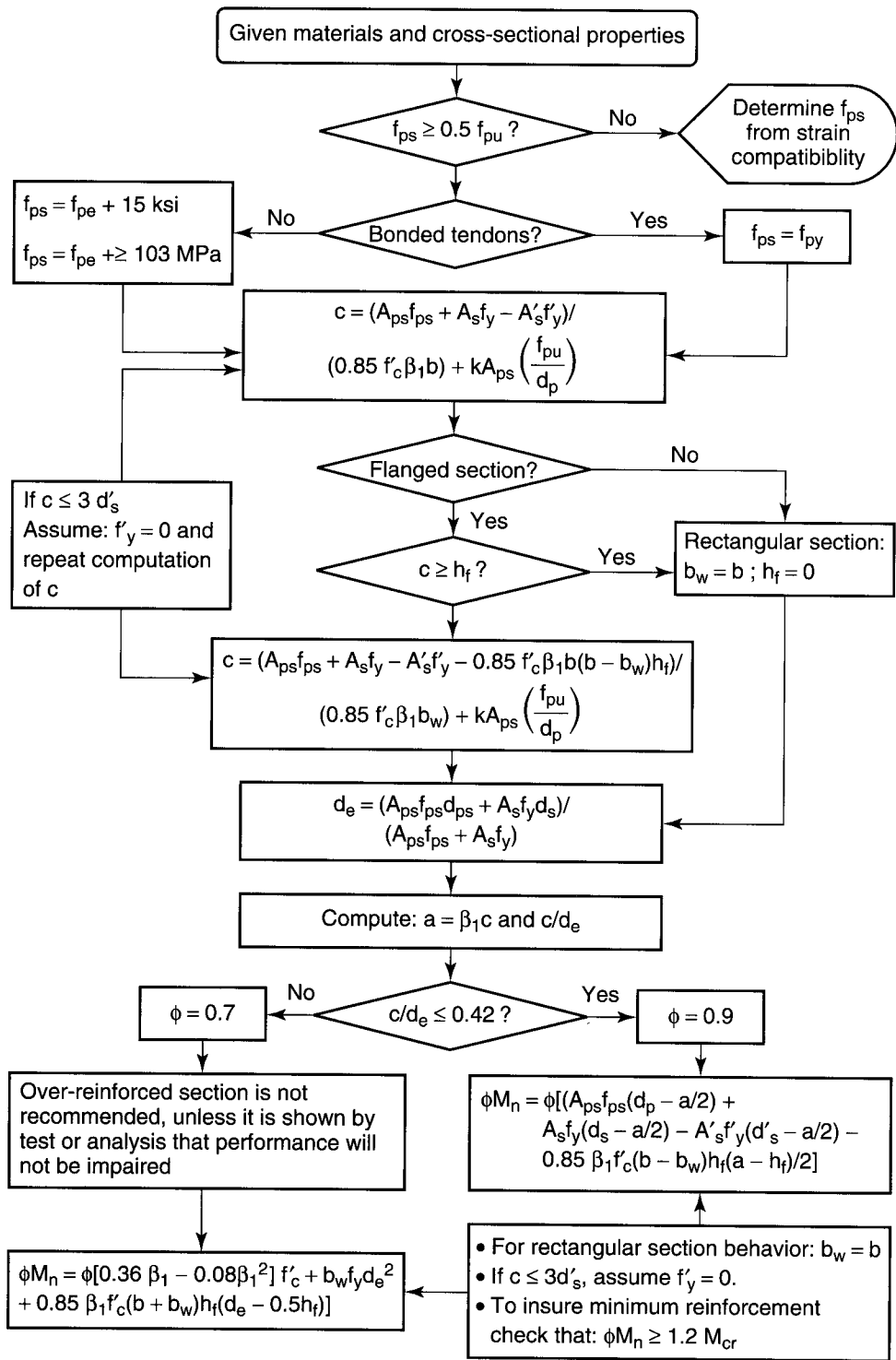
$A_{vf}$  = area of shear reinforcement crossing the shear plane within area  $A_{cv}$

$\phi$  = strength reduction factor = 0.90.

Limit  $A_{vf}$  to cases in which  $v_{uh}/\phi$  is greater than 100 psi.

Figure 12.10 gives flowchart (Ref. 12.15) for steps to be followed in determining the nominal moment strength, namely, the nominal bending resistance for bonded and unbonded tendons.

13. Maximum allowable spacing of web shear reinforcement:



**Figure 12.10** Nominal moment strength of prestressed section with bonded and unbonded reinforcement (Ref. 12.15).

- (a) If  $v_u < 0.125 f'_c$ ,  $s = 0.8 d_v \leq 24$  in.  
 (b) If  $v_u > 0.125 f'_c$ ,  $s = 0.4 d_v \leq 12$  in.

Note that the design yield strength of non-prestressed transverse reinforcement should not exceed 60.0 ksi. The design yield strength of prestressed transverse reinforcement should be taken as the effective prestress after allowing for all prestress losses plus 60.0 ksi, but not greater than  $f_{py}$ .

For Dowel reinforcement spacing:

$$\text{If } A_v \geq \frac{0.05 b_v}{f_{yt}} \text{ where } b_v = \text{width of interface and spacing as presented in item 13.}$$

## 12.9 LRFD DESIGN OF BULB-TEE BRIDGE DECK

### Example 12.1

Design for flexure an interior beam of a 120 ft (36.6 m) simply supported AASHTO-PCI bulb-tee composite bridge deck with no skews (adapted from Ref. 12.11). The superstructure is composed of six pretensioned beams at 9'-0" (2.74 m) on centers as shown in Figure 12.11. The bridge has an 8-in. (203-mm) situ-cast concrete deck with the top  $\frac{1}{2}$ -in to be considered as wearing surface. The design live load is the HL-93 AASHTO-LRFD fatigue loading.

Assume the bridge is to be located in a low seismicity zone.

Given:

#### Maximum allowable stresses:

Deck  $f'_c = 4000$  psi, normal weight

$$f_c = 0.60 f'_c = 2400 \text{ psi}$$

Bulb-tee  $f'_c = 6500$  psi

$$f'_{ci} = 5500 \text{ psi}$$

$$f_c = 0.60 f'_c = 3900 \text{ psi, Service III}$$

$$f_c = 0.45 f'_c = 2925 \text{ psi, Service I}$$

$$f'_{ci} = 0.60 f'_c = 3480 \text{ psi}$$

$$f_t = 6 \sqrt{f'_c} = 484 \text{ psi}$$

$$f_{pu} = 270,000 \text{ psi}$$

$$f_{py} = 0.90 f_{pu} = 243,000 \text{ psi}$$

#### Section Properties

$$A_c = 767 \text{ in.}^2$$

$$h = 72 \text{ in.}$$

$$I_c = 545,894 \text{ in.}^4$$

$$c_b = 36.60 \text{ in.}$$

$$c_t = 35.40 \text{ in.}$$

$$S_b = 14,915 \text{ in.}^3$$

$$S'_t = 15,421 \text{ in.}^3$$

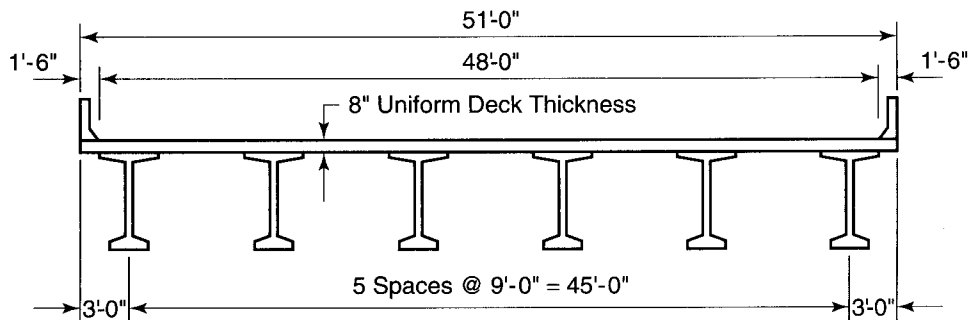


Figure 12.11 Bulb-tee Bridge Deck Cross Section in Example 12.1 (Ref. 12.11)

$$f_{pi} = 0.75 f_{pu} = 202,500 \text{ psi}$$

$$f_y = f_{yt} = 60,000 \text{ psi}$$

$$E_{ps} = 28.5 \times 10^6 \text{ psi}$$

$$E_s = 29.0 \times 10^6 \text{ psi.}$$

$$r^2 = \frac{I_c}{A_c} = \frac{545,894}{767} = 712 \text{ in.}^2$$

$$W_D = 799 \text{ plf.}$$

**Solution:**

**1. Transformed Deck slab controlling width**

Compute the transformed flange width:

$$E_{cs} = 33w^{1.5} \sqrt{f'_c} = 33 \times (1.5)^{1.5} \sqrt{4000} = 3830 \text{ ksi}$$

$$E_{ci} \text{ at transfer} = 33(1.5)^{1.5} \sqrt{5500} = 4500 \text{ ksi}$$

$$E_{ce} \text{ at service} = 33(1.5)^{1.5} \sqrt{6500} = 4890 \text{ ksi}$$

Effective flange width is the lesser of

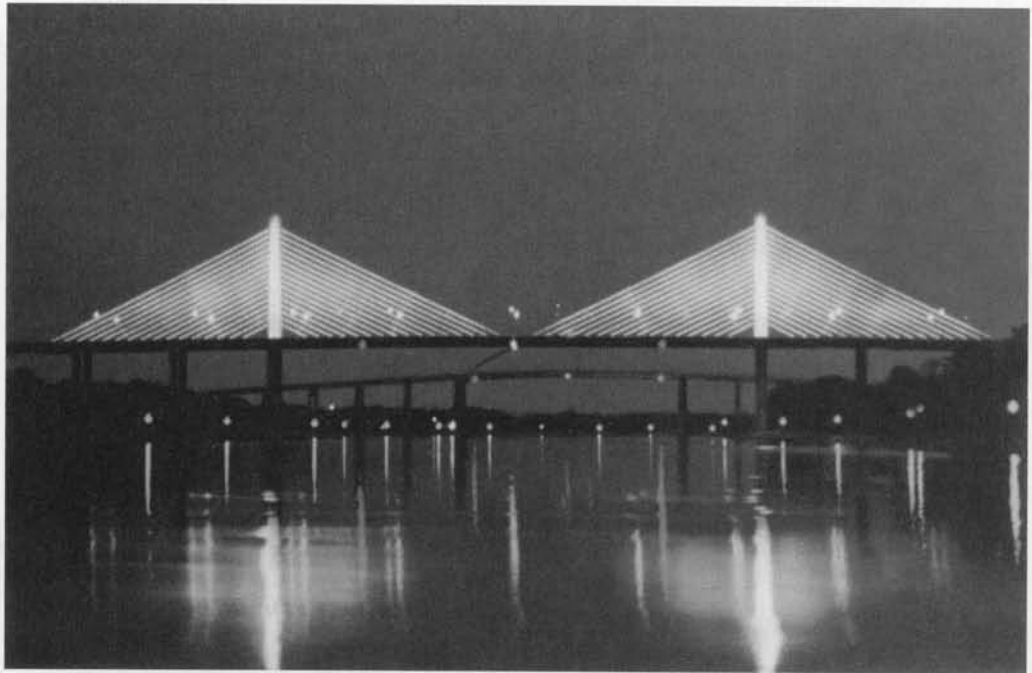
(i)  $\left(\frac{1}{4}\right)$  span =  $\frac{120 \times 12}{4} = 360 \text{ in.}$

(ii)  $12 h_f +$  greater of web thickness or  $\frac{1}{2}$ -beam top flange width,  $b = 12 \times 7.5 + 0.5 \times 42 = 111 \text{ in.}$

(iii) average spacing between beams =  $9 \times 12 = 108 \text{ in.}$   
hence, controlling flange width = 108 in.

$$\text{Modular ratio } n_s = \frac{E_{cs}}{E_c} = \frac{3830}{4890} = 0.78$$

$$\text{Transformed width } b_m = n_s b = 0.78 \times 108 = 84 \text{ in.}$$



**Photo 12.4** Chesapeake and Delaware Canal cable-stayed bridge on S.R. 1. Length 4650 ft. with 12-ft. deep precast girders carrying a 112-ft. wide roadway; typical spans are 150 ft. with precast box piers (Courtesy Figg Engineering Group, Tallahassee, Florida)



**2. Properties of composite section**

Disregard as insignificant the contribution of the deck concrete haunch to  $I'_c$  which is needed because of the precast element camber.

$$A'_c = 1397 \text{ in.}^2$$

$$h = 80 \text{ in.}$$

$$I_{cc} = 1,095,290 \text{ in.}^4$$

$$c_{bc} = 54.6 \text{ in. to the bottom fibers}$$

$$c_{tc} = 72 - 54.6 = 17.4 \text{ in. - precast}$$

$$c_{tsc} = 80 - 54.6 = 25.4 \text{ in. - deck top}$$

$$S_{bc} = \frac{1,095,290}{54.6} = 20,060 \text{ in.}^3$$

$$S'_c = \frac{1,095,290}{17.4} = 62,950 \text{ in.}^3$$

$$S_c^{ts} = \frac{1,095,290}{25.4 \times 0.78} = 55,284 \text{ in.}^3$$

**3. Bending moments and shear forces**

$$\text{Slab: } W_{SD1} = \frac{8}{12} \times 9 \times 150 = 900 \text{ lb/ft}$$

$$\text{Barrier weight: } W_{SD2} = \frac{2 \text{ barriers (300 lb/ft)}}{6 \text{ beams}} = 100 \text{ lb/ft}$$

$$2 \text{ in. future-wearing surface: } W_{SD3} = \frac{2}{12} \times \frac{48 \text{ ft}}{6 \text{ beams}} \times 150 = 200 \text{ lb/ft}$$

Live load (truck load) in LRFD would be based on HL-93 truck fatigue loading.

Clear width from figure 12.12 = 48 ft (14.6 cm)

$$\text{Number of lanes} = \frac{48}{12} = 4 \text{ lanes}$$

**(a) Distribution factor for moment**

For two or more lanes loaded (Ref. 12.3), the distribution factor for bending moment (Table 12.3b)

$$\text{DFM} = 0.075 + \left(\frac{S}{9.5}\right)^{0.6} \left(\frac{S}{L}\right)^{0.2} \left(\frac{K_g}{12f_s^2L}\right)^{0.1}$$

provided that

beam spacing: $3.5 \leq S \leq 16$	Actual $S = 9.0 \text{ ft}$	O.K.
deck slab: $4.5 \leq T_s \leq 12$	Actual $T_s = 7.5 \text{ in.}$	O.K.
span: $20 \leq L \leq 240$	Actual $L = 120 \text{ ft}$	O.K.
no. of beams: $N_b > 4$	Actual $N_b = 6$	O.K.

$e_g$  = distance between the center of gravity of the beam and the slab

$$= \frac{7.5}{2} + 0.5 + 35.4 = 39.65 \text{ in.}$$

$$n = \frac{E_c}{E_{sc}} = \frac{4890}{3830} = 1.28$$

$$K_g = n(I_c + A_c e_g^2)$$

$$= 1.28 [545,894 + 767 (39.65)^2] = 2,242,191 \text{ in.}^4$$

hence,

$$\begin{aligned} \text{DFM} &= 0.075 + \left(\frac{9}{9.5}\right)^{0.6} \left(\frac{9}{120}\right)^{0.2} \left[ \frac{2,242,191}{12(7.5)^3(120)} \right]^{0.1} \\ &= 0.732 \text{ lanes/beam} \end{aligned}$$

For one design lane loaded, from Table 12.3b,

$$\begin{aligned} \text{DFM} &= 0.06 + \left(\frac{S}{14}\right)^{0.4} \left(\frac{S}{L}\right)^{0.3} \left(\frac{K_g}{12L^3}\right)^{0.1} \\ &= 0.06 + \left(\frac{9}{14}\right)^{0.4} \left(\frac{9}{120}\right)^{0.3} \left[ \frac{2,242,191}{12(7.5)^3(120)} \right]^{0.1} = 0.499 \text{ lanes/beam;} \end{aligned}$$

consequently, the case of two or more lanes loaded controls so that the DFM = 0.732 lanes per beam.

*Fatigue Moments:*

The moment is taken for a single design truck having the same axle weight as in all other limit states, but with a constant spacing of 30 ft between the 32-kip axles. A multiple lane factor of 1.2 for fatigue is used to reduce the controlling DFM factor. From table 12.2a, the load factor is 0.75 and the impact factor (IM) for fatigue = 15%.

Hence, the fatigue truckload bending moment becomes:

$$\begin{aligned} M_f &= (\text{bending moment per lane}) (\text{DFM}/1.2)(1 + \text{IM}) \\ \text{or } M_f &= (\text{bending moment per lane}) \left(\frac{0.499}{1.2}\right)(1 + 0.15) \\ &= (\text{bending moment per lane}) (0.415)(1 + 0.15) \\ &= (0.478) (\text{bending moment per lane}) \end{aligned}$$

**(b) Distribution factor for shear**

From Table 12.3(a),

For two or more lanes loaded

$$\text{DFV} = 0.2 + \left(\frac{S}{12}\right) - \left(\frac{S}{36}\right)^2$$

provided that:

beam spacing: $3.5 \leq S \leq 16$	Actual $S = 9.0$ ft	O.K.
deck slab: $4.5 \leq T_s \leq 12$	Actual $T_s = 7.5$ in.	O.K.
span: $20 \leq L \leq 240$	Actual $L = 120$ ft	O.K.
$10,000 \leq K_g \leq 7,000,000$	Actual $K_g = 2,242,191$ in. <sup>4</sup>	O.K.

$$\text{hence, } \text{DFV} = 0.2 + \left(\frac{9}{12}\right) - \left(\frac{9}{36}\right)^2 = 0.887 \text{ lanes/beam.}$$

For one design lane loaded (Table 12.3a)

$$\text{DFV} = 0.36 + \left(\frac{S}{25.0}\right) = 0.36 \left(\frac{9.0}{25.0}\right) = 0.720 \text{ lanes/beam;}$$

consequently, the case of two or more lanes loaded controls and DFV = 0.887 lanes per beam.

**4. Load Combinations**

Total factored load,  $Q = \eta \sum \gamma_i q_i$

where  $\eta$  = a factor relating to ductility, redundancy and operational importance.

$\gamma_i$  = load factors

$q_i$  = special loads;

use  $\eta = 1.0$  for all practical purposes in this example.

Investigate all the load combinations from table 12.2(a) and (b). The cases that control are as follows:

- (a) Service I for compressive stresses in the prestressed concrete components:  
 $Q = 1.0 (DC + DW) + 1.0 (LL + IM)$
- (b) Service III for tensile stresses in the prestressed concrete components:  
 $Q = 1.0 (DC + DW) + 0.8 (LL + IM)$
- (c) Strength I for ultimate strength:

$$\text{Maximum } Q = 1.25 DC + 1.50 DW + 1.75 (LL + IM)$$

$$\text{Minimum } Q = 0.90 DC + 0.65 DW + 1.75 (LL + IM)$$

- (d) Fatigue for checking stress range in the strands

$$Q = 0.75 (LL + IM)$$

(The fatigue  $Q$  is a special load combination for checking the tensile stress range in the strands due to live load and dynamic allowance.)

### 5. Unfactored shear forces and bending moments

- (a) *Truck Loads*

Truck load shear force:

$$\begin{aligned} V_{LT} &= (\text{shear force per lane})(DFV)(1 + IM) \\ &= (\text{shear force per lane})(0.887)(1 + 0.33) \\ &= 1.180 (\text{shear force per lane}) \text{ kips.} \end{aligned}$$

Truck load bending moment:

$$\begin{aligned} M_{LT} &= (\text{moment per lane})(DFM)(1 + IM) \\ &= (\text{moment per lane})(0.732)(1 + 0.33) \\ &= 0.974 (\text{moment per lane}) \text{ ft-kips.} \end{aligned}$$

$$LT = \text{Truck live load}$$

- (b) *Lane Loads*

For lane loads, no dynamic allowance is applied, hence,

$$\begin{aligned} V_{LL} &= (\text{shear force per lane})(DFV) \\ &= (\text{shear force per lane})(0.887) \text{ kips} \end{aligned}$$

$$\begin{aligned} M_{LL} &= (\text{moment per lane})(DFM) \\ &= (\text{moment per lane})(0.732) \text{ ft-kips.} \end{aligned}$$

The lane loads from Figure 12.4, the load on this bridge is as follows in Figure 12.13.

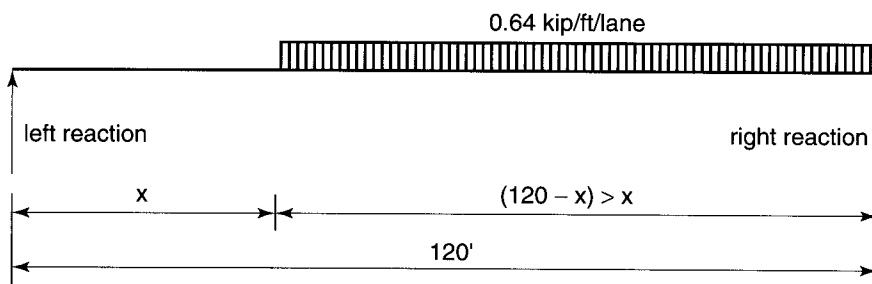
### 6. Computation of moments and shears

- (a) *Lane live load* ( $DFV = 0.887$ ,  $DFM = 0.732$ )

- (i) *Support section:*

shear at the left support ( $x = 0$ ) from equation 12.6(a) and Figure 12.12:

$$\begin{aligned} V_{LL} &= \frac{0.64}{2L} (L - x)^2 (DFV) \\ &= \frac{0.64}{2 \times 120} (120)^2 (0.887) = 34.1 \text{ kips} \end{aligned}$$



**Figure 12.12** Truck load per lane

From equation 12.6(b), and  $DFM = 0.732$

$$M_{LL} = \frac{0.64(x)(L - x)}{2} (DFM) = 0 \text{ ft-kip}$$

**(ii) Section at 24 ft from support:**

As an example, find  $V_{LL}$  and  $M_{LL}$  at  $x = 24$  ft from the left support.

$$V_{LL} = \frac{0.64}{2 \times 120} (120 - 24)^2 (0.887) = 21.8 \text{ kips}$$

$$M_{LL} = \frac{0.64(24)(120 - 24)}{2} (0.732) = 539.7 \text{ ft-kip}$$

**(b) Truck live load ( $DFV = 1.180$ ,  $DFM = 0.974$ )**

Here, the impact factor  $IM = 33\%$  has to be included, hence, larger  $DFV$  and  $DFM$  values.

**(i) Support sections:**

From Table 12.4,

$$\begin{aligned} V_{LT} &= \frac{72[(L - x) - 9.33]}{L} (DFV) \\ &= \frac{72[(120 - 0.0) - 9.33]}{120} (1.180) = 78.1 \text{ kips} \end{aligned}$$

From Table 12.5,

$$\begin{aligned} M_{LT} &= \frac{72(x)[(L - x) - 9.33]}{L} (DFM) \\ &= 0 \text{ ft-kip for the support moment.} \end{aligned}$$

**(ii) Section at 24 ft from support:**

$$V_{LT} = \frac{72[(120 - 24) - 9.33]}{120} (1.180) = 61.4 \text{ kips}$$

$$M_{LT} = \frac{72(24)[(120 - 24) - 9.33]}{120} (0.974) = 1215.0 \text{ ft-kip}$$

**(c) Fatigue moment at 24 ft ( $DFF = 0.478$ )**

From Table 12.7,

$$M_f = \frac{72(x)[(L - x) - 18.22]}{L} (DFF)$$

From before,  $DFF = 0.478$

hence,

$$M_f = \frac{72(24)[(120 - 24) - 18.22]}{120} (0.478) = 535.8 \text{ ft-kip}$$

**(d) Shears and moments due to dead loads:**

The loads to be considered are beam weight ( $W_D$ ) plus deck slab and haunches ( $W_{SD1}$ ), and future wearing surface ( $W_{SD3}$ ).

The beam is simply supported, hence, the shear and moment at any cross section along the span are:

$$V_x = W_D(0.5L - x)$$

$$M_x = 0.5W_Dx(L - x)$$

As an example, consider a section at 24 ft from the left support and compute the shear and moment due to self-weight  $W_D = 0.799$  Kip/ft:

$$V_x = 0.799(0.5 \times 120 - 24) = 28.8 \text{ kips}$$

$$M_x = 0.5 \times 0.799 \times 24(120 - 24) = 920.4 \text{ ft-kip.}$$

Tables 12.10 and 12.11 (Ref. 12.11) list the forces and moments required for the design of the interior beam elements. It should be noted that long-hand computations to develop such a table are time consuming. Computer programs developed by several state DOTs are available, some on the internet, such as the Washington State DOT Program.

## 7. Design of the Bulb-tee prestressed interior beam

### (1) Selection of Prestressing Strands

For Service-III load combination, bottom fiber stress  $f_b$  is:

$$f_b = \frac{M_D + M_S}{S_b} + \frac{M_b + M_{WS} + 0.8(M_{LT} + M_{LL})}{S_{bc}}$$

where  $M_D$  = unfactored self-weight moment, ft-kip

$M_S$  = unfactored moment due to slab and haunch weight, ft-kip

$M_b$  = unfactored barrier moment, ft-kip

$M_{WS}$  = unfactored future wearing surface moment, ft-kip

$M_{LT}$  = unfactored truck load moment, ft-kip

$M_{LL}$  = unfactored lane load moment, ft-kip

From before,  $S_b = 14,915 \text{ in.}^3$

$$S_{bc} = 20,090 \text{ in.}^3$$

From Tables 12.10 and 12.11,

Midspan stresses at bottom fibers at service:

$$\begin{aligned} f_{bc} &= \frac{(1438.2 + 1659.6)}{14,915} (12) + \frac{(180 + 360) + 0.8(1830.3 + 843.2)}{20,090} (12) \\ &= 2.50 + 1.60 \cong 4.10 \text{ ksi (T).} \end{aligned}$$

The 4.10 ksi (T) will be neutralized by prestressing the beam. Maximum allowable tensile stress:

$$f_t = 6.0\sqrt{f'_c} \text{ psi} = 6\sqrt{6500} = 484 \text{ psi} = 0.484 \text{ ksi}$$

Required prestress compressive stress at the bottom fibers:

$$f_{cb} = (4.1 - 0.48) = 3.62 \text{ ksi}$$

**Table 12.10** LRFD Service Shear and Moment Due to Dead Load

Distance <i>X</i>	Section <i>X/L</i>	Beam Weight $W_D$		(Slab + Haunch) Weight $W_{SD1}$		Barrier Weight $W_{DS2}$		Wearing Surface $W_{SD3}$	
		Shear	Moment $M_g$	Shear	Moment $M_s$	Shear	Moment $M_b$	Shear	Moment $M_{ws}$
ft		kips	ft-kips	kips	ft-kips	kips	ft-kips	kips	ft-kips
0	0.0	47.9	0.0	55.3	0.0	6.0	0.0	12.0	0.0
6.00*	0.05	43.1	274.3	49.8	315.3	5.4	34.2	10.8	68.4
12	0.1	38.4	517.8	44.3	597.5	4.8	64.8	9.6	129.6
24	0.2	28.8	920.4	33.2	1,062.1	3.6	115.2	7.2	230.4
36	0.3	19.2	1,208.1	22.1	1,394.1	2.4	151.2	4.8	302.4
48+	0.4	9.6	1,380.7	11.1	1,593.2	1.2	172.8	2.4	345.6
60	0.5	0.0	1,438.2	0.0	1,659.6	0.0	180.0	0.0	360.0

\*Critical section for shear

+ Harp point

Assume that the distance from the centroid of the prestressing reinforcement and the section bottom fibers =  $0.05h$

$$= (0.05)(72) = 3.6 \text{ in; use 4.0 in., hence } e_c = 36.6 - 4.0 = 32.6 \text{ in.}$$

As presented in the examples in Chapter 4,

$$f_{bp} \text{ due to prestress} = \frac{P_e}{A_c} + \frac{P_e \times e_c}{S_b}$$

$$\text{or } f_{bp} = \frac{P_e}{767} + \frac{P_e \times 32.6}{14,915} = 3.62 \text{ ksi}$$

**Table 12.11** LRFD Service Shear and Moment Due to Truck and Lane Loads

Distance <i>X</i>	Section <i>X/L</i>	Truck Load with Impact $W_{LT+I}$		Lane Load $W_{LL}$		Fatigue Truck with Impact $W_f$
		Shear $V_{LT}$	Moment $M_{LT}$	Shear $V_{LL}$	Moment $M_{LL}$	Moment $M_f$
ft		kips	ft-kips	kips	ft-kips	ft-kips
0	0.0	78.1	0.0	34.1	0.0	0.0
6.00*	0.05	73.8	367.8	30.6	160.2	165.0
12	0.1	69.6	691.6	27.5	303.6	309.2
24	0.2	61.4	1,215.0	21.8	539.7	535.8
36	0.3	52.7	1,570.2	16.6	708.3	692.7
48+	0.4	44.2	1,778.9	12.2	809.5	776.2
60	0.5	35.7	1,830.2	8.5	843.3	776.9

\*Critical section for shear

+ Harp point

to give prestressing force  $P_e = 1037$  kips  
 Assume total prestress loss = 25%

$$P_i = \frac{1037}{1 - 0.25} = 1383 \text{ kips}$$

assume using  $\frac{1}{2}$  in.-dia 7-wire 270-K low-relaxation strands ( $A_{ps} = 0.153 \text{ in.}^2$ )

$$\text{Required number of strands} = \frac{1383}{0.153 \times 202.5} = 44.6 \text{ strands.}$$

After two trials and adjustments, 48 strands with the configuration shown in Figure 12.13 are tried. Less than 48 strands result in tensile stresses at the bottom fibers at service which exceed the maximum allowable  $f_t = 484$  psi. Twelve strands are harped at 0.4 L. Accordingly, 36 strands remain straight at the beam (see Figure 12.13).

From data,  $c_b = 36.60$  in. and  $c_t = 72 - 36.60 = 35.40$  in.

$$e_e = c_b - [2 \times 70 + 2 \times 68 + 2 \times 66 + 2 \times 64 + 2 \times 62 + 2 \times 60 + 4 \times 8 + 8 \times 6 + 12 \times 4 + 12 \times 2] / 48$$

$$= 36.60 - 19.42 = 17.28 \text{ in.}$$

$$e_c = c_b - [2 \times 12 + 12 \times 4 + 8 \times 6 + 8 \times 4 + 2 \times 10 + 2 \times 12 + 2 \times 14 + 2 \times 16 + 2 \times 18 + 2 \times 20] / 48$$

$$= 36.6 - 6.92 = 29.68 \text{ in.}$$

Given  $f_{pi} = 0.75 f_{pu} = 202,500$  psi,

$$P_i = (48)(0.153)(202.5) = 1488 \text{ kips.}$$

After running a detailed step-by-step analysis of prestress losses as in chapter 3, Section 3.9, the total prestress loss was determined to be 26.4%.

$$f_{pe} = 202.5(1 - 0.264) = 149.0 \text{ ksi}$$

hence,  $P_e = 1488(1 - 0.264) = 1095.0$  kips

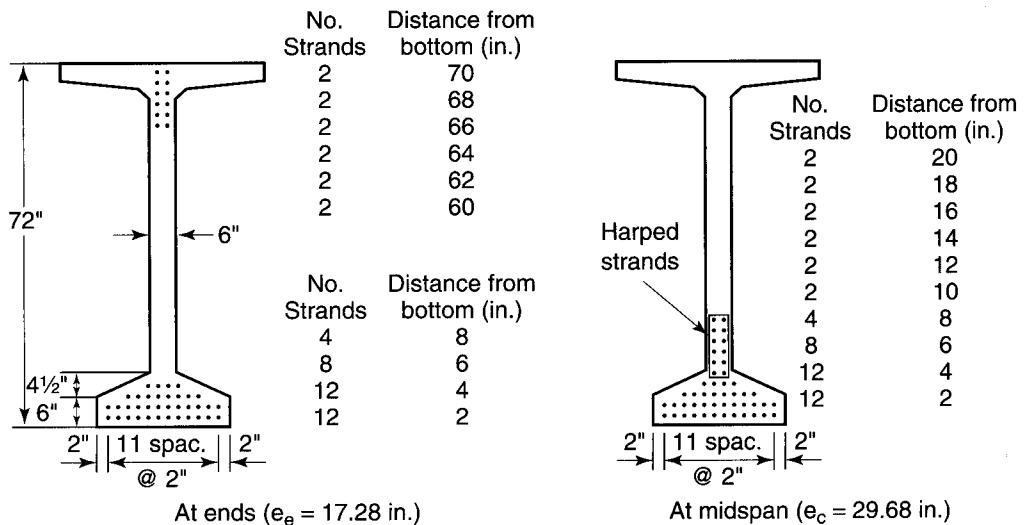


Figure 12.13 Bulb-Tee Prestressing Strand Pattern

**(2) Check of Concrete Unfactored Stresses****(a) Stresses at Transfer**

Initial  $f_{pi} = 0.7 f_{pu} = 0.7 \times 270 = 202.5$  ksi. Common practice assumes that initial relaxation losses at prestressing amount to 9 to 10%. Use 10% reduction in  $f_{pi}$ .

$$P_i = 0.90 \times 1488 = 1339 \text{ kips}$$

Hence,  $P_i = (0.9)(202.5)(0.153 \times 48) = 1338$  kips

**(i) Support Section**

From Chapter 4, Equation 4.1 (a),

$$\begin{aligned} f^t &= -\frac{P_i}{A_c} \left( 1 - \frac{e_e c_t}{r^2} \right) - \frac{M_D}{S^t} \\ &= -\frac{1338}{767} \left( 1 - \frac{17.28 \times 35.4}{712} \right) - 0 = -0.25 \text{ ksi (C), no tension, O.K.} \end{aligned}$$

$$\begin{aligned} f_b &= -\frac{P_i}{A_c} \left( 1 + \frac{e_e c_b}{r^2} \right) + \frac{M_D}{S_b} \\ &= -\frac{1339}{767} \left( 1 + \frac{17.28 \times 36.3}{712} \right) + 0 \\ &= 3.29 \text{ ksi (C) } < \text{allowable } f_c = 3.48 \text{ ksi O.K.} \end{aligned}$$

**(ii) Midspan Section**

$$\begin{aligned} f^t &= -\frac{1338}{767} \left( 1 - \frac{29.68 \times 36.60}{712} \right) - \frac{1438 \times 12}{15,421} \\ &= 0.917 - 1.119 = -0.202 \text{ ksi (C), no tension allowed, hence, O.K.} \end{aligned}$$

$$\begin{aligned} f_b &= -\frac{1339}{767} \left( 1 + \frac{29.68 \times 36.6}{712} \right) + \frac{1438 \times 12}{14,915} \\ &= -4.513 + 1.157 = -3.356 \text{ ksi (C) } < \text{than allowable } f'_{ci} = 5.50 \text{ ksi, O.K.} \end{aligned}$$

**(b) Stresses at Service:****(i) Midspan Section:**

From chapter 4, Equations 4.3(a) and 4.3(b):

$$f^t = -\frac{P_e}{A_c} \left( 1 - \frac{e_e c_t}{r^2} \right) - \frac{M_T}{S^t} \leq f_c$$

$$f_b = -\frac{P_e}{A_c} \left( 1 + \frac{e_e c_b}{r^2} \right) + \frac{M_T}{S_{cb}} \leq f_t$$

Since the loads are placed at different stages of construction, for Service-I precast sections,

$$\begin{aligned} f^t &= -\frac{P_e}{A_c} \left( 1 - \frac{e_e c_t}{r^2} \right) - \frac{M_D + M_S}{r^2} - \frac{M_{WS} + M_b}{S^t} \\ &= -\frac{1095}{767} \left( 1 - \frac{29.68 \times 35.40}{712} \right) - \frac{(1438 + 1660)12}{15,421} - \frac{(360 + 180)12}{62,950} \\ &= 0.679 - 2.411 - 0.103 = -1.835 \text{ ksi (C)} \end{aligned}$$

< Service allowable  $f_c = 2925$  psi O.K.

$$\begin{aligned} f_b &= -\frac{1095}{767} \left( 1 + \frac{29.68 \times 36.60}{712} \right) + \frac{(1438 + 1660)12}{14,915} + \frac{(360 + 180)12}{20,060} \\ &= -3.605 + 2.493 + 0.323 = -0.789 \text{ ksi (C) O.K.} \end{aligned}$$



**(3) Including stresses due to the transient lane and truck loads**

A factor of 0.80 is used for Type III loading (Table 12.2a)

$$f^t = -1.835 - \frac{0.8(1830 + 843)12}{62,950}$$

$$= -1.835 - 0.408 = -2.243 \text{ ksi (C)} < \text{Service-III } f_c = 3900 \text{ psi O.K.}$$

$$f_b = -0.789 + \frac{0.8(1830 + 843)12}{20,060}$$

$$= -0.789 + 1.279 = 0.490 \text{ ksi (T)} \approx \text{Allowable } f_t = 0.484, \text{ O.K.}$$

**(4) Concrete stresses at top deck fibers****(i) Under permanent Service I loads**

$$f_c^{fs} = \frac{M_{ws} + M_b}{S_c^t} = \frac{(360 + 180)12}{55,284}$$

$$= -0.117 \text{ ksi (c)} < \text{allowable } f_c = 2.4 \text{ ksi O.K.}$$

**(ii) Under permanent and transient lane and truck loads, Service I:**

$$f_c^{fs} = \frac{M_{ws} + M_b}{S_c^t} + \frac{M_{LT} + M_{LL}}{S_c^t}$$

$$= -0.117 - \frac{(1830 + 843)12}{55,284}$$

$$= -0.697 \text{ ksi (C)} < \text{allowable } f_c = 2.4 \text{ ksi, O.K.}$$

**(5) Concrete Stresses at beam bottom fibers, Service III (See step 3)**

$$f_b = -\frac{P_e}{A_c} \left( 1 + \frac{e_c c_b}{r^2} \right) + \frac{M_D + M_S}{S_b} + \frac{(M_{ws} + M_B) + 0.8(M_{LT} + M_{LL})}{S_{bc}}$$

$$= -\frac{1095}{767} \left( 1 + \frac{29.68 \times 36.60}{712} \right) + \frac{(1438 + 1660)12}{14,915}$$

$$+ \frac{[(360 + 180) + 0.8(1830 + 843)]12}{20,060}$$

$$= -3.605 + 2.492 + 1.603 = 0.490 \text{ ksi (T)} \cong \text{allowable } f_t = 0.484 \text{ ksi, O.K.}$$

**(6) Fatigue stresses**

LRFD specifies that in regions of compressive stress due to permanent loads and prestress, fatigue is only considered if the compressive stress is less than twice the maximum tensile live load stress resulting from the fatigue:

Thus, for permanent loads only, the term  $(M_{LT} + M_{LL})/S_c^t$  is taken out to give:

$$f_b = -\frac{P_e}{A_c} \left( 1 + \frac{e_c c_b}{r^2} \right) + \frac{M_D + M_S}{S_b} + \frac{(M_{ws} + M_B)}{S_{bc}}$$

$$= -3.605 + 2.492 + \frac{(360 + 180)12}{20,060} = -0.790 \text{ ksi (c) O.K.}$$

From table 12.11, fatigue moment  $M_f = 777$  ft-kips,  
Tensile fatigue stress at the bottom fibers,

$$f_b = \frac{0.75M_f}{S_{bc}} = \frac{0.75 \times 777 \times 12}{20,060} = 0.348 \text{ ksi (T)}$$

Since twice  $0.348 = 0.696 < 0.790$  ksi (which is a compressive stress), a fatigue check is unnecessary.

From the forgoing computations, the flexural design is O.K. at the initial and service load conditions. To be complete and also determine the reserve strength available for overload conditions, the limit state at failure design is necessary as in the following section. The total design has to include shear, torsion, if any, and serviceability as in Example 12.2.

### 8. Ultimate strength (Limit state of failure)

#### (a) Nominal flexural resistance moment

From Tables 12.2 (a) and (b) total factored moment for Strength I Load:

$$M_u = 1.25DC + 1.5DW + 1.75(LL + IM)$$

From Table 12.10

$$M_u = 1.25(1438 + 1660) + 1.5(360 + 180) + 1.75(1830 + 843) = 9316 \text{ ft-kip}$$

$$\text{Required } M_r = \frac{M_u}{\phi} = \frac{9316}{1.0} = 9316 \text{ ft-kip}$$

Average stress in the prestressing reinforcement when  $f_{pe} \geq 0.5 f_{pu}$ , from

$$\text{equation 12.9: } f_{ps} = f_{pu} \left( 1 - k \frac{c}{d_p} \right) \text{ where } k = 2 \left( 1.04 - \frac{f_{py}}{f_{pu}} \right).$$

For the depth of the compressive block, use slab  $f'_c = 4.0$  ksi.

$k = 0.28$  for low-relaxation steel

$$d_p = (\text{h-cover to c.g.s.}) = [(72 + 8) - 6.92] = 73.08 \text{ in.}$$

$b =$  effective compression flange width =  $9' - 0'' = 108$  in.

$$A_{ps} = 48 \times 0.153 = 7.344 \text{ in.}^2$$

$$f_{pu} = 270 \text{ ksi}$$

From equation 12.10,

$$\begin{aligned} c &= \frac{A_{ps} f_{pu} + A_s f_y - A'_s f'_y}{0.85 f'_c \beta_1 b + k A_{ps} \frac{f_{pu}}{d_p}} \\ &= \frac{7.344 + 0 - 0}{0.85 \times 4.0 \times 0.85 \times 108 + 0.28 \times 7.344 \left( \frac{270}{73.08} \right)} \\ &= 6.20 \text{ in.} < t_s = 7.5 \text{ in.} \\ a &= \beta_1 c = 0.85 \times 6.20 = 5.27 \text{ in.,} \end{aligned}$$

hence, neutral axis is within the flange and the section is considered rectangular.

Average design reinforcement strength  $f_{ps}$ :

$$f_{ps} = 270 \left( 1 - 0.28 \frac{6.20}{73.08} \right) = 263.6 \text{ ksi}$$

$$\text{nominal flexural resistance } M_r = A_{ps} f_{ps} \left( d - \frac{a}{2} \right)$$

$$M_n = M_r = 7.344 \times 263.6 \left( 73.08 - \frac{5.27}{2} \right) \left( \frac{1}{12} \right)$$

$$= 11,364 \text{ ft-kips} > \text{required } M_n = 9316 \text{ ft-kip} \quad \text{O.K.}$$

$\frac{c}{d_e} \leq 0.42$  for ductile behavior discussed in section 12.3.1 and table 12.1 (a).

$$\text{Actual } \frac{c}{d_e} = \frac{6.20}{73.08} = 0.085 < 0.42 \quad \text{O.K.}$$

**(b) Minimum reinforcement**

As discussed in section 12.3.4, the minimum reinforcement has to be the lesser of  $1.2 M_{cr}$  or  $1.33 M_u$  required by the applicable load combinations. See also flow-chart Figure 12.11 and Tables 12.10 and 12.11.

$$f_r = 7.5\sqrt{f'_c} = 7.5\sqrt{6500} = 605 \text{ psi} = 0.6 \text{ ksi}$$

$f_{ce}$  = compressive stress due to effective prestress only at the bottom fibers as defined in section 12.3.4,

$$= -\frac{P_e}{A_c} \left( 1 + \frac{e_c c_b}{r^2} \right) = -3.606 \text{ ksi from before.}$$

$$\text{Non-composite } M_{dnc} = M_D + M_S = 1438 + 1660 = 3098 \text{ ft-kip}$$

$$S_{bc} = 20,060 \text{ in.}^4$$

$$S_b = 14,915 \text{ in.}^4$$

From equation 12.13,

$$\begin{aligned} M_{cr} &= (f_r + f_{ce})S_b - M_{dnc} \left( \frac{S_{bc}}{S_b} - 1 \right) \\ &= (0.6 + 3.6) \frac{14,915}{12} - 3098 \left( \frac{20,060}{14,915} - 1 \right) \\ &= 5220 - 1069 = 4151 \text{ ft-kip} \end{aligned}$$

$$1.2 M_{cr} = 1.2 \times 4151 = 4981 \text{ ft-kip}$$

$$1.33 M_u = 1.33 \times 9316 = 12,390 \text{ ft-kip} > 4981 \text{ ft-kip}$$



**Photo 12.5** Hanging Lake Viaduct, Glenwood Canyon, Colorado, total length 1297 ft., consisting of 34 spans, primarily 200-ft. lengths (Courtesy Figg Engineering Group, Tallahassee, Florida)

hence, the lesser of the two moments controls, namely,  $1.2 M_{cr} = 4981$ .  
 $M_n$  or  $M_r = 11,364 > 4981$  O.K.

### 9. *Pretensioned Anchorage Zone*

The zone reinforcement is designed using the force in the strands just prior to release transfer. The LRFD specifications require that the bursting resistance,  $P_r$ , should not be less than 4.0% of the force in the strands,  $F_{pi}$ , before release, namely:

$$P_r = f_s A_s \geq 0.04 F_{pi}$$

$$F_{pi} = 48 \times 0.153 \times 202.5 = 1488 \text{ kips}$$

$$P_r = 0.04 \times 1488 = 59.5 \text{ kips}$$

Use a stress,  $f_s$ , in the anchorage reinforcement not exceeding 20 ksi.

$$\text{Required area} = 59.5/20 = 2.98 \text{ in.}^2$$

$$\text{Try No. 5 closed ties; } A_s = 2 \times 0.31 = 0.62 \text{ in.}^2$$

$$\text{Number of ties} = 2.98/0.62 = 4.8$$

Distance within which anchorage reinforcement has to be provided from beam end =  $h/5 = 72/5 = 14.4$  in.

Use No. 5 closed ties at 3 in. center-to-center, with the first tie starting at 2 in. from the beam end.

#### **Conclusion:**

Accept the design of the bulb-tee bridge for flexure. For the design to be complete, design for shear, interface shear transfer and deflection/camber checks have to be performed as in Example 12.2.

## 12.10 LRFD SHEAR AND DEFLECTION DESIGN

### Example 12.2

Design the web shear reinforcement for the bulb-tee beam in Example 12.1 at the critical section near the supports and the interface shear transfer reinforcement at the interface plane between the precast section and the deck situ-cast concrete. Also, verify if the span deflection is within the allowable limits.

#### **Solution:**

#### 1. *Web Shear Design*

##### (a) *Strain at centroid level of reinforcement*

$$\phi = 0.90$$

$$e_e = 17.28 \text{ in.}$$

Provide web steel when  $V_u > 0.5\phi (V_c + V_p)$

Critical section is the greater of  $0.5 d_v \cot\theta$  or  $d_v$

$$d_e = d_c = h - e_e = 80.0 - 17.28 = 62.72 \text{ in.}$$

$$d_v = \left( d_e - \frac{a}{2} \right) = 62.72 - \frac{5.27}{2} = 60.08 \text{ in.}$$

$$\geq 0.9d_e = 0.9 \times 62.72 = 56.45 \text{ in.}$$

$$\geq 0.72h = 0.72 \times 80 = 57.6 \text{ in.}$$

$$d_v = 60.08 \text{ in. controls as the largest of the three values}$$

Assume  $\theta = 23^\circ$  for a first trial

$$0.5d_v \cot\theta = 0.5 \times \cot 23^\circ$$

$$= 70.77 > 60.08 \text{ in., use } d_v = 60.08 \text{ in the } \epsilon_x \text{ equation}$$

As the support bearing width is not yet determined, assume it conservatively = 0. Consequently, the critical section for shear is 74.35 in.  $\cong$  6.2 ft from the support, being larger than the dimension  $d_v = 60.08$  in. as stipulated by the LRFD AASHTO requirement; hence distance 74.35 in. controls for the critical shear section.

$$\frac{x}{L} = \frac{6.2}{120} \cong 0.05L \text{ from the support face.}$$

From equation 12.23,

$$V_c = \beta (\text{psi}) \sqrt{f'_c} b_v d_v$$

In order to determine the value of  $\beta$  several computations have to be performed. Reinforcement strain  $\epsilon_x$  from equation 12.28 is initially using either Equations 12.28(a) or (b). Try Equation 12.28(a),

$$\epsilon_x = \frac{\frac{M_u}{d_v} + 0.5N_u + 0.5V_u \cot\theta - A_{ps}f_{po}}{2[E_s A_s + E_{ps} A_{ps}]} \leq 0.002$$

At plane 0.05L, from Table 12.10

$$M_u = 1.25(275 + 315 + 34) + 1.5(68) + 1.75(368 + 160) = 1802 \text{ ft-kip}$$

Corresponding shear:

$$V_u = 1.25(43 + 50 + 5) + 1.50(11) + 1.75(74 + 31) = 323 \text{ kips}$$

$$N_u = \text{applied normal force at } 0.05L \text{ plane} = 0$$

$$f_{po} = \text{jacking stress} \cong 0.70 f_{pu}$$

$$= f_{pe} + \frac{\bar{f}_{ce} E_{ps}}{E_c}. \text{ It can however, be conservatively taken}$$

as the effective prestress  $f_{pe}$

$\bar{f}_{ce}$  = concrete compressive stress at the centroid of the composite section due to both prestressing and the bending moments resisted by the precast section acting alone.

Distance from the c.g.c. of the composite section to the c.g.c. of the precast section.

$$c_1 = c_{bc} - c_b = 54.6 - 36.6 = 18.0 \text{ in.}$$

At the critical section  $e_{el} = 18.9$  in.

$$\text{Section modulus } S_1 = \frac{I_c}{c_1} = \frac{545,894}{18.0} = 30,327 \text{ in.}^4$$

$$e_e = 17.28 \text{ in.}$$

$$r^2 = 712 \text{ in.}^2$$

$$\begin{aligned} \bar{f}_{ce} &= -\frac{P_e}{A_c} \left( 1 - \frac{e_e c_1}{r^2} \right) - \frac{(M_D + M_{SD})}{S_1} \\ &= -\frac{1095}{767} \left( 1 - \frac{18.9 \times 18.0}{712} \right) - \frac{(275 + 315)(12)}{30,327} \\ &= -0.746 - 0.233 = -0.979 \text{ ksi (c)} \end{aligned}$$

$$f_{pe} = \frac{1095}{48 \times 0.153} = 149.0 \text{ ksi}$$

$$E_c = 4890 \text{ ksi}$$

$$V_u = 323 \text{ kips}$$

$$M_u = 1802 \text{ kip-ft}$$

$$A_{ps} = 48 \times 0.153 = 7.344$$

$V_u = 323$  kips,  $V_p = 24.5$  kips from Fig. 12.13 and the computations from the slope of the harped tendon to follow.

From Equation 12.29

$$f_{po} = 149.0 + 0.979 \times 28,500/4890 = 155.0 \text{ ksi}$$

$$\text{or } f_{po} = 0.70 f_{pu} = 0.7 \times 270 = 189.0 \text{ ksi}$$

Use  $f_{pe} = 155$  ksi in the computations.

Assume that the section contains at least the minimum  $A_v$  to be verified later, using Equation 12.28 (a) for a first trial and no longitudinal mild steel, calculate the strain  $\epsilon_x$  as follows:

$$\begin{aligned} \epsilon_x &= \frac{\left( \frac{M_u}{d_v} + 0.5 N_u + 0.5(V_u - V_p) \cot \theta - A_{ps} f_{po} \right)}{2(E_s A_s + E_p A_{ps})} \\ &= \frac{\frac{1802 \times 12}{60.08} + 0 + 0.5(323 - 24.5) \cot 23^\circ - 7.344 \times 155}{2(0 + 28,500 \times 7.344)} \\ &= \frac{-426.8}{418,608} = \text{negative value.} \end{aligned}$$

hence, Eq. 12.28(c) would have to be used:

$$\epsilon_x = \frac{\left( \frac{M_u}{d_v} + 0.5 N_u + 0.5(V_u - V_p) \cot \theta - A_{ps} f_{po} \right)}{2(E_c A_c + E_s A_s + E_p A_{ps})}$$

$A_c$  = area of the concrete section on the flexural tension side of the member as shown in Figure 12.9. Hence, from Figure 12.15 of the flanged section used in this example,

$$A_c = 26 \times 6 + \frac{1}{2} (26 - 6) \times 4.5 + 6 \times 4.5 + 6 \times 25.5 = 156 + 45 + 27 + 153 = 381 \text{ in.}^2$$

$E_c = 4890$  ksi from before when the concrete is beyond the 28 day strength

Hence,

$$\begin{aligned} \epsilon_x &= \frac{\frac{1602 \times 12}{60.08} + 0 + 0.5(323 - 24.5) \cot 23^\circ - 7.344 \times 155}{2(4890 \times 381 + 0 + 28,500 \times 7.344)} \\ &= \frac{-426.8}{4145 \times 10^3} = -0.10 \times 10^{-3} \text{ in./in.} \end{aligned}$$

Use  $1000\epsilon_x = -0.10$  in Table 12.8(a).

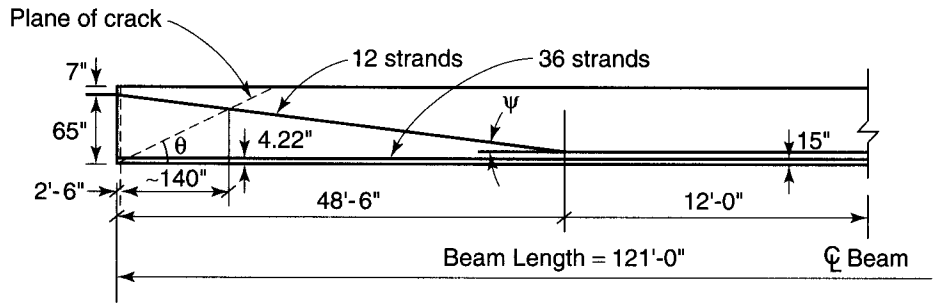
**(b) Web shear strength,  $V_o$  from  $\theta - \beta$  analysis.**

$$V_u = 323 \text{ kips}$$

From equation 12.15(b)

$$\text{Shear stress } \nu = \frac{(V_u - \phi V_p)}{\phi b_v d_v}, \quad \text{where } \phi = 0.90 \text{ for shear}$$

$$f_{pe} \text{ from before} = 149.0 \text{ ksi}$$



**Figure 12.14** Beam tendon geometry

Figure 12.14 shows the inclination angle,  $\psi$ , of the 12 harped strands,

$$\sin \psi = \frac{(65 - 15)}{48.5 \times 12} = 0.086$$

Harped tendon force =  $12 \times 0.153 \times 155.0 = 284.6$  kips

$$V_p = 284.6 \sin \theta = 284.6 \times 0.086 = 24.5 \text{ kips}$$

$$\text{Required } v = \frac{323 - 0.9 \times 24.5}{0.9 \times 6 \times 60.08} = 0.93 \text{ ksi}$$

$$\text{Ratio } \frac{v}{f'_c} = \frac{0.93}{6.5} = 0.143$$

Entering Table 12.8 (a) for the values of  $1000\varepsilon_x = -0.10$  and  $(v_u/f'_c) = 0.143$ , we get  $\theta = 23.3^\circ$ , which is close to the value of  $23^\circ$  assumed, and  $\beta = 2.80$ .

Hence,  $V_c = 0.0316\beta\sqrt{f'_c} b_v d_v$

$$= 0.0316 \times 2.80 \sqrt{6.5} \times 6 \times 60.08 = 81.3 \text{ kips}$$

**(c) Selection of web reinforcement**

From equation 12.26, check whether web reinforcement is needed, namely, if  $V_u > 0.5\phi(V_c + V_p)$

$$0.5\phi(V_c + V_p) = 0.5 \times 0.9(81.3 + 24.5) = 47.6 \text{ kips}, < V_u = 323 \text{ kips}$$

Use web steel.

$$\text{Required } V_s = \frac{V_u}{\phi} - V_c - V_p = \left(\frac{323}{0.9}\right) - 81.3 - 24.5 = 253.0 \text{ kips}$$

From Equation 12.25,

$$\text{Available } V_s = \frac{A_v f_y d_v \cot \theta}{s}$$

Trying No. 4 stirrups,  $A_v = 2 \times 0.20 = 0.40 \text{ in.}^2$

$$\cot \theta = \cot 23^\circ = 2.356$$

$$\text{hence, } 253.0 = \frac{0.4 \times 60.0 \times 60.08 \times 2.475}{s}, \quad \text{giving } s = 13.4 \text{ in.}$$

**(i) Maximum allowable web stirrup spacing:**

$$\text{If } v_u < 0.125 f'_c \quad s = 0.8 d_v \leq 24 \text{ in.}$$

$$\text{If } v_u > 0.125 f'_c \quad s = 0.4 d_v \leq 12 \text{ in.}$$

Limit  $v_u = 0.125 f'_c = 0.125 \times 6.5 = 0.81$  ksi

Actual  $v_u = 0.93$  ksi  $>$  limit  $v_u = 0.81$ , hence use  $s = 0.40 d_v = 0.40 \times 60.08 = 24$  but not to exceed 12 in. c/c.

Therefore, space the transverse web reinforcement at 12 in. c/c.

**(ii) Minimum area of transverse reinforcement:**

$$A_v/ft = 0.0316 \sqrt{f'_c} \frac{b_v s}{f_{yt}}$$

$$= 0.0316 \sqrt{6.5} \left( \frac{6 \times 12}{60} \right) = 0.10 \text{ in.}^2/\text{ft}$$

Use No. 4 stirrups at 12 in. center-to-center with the spacing to be increased along the span.

**(iii) Maximum shear resistance:**

To ensure that the concrete in the web does not crush prior to yielding of the stirrups,

$$(V_n - V_p) \leq 0.25 f'_c b_v d_v$$

$$(V_n - V_p) = V_c + V_s = 75.0 + 253.0 = 335.8 \text{ kips}$$

$$0.25 f'_c b_v d_v = 0.25 \times 6.5 \times 6 \times 60.08 = 585.8 \text{ kips} > 335.8, \text{ O.K.}$$

**2. Interface shear transfer**

**(a) Dowel reinforcement design**

Assume that the critical section for shear transfer is the same as the vertical shear at plane  $0.05 L$  from the support face.

From load combination Strength I:

$$V_u = 1.25(5.4) + 1.5(10.8) + 1.75(73.8 + 30.6)$$

$$= 205.5 \text{ kips}$$

$$d_v = 74.35 \text{ in.}$$

$$V_{uh} = \frac{205.5}{74.35} = 2.76 \text{ kip/in.}$$

$$\text{Required } V_n = \frac{V_{uh}}{\phi} = \frac{2.76}{0.9} = 3.07 \text{ kip/in.}$$

From Equation 12.32,

$$\text{available } V_n = c A_{cv} + \mu [A_{vf} f_y + P_c]$$

For concrete placed clean, hardened concrete with interface contact not intentionally roughened,

$$c = 0.075 \text{ ksi} \quad \mu = 0.6$$

$$b_v = \text{contact width between slab and precast flange top} = 42 \text{ in.}$$

$$\frac{A_{cv}}{\text{in. depth}} = 42.0 \times 1.0 = 42.0 \text{ in.}^2$$

hence,  $3.07 = 0.075 \times 42.0 + 0.6(A_{vf} \times 60 + 0)$  to give  $A_{vf} \approx 0.0 \text{ in.}^2/\text{in.}$ ,  $< A_v = 0.40 \text{ in.}^2$  at 12 in. c/c vertical stirrups.

On this basis, no special additional dowel reinforcement is needed. LRFD, however, also requires that if the width  $b_v$  exceeds 36 in., a minimum of four bars are required as dowel reinforcement. Thus, use also two No. 3 dowels at 12 in. c/c in addition to the No. 4 vertical stirrups at 12 in. c/c, to give total  $A_{vf} = 0.62 \text{ in.}^2/\text{ft}$ .

**(b) Maximum and minimum dowel reinforcement**

$$f'_c = 4.0 \text{ ksi for the deck concrete}$$

$$\text{Actual provided } V_n = 0.075 \times 42 + 0.6 \left( \frac{0.62}{12} \times 60 \right) = 5.01 \text{ kips/in.}$$



From Equations 12.36 (a) and (b), the maximum allowable:

$$0.2f'_c A_{cv} = 0.2 \times 4.0 \times 42.0 = 33.6 \text{ kip/in.}$$

In both cases, more than provided  $V_n$ , O.K.

### 3. LRFD Minimum Longitudinal Reinforcement

The longitudinal reinforcement at *each* beam section along the span has to satisfy equation 12.29:

$$A_s f_s + A_{ps} f_{ps} \geq \frac{M_u}{d_v \phi_f} + 0.5 \frac{N_u}{\phi_c} + \left( \frac{V_u}{\phi_v} - 0.5V_s - V_p \right) \cot \theta$$

From Tables 12.8 and 12.9 at  $x = 0$  from support,  $V_u = 1.25(47.9 + 55.3 + 6.0) + 1.50(12.0) + 1.75(78.1 + 33.9) = 350 \text{ kip}$

$V_s$  based on only the No. 4 stirrups = 260.4 kips

$$M_u = 0$$

$$N_u = 0$$

$$\cot \theta = \cot 22^\circ = 2.475$$

$$\text{hence, } \frac{M_u}{d_v \phi_f} + 0.5 \frac{N_u}{\phi_c} + \left( \frac{V_u}{\phi_v} - 0.5V_s - V_p \right) \cot \theta$$

$$= 0 + 0 + \left( \frac{350}{0.9} - 0.5 \times 253.0 - 24.5 \right) (2.356) = 560.5 \text{ kips}$$

Number of straight strands at the support = 36

Number of draped strands at the support = 12

From the assumed crack plane intersection with the strands in Figure 12.14, the distance of the intersection from the support =  $6 + 4.22 \cot 23^\circ = 15.9 \text{ in.}$  where the strand stops at 6 in. from face of the support.

Transfer length =  $60 \times \text{strand diameter} = 30 \text{ in.}$

The available prestress of the 36 straight strands at the support face is a portion of the effective prestress,  $f_{pe}$ .

$$\text{Hence, use } f_{pe} = 149.0 \times \frac{15.9}{30.0} = 79.0 \text{ ksi}$$

For the top draped strands, the crack in Figure 12.15 intersects the strands at a distance  $\cong 140 \text{ in.}$  from the support face (compute from geometry of the dimensions in Figure 12.14). Consequently the effective prestress can be approximated at  $f_{pe} = 149.0 \text{ ksi.}$

$$A_s f_s + A_{ps} f_{ps} = 0 + 36 \times 0.153(79.0) + 12 \times 0.153(149.0)$$

$$= 435.1 + 273.6 = 708.7 \text{ kips}$$

$> 560.5 \text{ kips}$ , hence, no additional longitudinal reinforcement is needed.

### 4. Deflection and camber

#### (i) Immediate deflection due to permanent loads

Compute the camber and deflection of the beam as detailed in the discussions and numerous examples of chapter 7.

From the deflection table in Figure 7.6,

$$\text{Midspan } \delta = \frac{PL^2}{8E_c I_g} \left[ e_c + (e_e - e_c) \frac{4}{3} \frac{a^2}{L^2} \right]$$

$$\text{here, } a = \frac{L}{2}$$

$$\delta = \frac{PL^2}{E_c I_g} \left[ \frac{e_c}{8} + \frac{(e_e - e_c)}{24} \right]$$

From Example 12.1:

$$\begin{array}{ll}
 P_i = 1488 \text{ kips} & I_{cc} = 1,095,290 \text{ in.}^4 \\
 e_c = 29.68 \text{ in.} & w_{s+h} = 0.922 \text{ kip/ft} \\
 e_e = 17.7 \text{ in.} & w_{\text{barrier}} = 0.300 \text{ kip/ft} \\
 E_{ci} = 4620 \text{ ksi} & A_c = 767 \text{ in.}^2 \\
 E_{ce} = 4890 \text{ ksi} & S_b = 14,915 \text{ in.}^3 \\
 w_D = 0.779 \text{ kip/ft} & S^t = 15,421 \text{ in.}^3 \\
 & I_c = 545,897 \text{ in.}^4
 \end{array}$$

$$\begin{aligned}
 \delta_i &= \frac{1488(120 \times 12)^2}{4620 \times 545,897} \left[ \frac{29.68}{8} + \frac{(17.7 - 29.68)}{24} \right] \\
 &= 1.22 (3.71 - 0.50) = 3.92 \text{ in. } \uparrow \text{ (camber)}
 \end{aligned}$$

$$w_D \text{ per inch} = 0.799/12 = 0.065 \text{ kip/in.}$$

$$\begin{aligned}
 \delta_D &= \frac{5wL^4}{384E_{ci}I_g} = \frac{5(0.065)(120 \times 12)^4}{384 \times 4620 \times 545,894} \\
 &= 1.44 \text{ in. } \downarrow
 \end{aligned}$$

$$w_{s+h} = 0.922 \text{ kip/ft} = 0.077 \text{ kip/in.}$$

$$\delta_D = \frac{5(0.077)(120 \times 12)^4}{384 \times 4888 \times 545,894} = 1.61 \text{ in. } \downarrow$$

$$w_{\text{barrier}} = 0.300 \text{ kip/ft} = 0.025 \text{ kip/in.}$$

$$\delta_D = \frac{5(0.025)(120 \times 12)^4}{384 \times 4888 \times 1,095,290} = 0.26 \text{ in. } \downarrow$$

**(ii) Immediate deflection due to transient loads**

Live load deflection limit =  $L/800$ .

LRFD specifications require that all the bridge deck beams be assumed to deflect equally under applied live load and impact. They also stipulate that the long-term deflection may be taken as four times the immediate deflection. This stipulation is too general and the designer is well-advised to use other more refined methods. The larger is the span the more is the needed accuracy. It should be emphasized that computed deflection values can differ from actual deflections by as much as 30 to 40% depending on the concrete modulus and stress-strain relationship assumed and the degree of accuracy of the method used in the computation.

The following deflection computation methods from chapter 7 can give reasonable step-by-step values during the loading history

- PCI multipliers method (Sec. 7.7.1)
- Incremental time-step method (Sec. 7.7.2)
- Approximate time-step method (Sec. 7.7.3)

From Figure 12.11 in Example 12.1, the number of bridge beams = 6 and the number of lanes = 4

$$\begin{aligned}
 \text{DFD} &= \text{distribution factor for deflection} \\
 &= \text{number of lanes divided by number of beams} \\
 &= \frac{4}{6} = 0.667 \text{ lanes/beam}
 \end{aligned}$$

It is more conservative to use moment distribution factor  $\text{DFM} = 0.732$

**Table 12.12** Long-Term Camber and Deflection

	Transfer $\delta_p$ (in.)	Non- composite PCI Multipliers	Composite PCI Multipliers	$\delta_{final}$ (in.)
Prestress	3.92 $\uparrow$	1.80	2.20	8.62 $\uparrow$
$W_d$	-1.44 $\downarrow$	1.85	2.40	-3.47 $\downarrow$
	Net 2.48 $\uparrow$			Net 5.15 $\uparrow$
$w_{S+H}$	-1.61 $\downarrow$	1.85	2.40	-3.84 $\downarrow$
$w_{barrier}$	-0.26 $\downarrow$	1.85	2.30	-0.60 $\downarrow$
$\delta_{LL}$	-0.41 $\downarrow$			-0.41 $\downarrow$
$\delta_{Lt}$	-0.78 $\downarrow$			-0.78 $\downarrow$
Final $\delta$	2.48 $\uparrow$			+0.48 $\downarrow$

Design lane load,  $W = 0.64$  DFM

$$= 0.64 \text{ kip/ft (0.732)} = 0.468 \text{ kip/ft/beam}$$

$$= 0.039 \text{ kip/in./beam}$$

$$\delta_{LL} = \frac{5}{384E_cI_{cc}} = \frac{5(0.039)(120 \times 12)^4}{384 \times 4888 \times 1,095,290} = 0.41 \text{ in. } \downarrow$$

The transient truck load and impact deflection is determined from influence lines of wheel position for maximum moment. For a 120-ft span, the 72 kip



**Photo 12.6** West Kowloon Expressway Viaduct, Hong Kong, 1997. 4.2-Km dual three-lane causeway connecting Western Harbor Crossing to new airport (Courtesy Institution of Civil Engineers, London)

resultant of the axial loads falls at 2.33 ft from the midspan. The deflection at midspan = 0.8 in. ↓

$$\delta_{LT} = 0.8(IM)(DFM) = 0.8(1.33)(0.732) = 0.78 \text{ in.} \downarrow$$

Using the PCI multipliers from Table 7.1, a summary of the long-term cambers and deflections are given in Table 12.11.

$$\text{Allowable deflection } \delta = \frac{L}{800} = \frac{120 \times 12}{800} = 1.80 \text{ in. (down)}$$

$$> \text{ actual} = 0.49 \text{ in. O.K.}$$

Adopt the bridge deck design of the interior beam in Example 12.1 and 12.2.

## 12.11 STANDARD AASHTO FLEXURAL DESIGN OF PRESTRESSED BRIDGE DECK BEAMS (LFD)

### Example 12.3

Design for flexure, an interior beam of the bridge deck in Example 12.1 (adopted from Ref. 12.11) using the standard AASHTO Design Specifications for HS-20 lane and truck loads. Use the same data and allowable stresses of the materials as in the indicated example except where they differ from the LRFD allowable stresses.

#### Solution:

#### 1. Transformed deck slab controlling width

From example 12.2 Step 1,

$$E_{cs} = 3830 \text{ psi}$$

$$E_{ci} = 4620 \text{ psi at transfer}$$

$$E_{ce} = 4890 \text{ psi at service}$$

Average spacing between beams = 108 in.

Transformed flange width  $b_m = 84$  in.

#### 2. Properties of Section

*Non-Composite*

$$A_c = 767 \text{ in.}^2$$

$$h = 72 \text{ in.}$$

$$I_c = 545,894 \text{ in.}^4$$

$$c_b = 36.60 \text{ in.}$$

$$c_t = 35.40 \text{ in.}$$

$$r^2 = 1051 \text{ in.}^2$$

$$S_b = 14,915 \text{ in.}^3$$

$$S_t = 15,421 \text{ in.}^3$$

*Composite*

$$A_c = 1402 \text{ in.}^2$$

$$h = 80 \text{ in.}$$

$$I_{cc} = 1,095,290 \text{ in.}^4$$

$$c_{bc} = 54.6 \text{ in.}$$

$$c_{tc} = 17.4 \text{ in.}$$

$$c_{tsc} = 25.4 \text{ in.}$$

$$r^2 = 712 \text{ in.}^2$$

$$S_{bc} = 20,060 \text{ in.}^3$$

$$S_c^t = 62,950 \text{ in.}^3$$

$$S_c^b = 55,284 \text{ in.}^3$$

#### 3. Bending moment and shear forces

self-weight

$$W_D = 799 \text{ lb/ft}$$

slab

$$W_{SD1} = 900 \text{ lb/ft}$$

0.5 " haunch

$$= 22 \text{ lb/ft}$$

Barrier weight

$$W_{SD2} = 100 \text{ lb/ft}$$

2-in. future wearing surface

$$W_{SD3} = 200 \text{ lb/ft}$$

Live load (truck load) in AASHTO standard specifications would be based on HS-20 trucks.

Number of lanes =  $48/12 = 4$  lanes

**(a) Distribution factor for moment**

Live load in the standard specifications is *either* the standard truck or lane loading corresponding to HS-20. In LRFD, both have to be used in the design. From Section 12.2.2, the live load distribution factor for moment for a precast beam is  $DF_m = S/5.5 = 9.0/5.5 = 1.636$  wheels per beam, where  $S$  = average spacing between beams in feet.

$$\frac{1}{2} DF_m = 0.818 \text{ lanes per beam}$$

$$\begin{aligned} \text{the live load impact factor } I &= \frac{50}{L + 125} \leq 30\% \quad \text{or,} \\ &= \frac{50}{120 + 150} = 0.204 \end{aligned}$$

In LRFD, This factor has a maximum 33% value hence,

$$\begin{aligned} V_{LL+I} &= (\text{shear force per lane}) (DFM) (1 + I) \\ &= (\text{shear force per lane}) (0.818) (1 + 0.204) \text{ kips} \\ &= (\text{shear force per lane}) (0.985) \text{ kips} \\ M_{LL+I} &= (\text{moment per lane}) (DFM) (1 + I) \\ &= (\text{moment per lane}) (0.818) (1 + 0.204) \text{ kips} \\ &= (\text{moment per lane}) (0.985) \text{ kips.} \end{aligned}$$

Load contributions from Equation 12.5 and Table 12.1 show that load combination Group I controls.

$$\text{Group I service load design} = 1.00 D + 1.00 (L + I)$$

$$\text{Group I factored load design} = 1.3 [1.00D + 1.67(L + I)]$$

**(b) Shear and bending moments**

$$V_x = (w) (0.5 L - X)$$

$$M_x = 0.5 (w) (X) (L - X)$$

As an example, the following are computations for the shear and moment at midspan, at the support and at the critical shear section:

At midspan,  $V_x = 0$

$$M_D = 0.5(0.799) (60) (60) = 1438 \text{ ft-kip}$$

At support,  $V = 0.799(60) = 47.9$  kip

At critical shear section,

The cgs of the prestressing steel is  $e = 17.1$  in. near the support section (see subsequent computations)

$$d = 80 - 17.1 = 62.9 \text{ in.} > 0.80 h = 64 \text{ in.}$$

Use  $d = 64.0$  in.

Critical shear section at  $h/2 = 80/2 = 40$  in. = 3.33 ft

$$V_{3.33} = 0.799 [(0.5) (120) - 3.33] = 45.3 \text{ kips}$$

$$M_{3.33} = 0.5(0.799) (3.33) (120 - 3.33) = 155.4 \text{ ft-kip}$$

**Table 12.12** Standard AASHTO (LFD) Service Shear and Moment Due to Dead Load

Distance <i>X</i>	Section <i>X/L</i>	Beam Weight $W_D$		(Slab + Haunch) Weight $W_{SD1}$		Barrier Weight $W_{SD2}$		Wearing Surface $W_{SD3}$		Live Load Plus Impact	
		Shear $V_g$	Moment $M_g$	Shear $V_s$	Moment $M_s$	Shear $V_b$	Moment $M_b$	Shear $V_{WS}$	Moment $M_{WS}$	Shear $V_{LL+I}$	Moment $M_{LL+I}$
ft		kips	ft-kips	kips	ft-kips	kips	ft-kips	kips	ft-kips	kips	ft-kips
0	0.0	47.9	0.0	55.3	0.0	6.0	0.0	12.0	0.0	65.4	0.0
3.33*	0.028	45.3	155.4	52.2	179.3	5.7	19.4	11.3	38.9	63.6	211.5
12	0.1	38.4	517.8	44.3	597.5	4.8	64.8	9.6	129.6	58.3	699.7
24	0.2	28.8	920.4	33.2	1,062.1	3.6	115.2	7.2	230.4	51.2	1,229.1
36+	0.3	19.2	1,208.1	22.1	1,394.1	2.4	151.2	4.8	302.4	44.1	1,588.4
48	0.4	9.6	1,380.7	11.1	1,593.2	1.2	172.8	2.4	345.6	37.0	1,799.6
60	0.5	0.0	1,438.2	0.0	1,659.6	0.0	180.0	0.0	360.0	29.9	1,851.6

\*Critical section for shear

+Harp point

The values for shear and moment for all permanent and transient loads are tabulated in Table 12.12 (Ref. 12.11). Compare the tabulated values with those computed by the LRFD method in Table 12.9 and 12.10.

#### 4. Design of Bulb-Tee Prestressed Interior Beam

##### 1. Selection of prestressing strands

Due to applied gravity loads, the unfactored stress at bottom fibers:

$$f_b = \frac{M_D + M_{SD1}}{S_b} + \frac{M_{SD2} + M_{SD3} + M_{LL+I}}{S_{bc}}$$

$$= \frac{(1438 + 1660)12}{14,915} + \frac{(180 + 360 + 1852)12}{20,060} = 3.923 \text{ ksi}$$

Allowable tensile stress  $f_t = 6\sqrt{f'_c} = 6\sqrt{6500} = 484 \text{ psi} = 0.484 \text{ ksi}$

Required precompressive stress at the bottom fibers after losses =  $(f_b - f_t)$

$$f_{bp} = 3.923 - 0.484 = 3.439 \text{ ksi}$$

Assume that the tendon c.g.s. is at a distance  $y_b = 4 \text{ in.}$  from the bottom fibers.

$$e_c = c_c - y_b = 36.60 - 4.00 = 32.60 \text{ in.}$$

$$f_{bp} \text{ due to prestress} = \frac{P_e}{A_c} + \frac{P_e e_c}{S_b} \text{ or } 3.439 = \frac{P_e}{767} + \frac{P_e \times 32.6}{14,915}$$

$$P_e = 986 \text{ kips}$$

Assume total prestress loss = 25%

$$P_i = \frac{986}{1 - 0.25} = 1315 \text{ kips}$$

Assume using 1/2-in. diameter 7-wire 270-K low-relaxation strands ( $A_{ps} = 0.153 \text{ in.}^2$ ),

$$\text{Required number of strands} = \frac{1315}{0.153 \times 202.5} = 42.44 \text{ strands}$$

Try 44 strands.

After trials and adjustments, assume that the strands pattern is as shown in Figure 12.16 with 10 strands harped at 48 ft from the support.

From data,  $c_b = 36.60 \text{ in.}$  and  $c_t = 72 - 36.60 = 35.40 \text{ in.}$

$$e_e = c_b - [2 \times 70 + 2 \times 68 + 2 \times 66 + 2 \times 64 + 2 \times 62 + 2 \times 8 + 8 \times 6 + 12 \times 4 + 12 \times 2] / 44 = 36.60 - 18.09 = 18.51 \text{ in.}$$

$e_{3.33} = 17.1 \text{ in.}$  at the critical shear section.

$$e_c = c_b - [2 \times 16 + 2 \times 14 + 2 \times 12 + 2 \times 10 + 4 \times 8 + 8 \times 6 + 12 \times 4 + 12 \times 2] / 48 = 36.6 - 5.81 = 30.79 \text{ in.}$$

Computing the total losses in prestress by the detailed method and the examples of Chapter 3, the total loss of prestress was 24.9%.

$$f_{pe} \text{ before losses} = 0.75(270) = 202.5 \text{ ksi}$$

hence, adjusted  $f_{pe} = 202.5(1 - 0.249) = 152.1 \text{ ksi}$

$$P_e = 48(0.153)(152) = 1024 \text{ kips}$$

Common practice assumes that a prestress relaxation and other losses at prestressing amount to 9 to 10%

Use 9% here to get  $f_{pi} = 202.5(1 - 0.09) = 184.3 \text{ ksi}$

$$P_i = 44(0.153)(184.3) = 1240 \text{ kips}$$

From Example 12.2,

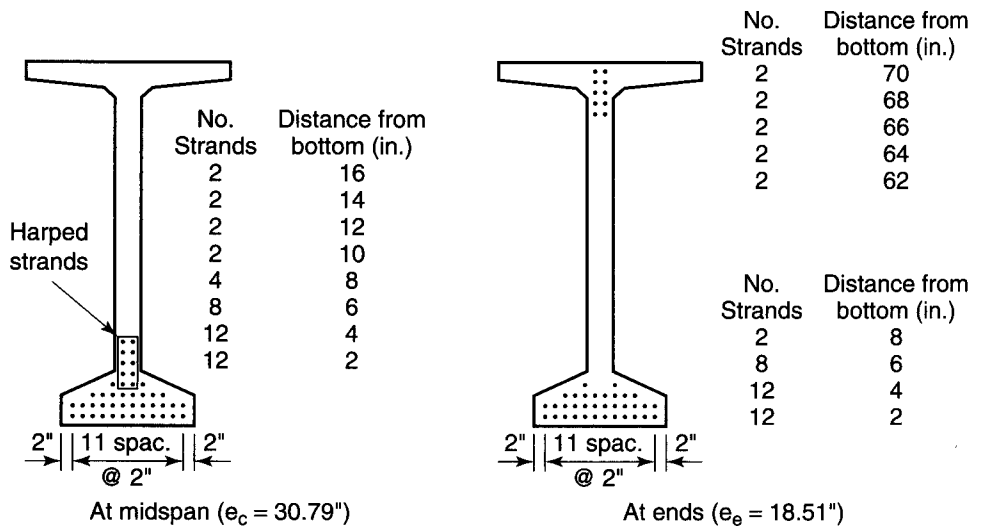
$$f_{ci} = 0.6 f'_c = 0.6(5500) = 3300 \text{ psi (c)}$$

$$f_{ti} = 7.5 \sqrt{f'_{ci}} = 7.5 \sqrt{5500} = 556 \text{ psi (T)}$$

If the computed tensile stress at transfer exceeds 200 psi or  $3\sqrt{f'_{ci}} = 220 \text{ psi}$ , whichever is small, bonded reinforcement has to be provided to resist the total tensile force in the concrete, computed on the basis of uncracked section.

**2. Check of concrete unfactored stresses**

The standard AASHTO allowable stresses are as follows, Case I for all load combinations:



**Figure 12.15** Bulb-tee prestressing strand pattern

$$\text{Precast beam } f_c = 0.60 f'_c = 0.6(6500) = 3900 \text{ psi}$$

$$\text{Deck slab } f_c = 0.60 f'_c = 0.6(4000) = 2400 \text{ psi}$$

Case (II) for effective pretension force + permanent dead loads:

$$\text{Precast beam } f_c = 0.40 f'_c = 0.4(6000) = 2400 \text{ psi}$$

$$\text{Deck slab } f_c = 0.40 f'_c = 0.4(4000) = 1600 \text{ psi}$$

Case (III) for live load +  $\frac{1}{2}$  (pretensioning force + dead load)

$$\text{Precast beam } f_c = 0.40 f'_c = 0.4(6500) = 2600 \text{ psi}$$

$$\text{Deck slab } f_c = 0.40 f'_c = 0.4(4000) = 1600 \text{ psi}$$

$$\text{Allowable tension } f_t = 6\sqrt{f'_{ci}} = 6\sqrt{6500} = 484 \text{ psi}$$

$$\text{Allowable } f_i \text{ at transfer} = 3\sqrt{f'_c} = 242 \text{ psi}$$

**a. Stresses at Transfer**

Initial  $f_{pi} = 0.7 f_{pu} = 202.5$  ksi. Common practice assumes that initial relaxation losses at prestressing amount to 9 to 10%. Use 9% reduction in  $f_{pi}$ .

hence,  $P_i = (0.9)(202.5)(0.153 \times 48) = 1338$  kips

**i. Support Section**

From Chapter 4, Equation 4.1 (a),

$$\begin{aligned} f^t &= -\frac{P_i}{A_c} \left( 1 - \frac{e_c c_t}{r^2} \right) - \frac{M_D}{S^t} \\ &= -\frac{1240}{767} \left( 1 - \frac{18.51 \times 35.40}{712} \right) - 0 = -0.129 \text{ ksi (C), O.K.} \end{aligned}$$

$$\begin{aligned} f_b &= -\frac{P_i}{A_c} \left( 1 + \frac{e_c c_b}{r^2} \right) + \frac{M_D}{S^t} \\ &= -\frac{1240}{767} \left( 1 + \frac{18.51 \times 36.30}{712} \right) + 0 \\ &= -3.14 \text{ ksi (C)} \cong f_{ci} = 3.3 \text{ ksi O.K.} \end{aligned}$$

**(ii) Midspan Section.**

$$\begin{aligned} f^t &= -\frac{1240}{767} \left( 1 - \frac{30.79 \times 35.40}{712} \right) - \frac{1438 \times 12}{15,421} \\ &= 0.858 - 1.119 = -0.261 \text{ ksi (C), no tension allowed, hence, O.K.} \end{aligned}$$

$$\begin{aligned} f_b &= -\frac{1240}{767} \left( 1 + \frac{30.79 \times 36.60}{712} \right) + \frac{1438 \times 12}{14,915} \\ &= -4.175 + 1.157 = -3.018 \text{ ksi (C)} < 3.300 \text{ ksi allowed O.K.} \end{aligned}$$

**b. Stresses at Service load:**

**(i) Midspan Section precast section fiber stresses:**

concrete stress at top fibers at midspan due to all loads:

$$f^t = -\frac{P_e}{A_c} \left( 1 - \frac{e_c c_t}{r^2} \right) - \frac{M_D + M_{DS1}}{S^t} - \frac{M_{DS2} + M_{DS3}}{S^t_c} - \frac{M_{LL+I}}{S^t_c}$$

$$e_c = 30.79 \text{ in.} \quad e_e = 18.51 \text{ in.}$$

From the moment values at midspan tabulated in table 12.10 for load combinations:





**Photo 12.7** Natchez Parkway Arches, Nashville Tennessee, America's first segmental arch bridge; principal arch span is 582-ft. long and has a vertical clearance of 137 ft (Courtesy Figg Engineering Group, Tallahassee, Florida)

Case (I):

$$f^t = -\frac{1024}{767} \left( 1 - \frac{30.79 \times 35.40}{712} \right) - \frac{(1438 + 1660)12}{15,421} - \frac{(360 + 180)12}{62,950} - \frac{(1852)12}{62,950}$$

$$= 0.708 - 2.411 - 0.103 - 0.353 = -2.159 \text{ ksi (C)}$$

Case (II):

$$f^t = 0.708 - 2.411 - 0.103 = -1.806 \text{ ksi (C)}$$

Case (III):

$$f^t = 0.5(0.708 - 2.411 - 0.103) = -1.256 \text{ ksi (C)}$$

All compressive stress are less than the allowable  $f_c = 3900$  psi O.K.

(ii) Midspan section bottom fiber stresses

$$f_b = -\frac{P_e}{A_c} \left( 1 + \frac{e_c c_b}{r^2} \right) + \frac{M_D + M_{DS1}}{S_b} + \frac{M_{DS2} + M_{DS3}}{S_{bc}} + \frac{M_{LL+I}}{S_{bc}}$$

$$f_b = -\frac{1024}{767} \left( 1 + \frac{30.79 \times 36.60}{712} \right) + \frac{(1438 + 1660)12}{14,915} + \frac{(360 + 180)12}{20,060} + \frac{(1852)12}{20,060}$$

$$= -3.437 + 2.493 + 0.323 + 1.10 = 0.486 \text{ ksi (T)}$$

$$\cong \text{allowable } f_t = 0.484 \text{ ksi O.K.}$$

(iii) *Midspan slab top-fiber stresses, assuming concrete strength same as of the pre-cast beam*

Case (I):

$$f^t = -\frac{M_D + M_{DS1}}{S_b} - \frac{M_{LL+I}}{S_{bc}}$$

$$f^t = -\frac{(180 + 360)}{55,284} - \frac{1852(12)}{55,284} = -0.117 - 0.402$$

$$= -0.519 \text{ ksi (C)} < \text{allowable } f_c = 2400 \text{ ksi} \quad \text{O.K.}$$

Case (II):

$$f^t = -0.117 \text{ ksi (C)} \quad \text{O.K.}$$

Case (III):

$$f^t = 0.5(-0.117) - 0.402 = -0.461 \text{ ksi (C)} \quad \text{O.K.}$$

$$E_c = 33 W^{1.5} \sqrt{f'_c}$$

$$\text{Modular ratio} = \frac{\sqrt{4000} \text{ (slab)}}{\sqrt{6500} \text{ (beam)}} = 0.78$$

Hence reduce these stresses by the 0.78 multiplier in order to get the true stresses at the top slab fibers.

### 3. Ultimate Strength (Limit State at Failure)

#### a. Normal flexural resistance moment

$$M_U = 1.3 [M_D + M_{SD1} + M_{SD2} + M_{SD3} + 1.67 (M_{LL+I})]$$

$$= 1.3(1438 + 1660 + 180 + 360 + 1.67 \times 1852) = 8750 \text{ ft-kip}$$

From equation 12.9(c)

$$f_{ps} = f_{pu} \left[ 1 - \frac{\gamma}{\beta_1} \rho \frac{f_{pu}}{f'_c} \right]$$

For the depth of the compressive block use the slab  $f'_c = 4.0 \text{ ksi}$ ,  $\beta_1 = 0.85$

$$\gamma = 0.28 \text{ for low-relaxation strands}$$

$$b = \text{flange width} = 108 \text{ in.}$$

$$e_c = 30.79 \text{ in.}, \quad c_b = 36.60,$$

hence,  $y_b = 36.60 - 30.79 = 5.81 \text{ in.}$

$d_p$  = distance from the top of the deck to the centroid of the prestressing strands.

$$= \text{beam depth (h)} + \text{haunch} + \text{slab thickness } (h_f - y_b)$$

$$= 72 + (0.5 + 7.5) - 5.81 = 74.19 \text{ in.}$$

$$A_{ps} = 44(0.153) = 6.732 \text{ in.}^2$$

$$\rho = \frac{A_{ps}}{bd_p} = \frac{6.732}{108 \times 74.19} = 0.00084$$

Consequently,

$$f_{ps} = 270 \left[ 1 - \frac{0.28}{0.85} 0.00084 \frac{270}{4.0} \right] = 265.0 \text{ ksi}$$

$$a = \frac{A_{ps} f_{ps}}{0.85 f'_c b} = \frac{6.732 \times 265.0}{0.85 \times 4.0 \times 108} = 4.86 \text{ in.} < 7.5 \text{ in.}$$

hence design as rectangular section.

$$\begin{aligned} \text{Available } M_U &= \phi M_n = A_{ps} f_{ps} \left( d - \frac{a}{2} \right) \\ &= 1.0 \left[ 6.732 (265.0) \left( 74.19 - \frac{4.86}{2} \right) \right] \\ &= 128,018 \text{ in.-kip} > \text{required } M_U = 8750 \text{ ft-kip, O.K.} \\ c &= a/\beta_1 = 4.86/0.85 = 5.72 \text{ in.} \end{aligned}$$

$c/d_t = 5.72/74.19 = 0.24 < 0.42$  limit in Sec. 12.3.1; hence, the section is tension controlled and  $\phi = 1.0$  is verified.

**b. Maximum Reinforcement**

$$\begin{aligned} \rho \frac{f_{ps}}{f'_c} &\leq 0.36\beta_1 \leq 0.36 \times 0.85 = 0.306 \\ \rho \frac{f_{ps}}{f'_c} &= 0.00084 \times \frac{265}{4.0} = 0.0557 < 0.306 \quad \text{O.K.} \end{aligned}$$

**c. Minimum Reinforcement**

The total amount of pretensioned and post-tensioned reinforcement should be adequate to develop an ultimate moment such that

$$\phi M_n \geq 1.2 M_{cr}$$

From equation 12.13,

$$M_{cr} = (f_r + f_{ce})S_b - M_{dnc} \left[ \frac{S_{bc}}{S_b} - 1 \right]$$

$$f_r = 7.5\sqrt{f'_c} = 7.5\sqrt{6500} = 605 \text{ psi} = 0.605 \text{ ksi}$$

Concrete stress due to prestressing only, after all losses is  $f_b = 3.437 \text{ ksi (C)}$

$M_{dnc}$  = non-composite dead load moment due to beam self-weight and slab weight

$$= 1438 + 1660 = 3098 \text{ ft-kip}$$

$$1.2 M_{cr} = 1.2 \left[ \frac{1}{12} (0.605 + 3.437) 20,060 - 3098 \left( \frac{20,060}{14,915} - 1 \right) \right] = 6896 \text{ ft-kip}$$

It should be noted that contrary to the LRFD specifications, the standard specification stipulates that this requirement has to be satisfied only at the critical section.

**d. Pretensioned anchorage zone**

Before initial losses,  $f_{pi} = A_{ps}(0.75 f_{pu})$

$$= 6.732(0.75 \times 270) = 1363 \text{ kips}$$

$$4\% f_{pi} = 0.04 \times 1363 = 54.5 \text{ kips}$$

Allowable  $f_s = 20 \text{ ksi}$

$$\text{Hence, required } A_v = \frac{54.5}{20} = 2.73 \text{ in.}^2$$

Try No. 5 vertical stirrups in the rectangular anchorage zone region

$$A_v = 2 \times 0.305 = 0.61 \text{ in.}^2$$

$$\text{No. of stirrups} = \frac{2.73}{0.61} = 4.5$$

$$\text{Precast Section } d_p = (h - y_b) = 72 - 5.81 = 66.19 \text{ in.}$$

$$d_v = \left( d_p - \frac{a}{2} \right) = 66.19 - \frac{4.86}{2} = 63.76 \text{ in.}$$

Distance within which anchorage reinforcement has to be provided

$$= \frac{d_v}{4} = \frac{63.76}{4} = 15.94 \text{ in.}$$

Use five # 5 closed U-stirrups at 3 in. center-to-center at each beam end.

## 12.12 STANDARD AASHTO SHEAR-REINFORCEMENT DESIGN OF BRIDGE DECK BEAMS

### Example 12.4

Design for shear, an interior beam of the bridge deck in Example 12.3 using the standard AASHTO design specifications for HS-20 Lane and Truck loads. Use the same data and allowable stresses of the materials as in the indicated example. Use the refined flexural and web shear approach for determining the nominal strength of the plain concrete in the web. Also design the interface shear transfer reinforcement and check the deflection and camber of the beam.

### Solution:

#### 1. Shear Reinforcement

The AASHTO standard specification follows the ACI-318 code for shear and torsion which are detailed in Chapter 5, Sections 5.5 and 5.6 as well Section 5.18 for torsion.

$$V_s \leq \phi (V_c + V_s), \text{ where } \phi = 0.90 \text{ vs. } \phi = 0.85 \text{ in ACI.}$$

Other strength reduction factors,  $\phi$ , also differ from the ACI factors. The computations have to be based on a factored shear value at a distance  $1/2 h$  from the face of the support. The nominal shear strength,  $V_c$ , of the plain concrete in the web has to be the lesser of the flexural shear,  $V_{ci}$ , and the web shear,  $V_{cw}$ .

#### a. Flexural shear, $V_{ci}$

From Equation 5.11,

$$V_{ci} = 0.6\lambda \sqrt{f'_c} b_w d_p + V_d + \frac{V_i}{M_{\max}} (M_{cr}) \geq 1.7\lambda \sqrt{f'_c} b_w d_p$$

where  $b_w = 6 \text{ in.}$

From table 12.12 for standard AASHTO loads in Example 12.3

$$\begin{aligned} V_d &= \text{total unfactored dead load at the critical section} \\ &= 45.3 + 52.2 + 5.7 + 11.3 = 114.5 \text{ kips} \end{aligned}$$

$$V_{LL+i} \text{ (unfactored)} = 63.6 \text{ kips}$$

$$\begin{aligned} V_U &= \text{factored shear force at the critical section} \\ &= 1.3(V_d + 1.67V_{LL+i}) \\ &= 1.3(114.5 + 1.67 \times 63.6) = 286.9 \text{ kips} \end{aligned}$$

$$M_d = 155.4 + 179.3 + 19.4 + 38.9 = 393.0 \text{ kips}$$

$$M_{LL+i} = 211.5 \text{ kips}$$

$$\begin{aligned} M_U &= 1.3 (M_d + 1.67 M_{LL+i}) \\ &= 1.3(393.0 + 1.67 \times 211.5) = 970.1 \text{ ft-kips} \end{aligned}$$

$$\begin{aligned} V_i &= \text{factored shear force at the section due to externally} \\ &\quad \text{applied loads occurring simultaneously with } M_{\max}. \\ &= (V_U - V_D) = 286.9 - 114.5 = 172.4 \text{ kips. This is on the} \\ &\quad \text{conservative side since the factored } V_U \text{ is reduced} \end{aligned}$$

by the unfactored  $V_d$ .

$$M_{\max} = (M_U + M_d) = 970.1 - 393.0 = 577.1 \text{ ft-kip}$$

From equation 5.12,

$$M_{cr} = S_{bc} (6\sqrt{f'_c} + f_{ce} - f_d). \text{ Note that the factor "6" in the term } 6\sqrt{f'_c} \text{ is conservative and maybe unjustified since the modulus of rupture, } f_r, \text{ is taken as } 7.5\sqrt{f'_c} \text{ and tests indicate even higher values.}$$

$f_{ce}$  = compressive stress due to prestress after losses at the extreme fibers of the section where tensile stress is caused by externally applied load.

$$= -\frac{P_e}{A_c} \left( 1 + \frac{e_{e1}c_b}{r^2} \right), \text{ where } e_{e1} = 19.5 \text{ in. at the critical section}$$

$$= -\frac{1024}{767} \left( 1 + \frac{19.5 \times 36.60}{712} \right) = -2.673 \text{ ksi (C)}$$

$f_d$  = stress due to unfactored dead load at the extreme fibers of the section where tensile stress is caused by externally applied load

$$= \left[ \frac{(155.4 + 179.3)(12)}{14,915} + \frac{(19.4 + 38.9)12}{20,060} \right] = 0.304 \text{ ksi}$$

$$\text{Hence, } M_{cr} = \frac{20,060}{12} \left( \frac{6\sqrt{6500}}{1000} + 2.673 - 0.304 \right) = 4776 \text{ ft-kip}$$

$y_b$  = distance of cgs of the prestressing strands at the critical section from the bottom fibers = 17.12 in.

$$d_{pc} = h_c - y_b = 80 - 17.12 = 62.88 \text{ in.}$$

$$0.8 h_c = 64 \text{ in., controls}$$

$$\text{used } d_p = 64 \text{ in.}$$

Hence,

$$V_{ci} = \frac{0.6\sqrt{6500}(6.0 \times 64)}{1000} + 114.5 - \frac{172.4 \times 4776}{577.1} = 1,559.8 \text{ kips}$$

$$\text{Minimum } V_{ci} = 1.7\sqrt{f'_c} b_w d$$

$$= \frac{0.6\sqrt{6500}(6.0 \times 64)}{1000} = 52.6 \text{ kips} \ll 1,559.8 \text{ kips O.K.}$$

**b. Web shear  $V_{cw}$**

From Equation 5.15,

$$V_{cw} = (3.5\lambda\sqrt{f'_c} + 0.3\bar{f}_c)b_w d_p + V_p$$

where  $f'_c$  is termed as  $F_{pc}$  in AASHTO notation. It is the concrete stress at the centroid of the section resisting all externally applied load.

$$\bar{f}_c = -\frac{P_e}{A_c} \left( 1 - \frac{e_{e1}(c_{bc} - c_b)}{r^2} \right) + \frac{M_D(c_{bc} - c_b)}{I_c}$$

From section properties,  $c_{bc} = 54.6$  in. and  $c_b = 36.6$  in.

$$\bar{f}_c = -\frac{1024}{767} \left( 1 - \frac{19.5(54.60 - 36.60)}{712} \right) + \frac{334.7 \times 12(54.60 - 36.60)}{545,894}$$

$$= -0.676 + 0.132 = -0.545 \text{ ksi (C)}$$

$V_p$  = vertical component of prestressing force.

From Figure 12.15, the tangent of angle  $\psi$  subtended by the 10 harped

$$\text{tendons} \cong \frac{65 - 15}{48.5 \times 12} \cong \sin \psi \cong 0.086$$

$$V_p = A_{ps} f_{pe} \sin \psi = (10 \times 0.153) 149.0 \times 0.086 = 19.61 \text{ kips}$$

Hence,

$$\begin{aligned} V_{cw} &= \left( \frac{3.5 \times 1.0 \sqrt{6500}}{1000} + 0.3 \times 0.545 \right) 6.0 \times 64 + 19.61 \\ &= 171.15 + 19.61 = 190.8 \text{ kips, controls since it is less than } V_{ci} \end{aligned}$$

### c. Selection of web steel

$$V_c = 190.8 \text{ kips}$$

$$V_U < \phi (V_c + V_s) \quad \text{or,} \quad V_s = \left( \frac{V_U}{\phi} - V_c \right)$$

$$\text{Required } V_s = \frac{286.9}{0.90} - 190.8 = 128.0 \text{ kips}$$

$$\text{Maximum allowable } V_s = 8\sqrt{f'_c} b_w d_v = 9\sqrt{6500} \frac{6.0 \times 64}{1000} = 247.7 \text{ kips}$$

> 128.0 kips O.K. (the section depth adequate for shear).

$$V_s = \frac{A_v f_y d_v}{s}$$

$$\text{Required } \frac{A_v}{s} = \frac{V_s}{f_y d_v} = \frac{128.0}{60.0 \times 64.0} = 0.033 \text{ in.}^2/\text{ft} = 0.0028 \text{ in.}^2/\text{in.}$$

$$\text{Minimum } \frac{A_v}{s} = \frac{50b_w}{f_y} = \frac{(50 \times 6.0)}{60,000} = 0.005 \text{ in.}^2/\text{in.}, \text{ controls.}$$

Using No. 4 two-legged U-stirrups in the rectangular end section,  $A_v = 2 \times 0.20 = 0.40 \text{ in.}^2$

$$\text{Spacing } s = \frac{A_v}{\text{unit } A_v} = \frac{0.40}{0.005} = 80 \text{ in.}$$

Maximum allowable spacing  $s = 0.75 h_c$  or 24 in.

$$= 0.75(72 + 7.5 + 0.5) = 60 \text{ in. or } 24 \text{ in.}$$

Use No. 4 U-stirrups at 12 in. center-to-center in the rectangular end block section over a width  $= h = 80$  in. Beyond the end of the anchorage block, stirrups would no longer be needed. However, it is useful to use minimum vertical mesh reinforcement in the web along the span. The 12-in. spacing is necessitated by the interface horizontal shear requirement.

## 2. Interface shear reinforcement

Determine the interface shear force for the critical section at  $\frac{1}{2} h_c$  from the support.

### a. Contact surface roughened or minimum ties used

$$V_U = 286.9 \text{ kips} < V_{nh}$$

$V_{nh}$  = nominal horizontal shear strength

$$\cong \frac{V_U}{\phi} = \frac{286.9}{0.9} = 318.8 \text{ kips}$$

Allowable  $V_{nh} = b_v d_{pc}$  where

$b_c$  = width of cross-section at the contact surface being investigated for horizontal shear = 42.0 in.

$d_{pc}$  = 62.88 in. from before

$$\text{Available } V_{nh} = \frac{80(42.0 \times 62.88)}{1000} = 211.3 \text{ kips} < 318.9 \text{ kips}$$

hence, dowel reinforcement is needed.

**b. Minimum ties provided and contact surface roughened**

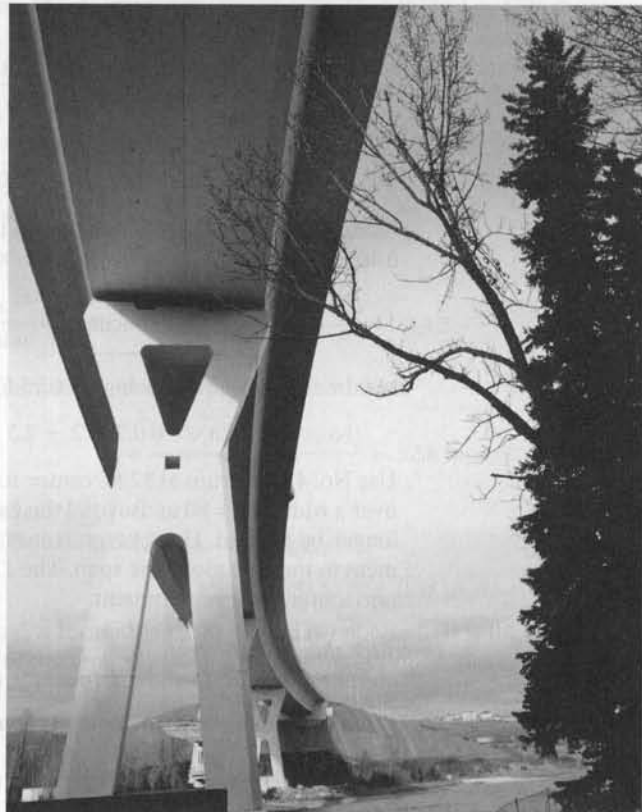
$$V_{nh} = 350b_v d_{pc} = \frac{350(42.0 \times 62.88)}{1000} = 924.3 \text{ kips} > 318.8 \text{ kips O.K.}$$

Use  $V_{nh} = 318.8$  kips  
From equation 5.33,

$$\text{Minimum } A_{vh} = \frac{50b_v l_{vh}}{f_y} = \frac{50b_v s}{f_y} \text{ per dowel}$$

Assume 12-in. dowel spacing,

$$\text{Minimum } A_{vh} \text{ per dowel} = \frac{(50)(42 \times 12)}{60,000} = 0.42 \text{ in.}^2/\text{ft}$$



**Photo 12.8** Pier support for Stoney Trail Bow River segmental Bridge, Calgary, Alberta, span 1562 ft, deck width 69 ft, the deck rises 89 to 118 ft above the river valley (Courtesy James Skeet-Reid Crowther Engineering, Calgary)

Available dowels form shear reinforcement:

$$= \text{No. 4 U-stirrups at 12 in. c./c.} = 0.40 \text{ in.}^2/\text{ft} \quad \text{O.K.}$$

Beyond the rectangular end block zone of 80 in., add in the web additional #4 dowels at 12 in. c./c. to compliment the single #4 bars available in the 6-in. thick web.

$$\text{Maximum allowable spacing} = 4 b_w = 4 \times 6 = 24 \text{ in.} \quad \text{O.K.}$$

Note that the vertical web shear reinforcement is utilized here to provide for the required dowel reinforcement.

### 3. Deflection Computations

The deflection computations are similar to those given in Example 12.2 except that in the standard AASHTO specifications, fatigue live load for deflection is disregarded. From Table 12.11, Example 12.2, the final long-term deflection becomes:

$$\delta = -8.62 + 3.46 + 3.86 + 0.60 + 0.41 = -0.29 \text{ in. (camber)}$$

$$< \frac{L}{800} = \frac{120 \times 12}{800} = 1.80 \text{ in.} \quad \text{O.K.}$$

Adopt the bridge-deck design of the interior prestressed beam in Examples 12.3 and 12.4.

## 12.13 SHEAR AND TORSION REINFORCEMENT DESIGN OF A BOX-GIRDER BRIDGE

### Example 12.5

A single span composite two-lane box girder bridge has a span of 90'-0" (27.5m). The deck is composed of seven AASHTO BIII-48 box beams at 4'-0" on centers to form a 28'-0" bridge deck with a traffic pathway width = 25'-0" as shown in Figure 12.16. Each beam is subjected to a factored shear  $V_U = 140$  kips at the critical support section, a corresponding moment at that section = 320 ft-kip and a torsional moment  $T_U = 165$  ft-kip.

Design the shear and torsional reinforcement for this bridge section, using the LRFD expressions, given:

$$f'_c = 5.0 \text{ ksi}$$

$$f'_{ci} = 4.0 \text{ ksi}$$

$$f_{pu} = 270.0 \text{ ksi}$$

$$f_{py} = 0.90 f_{pu} = 243.0 \text{ ksi}$$

$$f_{pi} < 0.75 f_{pu} = 202.5 \text{ ksi}$$

$$\text{Total prestress loss} = 22\%$$

$$f_y = 60.0 \text{ ksi}$$

$$E_{ps} = 28,500 \text{ ksi}$$

$$E_s = 29,000 \text{ ksi}$$

$$A_c = 813 \text{ in.}^2$$

$$h = 39 \text{ in.}$$

$$I_g = 168,367 \text{ in.}^4$$

$$c_b = 19.29 \text{ in.}$$

$$c_t = 19.71 \text{ in.}$$

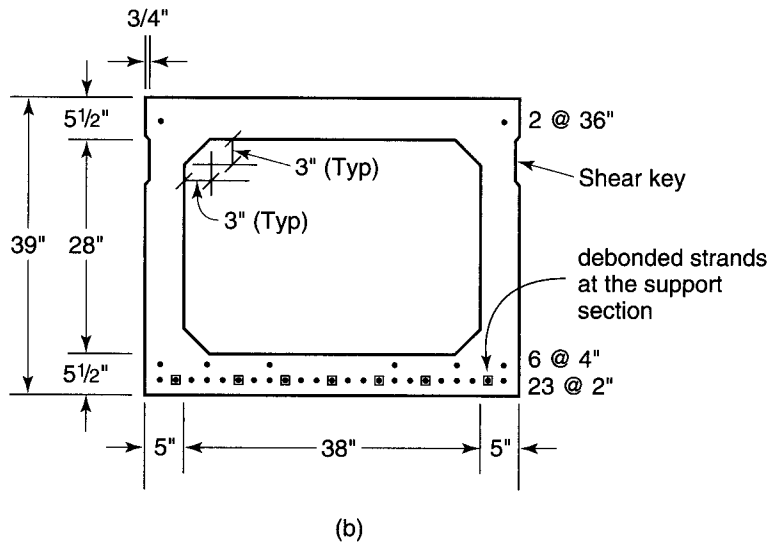
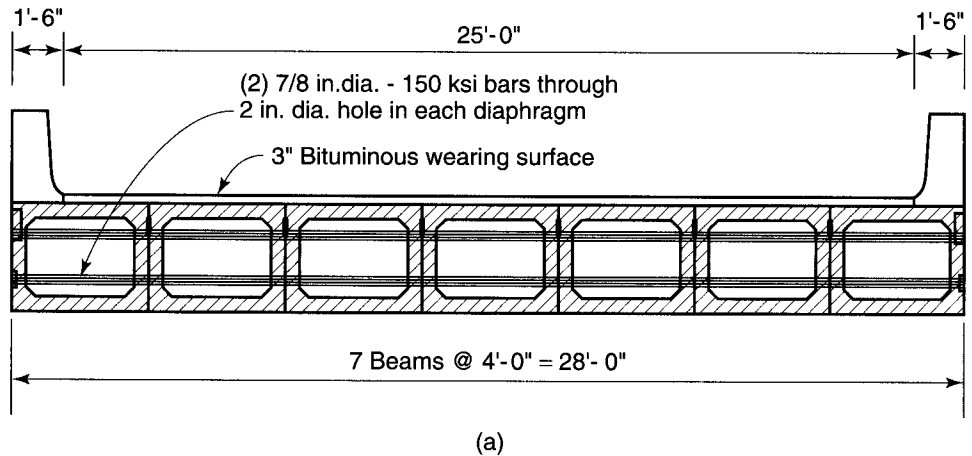
$$S_b = 8,721 \text{ in.}^3$$

$$S^t = 8,542 \text{ in.}^3$$

$$E_{ci} = 3840 \text{ ksi}$$

$$E_c = 4290 \text{ ksi}$$





**Figure 12.16** Two-Lane Box-Girder Bridge. (a) Roadway cross section, (b) Cross section of a component beam unit at midspan and at end sections. The end section has seven strands de-bonded.

**Solution:**

**1. Effective shear depth,  $d_v$**

The strands are horizontal,  $V_p = 0$

From Figure 12.17,

$$\begin{aligned} \text{At midspan, } A_{ps} &= 31 \frac{1}{2}\text{-in. dia., 7-wire, low-relaxation 270-K strands} \\ &= 4.437 \text{ in.}^2 \text{ at the bottom fibers.} \end{aligned}$$

$$\text{At support, } A_{ps} = 24 \text{ stands, since 7 are de-bonded} = 3.366 \text{ in.}^2$$

Midspan c.g.s. of strands from bottom:

$$y_{bc} = \frac{23 \times 2 + 6 \times 4 + 2 \times 36}{31} = 4.58 \text{ in.}$$

$$\text{Midspan } d_p = h - y_{bc} = 39.0 - 4.58 = 34.42 \text{ in.}$$

Support cgs of strands from bottom:

$$y_{be} = \frac{(23 - 7)2 + 6 \times 4 + 2 \times 36}{31 - 7} = 5.33 \text{ in.}$$

support  $d_p = h - y_{be} = 39.0 - 5.33 = 33.67 \text{ in.}$

$$\text{where, } d_c = \frac{A_{ps}f_{ps}d_p + A_s f_y d}{A_{ps}f_{ps} + A_s f_y}$$

$d_v$  = effective shear depth

= distance between resultants of tensile and compressive forces, but not less than  $0.90d_c$  or  $0.72h$ .

To determine the neutral axis depth,  $c$ , and the equivalent rectangular block depth,  $a$ , use the midspan section for the computations as the section of maximum moment ( $M_U = 0$  at support).

Assume the neutral axis within the  $5\frac{1}{2}$  in. "flange."

$$c = \frac{A_{ps}f_{pu} + A_s f_y - A'_s f'_y}{0.85f'_c \beta_1 b + kA_{ps} \left( \frac{f_{pu}}{d_p} \right)} = \frac{4.437(270) + 0 + 0}{0.85 \times 5.0 \times 0.80 \times 48 + 0.28 \times 4.437 \left( \frac{270}{34.42} \right)}$$

$$= 6.95 \text{ in.}$$

$$a = \beta_1 c = 0.80 \times 6.95 = 5.56 \text{ in.} > 5.5 \text{ in., hence treat as a flanged}$$

section with width  $b$  = web width  $b_w$

$$b_w = 2 \times 5 = 10 \text{ in.}$$

$$c = \frac{A_{ps}f_{pu} + A_s f_y - A'_s f'_y - 0.85f'_c \beta_1 (b - b_w) h_f}{0.85f'_c \beta_1 b_w + kA_{ps} \left( \frac{f_{pu}}{d_p} \right)}$$

$$= \frac{4.437 \times 270 + 0 - 0 - 0.85 \times 0.80 \times 5.0(48 - 10)5.5}{0.85 \times 5.0 \times 0.80 \times 10 + 0.28 \times 4.437 \left( \frac{270}{34.42} \right)}$$

$$= 11.14 \text{ in.} > 5.5 \text{ in.} \quad \text{O.K.}$$

$$a = \beta_1 c = 0.80 \times 11.14 = 8.91 \text{ in.}$$

$$f_{ps} = f_{pu} \left( 1 - k \frac{c}{d_p} \right) = 270 \left( 1 - 0.28 \left\{ \frac{11.14}{34.4} \right\} \right) = 245.4 \text{ ksi}$$

$$d_v = \left( d_p - \frac{a}{2} \right) = 33.67 - \frac{8.91}{2} = 29.22 \text{ in.}$$

$$0.9 d_c = 0.9 \times 33.67 = 30.30 \text{ in. (controls)}$$

$$0.72h = 0.72 \times 39 = 28.08 \text{ in.}$$

## 2. Angle of inclination $\theta$ of the diagonal compression struts

Critical section near the support is the larger of  $0.5d_v \cot \theta$  or  $d_v$  from the face of the support.  $\theta$  is obtained from Table 12.8 using the values of  $v/f'_c$  and  $\epsilon_x$ .

From equation 12.43(a),

$$v = \frac{V_u - \phi V_p}{\phi b_v d_v} + \frac{T_p p_h}{\phi A_{oh}^2}$$

$$\phi = 0.9 \text{ from Table 12.1(a)}$$

$$A_{oh} = (48 - 2 \times 1.5 \text{ for clear cover} - 2 \times 0.25 \text{ for stirrups}) \times$$

$$(39 - 2 \times 1.5 - 2 \times 0.25) = 44.5 \times 35.5 = 1580 \text{ in.}^2$$

$$p_h = 2(44.5 + 35.5) = 160 \text{ in.}$$

$$b_v = 2 \times 5 = 10 \text{ in.}$$

$$v = \frac{140 - 0}{0.9 \times 10 \times 30.3} + \frac{165 \times 12 \times 160}{0.9(1580)^2}$$

$$= 0.515 + 0.141 = 0.656 \text{ ksi}$$

$$\frac{v}{f'_c} = \frac{0.656}{5.0} = 0.131$$

For torsion adjustment, change the numerator in Eqs. 12.28(a), (b), and (c) to the following from Eq. 12.43(b):

$$\frac{M_u}{d_u} + 0.5N_u + 0.5V_u \cot \theta \sqrt{V_u^2 + \left(\frac{p_h T_u}{2A_o}\right)^2} - A_{ps} f_{po}$$

Use  $f_{po} \cong f_{pe} = f_{pi}(1 - 0.22) = 202.5 \times 0.78 = 157.9 \text{ ksi}$

$$N_u = 0, V_p = 0, V_u = 140 \text{ kips}, T_u = 165 \text{ ft-kip}, M_u = 320 \text{ ft-kip.}$$

$$A_o \cong 0.85A_{oh} = 0.85 \times 1580 = 1343 \text{ in.}^2$$

Try  $\theta = 23.5^\circ$  for a first trial;  $\cot 23.5^\circ = 2.30$

Trying Equation 12.28(a) for less than minimum longitudinal tensile reinforcement case,

$$\epsilon_x = \frac{\frac{320 \times 12}{30.3} + 0 + 0.5 \cot 23.5^\circ \sqrt{(140)^2 + \left(\frac{160 \times 165 \times 12}{2 \times 1343}\right)^2} - (3.366 \times 157.9)}{2(0 + 28,500 \times 3.366)}$$

$$= -1.01 \times 10^{-3} \text{ in./in.} < 0.002 \text{ in./in.} \quad \text{but negative.}$$

Hence, the longitudinal tensile strain,  $\epsilon_x$ , has to be computed adjusting Equation 12.28(c) for the torsional moment,  $T_u$ , from Equation 12.43(b), namely,

$$\epsilon_x = \frac{\left(\frac{M_u}{d_v} + 0.5 N_u + 0.5 \cot \theta \sqrt{V_u^2 + \left(\frac{p_h T_u}{2 A_o}\right)^2} - A_{ps} f_{po}\right)}{2(E_c A_c + E_s A_s + E_p A_{ps})}$$

where

$A_c$  = area of concrete in the flexural tension side of the member (Fig. 12.9) and box girder vertical walls (Fig. 12.18)

$$A_o = 0.85 A_{oh} = 0.85 \times 1580 \text{ in.}^2 = 1343 \text{ in.}^2$$

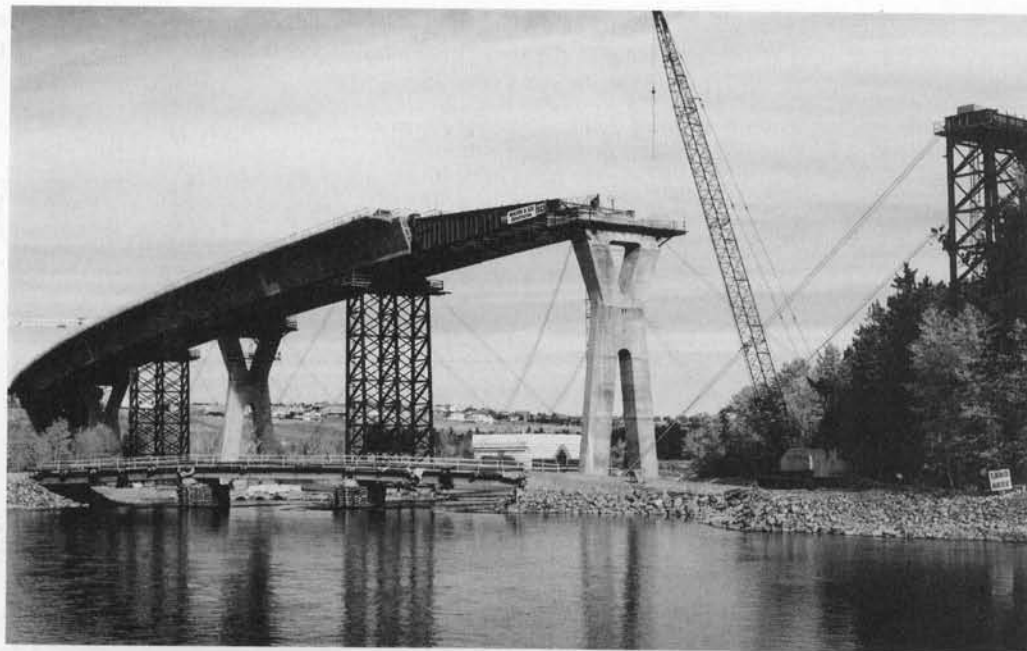
$$c = 11.14 \text{ in.}, \quad d_p = 33.67 \text{ in.}, \quad b_w = 2 \times 5 \text{ in.} = 10 \text{ in.}$$

$$A_c = 10(33.67 - 11.14) = 225.3 \text{ in.}^2$$

$$\epsilon_x = \frac{\frac{320 \times 12}{30.3} + 0 + 0.5 \times 2.30 \sqrt{(140)^2 + \left(\frac{160 \text{ in.} \times 165 \times 12}{2 \times 1343 \text{ in.}^3}\right)^2} - 3.366 \text{ in.}^2 \times 157.9 \text{ ksi}}{2(4290 \text{ ksi} \times 225.3 \text{ in.}^2 + 0 + 28,500 \text{ ksi} \times 3.366 \text{ in.}^2)}$$

$$= \frac{126.73 + 0.5 \times 2.30 \times 183.06 - 531.49}{2 \times 1.062,468} = -0.086 \times 10^{-3}$$

Enter Table 12.8 (a) with  $(1000 \epsilon_x = 0.086)$  and  $\left(\frac{v}{\sqrt{f'_c}} = 0.131\right)$  to get  $\theta = 23.3^\circ$  and  $\beta = 2.787$ , say, 2.79



**Photo 12.9** Launching the segmental bridge segments for Stoney Trail Bow River segmental Bridge, Calgary, Alberta, span 1562 ft, deck width 69 ft, the deck rises 89 to 118 ft above the river valley (Courtesy James Skeet-Reid Crowther Engineering, Calgary)

### 3. Design of transverse closed stirrups

$$\begin{aligned}
 V_c &= 0.0316\beta\sqrt{f'_c} b_v d_v \text{ using ksi units} \\
 &= 0.0316 \times 2.79 \sqrt{5.0} (10 \times 30.3) = 59.7 \text{ kips} < 140 \text{ kips} \\
 &\text{hence web shear reinforcement is necessary.}
 \end{aligned}$$

From equation 12.40(a)

$$\begin{aligned}
 \frac{A_v}{s} &= \frac{V_n - (0.0361\beta\sqrt{f'_c} b_v d_v + V_p)}{f_y d_v \cot \theta} \\
 &= \frac{140}{0.9} - (0.0316 \times 2.79 \sqrt{5.0} \times 10 \times 30.3 + 0) \\
 &= \frac{\quad}{60.0 \times 30.3 \times 2.3} \\
 &= 0.023 \text{ in.}^2/\text{in.}/\text{two legs.}
 \end{aligned}$$

From equation 12.40(b),

$$\begin{aligned}
 \frac{A_t}{s} &= \frac{T_n}{2A_0 f_{yt} \cot \theta} = \frac{165 \times 12}{2 \times 1343 \times 60 \times 2.3} = 0.006 \text{ in.}^2/\text{in.}/\text{one leg} \\
 \frac{A_{vt}}{s} &= \frac{A_v}{s} + 2 \frac{A_t}{s} = 0.023 + 2(0.006) = 0.035 \text{ in.}^2/\text{in.}/\text{two legs}
 \end{aligned}$$

Trying No. 4 closed stirrups with each of the two legs of a stirrup in each vertical wall.

$$\text{spacing } s = \frac{2 \times 0.20}{0.035} = 11.4 \text{ in.}$$

Maximum allowable  $s = 12 \text{ in.}$

Use No. 4 closed stirrups at 10 in. center to center throughout the span. Note that the spacing of the transverse reinforcement can be increased along the span if the shear and torsion envelopes warrant it.

#### 4. Longitudinal reinforcement check

From Equation 12.40,

$$(A_s f_y + A_{ps} f_{ps}) \geq \frac{M_u}{\phi_f d_v} + 0.5 \frac{N_u}{\phi_c} + \cot \theta \sqrt{\left( \frac{V_U}{\phi_v} + 0.5 V_s - V_p \right)^2 + \left( \frac{0.45 T_u p_o}{\phi_v 2 A_o} \right)^2}$$

$$A_{ps} f_{ps} = 3.366 \times 245.5 = 826 \text{ kips}$$

$$A_o \approx 0.85 A_{oh} = 0.85 \times 1580 = 1343 \text{ in.}^2$$

$$p_o \approx 0.85 p_h = 0.85 \times 160 = 136 \text{ in.}$$

$$V_s = \frac{A_v f_y d_v}{s} = \frac{0.40 \times 60 \times 30.3}{6.75} = 108 \text{ kips.}$$

Hence,

$$\begin{aligned} \frac{320 \times 12}{0.9 \times 30.2} + 0 + 2.30 \sqrt{\left( \frac{140}{0.9} + 0.5 \times 102 \right)^2 + \left( \frac{0.45 \times 165 \times 12 \times 136}{0.9 \times 2 \times 1343} \right)^2} \\ = 140.8 + 2.3(212.6) = 630 \text{ kips} < 826 \text{ kips.} \end{aligned}$$

Hence no additional longitudinal reinforcement is needed. Adopt the No. 4 vertical ties at 10 in. on centers in each of the two beam box walls. Each vertical transverse tie, if not in a single piece, has to be fully developed to satisfy the development length requirements of the specifications.



**Photo 12.10** State Route 509 Elevated Single-Point Urban Interchange, Tacoma, Washington: a situ-cast post-tensioned box girder bridge featuring tight radius curved exterior webs; the footprint of the interchange is approximately two football fields in size (Designed by BERGER/ABAM Engineers, Federal Way, Washington, courtesy Robert Mast, Senior Principal)



**Photo 12.11** Valley Ave. Bridge, Fife, Washington: 4-span bridge consisting of two structural types, situ-cast post-tensioned concrete box girder with precast prestressed end girders (Designed by BERGER/ABAM Engineers, Federal Way, Washington, courtesy Robert Mast, Senior Principal)

## 12.14 LRFD MAJOR DESIGN EXPRESSIONS IN SI FORMAT

Eq. 12.9(a):

$$f_{ps} = f_{pu} \left( 1 - k \frac{c}{d_p} \right)$$

$$k = 2 \left( 1.04 - \frac{f_{py}}{f_{pu}} \right)$$

For non-bonded tendons,

$$f_{ps} = f_{pe} + 1.5 \frac{L}{d_p} E_{ps} \epsilon_{cu} \left( \frac{d_p}{c} - 1.0 \right) \frac{L_1}{L_2}$$

$< 0.94 f_{py}$  where  $L_1 =$  span and tendon length

$L_2 =$  stresses in MPa.

Eq. 12.12(a):

$$\frac{c}{d_e} \leq 0.42$$

$$\text{Moment distribution factor } p_d = 20 \left( 1 - 2.36 \frac{c}{d_e} \right)$$

Eq. 12.24(a)

$$V_c = 0.083\beta \sqrt{f'_c} b_v d_v$$

where  $b$  and  $d_y$  (mm),  $f'_c$  (MPa)

Eq. 12.29, when torsion is present,

$$(A_s f_y + A_{ps} f_{ps}) \geq \frac{M_u}{d_v \phi_f} + \frac{0.5N_u}{\phi_c} + \cot \theta \sqrt{\left( \frac{V_u}{\phi_v} - 0.5V_p \right)^2 + \left( \frac{0.45T_u P_h}{2A_o \phi_v} \right)^2}$$

Eq. 12.35:

$$A_{vf} = 0.35b_v \frac{s}{f_y}, \text{ where } b_v, s \text{ (mm).}$$

Eq. 12.38:

$$V_u = \sqrt{V_u^2 + \left( \frac{0.9p_h T_u}{2A_o} \right)^2}$$

where  $V_u$  (Newton),  $T_u$  (N-mm),  $A_o$  (mm<sup>2</sup>).

Eq. 12.40(b):

$$\frac{A_t}{s} = \frac{T_n}{2A_o f_y \cot \theta} \text{ where } s \text{ (mm).}$$

## SELECTED REFERENCES

- 12.1 ASCE, "Minimum Design Loads for Buildings and Other Structures," ANSI-ASCE 7-95 Standard, American Society of Civil Engineers, Reston, VA, 1995, pp. 214.
- 12.2 AASHTO, "Standard Specifications for Highway Bridges," 18th Ed., Supplements, American Association of State Highway and Transportation Officials, Washington, D.C., 2006–2009.
- 12.3 AASHTO, "LRFD Bridge Design Specifications," American Association of State Highway and Transportation Officials, Washington, D.C., 2004.
- 12.4 ACI, "Building Code Requirements for Structural Concrete (ACI 318-08) and Commentary (ACI 318R-08), American Concrete Institute, Farmington Hills, MI.
- 12.5 Nawy, E.G., *Reinforced Concrete—A Fundamental Approach*, 6th Ed., Prentice Hall, Upper Saddle River, NJ., 2009, 936 pp.
- 12.6 Collins, M. P., and Mitchell, D., *Prestressed Concrete Structures*, Prentice Hall, Upper Saddle River, NJ, 1991.
- 12.7 Collins, M. P., and Mitchell, D., "Shear and Torsion Design of Prestressed and Non-Prestressed Concrete Beams," *PCI Journal*, Precast/Prestressed Concrete Institute, Chicago, 1980, pp. 12–100.

- 12.8** Hsu, T. T. C., *Torsion in Reinforced Concrete*, Van Nostrand Reinhold, New York, 1983.
- 12.9** Hsu, T. T. C., "Torsion in Structural Concrete—Uniformly Prestressed Members Without Web Reinforcement," *PCI Journal*, V. 13, Precast/Prestressed Concrete Institute, Chicago, 1968, pp. 34–44.
- 12.10** Hsu, T. T. C., *Unified Theory of Reinforced Concrete*, CRC Press, Boca Raton, FL, 1993.
- 12.11** PCI, *Bridge Design Manual*, Precast/Prestressed Concrete Institute, Chicago, 1999.
- 12.12** PTI, *Post-Tensioning Manual*, 5th Ed., Post-Tensioning Institute, Phoenix, AZ, 1991.
- 12.13** Kudlapur, S. T., and Nawy, E. G., "Early Age Shear Friction Behavior of High Strength Concrete Layered Systems at Subfreezing Temperatures," Proceedings, *Symposium on Designing Concrete Structures for Serviceability and Safety*, ACI SP-133.9, E. G. Nawy and A. Scanlon, ed., American Concrete Institute, Farmington Hills, MI, 1992, pp. 159–185.
- 12.14** Naaman, A. E., "Unified Design Recommendations for Reinforced, Prestressed and Partially Prestressed Concrete Bending and Compression Members," *ACI Structural Journal*, American Concrete Institute, Farmington Hills, MI, March–April 1992, pp. 200–210.
- 12.15** Naaman, A. E., "Unified Bending Strength Design of Concrete Members: AASHTO-LRFD Code," *Journal of Structural Engineering*, American Society of Civil Engineers, Reston, VA, June 1995, pp. 964–970.
- 12.16** Mast, R. F., "Unified Design Provisions for Reinforced and Prestressed Concrete Flexural and Compression Members," *ACI Structural Journal*, American Concrete Institute, Farmington Hills, MI, April 1992, pp. 185–199.
- 12.17** Badie, S. S., Baishya, M. C., and Tadros, M. K., "NUDECK—An Efficient and Economical Precast Prestressed Bridge Deck System," *PCI Journal*, Vol. 43 No. 5, Precast/Prestressed Concrete Institute, Chicago, September–October 1998, pp. 56–71.
- 12.18** Ma, Z., Huo, X., and Tadros, M. K., "Restraint Moment in Precast/Prestressed Concrete Continuous Bridges," *PCI Journal*, Vol. 43, No. 6, Precast/Prestressed Concrete Institute, Chicago, November–December 1998, pp. 40–57.
- 12.19** Nawy, E. G., editor-in-chief, *Concrete Construction Engineering Handbook*, 2nd Ed., CRC Press, Boca Raton, FL, 2008, pp. 1–1560.
- 12.20** Nawy, E. G., *Fundamentals of High Performance Concrete*, 2nd Ed., John Wiley & Sons, New York, 2001, 466 p.
- 12.21** Hsu, T. T. C., Zhu, R. H. and Lee, J. Y., "A Critique on the Modified Compression Field Theory," Presented at the 78<sup>th</sup> Annual Meeting of the Transportation Research Board, Washington, D.C., January 10–14, 23 pp.
- 12.22** Nawy, E. G., "Concrete—The Sustainable Infrastructure Material for the 21<sup>st</sup> Century," Keynote Address Paper, No. E-C103, Transportation Research Board, National Research Council, Washington, D.C., September 2006, pp. 1–23.
- 12.23** Nawy, E. G., "Concrete—The Sustainable Infrastructure Material for the 21<sup>st</sup> Century," Keynote Address Paper, Proceedings, The First International Conference on Recent Advances in Concrete Technology, Crystal City, Washington, D.C., September 19, 2007, pp. 1–24.

## PROBLEMS FOR SOLUTION

- 12.1** Design for flexure a 100 ft (30.5m) simply supported AASHTO-PCI bulb-tee composite bridge deck with no skews using the LRFD AASHTO specifications. The superstructure is composed of six pretensioned beams at 9'-0" (2.74 m) on centers. The bridge has an 8 in. (203 mm) situ-cast concrete deck with the top one half inch to be considered as wearing surface. The design live load is the HL-93 AASHTO-LRFD fatigue loading. Assume the bridge is to be located in a low seismicity zone. Given, the following maximum allowable stresses:

Deck	$f'_c = 4000$ psi, normal weight
	$f_c = 0.60 f'_c = 2400$ psi
Bulb-tee	$f'_c = 6500$ psi



$$f'_{ci} = 5500 \text{ psi}$$

$$f_c = 0.60 f'_c = 3900 \text{ psi, Service III}$$

$$f_c = 0.45 f'_c = 2925 \text{ psi, Service I}$$

$$f_{ci} = 0.60 f'_c = 3480 \text{ psi}$$

$$f_t = 6\sqrt{f'_c} = 484 \text{ psi}$$

$$f_{pu} = 270,000 \text{ psi}$$

$$f_{py} = 0.90 f_{pu} = 243,000 \text{ psi}$$

$$f_{pi} = 0.75 f_{pu} = 202,500 \text{ psi}$$

$$f_y = 60,000 \text{ psi}$$

$$E_{ps} = 28.5 \times 10^6 \text{ psi}$$

$$E_s = 29.0 \times 10^6 \text{ psi.}$$

- 12.2** Design the web shear reinforcement for the bulb-tee beam in Problem 12.1 at the critical section near the supports and the interface shear transfer reinforcement at the interface plane between the precast section and the deck situ-cast concrete. Also, verify if the span deflection is within the allowable limits.
- 12.3** A single-span two-lane unskewed AASHTO Type BIII-48 bridge has an overall span of 96 ft and the cross-section shown in Figure P12.1 (Adapted from the PCI Manual - Ref. 12.11). The total deck width is 28 ft and the clear roadway is 25 ft wide. The deck has a 3-in. bituminous wearing surface. Design for flexure and shear an interior box element using the AASHTO LRFD specifications in the design. Given:

Effective span = 95 ft.

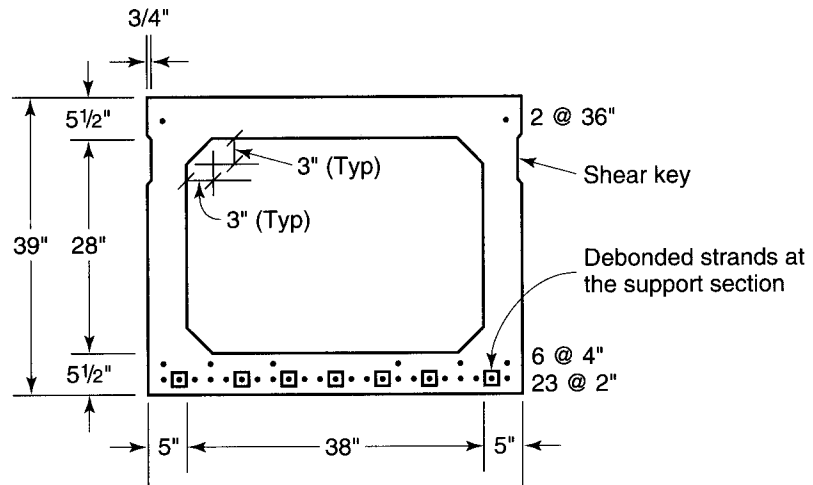
$$f'_c = 5000 \text{ psi, normal weight}$$

$$f_c = 0.60 f'_c = 3000 \text{ psi, Service III}$$

$$f_c = 0.45 f'_c = 2250 \text{ psi, Service I}$$

$$f_{ci} = 0.60 f'_c = 3000 \text{ psi}$$

$$f_t = 6\sqrt{f'_c} = 424 \text{ psi}$$



**Figure P12.1** Box Beam Geometry

$$f_{pu} = 270,000 \text{ psi}$$

$$f_{py} = 0.90 f_{pu} = 243,000 \text{ psi}$$

$$f_{pi} = 0.75 f_{pu} = 202,500 \text{ psi}$$

$$f_y = 60,000 \text{ psi}$$

$$E_{ps} = 28.5 \times 10^6 \text{ psi}$$

$$E_s = 29.0 \times 10^6 \text{ psi.}$$

Section Properties:

$$A_c = 813 \text{ in.}^2$$

$$h = 39 \text{ in.}$$

$$I_c = 168,367 \text{ in.}^4$$

$$c_b = 19.29 \text{ in.}$$

$$c_t = 19.71 \text{ in.}$$

$$S_b = 8728 \text{ in.}^3$$

$$S_t = 8542 \text{ in.}^3$$

$$W_D = 847 \text{ lb/ft.}$$

- 12.4** Solve Problem 12.3 using the AASHTO Standard specifications for both flexure, shear and deflection.

# 13



## SEISMIC DESIGN OF PRESTRESSED CONCRETE STRUCTURES

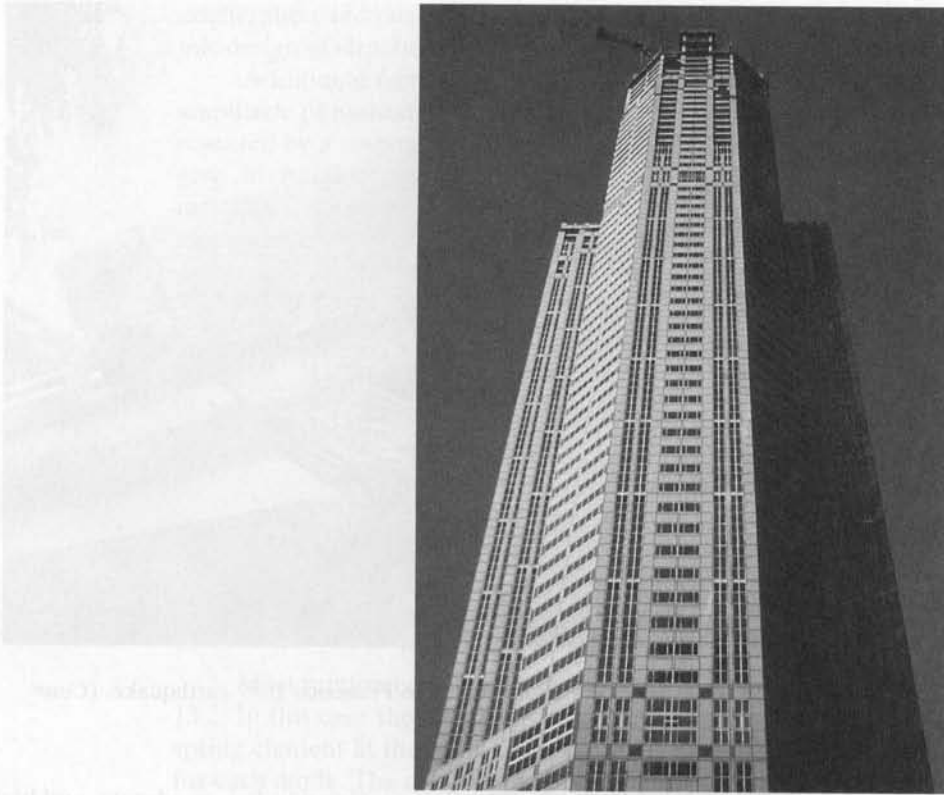
### 13.1 INTRODUCTION: MECHANISM OF EARTHQUAKES

The earth crust is composed of several layers of hard “tectonic” plates, called *lithospheres*, which float on the softer, underpinning, fluid medium called *mantle*. These plates or rock masses, when fractured, *form fault lines*. The adjoining plates or rock masses are prevented by the interacting frictional forces from moving past one another most of the time. However, when this frictional ultimate resistance is reached because of the continuous motion of the underlying fluid, any two plates can impact on one another, generating seismic waves that can cause large horizontal and vertical ground motions. These ground motions translate into inertia forces in structures.

The length and width of a fault are interrelated to the magnitude of the earthquake. The fault is the cause rather than the result of the earthquake. A fault can cause an earthquake due to the following reasons (Ref. 13.5):

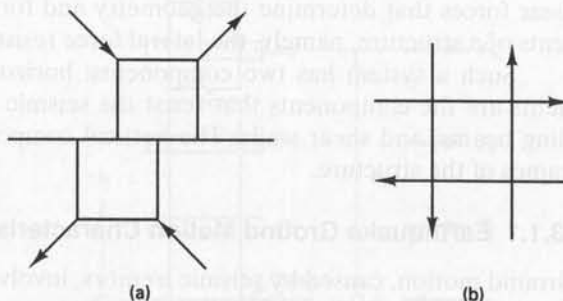
1. Cumulative strain in the fault over a long period of time reaches the rupture level.
2. Slip of the tectonic plates at the fault zones causes a rebound, as in Fig. 13.1(a),

Northridge, California, 1994 earthquake structural failure. (Courtesy, Dr. Murat Saatcioglu.)



**Photo 13.1** 311 S. Wacker Street, Chicago, 12,000 concrete (Courtesy Portland Cement Association.)

3. Sudden push and pull forces at the fault lead to reverse moment couples, as in Fig. 13.1(b). The moment caused by these couples as a measure of earthquake size can be termed the *seismic moments*. The magnitude is equal to rock rigidity  $\times$  fault area  $\times$  amount of slip. The range of slip velocity in such faults as the San Andreas Fault in California is 30 to 100 mm per year. On this basis, a slippage or horizontal motion of 3 m at such faults in one single earthquake is expected to occur at intervals of 30 to 100 years.



**Figure 13.1** Mechanism of earthquakes: (a) slip of tectonic plates; (b) reverse moment couples.



**Photo 13.2** Bridge girder collapse in the San Francisco 1989 earthquake. (Courtesy Portland Cement Association.)

Earthquakes may be characterized by three categories: low, moderate, and high intensity. The intensity is governed by ground motion accelerations, represented by response spectra and coefficients derived from such spectra. A structure is expected to respond essentially elastically to low-intensity earthquakes. In such a case, the stresses are expected to remain within the elastic range, with a slight possibility of developing limited inelasticity with no appreciable structural or non-structural damage. Structural response is expected to be inelastic under high-intensity earthquakes having an intensity of 5 or higher on the Richter scale and in regions close to the epicenter. For the design of structures in seismic zones, two methods are presented in the IBC 2009 code, the spectral response method and the equivalent lateral force method. The latter has certain limitations that will be discussed later.

A detailed discussion of the subject of earthquakes is beyond the scope of this book since the primary aim of this chapter is the proportioning of seismic resistant components of concrete structures. However, some of the basic underlying characteristics are important to cover. They are intended to help define the magnitude of the lateral seismic base shear forces that determine the geometry and form of the earthquake resisting components of a structure, namely, the lateral force resisting system (LFRS).

Such a system has two components: horizontal and vertical. The horizontal elements are the components that resist the seismic forces. They can be diaphragms, coupling beams, and shear walls. The vertical component comprises the walls and vertical frames of the structure.

### 13.1.1 Earthquake Ground Motion Characteristics

Ground motion, caused by seismic tremors, involves acceleration, velocity, and displacement. These are in the majority amplified, thereby producing forces and displacements, which can exceed those which the structure is able to sustain (Ref. 13.13). The maximum value of the ground motion magnitude, namely, the peak ground velocity, peak ground

acceleration and peak ground displacement become the principal parameters in the seismic design of structures.

Additional factors also affect the response of a structure. They include frequency, amplitude of motion, shaking duration, and site soil characteristics. These can all be represented by a response spectrum which idealizes a structure into a dampened, single degree of freedom system (SDF) oscillating at various periods and frequencies. The maximum vibration magnitude reached during any time duration after the base ground motion is its spectral value.

### 13.1.2 Fundamental Period of Vibration

The basic natural period  $T$  of a simple one-degree-of-freedom system is the time required to complete one whole cycle during dynamic loading. In other words, it is the time required for a phase angle  $\omega t$  to travel from 0 to  $2\pi$ , where  $\omega$  is the angular frequency of the system. Hence  $\omega t = 2\pi$ , leading to the expression

$$T = \frac{2\pi}{\omega} = 2\pi \left( \frac{m}{k} \right)^{1/2} \quad (13.1)$$

where  $m$  = mass of system

$k$  = spring constant and damping is not considered

Most reinforced concrete structures are multidegrees-of-freedom systems, as in Fig. 13.2. In this case the structural mass can be assumed to be concentrated in the vertical spring element at the floor level, resulting in multiple modes with frequencies (periods) for each mode. The compound natural period  $T$  is then evaluated with due consideration given to the distribution of mass and stiffness. Codes require that  $T$  be established using the structural properties and deformation characteristics of the resisting elements in a properly substantiated analysis using expressions such as those given by the International Building Code—IBC 2009 (Ref. 13.2), or The Uniform Building Code (Ref. 13.3) integrated into the IBC provisions.

Since a structure is composed of a series of single degrees of freedom components subjected to the *same* base motion, a series of maximum values related to the SDF system's fundamental periods,  $T$ , would ensue. These, in turn, form a spectral curve for that base ground motion. By knowing the base motion, the SDF fundamental period and the percent critical damping, one can obtain from the applicable curve the maximum acceleration, velocity, and displacement relative to the base (Ref. 13.14). Evidently, computer

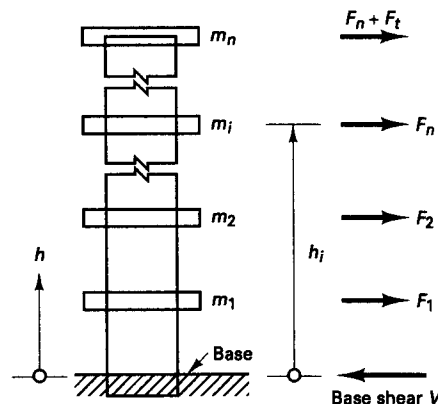


Figure 13.2 Modeling multistory structures.



**Photo 13.3** Northridge, California, 1994 earthquake structural failure. (Courtesy Dr. Murat Saatcioglu.)

use is needed to obtain a complete spectral response of the multi-degree state of a structure.

It should be recognized that a structure is designed to resist earthquake motion such that it is able to sustain and survive the earthquake through large inelastic deformations and energy dissipation through cracking and limited local material failure, but without loss of stability. It would be highly uneconomical to design the lateral force resisting system to the earthquake forces such that the structure deforms only elastically as a result of these forces. The codes have this as a basic philosophy particularly for major earthquakes in which some structural damage can result.

### 13.1.3 Design Philosophy

The International Building Code (IBC 2009, Ref 13.2) on seismic design consolidates the three major existing regional codes into one major document that is now universally adopted covering the work of the following regional codes:

1. Building Officials Code Administration International (BOCA)
2. International Conference of Building Officials (ICBO): Uniform Building Code (UBC)
3. Southern Building Code Congress International (SBCCI)

Underlying its seismology design provisions are:

1. Recommended design levels related to effective peak accelerations that can resist minor earthquakes without damage, moderate earthquakes without structural damage, and major earthquakes in which some structural damage can result.
2. Minimum design criteria for all types of buildings, low and high rise, with and without shear walls.
3. Spectral response values for various ground motion intensities, mainly within the elastic range.
4. Provide design criteria for lateral ground motion, unidirectional and bi-directional, addressing them one at a time.
5. Limit the story drift and displacement magnitudes of the building structures within acceptable ranges, through control of stiffness of components and shear walls, diaphragms, and coupling beams.

## 13.2 SPECTRAL RESPONSE METHOD

### 13.2.1 Spectral Response Acceleration Maps

As discussed in Ref. 13.15, prior to the Northridge and Kobe earthquakes, the Uniform Building Code (UBC) provisions performed satisfactorily in the United States in past earthquakes. The failures in these two cases were determined to be due to “related configurations of the structural systems, inadequate connection detailing, incompatibility of deformations and design or construction deficiencies. They were not due to deficiency in strength (Structural Engineers Association of California, 1995).

The UBC provisions incorporated in the International Building Code (IBC) are based on consideration of the site conditions of the structure and the application of maximum considered earthquake ground motion maps for site class B, prepared by the United States Geological Survey (USGS). The equivalent maximum considered earthquake ground motion values for the ceiling were determined to be 1.50 g for the short period and 0.60 g for the long period (Ref. 13.15).

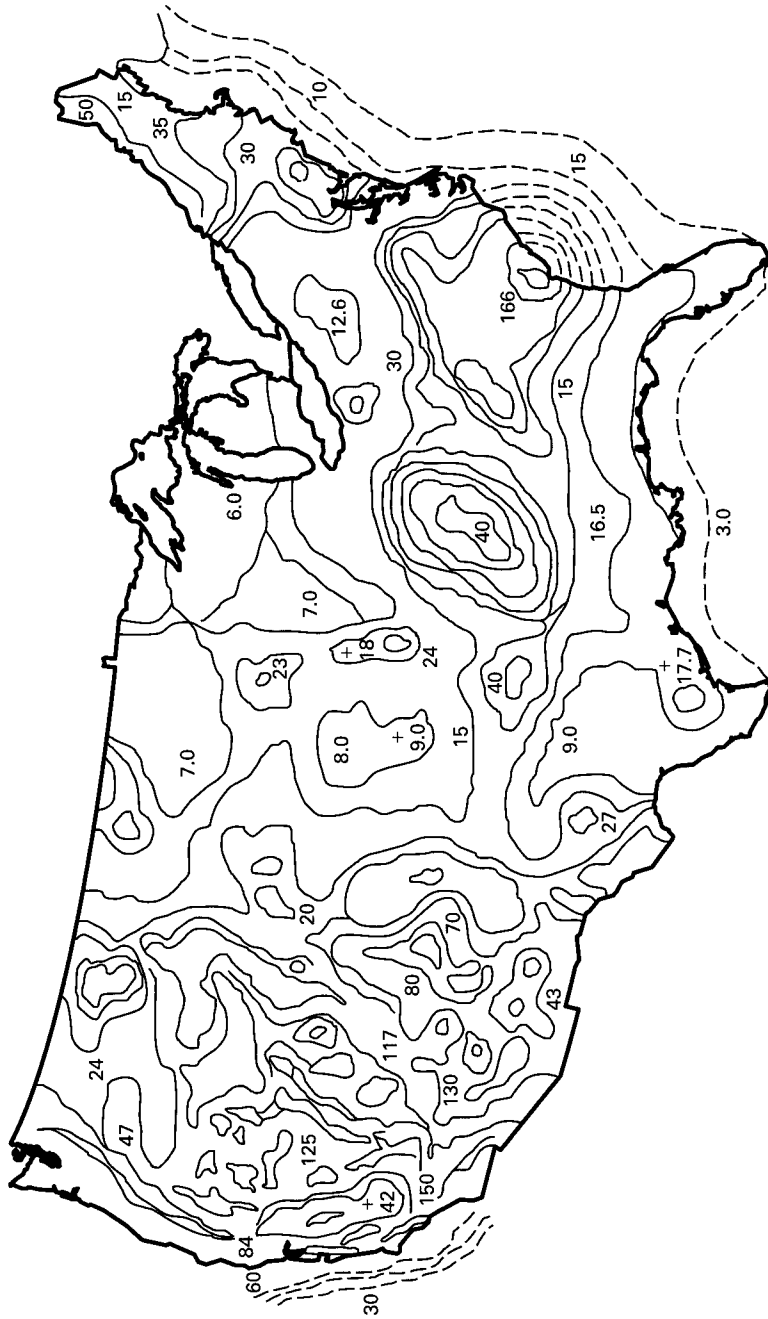
The high seismicity regions, where the maximum considered earthquake ground motion values are greater than 0.75 g for the 1.0 sec, peak acceleration additional requirements are imposed on irregular structures exceeding five stories in height and a period  $T$  in excess of 0.5 sec, such as increasing the ground motion spectral acceleration values by 50 percent. The USGS large-scale maps for the 1.0 sec and the 0.2 sec levels of spectral response acceleration, site-B class, and 5 percent critical damping are condensed and abridged in Figs. 13.3(a) and (b) for general guidance. They show the relative values of the peak spectral response accelerations at the two ground motion levels of 0.2 and 1.0 sec. Values have to be extrapolated linearly from the USGS large-scale maps for use in the seismic design of structures.

### 13.2.2 Seismic Design Parameters

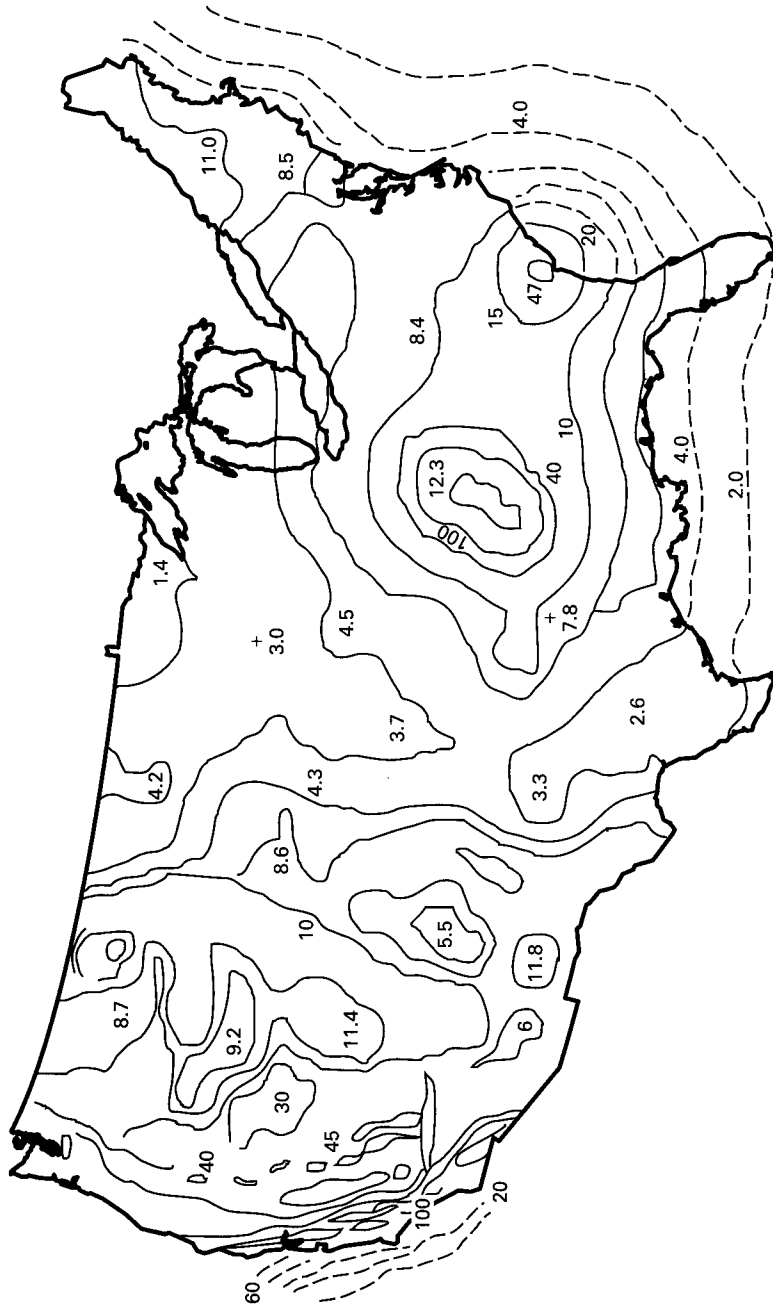
Both the spectral response method and the equivalent lateral force method are based on the same code principles and formulations presented in this chapter. Sites are classified into six categories A, B, C, D, E, and F as shown in Table 13.1 on site properties.

Ground motion accelerations and the maximum considered earthquake spectral response acceleration are considered at 1.0 sec period ( $S_1$ ) and at short periods ( $S_s$ ) such as 0.2 sec obtained from seismic contour maps discussed in Section 13.2.1.





**Figure 13.3(a)** Maximum considered earthquake ground motion for the United States, 0.2 sec. Spectral response acceleration  $S_s$  as a percent of gravity, site-class B with 5 percent critical damping.



**Figure 13.3(b)** Maximum considered earthquake ground motion for the United States, 1.0 sec. Spectral response acceleration  $S_1$  as a percent of gravity, site-class B with 5 percent critical damping.

**Table 13.1** Site Class Definitions and Classifications

Site Class	Soil Profile Name	Average Properties in Top 100Ft (30 m), As in Section 1615.1.5		
		Soil Shear Wave Velocity, $V_s$ (ft/S)	Standard Penetration Resistance, $N$	Soil Unconfined Shear Strength $S_U$ (PSF)
A	Hard rock	$V_s > 5,000$	not applicable	not applicable
B	rock	$2,500 \leq V_s \leq 5,000$	not applicable	not applicable
C	Very dense soil and soft Rock	$1,200 \leq V_s \leq 2,500$	$N > 50$	$S_U > 2,000$
D	Stiff soil profile	$600 \leq V_s \leq 2,500$	$15 \leq N \leq 50$	$1,000 \leq S_U \leq 2,000$
E	Soft soil profile	$V_s < 600$	$N < 15$	$S_U < 1,000$
E		Any profile with more than 10 ft of soil having the following characteristics: -plasticity index $PI > 20$ ; -moisture content $w > 40\%$ and -unconfined shear strength $S_U < 500$ psf		
F		Any profile containing soil having one or more of the following characteristics: 1. Soils vulnerable to potential failure or collapse under seismic loading such as liquefiable soils, quick and highly sensitive clays, collapsible weakly cemented soils. 2. Peats and/or highly organic clays ( $H > 10$ ft of peat and/or highly organic clay where $H$ = thickness of soil) 3. Very high plasticity clays ( $H > 25$ ft with plasticity index $PI > 75$ ) 4. Very thick soft/medium stiff clays ( $H > 120$ ft)		

For  $S_1$ : 1 ft/sec = 304.8 mm/sec; 1 psf = 0.0479 kP; 1 ft. = 305 mm.

Steps and expressions for classifying and determining their values are detailed in Ref. 13.2

$$S_{MS} = F_a S_s \quad (13.2a)$$

$$S_{M1} = F_v S_1 \quad (13.2b)$$

where,

$F_a$  = Site coefficient from Table 13.2a

$F_v$  = Site coefficient from Table 13.2b

$S_s$  = Mapped spectral acceleration for short periods (See Ref. 13.2 for map contour values)

$S_1$  = Mapped spectral acceleration for 1.0-sec periods (See Ref. 13.2 for map contour values)

**Table 13.2(a)** Values of Site Coefficient  $F_a$  as a Function of Site Class and Mapped Spectral Response Acceleration at Short Periods ( $S_s$ )

Site Class	Mapped Spectral Response Acceleration at Short Periods				
	$S_s \leq 0.25$	$S_s = 0.50$	$S_s = 0.75$	$S_s = 1.00$	$S_s \geq 1.25$
A	0.8	0.8	0.8	0.8	0.8
B	1.0	1.0	1.0	1.0	1.0
C	1.2	1.2	1.1	1.0	1.0
D	1.6	1.4	1.2	1.1	1.0
E	2.5	1.7	1.2	0.9	0.9
F	Note b	Note b	Note b	Note b	Note b

**Table 13.2(b)** Values of Site Coefficient  $F_V$  as a Function of Site Class and Mapped Spectral Response Acceleration at 1.0 Sec Periods ( $S_1$ )

Site Class	Mapped Spectral Response Acceleration at 1.0-Sec Periods				
	$S_1 \leq 0.1$	$S_1 = 0.2$	$S_1 = 0.3$	$S_1 = 0.4$	$S_1 \geq 0.5$
A	0.8	0.8	0.8	0.8	0.8
B	1.0	1.0	1.0	1.0	1.0
C	1.7	1.6	1.5	1.4	1.3
D	2.4	2.0	1.8	1.6	1.5
E	3.5	3.2	2.8	2.4	2.4
F	Note b	Note b	Note b	Note b	Note b

NOTES: a—Straight line interpolation for intermediate values are to be made.

b—Site geotechnical investigation and dynamic site response analyses are to be performed

The design spectral response accelerations at short periods ( $S_S$ ) and at 1 sec ( $S_1$ ) are to be adjusted for site class effect ( $S_{MS}$ ) at short periods and ( $S_{M1}$ ) for 1 sec based on Table 13.1 in conjunction with Tables 13.2(a) and 13.2(b) for site coefficients.

The maximum considered earthquake spectral response for short and one second periods are respectively defined by the following expressions where for 5 percent damped design, the spectral response acceleration becomes:

$$S_{DS} = \frac{2}{3} S_{MS} \quad (13.3a)$$

$$S_{D1} = \frac{2}{3} S_{M1} \quad (13.3b)$$

### 13.2.3 Earthquake Design Load Classifications and Seismic Categories

Structures in seismic areas have to be classified in separate categories than those that are subjected to low or negligible seismic loads. Regardless of the period of vibration of the structure they are classified as in tables 13.3 (a) and 13.3 (b) for short period response acceleration and 1-second response acceleration respectively.

The IBC 2009 assigns four seismic occupancy categories, I, II, III, and IV. They are defined by the magnitude of the seismic response acceleration, namely, the short period response  $S_{DS}$  of 0.2 seconds and the 1-second period response  $S_{D1}$ . Tables 13.3 (a) and 13.3 (b) list the design categories A, B, C, and D corresponding to the  $S_{DS}$  and  $S_{D1}$  levels. The Code stipulates that Occupancy Category I, II, or III structures located where the map spectral response acceleration parameter at 1-second period,  $S_{D1}$ , is greater than or equal to 0.75, that structure should be assigned Seismic Design Category E. Occupancy

**Table 13.3(a)** Seismic Design Category Based on Short Period Response Accelerations

Value of $S_{DS}$	Occupancy Category		
	I or II	III	IV
$S_{DS} < 0.167g$	A	A	A
$0.167g \leq S_{DS} < 0.33g$	B	B	C
$0.33g \leq S_{DS} < 0.50g$	C	C	D
$0.50g \leq S_{DS}$	D	D	D

**Table 13.3(b)** Seismic Design Category  
Based on 1 Second Period Response Accelerations

Value of $S_{D1}$	Occupancy Category		
	I or II	III	IV
$S_{D1} < 0.067g$	A	A	A
$0.067g \leq S_{D1} < 0.133g$	B	B	C
$0.133g \leq S_{D1} < 0.20g$	C	C	D
$0.20g \leq S_{D1}$	D	D	D

Category IV structures located where the mapped spectral response acceleration parameter at 1-second period  $S_{D1}$ , is greater than or equal to 0.75, the structure should be assigned to Seismic design Category F.

All other structures should be assigned to a seismic design category based on their occupancy category and the design spectral response coefficients  $S_{DS}$  and  $S_{D1}$  as defined in Equations 13.3 (a) and (b) or the site-specific procedures of ASCE 7. But each structure should be assigned to more severe seismic category in accordance with Tables 13.3 (a) or 13.3 (b) irrespective of the fundamental period of vibration,  $T$ .

To amplify, there are exceptions that allow for the Seismic Design Category to be determined from Table 13.3 (a) alone. In order to use this exception,  $S_1$  must be less than 0.75 and all of the following requirements have to be met (Ref. 13.13).

1. The approximate fundamental period of vibration,  $T_a$ , as determined by Equation 13.13 in each of the two orthogonal directions is less than  $0.8 T_S$ , where  $T_S = S_{D1}/S_{DS}$ .
2. The fundamental period of the structure that is used to calculate the story drift in the two orthogonal directions is less than  $T_S$ .
3. The seismic response coefficient,  $C_S$ , is determined by Equation 13.9.
4. The diaphragms are rigid, or where diaphragms are considered flexible, the spacing between vertical elements of the lateral force-resisting system does not exceed forty feet.

The FEMA 302 Parts 1 and 2 defined seismic regions as follows in Ref. 13.15:

**Region 1—Regions of Negligible Seismicity with Very Low Probability of Collapse of the Structure (No Spectral Values)**

**Region definition:** Regions for which  $S_S < 0.25g$  and  $S_1 < 0.10g$ .

**Design values:** No spectral ground motion values required. Use a minimum lateral force level of 1 percent of the dead load for seismic design Category A.

**Region 2—Regions of Low and Moderate to High Seismicity (Probabilistic Map Values)**

**Region definition:** Regions for which  $0.25g < S_S < 1.5g$  and  $0.25g < S_1 < 0.60g$ .

**Maximum considered earthquake map values:** Use  $S_S$  and  $S_1$  map values.

**Transition between Regions 2 and 3—**Use values of  $S_S = 1.5g$  and  $S_1 = 0.60g$ .

### Region 3—Regions of High Seismicity Near Known Faults (Deterministic Values)

**Regional definition:** Regions for which  $1.5 \text{ g} < S_S$  and  $0.60 \text{ g} < S_1$ .

The structural analysis based on the worst load combinations should be the basis for determining the seismic forces  $E$  for combined gravity and seismic load effects when they are additive and the maximum seismic load effect  $E_m$ . The value of  $E$  and  $E_m$  are determined from the following expressions detailed in Ref. 13.2 for additive seismic force and dead load:

$$E = \rho Q_E + 0.2 S_{DS} D \quad (13.4a)$$

$$E = \Omega_o Q_E + 0.2 S_{DS} D \quad (13.4b)$$

For counteracting seismic forces and dead load:

$$E = \rho Q_E - 0.2 S_{DS} D \quad (13.5a)$$

$$E = \Omega_o Q_E - 0.2 S_{DS} D \quad (13.5b)$$

where,  $E$  = combined effect of horizontal and vertical earthquake-induced forces  
 $\rho$  = reliability factor based on system redundancy = 1.0 for categories A, B, and C  
 $Q_E$  = effect of horizontal seismic forces  
 $S_{DS}$  = spectral response acceleration at short periods obtained from IBC Sec. 1613.5.4.  
 $\Omega_o$  = system over-strength factor given in Table 13.4  
 $D$  = effect of dead load

#### 13.2.4 Redundancy

A redundancy coefficient  $\rho$  has to be assigned to all structures based on the extent of structural redundancy inherent in the lateral force resisting system. For structures in seismic design categories A, B, and C, the value of the redundancy coefficient  $\rho$  is to be taken as 1.0. For structures in seismic design categories D, E, and F, the redundancy coefficient  $\rho$  has to be taken as the largest of the values  $\rho_1$  computed at each story level “ $i$ ” of the structure in accordance with the expression

$$\rho_1 = 2 - \frac{20}{r_{\max i} \sqrt{A_i}} \quad (13.6a)$$

In SI Units, the expression becomes

$$\rho_1 = 2 - \frac{6.1}{r_{\max i} \sqrt{A_i}} \quad (13.6b)$$

where

$r_{\max i}$  = ratio of the design story shear resisted by the most heavily loaded single element in the story to the total story shear for a given loading condition,  
 $A_i$  = Floor area in square feet ( $\text{m}^2$ ) of the diaphragm level immediately above the story

The value of  $\rho$  cannot be less than 1.0 and need not exceed 1.5.

#### 13.2.5 General Procedure Response Spectrum

The design response can be idealized by the fundamental period-response acceleration relationship shown in Fig. 13.4 for three fundamental period levels.

**Table 13.4** Design Coefficients and Factors for Basic Seismic-Force-Resisting Systems  
(abridged from Ref. 13.4)

BASIC SEISMIC-FORCE-RESISTING SYSTEM	RESPONSE MODIFICATION COEFFICIENT $R^a$	SYSTEM OVER-STRENGTH FACTOR $\Omega_o$	DEFLECTION AMPLIFICATION FACTOR, $c_d^b$	SYSTEM LIMITATIONS AND BUILDING HEIGHT LIMITATIONS (FT) BY SEISMIC DESIGN CATEGORY <sup>c</sup> AS DETERMINED IN IBC SECTION 1616.				
				A & B	C	D <sup>d</sup>	E <sup>e</sup>	F <sup>f</sup>
<b>Bearing Wall System</b>								
Special reinforced concrete shear walls	5	2.5	5	NL	NL	160	160	100
Ordinary reinforced concrete shear walls	4	2.5	4	NL	NL	NP	NP	NP
Detailed plain concrete shear walls	2	2.5	2	NL	NL	NP	NP	NP
Ordinary plain concrete shear walls	1.5	2.5	1.5	NL	NP	NP	NP	NP
Ordinary precast shear wall	3	2.5	3	NL	NP	NP	NP	ND
<b>Building Frame System</b>								
Ordinary reinforced concrete shear walls	5	2.5	4.5	NL	NL	NP	NP	NP
Detailed plain concrete shear walls	2	2.5	2.5	NL	NL	NP	NP	NP
Ordinary plain concrete shear walls	1½	2.5	1½	NL	NP	NP	NP	NP
Indeterminate precast shear wall	5	2.5	4½	NL	NL	40	40	40
<b>Moment Resistant Frames</b>								
Special reinforced concrete moment frames	8	3	5.5	NL	NL	NL	NL	NL
Intermediate reinforced concrete moment frames	5	3	4.5	NL	NL	NP	NP	NP
Ordinary reinforced concrete moment frames	3	3	2.5	NL <sup>h</sup>	NP	NP	NP	NP
<b>Dual System with Special Moment Frames</b>								
Special reinforced concrete shear wall	7	2.5	5½	NL	NL	NL	NL	NL
Ordinary reinforced concrete shear wall	6	2.5	5	NL	NL	NP	NP	NP
Special reinforced masonry wall	5½	3	5					
<b>Dual System with Intermediate Moment Frames</b>								
Special reinforced concrete shear wall	6½	2.5	5	NL	NL	160	100	100
Ordinary reinforced concrete shear wall	5.5	2.5	4.5	NL	NL	NP	NP	NP
Ordinary reinforced masonry shear wall	3	3	2½	NL	160	NP	NP	NP
Shear Wall-Frame interactive system with ordinary reinforced concrete moment frames and ordinary reinforced concrete shear walls	4½	2.5	4	NL	NP	NP	NP	NP

For SI, 1 ft = 305 mm

<sup>a</sup>Response modification coefficient  $R$ , for use throughout

<sup>b</sup>Deflection amplification factor,  $C_d$

<sup>c</sup>NL = not limited and NP = not permitted

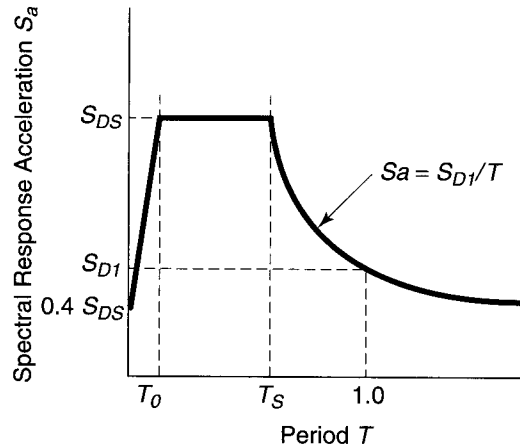
<sup>d</sup>limited to buildings with a height of 240 ft or less.

<sup>e</sup>limited to buildings with a height of 160 ft or less.

<sup>f</sup>Ordinary moment frame is permitted to be used in lieu of Intermediate moment frame in Seismic Design Categories B, and C.

<sup>g</sup>The tabulated value of the overstrength factor,  $\Omega_o$  may be reduced by subtracting ½ for structures with flexible diaphragms but shall not be taken as less than 2.0 for any structure.

<sup>h</sup>Ordinary moment frames of reinforced concrete are not permitted as a part of the seismic-force-resisting system in Seismic Design Category B structures founded on Site-Class E or F soils



**Figure 13.4** Design response spectrum.

1. For periods in seconds less than or equal to  $T_o$ , the design spectral response acceleration  $S_a$  is determined from the following equation:

$$S_a = 0.6 \frac{S_{DS}}{T_o} T + 0.4 S_{DS} \quad (13.7a)$$

2. For periods greater than or equal to  $T_o$ , and less than or equal to  $T_s$ , the design spectral response acceleration  $S_a$ , is taken equal to  $S_D$ .
3. For periods greater than  $T_s$ , the design spectral response acceleration,  $S_a$ , is determined from the expression:

$$S_a = \frac{S_{D1}}{T} \quad (13.7b)$$

where,

$S_{DS}$  = the design spectral response acceleration at short periods

$S_{D1}$  = the design spectral response acceleration at 1-sec periods

$T$  = Fundamental period (in seconds) of the structure

$T_o = 0.2 S_{D1}/S_{DS}$

$T_s = S_{D1}/S_{DS}$

The sites have to be classified for determining the shear wave velocity and the maximum considered earthquake ground motion. Details are given in the IBC (Ref. 13.2) section 1615.

## 13.3 EQUIVALENT LATERAL FORCE METHOD

### 13.3.1 Horizontal Base Shear

In this method, a building is considered fixed at the base. The seismic base shear,  $V$ , in a given direction is determined from the expression(Ref. 13.2):

$$V = C_s W \quad (13.8)$$

where,

$C_s$  = seismic response coefficient

$W$  = The effective seismic weight of the structure, including the total dead loads and other loads listed herein:



1. In areas used for storage, a minimum of 25 percent of the reduced floor live load (floor live load in public garages and open parking structures need not be included).
2. Where an allowance for partition load is included in the floor load design, the actual partition weight or a minimum weight of 10 psf (500 Pa/m<sup>2</sup>) of floor area, whichever is greater.
3. Total operating weight of permanent equipment.
4. 20 percent of flat roof snow load where the flat roof snow load exceeds 30 psf.

$$C_S = \frac{S_{DS}}{(R/I)} \quad (13.9)$$

But  $C_S$  cannot exceed the value:

$$C_S = \frac{S_{D1}}{\left(\frac{R}{I}\right)T} \quad (13.10)$$

nor can it be taken less than:

$$C_S = 0.044 S_{DS} \quad (13.11)$$

where,

$S_{DS}$  = Design spectral response acceleration at short period as determined in Section 13.2.2

$R$  = Response modification factor from Table 13.4

$I$  = Occupancy importance factor from Table 13.5

$T$  = fundamental period of building (seconds)

For buildings and structures in seismic design categories E or F and in buildings and structures for which the 1-sec spectral response,  $S_1$  is equal to or greater than 0.6  $g$ , the value of the seismic coefficient  $C_S$  should not be taken less than:

$$C_S = \frac{0.5S_1}{R/I} \quad (13.12)$$

The fundamental period  $T$  in the direction under consideration has to be determined by analysis based on the structural and deformational characteristics of the resisting element. In lieu of an analysis, an approximate fundamental period  $T_a$ , in seconds, can be used from the following expression:

$$T_a = C_T h^{3/4} \quad (13.13)$$

where,

$C_T$  = Building Period Coefficient

- 0.035 for moment resisting frame systems of steel in which the frames resist 100 percent of the required seismic force and are not enclosed or adjoined by more rigid components that will prevent the frames from deflecting when subjected to seismic forces (the metric coefficient is 0.085)
  - 0.030 for moment resisting frame systems of reinforced concrete in which the frames resist 100 percent of the required seismic force and are not enclosed or adjoined by more rigid components that will prevent the frames from deflecting when subjected to seismic forces (the metric coefficient is 0.073)
  - 0.030 for eccentrically braced steel frames (the metric coefficient is 0.073)
  - 0.020 for all other building systems (the metric coefficient is 0.049)
- $h_n$  = the height (ft or m) above the base to the highest level of the building.

**Table 13.5(a)** Occupancy of Buildings and other Structures for Floods, Wind, Snow, Earthquake and Ice Loads

Occupancy Category	Nature of Occupancy
I	Buildings and other structures that represent a low hazard to human life in the event of failure, including, but not limited to: <ul style="list-style-type: none"> <li>• Agricultural facilities</li> <li>• Certain temporary facilities</li> <li>• Minor storage facilities</li> </ul>
II	All buildings and other structures except those listed in Occupancy Categories I, III, and IV
III	Buildings and other structures that represent a substantial hazard to human life in the event of failure, including, but not limited to: <ul style="list-style-type: none"> <li>• Buildings or structures whose primary occupancy is public assembly with an occupant load greater than 300.</li> <li>• Buildings and other structures containing elementary school or day care facilities with an occupant load greater than 250.</li> <li>• Buildings and other structures containing adult education facilities, such as colleges and universities with an occupant load greater than 500.</li> <li>• Group I-2 occupancies with an occupant load of 50 or more resident patients but not having surgery or emergency treatment facilities.</li> <li>• Group I-3 occupancies.</li> <li>• Any other occupancy with an occupant load greater than 5000<sup>a</sup>.</li> <li>• Power generating stations, water treatment facilities for potable water, waste water treatment facilities and other public utilities facilities not included in occupancy category IV.</li> <li>• Buildings and other structures not included in occupancy category IV containing sufficient quantities of toxic or explosive substances to be dangerous to the public if released.</li> </ul>
IV	Buildings and other structures designated as essential facilities, including, but not limited to: <ul style="list-style-type: none"> <li>• Group I-2 occupancies having surgery or emergency treatment facilities.</li> <li>• Fire, rescue, ambulance and police stations or emergency treatment facilities.</li> <li>• Designated earthquake, hurricane or other emergency shelters.</li> <li>• Designated emergency preparedness, communications, and operations centers and other facilities required for emergency response.</li> <li>• Power-generating stations and other public utility facilities required as emergency backup facilities for Occupancy Category IV structures.</li> <li>• Structures containing highly toxic materials as defined by Section 307 where the quantity of the material exceeds the maximum allowable quantities of Table 307.1 (2) of Ref. 13.2.</li> <li>• Aviation control towers, air traffic control centers and emergency aircraft hangers.</li> <li>• Building and other structures having critical national defense functions.</li> <li>• Water storage facilities and pump structures required to maintain water pressure for fire suppression.</li> </ul>

<sup>a</sup>Reference 13.2

**Table 13.5(b)** Importance Factors\*

Occupancy Category	I
I or II	1.0
III	1.25
IV	1.5

\* Reference 13.2

In cases where moment resisting frames do not exceed 12 stories in height and having a minimum story height of 10 ft (3 m), an approximate period  $T_a$  in seconds in the following form can be used:

$$T_a = 0.1 N \tag{13.14}$$

where

$N$  = number of stories

The computed fundamental period,  $T$ , cannot exceed the product of the coefficient,  $C_n$ , in Table 13.6 for the upper limit on the computed period times the approximate fundamental period,  $T_a$ . The base shear  $V$  is to be based on a fundamental period,  $T$ , in seconds, of 1.2 times the coefficient for the upper limit on the calculated value,  $C_w$  taken from Table 13.6 times the approximate fundamental period  $T_a$ .

**13.3.2 Vertical Distribution of Forces**

The lateral force  $F_x$  (kips or kN) induced at any level can be determined from the following expressions:

$$F_x = C_{vx} V \tag{13.15a}$$

$$C_{vx} = \frac{W_x h_x^k}{\sum_{i=1}^n W_i h_i^k} \tag{13.15b}$$

where

$C_{vx}$  = vertical distribution factor

$V$  = total design lateral force or shear at the base of the building (kips or kN),

$W_i$  and  $W_x$  = the portion of the total gravity load of the building,  $W$ , located or assigned to level  $i$  or  $x$

$h_i$  and  $h_x$  = the height (ft or m) from the base to level  $i$  or  $x$

$k$  = a distribution exponent related to the building period as follows:

**Table 13.6** Coefficient for Upper Limit On Computed Fundamental Period

Design Spectral Response Acceleration at 1-sec period, $S_{D1}$	Coefficient $C_u$
$\geq 0.4$	1.2
0.3	1.3
0.2	1.4
0.15	1.5
$\leq 0.1$	1.7

- For buildings having a period of 0.5 sec or less,  $k = 1$
- For buildings having a period of 2.5 sec or more,  $k = 2$
- for buildings having a period between 0.5 and 2.5 seconds,  $k$  shall be 2 or shall be determined by linear interpolation between 1 and 2

### 13.3.3 Horizontal Distribution of Story Shear $V_x$

The seismic design story horizontal shear in any story,  $V_x$  (kips or kN) should be determined from the following expression:

$$V_x = \sum_{i=1}^x F_i \quad (13.16)$$

where

$F_i$  = the portion of the seismic base shear,  $V$  (kips or kN) introduced at level  $i$ .

### 13.3.4 Rigid and Flexible Diaphragms

- (a) *Rigid diaphragms*: The seismic design story shear,  $V_x$ , has to be distributed to the various vertical elements of the system in the story under consideration. This distribution is to be based on the relative stiffness of the vertical resisting elements and the diaphragms.
- (b) *Flexible Diaphragms*: The seismic design story shear,  $V_x$ , in this case has to be distributed to the various vertical elements based on the tributary area of the diaphragms to each line of resistance. The vertical elements of the lateral force resisting system can be considered to be in the same line of resistance, if the maximum out of plane offset between such elements is less than 5 percent of the building's dimension *perpendicular* to the direction of the lateral load.

### 13.3.5 Torsion

If the diaphragms are not flexible, the design has to include the torsional moment  $M_t$  (Kip-ft or kN-m) resulting from the difference in location between the center of mass and the center of stiffness. Dynamic amplification of torsion for structures in seismic design category C, D, E or F has to be accounted for by multiplying the torsional moments by a torsional amplification factor presented in Ref. 13.2, Sec. 1613.5.3.

### 13.3.6 Story Drift and the P-Delta Effect

- (a) *Drift*: The design story drift,  $\Delta$ , is computed as the difference between the deflections of the center of mass at the top and bottom of the story being considered. If allowable stress design is used  $\Delta$  is computed using earthquake forces without dividing by 1.4. The deflection of level  $X$  is to be determined from the following expression,

$$\delta_x = \frac{C_d \delta_{xe}}{I} \quad (13.17)$$

where,

$C_d$  = Deflection amplification factor (Table 13.4)

$\delta_x$  = Deflections (in. or mm) determined by an elastic analysis of the seismic forces resisting system.

$I$  = Occupancy importance factor (Table 13.5)

The design story drift,  $\Delta$ , has to be increased by an incremental factor relating to the P-delta effects. The redundancy coefficient,  $\rho$ , in the case of drift should be taken as 1.0.

- (b) *P-delta effects*: The P-delta effects can be disregarded if the stability coefficient,  $\theta$ , from the following expression is equal or less than 0.10,

$$\theta = \frac{P_x \Delta}{V_x h_{sx} C_d} \quad (13.18)$$

where,

$P_x$  = The total unfactored vertical design load at and above Level  $x$  (kip or kN); when computing the vertical design load for purposes of determining P-delta, the individual load factors need not exceed 1.0

$\Delta$  = The design story drift (in. or mm) occurring simultaneously with  $V_x$

$V_x$  = The seismic shear force (kip or kN) acting between level  $x$  and  $x - 1$

$h_{sx}$  = The story height (ft or m) below level  $x$

$C_d$  = The deflection amplification factor in Table 13.4.

The stability coefficient,  $\theta$ , shall not exceed  $\theta_{\max}$  determined as follows:

$$\theta_{\max} = \frac{0.5}{C_d \beta} \leq 0.25$$

where:

$\beta$  = The ratio of shear demand to shear capacity for the story between level  $x$  and  $x - 1$ . Where the ratio  $\beta$  is not calculated, a value of  $\beta = 1.0$  shall be used.

When the stability coefficient,  $\theta$ , is greater than 0.10 but less than or equal to  $\theta_{\max}$ , inter-story drifts and element forces shall be computed including P-delta effects. To obtain the story drift for including the P-delta effect, the design story drift shall be multiplied by  $1.0/(1 - \theta)$ .

**Table 13.7** Allowable Story Drift,  $\Delta$  (in. or mm)<sup>a,b,c,d,e</sup>

Building	Occupancy Group		
	I or II	III	IV
Structures, other than masonry shear wall structures, 4 stories or less with interior walls, partitions, ceilings and exterior wall systems that have been designed to accommodate the story drifts.	$0.025h_{sx}$ <sup>c</sup>	$0.020h_{sx}$	$0.015h_{sx}$
Masonry cantilever shear wall structures <sup>c</sup>	$0.010h_{sx}$	$0.010h_{sx}$	$0.010h_{sx}$
Other masonry shear wall buildings	$0.007h_{sx}$	$0.007_{sx}$	$0.007_{sx}$
All other buildings	$0.020h_{sx}$	$0.015h_{sx}$	$0.010h_{sx}$

<sup>a</sup>  $h_{sx}$  is the story height below Level  $x$ .

<sup>b</sup> For seismic force-resisting systems comprised solely of moment frames in Seismic Design Categories D, E, and F, the allowable story drift shall comply with the requirements of ASCE 7-05 Section 12.12.1.1.

<sup>c</sup> There shall be no drift limit for single story structures with interior walls, partitions, ceilings, and exterior wall systems that have been designed to accommodate the story drifts. The structure separation requirement of ASCE 7-05 Section 12.12.3 is not waived.

<sup>d</sup> Structure in which the basic structural system consists of masonry shear walls designed as vertical elements cantilevered from their base or foundation support which are so constructed that moment transfer between shear walls (coupling) is negligible.

<sup>e</sup> Reference 13.2, 13.4

When  $\theta$  is greater than  $\theta_{\max}$ , the structure is potentially unstable and has to be re-designed.

The allowable story drifts are given in Table 13.7.

### 13.3.7 Overturning

Ground motion can result in overturning of a structure. At any story, the increment of overturning moment in the story under consideration would have to be distributed to the various vertical force-resisting elements, in the same proportion as the distribution of the horizontal shear forces to these elements. The overturning moment at level  $x$ ,  $M_x$  (kip-ft or kN-m), is determined from the following expression:

$$M_x = \tau \sum_{i=x}^n F_i (h_i - h_x) \quad (13.19)$$

where

$F_i$  = Portion of  $h_i$  and  $h_x$  = height (ft or m) from the base to the level  $i$  or  $x$ .

$\tau$  = Overturning moment reduction factor

= 1.0 for the top 10 stories

= 0.8 for the 20th story from the top and below

= values between 1.0 and 0.8 determined by a straight line interpolation for stories between the 20th and 10th stories below the top. The seismic base shear,  $V$ , is induced at level  $i$ .

### 13.3.8 Simplified Analysis Procedure for Seismic Design of Buildings

This procedure can be used for structures in seismic use group I, subject to the following limitations, otherwise either the method in Section 13.2 or this section has to be used.

1. Buildings of light-framed construction not exceeding *three* stories in height, excluding basement.
2. Buildings of any construction other than light framed, not exceeding two stories in height, excluding basement.

The seismic base shear,  $V$ , can be computed from the following expression,

$$V = \frac{1.2S_{DS}}{R} W \quad (13.20)$$

where

$S_{DS}$  = Design elastic response acceleration at short periods as determined from Section 13.2

$R$  = Response modification factor from Table 13.4

$W$  = The effective seismic weight of the structure, including the total dead load and other loads listed below.

In areas used for storage, a minimum of 25 percent of the reduced floor live load (floor live load in public garages and open parking structures need not be included.)

1. Where an allowance for partition load is included in the floor load design, the actual partition weight of 10 psf of floor area, whichever is greater.
2. Total weight of permanent operating equipment.
3. 20 percent of flat roof snow load where flat snow load exceeds 30 psf (1.44 kN/m<sup>2</sup>).

The vertical distribution of forces at each level would be computed from the following expression:

$$F_x = \frac{1.2S_{DS}}{R} W_x \quad (13.21)$$

where,

$W_x$  = The portion of the effective seismic weight of the total structure,  $W$ , at story level  $x$ .

For structures satisfying this section, the design story drift,  $\Delta$ , is taken as 1 percent of the story height unless a more exact analysis is made.

Table 13.8 gives the requirements for each story resisting more than 35% of the base shear. Table 13.9 outlines the category occupancy cases and conditions where analytical procedures are permitted in the design.

### 13.3.9 Other Aspects in Seismic Design

The discussion presented in the previous sections is intended only to highlight the most important basic considerations for establishment of the seismic basic shear force values and their distribution over the height of a structure, at all story levels. The scope of this book does not permit more coverage of other essential topics such as modeling, model forces, deflections and drifts, diaphragms, coupling beams, interconnecting shear walls, connections, irregularity of structures, out-of-plane loading, torsion, and foundations.

Through a careful review of the details presented, the numerical examples and solving the assignments, the reader becomes well equipped to handle the design requirement aspects of the topics listed. The International Building Code—IBC 2009 (Ref. 13.2) detailed provisions give all the additional provisions and guidance needed for safe complete designs of concrete structures that can successfully resist severe earthquakes. The ensu-

**Table 13.8** Requirements for Each Story Resisting More than 35% of the Base Shear\*

Lateral Force-Resisting Element	Requirement
Braced Frames	Removal of an individual brace, or connection thereto, would not result in more than a 33% reduction in story strength, nor does the resulting system have an extreme torsional irregularity (horizontal structural irregularity)
Moment Frames	Loss of moment resistance at the beam-to-column connections at both ends of a single beam would not result in more than a 33% reduction in story strength, nor does the resulting system have an extreme torsional irregularity (horizontal structural irregularity)
Shear Walls or Wall Pier with a height-to-length ratio of greater than 1.0	Removal of a shear wall or wall pier with a height-to-length ratio greater than 1.0 within any story, or collector connections thereto, would not result in more than 33% reduction in story strength, nor does the resulting system have an extreme torsional irregularity (horizontal structural irregularity)
Cantilever Columns	Loss of moment resistance at the base connections of any single cantilever column would not result in more than 33% reduction in story strength, nor does the resulting system have an extreme torsional irregularity (horizontal structural irregularity type)
Other	No requirements

\* Reference 13.4

**Table 13.9** Permitted Analytical Procedures \* #

Seismic Design Category	Structural Characteristics	Equivalent Lateral Force Analysis	Modal Response Spectrum Analysis	Seismic Response History (ASCE 7 Procedure)
<b>B, C</b>	Occupancy Category I or II buildings of light-framed construction not exceeding 3 stories in height	P <sup>#</sup>	P	P
	Other Occupancy Category I or II buildings not exceeding 2 stories in height	P	P	P
	All other structures	P	P	P
<b>D, E, F</b>	Occupancy Category I or II buildings of light-framed construction not exceeding 3 stories in height	P	P	P
	Other Occupancy Category I or II buildings not exceeding 2 stories in height	P	P	P
	Regular structures with $T < 3.5T_s$ and all structures of light-frame construction	P	P	P
	Irregular structures with $T < 3.5T_s$ and having only horizontal irregularities Type 2, 3, 4, or 5 of Table 32.2-9 or vertical irregularities Type 4, 5a, or 5b of Table 32.2-10	P	P	P
	All other structures	NP <sup>#</sup>	P	P

\* Reference 13.4

# P= Permitted, NP = Not permitted

ing sections will present ACI 318-08 code provisions for proportioning and detailing of reinforced concrete elements that can withstand Seismic loading through conformity with the IBC 2009 requirements.

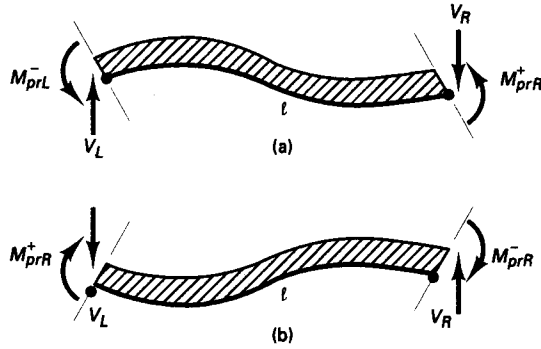
## 13.4 SEISMIC SHEAR FORCES IN BEAMS AND COLUMNS OF A FRAME: STRONG COLUMN–WEAK BEAM CONCEPT

### 13.4.1 Probable Shears and Moments

Shear failure in reinforced concrete members is regarded as brittle failure. Therefore, in designing earthquake-resistant structures, it is important to provide excess shear capacity over and above that corresponding to flexural failure. The ACI 318-05 requirements are based on the strong column-weak beam concept subsequently discussed. Hence, plastification of the critical regions at the ends of the beams will have to be considered as a possible loading condition.

The shear force is then computed based on the moment resistances in the developed plastic hinges, labeled as probable moment resistance,  $M_{pr}$ , developed when the longitudinal flexural steel enters into the hardening stage. Consequently, in the computation of the probable moment resistance,  $1.25 f_y$  is used as the stress in the longitudinal reinforcement. This is because the development of inelastic rotation at the faces of the





**Figure 13.5** Seismic moments and shears at beam ends: (a) sidesway to the left; (b) sidesway to the right

joints is associated with strains in the flexural reinforcement well in excess of the yield strain. As a result, the joint shear force generated by the flexural reinforcement is computed for an increased stress  $\lambda_o f_y$  where  $\lambda_o = 1.25$ , namely, an increase in stress of 25 percent. In order to absorb the energy that can cause plastic hinging, the earthquake resistant frame has to be ductile in part through confinement of the longitudinal reinforcement of the columns and the beam-column joints and in part through the provision of the excess shear capacity previously discussed.

Fig. 13.5 shows the deformed geometry of and the moment and shear forces for a beam subjected to gravity loading and reversible side-sway. If the intensity of gravity load is  $W_u$  then, ACI 318-08 stipulates:

$$W_u = 1.2D + 1.6L + 1.4E$$

**13.4.1.1 Factored Loads**

The IBC (Sec. 1605.2) stipulates the following load combinations; they are comparable to the ACI factored loads in Section 4.11.2:

$$\begin{aligned}
 &1.4D \\
 &1.2D + 1.6L + 0.5(L_r \text{ or } S \text{ or } R) \\
 &1.2D + 1.6L(L_r \text{ or } S) + (f_1L \text{ or } 0.8W) \\
 &1.2D + 1.3W + f_1L + 0.5(L_r \text{ or } S \text{ or } R) \\
 &1.2D + 1.0E + (f_1L \text{ or } f_2S) \\
 &0.9D \pm (1.0E \text{ or } 1.3W)
 \end{aligned}
 \tag{13.22}$$

where,

- $f_1 = 1.0$  for floors in places of public assembly, for live loads in excess of 100 lb/ft<sup>2</sup> (4,79 kN/m<sup>2</sup>), and for parking garage live load
- = 0.5 for other live loads
- $f_2 = 0.7$  For roof configurations (such as saw tooth) that do not shed snow off the structure
- = 0.2 for other roof configurations
- $L$  = Live load except roof load
- $L_r$  = Roof live load including any live load reduction
- $R$  = Rain load
- $S$  = Snow load
- $W$  = Wind load

The seismic shear forces are:



**Photo 13.4** Skybridge, Vancouver, Canada, a 2020-ft long cable-stayed bridge and the world's longest transit bridge. (Courtesy Portland Cement Association.)

$$V_L = \frac{M_{prL}^- + M_{prR}^+}{l} + \frac{1.2D + 1.6L}{2} \quad (13.23)$$

$$V_R = \frac{M_{prL}^+ + M_{prR}^-}{l} - \frac{1.2D + 1.6L}{2} \quad (13.24)$$

where  $l$  = span,  $L$  and  $R$  subscripts = left and right ends and  $M_{pr}$  = probable moment strength at the end of the beam based on steel reinforcement tensile strength of  $1.25 f_y$  and strength reduction factor  $\phi = 1.0$ . These instantaneous moments,  $M_{pr}$  should be computed on the basis of equilibrium of moments at the joint where the beam moments are equal to the probable moments of resistance.

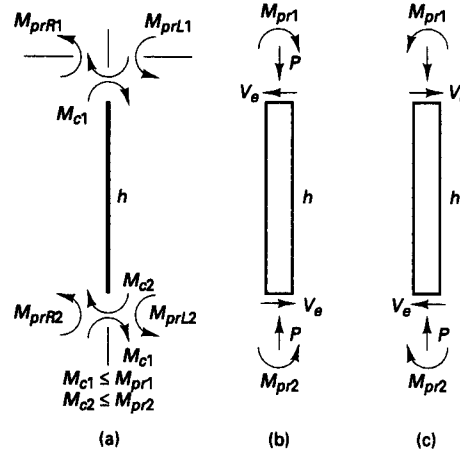
The shear forces in the columns are computed in a similar manner so that the horizontal shear force,  $V_e$  at top and bottom of the column is

$$V_e = \frac{M_{pr1} + M_{pr2}}{h} \quad (13.25)$$

except that end moments for columns  $M_{pr1}$  and  $M_{pr2}$  need not be greater than the moments generated by the  $M_{pr}$  of beams framing into the beam-column joint.  $h$  = column height and the subscripts 1 and 2 indicate the top and bottom column end moments respectively as seen in Figure 13.6. The sense of moments at the joints is shown in Figure 13.7.

### 13.4.2 Strong Column Weak Beam Concept

As previously stated, U.S. seismic codes require that earthquake induced energy be dissipated by plastic hinging of the beams rather than the columns. This hypothesis is due to the fact that compression members such as columns have lower ductility than flexure-dominant beams. If the columns are not stronger than the beams framing into a joint,



**Figure 13.6** Seismic moments and shears at column ends: (a) joint moments (b) sway to right; (c) sway to left.

inelastic action can develop in the column, and if large enough, can cause the column to collapse. Furthermore, the consequence of a column failure is far more severe than a local beam failure. Therefore, the ACI 318-08 Code as well as the IBC stipulates “strong columns and weak beams”. This is ensured by the following inequality

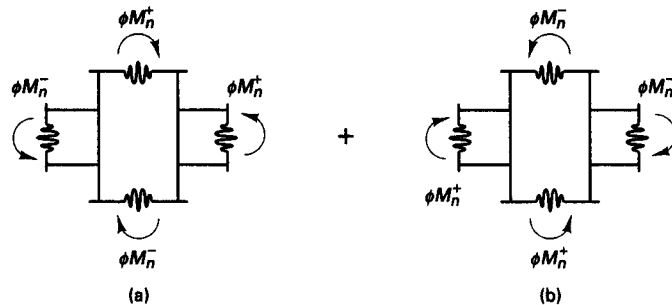
$$\sum M_{nc} \geq \left(\frac{6}{5}\right) \sum M_{nb} \tag{13.26}$$

where  $\sum M_{col}$  = sum of nominal flexural strengths of columns framing into joint, calculated for factored axial forces consistent with the direction of lateral forces considered, resulting in lowest flexural strength.

$\sum M_{bm}$  = sum of moments, at the face of the joint, corresponding to the nominal flexural strengths of the beams framing into that joint.

For a joint subjected to reversible base shear forces, as shown in Fig. 13.7, Eq. 13.26 becomes

$$(\phi M_n^+ + \phi M_n^-)_{col} \geq \frac{6}{5} (\phi M_n^+ + \phi M_n^-)_b \tag{13.27}$$



$$(\phi M_n^+ + \phi M_n^-)_{col} \geq \left(\frac{6}{5}\right) (\phi M_n^+ + \phi M_n^-)_{bm}$$

**Figure 13.7** Seismic moment summation at beam-column joint: (a) sidesway to left; (b) sidesway to right.

where  $\phi = 0.90$  for beams  
 $= 0.65$  for tied and  $0.75$  for spiral columns.  
 $= 0.90$  to  $0.65$  for beam-columns.

### 13.5 ACI CONFINING REINFORCEMENTS FOR STRUCTURAL CONCRETE MEMBERS

Members in frames designed for seismic regions can be classified into two categories for proportioning transverse reinforcement as follows:

- (a) Members with factored axial compressive force  $P_u$  not exceeding  $(A_g f'_c/10)$  are treated as beams.
- (b) Members with factored axial compressive force  $P_u$  greater than  $(A_g f'_c/10)$  are treated as columns.

#### 13.5.1 Longitudinal Reinforcement in Compression Members

1. In seismic design, when the factored axial load  $P_u$  is negligible or significantly less than  $A_g f'_c/10$ , the member is considered a flexural member (beam). If  $P_u > A_g f'_c/10$ , the member is considered beam-column, because it is subjected to both axial and flexural loads as columns and shear walls are.
2. The shortest cross-sectional dimension  $\geq 12$  in. (300 mm).
3. The limitation on the longitudinal reinforcement ratio in the beam-column element is  $0.01 \leq \rho_g = A_v/A_g \leq 0.06$ . For practical considerations, an upper limitation of 6 percent is too excessive, because it results in impractical congestion of longitudinal reinforcement. A practical maximum total percentage  $\rho_g$  of 3.5 percent to 4.0 percent should be a reasonable limit.
4. A minimum percentage of longitudinal reinforcement in flexural members (beams) for sections requiring tensile reinforcement.

$$\rho \geq \frac{3\sqrt{f'_c}}{f_y} \geq \frac{200}{f_y} \leq 0.025 \quad (13.28)$$

But under no condition should the value of  $\rho$  exceed 0.025. The stresses  $f'_c$  and  $f_y$  in these expressions are in psi units. All reinforcement has to be continued through the joint. At least two bars have to be continuously provided *both* at top and bottom.

5. Beams should have at least two of the longitudinal bars continued along both the top and the bottom faces. These bars should be developed at the face of the support.
6. Columns having clear height-to-maximum-plan-dimension ratio of *five* or less should be designed in shear such that not less than the smaller of (a) and (b) :
  - (a) The sum of the shear associated with development of nominal moment strengths of the member at each restrained end of the clear span and the shear calculated for factored gravity loads;
  - (b) The maximum shear obtained from design load combinations that include modulus E, with E assumed to be twice the modulus prescribed by the governing code for earthquake resistant design.
7. Where design forces have been magnified to account for overstrength of the vertical elements of seismic-force-resisting system, the limit of  $(A_g f'_c/10)$  should be changed to  $(A_g f'_c/4)$  and the transverse reinforcement should extend into the discontinued member for at least a distance  $I_d$  of the largest longitudinal column bar required in the design.



**Photo 13.5** Column localized damage in a high-rise frame building, Los Angeles 1994 Earthquake. (Courtesy Portland Cement Association.)

8. Columns supporting reactions from discontinuous stiff members, such as walls, should be provided with transverse reinforcement at a spacing,  $s_o$ , over the full height beneath the level at which the discontinuity occurs if portion of the factored axial compressive force in these members related to earthquake effects exceeded  $(A_g f'_c/10)$ . Where design forces have been magnified to account for overstrength of the vertical elements of the service-force-resisting system, the limit of  $(A_g f'_c/10)$  should be changed to  $(A_g f'_c/4)$  according to the ACI 318-08 Code. This transverse reinforcement should extend above and below the column as stipulated in this chapter.
9. Main reinforcement should be chosen on the basis of the strong column-weak beam concept of the ACI Code, namely,  $\Sigma M_{nc} \geq 6/5 \Sigma M_{nb}$
10. The nominal moment strength requirements are:
  - (a)  $M_n^+$  at joint face  $\geq 1/2 M_n^-$  at that face.
  - (b) Neither the negative nor the positive moment strength at *any* section along the span can be less than *one quarter* the maximum moment strength provided at the face of either joint. Hence, at joint face:

$$M_n^+ \geq \frac{1}{2} M_a \quad (13.29a)$$

at any section:

$$M_n^+ \geq \frac{1}{4} (M_a^-)_{\max} \quad (13.29b)$$

$$M_n^- \geq \frac{1}{4} (M_a^+)_{\max} \quad (13.29c)$$

11. For coupling beams with aspect ratio  $l_n/h < 2$ , and with factored shear force  $V_u$  exceeding  $4\sqrt{f'_c} A_{cp}$  has to be reinforced with *two* intersecting groups of diagonally placed bars, symmetrical about the midspan, where  $A_{cp}$  = area of concrete resisting shear.
12. Prestressing steel should be unbonded in potential plastic hinge regions. The calculated strain in the prestressing steel under the design displacement procedure should be less than one percent.
13. Prestressing steel should not contribute to more than one quarter of the positive and negative flexural strength at the critical section in a plastic hinge region and should be anchored at or beyond the external face of the joint.

### 13.5.2 Transverse Confining Reinforcement

Transverse reinforcement in the form of closely spaced hoops (ties) or spirals has to be adequately provided. The aim is to produce adequate rotational capacity within the elastic hinges that may develop as a result of the seismic forces.

1. For column spirals, the minimum volumetric ratio of the spiral hoops needed for the concrete core confinement cannot be less than the larger of:

$$\rho_s \geq \frac{0.12 f'_c}{f_{yt}} \quad (13.30a)$$

or

$$\rho_s \geq 0.45 \left( \frac{A_g}{A_{ch}} - 1 \right) \frac{f'_c}{f_{yt}} \quad (13.30b)$$

whichever is greater, where

$\rho_s$  = ratio of volume of spiral reinforcement to the core volume measured out to out.

$A_g$  = gross area of the column section.

$A_{ch}$  = core area of section measured to the outside of the transverse reinforcement (sq. in.).

$f_{yt}$  = specified yield of transverse reinforcement, psi.

2. For column rectangular hoops, the total cross-sectional area within spacing  $s$ , cannot be less than the larger of:

$$A_{sh} \geq 0.09 s b_c \frac{f'_c}{f_{yt}} \quad (13.31a)$$

or

$$A_{sh} \geq 0.3 s b_c \left( \frac{A_g}{A_{ch}} - 1 \right) \frac{f'_c}{f_{yt}} \quad (13.31b)$$

where

$A_{sh}$  = total cross-sectional area of transverse reinforcement (including cross ties) within spacing  $s$  and perpendicular to dimension  $h_c$ .

$b_c$  = cross-sectional dimension of member core measured c.-c. of confining reinforcement, in., as in Figure 13.13.

$h_x$  = maximum horizontal spacing of hoops or ties on all faces of the column, in.

$A_{ch}$  = cross-sectional area of structural member, measured out-to-out of transverse reinforcement

$s$  = spacing of transverse reinforcement measured along the longitudinal axis of the member, in.

$s_{max} \leq$  one-quarter of the smallest cross-sectional dimension of the member or 6 times the diameter of longitudinal reinforcement,

$$\text{Also} \quad s_o = 4 + \left( \frac{14 - h_x}{3} \right)$$

$s_o$  = longitudinal spacing of the transverse reinforcement within length  $l_o$ . Its value should not exceed 6 in. and need not be taken less than 4 in.

Additionally, if the thickness of the concrete outside the confining transverse reinforcement exceeds 4 in., additional transverse reinforcement has to be provided at a spacing not to exceed 12 in. The concrete cover on the additional reinforcement should not exceed 4 in.

3. The confining transverse reinforcement in *columns* should be placed on *both* sides of a potential hinge over a distance  $l_o$ . The largest of the following three conditions governs  $l_o$ :
  - (a) depth of member at joint face
  - (b) one-sixth of the clear span
  - (c) 18 in.

Increase the distance  $l_o$  by 50% or more in locations of high axial loading and flexural demand such as at the base of a building. When transverse reinforcement is not provided throughout the column length, the remainder of the column length has to contain spiral or hoop reinforcement with spacing not exceeding the smaller of six times the diameter of the longitudinal bars or 6 in.

4. For beam confinement, the confining transverse reinforcement at *beam* ends should be placed over a length equal to *twice* the member depth  $h$  from the face of the joint on either side or of any other location where plastic hinges can develop. The maximum hoop spacing should be the smallest of the following four conditions:
  - (a) One-fourth effective depth  $d$ .
  - (b)  $8 \times$  diameter of longitudinal bars.
  - (c)  $24 \times$  diameter of the hoop.
  - (d) 12 in. (300 mm).

IBC requires that the spacing of the confining loops in the plasticity zone of the beam not exceed 4 in. Figure 13.13(a) from Ref. 13.14 summarizes typical detailing requirements for a confined column in a monolithic ductile connection and Figure 13.13(b) from Ref. 13.24 for a hybrid precast prestressed assembly.

5. Reduction in confinement at joints: a 50 percent reduction in confinement and an increase in the minimum tie spacing to 6 in. is allowed by the ACI Code, if a monolithic joint is confined on all *four* faces by adjoining beams with each beam wide enough to cover three quarters of the adjoining face.
6. The yield strength of reinforcement in seismic zones should not exceed 60,000 psi.

### 13.5.3 Horizontal Shear at the Joint of Beam–Column Connections

Test of joints and deep beams have shown that shear strength is not as sensitive to joint shear reinforcement as for that along the span. On this basis, the ACI Code has assumed the joint strength as a function of only the compressive strength of the concrete and requires a minimum amount of transverse reinforcement in the joint. The effective area  $A_j$  within the joint should in no case be greater than the column cross-sectional area.

The minimal shear strength of the joint should not be taken greater than the forces  $V_n$  specified below for normal weight concrete,

1. Confined on all faces by beams framing into the joint,

$$V_n \leq 20 \lambda \sqrt{f'_c} A_j \quad (13.32a)$$

2. Confined on three faces or on two opposite faces,

$$V_n \leq 15 \lambda \sqrt{f'_c} A_j \quad (13.32b)$$

3. All other cases,

$$V_n \leq 12 \lambda \sqrt{f'_c} A_j \quad (13.32c)$$

A framing beam in a monolithic joint is considered to provide confinement to the joint only if at least three-quarters of the joint is covered by the beam.

The value of allowable  $V_n$  should be reduced by 25 percent if lightweight concrete is used. Also, test data indicates that the value in Eq. 13.32c is unconservative when applied to corner joints.  $A_j$  = effective cross-sectional area within a joint as in Figure 13.8, in a plane parallel to the plane of reinforcement generating shear at the joint. The reversible seismic forces at the joint are shown in Figure 13.9. The ACI Code assumes that the horizontal shear in the joint is determined on the basis that the stress in the flexural tensile steel =  $1.25 f_y$ . Figure 13.9 shows the forces acting on a beam-column connection at the joint.

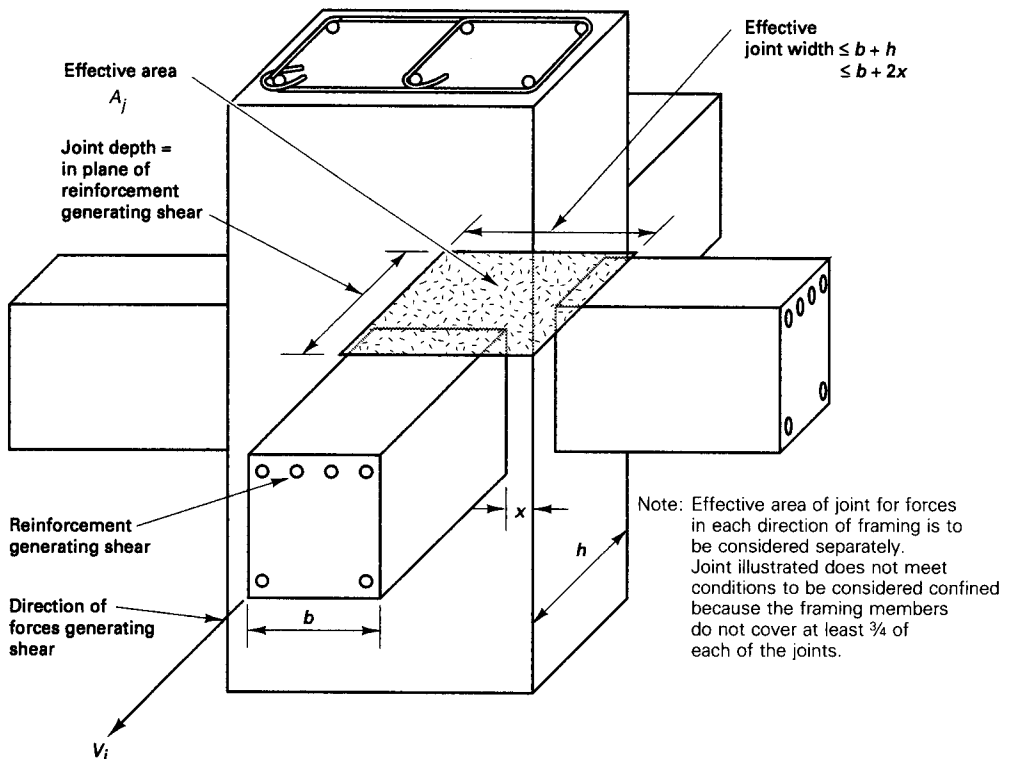
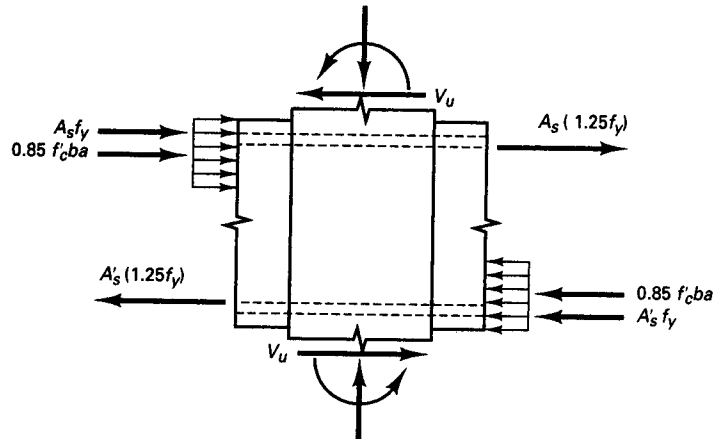


Figure 13.8 Seismic effective area of joint (Ref. 13.1).





**Figure 13.9** Reversible forces at beam-column joint connection. ( $V_u$  = horizontal shear at joint).

For slab-column connections of two-way slabs without beams, slab shear reinforcement should be based on  $V_n \leq 6\sqrt{f'_c} b_o d$  provided that  $V_s \geq 3\sqrt{f'_c} b_o d$ , and should extend at least 4 times the slab thickness from the face of the support.

### 13.5.4 Development of Reinforcement

For bars of sizes No. 3 through 11 terminating at an exterior joint with standard 90° hooks in normal concrete, the development length  $\ell_{dh}$  beyond the column face, as required by the ACI 318 Code, should not be less than the largest of following:

$$\ell_{dh} \geq f_y d_b / (65 \sqrt{f'_c}) \quad (13.33a)$$

$$\ell_{dh} \geq 8 d_b \quad (13.33b)$$

where  $d_b$  = bar diameter

$$\ell_{dh} \geq 6 \text{ in.} \quad (13.33c)$$

The development length provided beyond the column face must be no less than  $\ell_d = 2.5 \ell_{dh}$  when the depth of concrete cast in a monolithic joint in one lift beneath the bar  $\leq 12$  in., or  $\ell_d = 3.5 \ell_{dh}$  when the depth of concrete cast in one lift beneath the bar exceeds 12 in.

For lightweight concrete,  $\ell_{dh}$  for a bar with a standard 90° hook should not be less than the largest of  $10 d_b$ ,  $7\frac{1}{2}$  in. and 1.25 times the length required by Equation 13.33(a).

All straight bars terminated at a joint are required to pass through the confined core of the column or shear wall boundary member. Any portion of the straight embedment length not within the confined core should be increased by a factor of 1.6.

### 13.5.5 Allowable Shear Stresses in Structural Walls, Diaphragms, and Coupling Beams

#### 1. Structural Walls and Diaphragms

High shear walls, that is, structural walls, with height-to-depth ratio in excess of 2.0 essentially act as vertical cantilever beams. As a result, their strength is principally determined by flexure rather than by shear.

**Flexural considerations:**

**(a) Displacement-based Approach:** For walls or piers continuous in cross section from the base of the structure to the top of the wall and designed to have a single critical section for flexure and axial loads, the compressive zones have to be reinforced with boundary elements with a geometry defined as follows:

$$c \geq \frac{l_w}{600 (\delta_u/h_w)} \quad (13.34a)$$

but that  $\delta_u/h_w$  is taken not less than 0.007. The reinforcement has to extend vertically along the wall a distance not less than the larger of  $l_w$  or  $M_u/4V_u$  from the critical section.

$c$  = distance from the extreme compression fibers to the neutral axis computed from the factored axial force and nominal moment strength.

$h_w$  = height of entire wall.

$\delta_u$  = design displacement

**(b) Stress-based Approach:** This alternative design procedure requires that boundary elements in structural walls have to be provided whenever the extreme fiber compressive stresses exceed  $0.20 f'_c$ . The boundary elements have to extend along the vertical boundaries of the entire wall and around the edges of openings. They can be discontinued where the computed compressive stress is less than  $0.15 f'_c$ . The stresses are computed for factored forces using a linearly elastic model and cross-section properties.

It should be noted that when boundary elements are required, the wall is essentially detailed in a similar manner in both approaches.

**Shear considerations:**

If the shear wall is subjected to factored in-plane seismic shear forces  $V_{uh} > A_{cv} \lambda \sqrt{f'_c}$ , then it should be reinforced with a reinforcement percentage  $\rho_v \geq 0.0025$ . Spacing of the reinforcement each way should not exceed 18 in. center to center. If  $V_{uh} < A_{cv} \lambda \sqrt{f'_c}$ , the reinforcement percentage can be reduced to 0.0012 for No. 5 bars or less in diameter and 0.0015 for larger deformed bar sizes. Reinforcement provided for shear strength has to be continuous and distributed across the shear plane.

At least two curtains of reinforcement are needed in such a wall if the in-plane factored shear forces exceed a value of  $2 A_{cv} \lambda \sqrt{f'_c}$ .

where

$\rho_t = A_{sv}/A_{cv}$   
 $A_{cv}$  = net area of concrete cross section = thickness  $\times$  length of section in direction of shear considered.  
 $A_{sv}$  = projection on  $A_{cv}$  of area of distributed shear reinforcement crossing the plane  $A_{cv}$ .

The nominal shear strength  $V_n$  of structural walls and diaphragms of high-rise buildings with aspect ratio greater than 2 should not exceed the shear force computed from:

$$V_n = A_{cv} (2 \lambda \sqrt{f'_c} + \rho_t f_y) \quad (13.34b)$$

where

$\rho_n$  = ratio of distributed shear reinforcement of a plane perpendicular to the plane of  $A_{cv}$ .

For low-rise walls with aspect ratio  $h_w/l_w$  less than 2, the ACI Code requires that the coefficient in Eq. 13.34b be increased linearly up to a value of 3 when the  $h_w/l_w$  ratio



**Photo 13.6** Northridge, California, 1994 earthquake structural failure. (Courtesy Dr. Murat Saatcioglu.)

reaches 1.5 in order to account for the higher shear capacity of low-rise walls. In other words,

$$V_n = A_{cv} (\alpha_c \lambda \sqrt{f'_c} + \rho_t f_y) \quad (13.34c)$$

where

$$\alpha_c = 2 \text{ when } h_w/l_w \geq 2 \text{ and } \alpha_c = 3 \text{ when } h_w/l_w = 1.5; V_u = \phi V_n$$

$\phi = 0.6$  for designing the joint, if nominal shear is less than the shear corresponding to the development of the nominal flexural strength of that corresponding to the development of the nominal flexural strength of the member.

The nominal flexural strength is determined considering the most critical factored axial loads including earthquake effects. The maximum allowable nominal unit shear strength in structural walls is  $8A_{cv} \lambda \sqrt{f'_c}$  where  $A_{cv}$  is the total cross-sectional area (in.<sup>2</sup>) previously defined and  $f'_c$  is in psi. However, the nominal shear strength of any one of the individual wall piers can be permitted to have a maximum value of  $10 A_{cp} \lambda \sqrt{f'_c}$ , where  $A_{cp}$  is the cross-sectional area of the individual pier.

## 2. Coupling Beams:

The provisions for allowable shear stresses in coupling beams are as follows. Coupling beams are structural elements connecting structural walls to provide additional stiffness and energy dissipation. In many cases, geometrical limits result in coupling beams whose depth to clear span ratio is high (Ref. 13.1, 13.2). Hence, they can be con-

trolled by shear and subjected to strength and stiffness deterioration in earthquakes. To reduce the extent of the deterioration, the span to depth ratio  $l_n/d$  is limited to a value of 4.0 except in cases of special moment frames in which the width to depth ratio cannot be less than 0.30. Coupling beams should only be used in locations where damage to them would not impair the vertical load carrying capacity of the structure or the integrity of the non-structural components and their connection to the structure (Ref. 13.1).

If the factored shear force  $V_u$  exceeds  $4 \lambda \sqrt{f'_c} A_{cp}$ , two intersecting groups of diagonally-placed bars symmetrical about the midspan have to be used. This requirement can be waived if it can be demonstrated that their stiffness loss does not impair the vertical load carrying capacity of the structure. The nominal shear strength,  $V_n$ , is determined from the following expression.

$$V_n = 2A_{vd} f_y \sin \alpha \leq 10 \lambda \sqrt{f'_c} A_{cp} \quad (13.35)$$

where  $A_{cp}$  is the cross-sectional area of the beam, and  $A_{vd}$  is the total area of reinforcement in each group of diagonal bars in a diagonally reinforced beam.

$\alpha$  = angle between the diagonally placed bars and the longitudinal axis of the coupling beams.

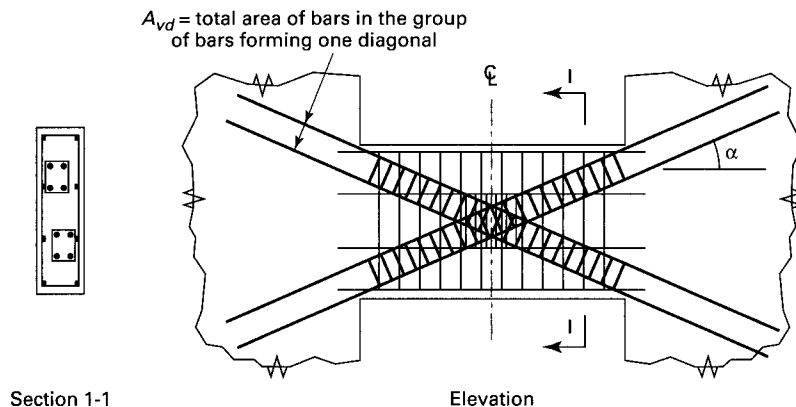
For coupling beams when reinforced with intersecting groups of diagonally placed bars, each group has to consist of a minimum of four bars provided in two or more layers. The diagonal bars have to be embedded into the wall not less than 1.25 times the development length  $l_d$  for steel yield strength  $f_y$  in tension. Each group of the diagonal bars have to be enclosed in transverse reinforcement having out-to-out dimensions not smaller than  $b_w/2$  parallel to  $b_w$  and  $b_w/5$  in all other sides. The transverse reinforcement should have spacing measured parallel to the diagonal bars not exceeding six times the diameter of the diagonal bar but not exceeding 6 inches along the entire length of the longitudinal bar. The nominal shear  $V_n$  is determined from the above expression:

$$V_n = 2 A_{vd} f_y \sin \alpha \leq 10 \lambda \sqrt{f'_c} A_{cw}$$

where  $\alpha$  is the angle between the diagonal bars and the longitudinal axis of the coupling beam.

In the case of structural diaphragms, the nominal shear in the diaphragm is limited to  $V_n \leq 8 A_{cv} \lambda \sqrt{f'_c}$ .

A typical illustration of a diagonally reinforced coupling beam is shown in Fig. 13.10. The diagonally-placed bars have to be developed in tension within the wall and also considered to contribute to the nominal flexural strength of the coupling beam.



**Figure 13.10** Coupling Beam with Diagonally Oriented Reinforcement

## 13.6 SEISMIC DESIGN CONCEPTS IN HIGH-RISE BUILDINGS AND OTHER STRUCTURES

### 13.6.1 General Concepts

The design of concrete structures in seismic regions has to take into consideration the impact of the large reversible seismic horizontal forces that act on a structure during an earthquake. For the main elements of a structure to service such high-intensity forces, the structure must have adequate ductility in the joints of the principal components or in the response of solid vertical elements such as structural shear walls to ground motion. Excessive strength is not necessarily desirable or essential in earthquake-resistant design. Inelastic response can overcome service damage if adequate ductility is available through proper design and confinement. Shear strength has to exceed the flexural strength of the components and joints in order that shear deformations do not occur as a result of significant loss of stiffness and strength (Ref 13.17).

The failure due to severe ground motion is accentuated in stories with sudden stiffness changes. The dynamic response of the total structure is determined by the flexible stories. Since loss of stiffness results in large inelastic deformations, such deformations, if of sufficient magnitude, would lead to the collapse of the total structure. Therefore, the design has to proportion the detailing of the members to such a degree that the components can tolerate the expected large inelastic deformations without rupture. Such detailing will be discussed in subsequent sections.

In the design of high-rise buildings, a number of analytical tools are usually used to identify the required strength and probable deformations demand (Refs. 13.14, 13.16, 13.17). The required strength is the factored load or required ultimate strength of the component along the lateral load path (“ductile-link”) that is expected to absorb the anticipated post-yield deformation. The strength of this “ductile-link” is usually developed by combining load effects (D, L, E, etc.), although moment redistribution may be used to attain a more rational development of the system (Ref. 13.17). The *design* earthquake load (E) must exceed that required by the IBC or other controlling codes. Typically, the strength of this “ductile-link” is developed from site-specific ground motion studies.

The probable deformation demand is the level of deformability likely to be imposed on a structure and most importantly on the component that is expected to deform in the post-yield range during a catastrophic earthquake. Deformation objectives will be many times greater than those associated with the objective strength level. The designer should endeavor to have those post-yield deformations occur where they are likely to create the least potential for collapse of the structure and minimize component damage. It is for this reason that the weak beam/strong column philosophy is adopted in the design of special moment frames, be they constructed of concrete or steel. The brief design examples that are in subsequent sections will presume that the level of strength and deformation required of the “ductile-link” has been determined. The development of the ductile-link is essential to the success of the adopted seismic bracing system, but it is not sufficient. The other members along the lateral load path must be protected so that they do not fail as the ductile-link deforms. This member protection hypothesis is generically referred to as *capacity-based design* (Ref. 13.16, 13.17).

### 13.6.2 Ductility of Elements and Plastic Hinging

Ductility is an essential property in structures which have to respond to inelasticity in severe earthquakes. It is measured in terms of strain, displacement, and rotation. High ductility enables a member or a joint to sustain plastic strains without a significant reduction of stress. Hence, large rotations are essential as a measure of curvature if discontinuity, unsustainable displacements, or rupture are to be avoided. Three measures of ductility are identified:

(a) Strain ductility defined by

$$\mu_e = \frac{\epsilon}{\epsilon_y} \quad (13.36a)$$

where  $\epsilon$  = maximum sustainable strain  
 $\epsilon_y$  = yield strain ductility

(b) Curvature ductility defined by:

$$\mu_\phi = \frac{\phi_m}{\phi_y} \quad (13.36b)$$

where  $\phi_m$  = maximum sustainable curvature  
 $\phi_y$  = yield curvature

(c) Displacement ductility defined by:

$$\mu_\Delta = \frac{\Delta}{\Delta_y} \quad (13.36c)$$

where  $\Delta$  = maximum sustainable displacement =  $\Delta_y + \Delta_p$   
 $\Delta_y$  = yield displacement  
 $\Delta_p$  = plastic displacement

The values of all these ductility factors have to be considerably greater than 1.0 for inelastic behavior to be sustainable. Ductility can effectively be achieved through adequate confinement as stipulated in the *ACI 318-08 code* (Ref. 13.1) and the *International Building Code, IBC 2009* (Ref. 13.2)

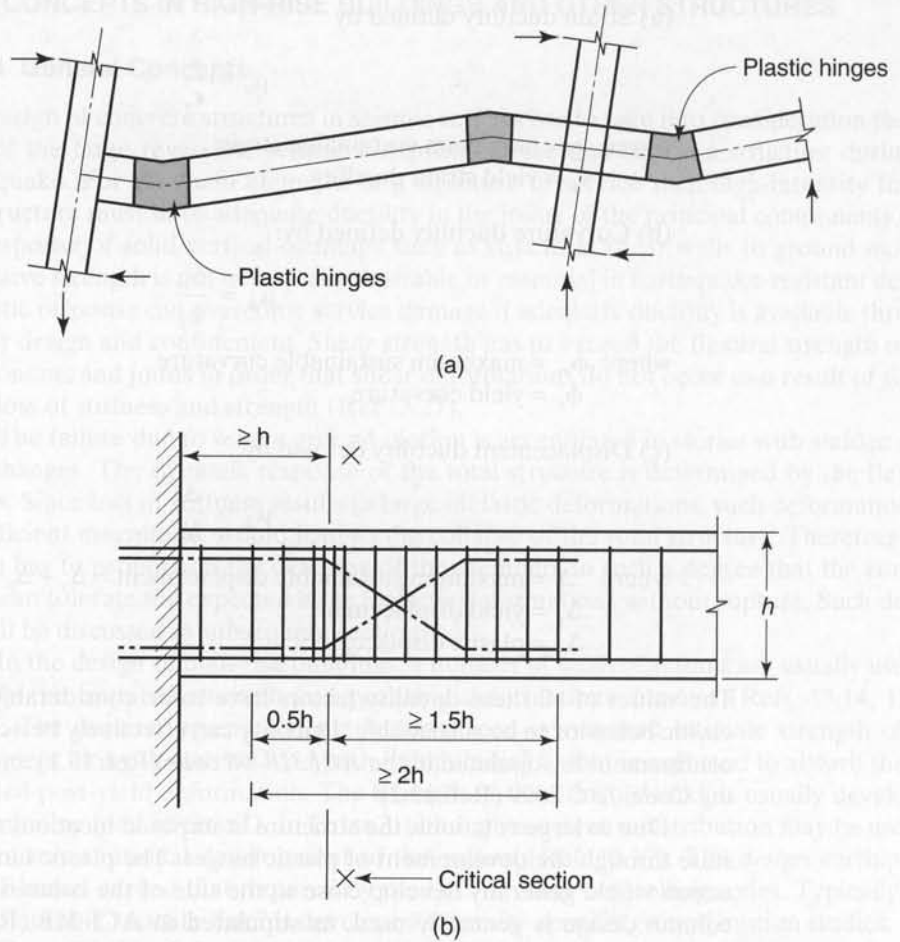
Due to large rotations, the structure at imposed locations reaches the limit ultimate state through the development of plastic hinges. The plastic hinges generated by seismic action would generally develop close to the side of the column since weak beam–strong column design is generally used, as stipulated in ACI 318 (Ref. 13.1). For the plastic hinge to develop in the beams rather than the columns of a multistory frame, special confinements have to be provided over a beam's length ahead of the columns face, equal to twice the beam depth. Figure 13.11 (a) and (b) schematically demonstrate the imposed locations of the plastic hinges in monolithic construction.

Hence, the columns would be large enough to resist the design seismic forces while the beams possess the required ductility to respond to the seismic strains imposed by the earthquake. In the case of using precast ductile moment resisting frames, a hybrid connection can be used and proportioned by a capacity-based design. An example is the Dywidag Ductile Assembly described in Section 13.7.2 or a dual system as in Section 13.7.5, providing a large level of energy dissipation.

### 13.6.3 Ductility Demand Due to Drift Effect

As the multistory floors drift in response to the horizontal seismic force, the drift increases in the lower levels due to the  $P$ - $\Delta$  effect. The plastic rotation demand increases. If ignoring the  $P$ - $\Delta$  effect results in inelastic drift significantly larger than 1.5 percent of the story height, the drift, with the  $P$ - $\Delta$  influence, would be considerably magnified. In such a case, the plastic rotation demands in both beams and first-story columns would exceed the levels achieved with normal detailing in seismic design (Ref. 13.17).

It must be emphasized that design joint deformations associated with shear and bond mechanisms should *not* result in excessive drift. This is because large shear forces can develop in the beam-column joints under seismic action regardless whether plastic hinges develop close to the column face or ahead in the beam span. In order to prevent



**Figure 13.11** Imposed Plastic Hinge Locations: (a) Transformed hinge location in monolithic construction (b) critical hinge section.

shear failure at the joint, both vertical and horizontal shear reinforcement is necessary, with the horizontal reinforcement significantly more than is normally provided by ties or hoops. Also, full anchorage development lengths or bond mechanisms have to be ensured in the reinforcement embedded within the beam-column joint.

## 13.7 STRUCTURAL SYSTEMS IN SEISMIC ZONES

In general, three systems are applicable in medium- and high-seismicity zones

1. Structural ductile frames
2. Shear wall systems
3. Dual systems, which are a combination of the two

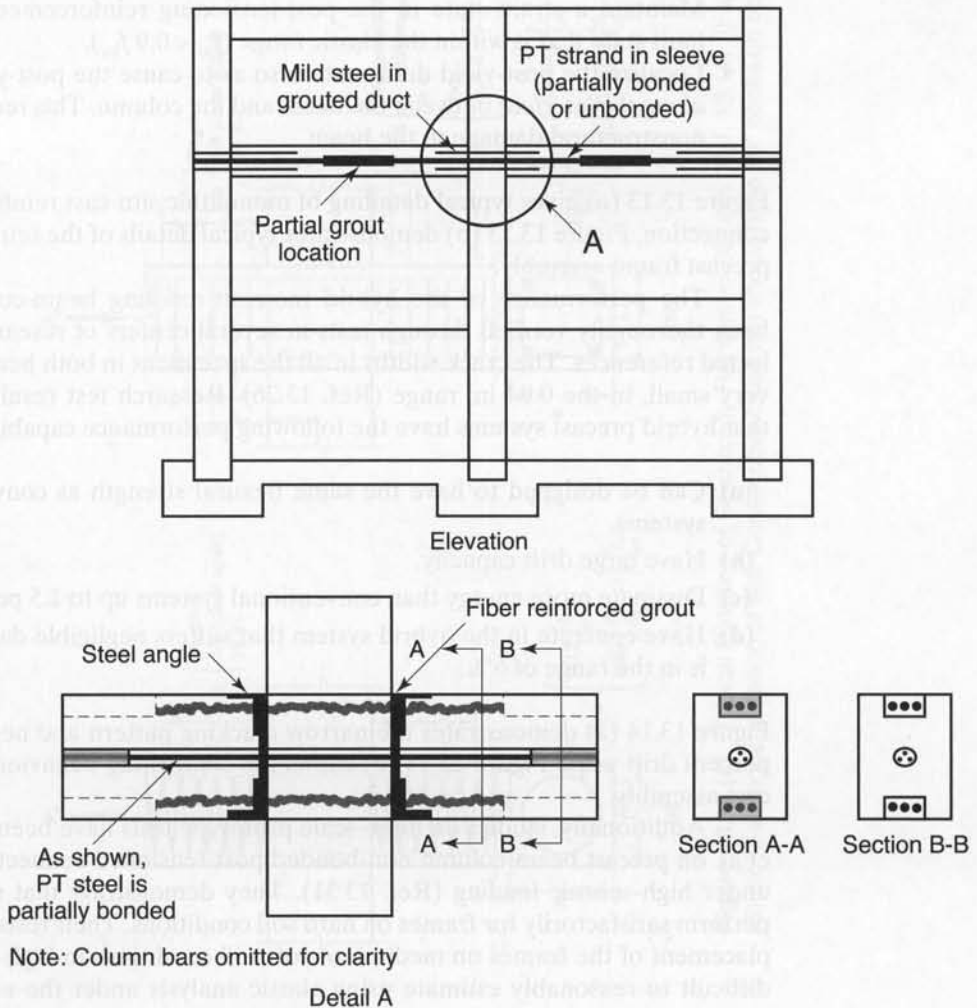
### 13.7.1 Structural Ductile Frames

Present building codes when used in high-seismicity zones have generally been limited to situ-cast special moment resisting ductile frame and shear walls. From the discussion in Sections 13.6.2 and 13.6.3 it is clear that the beam-column connection is the major part of

the frame that has to sustain large seismically imposed deformations. Both reinforced and monolithic prestressed concrete frames have been designed and built for some time (Ref. 13.13, 13.14, 13.17).

Precast concrete, on the other hand, has traditionally been viewed as an assembly of components that attempts to emulate a situ-cast structure. This approach disregards the advantages presented by the discrete elements that make up a total precast structure. If, by design, a post-yield deformation can be imposed to occur where precast elements are joined, damage to the structure can be significantly reduced. This is because a weakened plane already exists at the point where a post-yield rotation has to be accommodated. A monolithically cast element, on the other hand, must crack, usually along *several* planes, in order to accommodate the required rotation. Given this advantage, precast concrete structures can be created capable of surviving earthquakes with lower levels of damage than those created from other materials or by other processes.

The use of precast prestressed concrete elements in ductile frame construction is coming of age. Extensive research is available to justify use of precast elements safely in ductile beam-column frames in high seismicity zones (Ref. 13.18–13.27). Figure 13.12 from Ref. 13.18 shows a hybrid connection. The connection would have well-bonded



**Figure 13.12** Precast Hybrid Moment Connection (Ref. 13.18)



mild (ductile) steel reinforcing bars at top and bottom of the beam and high-strength prestressing tendons at mid-depth of the beam. The mild steel is intended to dissipate the seismic energy by yielding. The prestressing steel provides the shear resistance from the friction developed by the prestressing force. The system is defined as hybrid because of using two types of reinforcement.

The hybrid system is the evolution of an assemblage of precast concrete components by post-tensioning that was first proposed in New Zealand in the early 1970s. The hybrid system was developed largely through an interactive test program (Ref. 13.17, 13.22, 13.23). The objective of the tests performed was to improve upon the energy dissipation characteristics of assemblies connected exclusively by post-tensioning (Ref. 13.24).

The basic objectives of the hybrid system are to mainly accomplish the following results:

- Balance the restoring force provided by the concentric post-tensioning with the strength developed by the mild steel so that a restorative or self-centering force exists after the earthquake. This should reduce the potential for permanent deformation.
- Maintain a strain state in the post-tensioning reinforcement at the deformation limit state that is within the elastic range ( $f_{ps} < 0.9 f_{pu}$ ).
- Localize the post-yield deformation so as to cause the post-yield rotation to occur *along the interface* between the beam and the column. This reduces the potential for nonstructural damage to the beam.

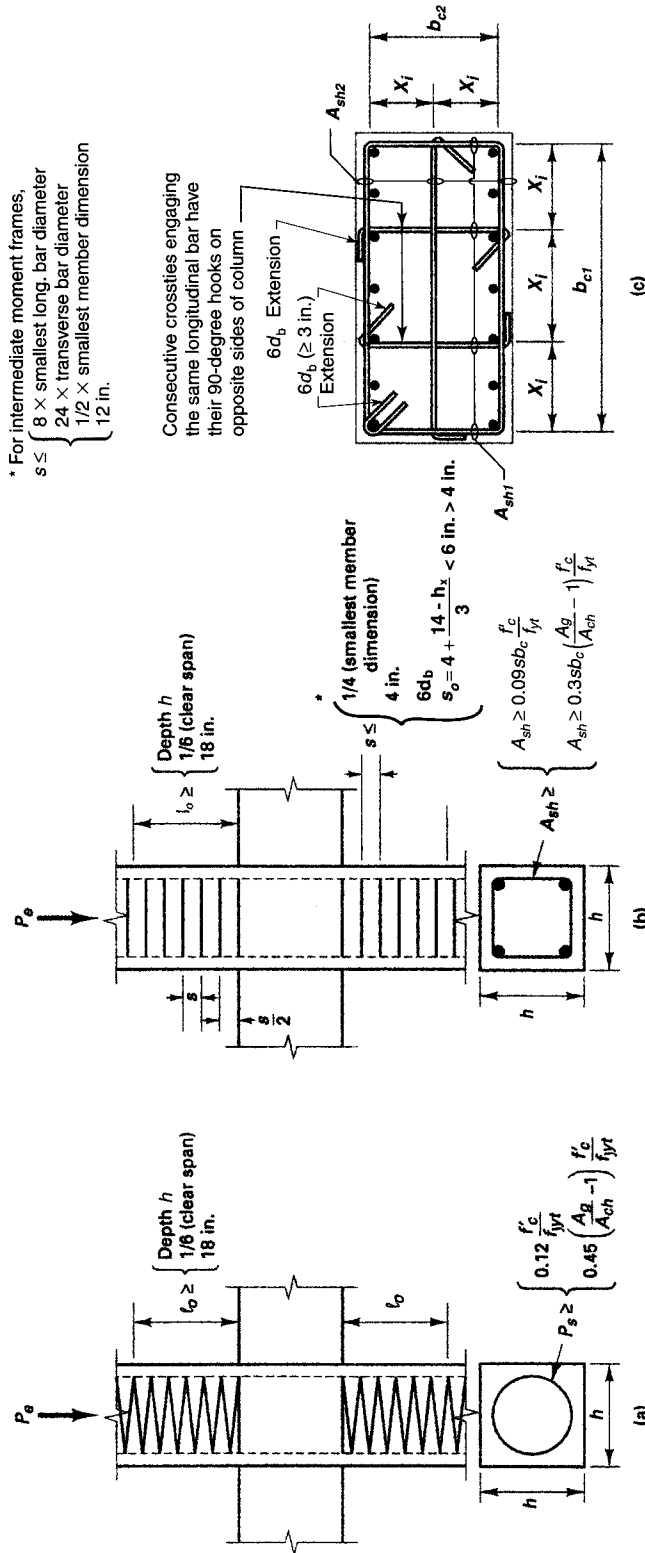
Figure 13.13 (a) gives typical detailing of monolithic situ-cast reinforced concrete ductile connection. Figure 13.13 (b) demonstrates typical details of the reinforcement in a hybrid precast frame assembly.

The performance of the hybrid moment-resisting beam-column connection has been thoroughly verified through tests in several centers of research as listed in the selected references. The crack widths in all the specimens in both beams and columns were very small, in the 0.04 in. range (Ref. 13.26). Research test results have demonstrated that hybrid precast systems have the following performance capabilities:

- (a) Can be designed to have the same flexural strength as conventionally reinforced systems.
- (b) Have large drift capacity.
- (c) Dissipate more energy than conventional systems up to 1.5 percent drift.
- (d) Have concrete in the hybrid system that suffers negligible damage even if the drift is in the range of 6%.

Figure 13.14 (a) demonstrates the narrow cracking pattern and negligible damage at 3.5 percent drift while Figure 13.14 (b) shows the contrasting behavior of the monolithically cast assembly.

Additionally, studies on large-scale prototype tests have been conducted by Pessiki et al. on precast beam-column non-bonded post-tensioned connections in ductile frames under high-seismic loading (Ref. 13.31). They demonstrate that such assemblages can perform satisfactorily for frames on hard soil conditions. Their tests also indicate that displacement of the frames on medium or soft soil conditions in high-seismicity regions are difficult to reasonably estimate using elastic analysis under the equivalent lateral base force code approach.



**Figure 13.13** (a) Typical Detailing of Seismically Reinforced Column (Ref. 13.14) (i) spirally confined, (ii) confined with rectangular hoops, (iii) cross-sectional detailing of ties. Consecutive cross ties should have 90° hooks on opposite sides.

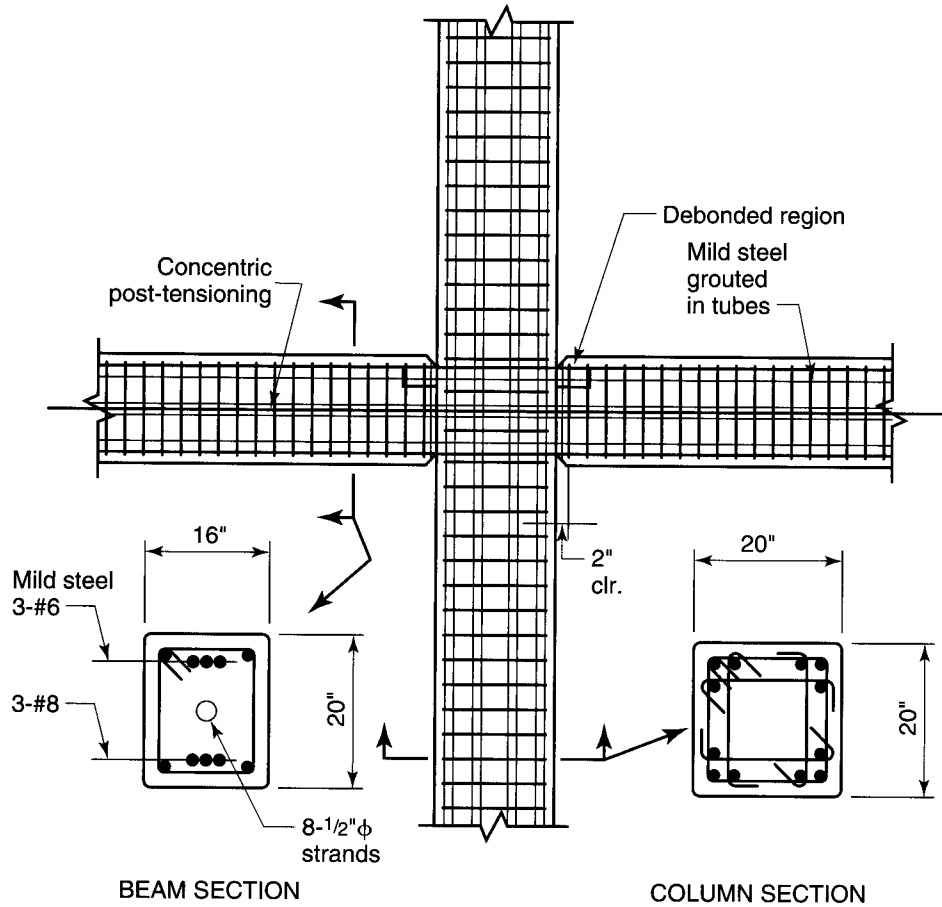


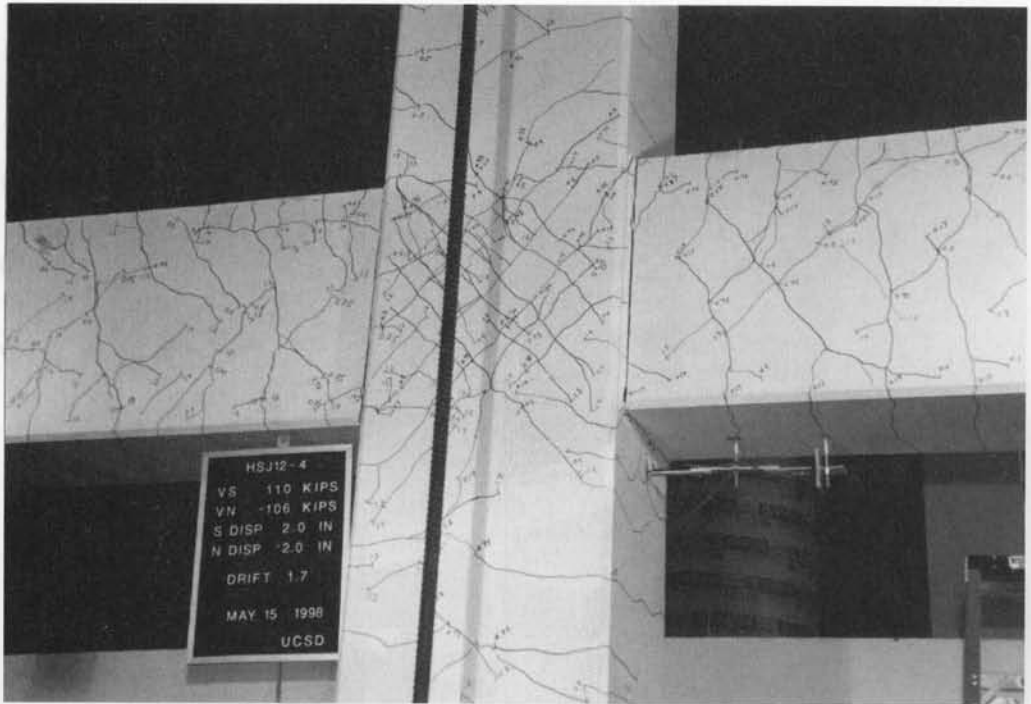
Figure 13.13 (b) Hybrid Frame Assembly (Ref. 13.24)

### 13.7.2 Dywidag Ductile Beam–Column Connection: DDC Assembly

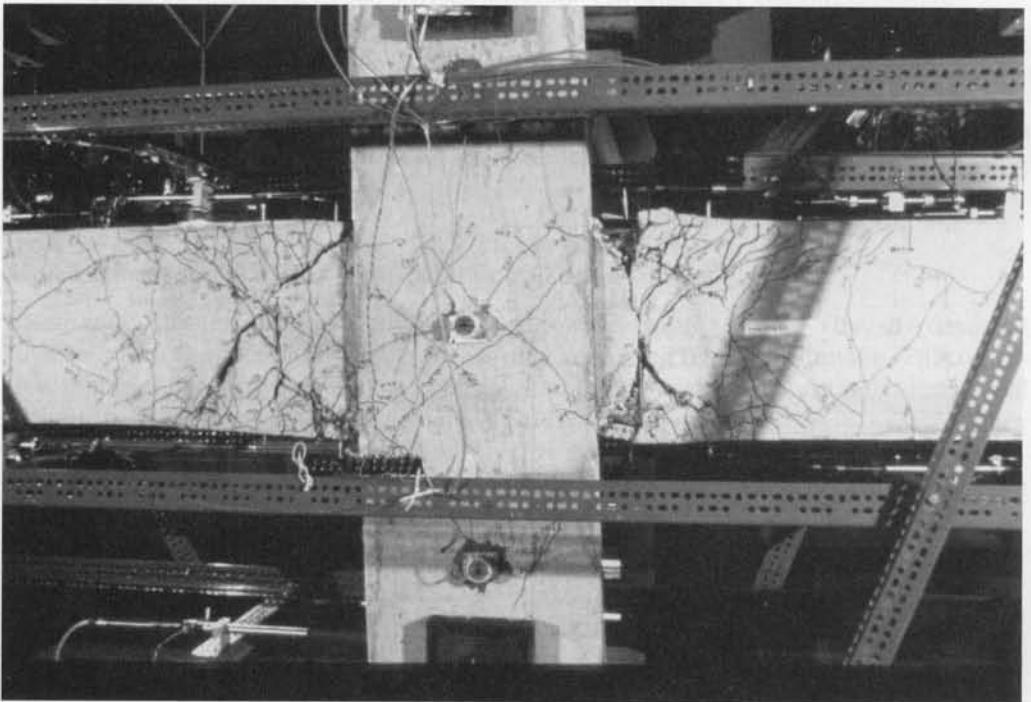
The DDC assembly was developed by Dr. R. E. Englekirk (Ref. 13.19) and produced by Dywidag Systems International (DSI). It allows the precast concrete beams to be bolted to the column, simplifying construction while at the same time improving seismic behavior. The system seems to satisfy the ductility requirements for both the shear forces at the column joint and the deformation and rotational ductility requirements in high seismicity zones. The design is also simple and easy.

The assembly consists of ductile rods embedded in the concrete column. The precast beam contains high-strength ( $F_{ymin} = 120$  ksi) Dywidag Bars<sup>®</sup> connected to a transfer block. The beam is connected to the column by high-strength steel bolts ( $1\frac{1}{2}$  in.  $\phi$ -A490). The flexural strength of the beam is limited by the capacity of the ductile rod ( $F_y = 141$  kips). The other components along the load path are designed to the probable strength of the ductile rod ( $1.25 F_y$ ), a capacity-based approach. Shear is transferred by steel-to-steel friction at the interface (transfer block to ductile rod) and bearing of the head of the ductile rod on the confined concrete of the column.

Figure 13.15 illustrates a typical single DDC assembly unit with the high-strength bolts connecting the precast prestressed beams to the assembly embedded in the columns at the joint. Example 13.4 gives the design computational steps for a typical ductile connection in a high-rise frame building. Figure 13.16 gives an example of this application to

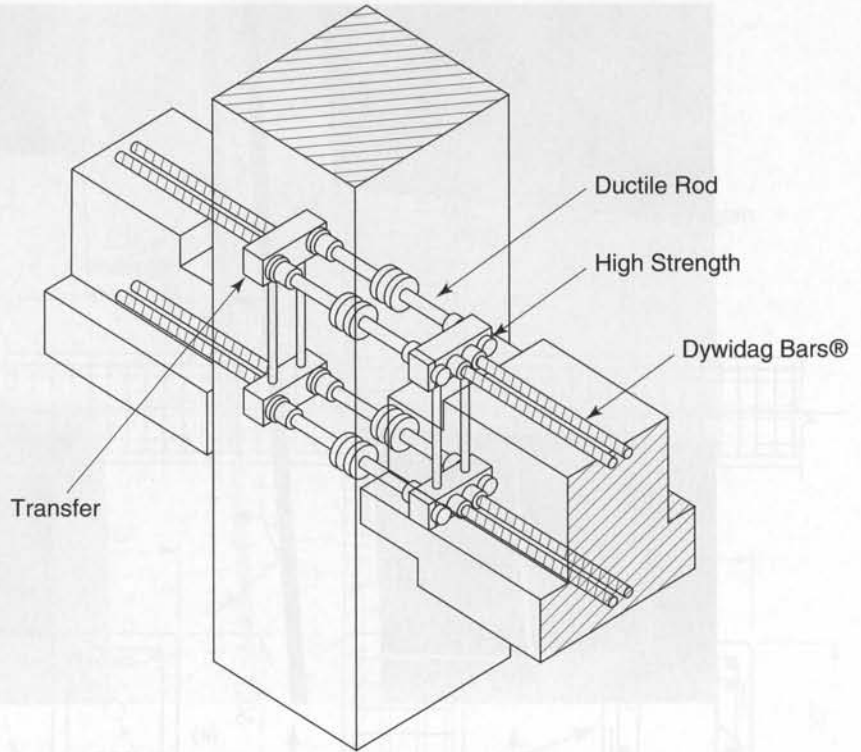


(a)

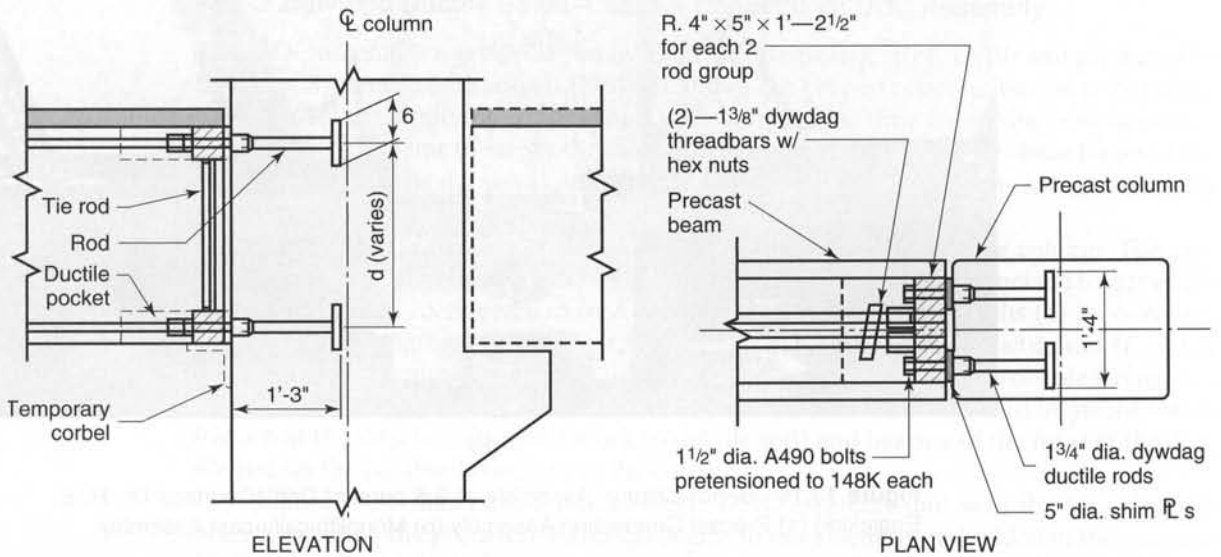


(b)

**Figure 13.14** Beam-Column Assembly at 3.5 percent Drift (Courtesy Dr. R. E. Englekirk) (a) Precast Connection Assembly (b) Monolithically-cast Assembly



**Figure 13.15** DDC Assembly, Tensile Strength at Yield = 282 Kips (Courtesy Dywidag-Systems International and Dr. R. E. Englekirk)



**Figure 13.16** Beam-to-Column Connection showing Dywidag Ductile Connector Details (Ref. 13.19)

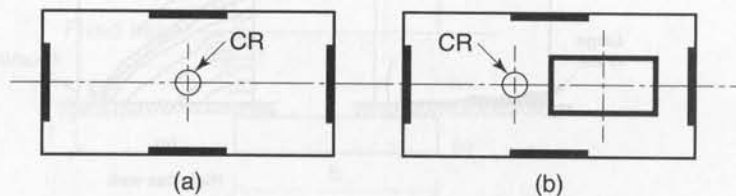


**Photo 13.7** Wilern Center Parking Structure, Los Angeles, California (Courtesy Dr. Robert E. Englekirk).

a parking garage in high seismicity zones showing beams-to-column DDC details in a parking garage (Ref. 13.19). Photo 13.7 shows the ductile garage frame structure at completion.

### 13.7.3 Structural Walls in High-Seismicity Zones (Shear Walls)

Shear walls form efficient and reliable lateral force resisting systems. They are designed to account for the total lateral base shear force generated by an earthquake. This condition assumes that the wall has an adequate foundation, which can transmit deformational actions from the structure to the ground without rocking to any measurable extent. They also provide torsional stability to the multi-story system. Figure 13.17 shows a typical torsional stability arrangement of walls both in the E-W and N-S directions, with Figure 13.17 (b) the torsional stability provided by an interior core.

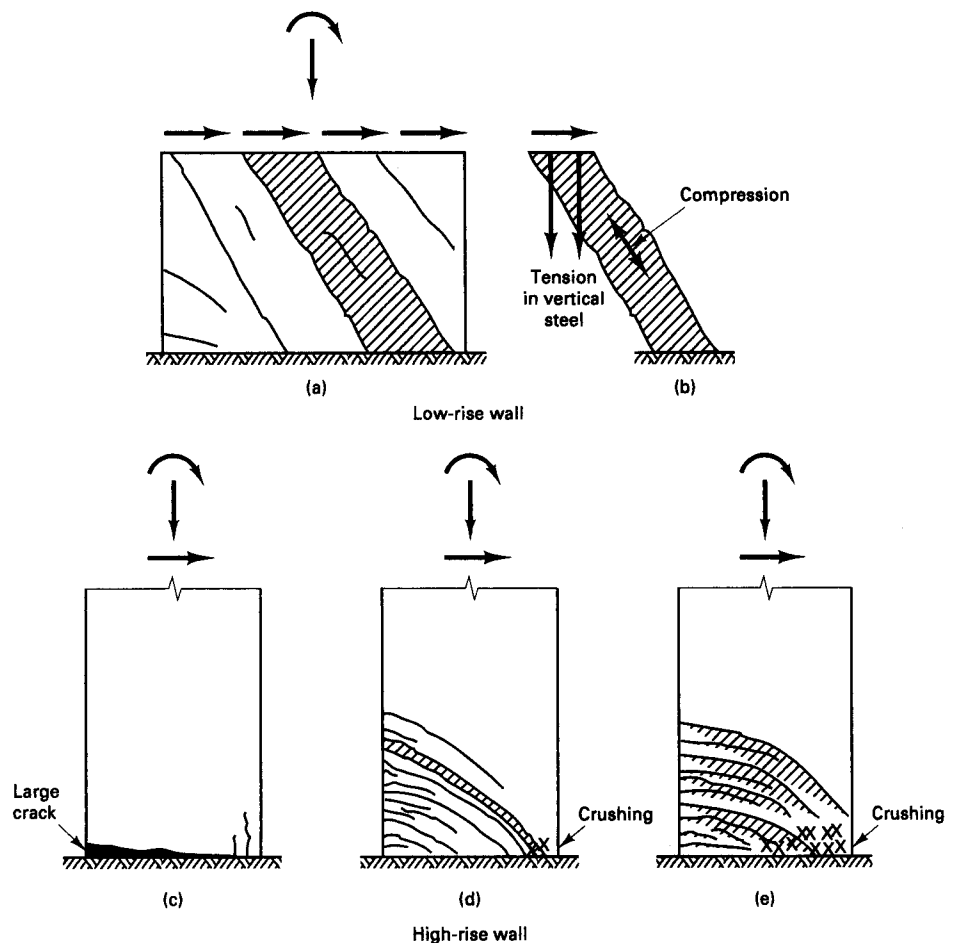


**Figure 13.17** Torsionally Stable Shear Wall Systems (a) Boundary walls arrangement with concentric resistance center; (b) Core wall system with eccentric resistance center.

Structural (shear) walls have been successfully used for more than 35 years. They are essentially vertical cantilevers designed to receive lateral forces from diaphragms or coupling beams and then transmit the forces to the ground. The forces in these walls may often be predominantly shear forces for low-rise buildings. Slender walls will also undergo significant bending, mainly flexural stresses.

One of the main objectives of the structural analysis is to determine in what proportion the applied wind or seismic forces are distributed among the various shear walls. For the case where no ductile moment frames are present, one can assume that each floor diaphragm displaces in its plane as a rigid body. In such an analysis, the magnitude of lateral displacement becomes the dominant factor in determining the proportion of loads resisted by each wall.

If the wall is treated as a *deep* vertical beam cantilevering from the foundation, shear deformations become a major component of the displacement and have to be taken into account. Based on the analysis by Aswad et al. in Ref. 13.28, it has been shown that the “beam element” method including the shear deformations is quite accurate for evaluating the shear and overturning moments in plan layouts with shear walls. Figure 13.18 shows the modes of failure of structural walls subjected to seismic lateral loading.

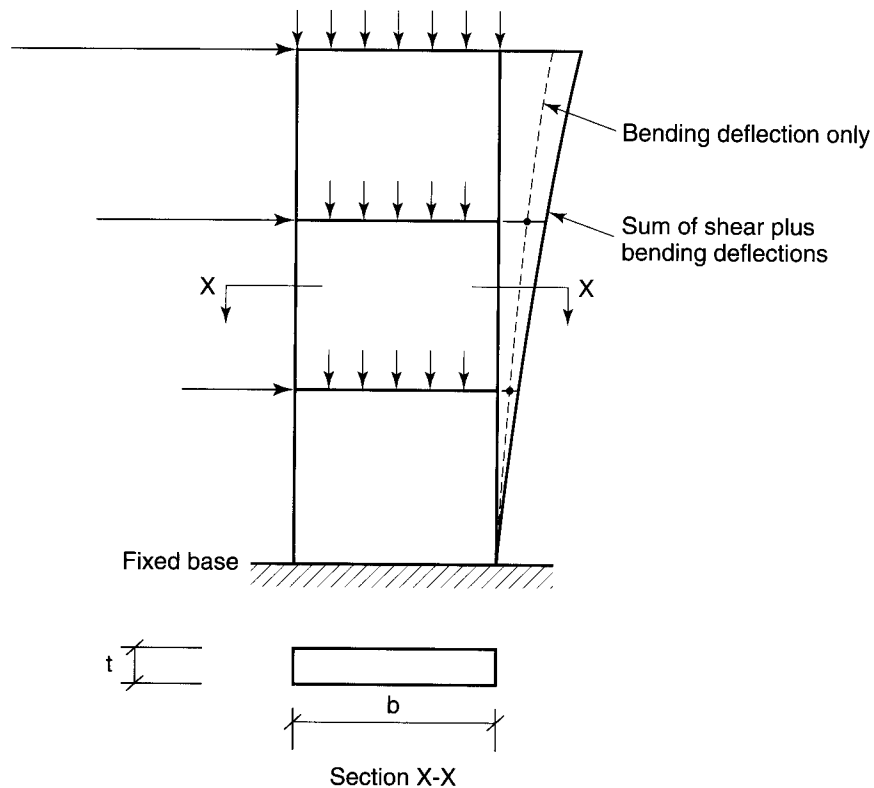


**Figure 13.18** Typical failure modes of structural walls: (a) Shear cracking pattern; (b) compression strut between cracks; (c) fracture of the reinforcement; (d) flexure-shear failure pattern; (e) failure by crushing of concrete.

Figure 13.19 schematically illustrates the drift due to both bending and shear, and Figure 13.20 shows a precast shear wall connection to the foundation using a Dywidag threaded bar connector. For small uplift forces, Figure 13.21 gives a typical welded angle connector to the foundation.

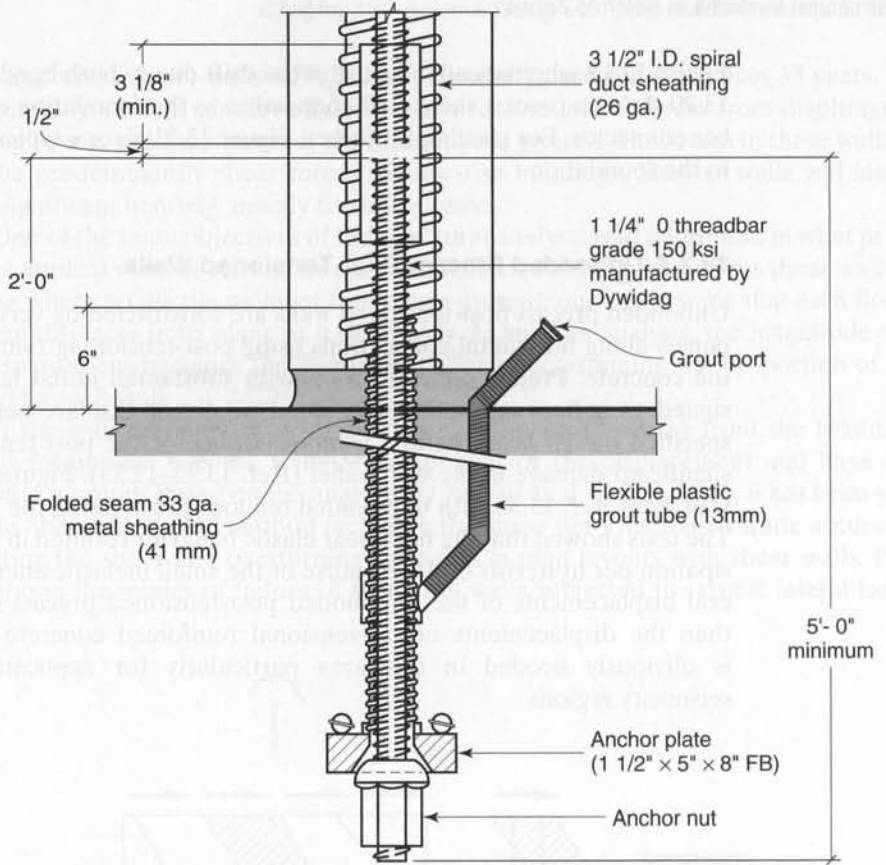
### 13.7.4 Unbonded Precast Post-Tensioned Walls

Unbonded precast post-tensioned walls are constructed by vertically joining precast wall panels along horizontal connections using post-tensioning reinforcement not bonded to the concrete. Precast concrete walls with substantial initial lateral stiffness can be designed to soften and satisfy estimated nonlinear displacement demands under code-specified design level motion, *without yielding* in the post-tensioning reinforcement or significant damage in the wall panel (Ref. 13.32–13.33). Figure 13.22 shows a prototype wall from Ref. 13.33 with unbounded tendons prestressing the six structural wall panels. The tests showed that the nonlinear elastic behavior resulted in small inelastic energy dissipation per hysteresis cycle. Because of the small inelastic energy dissipation, larger lateral displacements of the unbounded post-tensioned precast concrete walls are larger than the displacements of conventional reinforced concrete systems. More research is obviously needed in this area particularly for application to designs in high-seismicity regions.

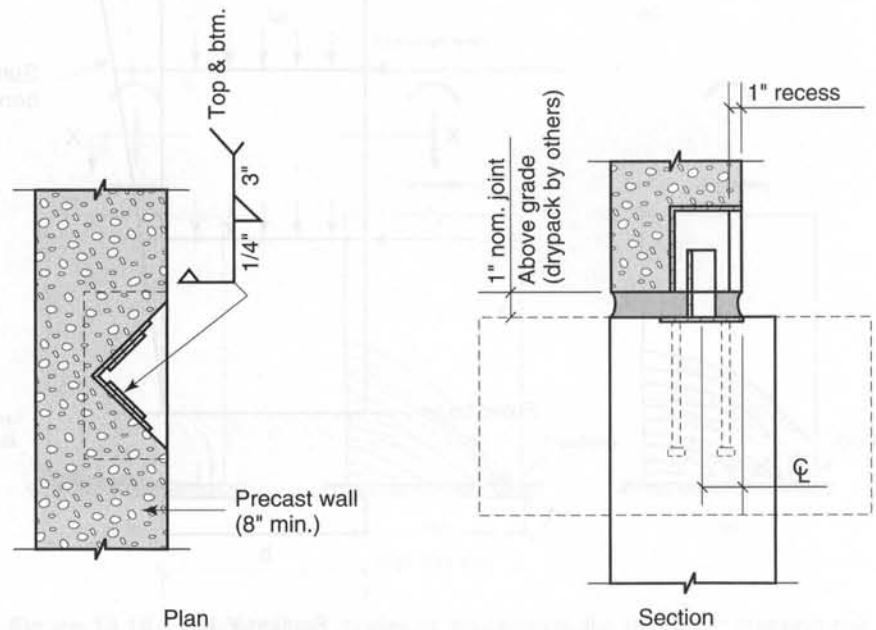


**Figure 13.19** Schematic of shear wall drift due to bending and shear

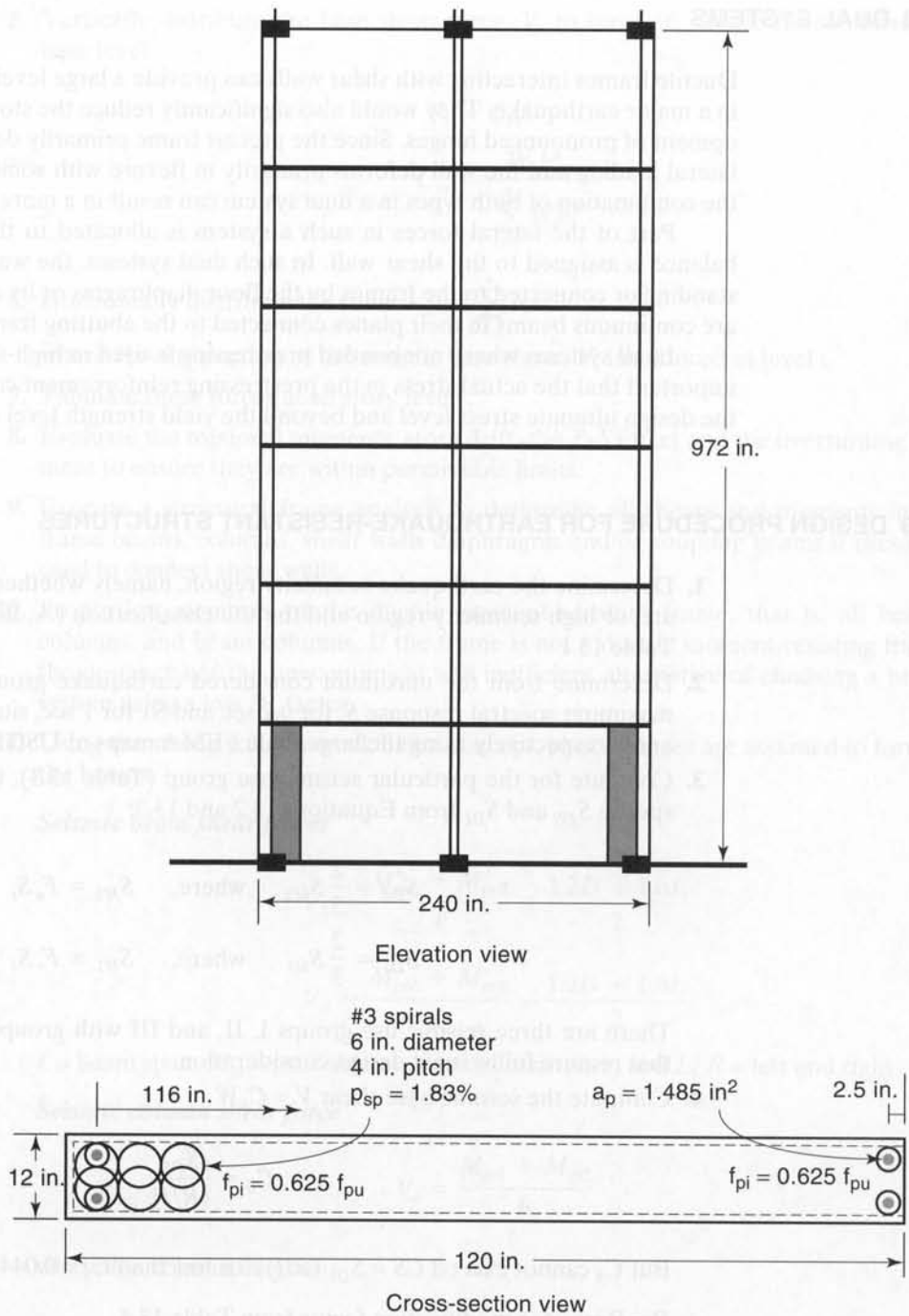




**Figure 13.20** Precast shear wall connection to continuous foundation using Dywidag threaded bar connector



**Figure 13.21** Welded angle connection of precast shear wall to continuous foundation



**Figure 13.22** Post-tensioned unbounded precast shear wall (Ref. 13.33)

### 13.8 DUAL SYSTEMS

Ductile frames interacting with shear walls can provide a large level of energy dissipation in a major earthquake. They would also significantly reduce the story drift and the development of pronounced hinges. Since the precast frame primarily deforms in shear due to lateral loading and the wall deforms primarily in flexure with some shear deformations, the combination of both types in a dual system can result in a more efficient structure.

Part of the lateral forces in such a system is allocated to the ductile frame. The balance is assigned to the shear wall. In such dual systems, the walls can be either free-standing or connected to the frames by the floor diaphragms or by coupling beams which are continuous beams in their planes connected to the abutting frames.

In all systems where nonbonded prestressing is used in high-seismicity regions, it is important that the actual stress in the prestressing reinforcement can achieve and sustain the design ultimate stress level and beyond the yield strength level of  $1.25 f_{py}$ .

### 13.9 DESIGN PROCEDURE FOR EARTHQUAKE-RESISTANT STRUCTURES

1. Determine the earthquake seismicity region, namely whether it is in a low, moderate, or high seismicity region and the site classification (A, B, C, D, E, and F) from Table 13.1
2. Determine from the maximum considered earthquake ground motion maps, the maximum spectral response  $S_s$  for 0.2 sec and  $S_1$  for 1 sec, site-class B, Figure 13.3a and b respectively using the large scale FEMA maps of USGS (Ref. 13.15)
3. Compute for the particular seismic use group (Table 13.3), the design spectral response  $S_{DS}$  and  $S_{D1}$  from Equations 13.2 and 13.3:

$$S_{DS} = \frac{2}{3} S_{MS} \quad \text{where,} \quad S_{MS} = F_a S_s$$

$$S_{D1} = \frac{2}{3} S_{M1} \quad \text{where,} \quad S_{M1} = F_v S_1$$

There are three seismic use groups I, II, and III with groups II and III structures that require full seismic design consideration.

4. Compute the seismic base shear  $V = C_s W$

$$C_s = \frac{S_{DS}}{(R/I)}$$

But  $C_s$  cannot exceed  $CS = S_{D1}/(R/I)T$  or less than  $C_s = 0.044 C_{DS}I$

$R$  = Response modification factor from Table 13.4

$I$  = Occupancy importance factor from Table 13.5

$T$  = Fundamental period of vibration of a structure, Sec. 13.3.1,  $T_a = C_T h^{\frac{3}{4}}$

where,  $C_T$  = building period coefficient ranging between 0.035 – 0.020 as given in the text.

In cases where moment resisting frames do not exceed twelve stories in height, an approximate period  $T_a = 0.1 N$  can be used where  $N$  = number of stories.

For structures in seismic design categories E or F and for other structures having a spectral response  $S_1 \geq 0.6 g$ , the value of  $C_s \geq (0.5S_1)/(R/I)$

5. Vertically distribute the base shear force,  $V$ , to forces  $F_x$  to the floors above the base level:

$$F_x = C_{vx}V$$

$$C_{vx} = \frac{W_x h_x^k}{\sum_{i=1}^n W_i h_i^k}$$

6. Horizontally distribute the shear  $V_x = \sum_{i=1}^x F_i$

where  $F_i$  = the portion of the seismic base shear,  $V$ , introduced at level  $i$ .

7. Tabulate these forces at all story levels.
8. Evaluate the torsional moments, story drift, the  $P$ - $\Delta$  effect and the overturning moment to ensure they are within permissible limits.
9. Execute a structural frame analysis to determine all shears and moments in the frame beams, columns, shear walls diaphragms and/or coupling beams if these are used to connect shear walls.
10. Proportion members of the ductile moment-resistant frame, that is, all beams, columns, and beam-columns. If the frame is not a ductile moment-resisting frame, the designer has the uneconomical and inefficient alternative of choosing a brittle system using a low  $R_w$  factor.
11. Using the strong column-weak beam concept, plastic hinges are assumed to form in the beams.

#### ***Seismic beam shear forces***

$$V_L = \frac{M_{prL}^- + M_{prR}^+}{\ell} + \frac{1.2D + 1.6L}{2}$$

$$V_R = \frac{M_{prL}^+ + M_{prR}^-}{\ell} - \frac{1.2D + 1.6L}{2}$$

$\ell$  = beam span,  $M_{pr}$  = probable moment of resistance, and  $L, R$  = left and right.

#### ***Seismic column shear force***

$$V_e = \frac{M_{pr1} + M_{pr2}}{h}$$

where  $h$  = column height.

$$\sum M_{nc} \geq \frac{6}{5} \sum M_{nb}$$

at joint to ensure hinges form in the beams; hence

$$(\phi M_n^+ + \phi M_n^-)_{nc} \geq \frac{6}{5} (\phi M_n^+ + \phi M_n^-)_{nb}$$

The nominal moment strengths  $M_n$  have to be evaluated and the member proportioned prior to evaluating the seismic beam shear forces.

Beam: flexural design,  $P_u$  insignificant  
 Column: combined bending and axial load  $P_u$   
 Beam-column:  $P_u > A_g f'_c / 10$   
 Shortest cross-sectional dimension  $\geq 12$  in.

## 12. Longitudinal reinforcement

Beam-column or columns

$$0.01 \leq \rho_g = \frac{A_s}{A_g} \leq 0.06$$

For practical considerations,  $\rho_g \leq 0.035$ .

Beam (positive reinforcement):

$$\rho_{\min} \geq \frac{200}{f_y} \geq \frac{3\sqrt{f'_c}}{f_y}$$

Beam (flange in tension):

$$\rho_{\min} \geq \frac{200}{f_y} \geq \frac{6\sqrt{f'_c}}{f_y}$$

The factor value, 6, in the numerator instead of 3 is because a flange width twice the web width or more is used.

where  $f_y$  is in psi units.  $\rho$  should never exceed 0.025.

For proportioning reinforcement in beams, the nominal moment strength requirements are

- (a)  $M_n^+$  at face of joint  $\geq \frac{1}{2} M_n^-$  at the face.
- (b)  $M_n^+$  or  $M_n^-$  at any section  $\geq \frac{1}{4} M_{a,\max}$  at the face.

## 13. Transverse confining reinforcement

(a) Spirals

$$\rho_s \geq \frac{0.12f'_c}{f_{yh}} \quad \text{or} \quad \rho_s \geq 0.45 \left( \frac{A_g}{A_{ch}} - 1 \right) \frac{f'_c}{f_{yt}}$$

whichever is greater.

$A_g$  = gross area

$A_{ch}$  = core area to outside of spirals

$f_{yt}$  = specified yield strength

(b) Rectangular hoops in columns: Total cross-sectional area within spacing  $s$ :

$$\begin{aligned} A_{sh} &\geq 0.09 s h_c \frac{f'_c}{f_{yt}} \\ &\geq 0.3 s h_c \left( \frac{A_g}{A_{ch}} - 1 \right) \frac{f'_c}{f_{yt}} \end{aligned}$$

whichever is greater.

$A_{sh}$  = total cross-sectional area of transverse reinforcement (including cross ties) within spacing  $s$  and perpendicular to dimension  $h_c$

$h_c$  = cross-sectional dimension of column core, in.

$s$  = spacing of transverse hoops

$s_{\max}$  = one-quarter of the smallest cross-sectional dimension or 4 in., whichever is smaller, but not to exceed 6 in.

*Placement of confining reinforcement:* Place confining reinforcement on either side of potential hinge over a distance the largest of

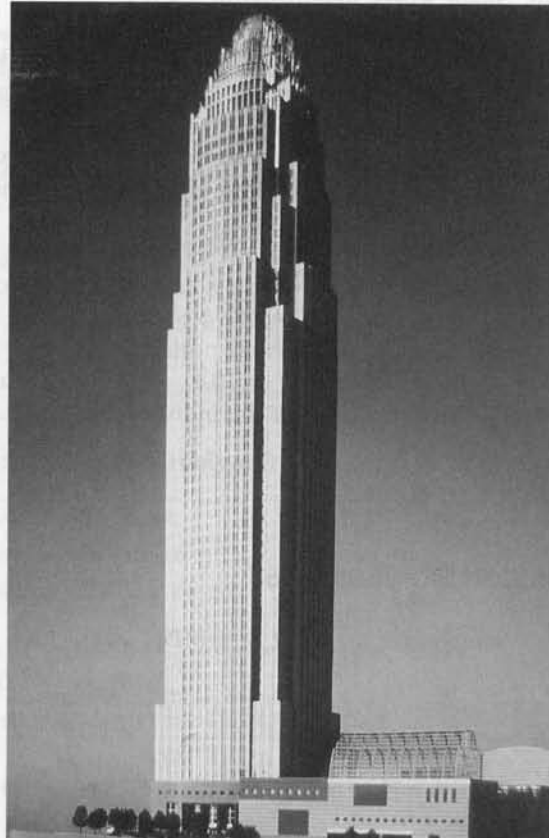
- (i) Depth of member at joint face
- (ii) One-sixth clear span
- (iii) 18 in.

The spacing of the ties in the balance of column height follows normal column tie requirements.

- (c) *Confining reinforcement in beam ends:* Should be placed on a length =  $2h$  on both sides of the joint if it is internal; otherwise, maximum hoop spacing, smallest of

- (i) One-quarter effective depth  $d$
- (ii)  $8 \times$  diameter of longitudinal bar
- (iii)  $24 \times$  diameter of hoop
- (iv) 12 in.

IBC requires that spacing in ductile frames at the plasticity region not exceed 4 in. The ties in the balance of the beam span follow the standard shear web reinforcement requirements. If the joint is confined on all four sides, 50 percent reduction in confinement and increase in minimum tie spacing to 6 in. in the columns are allowed. No smooth bar reinforcement is allowed in seismic structures.



**Photo 13.8** NCNB Tower, Charlotte, North Carolina, 9000-psi concrete. (Courtesy Portland Cement Association.)

**14. Beam-column connections (joints):** Normal concrete nominal shear strength  $V_n$  at a joint:

- (a) Confined on all faces:  $V_n \leq 20\sqrt{f'_c} A_j$
- (b) Confined on three faces or two opposite faces:  $V_n \leq 15\sqrt{f'_c} A_j$
- (c) All other cases:  $V_n \leq 12\sqrt{f'_c} A_j$

where  $A_j$  is effective area at joint (Fig. 13.8). The value of allowable  $V_n$  should be reduced by 25% for lightweight concrete. Note from Fig. 13.9 that the horizontal shear in the joint is determined by assuming a stress =  $1.25f_y$  in the tensile reinforcement.

**15. Development length of reinforcing bars:** For bar sizes Nos. 3 to 11 without hooks, the largest of

$$\ell_d = 2.5\ell_{dh} \text{ when concrete below bars } \leq 12 \text{ in.}$$

$$\ell_d = 3.5\ell_{dh} \text{ when concrete below bars } \geq 12 \text{ in.}$$

where for normal-weight concrete

$$\begin{aligned} \ell_{dh} &\geq f_y d_b / (65\sqrt{f'_c}) \\ &\geq 8d_b \\ &\geq 6 \text{ in.} \end{aligned}$$

When standard 90° hooks are used,  $\ell_d = \ell_{dh}$ . Any portion of straight embedment length not within the confined core should be increased by a factor of 1.6.

**16. Shear walls: height/depth > 2.0**

- (i) Minimum  $\rho_v = 0.0025$  if  $V_{uh} > A_{cv} \sqrt{f'_c}$ . At least two curtains of reinforcement needed if in-plane factored shear force  $V_{uh} > 2A_{cv} \sqrt{f'_c}$ , where  $A_{cv}$  = net area of concrete cross section = thickness  $\times$  length of section in direction of the considered shear.
- (ii) If extreme fiber compressive stresses exceed  $0.2f'_c$ , shear walls have to be provided with boundary elements along their vertical boundaries and around the edges of openings.
- (iii) Available  $V_n = A_{cv} (2\sqrt{f'_c} + \rho_t f_y)$  for  $h_w/\ell_w \geq 2.0$ . For  $h_w/\ell_w < 2$ , the factor of 2 inside the parenthesis varies linearly from 3.0 for  $h_w/\ell_w = 1.5$  to 2.0 for  $h_w/\ell_w = 2.0$ ;  $V_u = \phi V_n$ , where  $\phi = 0.60$ .
- (iv) Maximum allowable nominal unit shear  $V_n = 8A_{cv} \sqrt{f'_c}$  for total wall, but can be increased to  $V_n = 10A_{cp} \sqrt{f'_c}$  for an individual pier, where  $A_{cp}$  is the cross-sectional area of the individual pier.

Figure 13.23 gives a logic flowchart for the preceding sixteen steps.

### 13.10 SI SEISMIC DESIGN EXPRESSIONS

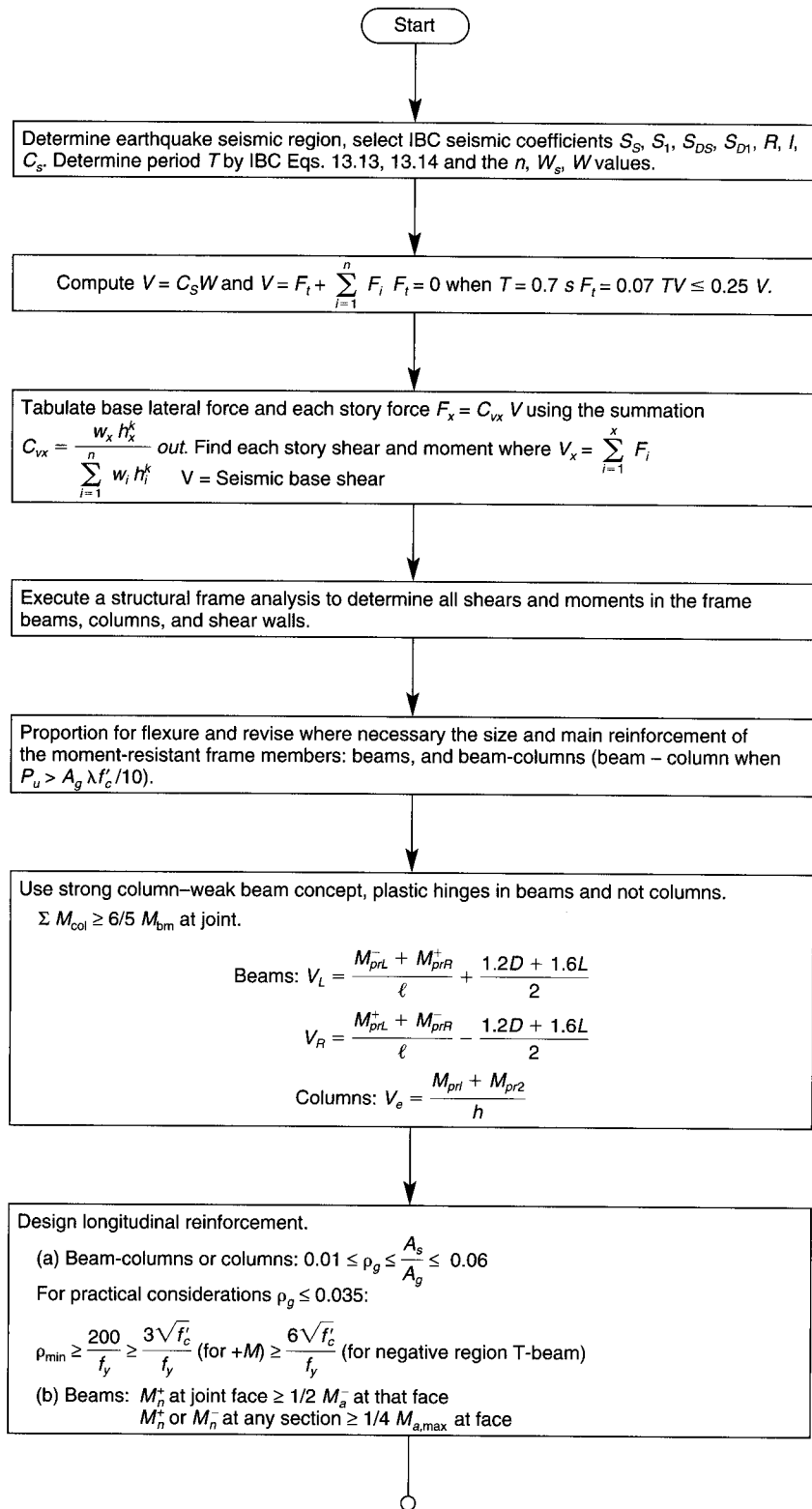
compressive strength  $f'_c \geq 20$  MPa

$$E_c = w_c^{1.5} 0.043 \sqrt{f'_c} \text{ MPa}$$

$$E_s = 200,000 \text{ MPa}$$

$$\text{Equation 13.22} \quad V_L = \frac{M_{prL}^- + M_{prR}^+}{\ell} + \left( \frac{1.2D + 1.4L}{2} \right)$$

$$\text{Equation 13.23} \quad V_R = \frac{M_{prL}^+ + M_{prR}^-}{\ell} - \left( \frac{1.2D + 1.4L}{2} \right)$$



**Figure 13.23** Flowchart for seismic design of ductile monolithic (strong column-weak beam concept) structures.



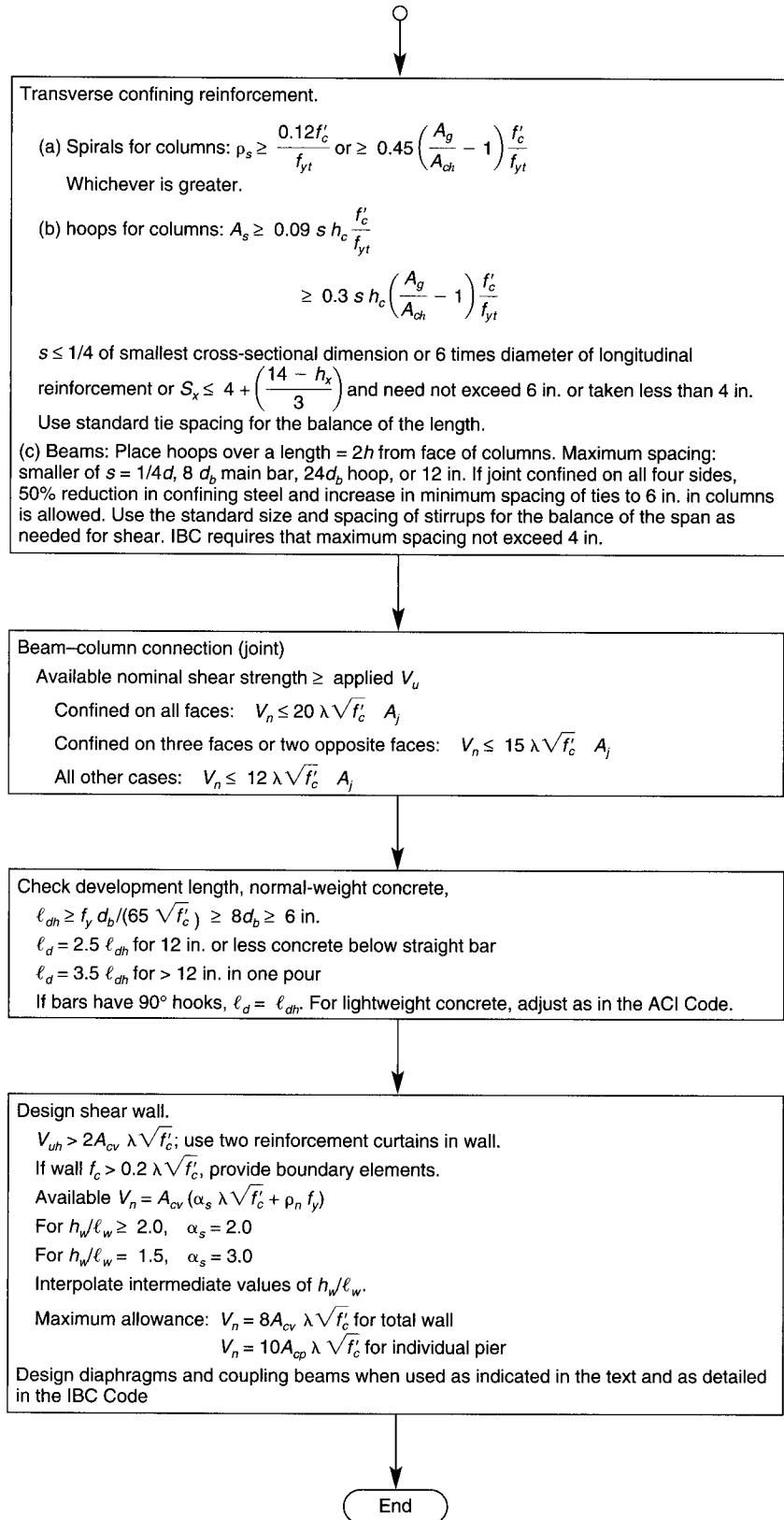


Figure 13.23 Continued



**Photo 13.9** Masonry collapse in Los Angeles earthquake, 1994. (Courtesy Portland Cement Association.)

Equation 13.24 
$$V_e = \frac{M_{pr1} + M_{pr2}}{h}$$

Equation 13.27 
$$(\phi M_n^+ + \phi M_n^-)_{col} \geq \frac{6}{5} (\phi M_n^+ + \phi M_n^-)_{bm}$$

$\phi = 0.9$  for beams and 0.7 or 0.75 for columns.

Equation 13.28

$$\text{For positive moment: } \rho \geq \frac{\sqrt{f'_c}}{4f_y} \geq \frac{1.4}{f_y}$$

where  $f'_c, f_y$  are in MPa

Equation 13.29(a)

$$\text{At joint face: } M_n^+ \geq \frac{1}{2} M_n^-$$

At any section:

Equation 13.29(b) 
$$M_a^+ \geq \frac{1}{4} (M_a^-)_{max}$$

Equation 13.29(c) 
$$M_a^- \geq \frac{1}{4} (M_a^+)_{max}$$

## 13.11 SEISMIC BASE SHEAR AND LATERAL FORCES AND MOMENTS BY THE IBC APPROACH

### Example 13.1:

A moment-resisting, five-story building with shear walls is idealized as in Figure 13.2. Each floor has a weight  $W_s$  and a height  $h = 9'-6''$  (2.9 m). Compute the seismic base shear,  $V$ , and the overturning moment,  $M$ , at each story level in terms of single floor weight  $W_s$ , assuming

the idealized mass of each floor is  $W_s$ . Consider the structure to be a building in seismic occupancy category II, site-class B, design category B and seismic use group II.

Given: Response modification factor  $R = 3.0$

Occupancy importance factor  $I = 1.25$

Use the equivalent lateral force method in the solution.

**Solution:**

**(a) Spectral response period and base shear**

Total building height =  $5 \times 9.5 = 47.5$  ft

From the FEMA ground motion maps (Figure 13.3) spectral response accelerations

$S_1 = 0.42$  sec and  $S_S = 0.85$  sec, with a site-B class and 5 percent damping.

Adjusted spectral response accelerations for site class effects: from Tables 13.2(a) and (b),

for  $S_1 = 0.42$  sec,  $F_v = 1.0$  and for  $S_S = 0.85$  sec,  $F_a = 1.0$

From Equations 13.2(a) and (b),

$$S_{MS} = F_a S_S = 1.0 \times 0.85 = 0.85$$

$$S_{M1} = F_v S_1 = 1.0 \times 0.42 = 0.42$$

For 5 percent damped design spectral response acceleration using Eqs. 13.3(a) and (b),

$$S_{DS} = \frac{2}{3} S_{MS} = \frac{2}{3} 0.85 = 0.567$$

$$S_{D1} = \frac{2}{3} S_{M1} = \frac{2}{3} 0.42 = 0.278$$

The seismic base shear  $V$  from Eq. 13.8 is  $V = C_S W = C_S (5W_s)$  for the five stories where  $W_s$  is the idealized weight of each story.

From Table 13.4, the response modification coefficient for ordinary reinforced concrete moment frame is given as  $R = 3$ .

The occupancy importance factor for building category II from Table 13.5 is:  $I = 1.25$ .

$$\text{From Eq. 13.9, } C_S = \frac{S_{DS}}{(R/I)} = \frac{0.567}{3/1.25} = 0.236,$$

$$\text{But } C_S \text{ cannot exceed the value: } C_S = \frac{S_{D1}}{\left(\frac{R}{I}\right)T} \text{ from Eq. 13.10.}$$

For  $S_{D1} = 0.278$  and from Table 13.6,  $C_u \cong 1.32$ .

For moment resistant concrete frame systems, a building period coefficient  $C_T = 0.022$  will be used in this example. (See Sec. 13.3.1)

From Eq. 13.13, the approximate fundamental period,

$$T_a = C_T h^{3/4} = 0.022 (47.5)^{3/4} = 0.396 \text{ sec}$$

Maximum allowable  $T_a = C_u T_a = 1.32 \times 0.396 = 0.523$  sec

For computing the base shear  $V$ ,  $T = 1.2 \times 0.523 = 0.63$ .

$$C_S = \frac{S_{D1}}{\left(\frac{R}{I}\right)T} = \frac{0.278}{\left(\frac{3}{1.25}\right)0.63} = 0.184 \text{ sec}$$

From Eq. 13.11,  $C_s$  cannot be less than  $C_s = 0.044 S_{DS} = 0.044 \times 0.567 = 0.025$   
Hence,  $C_s = 0.184$  sec controls.

$\therefore$  base shear  $V = C_s W = C_s (5W_s) = 0.184 \times 5 W_s = 0.92 W_s$

**(b) Vertical Distribution of Forces and Overturning Moments:**

From Eqs. 13.15 (a) and (b), the lateral force induced at any story level is:

$$F_x = C_{vx} V \quad \text{where,} \quad C_{vx} = \frac{W_x h_x^k}{\sum_{i=1}^n W_i h_i^k}$$

$$k = \frac{0.63 - 0.50}{0.50} \times 1.0 + 1.0 = 1.26 \quad (\text{by linear interpolation})$$

Since  $h$  is constant for all the floors,  $C_{vx}$  becomes  $\frac{W_x}{\sum_{i=1}^n W_i}$  where  $i = 5$  at the top floor.

$$\sum_{i=1}^n = 1W_s + 2W_s + 3W_s + 4W_s + 5W_s = 15W_s$$

Lateral force  $F_x = C_{vx} V = 0.92 C_i W_s$

Overturning moment from Eq. 13.19 is  $M_x = \tau \sum_{i=x}^n F_i (h_i - h_x)$  for the top ten stories,  
overturning moment reduction factor  $\tau = 1.0$ .

$$\text{Hence, } M_x = \sum_{i=x}^n F_i (h_i - h_x)$$

Computing and tabulating the story forces  $F_i$  and the overturning moment  $M_i$  for all stories,



**Photo 13.10** Overpass collapse in 1971 Los Angeles earthquake. (Courtesy Portland Cement Association.)

Floor	$C_i$	Lateral force $F_i = 0.92W_s C_i$	Story Shear	Story Moment
(1)	(2)	(3)	(4)	(5)
5	$C_5 = \frac{5W_s}{15W_s} = 0.333$	$0.3064W_s$	0	0
4	$C_4 = \frac{4}{15} = 0.267$	$0.2456W_s$	$0.3064W_s$	$0.3064W_s h$
3	$C_3 = \frac{3}{15} = 0.200$	$0.1840W_s$	$0.5520W_s$	$0.8584W_s h$
2	$C_2 = \frac{2}{15} = 0.133$	$0.1224W_s$	$0.7360W_s$	$1.5944W_s h$
1	$C_1 = \frac{1}{15} = 0.067$	$0.0616W_s$	$0.8584W_s$	$2.4528W_s h$
Wall base	$C_0 = 0$	0	$0.9200W_s$	$3.3728W_s h$

hence seismic base shear  $V = 0.9200W_s$ . The moments at each story level are tabulated in column (5).

## 13.12 SEISMIC SHEAR WALL DESIGN AND DETAILING

### Example 13.2

Design by the ACI 318 Code the reinforcement for a shear wall in a multibay, ductile frame, twelve-story structure (adapted from Ref. 13.9) having a total height  $h_w = 148$  ft (45 m) and having equal spans of 22 ft (6.7 m). Except for the ground story, which is 16 ft (4.88 m) high, all other stories have 12 ft (3.67 m) heights. The total gravity factored load on the shear wall is  $W_u = 4,800,000$  lb (21.4 MN). The factored moment at the base of the wall due to seismic loads from the lateral load analysis of the transverse frames is  $M_u = 554 \times 10^6$  in.-lb (62.6 MN-m). The maximum axial force on the boundary element is  $P_u = 4,500,000$  lb (20 MN). The horizontal shear force at the base is 885,000 lb (3940 kN).

Given:

$$\text{wall length (horizontally)} = 26' - 2'' = 26.17 \text{ ft} = 314 \text{ in. (7980 mm)}$$

$$\text{thickness } t = 20 \text{ in.} = 1.67 \text{ ft (508 mm)}$$

$$\text{boundary element width} = 32 \text{ in. (813 mm)}$$

$$\text{depth} = 50 \text{ in. (1270 mm)}$$

$$A_s = 39 \text{ No. 11 bars (39 bars of 35-mm diameter)}$$

in each boundary element

$$f'_c = 4000 \text{ psi (27.6 MPa), normal weight}$$

$$f_y = 60,000 \text{ psi (414 MPa)}$$

Use  $\phi = 0.60$  as the strength reduction factor for shear in this example.

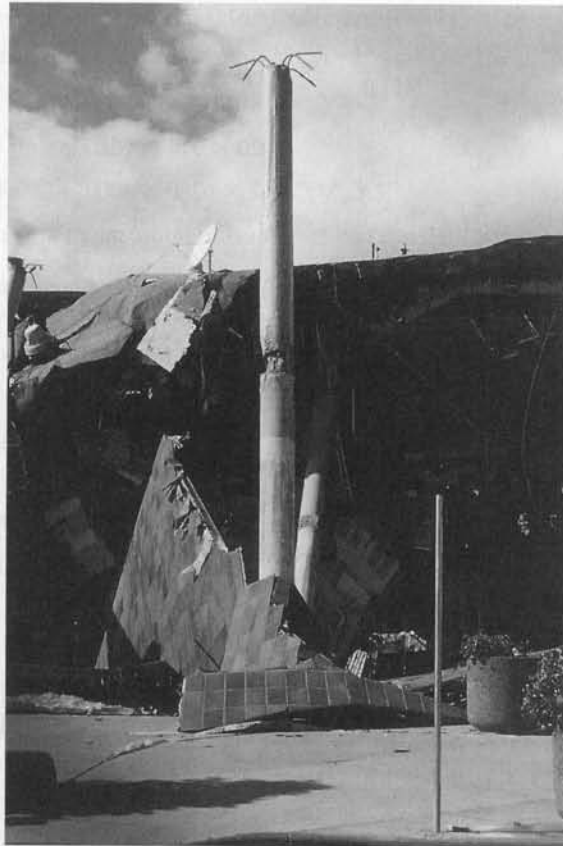
**Solution:**

- Wall geometry and forces:**  $\ell_n = 22$  ft (6.7 m),  $\ell_w$  (horizontal dimension) = 26.17 ft,  $b_{\text{web}} = 20$  in. = 1.67 ft, and  $b_{\text{bound}} = 32$  in. = 2.67 ft.

$$\text{factored } W_u = 4,800,000 \text{ lb (21.4 MN)}$$

$$M_u = 554 \times 10^6 \text{ in. lb (62.6 MN-m)}$$

$$P_u = 4,500,000 \text{ lb (20 MN)}$$



**Photo 13.11** Northridge, California, 1994 earthquake structural failure. (Courtesy Dr. Murat Saatcioglu.)

2. **Boundary element check:**  $\ell_w = 26.17$  ft,  $b = 1.67$  ft,  $P_u = 4,500,000$  lb, and  $M_u = 550 \times 10^6$  in.-lb. Assume that the wall will not be provided with confinement over its entire section.

$$\text{gross } I_g = \frac{bh^3}{12} = \frac{1.67(26.17)^3}{12} = 2495 \text{ ft}^4$$

$$A_g = 1.67 \times 26.17 = 43.7 \text{ ft}^2$$

$$f_c = -\frac{P}{A} \pm \frac{M_c}{I}, \quad c = \frac{26.17}{2} \times 12 = 157 \text{ in. (3990 mm)}$$

Concrete compressive stress in the wall is

$$\begin{aligned} f_c &= \frac{4,800,000}{43.7(12)^2} - \frac{554 \times 10^6 \times 157}{2494(12)^4} \\ &= -763 - 1682 = -2445 \text{ psi (C) (16.8 MPa)} \end{aligned}$$

Maximum allowable  $f_c = 0.2 f'_c = 0.2 \times 4000 = 800$  psi (5.52 MPa) in compression if a boundary element is not required. Hence boundary elements are needed subject to the confinement and loading requirements of Section 13.5.

3. **Longitudinal and transverse reinforcement:** Check if two curtains of reinforcement are needed, that is, if in-plane factored shear  $> 2A_{cv} \sqrt{f'_c}$  (Section 13.5.5).

$$V_u = 885,000 \text{ lb}$$

$A_{cv}$  = area bound by web thickness and length of section in direction of shear force

$$= 20 \times 314 = 6280 \text{ in.}^2$$

$$2A_{cv}\sqrt{f'_c} = 2 \times 6280 \sqrt{4000} = 799,400 \text{ lb (353 kN)} < V_u = 885,000 \text{ lb}$$

Hence two curtains of reinforcement are required.

$$\min \rho_v = \frac{A_{sv}}{A_{cv}} = \rho_n = 0.0025 \quad \text{and} \quad \max s = 18 \text{ in.}$$

$$A_{cv} \text{ per ft of wall} = 20 \times 12 = 240 \text{ in.}^2$$

$$\text{required } A_s \text{ in each direction} = 0.0025 \times 240 = 0.60 \text{ in.}^2/\text{ft}$$

Trying No. 5 bars (15.8-mm diameter),  $A_s = 2(0.31) = 0.62 \text{ in.}^2$  in two curtains.

$$s = \frac{\text{one bar area}}{\text{required } A_s/12 \text{ in.}} = \frac{0.62}{0.60/12}$$

$$= 12.4 \text{ in. (315 mm)} < 18 \text{ in. limit} \quad \text{O.K.}$$

Use  $s = 12 \text{ in.}$

#### **Check for shear reinforcement capacity**

A check is needed in order to determine that the No. 5 bars in two curtains at 12 in. c-c both ways are adequate for the wall section to sustain the applied shear force at the base. The shear wall aspect ratio is

$$\frac{h_w}{\ell_w} = \frac{148}{26.17} = 5.66 > 2$$

Hence from Eq. 13.34 b

$$\phi V_n = \phi A_{cv} (2\sqrt{f'_c} + \rho_t f_y)$$

where  $\phi = 0.60$  in this example; otherwise, refer to the ACI 318-02 Code for other conditions.

$$A_{cv} = 20(26.17 \times 12) = 6280 \text{ in.}^2$$

$$\rho_t = \frac{2(0.31)}{20 \times 12} = 0.0026$$

$$\text{available } \phi V_n = 0.60 \times 6280 (2\sqrt{4000} + 0.0026 \times 60,000)$$

$$= 1,065,000 \text{ lb} > V_u = 885,000 \text{ lb (4.7 MN} > \text{required 3.9 MN)}$$

Hence the wall section is adequate. Therefore, use two curtains of No. 5 bars spaced at 12 in. c-c in both horizontal and vertical directions.

**4. Boundary element check if acting as a short column under factored vertical forces due to gravity and lateral loads:**  $P_u$  acting on wall = 4,500,000 lb. From before,  $b = 32 \text{ in.}$ ,  $h = 50 \text{ in.}$ ,  $A_s = 39$  No. 11 bars =  $39 \times 1.56 = 60.84 \text{ in.}^2$  (35,100 mm<sup>2</sup>) in each boundary element.

$$\rho_{st} = \frac{A_s}{A_g} = \frac{60.84}{32 \times 50} = 0.038$$

$$\rho_{\min} = 0.01 < \rho_{st} < \rho_{\max} = 0.06 \text{ O.K.}$$

The axial load capacity of the boundary element acting as a short column is

$$\phi P_{n(\max)} = 0.80 \phi [0.85f'_c (A_g - A_{st}) + A_{st}f_y]$$

$$= 0.80 \times 0.65 [0.85 \times 4000 (1600 - 60.84) + 60.84 \times 60,000]$$

$$= 4,619,443 \text{ lb} > P_u = 4,500,000 \text{ lb} \quad \text{O.K.}$$

5. **Boundary element transverse confining reinforcement:**  $b_w = 20$  in.,  $b_b = 32$  in.,  $h$  or  $\ell_w = 314$  in., and  $A_g = 1600$  in.<sup>2</sup>. From Eqs. 13.31(a) and (b)

$$\rho_s \geq \frac{0.12f'_c}{f_{yt}}$$

and

$$A_{sh} \geq 0.3 sb_c \left( \frac{A_g}{A_{ch}} - 1 \right) \frac{f'_c}{f_{yt}}$$

Assume No. 5 hoops and crossties spaced at 4 in. c-c.

- (a) *Short direction*

$$b_{c1} = 50 - 2 \left( 1.5 + \frac{5}{16} \right) = 46.37 \text{ in.}$$

$$b_{c2} = 32 - 2 \left( 1.5 + \frac{5}{16} \right) = 28.37 \text{ in.}$$

$$A_{ch} = 46.33 \times 28.37 = 1314 \text{ in.}^2 \text{ (core area)}$$

$$A_{sh} = \frac{0.09f'_c s b_{c1}}{f_{yt}} = \frac{0.09 \times 4000 \times 4 \times 46.37}{60,000} = 1.08 \text{ in.}^2$$

$$A_{sh} = 0.3 \times 4 \times 46.37 \left( \frac{1600}{1314} - 1 \right) \frac{4000}{60,000} = 0.80 \text{ in.}^2$$

$A_{sh} = 1.08$  in.<sup>2</sup> governs.

Use three No. 5 crossties, for a total of five legs being provided including the hoop, every 4 in. along the boundary length (wall length  $\ell_w$ ).  $A_{sh}$  provided =  $5 \times 0.31 = 1.55$  in.<sup>2</sup>, O.K., on the conservative side

- (b) *Longitudinal direction*

$$b_{c2} = 28.37 \text{ in.}, \quad A_{ch} = 1314 \text{ in.}^2$$

or 
$$A_{sh} = \frac{0.12f'_c b_{c2} s}{f_{yt}} = \frac{0.12 \times 4000 \times 4 \times 28.37}{60,000} = 0.91 \text{ in.}^2$$

$$A_{sh} = 0.3 \times 4 \times 28.37 \left( \frac{1600}{1314} - 1 \right) \frac{4000}{60,000} = 0.49 \text{ in.}^2$$

$A_{sh} = 0.91$  in.<sup>2</sup> (587 mm<sup>2</sup>) controls. With one No. 5 crosstie, a total of three legs is provided every 4 in. c-c.  $A_{sh}$  provided =  $3 \times 0.31 = 0.93$  in.<sup>2</sup> (600 mm<sup>2</sup>).

6. **Check for maximum hoop spacing:**

$$s \leq \frac{1}{4} \times 32 = 8 \text{ in.}$$

$$s \leq 6 \text{ times dia. of longitudinal bar} = 6 \times \frac{11}{8} = 8.25 \text{ in.}$$

$$h_x = \frac{32 - [2(1\frac{1}{2} + \frac{1}{4}) + 5(\frac{11}{8})]}{4} = 5.4 \text{ in.}$$

$$s_o \leq 4 + \left( \frac{14 - h_x}{3} \right) = 4 + \left( \frac{14 - 5.4}{3} \right) = 6.9 \text{ in.} < 6.0 \text{ in. within length } \ell_o$$

Maximum spacing of cross-ties or hoops = 4 in. (100 mm)

7. **Development of reinforcement:** Development length of No. 5 horizontal bars assuming no hooks are used within the boundary element: From Eqs. 13.33(a), b, and c,

$$\ell_{dh} \geq \frac{f_y d_b}{65 \sqrt{f'_c}} = \frac{60,000 \times 0.625}{65 \sqrt{4000}} = 9 \text{ in.}$$

$$\geq 8d_b = 8 \times 0.625 = 5 \text{ in.}$$

$$\geq 6 \text{ in.}$$





**Photo 13.12** Interfirst Plaza, Dallas, Texas, 10,000-psi concrete. (Courtesy Portland Cement Association.)

$$\ell_{dh} = 9 \text{ in. (229 mm) governs}$$

$$\ell_d = 3.5\ell_{dh} = 3.5 \times 9 \cong 32 \text{ in. (815 mm)}$$

If bars are straight as in this example, ensure that development length is provided. If 90° hooks are used,  $\ell_d = \ell_{dh} = 9$  in. Note that no lap splices should be allowed for the No. 5 horizontal bars.

**8. Verify adequacy of shear wall section at its base under combined axial load and bending in its plane:** From before,

Actual  $P_u = 4,800,000$  lb (total gravity factored load)

Actual  $M_u = 554 \times 10^6$  in.-lb,  $e = \frac{M_u}{P_u} = 115$  in.,  $b_{web} = 20$  in.,  $b_{bound} = 32$  in.

$$P_n = \frac{4,800,000}{0.65} = 7,384,615 \text{ lb}$$

$$M_n = \frac{554 \times 10^6}{0.65} = 852 \times 10^6 \text{ in.-lb}$$

$\ell_w = 26.17$  ft = 314 in., wall height  $h_w = 148$  ft = 1776 in. (45 m)

column action  $\phi = 0.65$ , beam action  $\phi = 0.90$

no. of longitudinal bars in wall plane = 116 composed of two rows (39 No. 11 bars)

for both boundary elements and two curtains of No. 5 bars at 12 in. center-to-center over  $\ell_w = 314$  in.

total  $A_{st}$  in the lateral cross section =  $2 \times 60.84 + 2(18 \times 0.31) = 132.8 \text{ in.}^2$

$A_g = 2(32 \times 50) + 20(314 - 2 \times 50) = 7480 \text{ in.}^2$  (4,830,000 mm<sup>2</sup>)

$$\rho = \frac{132.8}{7480} = 0.0178 > 0.01 \text{ and } < 0.06 \text{ O.K.}$$

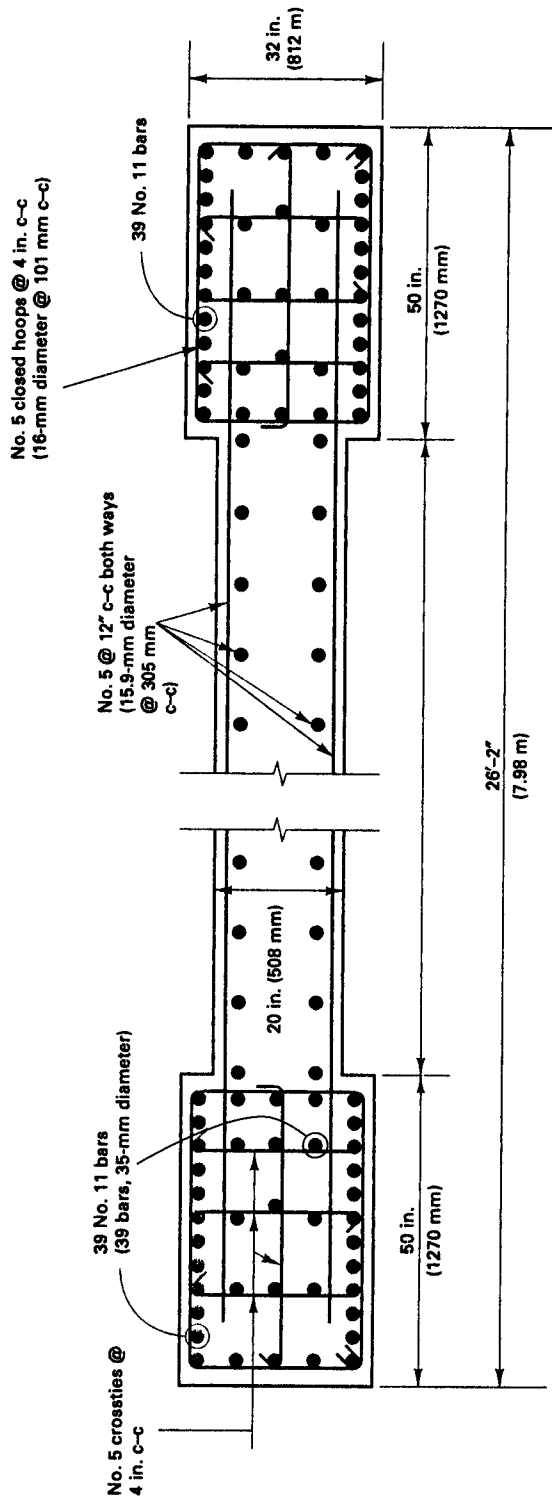


Figure 13.24 Plan and detailing of shear wall in Example 13.2.

$$P_n = \frac{7,384,615}{4000 \times 7480} = 0.247$$

Enter Figure 9.24(a) in Ref. 13.14 with  $P_n/(f'_c A_g) = 0.247$  and  $\rho = 0.0178$ . This gives a value of  $M_n/f'_c A_g h = 0.19$ .

Hence, available  $M_n = 0.19 \times 4000 \times 7480 \times 314 = 1785 \times 10^6$  in.-lb  $\gg$  Required  $M_n = 852 \times 10^6$  in.-lb, O.K.

### 13.13 EXAMPLE 13.3 STRUCTURAL PRECAST WALL BASE CONNECTION DESIGN

A precast structural (shear) wall for a five-story building in a moderate seismicity zone is  $b = 8$  in. (203 mm) thick (Ref. 13.29). The length of the interior wall is 24 ft (7.32 m) and the height of each story is 13'-0" (3.96 m). Structural analysis showed that the wall is subjected to a factored seismic base shear force  $V_u = LF(V_e) = 157.4$  kips (582 kN) and a factored overturning Case II base moment  $M_u = LF(M_e) = 7114$  ft-kip (9645 kN-m). The total weight of each floor including attached masses is 2,400 kips (10,675 kN). Design the connection at the base of the wall assuming that it is so reinforced that the neutral axis obtained by trial and adjustment and strain compatibility analysis is  $c = 17.62$  in. (447 mm). Use either welded connection as in Figure 13.21 having a rated capacity of 25 kips per connection (111 kN) or Dywidag rods grade 150 ksi (1034 MPa) with thread bar couplers as in Fig. 13.20. Case I factored overturning moment  $M_u = 6941$  ft-kip (9410 kN-m).

Given:

Sliding shear friction coefficient  $\mu = 0.60$

Maximum allowable horizontal concrete shear interaction stress (sliding friction):

$$f_{cv} = 1200 \text{ psi (8.2 MPa)}$$

$$f'_c = 5,000 \text{ psi (34.5 MPa) for shear wall and for grout (dry pack)}$$

**Solution:** The system forces acting on the structural wall are shown in Figure 13.25. The ACI load factors governing the design are:

- Load Case I LF: = 1.2D + 1.0E + ( $f_1$  L or  $f_2$  S)
- Load Case II LF: = 0.9D  $\pm$  (1.0E or 1.6W)

Usually, Load Case II controls the majority of design cases for gravity walls. Use case II for seismic effects. As given in the problem statement, computer analysis using strain compatibility and trial and adjustment for the reinforcement used in the wall (Ref. 13.29) gave the following factored overturning moment:

Seismic overturning moment = 7114 ft-kip (Case II)

and a neutral axis depth  $c = 17.62$  in.

Actual Seismic Shear:

$$V_u = 157.4 \text{ kips}$$

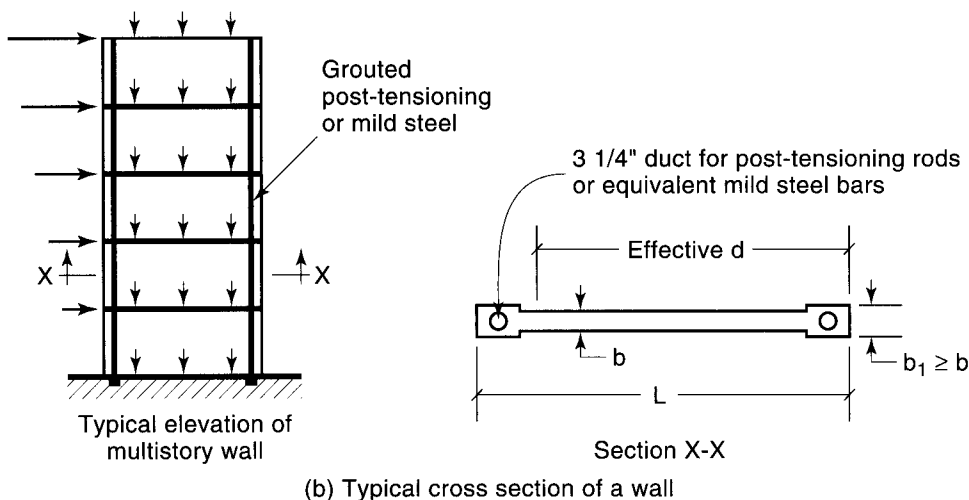
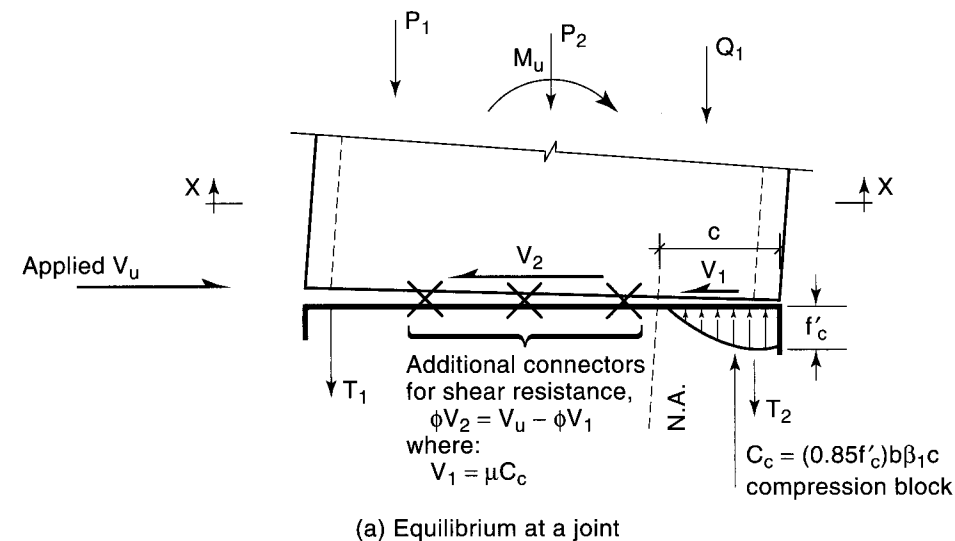
$$V_n = \frac{V_u}{\phi} = \frac{157.4}{0.75} = 209.8 \text{ kips (930 kN)}$$

$$C_c = 0.85 f'_c b \beta_1 c = \frac{1}{1000} (0.85 \times 5000 \times 8 \times 0.80 \times 17.62) = 476.5 \text{ kips.}$$

From Figure 13.25, the sliding friction contribution,

$$V_1 = \mu C_c = 0.60 \times 476.5 = 285.9 \text{ kips.}$$

Upper bound of  $V_1 = [($  wall thickness  $b)$  (N.A. depth  $c)$  (allowable horizontal frictional stress  $f_{cv})]$



**Figure 13.25** Equilibrium forces and stresses at base of structural wall

$$V_1 = \frac{1}{1000} (8.0 \times 17.62 \times 1200) = 169.2 \text{ kips} \leftarrow \text{controls} (< 285.9 \text{ kips}).$$

$$\text{Net } V_2 = \text{Actual } V_n - V_1 = 209.8 - 169.2 = 40.6 \text{ kips.}$$

Hence, required horizontal force contribution for designing the connection at the wall base is 40.6 kips.

If a welded connection is used with the given rated shear capacity of 25 kips, two welded connections have to be used per wall, which is the minimum per panel (see Figure 13.21).

If Dywidag connector and *grouted* post-tensioning is used throughout the wall height, use Dywidag type A722, Grade 150 ksi connectors with minimum yield strength of 120 ksi ( $f_{pu} = 150$  ksi and effective pull after seating losses = 0.75 in. minimum). Grout the horizontal joint as in Figure 13.20.

The vertical flexural reinforcement in the precast 8-in. wall panel elements is a typical  $6 \times 6 - W5 \times W5$  welded wire fabric reinforcement for such standard flexural wall design.

It should be noted that the design engineer has to consult with the local precasters for the appropriate connection configuration and its rated capacity.

### 13.14 DESIGN OF PRECAST PRESTRESSED DUCTILE FRAME CONNECTION IN A HIGH-RISE BUILDING IN HIGH-SEISMICITY ZONE USING DYWIDAG DUCTILE CONNECTION ASSEMBLY (DDC)

#### Example 13.4

Design a typical ductile precast prestressed concrete moment-resisting frame connection in a thirty-nine-story high rise building in a high-intensity seismic zone with design data from Ref. 3.21. Use the Dywidag ductile connector assembly (DDC) described in Section 13.7.2 and Figure 13.15, namely, 282 kips capacity per single assembly. The frame analysis output for this connection gave a factored moment  $M_u = 1,150$  ft-kip (1559 kN-m) and a post-yield rotation  $\theta_p = 3.0$  percent. The floors are post-tensioned slabs with 200 psi stress limit in the slab concrete at service. The 5 1/2 in. thick slab panels were 18 ft  $\times$  27 ft on the average, prestressed both ways.

Given:

Precast beam span (L):	18 feet (5.49 m)
Clear Span ( $L_{cl}$ ):	15 feet (4.57 m)
Story Height:	9ft 8 in. (2.95 m)
Column Size:	36 in. $\times$ 36 in. (914 mm $\times$ 914 mm)
Beam Size:	30 in. $\times$ 36 in. (762 mm $\times$ 914 mm) : [b $\times$ h]
Center to Center of Ductile Rods:	2.33 ft (710 mm) : [d-d']
Objective Strength	1150 ft-kips (1559 kN-m) : [ $M_u$ ]
Objective Post-Yield Rotation:	3% ( $\theta_p$ )
$f'_c = 5000$ psi (34.5 MPa), normal weight	Load intensity on precast beam:
$f_y = f_{yt} = 60,000$ psi (414 MPa)	Slab $w_D = 0.70$ K/ft
$f_{pu} = 270,000$ psi (1861 MPa)	$w_L = 0.16$ K/ft
$f_{ps} \leq 0.90 f_{pu}$	
$f_{pe} = 162,000$ psi (1117 MPa)	
$E_s = 29,000,000$ psi (200,000 MPa)	
$E_{ps} = 28,000,000$ psi (193,000 MPa)	
Maximum concrete stress, $f_c$ , at post-tensioning = 1000 psi (6.9 MPa)	

Note that  $\lambda_o f_y = 1.25 f_y$  due to probable seismic increase in the longitudinal reinforcement strain at the joint well beyond the yield strain, as stipulated in the ACI 318 and IBC 2009 codes (see Sec. 13.4.1).

**Solution:**

**1. Determine nominal capacity of a double DDC connection.**

$$T_y = 2(282) = 564 \text{ kips}$$

$$M_n = T_y(d - d') = 564(2.33) = 1314 \text{ ft-kips}$$

$$M_u = \phi M_n = 0.9(1314) = 1183 \text{ ft-kips} > 1150 \text{ ft-kips}$$

As discussed in Sec. 13.6 and 13.7, it is important to note that a *capacity-based approach* is being used in order to develop the strength required along the seismic load path.

**2. Determine the shear imposed on the connector at probable demand of the DDC assembly.**

$$\text{Beam } w_D = \frac{30 \times 36}{144} (0.150) = 1.13 \text{ K/ft}$$

$$W_D = 1.13 \text{ k/ft. (beam)} + 0.70 \text{ k/ft. (slab)} = 1.83 \text{ k/ft.}$$



**Photo 13.13** Paramount Apartments, San Francisco, CA: the first hybrid precast prestressed concrete moment-resistant 39 floor high-rise frame building in high seismicity zone, 2002, Ref. 13.21 and Examples 13.4 and 13.5. (Photo 1.17 lists acknowledgements for both photos, courtesy Charles Pankow Builders Ltd.)

The subscripts *pr* denote the probable seismic force, shear, or moment.  
From Eq. 4.31(e), controlling  $U = 1.2D + 1.0E + 1.0L$

$L_{cl}$  = clear span

$$\begin{aligned} V_{bpr} &= \left( \frac{M_A + M_B}{L_{cl}} \right) + [1.2(1.83) + 1.0(0.16)] \frac{L_{cl}}{2} \\ &= \frac{1.25(2)(1314)}{15} + 17.67 \\ &= 237 \text{ kips} \end{aligned}$$

where  $M_A$  and  $M_B$  are the probable flexural strengths that can be developed in the beams at the column face ( $1.25 M_n$ ). Dead and live loads are factored.  
Required friction factor between transfer block and face of ductile rod,

$$f_v = \frac{V_b}{1.25T_y} = \frac{237}{(1.25)564} = 0.34$$

Note that class-A slip critical connectors develop a friction factor of 0.33 (AISC Specifications) but this includes a safety factor of about 40 percent (Ref. 13.16). Observe also that the available friction increases in direct proportion to the tensile load developed in the ductile rod.

3. Check the induced bearing pressure ( $\rho$ ) under a ductile rod at the probable strength of the ductile rod.

$$\text{Shear/bolt} = \frac{V_{bpr}}{4} = \frac{237}{4} = 59.3 \text{ kips}$$

$$\rho = \frac{59.3}{2.95 \times 2.95} = 6.81 \text{ ksi}$$

Note that the shear transfer mechanism is assumed conservatively to flow through the compression node (Figure 13.26). The bearing area under the ductile rod is confined on all sides. On the open face where it meets the beam, an oversized washer is provided to accomplish this objective.

$$\text{Allowable nominal bearing pressure } \rho_{\text{allow}} = 1.7 f'_c$$

$$= 1.7(5) = 8.5 \text{ ksi}$$

$$\phi \rho_{\text{allow}} = 0.7(8.5) = 6.0 \text{ ksi}$$

4. Design of shear reinforcement for the beam.

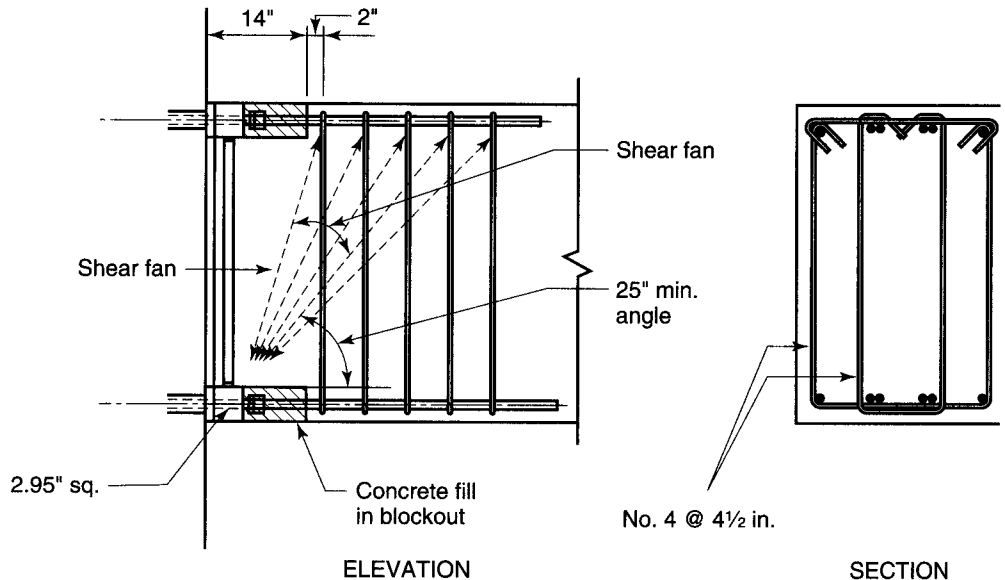
$$V_{bpr} = 237 \text{ kips} \quad (\text{see step 2})$$

$$v_u = \frac{V_{bpr}}{bd} = \frac{237}{30(33)} = 0.24 \text{ ksi}$$

It should be noted that since inelastic behavior will not occur in the beam, the ability of the concrete to carry shear is not diminished (Ref. 13.17). Hence,  $v_c = 2\sqrt{f'_c} = 2\sqrt{5000} = 141 \text{ psi} = 0.141 \text{ ksi}$ .

$$v_s = \frac{v_{upr}}{\phi} - v_c$$

$$= \frac{0.24}{0.75} - 0.141 = 0.179 \text{ ksi}$$



**Figure 13.26** Shear transfer mechanism in the discontinuous region of a DDC® frame beam (Ref. 13.21)

$$s = \frac{A_v f_{yt}}{v_s b} = \frac{0.4(60)}{0.179(30)} = 4.47 \text{ in. c./c.}$$

Provide #4 closed U-stirrups (ties) at  $4\frac{1}{2}$  in. c./c. as shown in Fig. 13.26 to cover the shear fans zone.

It is suggested that the first two stirrups should be hoop sets and include an inner hoop set to provide lateral support for the flexural bars (see Figure 13.26). The first hoop set should be placed at the edge of the blockout. The shear fan describes the shear transfer mechanism in this discontinuous region.

*Shear transfer in the Discontinuous Region*

A shear fan describes the shear transfer mechanism in this discontinuous region. Capacity of one #4 tie set:

$$V_s = A_v f_{yt} = 0.4(60) = 24 \text{ kips}$$

$$\text{Number Required} = \frac{237}{24} \cong 10$$

Provide five double-#4 closed U-stirrup sets within the shear fan region.

**5. Load transfer mechanism within the joint.**

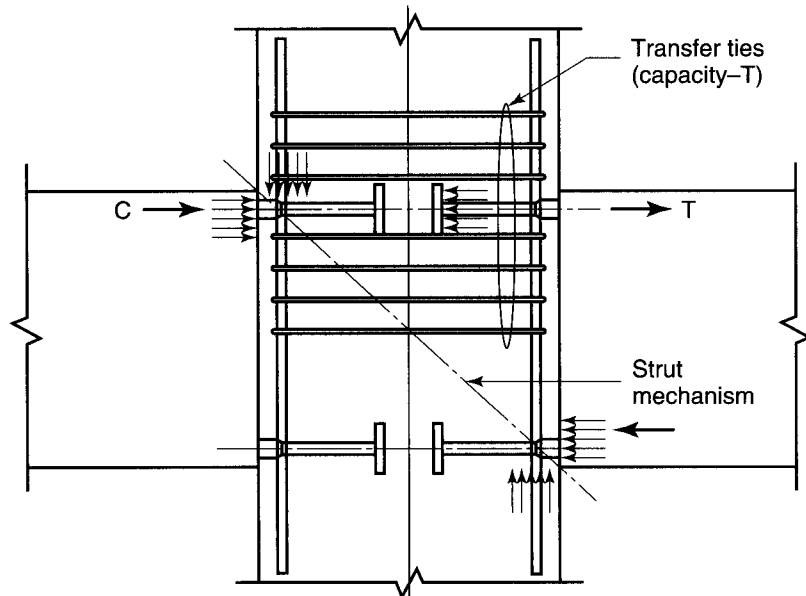
The bearing plate on the interior end of the ductile rod develops the tensile strength of the rod in bearing. Joint behavior is significantly improved because this load transfer mechanism does not slip, as a conventional bar will as it debonds when subjected to load reversals.

*Bearing on the end plate:*

$$\lambda_o R = 1.25 \left( \frac{564}{4} \right) = 176.5 \text{ kips}$$

$$\text{Bearing stress } \rho = \frac{176.5}{28} = 6.3 \text{ ksi} \cong 6.0 \text{ ksi, O.K.}$$

where the DDS plate area = 28 in.<sup>2</sup>



**Figure 13.27** Load path within the beam-column joint of a DDC assembly (Ref. 13.21)





**Photo 13.14** Failure of piers at Hanshin Highway Bridge, Kobe Earthquake, Japan, 1995 (Courtesy Professor Megumi Tominaga, Kyoto University, Japan)

#### *Load transfer within a beam-column joint*

It is accomplished through the activation of a strut mechanism and a truss mechanism (Ref. 13.17, 13.22). As seen from Figure 13.27; The strut mechanism is activated by bearing on the column face in the case of the compression side at the peak load. On the tension side the load is delivered to the truss mechanism. Since the stiffer load path is, at least initially, through the strut mechanism, it is advisable to provide a sufficient number of ties in the vicinity of the ductile rod to transfer the developed rod force to the node region. The suggested tie force ( $T_T$ ) is:

$$T_T = 4(\lambda_o R) = 4(176.4) = 706 \text{ kips}$$

where  $\lambda_o = 1.25$  for probable increase of 25%.

$$A_T = \frac{706}{60} = 11.7 \text{ in.}^2$$

Use seven triple-#5 tie sets  $7(3 \times 0.62) = 13.02 \text{ in.}^2 > 11.7 \text{ in.}^2$ , OK—*three above and four below* the ductile rods. Tie sets should be located within a  $65^\circ$  angle of the ductile rod bearing area.

#### *Joint Shear Stress—ACI 318 Code basis*

$$V_{bpr} = \frac{\lambda_o M_n}{L_c/2} = \frac{1.25(1314)}{7.5} = 219 \text{ kips}$$

$$V_{cpr} = \frac{V_{bpr} L}{h} = \frac{219(18)}{9.67} = 408 \text{ kips}$$

$$V_{jh} = 2\lambda_o T_y - V_{cpr} = 2(1.25)(564) - 408 = 1002 \text{ kips}$$

$$v_{jh} = \frac{V_{jh}}{A_j} = \frac{1002}{36(36)} = 0.773 \text{ ksi}$$

$$v_{jh \text{ allow}} = 15\phi\sqrt{f'_c} = 15(0.75)\sqrt{5000} = 0.80 \text{ ksi} > 0.773 \text{ ksi, O.K.}$$

#### **6. Column Design Criterion**

Design of the column follows standard situ-cast concrete design procedures using the strong column-weak beam requirement in the ACI Code:

$$\Sigma M_{nc} > \frac{6}{5} \Sigma M_{nb}$$

Alternatively, and consistent with the capacity design approach, the moment demand can be developed directly from probable column shears.

$$M_{nc} \geq \frac{h_c}{2} (V_{cpr})$$

where  $h_c$  is the clear height of the column.

$$\begin{aligned} M_{nc} &= \frac{9.67}{2} (408) \\ &= 1972 \text{ ft-kips} \end{aligned}$$

Once the nominal axial load  $P_n$  is entered from the computer analysis output, the column is designed in the usual manner as outlined in Chapter 8.

#### 7. Post-yield deformability

The portion of the ductile rod, which was designed to absorb post-yield deformations, is 9 in. long. The elongation required of the ductile rod ( $\Delta_\epsilon$ ) is:

$$\begin{aligned} \Delta_\epsilon &= \theta_p \frac{(d - d')}{2} = 0.03(14) = 0.42 \text{ in.} \\ \epsilon_p &= \frac{0.42}{9} = 0.047 \end{aligned}$$

The strain associated with the fracture of the ductile rod is in excess of 50 percent or 0.50, hence O.K.

### 13.15 DESIGN OF PRECAST PRESTRESSED DUCTILE FRAME CONNECTION IN A HIGH-RISE BUILDING IN HIGH-SEISMICITY ZONE USING A HYBRID CONNECTOR SYSTEM

#### Example 13.5:

Design a typical moment-resisting connection for the ductile frame building in Example 13.4 using a hybrid system as described in Section 13.7.1. Use both well-bonded mild reinforcing bars at top and bottom of the frame beams with debonding at the column face and concentric post-tensioning steel reinforcement at their mid-depth. Given:

Beam size: 24 in.  $\times$  36 in. (610 mm  $\times$  914 mm)

$f'_c = 5000$  psi (34.5 MPa), normal weight

$f_y = 60,000$  psi (414 MPa)

$f_{pu} = 270,000$  psi (1861 MPa)

$f_{ps} \leq 0.90 f_{pu}$

$f_{pe} = 162,000$  psi (1117 MPa)

$E_s = 29,000,000$  psi (200,000 MPa)

$E_{ps} = 28,000,000$  psi (193,000 MPa)

Maximum concrete stress,  $f_c$ , at post-tensioning = 1000 psi (6.9 MPa)

**Solution:** The design procedure in this example differs in that the beam width here does not need to be a function of the hardware as is the case for the DDC in the previous example.

It is important to note in this example also that a *capacity-based* approach is used in order to develop the strength required along the seismic load path.

#### 1. Determine the amount of post-tensioning required.

The post-tensioning should be capable of resisting about 60 percent of the moment demand. The balance is to be resisted by the mild steel reinforcement.

$$M_u = 1150 \text{ ft-kips}$$

$$M_n = \frac{M_u}{\phi} = \frac{1150}{0.9} = 1278 \text{ ft-kips}$$

$$M_{nps} = 0.6(1278) = 767 \text{ ft-kips}$$

Assume that the effective lever arm is about 16 in.  $(h/2 - a/2) = 1.33 \text{ ft}$ .

$$T_{nps} = \frac{M_{nps}}{\left(\frac{h}{2} - \frac{a}{2}\right)} = \frac{767}{1.33} = 576 \text{ kips}$$

$$A_{ps} = \frac{T_{nps}}{f_{pe}} = \frac{576}{162} = 3.56 \text{ in.}^2$$

Use 0.6 in. diameter strands,  $A_{ps} = 0.213 \text{ in.}^2 / \text{strand}$ .

$$\text{Required number of strands, } N = \frac{3.56}{0.213} = 16.7$$

It should be noted that the selection of the amount of post-tensioning is fairly arbitrary. The objective is to provide a restoring force (see design objectives) and satisfy objective strength requirements. The designer may select a 17-strand tendon or opt to use a 19-strand tendon. The latter will be used in this example since a 19-strand tendon anchorage is available and would be used for either choice. Also observe that post-tensioning strands are more cost effective than Grade 60 reinforcing when developed as described in Figure 13.13(b). The consequence associated with the use of proportionately higher amounts of post-tensioning is the loss of some energy dissipation.

$$A_{ps} = 19(0.213) = 4.05 \text{ in.}^2$$

$$T_{ps} = A_{ps}f_{pe} = 4.05(162) = 656 \text{ kips}$$

$$a = \frac{T_{ps}}{0.85 f'_c b} = \frac{656}{0.85(5)24} = 6.43 \text{ in.} \quad (\text{from data, } b = 24 \text{ in.})$$

$$M_{nps} = T_{ps} \left(\frac{h}{2} - \frac{a}{2}\right) = \frac{656(18 - 3.21)}{12} = 813 \text{ ft-kips}$$

Check compressive stress on the concrete  $= P_e/A_c$

$$\frac{P_e}{A_c} = \frac{T_{ps}}{A_g} = \frac{656}{24(36)} = 0.76 \text{ ksi}$$

Note that the post-tensioning stress level in the concrete should not exceed 1000 psi. This is because stress compatibility with the other components of the structure will become more of a problem and system shortening is likely to be excessive. In the building being designed and used in this example (Ref. 13.21), the floor slab is post-tensioned and the level of effective post-tensioning in the floor will be on the order of 200 psi (or less).

### 2. Determine the amount of mild steel required to attain the objective strength.

$$M_{ns} = M_n - M_{nps} = 1278 - 813 = 465 \text{ ft.kips}$$

$$T_{ns} = \frac{M_{ns}}{d - d'} = \frac{465}{(33 - 3)/12} = 186 \text{ kips} \quad (d' = 3 \text{ in.})$$

$$A_s = \frac{T_{ns}}{f_y} = \frac{186}{60} = 3.1 \text{ in.}^2$$

Hence, provide four No. 8 bars ( $A_s = 3.16 \text{ in.}^2/M_{ns} = 474 \text{ ft.-kips}$ ).

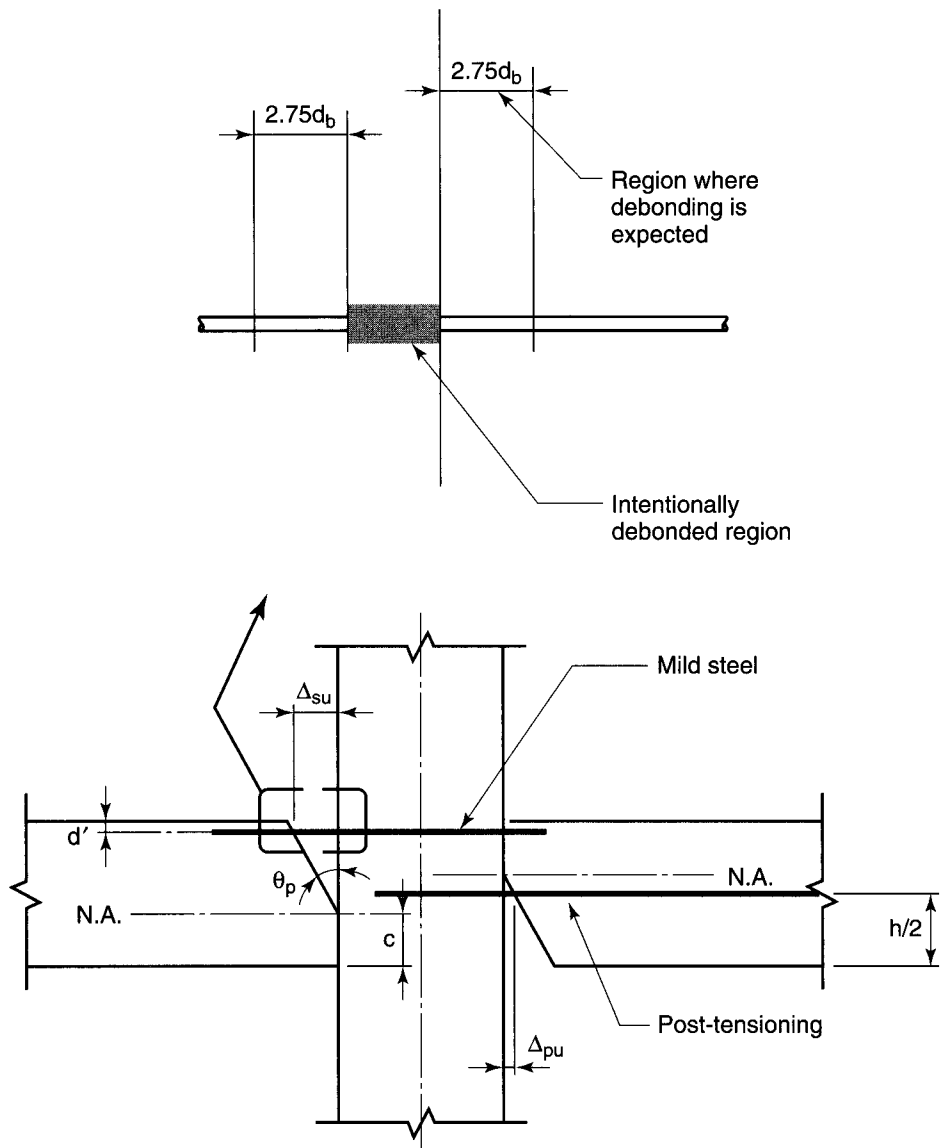
Available  $T_{ns} = 3.16 \times 60 = 190 \text{ kips}$

### 3. Limit state at ultimate strength.

The original design guidelines for this construction system (Ref. 13.18) require that the flexural overstrength (probable strength) provided by the mild steel be less than

that provided by the post-tensioning steel. This provision is intended to produce the objective of a self-restoring bracing system. The mild steel reinforcing bars are debonded at the beam-column interface as in Figure 13.28. This is because the precast beam will tend to separate or “lift-off” the column, introducing large strains in the mild steel in this region. The extent of the debonding determines the strain/stress induced in the mild steel when the deformation limit state is reached. It should be noted that as the strain limit in the mild steel reinforcing bars is approached, their stress level becomes on the order of approximately 105 ksi. The probable strain in the mild steel would be comfortably less than the strain limit state at the deformation limit state.

Determine the mild steel stress at a post-yield rotation of 3% (see stress-strain diagram in Figure 2.18 and Ref. 13.19). The unbonded mild steel length includes a region of probable debonding of  $2.75 d_b$  on either side of the intentionally debonded region. If the intentionally debonded length is 6 in., the total debonded length becomes:



**Figure 13.28** Reinforcing elongation at post-yield rotation limit state hybrid beam subassembly (Ref. 13.21)

$$L_u + 5.5d_b = 6 + 5.5(1) = 11.5 \text{ in.}$$

The strain states in the mild and post-tensioned steel are developed from the post-yield deformation state of the connection in Fig. 13.28 and the stress-strain diagram of the mild steel reinforcement in Figure 2.16 or 2.18b of Chapter 2. The process is an iterative trial-and-adjustment procedure since the location of the neutral axis and steel strain states are mutually dependent. A reasonable estimate of the neutral axis is possible.  $T_{ps}$  will increase by about 25% to about 200 ksi.  $T_{ns}$  will increase by about 67 percent (100/60), which is the increase transmitted to the concrete at the compression side due to the probable seismic load. The compressive force that must be resisted by the concrete is:

**(a) Mild steel reinforcement**

For equilibrium,  $T_{ns} = C'_s$

$$\begin{aligned} C &= 1.25 T_{ps} + 1.67 T_{ns} - C'_s = 1.25 T_{ps} + 0.67 T_{ns} \\ &= 1.25(656) + 0.67(190) = 820 + 127 = 947 \text{ kips} \end{aligned}$$

$$a = \frac{947}{0.85(5)(24)} = 9.3 \text{ in.}$$

$$c = \frac{a}{\beta_1} = \frac{9.3}{0.80} = 11.6 \text{ in.}$$

Assume  $c = 11.6$  in. for this trial cycle

$$\Delta_{su} = \theta_p(d - c) = 0.03(33 - 11.5) = 0.645 \text{ in.} \quad (\text{elongation of the mild steel})$$

$$\Delta\epsilon_s = \frac{\Delta_{su}}{L_u + 5.5d_b} = \frac{0.645}{11.5} = 0.056$$

$$\epsilon_{su} = 0.056 + \epsilon_y = 0.058$$

$$f_{su} \cong 100 \text{ ksi} \quad (\text{Refer to Figure 2.16 or Figure 2.18b})$$

**(b) Prestressing steel reinforcement**

$$\Delta_{pu} = \theta_p \left( \frac{h}{2} - c \right) = 0.03(18 - 11.6) = 0.195 \quad (\text{elongation required of the post-tensioning tendon})$$

$$\Delta\epsilon_{pu} = \frac{\Delta_{pu}}{L/2} = \frac{0.195}{18(12)(0.5)} = 0.0018$$

$$\Delta f_{ps} = \Delta\epsilon_{pu} E_{ps} = 0.0018(28,000) = 50 \text{ ksi}$$

$$f_{psu} = f_{pse} + \Delta f_{pe} = 162 + 50 = 212 \text{ ksi} < 0.9 f_{pu} \quad (\text{Refer to Figure 2.16 or Figure 2.18b})$$

$$T_{su} = A_s f_{su} = 3.16(60 + 40) = 3.16(100) = 316 \text{ kips}$$

$$T_{psu} = A_{ps} f_{psu} = 4.05(212) = 859 \text{ kips}$$

$$C = T_{psu} + T_{su} - C'_s = 859 + 316 - 190 = 985 \text{ kips}$$

$$a = \frac{985}{0.85(5)(24)} = 9.65 \text{ in.}$$

$$c = \frac{9.65}{0.8} = 12 \text{ in.} \quad (\text{which is close to the } c = 11.6 \text{ in., hence O.K.})$$

$$\begin{aligned} M_{pr} &= T_{psu} \left( \frac{h}{2} - \frac{a}{2} \right) + (T_{su} - T_{ns}) \left( d - \frac{a}{2} \right) + T_{ns} (d - d') \\ &= 212(4.05)(18 - 4.83) + 40(3.16)(33 - 4.83) + 60(3.16)(30) \\ &= 11,308 + 3561 + 5688 \\ &= 20,560 \text{ in.-kips} = 1713 \text{ ft-kips} \end{aligned}$$

$$M_{su} = 3561 + 5688 = 9249 \text{ in.-kips} < M_{psu} = 11,308 \text{ in.-kips}$$

$$\text{Overstrength factor achieved} = \frac{M_{pr}}{M_n} = \frac{1713}{1278} = 1.34, \text{ O.K.}$$

Verification of  $\phi = 0.90$  value:

$c/d_t = 12/33 = 0.363 < 0.375$  in Figure 4.45, hence the section is tension controlled, and the value of  $\phi = 0.90$  is verified.

**4. Verify that the capacity of the joint is sufficient.**

Comparing with the ACI 318 Code requirements, the ratio of probable strength ( $M_{pr}$ ) to nominal strength ( $M_n$ ) is 1.33 for the hybrid beam as opposed to the 1.25 stipulated by the ACI for conventional cases. This would probably be the conclusion resulting from the analysis of a conventionally reinforced frame beam at a post-yield rotation demand of 3 percent.

$$T_{ps-pr} = 1.25(162)(4.05) = 820 \text{ kips}$$

$$T_{s-pr} = 1.25(60)(3.16) = 237 \text{ kips}$$

$$T_s = A_s f_y = 60 \times 3.16 = 190 \text{ kips}$$

$$a = \frac{T_{ps-pr} + 0.25T_s}{0.85f'_c b} = \frac{867}{0.85(5)(24)} = 8.5 \text{ in.}$$

$$\begin{aligned} M_{pr} &= T_{ps-pr} \left( \frac{h}{2} - \frac{a}{2} \right) + T_s (d - d') + 0.25T_s \left( d - \frac{a}{2} \right) \\ &= 820(18 - 4.25) + 190(33 - 3) + 47(33 - 4.25) \\ &= 18,326 \text{ in.-kips} \end{aligned}$$

$$V_{b-pr} = \frac{M_{pr}}{L/2} = \frac{18,326}{9(12)} = 170 \text{ kips}$$

$$V_{c-pr} = \frac{V_{b-pr} L}{h} = \frac{170(18)}{9.67} = 316 \text{ kips}$$

$$\begin{aligned} V_j &= T_{ps-pr} + 2T_{s-pr} - V_{c-pr} \\ &= 820 + 2(237) - 316 = 978 \text{ kips} \end{aligned}$$

$$v_j = \frac{V_j}{A_j} = \frac{978}{36(36)} = 0.75 \text{ ksi}$$

$$v_{j-allow} = \phi 15 \sqrt{f'_c} = 0.75(15) \sqrt{5000} = 795 \text{ psi} = 0.80 \text{ ksi} > 0.75 \text{ ksi, O.K.}$$

**5. Design the shear reinforcement for the beam.**

Since post-yield behavior is anticipated in the end of the beam, the procedures used for the design of a monolithically cast "special" concrete frame beam are required. From step 4,

$$V_{b-pr} = 170 \text{ kips}$$

$$v_{b-pr} = \frac{V_{b-pr}}{bd} = \frac{170}{24(33)} = 0.215 \text{ ksi}$$

**(a) Hinge region:**

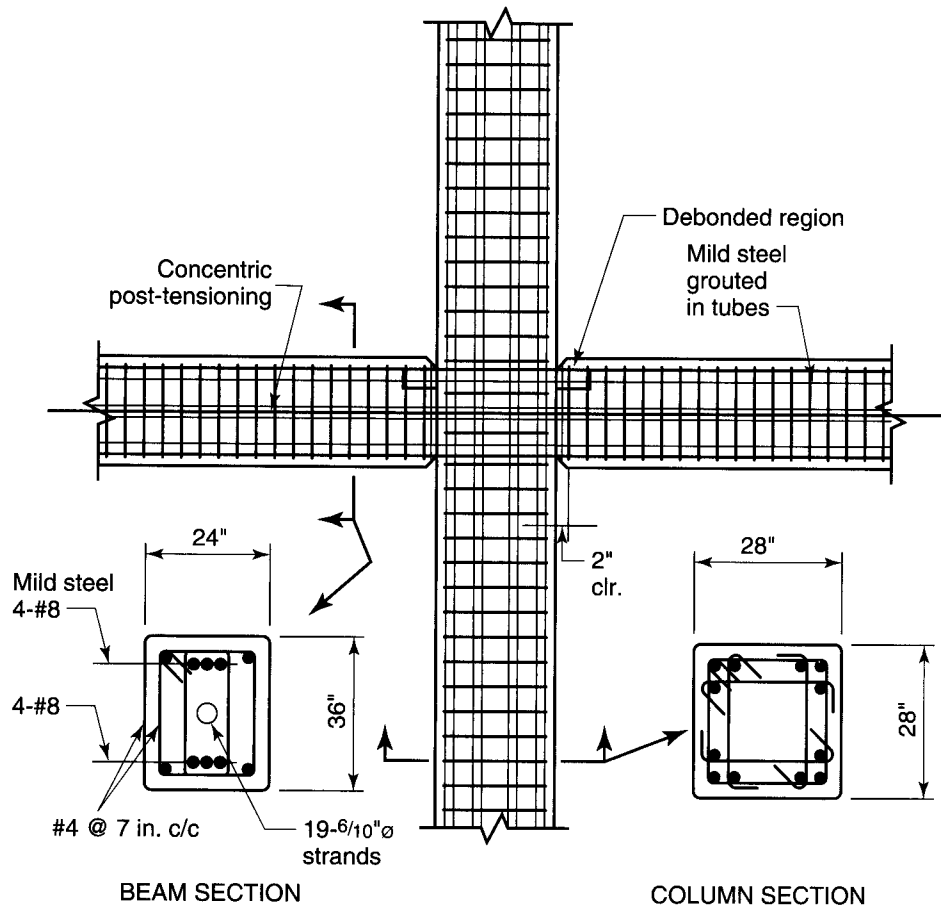
Disregard in the hinge region the shear strength of the plain concrete, namely,  $v_c = 0$ .

$$v_s = 0.215 \text{ ksi}$$

Trying two No. 4 stirrup sets,  $A_v = 0.20 \text{ in.}^2$ /one leg of a stirrup.

$$s = \frac{\phi f_{yt} A_v}{v_s b} = \frac{0.75(60)(4)(0.20)}{0.215(24)} = 6.98 \text{ in.}$$

where  $s$  is the maximum spacing of stirrups and  $A_v$  is the stirrup area.



**Figure 13.29** Schematic of the hybrid ductile beam–column connection in Example 13.5

Provide two No. 4 closed U-stirrups (hoops) at 7 in. center-to-center in the hinge region.

(b) *Outside the hinge region:*

Assume double No. 4 U-stirrups,  $A_v = 0.40 \text{ in.}^2$  per stirrup.

$$v_c = 2\sqrt{f'_c} = 141 \text{ psi} = 0.141 \text{ ksi}$$

$$v_s = \frac{v_{b-pr}}{\phi} - v_c = \frac{0.215}{0.75} - 0.141 = 0.146 \text{ ksi}$$

$$s = \frac{f_y A_v}{v_s b} = \frac{60(2 \times 0.40)}{0.146(24)} = 13.69 \text{ in. c./c.}$$

Provide double No. 4 U-stirrups at 14 in. center-to-center outside the hinge region which do not necessarily have to be hooped. Figure 13.29 schematically shows details of the ductile beam–column connection designed in this example. The first three sets of stirrups at 12 in. c. toc.

## SELECTED REFERENCES

- 13.1** ACI Committee 318, *Building Code Requirements for Structural Concrete (ACI 318–08) and Commentary (ACI 318R–08)*. American Concrete Institute, Farmington Hills, MI, 2008, pp. 465.

- 13.2 International Code Council, *International Building Codes 2009 (IBC)*, Joint UBC, BOCA, SBCCI, Whittier, CA, 2009, 667 p.
- 13.3 International Conference of Building Officials, *Uniform Building Code (UBC)*, Vol. 2, ICBO, Whittier, CA, 1997.
- 13.4 ASCE Standard 7-05, *Minimum Design Loads for Buildings and Other Structures*, American Society of Civil Engineers, Reston, VA, 2005, pp. 110–125.
- 13.5 Norris, H. C., Hansen, R. J., Holley, M. J., Biggs, J. M., Namyet, S., and Minami, K., *Structural Design for Dynamic Loads*, McGraw-Hill, New York, 1959.
- 13.6 Englekirk, R. E., and Hart, G. C., *Earthquake Design of Concrete Masonry Buildings*, Vols. I & II, Prentice Hall, Upper Saddle River, N.J., 1982.
- 13.7 Schneider, R. R., and Dickey, W. L., *Reinforced Masonry Design*, Prentice Hall, Upper Saddle River, N.J., 1994.
- 13.8 Clough R. W., “Dynamic Effects of Earthquakes,” *Proc. ASCE*, Vol. 86, ST4, New York, April 1960, pp. 49–65.
- 13.9 Ghosh, S. K., “Special Provisions for Seismic Design,” PCA Publication, *Notes on ACI318-89 Code*, Chapter 31, Portland Cement Association, Skokie, IL, 1990, pp. 31–1 to 31–81.
- 13.10 Derecho, A. T., Fintel, M., and Ghosh, S. K., “Earthquake-resistant Structures,” Ch. 12 in *Handbook of Concrete Engineering*, 2nd ed., Van Nostrand Reinhold, New York, 1985, pp. 411–513.
- 13.11 Borg, S. E., *Earthquake Engineering-Damage Assessment and Structural Design*, John Wiley & Sons, New York, 1983.
- 13.12 Wakabayashi, M., *Design of Earthquake-resistant Buildings*, McGraw-Hill, New York, 1986.
- 13.13 Naja, W. M., and Bane, C. T., “Seismic Resisting Construction” Chapter 26, in E. G. Nawy, editor-in-chief, *Concrete Construction Engineering Handbook*, 2nd Ed. CRC Press, Boca Raton, FL, 2008, 1560 p. (CH 32, pp. 1–70).
- 13.14 Nawy, E. G., *Reinforced Concrete—A Fundamental Approach*, 6th Ed., Prentice Hall, Upper Saddle River, N.J., 2009, pp. 936.
- 13.15 Federal Emergency Management Agency (FEMA), “NEHRP Recommended Provisions for Seismic Regulations for New buildings and Other Structures,” FEMA 302, Part I & II, Building Seismic Safety Council, Washington, D.C., 1998.
- 13.16 Englekirk, R. E., *Steel Structures—Controlling Behavior through Design*, John Wiley & Sons, New York, 1994.
- 13.17 Pauley, T., and Priestely, M. J. N., *Seismic Design of Reinforced Concrete and Masonry Walls*, John Wiley & Sons, New York, 1992, 744 pp.
- 13.18 Cheok, G. S., Stone, W. C. and Nakaki, S. D., “Simplified Design Procedure for Hybrid Precast Concrete Connection,” NISTIR Report No. 5765, National Institute of Standards and Technology, Gaithersburg, MD, February 1996, 82 pp.
- 13.19 Englekirk, R. E., “An Innovative Design Solution for Precast Prestressed Concrete Buildings in High Seismic Zones,” Vol. 41 No. 4, *PCI Journal*, Precast/Prestressed Concrete Institute, Chicago, IL, July/August 1996, pp. 44–53.
- 13.20 Ghosh, S. K., Nakaki, S. W., and Krishnan, K., “Precast Structures in Regions of High Seismicity: 1997 UBC Design Provisions,” Vol. 42, No. 6, *PCI Journal*, Precast/Prestressed Concrete Institute, Chicago, IL, November–December 1997, pp. 76–93.
- 13.21 Englekirk, R. E., Design of Paramount Apartments: Thirty-Nine Story Ductile Frame Precast Prestressed Concrete Building in San Francisco. Private Communication, 1999.
- 13.22 Englekirk, R. E., and Llovet, D., “Cyclic Test of Cast-in-Place High Strength Beam-Column Joints,” Concrete International, American Concrete Institute, Farmington Hills, MI, 1999.
- 13.23 Choek, G. S., and Lew, H. S., “Model Precast Beam-to-Column Connections Subject to Cyclic Loading,” *PCI Journal*, Vol. 38, No 4, July–August 1993, Chicago, IL: Precast/Prestressed Concrete Institute, Chicago, IL, July/August, pp. 80–100.
- 13.24 Choek, G. S., and Stone, W. C., and Kunnath, S. K., “Seismic Response of Precast Prestressed Concrete Frames with Hybrid Connections,” *ACI Structural Journal*, American Concrete Institute, Farmington Hills, MI, September/October 1998, pp. 527–546.



- 13.25** Priestly, M. J. N. and Marcie, G. A., "Seismic Tests of Precast Beam-to-Column Joint Subassemblies with Unbonded Tendons," *PCI Journal*, Vol. 41 No. 1, Precast/Prestressed Concrete Institute, Chicago, IL, January–February, 1996, pp. 64–81.
- 13.26** Stone, W. C., Choek, G. S., and Stanton, J. F., "Performance of Hybrid Moment-Resisting Precast Beam-Column Concrete Connections Subjected to Cyclic Loading," Title 92-S22, *ACI Structural Journal*, American Concrete Institute, Farmington Hills, MI, March–April, 1995, pp. 229–249.
- 13.27** Stanton, J., Stone, W. C., and Choek, G. S., "A Hybrid Reinforced Precast Frame for seismic Regions," *PCI Journal*, Precast/Prestressed Concrete Institute, Chicago, IL, March–April, 1997, pp. 20–32.
- 13.28** Aswad, G. S., Djazmati and Aswad, A., "Comparison of Shear Wall Deformations and forces Using Two Approaches," *PCI Journal*, Vol. 44, No. 1, Precast/Prestressed Concrete Institute, Chicago, IL, January–February, 1999, pp. 34–46.
- 13.29** Aswad, A., Private Communication and "Analysis of Reinforced or Post-Tensioned Shear Walls," SHEARWAL Computer Program, Version 2.1, Jacques and Aswad Inc., Denver, CO, 1990.
- 13.30** Cleland, N. M., "Design for Lateral Resistance with Precast Concrete Shear Walls," Col. 42, No. 5, *PCI Journal*, Precast/Prestressed Concrete Institute, Chicago, IL, September–October 1997, pp. 44–63.
- 13.31** Pessiki, S. et al. "Seismic Analysis, Behavior and Design of Unbonded Post-Tensioned Precast Concrete Frames." Report No. EQ-97-02, Dept. of Civil and Environmental Engineering, Lehigh University, Bethlehem, PA, November 1997, pp. 1–315.
- 13.32** Pessiki, S. et al. "Analytical Modeling and Lateral Load Behavior of Unbonded Post-Tensioned Precast concrete walls," Reports No. EQ-96-02, Dept. of Civil and Environmental Engineering, Lehigh University, Bethlehem, PA, November 1996, pp. 1–192.
- 13.33** Pessiki, S. et al. "Seismic Design and Response evaluation of Unbonded Post-Tensioned Precast Concrete Walls" Report No. EQ-97-01, Dept. of Civil and Environmental Engineering, Lehigh University, Bethlehem, PA, November 1997, pp. 185.
- 13.34** Englekirk, R. E., "Design-Construction of the Paramount –A 30 Story Precast Prestressed Concrete Apartment Building," *PCI Journal*, Precast/Prestressed Concrete Institute, Chicago, IL, July–August 2002, pp. 56–69
- 13.35** Nawy, E. G., "Discussion – The Paramount Building," *PCI Journal*, Precast/Prestressed Concrete Institute, Chicago, IL, November–December 2002, p. 116
- 13.36** ACI Committee 340, *ACI Design Handbook—Design of Structural Reinforced Concrete Elements with the Strength Design Method*, ACI SP-17, American Concrete Institute, Farmington Hills, MI, 1997, pp. 482.
- 13.37** Englekirk, R. E., "Seismic Design of Reinforced and Precast Concrete Buildings," Publ. John Wiley and Sons, Inc., 2003, pp. 825.

### PROBLEMS FOR SOLUTION

- 13.1** A 3 x 18 panel ductile, moment-resistant frame category-II site-class B frame building has a ground story 15 ft. high (4.6 m) and ten upper stories of equal height of 11'-6" (3.5 m). Compute the seismic base shear  $V$  and the overturning moment at each story level in terms of the weight  $W_s$  of each floor. Use the equivalent lateral force method in the solution. Given:

$$S_1 = 0.34 \text{ sec}, S_s = 0.90 \text{ sec } R = 5,$$

$$W_s \text{ per floor} = 2400 \text{ kips (9560 kN)}$$

- 13.2** A moment-resisting ductile frame building is located in a high-seismic-intensity zone. The earthquake forces are resisted equally as a dual system by the ductile frame and a monolithic reinforced concrete shear wall over the total height of the building. The geometry of the structure is given below. Design the shear wall assuming that the magnitude of the loads, forces and moments applied to the wall are 110 percent of the values used in Ex. 13.2. Given:

floors have slabs of thickness  $h_f = 7$  in. (178 mm)

clear beam spans in both longitudinal and transverse directions = 20'-0" (6.1 m)

shear wall base length  $l_w = 25$  ft (39.6 m)

shear wall height  $h_w = 130$  ft (39.6 m)

$f'_c = 5000$  psi, normal weight (34.5 MPa)

$f_{yv} = f_{yh} = 60,000$  psi (414 MPa),

Sketch the wall reinforcement.

- 13.3** A precast shear wall in a moderate seismicity zone for a six story frame building has a wall thickness of 10 in. (254 mm). The height of each story is 11'-6" (3.5 m) and the wall segments extend the height of the building and prestressed vertically. The wall is subjected to a factored seismic base shear  $V_u = 210$  kips (1048 kN) and a factored overturning moment  $M_e = 8000$  ft-kip (12,150 kN-m) for Case II loading as controlling in this case (gravity load dominant). The total weight of each floor including any attached masses is 2800 kips (12,454 kN). Design the connection at the base of the wall assuming that the neutral axis obtained by strain-compatibility analysis is  $c = 21.5$  in. (546 mm). Given:

sliding coefficient  $\mu = 0.60$

beams size: 24 in.  $\times$  28 in. (610 mm  $\times$  711 mm)

effective beam spans: 22 ft 6 in. (6.9 m)

allowable horiz. shear stress  $f_{cv} = 1200$  psi (8.3 MPa)

$f'_c = 5000$  psi, normal weight (34.5 MPa)

$f_y = f_{yt} = 60,000$  psi (414 MPa)

Use a Dywidag connector system.

- 13.4** Design a ductile precast prestressed concrete moment-resistant connection of a ductile frame in a high intensity seismic zone subjected to a factored seismic moment  $M_u = 1350$  ft-kip (1831 kN-m) and a post-yield rotation  $\theta_p = 2.75$  percent. The frame precast beams have spans of 20'-0" and the clear spans are 17'-4" (5.3 m). Each story height is 9'-0" (2.74 m). Use the Dywidag Ductile Connection assembly (DDC) in your solution. Given:

column sizes: 38 in.  $\times$  38 in. (965 mm  $\times$  965 mm)

center to center Ductile Rods,  $(d - d')$ : 27 in. (686 mm)

$f'_c = 5000$  psi, normal weight concrete (34.5 MPa)

- 13.5** Design the moment resisting connection in Problem 13.4 as a hybrid connection using both mild steel and prestressing post-tensioned reinforcement. Given:

$f'_c = 5000$  psi, normal weight concrete (34.5 MPa)

$f_y = f_{yt} = 60,000$  psi (414 MPa)

$f_{pu} = 270,000$  psi (1862 MPa)

$f_{ps} = < 0.90 f_{pu}$  (determine from compatibility analysis)

$f_{pe} = 160,000$  psi (1103 MPa)

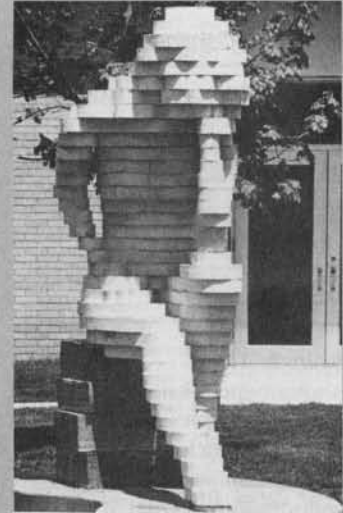
$E_s = 29,000$  ksi (200,000 MPa)

$E_{ps} = 28,000$  ksi (193,000 MPa)

$f_c = 1000$  psi (6.9 MPa) maximum concrete stress at post-tensioning



# A



## UNIT CONVERSIONS, DESIGN INFORMATION, PROPERTIES OF REINFORCEMENT

**Table A-1** Conversion to International System of Units (SI)

To convert from	to	Multiply by
<b>Length</b>		
inch (in.)	millimeter (mm)	25.4
inch (in.)	meter (m)	0.0254
foot (ft)	meter (m)	0.3048
yard (yd)	meter (m)	0.9144
<b>Area</b>		
square foot (sq ft)	square meter (sq m)	0.09290
square inch (sq in.)	square millimeter (sq mm)	645.2
square inch (sq in.)	square meter (sq m)	0.0006452
square yard (sq yd)	square meter (sq m)	0.8361
<b>Volume</b>		
cubic inch (cu in.)	cubic meter (cu m)	0.00001639
cubic foot (cu ft)	cubic meter (cu m)	0.02832
cubic yard (cu yd)	cubic meter (cu m)	0.7646
gallon (gal) Can. liquid*	liter	4.546
gallon (gal) Can. liquid*	cubic meter (cu m)	0.004546

"Reflections"—High strength polymer concrete sculpture at Rutgers University. Work by R. H. Karol, the civil engineering class of 1982, and the author.

Table A-1 Continued

To convert from	to	Multiply by
gallon (gal) U.S. liquid*	liter	3.785
gallon (gal) U.S. liquid*	cubic meter (cu m)	0.003785
<b>Force</b>		
kip	kilogram (kgf)	453.6
kip	newton (N)	4448.0
pound (lb)	kilogram (kgf)	0.4536
pound (lb)	newton (N)	4.448
<b>Pressure or Stress</b>		
kips/square inch (ksi)	megapascal (MPa)**	6.895
pound/square foot (psf)	kilopascal (kPa)**	0.04788
pound/square inch (psi)	kilopascal (kPa)**	6.895
pound/square inch (psi)	megapascal (MPa)**	0.006895
pound/square foot (psf)	kilogram/square meter (kgf/sq m)	4.882
<b>Mass</b>		
pound (avdp)	kilogram (kg)	0.4536
ton (short, 2000 lb)	kilogram (kg)	907.2
ton (short, 2000 lb)	tonne (t)	0.9072
grain	kilogram (kg)	0.00006480
tonne (t)	kilogram (kg)	1000
<b>Mass (weight) per Length</b>		
kip/linear foot (klf)	kilogram/meter (kg/m)	0.001488
pound/linear foot (plf)	kilogram/meter (kg/m)	1.488
pound/linear foot (plf)	newton/meter (N/m)	14.593
<b>Mass per volume (density)</b>		
pound/cubic foot (pcf)	kilogram/cubic meter (kg/cu m)	16.02
pound/cubic yard (pcy)	kilogram/cubic meter (kg/cu m)	0.5933
<b>Bending Moment or Torque</b>		
inch-pound (in.-lb)	newton-meter	0.1130
foot-pound (ft-lb)	newton-meter	1.356
foot-kip (ft-k)	newton-meter	1356
<b>Temperature</b>		
degree Fahrenheit (deg F)	degree Celsius (C)	$t_C = (t_F - 32)/1.8$
degree Fahrenheit (deg F)	degree Kelvin (K)	$t_K = (t_F + 459.7)/1.8$
<b>Energy</b>		
British thermal unit (Btu)	joule (j)	1056
kilowatt-hour (kwh)	joule (j)	3,600,000
<b>Power</b>		
horsepower (hp) (550 ft lb/sec)	watt (W)	745.7
<b>Velocity</b>		
mile/hour (mph)	kilometer/hour	1.609
mile/hour (mph)	meter/second (m/s)	.04470
<b>Other</b>		
Section modulus (in. <sup>3</sup> )	mm <sup>3</sup>	16.387
Moment of inertia (in. <sup>4</sup> )	mm <sup>4</sup>	416.231
Coefficient of heat transfer (Btu/ft <sup>2</sup> /h/°F)	W/m <sup>2</sup> /°C	5.678
Modulus of elasticity (psi)	MPa	0.006895
Thermal conductivity (Btu-in./ft <sup>2</sup> /h/°F)	Wm/m <sup>2</sup> /°C	0.1442
Thermal expansion (in./in./°F)	mm/mm/°C	1.800
Area/length (in. <sup>2</sup> /ft)	mm <sup>2</sup> /m	2116.80

\*One U.S. gallon equals 0.8321 Canadian gallon.

\*\*A pascal equals one newton/square meter.

**Table A-2** Recommended Minimum Floor Live Loads\*

Uniformly Distributed Loads		Uniformly Distributed Loads	
Occupancy or Use	Live Load (psf)	Occupancy or Use	Live Load (psf)
Apartments ( <i>see Residential</i> )	150	Hotels ( <i>see Residential</i> )	
Armories and drill rooms		Libraries:	
Assembly halls and other places of assembly:		Reading rooms	60
Fixed seats	60	Stack rooms (books & shelving at 65 pcf) but not less than.	150
Movable seats	100	Corridors, above first floor	80
Platforms (assembly)	100	Manufacturing:	
Balcony (exterior)	100	Light	125
On one- and two-family residences only and not exceeding 100 sq ft	60	Heavy	250
Bowling alleys, poolrooms, and similar recreational areas	75	Marquees and canopies	75
Corridors:		Office buildings:	
First floor	100	Offices	50
Other floors, same as occupancy served except as indicated		Lobbies	100
Dance halls and ballrooms	100	File and computer rooms require heavier loads based upon anticipated occupancy	
Dining rooms and restaurants	100	Penal institutions:	
Dwellings ( <i>see Residential</i> )		Cell blocks	40
Fire escapes	100	Corridors	100
On multi- or single-family residential buildings only	40	Residential:	
Garages (passenger cars only)	50	Dwellings (one- and two-family)	
For trucks and buses use AASHTO lane loads (1)		Uninhabitable attics without storage	10
Grandstands ( <i>see Stadium and arena bleachers</i> )		Uninhabitable attics with storage	20
Gymnasiums, main floors and balconies	100	Habitable attics and sleeping areas	30
Hospitals:		All other areas	40
Operating rooms, laboratories	60	Hotels and multifamily houses:	
Private rooms	40	Private rooms and corridors serving them	40
Wards	40	Public rooms and corridors serving them	100
Corridors, above first floor	80		

Table A-2 Continued

Uniformly Distributed Loads		Concentrated Loads	
Occupancy or Use	Live Load (psf)	Location	Load (lb)
Schools:			
Classrooms	40	Elevator machine room grating (on area of 4 sq in)	300
Corridors above first floor	80	Finish light floor plate construction (on area of 1 sq in)	200
Sidewalks, vehicular driveways, and yards, subject to trucking (2)		Garages	(4)
Stadiums and arena bleachers (3)	250	Office floors	2000
Stairs and exitways	100	Scuttles, skylight ribs, and accessible ceilings	200
Storage warehouse:	100	Sidewalks	8000
Light	125	Stair treads (on area of 4 sq in at center of tread)	300
Heavy	250		
Stores:			
Retail:			
First floor	100	(1) American Association of State Highway and Transportation Officials.	
Upper floors	75	(2) AASHTO lane loads should also be considered where appropriate.	
Wholesale, all floors	125	(3) For detailed recommendations, see Assembly Seating, Tents and Air Supported Structures, ANSI/NFPA 102-1978 [Z20.3].	
Walkways and elevated platforms (other than exitways)	60	(4) Floors in garages or portions of buildings used for storage of motor vehicles shall be designed for the uniformly distributed live loads shown or the following concentrated loads: (1) for passenger cars accommodating not more than nine passengers, 2000 pounds acting on an area of 20 in. <sup>2</sup> (2) mechanical parking structures without slab or deck, passenger cars only, 1500 pounds per wheel; (3) for trucks or buses, maximum axle load on an area of 20 in. <sup>2</sup>	

\*Source: American National Standard ANSI A58.1-1982.

Local building codes take precedence.

**Table A-3** Dead Weights of Floors, Ceilings, Roofs, and Walls

<b>Floorings</b>	<b>Weight (psf)</b>		
Normal weight concrete topping, per inch of thickness			12
Sand-lightweight (120 pcf) concrete topping, per inch			10
Lightweight (90–100 pcf) concrete topping, per inch			8
$\frac{7}{8}$ in. hardwood floor on sleepers clipped to concrete without fill			5
$\frac{1}{2}$ in. terrazzo floor finish directly on slab			19
$\frac{1}{2}$ in. terrazzo floor finish on 1 in. mortar bed			30
1 in. terrazzo finish on 2 in. concrete bed			38
$\frac{3}{4}$ in. ceramic or quarry tile on $\frac{1}{2}$ in. mortar bed			16
$\frac{3}{4}$ in. ceramic or quarry tile on 1 in. mortar bed			22
$\frac{1}{4}$ in. linoleum or asphalt tile directly on concrete			1
$\frac{1}{4}$ in. linoleum or asphalt tile on 1 in. mortar bed			12
$\frac{3}{4}$ in. mastic floor			9
Hardwood flooring, $\frac{7}{8}$ in. thick			4
Subflooring (soft wood), $\frac{3}{4}$ in. thick			2 $\frac{1}{2}$
Asphaltic concrete, 1 $\frac{1}{2}$ in. thick			18
<hr/>			
<b>Ceilings</b>			
$\frac{1}{2}$ in. gypsum board			2
$\frac{5}{8}$ in. gypsum board			2 $\frac{1}{2}$
$\frac{3}{4}$ in. plaster directly on concrete			5
$\frac{3}{4}$ in. plaster on metal lath furring			8
Suspended ceilings			2
Acoustical tile			1
Acoustical tile on wood furring strips			3
<hr/>			
<b>Roofs</b>			
Ballasted inverted membrane			16
Five-ply felt and gravel (or slag)			6 $\frac{1}{2}$
Three-ply felt and gravel (or slag)			5 $\frac{1}{2}$
Five-ply felt composition roof, no gravel			4
Three-ply felt composition roof, no gravel			3
Asphalt strip shingles			3
Rigid insulation, per inch			$\frac{1}{2}$
Gypsum, per inch of thickness			4
Insulating concrete, per inch			3
<hr/>			
<b>Walls</b>	Un-plastered	One side plastered	Both sides plastered
4 in. brick wall	40	45	50
8 in. brick wall	80	85	90
12 in. brick wall	120	125	130
4 in. hollow normal weight concrete block	28	33	38
6 in. hollow normal weight concrete block	36	41	46
8 in. hollow normal weight concrete block	51	56	61
12 in. hollow normal weight concrete block	59	64	69



Table A-3 *Continued*

Walls	Un-plastered	One side plastered	Both sides plastered
4 in. hollow lightweight block or tile	19	24	29
6 in. hollow lightweight block or tile	22	27	32
8 in. hollow lightweight block or tile	33	38	43
12 in. hollow lightweight block or tile	44	49	54
4 in. brick 4 in. hollow normal weight block backing	68	73	78
4 in. brick 8 in. hollow normal weight block backing	91	96	101
4 in. brick 12 in. hollow normal weight block backing	119	124	129
4 in. brick 4 in. hollow lightweight block or tile backing	59	64	69
4 in. brick 8 in. hollow lightweight block or tile backing	73	78	83
4 in. brick 12 in. hollow lightweight block or tile backing	84	89	94
4 in. brick, steel or wood studs, $\frac{5}{8}$ in. gypsum board	43		
Windows, glass, frame and sash	8		
4 in. stone	55		
Steel or wood studs, lath, $\frac{3}{4}$ in. plaster	18		
Steel or wood studs, $\frac{5}{8}$ in. gypsum board each side	6		
Steel or wood studs, 2 layers $\frac{1}{2}$ in. gypsum board each side	9		

**Table A-4** Area of Bars in a 1-Foot-wide Slab Strip

Spacing, in.	Cross Section Area of Bar, $A_s$ (or $A'_s$ ), in. <sup>2</sup>														Spacing, in.
	#3	#4	#5	#6	#7	#8	#9	#10	#11	#14	#18				
4	0.33	0.60	0.93	1.32	1.80	2.37	3.00	3.81	4.68					4	
4½	0.29	0.53	0.83	1.17	1.60	2.11	2.67	3.39	4.16		6.00			4½	
5	0.26	0.48	0.74	1.06	1.44	1.90	2.40	3.05	3.74		5.40		9.60	5	
5½	0.24	0.44	0.68	0.96	1.31	1.72	2.18	2.77	3.40		4.91		8.73	5½	
6	0.22	0.40	0.62	0.88	1.20	1.58	2.00	2.54	3.12		4.50		8.00	6	
6½	0.20	0.37	0.57	0.81	1.11	1.46	1.85	2.34	2.88		4.15		7.38	6½	
7	0.19	0.34	0.53	0.75	1.03	1.35	1.71	2.18	2.67		3.86		6.86	7	
7½	0.18	0.32	0.50	0.70	0.96	1.26	1.60	2.03	2.50		3.60		6.40	7½	
8	0.17	0.30	0.47	0.66	0.90	1.19	1.50	1.91	2.34		3.38		6.00	8	
8½	0.16	0.28	0.44	0.62	0.85	1.12	1.41	1.79	2.20		3.18		5.65	8½	
9	0.15	0.27	0.41	0.59	0.80	1.05	1.33	1.69	2.08		3.00		5.33	9	
9½	0.14	0.25	0.39	0.56	0.76	1.00	1.26	1.60	1.97		2.84		5.05	9½	
10	0.13	0.24	0.37	0.53	0.72	0.95	1.20	1.52	1.87		2.70		4.80	10	
10½	0.13	0.23	0.35	0.50	0.69	0.90	1.14	1.45	1.78		2.57		4.57	10½	
11	0.12	0.22	0.34	0.48	0.65	0.86	1.09	1.39	1.70		2.45		4.36	11	
11½	0.11	0.21	0.32	0.46	0.63	0.82	1.04	1.33	1.63		2.35		4.17	11½	
12	0.11	0.20	0.31	0.44	0.60	0.79	1.00	1.27	1.56		2.25		4.00	12	
13	0.10	0.18	0.29	0.41	0.55	0.73	0.92	1.17	1.44		2.08		3.69	13	
14	0.09	0.17	0.27	0.38	0.51	0.68	0.86	1.09	1.34		1.93		3.43	14	
15	0.09	0.16	0.25	0.35	0.48	0.63	0.80	1.02	1.25		1.80		3.20	15	
16	0.08	0.15	0.23	0.33	0.45	0.59	0.75	0.95	1.17		1.69		3.00	16	
17	0.08	0.14	0.22	0.31	0.42	0.56	0.71	0.90	1.10		1.59		2.82	17	
18	0.07	0.13	0.21	0.29	0.40	0.53	0.67	0.85	1.04		1.50		2.67	18	

**Table A-5** Properties and Design Strengths of Prestressing Strand and Wire

<b>Seven-Wire Strand, <math>f_{pu} = 270</math> ksi</b>						
Nominal Diameter, in.	3/8	7/16	1/2	9/16	0.600	
Area, sq in.	0.085	0.115	0.153	0.192	0.215	
Weight, plf	0.29	0.40	0.53	0.65	0.74	
0.7 $f_{pu} A_{ps}$ , kips	16.1	21.7	28.9	36.3	40.7	
0.75 $f_{pu} A_{ps}$ , kips	17.2	23.3	31.0	38.9	43.5	
0.8 $f_{pu} A_{ps}$ , kips	18.4	24.8	33.0	41.4	46.5	
$f_{pu} A_{ps}$ , kips	23.0	31.0	41.3	51.8	58.1	

<b>Seven-Wire Strand, <math>f_{pu} = 250</math> ksi</b>						
Nominal Diameter, in.	1/4	5/16	3/8	7/16	1/2	0.600
Area, sq in.	0.036	0.058	0.080	0.108	0.144	0.215
Weight, plf	0.12	0.20	0.27	0.37	0.49	0.74
0.7 $f_{pu} A_{ps}$ , kips	6.3	10.2	14.0	18.9	25.2	37.6
0.8 $f_{pu} A_{ps}$ , kips	7.2	11.6	16.0	21.6	28.8	43.0
$f_{pu} A_{ps}$ , kips	9.0	14.5	20.0	27.0	36.0	53.8

<b>Three- and Four-Wire Strand, <math>f_{pu} = 250</math> ksi</b>				
Nominal Diameter, in.	1/4	5/16	3/8	7/16
No. of wires	3	3	3	4
Area, sq in.	0.036	0.058	0.075	0.106
Weight, plf	0.13	0.20	0.26	0.36
0.7 $f_{pu} A_{ps}$ , kips	6.3	10.2	13.2	18.6
0.8 $f_{pu} A_{ps}$ , kips	7.2	11.6	15.0	21.2
$f_{pu} A_{ps}$ , kips	9.0	14.5	18.8	26.5

<b>Prestressing Wire</b>										
Diameter, in.	0.105	0.120	0.135	0.148	0.162	0.177	0.192	0.196	0.250	0.276
Area, sq in.	0.0087	0.0114	0.0143	0.0173	0.0206	0.0246	0.0289	0.0302	0.0491	0.0598
Weight, plf	0.030	0.039	0.049	0.059	0.070	0.083	0.098	0.10	0.17	0.20
Ult. strength, $f_{pu}$ , ksi	279	273	268	263	259	255	250	250	240	235
0.7 $f_{pu} A_{ps}$ , kips	1.70	2.18	2.68	3.18	3.73	4.39	5.05	5.28	8.25	9.84
0.8 $f_{pu} A_{ps}$ , kips	1.94	2.49	3.06	3.64	4.26	5.02	5.78	6.04	9.42	11.24
$f_{pu} A_{ps}$ , kips	2.43	3.11	3.83	4.55	5.33	6.27	7.22	7.55	11.78	14.05

**Table A-6** Properties and Design Strengths of Prestressing Bars

<b>Smooth Prestressing Bars, <math>f_{pu} = 145</math> ksi*</b>						
<b>Nominal Diameter, in.</b>	<b>3/4</b>	<b>7/8</b>	<b>1</b>	<b>1 1/8</b>	<b>1 1/4</b>	<b>1 3/8</b>
Area, sq in.	0.442	0.601	0.785	0.994	1.227	1.485
Weight, plf	1.50	2.04	2.67	3.38	4.17	5.05
0.7 $f_{pu} A_{ps}$ , kips	44.9	61.0	79.7	100.9	124.5	150.7
0.8 $f_{pu} A_{ps}$ , kips	51.3	69.7	91.0	115.3	142.3	172.2
$f_{pu} A_{ps}$ , kips	64.1	87.1	113.8	144.1	177.9	215.3
<b>Smooth Prestressing Bars, <math>f_{pu} = 160</math> ksi*</b>						
<b>Nominal Diameter, in.</b>	<b>3/4</b>	<b>7/8</b>	<b>1</b>	<b>1 1/8</b>	<b>1 1/4</b>	<b>1 3/8</b>
Area, sq in.	0.442	0.601	0.785	0.994	1.227	1.485
Weight, plf	1.50	2.04	2.67	3.38	4.17	5.05
0.7 $f_{pu} A_{ps}$ , kips	49.5	67.3	87.9	111.3	137.4	166.3
0.8 $f_{pu} A_{ps}$ , kips	56.6	77.0	100.5	127.2	157.0	190.1
$f_{pu} A_{ps}$ , kips	70.7	96.2	125.6	159.0	196.3	237.6
<b>Deformed Prestressing Bars</b>						
<b>Nominal Diameter, in.</b>	<b>5/8</b>	<b>1</b>	<b>1</b>	<b>1 1/4</b>	<b>1 1/4</b>	<b>1 3/8</b>
Area, sq. in.	0.28	0.85	0.85	1.25	1.25	1.58
Weight, plf	0.98	3.01	3.01	4.39	4.39	5.56
Ult. strength, $f_{pu}$ , ksi	157	150	160*	150	160*	150
0.7 $f_{pu} A_{ps}$ , kips	30.5	89.3	95.2	131.3	140.0	165.9
0.8 $f_{pu} A_{ps}$ , kips	34.8	102.0	108.8	150.0	160.0	189.6
$f_{pu} A_{ps}$ , kips	43.5	127.5	136.0	187.5	200.0	237.0
Stress-strain characteristics (all prestressing bars):						
For design purposes, following assumptions are satisfactory:						
$E_s = 29,000$ ksi						
$f_y = 0.95 f_{pu}$						
*Verify availability before specifying						

**Table A-7** Moments in Beams with Fixed Ends

Loading	Moment at A	Moment at center	Moment at B
	$-\frac{Pl}{8}$	$+\frac{Pl}{8}$	$-\frac{Pl}{8}$
	$-Pl/a(1-a)^2$		$-Pla^2(1-a)$
	$-\frac{2Pl}{9}$	$+\frac{Pl}{9}$	$-\frac{2Pl}{9}$
	$-\frac{5Pl}{16}$	$+\frac{3Pl}{16}$	$-\frac{5Pl}{16}$
	$-\frac{Wl}{12}$	$+\frac{Wl}{24}$	$-\frac{Wl}{12}$
	$-\frac{Wl(1+2a-2a^2)}{12}$	$+\frac{Wl(1+2a+4a^2)}{24}$	$-\frac{Wl(1+2a-2a^2)}{12}$
	$-\frac{Wl(3a-2a^2)}{12}$	$+\frac{Wl a^2}{6}$	$-\frac{Wl(3a-2a^2)}{12}$
	$-\frac{Wl a(6-8a+3a^2)}{12}$		$-\frac{Wl a^2(4-3a)}{12}$
	$-\frac{5Wl}{48}$	$+\frac{3Wl}{48}$	$-\frac{5Wl}{48}$
	$-\frac{Wl}{10}$		$-\frac{Wl}{15}$
W = Total load on beam			

Table A-8 Camber (Deflection) and Rotation Coefficients for Prestress Force and Loads\*

Prestress Pattern	Equivalent Moment or Load	Equivalent Loading	Camber		End Rotation	
			+	↑	↙+	↘
(1)	$M = Pe$		$+$	$+$	$+$	$+$
(2)	$M = Pe$		$+$	$+$	$+$	$+$
(3)	$M = Pe$		$+$	$+$	$+$	$+$
(4)	$M = \frac{4Pe'}{l}$ $N = \frac{4Pe'}{l}$		$+$	$+$	$+$	$+$
(5)	$N = \frac{Pe'}{b/l}$		$+$	$+$	$+$	$+$

Table A-8 Continued

<p>(6)</p>	$w = \frac{8 Pe'}{l^2}$		$+\frac{5w^4}{384 EI}$	$+\frac{w^3}{24 EI}$	$-\frac{w^3}{24 EI}$
<p>(7)</p>	$w = \frac{8 Pe'}{l^2}$		$+\frac{5w^4}{768 EI}$	$+\frac{9w^3}{384 EI}$	$-\frac{7w^3}{384 EI}$
<p>(8)</p>	$w = \frac{8 Pe'}{l^2}$		$+\frac{5w^4}{768 EI}$	$+\frac{7w^3}{384 EI}$	$-\frac{9w^3}{384 EI}$
<p>(9)</p>	$w = \frac{4 Pe'}{(0.5 - b) l^2}$ $w_1 = \frac{w}{b} (0.5 - b)$		$\left[ \frac{5}{8} - \frac{b}{2} (3 - 2b^2) \right] \frac{w^4}{48 EI}$	$+\frac{(1 - b) (1 - 2b) w^3}{24 EI}$	$-\frac{(1 - b) (1 - 2b) w^3}{24 EI}$
<p>(10)</p>	$w = \frac{4 Pe'}{(0.5 - b) l^2}$ $w_1 = \frac{w}{b} (0.5 - b)$		$\left[ \frac{5}{16} - \frac{b}{4} (3 - 2b^2) \right] \frac{w^4}{48 EI}$	$\left[ \frac{9}{8} - b (2 - b)^2 \right] \frac{w^3}{48 EI}$	$\left[ \frac{7}{8} + b (2 - b^2) \right] \frac{w^3}{48 EI}$
<p>(11)</p>	$w = \frac{4 Pe'}{(0.5 - b) l^2}$ $w_1 = \frac{w}{b} (0.5 - b)$		$\left[ \frac{5}{16} - \frac{b}{4} (3 - 2b^2) \right] \frac{w^4}{48 EI}$	$\left[ \frac{7}{8} - b (2 - b)^2 \right] \frac{w^3}{48 EI}$	$\left[ \frac{9}{8} + b (2 - b)^2 \right] \frac{w^3}{48 EI}$

\* The tabulated values apply to the effects of prestressing. By adjusting the directional notation, they may also be used for the effects of loads.  
 For patterns 4-11, superimpose on 1, 2, or 3 for other C.G. locations.

**Table A-9** Presumptive Bearing Capacity (tons/ft<sup>2</sup>)

Type of Soil	Bearing Capacity
Massive crystalline bedrock, such as granite, diorite, gneiss, and trap rock	100
Foliated rocks, such as schist or slate	40
Sedimentary rocks, such as hard shales, sandstones, limestones, and siltstones	15
Gravel and gravel-sand mixtures (GW and GP soils)	
Densely compacted	5
Medium compacted	4
Loose, not compacted	3
Sands and gravelly sands, well graded (SW soil)	
Densely compacted	3 $\frac{3}{4}$
Medium compacted	3
Loose, not compacted	2 $\frac{1}{4}$
Sands and gravelly sands, poorly graded (SP soil)	
Densely compacted	3
Medium compacted	2 $\frac{1}{2}$
Loose, not compacted	1 $\frac{3}{4}$
Silty gravels and gravel-sand-silt mixtures (GM soil)	
Densely compacted	2 $\frac{1}{2}$
Medium compacted	2
Loose, not compacted	1 $\frac{1}{2}$
Silty sand and silt-sand mixtures (SM soil)	2
Clayey gravels, gravel-sand-clay mixtures, clayey sands, sand-clay mixtures (GC and SC soils)	2
Inorganic silts, and fine sands; silty or clayey fine sands and clayey silts, with slight plasticity; inorganic clays of low to medium plasticity; gravelly clays; sandy clays; silty clays; lean clays (ML and CL soils)	1
Inorganic clays of high plasticity, fat clays; micaceous or diatomaceous fine sand or silty soils, elastic silts (CH and MH soils)	1



Table A-10 Standard Wire Reinforcement

Smooth	W&D Size	Deformed	U.S. Customary			Area (in. <sup>2</sup> /ft of width for various spacings)						
			Nominal diameter (in.)	Nominal area (in. <sup>2</sup> )	Nominal weight (lb/ft)	Center-to-center spacing (in.)						
						2	3	4	6	8	10	12
W31		D31	0.628	0.310	1.054	1.86	1.24	0.93	0.62	0.465	0.372	0.31
W30		D30	0.618	0.300	1.020	1.80	1.20	0.90	0.60	0.45	0.366	0.30
W28		D28	0.597	0.280	0.952	1.68	1.12	0.84	0.56	0.42	0.336	0.28
W26		D26	0.575	0.260	0.934	1.56	1.04	0.78	0.52	0.39	0.312	0.26
W24		D24	0.553	0.240	0.816	1.44	0.96	0.72	0.48	0.36	0.288	0.24
W22		D22	0.529	0.220	0.748	1.32	0.88	0.66	0.44	0.33	0.264	0.22
W20		D20	0.504	0.200	0.680	1.20	0.80	0.60	0.40	0.30	0.24	0.20
W18		D18	0.478	0.180	0.612	1.08	0.72	0.54	0.36	0.27	0.216	0.18
W16		D16	0.451	0.160	0.544	0.96	0.64	0.48	0.32	0.24	0.192	0.16
W14		D14	0.422	0.140	0.476	0.84	0.56	0.42	0.28	0.21	0.168	0.14
W12		D12	0.390	0.120	0.408	0.72	0.48	0.36	0.24	0.18	0.144	0.12
W11		D11	0.374	0.110	0.374	0.66	0.44	0.33	0.22	0.165	0.132	0.11
W10.5			0.366	0.105	0.357	0.63	0.42	0.315	0.21	0.157	0.126	0.105
W10		D10	0.356	0.100	0.340	0.60	0.40	0.30	0.20	0.15	0.12	0.10
W9.5			0.348	0.095	0.323	0.57	0.38	0.285	0.19	0.142	0.114	0.095
W9		D9	0.338	0.090	0.306	0.54	0.36	0.27	0.18	0.135	0.108	0.09
W8.5			0.329	0.085	0.289	0.51	0.34	0.255	0.17	0.127	0.102	0.085
W8		D8	0.319	0.080	0.272	0.48	0.32	0.24	0.16	0.12	0.096	0.08
W7.5			0.309	0.075	0.255	0.45	0.30	0.225	0.15	0.112	0.09	0.075
W7		D7	0.298	0.070	0.238	0.42	0.28	0.21	0.14	0.105	0.084	0.07
W6.5			0.288	0.065	0.221	0.39	0.26	0.195	0.13	0.097	0.078	0.065
W6		D6	0.276	0.060	0.204	0.36	0.24	0.18	0.12	0.09	0.072	0.06
W5.5			0.264	0.055	0.187	0.33	0.22	0.165	0.11	0.082	0.066	0.055
W5		D5	0.252	0.050	0.170	0.30	0.20	0.15	0.10	0.075	0.06	0.05
W4.5			0.240	0.045	0.153	0.27	0.18	0.135	0.09	0.067	0.054	0.045
W4		D4	0.225	0.040	0.136	0.24	0.16	0.12	0.08	0.06	0.048	0.04
W3.5			0.211	0.035	0.119	0.21	0.14	0.105	0.07	0.052	0.042	0.035
W3			0.195	0.030	0.102	0.18	0.12	0.09	0.06	0.045	0.036	0.03
W2.9			0.192	0.029	0.098	0.174	0.116	0.087	0.058	0.043	0.035	0.029
W2.5			0.178	0.025	0.085	0.15	0.10	0.075	0.05	0.037	0.03	0.025
W2			0.159	0.020	0.068	0.12	0.08	0.06	0.04	0.03	0.024	0.02
W1.4			0.135	0.014	0.049	0.084	0.056	0.042	0.028	0.021	0.017	0.014

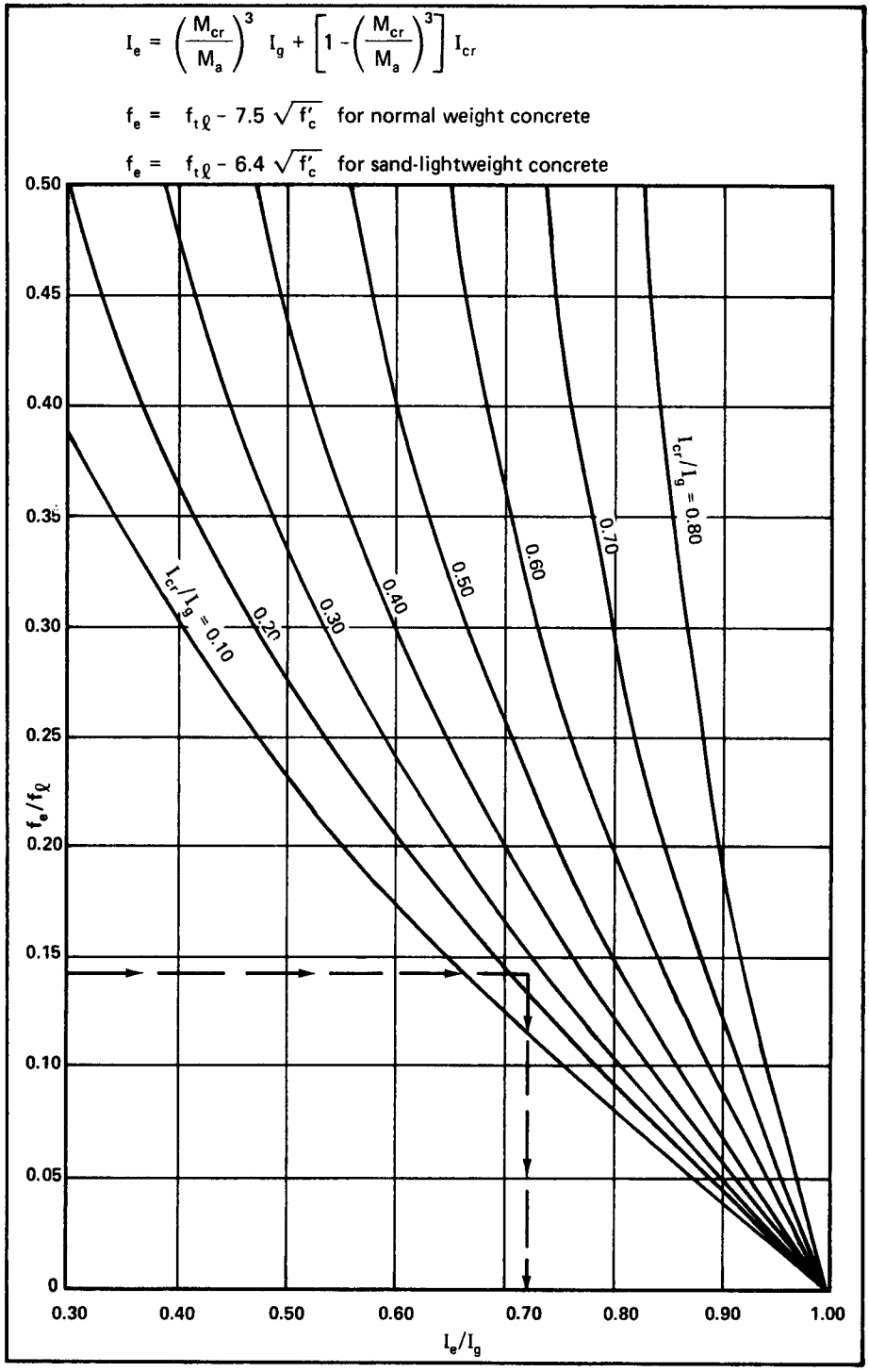


Figure A-1 Effective moment of inertia


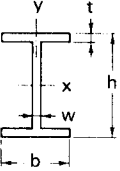
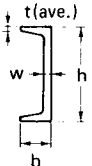

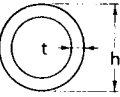
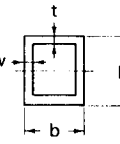
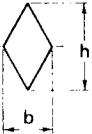
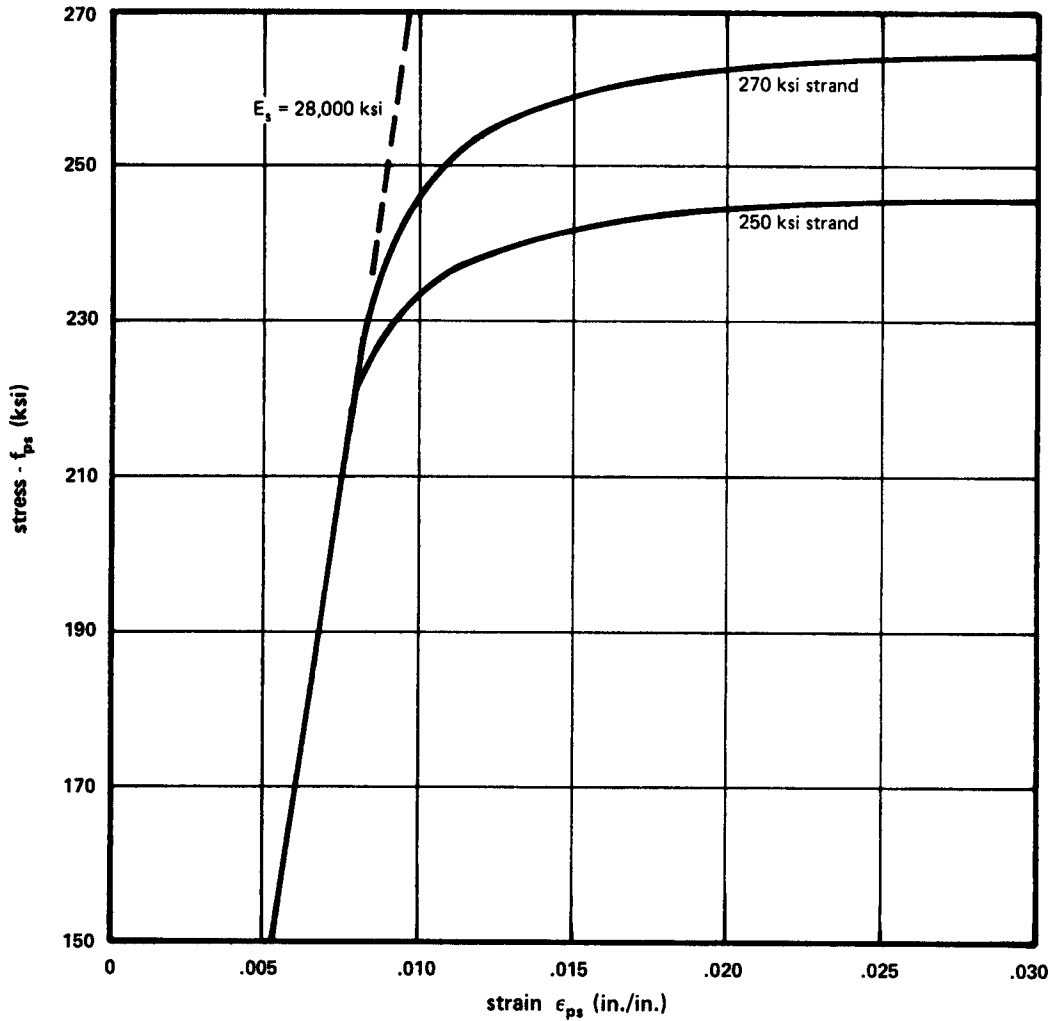
Section	Geometric section modulus, $Z_s$ , in. <sup>3</sup>	Shape factor
	$\frac{bh^2}{4}$	1.5
	x-x axis: $bt(h-t) + \frac{w}{4}(h-2t)^2$	1.12 (approx)
	y-y axis: $\frac{b^2t}{2} + \frac{(h-2t)w^2}{4}$	1.55 (approx)
	$bt(h-t) + \frac{w(h-2t)^2}{4}$	1.12 (approx)
	$\frac{h^3}{6}$	1.70
	$\frac{h^3}{6} \left[ 1 - \left( 1 - \frac{2t}{h} \right)^3 \right]$ $th^2$ for $t \ll h$	$\frac{16}{3\pi} \left[ \frac{1 - \left( 1 - \frac{2t}{h} \right)^3}{1 - \left( 1 - \frac{2t}{h} \right)^4} \right]$ 1.27 for $t \ll h$
	$\frac{bh^2}{4} \left[ 1 - \left( 1 - \frac{2w}{b} \right) \left( 1 - \frac{2t}{h} \right)^2 \right]$	1.12 (approx) for thin walls
	$\frac{bh^2}{12}$	2

Figure A-2 Geometric section moduli and shape factors



These curves can be approximated by the following equations:

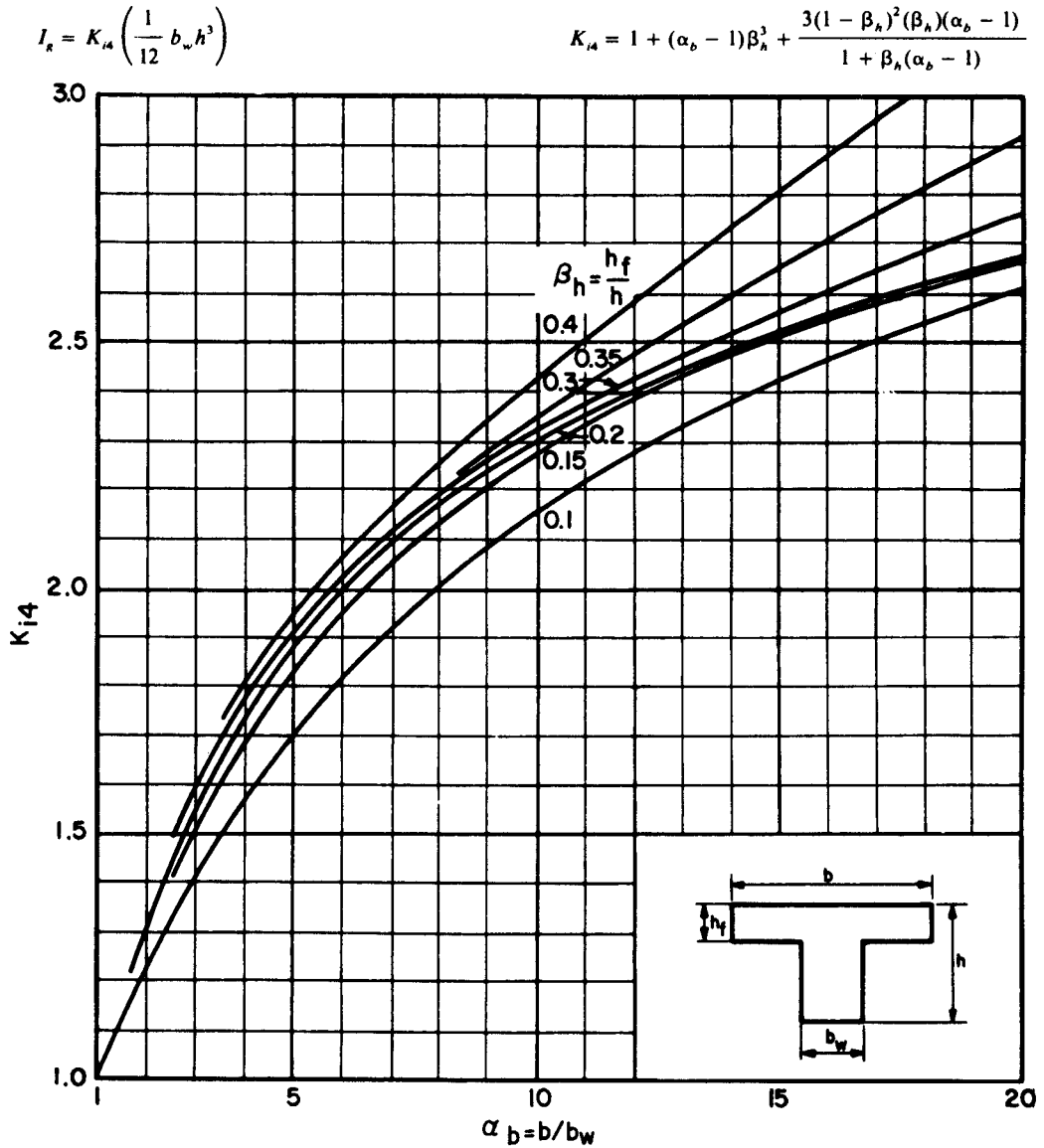
$$\epsilon_{ps} \leq 0.008: \quad f_{ps} = 28,000 \epsilon_{ps} \text{ (ksi)}$$

$\epsilon_{ps} > 0.008$ :

$$250 \text{ ksi strand: } f_{ps} = 248 - \frac{0.058}{\epsilon_{ps} - 0.006} < 0.98 f_{pu} \text{ (ksi)}$$

$$270 \text{ ksi strand: } f_{ps} = 268 - \frac{0.075}{\epsilon_{ps} - 0.0065} < 0.98 f_{pu} \text{ (ksi)}$$

**Figure A-3** Typical stress-strain curve, 7-wire stress-relieved and low-relaxation prestressing strand



Example: For the T-beam shown, find the moment of inertia  $I_r$ :

$$\alpha_b = b/b_w = 143/15 = 9.53$$

$$\beta_h = h_f/h = 8/36 = 0.22$$

Interpolating between the curves for  $\beta_h = 0.2$  and 0.3, read  $K_{i4} = 2.28$

$$I_r = K_{i4} \frac{b_w h^3}{12} = 2.28 \frac{15(36)^3}{12} = 133,000 \text{ in.}^4$$

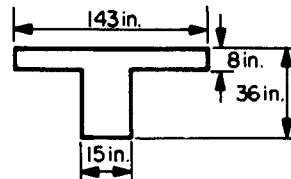
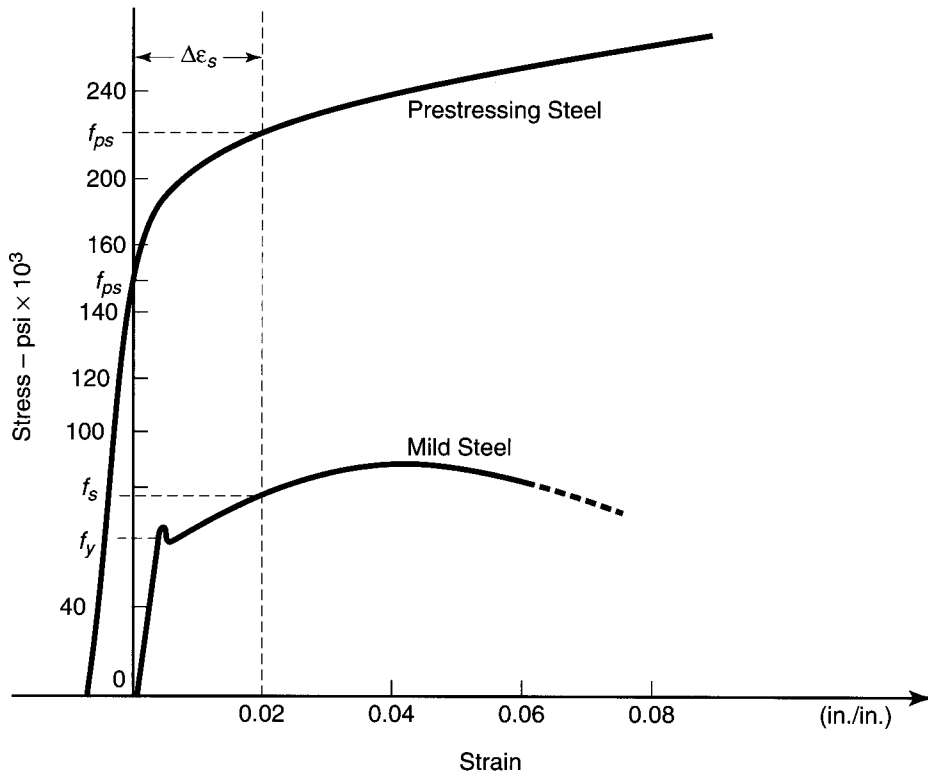


Figure A-4 Gross moment of inertia of T sections



**Figure A-5** Stress-strain diagram for prestressing steel strands in comparison with mild steel bar reinforcement

$$\rho \geq 0.45 \left( \frac{A_g}{A_c} - 1 \right) \frac{f'_c}{f_{yt}} \quad \text{and} \quad \geq 0.12 \frac{f'_c}{f_{yt}}$$

$A_g/A_c$	$f_{yt} = 40,000$ psi			$f_{yt} = 60,000$ psi		
	$f'_c = 4000$ psi	$f'_c = 6000$ psi	$f'_c = 8000$ psi	$f'_c = 4000$ psi	$f'_c = 6000$ psi	$f'_c = 8000$ psi
	$\rho_s$					
1.1	0.012	0.018	0.024	0.008	0.012	0.016
1.2	0.012	0.018	0.024	0.008	0.012	0.016
1.3	0.014	0.020	0.027	0.009	0.014	0.018
1.4	0.018	0.027	0.036	0.012	0.018	0.024
1.5	0.023	0.034	0.045	0.015	0.023	0.030
1.6	0.027	0.041	0.054	0.018	0.027	0.036
1.7	0.032	0.047	0.063	0.021	0.032	0.042
1.8	0.036	0.054	0.072	0.024	0.036	0.048
1.9	0.041	0.081	0.027	0.027	0.041	0.054
2.0	0.045	0.068	0.090	0.030	0.045	0.060
2.1	0.050	0.074	0.099	0.033	0.050	0.066
2.2	0.054	0.081	0.108	0.036	0.054	0.072
2.3	0.058	0.088	0.117	0.039	0.058	0.078
2.4	0.063	0.094	0.126	0.042	0.063	0.084
2.5	0.067	0.101	0.135	0.045	0.067	0.090

**Figure A.6** Volumetric ratio of spiral reinforcement  $\rho_s$  for concrete confinement (Ref. 13.36).

$$\rho_c \geq \frac{A_{sh}}{sh_c} \geq 0.3 \left( \frac{A_g}{A_{ch}} - 1 \right) \quad \text{and} \quad \geq 0.09 \frac{f'_c}{f_{yt}}$$

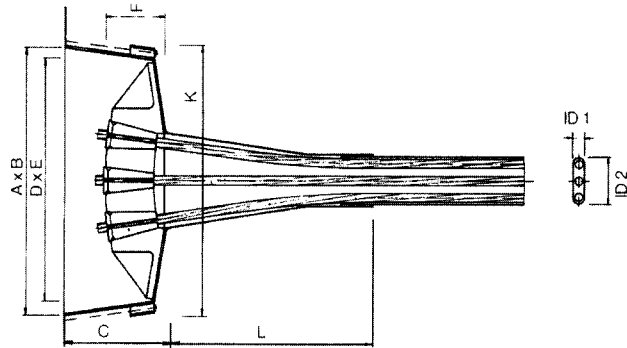
$A_g/A_{ch}$	$f_{yt} = 40,000$ psi			$f_{yt} = 60,000$ psi		
	$f'_c = 4000$ psi	$f'_c = 6000$ psi	$f'_c = 8000$ psi	$f'_c = 4000$ psi	$f'_c = 6000$ psi	$f'_c = 8000$ psi
	$\rho_s$					
1.1	0.009	0.014	0.018	0.006	0.009	0.012
1.2	0.009	0.014	0.018	0.006	0.009	0.012
1.3	0.009	0.014	0.018	0.006	0.009	0.012
1.4	0.012	0.018	0.024	0.008	0.012	0.016
1.5	0.015	0.023	0.030	0.010	0.015	0.020
1.6	0.018	0.027	0.036	0.012	0.018	0.024
1.7	0.021	0.032	0.042	0.014	0.021	0.028
1.8	0.024	0.036	0.048	0.016	0.024	0.032
1.9	0.027	0.041	0.054	0.018	0.027	0.036
2.0	0.030	0.045	0.060	0.020	0.030	0.040
2.1	0.033	0.050	0.066	0.022	0.033	0.044
2.2	0.036	0.054	0.072	0.024	0.036	0.048
2.3	0.039	0.058	0.078	0.026	0.039	0.052
2.4	0.042	0.063	0.084	0.028	0.042	0.056
2.5	0.045	0.067	0.090	0.030	0.045	0.060

**Figure A.7** Area percentage of rectilinear hoop reinforcement  $\rho_c$  for concrete confinement (Ref. 13.36).

$\rho$	$M_{pr} = K_{pr} F$ ft-kips			$F = bd^2/12000$		$\rho = A_s/bd$	
	$f_y = 40,000$ psi					$f_y = 60,000$ psi	
	$f'_c = 4000$ psi	$f'_c = 6000$ psi	$f'_c = 8000$ psi	$f'_c = 4000$ psi	$f'_c = 6000$ psi	$f'_c = 8000$ psi	
	$K_{pr}$ (psi)						
0.003	147	148	148	218	220	221	
0.004	194	196	197	287	291	293	
0.005	241	244	245	354	361	365	
0.006	287	291	293	420	430	435	
0.007	332	338	341	484	498	505	
0.008	376	384	388	547	565	574	
0.009	420	430	435	608	630	641	
0.010	463	475	482	667	695	709	
0.011	506	520	528	725	758	775	
0.012	547	565	574	781	821	840	
0.013	588	609	619	835	882	905	
0.014	628	652	664	888	942	969	
0.015	667	695	709	939	1001	1032	
0.016	706	737	753	988	1059	1094	
0.017	744	779	797	1036	1116	1155	
0.018	781	821	840	1082	1171	1216	
0.019	817	862	884	1126	1226	1276	
0.020	853	902	926	1169	1279	1335	
0.021	888	942	969	1210	1332	1393	
0.022	922	981	1011		1383	1450	
0.023	956	1020	1053		1433	1506	
0.024	988	1059	1094		1482	1562	
0.025	1020	1097	1135		1530	1616	
0.026	1051	1134	1176		1577	1670	
0.027	1082	1171	1216		1623	1723	
0.028	1112	1208	1256		1668	1776	
0.029	1141	1244	1295			1827	
0.030	1169	1279	1335			1878	
0.031	1197	1314	1373			1928	
0.032	1224	1349	1412			1976	
0.033	1250	1383	1450				
0.034	1275	1417	1487				
0.035	1300	1450	1525				

Figure A.8 Probable seismic moment strengths for beams (Ref. 13.36).





Flat Anchorage FA

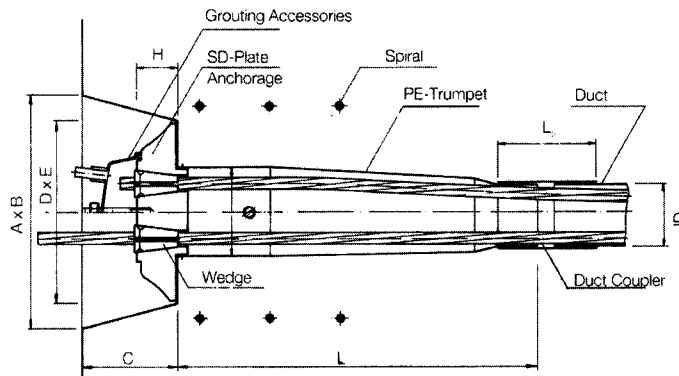


Plate Anchorage SD

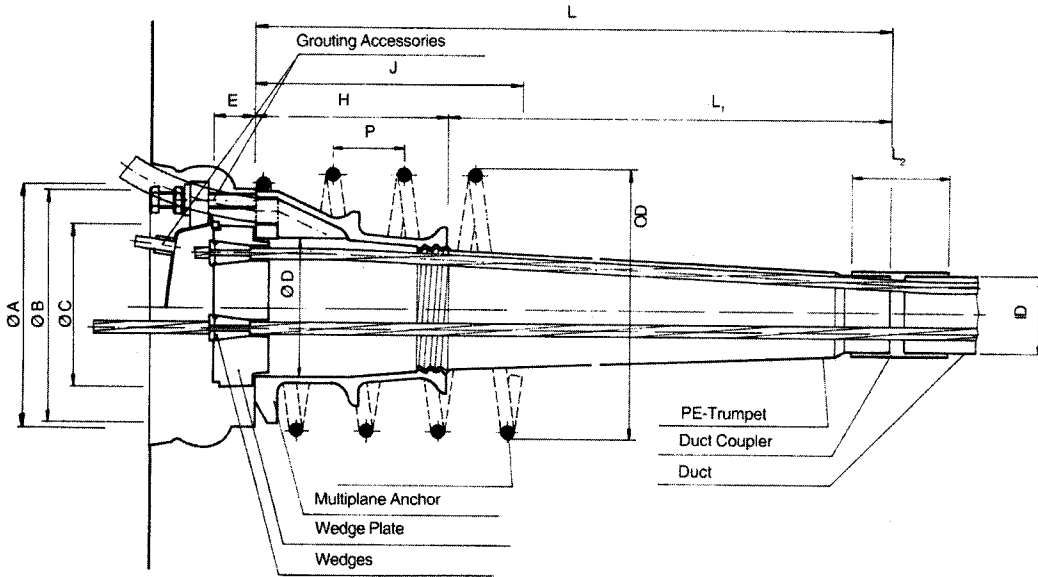
**Flat Anchorage FA**

**Combination Plate Anchorage SD**

Tendon Size	3-0.6" or 4-0.5"	4-0.6" or 5-0.5"	Tendon Size	3-0.6" or 4-0.5"	4-0.6" or 5-0.5"	4-0.6"	5-0.6" or 7-0.5"	6-0.6" or 8-0.5"	7-0.6" or 9-0.5"		
<b>Flat Anchor</b>	D	10 \ 255	13 \ 330	<b>Comb. Plate</b>	D	4-15/16 \ 125	5-5/16 \ 135	5 \ 127	5-7/8 \ 150	6-1/2 \ 165	6-11/16 \ 170
	E	4 \ 100	4 \ 100		E	5-1/2 \ 140	6-5/16 \ 160	9 \ 229	7-1/16 \ 180	8-1/16 \ 205	8-1/2 \ 215
	F	2-1/4 \ 57	2-1/4 \ 57		H	1-5/8 \ 41	1-5/8 \ 41	2 \ 51	1-9/16 \ 40	1-3/4 \ 44	1-3/4 \ 44
<b>Transition</b>	K	12-1/4 \ 310	--	<b>Transition</b>	Ø	2-9/16 \ 65	2-15/16 \ 75	2-13/16 \ 72	3-3/8 \ 85	3-3/4 \ 95	3-3/4 \ 95
	L	4-1/2 \ 115	8-5/8 \ 220		L	11-3/8 \ 290	10-7/16 \ 265	11 \ 280	14 \ 355	15-15/16 \ 405	15-15/16 \ 405
<b>Pocket Former</b>	A	10-3/4 \ 275	13-3/4 \ 350	<b>Pocket Former</b>	A	6-1/2 \ 165	6-1/2 \ 165	7-1/16 \ 179	7-1/16 \ 180	7-7/8 \ 200	7-7/8 \ 200
	B	4-1/2 \ 115	4-7/8 \ 124		B	7-5/16 \ 185	7-5/16 \ 185	9-7/8 \ 251	8-1/4 \ 210	9-7/16 \ 240	9-7/16 \ 240
	C	5-1/2 \ 140	5-7/8 \ 148		C	3-15/16 \ 100	3-15/16 \ 100	5-1/8 \ 130	3-15/16 \ 100	4-5/16 \ 110	4-5/16 \ 110
<b>Duct</b>	ID1	1 \ 25	1 \ 25	<b>Duct</b>	ID	1-9/16 \ 40	1-13/16 \ 46	2 \ 51	2-1/16 \ 52	2-7/16 \ 62	2-7/16 \ 62
	ID2	3 \ 75	3 \ 75		L2	8 \ 200	8 \ 200	4 \ 100	8 \ 200	8 \ 200	8 \ 200

All dimensions are nominal and are expressed in inch \ mm. Technical data subject to change.

**Figure A-9** Dywidag flat anchorage for prestressing strands (Courtesy Dywidag Systems International).



Anchorage Size	5-0.6" or 7-0.5"	7-0.6" or 9-0.5"	9-0.6" or 12-0.5"	12-0.6" or 15-0.5"	15-0.6" or 20-0.5"	19-0.6" or 27-0.5"	27-0.6" or 37-0.5"	37-0.6" or 59-0.5"
Min. Block-out Dia. A	7 \ 179	8 \ 203	9 \ 229	10 \ 254	11 \ 279	12 \ 305	13-1/2 \ 343	16 \ 407
Transition Length	12-3/8 \ 314	13-7/16 \ 341	15-3/4 \ 400	20 \ 508	22-5/8 \ 575	25-3/16 \ 640	27-5/8 \ 702	35 \ 890
Anchor Dia. B	5-15/16 \ 150	6-11/16 \ 170	7-1/2 \ 190	8-5/8 \ 220	9-7/8 \ 250	11 \ 280	12-3/8 \ 315	14-1/8 \ 360
D	3-9/16 \ 90	3-7/8 \ 98	4-7/16 \ 113	5-1/16 \ 128	5-13/16 \ 148	6-3/8 \ 162	7-1/2 \ 190	8-1/2 \ 220
H	3-9/16 \ 90	3-15/16 \ 100	4-15/16 \ 125	7-1/16 \ 180	7-7/8 \ 200	8-5/8 \ 220	9-7/16 \ 240	12-1/2 \ 320
Wedge Plate C	5-1/8 \ 130	5-1/8 \ 130	5-1/2 \ 140	6-5/16 \ 160	7-1/16 \ 180	7-7/8 \ 200	9-7/16 \ 240	10-2/3 \ 270
E	2 \ 50	1-9/16 \ 40	1-11/16 \ 43	1-11/16 \ 43	2 \ 50	2-3/16 \ 55	2-15/16 \ 75	3-1/2 \ 90
Trumpet L1	8-7/8 \ 225	9-1/2 \ 241	10-13/16 \ 275	12-7/8 \ 327	14-3/4 \ 375	16-1/2 \ 419	18-1/8 \ 460	22-1/2 \ 600
Rebar Spiral * Size	# 4 \ 15M	# 4 \ 15M	# 4 \ 15M	# 5 \ 15M	# 5 \ 15M	# 5 \ 15M	# 6 \ 20M	# 7 \ 22M
Grade	60 KSI \ 400 MPa	60 KSI \ 400 MPa	60 KSI \ 400 MPa	60 KSI \ 400 MPa	60 KSI \ 400 MPa	60 KSI \ 400 MPa	60 KSI \ 400 MPa	60 KSI \ 400 MPa
Pitch	1-7/8 \ 50	1-7/8 \ 50	1-7/8 \ 50	2-1/4 \ 55	1-7/8 \ 50	1-7/8 \ 50	2-1/4 \ 55	2-3/8 \ 60
J	10 \ 255	10-1/2 \ 265	10-5/8 \ 270	14 \ 355	14-3/4 \ 365	15 \ 380	16-5/8 \ 420	18 \ 460
OD	7-3/4 \ 190	9 \ 230	9-1/2 \ 240	11-1/4 \ 285	12-1/2 \ 315	14-1/2 \ 365	17 \ 430	22 \ 560
Duct ID	2 \ 50	2-3/8 \ 60	3 \ 75	3-3/8 \ 85	3-3/4 \ 95	4 \ 100	4-1/2 \ 115	5-1/8 \ 130
Duct Coupler L2	8 \ 200	8 \ 200	8 \ 200	8 \ 200	8 \ 200	8 \ 200	8 \ 200	12 \ 300
Grout Requirements gal/ft \ l/m	0.12 \ 1.5	0.17 \ 2.1	0.28 \ 3.46	0.35 \ 4.39	0.44 \ 5.48	0.47 \ 5.80	0.58 \ 7.25	0.72 \ 8.90

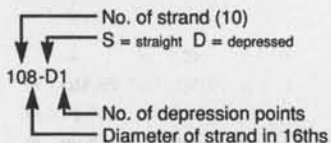
Spiral required in "local anchor" zone.  
 \ dimensions are nominal and are expressed in inch \ mm. Technical data subject to change.

**Figure A-10** Dywidag multiple anchorage for prestressing strands (Courtesy Dywidag Systems International)





**Strand Pattern Designation**



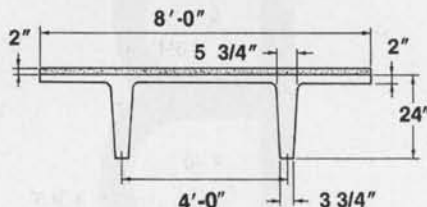
Safe loads shown include dead load of 10 psf for untopped members and 15 psf for topped members. Remainder is live load. Long-time cambers include superimposed dead load but do not include live load.

**Key**

- 173 — Safe superimposed service load, psf
- 0.5 — Estimated camber at erection, in.
- 0.7 — Estimated long-time camber, in.

**DOUBLE TEE**

**8'-0" x 24"**  
**Normal Weight Concrete**



$f'_c = 5,000$  psi  
 $f_{pu} = 270,000$  psi

**Section Properties**

	Untopped	Topped
A	401 in. <sup>2</sup>	—
I	20,985 in. <sup>4</sup>	27,720 in. <sup>4</sup>
$y_b$	17.15 in.	19.27 in.
$y_t$	6.85 in.	6.73 in.
$Z_b$	1,224 in. <sup>3</sup>	1,438 in. <sup>3</sup>
$Z_t$	3,063 in. <sup>3</sup>	4,119 in. <sup>3</sup>
wt	418 plf	618 plf
	52 psf	77 psf
V/S	1.41 in.	

**8DT24**

**Table of safe superimposed service load (psf) and cambers**

**No Topping**

Strand Pattern	$e_o$ $e_c$	Span, ft.																								
		30	32	34	36	38	40	42	44	46	48	50	52	54	56	58	60	62	64	66	68	70	72	74		
68-S	11.15	173	147	126	108	92	79	68	58	50	43	36	30													
	11.15	0.5	0.6	0.6	0.7	0.7	0.7	0.7	0.7	0.7	0.6	0.6	0.5													
88-S	9.15	180	155	134	116	100	87	76	66	57	49	43	36	31												
	9.15	0.7	0.7	0.8	0.8	0.8	0.8	0.8	0.9	0.8	0.8	0.8	0.7	0.6	0.5											
88-D1	9.15			190	166	146	129	114	100	89	79	70	62	54	48	42	37	32								
	14.40			1.1	1.2	1.3	1.4	1.5	1.5	1.6	1.6	1.6	1.6	1.5	1.4	1.3	1.2									
108-D1	7.15							145	129	116	103	92	83	74	66	59	53	47	42	37	32					
	14.15							1.7	1.8	1.9	2.0	2.0	2.1	2.1	2.1	2.0	2.0	1.8	1.7	1.5						
128-D1	5.48																	83	75	68	61	55	49	44	40	35
	13.90																	2.5	2.5	2.5	2.5	2.4	2.3	2.1	1.9	1.9
148-D1	4.29																					61	55	50	45	45
	13.65																	2.7	2.7	2.5	2.3	2.1	1.8	1.5	1.1	0.6

**8DT24 + 2**

**Table of safe superimposed service load (psf) and cambers**

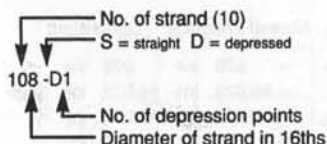
**2" Normal Weight Topping**

Strand Pattern	$e_o$ $e_c$	Span, ft.																							
		26	28	30	32	34	36	38	40	42	44	46	48	50	52	54	56	58	60	62	64				
48-S	14.15	183	149	122	100	82	66	53	42	33															
	14.15	0.4	0.4	0.4	0.5	0.5	0.5	0.5	0.5	0.5															
68-S	11.15		175	147	123	103	86	72	60	49	39														
	11.15		0.5	0.6	0.6	0.7	0.7	0.7	0.7	0.7	0.7														
68-D1	11.15				184	156	133	113	96	81	69	58	48	39											
	14.65				0.7	0.8	0.9	0.9	1.0	1.0	1.0	1.0	1.0	1.0											
88-D1	9.15					190	165	143	124	107	93	80	69	59	51	43									
	14.40					1.1	1.2	1.3	1.4	1.5	1.5	1.6	1.6	1.6	1.6	1.6									
108-D1	7.15								142	124	109	96	84	74	64	56	48								
	14.15								1.7	1.8	1.9	2.0	2.0	2.1	2.1	2.1	2.1								
128-D1	5.48																	74	65	57	49				
	13.90																	2.5	2.5	2.5	2.5				

Strength based on strain compatibility; bottom tension limited to  $12\sqrt{f'_c}$ ; Shaded values require release strengths higher than 3500 psi.

**Figure B-1** 8'-0" x 24" Double Tee (Courtesy PCI, Ref. 4.9)

## Strand Pattern Designation



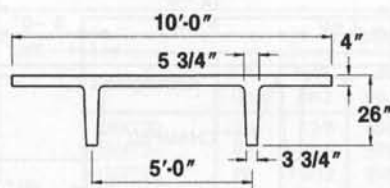
Because these units are pretopped and are typically used in parking structures, safe loads shown do not include any superimposed dead loads. Loads shown are live load. Long-time cambers do not include live load.

## Key

- 196 — Safe superimposed service load, psf  
0.4 — Estimated camber at erection, in.  
0.5 — Estimated long-time camber, in.

PRETOPPED  
DOUBLE TEE

10'-0" x 26"



## Section Properties

Normal Weight    Lightweight

A	=	689 in. <sup>2</sup>	689 in. <sup>2</sup>
I	=	30,716 in. <sup>4</sup>	30,716 in. <sup>4</sup>
y <sub>b</sub>	=	20.29 in.	20.29 in.
y <sub>t</sub>	=	5.71 in.	5.71 in.
Z <sub>b</sub>	=	1,514 in. <sup>3</sup>	1,514 in. <sup>3</sup>
Z <sub>t</sub>	=	5,379 in. <sup>3</sup>	5,379 in. <sup>3</sup>
wt	=	718 plf	550 plf
		72 psf	55 psf
V/S	=	2.05 in.	2.05 in.

$f'_c = 5,000 \text{ psi}$

$f_{pu} = 270,000 \text{ psi}$

## 10DT26

Table of safe superimposed service load (psf) and cambers

No Topping

Strand Pattern	e <sub>c</sub>	Span, ft.																					
		26	28	30	32	34	36	38	40	42	44	46	48	50	52	54	56	58	60	62	64	66	68
68-S	14.29	196	161	133	109	90	74	60	49	39	30												
	14.29	0.4	0.4	0.4	0.4	0.5	0.5	0.5	0.4	0.4	0.4												
88-S	12.29		169	142	119	100	83	69	57	47	38	30											
	12.29		0.5	0.5	0.6	0.6	0.6	0.6	0.6	0.6	0.5	0.4											
88-D1	12.29			200	170	146	125	107	91	78	66	56	47	39	32								
	17.54			0.7	0.8	0.9	0.9	1.0	1.0	1.0	1.0	0.9	0.9	0.8									
108-D1	10.29				189	163	142	123	107	93	80	69	60	51	43	36							
	17.29				1.1	1.1	1.2	1.3	1.3	1.4	1.4	1.4	1.3	1.3	1.2	1.1							
128-D1	8.62								134	118	103	90	79	69	60	52	45	38	32				
	17.04								1.6	1.6	1.7	1.7	1.7	1.7	1.6	1.5	1.4	1.3					
148-D1	7.43												98	87	76	67	59	51	45	38	33		
	16.79												2.0	2.1	2.1	2.1	2.1	2.0	1.9	1.7	1.5		

## 10LDT26

Table of safe superimposed service load (psf) and cambers

No Topping

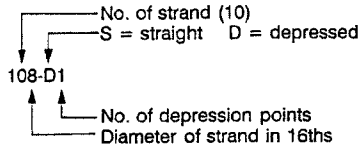
Strand Pattern	e <sub>c</sub>	Span, ft.																						
		28	30	32	34	36	38	40	42	44	46	48	50	52	54	56	58	60	62	64	66	68	70	72
68-S	14.29	175	146	123	104	88	74	63	53	44	36	30												
	14.29	0.6	0.7	0.7	0.8	0.8	0.9	0.9	0.9	0.9	0.9	0.8												
88-S	12.29		183	156	133	113	97	83	71	61	52	44	37	31										
	12.29		0.8	0.9	1.0	1.0	1.1	1.1	1.2	1.2	1.2	1.2	1.1	1.0										
88-D1	12.29			184	159	138	120	105	92	80	70	61	53	46	39	34								
	17.54			1.3	1.4	1.5	1.7	1.7	1.8	1.9	1.9	1.9	1.9	1.9	1.8	1.7								
108-D1	10.29				177	155	137	121	106	94	83	73	65	57	50	44	38	33						
	17.29				1.8	2.0	2.1	2.2	2.3	2.5	2.6	2.6	2.6	2.6	2.6	2.5	2.4	2.3						
128-D1	8.62												104	93	83	74	66	59	52	46	41	36	31	
	17.04												3.0	3.1	3.2	3.3	3.3	3.4	3.3	3.2	3.1	3.0	2.8	
148-D1	7.43																	73	65	58	52	47	41	37
	16.79																	4.0	4.0	4.0	4.0	4.0	3.8	3.6

Strength based on strain compatibility; bottom tension limited to  $12\sqrt{f'_c}$ ;

Shaded values require release strengths higher than 3500 psi.

Figure B-2 10'-0" x 26" Double Tee (Courtesy PCI, Ref. 4.9)

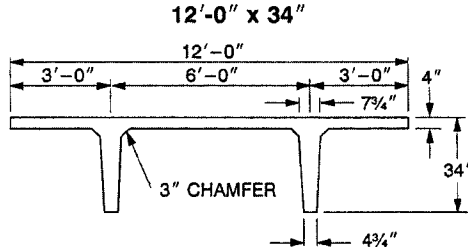
**Strand Pattern Designation**



Because these units are pretopped and are typically used in parking structures, safe loads shown do not include any superimposed dead loads. Loads shown are live load. Long-time cambers do not include live load.

- Key**  
 176 — Safe superimposed service load, psf  
 0.8 — Estimated camber at erection, in.  
 1.1 — Estimated long-time camber, in.

**PRETOPPED DOUBLE TEE**



$f'_c = 5,000$  psi  
 $f_{pu} = 270,000$  psi

**Section Properties**

	Normal Weight	Lightweight
A	= 978 in <sup>2</sup>	978 in <sup>2</sup>
I	= 86,072 in <sup>4</sup>	86,072 in <sup>4</sup>
y <sub>b</sub>	= 25.77 in.	25.77 in.
y <sub>t</sub>	= 8.23 in.	8.23 in.
S <sub>b</sub>	= 3,340 in <sup>3</sup>	3,340 in <sup>3</sup>
S <sub>t</sub>	= 10,458 in <sup>3</sup>	10,458 in <sup>3</sup>
wt	= 1,019 plf	781 plf
	85 psf	65 psf
V/S	= 2.39 in.	2.39 in.

**12DT34**

**Table of safe superimposed service load (psf) and cambers (in.)** **No Topping**

Strand Pattern	e <sub>s</sub> , in. e <sub>c</sub> , in.	Span, ft																							
		42	44	46	48	50	52	54	56	58	60	62	64	66	68	70	72	74	76	78	80	82	84	86	
128-D1	14.10	176	155	135	119	104	91	79	69	59	51	43	36	30											
	22.52	0.8	0.8	0.9	0.9	0.9	0.9	0.9	0.8	0.8	0.7	0.7	0.6	0.5											
148-D1	12.91	187	165	146	129	114	101	89	78	68	60	52	44	38	32	26									
	22.27	1.0	1.0	1.1	1.1	1.1	1.1	1.1	1.1	1.1	1.0	1.0	0.9	0.7	0.6	0.4									
168-D1	12.77	196	174	155	138	123	110	97	86	76	67	59	52	45	39	33	28								
	22.02	1.2	1.3	1.3	1.4	1.4	1.4	1.4	1.4	1.4	1.4	1.3	1.2	1.1	1.0	0.8	0.6								
188-D1	11.38	178	160	143	128	115	102	91	82	73	64	57	50	43	38	32	27								
	21.77	1.5	1.5	1.6	1.6	1.7	1.7	1.7	1.7	1.7	1.6	1.5	1.5	1.4	1.2	1.1	0.9	0.6							
208-D1	10.27	131	118	106	95	85	76	68	61	54	47	41	36	31	26										
	21.52	1.8	1.9	1.9	1.9	1.9	1.9	1.9	1.9	1.9	1.9	1.8	1.5	1.3	1.1	0.9	0.6								
228-D1	9.36	109	98	88	79	71	64	57	50	44	39	34	29												
	21.27	2.1	2.1	2.1	2.1	2.1	2.0	1.9	1.7	1.6	1.4	1.1	0.8												

**12LDT34**

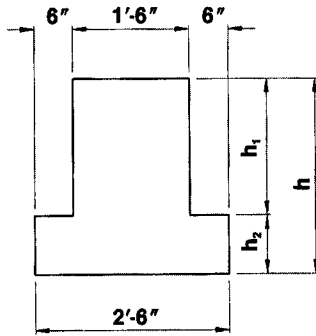
**Table of safe superimposed service load (psf) and cambers (in.)** **No Topping**

Strand Pattern	e <sub>s</sub> , in. e <sub>c</sub> , in.	Span, ft																							
		42	44	46	48	50	52	54	56	58	60	62	64	66	68	70	72	74	76	78	80	82	84	86	
128-D1	14.10	193	171	152	135	120	107	95	85	76	67	59	52	46	40	35	30	26							
	22.52	1.3	1.4	1.5	1.5	1.6	1.6	1.7	1.7	1.7	1.7	1.7	1.6	1.6	1.5	1.4	1.2	1.0							
148-D1	12.91	182	162	146	130	117	105	94	85	76	68	61	54	48	42	37	33	28							
	22.27	1.7	1.8	1.9	2.0	2.0	2.1	2.1	2.1	2.1	2.1	2.1	2.1	2.1	2.0	1.9	1.8	1.6	1.4						
168-D1	12.77	191	172	155	139	126	114	103	93	84	76	68	61	55	49	44	39	34	30	26					
	22.02	2.1	2.2	2.3	2.4	2.5	2.6	2.7	2.7	2.7	2.7	2.7	2.7	2.6	2.5	2.4	2.3	2.1	1.9	1.6					
188-D1	11.38	144	131	119	108	98	89	81	73	66	60	54	48	43	39	34	30	26							
	21.77	2.7	2.8	2.9	3.0	3.1	3.2	3.2	3.2	3.1	3.2	3.2	3.2	3.1	3.0	2.9	2.8	2.6	2.4	2.1					
208-D1	10.27	102	93	85	77	70	64	58	52	47	42	38													
	21.52	3.5	3.6	3.6	3.6	3.6	3.6	3.6	3.6	3.6	3.6	3.6	3.6	3.6	3.6	3.6	3.5	3.4	3.3	3.1	2.9				
228-D1	9.36	80	73	67	61	56	51	47	43	39	35	31	28												
	21.27	4.1	4.1	4.1	4.0	3.9	3.8	3.6	3.5	3.4	3.3	3.2	3.1	3.0	2.9	2.8	2.6	2.4	2.2	2.0	1.8	1.6	1.4	1.2	1.0

Strength based on strain compatibility; bottom tension limited to  $12\sqrt{f'_c}$ ; see pages 2-2-2-6 for explanation. Shaded values require release strengths higher than 3500 psi.

**Figure B-3** Pretopped 12'-0" x 34" Double Tee (Courtesy PCI, Ref. 4.9)

### INVERTED TEE BEAMS



$f'_c = 5,000$  psi  
 $f_{pu} = 270,000$  psi  
 ½ in. diameter  
 low-relaxation strand

Normal Weight Concrete

Section Properties								
Designation	h (in.)	h <sub>1</sub> /h <sub>2</sub> (in.)	A (in. <sup>2</sup> )	I (in. <sup>4</sup> )	y <sub>b</sub> (in.)	Z <sub>b</sub> (in. <sup>3</sup> )	Z <sub>t</sub> (in. <sup>3</sup> )	wt (plf)
30IT20	20	12/8	456	15,240	8.74	1,744	1,354	475
30IT24	24	12/12	576	26,352	10.50	2,510	1,952	600
30IT28	28	16/12	648	41,824	12.22	3,423	2,650	675
30IT32	32	20/12	720	62,400	14.00	4,457	3,467	750
30IT36	36	24/12	792	88,678	15.82	5,605	4,394	825
30IT40	40	24/16	912	121,923	17.47	6,979	5,412	950
30IT44	44	28/16	984	162,161	19.27	8,415	6,557	1,025
30IT48	48	32/16	1,056	210,199	21.09	9,967	7,811	1,100
30IT52	52	36/16	1,128	266,627	22.94	11,623	9,175	1,175
30IT56	56	40/16	1,200	332,032	24.80	13,388	10,642	1,250
30IT60	60	44/16	1,272	406,997	26.68	15,255	12,215	1,325

**Key**

- 8,428 — Safe superimposed service load, plf
- 0.4 — Estimated camber at erection, in.
- 0.2 — Estimated long-time camber, in.

1. Check local area for availability of other sizes.
2. Safe loads shown include 50% dead load and 50% live load. 800 psi top tension has been allowed, therefore additional top reinforcement is required.
3. Safe loads can be significantly increased by use of structural composite topping.

**Table of safe superimposed service load (plf) and cambers**

Designation	No. Strand	e	Span, ft.																	
			18	20	22	24	26	28	30	32	34	36	38	40	42	44	46	48	50	
30IT20	14	6.65	8,428	6,736	5,485	4,533	3,792	3,204	2,730	2,342	2,020	1,751	1,523	1,332	1,167	1,024				
			0.4	0.5	0.6	0.7	0.9	1.0	1.1	1.2	1.3	1.4	1.4	1.5	1.6	1.6				
			0.2	0.2	0.2	0.3	0.3	0.3	0.3	0.3	0.3	0.3	0.3	0.3	0.3	0.3	0.2			
30IT24	17	7.67	9,736	7,942	6,578	5,516	4,673	3,994	3,437	2,976	2,592	2,269	1,993	1,755	1,550	1,370	1,212	1,073		
			0.4	0.5	0.6	0.7	0.8	0.9	1.0	1.1	1.2	1.2	1.3	1.4	1.4	1.5	1.5	1.5		
			0.2	0.2	0.2	0.2	0.3	0.3	0.3	0.3	0.3	0.3	0.3	0.3	0.3	0.2	0.2	0.2	0.1	0.0
30IT28	20	9.06	9,087	7,643	6,497	5,573	4,816	4,189	3,664	3,219	2,839	2,513	2,334	1,990	1,776	1,588				
			0.6	0.6	0.7	0.8	0.9	1.0	1.1	1.2	1.2	1.3	1.4	1.4	1.5	1.5				
			0.2	0.2	0.3	0.3	0.3	0.3	0.3	0.3	0.3	0.3	0.3	0.3	0.3	0.3	0.3	0.3	0.3	0.2
30IT32	23	10.50	8,647	7,436	6,445	5,623	4,935	4,352	3,855	3,426	3,055	2,732	2,448	2,201						
			0.7	0.7	0.8	0.9	1.0	1.1	1.2	1.2	1.3	1.4	1.4	1.5	1.5					
			0.2	0.3	0.3	0.3	0.3	0.3	0.3	0.4	0.4	0.4	0.4	0.4	0.4	0.4	0.4	0.4	0.4	0.3
30IT36	24	12.32	9,492	8,243	7,207	6,340	5,605	4,978	4,439	3,971	3,563	3,205	2,892							
			0.7	0.7	0.8	0.9	1.0	1.1	1.2	1.3	1.3	1.3	1.4							
			0.2	0.2	0.3	0.3	0.3	0.3	0.3	0.3	0.3	0.3	0.3	0.3	0.3	0.3	0.3	0.3	0.3	0.3
30IT40	30	12.92	9,077	7,994	7,077	6,295	5,621	5,037	4,528	4,081	3,687									
			0.8	0.8	0.9	1.0	1.1	1.2	1.2	1.3	1.4									
			0.3	0.3	0.3	0.4	0.4	0.4	0.4	0.4	0.4	0.4	0.4	0.4	0.4	0.4	0.4	0.4	0.4	0.4
30IT44	30	14.73	9,659	8,564	7,629	6,825	6,127	5,519	4,985	4,514										
			0.7	0.8	0.9	1.0	1.0	1.1	1.2	1.3	1.3	1.4								
			0.3	0.3	0.3	0.3	0.3	0.3	0.3	0.3	0.3	0.3	0.3	0.3	0.3	0.3	0.3	0.3	0.3	0.3
30IT48	33	16.17	9,222	8,262	7,431	6,705	6,068	5,506												
			0.8	0.9	1.0	1.0	1.1	1.2	1.2	1.3	1.3	1.4								
			0.3	0.3	0.3	0.3	0.3	0.3	0.3	0.3	0.3	0.3	0.3	0.3	0.3	0.3	0.3	0.3	0.3	0.3
30IT52	36	17.62	9,836	8,858	8,004	7,255	6,594													
			0.9	0.9	1.0	1.1	1.1	1.2	1.2	1.3	1.3	1.4								
			0.3	0.3	0.3	0.3	0.3	0.3	0.3	0.3	0.3	0.3	0.3	0.3	0.3	0.3	0.3	0.3	0.3	0.3
30IT56	39	19.06	9,407	8,538	7,770															
			1.0	1.0	1.1															
			0.3	0.4	0.4															
30IT60	42	20.49	9,917	9,036																
			1.0	1.0																
			0.3	0.4																

Figure B-4 Inverted Tee Beam Sections (Courtesy PCI, Ref. 4.9)



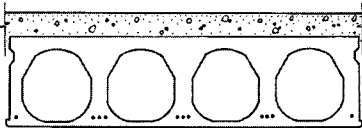
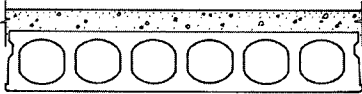
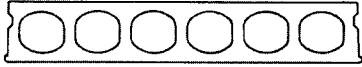
## HOLLOW-CORE SLABS

**Section Properties — normal weight concrete**

**Dy-Core**

Trade name: Dy-Core®

Licensing Organization: Dy-Core Systems, Inc., Vancouver, British Columbia



Section width x depth	Untopped				With 2" topping		
	A in. <sup>2</sup>	y <sub>b</sub> in.	I in. <sup>4</sup>	wt psf	y <sub>b</sub> in.	I in. <sup>4</sup>	wt psf
4'-0" x 6"	151	3.11	683	40	4.54	1,552	65
4'-0" x 8"	190	3.95	1,568	51	5.54	3,130	76
4'-0" x 10"	216	5.10	2,892	58	6.80	5,097	83
4'-0" x 12"	262	6.34	4,875	71	8.01	7,823	96
4'-0" x 15"	289	7.34	8,701	78	9.36	13,776	103

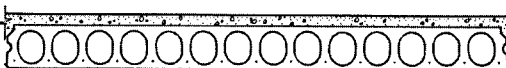
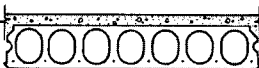
Note: All sections not available from all producers. Check availability with local manufacturers.

**Section Properties — normal weight concrete**

**Dynaspan**

Trade name: Dynaspan®

Equipment Manufacturers: Dynamold Corporation, Salina, Kansas

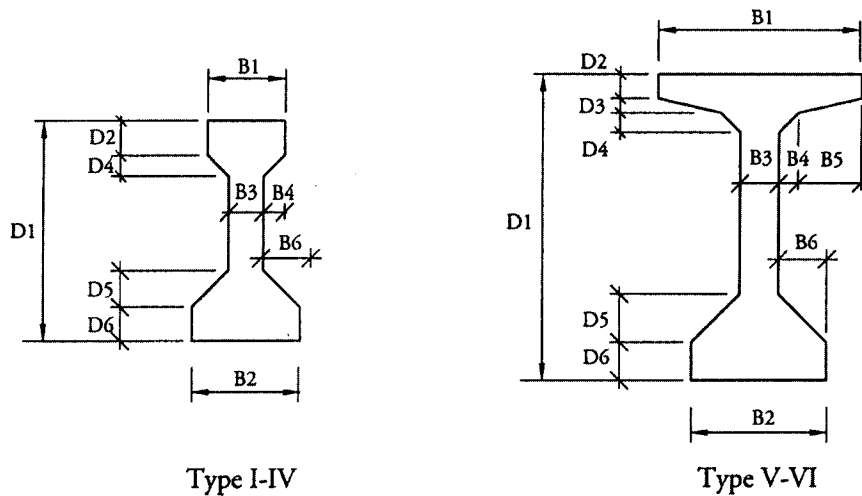


Section width x depth	Untopped				With 2" topping		
	A in. <sup>2</sup>	y <sub>b</sub> in.	I in. <sup>4</sup>	wt psf	y <sub>b</sub> in.	I in. <sup>4</sup>	wt psf
4'-0" x 4"	133	2.00	235	35	3.08	689	60
4'-0" x 6"	165	3.02	706	43	4.25	1,543	68
4'-0" x 8"	233	3.93	1,731	61	5.16	3,205	86
4'-0" x 10"	260	4.91	3,145	68	6.26	5,314	93
8'-0" x 6"	338	3.05	1,445	44	4.26	3,106	69
8'-0" x 8"	470	3.96	3,525	61	5.17	6,444	86
8'-0" x 10"	532	4.96	6,422	69	6.28	10,712	94
8'-0" x 12"	615	5.95	10,505	80	7.32	16,507	105

Note: All sections not available from all producers. Check availability with local manufacturers.

**Figure B-5** Hollow Core Slab Sections (Courtesy PCI, Ref. 4.9)

### AASHTO I-Beams



#### Dimensions (inches)

Type	D1	D2	D3	D4	D5	D6	B1	B2	B3	B4	B5	B6
I	28.0	4.0	0.0	3.0	5.0	5.0	12.0	16.0	6.0	3.0	0.0	5.0
II	36.0	6.0	0.0	3.0	6.0	6.0	12.0	18.0	6.0	3.0	0.0	6.0
III	45.0	7.0	0.0	4.5	7.5	7.0	16.0	22.0	7.0	4.5	0.0	7.5
IV	54.0	8.0	0.0	6.0	9.0	8.0	20.0	26.0	8.0	6.0	0.0	9.0
V	63.0	5.0	3.0	4.0	10.0	8.0	42.0	28.0	8.0	4.0	13.0	10.0
VI	72.0	5.0	3.0	4.0	10.0	8.0	42.0	28.0	8.0	4.0	13.0	10.0

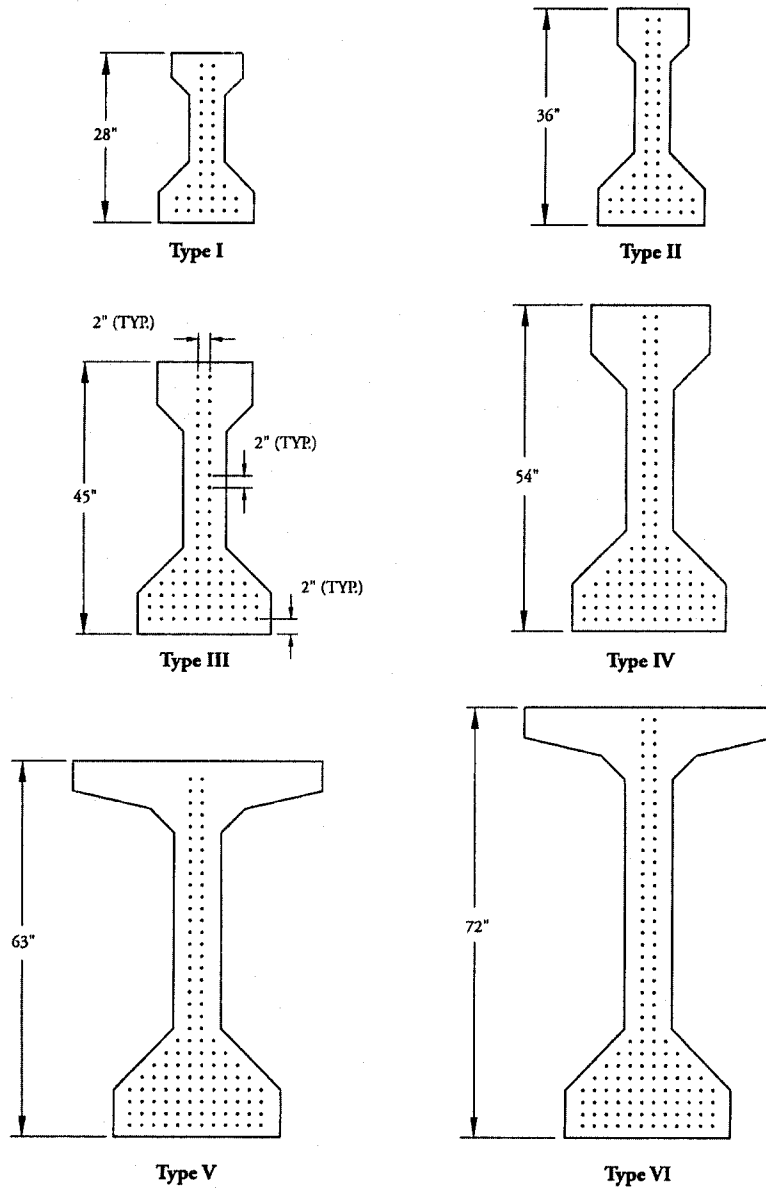
#### Properties

Type	Area in. <sup>2</sup>	$y_{\text{bottom}}$ in.	Inertia in. <sup>4</sup>	Weight kip/ft	Maximum Span,* ft
I	276	12.59	22,750	0.287	48
II	369	15.83	50,980	0.384	70
III	560	20.27	125,390	0.583	100
IV	789	24.73	260,730	0.822	120
V	1,013	31.96	521,180	1.055	145
VI	1,085	36.38	733,320	1.130	167

\*Based on simple span, HS-25 loading and  $f'_c = 7,000$  psi.

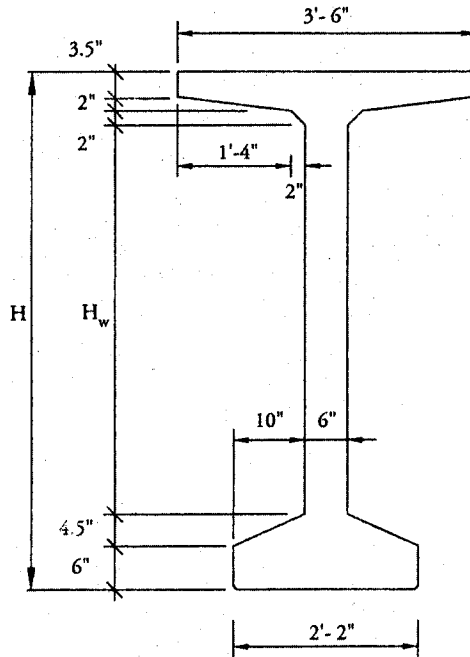
Figure B-6 (a) AASHTO/PCI Standard Bridge Sections (Courtesy PCI, Ref. 12.11)

**AASHTO I-Beams**



**Figure B-6 (b)** Possible Strand Arrangement for Sections in Figure C-6 (a)

**AASHTO-PCI Bulb-Tees**



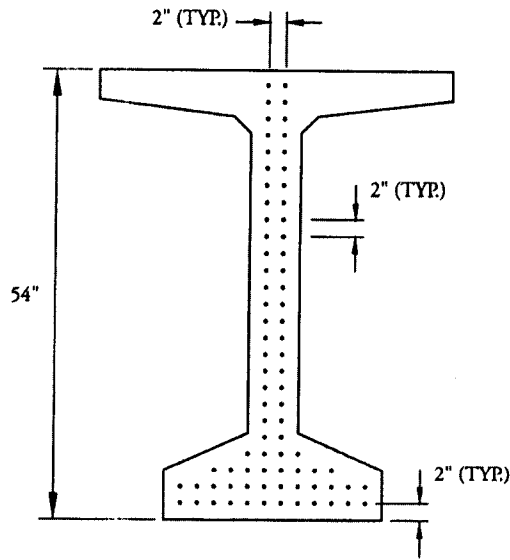
**Properties**

Type	H in.	H <sub>w</sub> in.	Area in. <sup>2</sup>	Inertia in. <sup>4</sup>	y <sub>bottom</sub> in.	Weight kip/ft	Maximum Span,* ft
BT-54	54	36	659	268,077	27.63	0.686	114
BT-63	63	45	713	392,638	32.12	0.743	130
BT-72	72	54	767	545,894	36.60	0.799	146

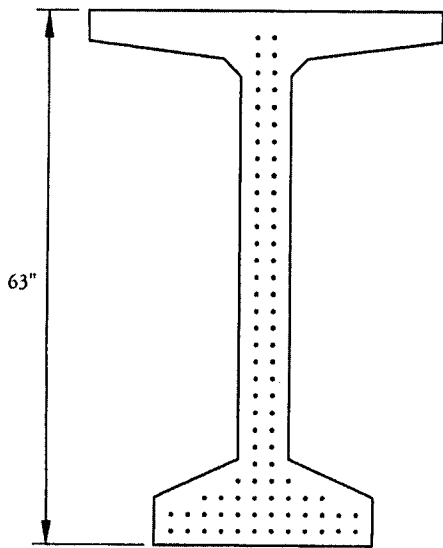
\*Based on simple span, HS-25 loading and f<sub>c</sub>' = 7,000 psi.

**Figure B-7 (a)** AASHTO/PCI Bulb Tees (Courtesy PCI, Ref. 12.11)

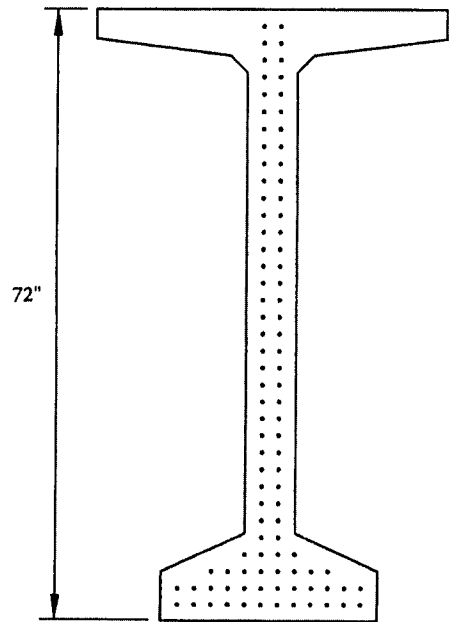
**AASHTO-PCI Bulb-Tees**



**BT-54**

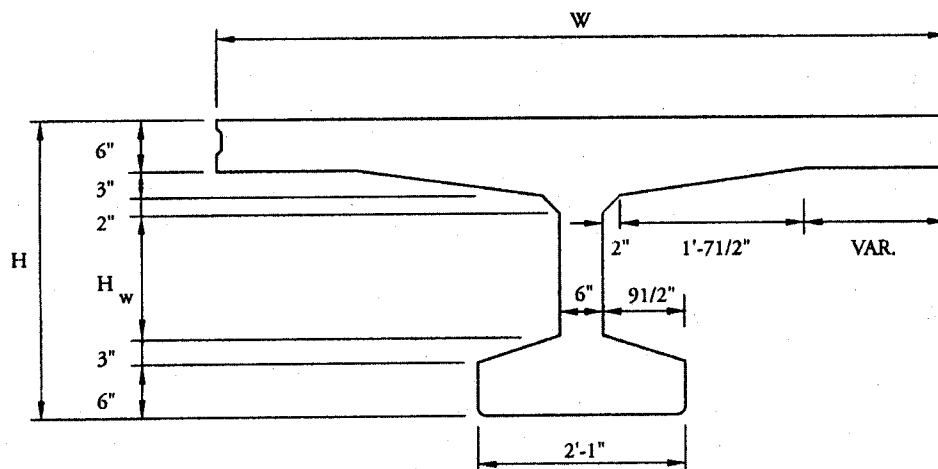


**BT-63**



**BT-72**

**Figure B-7 (b)** Possible Strand Arrangement for Sections in Figure C-7 (a)

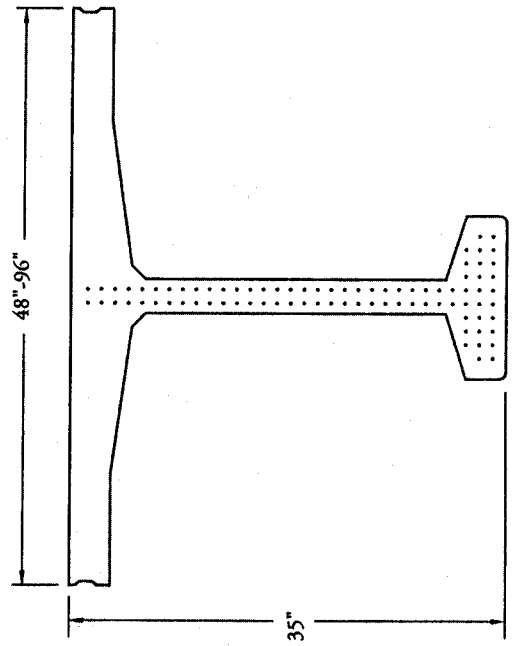
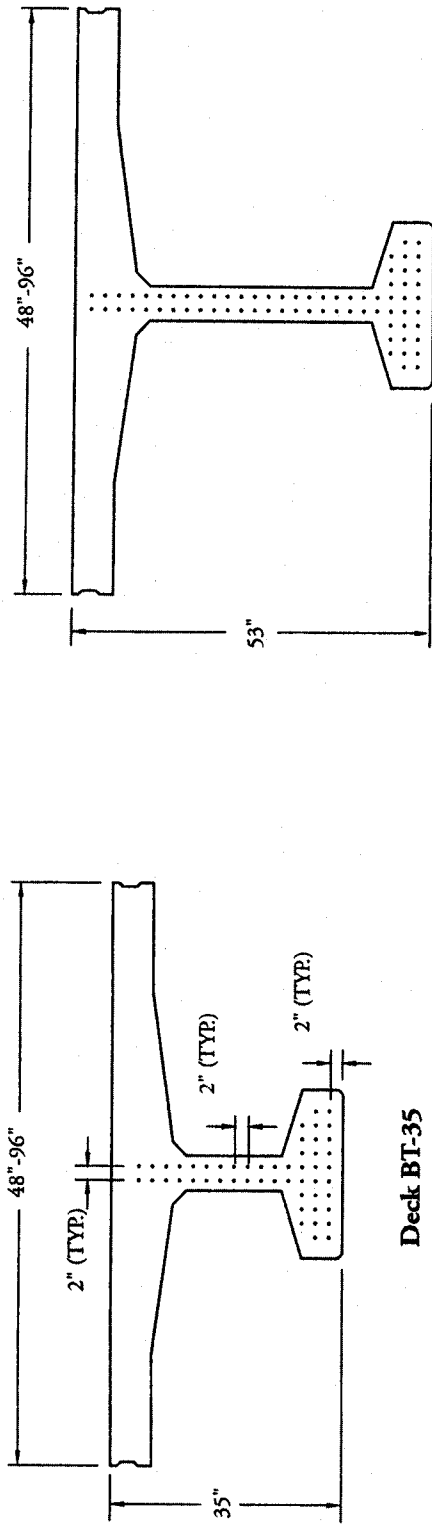
**Deck Bulb-Tees****Dimensions and Properties**

H in.	H <sub>w</sub> in.	W in.	Area in. <sup>2</sup>	Inertia in. <sup>4</sup>	y <sub>bottom</sub> in.	Weight kip/ft	Maximum Span* ft
35	15	48	677	101,540	21.12	0.75	100
		72	823	116,071	23.04	0.91	78
		96	967	126,353	24.37	1.07	65
53	33	48	785	294,350	31.71	0.87	145
		72	931	335,679	34.56	1.03	121
		96	1,075	365,827	36.63	1.19	105
65	45	48	857	490,755	38.55	0.95	168
		72	1,003	559,367	41.95	1.11	148
		96	1,147	610,435	44.46	1.27	130

\*Based on simple span, HS-25 loading and  $f'_c = 7,000$  psi.

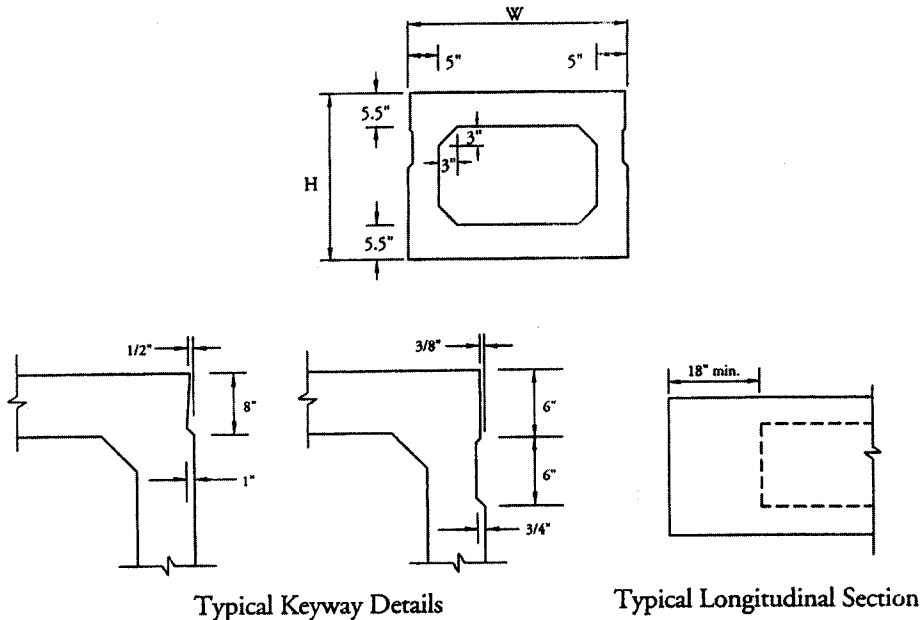
**Figure B-8 (a)** AASHTO/PCI Shallow Bridge Deck Bulb Tees (Courtesy PCI, Ref. 12.11)

**Deck Bulb-Tees**



**Figure B-8 (b)** Possible Strand Arrangement for Sections in Figure C-8 (a)

### AASHTO Box Beams



**Dimensions (inches)**

Type	W	H
BI-36	36	27
BI-48	48	27
BII-36	36	33
BII-48	48	33
BIII-36	36	39
BIII-48	48	39
BIV-36	36	42
BIV-48	48	42

**Properties**

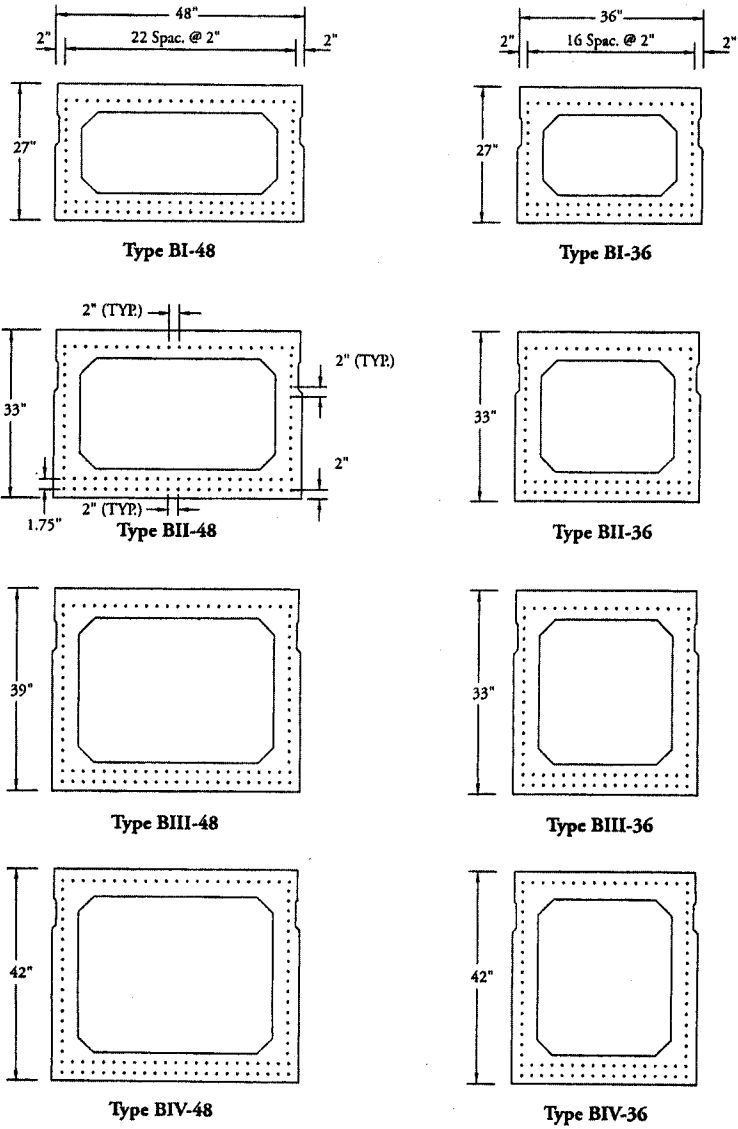
Type	Area in. <sup>2</sup>	$y_{\text{bottom}}$ in.	Inertia in. <sup>4</sup>	Weight kip/ft	Max. Span* ft
BI-36	560.5	13.35	50,334	0.584	92
BI-48	692.5	13.37	65,941	0.721	92
BII-36	620.5	16.29	85,153	0.646	107
BII-48	752.5	16.33	110,499	0.784	108
BIII-36	680.5	19.25	131,145	0.709	120
BIII-48	812.5	19.29	168,367	0.846	125
BIV-36	710.5	20.73	158,644	0.740	124
BIV-48	842.5	20.78	203,088	0.878	127

\*Based on simple span, HS-25 loading and  $f'_c = 7,000$  psi.

Figure B-9 (a) AASHTO/PCI Bridge Box Girders (Courtesy PCI, Ref. 12.11)



**AASHTO Box Beams**



**Figure B-9 (b)** Possible Strand Arrangement for Sections in Figure C-9 (a)

# INDEX

- AASHTO: 71, 74, 130, 140, 161, 165, 168, 169, 220, 742, 744, 750, 758, 764, 780, 820
  - design, concrete bridges, 742
  - LFD, 744, 748
  - LRFD specifications, 753, 754, 756
  - sections, 116–119
  - standard specifications, 741
  - truck loads, 745
- Abeles, P.W., 6, 28, 72, 220, 321, 416, 713, 741
- Acceleration, 829
  - maps, 830, 831
- ACI, 71, 79, 130, 161, 185, 187, 200, 413, 415, 443, 557, 559, 704, 741, 744, 759, 763, 820
  - ACI Committee 318: 71, 104, 148, 152, 219, 235, 298, 302, 336, 519, 552, 573, 629, 705, 715, 849, 851, 900
  - ACI Committee 435: 72, 104, 220
- ACI-ASCE, 74, 80, 82, 104, 228
- Aggregates
  - shrinkage of, 48
- Allowable deflections, 453, 454
- Allowable stresses
  - concrete, 59, 60
  - steel, 59, 60
- Analysis, flexural, 107
- Anchorage zone design, 141, 145
- ANSI, 182, 220
- ANSI/ASCE, 705
- Arthur, P.D., 416
- ASCE, 740, 741, 820
- ASTM, 70, 71
- ASTM Specification, 50
- Aswad, A., 868, 902
- Aswad, G.S., 868, 902
- Badie, S.S., 821
- Baishya, M.C., 821
- Baker, A.L.L., 181, 220, 416, 408
- Balaguru, P.N., 71, 220
- Balancing effects, 15
- Bardhan-Roy, B.K., 28, 70, 72, 220, 416, 715, 741
- Bars
  - prestressing, 53, 54
  - reinforcing, 50, 51
- Base restraint, 672
- Basic concepts of prestressing, 7
- Bazant, 497
- Beams
  - constant eccentricity, 113
  - continuous, 341, 358, 405
  - variable eccentricity, 115
  - weak beam-strong column concept, 847
- Bearing stresses, 634, 638
- Biaxial bending, 531
- Billington, D.P., 713, 724, 740
- Blair, H., 708, 741
- Blair, K., 630
- Borg, S.E., 901
- Branson, D.E., 49, 71, 104, 427, 451, 496
- Breen, J.E., 144, 220
- Bridges
  - AASHTO sections, 935–942

- Bridges (*cont.*)
  - cable-stayed, 3, 7, 11, 506
  - segmental, 3, 7
- Brondum-Nielsen, T., 741
- Burdet, O., 144, 220
- Burns, N.H., 28, 220, 630
- Bursting stresses, 140
  
- Cantilever factor, 677
- CEB, 74
- CEB-FIP, 130
- Center-of-pressure line (C-line), 13
- Chakrabarti, P., 571, 630
- Chan, T.C., 658
- Chen, B., 39, 41, 72
- Chen, K.C., 219, 235, 336
- Chiang, J.Y., 219, 479, 497
- Choek, G.S., 901, 902
- Circular prestressing, 70
- Circular tanks, 660
- Cleland, N.M., 902
- C-line, 12, 21, 347, 350, 362
- Clough, D.P., 659
- Clough, R.W., 901
- Cohn, M.Z., 104, 408, 416, 479, 497, 630
- Collins, M.P., 148, 149, 220, 287, 289, 290, 292, 337, 762, 763, 820
- Columns
  - behavior, 501
  - load contour method, 530
  - modified, 540
  - nonslender, 508
  - P- $\Delta$  effect, 523
  - reciprocal load method for biaxial bending, 540
  - slender, 515, 525
  - strength of, 507
- Combined slide and pin, 679
- Compatibility, 198, 298
- Composite beams
  - elastic flexural stresses in, 158, 162, 242
  - section properties of, 115–119
  - shear transfer in, 242
- Composite members, 635
- Composite sections, 118, 152, 165, 242
- Compression-controlled state, 198, 759
- Concordant tendon, 354
- Concrete, 31
  - compressive strength, 32, 36, 39
  - creep properties, 43
  - modulus of rupture, 422
  - shear strength, 35
  - stress-strain diagram, 36
  - stress-strain properties of, 467
  - tensile strength, 33
- Confining reinforcement, 849
  - transverse, 849, 851
- Connections
  - dapped-end beam, 640
  - details of, 651
  - tolerances for, 634, 635
- Continuous beams, 340, 341
- Corbels, 263, 647
- Corbel design by strut-and-tie method, 327, 329
- Corley, W.G., 408, 416
- Cornell, C.A., 182, 220
- Coupling beams, 856
- Crack control, 479, 480
- Cracking
  - beam behavior before cracking, 420, 423
  - beams, 427, 443, 479
  - inclined, 228
  - longitudinal, 140
  - tension members, 548
- Crack width
  - calculation of, 708
- Crack widths
  - calculation of, 480, 481
  - tank walls, 708
  - tolerable, 485
- Creasy, L.R., 661, 677, 694, 740 (Ref. 11.2)
- Creep
  - coefficient, 46
  - concrete, 43
  - in long-term deflections, 437, 444, 454
  - losses, 80
- Crom, J.S. Sr., 660
- Cross, H., 630
- Curing, 47
- Curvature
  - beams, 423, 429, 440, 452
  - creep, 450
  - instantaneous, 419, 426
  
- Danesi, R., 408, 416
- Decompression, 110, 111
- Deep beams by strut-and-tie method, 320, 322, 325
- Deflections
  - allowable, 453, 454
  - of flat plates, 610
  - incremental, 429

- time-step method for, 448
- of two-way slabs and plates, 617
- Deformation
  - of concrete, 33
- Derecho, A.T., 901
- Design aids, 905
- Design information, 903
- Diagonal shear cracking, 228
- Diaphragms, 841, 854, 857
- Dikshit, O.P., 630
- Dilger, W.H., 104, 496
- Dill, R.E., 5
- Djazmati, C., 868, 902
- Dobell, C., 28
- Doehring, C.W., 5
- Double-T beams, 116, 117
- Drift, 841, 842
- Dual systems, 872
- Ductile frames, 858, 860, 890, 895
- Ducts, 66
- Dywidag ductile connection assembly (DDC), 65, 864, 890
  
- Earthquake ground motion, 826, 829
- Eccentricity
  - limits of, 122
  - variation of, 115
- Economics of prestressed concrete, 4
- Effective prestress, 73, 93, 97, 100
- Elastic deformation, 75
- Elastic modulus
  - of concrete, 36
  - of steel, 56
- Elastic shortening losses, 75
- Ellingwood, B., 182, 220
- Empty tank technique, 671
- End-block reinforcement, 173
- Englekirk, R.E., 864, 866, 867, 897, 901, 902 (Ref. 13.21, 13.22)
- Equivalent frame method
  - for deflection, 563, 610, 611
  - for flexural analysis, 543, 547
- Equivalent lateral force method in seismic design, 837
- Equivalent load method, 16, 22, 347, 348, 351, 352
- Ezeldin, A., 220
  
- Factored loads, 846
- Failure
  - shear compression, 231
  
- Federal Emergency Management Agency (FEMA), 901
- Federal Highway Administration, 220
- FIP, 74
- First-order second-moment (FOSM) method, 182
- Fixity at wall foot, 695, 736
- Fixity of dome support, 712
- Flange width, effective, 161
- Flat dome, 712
- Flat-plate slabs, 592
- Flexural strength
  - of beams, 178
- Flexural stresses, 59, 106
  - allowable in concrete, 59
  - allowable in steel, 59
- Flexure-shear cracking, 225
- Form factor, 677
- Frames, indeterminate, 379
- Freely sliding, 659, 662, 664, 692
- Freudenthal, A.M., 71
- Freysinnet, E., 6, 28
- Frictional losses, 85
- Furlong, R.W., 408, 416, 659
  
- Gadebeku, B.K., 220
- Gadebeku, C., 144, 145
- Galambos, T.V., 182, 220
- Gas load, 662
- Gergely, P., 220
- Gerwick, B.C. Jr., 28, 220, 361, 416, 550
- Gesund, H., 630
- Ghali, A., 104, 496, 740
- Ghosh, S.K., 901
- Goodkind, H., 219
- Gouwens, A.J., 630
- Grosco, J., 406, 416
- Grouting tendons, 64
- Gustafson, D.P., 630
- Guyon, Y., 6, 28, 220
  
- Hemabom, R., 630
- Hemispherical dome, 709, 712
- Hewett, W.H., 5, 660
- High-rise buildings, 855, 858, 895
- Hinges, plastic, 401, 405, 408
- Historical development of prestressing, 5
- Hoffman, E.S., 630
- Hoop stress, 673
- Horizontal base shear, 837
- Horizontal interface shear, 768
- Hsu, T.T.C., 285, 288, 295, 302, 337, 762, 821

- Hsu, C.T.T., 525, 526, 536  
Huang, P.T., 220, 479, 480, 497  
Hung, T.Y., 630
- Indeterminate  
    beams, 341, 363, 401  
    frames, 379, 401  
Influence coefficients, 403, 405, 669, 670  
Initial prestress, 10, 11  
Institute of Structural Engineers, 28  
International Building Code (IBC2009),  
    413, 416, 751, 826, 828, 901  
Itaya, R., 630
- Jack, hydraulic, 63  
Jackson, P.H., 5  
Johansen, K.W., 616
- Kern of the cross-section, 130, 134, 135  
Kudlapur, S.T., 821  
Kunnath, S.K., 862, 901 (Ref. 13.24)
- Ledges, 647  
Lee, J.Y., 821  
Leonhardt, F., 6  
Lew, H.S., 901  
Lift slabs, 861  
Limit analysis, 401  
Lin, T.Y., 6, 28, 104, 220, 416, 550, 630  
Linear elastic anchorage zone analysis,  
    144  
Linear transformation, 354  
Liquid load, 661  
Llovet, D., 901  
Load-and-resistance-factor-design  
    (LRFD) method, 182  
Load balancing, 22  
    for beams, 347, 358  
    for slabs, 567, 577  
Load-balancing method for beams, 15  
Load combinations, 846  
Load contour method of biaxial bending,  
    540  
Load factors, ACI, 185  
Losses  
    anchorage seating, 88  
    creep, 80  
    elastic shortening, 76  
    friction, 85  
    relaxation, 78, 80  
    shrinkage, 83  
Loss of prestress, 73
- LRFD  
    AASHTO design, concrete bridges, 742  
Lund, J., 5
- Magnel, G., 6, 28  
Maher, M.H., 39, 41, 72  
Mansfield, E.H., 622, 630  
Marshall, W.T., 220  
Martin, L.D., 496  
Mast, R.F., 773, 818, 819, 821 (Ref. 12.16)  
Mattock, A.H., 143, 218, 235, 332, 408, 416,  
    659  
McGee, W.D., 332  
McGregor, J.G., 182, 220  
Mehta, P.K., 71  
Membrane coefficients, 677, 680–693  
Mikhailov, V., 6  
Mindess, S., 71  
Mirza, S.A., 659  
Mitchell, D., 148, 149, 220, 287, 289, 290,  
    291, 337, 762, 763, 820  
Modified load contour method for biaxial  
    bending, 542  
Moment distribution, 351, 352  
    carryover factor, 597, 598  
Moment magnification factor for columns,  
    520  
Moment of inertia, effective, 427  
Moment redistribution, 361  
Morgan, N., 630  
Moriadith, F.L., 652  
Multipliers for deflection, 446
- Naaman, A.E., 28, 220, 759, 773, 774, 778,  
    821  
Naja, W.M., 834, 861, 901  
Nakaki, S.D., 861, 901 (Ref. 13.18)  
Nawy, E.G., 28, 39, 41, 62, 66, 71, 72, 104,  
    144, 145, 202, 219, 220, 266, 336, 408,  
    479, 480, 496, 550, 573, 574, 708, 741,  
    751, 763, 821, 901  
Neville, A.M., 71  
Nilson, A.H., 220, 416, 451, 496, 630  
Nonprestressed steel, 50  
    in beams, 50  
    in columns, 50  
    in slabs, 51, 52  
Norris, H.C., 901
- Occupancy, seismic, 833, 834  
One-way slabs, 570  
Overturning, 843

- Park, R., 416
- Partial prestressing, 179
- Paulay, J., 416
- Pauley, T., 901
- PCI, 74, 83, 104, 117, 120, 130, 220, 245, 259, 303, 336, 337, 416, 446, 496, 550, 635, 640, 651, 659, 661, 704, 741, 780, 786, 803, 821
  - connection details, 651–658
  - deflection multipliers, 454, 468
- Period of vibration, 827
- Pessiki, S., 862, 869, 871, 902 (Refs. 13.31–13.33)
- Pinned wall foot, 671, 695, 697
- Plastic hinges, 305, 308, 401
- Plasticity equilibrium torsion, 293
- Plates
  - carryover factors, 596, 597
  - fixed-end moments, 570
  - torsional stiffness, 564
- Poisson's ratio for concrete, 668, 671, 675
- Popovics, S., 70
- Portland Cement Association, 71, 678, 740
- Post-tensioning, 62
- Post-Tensioning Institute, 71, 104, 144, 219, 550, 629, 659, 704, 741, 821
- Potyondy, G.J., 62, 72, 202, 219, 408, 416, 474, 480, 496
- Precast prestressed frames in high seismicity zones, 852, 864
- Precast tanks, 704, 705
- Preload, 663, 665, 715
- Pressure, center of, 13
- Pressure grouting, 64
- Preston, R.L., 630, 708, 741
- Pretensioning, 61
- Priestley, M.J.N., 902
- Primary moments, 344
- Principal stresses in beams, 232
- Probable shears and moments, 845
- Profile of tendons, 129, 132, 133
  - of steel, 78
- Restrained wall foot, 662
- Reynolds, C.E., 569, 570, 571, 630
- Rice, P.F., 630
- Ring force, 674, 676
- Roberts, C., 144, 220
- Roll, F., 71
- Roof, 708
- Ross, A.D., 71
- Rotation, 402
- Safety, 742
  - structural, 181
- Salek, F., 408, 416
- Sanders, D., 144, 220
- Sauer, J.A., 71
- Sawyer, H.A., 408
- Schneider, R.R., 897
- Scordelis, A.C., 630
- Secondary moments, 344
- Section modulus, 108
- Seismic design, 824
- Seismic forces, 751
- Semisliding, 733
- Serviceability, 418, 420, 453, 479
- Shaikh, A.F., 447, 451, 496
- Shear, 223
- Shear design by ACI code, 228, 235, 240, 246
- Shear friction theory, 264, 266
- Shear-moment transfer, 583
- Shear reinforcement
  - in beams, 234, 266
  - in slabs, 582, 585
- Shear wall, 855, 879
  - design, 882
- Shells, 660, 664, 709
- Shrinkage
  - of concrete, 48
  - losses, 83
- SI conversion table, 905–906
- Siess, C.P., 234, 336
- Sign convention, 107, 680
- Slabs
  - deflection of two-way, 586
  - flat-plate, 592
  - shear-moment transfer, 583
  - types of, 554, 555
- Slender columns
  - ACI design method for, 525
- Smulski, E., 416
- Soogswang, K., 235, 336

- Sozen, M.A., 220, 234, 336
- Spalling zone, 141
- Span-depth ratios, flat plates, 570
- Spectral response, 829
- Standard sections, 115
- Stanton, J.F., 861, 902
- Steedman, J.C., 569, 570, 571, 630
- Steel
  - low-relaxation, 54
  - relaxation of, 56, 78
  - strands, 54
  - stress-relieved, 54
  - wires, 54
- Steiner, G.R., 5
- Stirrups, 241, 248, 250
- Stone, W.C., 220, 901, 902
- Story height drift, 841
- Strain, 36, 43
- Strain compatibility analysis, 209
  - strain limits design approach, 191, 759, 760
  - strain limits, 191, 192, 759
- Strength
  - concrete, 31, 35, 59
  - flexural, beams, 188
  - nominal, 181, 186
  - of prestressing steel, 53, 54
  - reduction factor, 507
  - reduction factors, ACI, 185
  - reinforcing bars, 50, 51, 52
  - tanks, 705
- Stress block, rectangular, 190
- Stress distribution, 183
- Stress-strain properties of
  - concrete, 36, 37, 421, 467
  - prestressing steel, 51, 56, 441
  - reinforcing bars, 51
- Strong column-weak beam concept, 845, 847, 873
- Structural (shear) walls, 854
- Strut-and-tie anchorage zone design, 144
- Strut stress path in post-tensioned anchorage zone, 144
- Strut-and-tie hypothesis for corbels and deep beams, 317, 318, 322, 324
- Subsoil support, 699
- Support displacement method, 344–348
- Tadros, M.K., 104, 425, 496, 741, 821
- Tanks
  - circular prestressing, 69, 704, 715
  - influence coefficients, 680–693
  - moments, 663
  - radial stress, 663
  - roof dome, 708
  - toe, 699, 700
  - vertical prestressing, 736
  - wall, 679, 716, 717
- Taylor, F.W., 416
- Tendon profile, concordant, 354
- Tensile strength
  - concrete, 31
  - prestressing steel, 54
  - reinforcing bars, 50, 51
- Tension-controlled state, 192, 759
- Tension members, 500
  - behavior of, 546
  - design of, 548
  - linear, 548
- Thickness of walls, 706, 707
- Thompson, S.E., 416
- Thornton, K., 416
- Time-step method, incremental, 448
- Timoshenko, S., 668, 671, 713, 740
- Torsion
  - in beams, 286, 298, 308
  - compression field theory, 289
  - cracking, 290, 292
  - design for, 298, 304
  - equilibrium in element theory, 294
  - reinforcement requirements, 303
  - skew-bending theory, 285
  - space-truss analogy theory, 287
- Transformation, linear, 355
- Ukadike, M.M., 71, 266, 336
- Unbonded post-tensioned precast concrete
  - precast shear walls, 867, 888
  - wall-base bolting, 870
  - wall base connection, 888
  - wall base grouting, 889
- Unified design approach (*See* Strain limits design approach)
- Uniform Building Code (UBC), 413, 416, 829, 901
- Vertical moments, 679, 696
- Vertical prestressing, 679, 715
- Vessey, J.V., 630, 708, 741 (Ref. 11.14)
- Wakabayashi, M., 622, 696
- Walters, D.B., 630

- Water-cement ratio, 48  
Web reinforcement, minimum, 238  
Web-shear cracking, 231  
Wheel load distribution, 748  
Wheen, R.J., 552  
Wilhelm, W.J., 552  
Wind loads, 751  
Wire mesh, welded, 51  
Wires for prestressing, 54, 55, 56  
Woinowsky-Krieger, S., 668, 671, 713, 740  
Wollman, G., 144, 220  
Yong, Y.K., 144, 145, 220  
Young, J.F., 71  
Zhu, R.H., 821  
Zia, P., 285, 336  
Zwoyer, E.M., 234, 336





$V_j$  = factored shear force at section due to externally applied loads occurring simultaneously with  $M_{\max}$ .

$V_n$  = nominal shear strength.

$w_u$  = factored load per unit length of beam or per unit area of slab.

$x$  = shorter overall dimension of rectangular part of cross section.

$x_1$  = shorter center-to-center dimension of closed rectangular stirrup.

$y$  = longer overall dimension of rectangular part of cross section.

$y_t$  = distance from centroidal axis of gross section, neglecting reinforcement, to extreme fiber in tension.

$y_1$  = longer center-to-center dimension of closed rectangular stirrup.

$\alpha$  = total angular change of prestressing tendon profile in radians from tendon jacking end to any point  $x$ .

$\alpha$  = ratio of flexural stiffness of beam section to flexural stiffness of a width of slab bounded laterally by centerlines of adjacent panels (if any) on each side of the beam.

$$= \frac{E_{cb}I_b}{E_{ca}I_s}$$

$\alpha_m$  = average value of  $\alpha$  for all beams on edges of a panel.

$\beta_d$  = ratio of dead load per unit area to live load per unit area (in each case without load factors).

$\beta_d$  = ratio of maximum factored dead load moment to maximum factored total load moment, always positive.

$\beta$  = a ratio of clear spans in long to short direction of two-way slabs.

$\gamma_f$  = fraction of unbalanced moment transferred by flexure at slab-column connections.

$\gamma_p$  = factor for type of prestressing tendon.

$$= 0.55 \text{ for } f_{py}/f_{pu} \text{ not less than } 0.80$$

$$= 0.40 \text{ for } f_{py}/f_{pu} \text{ not less than } 0.85$$

$$= 0.28 \text{ for } f_{py}/f_{pu} \text{ not less than } 0.90$$

$\gamma_v$  = fraction of unbalanced moment transferred by eccentricity of shear at slab-column connections.

$$= 1 - \gamma_f$$

$\delta_{ns}$  = moment magnification factor for frames braced against sidesway, to reflect effects of member curvature between ends of compression member.

$\delta_s$  = moment magnification factor for frames not braced against sidesway, to reflect lateral drift resulting from lateral and gravity loads.

$\mu$  = curvature friction coefficient.

$\xi_{(xi)}$  = time-dependent factor for sustained load.

$\rho_{(rho)}$  = ratio of nonprestressed tension reinforcement.

$$= A_s/bd$$

$\rho'$  = ratio of nonprestressed compression reinforcement

$$= A'_s/bd$$

$\rho_b$  = reinforcement ratio producing balanced strain conditions.

$\rho_p$  = ratio of prestressed reinforcement.

$$= A_{ps}/bd_p$$

$\rho_t$  =  $A_{sv}/A_{cv}$ ; where  $A_{sv}$  is the projection on  $A_{cv}$  of area of distributed shear reinforcement crossing the plane of  $A_{cv}$ .

$\theta$  = angle of compression diagonals in truss analogy for torsion.

$\phi$  = strength reduction factor.

$$\omega = \rho f_y / f'_c$$

$$\omega' = \rho' f_y / f'_c$$

$$\omega_p = \rho_p f_{pe} / f'_c$$

$$\omega_{pw}, \omega_w, \omega'_w$$

= reinforcement indices for flanged sections computed as for  $\omega, \omega_p$ , and  $\omega'$  except that  $b$  shall be the web width, and reinforcement area shall be that required to develop compressive strength of web only.

To convert from	to	multiply by
<b>Length</b>		
inch (in.)	millimeter (mm)	25.4
inch (in.)	meter (m)	0.0254
foot (ft)	meter (m)	0.3048
yard (yd)	meter (m)	0.9144
<b>Area</b>		
square foot (sq. ft)	square meter (sq m)	0.09290
square inch (sq. in.)	square millimeter (sq mm)	645.2
square inch (sq. in.)	square meter (sq m)	0.0006452
square yard (sq yd)	square meter (sq m)	0.8361
acre (A)	hectare (ha) = 10,000 sq m	0.4047
<b>Volume</b>		
cubic inch (cu in.)	cubic meter (cu m)	0.00001639
cubic foot (cu ft)	cubic meter (cu m)	0.02832
cubic yard (cu yd)	cubic meter (cu m)	0.7646
gallon (gal) Can. liquid*	liter	4.546
gallon (gal) Can. liquid*	cubic meter (cu m)	0.004546
gallon (gal) U.S. liquid*	liter	3.785
gallon (gal) U.S. liquid*	cubic meter (cu m)	0.003785
<b>Force</b>		
kip	kilogram (kgf)	453.6
kip	newton (N)	4448.0
pound (lb)	kilogram (kgf)	0.4536
pound (lb)	newton (N)	4.448
<b>Pressure or Stress</b>		
kips/square inch (ksi)	megapascal (MPa)**	6.895
pound/square foot (psf)	kilopascal (kPa)**	0.04788
pound/square inch (psi)	kilopascal (kPa)**	6.895
pound/square inch (psi)	megapascal (MPa)**	0.006895
pounds/square foot (psf)	kilogram/square meter (kgf/sq m)	4.882
<b>Mass</b>		
pound (avdp)	kilogram (kg)	0.4536
ton (short, 2000 lb)	kilogram (kg)	907.2
ton (short, 2000 lb)	tonne (t)	0.9072
grain	kilogram (kg)	0.00006480
tonne (t)	kilogram (kg)	1000
<b>Mass (weight per Length)</b>		
kip/linear foot (klf)	kilogram/meter (kg/m)	1488
pound/linear foot (plf)	kilogram/meter kg/m	1.488
pound/linear foot (plf)	newton/meter (N/m)	14.593
<b>Mass per volume (density)</b>		
pound/cubic foot (pcf)	kilogram/cubic meter (kg/cu m)	16.02
pound/cubic yard (pcy)	kilogram/cubic meter (kg/cu m)	0.5933
gallon per yd <sup>3</sup>	Kg/m <sup>3</sup>	4.985
oz per yd <sup>3</sup>	Kg/m <sup>3</sup>	0.037
<b>Bending Moment or Torque</b>		
inch-pound (in.-lb)	newton-meter	0.1130
foot-pound (ft-lb)	newton-meter	1.356
foot-kip (ft-k)	newton-meter	1356
<b>Temperature</b>		
degree Fahrenheit (deg F)	degree Celsius (C)	$t_c = (t_f - 32)/1.8$
degree Fahrenheit (deg F)	degree Kelvin (K)	$t_K = (t_f + 459.7)/1.8$
<b>Energy</b>		
British thermal unit (Btu)	joule (j)	1056
kilowatt-hour (kwh)	joule (j)	3,600,000
<b>Power</b>		
horsepower (hp) (550 ft lb/sec)	watt (W)	745.7
<b>Velocity</b>		
mile/hour (mph)	kilometer/hour	1.609
mile/hour (mph)	meter/second (m/s)	0.4470
<b>Other</b>		
Section modulus (in. <sup>3</sup> )	mm <sup>3</sup>	16,387
Moment of inertia (in. <sup>4</sup> )	mm <sup>4</sup>	416,231
Coefficient of heat transfer (Btu/ft <sup>2</sup> /h/°F)	W/m <sup>2</sup> /°C	5.678
Modulus of elasticity (psi)	MPa	0.006895
Thermal conductivity (BTU-in./ft <sup>2</sup> /h/°F)	Wm/m <sup>2</sup> /°C	0.1442
Thermal expansion in./in./°F	mm/mm/°C	1.800
Area/length (in. <sup>2</sup> /ft)	mm <sup>2</sup> /m	2116.80

\*One U.S. gallon equals 0.8321 Canadian gallon

\*\*A pascal equals one newton/square meter

# PRESTRESSED CONCRETE

## A FUNDAMENTAL APPROACH

FIFTH EDITION UPDATE

ACI, AASHTO, IBC 2009 Codes Version

EDWARD G. NAWY

A state-of-the-art book by a national and international expert on concrete structures and materials, this updated fifth edition of *Prestressed Concrete: A Fundamental Approach* reflects the very latest ACI 318-08, the International Building Code IBC 2009, and the AASHTO 2004-08. It puts at the disposal of the user the author's many years of professional and academic know-how in design, construction, and forensic engineering.

This book is different from most because its major topics of material behavior, prestress losses, flexure, shear, torsion, and deflection-camber are sequentially self-contained and can be covered in one semester at the advanced senior and graduate levels. It uniquely follows procedures given in over 20 flow charts and 400 illustrations that simplify the understanding and application of the subject in design, using both customary US and SI units in the examples.

### Additionally, you will find:

- All design examples presented in this edition update conform to the ACI 318-08 Strain Limits Method and AASHTO in the flexural design of prestressed concrete members.
- A detailed revised chapter on the seismic design of ductile prestressed and precast concrete beams and shear walls in high seismicity zones conforming to ACI 318-08 Code and the IBC 2009 Code including in the chapter the new seismic tables and factors.
- A new section on the strut-and-tie design of corbels and deep beams.
- A detailed chapter on the design of statically indeterminate structures.
- A revised chapter containing the latest ACI and AASHTO provisions on the design of anchorage end blocks in post-tensioned beams using the strut-and-tie method.
- A revised chapter on slender columns, including a simplified load-contour bi-axial bending method.
- A chapter with comprehensive design examples on LRFD and standard design of bridge deck members for flexure, shear and torsion, conforming to the latest AASHTO specifications.
- A comprehensive chapter on the design of prestressed concrete tanks and shell roofs, rarely found in any other textbooks.

Prentice Hall  
is an imprint of

PEARSON

[www.pearsonhighered.com](http://www.pearsonhighered.com)



### ABOUT THE AUTHOR

**Dr. Edward G. Nawy** is a distinguished professor attaining the emeritus professorship status this year after 50 years of service in the Department of Civil and Environmental Engineering at Rutgers, The State University of New Jersey. He has been active in the ACI, PCI, and TRB since the 1960s and is internationally recognized for his extensive work in the fields of reinforced and prestressed concrete, particularly in the areas of crack and deflection control. Dr. Nawy has published more than 175 papers in numerous technical journals worldwide and is the author of *Reinforced Concrete: A Fundamental Approach*, Sixth Edition, 2009, *Prestressed Concrete: A Fundamental Approach*, updated Fifth Edition, 2010, both published by Prentice Hall, *Fundamentals of High Performance Concrete*, Second Edition, 2001, published by John Wiley and Sons, and *Concrete Construction Engineering Handbook*, Second Edition, 2008, published by CRC Press. He is the recipient of several major awards, including the Henry L. Kennedy Award of the ACI, the ACI Concrete Research Council Award, and the ACI Design Practice Award, honorary professorship with the Nanjing Institute of Technology, honorary membership of the ACI, and emeritus membership of the Transportation Research Board Committee on Concrete Properties of the National Research Council. Dr. Nawy has been an Evaluator for the Accreditation Board for Engineering and Technology (ABET). He is a licensed Professional Engineer in the states of New York, New Jersey, Pennsylvania, California, and Florida, a Chartered Civil Engineer overseas, and has been a consultant in structural and forensic engineering to agencies throughout the United States.

ISBN-13: 978-0-13-608150-0  
ISBN-10: 0-13-608150-9

